INTRODUCTION TO THE FINITE ELEMENT METHOD

4TH EDITION

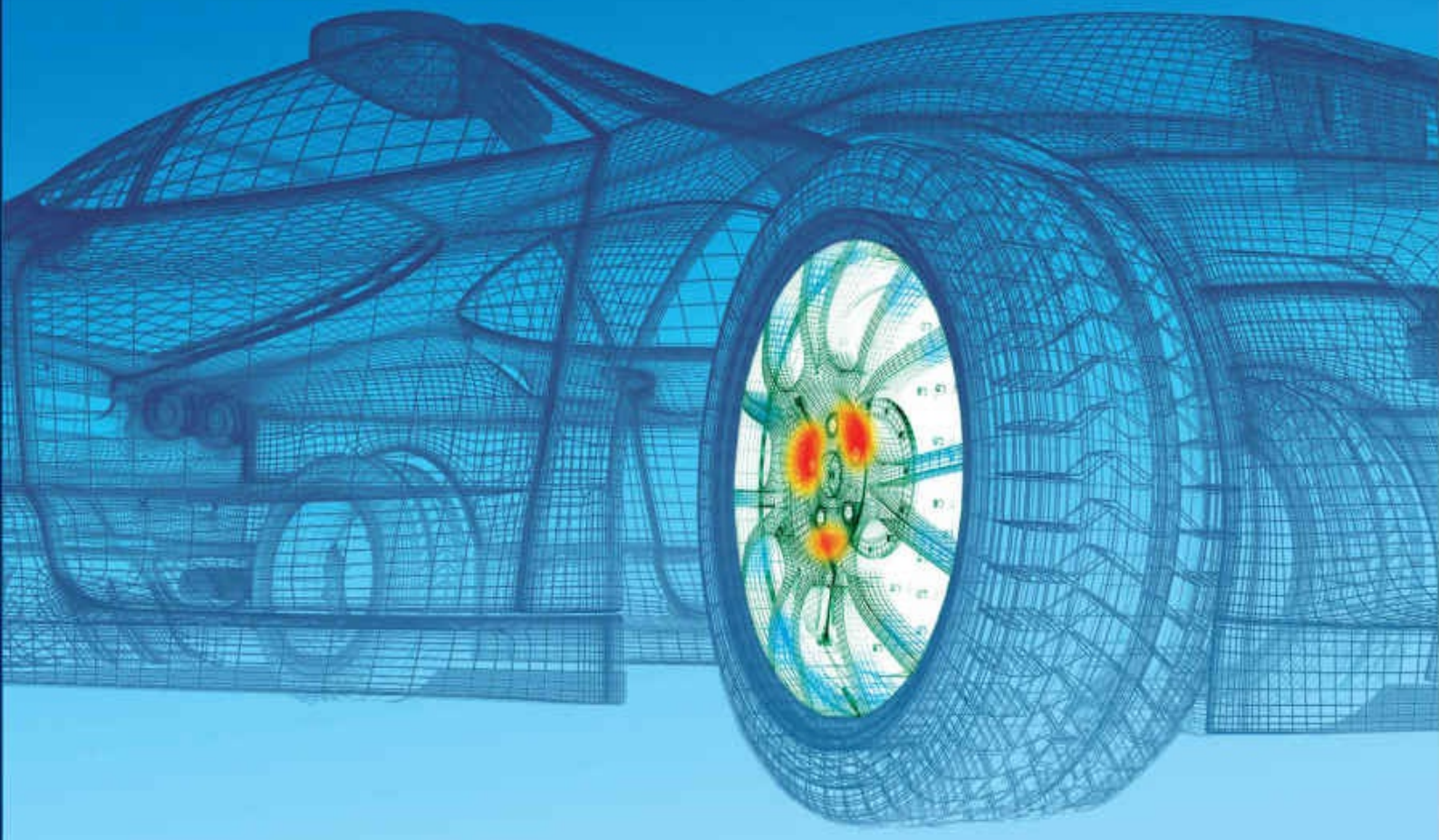

J. N. REDDY

Mc Graw Hill Education

About the Author

J. N. Reddy, Ph.D., is the Oscar S. Wyatt Endowed Chair Professor, a Distinguished Professor, and a Regents Professor of Mechanical Engineering at Texas A&M University. He is a highly cited researcher with an h-index of 100 (per Google Scholar) and the author of 21 books and over 650 journal papers. Dr. Reddy is known worldwide for his significant contributions to the field of applied mechanics for more than 40 years through the authorship of widely used textbooks on linear and nonlinear finite element analysis, variational methods, composite materials and structures, and continuum mechanics. His pioneering work on the development of shear deformation theories that bear his name in the literature, the *Reddy third-order plate theory* and the *Reddy layerwise theory*, has had a major impact and led to new research developments and applications. Some of his ideas on shear deformation and on penalty finite element models of fluid flows have been implemented in commercial finite element computer programs like ABAQUS, NISA, and HyperXtrude. Dr. Reddy is a Fellow of all major professional societies of engineering (ASME, AIAA, ASCE, AAM, ASC, USACM, IACM), and has received top mechanics medals from these and other societies (ASME Medal, Raymond D. Mindlin Medal, Theodore von Karman Medal, John von Neumann Medal, William Prager Medal, O. C. Zienkiewicz Medal). He is a Member of the U.S. National Academy of Engineering and a Foreign Fellow of the Canadian Academy of Engineering, Indian National Academy of Engineering, and Brazilian National Academy of Engineering. For additional details, visit http://mechanics.tamu.edu.

That which is not given is lost.

Introduction to the Finite Element Method

J. N. Reddy
Department of Mechanical Engineering
Texas A&M University
College Station, Texas

Fourth Edition

New York Chicago San Francisco
Athens London Madrid
Mexico City Milan New Delhi
Singapore Sydney Toronto

ISBN: 978-1-25-986191-8
MHID: 1-25-986191-0

The material in this eBook also appears in the print version of this title: ISBN: 978-1-25-986190-1, MHID: 1-25-986190-2.

eBook conversion by codeMantra
Version 1.0

To my teachers and students everywhere,
who taught me all that I know.

Contents

Preface to the Fourth Edition

The most important step in the analysis of any system or component thereof is an understanding of its functionalities (i.e., knowing the goal of the study), identification of the domain and its material constitution, stimuli placed on the system, and boundary conditions. Consistent with the goal of the study, one selects an appropriate mathematical model (i.e., set of equations that govern the response of the system). The selection of a realistic mathematical model is directly connected to the ability to convert it into a numerical model which preserves the physical features that the mathematical model embodies and enables us to systematically evaluate various parameters of the system. Numerical simulations aid the selection of designs and manufacturing processes in such a way as to maximize the reliable functionality of products and minimize the cost of production, distribution, and repairs.

Mathematical models are developed using laws of physics and assumptions concerning a system's behavior. Courses taken during their studies on continuum mechanics, materials science, experimental methods, and dynamical systems, among others, provide engineers with the theoretical background needed to formulate suitable mathematical models and understand the behavior of some simple systems. On the other hand, courses on numerical methods prepare them to see how the mathematical models are translated into engineering solutions. In addition, in cases where physical experiments are prohibitively expensive, numerical simulations are the only alternative, especially when the phenomena are governed by differential equations with variable coefficients, to evaluate various design and manufacturing options. It is in this context that a course on the finite element method proves to be very useful.

The present book, *Introduction to the Finite Element Method*, first published in 1984, is an introduction to the method as applied to linear, one- and two-dimensional problems of engineering and applied sciences. The method is introduced via a number of commonly encountered differential equations that arise in various specialties of science and

engineering. One of the main features of the book is that the method is presented in its most general form (i.e., not as a method only for structural engineers) so that engineers and scientists from all disciplines can understand the steps involved in converting differential equations into a suitable set of algebraic equations among variables of interest. In doing this, simple explanations of both the physics involved and mathematics needed are given priority over problem complexity. Another strong feature of the book is to make the reader think about and understand the material, rather than memorize and "plug and chug." Various editions of the book have been adopted by many academic institutions in the United States and around the world, and it has been used by a countless number of students, engineers, and researchers for three generations.

The present edition closely resembles its immediate previous edition. The main changes are the addition of material on work and energy methods in Chapter 2, additional explanation in Chapter 3 on how to set up element equations using physical principles but without differential equations, additional examples of heat transfer, fluid mechanics, and solid mechanics problems in Chapter 4, applications to circular plates in Chapter 5, expansion of the material on trusses and frames in Chapter 6, and expanded material on viscous flows, elasticity, and 3-D finite elements in Chapters 11, 12, and 13, respectively. In the present edition, the chapter on plate bending is omitted because it is an advanced topic for a first course (and there is more than enough material to cover in a first course). Every chapter has undergone changes in terms of explanation, examples, and exercise problems. The book is largely self-contained, and it may be used as a textbook for a first course on the finite element method at undergraduate and graduate levels. A solutions manual has also been prepared for the book, and it is available from the publisher to certified teachers who adopt the book as a text. Fortran and MATLAB source codes used in the book (FEM1D and FEM2D) and their executable programs with example data files are available, free of charge, from the author's website, *http://mechanics.tamu.edu*.

Since the publication of the first to the third editions, many users of the book have communicated their compliments as well as errors they found, for which the author thanks them. All of the errors known to the author have been corrected in the current edition. Manuscript of this edition was proofread by Archana Arbind, Parisa Khodabakhshi, Jinseok Kim, Namhee Kim, and Michael Powell; the author is grateful for their help and constructive comments. The author also thanks the following professional colleagues, among many others, for their friendship, encouragement, and

constructive comments on the book over the years:

Hasan Akay, Purdue University at Indianapolis
David Allen, Texas A&M University, College Station
Narayana Aluru, University of Illinois at Urbana-Champaign
Marcilio Alves, University of São Paulo, Brazil
Marco Amabili, McGill University, Canada
Ronald Averill, Michigan State University
Ted Belytschko, Northwestern University
K. Chandrashekara, Missouri University of Science and Technology
A. Ecer, Purdue University at Indianapolis
Antonio Ferreira, University of Porto, Portugal
Somnath Ghosh, Johns Hopkins University
S. Gopalakrishna, Indian Institute of Science, Bangalore
Antonio Grimaldi, University of Rome II, Italy
Norman Knight, Jr., Clemson University
Filis Kokkinos, Technological Educational Institute of Athens, Greece
A. V. Krishna Murty, Indian Institute of Science, Bangalore
R. Krishna Kumar, Indian Institute of Technology, Madras
H. S. Kushwaha, Bhabha Atomic Research Centre, India
K. Y. Lam, Nanyang Technological University, Singapore
J. K. Lee, Ohio State University
K. M. Liew, City University of Hong Kong
C. W. Lim, City University of Hong Kong
Franco Maceri, University of Rome II, Italy
C. S. Manohar, Indian Institute of Science, Bangalore
Antonio Miravete, Zaragoza University, Spain
J. T. Oden, University of Texas at Austin
Alan Palazzolo, Texas A&M University
P. C. Pandey, Indian Institute of Science, Bangalore
Glaucio Paulino, University of Illinois at Urbana-Champaign
Siva Prasad, Indian Institute of Technology, Madras
A. Rajagopal, Indian Institute of Technology, Hyderabad
Jani Romanoff, Aalto University, Finland
Debasish Roy, Indian Institute of Science, Bangalore
Samit Roy, University of Alabama, Tuscaloosa
Elio Sacco, University of Cassino, Italy

Martin Sadd, University of Rhode Island
Rüdger Schmidt, University of Aachen, Germany
E. C. N. Silva, University of São Paulo, Brazil
Arun Srinivasa, Texas A&M University
Sivakumar Srinivasan, Indian Institute of Technology, Madras
Fanis Strouboulis, Texas A&M University
Karan Surana, University of Kansas
Liqun Tang, South China University of Technology
Vinu Unnikrishnan, University of Alabama, Tuscaloosa
C. M. Wang, National University of Singapore
John Whitcomb, Texas A&M University
Y. B. Yang, National Taiwan University

J. N. Reddy, Ph.D.

To raise new questions, new possibilities, to regard old problems from a new angle, requires creative imagination and marks real advance in science.

— Albert Einstein

The art and science of asking questions is the source of all knowledge.

— Thomas Berger

Preface to the Third Edition

The third edition of the book, like the previous two editions, represents an effort to select and present certain aspects of the finite element method that are most useful in developing and analyzing linear problems of engineering and science. In revising the book, students taking courses that might use this book as the textbook have been kept in mind. This edition is prepared to bring more clarity to the concepts discussed while maintaining the necessary mathematical rigor and providing physical interpretations and engineering applications at every step.

This edition of the book is a revision of the second edition, which was well received by engineers as well as researchers in the fields of engineering and science. Most of the revisions in the current edition took place in Chapters 1 through 6. Chapter 5 on error analysis from the second edition is eliminated and a section on the same is added to Chapter 14. Chapter 3 from the second edition is now divided into two chapters, Chapter 3 on theoretical formulation and Chapter 4 on applications. Chapter 4 on beams from the second edition now became Chapter 5 in the current edition, making the total number of chapters in both editions the same. Another change is the interchanging of Chapters 10 and 11 to facilitate the natural transition from plane elasticity to plate bending (Chapter 12). In all chapters, material is added and reorganized to aid the reader in understanding the concepts. Chapters 1, 2, and 3 have extensive modifications that should help the reader. The discussion on nonlinear formulations of Chapter 14 is brief since the material is now available in textbook form in the author's recent publication, *Introduction to Nonlinear Finite Element Analysis* (Oxford University Press, 2004).

Most people who have used the earlier editions of the book liked the "differential equations approach" adopted here. This is natural because everyone, engineer or scientist, is looking for a way to solve differential equations arising in the study of physical phenomena. It is hoped that the third edition of the book serves the student even better than the previous editions in understanding the finite element method as applied to linear

problems of engineering and science.

The author has benefited by teaching an introductory course from this book for many years. While it is not possible to name the hundreds of students and colleagues who have contributed to the author's ability to explain concepts in a clear manner, the author expresses his sincere appreciation to all of them.

J. N. Reddy, Ph.D.

Tejasvi naavadhitamastu
(Let our learning be radiant)

Preface to the Second Edition

This second edition has the same objectives as the first, namely, an introduction to the finite element method as applied to linear, one- and two-dimensional problems of engineering and applied sciences. The revisions are mainly in the form of additional details, expansion of the topics discussed, and the addition of a few topics to make the coverage more complete.

The major organizational change from the first edition is the division of its five chapters into fourteen chapters here. These chapters are grouped into four parts. This reorganization should aid instructors in selecting suitable material for courses. Other organizational changes include putting problem sets at the ends of chapters, providing a chapter summary for each, and reviewing pertinent equations and text in each chapter instead of referring to several chapters back. In addition, example problems in Chapters 3 and 8 are presented in separate sections on heat transfer, fluid flow, and solid mechanics.

Additional details are provided on the construction of the weak forms, time approximations (e.g., accuracy and stability of schemes, and mass lumping), alternative finite element formulations, and nonlinear finite element models. The new topics include sections on trusses and frames, the Timoshenko beam element, eigenvalue problems, and classical plate bending elements. All these changes are also reflected in the revised computer programs FEM1DV2 and FEM2DV2 (revised versions of the FEM1D, FEM2D and PLATE programs in the first edition). Therefore the sections on computer implementation and applications of FEM1DV2 and FEM2DV2 have also been modified extensively. These changes are accompanied by the addition of several figures, tables, and examples.

These extensive changes have resulted in a second edition that is 60% larger. In the interest of keeping the cost of the book within reasonable limits while retaining the basic approach and technical details, certain portions of the original manuscript have been omitted. More specifically, answers to selective problems have been included at the end of the

problem statements themselves, rather than in a separate section. Interested readers and instructors can obtain a copy of the executable programs on a diskette from the author. Fortran source programs can also be purchased from the author.

There is no doubt that this edition is more complete and thorough than the first. It can be used as a textbook for an introductory and/or intermediate level course on the finite element method at senior undergraduate as well as graduate levels. Students of engineering and applied sciences should feel comfortable with the coverage in the book.

The author gratefully acknowledges help in reading the manuscript and suggestions for constructive changes from several colleagues. These include: Hasan Akay, Purdue University at Indianapolis; Norman Knight, Jr., Clemson University; J. K. Lee, Ohio State University; William Rule, University of Alabama; Martin Sadd, University of Rhode Island; John Whitcomb, Texas A&M University; and the author's research students: Ronald Averill, Filis Kokkinos, Y. S. N. Reddy, and Donald Robbins. It is a great pleasure to acknowledge the typing of the manuscript by Mrs. Vanessa McCoy (Virginia Tech), without whose patience and cooperation this work would not have been completed. The author is grateful to the colleagues in the Department of Engineering Science and Mechanics of Virginia Polytechnic Institute and State University for their support and friendship throughout the author's tenure there.

J. N. Reddy, Ph.D.

Preface to the First Edition

The motivation which led to the writing of the present book has come from my many years of teaching finite element courses to students from various fields of engineering, meteorology, geology and geophysics, physics, and mathematics. The experience gained as a supervisor and consultant to students and colleagues in universities and industry, who have asked for explanations of the various mathematical concepts related to the finite element method, helped me introduce the method as a variationally based technique of solving differential equations that arise in various fields of science and engineering. The many discussions I have had with students who had no background in solids and structural mechanics gave rise to my writing a book that should fill the rather unfortunate gap in the literature.

The book is designed for senior undergraduate and first-year graduate students who have had a course in linear algebra as well as in differential equations. However, additional courses (or exposure to the topics covered) in mechanics of materials, fluid flow, and heat transfer should make the student feel more comfortable with the physical examples discussed in the book.

In the present book, the finite element method is introduced as a variationally based technique of solving differential equations. A continuous problem described by a differential equation is put into an equivalent variational form, and the approximate solution is assumed to be a linear combination, $\Sigma c_j \phi_j$, of approximation functions ϕ_j. The parameters c_j are determined using the associated variational form. The finite element method provides a systematic technique for deriving the approximation functions for simple subregions by which a geometrically complex region can be represented. In the finite element method, the approximation functions are piece-wise polynomials (i.e., polynomials that are defined only on a subregion, called an element).

The approach taken in the present book falls somewhere in the middle of the approaches taken in books that are completely mathematical and

those approaches that are more structural-mechanics-oriented. From my own experience as an engineer and self-taught applied mathematician, I know how unfortunate outcomes may be arrived at if one follows a "formula" without deeper insight into the problem and its approximation. Even the best theories lead ultimately to some sort of guidelines (e.g., which variational formulation is suitable, what kind of element is desirable, what is the quality of the approximation, etc.). However, without a certain theoretical knowledge of variational methods one cannot fully understand various formulations, finite-method models, and their limitations.

In the present study of variational and finite element methods, advanced mathematics are intentionally avoided in the interest of simplicity. However, a minimum of mathematical machinery that seemed necessary is included in Chapters 1 and 2. In Chapter 2, considerable attention is devoted to the construction of variational forms since this exercise is repeatedly encountered in the finite element formulation of differential equations. The chapter is concerned with two aspects: first, the selection of the approximation functions that meet the specified boundary conditions; second, the technique of obtaining algebraic equations in terms of the undetermined parameters. Thus, Chapter 2 not only equips readers with certain concepts and tools that are needed in Chapters 3 and 4, but it also motivates them to consider systematic methods of constructing the approximation functions, which is the main feature of the finite element method.

In introducing the finite element method in Chapters 3 and 4, the traditional solid mechanics approach is avoided in favor of the "differential equation" approach, which has broader interpretations than a single special case. However, when specific examples are considered, the physical background of the problem is stated. Since a large number of physical problems are described by second- and fourth-order ordinary differential equations (Chapter 3), and by the Laplace operator in two dimensions (Chapter 4), considerable attention is devoted to the finite element formulation, the derivation of interpolation functions, and the solution of problems described by these equations. Representative examples are drawn from various fields of engineering, especially from heat transfer, fluid mechanics, and solid mechanics. Since this book is intended to serve as a textbook for a first course on the finite element method, advanced topics such as nonlinear problems, shells, and three-dimensional analyses are omitted.

Since the practice of the finite element method ultimately depends on

one's ability to implement the technique on a digital computer, examples and exercises are designed to let the reader actually compute the solutions of various problems using computers. Ample discussion of the computer implementation of the finite element method is given in Chapters 3 and 4. Three model programs (FEM1D, FEM2D, and PLATE) are described, and their application is illustrated via several examples. The computer programs are very easy to understand because they are designed along the same lines as the theory presented in the book. The programs are available for mainframe and IBM PC compatibles from the author for a small charge.

Numerous examples, most of which are applications of the concepts to specific problems in various fields of engineering and applied science, are provided throughout the book. The conclusion of the examples is indicated by the symbol Δ. At appropriate intervals in the book an extensive number of exercise problems is included to test and extend the understanding of the concepts discussed. For those who wish to gain additional knowledge of the topics covered in the book, many reference books and research papers are listed at the end of each chapter.

There are several sections that can be skipped in a first reading of the book (such sections are marked with an asterisk); these can be filled in wherever needed later. The material is intended for a quarter or a semester course, although it is better suited for a semester course.

The following schedule of topics is suggested for a first course using the present textbook:

Undergraduate		Graduate	
Chapter 1	Self-study	Chapter 1	Self-study
Chapter 2	Section 2.1 (self)	Chapter 2	Section 2.1 (self)
	Section 2.2		Section 2.2
	Sections 2.3.1–2.3.3		Section 2.3
Chapter 3	Sections 3.1–3.4	Chapter 3	Sections 3.1–3.7
	Sections 3.6–3.7		
Chapter 4	Sections 4.1–4.4	Chapter 4	Sections 4.1–4.8
	Section 4.7		
	Sections 4.8.1–4.8.4	Chapter 5	Term Paper

Due to the intimate relationship between Sections 3.5 and 4.6, 3.6 and 4.7,

and 3.7 and 4.8, they can be covered simultaneously. Also, it is suggested that Sections 3.6 and 3.7 (hence, 4.7 and 4.8) be covered after Section 3.2.

The author wishes to thank all those students and colleagues who have contributed by their advice and criticism to the improvement of this work. The author is also thankful to Vanessa McCoy for the skillful typing of the manuscript, to Mr. N. S. Putcha and Mr. K. Chandrashekhara for proofreading the pages, and to the editors Michael Slaughter and Susan Hazlett for their help and cooperation in publishing the manuscript.

J. N. Reddy, Ph.D.

Tejasvi naavadhitamastu
(Let our learning be radiant)

Symbols and Conversion Factors

The symbols that are used throughout the book for various important quantities are defined in the following list. In some cases, the same symbol has different meanings in different parts of the book; which meaning should be clear from the context.

Symbol	Meaning
$\mathbf{a}$	Acceleration vector, $\frac{D\mathbf{v}}{Dt}$
a_{ij}	Coefficients of matrix $[A] = \mathbf{A}$
c_v, c_p	Specific heat at constant volume and pressure, respectively
C	Concentration
C_{ij}, c_{ij}	Elastic stiffness coefficients
C_{ijkl}, c_{ijkl}	Elastic stiffness coefficients
d	Diameter
ds, dS	Surface elements
dA	Area element $(= dxdy)$
dv	Volume element $(= dxdydz)$
D, D_i	Diffusion coefficients
$\mathbf{D}$	Symmetric part of the velocity gradient tensor; that is, $\mathbf{D} = \frac{1}{2}\left[(\boldsymbol{\nabla}\mathbf{v})^{\mathrm{T}} + \boldsymbol{\nabla}\mathbf{v}\right]$
D_{ij}	Rectangular cartesian components of $\mathbf{D}$
D/Dt	Material time derivative, $\frac{D}{Dt} = \frac{\partial}{\partial t} + \mathbf{v} \cdot \boldsymbol{\nabla}$
$\hat{\mathbf{e}}$	Unit vector
$\hat{\mathbf{e}}_A$	Unit basis vector in the direction of vector $\mathbf{A}$
$\mathbf{e}_i$	Basis vector in the x_i-direction
$(\hat{\mathbf{e}}_r, \hat{\mathbf{e}}_\theta, \hat{\mathbf{e}}_z)$	Basis vectors in the (r, θ, z) system
$(\hat{\mathbf{e}}_x, \hat{\mathbf{e}}_y, \hat{\mathbf{e}}_z)$	Basis vectors in the (x, y, z) system
$(\hat{\mathbf{e}}_1, \hat{\mathbf{e}}_2, \hat{\mathbf{e}}_3)$	Basis vectors in the (x_1, x_2, x_3) system
E	Young's modulus (modulus of elasticity)
E_1, E_2, E_3	Young's moduli for orthotropic materials
f	Load per unit length of a bar
$\mathbf{f}$	Body force vector
f_x, f_y, f_z	Body force components in the x, y, and z directions
g	Acceleration due to gravity; internal heat generation per unit volume
G	Shear modulus (modulus of rigidity)
G_{12}, G_{13}, G_{23}	Shear moduli for orthotropic materials

h	Thickness; heat transfer coefficient
H	Heat input to the system; height of the beam
I	Second moment of area of a beam; current density
$\mathbf{I}$	Unit second-order tensor
I_1, I_2, I_3	Invariants of a second-order tensor
J	Determinant of $\mathbf{J}$ (Jacobian)
$\mathbf{J}$	Jacobian (of transformation) matrix
k	Spring constant; thermal conductivity
$\mathbf{k}$	Thermal conductivity tensor
k_e	Electrical conductivity
K	Kinetic energy
L	Length
M	Bending moment in beam problems
$\hat{\mathbf{n}}$	Unit normal vector in the current configuration
n_i	ith component of the unit normal vector $\hat{\mathbf{n}}$
(n_x, n_y, n_z)	Components of the unit normal vector $\hat{\mathbf{n}}$
N	Axial force in beam problems
$\hat{\mathbf{N}}$	Unit normal vector in the reference configuration
N_I	Ith component of the unit normal vector $\hat{\mathbf{N}}$
p	Internal pressure of a pressure vessel; thermodynamic or hydrostatic pressure
P	Hydrostatic pressure; point load in beams; perimeter
q	Distributed transverse load on a beam
q_0	Intensity of the distributed transverse load in beams
q_n	Heat flux normal to the boundary, $q_n = \boldsymbol{\nabla} \cdot \hat{\mathbf{n}}$
$\mathbf{q}$	Heat flux vector; diffusion flux
Q	Mass flow rate; volume rate of flow
Q_e	Rate of heat due to current density
r	Radial coordinate in the cylindrical polar system; $r = \lvert\mathbf{r}\rvert$
$\mathbf{r}$	Position vector in cylindrical coordinates, $\mathbf{x}$
(r, θ, z)	Cylindrical coordinate system
R	Residual in the approximation; radius
t	Time
$\mathbf{t}$	Stress vector; traction vector
$\mathbf{t}_i$	Stress vector on x_i-plane, $\mathbf{t}_i = \sigma_{ij}\hat{\mathbf{e}}_j$
T	Temperature; torque

$\mathbf{u}$	Displacement vector
(u, v, w)	Displacements in the (x, y, z) coordinate system
(u_1, u_2, u_3)	Displacements in the (x_1, x_2, x_3) coordinate system
(u_r, u_θ, u_z)	Displacements in the (r, θ, z) coordinate system
U	Internal (or strain) energy
v	Velocity, $v = \lvert\mathbf{v}\rvert$
v_n	Projection of $\mathbf{v}$ onto $\hat{\mathbf{n}}$, $v_n = \mathbf{v} \cdot \hat{\mathbf{n}}$
(v_1, v_2, v_3)	Components of velocity vector $\mathbf{v}$ in (x_1, x_2, x_3) system
(v_r, v_θ, v_z)	Components of velocity vector $\mathbf{v}$ in (r, θ, z) system
$\mathbf{v}$	Velocity vector, $\mathbf{v} = \frac{D\mathbf{x}}{Dt}$
$\mathbf{v}_n$	Velocity vector normal to the plane (whose normal is $\hat{\mathbf{n}}$)
V	Shear force in beam problems; scalar potential of body forces
W	Power input
$\mathbf{x}$	Position vector in the current configuration
(x, y, z)	Rectangular Cartesian coordinates
(x_1, x_2, x_3)	Rectangular Cartesian coordinates

Greek symbols

Symbol	Meaning
α	Angle; coefficient of thermal expansion; kinetic energy coefficient
β	Heat transfer coefficient
γ	Shear strain in one-dimensional problems; penalty parameter
Γ	Total boundary
δ	Dirac delta; variational symbol
δ_{ij}	Components of the unit tensor, $\mathbf{I}$ (Kronecker delta)
ϵ	Tolerance specified for steady-state solution
$\boldsymbol{\varepsilon}$	Infinitesimal strain tensor, $\boldsymbol{\varepsilon} = \frac{1}{2}\left[(\boldsymbol{\nabla}_0\mathbf{u})^{\mathrm{T}} + \boldsymbol{\nabla}_0\mathbf{u}\right]$
ϵ	Total energy stored per unit mass
ε_{ij}	Rectangular components of the infinitesimal strain tensor
ε_{ijk}	Alternating symbol
$\varepsilon_{rr}, \varepsilon_{\theta\theta}, \varepsilon_{r\theta}, \cdots$	Components of the infinitesimal strain tensor in the cylindrical coordinate system (r, θ, z)
ζ	Natural (normalized) coordinate
η	Natural (normalized) coordinate

θ	Angular coordinate in the cylindrical and spherical coordinate systems; angle; absolute temperature
θ_n, θ_s	Angles corresponding to maximum normal stress and maximum shear stress, respectively
λ	Lamé constant; eigenvalue; Lagrange multiplier
$\lambda_1, \lambda_2, \lambda_3$	Eigenvalues of a 3×3 matrix
Λ	Parameter introduced in Timoshenko beam element
μ	Lamé constant; viscosity; parameter used in Timoshenko beam element
ν	Poisson's ratio
ν_{ij}	Poisson's ratios for orthotropic materials
ξ	Natural (normalized) coordinate
Π	Total potential energy
ρ	Mass density
σ	Stress in one-dimensional problems; Boltzman constant
$\boldsymbol{\sigma}$	Stress tensor
σ_{ij}	Components of the stress tensor in the rectangular coordinate system (x_1, x_2, x_3)
σ_n, σ_s	Normal and shear stresses on a plane with normal $\hat{\mathbf{n}}$
$\sigma_{rr}, \sigma_{\theta\theta}, \sigma_{r\theta}, \cdots$	Components of the stress tensor $\boldsymbol{\sigma}$ in the cylindrical coordinate system (r, θ, z)
τ	Shear stress
$\boldsymbol{\tau}$	Viscous stress tensor
ϕ	A typical scalar function; velocity potential; angular coordinate in the spherical coordinate system
ϕ_i	Hermite cubic interpolation functions
ψ	Warping function; stream function
ψ_i	Lagrange interpolation functions
Ψ	Prandtl stress function
ω	Natural frequency; angular velocity
Ω	Domain of a problem
$\boldsymbol{\Omega}$	Spin tensor or skew symmetric part of the velocity gradient tensor, $(\boldsymbol{\nabla}\mathbf{v})^{\mathrm{T}}$; that is, $\boldsymbol{\Omega} = \frac{1}{2}\left[(\boldsymbol{\nabla}\mathbf{v})^{\mathrm{T}} - \boldsymbol{\nabla}\mathbf{v}\right]$
ω_i	Components of vorticity vector $\boldsymbol{\omega}$ in the rectangular coordinate system (x_1, x_2, x_3)
$\omega_x, \omega_y, \omega_z$	Components of vorticity vector $\boldsymbol{\omega}$ in the rectangular coordinate system (x, y, z)

Other symbols

$\boldsymbol{\nabla}$	Gradient operator with respect to $\mathbf{x}$
∇^2	Laplace operator, $\nabla^2 = \boldsymbol{\nabla} \cdot \boldsymbol{\nabla}$
∇^4	Biharmonic operator, $\nabla^4 = \nabla^2 \nabla^2$
[ ]	Matrix of components of the enclosed tensor
{ }	Column of components of the enclosed vector
·	Symbol for the dot product or scalar product
×	Symbol for the cross product or vector product

Table 1 Conversion factors.

Quantity	US customary unit	SI equivalent
Mass	lb (mass)	0.4536 kg
Length	in	25.4 mm
	ft	0.3048 m
Density	lb/in^3	27.68×10^3 kg/m^3
	lb/ft^3	16.02 kg/m^3
Force	lb (force)	4.448 N
	kip (10^3 lb)	4.448 kN
Pressure or stress	lb/in^2 (psi)	6.895 kN/m^2
	ksi (10^3psi)	6.895 MN/m^2
	msi (10^6psi)	6, 895 MN/m^2
Moment or torque	lb in	0.1130 Nm
	lb ft	1.356 Nm
Power	ft lb/s	1.356 W
	hp (550 ft lb/s)	745.7 W
Temperature	°F	0.5556°C
Conversion formula	$°F = \frac{5}{9}°C + 32°F$	

s = second; lb = pound; in = inch; ft = foot; hp = horsepower;
kg = kilogram (= 10^3 grams); m = meter; mm = millimeter (10^{-3} m);
N = newton; W = watt; Pa = pascal = N/m^2;
kN = 10^3 N; MN = 10^6 N; MPa = 10^6 Pa; GPa = 10^9 Pa.

Ignorance more frequently begets confidence than does knowledge: it is those who know little, and not those who know much, who so positively assert that this or that problem will never be solved by science.

— Charles Darwin

Science can purify religion from error and superstition. Religion can purify science from idolatry and false absolutes.

— Pope John Paul II

A yogi seated in a Himalayan cave allows his mind to wander on unwanted things. A cobbler, in a corner at the crossing of several busy roads of a city, is absorbed in mending a shoe as an act of service. Of these two, the latter is a better yogi than the former.

— Swami Vivekananda

Note: The quotes by various people included in this book were found at different websites. For example, visit:

http://naturalscience.com/dsqhome.html
http://thinkexist.com/quotes/david_hilbert/
http://www.yalescientific.org/2010/10/from-the-editor-imagination-in-science/
https://www.brainyquote.com/quotes/topics/topic_science.html

The author cannot vouch for the accuracy of the quotes; he is motivated to include them at various places in his book for their wit and wisdom.

1 General Introduction

Mathematics is the language with which God has written the universe.

— Galileo Galilei

1.1 Background

One of the most important things engineers and scientists do is to model physical phenomena. Virtually every phenomenon in nature—whether aerospace, biological, chemical, geological, or mechanical—can be described, with the aid of the laws and axioms of physics or other fields, in terms of algebraic, differential, and/or integral equations relating various quantities that describe the phenomenon. Determining the stress distribution in a pressure vessel with oddly shaped holes and stiffeners and subjected to mechanical, thermal, and/or aerodynamic loads; finding the concentration of pollutants in lakes or in the atmosphere; and simulating weather in an attempt to understand and predict the formation of thunderstorms, tsunamis, and tornadoes are a few examples of many important practical problems that engineers deal with.

Analytical descriptions of physical or physiological processes in terms of pertinent variables are termed *mathematical models*. Mathematical models of a process are developed using assumptions concerning how the process works and using appropriate axioms or laws governing the process, and they are often characterized by very complex set of algebraic, differential, and/or integral equations posed on geometrically complicated domains. Consequently, the processes to be studied, until the advent of electronic computation, were drastically simplified so that their mathematical models can be evaluated analytically. Over the last three decades, however, computers have made it possible, with the help of suitable mathematical models and numerical methods, to analyze many practical problems of engineering. The use of a numerical method and a computer to evaluate the mathematical model of a process and estimate its characteristics is called a *numerical simulation*. There now exists a new and growing body of knowledge connected with the development of mathematical models and use of numerical simulations of physical

systems, and it is known as *computational mechanics* [1].

Any numerical simulation, such as the one by the finite element method, is not an end in itself but rather an aid to design and manufacturing. There are several reasons why an engineer or a scientist should study a numerical method, especially the finite element method. They are listed here.

1. Analysis of most practical systems involve complicated domains (both geometry and material constitution), loads, boundary conditions, and interactions between various aspects of the system response that forbid the development of analytical solutions. Therefore, the only alternative is to find approximate solutions using numerical methods.
2. A numerical method, with the advent of a computer, can be used to investigate the effects of various parameters (e.g., geometry, material parameters, loads, interactions, and so on) of the system on its response to gain a better understanding of the system being analyzed. It is costeffective and saves time and material resources compared to the multitude of physical experiments required to gain the same level of understanding.
3. Because of the power of numerical methods and electronic computation, it is possible to include most relevant features in a mathematical model of a physical process, without worrying about its solution by exact means.
4. Those who are quick to use a computer program rather than *think* about the problem to be analyzed may find it difficult to interpret or explain the computer-generated results. Even to develop proper input data to the computer program, a good understanding of the underlying theory of the problem as well as the numerical method (on which the computer program is based) is required.
5. The finite element method and its generalizations are the most powerful computer methods ever devised to analyze practical engineering systems. Today, finite element analysis is an integral and major component in many fields of engineering design and manufacturing. Major established industries such as the automobile, aerospace, chemical, pharmaceutical, petroleum, electronics and communications, as well as emerging technologies such as nanotechnology and biotechnology rely on the finite element method to simulate complex phenomena at different scales for design and manufacture of high-technology products.

1.2 Mathematical Model Development

A *mathematical model* can be broadly defined as a set of equations that expresses the essential features of a physical system in terms of variables that describe the system. The mathematical models of physical phenomena are often based on fundamental scientific laws of physics such as the principle of conservation of mass, the principles of balance of linear and angular momentum, and the principle of balance of energy [2, 3]. The equations resulting from these principles are supplemented by equations that describe the constitutive behavior and by boundary and/or initial conditions. Next, we consider three simple examples drawn from dynamics, heat transfer, and solid mechanics to illustrate how mathematical models of physical problems are formulated. *All mathematical models are not the exact representation of the physics; they are just models.*

Example 1.2.1

Problem statement (Planar motion of a pendulum): A simple pendulum (such as the one used in a clock) consists of a bob of mass m (kg) attached to one end of a rod of length ℓ (m) with the other end pivoted to a fixed point O, as shown in Fig. 1.2.1(a). Make necessary simplifying assumptions to derive the governing equation for the simplest linear motion of the pendulum. Also, determine the analytical solution of the resulting equation for the case in which the initial conditions on the angular displacement θ and its derivative are specified.

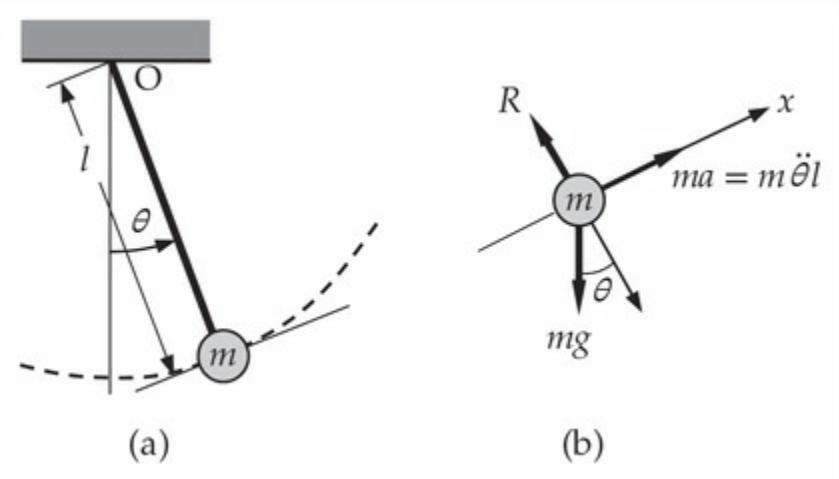

Fig. 1.2.1 Simple pendulum.

Solution: In order to derive the governing equation of the problem, we must make certain assumptions concerning the system (the bob and rod), consistent with the goal of the analysis. If the goal is to study the simplest linear motion of the pendulum, we assume that the bob as well as the rod are rigid (i.e., not deformable) and the rod is massless (i.e., compared to the mass of the bob). In addition, we assume that there is no friction at the pivot point O and the resistance offered by the surrounding medium to the pendulum is also negligible.

Under these assumptions, the equation governing the motion of the system can be formulated using the *principle of conservation of linear momentum* (or simply Newton's second law), which states, in the present case, that *the vector sum of externally applied forces on a system is equal to the time rate of change of the linear momentum* (mass times velocity) *of the system*:

$$\mathbf{F} = \frac{d}{dt}(m\mathbf{v}) = m\mathbf{a} \tag{1.2.1}$$

where **F** is the vector sum of all forces acting on the system, m is the mass of the system, **v** is the velocity vector, and **a** is the acceleration vector of the system. To write the equation governing the angular motion, we set up a coordinate system, as shown in Fig. 1.2.1(b). Applying Newton's second law to the x-direction [note that the dynamic equilibrium of forces in the y-direction gives the reaction force R (N) in terms of the weight mg of the bob], we obtain

$$F_x = m\frac{dv_x}{dt}, \quad \text{where} \quad F_x = -mg\sin\theta, \quad v_x = \ell\frac{d\theta}{dt} \tag{1.2.2}$$

and θ is the angular displacement (radians), v_x is the component of velocity (m/s) along the x coordinate, and t denotes time (sec). Thus, the equation for angular motion becomes

$$-mg\sin\theta = m\ell\frac{d^2\theta}{dt^2} \quad \text{or} \quad \frac{d^2\theta}{dt^2} + \frac{g}{\ell}\sin\theta = 0 \tag{1.2.3}$$

Equation (1.2.3) is nonlinear on account of the term $\sin\theta$. For small angular motions (consistent with the goal of the study), $\sin\theta$ is approximated as $\sin\theta \approx \theta$ (i.e., linearized). Thus, the angular motion is described by the linear differential equation

$$\frac{d^2\theta}{dt^2} + \frac{g}{\ell}\theta = 0 \tag{1.2.4}$$

Equations (1.2.3) and (1.2.4) represent mathematical models of nonlinear and linear motions, respectively, of a rigid pendulum. Their solution requires knowledge of conditions at time $t = 0$ on θ and its time derivative $\dot{\theta}$ (angular velocity). These conditions are known as the *initial conditions*. Thus, the linear problem involves solving the differential equation in Eq. (1.2.4) subjected to the initial conditions

$$\theta(0) = \theta_0, \qquad \frac{d\theta}{dt}(0) = v_0 \tag{1.2.5}$$

The problem described by Eqs. (1.2.4) and (1.2.5) is called an *initial-value problem* (IVP).

The linear problem described by Eqs. (1.2.4) and (1.2.5) can be solved analytically. The general analytical solution of the linear equation in Eq. (1.2.4) ($\ddot{\theta} + \lambda^2\theta = 0$) is

$$\theta(t) = A \sin\lambda t + B \cos\lambda t, \quad \lambda = \sqrt{\frac{g}{\ell}} \tag{1.2.6}$$

where A and B are constants of integration, which can be determined using the initial conditions in Eq. (1.2.5). We obtain

$$A = \frac{v_0}{\lambda}, \quad B = \theta_0 \tag{1.2.7}$$

and the solution to the linear problem becomes

$$\theta(t) = \frac{v_0}{\lambda}\sin\lambda t + \theta_0 \cos\lambda t \tag{1.2.8}$$

For zero initial velocity ($v_0 = 0$) and nonzero initial position θ_0, we have

$$\theta(t) = \theta_0 \cos\lambda t \tag{1.2.9}$$

which represents a simple harmonic motion.

If we were to solve the nonlinear equation, Eq. (1.2.3), subject to the conditions in Eq. (1.2.5), we may consider using a numerical method because it is not possible to solve Eq. (1.2.3) exactly for large values of θ. We will revisit this issue in the sequel.

Example 1.2.2

Problem statement (One-dimensional heat flow): Derive the governing equations (i.e., develop the mathematical model) of steady-state heat transfer through a cylindrical bar of nonuniform cross section, as shown in Fig. 1.2.2(a). Assume that there is a heat source within the rod generating energy at a rate of f(W/m). In practice, such energy source can be due to nuclear fission or chemical reactions taking place along the length of the bar, or due to the passage of electric current through the medium (i.e., volume heating). Assume that temperature is uniform at any section of the bar, $T = T(x)$. Due to the difference between the temperatures of the bar and the surrounding medium, there is convective heat transfer across the surface of the body and at the right end. Also, analytically solve the resulting equation for constant material and geometric parameters and uniform internal heat generation f. The bar is subject to a known temperature T_0 (°C) at the left end and exposed, both on the surface and at the right end, to a medium (such as cooling fluid or air) at temperature T_∞.

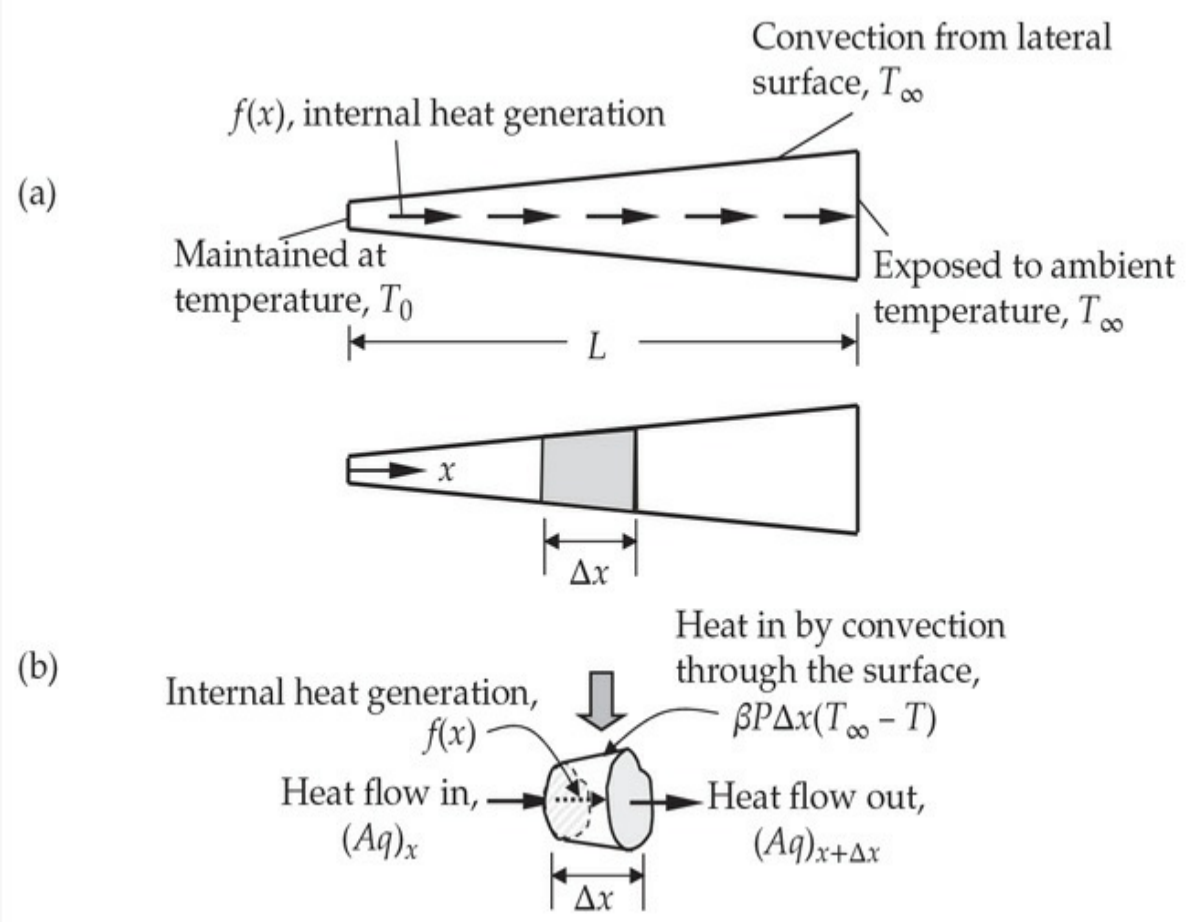

Fig. 1.2.2 One-dimensional heat flow in a bar.

Solution: The principle of balance of energy, also known as the *first law of thermodynamics*, can be used to derive the governing equations of the problem. The principle of balance of energy requires that *the rate of change (increase) of internal energy is equal to the sum of heat gained by conduction, convection, and internal heat generation* (radiation not included). For a steady process the time rate of internal energy is zero.

Consider a volume element of length Δx and having an area of cross section $A(x)$ (m^2) at a distance x along the length of the bar, as shown in Fig. 1.2.2(b). If q denotes the heat flux (heat flow per unit area, W/m^2), then $[Aq]_x$ is the net heat flow into the volume element at x, $[Aq]_{x+\Delta x}$ is the net heat flow out of the volume element at $x + \Delta x$, and $\beta P \Delta x(T_\infty - T)$ is the heat flow through the surface into the bar. Here β denotes the film (that is formed between the bar and the medium around) conductance [$W/(m^2 \cdot °C)$], T_∞ is the temperature of the surrounding medium, and P is the perimeter (m) of the bar. Then the energy balance gives

$$[Aq]_x - [Aq]_{x+\Delta x} + \beta P \Delta x(T_\infty - T) + f\Delta x = 0 \tag{1.2.10}$$

Dividing throughout by Δx,

$$-\frac{[Aq]_{x+\Delta x} - [Aq]_x}{\Delta x} + \beta P(T_\infty - T) + f = 0$$

and taking the limit $\Delta x \to 0$, we obtain

$$-\frac{d}{dx}(Aq) + \beta P(T_\infty - T) + f = 0 \tag{1.2.11}$$

We can relate the heat flux q (W/m^2) to the temperature gradient using a material law. Such a relation is provided by the *Fourier law*

$$q(x) = -k\frac{dT}{dx} \tag{1.2.12}$$

where k denotes the thermal conductivity [$W/(m \cdot °C)$] of the material. The minus sign on the right side of the equality in Eq. (1.2.12) indicates that heat flows from high temperature to low temperature. Equation (1.2.12) is a *constitutive relation* between the heat flux and the temperature gradient.

Now using the Fourier law, Eq. (1.2.12) in Eq. (1.2.11), we arrive at the *heat conduction equation*

$$\frac{d}{dx}\left(kA\frac{dT}{dx}\right) + \beta P(T_\infty - T) + f = 0 \tag{1.2.13}$$

which can also be written as

$$-\frac{d}{dx}\left(kA\frac{dT}{dx}\right)+\beta P(T-T_\infty)=f \tag{1.2.14}$$

Equation (1.2.14) is a linear, nonhomogeneous (because the right-hand side is nonzero), second-order differential equation with variable coefficients (because, in general, kA is a function of x), which can be solved with known conditions on temperature T or heat Aq (not both) at a boundary point (e.g., ends of the bar). The known end conditions for the present case can be expressed as

$$T(0)=T_0, \quad \left[kA\frac{dT}{dx}+\beta A(T-T_\infty)\right]_{x=L}=0 \tag{1.2.15}$$

These conditions are called *boundary conditions* because they represent conditions at the boundary points of the bar. The first condition in Eq. (1.2.15) is obvious. The second condition represents the balance of heat due to conduction $[kA(dT/dx)]$ and convection $[\beta A(T-T_\infty)]$. The problem described by Eqs. (1.2.14) and (1.2.15) is called, for obvious reasons, a *boundary-value problem* (BVP). This completes the mathematical model development of the problem.

Equations (1.2.14) and (1.2.15) can be simplified for various special cases. First let

$$u\equiv T-T_\infty, \quad a\equiv kA\ (\mathrm{W\cdot m/^\circ C}), \quad c\equiv \beta P\ [\mathrm{W/(m\cdot^\circ C)}] \tag{1.2.16}$$

so that Eqs. (1.2.14) and (1.2.15) can be written as (note that a and c are always positive in heat transfer problems)

$$-\frac{d}{dx}\left(a\frac{du}{dx}\right)+cu=f \tag{1.2.17}$$

$$u(0)=T(0)-T_\infty=T_0-T_\infty\equiv u_0, \quad \left[a\frac{du}{dx}+\beta Au\right]_{x=L}=0 \tag{1.2.18}$$

Now if $a = kA$ and $c = \beta P$ are constant (e.g., homogeneous and isotropic bar of constant cross section) and no internal heat generation (i.e., $f = 0$), Eqs. (1.2.17) and (1.2.18) become

$$-\frac{d^2u}{dx^2}+m^2u=0, \quad m\equiv\sqrt{\frac{c}{a}}=\sqrt{\frac{\beta P}{kA}}, \quad 0<x<L \tag{1.2.19}$$

$$u(0) = u_0, \quad \left[\frac{du}{dx} + \frac{\beta}{k}u\right]_{x=L} = 0 \tag{1.2.20}$$

The general solution of Eq. (1.2.19) ($u'' - m^2u = 0$) is

$$u(x) = C_1 \cosh mx + C_2 \sinh mx \tag{1.2.21}$$

where C_1 and C_2 are constants of integration, which can be determined using the boundary conditions in Eq. (1.2.20). We have [$\sinh x = (e^x - e^{-x})/2$ and $\cosh x = (e^x + e^{-x})/2$]

$$C_1 = u_0, \quad C_2 = -u_0\left[\frac{\sinh mL + (\beta/mk)\cosh mL}{\cosh mL + (\beta/mk)\sinh mL}\right] \tag{1.2.22}$$

Hence, the solution of Eqs. (1.2.19) and (1.2.20) becomes

$$u(x) = u_0\left[\frac{\cosh m(L-x) + (\beta/mk)\sinh m(L-x)}{\cosh mL + (\beta/mk)\sinh mL}\right] \tag{1.2.23}$$

The last example of this section is concerned with the mathematical formulation of the axial deformation of a bar of variable cross section. The term *bar* is used in solid and structural mechanics to mean a structural element that carries only axial (tensile as well as compressive) loads and undergoes axial deformation. Practical examples of the problem are provided by the deformation of a slender body under its own weight, a concrete pier supporting a bridge, a fiber embedded in a matrix material, a pile in a soil, among others.

Example 1.2.3

Problem statement (Deformation of a bar embedded in a matrix material): Consider a pile embedded in an elastic material and subjected to an axial force Q_0. The resistance offered by the surrounding material to the movement of the bar is assumed to be linearly proportional to the displacement, u. Thus, the force per unit surface area of the rod is $m_j u$, where m_j, represents the proportionality parameter. The weight of the body, $f(x)$ measured per unit length, is assumed to be negligible compared to the applied load Q_0, but include it in the derivation for generality. Derive the governing equation of the problem.

Solution: First, we know that the significant load taken by a pile is vertical. So the axial deformation and stress will be the significant quantities, and the lateral deformation due to the Poisson effect may be neglected. Second, we wish to consider the static case. The governing equations of this simplified problem can be obtained using Newton's second law and a uniaxial stress-strain (constitutive) relation for the material of the bar. The reader should note the similarity in the derivation of the equations of this solid mechanics problem with the heat flow problem discussed earlier.

Figure 1.2.3 shows an element of length Δx with axial forces acting at both ends of the element, where σ_x denotes stress (i.e., force per unit area; N/m^2) in the x direction, which is taken positive upward; $f(x)$ denotes the body force measured per unit length (N/m). Hence, $[A\sigma_x]_x$ is the net tensile force on the volume element at x and $[A\sigma_x]_{x+\Delta x}$ is the net tensile force at $x + \Delta x$. The resistance of the surrounding medium is $m_j uP$ per unit length in the direction opposite to the force Q_0, where P is the perimeter. Then setting the sum of the forces to zero (i.e., applying Newton's second law in the x-direction) yields

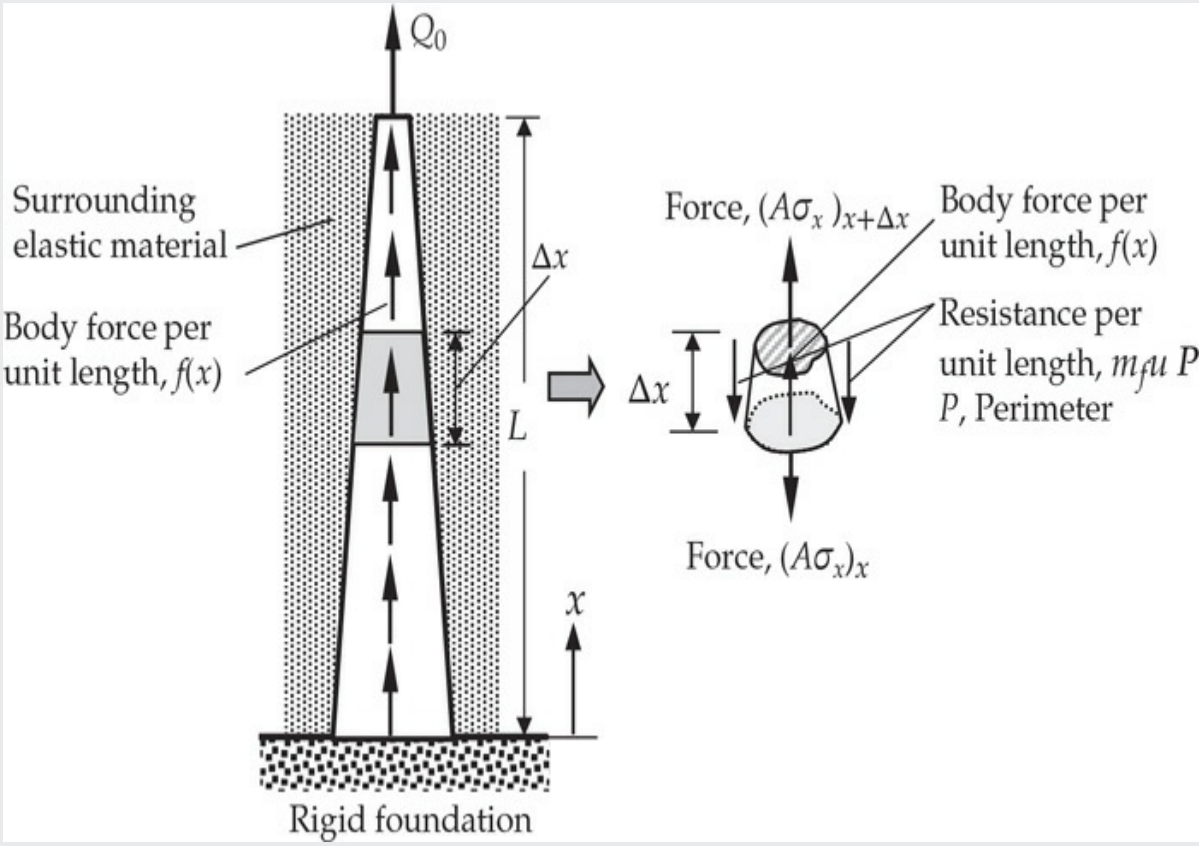

Fig. 1.2.3 Axial deformation of a bar.

$$-[A\sigma_x]_x + [A\sigma_x]_{x+\Delta x} + f\Delta x - m_f u P \Delta x = 0$$

Dividing throughout by Δx and taking the limit $\Delta x \to 0$, we obtain

$$\frac{d}{dx}(A\sigma_x) - cu + f(x) = 0 \tag{1.2.24}$$

where $c = m_f P$.

The stress σ_x can be related to the axial displacement using *Hooke's law* and straindisplacement relation

$$\sigma_x = E\varepsilon_x, \quad \varepsilon_x = \frac{du}{dx} \tag{1.2.25}$$

where E is Young's modulus (N/m^2), $u(x)$ denotes the axial displacement (m) and ε_x is the axial strain (m/m). Again, Eq. (1.2.25) represents a constitutive equation. Note that a system can have several constitutive relations, each depending on the phenomenon being studied. The study of heat transfer in a bar required us to employ Fourier's law to relate temperature gradient to heat flux, and the study of deformation of the same bar subjected to axial forces requires us to use Hooke's law to connect stress to displacement gradient.

Now using Eq. (1.2.25) in Eq. (1.2.24), we arrive at the equilibrium equation in terms of the displacement

$$-\frac{d}{dx}\left(EA\frac{du}{dx}\right) + cu = f, \quad 0 < x < L \tag{1.2.26}$$

This second-order equation can be solved using known boundary conditions at $x = 0$ and $x = L$. The boundary conditions of a bar involve specifying either the displacement u or the force $A\sigma_x$ at a boundary point.

The boundary conditions of the problem at hand can be inferred from Fig. 1.2.3. We have

$$u(0) = 0, \quad \left[EA\frac{du}{dx}\right]_{x=L} = Q_0 \tag{1.2.27}$$

where Q_0 is the load applied at the top. The second boundary condition in Eq. (1.2.27) represents the force equilibrium at $x = L$. Equations (1.2.26) and (1.2.27) may not admit an analytical solution when $a = EA = a(x)$, requiring us to seek approximate solutions using numerical methods.

The analytical solution of Eq. (1.2.26) subject to the boundary

conditions in Eq. (1.2.27) may be found for the simple case in which $a \equiv EA$ and $f = f_0$ are constant (homogeneous and uniform cross section pier) and $c = 0$ (i.e., the bar is not embedded in an elastic medium). The general solution of Eq. (1.2.26) in this case is given by

$$u(x) = \frac{1}{EA}\left(-\frac{f_0}{2}x^2 + C_1 x + C_2\right) \tag{1.2.28}$$

Use of the boundary conditions in Eq. (1.2.27) give $C_1 = Q_0 + f_0 L$ and $C_2 = 0$. Then the vertical displacement and stress in the pier (or pile) become

$$u(x) = \frac{1}{EA}\left[\frac{f_0}{2}(2Lx - x^2) + Q_0 x\right], \quad \sigma_x = \frac{f_0 L}{A}\left(1 - \frac{x}{L}\right) + \frac{Q_0}{A} \tag{1.2.29}$$

1.3 Numerical Simulations

While the derivation of the governing equations for most problems is not unduly difficult (in fact, for most problems they can be found in textbooks), their solution by exact methods of analysis is often difficult due to geometric and material complexities. In such cases, numerical methods of analysis provide a means of finding solutions. By a *numerical simulation* of a process, we mean the solution of the governing equations (or mathematical model) of the process using a numerical method and a computer. Numerical methods typically transform differential equations governing a continuum to a set of algebraic relations among the values of dependent variables of a discrete model of the continuum, and these algebraic equations are solved using computers.

There exist a number of numerical methods, many of which are developed to solve differential equations. In the finite difference approximation of a differential equation, the derivatives in the latter are replaced by difference quotients (or the function is expanded in a Taylor series) that involve the values of the solution at discrete mesh points of the domain. The resulting algebraic equations are solved for the values of the solution at the mesh points after imposing the boundary conditions. We note that the finite difference method is *not* based on the concept of minimization of error introduced in the approximation of the differential equation. It simply provides a means to compute a solution.

In the solution of a differential equation by a classical variational

method, the equation is expressed as an equivalent weighted-integral statement, which often means making the error in the approximation of the differential equation orthogonal to the set of weight functions. In solid mechanics, the integral statement is equivalent to an energy principle [4]. Then the approximate solution over the domain is assumed to be a linear combination ($\sum_j c_j \phi_j$) of appropriately chosen approximation functions ϕ_j and coefficients c_j to be determined. The coefficients c_j are determined such that the integral statement is satisfied. Various variational methods, for example, the Ritz, Galerkin, collocation, and least-squares methods, differ from each other in the choice of the integral form and weight functions. A more detailed discussion of variational methods is presented in Chapter 2 (also, see [4]). The classical variational methods, which are truly *meshless methods*, are powerful methods that provide globally continuous solutions but suffer from the drawback that the approximation functions for problems with arbitrary domains are difficult to construct. The modern meshless methods seem to provide a way to construct approximation functions for arbitrary domains, but they also have their own disadvantages.

Next, we consider two examples of numerical simulations, one for an initialvalue problem (IVP) and another for a boundary-value problem (BVP), using the finite difference method to give the reader a taste of numerical methods and, in the process, introduce the finite difference method. The examples discussed here are based on the problems introduced in Examples 1.2.1 and 1.2.2. Mathematically, the bar problem of Example 1.2.3 is the same as the heat transfer problem of Example 1.2.2; therefore, its numerical solution is not discussed here.

Example 1.3.1

Problem statement (The pendulum problem): Consider Eq. (1.2.4) governing the simple planar motion of a pendulum subject to the initial conditions in Eq. (1.2.5). Use the forward and backward finite difference methods to formulate discretized forms of the equation. Obtain numerical solutions for three different time steps, $\Delta t = 0.05$, $\Delta t = 0.025$, and $\Delta t = 0.001$, and compare them graphically with the exact linear solution. Take $\ell = 2.0$, $g = 32.2$, $\theta_0 = \pi/4$, and $v_0 = 0$ in the numerical computation.

Solution: We begin with the following general first-order differential equation [of which Eq. (1.2.4) is a special case]

$$\frac{du}{dt} = f(t,u), \quad 0 < t < T; \quad u(0) = u_0 \tag{1.3.1}$$

where f is a known function of the unknown, u. Equation (1.3.1) must be solved for $t > 0$ subject to the initial (i.e., time $t = 0$) condition $u(0) = u_0$. We approximate the derivative at time $t = t_i$ by

$$\left(\frac{du}{dt}\right)\Big|_{t=t_i} \approx \frac{u(t_{i+1}) - u(t_i)}{t_{i+1} - t_i} \tag{1.3.2}$$

We note that the derivative at $t = t_i$ is replaced by its definition except that we did not take the limit $\Delta t \equiv t_{i+1} - t_i \to 0$; that is why it is an approximation. We also note that the slope of u at t_i in Eq. (1.3.2) is based on values of u at t_i and t_{i+1}. We can also take it to be the slope at $t = t_{i+1}$

$$\left(\frac{du}{dt}\right)\Big|_{t=t_{i+1}} \approx \frac{u(t_{i+1}) - u(t_i)}{t_{i+1} - t_i} \tag{1.3.3}$$

The formula in Eq. (1.3.2) is called, for obvious reasons, *forward difference*, while that in Eq. (1.3.3) is called *backward difference*. The forward difference scheme is also known as *Euler's explicit scheme* or *first-order Runge–Kutta method*. For increasingly small values of Δt, we hope that both approximations have a decreasingly small error in the computation of the slope. However, the two schemes will have different numerical convergence and stability behavior, as will be discussed in more detail in Chapter 7.

Substituting Eq. (1.3.2) into Eq. (1.3.1) at $t = t_i$, we obtain the forward difference formula

$$u_{i+1} = u_i + \Delta t\, f(u_i, t_i), \quad u_i = u(t_i), \quad \Delta t = t_{i+1} - t_i \tag{1.3.4}$$

Equation (1.3.4) can be solved, starting from the known value u_0 of $u(t)$ at $t = 0$, for $u_1 = u(t_1) = u(\Delta t)$. This process can be repeated to determine the values of u at times $t = \Delta t, 2\Delta t, \ldots, n\Delta t$. Of course, there are higher-order finite difference schemes that are more accurate than the Euler's scheme and we will not discuss them as they are outside the scope of this study. Note that we are able to convert the ordinary differential equation, Eq. (1.3.1), to an algebraic equation, Eq. (1.3.4), which needs to be evaluated at different times to construct the time history of $u(t)$.

We now apply Euler's explicit scheme to the second-order equation

(1.2.4) subjected to the initial conditions in Eq. (1.2.5). To apply the procedure described above to the equation at hand, we rewrite Eq. (1.2.4) as a pair of first-order differential equations (note that $v_x = \ell v$)

$$\frac{d\theta}{dt} = v, \quad \frac{dv}{dt} = -\lambda^2\theta \quad (\lambda^2 = g/\ell) \tag{1.3.5}$$

which are *coupled* (i.e., one cannot be solved without the other). Applying the scheme of Eq. (1.3.4) to the equations at hand, we obtain

$$\theta_{i+1} = \theta_i + \Delta t\, v_i; \quad v_{i+1} = v_i - \Delta t\, \lambda^2\theta_i \tag{1.3.6}$$

The expressions for θ_{i+1} and v_{i+1} in Eq. (1.3.6) are repeatedly computed using the known solution (θ_i, v_i) from the previous time step. At time $t = 0$, we use the known initial values (θ_0, v_0). Thus, one needs a computer and a computer language like MATLAB, Fortran, or C++ to implement the logic of repeatedly computing θ_{i+1} and v_{i+1} with the help of Eq. (1.3.6).

The numerical solutions of Eq. (1.3.6) for three different time steps, $\Delta t = 0.05$, $\Delta t = 0.025$ and $\Delta t = 0.001$, along with the exact linear solution in Eq. (1.2.9) (with $\ell = 2.0$, $g = 32.2$, $\theta_0 = \pi/4$, $v_0 = 0$) are presented in Fig. 1.3.1. The accuracy of the numerical solutions is dependent on the size of the time step; the smaller the time step the more accurate the solution is. For large time steps the solution may even diverge from the true solution.

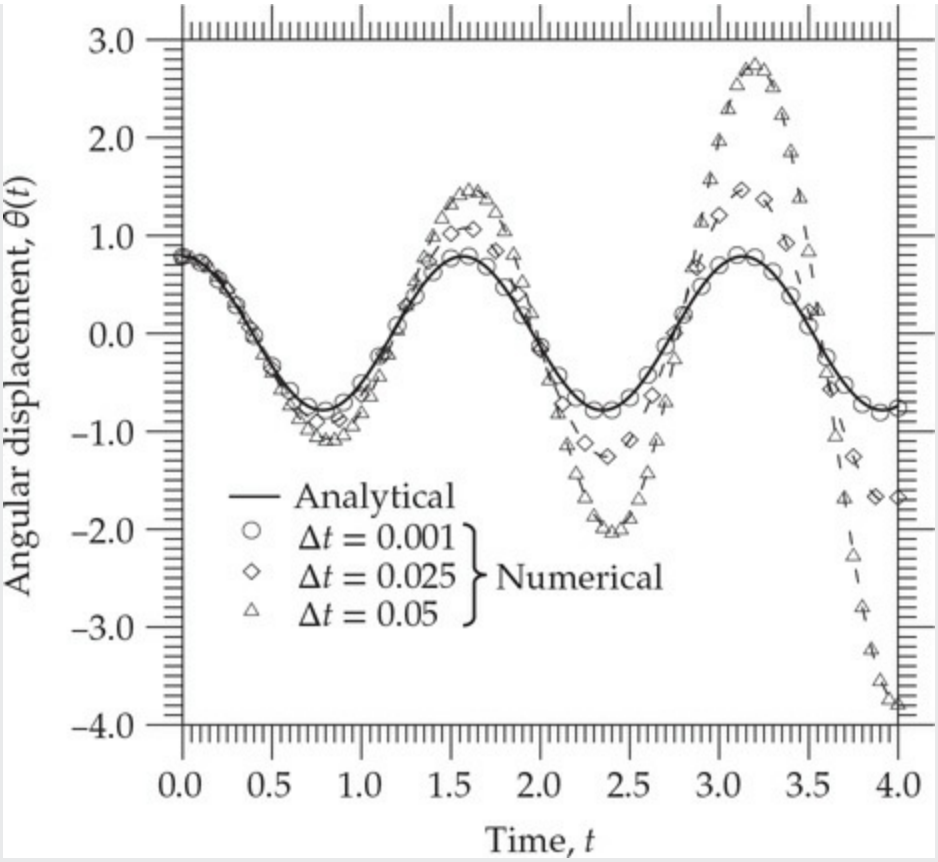

Fig. 1.3.1 Comparison of the numerical solutions $\theta(t)$ obtained with Euler's scheme with the analytical solution of the simple pendulum (linearized equations).

Example 1.3.2

Problem statement (The heat flow problem): Consider the boundary-value problem of **Example 1.2.2**. Use the centered difference method to determine the numerical solution of Eq. (1.2.19):

$$-\frac{d^2\theta}{dx^2} + m^2\,\theta = 0, \quad m = \sqrt{\frac{\beta P}{kA}}, \quad 0 < x < L$$

Solution: First we divide the domain $(0, L)$ into a finite set of N intervals of equal length Δx, as shown in Fig. 1.3.2(b). Then we approximate the second derivative of $\theta = T - T_\infty$ directly using the centered difference scheme [error is of order $O(\Delta x)^2$]

$$\left(\frac{d^2\theta}{dx^2}\right)_{x=x_i} \approx \left(\frac{\theta_{i-1} - 2\theta_i + \theta_{i+1}}{(\Delta x)^2}\right) \tag{1.3.7}$$

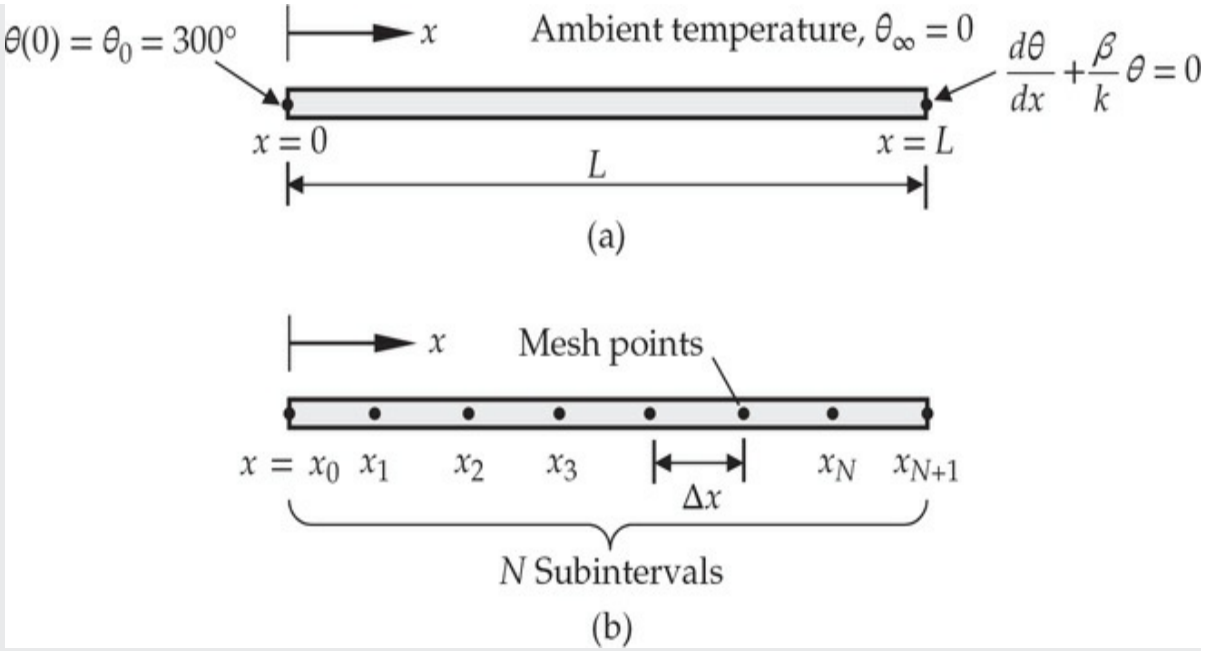

Fig. 1.3.2 Heat transfer in a bar and a typical finite difference mesh.

This approximation involves three points, called mesh points, at which function evaluations are required. The mesh points are separated by a distance of Δx. Using the above approximation in Eq. (1.2.19), we obtain

$$-(\theta_{i-1} - 2\theta_i + \theta_{i+1}) + (m\Delta x)^2\theta_i = 0 \text{ or } -\theta_{i-1} + [2 + (m\Delta x)^2]\theta_i - \theta_{i+1} = 0 \qquad (1.3.8)$$

Equation (1.3.8) is valid for any mesh point $x = x_i$, $i = 1, 2, \ldots, N$, at which the solution is not known. The formula contains values of θ at three mesh points $x = x_{i-1}$, x_i, and $x = x_{i+1}$ at a time. Note that Eq. (1.3.8) is not used at mesh point $x = x_0 = 0$ because the temperature is known there, as given in Eq. (1.2.20). However, use of Eq. (1.3.8) at mesh point $x = x_N = L$ requires the knowledge of the fictitious value θ_{N+1} (as we see in the sequel, we never have to deal with such fictitious values in the finite element method). The forward finite difference approximation of the second boundary condition in Eq. (1.2.20) at mesh point $x_N = L$ can be used to determine θ_{N+1}:

$$\frac{\theta_{N+1} - \theta_N}{\Delta x} + \frac{\beta}{k}\theta_N = 0 \Rightarrow \theta_{N+1} = \left(1 - \frac{\beta\Delta x}{k}\right)\theta_N \qquad (1.3.9)$$

Application of the formula in Eq. (1.3.7) to mesh points at $x_1, x_2, \ldots, x_N$ yields

$$
\begin{aligned}
-\theta_0 + D\theta_1 - \theta_2 &= 0 \\
-\theta_1 + D\theta_2 - \theta_3 &= 0 \\
-\theta_2 + D\theta_3 - \theta_4 &= 0 \\
\cdots \quad \cdots \quad \cdots & \\
-\theta_{N-1} + D\theta_N - \theta_{N+1} &= 0
\end{aligned}
\tag{1.3.10}
$$

where $D = [2 + (m\Delta x)^2]$. Equation (1.3.9) can be used to eliminate θ_{N+1} from the last equation in (1.3.10). Then Eq. (1.3.10) consists of N equations in N unknowns, $\theta_1, \theta_2, \ldots, \theta_N$.

As a specific example, consider a steel rod of diameter $d = 0.02$ m, length $L = 0.05$ m, and thermal conductivity $k = 50$ W/(m·°C). Suppose that the temperature at the left end is $T_0 = 320$°C, ambient temperature is $T_\infty = 20$°C, and film conductance (or heat transfer coefficient) $\beta = 100$ W/(m^2·°C). For this data, we have

$$
\frac{\beta}{k} = 2, \quad m^2 = \frac{\beta P}{kA} = \frac{\beta(\pi d)}{k(\pi d^2/4)} = 400, \quad \theta_0 \equiv \theta(0) = T(0) - T_\infty = 300°\text{C}
$$

For a subdivision of four intervals ($N = 4$), we have $\Delta x = 0.0125$ m, $D = 2 + (20 \times 0.0125)^2 = 2.0625$, and $D - 1 + (\beta\Delta x/k) = 1.0875$. For this case, there are four equations in four unknowns:

$$
\begin{aligned}
2.0625\,\theta_1 - \theta_2 &= 300 \\
-\theta_1 + 2.0625\,\theta_2 - \theta_3 &= 0 \\
-\theta_2 + 2.0625\,\theta_3 - \theta_4 &= 0 \\
-\theta_3 + 1.0875\,\theta_4 &= 0
\end{aligned}
\tag{1.3.11}
$$

The above *tridiagonal* system of algebraic equations can be solved using the Gauss elimination method (this is where we need a computer!). The solution is given by

$$
\{\theta\} = \{245.81,\ 206.98,\ 181.10,\ 166.52\}^{\mathrm{T}} \tag{1.3.12}
$$

The analytical solution at the same points is

$$
\{\theta\} = \{248.75,\ 213.13,\ 190.90,\ 180.66\}^{\mathrm{T}} \tag{1.3.13}
$$

The maximum error is about 7.8%. When the number of mesh points is doubled, the maximum error goes down to 4.2%, and it is 1% when the number of mesh points is increased to 32 (results are not included here for these cases).

1.4 The Finite Element Method

1.4.1 The Basic Idea

The finite element method is a numerical method like the finite difference method, but is more general and powerful in its application to real-world problems, which may involve multi-physics and complicated geometry and boundary conditions. In the finite element method, a given domain is viewed as a collection of subdomains, and over each subdomain the governing equation is approximated by any of the traditional variational methods or any method that is suitable. The main reason behind seeking approximate solutions on a collection of subdomains is the fact that it is easier to represent a complicated function as a collection of simple polynomials, as can be seen from Fig. 1.4.1. Of course, each individual segment of the solution should fit with its neighbors in the sense that the function and possibly its derivatives up to a chosen order are continuous (i.e., single-valued) at the connecting points. These ideas will be more clear in the sequel.

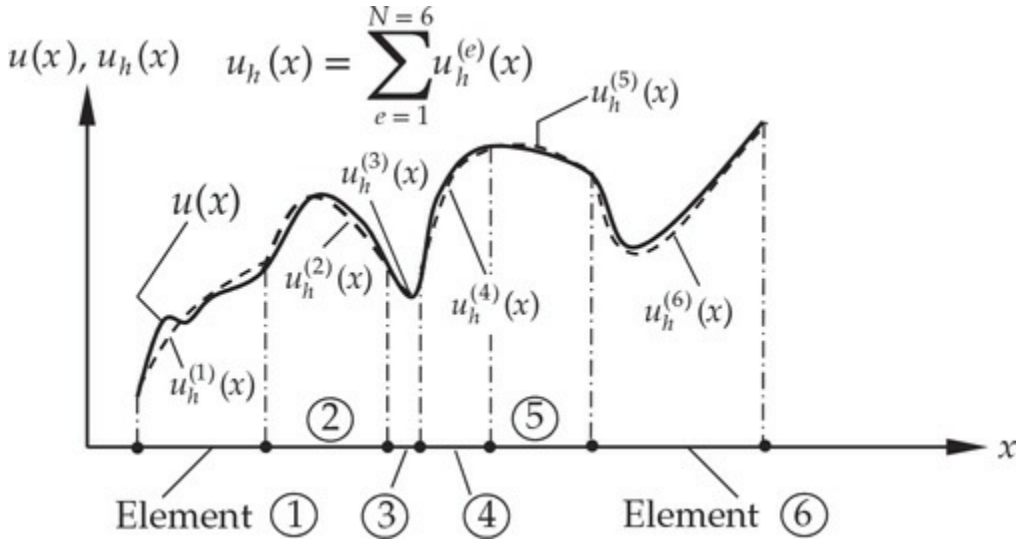

Fig. 1.4.1 Piece-wise approximation of a function.

1.4.2 The Basic Features

The finite element method is endowed with three distinct features that account for its superiority over other competing methods. These features are outlined next.

1. A geometrically complex domain Ω of the problem, such as the one

in Fig. 1.4.2(a), is represented as a collection, called *mesh*, of geometrically simple subdomains as indicated in Fig. 1.4.2(b). A subdomain is called a *finite element* [see Fig. 1.4.2(c)]. Here the word "domain" refers to the geometric region over which the equations are solved. Note that not all geometric shapes can qualify as finite elements; only those shapes that allow the derivation of the approximation functions can qualify as finite elements. In reality, the discretized domain is a collection of points, as shown in Fig. 1.4.2(d).

2. Over each finite element, algebraic relations between the values of the duality pairs (i.e., cause and effect or primary and secondary degrees of freedom) of the problem at element nodes are derived using (a) statements equivalent to the governing equations of the problem and (b) a method of approximation. Alternatively, one may use physical principles directly to obtain the relationships. In principle, any suitable method of approximation can be used to derive the algebraic relations. The set of resulting algebraic equations among the nodal values of the duality pairs (e.g., displacements and forces) is termed a *finite element model*.
3. The equations from all elements, $\bar{\Omega}^e \equiv \Omega^e \cup \Gamma^e$, are assembled (i.e., elements are put back into their original positions of the mesh) using (a) continuity of the primary variables (e.g., displacements) and (b) balance of secondary variables (e.g., forces).

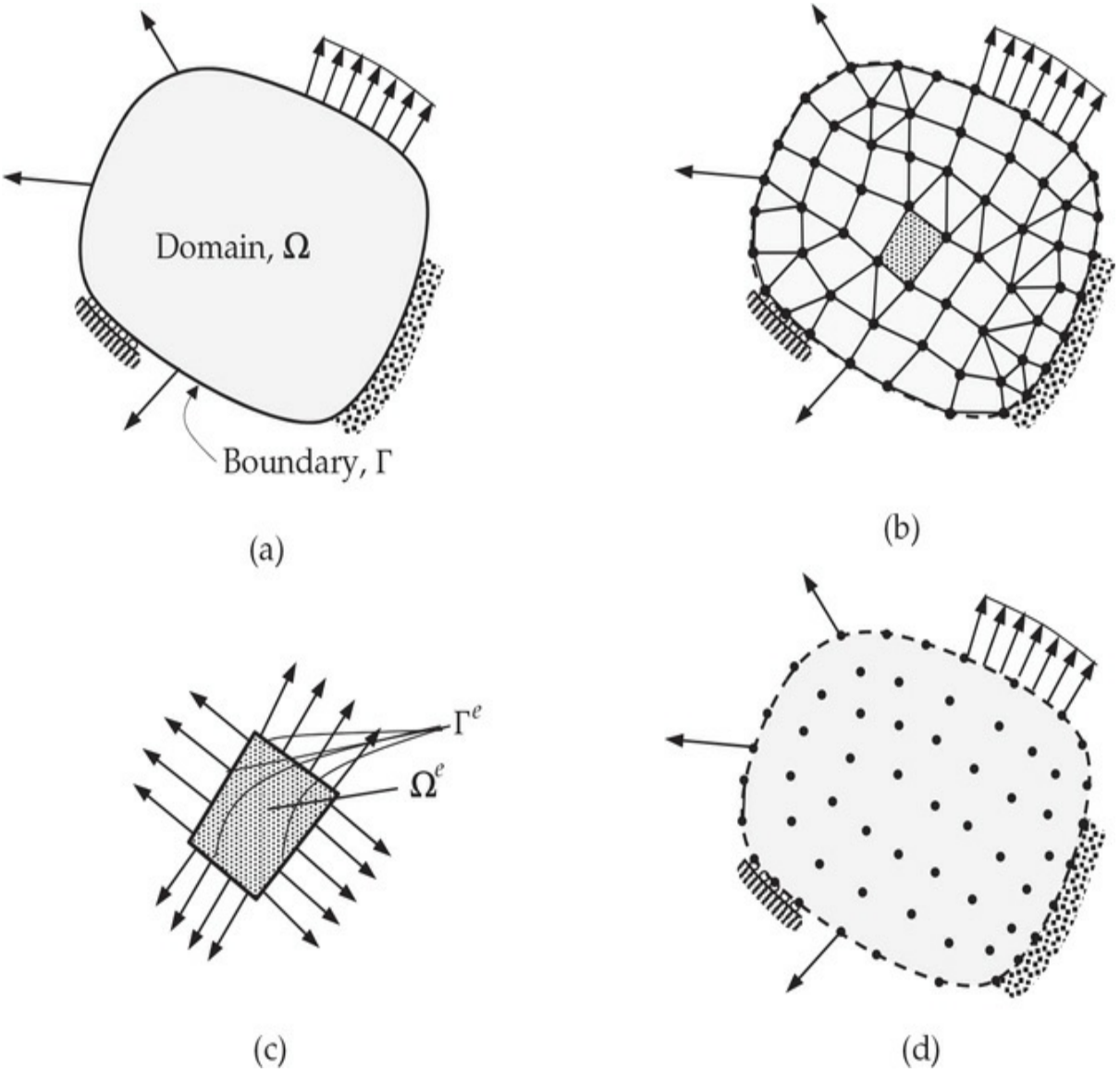

Fig. 1.4.2 Discretization of a two-dimensional domain. (a) Original domain with boundary. (b) Representation of the domain by a collection of triangles and quadrilateral elements. (c) A typical element with domain and boundary. (d) Representation of the domain by a collection of nodes.

These statements may not make complete sense to the reader until some specific examples to illustrate the features are discussed in the coming pages.

Approximations enter engineering analysis at several stages. The division of the whole domain into finite elements may not be exact (i.e., the assemblage of elements, $\Omega_h = \cup_{e=1}^{N} \bar{\Omega}^e$, where N is the number of elements, does not exactly match the original domain Ω), introducing error in the domain (hence in the boundary data) being modelled. The second stage is when element equations are derived. Typically, the dependent

unknowns (u) of the problem are approximated using the basic idea that any continuous function can be represented by a linear combination of known functions ϕ_i and undetermined coefficients c_i($u \approx u_h = \sum c_i \phi_i$). Algebraic relations among the undetermined coefficients c_i are obtained by satisfying the governing equations in a weighted-integral sense over each element. The approximation functions ϕ_i are often taken to be polynomials and they are derived using concepts from interpolation theory. Therefore, they are also termed *interpolation functions*. Thus approximation errors in the second stage are introduced both in representing the solution u as well as in evaluating the integrals. Finally, errors are introduced in solving the assembled system of equations. Obviously, some of the errors discussed above can be zero. When all errors are zero, we obtain the exact solution of the problem (not the case in most problems in two and three dimensions).

Next, the basic ideas and some terminology of the finite element method are introduced via several simple examples. The reader should try to understand the basic features rather than to question the use of an approximation method to solve such a simple problem (which can possibly be solved exactly without using the finite element method).

The following example is an expansion of an article written by the author for a student magazine at the University of Oklahoma [5, 6]. This simple example illustrates the basic steps involved in a finite element analysis.

Example 1.4.1

Problem statement: Consider the problem of determining the perimeter (a quantity of interest) of a circle of radius R, as shown in Fig. 1.4.3(a). *Pretend* that we do not know the formula ($P = 2\pi R$) for the perimeter P (circumference) of a circle. Babylonians estimated the value of the perimeter of a circle by approximating it by straight line segments, whose lengths they were able to measure. Obtain the approximate value of the circumference by representing it as a sum of the lengths of the line segments.

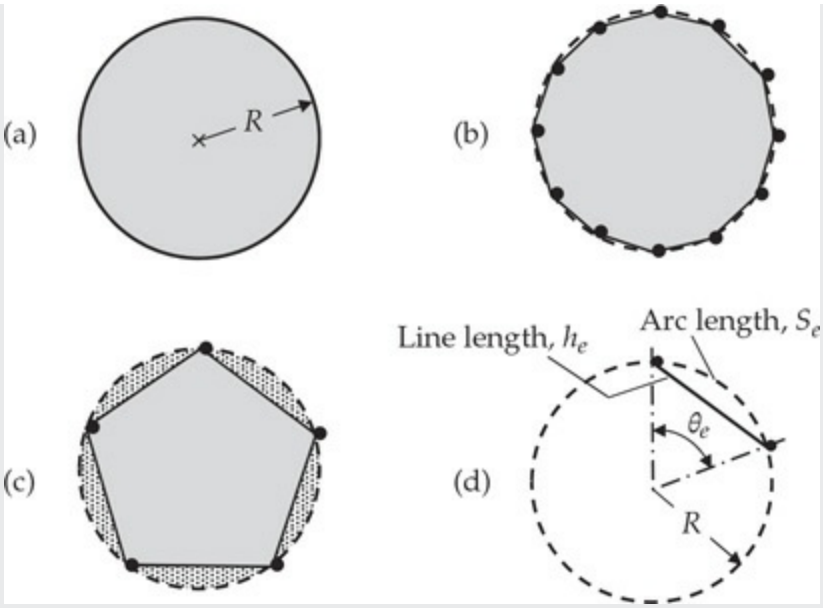

Fig. 1.4.3 Determination of the perimeter of a circle.

Solution: The three basic features of the finite element method in the present case take the following form. First, the division of the perimeter of a circle into a collection of line segments. In theory, we need infinite number of such line elements to represent the perimeter; otherwise, the value computed will have some error. Second, writing an equation for the quantity of interest (perimeter) over an element (line segment) in this case is exact, because the approximated perimeter is a straight line. Third, the assembly of elements amounts to simply adding the element lengths to obtain the total value. Although this is a trivial example, it illustrates several (but not all) ideas and steps involved in the finite element analysis of a problem. We outline the steps involved in computing an approximate value of the perimeter of the circle. In doing so, we introduce certain terms that are used in the finite element analysis of any problem.

1. *Finite element discretization*. First, the domain (i.e., the perimeter of the circle) is represented as a collection of a finite number *n* of subdomains, namely, line segments, as shown in Fig. 1.4.3(b). This is called *discretization of the domain*. Each subdomain (i.e., line segment) is called an *element*. The collection of elements is called the *finite element mesh*. The elements are connected to each other at points called *nodes*. In the present case, we discretize the perimeter into a mesh of five ($n = 5$) line segments, as shown in Fig. 1.4.3(c). The line segments can be of different lengths. When all elements are of the same length, the mesh is said to be *uniform*; otherwise, it is called a *nonuniform* mesh.

2. *Element equations*. A typical element (i.e., line segment, Ω_e) is isolated and its required properties, i.e., length, are computed by some appropriate means. Let h_e be the length of element Ω_e in the mesh. For a typical element Ω_e, h_e is given, as can be seen from Fig. 1.4.3(d), by

$$h_e = 2R \sin \frac{1}{2}\theta_e \tag{1.4.1}$$

where R is the radius of the circle and $\theta_e < \pi$ is the angle subtended by the line segment. The above equations are called *element equations*. Ancient mathematicians most likely made measurements, rather than using Eq. (1.4.1), to find h_e (they did not know π).

3. *Assembly of element equations and solution*. The approximate value of the perimeter of the circle is obtained by putting together the element properties in a meaningful way; this process is called the *assembly* of the element equations. It is based, in the present case, on the simple idea that the total perimeter of the polygon Ω_h (assembly of elements) is equal to the sum of the lengths of individual elements:

$$P_n = \sum_{e=1}^{n} h_e \tag{1.4.2}$$

Then P_n represents an approximation to the actual perimeter, P. If the mesh is uniform, or h_e is the same for each of the elements in the mesh, then $\theta_e = 2\pi/n$, and we have

$$P_n = n\left(2R \sin \frac{\pi}{n}\right) \tag{1.4.3}$$

4. *Convergence and error estimate*. For this simple problem, we know the exact solution: $P = 2\pi R$. We can estimate the error in the approximation and show that the approximate solution P_n converges to the exact value P in the limit as $n \to \infty$. Consider a typical element Ω_e . The error in the approximation is equal to the difference between the length of the sector and that of the line segment [see Fig. 1.4.3(d)]

$$E_e = |S_e - h_e| \tag{1.4.4}$$

where $S_e = R\theta_e$ is the length of the sector. Thus, the error estimate for an element in the mesh is given by

$$E_e = R\left(\frac{2\pi}{n} - 2\sin\frac{\pi}{n}\right) \tag{1.4.5}$$

The total error (called *global* error) is given by multiplying E_e by n:

$$E = nE_e = 2R\left(\pi - n\sin\frac{\pi}{n}\right) = 2\pi R - P_n = P - P_n \tag{1.4.6}$$

We now show that E goes to zero as $n \to \infty$. Letting $x=1/n$, we have

$$P_n = 2Rn\sin\frac{\pi}{n} = 2R\frac{\sin\pi x}{x}$$

and

$$\lim_{n\to\infty} P_n = \lim_{x\to 0}\left(2R\frac{\sin\pi x}{x}\right) = \lim_{x\to 0}\left(2\pi R\frac{\cos\pi x}{1}\right) = 2\pi R \tag{1.4.7}$$

Hence, E_n goes to zero as $n \to \infty$. This completes the proof of convergence.

It should be recalled, from a first course on statics of rigid bodies, that the calculation of the mass center or the geometric centroid (quantity of interest) of an irregular volume makes use of the so-called method of composite bodies, in which a body is conveniently divided (mesh discretization) into several parts (elements) of simple shape for which the mass and the center of mass (element properties) can be computed readily. The center of mass of the whole body is then obtained using the *principle of moments* or *Varignon's theorem* (a basis for the assembly of element equations):

$$(m_1 + m_2 + \cdots + m_n)\bar{X} = m_1\bar{x}_1 + m_2\bar{x}_2 + \cdots + m_n\bar{x}_n \tag{1.4.8}$$

where $\bar{X}$ is the x-coordinate of the center of mass of the whole body, m_e is the mass of the eth part, and $\bar{x}_e$ is the x-coordinate of the center of mass of the eth part. Similar expressions hold for the y and z coordinates of the center of mass of the whole body. Analogous relations hold for composite lines, areas, and volumes, wherein the masses are replaced by lengths, areas, and volumes, respectively. When a given body is not expressible in

terms of simple geometric shapes (elements) for which the mass and the center of the mass can be represented mathematically, it is necessary to use a method of approximation to represent the "properties" of an element. The next example illustrates the approximate determination of the geometric centroid of an irregular plane region.

Example 1.4.2

Problem statement (Geometric centroid of an irregular body): Determine the geometric centroid $(\bar{X}, \bar{Y})$ of the irregular plane region shown in Fig. 1.4.4(a).

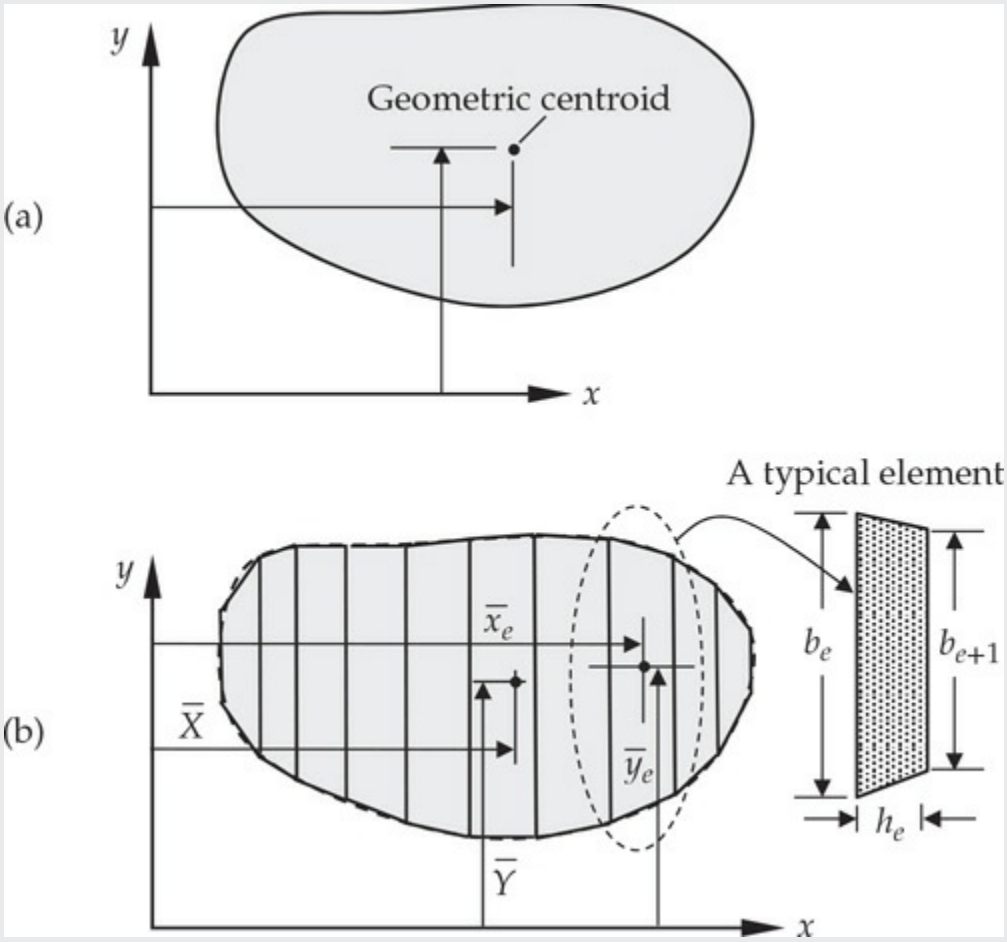

Fig. 1.4.4 Determination of the centroid of an irregular region.

Solution: The plane region can be divided into a finite number of trapezoidal strips (elements), a typical element having width h_e and heights b_e and b_{e+1}, as indicated in Fig. 1.4.4(b). The area of the eth strip is given by

$$A_e = \frac{1}{2} h_e (b_e + b_{e+1}) \tag{1.4.9}$$

The area A_e is an approximation of the true area of the element because $(b_e + b_{e+1})/2$ is an estimated average height of the element. The coordinates of the centroid of the region are obtained by applying the moment principle:

$$\bar{X} = \frac{\sum_e A_e \bar{x}_e}{\sum_e A_e}, \quad \bar{Y} = \frac{\sum_e A_e \bar{y}_e}{\sum_e A_e} \tag{1.4.10}$$

where $\bar{x}_e$ and $\bar{y}_e$ are the coordinates of the centroid of the eth element with respect to the coordinate system used for the whole body. It should be noted that the accuracy of the approximation will be improved by increasing the number of strips (i.e., decreasing their width, h_e).

When the center of mass is required, A_e in the above equations is replaced by the mass $m_e = \rho_e A_e$, ρ_e being the mass density of the eth element. For a homogeneous body, ρ_e is the same for all elements, and therefore Eq. (1.4.10) also gives the coordinates of the center of mass of a homogeneous body.

The two examples considered above illustrate how the idea of piecewise approximation is used to approximate irregular geometry and calculate required quantities. Thus, subdividing a geometrically complex domain into parts that allow the evaluation of desired quantities is a very natural and practical approach. The idea can be extended to approximate functions representing physical quantities. For example, the temperature variation in a two-dimensional domain can be viewed as a curved surface, and it can be approximated over any part of the domain, that is, over a subdomain, by a polynomial of desired degree. A curved surface over a triangular subregion may be approximated by a planar surface, as shown in Fig. 1.4.5. Such ideas form the basis of finite element approximations.

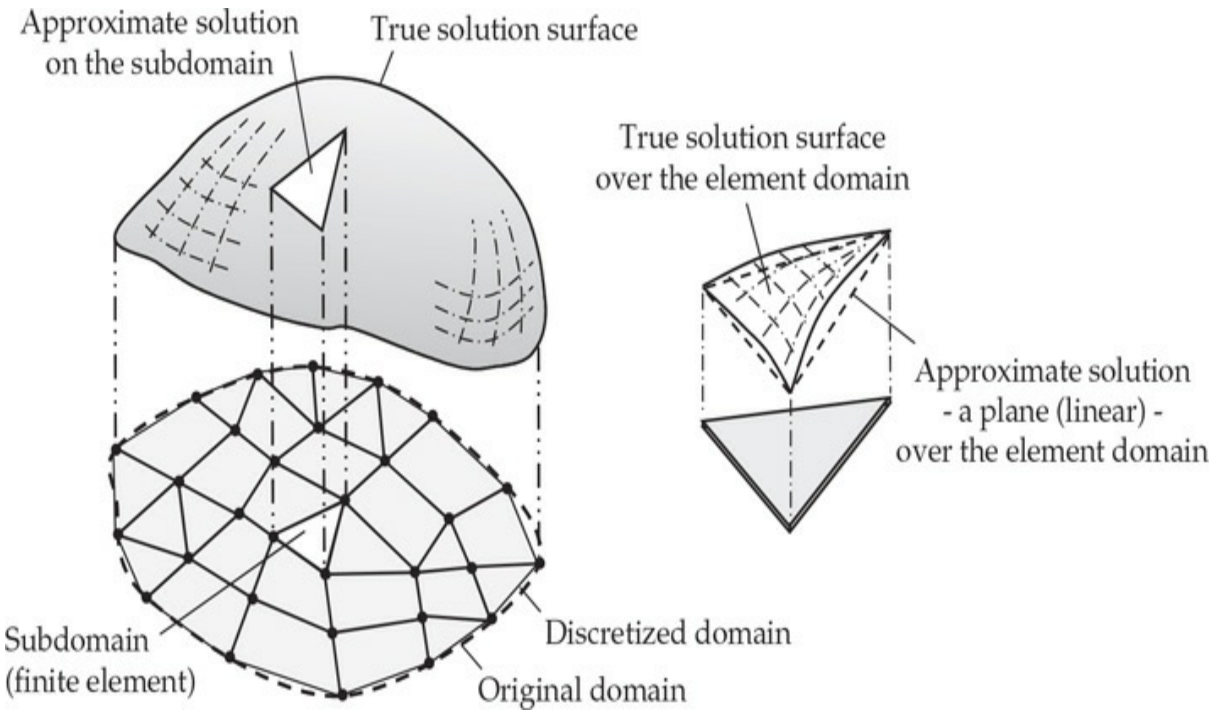

Fig. 1.4.5 Approximation of a curved surface by a planar surface.

The next example illustrates this idea of approximation for a one-dimensional continuous system described by an ordinary differential equation. The problem is one of axisymmetric radial heat flow in a long composite cylinder. Heat dissipation from a wire (with two insulations) carrying an electric current and heat flow across a thick-walled composite cylindrical tube are typical examples of the problem.

Example 1.4.3

Problem statement (Solution of a differential equation): Consider the temperature variation in a long composite cylinder consisting of two coaxial layers in perfect thermal contact, as shown in Fig. 1.4.6(a). Because of the long and axisymmetric geometry, boundary conditions, material and loading, the temperature T is independent of the axial coordinate z and angular coordinate θ; that is, every radial line has the same temperature T at any radial distance r, $T = T(r)$. Divide the radius into a finite number of subdomains and determine an approximation $T_e(r)$ of $T(r)$ over the eth subdomain.

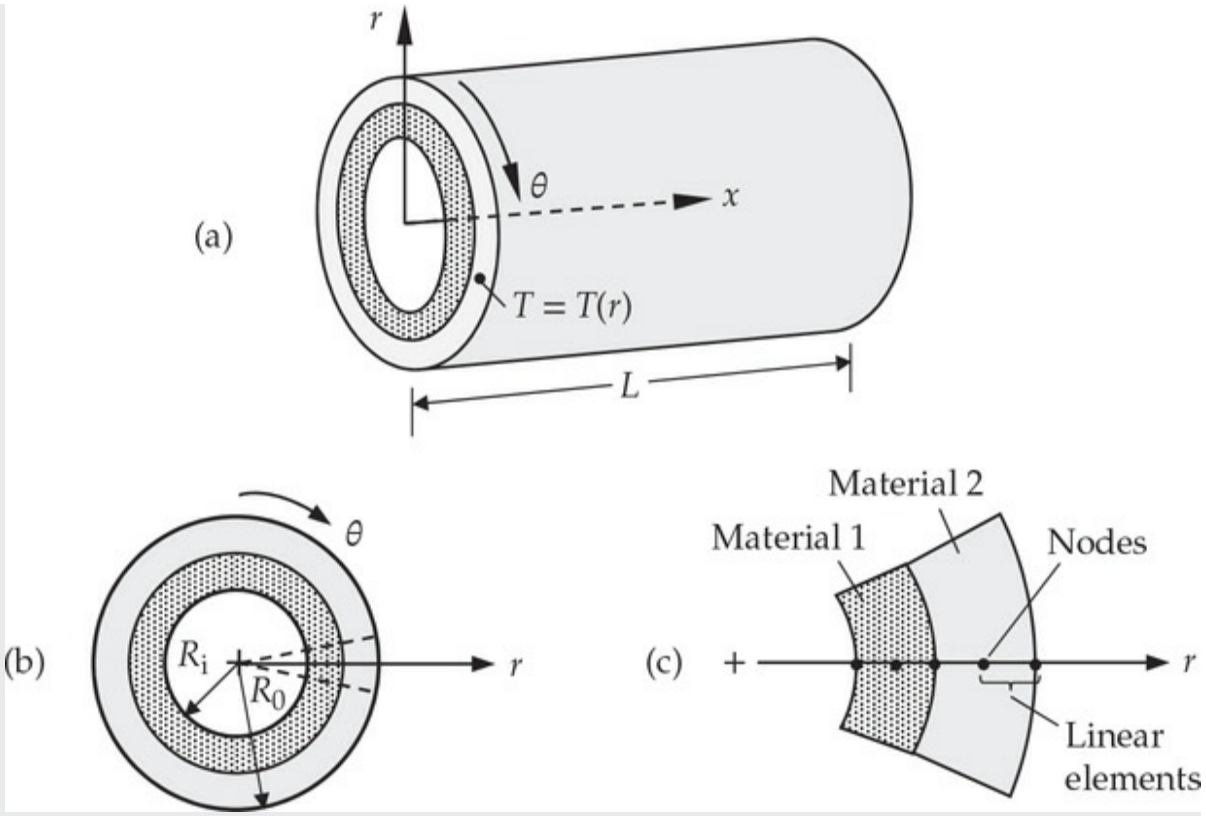

Fig. 1.4.6 (a) Coaxial cylinder made of two different materials. (b) Typical cross section of the composite cylinder. (c) Finite element discretization by line segments (linear elements).

Solution: The equation governing the axisymmetric heat transfer in a long cylinder can be formulated using the principle of balance of energy (as was done in **Example 1.2.2**), and it is given by

$$-\frac{1}{r}\frac{d}{dr}\left(rk\frac{dT}{dr}\right)=g(r) \tag{1.4.11}$$

Equation (1.4.11) is subject to appropriate boundary conditions. For example, consider the case in which $dT/dr = 0$ at $r = R_i$ and $T = T_0$ at $r = R_0$:

$$kr\frac{dT}{dr}=0 \quad \text{at} \quad r=R_i; \quad T(r)=T_0 \quad \text{at} \quad r=R_0 \tag{1.4.12}$$

Here k denotes the thermal conductivity, which varies from layer to layer, R_i and R_0 are the inner and outer radii of the cylinder, as shown in Fig. 1.4.6(b), and g is the rate of energy generation in the medium. When it is difficult to obtain an exact solution of Eqs. (1.4.11) and (1.4.12), either because of complex geometry and material properties or because $g(r)$ is a

complicated function that does not allow exact evaluation of its integral, we seek an approximate one. In the finite element method, the domain (R_i,R_0) is divided into N subintervals as indicated in Fig. 1.4.6(c), and the approximate solution is sought in the form

$$
\begin{aligned}
T_1(r) &= \sum_{j=1}^{n} T_j^{(1)} \psi_j^{(1)}(r), \quad R_i \le r \le R_i + h_1 \text{ (first interval)} \\
T_2(r) &= \sum_{j=1}^{n} T_j^{(2)} \psi_j^{(2)}(r), \quad R_i + h_1 \le r \le R_i + h_1 + h_2 \text{ (second interval)} \\
&\vdots \\
T_N(r) &= \sum_{j=1}^{n} T_j^{(N)} \psi_j^{(N)}(r), \quad R_i + h_1 + \cdots + h_{N-1} \le r \le R_0 \text{ (Nth interval)}
\end{aligned}
\tag{1.4.13}
$$

where h_e denotes the length of the eth interval, T_j (the element label 'e' is omitted in the interest of brevity) is the value of the temperature $T_e(r)$ at the jth geometric point, called *node*, of the eth interval, ψ_j are the approximation functions on the eth interval, and T_j are the unknown nodal values. Thus, the continuous function $T(r)$ is approximated in each subinterval by a desired degree of approximating polynomials, and the polynomial is expressed in terms of the values of the function at a selected number of points in the interval. The number of points is equal to the number of parameters in the polynomial. For example, a linear polynomial approximation of the temperature over the interval requires two values, and hence two points are identified in the interval. The end points of the interval are selected for this purpose because they also define the length of the interval, as can be seen from Fig. 1.4.7. For higher-order polynomial approximations, additional nodes are identified inside the element domain. The importance of these geometric points (i.e., nodes) is that they are the base points required to define the approximating polynomials. The nodal values T_j are determined such that $T_e(r)$ satisfies the differential equation in Eq. (1.4.11) and boundary conditions in Eq. (1.4.12) in some sense, often in an integral sense over each element:

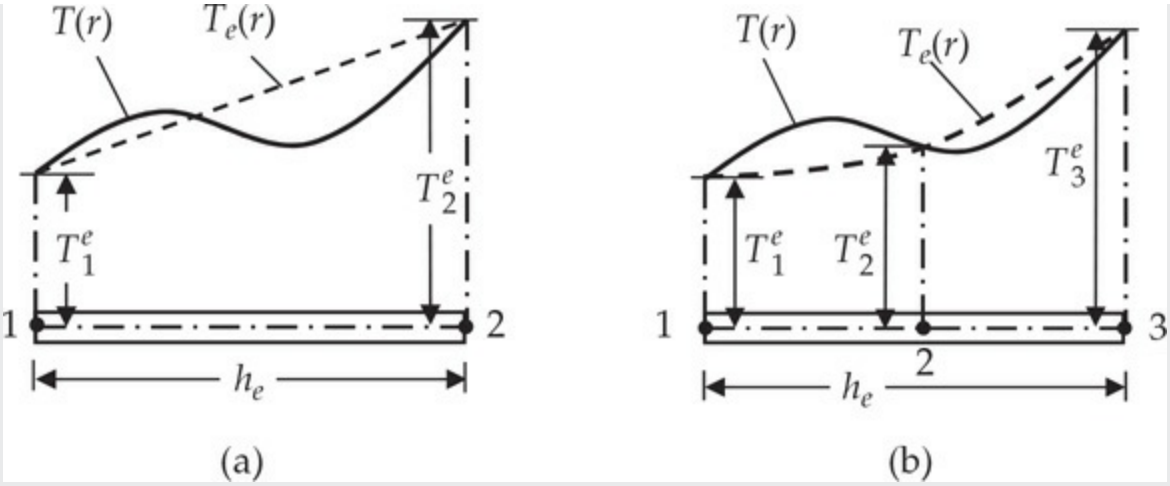

Fig. 1.4.7 (a) Linear approximation $T_e(r)$ of a function $T(r)$ over an element (b) Quadratic approximation $T_e(r)$ of $T(r)$.

$$0 = \int_{r_a}^{r_b} w_i(r) \left[-\frac{1}{r}\frac{d}{dr}\left(rk\frac{dT_e}{dr}\right) - g(r) \right] rdr \qquad (1.4.14)$$

for all independent choices of the weight functions, ω_i, $_{\text{i}}$ = 1, 2, ..., n. Often we select $\omega_i = \psi_i (i = 1, 2, ..., n)$ to obtain n relations among then unknown nodal values of the element. These ideas will be discussed in more detail in Chapter 3.

The piecewise (i.e., element-wise) approximation of the solution allows us to include any discontinuous data, such as the material properties, and to use meshes of many lower-order elements or a mesh of few higher-order elements to represent large gradients of the solution. Polynomial approximations of the form (1.4.13) can be derived systematically for any assumed degree of variation. The satisfaction of the differential equation in a weighted-integral sense leads, for steady-state problems, to algebraic relations among nodal temperatures T_j and heats Q_j of the element. The algebraic equations of all elements are assembled (i.e., related to each other) such that the temperature is continuous and the heats are balanced at nodes common to elements. Then the assembled equations are solved for the nodal values of temperatures and heats, after imposing the boundary conditions of the problem. More details of this example will be presented in Chapter 3.

1.4.3 Some Remarks

In summary, in the finite element method a given domain is divided into

subdomains, called finite elements, and an approximate solution to the problem is developed over each element. The subdivision of a whole domain into parts has the following two advantages:

1. allows accurate representation of complex geometry and inclusion of dissimilar material properties, and
2. enables easy representation of the total solution by functions defined within each element that captures local effects (e.g., large gradients of the solution).

The three fundamental steps of the finite element method that are illustrated via the examples are as follows:

1. Divide the whole domain into parts (both to represent the geometry and solution of the problem).
2. Over each part, seek an approximation to the solution as a linear combination of nodal values and approximation functions and derive the algebraic relations among the nodal values of the solution over each part.
3. Assemble the parts and obtain the solution to the whole.

Although the above examples illustrate the basic idea of the finite element method, there are several other features that are either not present or not apparent from the examples. Some remarks are in order.

1. One can discretize the geometry of the domain, depending on its shape, into a mesh of more than one type of element (by shape or order). For example, in the approximation of an irregular domain, one can use a combination of rectangles and triangles. However, the element interfaces must be compatible in the sense that the solution is uniquely defined along the interface.
2. If more than one type of element is used in the representation of the domain, one of each kind should be isolated and its equations be developed.
3. The governing equations of problems considered in this book are differential equations. In most cases, the equations cannot be solved over an element for two reasons. First, they do not permit the exact solution. It is here that the variational methods come into play. Second, the discrete equations obtained in the variational methods cannot be solved independent of the remaining elements, because

the assemblage of the elements is subjected to certain continuity, boundary, and/or initial conditions.

4. There are two main differences in the form of the approximate solution used in the finite element method and that used in the classical variational methods (i.e., variational methods applied to the whole domain). First, instead of representing the solution u as a linear combination ($u_h = \sum_j c_j \phi_j$) in terms of arbitrary parameters c_j as in the variational methods, in the finite element method the solution is often represented as a linear combination ($u_h = \sum_j u_j \psi_j$) in terms of the values u_j of u_h (and possibly its derivatives as well) at the nodal points. Second, the approximate functions ψ_j in the finite element method are often polynomials that are derived using the interpolation theory. However, the finite element method is *not* restricted to the use of approximations that are algebraic polynomials. One may use nodeless variables and non-polynomial functions to approximate a function (like in meshless or element-free methods).
5. The number and the location of the nodes in an element depend on (a) the geometry of the element, (b) the degree of the polynomial approximation, and (c) the weighted-integral form of the equations. By representing the required solution in terms of its values at the nodes, one directly obtains the approximate solution at the nodes.
6. The assembly of elements, in a general case, is based on the idea that the solution (and possibly its derivatives in higher-order equations) is continuous at the interelement boundaries.
7. In general, the assemblage of finite elements is subjected to boundary and/or initial conditions. The discrete equations associated with the finite element mesh are solved only after the boundary and/or initial conditions have been imposed.
8. There are three sources of error in a finite element solution: (a) those due to the approximation of the domain (this was the only error present in the first two examples); (b) those due to the approximation of the solution; and (c) those due to numerical computation (e.g., numerical integration and round-off errors in a computer). The estimation of these errors, in general, is not simple. However, under certain conditions, they can be estimated for classes of elements and problems.
9. The accuracy and convergence of the finite element solution depend on the differential equation, its weighted-integral form, and the

element used. “Accuracy” refers to the difference between the exact solution and the finite element solution, while “convergence” refers to the accuracy as the number of elements in the mesh is increased.

10. For time-dependent problems, a two-stage formulation is usually followed. In the first stage, the differential equations are approximated by the finite element method to obtain a set of ordinary differential equations in time. In the second, the differential equations in time are solved exactly or further approximated by either variational methods or finite difference methods to obtain algebraic equations, which are then solved for the nodal values. Alternatively, the finite element method can be used at both stages of approximation.

11. The desktop computers of today are more powerful than the supercomputers that existed when the finite element method was first implemented. Consequently, the analysis time is considerably reduced, provided the mesh used to model the problem is adequate. Even the automatic mesh generation programs cannot guarantee meshes that are free of irregularly shaped elements or have sufficient number of elements in a region containing high gradients in the solution, both of which result in loss of accuracy or, in the case of nonlinear problems, non-convergence of solutions. A typical mesh of a practical problem is shown in Fig. 1.4.8.

12. Element-free methods that require no assembly (because there are no elements) are being developed. Such methods have applications in fracture mechanics and wave propagation problems where re-meshing is necessary.

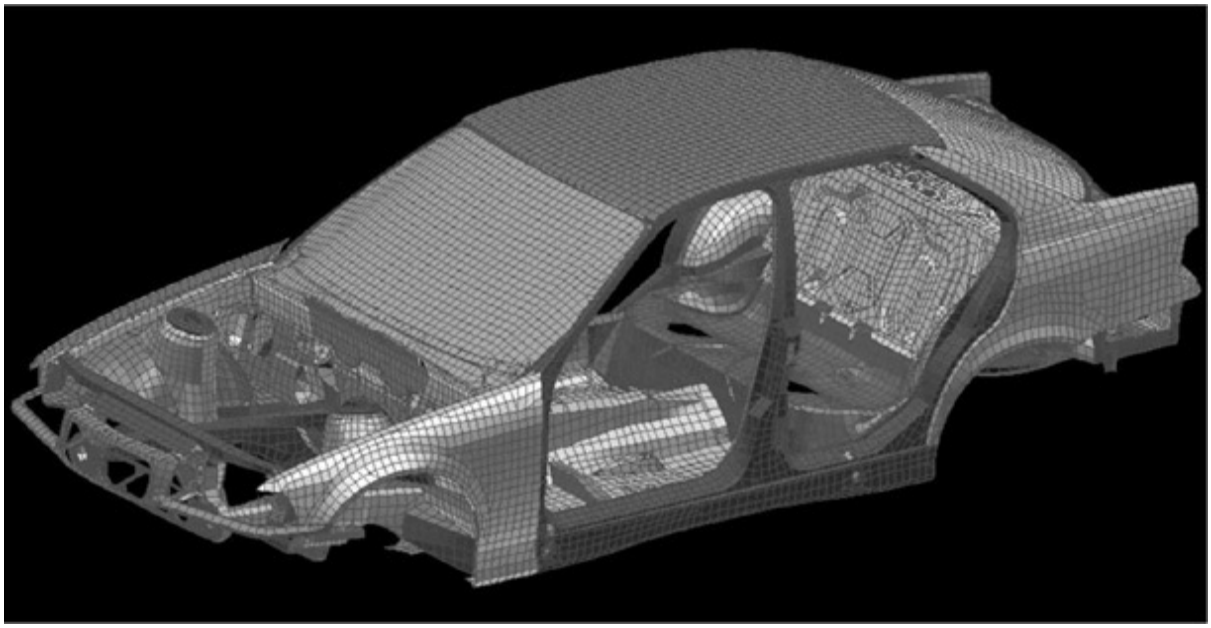

Fig. 1.4.8 A finite element mesh of an automobile body.

1.4.4 A Brief Review of the History of the Finite Element Method

The idea of representing a given domain as a collection of discrete parts is not unique to the finite element method. It was recorded that ancient mathematicians estimated the value of π by noting that the perimeter of a polygon inscribed in a circle approximates the circumference of the latter. They predicted the value of π to accuracy of almost 40 significant digits by representing the circle as a polygon of a finitely large number of sides (see Reddy [5, 6]). In modern times, the idea first found a home in structural analysis, where, for example, wings and fuselages are treated as assemblages of stringers, skins, and shear panels. In 1941, Hrenikoff [7] introduced the so-called framework method, in which a plane elastic medium was represented as a collection of bars and beams. The use of piecewise continuous functions defined over a subdomain to approximate an unknown function can be found in the work of Courant [8], who used an assemblage of triangular elements and the principle of minimum total potential energy to study the St. Venant torsion problem. Although certain key features of the finite element method can be found in the works of Hrenikoff [7] and Courant [8], its formal presentation is attributed to Argyris and Kelsey [9] and Turner et. al. [10]. The term “finite element” was first used by Clough [11]. Since its inception, the literature on finite element applications has grown exponentially, and today there are numerous books and journals that are primarily devoted to the theory and

application of the method. Additional information on the history of the finite element method can be found in [12–16].

In recent years, extensions and modifications of the finite element method have been proposed. These include the *partition of unity method* (PUM) of Melenk and Babuska [17], the *h-p cloud method* of Duarte and Oden [18], *meshless methods* advanced by Belytschko and his colleagues [19], and generalized finite element method (GFEM) detailed by Babuska and Strouboulis [20]. All of these methods and numerous other methods not named here are very closely related to the original idea.

1.5 The Present Study

This book deals with an introduction to the finite element method and its application to linear problems in engineering and applied sciences. Most introductory finite element textbooks written for use in engineering schools are intended for students of solid and structural mechanics, and these introduce the method as an offspring of matrix methods of structural analysis. A few texts that treat the method as a variationally based technique leave the variational formulations and the associated methods of approximation to an appendix. The approach taken in this book is one in which the finite element method is introduced as a numerical technique of solving classes of problems, each class having a common mathematical structure in the form of governing differential equations. This approach makes the reader understand the generality of the finite element method, irrespective of the reader's subject background. It also enables the reader to see the mathematical structure common to various physical problems, and thereby to gain additional insights into various engineering problems. Review of engineering problems that are governed by each class of equations will receive significant attention because the review helps the reader to understand the connection between the continuum problem and its discrete model.

1.6 Summary

Engineers develop conceptual and mathematical models of phenomena and systems that they wish to understand. The understanding may be used to develop and improve systems that contribute to the human convenience

and comfort. Mathematical models are developed using axioms and laws of nature that govern the phenomena. Mathematical models consist of algebraic, differential, and/or integral equations, and they are readily available for most problems in textbooks. Differential and integral equations are often difficult to solve exactly for the desired quantities of the system for a variety of input parameters (called data), necessitating the use of numerical methods.

In the numerical simulations of physical processes, we employ a numerical method and a computer to evaluate the mathematical model of the process. The finite element method is a powerful numerical method of solving algebraic, differential, and integral equations, and it is devised to study complex physical processes. The method is characterized by three basic features:

1. The domain of the problem is represented by a collection of simple subdomains, called *finite elements.* The collection of finite elements is called the *finite element mesh.*
2. Over each finite element, the physical process is approximated by functions of desired type (polynomials or otherwise), and algebraic equations relating physical quantities (duality pairs) at selective points, called nodes, of the element are developed. The set of algebraic equations is called a *finite element model.*
3. The element equations are assembled using continuity and "balance" of the physical quantities in the model.

In the finite element method one may seek an approximation u_h of u in the form

$$u(\mathbf{x}) \approx u_h(\mathbf{x}) = \sum_{j=1}^{n} u_j \psi_j(\mathbf{x}) + \sum_{j=1}^{m} c_j \phi_j(\mathbf{x})$$

where u_j are the values of u_h at the element nodes, ψ_j are the interpolation functions, c_j are coefficients that are *not* associated with nodes, and ϕ_j are the associated approximation functions. Direct substitution of such approximations into the governing differential equations does not always result, for an arbitrary choice of the data of the problem, in a necessary and sufficient number of equations for the undetermined coefficients u_j and c_j. Therefore, a procedure whereby a necessary and sufficient number of equations can be obtained is needed. One such procedure is provided by a

weighted-integral form of the governing equations. Chapter 2 is devoted to the study of weighted-integral formulations of differential equations and their solution by variational methods of approximation.

There is only one method of finite elements that is characterized by the three features stated above. Of course, there can be more than one finite element model of the same problem (i.e., governing equations). The type of model depends on the differential equations, methods used (i.e., the weighted-integral form used) to derive the algebraic equations for the undetermined coefficients over an element, and nature of the approximation functions used (but using the same three basic steps). Although the Ritz (or the weak-form Galerkin) method with polynomial approximations is used frequently to generate the finite element equations, any appropriate method and approximations can be used, in principle, to generate the algebraic equations. In this spirit, the collocation method, subdomain method, boundary integral methods, and so on can be used to generate the algebraic equations among discrete values of the primary and secondary variables. Each method results in a different finite element model of the same governing equations.

The basic theory of the finite element method can be found in more than three dozen textbooks. For the beginner, it is not necessary to consult any other books on the finite element method since the present book provides complete details of the method as applied to linear field problems, with examples drawn from fluid mechanics, heat transfer, solid and structural mechanics, and other field problems from engineering and applied sciences. For an introduction to nonlinear finite element analysis, the reader is referred to the author's book, *An Introduction to Nonlinear Finite Element Analysis* (2nd ed., Oxford University Press, 2015), which is a sequel to the present book, and it is prepared as a textbook with details that no other existing books can provide.

A summary of the basic equations of fluid mechanics, heat transfer, and solid mechanics is presented in Chapter 2. In studying these fields, we will come across a variety of physical quantities that describe the characteristics of the problem. Most of the quantities have dimensions and it is important to use units that are consistent throughout the study. For convenience of the readers, the dimensions of common physical quantities used herein are presented in Table 1.6.1. Each quantity is measured in terms of the primary quantities, such as length L, time T, mass M, and temperature Θ. Since Newton's law states that force is equal to the time rate of linear momentum (or mass times acceleration), it follows that $F = MLT^{-2}$ or $M = FL^{-1}\,T^{2}$. The equality between quantities in this discussion

is only to indicate the equivalence of the units and they are not mathematical formulas. For example, density $\rho = ML^{-3}$ means "the dimensions of a density are mass per unit of length cube." Inter-conversion of units between the metric (SI) and American (US) systems can be found in the Symbols and Conversion Factors section in the front of the book.

Table 1.6.1 Dimensions associated with common physical quantities.

Quantity	*FLT* System	*MLT* System	Quantity	*FLT* System	*MLT* System
Acceleration	LT^{-2}	LT^{-2}	Momentum	FT	MLT^{-1}
Angle	$F^0L^0T^0$	$M^0L^0T^0$	Power	FLT^{-1}	ML^2T^{-3}
Angular acceleration	T^{-2}	T^{-2}	Pressure	FL^{-2}	$ML^{-1}T^{-2}$
Angular velocity	T^{-1}	T^{-1}	Specific heat	$L^2T^{-2}\Theta^{-1}$	$L^2T^{-2}\Theta^{-1}$
Area	L^2	L^2	Specific wt.	FL^{-3}	$ML^{-2}T^{-2}$
Density	$FL^{-4}T^2$	ML^{-3}	Strain	$F^0L^0T^0$	$M^0L^0T^0$
Energy	FL	ML^2T^{-2}	Stress	FL^{-2}	$ML^{-1}T^{-2}$
Force	F	MLT^{-2}	Surface ten.	FL^{-1}	MT^{-2}
Frequency	T^{-1}	T^{-1}	Heat	FL	ML^2T^{-2}
Heat	FL	ML^2T^{-2}	Temperature	Θ	Θ
Length	L	L	Time	T	T
Mass	$FL^{-1}T^2$	M	Torque	FL	ML^2T^{-2}
Modulus of elasticity	FL^{-2}	$ML^{-1}T^{-2}$	Velocity	LT^{-1}	LT^{-1}
Moment of a force	FL	ML^2T^{-2}	Viscosity (dynamic)	$FL^{-2}T$	$ML^{-1}T^{-1}$
Moment of inertia (area)	L^4	L^4	Viscosity (kinematic)	L^2T^{-1}	L^2T^{-1}
Moment of inertia (mass)	FLT^2	ML^2	Volume	L^3	L^3
Momentum	FT	MLT^{-1}	Work	FL	ML^2T^{-2}

Problems

1.1 Newton's second law can be expressed as

$$\mathbf{F} = m\mathbf{a}$$

where **F** is the net force acting on the body, m is the mass of the body, and **a** is the acceleration of the body in the direction of the net force. Determine the mathematical model, that is, the governing equation of a free-falling body. Consider only the forces due to gravity and the air resistance. Assume that the air resistance is linearly proportional to the velocity of the falling body.

1.2 A cylindrical storage tank of diameter D contains a liquid at depth (or head) $h(x, t)$. Liquid is supplied to the tank at a rate of q_i (m^3/day) and drained at a rate of q_0 (m^3/day). Use the principle of conservation of mass to arrive at the governing equation of the flow problem.

1.3 Consider the simple pendulum of **Example 1.3.1**. Write a computer program to numerically solve the *linear* equation (1.2.4) using Euler's (or forward difference) finite difference scheme. Tabulate the numerical results for two different time steps $\Delta t = 0.05$ and $\Delta t = 0.025$ along with the exact linear solution.

1.4 Consider the simple pendulum of **Example 1.3.1**. Write a computer program to numerically solve the *nonlinear* equation (1.2.3) using Euler's (or forward difference) finite difference scheme. Tabulate the numerical results for two different time steps $\Delta t = 0.05$ and $\Delta t = 0.025$ along with the exact *linear* solution.

1.5 An improvement of Euler's method is provided by Heun's method, which uses the average of the derivatives at the two ends of the interval to estimate the slope. Applied to the equation

$$\frac{du}{dt} = f(t, u)$$

Heun's scheme has the form

$$u_{i+1} = u_i + \frac{\Delta t}{2}\left[f(t_i, u_i) + f(t_{i+1}, u^0_{i+1})\right], \quad u^0_{i+1} = u_i + \Delta t\, f(t_i, u_i)$$

The second equation is known as the *predictor* equation and the first equation is called the *corrector* equation. Apply Heun's method to Eq. (1.3.5) and obtain the numerical solution for $\Delta t = 0.05$.

1.6 Show that the backward difference approximation of the boundary condition in Eq. (1.2.20) yields

$$\theta_{N+1} = \left(1 + \frac{\beta \Delta x}{k}\right)^{-1} \theta_N$$

and that it is the same as that in Eq. (1.3.9) when $\frac{\beta \Delta x}{k} < 1$.

1.7 Write a computer program to solve the rod problem of **Example 1.3.2** using 8 intervals (i.e., $\Delta x = 0.00625$) and determine the solution at mesh points $x = 0.00625, 0.0125, 0.01875, \ldots, 0.05$ m.

1.8 Repeat **Problem 1.7** for 16 subdivisions and compare the finite difference solution with the analytical solution. *Ans:* The finite difference solutions are

$$\{\theta\} = \{285.36, 271.84, 259.37, 247.92, 237.44, 227.89, 219.22, 211.42, \ldots, 176.78\}^{\mathrm{T}}$$

The analytical solution at the same points is

$$\{\theta\} = \{285.56, 272.25, 259.99, 248.75, 238.48, 229.15, 220.71, 213.13, \ldots, 180.66\}^{\mathrm{T}}$$

References for Additional Reading

1. National Research Council, *Research Directions in Computational Mechanics*, National Academies Press, Washington, DC, 1991.
2. J. N. Reddy, *An Introduction to Continuum Mechanics with Applications*, 2nd ed., Cambridge University Press, New York, NY, 2013.
3. J. N. Reddy, *The Principles of Continuum Mechanics*, 2nd ed., Cambridge University Press, New York, NY, 2018.
4. J. N. Reddy, *Energy Principles and Variational Methods in Applied Mechanics*, 3rd ed., John Wiley & Sons, New York, NY, 2017.
5. J. N. Reddy, "The finite element method: A child of the computer age," *Sooner Shamrock* (Engineering Student Magazine at the University of Oklahoma), 23–26, Fall 1978.
6. J. N. Reddy, *An Introduction to the Finite Element Method*, 2nd ed., McGraw–Hill, New York, NY, 1993 (see Chapter 1).
7. A. Hrenikoff, "Solution of problems in elasticity by the framework method," *Journal of Applied Mechanics, Transactions of the ASME*, **8**, 169–175, 1941.
8. R. Courant, "Variational methods for the solution of problems of equilibrium and vibrations," *Bulletin of the American Mathematical*

Society, **49**, 1–23, 1943.

9. J. H. Argyris and S. Kelsey, *Energy Theorems and Structural Analysis*, Butterworth, London, UK, 1960 (first appeared in *Aircraft Engineering*), **26**, 1954 and **27**, 1955.
10. M. J. Turner, R. W. Clough, H. C. Martin, and L. J. Topp, "Stiffness and deflection analysis of complex structures," *Journal of Aeronautical Science*, **23**, 805–823, 1956.
11. R. W. Clough, "The finite element method in plane stress analysis," *Journal of Structures Division, ASCE, Proceedings of 2nd Conference on Electronic Computation*, 345–378, 1960.
12. I. Babuska, "Courant element: Before and after," *Finite Element Methods: Fifty Years of the Courant Element*, M. Krizek and P. Neittaanmäki (eds.), Marcel Dekker, New York, NY, 1994.
13. O. C. Zienkiewicz and Y. K. Cheung, *The Finite Element Method in Structural and Continuum Mechanics*, McGraw–Hill, London, UK, 1967.
14. J. T. Oden, *Finite Elements of Nonlinear Continua*, McGraw–Hill, New York, NY, 1972.
15. G. Strang and G. Fix, *An Analysis of the Finite Element Method*, Prentice Hall, Englewood Cliffs, NJ, 1973.
16. J. T. Oden and J. N. Reddy, *An Introduction to the Mathematical Theory of Finite Elements*, John Wiley & Sons, New York, NY, 1976.
17. J. M. Melenk and I. Babuska, "The partition of unity finite element method: Basic theory and applications," *Computer Methods in Applied Mechanics and Engineering*, **139**, 289–314, 1996.
18. C. A. Duarte and J. T. Oden, "An *h-p* adaptive method using clouds," *Computer Methods in Applied Mechanics and Engineering*, **139**, 237–262, 1996.
19. T. Belytschko, Y. Krongauz, D. Organ, M. Fleming, and P. Krysl, "Meshless methods: An overview and recent developments," *Computer Methods in Applied Mechanics and Engineering*, **139**, 3–47, 1996.
20. I. Babuska and T. Strouboulis, *The Finite Element Method and its Reliability*, Oxford University

2 Mathematical Preliminaries and Classical Variational Methods

The fact that an opinion has been widely held is no evidence whatever that it is not utterly absurd; indeed in view of the silliness of the majority of mankind, a widespread belief is more likely to be foolish than sensible.

— Bertrand Russell

2.1 General Introduction

2.1.1 Variational Principles and Methods

This chapter is devoted to a review of mathematical preliminaries that prove to be useful in the sequel and a study of integral formulations and more commonly used variational methods such as the Ritz, Galerkin, collocation, subdomain, and least-squares methods. Since the finite element method can be viewed as an element-wise application of a variational method, it is useful to learn how variational methods work. We begin with a discussion of the general meaning of the phrases "variational methods" and "variational formulations" used in the literature.

The phrase "direct variational methods" refers to methods that make use of variational principles, such as the principles of virtual work and the principle of minimum total potential energy in solid and structural mechanics, to determine approximate solutions of problems (see Oden and Reddy [1] and Reddy [2]). In the classical sense, a *variational principle* has to do with finding the extremum (i.e., minimum or maximum) or stationary values of a functional with respect to the variables of the problem. The functional includes all the intrinsic features of the problem, such as the governing equations, boundary and/or initial conditions, and constraint conditions, if any. In solid and structural mechanics problems, the functional represents the total energy of the system, and in other problems it is simply an integral representation of the governing equations.

Variational principles have always played an important role in mechanics. First, many problems of mechanics are posed in terms of

finding the extremum (i.e., minima or maxima) and thus, by their nature, can be formulated in terms of variational statements. Second, there are problems that can be formulated by other means, such as the conservation laws, but these can also be formulated by means of variational principles. Third, variational formulations form a powerful basis for obtaining approximate solutions to practical problems, many of which are intractable otherwise. The principle of minimum total potential energy, for example, can be regarded as a substitute to the equations of equilibrium of an elastic body, as well as a basis for the development of displacement finite element models that can be used to determine approximate displacement and stress fields in the body. Variational formulations can also serve to unify diverse fields, suggest new theories, and provide a powerful means to study the existence and uniqueness of solutions to problems. Similarly, Hamilton's principle can be used in lieu of the equations governing dynamical systems, and the variational forms presented by Biot replace certain equations in linear continuum thermodynamics.

2.1.2 Variational Formulations

The classical use of the phrase "variational formulations" refers to the construction of a functional (whose meaning will be made clear shortly) or a variational principle that is equivalent to the governing equations of the problem. The modern use of the phrase refers to the formulation in which the governing equations are translated into equivalent weighted-integral statements that are not necessarily equivalent to a variational principle. Even those problems that do not admit variational principles in the classical sense (e.g., the Navier–Stokes equations governing the flow of viscous or inviscid fluids) can now be formulated using weighted-integral statements.

The importance of variational formulations of physical laws, in the modern or general sense of the phrase, goes far beyond its use as simply an alternative to other formulations (see Oden and Reddy [1]). In fact, variational forms of the laws of continuum physics may be the only natural and rigorously correct way to think of them. While all sufficiently smooth fields lead to meaningful variational forms, the converse is not true: there exist physical phenomena which can be adequately modelled mathematically only in a variational setting; they are nonsensical when viewed locally.

The starting point for the discussion of the finite element method is differential equations governing the physical phenomena under study. As

such, we shall first discuss why integral statements of the differential equations are needed.

2.1.3 Need for Weighted-Integral Statements

In almost all approximate methods used to determine the solution of differential and/or integral equations, we seek the solution in the form

$$u(\mathbf{x}) \approx u_N(\mathbf{x}) = \sum_{j=1}^{N} c_j \phi_j(\mathbf{x}) \tag{2.1.1}$$

where u represents the solution of a particular differential equation and associated boundary conditions, and u_N is its approximation that is represented as a linear combination of unknown parameters c_j and known functions ϕ_j of position $\mathbf{x}$ in the domain Ω on which the problem is posed. We shall shortly discuss the conditions on ϕ_j. The approximate solution u_N is completely known only when c_j are known. Thus, we must find a means to determine c_j such that u_N satisfies the equations governing u. If somehow we can find u_N that satisfies the differential equation at every point $\mathbf{x}$ of the domain Ω and conditions on the boundary Γ of Ω, then $u_N(\mathbf{x}) = u(\mathbf{x})$, which is the exact solution of the problem. Of course, approximate methods are not about problems for which exact solutions can be determined by some methods of mathematical analysis; their role is to find an approximate solution of problems that do not admit analytical solutions. When the exact solution cannot be determined, the alternative is to find a solution u_N that satisfies the governing equations in an approximate sense. In the process of satisfying the governing equations approximately, we obtain (not accidentally but by planning) N algebraic relations among the N parameters $c_1, c_2, \ldots, c_N$. A detailed discussion of these ideas is given in the next few paragraphs in connection with a specific problem.

Consider the problem of solving the differential equation

$$-\frac{d}{dx}\left[a(x)\frac{du}{dx}\right] + c(x)u = f(x) \quad \text{for } 0 < x < L \tag{2.1.2}$$

subjected to the boundary conditions

$$u(0) = u_0, \quad \left[a(x)\frac{du}{dx}\right]_{x=L} = Q_L \tag{2.1.3}$$

where $a(x)$, $c(x)$ and $f(x)$ are known functions and $u0$ and Q_L are known parameters, and $u(x)$ is the function to be determined. The set $a(x)$, $c(x)$, $f(x)$, u_0 and Q_L is called the problem *data*. An example of the above problem is given by the heat transfer in an uninsulated rod (see Example 1.2.2 for additional details): $u = \theta$ denotes the temperature, $f(x) = Ag$ is the internal heat generation per unit length, $a(x) = kA$ is the thermal resistance, $c = \beta P$, $u_0 = \theta_0$ is the specified temperature at $x = 0$ and Q_L is the specified heat at $x = L$.

We seek an approximate solution over the entire domain $\Omega = (0, L)$ in the form

$$u_N \equiv \sum_{j=1}^{N} c_j \phi_j(x) + \phi_0(x) \tag{2.1.4}$$

where the c_j are coefficients to be determined, and $\phi_j(x)$ and $\phi_0(x)$ are functions chosen such that the specified boundary conditions of the problem are satisfied by the N-parameter approximate solution u_N. Note that the particular form in Eq. (2.1.4) has two parts: one containing the unknowns ($\sum c_j \phi_j$) and is termed the homogeneous part, and the other is the nonhomogeneous part (ϕ_0) that has the sole purpose of satisfying the specified boundary conditions of the problem. Since ϕ_0 satisfies the boundary conditions, the sum $\sum c_j \phi_j$ must satisfy, for arbitrary c_j, the homogeneous form of the boundary conditions (e.g., $u = u_0$ is said to be a nonhomogeneous boundary condition when $u_0 \neq 0$, and it is termed homogeneous boundary condition when $u_0 = 0$). Thus, in the present case, both of the specified boundary conditions are nonhomogeneous. The particular form in Eq. (2.1.4) is convenient in selecting ϕ_0 and ϕ_j. Thus, ϕ_0 and ϕ_j in the present case satisfy the conditions

$$\begin{aligned} &\phi_0(0) = u_0, \quad \left[a(x)\frac{d\phi_0}{dx}\right]_{x=L} = Q_L \\ &\phi_i(0) = 0, \quad \left[a(x)\frac{d\phi_i}{dx}\right]_{x=L} = 0, \quad i = 1, 2, \ldots, N \end{aligned} \tag{2.1.5}$$

As a specific example, first we consider the case in which $L = 1$, $u_0 = 0$, $Q_L = -15$, $a(x) = x$, $c(x) = 1$, $f(x) = x^3 - 72x + 36$, and $N = 2$. Then Eqs. (2.1.2) and (2.1.3) reduce to

$$-\frac{d}{dx}\left(x\frac{du}{dx}\right) + u = x^3 - 72x + 36, \quad 0 < x < 1$$
$$u(0) = 0, \quad \left[x\frac{du}{dx}\right]_{x=1} = -15 \tag{2.1.6}$$

We choose the two-parameter approximate solution in the form [lowest-order polynomials that satisfy the conditions in Eq. (2.1.5) with $u_0 = 0$ and $Q_L = -15$]

$$u_2 = c_1\phi_1(x) + c_2\phi_2(x) + \phi_0(x) \text{ with } \phi_0 = -15x, \ \phi_1(x) = x^2 - 2x, \ \phi_2 = (x^3 - 3x)$$

Substituting u_2 into the differential equation in Eq. (2.1.6), we obtain

$$-\frac{du_2}{dx} - x\frac{d^2u_2}{dx^2} + u_2 - f(x) = 0$$
$$c_2x^3 + c_1x^2 - 9c_2x^2 - x^3 - 6c_1x - 3c_2x + 2c_1 + 3c_2 + 57x - 21 = 0$$

Since this expression must hold for any value of x, the coefficients of the various powers of x must be zero, giving the following relations among c_1 and c_2:

$$c_2 - 1 = 0, \quad c_1 - 9c_2 = 0, \quad 6c_1 + 3c_2 = 57, \quad 2c_1 + 3c_2 = 21$$

From the first two relations, we obtain $c_1 = 9$ and $c_2 = 1$. The remaining two equations are consistent with the calculated values of c_1 and c_2 (i.e., all four equations are consistent). Hence the two-parameter solution (which coincides with the exact solution) is

$$u_2 = c_1\phi_1(x) + c_2\phi_2(x) + \phi_0(x) = x^3 + 9x^2 - 36x \tag{2.1.7}$$

Next consider the case in which $L = 1$, $u_0 = 0$, $Q_L = 1$, $a(x) = 1$, $c(x) = -1$, $f(x) = -x^2$, and $N = 2$. Then Eqs. (2.1.2) and (2.1.3) reduce to

$$-\frac{d^2u}{dx^2} - u = -x^2, \quad 0 < x < 1$$
$$u(0) = 0, \quad \left[\frac{du}{dx}\right]_{x=1} = 1 \tag{2.1.8}$$

We choose the approximate solution in the form

$$u_2 = c_1\phi_1 + c_2\phi_2 + \phi_0 \text{ with } \phi_0 = x,\ \phi_1(x) = x^2 - 2x,\ \phi_2 = (x^3 - 3x)$$

which satisfies the boundary conditions in Eq. (2.1.8) of the problem for any values of c_1 and c_2. Substituting u_2 into the differential equation in Eq. (2.1.8), we obtain

$$\begin{aligned} 0 &= -\frac{d^2u_2}{dx^2} - u_2(x) - f(x) \\ &= -c_2x^3 - c_1x^2 + 2c_1x - 3c_2x + x^2 - 2c_1 - x \end{aligned}$$

Since this expression must be zero for any value of x, the coefficients of the various powers of x must be zero, giving the following relations among c_1 and c_2 :

$$c_2 = 0, \quad -c_1 + 1 = 0, \quad 2c_1 - 3c_2 - 1 = 0, \quad c_1 = 0 \tag{2.1.9}$$

The above relations are inconsistent; hence, there is *no solution* to the equations.

The previous discussion indicates that the ability to obtain the solution to a differential equation as a linear combination of functions and undetermined parameters does not guarantee that one always obtains a solution; the ability to obtain a solution depends on the equation and its boundary conditions. However, instead of requiring the differential equation be satisfied pointwise, if we require it to be satisfied in a weighted-residual sense,

$$\int_0^L w_i(x)R(x, u_N)\,dx = 0, \quad i = 1, 2, \ldots, N \tag{2.1.10}$$

we obtain N algebraic relations to determine the N parameters, c_i (i = 1, 2, …, N). Here R denotes the *residual*,

$$R(x, u_N) \equiv -\frac{d}{dx}\left(a(x)\frac{du_N}{dx}\right) + c(x)u_N - f(x)$$

and w_i (i = 1, 2, …, N) is a set of linearly independent functions, called *weight functions*. To illustrate the idea, we consider the same two examples as discussed previously.

For the problem described by Eq. (2.1.6), the residual is given by

$$R(x, c_1, c_2) = c_2x^3 + c_1x^2 - 9c_2x^2 - x^3 - 6c_1x - 3c_2x + 2c_1 + 3c_2 + 57x - 21$$

For N = 2, we take w_1 = 1 and w_2 = x and obtain

$$\begin{aligned} 0 &= \int_0^1 1 \cdot R\,dx = -\frac{2}{3}c_1 - \frac{5}{4}c_2 + \frac{29}{4} \\ 0 &= \int_0^1 x \cdot R\,dx = -\frac{3}{4}c_1 - \frac{31}{20}c_2 + \frac{83}{10} \end{aligned} \tag{2.1.11}$$

or

$$\frac{2}{3}c_1 + \frac{5}{4}c_2 = \frac{29}{4}, \quad \frac{3}{4}c_1 + \frac{31}{20}c_2 = \frac{83}{10} \tag{2.1.12}$$

These two linearly independent equations can be solved for c_1 = 9 and c_2 = 1, giving the exact solution in Eq. (2.1.7).

For the problem described by Eq. (2.1.8), the residual is given by

$$R(x, c_1, c_2) = -c_2x^3 - c_1x^2 + 2c_1x - 3c_2x + x^2 - 2c_1 - x$$

For N = 2, we take w_1 = 1 and w_2 = x and obtain

$$\begin{aligned} 0 &= \int_0^1 1 \cdot R\,dx = -\frac{4}{3}c_1 - \frac{7}{4}c_2 + \frac{1}{6} \\ 0 &= \int_0^1 x \cdot R\,dx = -\frac{7}{12}c_1 - \frac{6}{5}c_2 + \frac{1}{12} \end{aligned} \tag{2.1.13}$$

or

$$\frac{4}{3}c_1 + \frac{7}{4}c_2 = \frac{1}{6}, \quad \frac{7}{12}c_1 + \frac{6}{5}c_2 = \frac{1}{12} \tag{2.1.14}$$

These two linearly independent equations can be solved for c_1 = 39/417 and c_2 = 10/417, and the approximate solution becomes

$$u_2(x) = \frac{39}{417}(x^2 - 2x) + \frac{10}{417}(x^3 - 3x) + x = \frac{1}{417}(10x^3 + 39x^2 - 525x) \qquad (2.1.15)$$

Although the solution $u_2(x)$ does not coincide with the exact solution, it is a good approximation (as will be discussed in the sequel).

The above discussion clearly demonstrates the need for weighted-integral statements of the type in Eq. (2.1.10); they provide means for obtaining as many algebraic equations as there are unknown coefficients in the approximate solution. This chapter deals with the construction of different types of integral statements used in different variational methods. The variational methods differ from each other in the choice of the weight functions w_i and/or the integral statement used, which in turn dictates the choice of the approximation functions ϕ_j. In the finite element method, a given domain is viewed as an assemblage of subdomains (i.e., finite elements), and an approximate solution is sought over each subdomain in the same way as in variational methods. Therefore, it is informative to review useful mathematical tools and study integral formulations and methods before we discuss the finite element method and its applications.

2.2 Some Mathematical Concepts and Formulae

2.2.1 Coordinate Systems and the Del Operator

In the analytical description of physical phenomena, a coordinate system in the chosen frame of reference is introduced, and various physical quantities involved in the description are expressed in terms of measurements made in that system. Vector and tensor quantities are expressed in terms of their components in that coordinate system. For example, a vector **A** in a three-dimensional space may be expressed in terms of its components (a_1, a_2, a_3) and *basis vectors* ($\mathbf{e}_1$, $\mathbf{e}_2$, $\mathbf{e}_3$) ($\mathbf{e}_i$ are not necessarily unit vectors) as

$$\mathbf{A} = a_1\mathbf{e}_1 + a_2\mathbf{e}_2 + a_3\mathbf{e}_3 \qquad (2.2.1)$$

2.2.1.1 Cartesian rectangular coordinates

When the basis vectors of a coordinate system are constants, i.e., with fixed lengths and directions, the coordinate system is called a *Cartesian coordinate system*. The general Cartesian system is oblique. When the Cartesian system is orthogonal, it is called *rectangular Cartesian*. The

rectangular Cartesian coordinates are denoted by

$$(x_1, x_2, x_3) \text{ or } (x, y, z) \tag{2.2.2}$$

The familiar rectangular Cartesian coordinate system is shown in Fig. 2.2.1. We shall always use a right-hand coordinate system. When the basis vectors are of unit lengths and mutually orthogonal, they are called *orthonormal*. In many situations an *orthonormal basis* simplifies calculations. We denote an orthonormal Cartesian basis by

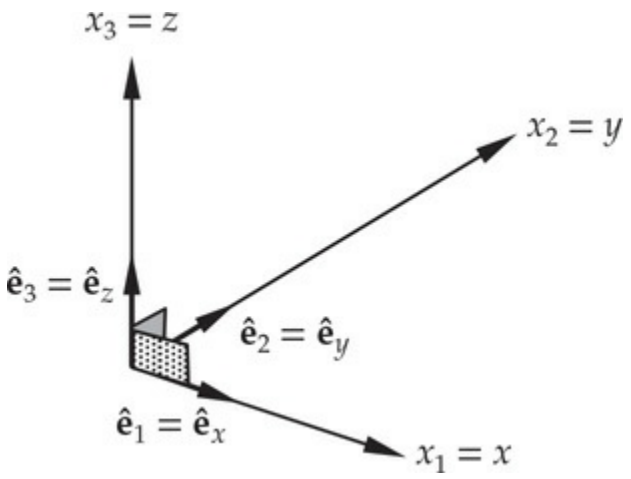

Fig. 2.2.1 A rectangular Cartesian coordinate system, $(x_1, x_2, x_3) = (x, y, z)$; $(\hat{\mathbf{e}}_1, \hat{\mathbf{e}}_2, \hat{\mathbf{e}}_3) = (\hat{\mathbf{e}}_x, \hat{\mathbf{e}}_y, \hat{\mathbf{e}}_z)$ are the unit basis vectors.

$$(\hat{\mathbf{e}}_1, \hat{\mathbf{e}}_2, \hat{\mathbf{e}}_3) \text{ or } (\hat{\mathbf{e}}_x, \hat{\mathbf{e}}_y, \hat{\mathbf{e}}_z) \tag{2.2.3}$$

For an orthonormal basis the vector **A** can be written as

$$\mathbf{A} = A_1\hat{\mathbf{e}}_1 + A_2\hat{\mathbf{e}}_2 + A_3\hat{\mathbf{e}}_3$$

where $\hat{\mathbf{e}}_i$ (i = 1, 2, 3) is the orthonormal basis, and A_i are the corresponding *physical components* (i.e., the components have the same physical dimensions as the vector). Although the analytical description depends upon the chosen coordinate system and may appear different in another type of coordinate system, one must keep in mind that *the laws of nature are independent of the choice of a coordinate system.*

2.2.1.2 Summation convention

It is useful to abbreviate a summation of terms by understanding that a repeated index means summation over all values of that index. Thus the summation

$$\mathbf{A} = \sum_{i=1}^{3} A_i \mathbf{e}_i$$

can be shortened to

$$\mathbf{A} = A_i \mathbf{e}_i \tag{2.2.4}$$

The repeated index is a *dummy index* and thus can be replaced by *any other symbol that has not already been used.* Thus we can also write

$$\mathbf{A} = A_i \mathbf{e}_i = A_m \mathbf{e}_m$$

and so on.

The "dot product" $\hat{\mathbf{e}}_i \cdot \hat{\mathbf{e}}_j$ and "cross product" $\hat{\mathbf{e}}_i \times \hat{\mathbf{e}}_j$ of base vectors in a righthanded system are defined by

$$\hat{\mathbf{e}}_i \cdot \hat{\mathbf{e}}_j \equiv \delta_{ij} = \begin{cases} 0, & \text{if } i \neq j \\ 1, & \text{if } i = j \end{cases} \tag{2.2.5}$$

$$\hat{\mathbf{e}}_i \times \hat{\mathbf{e}}_j \equiv \varepsilon_{ijk} \hat{\mathbf{e}}_k \tag{2.2.6}$$

where δ_{ij} is the *Kronecker delta* and ε_{ijk} is the *alternating symbol* or *permutation symbol*

$$\varepsilon_{ijk} = \begin{cases} 1, & \text{if } i,j,k \text{ are in cyclic order} \\ & \text{and not repeated } (i \neq j \neq k), \\ -1, & \text{if } i,j,k \text{ are not in cyclic order} \\ & \text{and not repeated } (i \neq j \neq k), \\ 0, & \text{if any of } i,j,k \text{ are repeated.} \end{cases} \tag{2.2.7}$$

Note that in Eq. (2.2.6), k is a dummy index, while i and j are not. The latter are called *free indices*. A free index can be changed to some other index only when it is changed in every expression of the equation to the same index. Thus, we can write Eq. (2.2.6) as

$$\hat{\mathbf{e}}_m \times \hat{\mathbf{e}}_j = \varepsilon_{mjk} \hat{\mathbf{e}}_k; \quad \hat{\mathbf{e}}_m \times \hat{\mathbf{e}}_n = \varepsilon_{mnk} \hat{\mathbf{e}}_k; \quad \hat{\mathbf{e}}_p \times \hat{\mathbf{e}}_q = \varepsilon_{pqk} \hat{\mathbf{e}}_k$$

2.2.1.3 The del operator

Differentiation of vector functions with respect to the coordinates is common
in science and engineering. Most of the operations involve the "del

operator", denoted by ∇. In a rectangular Cartesian system it has the form

$$\nabla \equiv \hat{\mathbf{e}}_x \frac{\partial}{\partial x} + \hat{\mathbf{e}}_y \frac{\partial}{\partial y} + \hat{\mathbf{e}}_z \frac{\partial}{\partial z} \tag{2.2.8}$$

It is important to note that the del operator has some of the properties of a vector but it does not have them all, because it is an operator. The operation $\nabla\phi(\mathbf{x})$ is called the *gradient* of a scalar function ϕ whereas $\nabla \times \mathbf{A}(\mathbf{x})$ is called the *curl* of a vector function $\mathbf{A}$. The operator $\nabla^2 \equiv \nabla \cdot \nabla$ is called the Laplace operator. In a 3-D rectangular Cartesian coordinate system it has the form

$$\nabla^2 = \frac{\partial^2}{\partial x^2} + \frac{\partial^2}{\partial y^2} + \frac{\partial^2}{\partial z^2} \tag{2.2.9}$$

We have the following relations between the rectangular Cartesian coordinates (x, y, z) and cylindrical coordinates (r, θ, z) (see Fig. 2.2.2):

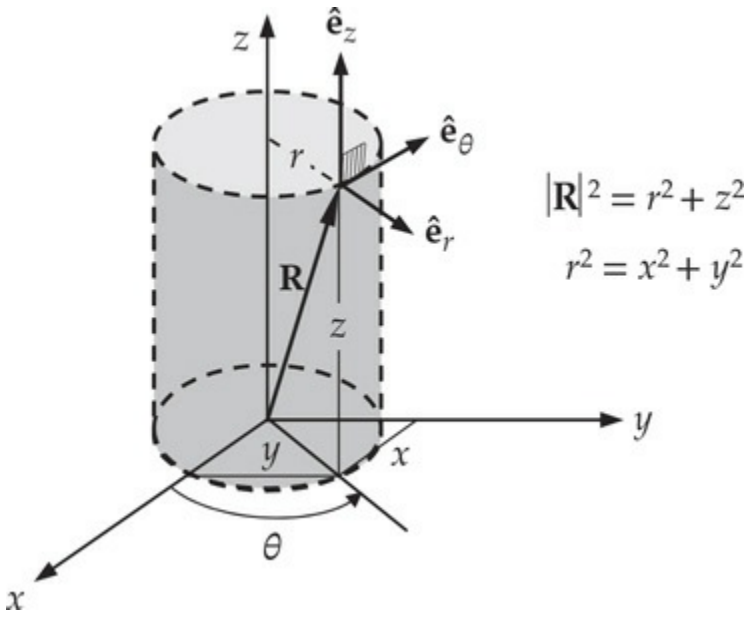

Fig. 2.2.2 Cylindrical coordinate system.

$$x = r\cos\theta, \quad y = r\sin\theta, \quad z = z \tag{2.2.10}$$

The base vectors in the two coordinate systems are related by

$$\hat{\mathbf{e}}_r = \cos\theta\,\hat{\mathbf{e}}_x + \sin\theta\,\hat{\mathbf{e}}_y, \quad \hat{\mathbf{e}}_\theta = -\sin\theta\,\hat{\mathbf{e}}_x + \cos\theta\,\hat{\mathbf{e}}_y, \quad \hat{\mathbf{e}}_z = \hat{\mathbf{e}}_z \tag{2.2.11}$$

Note that the base vectors of the cylindrical coordinate system are not constant; the direction of $\theta$and r-coordinates change as we move around

the cylindrical surface. Thus, we have

$$\frac{\partial \hat{\mathbf{e}}_r}{\partial \theta} = -\sin\theta\, \hat{\mathbf{e}}_x + \cos\theta\, \hat{\mathbf{e}}_y = \hat{\mathbf{e}}_\theta, \quad \frac{\partial \hat{\mathbf{e}}_\theta}{\partial \theta} = -\cos\theta\, \hat{\mathbf{e}}_x - \sin\theta \hat{\mathbf{e}}_y = -\hat{\mathbf{e}}_r \tag{2.2.12}$$

and all other derivatives of the base vectors are zero. The operators ∇ and ∇^2 in the cylindrical coordinate system are given by (see Reddy [2, 3])

$$\boldsymbol{\nabla} = \hat{\mathbf{e}}_r \frac{\partial}{\partial r} + \frac{1}{r}\hat{\mathbf{e}}_\theta \frac{\partial}{\partial \theta} + \hat{\mathbf{e}}_z \frac{\partial}{\partial z}, \quad \nabla^2 = \frac{1}{r}\left[\frac{\partial}{\partial r}\left(r\frac{\partial}{\partial r}\right) + \frac{1}{r}\frac{\partial^2}{\partial \theta^2} + r\frac{\partial^2}{\partial z^2}\right] \tag{2.2.13}$$

2.2.2 Boundary Value, Initial Value, and Eigenvalue Problems

The objective of most analysis is to determine unknown functions, called *dependent variables*, that are governed by a set of differential equations posed in a given domain Ω and some conditions on the boundary Γ of the domain Ω. Often, a domain not including its boundary is called an *open* domain. A domain Ω with its boundary Γ is called a *closed* domain and is denoted by $\bar{\Omega} = \Omega \cup \Gamma$.

A function u of several independent variables (or coordinates) (x, y, $\cdots$) is said to be of class $C^m(\Omega)$ in a domain Ω if all its partial derivatives with respect to (x, y, $\cdots$) of order up to and including m exist and are *continuous* in Ω. Thus, if u is of class C^0 in a two-dimensional domain Ω then u is continuous in Ω (i.e., $\partial u/\partial x$ and $\partial u/\partial y$ exist but may not be continuous). Similarly, if u is of class c_1, then u, $\partial u/\partial x$ and $\partial u/\partial y$ exist and are continuous (i.e., $\partial^2 u/\partial x^2$, $\partial^2 u/\partial y^2$, and $\partial^2 u/\partial y \partial x$ exist but may not be continuous).

When the dependent variables are functions of one independent variable (say, x), the domain is a line segment (i.e., one-dimensional) and the end points of the domain are called boundary points. When the dependent variables are functions of two independent variables (say, x and y), the domain is two-dimensional and the boundary is the closed curve enclosing it. In a threedimensional domain, dependent variables are functions of three independent variables (say x, y, and z) and the boundary is a two-dimensional surface.

As discussed in Section 1.2, a differential equation is said to describe a *boundary value problem* over the domain Ω if the dependent variable and possibly its derivatives are required to take specified values on the boundary Γ of Ω. An *initial value problem* is one in which the dependent variable and possibly its derivatives are specified initially (i.e., at time t =

0). Initial value problems are generally time-dependent problems. Examples of boundary and initial value problems were discussed in Section 1.2. A problem can be both a boundaryvalue and initial-value problem if the dependent variable is subject to both boundary and initial conditions. Another type of problem we encounter is one in which a differential equation governing the dependent unknown also contains an unknown parameter, and we are required to find both the dependent variable and the parameter such that the differential equation and associated boundary conditions are satisfied. Such problems are called *eigenvalue problems*. Examples of various types of problems we encounter in science and engineering are given below. The physics behind these equations will be explained later when these equations are actually analyzed.

2.2.2.1 Boundary value problems

Steady-state heat transfer in a fin and *axial deformation of a bar*: Find $u(x)$ that satisfies the second-order differential equation and *boundary conditions*:

$$-\frac{d}{dx}\left(a\frac{du}{dx}\right)+cu=f \quad \text{for} \quad 0<x<L$$
$$u(0)=u_0, \quad \left(a\frac{du}{dx}\right)_{x=L}=q_0 \tag{2.2.14}$$

The domain and boundary points are identified in Fig. 2.2.3.

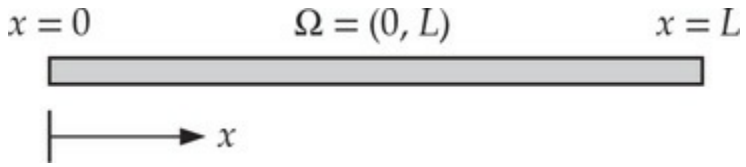

Fig. 2.2.3 A one-dimensional domain Ω = (0, *L*) and boundary points *x* = 0 and *x* = *L*.

Bending of elastic beams under transverse load: Find $w(x)$ that satisfies the fourthorder differential equation and *boundary conditions*:

$$\frac{d^2}{dx^2}\left(EI\frac{d^2w}{dx^2}\right)+cw=f \quad \text{for} \quad 0<x<L$$

$$w(0)=w_0, \quad \left(-\frac{dw}{dx}\right)_{x=0}=\theta_0 \tag{2.2.15}$$

$$\left[\frac{d}{dx}\left(EI\frac{d^2w}{dx^2}\right)\right]_{x=L}=V_0, \quad \left(EI\frac{d^2w}{dx^2}\right)_{x=L}=M_0$$

The domain and boundary points for this case are the same as shown in Fig. 2.2.3. However, the physics behind the equations is different, as we shall see shortly.

Steady heat conduction in a two-dimensional region and *transverse deflections of a membrane*: Find $u(x, y)$ that satisfies the second-order partial differential equation and *boundary conditions*:

$$-\left[\frac{\partial}{\partial x}\left(a_{xx}\frac{\partial u}{\partial x}\right)+\frac{\partial}{\partial y}\left(a_{yy}\frac{\partial u}{\partial y}\right)\right]+a_{00}u=f \quad \text{in } \Omega \tag{2.2.16}$$

$$u=u_0 \text{ on } \Gamma_u, \quad \left(a_{xx}\frac{\partial u}{\partial x}n_x+a_{yy}\frac{\partial u}{\partial y}n_y\right)=q_0 \text{ on } \Gamma_q \tag{2.2.17}$$

where (n_x, n_y) are the direction cosines on the unit normal vector $\hat{\mathbf{n}}$ to the boundary Γ_q. The domain Ω and two parts of the boundary Γ_u and Γ_q are shown in Fig. 2.2.4.

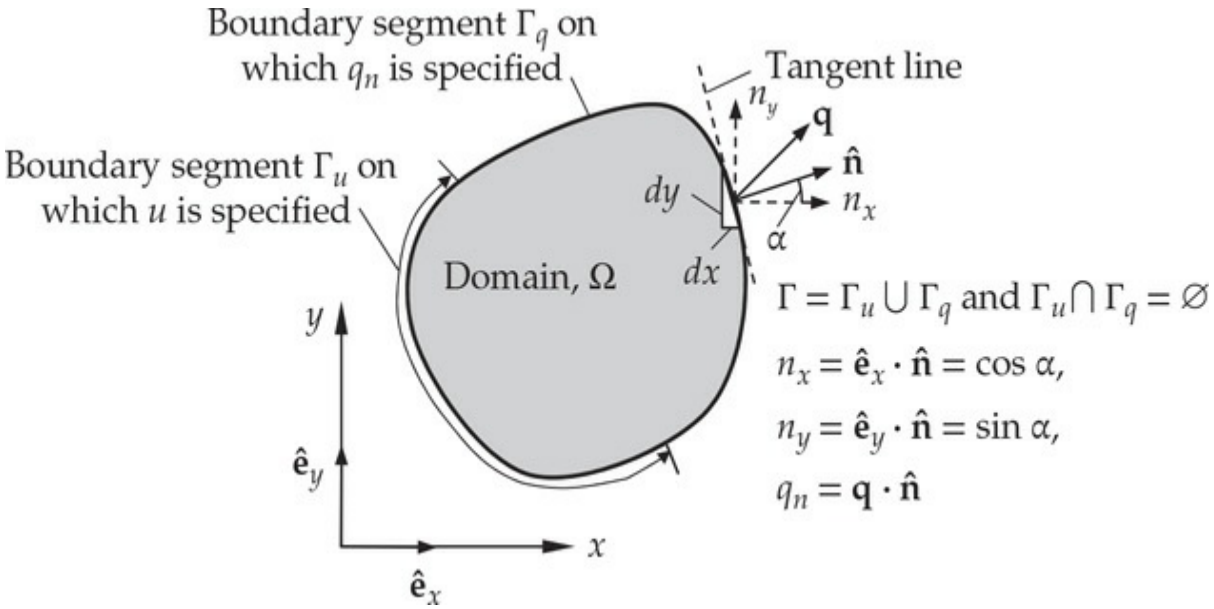

Fig. 2.2.4 Two-dimensional domain Ω with boundary Γ = Γ_u ∪ Γq and Γ_u

$\cap\, \Gamma q = \varnothing$.

2.2.2.2 Initial value problems

A general first-order equation: Find $u(t)$ that satisfies the first-order differential equation and *initial conditions*:

$$a\frac{du}{dt} + cu = f \quad \text{for} \quad 0 < t \le T \tag{2.2.18}$$

$$u(0) = u_0 \tag{2.2.19}$$

A general second-order equation: Find $u(t)$ that satisfies the second-order differential equation and *initial conditions*:

$$a\frac{du}{dt} + b\frac{d^2u}{dt^2} + cu = f \quad \text{for} \quad 0 < t \le T \tag{2.2.20}$$

$$u(0) = u_0, \quad \left(b\frac{du}{dt}\right)_{t=0} = v_0 \tag{2.2.21}$$

2.2.2.3 Boundary and initial value problems

Unsteady heat transfer in a rod: Find $u(x, t)$ that satisfies the partial differential equation and *initial* and *boundary conditions*:

$$\begin{gathered} -\frac{\partial}{\partial x}\left(a\frac{\partial u}{\partial x}\right) + cu + \rho\frac{\partial u}{\partial t} = f(x,t) \quad \text{for} \quad 0 < x < L,\ 0 < t \le T \\ u(0,t) = d_0(t), \quad \left(a\frac{\partial u}{\partial x}\right)_{x=L} = q_0(t), \quad u(x,0) = u_0(x) \end{gathered} \tag{2.2.22}$$

Unsteady motion of a membrane: Find $u(x, y, t)$ that satisfies the partial differential equation and *initial* and *boundary conditions*:

$$\begin{gathered} -\left[\frac{\partial}{\partial x}\left(a_{xx}\frac{\partial u}{\partial x}\right) + \frac{\partial}{\partial y}\left(a_{yy}\frac{\partial u}{\partial y}\right)\right] + a_{00}u + \rho\frac{\partial^2 u}{\partial t^2} = f(x,y,t) \quad \text{in } \Omega,\ 0 < t \le T \\ u = u_0(t) \text{ on } \Gamma_u, \quad \left(a_{xx}\frac{\partial u}{\partial x}n_x + a_{yy}\frac{\partial u}{\partial y}n_y\right) = q_0(t) \text{ on } \Gamma_q \\ u(x,y,0) = d_0, \quad \dot{u}(x,y,0) = v_0 \end{gathered} \tag{2.2.23}$$

where superposed dot indicates derivative with respect to time t.

2.2.2.4 *Eigenvalue problems*

Axial vibrations of a bar: Find $u(x)$ and λ that satisfy the differential equation and *boundary conditions*:

$$-\frac{d}{dx}\left(a\frac{du}{dx}\right)+cu-\lambda u=0 \quad \text{for} \quad 0<x<L$$
$$u(0)=0, \quad \left(a\frac{du}{dx}\right)_{x=L}=0 \tag{2.2.24}$$

Transverse vibrations of a membrane: Find $u(x, y)$ and λ that satisfy the partial differential equation and *boundary conditions*:

$$-\left[\frac{\partial}{\partial x}\left(a_{xx}\frac{\partial u}{\partial x}\right)+\frac{\partial}{\partial y}\left(a_{yy}\frac{\partial u}{\partial y}\right)\right]+a_{00}u-\lambda u=0 \quad \text{in } \Omega$$
$$u=0 \text{ on } \Gamma_u, \quad \left(a_{xx}\frac{\partial u}{\partial x}n_x+a_{yy}\frac{\partial u}{\partial y}n_y\right)=0 \text{ on } \Gamma_q \tag{2.2.25}$$

The values of λ are called *eigenvalues* and the associated functions u are called *eigenfunctions*. The set of specified functions and parameters (e.g., a, b, c, ρ, f, u_0, d_0, q_0, v_0 and so on) are called the *data* of the problem. Differential equations in which the right-hand side f is zero are called *homogeneous differential equations*, and boundary (initial) conditions in which the specified data is zero called homogeneous boundary (initial) conditions.

The *exact solution* of a differential equation is the function that identically satisfies the differential equation at every point of the domain and for all times $t > 0$, and satisfies the specified boundary and/or initial conditions.

2.2.3 Integral Identities

Integration by parts is used in the weak-form integral formulations of differential equations. In twoand three-dimensional cases, integration by parts amounts to using the gradient and divergence theorems. In this section, we derive some useful identities for use in the coming chapters.

2.2.3.1 *Integration by parts formulae*

Let p, q, u, v, and w be sufficiently differentiable functions of the coordinate x. Then the following integration by parts formulae hold:

$$\int_a^b w\frac{d}{dx}\left(p\frac{du}{dx}\right)dx = -\int_a^b p\frac{dw}{dx}\frac{du}{dx}dx - w(a)\left(p\frac{du}{dx}\right)_{x=a} + w(b)\left(p\frac{du}{dx}\right)_{x=b} \quad (2.2.26)$$

$$\begin{aligned}\int_a^b v\frac{d^2}{dx^2}\left(q\frac{d^2w}{dx^2}\right)dx &= \int_a^b q\frac{d^2v}{dx^2}\frac{d^2w}{dx^2}dx \\ &\quad - v(a)\left[\frac{d}{dx}\left(q\frac{d^2w}{dx^2}\right)\right]_{x=a} + v(b)\left[\frac{d}{dx}\left(q\frac{d^2w}{dx^2}\right)\right]_{x=b} \\ &\quad + \left(\frac{dv}{dx}\right)_{x=a}\left(q\frac{d^2w}{dx^2}\right)_{x=a} - \left(\frac{dv}{dx}\right)_{x=b}\left(q\frac{d^2w}{dx^2}\right)_{x=b} \quad (2.2.27)\end{aligned}$$

These relations can easily be established.

To establish the relation in Eq. (2.2.26), we begin with the identity

$$\frac{d}{dx}\left(w\cdot p\frac{du}{dx}\right) = \frac{dw}{dx}p\frac{du}{dx} + w\frac{d}{dx}\left(p\frac{du}{dx}\right) \quad (2.2.28)$$

Therefore, we have

$$\begin{aligned}\int_a^b w\frac{d}{dx}\left(p\frac{du}{dx}\right)dx &= \int_a^b \frac{d}{dx}\left(w\cdot p\frac{du}{dx}\right)dx - \int_a^b p\frac{dw}{dx}\frac{du}{dx}dx \\ &= -w(a)\left(p\frac{du}{dx}\right)_{x=a} + w(b)\left(p\frac{du}{dx}\right)_{x=b} - \int_a^b p\frac{dw}{dx}\frac{du}{dx}dx\end{aligned}$$

To establish the relation in Eq. (2.2.27), we begin with

$$\frac{d}{dx}\left[v\cdot\frac{d}{dx}\left(q\frac{d^2w}{dx^2}\right)\right] = \frac{dv}{dx}\frac{d}{dx}\left(q\frac{d^2w}{dx^2}\right) + v\frac{d^2}{dx^2}\left(q\frac{d^2w}{dx^2}\right)$$

Therefore, we have

$$\begin{aligned}\int_a^b v\frac{d^2}{dx^2}\left(q\frac{d^2w}{dx^2}\right)dx &= \int_a^b \frac{d}{dx}\left[v\cdot\frac{d}{dx}\left(q\frac{d^2w}{dx^2}\right)\right]dx - \int_a^b \frac{dv}{dx}\frac{d}{dx}\left(q\frac{d^2w}{dx^2}\right)dx \\ &= \left[v\cdot\frac{d}{dx}\left(q\frac{d^2w}{dx^2}\right)\right]_a^b - \int_a^b \frac{dv}{dx}\frac{d}{dx}\left(q\frac{d^2w}{dx^2}\right)dx \quad (2.2.29)\end{aligned}$$

Next, let $p = q$, $w = dv/dx$ and $u = dw/dx$ (in that order) in Eq. (2.2.25) and obtain

$$\int_a^b \frac{dv}{dx}\frac{d}{dx}\left(q\frac{d^2w}{dx^2}\right)dx = \left[\frac{dv}{dx}\cdot q\frac{d^2w}{dx^2}\right]_a^b - \int_a^b q\frac{d^2v}{dx^2}\frac{d^2w}{dx^2}\,dx \tag{2.2.30}$$

Substituting Eq. (2.2.30) into Eq. (2.2.29), we obtain

$$\begin{aligned}\int_a^b v\frac{d^2}{dx^2}\left(q\frac{d^2w}{dx^2}\right)dx &= \left[v\cdot\frac{d}{dx}\left(q\frac{d^2w}{dx^2}\right)\right]_a^b - \int_a^b \frac{dv}{dx}\frac{d}{dx}\left(q\frac{d^2w}{dx^2}\right)dx \\ &= \left[v\cdot\frac{d}{dx}\left(q\frac{d^2w}{dx^2}\right)\right]_a^b - \left[\frac{dv}{dx}\cdot q\frac{d^2w}{dx^2}\right]_a^b + \int_a^b q\frac{d^2v}{dx^2}\frac{d^2w}{dx^2}\,dx\end{aligned}$$

which is the same as the result in Eq. (2.2.27).

2.2.3.2 Gradient and divergence theorems

Equations governing most physical phenomena are derived in invariant form (i.e., independent of a particular coordinate system) using vectors, tensors, and the del operator (see Reddy [3] and Reddy and Rasmussen [4]). However, when we seek solutions to these equations, we must select a particular coordinate system and express all equations in that coordinate system. Integral formulations of these equations require integration by parts, which, in two and three dimensions, make use of the gradient and divergence theorems. Therefore, it is necessary to recall these integral identities and show their utility in establishing certain integral statements.

Let $F(\mathbf{x})$ and $\mathbf{G}(\mathbf{x})$ are, respectively, scalar and vector functions of class $C_0(\Omega)$ in a three-dimensional domain Ω, where $\mathbf{x}$ denotes the coordinates (i.e., position vector) of a generic point in Ω with respect to a rectangular Cartesian coordinate system (x_1, x_2, x_3). The following results can be specialized to two dimensions by simply restricting the index i on xi to 1 and 2.

Gradient theorem

$$\int_\Omega \nabla F\, d\Omega = \oint_\Gamma \hat{\mathbf{n}}\, F\, d\Gamma \tag{2.2.31}$$

where ∇ is the del operator defined in Eq. (2.2.8), $\hat{\mathbf{n}}$ denotes the unit vector normal to the surface Γ of the domain Ω, the circle on the boundary integral indicates that the integration is taken over the entire closed boundary, $d\Omega$ is a volume element, and $d\Gamma$ is a surface element. The component form of the above equation is given by

$$\int_{\Omega} \frac{\partial F}{\partial x_i}\, d\Omega = \oint_{\Gamma} n_i F\, d\Gamma \tag{2.2.32}$$

where n_i denotes the ith rectangular component of the unit normal vector $\hat{\mathbf{n}}$, that is, $n_i = \cos(x_i, \hat{\mathbf{n}})$. As a special case, Eq. (2.2.32) yields the following statements in two dimensions:

$$\int_{\Omega} \frac{\partial F}{\partial x}\, dxdy = \oint_{\Gamma} n_x F\, ds, \quad \int_{\Omega} \frac{\partial F}{\partial y}\, dxdy = \oint_{\Gamma} n_y F\, ds \tag{2.2.33}$$

where now ds denotes an element of the curve enclosing the two-dimensional domain. The direction cosines n_x and n_y of the unit vector $\mathbf{n}$ can be written as

$$n_x = \cos(x, \hat{\mathbf{n}}) = \hat{\mathbf{e}}_x \cdot \hat{\mathbf{n}}, \quad n_y = \cos(y, \hat{\mathbf{n}}) = \hat{\mathbf{e}}_y \cdot \hat{\mathbf{n}} \tag{2.2.34}$$

where $\hat{\mathbf{e}}_x$ and $\hat{\mathbf{e}}_y$ denote the unit basis vectors along the x and y coordinates, respectively, and $\cos(x, \hat{\mathbf{n}})$, for example, is the cosine of the angle between the positive x direction and the unit vector $\hat{\mathbf{n}}$.

Divergence theorem

$$\int_{\Omega} \nabla \cdot \mathbf{G}\, d\Omega = \oint_{\Gamma} \hat{\mathbf{n}} \cdot \mathbf{G}\, d\Gamma \tag{2.2.35}$$

Here the dot between vectors denotes the scalar product of the vectors. In component we have (summation on repeated indices is implied)

$$\int_{\Omega} \frac{\partial G_i}{\partial x_i}\, d\Omega = \oint_{\Gamma} n_i G_i\, d\Gamma \tag{2.2.36}$$

For two-dimensional case using the (x, y) coordinates, Eq. (2.2.35) has the explicit form

$$\int_{\Omega} \left(\frac{\partial G_x}{\partial x} + \frac{\partial G_y}{\partial y} \right) dxdy = \oint_{\Gamma} (n_x G_x + n_y G_y)\, ds \tag{2.2.37}$$

Let $w(\mathbf{x})$ and $u(\mathbf{x})$ be scalar functions of position $\mathbf{x}$ defined in a threedimensional domain Ω. Then the gradient and divergence theorems can be used to establish the following integral identities [the reader is asked to verify them; *hint*: $\nabla(wu) = (\nabla w)u + w(\nabla u)$]:

$$\int_\Omega w(\nabla u)\,d\Omega + \int_\Omega (\nabla w)\,u\,d\Omega = \int_\Gamma \hat{\mathbf{n}}\,w\,u\,d\Gamma \tag{2.2.38}$$

and [*hint:* $\nabla^2 = \nabla \cdot \nabla$ and $\nabla \cdot (\nabla u\, w) = \nabla^2 u\, w + \nabla u \cdot \nabla w$]

$$\int_\Omega (\nabla^2 u) w\,d\Omega + \int_\Omega \nabla u \cdot \nabla w\,d\Omega = \oint_\Gamma \frac{\partial u}{\partial n}\,w\,d\Gamma \tag{2.2.39}$$

where ∇^2 is the Laplace operator defined in Eq. (2.2.9), $\partial/\partial n$ denotes the normal derivative operator

$$\frac{\partial}{\partial n} \equiv \hat{\mathbf{n}} \cdot \nabla = n_i \frac{\partial}{\partial x_i} \tag{2.2.40}$$

and $d\Omega$ denotes a volume element in Ω. The component form of Eq. (2.2.38) in two dimensions is given by

$$\int_\Omega w \frac{\partial u}{\partial x}\,dxdy + \int_\Omega \frac{\partial w}{\partial x}\,u\,dxdy = \oint_\Gamma n_x\,w\,u\,ds \tag{2.2.41}$$

$$\int_\Omega w \frac{\partial u}{\partial y}\,dxdy + \int_\Omega \frac{\partial w}{\partial y}\,u\,dxdy = \oint_\Gamma n_y\,w\,u\,ds \tag{2.2.42}$$

The component form of Eq. (2.2.39) is given by

$$\int_\Omega \left(\frac{\partial^2 u}{\partial x^2} + \frac{\partial^2 u}{\partial y^2}\right) w\,dxdy + \int_\Omega \left(\frac{\partial u}{\partial x}\frac{\partial w}{\partial x} + \frac{\partial u}{\partial y}\frac{\partial w}{\partial y}\right) dxdy = \oint_\Gamma \left(n_x \frac{\partial u}{\partial x} + n_y \frac{\partial u}{\partial y}\right) w\,ds \tag{2.2.43}$$

If a_{xx}, a_{xy}, a_{yx}, a_{yy}, w, and u are continuous and sufficiently differentiable functions of (x, y), then we can use the identities in Eqs. (2.2.41) and (2.2.42) to show that

$$\begin{aligned}\int_\Omega w\left[\frac{\partial}{\partial x}\left(a_{xx}\frac{\partial u}{\partial x} + a_{xy}\frac{\partial u}{\partial y}\right) + \frac{\partial}{\partial y}\left(a_{yx}\frac{\partial u}{\partial x} + a_{yy}\frac{\partial u}{\partial y}\right)\right] dxdy \\ = -\int_\Omega \left[\frac{\partial w}{\partial x}\left(a_{xx}\frac{\partial u}{\partial x} + a_{xy}\frac{\partial u}{\partial y}\right) + \frac{\partial w}{\partial y}\left(a_{yx}\frac{\partial u}{\partial x} + a_{yy}\frac{\partial u}{\partial y}\right)\right] dxdy \\ + \oint_\Gamma w\left[n_x\left(a_{xx}\frac{\partial u}{\partial x} + a_{xy}\frac{\partial u}{\partial y}\right) + n_y\left(a_{yx}\frac{\partial u}{\partial x} + a_{yy}\frac{\partial u}{\partial y}\right)\right] ds\end{aligned} \tag{2.2.44}$$

2.2.4 Matrices and Their Operations

2.2.4.1 Definition of a matrix

Consider the system of linear algebraic equations

$$\begin{aligned} b_1 &= a_{11}x_1 + a_{12}x_2 + a_{13}x_3 \\ b_2 &= a_{21}x_1 + a_{22}x_2 + a_{23}x_3 \\ b_3 &= a_{31}x_1 + a_{32}x_2 + a_{33}x_3 \end{aligned} \tag{2.2.45}$$

We see that there are nine coefficients a_{ij}, $i, j = 1, 2, 3$ relating the three coefficients (b_1, b_2, b_3) to (x_1, x_2, x_3). The form of these linear equations suggests writing down the coefficients a_{ij} (jth components in the ith equation) in the rectangular array

$$\mathbf{A} = \begin{bmatrix} a_{11} & a_{12} & a_{13} \\ a_{21} & a_{22} & a_{23} \\ a_{31} & a_{32} & a_{33} \end{bmatrix}$$

This rectangular array **A** of numbers a_{ij} is called a *matrix*, and the quantities a_{ij} are called the *elements* of matrix **A**.

If a matrix has m rows and n columns, we will say that is m by n ($m \times n$), the number of rows always being listed first. The element in the ith row and jth column of a matrix **A** is generally denoted by a_{ij}, and we will sometimes designate a matrix by $\mathbf{A} = [A] = [a_{ij}]$. A square matrix is one that has the same number of rows as columns. An $n \times n$ matrix is said to be of *order n*. The elements of a square matrix for which the row number and the column number are the same (that is, a_{ii} for any fixed i) are called *diagonal elements*. A square matrix is said to be a *diagonal matrix* if all of the off-diagonal elements are zero. An *identity matrix* or its unit matrix, denoted by $\mathbf{I} = [I]$, is a diagonal matrix whose elements are all 1's. Examples of diagonal and identity matrices are:

$$\begin{bmatrix} 6 & 0 & 0 & 0 \\ 0 & 1 & 0 & 0 \\ 0 & 0 & 3 & 0 \\ 0 & 0 & 0 & -2 \end{bmatrix}, \qquad \mathbf{I} = \begin{bmatrix} 1 & 0 & 0 & 0 \\ 0 & 1 & 0 & 0 \\ 0 & 0 & 1 & 0 \\ 0 & 0 & 0 & 1 \end{bmatrix}$$

If the matrix has only one row or one column, we will normally use only a single subscript to designate its elements. For example,

$$\mathbf{X} = \begin{Bmatrix} x_1 \\ x_2 \\ x_3 \end{Bmatrix}, \quad \mathbf{Y} = \{y_1 \quad y_2 \quad y_3\}$$

denote a column matrix and a row matrix, respectively. Row and column matrices can be used to denote the components of a vector.

2.2.4.2 Matrix addition and multiplication of a matrix by a scalar

The *sum* of two matrices of the same size is defined to be a matrix of the same size obtained by simply adding the corresponding elements. If **A** is an $m \times n$ matrix and **B** is an $m \times n$ matrix, their sum is an $m \times n$ matrix, **C**, with

$$c_{ij} = a_{ij} + b_{ij} \quad \text{for all } i, j$$

A constant multiple of a matrix is equal to the matrix obtained by multiplying all of the elements by the constant. That is, the multiple of a matrix **A** by a scalar α, α**A**, is the matrix obtained by multiplying each of its elements with α:

$$\mathbf{A} = \begin{bmatrix} a_{11} & a_{12} & \dots & a_{1n} \\ a_{21} & a_{22} & \dots & a_{2n} \\ \vdots & \vdots & \dots & \vdots \\ a_{m1} & a_{m2} & \dots & a_{mn} \end{bmatrix}, \quad \alpha\,\mathbf{A} = \begin{bmatrix} \alpha a_{11} & \alpha a_{12} & \dots & \alpha a_{1n} \\ \alpha a_{21} & \alpha a_{22} & \dots & \alpha a_{2n} \\ \vdots & \vdots & & \vdots \\ \alpha a_{m1} & \alpha a_{m2} & \dots & \alpha a_{mn} \end{bmatrix}$$

Matrix addition has the following properties:

1. Addition is commutative: **A** + **B** = **B** + **A**.
2. Addition is associative: **A** + (**B** + **C**) = (**A** + **B**) + **C**.
3. There exists a unique matrix **0**, such that **A** + **0** = **0** + **A** = **A**. The matrix **0** is called *zero matrix*; all elements of it are zeros.
4. For each matrix **A**, there exists a unique matrix −**A** such that **A** + (−**A**) = **0**.
5. Addition is distributive with respect to scalar multiplication: α(**A** + **B**) = α**A** + α**B**.

2.2.4.3 Matrix transpose and symmetric and skew symmetric matrices

If **A** is an $m \times n$ matrix, then the $n \times m$ matrix obtained by interchanging its rows and columns is called the *transpose* of **A** and is denoted by $\mathbf{A}^T$. An example of a transpose is provided by

$$\mathbf{A}=\begin{bmatrix} 2 & -3 & 4 \\ 5 & 6 & 8 \\ 1 & 5 & 3 \\ -2 & 9 & 0 \end{bmatrix},\quad \mathbf{A}^{\mathrm{T}}=\begin{bmatrix} 2 & 5 & 1 & -2 \\ -3 & 6 & 5 & 9 \\ 4 & 8 & 3 & 0 \end{bmatrix}$$

The following basic properties of a transpose should be noted:

1. $(\mathbf{A}^{\mathrm{T}})^{\mathrm{T}} = \mathbf{A}$
2. $(\mathbf{A} + \mathbf{B})^{\mathrm{T}} = \mathbf{A}^{\mathrm{T}} + \mathbf{B}^{\mathrm{T}}$

A square matrix **A** of real numbers is said to be *symmetric* if $\mathbf{A}^{\mathrm{T}} = \mathbf{A}$. It is said to be *skew symmetric* or *antisymmetric* if $\mathbf{A}^{\mathrm{T}} = -\mathbf{A}$. In terms of the elements of **A**, these definitions imply that **A** is symmetric if and only if $a_{ij} = a_{ji}$, and it is skew symmetric if and only if $a_{ij} = -a_{ji}$. Note that the diagonal elements of a skew symmetric matrix are always zero since $a_{ij} = -a_{ij}$ implies $a_{ij} = 0$ for $i = j$. Examples of symmetric and skew symmetric matrices, respectively, are

$$\begin{bmatrix} 5 & -2 & 11 & 9 \\ -2 & 4 & 14 & -3 \\ 11 & 14 & 13 & 8 \\ 9 & -3 & 8 & 21 \end{bmatrix},\qquad \begin{bmatrix} 0 & -10 & 23 & 3 \\ 10 & 0 & 21 & 7 \\ -23 & -21 & 0 & 12 \\ -3 & -7 & -12 & 0 \end{bmatrix}$$

2.2.4.4 Matrix multiplication and quadratic forms

Consider a vector $\mathbf{A} = a_1\hat{\mathbf{e}}_1 + a_2\hat{\mathbf{e}}_2 + a_3\hat{\mathbf{e}}_3$ in a Cartesian system. We can represent **A** as a *product* of a row matrix with a column matrix:

$$\mathbf{A} = \{a_1 \quad a_2 \quad a_3\}\begin{Bmatrix} \hat{\mathbf{e}}_1 \\ \hat{\mathbf{e}}_2 \\ \hat{\mathbf{e}}_3 \end{Bmatrix}$$

Note that the vector **A** is obtained by multiplying the *i*th element in the row matrix with the *i*th element in the column matrix and adding them. This gives us a strong motivation for defining the product of two matrices (see Hildebrand [7]).

Let **x** and **y** be the vectors (matrices with one column)

$$\mathbf{x} = \begin{Bmatrix} x_1 \\ x_2 \\ \vdots \\ x_m \end{Bmatrix}, \quad \mathbf{y} = \begin{Bmatrix} y_1 \\ y_2 \\ \vdots \\ y_m \end{Bmatrix}$$

We define the product $\mathbf{x}^T\mathbf{y}$ to be the scalar

$$\mathbf{x}^T\mathbf{y} = \{x_1, x_2, \ldots, x_m\} \begin{Bmatrix} y_1 \\ y_2 \\ \vdots \\ y_m \end{Bmatrix} = x_1y_1 + x_2y_2 + \cdots + x_my_m = \sum_{i=1}^{m} x_iy_i \qquad (2.2.46)$$

It follows from Eq. (2.2.46) that $\mathbf{x}^T\mathbf{y} = \mathbf{y}^T\mathbf{x}$. More generally, let $\mathbf{A} = [a_{ij}]$ be $m \times n$ and $\mathbf{B} = [b^{ij}]$ be $n \times p$ matrices. The product **AB** is defined to be the $m \times p$ matrix $\mathbf{C} = [c^{ij}]$ with

$$c_{ij} = \{i\text{th row of } [\mathbf{A}]\} \begin{Bmatrix} j\text{th} \\ \text{column} \\ \text{of } \mathbf{B} \end{Bmatrix} = \{a_{i1}, a_{i2}, \ldots, a_{in}\} \begin{Bmatrix} b_{1j} \\ b_{2j} \\ \vdots \\ b_{nj} \end{Bmatrix}$$

$$= a_{i1}b_{1j} + a_{i2}b_{2j} + \cdots + a_{in}b_{nj} = \sum_{k=1}^{n} a_{ik}b_{kj} \qquad (2.2.47)$$

The linear equations in Eq. (2.2.45) can now be expressed with the help of the matrix notation as

$$\begin{Bmatrix} b_1 \\ b_2 \\ b_3 \end{Bmatrix} = \begin{bmatrix} a_{11} & a_{12} & a_{13} \\ a_{21} & a_{22} & a_{23} \\ a_{31} & a_{32} & a_{33} \end{bmatrix} \begin{Bmatrix} x_1 \\ x_2 \\ x_3 \end{Bmatrix} \quad \text{or} \quad \mathbf{B} = \mathbf{AX}$$

The following comments are in order on the matrix multiplication, wherein **A** denotes an $m \times n$ matrix and **B** denotes a $p \times q$ matrix:

1. The product **AB** is defined only if the number of columns n in **A** is equal to the number of rows p in **B**. Similarly, the product **BA** is defined only if $q = m$.
2. If **AB** is defined, **BA** may or may not be defined. If both **AB** and **BA** are defined, it is not necessary that they be of the same size.
3. The products **AB** and **BA** are of the same size if and only if both **A**

and **B** are square matrices of the same size.

4. The products **AB** and **BA** are, in general, not equal, **AB** ≠ **BA** (even if they are of equal size); that is, the matrix multiplication is not *commutative*.
5. For any real square matrix **A**, **A** is said to be *normal* if $\mathbf{A}\mathbf{A}^{\mathrm{T}} = \mathbf{A}^{\mathrm{T}}\mathbf{A}$; **A** is said to be *orthogonal* if $\mathbf{A}\mathbf{A}^{\mathrm{T}} = \mathbf{A}^{\mathrm{T}}\mathbf{A} = \mathbf{I}$.
6. Matrix addition is distributive with respect to matrix multiplication (note the order): (**A** + **B**)**C** = **AC** + **BC**.
7. If **A** is a square matrix, the powers of **A** are defined by $\mathbf{A}^2 = \mathbf{A}\mathbf{A}$, $\mathbf{A}^3 = \mathbf{A}\mathbf{A}^2 = \mathbf{A}^2\mathbf{A}$, and so on.
8. Matrix multiplication is associative: (**AB**)**C** = **A**(**BC**).
9. The product of any square matrix with the identity matrix is the matrix itself.
10. The transpose of the product is $(\mathbf{AB})\mathrm{T} = \mathbf{B}^{\mathrm{T}}\mathbf{A}^{\mathrm{T}}$ (note the order).

An expression of the form

$$Q = a_{11}x_1^2 + a_{22}x_2^2 + \cdots + a_{nn}x_n^2 + 2a_{12}x_1x_2 + 2a_{13}x_1x_3 + \cdots + 2a_{n-1,n}x_{n-1}x_n$$

where a_{ij} and x_i are real, is called a *quadratic form* in $x_1, x_2, \ldots, x_n$. If the quadratic form $\mathbf{x}^{\mathrm{T}}\mathbf{A}\mathbf{x}$ associated with a real symmetric matrix **A** is nonnegative for all real values of the variables x_i, and is zero only if each of those *n* variables is zero, then the quadratic form is said to be *positive definite* and the matrix **A** is said to be positive definite.

2.2.4.5 Inverse and determinant of a matrix

If **A** is an $n \times n$ matrix and **B** is any $n \times n$ matrix such that **AB** = **BA** = **I**, then **B** is called an *inverse* of **A**. If it exists, the inverse of a matrix is unique (a consequence of the associative law). If both **B** and **C** are inverses for **A**, then by definition,

$$\mathbf{AB} = \mathbf{BA} = \mathbf{AC} = \mathbf{CA} = \mathbf{I}$$

Since matrix multiplication is associative, we have

$$\begin{aligned}\mathbf{BAC} &= (\mathbf{BA})\mathbf{C} = \mathbf{IC} = \mathbf{C} \\ &= \mathbf{B}(\mathbf{AC}) = \mathbf{BI} = \mathbf{B}\end{aligned}$$

This shows that **B** = **C**, and the inverse is unique. The inverse of **A** is denoted by $\mathbf{A}^{-1}$. A matrix is said to be *singular* if it does not have an

inverse. If **A** is nonsingular, then the transpose of the inverse is equal to the inverse of the transpose: $(\mathbf{A}^{-1})^{\mathrm{T}} = (\mathbf{A}^{\mathrm{T}})^{-1}$.

Let $\mathbf{A} = [a_{ij}]$ be an $n \times n$ matrix. We wish to associate with **A** a scalar that in some sense measures the "size" of **A** and indicates whether or not **A** is nonsingular. The *determinant* of the matrix $\mathbf{A} = [a_{ij}]$ is defined to be the scalar $\det \mathbf{A} = |A|$ computed according to the rule

$$\det \mathbf{A} = |a_{ij}| = \sum_{i=1}^{n} (-1)^{i+1} a_{i1} |A_{i1}| \tag{2.2.48}$$

where $|A_{ij}|$ is the determinant of the $(n-1) \times (n-1)$ matrix that remains on deleting out the ith row and the first column of **A**. For convenience we define the determinant of a zeroth-order matrix to be unity. For 1×1 matrices the determinant is defined according to $|a_{11}| = a_{11}$. For a 2×2 matrix **A** the determinant is defined by

$$\mathbf{A} = \begin{bmatrix} a_{11} & a_{12} \\ a_{21} & a_{22} \end{bmatrix}, \quad |A| = \begin{vmatrix} a_{11} & a_{12} \\ a_{21} & a_{22} \end{vmatrix} = a_{11}a_{22} - a_{12}a_{21}$$

In the above definition special attention is given to the first column of the matrix **A**. We call it the expansion of $|A|$ according to the first column of **A**. One can expand $|A|$ according to any column or row:

$$|A| = \sum_{i=1}^{n} (-1)^{i+j} a_{ij} |A_{ij}| \text{ (for fixed } j) = \sum_{j=1}^{n} (-1)^{i+j} a_{ij} |A_{ij}| \text{ (for fixed } i) \tag{2.2.49}$$

where $|A_{ij}|$ is the determinant of the matrix obtained by deleting the ith row and jth column of matrix **A**.

We note the following properties of determinants:

1. $\det(\mathbf{AB}) = \det \mathbf{A} \cdot \det \mathbf{B}$.
2. $\det \mathbf{A}^{\mathrm{T}} = \det \mathbf{A}$.
3. $\det(\alpha \mathbf{A}) = \alpha^n \det \mathbf{A}$, where α is a scalar and n is the order of **A**.
4. If $\mathbf{A}'$ is a matrix obtained from **A** by multiplying a row (or column) of **A** by a scalar α, then $\det \mathbf{A}' = \alpha \det \mathbf{A}$.
5. If $\mathbf{A}'$ is the matrix obtained from **A** by interchanging any two rows (or columns) of **A**, then $\det \mathbf{A}' = -\det \mathbf{A}$.
6. If **A** has two rows (or columns) one of which is a scalar multiple of another (that is, linearly dependent), $\det \mathbf{A} = 0$.

7. If $\mathbf{A}'$ is the matrix obtained from $\mathbf{A}$ by adding a multiple of one row (or column) to another, then $\det \mathbf{A}' = \det \mathbf{A}$.

We now define singular matrices in terms of their determinants. A matrix is said to be *singular* if and only if its determinant is zero. By property 6 above the determinant of a matrix is zero if it has linearly dependent rows (or columns).

For an $n \times n$ matrix $\mathbf{A}$ the determinant of the $(n-1) \times (n-1)$ submatrix of $\mathbf{A}$ obtained by deleting row i and column j of $\mathbf{A}$ is called *minor* of a_{ij} and is denoted by $M_{ij}(\mathbf{A})$ (the same as $|A_{ij}|$). The quantity $\text{cof}_{ij}(\mathbf{A}) \equiv (-1)^{i+j} M_{ij}(\mathbf{A})$ is called the *cofactor* of a_{ij}. The determinant of $\mathbf{A}$ can be cast in terms of the minor and cofactor of a_{ij}

$$\det \mathbf{A} = \sum_{i=1}^{n} a_{ij} \, \text{cof}_{ij}(\mathbf{A}) \tag{2.2.50}$$

for any value of j.

The *adjunct* (also called *adjoint*) of a matrix $\mathbf{A}$ is the transpose of the matrix obtained from $\mathbf{A}$ by replacing each element by its cofactor. The adjunct of $\mathbf{A}$ is denoted by Adj $\mathbf{A}$.

Now we have the essential tools to compute the inverse of a matrix. If $\mathbf{A}$ is nonsingular (that is, $\det \mathbf{A} \neq 0$), the inverse $\mathbf{A}^{-1}$ of $\mathbf{A}$ can be computed according to

$$\mathbf{A}^{-1} = \frac{1}{\det \mathbf{A}} \text{Adj } \mathbf{A} \tag{2.2.51}$$

A numerical example of the calculation of determinant and inverse is presented next.

Example 2.2.1

Compute the determinant and inverse of the matrix

$$\mathbf{A} = \begin{bmatrix} 2 & 5 & -1 \\ 1 & 4 & 3 \\ 2 & -3 & 5 \end{bmatrix}$$

Solution: The minors are

$$M_{11}(\mathbf{A}) = \begin{vmatrix} 4 & 3 \\ -3 & 5 \end{vmatrix}, \quad M_{12}(\mathbf{A}) = \begin{vmatrix} 1 & 3 \\ 2 & 5 \end{vmatrix}, \quad M_{13}(\mathbf{A}) = \begin{vmatrix} 1 & 4 \\ 2 & -3 \end{vmatrix}$$

$$M_{21}(\mathbf{A}) = \begin{vmatrix} 5 & -1 \\ -3 & 5 \end{vmatrix}, \quad M_{22}(\mathbf{A}) = \begin{vmatrix} 2 & -1 \\ 2 & 5 \end{vmatrix}, \quad M_{23}(\mathbf{A}) = \begin{vmatrix} 2 & 5 \\ 2 & -3 \end{vmatrix}$$

$$M_{31}(\mathbf{A}) = \begin{vmatrix} 5 & -1 \\ 4 & 3 \end{vmatrix}, \quad M_{32}(\mathbf{A}) = \begin{vmatrix} 2 & -1 \\ 1 & 3 \end{vmatrix}, \quad M_{33}(\mathbf{A}) = \begin{vmatrix} 2 & 5 \\ 1 & 4 \end{vmatrix}$$

To compute the determinant, we use the definition in Eq. (2.2.48) and expand by the first column and obtain

$$|A| = \sum_{i=1}^{3} (-1)^{i+1} a_{i1} |A_{i1}| = a_{11} M_{11}(\mathbf{A}) - a_{21} M_{21}(\mathbf{A}) + a_{31} M_{31}(\mathbf{A})$$

$$= a_{11} \begin{vmatrix} 4 & 3 \\ -3 & 5 \end{vmatrix} - a_{21} \begin{vmatrix} 5 & -1 \\ -3 & 5 \end{vmatrix} + a_{31} \begin{vmatrix} 5 & -1 \\ 4 & 3 \end{vmatrix}$$

$$= 2[(4)(5) - (3)(-3)] + (-1)[(5)(5) - (-1)(-3)] + 2[(5)(3) - (-1)(4)]$$

$$= 2(20 + 9) - (25 - 3) + 2(15 + 4) = 74$$

We note that the determinant also can be computed by expanding by the first row:

$$|A| = a_{11} M_{11}(\mathbf{A}) - a_{12} M_{12}(\mathbf{A}) + a_{13} M_{13}(\mathbf{A}) = 2 \times 29 - 5 \times (-1) + (-1) \times (-11) = 74$$

To compute the inverse of the given matrix we first compute the cofactors:

$$\text{cof}_{11}(\mathbf{A}) = (-1)^2 M_{11}(\mathbf{A}) = 4 \times 5 - (-3)3 = 29$$
$$\text{cof}_{12}(\mathbf{A}) = (-1)^3 M_{12}(\mathbf{A}) = -(1 \times 5 - 3 \times 2) = 1$$
$$\text{cof}_{13}(\mathbf{A}) = (-1)^4 M_{13}(\mathbf{A}) = 1 \times (-3) - 2 \times 4 = -11$$
$$\text{cof}_{21}(\mathbf{A}) = (-1)^3 M_{21}(\mathbf{A}) = -[5 \times 5 - (-3)(-1)] = -22$$
$$\text{cof}_{22}(\mathbf{A}) = (-1)^4 M_{22}(\mathbf{A}) = [2 \times 5 - 2 \times (-1)] = 12$$
$$\text{cof}_{23}(\mathbf{A}) = (-1)^5 M_{23}(\mathbf{A}) = -[2 \times (-3) - 2 \times 5] = 16$$

and so on. Then the Adj (**A**) is given by cof11 (**A**) cof12 (**A**) cof13 (**A**)

$$\text{Adj}(\mathbf{A}) = \begin{bmatrix} \text{cof}_{11}(\mathbf{A}) & \text{cof}_{12}(\mathbf{A}) & \text{cof}_{13}(\mathbf{A}) \\ \text{cof}_{21}(\mathbf{A}) & \text{cof}_{22}(\mathbf{A}) & \text{cof}_{23}(\mathbf{A}) \\ \text{cof}_{31}(\mathbf{A}) & \text{cof}_{32}(\mathbf{A}) & \text{cof}_{33}(\mathbf{A}) \end{bmatrix}^{\mathrm{T}} = \begin{bmatrix} 29 & -22 & 19 \\ 1 & 12 & -7 \\ -11 & 16 & 3 \end{bmatrix}$$

The inverse of **A** can be now computed using Eq. (2.2.51):

$$\mathbf{A}^{-1} = \frac{1}{74}\begin{bmatrix} 29 & -22 & 19 \\ 1 & 12 & -7 \\ -11 & 16 & 3 \end{bmatrix}$$

It can be easily verified that $\mathbf{A}\mathbf{A}^{-1} = \mathbf{A}^{-1}\mathbf{A} = \mathbf{I}$.

2.3 Energy and Virtual Work Principles

2.3.1 Introduction

The field of solid and structural mechanics, unlike its counterparts (i.e., heat transfer and fluid mechanics), is endowed with special principles and theorems that are based on energy stored in and work done on the system. These principles form an alternative basis for deriving the governing equations of the solid continuum. More importantly, they can be used to directly obtain exact or approximate solutions to the equations governing the system. To present these ideas in a way for the reader to quickly understand and use, certain preliminary concepts must be introduced. For detailed presentations, the reader may consult the textbook by Reddy [2].

2.3.2 Work and Energy

Work done by a force (or moment) is defined to be the product of the force (or moment) and the displacement (or rotation) *in the direction* of the force (moment). Thus, if **F** is the force vector and **u** is the displacement vector, each having its own magnitude and direction, then the scalar product (or dot product) $\mathbf{F} \cdot \mathbf{u}$ gives the work done. The work done is a scalar with units of N-m (Newton meters). When the force and displacement are functions of position **x** in a domain Ω, then the integral of the product over the domain gives the work done:

$$W = \int_{\Omega} \mathbf{F}(\mathbf{x}) \cdot \mathbf{u}(\mathbf{x})\, d\Omega \tag{2.3.1}$$

where $d\Omega$ denotes a volume element of the body. If **F** is also a function of **u**, then

$$W = \int_{\Omega} \left(\int_{0}^{\mathbf{u}} \mathbf{F}(\mathbf{x}) \cdot d\mathbf{u}(\mathbf{x}) \right) d\Omega \tag{2.3.2}$$

To further understand the difference between work done by a force that is independent of the displacement and one that is a function of the displacement, consider a spring–mass system in static equilibrium [see Fig. 2.3.1(a)]. Suppose that the mass m is placed slowly (to eliminate dynamic effects) at the end of a *linear* elastic spring (i.e., the force in the spring is linearly proportional to the displacement in the spring). Under the action of the externally applied force of fixed magnitude F_0, the spring will elongate by an amount e_0, measured from its undeformed state. In this case, the force F_0 is due to gravity and it is equal to $F_0 = mg$. Clearly, F_0 is independent of the extension e_0 in the spring, and F_0 does not change during the course of the extension e going from 0 to its final value e_0 [see Fig. 2.3.1(b)]. The work done by F_0 in moving through de is $F_0\,de$. Then the total (external) work done by F_0 is

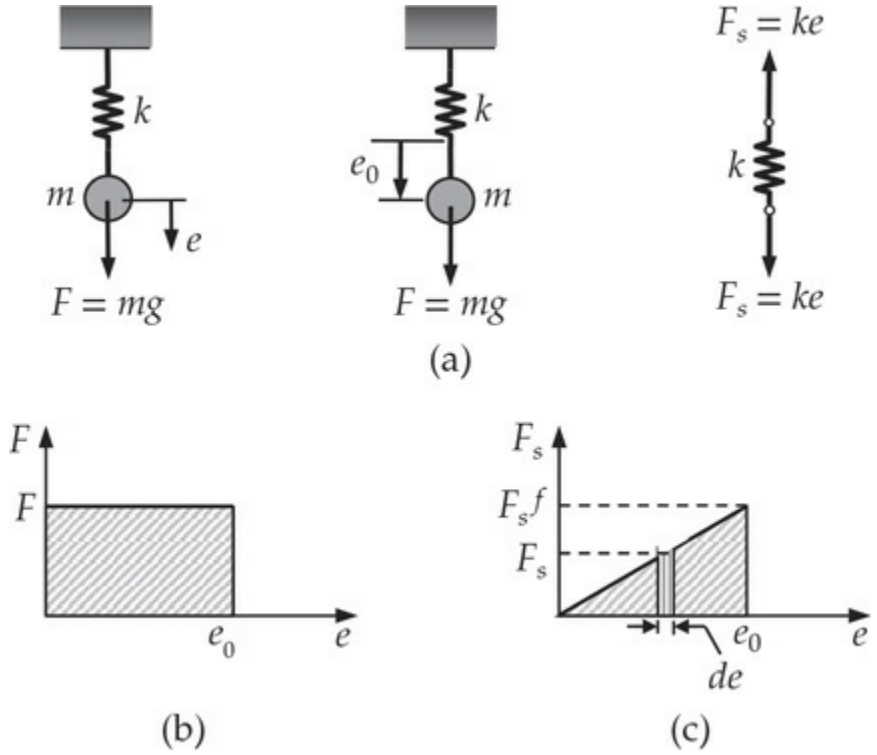

Fig. 2.3.1 A linear spring–mass system in equilibrium. (a) Elongation due to weight mg. (b) External work done. (c) Internal work done.

$$W_E = \int_0^{e_0} F_0\,de = F_0\,e_0$$

Next consider the force in the spring F_s. The force in the spring is proportional to the displacement in the spring. Therefore, the value of F_s

goes from 0 when $e = 0$ to its final value F_s^f when $e = e_0$ [see Fig. 2.3.1(c)]. The work done by F_s in moving through de is $F_s\, de$. The total (internal) work done by F_s is

$$W_I = \int_0^{e_0} F_s(e)\, de$$

Since the spring is assumed to behave linear, we have $F_s = ke$, where k is the spring constant. Then the work done by the spring force is

$$W_I = \int_0^{e_0} ke\, de = \frac{1}{2} k e_0^2$$

Clearly, $W_I \neq W_E$. However, at equilibrium, we have $F_s^f = F$, where F_s^f denotes the final force in the spring.

Now suppose that the spring is imagined to be elongated from e_0 to $e_0 + \Delta e$, Δe being infinitesimally small. Then the additional (or incremental) work done by $F = mg$ and $F_s = F_s(e_0)$ are simply

$$\Delta W_E = -F\Delta e = -mg\Delta e, \qquad \Delta W_I = F_s\, \Delta e = ke_0\, \Delta e$$

which shows that $\Delta W_I = -\Delta W_E$ since $F = F_s$.

A deformable body subjected to external forces develops internal forces that move through displacements produced by geometric changes in the body. Thus in the case of a deformable body, work is done by externally applied forces and internally developed forces. If $\mathbf{f}(\mathbf{x})$ is the body force (measured per unit volume) acting on a material particle occupying position $\mathbf{x}$ in a body with volume Ω, $\mathbf{t}$ is the surface force (measured per unit area) on the boundary Γ, and $\mathbf{u}$ is the displacement of the particle, then the work done on an interior particle is $\mathbf{f} \cdot \mathbf{u}$ and work done on a particle on the boundary is $\mathbf{t} \cdot \mathbf{u}$. The work done on all particles occupying the elemental volume $d\Omega$ is $\mathbf{f} \cdot \mathbf{u}\, d\Omega$, and the work done on all particles on the surface of the body is $\mathbf{t} \cdot \mathbf{u}\, d\Gamma$. Hence, the total external work done on the body, denoted by W_E, is the sum of the work done on all particles interior and on the surface of the body:

$$W_E = -\left[\int_\Omega \mathbf{f}(\mathbf{x}) \cdot \mathbf{u}(\mathbf{x})\, d\Omega + \oint_\Gamma \mathbf{t}(s) \cdot \mathbf{u}(s)\, d\Gamma\right] \tag{2.3.3}$$

The minus sign indicates that the work is expended on the body as opposed to the work stored in the body. In calculating the external work done, the applied forces (or moments) are assumed not to be functions of the displacements (or rotations) they cause in a body. Sometimes, W_E is called the potential energy due to the applied loads and is denoted by V_E.

Energy is defined as the capacity to do work. The energy stored in a body enables it with a capacity to do work. The internal work done by internal forces in moving through respective displacements is available as stored energy. However, internal forces are functions of the displacements (in fact, they are functions of the displacement gradients), as illustrated using the spring–mass system. The energy stored in the case of the previously discussed spring–mass system is entirely due to the stretching of the spring, and it is called the *strain energy*, $U = W_I$, which is available to restore the spring back to its original state when the external force causing the deformation is removed. Thus, energy is a measure of the capacity of all forces that can be associated with matter to perform work. Work is performed on a body through a change in energy.

Another form of energy is the kinetic energy. Consider Newton's second law of motion for a material particle, $\mathbf{F} = m(d\mathbf{v}/dt)$, where m is the fixed mass and $\mathbf{v}$ is the velocity of the particle. If $\mathbf{x}$ is the position vector of the particle with respect to a fixed frame, the work done by the force $\mathbf{F}$ in moving the particle through an infinitesimal distance $d\mathbf{r}$ is

$$dW = \mathbf{F} \cdot d\mathbf{x} = m\frac{d\mathbf{v}}{dt} \cdot d\mathbf{x} = m\frac{d\mathbf{v}}{dt} \cdot \mathbf{v}\, dt = m\frac{d}{dt}\left(\frac{1}{2}\mathbf{v} \cdot \mathbf{v}\right) dt = \frac{1}{2}mv^2 = \frac{dK}{dt}dt = dK$$

where $v = |\mathbf{v}|$, the magnitude of the velocity vector $\mathbf{v} = d\mathbf{x}/dt$ and K is the kinetic energy. Thus, the work done by a force is equal to the change (increase) in the kinetic energy.

2.3.3 Strain Energy and Strain Energy Density

For deformable elastic bodies under isothermal conditions and infinitesimal deformations, the internal energy per unit volume, denoted by U_0 and termed strain energy density, consists of only stored elastic strain energy (for rigid bodies, $U_0 = 0$). An expression for strain energy density can be derived as follows.

First, we consider axial deformation of a bar of area of cross section A. The free-body diagram of an element of length dx_1 of the bar is shown in

Fig. 2.3.2(a). Note that the element is in static equilibrium, and we wish to determine the work done by the internal force associated with stress σ_{11}^f, where the superscript *f* indicates that it is the final value of the quantity. Suppose that the element is deformed slowly so that axial strain varies from 0 to its final value ε_{11}^f. At any instant during the strain variation from $\varepsilon 11$ to $\varepsilon_{11} + d\varepsilon_{11}$, we assume that σ_{11} (due to ε_{11}) is kept constant so that equilibrium is maintained. Then the work done by the force $A\sigma_{11}$ in moving through the displacement $d\varepsilon_{11}dx_1$ is

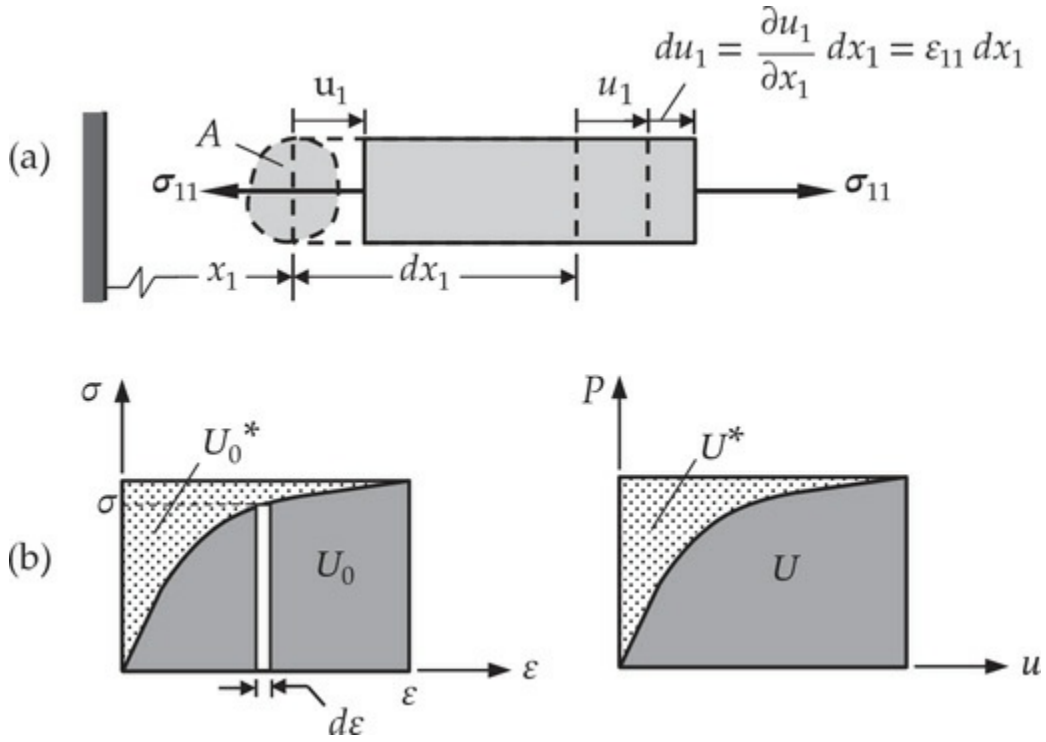

Fig. 2.3.2 Computation of strain energy for the uniaxially loaded member. (a) Work done by force ?11 *A*. (b) Definitions of strain energy density and complementary strain energy density and associated energies.

$$A\sigma_{11}\, d\varepsilon_{11}dx_1 = \sigma_{11}d\varepsilon_{11}\,(Adx_1) \equiv dU_0\,(Adx_1)$$

where dU_0 denotes the work done per unit volume in the element.

Referring to the stress–strain diagram in Fig. 2.3.2(b), dU_0 represents the elemental area *under* the stress–strain curve. The elemental area in the complement (in the rectangle formed by ε_{11} and σ_{11}) is given by $dU_0^* = \varepsilon_{11}\, d\sigma_{11}$ and it is called the complementary strain energy density of the bar of length dx_1. In the present study, we will not be dealing with the complementary strain energy. The total area under the curve, U_0, is

obtained by integrating from zero to the final value of the strain (during which the stress changes according to its relation to the strain):

$$U_0 = \int_0^{\varepsilon_{11}} \sigma_{11}\, d\varepsilon_{11}$$

where the superscript *f* is omitted as the expression holds for any value of ε.

The internal work done (or strain energy stored) by $A\sigma_{11}$ over the whole element of length *dx* during the entire deformation is

$$dU = \int_0^{\varepsilon_{11}} \sigma_{11} d\varepsilon_{11}(Adx_1) = U_0(Adx_1)$$

The total energy stored in the entire bar is obtained by integrating over the length of the bar:

$$U = \int_0^{L} AU_0\, dx_1$$

This is the internal energy stored in the body due to deformation of the bar and it is called the *strain energy*. We note that no stress–strain relation is used, except that the stress–strain diagrams shown in Fig. 2.3.2(b) implies that it can be nonlinear. When the stress–strain relation is linear, say $\sigma_{11} = E\varepsilon_{11}$, we have $U_0 = (1/2)E\varepsilon_{11}^2 = (1/2)\sigma_{11}\varepsilon_{11}$.

The aforementioned discussion can be extended to the three-dimensional case. Consider the rectangular parallelepiped element of sides dx_1, dx_2, and dx_3 taken from inside an elastic body Ω, as shown in Fig. 2.3.3(a). Suppose that the element is subjected to a system of stresses that vary slowly until they reach their final values, so that the equilibrium is maintained at all times. The forces due to the normal components of stresses are

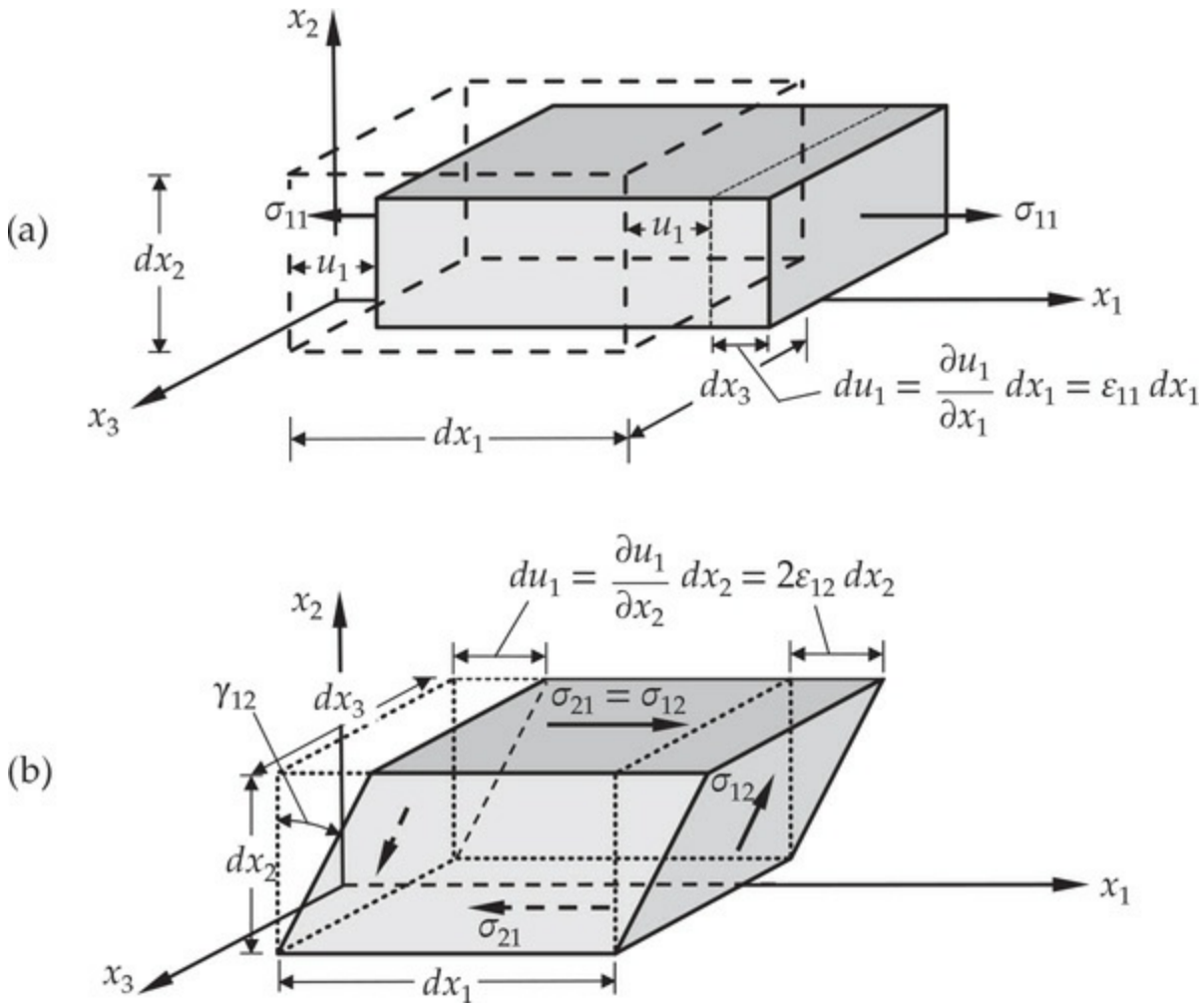

Fig. 2.3.3 Computation of strain energy for the three-dimensional case.

$$\sigma_{11}dx_2dx_3,\ \sigma_{22}dx_3dx_1,\ \sigma_{33}dx_1dx_2$$

and the forces due to the shear stresses on the six faces are

$$\sigma_{12}dx_2dx_3,\ \sigma_{13}dx_3dx_2,\ \sigma_{21}dx_1dx_3,\ \sigma_{23}dx_3dx_1,\ \sigma_{31}dx_1dx_2,\ \sigma_{32}dx_2dx_1$$

At any stage during the action of these forces, the faces of the infinitesimal parallelepiped will undergo displacements in the normal directions by the amounts $d\varepsilon_{11}dx_1$, $d\varepsilon_{22}dx_2$, and $d\varepsilon_{33}dx_3$, and distort by the amounts $2d\varepsilon_{12}dx_1$, $2d\varepsilon_{23}dx_2$, and
$2d\varepsilon_{31}dx_3$. As examples, the deformations caused by normal force $\sigma_{11}dx_2dx_3$ and shear force $\sigma_{21}dx_1dx_3$, each acting alone, are shown in Figs. 2.3.3(a) and (b), respectively (only final deformations are shown). The work done by individual forces can be summed to obtain the total work done by the simultaneous application of all of the forces, because, for example, an x_1 -

directed force does no work in the x_2 or x_3 directions. The work done, for instance, during the application of the force $\sigma_{11}dx_2dx_3$ is given by

$$(\sigma_{11}dx_2\, dx_3)(d\varepsilon_{11}dx_1) = \sigma_{11}d\varepsilon_{11}d\Omega$$

where $d\Omega = dx_1dx_2dx_3$. Similarly, the work done by the shear force $\sigma_{21}dx_1dx_3$ is given by

$$(\sigma_{21}dx_1\, dx_3)(2d\varepsilon_{21}dx_2) = 2\sigma_{21}d\varepsilon_{21}d\Omega$$

The internal work done by forces due to all stresses in varying slowly from zero to their final values is given by ($\sigma_{12} = \sigma_{21}$)

$$dU = \left(\int_0^{\varepsilon_{11}} \sigma_{11}\, d\varepsilon_{11} + \int_0^{\varepsilon_{12}} 2\sigma_{12}\, d\varepsilon_{12} + \cdots\right) d\Omega = \int_0^{\varepsilon_{ij}} \sigma_{ij}\, d\varepsilon_{ij}\, d\Omega = U_0 d\Omega \qquad (2.3.4)$$

where sum on the repeated indices is implied but the integral limit corresponds to a fixed i and j. The expression

$$U_0 = \int_0^{\varepsilon_{ij}} \sigma_{ij}\, d\varepsilon_{ij} \qquad (2.3.5)$$

is the strain energy per unit volume or simply the strain energy density. Thus, the total internal work done, that is the strain energy stored in the body, by forces due to all stress components σ_{ij} is given by the integral of U_0 over the volume of the body:

$$U = \int_\Omega U_0\, d\Omega \qquad (2.3.6)$$

Example 2.3.1

Consider a uniaxial bar of length L, constant area of cross section A, and constant Young's modulus E. Suppose that the axial displacement $u(x)$ is expressed in terms of the end displacements u_1 and u_2 along the length of the member as [see Fig. 2.3.4(a)]

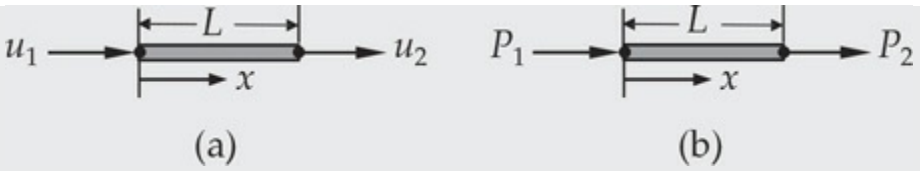

Fig. 2.3.4 Axial deformation of a bar.

$$u(x) = \left(1 - \frac{x}{L}\right)u_1 + \frac{x}{L}u_2 \tag{1}$$

Determine the strain energy density and strain energy in terms of (i) displacement u and (ii) end displacements u_1 and u_2.

Solution: The only strain the bar experiences is the axial strain ε, which is calculated from

$$\varepsilon = \frac{du}{dx} = \frac{u_2 - u_1}{L} \tag{2}$$

(i) The strain energy density is ($\sigma = E\varepsilon$)

$$U_0 = \int_0^{\varepsilon} \sigma \, d\varepsilon = \frac{E}{2}\varepsilon^2 = \frac{E}{2}\left(\frac{du}{dx}\right)^2 \tag{3}$$

The strain energy stored in the bar is

$$U = U_0 AL = \frac{EAL}{2}\left(\frac{du}{dx}\right)^2 \tag{4}$$

(ii) The strain energy density in terms of the end displacements of the bar is

$$U_0 = \frac{E}{2}(\varepsilon)^2 = \frac{E}{2}\left(\frac{u_2 - u_1}{L}\right)^2 = \frac{E}{2L^2}\begin{Bmatrix} u_1 \\ u_2 \end{Bmatrix}^{\mathrm{T}}\begin{bmatrix} 1 & -1 \\ -1 & 1 \end{bmatrix}\begin{Bmatrix} u_1 \\ u_2 \end{Bmatrix} \tag{5}$$

The strain energy stored in the bar becomes

$$U = \frac{EA}{2L}(u_2 - u_1)^2 = \frac{EA}{2L}\begin{Bmatrix} u_1 \\ u_2 \end{Bmatrix}^{\mathrm{T}}\begin{bmatrix} 1 & -1 \\ -1 & 1 \end{bmatrix}\begin{Bmatrix} u_1 \\ u_2 \end{Bmatrix} \tag{6}$$

Example 2.3.2

Determine the strain energy density U_0 and strain energy of a Bernoulli–Euler beam of length L, area of cross section A, moment of inertia I, and

modulus E. Assume that the material of the beam is linearly elastic, deformation is infinitesimal, and the displacement components at any point (x, y, z) in the beam can be expressed in terms of the two unknown (u, w) as follows:

$$u_1 = u(x) - z\frac{dw}{dx} \quad u_2 = 0, \quad u_3 = w(x) \tag{2.3.7}$$

Note that the beam is stretched and bent by external forces in the xz-plane only.

Solution: The only nonzero linear strain is

$$\varepsilon_{xx} = \frac{du}{dx} - z\frac{d^2w}{dx^2} \tag{2.3.8}$$

The strain energy density is

$$\begin{aligned} U_0 &= \int_0^{\varepsilon_{xx}} \sigma_{xx}\, d\varepsilon_{xx} = \int_0^{\varepsilon_{xx}} E\varepsilon_{xx}\, d\varepsilon_{xx} \\ &= \frac{E}{2}\varepsilon_{xx}^2 = \frac{E}{2}\left(\frac{du}{dx} - z\frac{d^2w}{dx^2}\right)^2 \end{aligned} \tag{2.3.9}$$

The strain energy U is given by

$$\begin{aligned} U &= \int_\Omega U_0\, d\Omega = \int_0^L \int_A \frac{E}{2}\left(\frac{du}{dx} - z\frac{d^2w}{dx^2}\right)^2 dA dx \\ &= \frac{1}{2}\int_0^L \left[A_{xx}\left(\frac{du}{dx}\right)^2 + D_{xx}\left(\frac{d^2w}{dx^2}\right)^2\right] dx \end{aligned} \tag{2.3.10}$$

where A_{xx} and D_{xx} are defined as (for the case in which E is at most a function of x)

$$A_{xx} = \int_A E\, dA = EA, \quad D_{xx} = \int_A z^2 E\, dA = EI$$

we have

$$U = \frac{1}{2}\int_0^L \left[EA\left(\frac{du}{dx}\right)^2 + EI\left(\frac{d^2w}{dx^2}\right)^2\right] dx \tag{2.3.11}$$

where we have used the fact (because x-axis is taken along the geometric

centroid)

$$\int_A z\,dA = 0$$

Example 2.3.3

Assume that the axial displacement $u(x)$ and transverse displacement $w(x)$ of the Bernoulli–Euler beam of **Example 2.3.2** are of the form

$$u(x) = \left(1 - \frac{x}{L}\right)u_1 + \frac{x}{L}u_2 \equiv \psi_1(x)u_1 + \psi_2(x)u_2 \tag{1}$$

$$\begin{aligned} w(x) &= \left[1 - 3\left(\frac{x}{L}\right)^2 + 2\left(\frac{x}{L}\right)^3\right]w_1 - x\left(1 - \frac{x}{L}\right)^2\theta_1 \\ &\quad + \left[3\left(\frac{x}{L}\right)^2 - 2\left(\frac{x}{L}\right)^3\right]w_2 - x\left[\left(\frac{x}{L}\right)^2 - \frac{x}{L}\right]\theta_2 \\ &\equiv \varphi_1(x)w_1 + \varphi_2(x)\theta_1 + \varphi_3(x)w_2 + \varphi_4(x)\theta_2 \end{aligned} \tag{2}$$

where (u_1, u_2, w_1, w_2) and (θ_1, θ_2) are the displacements and rotations of the two ends of the beam, as shown in Fig. 2.3.5. Express the strain energy of the Bernoulli–Euler beam theory in terms of the parameters (u_1, w_1, θ_1) and (u_2, w_2, θ_2).

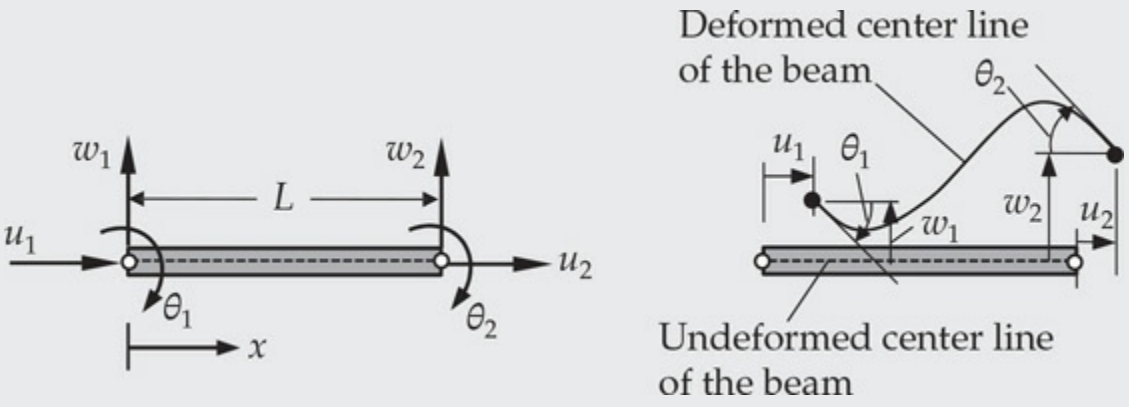

Fig. 2.3.5 A Bernoulli–Euler beam element with generalized displacement degrees of freedom.

Solution: The strain energy for the Bernoulli–Euler beam is given by Eq. (2.3.10). First we compute du/dx and d_2w/dx_2 in terms of the generalized displacements $(u_1, u_2, w_1, w_2, \theta_1, \theta_2)$:

$$\frac{du}{dx} = \frac{u_2 - u_1}{L},$$
$$\frac{d^2w}{dx^2} = -\frac{6}{L^2}\left(1 - 2\frac{x}{L}\right)w_1 - \frac{2}{L}\left(3\frac{x}{L} - 2\right)\theta_1 + \frac{6}{L^2}\left(1 - 2\frac{x}{L}\right)w_2 - \frac{2}{L}\left(3\frac{x}{L} - 1\right)\theta_2 \tag{3}$$

Then the strain energy due to stretching is

$$U_s = \frac{EA}{2}\int_0^L \left(\frac{du}{dx}\right)^2 dx = \frac{EA}{2L}(u_2 - u_1)^2 = \frac{EA}{2L}\begin{Bmatrix} u_1 \\ u_2 \end{Bmatrix}^{\mathrm{T}}\begin{bmatrix} 1 & -1 \\ -1 & 1 \end{bmatrix}\begin{Bmatrix} u_1 \\ u_2 \end{Bmatrix} \tag{4}$$

Next, we evaluate the integrals ($\xi = x/L$ and $dx = Ld\xi$):

$$\begin{aligned}
&\int_0^1 (1-2\xi)^2 L\,d\xi = \frac{L}{3}, \quad \int_0^1 (1-2\xi)(3\xi-2)L\,d\xi = -\frac{L}{2} \\
&\int_0^1 (3\xi-2)^2 L\,d\xi = L, \quad \int_0^1 (1-2\xi)(3\xi-1)L\,d\xi = -\frac{L}{2} \\
&\int_0^1 (3\xi-1)^2 L\,d\xi = L, \quad \int_0^1 (3\xi-2)(3\xi-1)L\,d\xi = \frac{L}{2}
\end{aligned} \tag{5}$$

Then the strain energy due to bending is

$$\begin{aligned}
U_b &= \frac{EI}{2}\int_0^L \left(\frac{d^2w}{dx^2}\right)^2 dx \\
&= \frac{EI}{L^3}(6w_1^2 - 6Lw_1\theta_1 - 12w_1w_2 - 6Lw_1\theta_2 + 2L^2\theta_1^2 + 6L\theta_1w_2 \\
&\quad + 2L^2\theta_1\theta_2 + 6w_2^2 + 6Lw_2\theta_2 + 2L^2\theta_2^2) \\
&= \frac{EI}{L^3}\begin{Bmatrix} w_1 \\ \theta_1 \\ w_2 \\ \theta_2 \end{Bmatrix}^{\mathrm{T}}\begin{bmatrix} 6 & -3L & -6 & -3L \\ -3L & 2L^2 & 3L & L^2 \\ -6 & 3L & 6 & 3L \\ -3L & L^2 & 3L & 2L^2 \end{bmatrix}\begin{Bmatrix} w_1 \\ \theta_1 \\ w_2 \\ \theta_2 \end{Bmatrix}
\end{aligned} \tag{6}$$

Thus, the strain energy due to stretching and bending of the beam ($U = U_s + U_b$) is

$$\begin{aligned}
U &= \begin{Bmatrix} u_1 \\ u_2 \end{Bmatrix}^{\mathrm{T}}\frac{EA}{2L}\begin{bmatrix} 1 & -1 \\ -1 & 1 \end{bmatrix}\begin{Bmatrix} u_1 \\ u_2 \end{Bmatrix} \\
&\quad + \begin{Bmatrix} w_1 \\ \theta_1 \\ w_2 \\ \theta_2 \end{Bmatrix}^{\mathrm{T}}\frac{EI}{L^3}\begin{bmatrix} 6 & -3L & -6 & -3L \\ -3L & 2L^2 & 3L & L^2 \\ -6 & 3L & 6 & 3L \\ -3L & L^2 & 3L & 2L^2 \end{bmatrix}\begin{Bmatrix} w_1 \\ \theta_1 \\ w_2 \\ \theta_2 \end{Bmatrix}
\end{aligned} \tag{7}$$

2.3.4 Total Potential Energy

When W_E involves only the work done by external forces that are independent of the deformation, we call it potential due to external loads and denote it by $V_E = W_E$ [see Eq. (2.3.3)]. The sum of the strain energy U and the potential due to external forces V_E is termed the *total potential energy*, and it is denoted by $\Pi = U + V_E$ (σ: $\varepsilon = \sigma_{ij}\, \varepsilon_{ij}$):

$$\Pi(\mathbf{u}) = U + V_E = \frac{1}{2}\int_{\Omega} \boldsymbol{\sigma}(\boldsymbol{\varepsilon}) : \boldsymbol{\varepsilon}\, d\Omega - \left[\int_{\Omega} \mathbf{f}\cdot\mathbf{u}\, d\Omega + \oint_{\Gamma} \mathbf{t}\cdot\mathbf{u}\, d\Gamma\right] \tag{2.3.12}$$

where Ω denotes the volume occupied by the body and Γ is its total boundary.

For example, the total potential energy expression for the Bernoulli–Euler beams (which include bars, i.e., members subjected to uniaxial forces as a special case) is

$$\Pi(u, w) = \frac{1}{2}\int_0^L \left[EA\left(\frac{du}{dx}\right)^2 + EI\left(\frac{d^2w}{dx^2}\right)^2\right] dx - \left\{\int_0^L \left[f(x)u(x) + q(x)w(x)\right] dx\right\} \tag{2.3.13}$$

where $f(x)$ is the distributed axial force along the line $z = 0$ and $q(x)$ is the transverse distributed load at $z = h/2$, both measured per unit length. The expression in Eq. (2.3.13) must be appended with any terms corresponding to the work done by external point forces and moments.

2.3.5 Virtual Work

The term *configuration* means the simultaneous positions of all material points of a body. A body with specific geometric constraints takes different configurations under different loads. The set of configurations that satisfy the geometric constraints (e.g., geometric boundary conditions) of the system is called the *set of admissible configurations* (i.e., every configuration in the set corresponds to the solution of the problem for a particular set of loads on the system). Of all admissible configurations only

one of them corresponds to the equilibrium configuration under a set of applied loads, and it is this configuration that also satisfies Newton's second law. The admissible configurations for a fixed set of loads can be obtained from infinitesimal *variations* of the true configuration (i.e., infinitesimal movement of the material points). During such variations, the geometric constraints of the system are not violated, and all applied forces are fixed at their actual equilibrium values. When a mechanical system experiences such variations in its equilibrium configuration, it is said to undergo *virtual displacements*. These displacements need not have any relationship with the actual displacements. The displacements are called virtual because they are *imagined* to take place (i.e., hypothetical) with the actual loads acting at their fixed values.

For example, consider a beam fixed at $x = 0$ and subjected to any arbitrary loading (e.g., distributed as well as point loads), as shown in Fig. 2.3.6. The possible geometric configurations the beam can take under the loads may be expressed in terms of the transverse deflection $w(x)$ and axial displacement $u(x)$. The support conditions require that

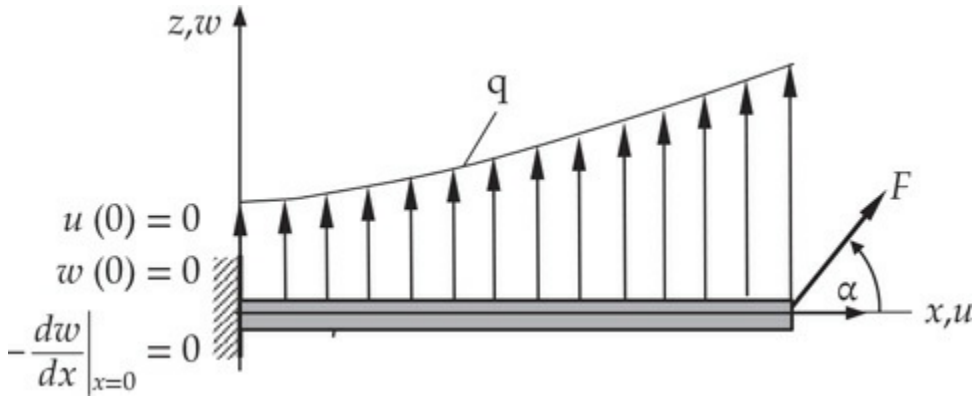

Fig. 2.3.6 A cantilever beam with a set of arbitrary loads.

$$w(0) = 0, \quad \left(-\frac{dw}{dx}\right)_{x=0} = 0, \quad u(0) = 0$$

These are called the *geometric* or *displacement boundary conditions*. Boundary conditions that involve specifying the forces applied on the beam are called *force boundary conditions*.

The set of all functions $w(x)$ and $u(x)$ that satisfy the geometric boundary conditions is the set of admissible configurations for this case. This set consists of pairs of elements $\{(u_i, w_i)\}$ of the form

$$u_1(x) = a_1 x, \quad w_1(x) = b_1 x^2$$
$$u_2(x) = a_1 x + a_2 x^2, \quad w_2(x) = b_1 x^2 + b_2 x^3$$

where a_i and b_i are arbitrary constants. The pair (u, w) that also satisfies, in addition to the geometric boundary conditions, the equilibrium equations and force boundary conditions (which require the precise nature of the applied loads) of the problem is the equilibrium solution. The virtual displacements, $\delta u(x)$ and $\delta w(x)$, must be necessarily of the form

$$\delta u_1 = a_1 x, \quad \delta w_1 = b_1 x^2; \quad \delta u_2 = a_1 x + a_2 x^2, \quad \delta w_2 = b_1 x^2 + b_2 x^3$$

and so on, which satisfy the homogeneous form of the specified geometric boundary conditions:

$$\delta w(0) = 0, \quad \left(\frac{d\delta w}{dx}\right)_{x=0} = 0, \quad \delta u(0) = 0$$

Thus, the virtual displacements at the boundary points at which the geometric conditions are specified (independent of the specified values) are necessarily zero.

The work done by the actual forces through a virtual displacement of the actual configuration is called *virtual work* done by actual forces. If we denote the virtual displacement by $\delta\mathbf{u}$, the virtual work done by a constant force **F** is given by

$$\delta W = \mathbf{F} \cdot \delta\mathbf{u}$$

The virtual work done by actual forces in moving through virtual displacements in a deformable body consists of two parts: virtual work done by internal forces, δW_I, and virtual work done by external forces, δW_E. These may be computed as discussed next.

Consider a deformable body of volume Ω and closed surface area Γ. Suppose that the body is subjected to a body force **f(x)** per unit volume of the body, a specified surface force **t**(s) per unit area on a portion Γ_σ of the boundary, and a specified displacement **u** on the remaining portion Γ_u of the boundary such that $\Gamma = \Gamma_u \cup \Gamma_\sigma$ and $\Gamma_u \cap \Gamma_\sigma$ is empty. For this case, the virtual displacement $\delta\mathbf{u}(\mathbf{x})$ is any function, small in magnitude (to keep the system in equilibrium), that satisfies the requirement

$$\delta\mathbf{u} = 0 \text{ on } \Gamma_u$$

The virtual work done by actual forces **f** and **t** in moving through the virtual displacement $\delta\mathbf{u}$ is

$$\delta W_E = -\left(\int_\Omega \mathbf{f}\cdot\delta\mathbf{u}\,d\Omega + \int_{\Gamma_\sigma} \mathbf{t}\cdot\delta\mathbf{u}\,d\Gamma\right) \tag{2.3.14}$$

The negative sign in front of the expression indicates that the work is performed *on* the body.

As a result of the application of the loads, the body develops internal forces in the form of stresses. These stresses also perform work when the body is given a virtual displacement. In this study, we shall be concerned mainly with only *ideal systems*. An ideal system is one in which no work is dissipated by friction. We assume that the virtual displacement $\delta\mathbf{u}$ is applied slowly from zero to its final value. Associated with the virtual displacement is the virtual strain, which can be computed according to the strain–displacement relation (for the linear case):

$$\delta\varepsilon = \frac{1}{2}\left[\nabla(\delta\mathbf{u}) + (\nabla(\delta\mathbf{u}))^{\mathrm{T}}\right] \tag{2.3.15}$$

The internal virtual work stored in the body per unit volume, analogous to the calculation of the strain energy density, is the virtual strain energy density:

$$\delta U_0 = \int_0^{\delta\varepsilon} \boldsymbol{\sigma} : d(\delta\varepsilon) = \int_0^{\delta\varepsilon_{ij}} \sigma_{ij}\,d(\delta\varepsilon_{ij}) = \sigma_{ij}\delta\varepsilon_{ij} \tag{2.3.16}$$

We note that the result in Eq. (2.3.16) is arrived without the use of a constitutive equation, because σ is not a function of $\delta\varepsilon$. The total internal virtual work stored in the body is denoted by δW_I, and it is equal to

$$\delta W_I = \int_\Omega \delta U_0\,d\Omega = \int_\Omega \sigma_{ij}\,\delta\varepsilon_{ij}\,d\Omega \tag{2.3.17}$$

Example 2.3.4

Consider the cantilever beam shown in Fig. 2.3.7. Assume virtual displacements $\delta u(x)$ and $\delta w(x)$ in the Bernoulli–Euler beam theory to be such that

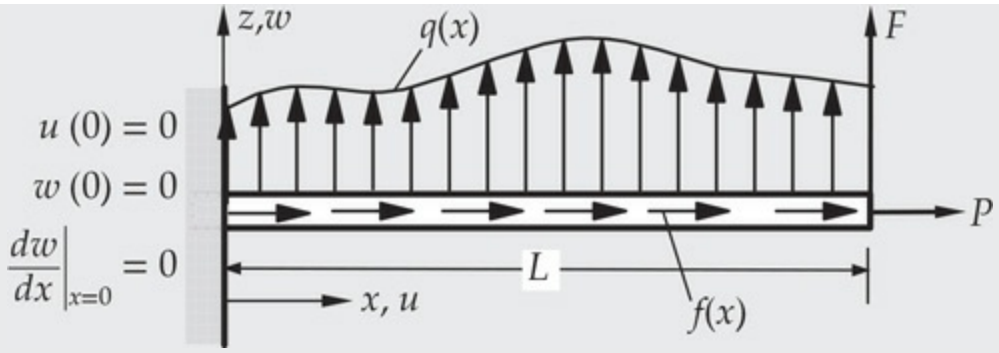

Fig. 2.3.7 A cantilever beam subjected to distributed and point loads.

$$\delta w(0) = 0, \quad \left.\frac{d\delta w}{dx}\right|_{x=0} = 0, \quad \delta u(0) = 0$$

Determine the external and internal virtual works done by actual forces in moving through virtual displacements for the Bernoulli–Euler beam theory. Express the results in terms of the usual stress resultants, applied external loads, and virtual displacements.

Solution: The total external virtual work done by the actual distributed force $q(x)$ in moving through virtual displacement $\delta w(x)$, distributed force $f(x)$ in moving through the virtual displacement $\delta u(x)$, point load F in moving through $\delta w(L)$, and point load P in moving through $\delta u(L)$ is given by

$$\delta W_E = -\left[\int_0^L (q\delta w + f\delta u)\,dx + F\delta w(L) + P\delta u(L)\right] \tag{2.3.18}$$

The virtual work done by internal forces in the Bernoulli–Euler beam theory is where the virtual strain is

$$\delta W_I = \int_0^L \int_A \sigma_{xx}\delta\varepsilon_{xx}\,dA dx \tag{2.3.19}$$

where the virtual strain is

$$\delta\varepsilon_{xx} = \frac{d\delta u}{dx} - z\frac{d^2\delta w}{dx^2} \tag{2.3.20}$$

The internal virtual work done in the Bernoulli–Euler beam theory is

$$\delta W_I = \int_0^L \int_A \sigma_{xx}\left(\frac{d\delta u}{dx} - z\frac{d^2\delta w}{dx^2}\right) dA dx$$
$$= \int_0^L \left(N\frac{d\delta u}{dx} - M\frac{d^2\delta w}{dx^2}\right) dx \tag{2.3.21}$$

where the stress resultants (N, M) are

$$N = \int_A \sigma_{xx}\, dA, \quad M = \int_A \sigma_{xx} z\, dA \tag{2.3.22}$$

The total virtual work expression is

$$\delta W = \delta W_I + \delta W_E$$
$$= \int_0^L \left(N\frac{d\delta u}{dx} - M\frac{d^2\delta w}{dx^2} - q\delta w - f\delta u\right) dx - F\delta w(L) - P\delta u(L) \tag{2.3.23}$$

Note that no constitutive law is used in arriving at the results in Eq. (2.3.23), but at the end N and M must be expressed in terms of the kinematic variables u, w, and $\theta x = -dw/dx$. If we assume linear elastic behavior $\sigma_{xx} = E\varepsilon_{xx}$ with E being independent of the thickness coordinate z, then

$$N = \int_A \sigma_{xx}\, dA = \int_A E\left(\frac{du}{dx} - z\frac{d^2w}{dx^2}\right) dx = EA\frac{du}{dx}$$
$$M = \int_A \sigma_{xx} z\, dA = \int_A E\left(\frac{du}{dx} - z\frac{d^2w}{dx^2}\right) z dx = -EI\frac{d^2w}{dx^2} \tag{2.3.24}$$

Note that u is decoupled from w because of the fact that the x-axis is taken along the geometric centroid of the beam (so that $\int_A z dA = 0$). In this case the expressions for the total virtual work done, which is denoted here by $\delta\Pi$ to distinguish it from δW (which is independent of the constitutive relation), are

$$\delta\Pi = \int_0^L \left(EA\frac{du}{dx}\frac{d\delta u}{dx} + EI\frac{d^2w}{dx^2}\frac{d^2\delta w}{dx^2} - q\delta w - f\delta u\right) dx$$
$$- F\delta w(L) - P\delta u(L) \tag{2.3.25}$$

2.3.6 The Principle of Virtual Displacements

In deformable bodies material points can move relative to one another and do internal work in addition to the work done by external forces. Thus we should consider the virtual work done by internal forces (i.e., stresses developed within the body) as well as the work done by external forces in moving through virtual displacements that are consistent with the geometric constraints.

Consider a continuum occupying the volume Ω (which is an open-bounded set of points in $\Re^3$, each point occupied by a material particle) and is in equilibrium under the action of body forces **f** and surface tractions **t**. Suppose that displacements are specified to be $\hat{\mathbf{u}}$, over portion Γ_u of the total boundary Γ of Ω; on the remaining boundary $\Gamma - \Gamma_u \equiv \Gamma_\sigma$, tractions are specified to be $\hat{\mathbf{t}}$. The boundary portions Γ_u and Γ_σ are disjoint (i.e., do not overlap), and their union is the total boundary, Γ. Let $\mathbf{u} = (u_1, u_2, u_3)$ be the displacement vector corresponding to the equilibrium configuration of the body, and let σ_{ij} and ε_{ij} be the associated stress and strain components, respectively, referred to rectangular Cartesian system (x_1, x_2, x_3). Throughout this discussion, we assume that the strains are infinitesimal and rotations are possibly moderate. We make no assumption concerning the constitutive behavior of the material body at the moment.

The set of admissible configurations is defined by sufficiently differentiable displacement fields that satisfy the geometric boundary conditions: $\mathbf{u} = \hat{\mathbf{u}}$ on Γ_u. Of all such admissible configurations, the actual one corresponds to the equilibrium configuration with the prescribed loads. In order to determine the displacement field **u** corresponding to the equilibrium configuration, we let the body experience a virtual displacement $\delta\mathbf{u}$ from the equilibrium configuration. The virtual displacements are arbitrary, continuous with continuous derivatives as dictated by the strain energy, and satisfy the homogeneous form of the specified geometric boundary conditions, $\delta\mathbf{u} = 0$ on Γ_u. The principle of virtual displacements states that *a continuous body is in equilibrium if and only if the virtual work done by all forces, internal and external, acting on the body is zero in a virtual displacement:*

$$\delta W = \delta W_I + \delta W_E = 0 \qquad (2.3.26)$$

where δW_I is the virtual work due to the internal forces and δW_E is the virtual work due to the external forces. For problems involving only mechanical stimuli, the internal virtual work is the same as the virtual strain energy, $\delta U = \delta W_I$.

The principle may be used to derive the equilibrium equations of deformable solids in terms of stresses or stress resultants. But more importantly, it forms the basis (i.e., weak form) to derive finite element models of all structural theories (e.g., theories of bars, beams, and plates).

Example 2.3.5

In **Example 2.3.2**, we have discussed the kinematics of the Bernoulli–Euler beam theory. Use the principle of virtual displacements to derive the governing equations of the Bernoulli–Euler beam theory. Assume that the beam rests on a linear elastic foundation with foundation modulus k and subjected to a distributed longitudinal load $f(x)$ and transverse load $q(x)$ (see Fig. 2.3.7).

Solution: The displacement field of a beam under the Bernoulli–Euler kinematic hypothesis is given by [see Eq. (2.3.7)]

$$u_1(x,y,z) = u(x) + z\theta_x, \quad u_2 = 0, \quad u_3(x,y,z) = w(x); \quad \theta_x \equiv -\frac{dw}{dx} \tag{1}$$

If we assume that the strains are small, the only nonzero strain is given by

$$\varepsilon_{xx} = \frac{du}{dx} + z\frac{d\theta_x}{dx} = \frac{du}{dx} - z\frac{d^2w}{dx^2} \tag{2}$$

Let the virtual displacements be δu and δw, which are completely arbitrary because there are no specified geometric boundary conditions for the problem at hand. Then the virtual strain $\delta\varepsilon_{xx}$ is given by

$$\delta\varepsilon_{xx} = \delta\left(\frac{du}{dx} + z\frac{d\theta_x}{dx}\right) = \frac{d\delta u}{dx} + z\frac{d\delta\theta_x}{dx} \tag{3}$$

Then the internal and external virtual works due to the virtual displacements δu and δw are given by

$$\delta W_E = -\left\{\int_0^L [f(x)\delta u + q(x)\delta w(x,h_t)]\,dx + \int_0^L (-F_s)\delta w(x,h_b)\,dx + P\delta u(L) + F\delta w(L)\right\}$$

$$= -\left\{\int_0^L [f(x)\delta u + q(x)\delta w(x)]\,dx - \int_0^L kw(x)\delta w(x)\,dx + P\delta u(L) + F\delta w(L)\right\} \quad (4)$$

$$\delta W_I = \int_0^L \int_A \sigma_{xx}\delta\varepsilon_{xx}\,dxdA$$

$$= \int_0^L \int_A \sigma_{xx}\left(\frac{d\delta u}{dx} - z\frac{d^2\delta w}{dx^2}\right)dxdA \quad (5)$$

where L is the length, h_t is the distance from the x-axis to the top of the beam, h_b is the distance from the x-axis to the bottom of the beam, and A is the cross-sectional area of the beam. The foundation reaction force F_s (acting downward) is replaced with $F_s = kw(x)$ using the linear elastic constitutive equation for the foundation.

The principle of virtual displacements requires that $\delta W = \delta W_I + \delta W_E = 0$, which gives

$$0 = \int_0^L \int_A \sigma_{xx}\left(\frac{d\delta u}{dx} - z\frac{d^2\delta w}{dx^2}\right)dAdx - \int_0^L [f\delta u + (q - kw)\,\delta w]\,dx - P\delta u(L) - F\delta w(L)$$

$$= \int_0^L \left(N\frac{d\delta u}{dx} - M\frac{d^2\delta w}{dx^2}\right)dx - \int_0^L [f\delta u + (q - kw)\,\delta w]\,dx - P\delta u(L) - F\delta w(L)$$

$$= \int_0^L \left(-\frac{dN}{dx}\delta u - \frac{d^2M}{dx^2}\delta w\right)dx - \int_0^L [f\delta u + (q - kw)\,\delta w]\,dx - P\delta u(L) - F\delta w(L) + \left[N\delta u + \frac{dM}{dx}\delta w - M\frac{d\delta w}{dx}\right]_0^L \quad (6)$$

where N and M are the stress resultants defined by

$$N = \int_A \sigma_{xx} dA, \quad M = \int_A \sigma_{xx} z \, dA \tag{7}$$

The Euler equations are obtained by setting the coefficients of δu and δw under the integral separately to zero:

$$\delta u: \qquad -\frac{dN}{dx} = f \tag{8}$$

$$\delta w: \qquad -\frac{d^2M}{dx^2} + kw = q \tag{9}$$

in $0 < x < L$.

We note that δu, δw, and $d\delta w/dx = \delta(dw/dx)$ appear in the boundary terms. Hence, u, w, and (dw/dx) are the primary variables of the theory, and their specification constitutes the displacement, geometric, or essential boundary conditions. Since nothing is said about the primary variables being specified, δu, δw, and $d\delta w/dx$ are arbitrary at

$$N = 0, \quad V \equiv \frac{dM}{dx} = 0, \quad M = 0 \text{ at } x = 0 \tag{10a}$$

$$N = P, \quad \frac{dM}{dx} = F, \quad M = 0 \text{ at } x = L \tag{10b}$$

A close examination of the steps involved in **Example 2.3.5** shows that the principle of virtual displacements can be used to derive the governing equations and associated boundary conditions of higher-order theories of beams, plates, and shells by (a) assuming a displacement expansion in powers of thickness coordinate with unknown generalized displacements, (b) computing the actual and virtual strains using a suitable measure, (c) using the principle of virtual displacements in an appropriate description of motion, (d) introducing stress resultants, and using the fundamental lemma of the calculus of variations (which requires integration by parts to relieve variations of the generalized displacements of any derivatives; see Reddy [2]).

2.3.7 The Principle of Minimum Total Potential Energy

The principle of virtual work discussed in the previous section is

applicable to any continuous body with arbitrary constitutive behavior (e.g., linear or nonlinear elastic materials). The principle of minimum total potential energy is obtained as a special case from the principle of virtual displacements when the constitutive relations can be obtained from a potential function. Here we restrict our discussion to materials that admit existence of a strain energy potential such that the stress is derivable from it. Such materials are termed *hyperelastic.*

For elastic bodies (in the absence of temperature variations), there exists a strain energy potential U_0 such that [see Eq. (2.3.5)]

$$\sigma_{ij} = \frac{\partial U_0}{\partial \varepsilon_{ij}} \tag{2.3.27}$$

The strain energy density U_0 is a function of strains at a point and is assumed to be positive definite. The statement of the principle of virtual displacements, $\delta W = 0$, can be expressed in terms of the strain energy density U_0 as

$$\begin{aligned} 0 = \delta W &= \int_\Omega \sigma_{ij}\, \delta\varepsilon_{ij}\, d\Omega - \left[\int_\Omega \mathbf{f} \cdot \delta\mathbf{u}\, d\Omega + \int_{\Gamma_\sigma} \hat{\mathbf{t}} \cdot \delta\mathbf{u}\, ds \right] \\ &= \int_\Omega \frac{\partial U_0}{\partial \varepsilon_{ij}} \delta\varepsilon_{ij}\, d\Omega + \delta V_E \\ &= \int_\Omega \delta U_0\, d\Omega + \delta V_E = \delta(U + V_E) \equiv \delta\Pi \end{aligned} \tag{2.3.28}$$

where

$$V_E = -\left[\int_\Omega \mathbf{f} \cdot \mathbf{u}\, d\Omega + \int_{\Gamma_\sigma} \hat{\mathbf{t}} \cdot \mathbf{u}\, ds \right] \tag{2.3.29}$$

is the potential energy due to external loads and U is the strain energy potential

$$U = \int_\Omega U_0\, d\Omega \tag{2.3.30}$$

The sum $V_E + U \equiv \Pi$ is called the *total potential energy,* and the statement

$$\delta\Pi \equiv \delta(U + V_E) = 0 \qquad (2.3.31)$$

is known as the *principle of minimum total potential energy*. It is a statement of the fact that the energy of the system is the minimum only at its equilibrium configuration **u**:

$$\Pi(\mathbf{u} + \alpha\mathbf{v}) \geq \Pi(\mathbf{u}) \text{ for all scalars } \alpha \text{ and admissible variations } \mathbf{v} \qquad (2.3.32)$$

The equality holds only for α = 0.

The principle of virtual displacements and the principle of minimum total potential energy (the minimum character of the total potential energy can be established, in general, for linear problems; for nonlinear problems it may not attain minimum at equilibrium) give, when applied to an elastic body, the equilibrium equations as the Euler equations. The main difference between them is that the principle of virtual displacements gives the equilibrium equations in terms of stresses or stress resultants, whereas the principle of minimum total potential energy gives them in terms of the displacements because, in the latter, constitutive and kinematic relations are used to replace the stresses (or stress resultants) in terms of the displacements. **Example 2.3.6** illustrates these ideas when applied to the Bernoulli–Euler beam theory.

Example 2.3.6

Consider the bending of a beam according to the Bernoulli–Euler beam theory (see Fig. 2.3.8). Construct the total potential energy functional and then determine the governing equation and boundary conditions. Also, examine if the functional Π(*u*, *w*) attains its minimum at equilibrium.

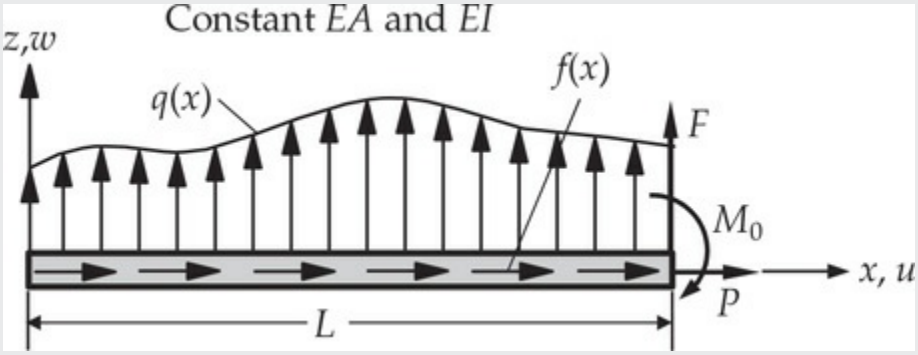

Fig. 2.3.8 A beam with applied loads.

Solution: From Eq. (5) of **Example 2.3.5** the virtual strain energy of the Bernoulli–Euler beam theory for the linear elastic case (i.e., obeys

Hooke's law, $\sigma_{xx} = E\varepsilon_{xx}$) is given by

$$\delta W_I = \delta U = \int_0^L \int_A \sigma_{xx}\delta\varepsilon_{xx}\, dAdx = \int_0^L \int_A E\varepsilon_{xx}\,\delta\varepsilon_{xx}\, dAdx$$
$$= \frac{1}{2}\delta\left[\int_0^L \int_A E\,(\varepsilon_{xx})^2\, dxdA\right]$$
$$= \frac{1}{2}\delta\left\{\int_0^L \int_A E\left(\frac{du}{dx} - z\frac{d^2w}{dx^2}\right)^2 dxdA\right\} \tag{1}$$

where L is the length, A is the cross-sectional area, I is the second moment of area about the axis (y) of bending, and E is the Young's modulus of the beam material. Thus, we have

$$U = \frac{1}{2}\left[\int_0^L \int_A E\left(\frac{du}{dx} - z\frac{d^2w}{dx^2}\right)^2 dxdA\right]$$
$$= \frac{1}{2}\int_0^L \left\{EA\left(\frac{du}{dx}\right)^2 + EI\left(\frac{d^2w}{dx^2}\right)^2\right\} dx \tag{2}$$

where the fact that the x-axis coincides with the centroidal axis is used; that is,

$$\int_A z\, dA = 0 \tag{3}$$

To compute the potential energy due to applied load, suppose that the beam is subjected to distributed axial force $f(x)$, distributed transverse load $q(x)$, horizontal point load P at $x = L$, transverse point load F at $x = L$, and bending moment M_0 at $x = L$, as shown in Fig. 2.3.8. Then the potential energy of applied forces is given by

$$V_E = -\left[\int_0^L (fu + qw)\, dx + Pu(L) + Fw(L) + M_0\left(-\frac{dw}{dx}\right)_{x=L}\right] \tag{4}$$

Note that $\theta_x = -dw/dx$ is the rotation in the counterclockwise sense.

The total potential energy of the beam is $\Pi = U + V_E$:

$$\Pi(u,w)=\frac{1}{2}\int_0^L\left[EA\left(\frac{du}{dx}\right)^2+EI\left(\frac{d^2w}{dx^2}\right)^2\right]dx$$
$$-\int_0^L(fu+qw)\,dx-\left[Pu(L)+Fw(L)-M_0\left.\frac{dw}{dx}\right|_{x=L}\right] \tag{5}$$

Applying the principle of minimum total potential energy, $\delta\Pi = 0$, and using the tools of variational calculus (see Reddy [2] for the properties of δ operator), we obtain

$$0=\delta\Pi=\int_0^L\left(EA\frac{du}{dx}\frac{d\delta u}{dx}+EI\frac{d^2w}{dx^2}\frac{d^2\delta w}{dx^2}\right)dx$$
$$-\int_0^L(f\delta u+q\delta w)\,dx-\left[P\,\delta u(L)+F\,\delta w(L)-M_0\left.\frac{d\delta w}{dx}\right|_{x=L}\right]$$
$$=\int_0^L\left[-\frac{dN}{dx}\delta u+\frac{d^2}{dx^2}\left(EI\frac{d^2w}{dx^2}\right)\delta w\right]dx$$
$$+[N\,\delta u]_0^L+\left[EI\frac{d^2w}{dx^2}\frac{d\delta w}{dx}\right]_0^L+\left[-\frac{d}{dx}\left(EI\frac{d^2w}{dx^2}\right)\delta w\right]_0^L$$
$$-\left[\int_0^L(f\delta u+q\delta w)\,dx+P\delta u(L)+F\delta w(L)-M_0\left.\frac{d\delta w}{dx}\right|_{x=L}\right] \tag{6}$$

where

$$N\equiv EA\frac{du}{dx} \tag{7}$$

An examination of the boundary terms resulting from integration by parts shows that the primary and secondary variables of the theory are,

$$\begin{aligned}&\text{Primary variables:} && u, && w, && -\frac{dw}{dx}\\ &\text{Secondary variables:} && N, && V\equiv\frac{dM}{dx}, && M\equiv -EI\frac{d^2w}{dx^2}\end{aligned} \tag{8}$$

The Euler equations resulting from the principle of the minimum total potential energy are

$$\delta u: \quad -\frac{d}{dx}\left(EA\frac{du}{dx}\right)-f=0 \tag{9}$$

$$\delta w: \quad \frac{d^2}{dx^2}\left(EI\frac{d^2w}{dx^2}\right) - q = 0 \tag{10}$$

Equations (9) and (10) are the same as Eqs. (8) and (9) of **Example 2.3.5**, except they are expressed here in terms of the displacements [see Eqs. (7) and (8) for the definitions of N, M, and V in terms of the displacements u and w].

The natural boundary conditions at the ends of the beam are dictated by the duality listed in Eq. (8). For example, when u is *not* specified at a boundary point, N must be known (or specified) at the point; when w is not specified, then V must be specified; and when $-(dw/dx)$ is not specified, M should be known. For the beam shown in Fig. 2.3.8, there are no specified geometric (or essential) boundary conditions. The known force (or natural) boundary conditions are [see Eqs. (10a) and (10b) of **Example 2.3.5**]

$$N(0) = 0, \;\; M(0) = 0, \;\; V(0) = 0; \quad N(L) = P, \;\; M(L) = M_0, \;\; V(L) = F \tag{11}$$

where N, M, and V are defined in Eqs. (7) and (8) in terms of the displacements u and w. Thus, *the principle of minimum total potential energy yields the equations of equilibrium as well as the natural boundary conditions in terms of the displacements.*

Now we examine if the total potential energy functional Π attains its minimum value at (u, w), where u and w satisfy the equations of equilibrium in Eqs. (9) and (10). We begin with Π at $\bar{u} = u + \alpha u_0$ and $\bar{w} = w + \beta w_0$, where α and β are real numbers and u_0 and w_0 are admissible variations of the displacements u and w (i.e., the variations u_0 and w_0 are arbitrary except that they vanish at the points where u and w are specified) and check if $\Pi(\bar{u}, \bar{w}) \geq \Pi(u, w)$ holds. We have

$$\Pi(\bar{u},\bar{w}) = \frac{1}{2}\int_0^L \left[EA\left(\frac{du}{dx}+\alpha\frac{du_0}{dx}\right)^2 + EI\left(\frac{d^2w}{dx^2}+\beta\frac{d^2w_0}{dx^2}\right)^2\right]dx$$
$$-\int_0^L \left[f(u+\alpha u_0)+q(w+\beta w_0)\right]dx$$
$$-\left[Pu(L)+\alpha Pu_0(L)+Fw(L)+\beta Fw_0(L)-M_0\left.\frac{dw}{dx}\right|_{x=L}-\beta M_0\left.\frac{dw_0}{dx}\right|_{x=L}\right]$$
$$=\frac{1}{2}\int_0^L \left[EA\left(\frac{du}{dx}\right)^2+EI\left(\frac{d^2w}{dx^2}\right)^2\right]dx-\int_0^L (fu+qw)\,dx$$
$$-\left[Pu(L)+Fw(L)-M_0\left.\frac{dw}{dx}\right|_{x=L}\right]+\int_0^L \beta EI\frac{d^2w}{dx^2}\frac{d^2w_0}{dx^2}\,dx$$
$$+\int_0^L \alpha EA\frac{du}{dx}\frac{du_0}{dx}\,dx+\frac{1}{2}\int_0^L\left[\alpha^2EA\left(\frac{du_0}{dx}\right)^2+\beta^2EI\left(\frac{d^2w_0}{dx^2}\right)^2\right]dx$$
$$-\int_0^L(\alpha fu_0+\beta qw_0)dx-\left[\alpha Pu_0(L)+\beta Fw_0(L)-\beta M_0\left.\frac{dw_0}{dx}\right|_{x=L}\right]$$

or

$$\Pi(\bar{u},\bar{w}) = \Pi(u,w)+\int_0^L \alpha EA\frac{du}{dx}\frac{du_0}{dx}\,dx$$
$$+\int_0^L \beta EI\frac{d^2w}{dx^2}\frac{d^2w_0}{dx^2}\,dx-\int_0^L(\alpha fu_0+\beta qw_0)dx$$
$$-\left[\alpha Pu_0(L)+\beta Fw_0(L)-\beta M_0\left.\frac{dw_0}{dx}\right|_{x=L}\right]+\mathcal{P} \qquad (12)$$

where $\mathcal{P}$ is the positive quantity (for nonzero u_0 and w_0):

$$\mathcal{P}=\frac{1}{2}\int_0^L\left[\alpha^2EA\left(\frac{du_0}{dx}\right)^2+\beta^2EI\left(\frac{d^2w_0}{dx^2}\right)^2\right]dx>0 \qquad (13)$$

First, we consider the following terms from Eq. (12):

$$\int_0^L \left(\alpha EA\frac{du}{dx}\frac{du_0}{dx} - \alpha f u_0\right)dx - \alpha P u_0(L)$$
$$= \alpha\int_0^L \left(-\frac{dN}{dx} - f\right)u_0\,dx - \alpha P u_0(L) + \alpha\left[N u_0\right]_0^L$$
$$= \alpha\left[N(L) - P\right]u_0(L) + N(0)u_0(0) = 0 \tag{14}$$

where the equation of equilibrium from Eq. (9), boundary conditions from Eq. (11), and

$$N = EA\frac{du}{dx}$$

are used in arriving at the last result.

Next, we consider the following terms from Eq. (12):

$$\beta\int_0^L \left(EI\frac{d^2w}{dx^2}\frac{d^2w_0}{dx^2} - qw_0\right)dx - \beta\left[Fw_0(L) - M_0\left.\frac{dw_0}{dx}\right|_{x=L}\right]$$
$$= \beta\int_0^L \left(-\frac{d^2M}{dx^2} - q\right)w_0\,dx + \beta\left[\frac{dM}{dx}w_0\right]_0^L$$
$$+ \beta\left[M\left(-\frac{dw_0}{dx}\right)\right]_0^L - \beta\left[Fw_0(L) - M_0\left.\frac{dw_0}{dx}\right|_{x=L}\right] = 0 \tag{15}$$

where the equilibrium equation in Eq. (10), the boundary conditions from Eq. (11), and

$$M = -EI\frac{d^2w}{dx^2}$$

are used in arriving at the result.

In view of the results in Eqs. (14) and (15), Eq. (12) takes the form

$$\Pi(\bar{u},\bar{w}) = \Pi(u,w) + \mathcal{P} \quad \text{or} \quad \Pi(\bar{u},\bar{w}) \geq \Pi(u,w) \tag{16}$$

Thus, the minimum character of Π is established (see Reddy [2] for additional details).

2.3.8 Castigliano's Theorem I

Castigliano's theorem allows one to compute displacements or loads at discrete points of a structural system. Carlo Alberto Castigliano (1847–

1884), an Italian mathematician and railroad engineer, was mainly concerned with linear elastic materials. The generalization of Castigliano's original theorem I to the case in which displacements are nonlinear functions of external forces is attributed to Friedrich Engesser (1848–1931), a German engineer. In the present study we consider Castigliano's theorem in a generalized form that are applicable to both linear and nonlinear elastic materials.

Suppose that the displacement field of a structure can be expressed in terms of the displacements (and possibly rotations) of a finite number of points $\mathbf{x}_i$ (i = 1, 2, …, N) in the body:

$$\mathbf{u}(\mathbf{x}) = \sum_{i=1}^{N} \mathbf{u}_i \phi_i(\mathbf{x}) \tag{2.3.33}$$

where $\mathbf{u}_i$ are unknown displacement parameters, called *generalized displacements*, and ϕ_i are known functions of position, called *interpolation functions* with the property that ϕ_i is unity at the ith point (i.e., $\mathbf{x} = \mathbf{x}_i$) and zero at all other points ($\mathbf{x}_j$, $j \neq i$). Then it is possible to represent the strain energy U and potential V_E due to applied loads in terms of the generalized displacements $\mathbf{u}_i$. The principle of minimum total potential energy can be expressed as

$$\delta\Pi = \delta U + \delta V_E = 0 \Rightarrow \delta U = -\delta V_E, \quad \text{or} \quad \frac{\partial U}{\partial \mathbf{u}_i} \cdot \delta \mathbf{u}_i = -\frac{\partial V_E}{\partial \mathbf{u}_i} \cdot \delta \mathbf{u}_i$$

where sum on repeated indices is implied. Since (only for conservative systems) $\partial V_E / \partial \mathbf{u}_i = -\mathbf{F}_i$, it follows that

$$\left(\frac{\partial U}{\partial \mathbf{u}_i} - \mathbf{F}_i \right) \cdot \delta \mathbf{u}_i = 0$$

Since $\delta \mathbf{u}_i$ are arbitrary, we have the result

$$\frac{\partial U}{\partial \mathbf{u}_i} = \mathbf{F}_i \quad \left(\frac{\partial U}{\partial u_{ij}} = F_{ij} \right) \tag{2.3.34}$$

where (u_{ij}, F_{ij}) are the displacement and force, respectively, at the ith point in the jth direction. Equation (2.3.34) is known as *Castigliano's theorem I*. For an elastic body, it states that the rate of change of strain energy with respect to a generalized displacement is equal to the associated generalized

force. When applied to a structure with point loads F_i (or moment M_i) moving through displacements u_i (or rotation θ_i), both having the same sense, Castigliano's theorem I takes the form

$$\frac{\partial U}{\partial u_i} = F_i, \quad \text{or} \quad \frac{\partial U}{\partial \theta_i} = M_i \tag{2.3.35}$$

It is clear from the derivation that Castigliano's theorem I is a special case of the principle of minimum total potential energy and hence that of the principle of virtual displacements. Castigliano's theorem I is derived using the principle of virtual displacements. Next, we consider two examples of application of Castigliano's theorem I that are relevant to the subject of the book (see Reddy [2] for additional examples).

Example 2.3.7

Use Castigliano's theorem I to determine the force-displacement relationships between the end displacements and forces of the uniaxial member shown in Fig. 2.3.9 (same as Fig. 2.3.4 of **Example 2.3.1**).

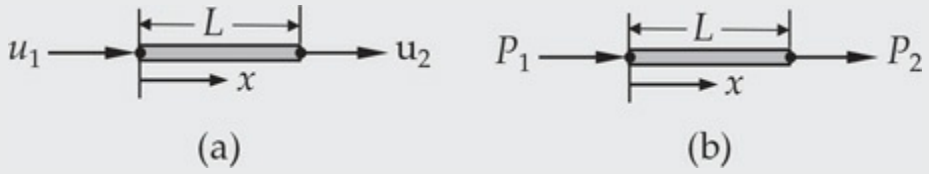

Fig. 2.3.9 Axial deformation of a bar. (a) End displacements. (b) End forces.

Solution: The strain energy of the axially loaded bar made of isotropic homogeneous material (Young's modulus E), length L, and constant cross section A is given in terms of the end displacements u_1 and u_2 in Eq. (6) of **Example 2.3.1** as

$$U = \frac{EA}{2L}(u_2 - u_1)^2 \tag{1}$$

Then by Castigliano's theorem I, we have

$$P_1 = \frac{\partial U}{\partial u_1} = \frac{EA}{L}(u_1 - u_2), \quad P_2 = \frac{\partial U}{\partial u_2} = \frac{EA}{L}(u_2 - u_1) \tag{2}$$

which can be expressed in matrix form as

$$\begin{Bmatrix} P_1 \\ P_2 \end{Bmatrix} = \frac{EA}{L}\begin{bmatrix} 1 & -1 \\ -1 & 1 \end{bmatrix}\begin{Bmatrix} u_1 \\ u_2 \end{Bmatrix} \tag{3}$$

Example 2.3.8

Use Castigliano's theorem I to determine the force-displacement relationships between the generalized displacements and forces of a straight beam of length L and constant bending stiffness EI shown in Fig. 2.3.10.

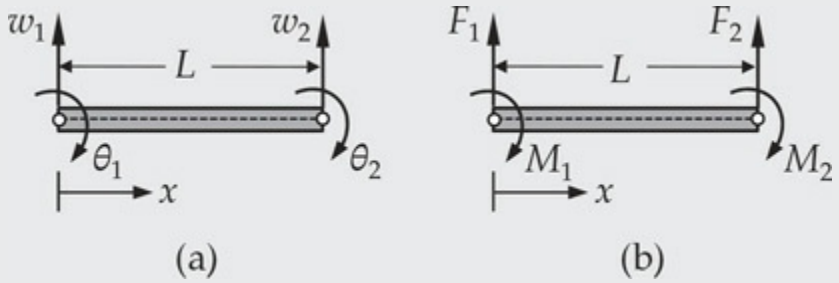

Fig. 2.3.10 Pure bending of a beam. (a) Generalized displacements. (b) Generalized forces.

Solution: The strain energy of a straight beam in pure bending according to the Euler–Bernoulli beam theory is given in terms of the generalized end displacements w_1, θ_1, w_2, and θ_2 in Eq. (6) of **Example 2.3.3** as

$$\begin{aligned} U = \frac{EI}{L^3}(&6w_1^2 - 6Lw_1\theta_1 - 12w_1w_2 - 6Lw_1\theta_2 + 2L^2\theta_1^2 + 6L\theta_1w_2 \\ &+ 2L^2\theta_1\theta_2 + 6w_2^2 + 6Lw_2\theta_2 + 2L^2\theta_2^2) \end{aligned} \tag{1}$$

Then by Castigliano's theorem I, we have

$$\begin{aligned} F_1 &= \frac{\partial U}{\partial w_1} = \frac{EI}{L^3}(12w_1 - 6L\theta_1 - 12w_2 - 6L\theta_2) \\ M_1 &= \frac{\partial U}{\partial \theta_1} = \frac{EI}{L^3}(-6Lw_1 + 4L^2\theta_1 + 6Lw_2 + 2L^2\theta_2) \\ F_2 &= \frac{\partial U}{\partial w_2} = \frac{EI}{L^3}(-12w_1 + 6L\theta_1 + 12w_2 + 6L\theta_2) \\ M_2 &= \frac{\partial U}{\partial \theta_2} = \frac{EI}{L^3}(-6Lw_1 + 2L^2\theta_1 + 6Lw_2 + 4L^2\theta_2) \end{aligned} \tag{2}$$

which can be expressed in matrix form as

$$\begin{Bmatrix} F_1 \\ M_1 \\ F_2 \\ M_2 \end{Bmatrix} = \frac{2EI}{L^3} \begin{bmatrix} 6 & -3L & -6 & -3L \\ -3L & 2L^2 & 3L & L^2 \\ -6 & 3L & 6 & 3L \\ -3L & L^2 & 3L & 2L^2 \end{bmatrix} \begin{Bmatrix} w_1 \\ \theta_1 \\ w_2 \\ \theta_2 \end{Bmatrix} \tag{3}$$

2.4 Integral Formulations of Differential Equations

2.4.1 Introduction

Recall from Section 2.1.3 that the motivation for the use of weighted-integral statements of differential equations comes from the fact that we wish to have a means to determine the unknown parameters c_j in the approximate solution $U_N = \sum_j^N c_j \phi_j$. The variational methods of approximation, e.g., the Ritz, Galerkin, least-squares, collocation, or, in general, weighted-residual methods to be discussed in Section 2.5, are based on weighted-integral statements of the governing equations. Since the finite element method is an element-wise application of a variational method, it is necessary to study the weighted-integral and the so-called weak-form integral statements of differential equations. All finite element models available in commercial codes are based on weak-form statements of differential equations. The weak-form integral statements facilitate, in a natural way, the identification of primary and secondary variables and inclusion of secondary variables into the statements.[1] As we shall see shortly, this classification plays a crucial role in the derivation of the approximation functions and the selection of the nodal degrees of freedom of the finite element model.

In this section, our primary objective is to construct weak forms of differential equations and to classify variables of the problem into primary type and secondary type and identify the form of the boundary conditions associated with the equations. In solid mechanics, the weak forms are the same as the principle of virtual displacements or the principle of minimum total potential energy when the constitutive relations are used.

2.4.2 Residual Function

Consider the problem of solving the differential equation

$$-\frac{d}{dx}\left[a(x)\frac{du}{dx}\right]+cu=f(x) \quad \text{for} \quad 0<x<L \tag{2.4.1}$$

for $u(x)$, which is subject to the boundary conditions

$$u(0)=u_0, \quad \left[a\frac{du}{dx}+\beta(u-u_\infty)\right]_{x=L}=Q_L \tag{2.4.2}$$

Here $a(x)$, $c(x)$, and $f(x)$ are known functions of the coordinate x; u_0, u_∞, β, and Q_L are known values, and L is the size of the one-dimensional domain. When the specified values are nonzero ($u_0 \neq 0$ or $Q_L \neq 0$), the boundary conditions are said to be nonhomogeneous; when the specified values are zero the boundary conditions are said to be homogeneous. The homogeneous form of the boundary condition $u(0) = u_0$ is $u(0) = 0$, and the homogeneous form of the boundary condition $[a(du/dx) + \beta(u - u_\infty)]_{x=L} = Q_L$ is $[a(du/dx) + \beta(u - u_\infty)]_{x=L} = 0$.

Equations of the type in Eq. (2.4.1) arise, for example, in the study of 1-D heat flow in a rod with surface convection (see Example 1.2.2), as shown in Fig. 2.4.1(a). In this case, $a = kA$, with k being the thermal conductivity and A the cross-sectional area, $c = \beta P$, with β being the heat transfer coefficient, P the perimeter of the rod, and L the length of the rod; f denotes the heat generation term, u_0 is the specified temperature at $x = 0$, Q_L is the specified heat at $x = L$, and u_∞ is the temperature of the surrounding medium. Another example where Eqs. (2.4.1) and (2.4.2) arise is provided by the axial deformation of a bar (see Example 1.2.3), as shown in Fig. 2.4.1(b). In this case, $a = EA$, with E being the Young's modulus and A the cross-sectional area, c is the spring constant associated with the shear resistance offered by the surrounding medium (as discussed in Example 1.2.3), and L is the length of the bar; f denotes the body force term, u_0 is the specified displacement at $x = 0$ ($u_0 = 0$), Q_L is the specified point load at $x = L$, and $u_\infty = 0$. Other physical problems are also described by the same equation, but with different meaning of the variables.

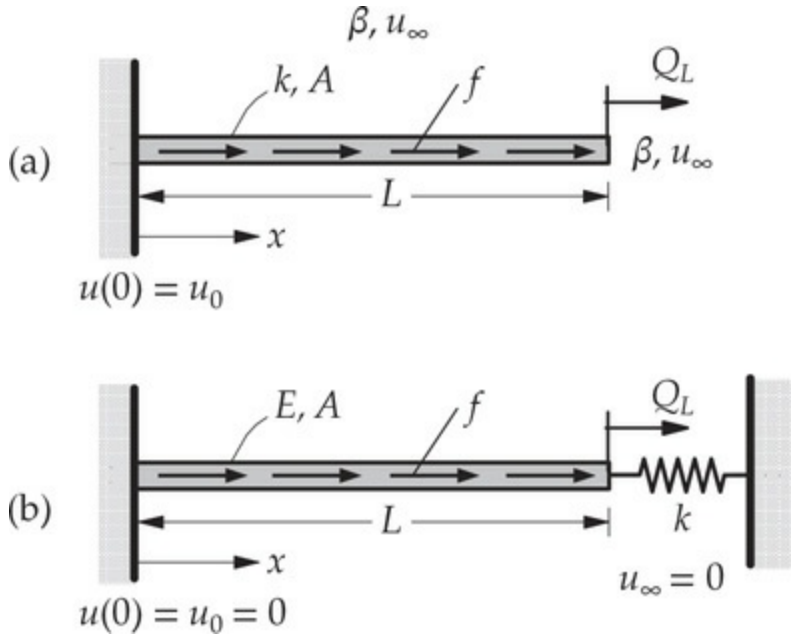

Fig. 2.4.1 (a) One-dimensional heat transfer in an uninsulated rod. (b) Axial deformation of a linear elastic bar.

We seek an approximation of $u(x)$ in the form

$$u(x) \approx u_n(x) = \sum_{j=1}^{n} c_j \phi_j(x) + \phi_0(x) \tag{2.4.3}$$

where, for the moment, we assume that the boundary conditions in Eq. (2.4.2) are identically satisfied by the choice of the approximation functions ϕ_j (x), and wish to determine the constants c_j such that the approximate solution *un* (x) satisfies the differential equation in Eq. (2.4.1). Substitution of *un* into Eq. (2.4.1) yields

$$-\frac{d}{dx}\left[a(x)\frac{du_n}{dx}\right] + cu_n = f(x) \quad \text{for} \quad 0 < x < L \tag{2.4.4}$$

Since the left side of the equality is now an approximate value, it is not equal, in general, to the right side (f) of the equality. The difference

$$0 \neq -\frac{d}{dx}\left[a(x)\frac{du_n}{dx}\right] + cu_n - f(x) \equiv R(x, c_1, c_2, \ldots, c_n) \quad \text{for} \quad 0 < x < L \tag{2.4.5}$$

is called the *residual* of approximation in the differential equation. It is a function of x and c_1, c_2, …, and c_n.

2.4.3 Methods of Making the Residual Zero

Any approximate method seeks to reduce R to zero in some meaningful sense and determine the unknown parameters c_j so that u_n in Eq. (2.4.3) is an acceptable approximation to the problem, i.e., satisfies Eq. (2.4.1). To determine c_j we must obtain a set of n linearly independent equations among c_j while forcing R equal to zero in whatever sense we choose. If we were able to make $R(x, c_1, c_2, \ldots, c_n)$ zero at every point of the domain $(0, L)$, then we would have obtained exact solution to the problem. Since it is not always possible to make R zero at every point of the domain, as discussed in Section 2.1.3, we must find an alternate way to make R zero and find n linearly independent relations among $(c_1, c_2, \ldots, n)$.

2.4.3.1 The collocation method

One possible acceptable sense in which R can be made zero is to require R to vanish at n selected points of the domain:

$$R(x_i, c_1, c_2, \ldots, c_n) = 0 \quad \text{for} \quad i = 1, 2, \ldots, n \tag{2.4.6}$$

2.4.3.2 The least-squares method

Another way to make R zero is to minimize the integral of the square of the residual (the squaring of R is to make it positive; otherwise, there is a possibility of positive and negative errors cancelling each other) with respect to c_i :

$$\text{minimize } I \equiv \int_0^L R^2\,dx \quad \text{or} \quad \frac{\partial}{\partial c_i}\int_0^L R^2\,dx = 2\int_0^L \frac{\partial R}{\partial c_i} R\,dx = 0 \tag{2.4.7}$$

for $i = 1, 2, \ldots, n$. The method based on Eq. (2.4.7) is called the *least-squares method*.

2.4.3.3 The general weighted-residual method

The least-squares method in Eq. (2.4.7) gives another idea, namely, weighting the residual with a linearly independent set of functions and setting it to zero. That is, determine the c_j by requiring R to vanish in a "weighted-residual" sense (i.e., making the residual orthogonal to a set of weight functions):

$$\int_0^L w_i(x)\, R(x, c_1, c_2, \cdots, c_n)\, dx = 0, \quad i = 1, 2, \ldots, n \tag{2.4.8}$$

where $\{w_i(x)\}$ are a set of linearly independent functions, called *weight functions*, which in general can be different from the set of approximation functions $\{\phi_i(x)\}$. This method is known as the *weighted-residual method*. Indeed, the weightedresidual statement in Eq. (2.4.8) includes, as special cases, the collocation method indicated in Eq. (2.4.6) as well as the least-squares method of Eq. (2.4.7). When $w_i = \delta(x - x_i)$, we obtain the result in Eq. (2.4.6), and when we set $w_i = (\partial R/\partial c_i)$ we obtain the result in Eq. (2.4.7). Various known special cases of Eq. (2.4.8) are listed below:

$$\begin{aligned}
&\textit{Petrov–Galerkin method:} && w_i = \psi_i \neq \phi_i \\
&\textit{Galerkin method:} && w_i = \phi_i \\
&\textit{Least-squares method:} && w_i = A(\phi_i),\ A = -\frac{d}{dx}\left[a(x)\frac{d}{dx}\right] + c \\
&\textit{Collocation method:} && w_i = \delta(x - x_i).
\end{aligned} \tag{2.4.9}$$

where x_i denotes the ith collocation point of the domain of the problem, and $\delta(\cdot)$ is the Dirac delta function, which is defined such that its value is zero for all nonzero values of its arguments:

$$\delta(x - x_0) = 0 \ \text{ when } \ x \neq x_0, \qquad \int_{-\infty}^{\infty} f(x)\delta(x - x_0)\, dx = f(x_0) \tag{2.4.10}$$

A simple geometric interpretation of the Galerkin method (a special case of the weighted-residual method) is possible. For example, consider a vector **u** in three-dimensional space, as illustrated in Fig. 2.4.2. We wish to find a twodimensional approximation to **u**. Of all the projections of the vector **u** to a two-dimensional space, the one that has the least amount of error (i.e., the best approximation) is the orthogonal projection $\mathbf{u}_h$ of **u** onto the two-dimensional plane.

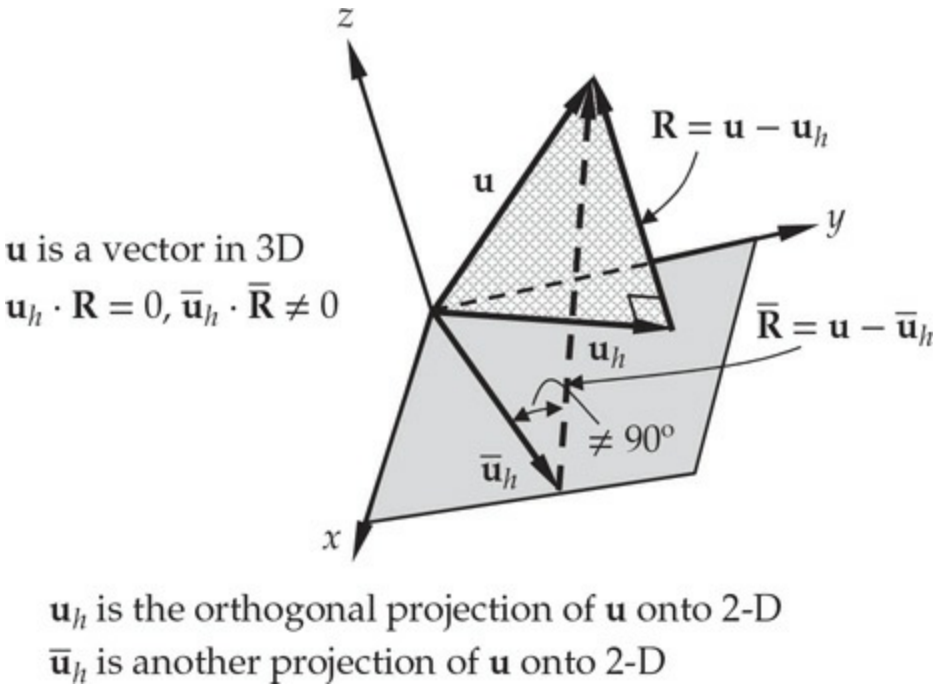

Fig. 2.4.2 Interpretation of the Galerkin method: the best approximation of a vector from 3-D space in a 2-D space is its orthogonal projection.

Due to the different choices of w_i – even when the ϕ_i used in Eqs. (2.4.6), (2.4.7), and (2.4.8) are the same – the system of algebraic equations will have different characteristics in different methods because of the choice of w_i. For linear differential equations of any order, only the least-squares method yields a system of matrix equations whose coefficient matrix is symmetric.

2.4.3.4 The subdomain method

We note that taking $w_i = 1$ in Eq. (2.4.8) does not yield n relations among $(c_1, c_2, \ldots, c_n)$; it yields only one equation. To obtain n equations, one may choose to divide the domain $(0, L)$ into n subintervals $I_1, I_2, \ldots, I_n$ and require the integral of the residual R be zero over each subinterval

$$\int_{I_i} R\,dx = 0, \quad i = 1, 2, \ldots, n \tag{2.4.11}$$

This method is known as the *subdomain method*, and it is the basis of the *finite volume technique* used in fluid dynamics.

2.4.3.5 The Ritz method

The method that is used the most in finite element model development and yet never acknowledged is the *Ritz method*. The Ritz method is originally presented as one in which a quadratic functional equivalent to the governing equation and certain boundary conditions is minimized with respect to the parameters (c_1, c_2, …, c_n) of the approximation. As discussed by Reddy [2], the method is applicable to any integral statement that is equivalent to the governing differential equations and the so-called natural boundary conditions of the problem. Such integral statement is known as the *weak form*, which is the topic of the next section. We shall return to the Ritz method in Section 2.5. The Ritz method is *not* a special case of the weighted-residual method.

2.4.4 Development of Weak Forms

At the outset it should be stated that weak forms can be developed for any differential equation of order 2 and higher. It is a statement equivalent to the differential equation being solved and part of the boundary conditions known as the natural boundary conditions, and requires "weakened differentiability" of the variables when compared to the original differential equation.

There are three steps in the development of the weak form of any differential equation. These steps are illustrated by means of the model differential equation, Eq. (2.4.1), and boundary conditions in Eq. (2.4.2).

Step 1: *The weighted-integral statement of the equation*. This step is the same as the weighted-residual statement of a differential equation. Move all terms of the differential equation to one side (so that it reads … = 0), multiply the entire equation with an arbitrary function w_i (x), and integrate over the domain $\Omega = (0, L)$ of the problem:

$$0 = \int_0^L w_i \left[-\frac{d}{dx}\left(a\frac{du_n}{dx} \right) + cu_n - f \right] dx \tag{2.4.12}$$

Recall that the expression in the square brackets is not identically zero since u is replaced by its approximation, u_n. Mathematically, Eq. (2.4.12) is a statement that the error in the differential equation (due to the approximation of the solution) is zero in the weighted-integral sense. The integral statement in Eq. (2.4.12) yields one algebraic equation among the parameters c_1, c_2, ⋯, c_n for each choice of w_i. By choosing n linearly

independent functions for w_i we obtain n equations for $c_1, c_2, \ldots, c_n$ of Eq. (2.4.3).

Note that the weighted-integral statement of any—first-order or higherorder—differential equation can be readily written. The weighted-integral statement is equivalent only to the differential equation and it does not include any boundary conditions. The weight function w_i in Eq. (2.4.12) can be any nonzero integrable function and has no differentiability requirements. Equation (2.4.12) is the basis of all of the weighted residual methods listed in Eq. (2.4.9).

Step 2: *Integration by parts to equally distribute differentiation between the dependent variables and the weight function and the identification of primary and secondary variables*. While the weighted-integral statement in Eq. (2.4.12) allows us to obtain the necessary number (n) of algebraic relations among c_j for n different choices of the weight function w_i, it requires that the approximation functions $\{\phi_i\}$ be such that u_n [see Eq. (2.4.3)] is differentiable as many times as called for in the original differential equation, Eq. (2.4.1), and satisfies the specified boundary conditions. If this is not a concern, one can proceed with the integral statement in Eq. (2.4.12) and obtain the necessary algebraic equations for $c_1, c_2, \ldots, c_n$ [using any one of the choices listed in Eq. (2.4.9) for w_i].

If we plan to use the approximation functions ϕ_i for w_i, it makes sense to shift half of the derivatives from u_n to w_i in the weighted-integral statement in Eq. (2.4.12) so that both are differentiated equally, and we have lesser (or weaker) continuity requirements on ϕ_i, $i = 1, 2, \ldots, n$. The resulting integral form is known, for obvious reasons, as the *weak form*. Of course, weakening the differentiability of u_n (and hence ϕ_i) is purely a mathematical (and perhaps computational) consideration. As will be seen shortly, the weak formulation has two desirable characteristics. First, it requires weaker, as already indicated, continuity of the dependent variable, and for self-adjoint equations (as is the case with problems studied in this book) it always results in a symmetric coefficient matrix. Second, the boundary conditions on the derivative of u_n of the problem are included in the weak form, and therefore the approximate solution u_n is required to satisfy boundary conditions[2] only on u_n. These two features of a weak form play an important role in the development of finite element models of a problem.

A word of caution is in order. The trading of differentiation from the

dependent variable to the weight function is also (in addition to the weakening the continuity requirements on ϕ_i) dictated by the need to include physically meaningful boundary terms into the weak form, regardless of the effect on the continuity requirements. Therefore, *trading of differentiation from the dependent variable to the weight function should not be performed if it results in boundary terms that are not physically meaningful.*

Returning to the integral statement in Eq. (2.4.12), we integrate the first term of the expression by parts to obtain

$$\begin{aligned} 0 &= \int_0^L \left\{ w_i \left[-\frac{d}{dx}\left(a\frac{du_n}{dx} \right) \right] + cw_i u_n - w_i f \right\} dx \\ &= \int_0^L \left(a\frac{dw_i}{dx}\frac{du_n}{dx} + cw_i u_n - w_i f \right) dx - \left[w_i \cdot a\frac{du_n}{dx} \right]_0^L \end{aligned} \tag{2.4.13}$$

where the integration by parts formula [see Eq. (2.2.26)] is used with $p = a$ on the first term to arrive at the second line of Eq. (2.4.13). Note that now the weight function w_i is required to be differentiable at least once. But this is not a concern because we plan to use $\{\phi_i\}$ for $\{w_i\}$ (in the Galerkin and Ritz methods).

An important part of step 2 is to identify the two types of variables every problem has (cause and effect). We shall term the variable appearing in the differential equation, namely u, as the *primary variable*. After trading differentiation between the weight function w_i and the variable u_n of the equation, examine the boundary expression(s) of the statement. The boundary expression(s) will involve both the weight function w_i and the dependent variable u_n (primary variable). Coefficients of the weight function (and possibly its derivatives for higher-order equations) in the boundary expression(s) are termed the *secondary variable(s*). Based on whether a primary variable is specified or secondary variable is specified in a boundary value problem, the boundary conditions are classified as *essential* and *natural* boundary conditions. The classification is important for both the variational methods of approximation considered in this chapter and the finite element formulations presented in the subsequent chapters.

The following rule is used to identify the essential and natural boundary conditions and their form. The specification of the primary variable u on the boundary constitutes the *essential boundary condition*

(EBC). The specification of the secondary variable on the boundary constitutes the *natural boundary condition* (NBC). For example, for the problem at hand the coefficient of the weight function w_i in the boundary expression is $a(du_n/dx)$; hence, $a(du_n/dx)$ is the secondary variable of the formulation. Specification of the secondary variable $a(du_n/dx)$ on the boundary constitutes the *natural boundary condition* (NBC).

The secondary variables always have physical meaning and are often quantities of interest. In the case of heat transfer problems, the secondary variable represents heat, Q. In the axial deformation of bars, $a(du_n/dx)$ represents a force. We shall denote the secondary variable by

$$Q \equiv \left(a \frac{du_n}{dx} \right) n_x \tag{2.4.14}$$

where n_x denotes the direction cosine, nx = cosine of the angle between the positive x axis and the normal to the boundary. For one-dimensional problems, the normal at the boundary points is always along the length of the domain. Thus, we have $n_x = -1$ at the left end and $n_x = 1$ at the right end of the domain.

It should be noted that the number and form of the primary and secondary variables depend on the order of the differential equation. The number of primary and secondary variables is always the same, and with each primary variable there is an associated secondary variable; that is, they always appear in pairs (e.g., displacement and force, temperature and heat, and so on). Only one member of the pair, either the primary variable or the secondary variable, may be specified at a point of the boundary. Thus, a given problem can have its specified boundary conditions in one of three categories: (1) all specified boundary conditions are of the essential type; (2) some of the specified boundary conditions are of the essential type and the remaining are of the natural type; or (3) all specified boundary conditions are of the natural type. For a single second-order equation, as in the present case, there is one primary variable u and one secondary variable Q. At a boundary point, only one element of the pair (u, Q) can be specified. For a fourth-order equation, such as that for the classical (i.e., Euler–Bernoulli or Bernoulli-Euler) theory of beams, there are two of each kind (i.e., two primary variables and two secondary variables), as will be illustrated later. In general, a $2m$th-order differential equation requires m integration-by-parts to transfer m derivatives from u_n to w_i and therefore there will be m boundary terms involving m primary

variables and m secondary variables; that is, m pairs of primary and secondary variables.

Returning to Eq. (2.4.13), we rewrite it using the notation of Eq. (2.4.14):

$$\begin{aligned} 0 &= \int_0^L \left(a \frac{dw_i}{dx} \frac{du_n}{dx} + c w_i u_n - w_i f \right) dx - \left[w_i \, a \frac{du_n}{dx} \right]_0^L \\ &= \int_0^L \left(a \frac{dw_i}{dx} \frac{du_n}{dx} + c w_i u_n - w_i f \right) dx - \left(w_i \, a \frac{du_n}{dx} n_x \right)_{x=0} - \left(w_i \, a \frac{du_n}{dx} n_x \right)_{x=L} \\ &= \int_0^L \left(a \frac{dw_i}{dx} \frac{du_n}{dx} + c w_i u_n - w_i f \right) dx - (w_i Q)_0 - (w_i Q)_L \end{aligned} \tag{2.4.15}$$

Equation (2.4.15) is called the *weak form* of the differential equation in Eq. (2.4.1). The word "weak" refers to the reduced (i.e. weakened) differentiability required of u_n in Eq. (2.4.15) when compared to the u_n in the weighted-integral statement in Eq. (2.4.12) or the differential equation in Eq. (2.4.1), where u_n is required to be twice-differentiable but only once-differentiable in Eq. (2.4.15).

Step 3: *Replace the expression for the secondary variables by their specified values and finalize the weak form*. The third and last step of the weak form development is to impose the actual boundary conditions of the problem under consideration. It is here that we require the weight function w_i to vanish at boundary points where the essential boundary conditions are specified; that is, w_i is required to satisfy the *homogeneous form* of the specified essential boundary conditions of the problem. That is, the weight function w_i is treated as a *virtual* change (or *variation*) of the primary variable u, $w_i \sim \delta u$. When a primary variable is specified at a point, the virtual change there must be zero. For the problem at hand, the boundary conditions are given by Eq. (2.4.2). By the rules of classification of boundary conditions, $u = u_0$ is the essential boundary condition and $(adu/dx)|_{x=L} = Q_L$ is the natural boundary condition. Thus, the weight function w_i, for $i = 1, 2, \ldots, n$, is required to satisfy

$$w_i(0) = 0, \quad \text{because} \quad u(0) = u_0 \tag{2.4.16}$$

Since $\omega_i(0) = 0$ and

$$Q(L) = \left(a\frac{du_n}{dx}n_x\right)\Big|_{x=L} = \left(a\frac{du_n}{dx}\right)\Big|_{x=L} = Q_L - \beta[u_n(L) - u_\infty] \tag{2.4.17}$$

Equation (2.4.15) reduces to the expression

$$0 = \int_0^L \left(a\frac{dw_i}{dx}\frac{du_n}{dx} + cw_iu_n - w_if\right)dx + \beta w_i(L)u_n(L) - w_i(L)Q_L - \beta w_i(L)u_\infty \tag{2.4.18}$$

which is the weak form equivalent to the differential equation in Eq. (2.4.1) and the natural boundary condition in Eq. (2.4.2). This completes the steps involved in the development of the weak form of a differential equation.

In summary, there are three steps in the development of a weak form. In the first step, we put all expressions of the differential equation on one side to define the residual of approximation and multiply the entire equation by a weight function and integrate over the domain of the problem. The resulting expression is called the weighted-integral form of the equation. In the second step, we use integration by parts to distribute differentiation evenly between the dependent variable and the weight function and use the boundary terms to identify the form of the primary and secondary variables. The integrationby-parts step should be performed only if the resulting boundary expression(s) lead to identification of physically meaningful secondary variable(s). In the third step, we modify the boundary terms by restricting the weight function to satisfy the homogeneous form of the specified essential boundary conditions and replacing the secondary variables by their specified values. Thus, the weak form of a differential equation is a weighted-integral statement equivalent to the differential equation but with weakened differentiability *and* it includes specified natural boundary conditions of the problem. Note that weak forms exist for all problems – linear or nonlinear – that are described by second and higher-order differential equations. However, not all problems admit the construction of a (quadratic) functional whose Euler equations are the governing equations.

It should be recalled that the primary purpose of developing a weightedintegral statement or the weak form of a differential equation is to obtain as many algebraic equations as there are unknown coefficients c_i in the approximation of the dependent variable u of the equation. For different choices of the weight function w_i, different sets of algebraic

equations are obtained. However, because of the restrictions placed on the weight function w_i in step 3 of the weak-form development, w_i belongs to the same vector space of functions as the approximation functions (i.e., $w_i \in \{\phi_i\}$). The resulting discrete model is known as the *Ritz model*.

2.4.5 Linear and Bilinear Forms and Quadratic Functionals

It is useful, although not necessary for the use of variational methods or the finite element method, to see the relation between the weak form and the minimum of a quadratic functional associated with the differential equation. Readers who find this section too mathematical to understand may skip it and go directly to Section 2.4.6 without the loss of continuity.

The weak form in Eq. (2.4.18) contains two types of expressions: those involving both the dependent variable u_n and the weight function w_i, and those involving only w_i. We shall denote these two types of expressions by $B(w_i, u_n)$ and $\ell(w_i)$, respectively:

$$B(w_i, u_n) = \int_0^L \left(a \frac{dw_i}{dx} \frac{du_n}{dx} + c w_i u_n \right) dx + \beta w_i(L) u_n(L)$$
$$\ell(w_i) = \int_0^L w_i f \, dx + w_i(L) Q_L + \beta w_i(L) u_\infty \tag{2.4.19}$$

Hence, the weak form in Eq. (2.4.18) can be expressed as

$$B(w_i, u_n) = \ell(w_i) \tag{2.4.20}$$

which is termed the *variational problem* associated with the Eqs. (2.4.1) and (2.4.2).

A characteristic of the expressions in Eq. (2.4.19) is that they are real numbers once the arguments w_i and u_n are assigned. Such expressions are known as *functionals*. In mathematics a functional $I(\cdot)$ is defined as a transformation that maps functions from a linear vector space[3] V into the field of real numbers $\Re$, i.e., $I : V \to \Re$. A functional $I(u)$ is said to be *linear* in u if and only if it satisfies the relation

$$I(\alpha u + \beta v) = \alpha I(u) + \beta I(v), \quad u, v \in V, \quad \alpha, \beta \in \Re \tag{2.4.21}$$

Here the symbol $\in$ means "an element of." Similarly, a functional $B(u, v)$ is said to be *bilinear* if it is linear in each of its arguments u and v:

$$B(\alpha u_1 + \beta u_2, v) = \alpha B(u_1, v) + \beta B(u_2, v) \text{ linear in the first argument}$$
$$B(u, \alpha v_1 + \beta v_2) = \alpha B(u, v_1) + \beta B(u, v_2) \text{ linear in the second argument} \quad (2.4.22)$$

where u, u_1, u_2, v, v_1, and v_2 are elements from a vector space V and α and β are real numbers. Note that a bilinear functional necessarily contains two arguments (dependent variables), and it must be linear with respect to each argument. A bilinear form is said to be *symmetric* if it satisfies the condition

$$J(\alpha u) = \alpha^2 J(u) \quad (2.4.24)$$

A *quadratic* functional $J(u)$ is one which satisfies the relation

$$J(\alpha u) = \alpha^2 J(u) \quad (2.4.24)$$

for all real numbers α.

Whenever $B(\cdot, \cdot)$ is bilinear and symmetric in its arguments and $\ell(\cdot)$ is linear in its argument, there exists a quadratic functional $I(u)$ defined by

$$I(u) = \frac{1}{2} B(u, u) - \ell(u), \; u \in V \quad (2.4.25)$$

such that seeking its minimum is equivalent to solving the variational problem in Eq. (2.4.20):

$$\delta I = 0 = B(\delta u, u) - \ell(\delta u), \quad \delta^2 I = B(\delta u, \delta u) > 0 \text{ for } \delta u \neq 0$$

Thus, the function u that minimizes $I(u)$ is the solution of Eq. (2.4.20) with $w_i = \delta u$ and $u_n = u$; conversely, the solution of Eq. (2.4.20) minimizes the functional $I(u)$. Mathematical proof of these assertions can be found in the book by Reddy [2, 4].

For solid mechanics problems, $I(u)$ represents the total potential energy functional, and $\delta I = 0$ is the statement of the *principle of the minimum total potential energy*: of all admissible functions u, the one that makes the total potential energy $I(u)$ a minimum also satisfies the differential equation(s) and natural boundary condition(s). In other words, the weak form of a differential equation is the same as the statement of the principle of minimum total potential energy. For problems outside solid mechanics, the functional $I(u)$, if exists, may not have any physical meaning, but it is still useful for mathematical analysis (e.g., in proving the existence and uniqueness of solutions).

As noted earlier, every differential equation admits a weighted-integral

statement, and a weak form exists provided the equation is of order 2 or higher. When the bilinear form is symmetric, we will also have a functional whose first variation set equal to zero is equivalent to the governing equations. However, the traditional variational methods and the finite element method use only an integral statement or a weak form of the equation(s) to be solved.

2.4.6 Examples of Weak Forms and Quadratic Functionals

Here, we consider some representative examples of differential equations in one and two dimensions, and develop their weak forms. These examples are of primary interest in the study of the finite element method in the coming chapters. All problems considered here correspond to one or more physical problems of science and engineering (see Reddy [2] for more details).

Example 2.4.1

Consider the differential equation in Eq. (2.4.1) and the boundary conditions in Eq. (2.4.2). Determine the quadratic functional associated with the problem.

Solution: The weak form for the problem is given by Eq. (2.4.18). It can be easily verified that $B(\cdot, \cdot)$ in Eq. (2.4.19) is bilinear and symmetric in w_i and u_n while $\ell(\cdot)$ is linear in w_i. Hence, the quadratic functional is given by Eq. (2.4.25) (set $w_i = u_n$):

$$I(u_n) = \frac{1}{2}B(u_n, u_n) - \ell(u_n)$$
$$= \frac{1}{2}\int_0^L \left[a\left(\frac{du_n}{dx}\right)^2 + cu_n^2\right]dx + \frac{1}{2}\beta[u_n(L)]^2 - \int_0^L fu_n\,dx - \beta u_n(L)u_\infty - Q_0u_n(L) \tag{2.4.26}$$

The next example illustrates the variational formulation of a fourth-order differential equation governing bending of elastic beams according to the Euler–Bernoulli beam theory (see Reddy [2] for detailed derivations).

Example 2.4.2

The governing equations of the Euler–Bernoulli beam theory [under the Euler-Bernoulli hypothesis that plane sections perpendicular to the axis of the beam before deformation remain (a) plane, (b) inextensible, and (c) perpendicular to the bent axis after deformation] are given by

$$-\frac{dV}{dx} + kw - q = 0, \quad \frac{dM}{dx} - V = 0, \quad 0 < x < L \tag{2.4.27}$$

where $w(x)$ denotes the transverse deflection of the beam, $V(x)$ is the shear force, $M(x)$ is the bending moment, $k(x)$ is the foundation modulus, $q(x)$ is the transverse distributed load, and L is the length of the beam, as shown in Fig. 2.4.3. Using the kinematics and Hooke's law, the bending moment and shear force can be related to the deflection w by

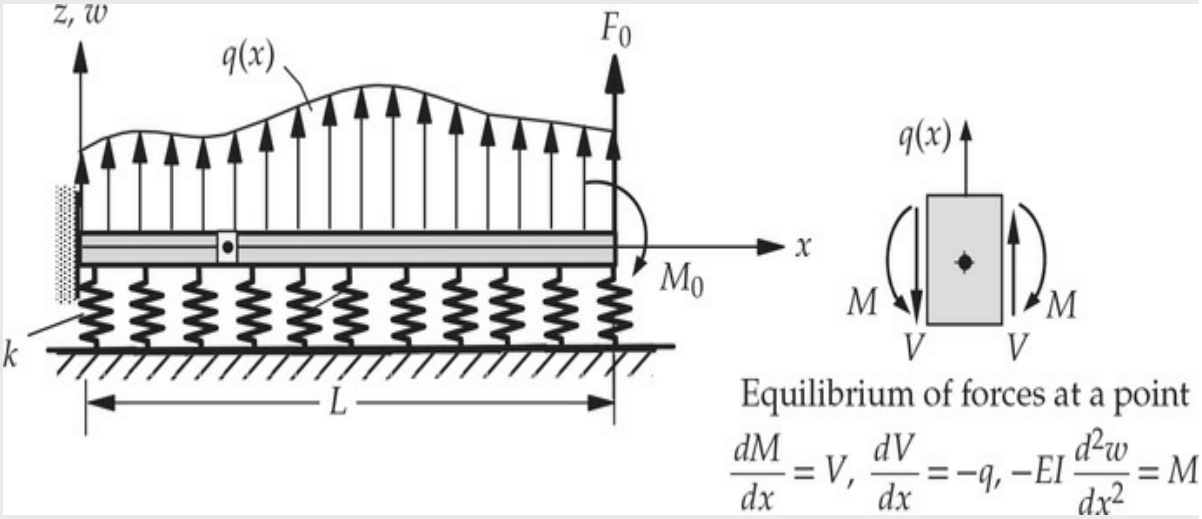

Fig. 2.4.3 A beam on elastic foundation and fixed at the left end, subjected to distributed transverse load, and point force and moment at the right end.

$$M = -EI\frac{d^2w}{dx^2}, \quad V = \frac{dM}{dx} = -\frac{d}{dx}\left(EI\frac{d^2w}{dx^2}\right) \tag{2.4.28}$$

where $E(x)I(x) > 0$ is the flexural rigidity of the beam (i.e., E is the modulus of elasticity and I is the second moment of area about the y-axis). Equations (2.4.27) and (2.4.28) can be combined into a single expression governing the deflection w as

$$\frac{d^2}{dx^2}\left(EI\frac{d^2w}{dx^2}\right) + kw - q = 0, \quad 0 < x < L \tag{2.4.29}$$

If the beam is clamped at the left end and subjected to a transverse point

load F_0 and bending moment M_0 at $x = L$, as indicated in Fig. 2.4.3, develop the weak form of the problem, identify the bilinear and linear forms, and determine the quadratic functional.

Solution: Since the equation contains a fourth-order derivative, we should integrate fourth-derivative term twice by parts to distribute the derivatives equally between the dependent variable w and the weight function v. In this case, v must be twice differentiable and satisfy the homogeneous form of essential boundary conditions. Multiplying Eq. (2.4.27) by v, and integrating the first term by parts twice with respect to x, we obtain

$$\textbf{Step 1:} \quad 0 = \int_0^L v\left[\frac{d^2}{dx^2}\left(EI\frac{d^2w}{dx^2}\right) + kw - q\right] dx$$

$$\textbf{Step 2:} \quad 0 = \int_0^L \left[\left(-\frac{dv}{dx}\right)\frac{d}{dx}\left(EI\frac{d^2w}{dx^2}\right) + kvw - vq\right] dx + \left[v\frac{d}{dx}\left(EI\frac{d^2w}{dx^2}\right)\right]_0^L$$

$$= \int_0^L \left(\frac{d^2v}{dx^2}EI\frac{d^2w}{dx^2} + kvw - vq\right) dx + \left[v\frac{d}{dx}\left(EI\frac{d^2w}{dx^2}\right) - \frac{dv}{dx}EI\frac{d^2w}{dx^2}\right]_0^L \tag{2.4.30}$$

From the last line, it follows that the specification of w and dw/dx constitutes the essential (geometric or static) boundary conditions, and the specification of

$$-\frac{d}{dx}\left(EI\frac{d^2w}{dx^2}\right) \text{ (shear force)} \quad \text{and} \quad -EI\frac{d^2w}{dx^2} \text{ (bending moment)} \tag{2.4.31}$$

constitutes the natural boundary conditions for the Euler–Bernoulli beam theory.

The boundary conditions can be expressed in terms of the deflection w as

$$w(0) = 0, \quad \theta(0) \equiv \left(-\frac{dw}{dx}\right)\Big|_{x=0} = 0$$
$$\left(-EI\frac{d^2w}{dx^2}\right)\Big|_{x=L} = M_0, \quad \left[-\frac{d}{dx}\left(EI\frac{d^2w}{dx^2}\right)\right]_{x=L} = F_0 \tag{2.4.32}$$

where M_0 is the bending moment and F_0 is the transverse load. Since w and $\theta = -dw/dx$ (both are primary variables) are specified at $x = 0$, we require the weight function v and its derivative dv/dx to be zero there:

$$v(0) = \left(\frac{dv}{dx}\right)\Big|_{x=0} = 0$$

The remaining two boundary conditions in Eq. (2.4.32) are natural boundary conditions, which place no restrictions on v and its derivatives.

Step 3: Thus, Eq. (2.4.30) becomes

$$0 = \int_0^L \left(EI\frac{d^2v}{dx^2}\frac{d^2w}{dx^2} + kvw - vq\right)dx - v(L)F_0 + \left(\frac{dv}{dx}\right)\Big|_{x=L} M_0 \qquad (2.4.33)$$

Variational Problem and Quadratic Functional: Equation (2.4.33) can be written in the form

$$B(v, w) = \ell(v) \qquad (2.4.34a)$$

$$B(v, w) = \int_0^L \left(EI\frac{d^2v}{dx^2}\frac{d^2w}{dx^2} + kvw\right)dx$$

$$\ell(v) = \int_0^L v\,q\,dx + v(L)F_0 - \left(\frac{dv}{dx}\right)\Big|_{x=L} M_0 \qquad (2.4.34b)$$

The functional, namely, the total potential energy of the beam, is obtained using

$$I(w) = \int_0^L \left[\frac{EI}{2}\left(\frac{d^2w}{dx^2}\right)^2 + \frac{k}{2}w^2 - wq\right]dx - w(L)F_0 + \left(\frac{dw}{dx}\right)\Big|_{x=L} M_0 \qquad (2.4.35)$$

Note that for the fourth-order equation, the essential boundary conditions involve not only the dependent variable but also its first derivative. As pointed out earlier, at any boundary point, only one of the two boundary conditions (essential or natural) can be specified. For example, if the transverse deflection w is specified at a boundary point then one cannot specify the shear force V at the same point, and vice versa. Similar comments apply to the slope $\theta = -dw/dx$ and the bending moment M. Note that in the present case, w and dw/dx are the primary variables, and V and M are the secondary variables.

The next example is concerned with the weak-form development of a pair of second-order differential equations in one dimension.

Example 2.4.3

Consider the following pair of coupled differential equations governing bending of straight beams according to the Timoshenko beam theory, in which the normality condition (c) of the Euler–Bernoulli beam theory is removed:

$$-\frac{d}{dx}\left[S\left(\frac{dw}{dx}+\phi\right)\right]+kw=q \tag{2.4.36a}$$

$$-\frac{d}{dx}\left(D\frac{d\phi}{dx}\right)+S\left(\frac{dw}{dx}+\phi\right)=0 \tag{2.4.36b}$$

where w is the transverse deflection, ϕ is the rotation of a transverse normal line, S is the shear stiffness ($S = K_s GA$; K_s is the shear correction coefficient, G is the shear modulus, and A is the area of cross section), $D = EI$ is the bending stiffness, k is the foundation modulus, and q is the distributed transverse load. Develop the weak form of the above equations using the three-step procedure, identify the linear and bilinear forms, and determine the associated quadratic functional.

Solution: We use the three-step procedure to each of the two differential equations to develop the weak forms.

Multiply the first equation with weight function v_1 and the second equation with weight function v_2 and integrate over the length of the beam:

Step 1a

$$0=\int_0^L v_1\left\{-\frac{d}{dx}\left[S\left(\frac{dw}{dx}+\phi\right)\right]+kw-q\right\}dx$$

Step 2a

$$\begin{aligned}0&=\int_0^L\left[\frac{dv_1}{dx}S\left(\frac{dw}{dx}+\phi\right)+kv_1w-v_1q\right]dx-\left[v_1\,S\left(\frac{dw}{dx}+\phi\right)\right]_0^L\\&=\int_0^L\left[\frac{dv_1}{dx}S\left(\frac{dw}{dx}+\phi\right)+kv_1w-v_1q\right]dx-v_1(L)\left[S\left(\frac{dw}{dx}+\phi\right)\right]_{x=L}\\&\quad+v_1(0)\left[S\left(\frac{dw}{dx}+\phi\right)\right]_{x=0}\end{aligned} \tag{2.4.37}$$

Step 1b

$$0 = \int_0^L v_2 \left[-\frac{d}{dx}\left(D\frac{d\phi}{dx} \right) + S\left(\frac{dw}{dx} + \phi \right) \right] dx$$

Step 2b

$$0 = \int_0^L \left[D\frac{dv_2}{dx}\frac{d\phi}{dx} + v_2 S\left(\frac{dw}{dx} + \phi \right) \right] dx - \left[v_2 D\frac{d\phi}{dx} \right]_0^L$$

$$= \int_0^L \left[D\frac{dv_2}{dx}\frac{d\phi}{dx} + v_2 S\left(\frac{dw}{dx} + \phi \right) \right] dx - v_2(L)\left[D\frac{d\phi}{dx} \right]_{x=L} + v_2(0)\left[D\frac{d\phi}{dx} \right]_{x=0} \quad (2.4.38)$$

Note that integration by parts was used such that the expression $dw/dx + \phi$ is preserved, as it enters the boundary term representing the shear force. Such considerations can only be used by knowing the mechanics of the problem at hand. Also, note that the pair of weight functions (v_1, v_2) satisfies the homogeneous form of specified essential boundary conditions on the pair (w, ϕ) (with the correspondence $v_1 \sim w$ and $v_2 \sim \phi$).

Step 3 An examination of the boundary terms shows that $w \sim v_1$ and $\phi \sim v_2$ are the primary variables, and the secondary variables are given by

$$S\left(\frac{dw}{dx} + \phi \right) \quad \text{(shear force)}, \qquad D\frac{d\phi}{dx} \quad \text{(bending moment)} \qquad (2.4.39)$$

To finalize the weak forms, we must take care of the boundary terms by considering a specific beam problem. Using the beam of Fig. 2.4.3, we see that $v_1(0) = 0$ and $v_2(0) = 0$, and

$$\left[S\left(\frac{dw}{dx} + \phi \right) \right]_{x=L} = F_0, \quad \left[D\frac{d\phi}{dx} \right]_{x=L} = M_0$$

Consequently, the weak forms in Eqs. (2.4.37) and (2.4.38) become

$$0 = \int_0^L \left[\frac{dv_1}{dx} S\left(\frac{dw}{dx} + \phi \right) + kv_1 w - v_1 q \right] dx - v_1(L) F_0 \qquad (2.4.40a)$$

$$0 = \int_0^L \left[\frac{dv_2}{dx} D\frac{d\phi}{dx} + v_2 S\left(\frac{dw}{dx} + \phi \right) \right] dx - v_2(L) M_0 \qquad (2.4.40b)$$

Variational Problem and Quadratic Functional: To write the variational problem of finding (w, ϕ) such that

$$B((v_1, v_2), (w, \phi)) = \ell((v_1, v_2)) \tag{2.4.41}$$

holds for all (v_1, v_2), we must combine the two weak forms into a single expression

$$0 = \int_0^L \left[\left(\frac{dv_1}{dx} + v_2 \right) S \left(\frac{dw}{dx} + \phi \right) + \frac{dv_2}{dx} D \frac{d\phi}{dx} + k v_1 w - v_1 q \right] dx - v_1(L) F_0 - v_2(L) M_0 \tag{2.4.42}$$

Thus, the bilinear and linear forms of the problem are given by

$$B((v_1, v_2), (w, \phi)) = \int_0^L \left[S \left(\frac{dv_1}{dx} + v_2 \right) \left(\frac{dw}{dx} + \phi \right) + D \frac{dv_2}{dx} \frac{d\phi}{dx} + k v_1 w \right] dx$$

$$\ell((v_1, v_2)) = \int_0^L v_1 \, q \, dx + v_1(L) F_0 + v_2(L) M_0 \tag{2.4.43}$$

Clearly, $B((v_1, v_2), (w, \phi))$ is symmetric in its arguments (i.e., interchange of v_1 with w and v_2 with ϕ yields the same expression). Hence the functional is given by

$$I((w, \phi)) = \frac{1}{2} \int_0^L \left[S \left(\frac{dw}{dx} + \phi \right)^2 + D \left(\frac{d\phi}{dx} \right)^2 + k w^2 \right] dx - \left(\int_0^L w \, q \, dx + w(L) F_0 + \phi(L) M_0 \right) \tag{2.4.44}$$

The first term in I denotes the strain energy stored due to traverse shear deformation, the second terms corresponds to the strain energy stored due to bending, and the third term is associated with the strain energy stored due to elastic foundation. The second line (with a minus sign) is the work done by externally applied loads.

The last example of this section is concerned with a second-order differential equation in two dimensions. The equation arises in a number of fields, including heat transfer, stream function or velocity potential formulation of inviscid flows, transverse deflections of a membrane, and torsion of a cylindrical member.

Example 2.4.4

Consider the problem of determining the solution $u(x, y)$ to the partial

differential equation

$$-\frac{\partial}{\partial x}\left(a_{xx}\frac{\partial u}{\partial x}\right)-\frac{\partial}{\partial y}\left(a_{yy}\frac{\partial u}{\partial y}\right)+a_{00}u=f \quad \text{in } \Omega \tag{2.4.45}$$

in a closed two-dimensional domain Ω with boundary Γ, as shown in Fig. 2.2.4. Here a_{00}, a_{xx}, a_{yy}, and f are known functions of position (x, y) in Ω. The function u is required to satisfy, in addition to the differential equation (2.4.45), the following boundary conditions on the boundary Γ of Ω:

$$u=\hat{u} \text{ on } \Gamma_u, \quad a_{xx}\frac{\partial u}{\partial x}n_x+a_{yy}\frac{\partial u}{\partial y}n_y=\hat{q} \text{ on } \Gamma_q \tag{2.4.46}$$

where the portions Γ_u and Γ_q are such that $\Gamma = \Gamma_u \cup \Gamma_q$, as shown in Fig. 2.2.4. Develop the weak form, identify the linear and bilinear forms, and determine the quadratic functional for the problem.

Solution: The three-step procedure applied to Eq. (2.4.45) yields:

Step 1:
$$0=\int_\Omega w\left[-\frac{\partial}{\partial x}\left(a_{xx}\frac{\partial u}{\partial x}\right)-\frac{\partial}{\partial y}\left(a_{yy}\frac{\partial u}{\partial y}\right)+a_{00}u-f\right]dxdy \tag{2.4.47a}$$

Step 2:
$$0=\int_\Omega\left(a_{xx}\frac{\partial w}{\partial x}\frac{\partial u}{\partial x}+a_{yy}\frac{\partial w}{\partial y}\frac{\partial u}{\partial y}+a_{00}wu-wf\right)dxdy$$
$$-\oint_\Gamma w\left(a_{xx}\frac{\partial u}{\partial x}n_x+a_{yy}\frac{\partial u}{\partial y}n_y\right)ds \tag{2.4.47b}$$

where we used integration by parts [see Eq. (2.2.43)] to transfer the differentiation from u to w so that both u and w have the same order derivatives. The boundary term shows that u is the primary variable while

$$a_{xx}\frac{\partial u}{\partial x}n_x+a_{yy}\frac{\partial u}{\partial y}n_y$$

is the secondary variable.

Step 3: The last step in the procedure is to impose the specified boundary conditions in Eq. (2.4.46). Since u is specified on Γ_u, then the weight function w is zero on Γ_u and arbitrary on Γ_q. Consequently, Eq. (2.4.47b) simplifies to

$$0 = \int_{\Omega} \left(a_{xx} \frac{\partial w}{\partial x} \frac{\partial u}{\partial x} + a_{yy} \frac{\partial w}{\partial y} \frac{\partial u}{\partial y} + a_{00} wu - wf \right) dxdy - \int_{\Gamma_q} w\hat{q}\, ds \qquad (2.4.48)$$

Variational Problem and Quadratic Functional: The weak form in Eq. (2.4.48) can be expressed as $B(w, u) = \ell(w)$, where the bilinear form and linear form are

$$B(w,u) = \int_{\Omega} \left(a_{xx} \frac{\partial w}{\partial x} \frac{\partial u}{\partial x} + a_{yy} \frac{\partial w}{\partial y} \frac{\partial u}{\partial y} + a_{00} wu \right) dxdy$$

$$\ell(w) = \int_{\Omega} w f\, dxdy + \int_{\Gamma_q} w\hat{q}\, ds \qquad (2.4.49)$$

The associated quadratic functional is

$$I(u) = \frac{1}{2} \int_{\Omega} \left[a_{xx} \left(\frac{\partial u}{\partial x} \right)^2 + a_{yy} \left(\frac{\partial u}{\partial y} \right)^2 + a_{00} u^2 \right] dxdy - \int_{\Omega} uf\, dxdy - \int_{\Gamma_q} \hat{q}u\, ds \qquad (2.4.50)$$

In the case of transverse deflections of a membrane (with $a_{00} = 0$), $I(u)$ represents the total potential energy.

2.5 Variational Methods

2.5.1 Introduction

Our objective in this section is to study the variational methods of approximation because they provide a background for the development of finite element models. The methods to be discussed here include the Ritz, Galerkin, and leastsquares methods. In all these methods, we seek an approximate solution in the form of a linear combination of suitable approximation functions ϕ_j and undetermined parameters c_j : $\sum_j c_j \phi_j$, as given in Eq. (2.4.3). The Ritz method uses the weak form, whereas the Galerkin method uses the weighted-integral form (step 1 of the weak-form development) to determine the parameters c_j. The least-squares method is based on the minimization of the integral of the square of the residual in the approximation of the differential equation. Various weighted-residual methods have been already introduced in Section 2.4.3. As we shall see in the coming chapters, finite element models in most cases (especially those

in the commercial codes) are based on an element-wise application of the Ritz method (i.e., the weak-form Galerkin method), which does not require a functional but only the variational statement, such as the one given in Eq. (2.4.20). Finite element models based on weighted-residual methods (e.g., Petrov–Galerkin, collocation, least-squares, and subdomain methods) are not found in commercial codes.

2.5.2 The Ritz Method

2.5.2.1 The basic idea

In the Ritz method, the coefficients c_j of the approximation are determined using the weak form of the problem, and hence, the choice of weight functions is restricted to the approximation functions, $w_i = \phi_i$. Recall that the weak form is equivalent to both the governing differential equation and the natural boundary conditions of the problem; hence, the weak form places weaker continuity requirements on the approximate solution u_n than the original differential equation or its weighted-integral statement. The method is described here for a linear variational problem (which is the same as the weak form).

Consider the variational problem resulting from the weak form: find the solution u such that

$$B(w,u) = \ell(w) \tag{2.5.1}$$

for all sufficiently differentiable functions w_i that satisfy the homogeneous form of specified essential boundary conditions on u. In general, $B(\cdot,\cdot)$ can be unsymmetric in w and u, and it can be even nonlinear in u[$B(\cdot,\cdot)$ is always linear in w]. When $B(\cdot,\cdot)$ is bilinear and symmetric in w and u and $\ell(\cdot)$ is linear, the variational (or weak) form in Eq. (2.5.1) is equivalent to minimization of the quadratic functional

$$I(u) = \frac{1}{2}B(u,u) - \ell(u) \tag{2.5.2}$$

The discrete problem consists of finding an approximate solution u_n such that

$$B(w_i,u_n) = \ell(w_i), \quad i = 1,2,\ldots,n \tag{2.5.3}$$

In the Ritz method, we seek an approximate solution to Eq. (2.5.1) in the form of a finite series [see Eq. (2.5.3)]

$$u_n = \sum_{j=1}^{n} c_j \phi_j + \phi_0 \tag{2.5.4}$$

where the constants $c_1, c_2, \ldots, c_n$, called the *Ritz coefficients*, are determined such that Eq. (2.5.3) holds for n different choices $\{w_i\}$, so that n independent algebraic relations among $c_1, c_2, \ldots, c_n$ are obtained. The functions $\{\phi_i\}$ and ϕ_0, called *approximation functions*, are chosen such that u_n satisfies the specified essential boundary conditions [recall that the specified natural boundary conditions are already included in the variational problem, Eq. (2.5.1), and hence in the functional $I(u_n)$]. The ith algebraic equation is obtained from Eq. (2.5.3) by substituting $w_i = \phi_i$ and u_n from Eq. (2.5.4) [and noting that $B(\cdot, \cdot)$ is bilinear]:

$$B\left(\phi_i, \sum_{j=1}^{n} c_j \phi_j + \phi_0\right) = \ell(\phi_i) \Rightarrow \sum_{j=1}^{n} B(\phi_i, \phi_j) c_j + B(\phi_i, \phi_0) = \ell(\phi_i)$$

or

$$\sum_{j=1}^{n} K_{ij} c_j = F_i, \quad i = 1, 2, \ldots, n \tag{2.5.5}$$

where

$$K_{ij} = B(\phi_i, \phi_j), \quad F_i = \ell(\phi_i) - B(\phi_i, \phi_0) \tag{2.5.6}$$

The algebraic equations in Eq. (2.5.5) can be expressed in matrix form as

$$\mathbf{Kc} = \mathbf{F} \tag{2.5.7}$$

As stated earlier, for symmetric bilinear forms the Ritz method can also be viewed as one that seeks a solution of the form in Eq. (2.5.4) in which the parameters c_j are determined by minimizing the quadratic functional $I(u_n)$. After substituting u_n from Eq. (2.5.4) for u into Eq. (2.5.2) and integrating, the functional I becomes an ordinary function of the parameters $c_1, c_2, \ldots, c_n$. Then the necessary condition for the minimization of $I(c_1, c_2, \ldots, c_n)$ is that its partial derivatives with respect to each of the parameters be zero:

$$\frac{\partial I}{\partial c_1}=0, \quad \frac{\partial I}{\partial c_2}=0, \quad \cdots, \quad \frac{\partial I}{\partial c_n}=0 \tag{2.5.8}$$

Thus there are n linear algebraic equations among unknowns (c_1, c_2, $\cdots$, c_n). These equations are exactly the same as those in Eq. (2.5.6) for all problems for which the variational problem in Eq. (2.5.1) is equivalent to $\delta I = 0$. Of course, when $B(\cdot, \cdot)$ is not symmetric, we do not have a quadratic functional. In other words, Eq. (2.5.5) is more general than (2.5.8), and they are the same when $B(\cdot, \cdot)$ is bilinear and symmetric. In all problems of interest in the present study, we shall have a symmetric bilinear form.

2.5.2.2 Approximation functions

In this section we discuss the properties of the set of approximation functions $\{\phi_i\}$ and ϕ_0 used in the n-parameter Ritz solution in Eq. (2.5.4). First, we note that u_n must satisfy only the specified essential boundary conditions of the problem, since the specified natural boundary conditions are included in the variational problem in Eq. (2.5.1). The particular form of u_n in Eq. (2.5.4) facilitates satisfaction of specified boundary conditions. To see this, suppose that the approximate solution is sought in the form

$$u_n = \sum_{j=1}^{n} c_j \phi_j(x)$$

and suppose that the specified essential boundary condition is $u(x_0) = u_0$. Then u_n must also satisfy the condition $u_n(x_0) = u_0$ at a boundary point $x = x_0$:

$$\sum_{j=1}^{n} c_j \phi_j(x_0) = u_0$$

Since c_j are unknown parameters to be determined, it is not easy to choose $\phi_j(x)$ such that the above relation holds for all c_j. If $u_0 = 0$, then we can select all ϕ_j such that $\phi_j(x_0) = 0$ and satisfy the condition $u_n(x_0) = 0$. By writing the approximate solution u_n in the form Eq. (2.5.4), a sum of a homogeneous part $\sum c_j \phi_j(x)$ and a nonhomogeneous part $\phi_0(x)$, we require $\phi_0(x)$ to satisfy the specified essential boundary conditions while the homogeneous part vanishes at the same boundary point where the essential

boundary condition is specified. This follows from

$$u_n(x_0) = \sum_{j=1}^{n} c_j \phi_j(x_0) + \phi_0(x_0)$$

$$u_0 = \sum_{j=1}^{n} c_j \phi_j(x_0) + u_0 \rightarrow \sum_{j=1}^{n} c_j \phi_j(x_0) = 0$$

which is satisfied, for arbitrary c_j, by choosing $\phi_j(x_0) = 0$.

If all specified essential boundary conditions are homogeneous (i.e., the specified value u_0 is zero), then ϕ_0 is taken to be zero and ϕ_j must still satisfy the homogeneous form of specified essential boundary conditions, $\phi_j(x_0) = 0$, $j = 1, 2, \ldots, n$. Note that the requirement that w_i be zero at the boundary points where the essential boundary conditions are specified is satisfied by the choice $w_i = \phi_i(x)$.

In summary, the approximation functions $\phi_i(x)$ and $\phi_0(x)$ are required to satisfy the following conditions:

1. (a) $\{\phi_i\}_{i=1}^{n}$ must be such that $B(\phi, \phi)$ is defined and nonzero [i.e., ϕ are sufficiently differentiable and integrable as required in the evaluation of $B(\phi_i, \phi_j)$]. (b) ϕ_i must satisfy the homogeneous form of the specified essential boundary conditions of the problem.
2. For any n, the set $\{\phi_i\}_{i=1}^{n}$ along with the columns (and rows) of $B(\phi, \phi)$ must be *linearly independent*.
3. The set $\{\phi_i\}$ must be *complete*. For example, when ϕ_i are algebraic polynomials, completeness requires that the set $\{\phi_i\}$ contain all terms of the lowest order admissible, and up to the highest order desired.
4. The only requirement on ϕ_0 is that it satisfy the specified essential boundary conditions. When the specified essential boundary conditions are zero, then ϕ_0 is identically zero. Also, for completeness reasons, ϕ_0 must be the lowest-order function that satisfies the specified essential boundary conditions.

2.5.2.3 Applications

Here, we consider a few examples of the application of the Ritz method. Because of the closeness of the Ritz method to the weak-form finite

element models, the reader should follow the steps in arriving at the algebraic equations for the unknown coefficients.

Example 2.5.1

Consider the differential equation

$$-\frac{d^2u}{dx^2} - u + x^2 = 0 \quad \text{for} \quad 0 < x < 1 \tag{2.5.9}$$

Determine n-parameter Ritz solutions using algebraic polynomials for the following two sets of boundary conditions:

$$\textbf{Set 1}: \quad u(0) = 0, \quad u(1) = 0 \tag{2.5.10}$$

$$\textbf{Set 2}: \quad u(0) = 0, \quad \left.\frac{du}{dx}\right|_{x=1} = 1 \tag{2.5.11}$$

Numerically evaluate the solutions for n = 1, 2, and 3.

Solution for Set 1 boundary conditions: The bilinear form and the linear functional associated with Eqs. (2.5.9) and (2.5.10) are

$$B(w,u) = \int_0^1 \left(\frac{dw}{dx}\frac{du}{dx} - wu\right) dx, \quad \ell(w) = -\int_0^1 w\,x^2\,dx \tag{2.5.12}$$

Since both of the specified boundary conditions are of the essential type and homogeneous, we have $\phi_0 = 0$. The algebraic equations for this case are given by

$$\sum_{j=1}^{n} K_{ij} c_j = F_i, \quad i = 1, 2, \ldots, n \tag{2.5.13a}$$

$$K_{ij} = B(\phi_i, \phi_j) = \int_0^1 \left(\frac{d\phi_i}{dx}\frac{d\phi_j}{dx} - \phi_i\phi_j\right) dx$$

$$F_i = \ell(\phi_i) = -\int_0^1 \phi_i\,x^2\,dx \tag{2.5.13b}$$

The same result as in Eqs. (2.5.13a) and (2.5.13b) can be obtained by minimizing the quadratic functional $I(u)$ in Eq. (2.4.26) [set a = 1, c = −1, $f = -x^2$, L = 1, Q_0 = 0, and β = 0]:

$$I(u) = \frac{1}{2}\int_0^1 \left[\left(\frac{du}{dx}\right)^2 - u^2 + 2x^2 u\right] dx$$

Substituting for $u \approx u_n$ from Eq. (2.5.4) with $\phi_0 = 0$ into the above functional, we obtain

$$I(c_1, c_2, \ldots, c_n) = \frac{1}{2}\int_0^1 \left[\left(\sum_{j=1}^{n} c_j \frac{d\phi_j}{dx}\right)^2 - \left(\sum_{j=1}^{n} c_j \phi_j\right)^2 + 2x^2\left(\sum_{j=1}^{n} c_j \phi_j\right)\right] dx$$

The necessary condition for the minimum of I, which is a function of n variables $c_1, c_2, \ldots, c_n$, is that its derivative with respect to each of the variables is zero:

$$\frac{\partial I}{\partial c_i} = 0 = \int_0^1 \left[\frac{d\phi_i}{dx}\left(\sum_{j=1}^{n} c_j \frac{d\phi_j}{dx}\right) - \phi_i\left(\sum_{j=1}^{n} c_j \phi_j\right) + \phi_i x^2\right] dx$$

$$0 = \sum_{j=1}^{n}\left[\int_0^1 \left(\frac{d\phi_i}{dx}\frac{d\phi_j}{dx} - \phi_i \phi_j\right) dx\right] c_j + \int_0^1 \phi_i x^2\, dx$$

$$= \sum_{j=1}^{n} K_{ij} c_j - F_i \quad \text{for } i = 1, 2, \ldots, n \tag{2.5.14}$$

Clearly, *Kij* and *Fi* are the same as those defined in Eq. (2.5.13b).

Next we discuss the choice of ϕ_i, which are required to satisfy the conditions $\phi_i(0) = \phi_i(1) = 0$. Clearly, the polynomial $(0 - x)(1 - x)$ vanishes at $x = 0$ and $x = 1$, and its first derivative is nonzero. Hence, we take $\phi 1 = x(1 - x)$. The next function in the sequence of complete functions is obviously $\phi_2 = x_2(1 - x)$ [or $\phi_2 = x(1 - x)^2$]. Thus, the following set of functions are admissible:

$$\phi_1 = x(1-x),\ \phi_2 = x^2(1-x), \ldots,\ \phi_i = x^i(1-x), \ldots,\ \phi_n = x^n(1-x) \tag{2.5.15}$$

The approximations

$$u_n = c_1 x(1-x) + c_2 x^2(1-x) + \cdots + c_n x^n(1-x) \tag{2.5.16a}$$

$$u_n = \hat{c}_1 x(1-x) + \hat{c}_2 x(1-x)^2 + \cdots + \hat{c}_n x(1-x)^n \tag{2.5.16b}$$

are equivalent. It should be noted that if one selects, for example, the functions $\phi_1 = x_2(1 - x)$, $\phi_2 = x_3(1 - x)$, and so on [not including $x(1 - x)$], the completeness requirement is violated, because the set cannot be

used to generate the linear term x of the exact solution, if the solution has such a term. As a rule (to achieve convergence of the solution with increasing number of terms in the sequence) one must start with the lowest-order admissible function and include all admissible higher-order functions up to the desired degree.

For the choice of approximation functions in Eq. (2.5.15), the matrix coefficients K_{ij} and vector coefficients F_i of Eq. (2.5.13b) can be computed as follows:

$$K_{ij} = \int_0^1 \{[ix^{i-1} - (i+1)x^i][jx^{j-1} - (j+1)x^j] - (x^i - x^{i+1})(x^j - x^{j+1})\}dx$$

$$= \frac{2ij}{(i+j)[(i+j)^2 - 1]} - \frac{2}{(i+j+1)(i+j+2)(i+j+3)} \tag{2.5.17a}$$

$$F_i = -\int_0^1 x^2(x^i - x^{i+1})dx = -\frac{1}{(i+3)(i+4)} \tag{2.5.17b}$$

for $i, j = 1, 2, \ldots, n$.

Next, we consider the one-, two-, and three-parameter approximations to illustrate how the Ritz solution converges to the exact solution of the problem [the reader may verify this by solving Eq. (2.5.9) subject to the boundary conditions in Eq. (2.5.10)]:

$$u(x) = \frac{\sin x + 2\sin(1-x)}{\sin 1} + x^2 - 2 \tag{2.5.18}$$

For $n = 1$, we have

$$K_{11} = \frac{3}{10}, \quad F_1 = -\frac{1}{20} \quad \rightarrow \quad c_1 = -\frac{1}{6} = -0.1667$$

The one-parameter Ritz solution is given by

$$u_1(x) = c_1\phi_1(x) = -\tfrac{1}{6}(x - x^2)$$

For $n = 2$, we have

$$\frac{1}{420}\begin{bmatrix} 126 & 63 \\ 63 & 52 \end{bmatrix}\begin{Bmatrix} c_1 \\ c_2 \end{Bmatrix} = -\frac{1}{60}\begin{Bmatrix} 3 \\ 2 \end{Bmatrix}$$

Solving the linear equations using Cramer's rule, we obtain

$$c_1 = -\frac{10}{123} = -0.0813, \quad c_2 = -\frac{21}{123} = -0.1707$$

The two-parameter Ritz solution is given by

$$u_2(x) = c_1\phi_1(x) + c_2\phi_2(x) = -0.0813(x - x^2) - 0.1707(x^2 - x^3)$$
$$= -0.0813x - 0.0894x^2 + 0.1707x^3$$

For $n = 3$, we have

$$\frac{1}{2520}\begin{bmatrix} 756 & 378 & 228 \\ 378 & 312 & 237 \\ 228 & 237 & 206 \end{bmatrix}\begin{Bmatrix} c_1 \\ c_2 \\ c_3 \end{Bmatrix} = -\frac{1}{420}\begin{Bmatrix} 21 \\ 14 \\ 10 \end{Bmatrix}$$

Note that the previously computed coefficients K_{ij} and F_i for $i, j = 1, 2$ remain unchanged and we only need to compute K_3i, $i = 1, 2, 3$ and F_3. The solution of the above equations is

$$c_1 = -0.0952, \quad c_2 = -0.1005, \quad c_3 = -0.0702$$

The three-parameter Ritz solution is given by

$$u_3(x) = c_1\phi_1(x) + c_2\phi_2(x) + c_3\phi_3(x)$$
$$= -0.0952(x - x^2) - 0.1005(x^2 - x^3) - 0.0702(x^3 - x^4)$$
$$= -0.0952x - 0.0053x^2 + 0.0303x^3 + 0.0702x^4$$

The values of the Ritz coefficients c_i, $i = 1, 2, \ldots, n$ for various values of n can be obtained by solving the matrix equation **Kc** = **F** with the coefficients *Kij* and *Fi* given by Eqs. (2.5.17a) and (2.5.17b). The Ritz coefficients and a comparison of the Ritz solution with the exact solution (2.5.18) are presented in Fig. 2.5.1 and Table 2.5.1. If the exact solution in Eq. (2.5.18) is expanded in a series in terms of powers of x, we note that it is an infinite series. However, the three-parameter Ritz solution is already a good approximation of the exact solution, as can be seen from Fig. 2.5.1.

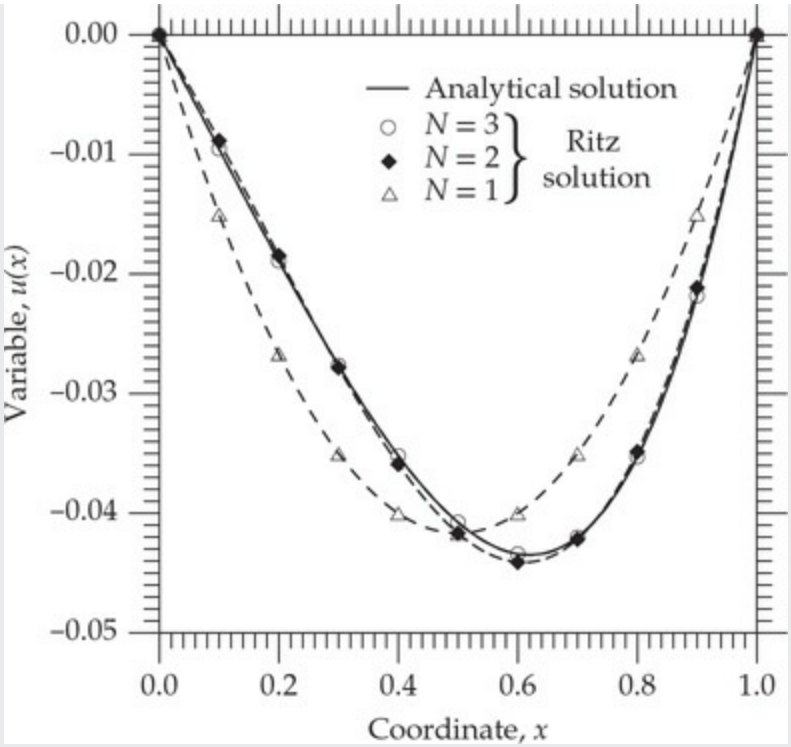

Fig. 2.5.1 Comparison of the Ritz solution with the exact solution of Eqs. (2.5.9) and (2.5.10) (the three-parameter Ritz solution and the exact solution do not differ on the scale of the plot).

Table 2.5.1 Comparison of the Ritz solution with the exact solution of

$$-\frac{d^2u}{dx^2} - u + x^2 = 0, \quad 0 < x < 1; \quad u(0) = u(1) = 0.$$

Ritz coefficients†			Ritz solution, $-10u$			Exact solution
n	c_i	x	$n=1$	$n=2$	$n=3$	
$n=1$:	$c_1=-0.1667$	0.0	0.0000	0.0000	0.0000	0.0000
		0.1	0.1500	0.0885	0.0954	0.0955
		0.2	0.2667	0.1847	0.1890	0.1890
$n=2$:	$c_1=-0.0813$	0.3	0.3500	0.2783	0.2766	0.2764
	$c_2=-0.1707$	0.4	0.4000	0.3590	0.3520	0.3518
		0.5	0.4167	0.4167	0.4076	0.4076
$n=3$:	$c_1=-0.0952$	0.6	0.4000	0.4410	0.4340	0.4342
	$c_2=-0.1005$	0.7	0.3500	0.4217	0.4200	0.4203
	$c_3=-0.0702$	0.8	0.2667	0.3486	0.3529	0.3530
		0.9	0.1500	0.2115	0.2183	0.2182
		1.0	0.0000	0.0000	0.0000	0.0000

†The four-parameter Ritz solution coincides with the exact solution up to four decimal places.

Solution for Set 2 boundary conditions: For the second set of boundary conditions in Eq. (2.5.11), the bilinear form is the same as that given in Eq. (2.5.1). The linear form and F_i are given by

$$\ell(w) = -\int_0^1 w\,x^2\,dx + w(1) \tag{2.5.19a}$$

$$F_i = -\int_0^1 x^2\,\phi_i(x)\,dx + \phi_i(1) \tag{2.5.19b}$$

The approximation function ϕ_0 is still zero because the specified essential boundary condition is zero; ϕ_i must be selected to satisfy the condition $\phi_i(0) = 0$. Clearly, $\phi_1(x) = x$, $\phi_2(x) = x^2$, $\cdots$, $\phi_n(x) = x^n$ meet the requirement. Thus, we have

$$u_n(x) = c_1 x + c_2 x^2 + \cdots + c_i x^i + \cdots + c_n x^n \tag{2.5.20}$$

The coefficients K_{ij} and F_i can be evaluated as

$$\begin{aligned} K_{ij} &= \int_0^1 (ijx^{i+j-2} - x^{i+j})\,dx = \frac{ij}{i+j-1} - \frac{1}{i+j+1} \\ F_i &= -\int_0^1 x^{i+2}\,dx + 1 = -\frac{1}{i+3} + 1 \end{aligned} \tag{2.5.21}$$

For example, for $n = 2$ we have

$$\frac{1}{60}\begin{bmatrix} 40 & 45 \\ 45 & 68 \end{bmatrix}\begin{Bmatrix} c_1 \\ c_2 \end{Bmatrix} = \frac{1}{20}\begin{Bmatrix} 15 \\ 16 \end{Bmatrix}$$

Solving the linear equations using Cramer's rule, we obtain

$$c_1 = \frac{180}{139} = 1.2950, \quad c_2 = -\frac{21}{139} = -0.1511$$

The two-parameter Ritz solution is given by

$$u_2 = c_1\phi_1 + c_2\phi_2 = 1.2950\,x - 0.1511\,x^2 \tag{2.5.22}$$

The exact solution for this case is given by

$$u(x) = \frac{2\cos(1-x) - \sin x}{\cos 1} + x^2 - 2 \tag{2.5.23}$$

A comparison of the Ritz solutions with the exact solution is presented in Table 2.5.2.

Table 2.5.2 Comparison of the Ritz solution in Eq. (2.5.22) with the exact solution in Eq. (2.5.23) of

$$-\frac{d^2u}{dx^2} - u + x^2 = 0,\ \ 0 < x < 1;\ \ u(0) = 0,\ \ \left(\frac{du}{dx}\right)\Big|_{x=1} = 1.$$

Ritz coefficients†			Ritz solution, $-10u$			Exact solution
n	c_i	x	$n=1$	$n=2$	$n=3$	
$n=1$:	$c_1 = 1.1250$	0.0	0.0000	0.0000	0.0000	0.0000
		0.1	0.1125	0.1280	0.1271	0.1262
		0.2	0.2250	0.2530	0.2519	0.2513
$n=2$:	$c_1 = 1.2950$	0.3	0.3375	0.3749	0.3740	0.3742
	$c_2 = -0.1511$	0.4	0.4500	0.4938	0.4934	0.4944
		0.5	0.5625	0.6097	0.6099	0.6112
$n=3$:	$c_1 = 1.2831$	0.6	0.6750	0.7226	0.7234	0.7244
	$c_2 = -0.1142$	0.7	0.7875	0.8325	0.8337	0.8340
	$c_3 = -0.0246$	0.8	0.9000	0.9393	0.9407	0.9402
		0.9	1.0125	1.0431	1.0443	1.0433
		1.0	1.1250	1.1439	1.1442	1.1442

†The four-parameter Ritz solution coincides with the exact solution.

Example 2.5.2

Consider the problem of finding the transverse deflection of a cantilever beam under a uniform transverse load of intensity q_0 per unit length and subjected to point load F_0 and bending moment M_0 at the free end (see **Example 2.3.6** for details). The governing equations according to the Euler–Bernoulli beam theory are

$$\frac{d^2}{dx^2}\left(EI\frac{d^2w}{dx^2}\right) - q_0 = 0 \ \text{ for } \ 0 < x < L, EI > 0 \tag{2.5.24}$$

$$w(0) = \left(\frac{dw}{dx}\right)\Big|_{x=0} = 0,\ \ \left(EI\frac{d^2w}{dx^2}\right)\Big|_{x=L} = -M_0,\ \ \left[\frac{d}{dx}\left(EI\frac{d^2w}{dx^2}\right)\right]\Big|_{x=L} = F_0 \tag{2.5.25}$$

The weak form of Eq. (2.5.24) subjected to the boundary conditions in Eq. (2.5.25) (which includes the specified natural boundary conditions)

was derived in **Example 2.4.2**, and is given by Eq. (2.4.33). Determine an n-parameter Ritz solution using algebraic polynomials and specialize the results for $n = 1$, 2, and 3.

Solution: We construct an n-parameter Ritz solution using the weak form in Eq. (2.4.33). Since the specified essential boundary conditions are homogeneous, $w(0) = 0$ and $(dw/dx)|_{x=0} = 0$, we set $\phi_0 = 0$. Next, we select algebraic approximation functions ϕ_i to satisfy the continuity conditions and homogeneous form of the specified essential boundary conditions. The lowest-order algebraic function that meets these conditions is $\phi_1 = x_2$. The next function in the sequence is $\phi_2 = x_3$. Thus we have the complete sequence

$$\phi_1 = x^2,\ \phi_2 = x^3,\ \ldots,\ \phi_i = x^{i+1},\ \ldots,\ \phi_n = x^{n+1} \tag{2.5.26}$$

The n-parameter Ritz approximation is

$$w_n(x) = \sum_{j=1}^{n} c_j \phi_j, \quad \phi_j = x^{j+1} \tag{2.5.27}$$

Substituting Eq. (2.5.27) for w and $v = \phi_i$ into Eq. (2.4.33), we obtain

$$\mathbf{Kc} = \mathbf{F} \tag{2.5.28a}$$

$$\begin{aligned} K_{ij} = B(\phi_i, \phi_j) &= \int_0^L EI(i+1)ix^{i-1}(j+1)jx^{j-1}\,dx \\ &= EI(L)^{i+j-1}\,\frac{ij(i+1)(j+1)}{(i+j-1)} \end{aligned} \tag{2.5.28b}$$

$$\begin{aligned} F_i = \ell(\phi_i) &= \int_0^L q_0 x^{i+1}\,dx + (L)^{i+1}F_0 - (i+1)(L)^i M_0 \\ &= q_0(L)^{i+2}\,\frac{1}{i+2} + (L)^{i+1}F_0 - (i+1)(L)^i M_0 \end{aligned} \tag{2.5.28c}$$

For $n = 1$, Eq. (2.5.28a) gives

$$c_1 = \left(\frac{q_0 L^4}{12EI} + \frac{F_0 L^3}{4EI} - \frac{M_0 L}{2EI}\right)$$

and the one-parameter Ritz solution is

$$w_1(x) = \left(\frac{q_0 L^4}{12EI} + \frac{F_0 L^3}{4EI} - \frac{M_0 L}{2EI} \right) \frac{x^2}{L^2} \tag{2.5.29}$$

For $n = 2$, we have

$$EI \begin{bmatrix} 4L & 6L^2 \\ 6L^2 & 12L^3 \end{bmatrix} \begin{Bmatrix} c_1 \\ c_2 \end{Bmatrix} = \frac{q_0 L^3}{12} \begin{Bmatrix} 4 \\ 3L \end{Bmatrix} + F_0 L^2 \begin{Bmatrix} 1 \\ L \end{Bmatrix} - M_0 L \begin{Bmatrix} 2 \\ 3L \end{Bmatrix}$$

Solving for c_1 and c_2, we obtain

$$c_1 = \frac{1}{24EI} (5q_0 L^2 + 12F_0 L - 12M_0), \quad c_2 = -\frac{1}{12EI} (q_0 L + 2F_0)$$

and the solution in Eq. (2.5.27) becomes

$$w_2(x) = \frac{q_0 L^4}{24EI} \left(5\frac{x^2}{L^2} - 2\frac{x^3}{L^3} \right) + \frac{F_0 L^3}{6EI} \left(3\frac{x^2}{L^2} - \frac{x^3}{L^3} \right) - \frac{M_0 L^2}{2EI} \frac{x^2}{L^2} \tag{2.5.30}$$

For $n = 3$, we obtain the matrix equation

$$EI \begin{bmatrix} 4 & 6L & 8L^2 \\ 6L & 12L^2 & 18L^3 \\ 8L^2 & 18L^2 & \frac{144}{5} L^4 \end{bmatrix} \begin{Bmatrix} c_1 \\ c_2 \\ c_3 \end{Bmatrix} = \frac{q_0 L^3}{60} \begin{Bmatrix} 20 \\ 15L \\ 12L^2 \end{Bmatrix} + F_0 L^2 \begin{Bmatrix} 1 \\ L \\ L^2 \end{Bmatrix} - M_0 L \begin{Bmatrix} 2 \\ 3L \\ 4L^2 \end{Bmatrix}$$

The solution of these equations when substituted into Eq. (2.5.27) for $N = 3$ gives

$$w_3(x) = \frac{q_0 L^4}{24EI} \frac{x^2}{L^2} \left(6 - 4\frac{x}{L} + \frac{x^2}{L^2} \right) + \frac{FL^3}{6EI} \left(3\frac{x^2}{L^2} - \frac{x^3}{L^3} \right) - \frac{M_0 L^2}{2EI} \frac{x^2}{L^2} \tag{2.5.31}$$

which coincides with the exact solution of Eqs. (2.5.24) and (2.5.25). Note that the oneparameter solution is exact when the beam is subjected to end moment M_0 only; the two-parameter solution is exact when the beam is subjected to both F_0 and M_0. If we try to compute the four-parameter solution without knowing that the three-parameter solution is exact for a beam subjected to distributed load q_0, point load F_0, and bending moment M_0, the parameters c_j ($j > 3$) will be zero.

Example 2.5.3

Consider the following partial differential equation governing two-dimensional heat transfer in a square region:

$$-k\left(\frac{\partial^2 T}{\partial x^2}+\frac{\partial^2 T}{\partial y^2}\right)=g_0 \quad \text{in} \quad \Omega=\{(x,y):0<(x,y)<1\} \tag{2.5.32}$$

with the following boundary conditions:

$$T=0 \quad \text{on sides } x=1 \quad \text{and} \quad y=1 \tag{2.5.33a}$$

$$\frac{\partial T}{\partial n}=0 \quad \text{on sides } x=0 \quad \text{and} \quad y=0 \tag{2.5.33b}$$

where g_0 is the rate of uniform heat generation in the region. Equation (2.5.32) is called generalized Poisson's equation (the standard Poisson's equation is $-\nabla^2 T = g_0$). Determine an n-parameter Ritz solution of the form

$$T_n=\sum_{i,j=1}^{n} c_{ij}\cos\alpha_i x\,\cos\alpha_j y, \quad \alpha_i=\frac{1}{2}(2i-1)\pi \tag{2.5.34}$$

Note that Eq. (2.5.34) involves a double summation.

Solution: The variational problem is of the form (see **Example 2.4.4**; set $u = T$, $a_1 = a_2 = k$, $a_0 = 0$, and $f = g_0$)

$$B(w,T)=\ell(w) \tag{2.5.35a}$$

$$B(w,T)=\int_0^1\int_0^1 k\left(\frac{\partial w}{\partial x}\frac{\partial T}{\partial x}+\frac{\partial w}{\partial y}\frac{\partial T}{\partial y}\right)dx\,dy$$

$$\ell(v)=\int_0^1\int_0^1 wg_0\,dx\,dy \tag{2.5.35b}$$

Note that the series in Eq. (2.5.34) involves a double summation, and the approximation functions have double subscripts, $\phi_{ij}(x, y) = \cos\alpha_i x \cos\alpha_j y$. Since the boundary conditions are homogeneous, we take $\phi_0 = 0$. Incidentally, ϕ_{ij} also satisfies the natural boundary conditions of the problem but that is not necessary to be admissible. While the choice $\hat{\phi}_{ij} = \sin i\pi x \sin j\pi y$ meets the essential boundary conditions, it is not

complete, because it cannot be used to generate the solution that *does not* vanish on the sides $x = 0$ and $y = 0$. Hence, $\hat{\phi}_i$ are not admissible.

The coefficients K_{ij} and F_i can be computed by substituting Eq. (2.5.34) into Eq. (2.5.35b). Since the double Fourier series has two summations, we introduce the notation

$$\begin{aligned} K_{(ij)(k\ell)} &= k\int_0^1\int_0^1 [(\alpha_i \sin\alpha_i x\cos\alpha_j y)(\alpha_k \sin\alpha_k x\cos\alpha_l y) \\ &\quad + (\alpha_j \cos\alpha_i x\sin\alpha_j y)(\alpha_\ell \cos\alpha_k x\sin\alpha_\ell y)]dxdy \\ &= \begin{cases} 0 & \text{if } i\neq k \text{ or } j\neq \ell \\ \frac{1}{4}k(\alpha_i^2+\alpha_j^2) & \text{if } i=k \text{ and } j=\ell \end{cases} \end{aligned} \tag{2.5.36a}$$

$$F_{ij} = g_0\int_0^1\int_0^1 \cos\alpha_i x\cos\alpha_j y\,dxdy = \frac{g_0}{\alpha_i\alpha_j}\sin\alpha_i\ \sin\alpha_j \tag{2.5.36b}$$

In evaluating the integrals, the following orthogonality conditions were used

$$\int_0^1 \sin\alpha_i x\ \sin\alpha_j x\,dx = \begin{cases} 0 & \text{if } i\neq j \\ \frac{1}{2} & \text{if } i=j \end{cases}$$

$$\int_0^1 \cos\alpha_i x\cos\alpha_j x\,dx = \begin{cases} 0 & \text{if } i\neq j \\ \frac{1}{2} & \text{if } i=j \end{cases}$$

Owing to the diagonal form of the coefficient matrix in Eq. (2.5.36a), we can readily solve for the coefficients c_{ij} (no sum on repeated indices):

$$c_{ij} = \frac{F_{ij}}{K_{(ij)(ij)}} = \frac{4g_0}{k}\frac{\sin\alpha_i\sin\alpha_j}{(\alpha_i^2+\alpha_j^2)\alpha_i\alpha_j} \tag{2.5.37}$$

The oneand two-parameter Ritz solutions are (the one-parameter solution has one term but the two-parameter solution has four terms)

$$T_1(x,y) = \frac{32g_0}{k\pi^4}\cos\tfrac{1}{2}\pi x\cos\tfrac{1}{2}\pi y \tag{2.5.38a}$$

$$\begin{aligned} T_2(x,y) = \frac{g_0}{k}\Big[&0.3285\cos\tfrac{1}{2}\pi x\cos\tfrac{1}{2}\pi y - 0.0219\Big(\cos\tfrac{1}{2}\pi x\cos\tfrac{3}{2}\pi y \\ &+ \cos\frac{3}{2}\pi x\cos\tfrac{1}{2}\pi y\Big) + 0.0041\cos\tfrac{3}{2}\pi x\cos\tfrac{3}{2}\pi y\Big] \end{aligned} \tag{2.5.38b}$$

If algebraic polynomials are to be used in the approximation of T, one can choose $\phi_1 = (1 - x)(1 - y)$ or $\phi_1 = (1 - x^2)(1 - y^2)$, both of which satisfy the (homogeneous) essential boundary conditions. However, the choice $\phi_1 = (1 - x^2)(1 - y^2)$ also meets the natural boundary conditions of the problem. The one-parameter Ritz solution for the choice $\phi 1 = (1 - x^2)(1 - y^2)$ is (see **Problem 2.18**)

$$T_1(x, y) = \frac{5g_0}{16k}(1 - x^2)(1 - y^2) \tag{2.5.39}$$

The exact solution of Eqs. (2.5.32), (2.5.33a), and (2.5.33b) is

$$T(x, y) = \frac{g_0}{2k}\left[(1 - y^2) + 4\sum_{n=1}^{\infty} \frac{(-1)^n \cos \alpha_n y \cosh \alpha_n x}{\alpha_n^3 \cosh \alpha_n}\right] \tag{2.5.40}$$

where $\alpha_n = \frac{1}{2}(2n - 1)\pi$. The Ritz solutions in Eqs. (2.5.38a), (2.5.38b), and (2.5.39) are compared with the exact solution in Eq. (2.5.40) in Fig. 2.5.2. The analytical solution is evaluated using 50 terms of the series in Eq. (2.5.40).

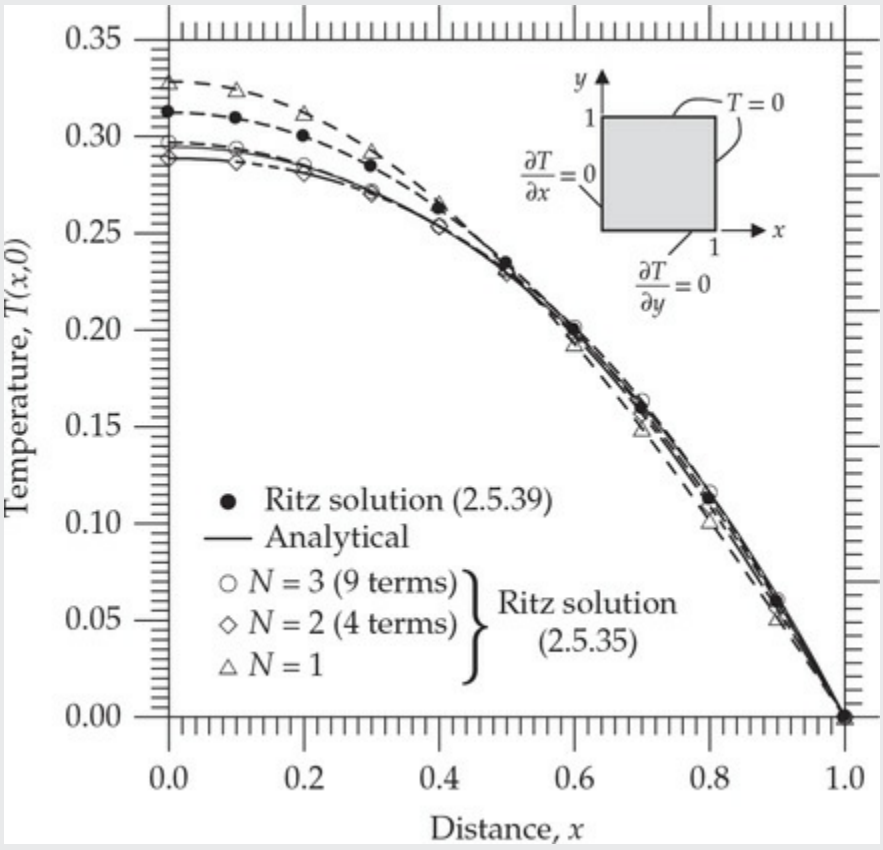

Fig. 2.5.2 Comparison of the Ritz solutions with the analytical solution of the Poisson equation in Eq. (2.5.32) with boundary conditions in Eqs.

(2.5.33a) and (2.5.33b) in two dimensions.

The next example deals with axial vibration of a bar (see Reddy [2]).

Example 2.5.4

Consider a uniform cross-section (A) bar of length L and modulus E, with the left end fixed and the right end connected to a rigid support via a linear elastic spring (with spring constant k), as shown in Fig. 2.5.3. Determine the first two natural axial frequencies, ?, of the bar using the Ritz method.

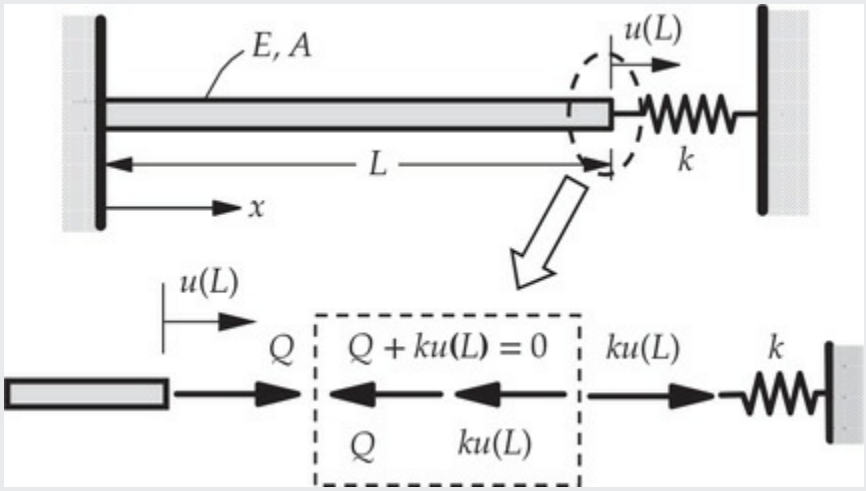

Fig. 2.5.3 A uniform bar with an end spring.

Solution: The differential equation and boundary conditions associated with the natural axial vibrations of a bar are:

$$-\frac{d}{dx}\left(EA\frac{du}{dx}\right) - \rho A\omega^2 u = 0, \quad 0 < x < L \tag{2.5.41}$$

$$u(0) = 0, \quad EA\frac{du}{dx} + ku = 0 \quad \text{at } x = L \tag{2.5.42}$$

The three-step procedure can be used to obtain the weak form

$$0 = \int_0^L \left(EA\frac{dw}{dx}\frac{du}{dx} - \rho A\omega^2 wu\right)dx + kw(L)u(L) \tag{2.5.43}$$

where w is the weight function. Clearly, $u(0) = 0$ is the essential boundary condition of the problem.

Next, we seek a n-parameter Ritz approximation (obviously, $\phi_0 = 0$)

$$u(x) \approx u_n(x) = \sum_{j=1}^{n} c_j \phi_j(x) \tag{2.5.44}$$

Substituting into Eq. (2.5.43), we obtain

$$0 = \sum_{j=1}^{n} \left[-\lambda \int_0^L \rho A \phi_i \phi_j \, dx + \left(\int_0^L EA \frac{d\phi_i}{dx} \frac{d\phi_j}{dx} \, dx + k\phi_i(L)\phi_j(L) \right) \right] c_j \tag{2.5.45}$$

where λ = ?2. In matrix form, we have

$$(\mathbf{A} - \lambda \mathbf{M})\,\mathbf{c} = 0 \tag{2.5.46}$$

where

$$A_{ij} = \int_0^L EA \frac{d\phi_i}{dx} \frac{d\phi_j}{dx} \, dx + k\phi_i(L)\phi_j(L), \quad M_{ij} = \int_0^L \rho A \phi_i \phi_j \, dx \tag{2.5.47}$$

Equation (2.5.46) represents a matrix eigenvalue problem of order $n \times n$ and we obtain n eigenvalues, λ_i, $i = 1, 2, \ldots, n$, by solving the eigenvalue problem.

For the problem at hand, the approximation functions $\phi_i(x)$ are required to be differentiable once with respect to x and vanish at $x = 0$. Hence, we choose

$$\phi_i(x) = \left(\frac{x}{L} \right)^i \tag{2.5.48}$$

Substituting ϕ_i from Eq. (2.5.48) into Eq. (2.5.47), we obtain

$$\begin{aligned} M_{ij} &= \int_0^L \rho A \phi_i \phi_j \, dx = \rho AL \left(\frac{1}{i+j+1} \right) \\ A_{ij} &= \int_0^L EA \frac{d\phi_i}{dx} \frac{d\phi_j}{dx} \, dx + k\phi_i(L)\phi_j(L) = \frac{EI}{L} \left(\frac{ij}{i+j-1} \right) + k \end{aligned} \tag{2.5.49}$$

Since we wish to determine two eigenvalues, we take $n = 2$ and obtain

$$M_{11}=\frac{\rho AL}{3},\quad M_{12}=\frac{\rho AL}{4},\quad M_{22}=\frac{\rho AL}{5}$$
$$A_{11}=\frac{EA}{L}+k,\quad A_{12}=\frac{EA}{L}+k,\quad A_{22}=\frac{4EI}{3L}+k$$

and the matrix eigenvalue problem in Eq. (2.5.46) becomes

$$\left(\frac{EA}{3L}\begin{bmatrix}3+3\alpha & 3+3\alpha\\ 3+3\alpha & 4+3\alpha\end{bmatrix}-\lambda\frac{\rho AL}{60}\begin{bmatrix}20 & 15\\ 15 & 12\end{bmatrix}\right)\begin{Bmatrix}c_1\\ c_2\end{Bmatrix}=\begin{Bmatrix}0\\ 0\end{Bmatrix} \tag{2.5.50}$$

where $\alpha = kL/EA$. The algebraic eigenvalue problem in Eq. (2.5.50) must be solved for $\lambda = \omega^2$ and c_i (hence, for the mode shape $u(x)$).

To carry out the remaining steps to obtain the numerical values for the natural frequencies, we take $\alpha = kL/EA = 1$. Then, for a nontrivial solution (i.e., $c_1 \neq 0$, $c_2 \neq 0$), we set the determinant of the coefficient matrix in Eq. (2.5.50) to zero:

$$\begin{vmatrix}2-\frac{\bar{\lambda}}{3} & 2-\frac{\bar{\lambda}}{4}\\ 2-\frac{\bar{\lambda}}{4} & \frac{7}{3}-\frac{\bar{\lambda}}{5}\end{vmatrix}=0,\quad \bar{\lambda}=\frac{\lambda\rho L^2}{E}=\frac{\omega^2\rho L^2}{E}$$

or

$$15\bar{\lambda}^2-640\bar{\lambda}+2400=0$$

The quadratic equation has two roots

$$\bar{\lambda}_1=4.1545,\quad \bar{\lambda}_2=38.512\ \rightarrow\ \omega_1=\frac{2.038}{L}\sqrt{\frac{E}{\rho}},\quad \omega_2=\frac{6.206}{L}\sqrt{\frac{E}{\rho}}$$

The eigenvectors (or mode shapes) are given by

$$u_2^{(i)}=c_1^{(i)}\frac{x}{L}+c_2^{(i)}\frac{x^2}{L^2}$$

where $c_1^{(i)}$ and $c_2^{(i)}$ are calculated from the equations [see Eq. (2.5.50)]

$$\begin{bmatrix}2-\frac{\bar{\lambda}_i}{3} & 2-\frac{\bar{\lambda}_i}{4}\\ 2-\frac{\bar{\lambda}_i}{4} & \frac{7}{3}-\frac{\bar{\lambda}_i}{5}\end{bmatrix}\begin{Bmatrix}c_1^{(1)}\\ c_2^{(1)}\end{Bmatrix}=\begin{Bmatrix}0\\ 0\end{Bmatrix}$$

The above pair of equations is linearly dependent. Hence, one of the two equations can be used to determine c_2 in terms of c_1 (or vice versa) for each value of λ. We obtain

$$\bar{\lambda}_1 = 4.1545: \quad c_1^{(1)} = 1.0000, \quad c_2^{(1)} = -0.6399 \quad \rightarrow \quad u_2^{(1)}(x) = \frac{x}{L} - 0.6399\frac{x^2}{L^2}$$

$$\bar{\lambda}_2 = 38.512: \quad c_1^{(1)} = 1.0000, \quad c_2^{(1)} = -1.4207 \quad \rightarrow \quad u_2^{(2)}(x) = \frac{x}{L} - 1.4207\frac{x^2}{L^2}$$

Plots of the two mode shapes are shown in Fig. 2.5.4.

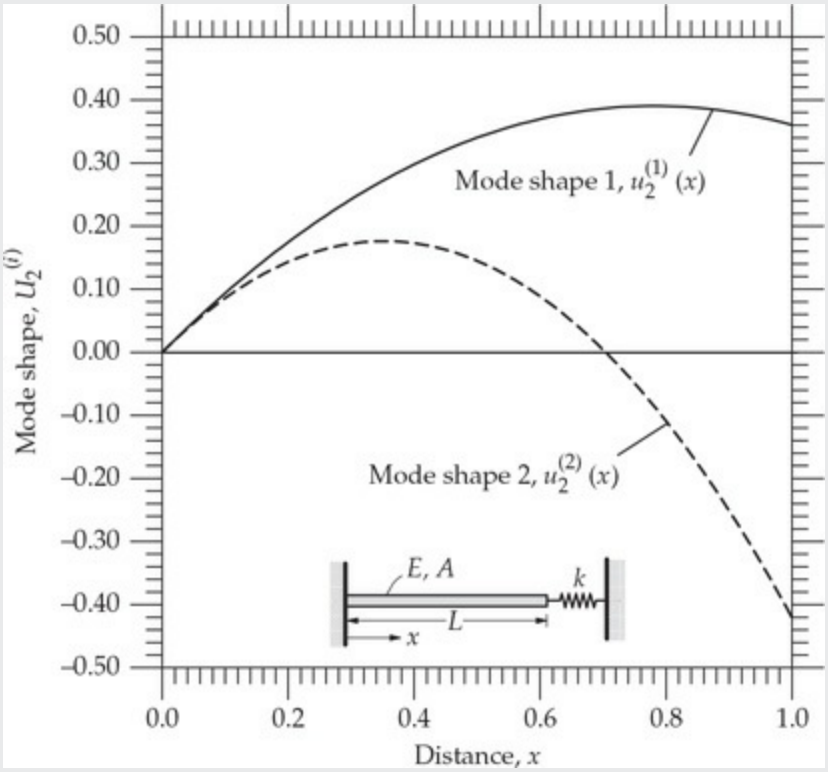

Fig. 2.5.4 First two mode shapes obtained by the Ritz method for the natural longitudinal vibrations of a spring-supported bar.

The exact values of λ are the roots of the transcendental equation (the reader may verify this by solving the problem analytically)

$$\lambda + \tan\lambda = 0$$

whose first two roots are ($\omega^2 = \lambda$)

$$\omega_1 = \frac{2.02875}{L}\sqrt{\frac{E}{\rho}}, \quad \omega_2 = \frac{4.91318}{L}\sqrt{\frac{E}{\rho}}$$

Note that the first approximate frequency is closer to the exact than the second.

If one selects ϕ_0 and ϕ_i to satisfy the natural boundary condition also, the degree of polynomials will inevitably go up. For example, the lowest-

order function that satisfies the homogeneous form (we still have $\phi_0 = 0$) of the natural boundary condition $u'(1) + u(1) = 0$ is

$$\hat{\phi}_1 = 3x - 2x^2$$

The one-parameter solution with the choice of $\hat{\phi}_1 = 3x - 2x^2$ gives $\lambda_1 = 50/12 = 4.1667$, which is no better than the two-parameter solution computed using $\phi_1 = x$ and $\phi_2 = x^2$. Of course, solution $c_1\hat{\phi}_1$ would yield a more accurate value for λ_1 than the solution $c_1\,\phi_1$. Although $c_1\hat{\phi}_1$ and $c_1\phi_1 + c_2\phi_2$ are of the same degree (polynomials), the latter gives better accuracy for λ_1 because the number of parameters is greater, which provides greater freedom to adjust the parameters c_i in satisfying the weak form.

The eigenvalues and mode shapes determined through eigenvalue analysis are also useful in determining the transient response. The general homogeneous solution to the transient problem is [see Eq. (2.5.44)]:

$$u_2(x,t) = (c_{11}\cos\omega_1 t + c_{12}\sin\omega_1 t)\,x + (c_{21}\cos\omega_2 t + c_{22}\sin\omega_2 t)\,x^2$$

where c_{1j} and c_{2j} are constants to be determined using the initial conditions.

2.5.3 The Method of Weighted Residuals

As noted in Section 2.4.3, one can always write the weighted-integral form of a differential equation, whether the equation is linear or nonlinear (in the dependent variables). The weak form can be developed if the equations are second-order or higher, even if they are nonlinear.

The weighted-residual method is a generalization of the Galerkin method in that the weight functions can be chosen from an independent set of functions, and it requires only the weighted-integral form to determine the parameters. Since the latter form does not include any of the specified boundary conditions of the problem, the approximation functions must be selected such that the approximate solution satisfies all of the specified boundary conditions. In addition, the weight functions can be selected independently of the approximation functions, but are required to be linearly independent so that the resulting algebraic equations are linearly independent.

We discuss the general method of weighted residuals first, and then

consider certain special cases that are known by specific names (e.g., the Galerkin method, the collocation method, the least-squares method and so on). Although a limited use of the weighted-residual method is made in this book, it is informative to have a knowledge of this class of methods for use in the formulation of certain nonlinear problems and non-self-adjoint problems.

The method of weighted residuals can be described in its generality by considering the operator equation

$$A(u) = f \quad \text{in} \quad \Omega \tag{2.5.51}$$

where A is an operator (linear or nonlinear), often a differential operator, acting on the dependent variable u, and f is a known function of the independent variables. Some examples of such operators are given below.

$$\begin{aligned}
&(1) \qquad A(u) = -\frac{d}{dx}\left(a\frac{du}{dx}\right) + cu \\
&(2) \qquad A(u) = \frac{d^2}{dx^2}\left(b\frac{d^2u}{dx^2}\right) \\
&(3) \qquad A(u) = -\left[\frac{\partial}{\partial x}\left(k_x\frac{\partial u}{\partial x}\right) + \frac{\partial}{\partial y}\left(k_y\frac{\partial u}{\partial y}\right)\right] \\
&(4) \qquad A(u) = -\frac{d}{dx}\left(u\frac{du}{dx}\right) \\
&(5) \qquad A(u,v) = u\frac{\partial u}{\partial x} + v\frac{\partial u}{\partial y} + \frac{\partial^2 u}{\partial x^2} + \frac{\partial}{\partial y}\left(\frac{\partial u}{\partial y} + \frac{\partial v}{\partial x}\right)
\end{aligned} \tag{2.5.52}$$

For an operator A to be *linear* in its arguments, it must satisfy the relation

$$A(\alpha u + \beta v) = \alpha A(u) + \beta A(v) \tag{2.5.53}$$

for any scalars α and β and dependent variables u and v. It can be easily verified that all operators in Eq. (2.5.52), except for those in (4) and (5), are linear. When an operator does not satisfy the condition in Eq. (2.5.53), it is said to be *nonlinear*.

The function u is not only required to satisfy the operator equation, Eq. (2.5.51), it is also required to satisfy the boundary conditions associated with the operator equation. From the examples considered so far, the boundary conditions associated with the operators defined in (1), (2), and (3) of Eq. (2.5.52) are obvious (see **Examples 2.4.1–2.4.3**). All operator

equations resulting from physical principles will be accompanied by a unique set of boundary conditions. The weak-form development (at the end of step 2) often tells what variables are involved in the specification of the boundary conditions.

In the weighted-residual method, the solution u is approximated, in much the same way as in the Ritz method, by the expression

$$u_n = \sum_{j=1}^{n} c_j \phi_j + \phi_0 \tag{2.5.54}$$

except that the requirements on ϕ_0 and ϕ_j in the weighted-residual method are more stringent than those in the Ritz method. Substitution of the approximate solution u_n into the left-hand side of Eq. (2.5.51) gives a function $A(u_n)$ that, in general, is not equal to the specified function f. The difference $A(u_n) - f$, called the *residual* of the approximation, is nonzero:

$$R \equiv A(u_n) - f = A\left(\sum_{j=1}^{n} c_j \phi_j + \phi_0\right) - f \neq 0$$

If A is a linear operator, then

$$R = A\left(\sum_{j=1}^{n} c_j \phi_j + \phi_0\right) - f = \sum_{j=1}^{n} c_j A(\phi_j) + A(\phi_0) - f \tag{2.5.55}$$

Note that the residual R is a function of position as well as of the parameters $c_1, c_2, \ldots, c_n$. In the weighted-residual method, as the name suggests, the parameters c_j are determined by requiring the residual R to vanish in the weighted-integral sense:

$$\int_{\Omega} \psi_i(x, y) R(x, y, c_1, c_2, \ldots, c_n)\, dx dy = 0 \quad (i = 1, 2, \ldots, n) \tag{2.5.56}$$

where Ω is a two-dimensional domain and ψi are *weight functions*, which, in general, are not the same as the approximation functions ϕ_i. The set $\{\psi_i\}$ must be a linearly independent set; otherwise, the equations provided by Eq. (2.5.56) will not be linearly independent and hence will not be solvable.

The requirements on ϕ_0 and ϕ_j for the weighted-residual method are

different from those for the Ritz method, which is based on the weak (integral) form of the differential equation. The differentiability requirement on ϕ_j in the weighted-residual method is dictated by the integral statement in Eq. (2.5.56), as opposed to the weak form in the Ritz method. Thus, ϕ_j must have nonzero derivatives up to the order appearing in the operator equation in Eq. (2.5.51). Since the weighted-integral form in Eq. (2.5.56) does not include any of the specified (either essential or natural) boundary conditions, we must also require u_n in Eq. (2.5.54) to satisfy all specified boundary conditions of the problem. Consequently, ϕ_0 is required to satisfy the homogeneous form of all specified boundary conditions of the problem. These requirements on ϕ_0 and ϕ_j will increase the order of the polynomial expressions used for the weighted-residual method. In general, the ϕ_j used in this method are higher-order functions than those used in the Ritz method, and the functions used in the latter may not satisfy the continuity (i.e., differentiability) requirements of the weighted-residual method. The case in which ψi is not equal to ϕ_i is known as the Petrov-Galerkin method.

2.5.3.1 The Galerkin method

For the choice of weight function ψ_i equal to the approximation function ϕ_i, the weighted-residual method is known as the Galerkin method. When A is a linear operator, the algebraic equations of the Galerkin approximation are

$$\sum_{j=1}^{N} A_{ij} c_j = F_i \tag{2.5.57a}$$

$$A_{ij} = \int_\Omega \phi_i A(\phi_j)\, dxdy, \quad F_i = \int_\Omega \phi_i [f - A(\phi_0)]\, dxdy \tag{2.5.57b}$$

We note that A_{ij} are not symmetric (i.e., $A_{ij} \neq A_{ji}$).

In general, the Galerkin method is *not* the same as the Ritz method. This should be clear from the fact that the former uses the weighted-integral form whereas the latter uses the weak form to determine the coefficients c_j. Consequently, the approximation functions used in the Galerkin method are required to be of higher order than those in the Ritz method. The method that uses the weak form in which the weight function is the same as the approximation function is sometimes called the *weak-*

form Galerkin method, but it is the same as the Ritz method. The Ritz and Galerkin methods yield the same solutions in two cases: (i) when the specified boundary conditions of the problem are all of the essential type, and therefore the requirements on ϕ_i in the two methods become the same and the weighted-integral form reduces to the weak form; and (ii) when the approximation functions of the Galerkin method are used in the Ritz method.

2.5.3.2 The least-squares method

In least-squares method, we determine the parameters c_j by minimizing the integral of the square of the residual R in Eq. (2.5.55):

$$\frac{\partial}{\partial c_i}\int_\Omega R^2(x, y, c_1, c_2, \cdots, c_n)\, dxdy = 0 \tag{2.5.58}$$

or

$$\int_\Omega \frac{\partial R}{\partial c_i} R\, dxdy = 0, \quad i = 1, 2, \ldots, n \tag{2.5.59}$$

Comparison of Eq. (2.5.59) with Eq. (2.5.56) shows that $\psi_i = \partial R/\partial c_i$. If A is a linear operator, we have $\psi_i = \partial R/\partial c_i = A(\phi_i)$, and Eq. (2.5.59) becomes

$$\sum_{j=1}^{N}\left[\int_\Omega A(\phi_i)A(\phi_j)\, dx\, dy\right] c_j = \int_\Omega A(\phi_i)[f - A(\phi_0)]\, dxdy$$

$$\sum_{j=1}^{N} A_{ij}c_j = F_i \tag{2.5.60a}$$

$$A_{ij} = \int_\Omega A(\phi_i)A(\phi_j)\, dx, \quad F_i = \int_\Omega A(\phi_i)[f - A(\phi_0)]\, dx \tag{2.5.60b}$$

Note that the coefficient matrix A_{ij} is symmetric whenever A is a linear operator, but it involves the same order of differentiation as in the governing differential equation $A(u) - f = 0$.

Example 2.5.5

Determine two-parameter Galerkin, Petrov-Galerkin, and least-squares approximation of the problem described by [see **Example 2.5.1** with Set 2 boundary conditions (BCs)]

$$-\frac{d^2u}{dx^2} - u + x^2 = 0, \quad u(0) = 0, \quad u'(1) = 1 \tag{2.5.61}$$

Compare the solutions with the two-parameter Ritz solution from **Example 2.5.1** in tabular form (u versus x).

Solution: For a weighted-residual method, ϕ_0 and ϕ_i should satisfy the following conditions:

$$\phi_0(0) = 0, \quad \phi_0'(1) = 1 \quad \text{(satisfy specified BCs)}$$
$$\phi_i(0) = 0, \quad \phi_i'(1) = 0 \quad \text{(satisfy homogeneous form of the specified BCs)}$$

For a choice of algebraic polynomials, we assume $\phi_0(x) = a + bx$ and use the two conditions on ϕ_0 to determine the constants a and b. We obtain

$$\phi_0(x) = x$$

Since there are two homogeneous conditions, we must assume at least a three-parameter polynomial to obtain a nonzero function, $\phi 1 = a + bx + cx^2$. Using the conditions on ϕ_i, we obtain ($b = -2c$) $\phi_1 = -cx(2 - x)$. The constant c can be set equal to unity because it will be absorbed into the parameter c_1. For ϕ_2, we can assume one of the forms

$$\phi_2 = a + bx + dx^3 \quad \text{or} \quad \phi_2 = a + cx^2 + dx^3$$

with $d \neq 0$; ϕ_2 does not contain all-order terms in either case, but the approximate solution is complete because $\{\phi_1, \phi_2\}$ contains all terms up to degree 3. Using the first choice above for ϕ_2, we obtain $\phi_2 = x^2\left(1 - \frac{2}{3}x\right)$. Recall from **Example 2.5.1** that the two-parameter Ritz approximation required the functions $\phi_1 = x$ and $\phi_2 = x^2$.

The residual in the approximation of the equation is

$$R = -\left(0 + \sum_{i=1}^{2} c_i \frac{d^2\phi_i}{dx^2}\right) - \left(\phi_0 + \sum_{i=1}^{2} c_i\phi_i\right) + x^2$$
$$= c_1(2 - 2x + x^2) + c_2(-2 + 4x - x^2 + \tfrac{2}{3}x^2) - x + x^2 \tag{2.5.62}$$

The Galerkin Method. Taking $\psi_i = \phi_i$, we have

$$\int_0^1 x(2-x)R\,dx = 0, \quad \int_0^1 x^2(1-\tfrac{2}{3}x)R\,dx = 0$$

or

$$u_{2G} = 1.2894x - 0.1398x^2 - 0.00325x^3 \tag{2.5.64}$$

whose solution is $c_1 = \frac{623}{4306}, c_2 = \frac{21}{4306}$. Hence the two-parameter Galerkin solution is

$$u_{2G} = 1.2894x - 0.1398x^2 - 0.00325x^3 \tag{2.5.64}$$

The Least-Squares Method. Taking $\psi_i = \frac{\partial R}{\partial c_i}$, we have

$$\int_0^1 (2-2x-x^2)R\,dx = 0, \quad -\int_0^1 (-2+4x+x^2-\tfrac{2}{3}x^2)R\,dx = 0$$

or

$$\tfrac{28}{15}c_1 - \tfrac{47}{90}c_2 - \tfrac{13}{60} = 0, \quad -\tfrac{47}{90}c_1 + \tfrac{253}{315}c_2 - \tfrac{1}{36} = 0 \tag{2.5.65}$$

The least-squares solution is given by (with $c_1 = \frac{1292}{9935}, c_2 = \frac{991}{19870}$)

$$u_{2LS} = 1.2601x - 0.08017x^2 - 0.03325x^3 \tag{2.5.66}$$

The two-parameter approximate solutions from Eqs. (2.5.22), (2.5.64), and (2.5.66) are compared in Table 2.5.3 with the exact solution, Eq. (2.5.23). The Ritz solution is nearly as good as the Galerkin and least-squares solutions even though the Ritz solution contains terms only up to quadratic whereas those of the Galerkin and least-squares methods contain cubic terms.

Table 2.5.3 Comparison of the Ritz, Galerkin, and least-squares solutions with the exact solution[a] of the boundary value problem in Eq. (2.5.61).

x	u_{exact}	u_{2R}	u_{2G}	u_{2LS}
0.0	0.0000	0.0000	0.0000	0.0000
0.1	0.1262	0.1280	0.1275	0.1252
0.2	0.2513	0.2529	0.2523	0.2485
0.3	0.3742	0.3749	0.3741	0.3699
0.4	0.4943	0.4938	0.4932	0.4891
0.5	0.6112	0.6097	0.6093	0.6058
0.6	0.7244	0.7226	0.7226	0.7200
0.7	0.8340	0.8324	0.8329	0.8314
0.8	0.9402	0.9393	0.9404	0.9397
0.9	1.0433	1.0431	1.0448	1.0449
1.0	1.1442	1.1439	1.1463	1.1467

[a]Subscripts have the following meanings: *R*, Ritz; *G*, Galerkin; *LS*, least-squares.

We close this section on variational methods with a note that the finite element models developed in the coming chapters are based on element-wise application of the Ritz (the same as the weak-form Galerkin) method. The finite element method allows, as will be seen shortly, a systematic construction of the approximation functions needed in the Ritz method for geometrically complex problems (the trick is to represent the domain as a collection of simple geometric shapes, called finite elements, that allow the derivation of the approximation functions).

2.6 Equations of Continuum Mechanics

2.6.1 Preliminary Comments

Since this book is concerned with the finite element solutions of differential equations arising mostly in engineering, although the basic developments are also valid for problems in applied sciences, it is useful to review the governing equations, including the boundary conditions (but not the initial conditions) of a continuum occupying a closed bounded region Ω with boundary Γ which serve as references in the coming chapters. Although sufficient background is given every time we consider a differential equation or a problem for analysis, the summary of equations included in this section serves as a quick reference. The equations are summarized under three subject areas of engineering that will receive

considerable attention in this book: heat transfer, fluid mechanics, and solid mechanics. Since the present exposure is only to summarize the equations, the readers may wish to consult books that contain detailed treatment of the subjects [3].

2.6.2 Heat Transfer

The principle of conservation of energy applied to a solid medium yields

$$\rho c_v \frac{\partial T}{\partial t} - \boldsymbol{\nabla} \cdot (k \boldsymbol{\nabla} T) = g \tag{2.6.1}$$

where ∇ is the del operator (see Section 2.2.1.3), T is the temperature, g is the rate of internal heat generation per unit volume, k is the conductivity of the (isotropic) solid, ρ is the density, and cv is the specific heat at constant volume. The expanded form of Eq. (2.6.1) (for constant k) in rectangular Cartesian system (x, y, z) is given by

$$\rho c_v \frac{\partial T}{\partial t} - k\left(\frac{\partial^2 T}{\partial x^2} + \frac{\partial^2 T}{\partial y^2} + \frac{\partial^2 T}{\partial z^2}\right) = g \tag{2.6.2}$$

In cylindrical coordinate system (r, θ, z), Eq.(2.6.1) takes the form

$$\rho c_v \frac{\partial T}{\partial t} - k\left[\frac{1}{r}\frac{\partial}{\partial r}\left(r\frac{\partial T}{\partial r}\right) + \frac{1}{r^2}\frac{\partial^2 T}{\partial \theta^2} + \frac{\partial^2 T}{\partial z^2}\right] = g \tag{2.6.3}$$

The second-order equations in Eqs. (2.6.1)–(2.6.3) are to be solved subjected to suitable boundary conditions. The boundary conditions involve specifying either the value of the temperature T or balancing the heat flux normal to the boundary $q_n = \hat{\mathbf{n}} \cdot \mathbf{q}$ at a boundary point:

$$T = \hat{T} \quad \text{or} \quad q_n + \beta(T - T_\infty) = \hat{q} \tag{2.6.4}$$

where $\hat{T}$ and $\hat{q}$ denote the specified temperature and heat flux, respectively. Heat flux vector $\mathbf{q}$ is related to the gradient of temperature by Fourier's heat conduction law (for the isotropic case)

$$\mathbf{q} = -k \nabla T \tag{2.6.5}$$

2.6.3 Fluid Mechanics

The equations governing flows of viscous incompressible fluids under

isothermal conditions are listed here (listing the conservation principles that give rise to the equations). Further, all nonlinear terms are omitted. In addition to the vector form, only the Cartesian component form is listed, and the summation convention of Section 2.2.1.2 is adopted.

Conservation of mass (Continuity equation)

$$\operatorname{div}(\rho \mathbf{v}) = 0, \quad \rho \frac{\partial v_i}{\partial x_i} = 0 \tag{2.6.6}$$

Conservation of linear momentum (equations of motion): ($\sigma_{ij} = \sigma_{ji}$)

$$\nabla \cdot \boldsymbol{\sigma} + \mathbf{f} = \rho \frac{\partial \mathbf{v}}{\partial t}, \quad \frac{\partial \sigma_{ji}}{\partial x_j} + f_i = \rho \frac{\partial v_i}{\partial t} \tag{2.6.7}$$

Constitutive relations

$$\boldsymbol{\sigma} = 2\mu \mathbf{D} - P\mathbf{I}, \quad \sigma_{ij} = 2\mu D_{ij} - P\delta_{ij} \tag{2.6.8}$$

Kinematic relations

$$\mathbf{D} = \frac{1}{2}\left[\nabla \mathbf{v} + (\nabla \mathbf{v})^{\mathrm{T}}\right], \quad D_{ij} = \frac{1}{2}\left(\frac{\partial v_i}{\partial x_j} + \frac{\partial v_j}{\partial x_i}\right) \tag{2.6.9}$$

Here **v** is the velocity vector, σ is the Cauchy stress tensor, **D** is the symmetric part of the velocity gradient tensor, *P* is the hydrostatic pressure, **f** is the body force vector, *ρ* is the density, and μ is the viscosity of the fluid. The boundary conditions involve specifying a velocity component v_i or stress vector component $t_i \equiv n_j \sigma_{ji}$ at a boundary point, where *nj* denote the direction cosines of a unit normal vector on the boundary

$$\mathbf{v} = \hat{\mathbf{v}} \text{ or } \hat{\mathbf{n}} \cdot \boldsymbol{\sigma} = \hat{\mathbf{t}}; \quad v_i = \hat{v}_i \text{ or } n_j \sigma_{ji} = \hat{t}_i \tag{2.6.10}$$

2.6.4 Solid Mechanics

Here we summarize the governing equations of a linearized, isotropic, elastic solid.

Momentum equations ($\sigma_{ji} = \sigma_{ij}$)

$$\nabla \cdot \sigma + \mathbf{f} = \rho \frac{d\mathbf{v}}{dt}, \quad \frac{\partial \sigma_{ji}}{\partial x_j} + f_i = \rho \frac{d\mathbf{v}}{dt} \tag{2.6.11}$$

Constitutive relations

$$\sigma = 2\mu\varepsilon + \lambda (\operatorname{tr} \varepsilon)\, \mathbf{I}, \quad \sigma_{ij} = 2\mu\varepsilon_{ij} + \lambda \varepsilon_{kk} \delta_{ij} \tag{2.6.12}$$

Kinematic relations

$$\varepsilon = \frac{1}{2}\left[\nabla \mathbf{u} + (\nabla \mathbf{u})^{\mathrm{T}}\right], \quad \varepsilon_{ij} = \frac{1}{2}\left(\frac{\partial u_i}{\partial x_j} + \frac{\partial u_j}{\partial x_i}\right) \tag{2.6.13}$$

Here **u** is the displacement vector, σ is the Cauchy stress tensor, ε is the symmetric part of the displacement gradient tensor, **f** is the body force vector, ρ is the density, and μ and λ are the Lamé (material) parameters. The boundary conditions involve specifying a displacement component u_i or stress vector component $t_i \equiv n_j \sigma_{ji}$ at a boundary point

$$\mathbf{u} = \hat{\mathbf{u}} \ \text{ or } \ \hat{\mathbf{n}} \cdot \sigma = \hat{\mathbf{t}}; \quad u_i = \hat{u}_i \ \text{ or } \ n_j \sigma_{ji} = \hat{t}_i \tag{2.6.14}$$

2.7 Summary

In this chapter, the following five major topics that are of immediate interest in the study of finite element method are covered:

1. A brief review of vectors, tensors, and matrices.
2. Concepts such as strain energy, total potential energy, and virtual work done as well as the energy principles of structural mechanics.
3. Weighted-integral and weak formulations of differential equations.
4. Solution of boundary value problems by the Ritz and weighted-residual (e.g., the Galerkin and least-squares) methods.
5. Summary of the governing equations of heat transfer, viscous incompressible fluid flows, and elastic solids under the assumptions of linearity.

These topics constitute essential prerequisites for the study of the finite element method and its applications.

The weighted-integral statements, including weak forms of differential equations and energy principles of structural mechanics (i.e., the principles

of virtual displacements and the minimum total potential energy), are a means to generate the necessary and sufficient number of algebraic equations to solve for the parameters (nodal as well as nodeless variables) in the approximate solution. To develop weak forms of second and higher-order differential equations, a three-step procedure is presented. In the case of structural mechanics, the energy principles are equivalent to the weak forms of the associated governing equations. Then the Ritz, Galerkin, subdomain, and least-squares methods are introduced to show how algebraic equations among the undetermined parameters of the approximation can be derived from the associated integral forms of the differential equations.

A few remarks are in order on the classical variational methods.

1. The traditional variational methods (e.g. Ritz, Galerkin, and least-squares) presented in Section 2.5 provide a simple means of finding spatially continuous approximate solutions to physical problems.
2. The finite volume method used in fluid dynamics is nothing but the finite element method where the residuals are made zero using the subdomain method. In other words, the finite volume technique is a subdomain finite element model.
3. The main limitation of classical variational methods that prevents them from being competitive with other methods is the difficulty encountered in constructing the approximation functions. The construction process becomes more difficult when the domain is geometrically complex. The so-called “meshless methods” are, in a sense, a return to the classical variational methods.
4. The classical variational methods can provide a powerful means of finding approximate solutions, provided one can find a way to systematically construct approximation functions for almost any geometry that depend only on the differential equation being solved and not on the boundary conditions of the problem. This property enables one to develop a computer program for a particular class of problem (each problem in the class differs from the others only in the data). Since the functions must be constructed for a geometrically complex domain, it seems that the region must be approximated as an assemblage of simple geometric shapes for which the construction of approximation functions becomes systematic and unique. The finite element method is based on this idea.
5. In the finite element method, a given domain is represented by a

collection of geometrically simple shapes (elements), and on each element of the collection, the governing equation is *formulated* using any one of the variational methods. The element equations are *assembled* together by imposing the continuity of the primary variables and balance of the secondary variables across interelement boundaries.

6. All commercially available finite element software is based on the weak-form Galerkin or the Ritz formulations with the choice of polynomial approximation functions.

Problems

2.1 Let **R** denote a position vector $\mathbf{R} = \mathbf{x} = x_i \hat{\mathbf{e}}_i$ (R_2 = *xi xi*) and **A** an arbitrary constant vector. Show that:

(a) $\nabla^2(R^p) = p(p+1)R^{p-2}$

(b) grad $(\mathbf{R} \cdot \mathbf{A}) = \mathbf{A}$

(c) div $(\mathbf{R} \times \mathbf{A}) = 0$

(d) $\text{div}\,(R\mathbf{A}) = \dfrac{1}{R}(\mathbf{R} \cdot \mathbf{A})$

2.2 Let **A** and **B** be continuous vector functions of the position **x** with continuous first derivatives, and let *F* and *G* be continuous scalar functions of position **x** with continuous first and second derivatives. Show that:

(a) $\nabla(\mathbf{A} \cdot \mathbf{x}) = \mathbf{A} + \nabla\mathbf{A} \cdot \mathbf{x}$

(b) $\nabla \cdot (F\mathbf{A}) = \mathbf{A} \cdot \nabla F + F\,\nabla \cdot \mathbf{A}$

2.3 Let **a** be a continuous second-order tensor function of the position **x** with continuous first derivatives, and let *u* be a continuous scalar function of the position **x** with continuous first and second derivatives. Show that

$$\begin{aligned}\nabla \cdot (\mathbf{a} \cdot \nabla u) = {} & \frac{1}{r}\frac{\partial}{\partial r}\left[r\left(a_{rr}\frac{\partial u}{\partial r} + a_{r\theta}\frac{1}{r}\frac{\partial u}{\partial \theta} + a_{rz}\frac{\partial u}{\partial z}\right)\right] \\ & + \frac{1}{r}\frac{\partial}{\partial \theta}\left(a_{\theta r}\frac{\partial u}{\partial r} + a_{\theta\theta}\frac{1}{r}\frac{\partial u}{\partial \theta} + a_{\theta z}\frac{\partial u}{\partial z}\right) \\ & + \frac{\partial}{\partial z}\left(a_{zr}\frac{\partial u}{\partial r} + a_{z\theta}\frac{1}{r}\frac{\partial u}{\partial \theta} + a_{zz}\frac{\partial u}{\partial z}\right)\end{aligned}$$

In **Problems 2.4–2.9**, construct the weak forms and, whenever

possible, the associated quadratic functionals (I).

2.4 A linear differential equation:

$$-\frac{d}{dx}\left[(1+2x^2)\frac{du}{dx}\right]+u=x^2$$

$$u(0)=1\,,\quad \left(\frac{du}{dx}\right)_{x=1}=2$$

2.5 A nonlinear equation:

$$-\frac{d}{dx}\left(u\frac{du}{dx}\right)+f=0 \quad \text{for} \quad 0<x<1$$

$$\left(u\frac{du}{dx}\right)\Big|_{x=0}=0 \quad u(1)=\sqrt{2}$$

2.6 The Euler-Bernoulli-von Kármán nonlinear theory of beams:

$$-\frac{d}{dx}\left\{EA\left[\frac{du}{dx}+\frac{1}{2}\left(\frac{dw}{dx}\right)^2\right]\right\}=f \quad \text{for} \quad 0<x<L$$

$$\frac{d^2}{dx^2}\left(EI\frac{d^2w}{dx^2}\right)-\frac{d}{dx}\left\{EA\frac{dw}{dx}\left[\frac{du}{dx}+\frac{1}{2}\left(\frac{dw}{dx}\right)^2\right]\right\}=q$$

$$u=w=0 \quad \text{at} \quad x=0,\ L; \quad \left(\frac{dw}{dx}\right)\Big|_{x=0}=0; \quad \left(EI\frac{d^2w}{dx^2}\right)\Big|_{x=L}=M_0$$

where EA, EI, f, and q are functions of x and M_0 is a constant. Here u denotes the axial displacement and w the transverse deflection of the beam.

2.7 A general second-order equation:

$$-\frac{\partial}{\partial x}\left(a_{11}\frac{\partial u}{\partial x}+a_{12}\frac{\partial u}{\partial y}\right)-\frac{\partial}{\partial y}\left(a_{21}\frac{\partial u}{\partial x}+a_{22}\frac{\partial u}{\partial y}\right)+f=0 \quad \text{in} \quad \Omega$$

$$u=u_0 \ \text{ on } \ \Gamma_1, \quad \left(a_{11}\frac{\partial u}{\partial x}+a_{12}\frac{\partial u}{\partial y}\right)n_x+\left(a_{21}\frac{\partial u}{\partial x}+a_{22}\frac{\partial u}{\partial y}\right)n_y=t_0 \ \text{ on } \ \Gamma_2$$

where $a_{ij}=a_{ji}$ $(i, j = 1, 2)$ and f are given functions of position (x, y) in a two-dimensional domain Ω and u_0 and t_0 are known functions on portions $\Gamma1$ and $\Gamma2$ of the boundary Γ: $(\Gamma1 + \Gamma2) = \Gamma$.

2.8 Two-dimensional heat transfer in an axisymmetric geometry:

$$-\left[\frac{1}{r}\frac{\partial}{\partial r}\left(rk\frac{\partial T}{\partial r}\right)+\frac{\partial}{\partial z}\left(k\frac{\partial T}{\partial z}\right)\right]=g \quad \text{in} \quad \Omega$$

$$T=\hat{T} \text{ on } \Gamma_T \quad \text{and} \quad q_n \equiv rk\left(\frac{\partial T_n}{\partial r}n_r+\frac{\partial T_n}{\partial z}n_z\right)=\hat{q}_n \text{ on } \Gamma_q$$

2.9 Governing equations for two-dimensional flow of viscous incompressible fluids:

$$-\mu\left[2\frac{\partial^2 v_x}{\partial x^2}+\frac{\partial}{\partial y}\left(\frac{\partial v_x}{\partial y}+\frac{\partial v_y}{\partial x}\right)\right]+\frac{\partial P}{\partial x}=f_x$$

$$-\mu\left[2\frac{\partial^2 v_y}{\partial y^2}+\frac{\partial}{\partial x}\left(\frac{\partial v_x}{\partial y}+\frac{\partial v_y}{\partial x}\right)\right]+\frac{\partial P}{\partial y}=f_y \quad \text{in } \Omega$$

$$\frac{\partial v_x}{\partial x}+\frac{\partial v_y}{\partial y}=0$$

$$v_x=\hat{v}_x, \quad v_y=\hat{v}_y \quad \text{on} \quad \Gamma_1$$

and

$$\left[\left(2\mu\frac{\partial v_x}{\partial x}-P\right)n_x+\mu\left(\frac{\partial v_x}{\partial y}+\frac{\partial v_y}{\partial x}\right)n_y\right]=\hat{t}_x$$

$$\left[\left(2\mu\frac{\partial v_y}{\partial y}-P\right)n_y+\mu\left(\frac{\partial v_x}{\partial y}+\frac{\partial v_y}{\partial x}\right)n_x\right]=\hat{t}_y \quad \text{on } \Gamma_2$$

2.10 Compute the coefficient matrix and the right-hand side of the *n*-parameter Ritz approximation of the equation

$$-\frac{d}{dx}\left[(1+x)\frac{du}{dx}\right]=0 \quad \text{for} \quad 0<x<1$$

$$u(0)=0, \quad u(1)=1$$

Use algebraic polynomials for the approximation functions. Specialize your result for $n = 2$ and compute the Ritz coefficients. *Answer:* $c_1 = \frac{55}{131}$ and $c_2 = -\frac{20}{131}$.

2.11 Use trigonometric functions for the two-parameter approximation of the equation in **Problem 2.10** and obtain the Ritz coefficients. *Answer:* $c_1 = -0.12407$ and $c_2 = 0.02919$ for a choice of functions.

2.12 A steel rod of diameter $d = 2$ cm, length $L = 25$ cm, and thermal conductivity $k = 50$ W/(m°C) is exposed to ambient air $T_\infty = 20$°C

with a heat-transfer coefficient $\beta = 64$ W/(m^2°C). Given that the left end of the rod is maintained at a temperature of $T_0 = 120$°C and the other end is exposed to the ambient temperature, determine the temperature distribution in the rod using a two-parameter Ritz approximation with polynomial approximation functions. The equation governing the problem is given by

$$-\frac{d^2\theta}{dx^2} + c\theta = 0 \quad \text{for} \quad 0 < x < 25 \text{ cm}$$

where $\theta = T - T_\infty$, T is the temperature, and c is given by

$$c = \frac{\beta P}{Ak} = \frac{\beta \pi D}{\frac{1}{4}\pi D^2 k} = \frac{4\beta}{kD} = 256 \text{ m}^2$$

P being the perimeter and A the cross-sectional area of the rod. The boundary conditions are

$$\theta(0) = T(0) - T_\infty = 100°\text{C}, \quad \left(k\frac{d\theta}{dx} + \beta\theta\right)\Big|_{x=L} = 0$$

Answer: For $L = 0.25$ m, $\phi_0 = 100$, $\phi_i = x^i$, the Ritz coefficients are $c_1 = -1,033.385$ and $c_2 = 2,667.261$.

2.13 Set up the equations for the n-parameter Ritz approximation of the following equations associated with a simply supported beam and subjected to a uniform transverse load $q = q_0$:

$$\frac{d^2}{dx^2}\left(EI\frac{d^2w}{dx^2}\right) = q \quad \text{for} \quad 0 < x < L$$

$$w = EI\frac{d^2w}{dx^2} = 0 \quad \text{at} \quad x = 0,\ L$$

Identify (a) algebraic polynomials and (b) trigonometric functions for ϕ_0 and ϕ_i. Compute and compare the two-parameter Ritz solutions with the exact solution for uniform load of intensity q_0.
Answer: (a) $c_1 = q_0 L_2 /(24EI)$ and $c_2 = 0$.

2.14 Repeat **Problem 2.13** for $q = q_0 \sin(?x/L)$, where the origin of the coordinate system is taken at the left end of the beam. *Answer:* $n = 2 : c_1 = c_2 L = 2q_0 L_2/(3EI\pi^3)$.

2.15 Repeat **Problem 2.13** for $q = Q_0\delta(x - \frac{1}{2}L)$, where $\delta(x)$ is the Dirac delta function (i.e., a point load Q_0 is applied at the center of the beam).

2.16 Develop the n-parameter Ritz solution for a simply supported beam under uniform transverse load using the Timoshenko beam theory. The governing equations are given in Eqs. (2.4.36a) and (2.4.36b). Use trigonometric functions to approximate w and ϕ.

2.17 Repeat **Problem 2.16** for a cantilever beam under uniform transverse load and an end moment M_0. Use algebraic polynomials to approximate w and ϕ.

2.18 Solve the Poisson equation governing heat conduction in a square region (see **Example 2.5.3**):

$$-k\nabla^2 T = g_0$$

$$T = 0 \quad \text{on sides} \quad x = 1 \quad \text{and} \quad y = 1$$

$$\frac{\partial T}{\partial n} = 0 \quad \text{(insulated) on sides} \quad x = 0 \quad \text{and} \quad y = 0$$

using a one-parameter Ritz approximation of the form

$$T_1(x, y) = c_1(1 - x^2)(1 - y^2)$$

Answer: $c_1 = \frac{5g_0}{16k}$.

2.19 Determine ϕ_i for a two-parameter Galerkin approximation with algebraic approximation functions of **Problem 2.12**.

2.20 Consider the (Neumann) boundary value problem

$$-\frac{d^2u}{dx^2} = f \quad \text{for} \quad 0 < x < L$$

$$\left(\frac{du}{dx}\right)\Big|_{x=0} = \left(\frac{du}{dx}\right)\Big|_{x=L} = 0$$

Find a two-parameter Galerkin approximation of the problem using trigonometric approximation functions, when (*a*) $f = f_0 \cos(\pi x/L)$ and (*b*) $f = f_0$. *Answer:* (a) $\phi_i = \cos(i\pi x/L)$, $c_1 = f_0L^2/\pi^2$, $c_i = 0$ for $i \neq 1$.

2.21 Find a one-parameter solution of the nonlinear equation

$$-2u\frac{d^2u}{dx^2}+\left(\frac{du}{dx}\right)^2=4 \quad \text{for} \quad 0<x<1$$

subject to the boundary conditions $u(0) = 1$ and $u(1) = 0$, and compare it with the exact solution $u_0 = 1 - x^2$. Use (a) the Galerkin method, (b) the least-squares method, and (c) the Petrov–Galerkin method with weight function $w = 1$. *Answer:* (a) $(c_1)_1 = 1$, and $(c_1)_2 = -3$.

2.22 Give a one-parameter Galerkin solution of the equation

$$-\nabla^2 u = 1 \quad \text{in} \quad \Omega \quad (= \text{unit square})$$

$$u = 0 \quad \text{on} \quad \Gamma$$

Use (a) algebraic and (b) trigonometric approximation functions. *Answer:* (b) $c_{ij} = \frac{16}{\pi^4}\frac{1}{ij(i^2+j^2)}$ (i, j odd), $\phi_{ij} = \sin i\pi x \sin j\pi y$

2.23 Repeat **Problem 2.22**(a) for an equilateral triangular domain. *Hint:* Use the product of equations of the lines representing the sides of the triangle for the approximation function. *Answer:* $c_1 = -\frac{1}{2}$.

2.24 Consider the differential equation

$$-\frac{d^2u}{dx^2} = \cos \pi x \quad \text{for} \quad 0<x<1$$

subject to the following three sets of boundary conditions:

(1) $u(0) = 0, \quad u(1) = 0$

(2) $u(0) = 0, \quad \left(\frac{du}{dx}\right)_{x=1} = 0$

(3) $\left(\frac{du}{dx}\right)_{x=0} = 0, \quad \left(\frac{du}{dx}\right)_{x=1} = 0$

Determine a three-parameter solution, with trigonometric functions, using (a) the Ritz method, (b) the least-squares method, and (c) collocation at $x = \frac{1}{4}, \frac{1}{2}$, and $\frac{3}{4}$, and compare with the exact solutions:

(1) $u_0 = \pi^{-2}(\cos \pi x + 2x - 1)$

(2) $u_0 = \pi^{-2}(\cos \pi x - 1)$

(3) $u_0 = \pi^{-2} \cos \pi x$

Answer: (1a) $c_i = \frac{4}{\pi^3 i(i^2-1)}$

2.25 Consider a cantilever beam of variable flexural rigidity, $EI = a_0[2 - (x/L)^2]$, and carrying a distributed load, $q = q_0[1 - (x/L)]$. Find a

three-parameter solution using the collocation method. *Answer:* $c_1 = -\frac{q_0 L^2}{4a_0}$ and $c_2 = \frac{q_0 L}{12a_0}$.

2.26 Consider the problem of finding the fundamental frequency of a circular membrane of radius a, fixed at its edge. The governing equation for axisymmetric vibration is

$$-\frac{1}{r}\frac{d}{dr}\left(r\frac{du}{dr}\right) - \lambda u = 0, \quad 0 < r < a$$

where λ is the frequency parameter and u is the deflection of the membrane. (a) Determine the trigonometric approximation functions for the Galerkin method, (b) use one-parameter Galerkin approximation to determine λ, and (c) use two-parameter Galerkin approximation to determine λ. *Answer:* (b) $\lambda = 5.832/a^2$; (c) $\lambda = 5.792/a^2$.

2.27 Find the first two eigenvalues associated with the differential equation

$$-\frac{d^2u}{dx^2} = \lambda u, \quad 0 < x < 1$$

$$u(0) = 0, \quad u(1) + u'(1) = 0$$

Use the least-squares method with algebraic polynomials. Use the operator definition to be $A = -(d_2/dx^2)$ to avoid increasing the degree of the characteristic polynomial for λ. *Answer:* $\lambda_1 = 4.212$ and $\lambda_2 = 34.188$.

2.28 Repeat **Problem 2.27** using the Ritz method with algebraic polynomials. *Answer:* $\lambda_1 = 4.1545$ and $\lambda_2 = 38.512$.

2.29 Consider the Laplace equation

$$-\nabla^2 u = 0, \quad 0 < x < 1, \quad 0 < y < \infty$$

$$u(0, y) = u(1, y) = 0 \quad \text{for} \quad y > 0$$

$$u(x, 0) = x(1 - x), \quad u(x, \infty) = 0, \quad 0 \le x \le 1$$

Assuming one-parameter approximation of the form

$$u(x, y) = c_1(y)x(1 - x)$$

find the differential equation for $c_1(y)$ and solve it exactly.

Answer: $U_1(x,y) = (x - x^2)e^{-\sqrt{10}y}$.

2.30 Find the first eigenvalue λ associated with the equation

$$-\nabla^2 u = \lambda u \text{ in } \Omega;\ u = 0 \text{ on } \Gamma$$

where Ω is a rectangle, $-a < x < a$ and $-b < y < b$, and Γ is its boundary. Assume oneparameter approximation of the form

$$u_1(x, y) = c_1(x)\phi_1(y) = c_1(x)(y_2 - b_2)$$

References for Additional Reading

1. J. T. Oden and J. N. Reddy, *Variational Methods in Theoretical Mechanics*, 2nd ed., Springer–Verlag, New York, NY, 1983.
2. J. N. Reddy, *Energy Principles and Variational Methods in Applied Mechanics*, 3rd ed., John Wiley & Sons, New York, NY, 2017.
3. J. N. Reddy, *An Introduction to Continuum Mechanics*, 2nd ed., Cambridge University Press, New York, NY, 2013.
4. J. N. Reddy and M. L. Rasmussen, *Advanced Engineering Analysis*, John Wiley & Sons, New York, NY, 1982; Krieger, Melbourne, FL, 1990.
5. J. N. Reddy, *Applied Functional Analysis and Variational Methods in Engineering*, McGraw–Hill, New York, 1986; Krieger, Melbourne, FL, 1991.
6. J. N. Reddy, *An Introduction to Nonlinear Finite Element Analysis*, Oxford University Press, Oxford, UK, 2015.
7. F. B. Hildebrand, *Methods of Applied Mathematics*, 2nd ed., Prentice–Hall, Engelwood Cliffs, NJ, 1965.
8. S. G. Mikhlin, *Variational Methods in Mathematical Physics*, Pergamon Press, New York, NY, 1964.
9. S. G. Mikhlin, *The Numerical Performance of Variational Methods*, Wolters–Noordhoff, Gröningen, The Netherlands, 1971.
10. K. Rektorys, *Variational Methods in Mathematics, Science and Engineering*, Reidel, Boston, MA, 1977.

[1] The primary variables are often the variables appearing in the differential equations.

[2] The two types of boundary conditions will be discussed in the following paragraphs.

[3] A set of dependent variables, called vectors, with certain rules of vector addition and scalar multiplication is defined as a linear vector space [5].

3 1-D Finite Element Models of Second-Order Differential Equations

If I have seen further than others, it is by standing upon the shoulders of giants.
— Isaac Newton

3.1 Introduction

3.1.1 Preliminary Comments

The traditional variational methods described in Chapter 2 (e.g., the Ritz and weighted-residual methods applied to the entire domain at once) cease to be effective because of a serious shortcoming, namely, the difficulty in constructing the approximation functions. The approximation functions, apart from satisfying continuity, linear independence, completeness, and boundary conditions, are arbitrary; the selection becomes even more difficult when the given domain is geometrically complex. Since the quality of the approximation is directly affected by the choice of the approximation functions, it is discomforting to know that there exists no systematic procedure to construct them for arbitrary domains in the traditional variational methods. Because of this shortcoming, despite the simplicity in obtaining approximate solutions, the traditional variational methods of approximation were never regarded as competitive computationally when compared with the finite difference schemes. The finite element method overcame the shortcomings of the traditional variational methods by providing a systematic procedure of constructing the approximation functions over certain geometric shapes (called finite elements) and using the shapes to represent the given domain.

3.1.2 Desirable Features of an Effective Computational Method

Ideally speaking, an effective computational method should have the

following features:

1. It should have a sound mathematical as well as physical basis (i.e., yield convergent solutions and be applicable to practical problems).
2. It should not have limitations with regard to the geometry, the physical composition of the domain, or the nature of the "loads."
3. The formulative procedure should be independent of the shape of the domain and the specific form (which is dictated by the physics) of the boundary conditions.
4. The method should be flexible enough to allow different degrees of approximation without reformulating the entire problem.
5. It should involve a systematic procedure that can be automated for use on digital computers.

3.1.3 The Basic Features of the Finite Element Method

The finite element method differs from the finite difference method in a fundamental way. The finite element method is a technique in which a dependent unknown is approximated as a linear combination of unknown parameters and known functions, whereas in the finite difference method the derivatives of the unknown are represented in terms of the values of the unknown. Thus, the finite difference method has no formal functional representation of the unknown itself; consequently, there are no evaluations of functions or their integrals, which can be considered as a positive aspect. However, there are associated drawbacks in imposing gradient boundary conditions and post-computation of gradients of the unknown. Further, the finite difference method only provides a means to compute solutions to problems described by differential equations but does not include the idea of minimizing the error in the approximation.

In a nutshell, the finite element method can be described as one that has the following three basic features:

1. Division of whole domain into subdomains, called *finite elements*, that enable a systematic derivation of the approximation functions as well as representation of complex domains.
2. Discretization of the mathematical model of the problem (i.e., derivation of algebraic relations from governing equations) in terms of the values of the unknowns at selective points, called *nodes*, over each finite element. This step requires the use of an approximation method in which an unknown is represented as a linear combination

of values of the unknown (and possibly its derivatives) at the nodes and suitable approximation functions, as discussed in Chapter 2. The element geometry and the position of the nodes in the element allow a systematic derivation of the approximation functions for each element. The approximation functions are often algebraic polynomials that are derived using interpolation theory. However, approximation functions need not be polynomials.

3. Assembly of the element equations to obtain a numerical analog of the mathematical model of the total problem being analyzed.

These three features, which constitute three major steps of the finite element formulation, are closely related. The geometry of the elements used to represent the domain of a problem should be such that the approximation functions can be uniquely derived. The approximation functions depend not only on the geometry but also on the number and location of the nodes in the element, and also on the quantities to be interpolated (e.g., dependent variables only or dependent variables and their derivatives). Once the approximation functions have been derived, the procedure to obtain algebraic relations among the unknown coefficients (which give the values of the dependent variable at the nodes) is exactly the same as that used in the Ritz and weighted-residual methods. Hence, a study of Chapter 2, especially the weak-form development and the Ritz method, makes the present study easier.

The finite element method not only overcomes the shortcomings of the traditional variational methods, but also is endowed with the features of an effective computational technique. The method is now recognized as the most general and practical engineering analysis tool in academia as well as in industry.

3.2 Finite Element Analysis Steps

3.2.1 Preliminary Comments

The basic steps involved in the finite element analysis of a problem are presented in Table 3.2.1.

Table 3.2.1 Steps involved in the finite element analysis of a typical problem.

1. Discretization (or subdivision) of the given domain into a collection of preselected finite elements, called *mesh generation*.
   (a) Construct the finite element mesh of preselected elements.
   (b) Number the nodes and elements.
   (c) Generate geometric properties (e.g., coordinates and element connectivity data).

2. Derivation of algebraic relations between the primary and secondary variables (the finite element model).

   Discrete systems:

   (a) Identify a typical element of the system.
   (b) Derive algebraic relationships between point (or nodal) variables associated with the primary variables and secondary variables (e.g., forces and displacements).

   Continuum problems:

   (a) Construct weak forms of the differential equations over a typical element $\tilde{\Omega}^e$.
   (b) Assume that a typical dependent variable $u(x)$ is approximated over $\tilde{\Omega}^e$ in the form

$$u(x) \approx u_h^e(x) = \sum_{j=1}^{n} u_j^e \psi_j^e(x)$$

   and substitute it into the weak forms of Step 2*a* to obtain element equations in the form $\mathbf{K}^e\mathbf{u}^e = \mathbf{F}^e$.
   (c) Select, if already available in the literature, or derive element interpolation functions $\psi_j(x)$ and compute the element matrices.

3. Assembly of element equations to obtain the equations of the whole problem.
   (a) Identify the inter-element continuity conditions among the *primary variables* (relationship between the local degrees of freedom and the global degrees of freedom—connectivity of elements) by relating element nodes to global nodes.
   (b) Identify the "equilibrium" conditions among the *secondary variables* (relationship between the local source or force components and the globally specified source components).
   (c) Assemble element equations using Steps 3(a) and 3(b).

4. Imposition of the boundary conditions of the problem.
   (a) Identify the specified global primary degrees of freedom.
   (b) Identify the specified global secondary degrees of freedom, if not already done in Step 3(b).

5. Solution of the assembled equations.

6. Postprocessing of the results.
   (a) Compute the gradient of the solution or other desired quantities from the primary degrees of freedom computed in Step 5.
   (b) Represent the results in tabular and/or graphical form.

3.2.2 Discretization of a System

Most engineered systems are usually assemblages of subsystems. The smallest part that serves as the "building block" for the system or its subsystems and whose "cause and effect" relationships, the meaning of which will be made clear in the sequel, can be uniquely described mathematically is called an *element*. If a system has several subsystems that are different from each other in terms of their geometry and behavior, then each such subsystem is an assemblage of a unique type of element. Thus, a system may be assemblage of different types of elements (i.e., parts that have different physical behavior). An automobile is an assemblage of, for example, frame, doors, engine, and so on. Each of them may be characterized in terms of their load-deflection behavior as frame elements, shell elements, or three-dimensional solid elements (see Fig. 1.4.8 for an example).

The phrase "discretization" in finite element analysis refers to representation of various parts of the system by a set of appropriate types of elements (e.g., frame element, shell element, or solid element). In general, such a representation is called a *finite element mesh*. In this introductory chapter, we will consider systems whose "cause and effect" can be described by only one type of element. Once we get comfortable, we can discuss multiple types of elements in a given system. In the following discussion, the word "domain" refers to the collection of material points of a continuous system whose physical behavior is of interest.

In the finite element method, the domain Ω of the problem is divided into a set of subdomains, called *finite elements*. The reason for dividing a domain into a set of subdomains is twofold. First, domains of most systems, by design, are a composite of geometrically and/or materially different parts, as shown in Fig. 3.2.1, and the solution on these subdomains is represented by different functions that are continuous at the interfaces of these subdomains. Therefore, it is appropriate to seek an approximation of the solution over each subdomain. Second, approximation of the solution over each element of the mesh is simpler than its approximation over the entire domain. Approximation of the geometry of the domain in the one-dimensional problems considered in this chapter is not a concern, since it is a straight line. We must, however, seek a suitable approximation of the solution over each finite element.

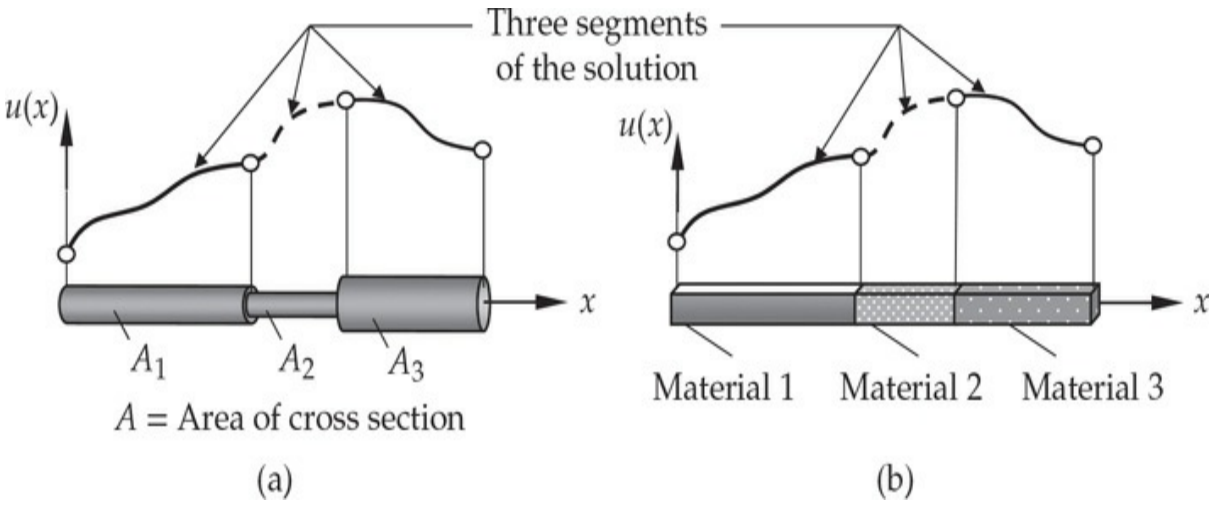

Fig. 3.2.1 (a) Bar with different areas of cross sections. (b) Bar made of multiple materials.

The number of elements into which the complete domain of the system is divided in a problem depends mainly on the geometry of the domain, the types of different physical behaviors the system exhibits, and the desired accuracy of the solution. In the one-dimensional problems to be discussed in this chapter, we shall consider, to begin with, only one type of behavior in each problem. In selecting a mesh, one often begins with a number of elements that are considered to be reasonable in predicting an accurate solution. Most often, the analyst has knowledge of the qualitative behavior of the solution, and this helps to choose a starting mesh. Whenever a problem is solved by the finite element method for the first time, one is required to investigate the convergence of the finite element solution by gradually *refining the mesh* (i.e., increasing the number of elements or the degree of approximation).

3.2.3 Derivation of Element Equations: Finite Element Model

In nature, all systems exhibit certain dualities in their behavior or response. For example, a force on a system induces displacement, while heat input to a system elevates its temperature. We call that force and displacements are dual to each other and heat and temperature are dual to each other. This is also referred to as the cause and effect. One element of the pair may be called the *primary variable* and the other the *secondary variable*; although the choice of the name given to each variable is arbitrary, the dualities are unique (i.e., if one element is dual to another element, these elements do not appear in other duality pairs again). In this book, we shall call the displacements as the primary variables and the corresponding forces as the

secondary variables. Similarly, temperature will be labelled as the primary variable and heat as the secondary variable. Mathematical representations of the relationships between primary and secondary variables are in the form of algebraic, differential, or integral equations, and they are derived with the aid of the laws of physics and constitutive relations. The finite element method is a technique of developing algebraic relations among the nodal values of the primary and secondary variables.

In most cases, the relationships between primary and secondary variables are in the form of differential equations. The objective of any numerical method is to convert these relationships to algebraic form so that one can determine the system response (e.g., force or displacement) associated with a given input to the system. The algebraic relationships for a typical element of a system, called *finite element equations* or *finite element model*, can be derived directly (i.e., without going through the differential relationships), in some simple cases, using the underlying physical principles (see Section 3.3). In all continuous systems, the differential equations can be used to derive the algebraic relationships between the primary and secondary variables. In the next section, we shall discuss the derivations of the element equations for discrete systems by a direct or physical approach. Assembly of element equations, imposition of boundary conditions, and solution of algebraic equations for nodal unknowns are presented. In Section 3.4, we systematically develop, starting with a representative differential equation, finite element equations of continuous systems. *The reader must have a good background in basic engineering subjects to understand the physical approach and appreciate the application of the general approach presented in Section 3.4 and in the subsequent chapters.*

3.3 Finite Element Models of Discrete Systems

3.3.1 Linear Elastic Spring

A linear elastic spring is a discrete element (i.e., not a continuum and not governed by a differential equation), as shown in Fig. 3.3.1(a). The load-displacement relationship of a linear elastic spring can be expressed as

$$F = k\delta \tag{3.3.1}$$

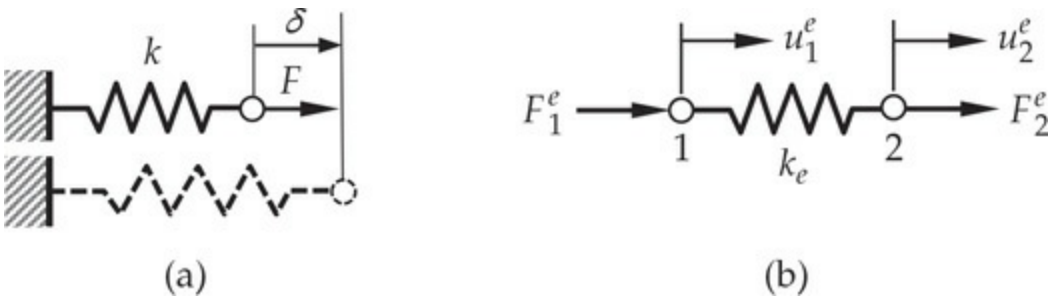

Fig. 3.3.1 (a) A linear spring. (b) A spring finite element.

where F is the force (N) in the spring, δ is the elongation (m) of the spring, and k is a constant, known as the *spring constant* (N/m). The spring constant depends on the elastic modulus, area of cross section, and number of turns in the coil of the spring. Often a spring is used to characterize the elastic behavior of complex physical systems.

A relationship between the end forces (F_1^e, F_2^e) and end displacements (u_1^e, u_2^e) of a typical spring element e shown in Fig. 3.3.1(b) can be developed with the help of the relation in Eq. (3.3.1). We note that all forces and displacements are taken positive to the right. The force F_1^e at node 1 is (compressive and) equal to the spring constant multiplied by the relative displacement of node 1 with respect to node 2, that is, $u_1^e - u_2^e$:

$$F_1^e = k_e(u_1^e - u_2^e) = k_e u_1^e - k_e u_2^e$$

Similarly, the force at node 2 is (tensile and) equal to elongation $u_2^e - u_1^e$ multiplied by k_e:

$$F_2^e = k_e(u_2^e - u_1^e) = -k_e u_1^e + k_e u_2^e$$

Note that the force equilibrium, $F_2^1 + F_1^2 + F_1^3$, is automatically satisfied by the above relations. These equations can be written in matrix form as

$$k_e \begin{bmatrix} 1 & -1 \\ -1 & 1 \end{bmatrix} \begin{Bmatrix} u_1^e \\ u_2^e \end{Bmatrix} = \begin{Bmatrix} F_1^e \\ F_2^e \end{Bmatrix} \quad \text{or} \quad \mathbf{K}^e\mathbf{u}^e = \mathbf{F}^e \tag{3.3.2}$$

Equation (3.3.2) is applicable to any spring element whose force-displacement relation is linear. Thus a typical spring in a network of springs of different spring constants obeys Eq. (3.3.2). The coefficient matrix $\mathbf{K}^e$ is termed stiffness matrix, $\mathbf{u}^e$ is the vector of displacements, and $\mathbf{F}^e$ is the force vector. We note that Eq. (3.3.2) is valid for any linear elastic spring, and it represents a relationship between point forces and displacements along the length of the spring. The end points are called

element nodes and F_i^e and u_i^e are the nodal force and displacement, respectively, of the *i*th node. We also note that *a spring element can only take loads and experience displacements along its length.* We consider an example of application of Eq. (3.3.2).

Example 3.3.1

Consider the spring assemblage shown in Fig. 3.3.2(a). Determine the displacement of the rigid block and forces in the springs. Assume that the rigid block is required to remain vertical (i.e., no tilting from its vertical position). Take k_1 = 100 N/m, k_2 = 50 N/m, k_3 = 150 N/m, and P = 6 N.

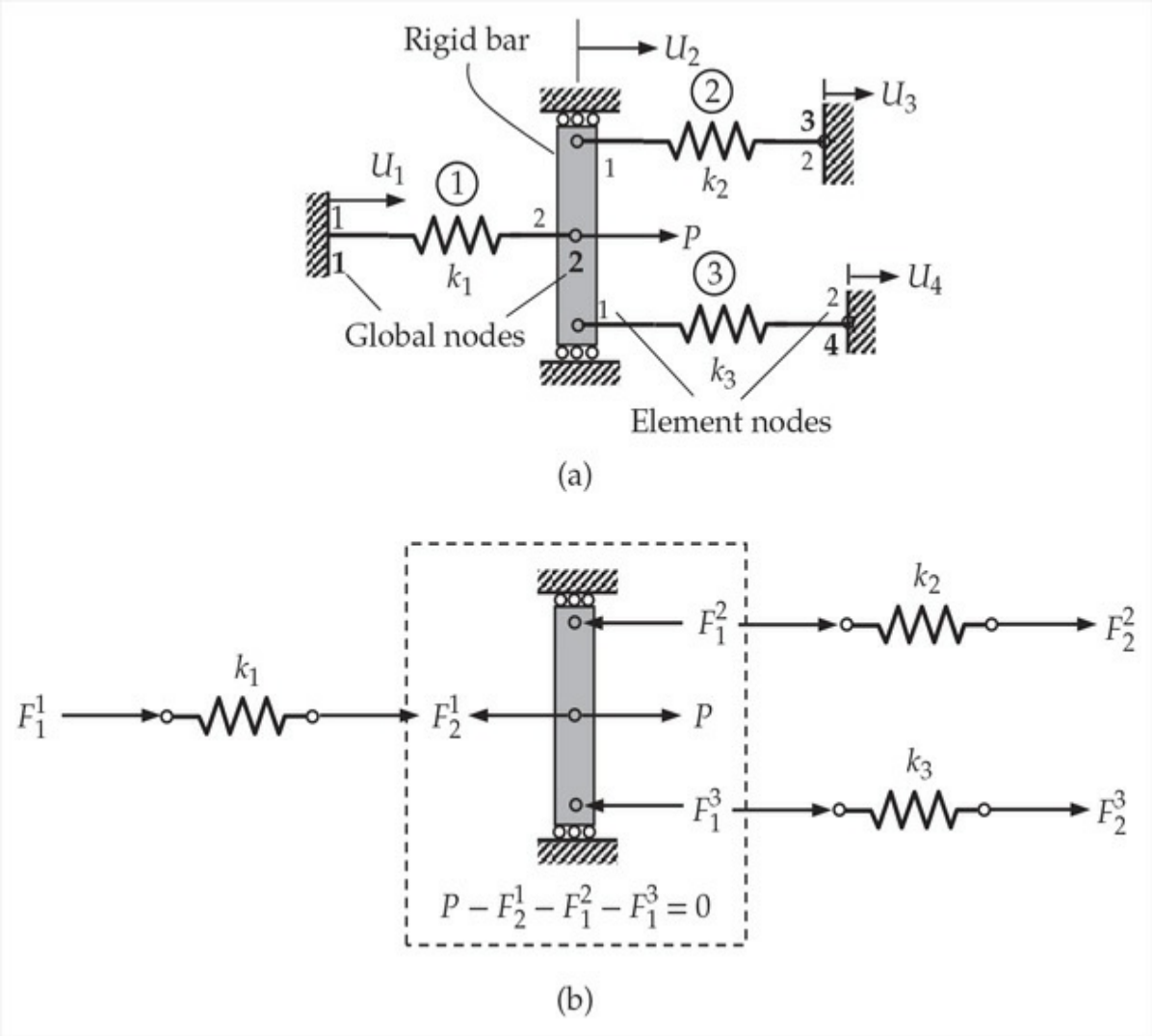

Fig. 3.3.2 (a) A three-spring system. (b) Free-body diagrams of the spring elements in the system.

Solution: There are three spring elements in the system, and each element

has two force-displacement relationships among the nodal forces and displacements. The element numbers are circled, the element node numbers are shown in lightface and the global node numbers are shown in boldface. The global displacements are shown in capital letters, U_I. Since the rigid block must remain vertical, all points on it will move horizontally by the same amount; hence, all global nodes on the block must have the same node number, say 2, as shown in Fig. 3.3.2(b). Each spring in the system has the same force-displacement relationship as in Eq. (3.3.2), except that the element number and spring constant will be different for different elements.

The three spring elements are connected at node 2 through a rigid block, as shown in Fig. 3.3.2(b). Hence, the continuity of displacements and equilibrium of forces at node 2 require

$$u_2^1 = u_1^2 = u_1^3 = U_2; \quad F_2^1 + F_1^2 + F_1^3 = F_2 \tag{3.3.3}$$

where capital letters without superscripts are used for the global quantities; the subscripts refer to the global node numbers. The equilibrium condition in Eq. (3.3.3) suggests that we must add the second equation of element 1, the first equation of element 2, and the first equation of element 3 together to replace the sum of three unknown forces $F_2^1 + F_1^2 + F_1^3$ with the known force $F_2 = P$. This process of using the continuity of displacements and balance of forces to arrive at exactly the same number of equations as the number of unknowns (before the imposition of boundary conditions) is called *assembly* of finite element equations of the system. Now we have four equations: the first equation of element 1, sum of the three equations stated above, the second equation of element 2, and the second equation of element 3:

$$\begin{aligned} k_1 U_1 - k_1 U_2 &= F_1^1 \\ -k_1 U_1 + (k_1 + k_2 + k_3) U_2 - k_2 U_3 - k_3 U_4 &= F_2^1 + F_1^2 + F_1^3 \\ -k_2 U_2 + k_2 U_3 &= F_2^2 \\ -k_3 U_2 + k_3 U_4 &= F_2^3 \end{aligned} \tag{3.3.4}$$

In matrix form, the above equations can be expressed as

$$\begin{bmatrix} k_1 & -k_1 & 0 & 0 \\ -k_1 & k_1+k_2+k_3 & -k_2 & -k_3 \\ 0 & -k_2 & k_2 & 0 \\ 0 & -k_3 & 0 & k_3 \end{bmatrix} \begin{Bmatrix} U_1 \\ U_2 \\ U_3 \\ U_4 \end{Bmatrix} = \begin{Bmatrix} F_1^1 \\ F_2^1 + F_1^2 + F_1^3 \\ F_2^2 \\ F_2^3 \end{Bmatrix} \tag{3.3.5}$$

Equation (3.3.5) is called *assembled system* of equations associated with the system of discrete springs shown in Fig. 3.3.2(a).

Alternatively, the assembly of element equations can be carried out by placing individual element equations directly into their proper locations in the assembled system (as is done in a computer program as soon as the element equations are generated). For example, element 1 has its first and second local degrees of freedom the same as the first and second global degrees of freedom (i.e., $u_1^1 = U_1$ and $u_2^1 = U_2$). Hence, we have

$$\begin{bmatrix} k_1 & -k_1 & 0 & 0 \\ -k_1 & k_1 & 0 & 0 \\ 0 & 0 & 0 & 0 \\ 0 & 0 & 0 & 0 \end{bmatrix} \begin{Bmatrix} U_1 \\ U_2 \\ U_3 \\ U_4 \end{Bmatrix} = \begin{Bmatrix} F_1^1 \\ F_2^1 \\ 0 \\ 0 \end{Bmatrix} \tag{3.3.6a}$$

Element 2 has its first and second local degrees of freedom the same as the second and third global degrees of freedom (i.e., $u_1^2 = U_2$ and $u_2^2 = U_3$). Hence, we have

$$\begin{bmatrix} 0 & 0 & 0 & 0 \\ 0 & k_2 & -k_2 & 0 \\ 0 & -k_2 & k_2 & 0 \\ 0 & 0 & 0 & 0 \end{bmatrix} \begin{Bmatrix} U_1 \\ U_2 \\ U_3 \\ U_4 \end{Bmatrix} = \begin{Bmatrix} 0 \\ F_1^2 \\ F_2^2 \\ 0 \end{Bmatrix} \tag{3.3.6b}$$

Finally, element 3 has its first and second local degrees of freedom the same as the second and fourth global degrees of freedom (i.e., $u_1^3 = U_2$ and $u_2^3 = U_4$). Hence, we have

$$\begin{bmatrix} 0 & 0 & 0 & 0 \\ 0 & k_3 & 0 & -k_3 \\ 0 & 0 & 0 & 0 \\ 0 & -k_3 & 0 & k_3 \end{bmatrix} \begin{Bmatrix} U_1 \\ U_2 \\ U_3 \\ U_4 \end{Bmatrix} = \begin{Bmatrix} 0 \\ F_1^3 \\ 0 \\ F_2^3 \end{Bmatrix} \tag{3.3.6c}$$

Adding (i.e., superposition of) these three global equations will yield the same result as in Eq. (3.3.5).

Next, we identify the boundary conditions and impose them on Eq. (3.3.5). From Fig. 3.3.2(a), it is clear that the displacements of global

nodes 1, 3, and 4 are zero, and the force at node 2 is specified to be P:

$$U_1 = U_3 = U_4 = 0, \qquad F_2^1 + F_1^2 + F_1^3 = P \tag{3.3.7}$$

Thus, there are four unknowns $(F_1^1, U_2, F_2^2, F_2^3)$ and four equations. The equations for the unknown forces contain the unknown displacement U_2, whereas equation 2 contains only the unknown displacement U_2 and known force P. Therefore, we use the second equation in Eq. (3.3.5) and determine U_2:

$$(k_1 + k_2 + k_3)\,U_2 = P \quad \text{or} \quad U_2 = \frac{P}{k_1 + k_2 + k_3} = 0.02 \text{ m} \tag{3.3.8}$$

Equations that involve only the unknown displacements are called *condensed equations for the displacements (or primary variables)*.

Once the displacements are known, the unknown forces F_1^1, F_2^2, and F_2^3 can be calculated from the remaining equations, that is, using equations 1, 3, and 4 of Eq. (3.3.5), which are termed the *condensed equations for forces (secondary variables)*:

$$\begin{aligned} F_1^1 &= -k_1 U_2 = -\frac{Pk_1}{k_1 + k_2 + k_3} = -2 \text{ N} \\ F_2^2 &= -k_2 U_2 = -\frac{Pk_2}{k_1 + k_2 + k_3} = -1 \text{ N} \\ F_2^3 &= -k_3 U_2 = -\frac{Pk_3}{k_1 + k_2 + k_3} = -3 \text{ N} \end{aligned} \tag{3.3.9}$$

It is easy to see that the equilibrium of global forces is satisfied: $F_1 + F_3 + F_4 + P = 0$.

The reaction forces at the supports can also be computed by reverting to the element equations:

$$\begin{aligned} F_1^1 &= k_1(u_1^1 - u_2^1) = -k_1 U_2 = -\frac{Pk_1}{k_1 + k_2 + k_3} \\ F_2^2 &= k_2(u_2^2 - u_1^2) = -k_2 U_2 = -\frac{Pk_2}{k_1 + k_2 + k_3} \\ F_2^3 &= k_3(u_2^3 - u_1^3) = -k_3 U_2 = -\frac{Pk_3}{k_1 + k_2 + k_3} \end{aligned} \tag{3.3.10}$$

3.3.2 Axial Deformation of Elastic Bars

For small axial deformations of a homogeneous and isotropic bar with uniform cross section, the element equations are obtained directly from the definitions of stress and strain and the stress-strain relation. For example, consider the free-body diagram of a bar element of length h_e, areas of cross section A_e, and modulus of elasticity E_e, and subjected to end forces Q_1^e and Q_2^e, as shown in Fig. 3.3.3.

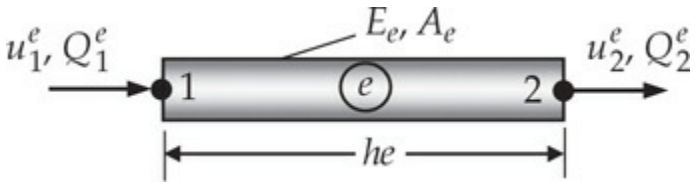

Fig. 3.3.3 A bar finite element.

From a course on mechanics of deformable solids, we have

$$\begin{aligned} &\text{strain, } \varepsilon^e = \text{elongation/original length} = \delta_e/h_e \\ &\text{stress, } \sigma^e = \text{modulus of elasticity} \times \text{strain} = E_e\,\varepsilon^e \\ &\text{load, } Q^e = \text{stress} \times \text{area of cross section} = \sigma^e A_e \end{aligned} \tag{3.3.11}$$

The strain defined above is the average (or engineering) strain. Mathematically, strain for one-dimensional problems is defined as $\varepsilon = du/dx$, u being displacement, which includes rigid body motion as well as elongation of the bar. The (compressive) force at the left end of the bar element is

$$Q_1^e = A_e\sigma_1^e = A_e E_e \varepsilon_1^e = A_e E_e \frac{u_1^e - u_2^e}{h_e} = \frac{A_e E_e}{h_e}(u_1^e - u_2^e)$$

where E_e is the Young's modulus of the bar element. Similarly, the force at the right end is

$$Q_2^e = \frac{A_e E_e}{h_e}(u_2^e - u_1^e)$$

In matrix form, these relations can be expressed as

$$k_e \begin{bmatrix} 1 & -1 \\ -1 & 1 \end{bmatrix} \begin{Bmatrix} u_1^e \\ u_2^e \end{Bmatrix} = \begin{Bmatrix} Q_1^e \\ Q_2^e \end{Bmatrix}, \quad k_e = \frac{A_e E_e}{h_e} \quad (\text{or } \mathbf{K}^e\mathbf{u}^e = \mathbf{Q}^e) \tag{3.3.12}$$

Equation (3.3.12) is identical to that in Eq. (3.3.2) for a linear elastic spring, with the equivalent spring constant of an elastic bar being $k_e = A_e E_e/h_e$. It is also the same as the one derived using Castigliano's theorem I in Example 2.3.7. This analogy holds only when the bar experiences linear variation of its displacement $u(x) = c_1 + c_2 x$. If a higher-order representation of the displacement is required, we cannot write the force-displacement relations in Eq. (3.3.9) directly; that is, the element equations of a quadratic finite element cannot be derived using Eq. (3.3.11) (Castigliano's theorem I can be used to derive it with a quadratic representation of the displacement field; see **Problem 3.29**).

Example 3.3.2

Consider a stepped bar supported by springs on both ends, as shown in Fig. 3.3.4(a). Determine the displacements in the springs and stresses in each portion of the stepped bar. Neglect the weight of the bar and assume that the bar experiences only axial displacements.

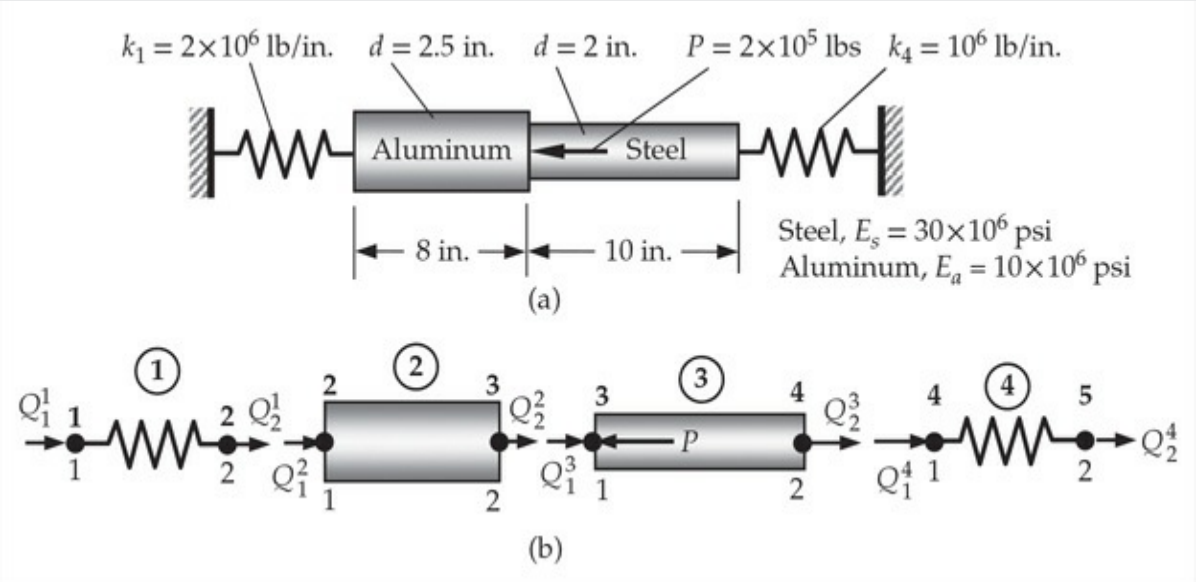

Fig. 3.3.4 (a) A spring-supported stepped bar system. (b) Free-body diagrams of the elements in the system.

Solution: There are two spring elements and two bar elements in the system, each element has two force-displacement relationships among the nodal forces and displacements. We wish to determine the displacements at global nodes 2, 3, and 4, and reaction forces at nodes 1 and 5—a total of five unknowns. Thus, we must eliminate three equations out of eight equations available to us. The free-body diagram provides the following

relations between element forces at nodes common to two (or more) elements. We have

$$Q_2^1 + Q_1^2 = 0, \quad Q_2^2 + Q_1^3 - P = 0, \quad Q_2^3 + Q_1^4 = 0 \tag{3.3.13}$$

These relations suggest that the second equation of element 1 must be added to the first equation of element 2, the second equation of element 2 must be added to the first equation of element 3, and the second equation of element 3 must be added to the first equation of element 4 to obtain the five equations expressed in terms of the global displacements:

$$U_1 = u_1^1, \quad U_2 = u_2^1 = u_1^2, \quad U_3 = u_2^2 = u_1^3, \quad U_4 = u_2^3 = u_1^4, \quad U_5 = u_2^4$$

We have

$$\begin{aligned}
k_1 U_1 - k_1 U_2 &= Q_1^1 \\
-k_1 U_1 + (k_1 + k_2) U_2 - k_2 U_3 &= Q_2^1 + Q_1^2 \\
-k_2 U_2 + (k_2 + k_3) U_3 - k_3 U_4 &= Q_2^2 + Q_1^3 \\
-k_3 U_3 + (k_3 + k_4) U_4 - k_4 U_5 &= Q_2^3 + Q_1^4 \\
-k_4 U_4 + k_4 U_5 &= Q_2^4
\end{aligned} \tag{3.3.14}$$

or in matrix form

$$\begin{bmatrix} k_1 & -k_1 & 0 & 0 & 0 \\ -k_1 & k_1 + k_2 & -k_2 & 0 & 0 \\ 0 & -k_2 & k_2 + k_3 & -k_3 & 0 \\ 0 & 0 & -k_3 & k_3 + k_4 & -k_4 \\ 0 & 0 & 0 & -k_4 & k_4 \end{bmatrix} \begin{Bmatrix} U_1 \\ U_2 \\ U_3 \\ U_4 \\ U_5 \end{Bmatrix} = \begin{Bmatrix} Q_1^1 \\ Q_2^1 + Q_1^2 \\ Q_2^2 + Q_1^3 \\ Q_2^3 + Q_1^4 \\ Q_2^4 \end{Bmatrix} \tag{3.3.15}$$

where $k_1 = 2 \times 10^6$ lb/in., $k_4 = 10^6$ lb/in., and

$$\begin{aligned}
k_2 &= \frac{A_2 E_2}{h_2} = \frac{\pi (2.5)^2 \times 10^7}{4 \times 8} = 6.136 \times 10^6 \text{ lb/in} \\
k_3 &= \frac{A_3 E_3}{h_3} = \frac{\pi (2)^2 \times 3 \times 10^7}{4 \times 10} = 9.425 \times 10^6 \text{ lb/in}
\end{aligned} \tag{3.3.16}$$

The boundary conditions and force balance conditions are

$$U_1 = 0, \quad U_5 = 0, \quad F_2 = 0, \quad F_3 = -P = -200 \times 10^3 \text{ lbs}, \quad F_4 = 0 \tag{3.3.17}$$

In view of these conditions, the condensed equations for the unknown

displacements are obtained by deleting the first and last rows and columns in Eq. (3.3.15):

$$10^6\begin{bmatrix} 8.136 & -6.136 & 0.000 \\ -6.136 & 15.561 & -9.425 \\ 0.000 & -9.425 & 10.425 \end{bmatrix}\begin{Bmatrix} U_2 \\ U_3 \\ U_4 \end{Bmatrix} = -\begin{Bmatrix} 0 \\ 2\times 10^5 \\ 0 \end{Bmatrix} \tag{3.3.18}$$

whose solution gives

$$U_2 = -6.252\times 10^{-2}\ \text{in.},\quad U_3 = -8.290\times 10^{-2}\ \text{in.},\quad U_4 = -7.495\times 10^{-2}\ \text{in.} \tag{3.3.19}$$

Thus, the first spring is in compression by 0.0625 in. and the second spring is elongated by 0.075 in.

The condensed equations for the unknown forces $F_1 = F_1^1$ and $F_5 = F_2^4$ are obtained from the first and last rows of Eq. (3.3.15) (and noting that $U_1 = U_5 = 0$):

$$\begin{Bmatrix} F_1 \\ F_5 \end{Bmatrix} = 10^6\begin{bmatrix} -2 & 0 & 0 \\ 0 & 0 & -1 \end{bmatrix}\begin{Bmatrix} U_2 \\ U_3 \\ U_4 \end{Bmatrix} = -10^6\begin{Bmatrix} 2U_2 \\ U_4 \end{Bmatrix} = 10^5\begin{Bmatrix} 1.2505 \\ 0.7495 \end{Bmatrix}\text{lbs} \tag{3.3.20}$$

Both forces act to the right. The element forces are

$$Q_1^1 = -Q_2^1 = Q_1^2 = -Q_2^2 = P + Q_1^3 = P - Q_2^3 = F_1 = 1.2504\times 10^5\ \text{lbs} \tag{3.3.21}$$

Hence, the stresses in the aluminum and steel bars are computed as

$$\begin{aligned} \sigma_a &= \frac{Q_2^2}{A_2} = -\frac{1.2505\times 10^5}{4.9087} = -25,475\ \text{lb/in.}^2\ \text{(compressive)} \\ \sigma_s &= \frac{Q_2^3}{A_3} = \frac{(2.0 - 1.2505)\times 10^5}{3.1416} = 23,858\ \text{lb/in.}^2\ \text{(tensile)} \end{aligned} \tag{3.3.22}$$

3.3.3 Torsion of Circular Shafts

Another problem that can be directly formulated as a discrete element is the torsion of a circular shaft shown in Fig. 3.3.5(a). From a course on mechanics of deformable solids, the angle of twist θ of an elastic, constant cross section, circular cylindrical member is related to torque T (about the longitudinal axis of the member) by

$$T = \frac{GJ}{L}\theta \equiv k\theta,\quad k = \frac{GJ}{L} \tag{3.3.23}$$

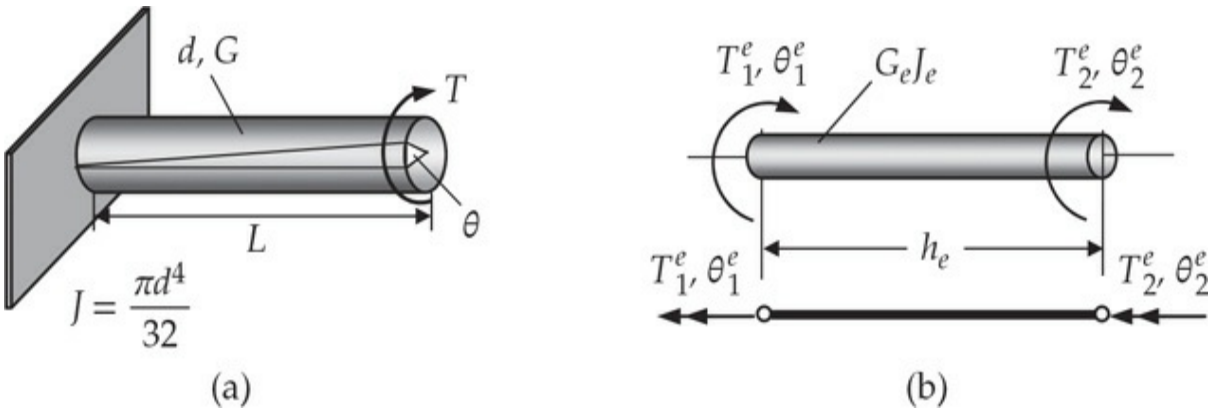

Fig. 3.3.5 (a) Torsion of a circular shaft. (b) Torsional finite element.

where J is the polar moment of area, L is the length, and G is the shear modulus of the material of the shaft. The above equation can be used to write a relationship between the end torques (T_1^e, T_2^e) and the end twists (θ_1^e, θ_2^e) of a circular cylindrical member of length h_e, as shown in Fig. 3.3.5(b):

$$T_1^e = k_e(\theta_1^e - \theta_2^e), \quad T_2^e = k_e(\theta_2^e - \theta_1^e), \quad k_e = \frac{G_e J_e}{h_e} \tag{3.3.24}$$

or, in matrix form,

$$k_e \begin{bmatrix} 1 & -1 \\ -1 & 1 \end{bmatrix} \begin{Bmatrix} \theta_1^e \\ \theta_2^e \end{Bmatrix} = \begin{Bmatrix} T_1^e \\ T_2^e \end{Bmatrix} \tag{3.3.25}$$

Once again, we have the same finite element equations with different symbols and for different physics. We can interpret that the torsional spring constant is equal
to $k_e = G_e J_e / h_e$. The nice part of using Eq. (3.3.24) is that it includes both kinematics and force balance. Consequently, solving indeterminate problems is very easy compared to the strength of materials approach.

Example 3.3.3

Consider a circular shaft AB consisting of a 10 in. long and 7/8 in. diameter steel cylinder, in which a 5 in. long, 5/8 in. diameter hole is drilled from end B. The shaft is attached at both ends to fixed rigid supports, and a 90 lb-ft torque is applied at its midsection, as shown in Fig. 3.3.6(a). Determine the amount of twist at the midsection and torque exerted on the shaft by each of the supports. Use the value $G = 11.5 \times 10^6$

psi for the shear modulus of steel.

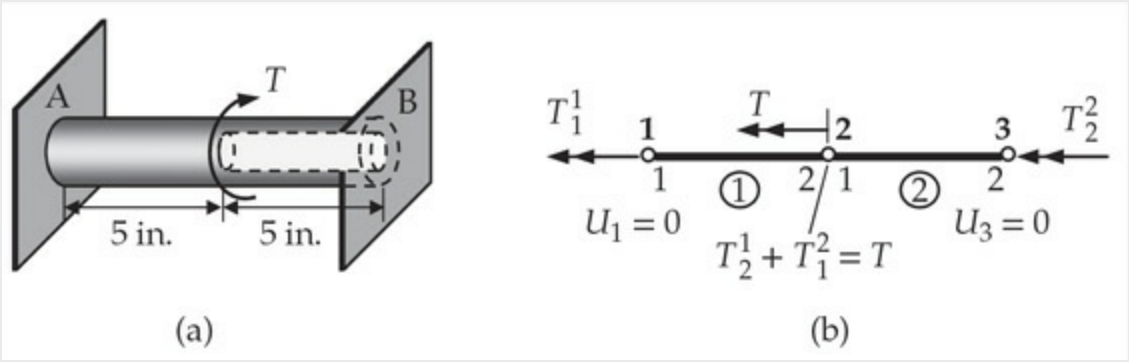

Fig. 3.3.6 (a) A steel circular shaft subjected to torque. (b) Finite element representation.

Solution: Divide the shaft into two elements of length 5 in. each, and label the element and global nodes and degrees of freedom, as shown in Fig. 3.3.6(b). The double-arrow notation used in Fig. 3.3.6(b) for the torque follows the right-hand rule (when thumb of the right hand is aligned with the double arrow, then the four fingers show the direction of the torque). Because of the equilibrium requirement on the torques at global node 2,

$$T_2^1 + T_1^2 = T \tag{1}$$

we must add the second equation of the first element to the first equation of the second element. The first equation of element 1 and the second equation of element 2 remain unchanged. The three equations can be written in matrix form as

$$\begin{bmatrix} k_1 & -k_1 & 0 \\ -k_1 & k_1 + k_2 & -k_2 \\ 0 & -k_2 & k_2 \end{bmatrix} \begin{Bmatrix} U_1 \\ U_2 \\ U_3 \end{Bmatrix} = \begin{Bmatrix} T_1^1 \\ T_2^1 + T_1^2 \\ T_2^2 \end{Bmatrix} \tag{2}$$

where

$$J_1 = \frac{\pi}{32}\left(\frac{7}{8}\right)^4 = 57.6 \times 10^{-3}\ \text{in.}^4, \quad J_2 = \frac{\pi}{32}\left[\left(\frac{7}{8}\right)^4 - \left(\frac{5}{8}\right)^4\right] = 42.6 \times 10^{-3}\ \text{in.}^4 \tag{3}$$

and

$$k_1 = \frac{G_1 J_1}{h_1} = \frac{1}{5}(11.5 \times 10^6)(57.6 \times 10^{-3}) = 132.48 \times 10^3$$
$$k_2 = \frac{G_2 J_2}{h_2} = \frac{1}{5}(11.5 \times 10^6)(42.6 \times 10^{-3}) = 97.98 \times 10^3 \quad (4)$$

The boundary conditions require $U_1 = U_3 = 0$. Hence, the condensed equation (i.e., equation for the primary unknown) U_2 is

$$U_2 = \frac{T}{k_1 + k_2} = \frac{90 \times 12}{230.46 \times 10^3} = 4.6863 \times 10^{-3} \text{ rad.} \quad (5)$$

To determine the reactions at the fixed ends, we use the first and last rows in Eq. (2):

$$Q_1^1 = -k_1 U_2 = -132.48 \times 4.6863 = -620.84 \text{ lb-in.} = -51.737 \text{ lb-ft}$$
$$Q_2^2 = -k_2 U_2 = -97.98 \times 4.6863 = -459.16 \text{ lb-in.} = -38.263 \text{ lb-ft} \quad (6)$$

where the minus sign indicates that the torques computed are in the direction opposite to the adopted notation (they are in the opposite direction to the applied torque).

3.3.4 Electrical Resistor Circuits

There is a direct analogy between network of mechanical springs and direct current electric resistor network. Ohm's law provides the relationship between flow of electric current I (amperes) through an ideal resistor and voltage drop V (volts) between the ends of the resistor:

$$V = IR \quad (3.3.26)$$

where R denotes the electric resistance (ohms) of the wire.

Kirchhoff's voltage rule states that the algebraic sum of the voltage changes in any loop must be equal to zero. Applied to a single resistor, the rule gives (see Fig. 3.3.7)

$$I_1^e R_e + V_2^e - V_1^e = 0, \quad I_2^e R_e + V_1^e - V_2^e = 0 \quad (3.3.27)$$

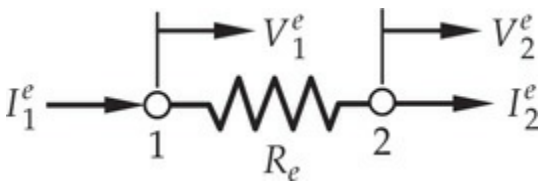

Fig. 3.3.7 Direct current electric element.

or in matrix form

$$\frac{1}{R_e}\begin{bmatrix} 1 & -1 \\ -1 & 1 \end{bmatrix}\begin{Bmatrix} V_1^e \\ V_2^e \end{Bmatrix} = \begin{Bmatrix} I_1^e \\ I_2^e \end{Bmatrix} \tag{3.3.28}$$

Thus, once again we have the same form of relationship between voltages and currents as in the case of springs. The quantity $1/R_e$ is known as the *electrical conductance.*

The assembly of resistor equations is based on the following rules:

1. Voltage is single-valued.
2. *Kirchhoff's current rule:* Sum of all currents entering a node is equal to zero.

Next we consider an example of the finite element analysis of a resistor network to illustrate the ideas.

Example 3.3.4

Consider the resistor circuit shown in Fig. 3.3.8(a), where the symbol Ω means ohms, the units of electrical resistance. Determine the currents in the loops and voltage at the nodes.

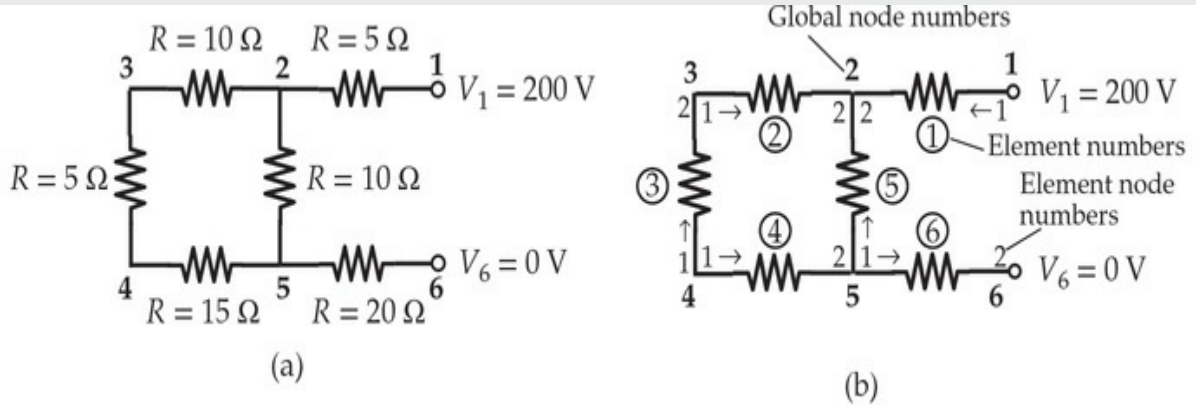

Fig. 3.3.8 (a) A resistor circuit. (b) Finite element mesh of the resistor circuit.

Solution: The element numbering, element node numbering, and global node numbering are indicated in Fig. 3.3.8(b). The element node numbering is important in assembling the element equations. The element

node numbers used in Fig. 3.3.7 indicate that current flows from node 1 to node 2 of the element. The element node numbering used in Fig. 3.3.8(b) indicates the assumed direction of currents.

Since the given resistor circuit is somewhat complicated, it is convenient to introduce the *connectivity matrix* that relates the element primary nodal degrees of freedom to the global primary degrees of freedom. The correspondence can be expressed through a matrix **B** whose coefficient b_{ij} in the ith row and jth column has the following meaning:

b_{ij} = the global node number corresponding to the jth element node number of the ith element (3.3.29)

For example, for the network shown in Fig. 3.3.8, the matrix **B** is of the order 6 × 2 (6 elements, each having no more than 2 primary degrees of freedom per element; for this one degree of freedom system, the number of nodes is the same as the number of primary degrees of freedom):

$$\mathbf{B} = \begin{array}{c} \begin{matrix} 1 & 2 \end{matrix} \\ \left[\begin{array}{cc} 1 & 2 \\ 3 & 2 \\ 4 & 3 \\ 4 & 5 \\ 5 & 2 \\ 5 & 6 \end{array}\right] \end{array} \begin{matrix} 1 \\ 2 \\ 3 \\ 4 \\ 5 \\ 6 \end{matrix} \tag{1}$$

The entries in the first column correspond to the first degree of freedom number of each element in the mesh and those in the second column correspond to the second degree of freedom of the element; each row corresponds a single element, with row number being the same as the element number. The matrix **B** can be used to assemble element coefficient matrices K_{ij}^{e} directly into the assembled matrix K_{IJ} as follows (note that the global nodes I and J must belong to the same element in order to have an entry in the global coefficient matrix; e.g., $K_{35} = 0$ and $K_{42} = 0$ because global nodes 3 and 5 do not belong to the same element and global nodes 2 and 4 do not belong to the same element; also, a global entry can have multiple entries added from different elements):

$K_{11} = K_{11}^{1}$, because local node 1 of element 1 corresponds to global node 1.

$K_{22} = K_{22}^{1} + K_{22}^{2} + K_{22}^{5}$, because local node 2 of elements 1, 2, and 5 corresponds to global node 2.

$K_{12} = K_{12}^{1}$, because local nodes 1 and 2 of element 1 correspond to global nodes 1 and 2, respectively. (2)

$K_{45} = K_{12}^{4}$, because local nodes 1 and 2 of element 4 correspond to global nodes 4 and 5, respectively.

$K_{42} = 0$, because there is no element whose nodes 1 and 2 correspond to the global nodes 4 and 2, respectively.

$K_{44} = K_{11}^{3} + K_{11}^{4}$, because node 1 of element 3 as well as node 1 of element 4 correspond to global node 4.

When more than one element is connected at a global node, the element coefficients are added together. For example, global node 5 appears in three rows (i.e., elements) of the matrix **B**, implying that all three elements are connected to a global node 5. Since global node 5 is the same as node 2 of element 4, node 1 of element 5, and node 1 of element 6, we have $F_5 = F_2^4 + F_1^5 + F_1^6 = I_2^4 + I_1^5 + I_1^6$. Similarly, $K_{55} = K_{22}^4 + K_{11}^5 + K_{11}^6$. For the off-diagonal coefficients, all we need to see is if both subscripts of the coefficient belong to the same row (i.e., from the same element). If they do not, then the global coefficient is zero. Thus, assembly by hand can be carried out by examining the finite element mesh of the problem. Inspection of **B** shows that all global coefficients come from a single element as there are no two rows that contain the same pair of two numbers. Thus, the assembled coefficient matrix is given by $(K_{ij}^e = K_{ji}^e)$

$$
\mathbf{K} = \begin{array}{c} \begin{matrix} 1 & 2 & 3 & 4 & 5 & 6 \end{matrix} \\ \left[\begin{matrix} K_{11}^{1} & K_{12}^{1} & 0 & 0 & 0 & 0 \\ & K_{22}^{1}+K_{22}^{2}+K_{22}^{5} & K_{21}^{2} & 0 & K_{21}^{5} & 0 \\ & & K_{11}^{2}+K_{22}^{3} & K_{21}^{3} & 0 & 0 \\ & & & K_{11}^{3}+K_{11}^{4} & K_{12}^{4} & 0 \\ & & & & K_{22}^{4}+K_{11}^{5}+K_{11}^{6} & K_{12}^{6} \\ \text{symm.} & & & & & K_{22}^{6} \end{matrix}\right] \end{array} \begin{matrix} 1 \\ 2 \\ 3 \\ 4 \\ 5 \\ 6 \end{matrix}
$$

$$
= \left[\begin{matrix} 0.2 & -0.2 & 0.0 & 0.0 & 0.0 & 0.0 \\ & 0.2+0.1+0.1 & -0.1 & 0.0 & -0.1 & 0.0 \\ & & 0.1+0.2 & -0.2 & 0.0 & 0.0 \\ & & & 0.2+0.0667 & -0.0667 & 0.0 \\ & & & & 0.0667+0.1+0.05 & -0.05 \\ \text{symm.} & & & & & 0.05 \end{matrix}\right] \tag{3}
$$

The right-hand-side vector is

$$
\mathbf{F}^{\mathrm{T}} = \left\{I_1^1,\ I_2^1 + I_2^2 + I_2^5,\ I_1^2 + I_2^3,\ I_1^3 + I_1^4,\ I_2^4 + I_1^5 + I_1^6,\ I_2^6\right\} \tag{4}
$$

The boundary conditions are $V_1 = 200$, $V_6 = 0$, and $\mathbf{F}^{\mathrm{T}} = \{I_1^1,\ 0,\ 0,\ 0,\ 0, I_2^6\}$. The condensed equations for the nodal voltages are obtained by moving the terms involving V_1 and V_6 to the right side and then deleting the first and last row and column of the 6×6 system:

$$
\left[\begin{matrix} 0.4 & -0.1 & 0.0000 & -0.1000 \\ -0.1 & 0.3 & -0.2000 & 0.0000 \\ 0.0 & -0.2 & 0.2667 & -0.0667 \\ -0.1 & 0.0 & -0.0667 & 0.2167 \end{matrix}\right] \left\{\begin{matrix} V_2 \\ V_3 \\ V_4 \\ V_5 \end{matrix}\right\} = \left\{\begin{matrix} 0.20\,V_1 \\ 0.00 \\ 0.00 \\ 0.05\,V_6 \end{matrix}\right\} \tag{5}
$$

The solution of these equations is given by (obtained with the aid of a computer)

$$
V_2 = 169.23,\quad V_3 = 153.85,\quad V_4 = 146.15,\quad V_5 = 123.08 \text{ (volts)} \tag{6}
$$

The condensed equations for the unknown currents at nodes 1 and 6 can be calculated from equations 1 and 6 of the system. We have

$$
\begin{aligned} I_1^1 &= 0.2V_1 - 0.2V_2 = 40 - 33.846 = 6.154 \text{ amps} \\ I_2^6 &= -0.05V_5 + 0.05V_6 = -6.154 \text{ amps} \end{aligned} \tag{7}
$$

The negative sign on I_1^6 indicates that the current is flowing out of global node 6.

The currents through each element can be calculated using the element equations in Eq. (3.3.28). For example, the nodal currents in resistor 5 are given by

$$\begin{Bmatrix} I_1^5 \\ I_2^5 \end{Bmatrix} = \begin{bmatrix} 0.1 & -0.1 \\ -0.1 & 0.1 \end{bmatrix} \begin{Bmatrix} 123.08 \\ 169.23 \end{Bmatrix} = \begin{Bmatrix} -4.615 \\ 4.615 \end{Bmatrix} \tag{8}$$

which indicates that the net current flow in resistor 5 is from its node 2 to node 1 (or global node 2 to global node 5), and its value is 4.615 amps (which is the same as 6.154 − 1.539). The finite element solutions for the voltages and currents are shown in Fig. 3.3.9.

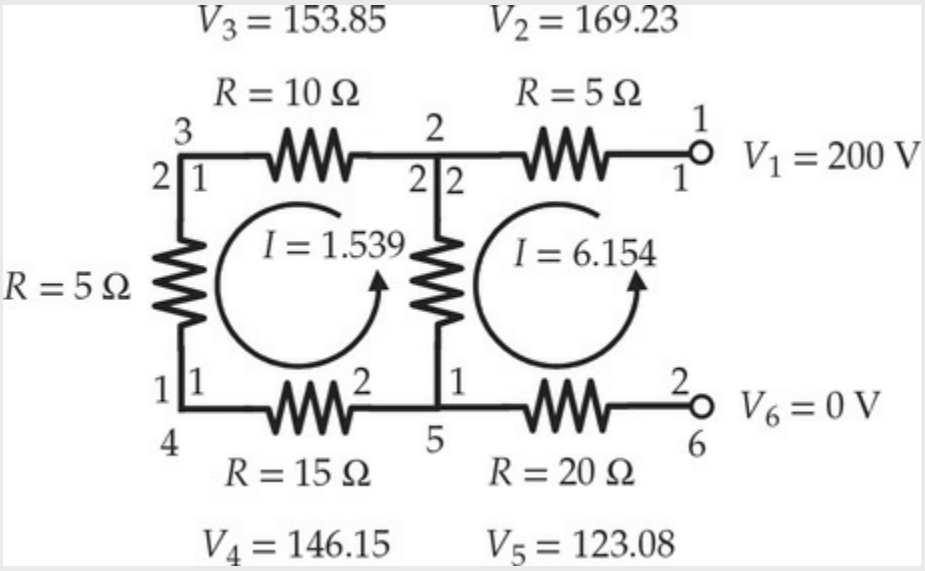

Fig. 3.3.9 The solution for currents and voltages obtained with the finite element method.

3.3.5 Fluid Flow Through Pipes

Another example of a discrete element is provided by steady, fully developed, flows of viscous incompressible fluids through circular pipes. The velocity of fully developed laminar flow of viscous fluids through a straight circular pipe of diameter d is given by (see Reddy [1], p. 178)

$$v_x = -\frac{d^2}{16\mu}\frac{dP}{dx}\left[1 - \left(\frac{2r}{d}\right)^2\right] \tag{3.3.30}$$

where r is the radial coordinate, dP/dx is the pressure gradient, d is the diameter of the pipe, and μ is the viscosity of the fluid [see Fig. 3.3.10(a)].

The volume rate of flow, Q, is obtained by integrating v_x over the pipe cross section. Thus the relationship between Q and the pressure gradient dP/dx is given by the equation

$$Q = -\frac{\pi d^4}{128\mu}\frac{dP}{dx} \tag{3.3.31}$$

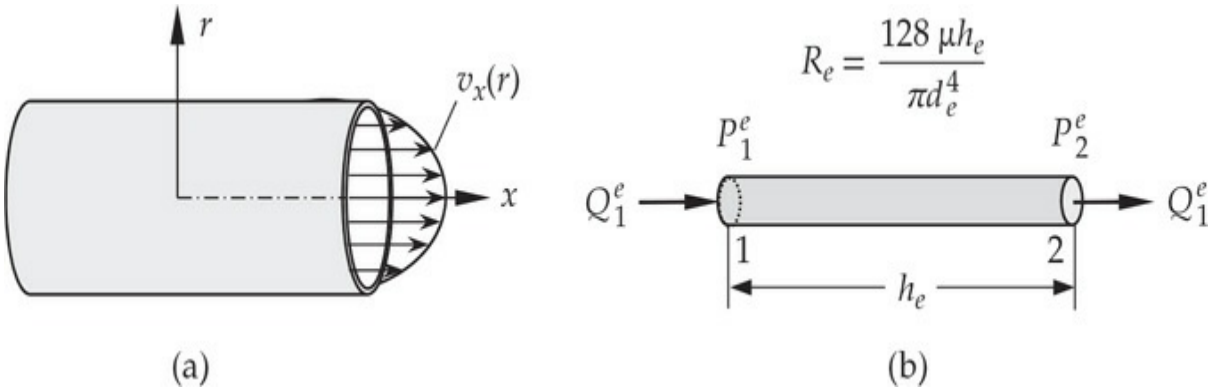

Fig. 3.3.10 Flow of viscous fluids through pipes.

The negative sign indicates that the flow is in the direction of the negative pressure gradient.

Equation (3.3.31) can be used to develop a relationship between the nodal values of the volume rate of flow, (Q_1^e, Q_2^e), and the pressure, (P_1^e, P_2^e), of a pipe element of length h_e and diameter d_e. The volume rate of flow entering node 1 is given by [see Fig. 3.3.10(b)]

$$Q_1^e = -\frac{\pi d_e^4}{128\mu h_e}(P_2^e - P_1^e) \tag{3.3.32a}$$

Similarly, the volume rate of flow entering node 2 is

$$Q_2^e = -\frac{\pi d^4}{128\mu h_e}(P_1^e - P_2^e) \tag{3.3.32b}$$

Thus, we have

$$\frac{\pi d_e^4}{128\mu h_e}\begin{bmatrix} 1 & -1 \\ -1 & 1 \end{bmatrix}\begin{Bmatrix} P_1^e \\ P_2^e \end{Bmatrix} = \begin{Bmatrix} Q_1^e \\ Q_2^e \end{Bmatrix} \tag{3.3.33}$$

The constant $R_e = 128\mu h_e/\pi d_e^4$ is called the *pipe resistance*, in analogy with the electrical resistance [see Eq. (3.3.27)].

3.3.6 One-Dimensional Heat Transfer

The direct approach can also be used to develop finite element models of one-dimensional heat transfer. The relations between temperatures and heats at the ends of a surface insulated solid bar or two surfaces of a plane wall can be developed using the basic principles of heat transfer. We have

$$\text{temperature gradient} = \text{difference in temperature}/\text{length}$$

$$\text{heat flux, } q = \text{conductivity} \times (-\text{temperature gradient})$$

$$\text{heat, } Q = \text{heat flux} \times \text{area of cross section}$$

Then, if there is no internal heat generation and the temperature is assumed to vary linearly between the ends of the bar of length (or plane wall of thickness) h_e, cross-sectional area A_e, and conductivity k_e, the heats at the left and right ends of the bar are

$$Q_1^e = A_e q_1^e = -A_e k_e \frac{T_2^e - T_1^e}{h_e} = \frac{A_e k_e}{h_e}(T_1^e - T_2^e)$$

$$Q_2^e = A_e q_2^e = -A_e k_e \frac{T_1^e - T_2^e}{h_e} = \frac{A_e k_e}{h_e}(T_2^e - T_1^e)$$

Technically, both Q_1^e and Q_2^e are heat inputs. In matrix form, we have

$$\frac{A_e k_e}{h_e}\begin{bmatrix} 1 & -1 \\ -1 & 1 \end{bmatrix}\begin{Bmatrix} T_1^e \\ T_2^e \end{Bmatrix} = \begin{Bmatrix} Q_1^e \\ Q_2^e \end{Bmatrix} \tag{3.3.34}$$

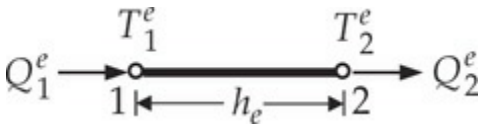

The similarity between Eq. (3.3.28) of an electric resistor and Eq. (3.3.34) of one-dimensional heat transfer allows us to identify the *thermal resistance* R_{th}^e as

$$R_{th}^e = \frac{h_e}{k_e A_e} \tag{3.3.35}$$

Then Eqs. (3.3.28) and (3.3.34) are the same with the following correspondence:

$$R_e \sim R_{th}^e, \quad I_i^e \sim Q_i^e, \quad V_i^e \sim T_i^e \tag{3.3.36}$$

This allows us to model complicated problems involving both series and parallel thermal resistances. Typical problems and their electrical analogies are shown in Fig. 3.3.11.

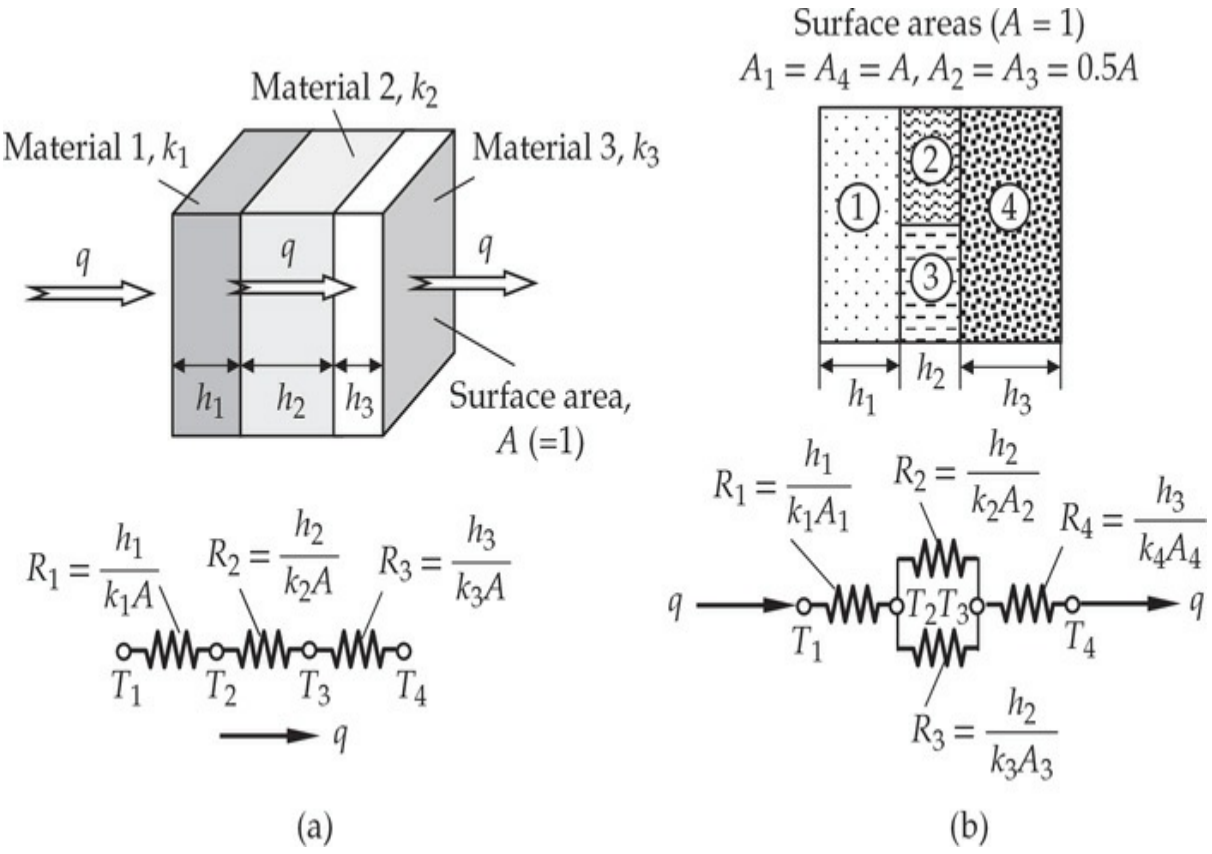

Fig. 3.3.11 One-dimensional heat transfer through composite walls and their thermal circuits.

Example 3.3.5

A composite wall consists of three materials, as shown in Fig. 3.3.12. The inside wall temperature is 200°C and the outside air temperature is 50°C with a convection coefficient of β = 10 W/(m^2 · K). Determine the temperature along the composite wall using the minimum number of finite elements.

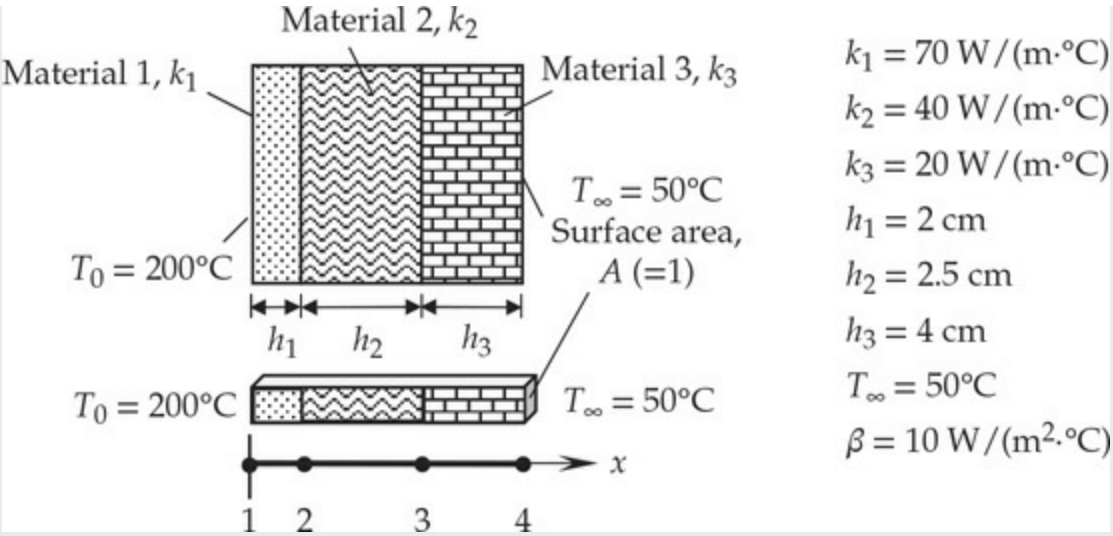

Fig. 3.3.12 Heat transfer problem discussed in Example 3.3.5.

Solution: Since there are three walls with different conductivities, we shall use three elements to model the problem. The element matrices are

$$\mathbf{K}^1 = \frac{k_1 A}{h_1}\begin{bmatrix} 1 & -1 \\ -1 & 1 \end{bmatrix} = \frac{70\times 1}{0.02}\begin{bmatrix} 1 & -1 \\ -1 & 1 \end{bmatrix} = \begin{bmatrix} 3500 & -3500 \\ -3500 & 3500 \end{bmatrix}$$

$$\mathbf{K}^2 = \frac{k_2 A}{h_2}\begin{bmatrix} 1 & -1 \\ -1 & 1 \end{bmatrix} = \frac{40\times 1}{0.025}\begin{bmatrix} 1 & -1 \\ -1 & 1 \end{bmatrix} = \begin{bmatrix} 1600 & -1600 \\ -1600 & 1600 \end{bmatrix} \qquad (1)$$

$$\mathbf{K}^3 = \frac{k_3 A}{h_3}\begin{bmatrix} 1 & -1 \\ -1 & 1 \end{bmatrix} = \frac{20\times 1}{0.04}\begin{bmatrix} 1 & -1 \\ -1 & 1 \end{bmatrix} = \begin{bmatrix} 500 & -500 \\ -500 & 500 \end{bmatrix}$$

where the area of cross section is taken to be unity, that is, unit surface area of the plane wall is used.

The heat balance conditions between walls can be expressed as

$$Q_2^1 + Q_1^2 = 0, \quad Q_2^2 + Q_1^3 = 0 \qquad (2)$$

These require us to add the second equation of the first wall to the first equation of the second wall, and the second equation of the second wall to the first equation of the third wall to get rid of the extra unknowns $Q_2^1 = -Q_1^2$ and $Q_2^2 = -Q_1^3$. Thus, the assembled finite element equations are

$$\begin{bmatrix} 3,500 & -3,500 & 0 & 0 \\ -3,500 & 3,500+1,600 & -1,600 & 0 \\ 0 & -1,600 & 1,600+500 & -500 \\ 0 & 0 & -500 & 500 \end{bmatrix} \begin{Bmatrix} U_1 \\ U_2 \\ U_3 \\ U_4 \end{Bmatrix} = \begin{Bmatrix} Q_1^1 \\ 0 \\ 0 \\ Q_2^3 \end{Bmatrix} \qquad (3)$$

To identify the boundary conditions of the problem, we assume that the left surface of the composite wall is maintained at temperature T_0 while the right surface is exposed to ambient temperature T_∞. Therefore, the boundary conditions become

$$T(0) = T_0 \rightarrow U_1 = T_0 \text{ and } \left[k_3 \frac{dT}{dx} + \beta (T - T_\infty)\right]_{x=L} = 0 \rightarrow Q_2^3 + \beta (U_4 - T_\infty) = 0 \quad (4)$$

where $L = h_1 + h_2 + h_3$ and β is the heat transfer coefficient between the surface and the surroundings. Consistent with the notation, we have assumed that $T(L) = U_4 > T_\infty$. The boundary conditions can be expressed as

$$U_1 = T_0 = 200, \quad Q_2^3 = -\beta (U_4 - T_\infty) = -10U_4 + 500 \quad (5)$$

Hence, the condensed equations for the unknown primary variables (i.e., temperatures) are

$$\begin{bmatrix} 5,100 & -1,600 & 0 \\ -1,600 & 2,100 & -500 \\ 0 & -500 & 500 \end{bmatrix} \begin{Bmatrix} U_2 \\ U_3 \\ U_4 \end{Bmatrix} = \begin{Bmatrix} 3,500 \times 200 \\ 0 \\ -10U_4 + 500 \end{Bmatrix} \quad (6)$$

Taking the unknown U_4 from the right side to the left side of the equation, we obtain

$$\begin{bmatrix} 5,100 & -1,600 & 0 \\ -1,600 & 2100 & -500 \\ 0 & -500 & 510 \end{bmatrix} \begin{Bmatrix} U_2 \\ U_3 \\ U_4 \end{Bmatrix} = \begin{Bmatrix} 7 \times 10^5 \\ 0 \\ 500 \end{Bmatrix} \quad (7)$$

The solution of these equations is given by

$$U_1 = 200°\text{C}, \quad U_2 = 199.58°\text{C}, \quad U_3 = 198.67°\text{C}, \quad U_4 = 195.76°\text{C} \quad (8)$$

The unknown heat Q_1^1 (per unit area) can be computed from the first row of the assembled equations

$$Q_1^1 = 3{,}500U_1 - 3{,}500U_2 = 3{,}500 \times 200 - 3{,}500 \times 199.58354 = 1{,}457.6 \text{ W/m}^2 \text{ (heat in)} \quad (9)$$

The heat Q_2^3 can be computed from the last row of the assembled equations

$$Q_2^3 = -10 (U_4 - 50) = -10(195.76 - 50) = -1{,}457.6 \text{ W/m}^2 \text{ (heat out)} \quad (10)$$

The exact solution for one-dimensional heat flow through a composite wall can be derived by solving the governing equation

$$-kA\frac{d^2T}{dx^2}=0 \tag{11}$$

in each portion of the wall and applying the interface and boundary conditions. The solution is given by

$$T_{\text{exact}}(x)=\begin{cases} A_1+A_2x, & 0<x<h_1 \\ B_1+B_2x, & h_1<x<h_1+h_2 \\ C_1+C_2x, & h_1+h_2<x<h_1+h_2+h_3 \end{cases} \tag{12}$$

$$A_1=T_0,\ \ A_2=\frac{T_\infty-T_0}{\Delta},\ \ B_1=T_0+h_1\left(1-\frac{k_1}{k_2}\right)A_2$$

$$B_2=\frac{k_1}{k_2}A_2,\ \ C_1=T_\infty-k_1\left(\frac{1}{\beta}+\frac{L}{k_3}\right)A_2,\ \ C_2=\frac{k_2}{k_3}B_2 \tag{13}$$

$$\Delta=k_1\left(\frac{h_1}{k_1}+\frac{h_2}{k_2}+\frac{h_3}{k_3}+\frac{1}{\beta}\right)$$

The finite element solution for the nodal temperatures and heats matches with the exact solution.

3.4 Finite Element Models of Continuous Systems

3.4.1 Preliminary Comments

In the subsections that follow, our objective is to introduce many fundamental ideas that form the basis of the finite element method. In doing so, we postpone some issues of practical and theoretical complexity to later sections of this chapter and to subsequent chapters. The basic steps of a finite element analysis are introduced via a model second-order differential equation, which represents a mathematical model of most systems that can be idealized as one-dimensional systems (e.g., see Examples 1.2.2 and 1.2.3).

3.4.2 Model Boundary Value Problem

Consider the problem of finding the function $u(x)$ that satisfies the differential equation

$$-\frac{d}{dx}\left(a\frac{du}{dx}\right)+cu-f=0 \quad \text{for} \quad 0<x<L \tag{3.4.1}$$

and the boundary conditions

$$u(0)=u_0, \qquad \left(a\frac{du}{dx}\right)\Big|_{x=L}=Q_L \tag{3.4.2}$$

where $a = a(x)$, $c = c(x)$, $f = f(x)$, u_0, and Q_L are known quantities, called the *data* of the problem. Equation (3.4.1) arises in connection with the analytical description of many physical processes. For example, conduction and convection heat transfer in the bar shown in Fig. 3.4.1(a), flow through channels and pipes, transverse deflection of cables, axial deformation of bars shown in Fig. 3.4.1(b), and many other physical processes are described by Eq. (3.4.1). A sample list of field problems described by Eq. (3.4.1) when $c(x) = 0$ is presented in Table 3.4.1. Thus, if we can develop a numerical procedure by which Eq. (3.4.1) can be solved for all possible boundary conditions, the procedure can be used to solve all field problems listed in Table 3.4.1. This fact provides us with the motivation to use Eq. (3.4.1) as the model second-order equation in one dimension.

The mathematical problem consists of solving the differential equation in Eq. (3.4.1) in the one-dimensional domain $\Omega = (0, L)$, subject to a suitable set of specified boundary conditions at the boundary points $x = 0$ and $x = L$, as shown in Fig. 3.4.1(c). As already shown in Chapter 2, the boundary conditions associated with a differential equation emerge in a natural way during the weak-form development of the differential equation. The finite element analysis of the equation requires division of $\Omega = (0, L)$ into a set of subintervals $\Omega^e = (x_a^e, x_b^e)$ (see Fig. 3.4.2), development of the weak form of the differential equation over Ω^e, and application of the Ritz method to derive algebraic equations among the nodal values of $u(x)$ and its dual variable, $a(du/dx)$. A detailed discussion of these ideas is presented next.

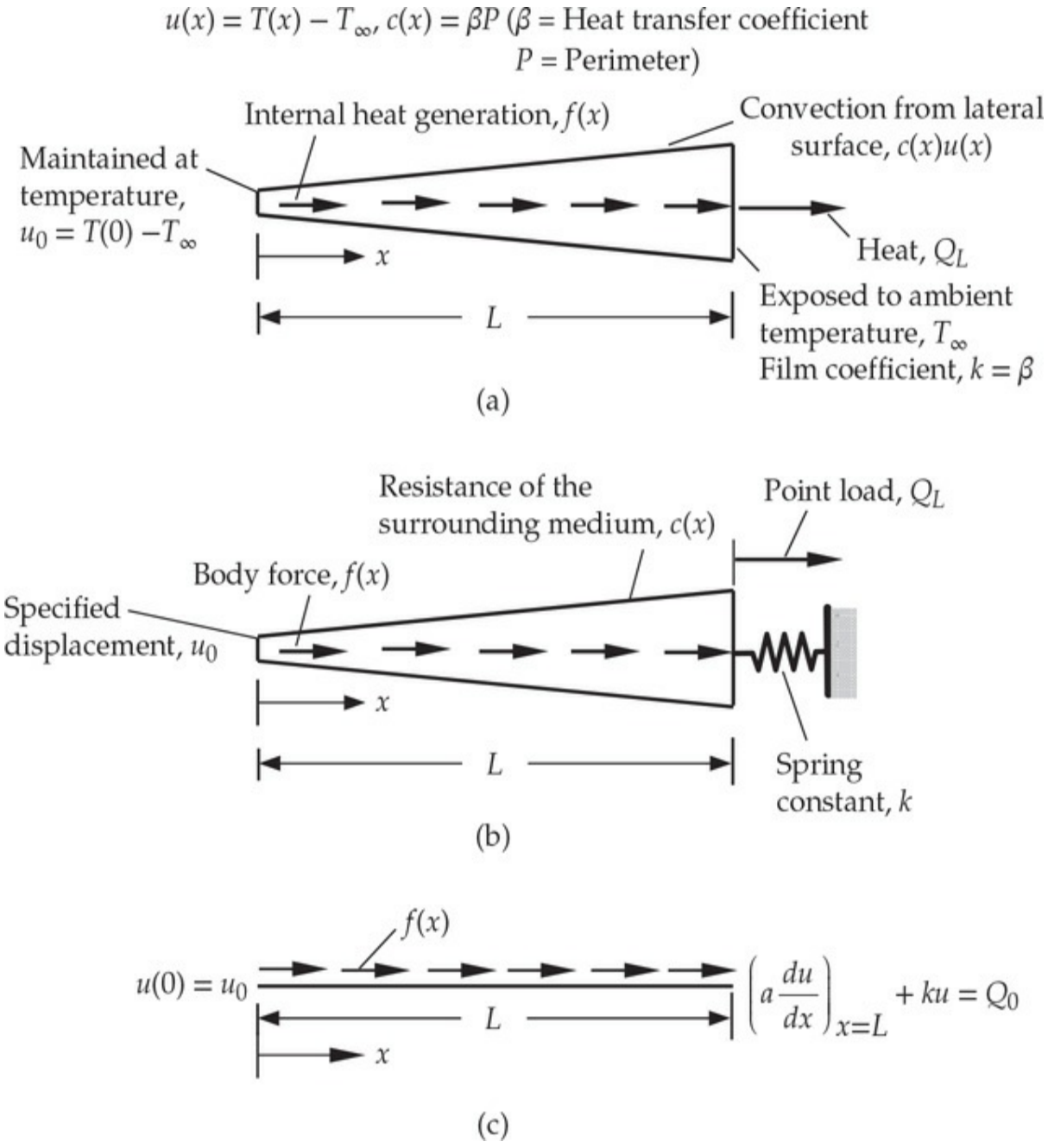

Fig. 3.4.1 (a) Heat transfer in a fin. (b) Axial deformation of a bar. (c) Mathematical idealization of the problem in (a) or (b).

3.4.3 Derivation of Element Equations: The Finite Element Model

The domain and its subdivision into a collection of finite elements are shown in Fig. 3.4.2(a) and (b), respectively. A typical element, $\Omega^e = (x_a^e, x_b^e)$, is located between points A and B with coordinates $x = x_a^e$ and $x = x_b^e$ and its length is $h_e = x_b^e - x_a^e$. The collection of finite elements

in a domain is called the *finite element mesh* of the domain. To obtain the Ritz equations for the nodal values of $u(x)$, we focus on solving Eq. (3.4.1) subject to the boundary conditions $u(x_a^e) = u_a^e$ and $u(x_b^e) = u_b^e$ using the Ritz method. The main difference here is that we apply a variational method over a finite element Ω^e as opposed to the total domain Ω. This step results in *the finite element model*, $\mathbf{K}^e \mathbf{u}^e = \mathbf{F}^e$.

The derivation of finite element equations, that is, algebraic relations among the unknown parameters of the finite element approximation, involves the following three steps:

1. Construct the weighted-residual or weak form of the differential equation.
2. Assume the form of the approximate solution over a typical finite element.
3. Derive the finite element equations by substituting the approximate solution into the weighted-residual or weak form.

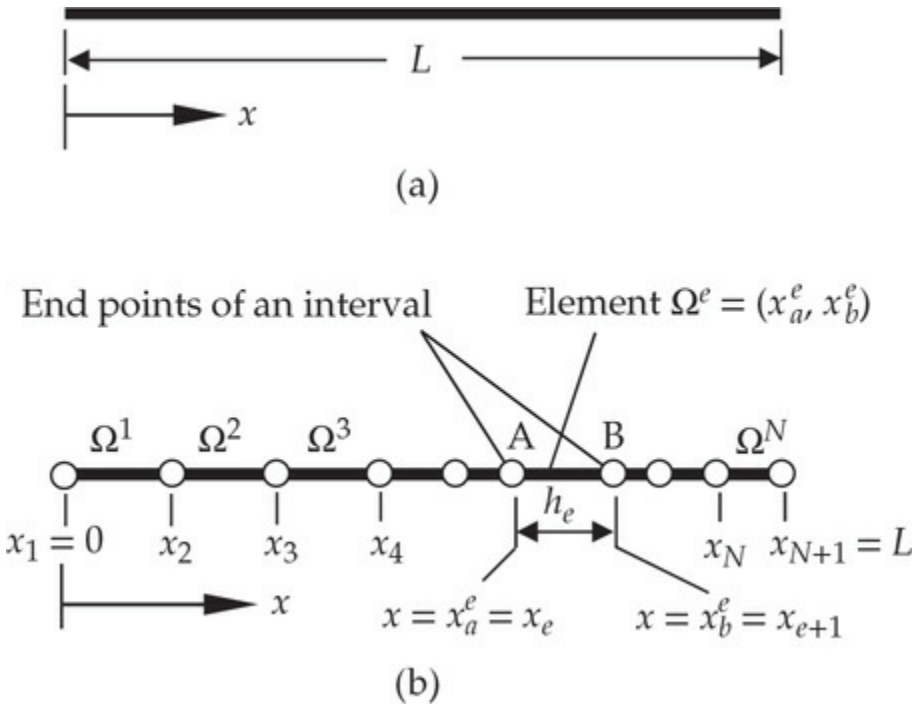

Fig. 3.4.2 (a) Whole domain. (b) Finite element discretization (mesh).

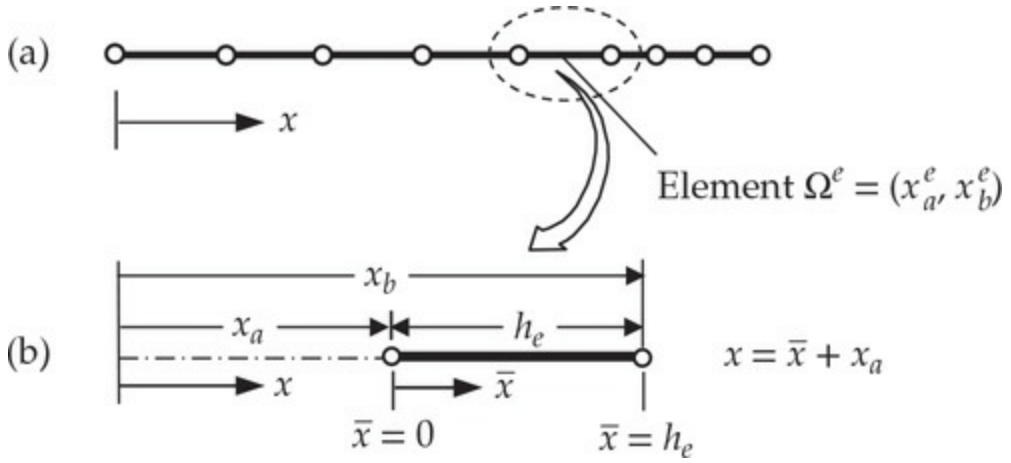

Fig. 3.4.3 (a) The finite element mesh of the domain. (b) A typical finite element isolated from the mesh.

A typical element $\Omega^e = (x_a^e, x_b^e)$ is isolated from the mesh [see Fig. 3.4.3(a) and (b)]. We seek an approximate solution to the governing differential equation over the element. In principle, any method of solution that allows the derivation of necessary algebraic relations among the duality pairs at all nodes of the element can be used. In this book we develop the algebraic equations using the Ritz (i.e., the weak-form Galerkin) method.

3.4.3.1 Weak-form development

The weak-form development was discussed in detail in Sections 2.4.4–2.4.6. Here we review the three steps in the derivation of the weak form associated with the model differential equation over a *typical element* of the mesh. We begin with the polynomial approximation of the solution within a typical finite element Ω^e to be of the form:

$$u_h^e(x) = \sum_{j=1}^{n} u_j^e \psi_j^e(x) \tag{3.4.3}$$

where u_j^e are the values of the solution $u(x)$ at the nodes of the finite element Ω^e, and $\psi_j^e(x)$ are the approximation functions over the element. The superscript e refers to element Ω^e while the subscript h on the approximate solution u_h^e refers to a mesh parameter (such as the length of the element). The particular form in Eq. (3.4.3) will be derived in the next section. Note that the approximation in Eq. (3.4.3) differs from the one used in the Ritz method in that $c_j\varphi_j(x)$ is now replaced with $u_j^e\psi_j^e(x)$, and u_j^e

plays the role of undetermined parameters and ψ_j^e the role of approximation functions over an element Ω^e. As we shall see later, writing the approximation in terms of the nodal values of the solution is necessitated by the fact that the continuity of $u(x)$ between elements can be readily imposed by equating the nodal values from all elements connected at the node. In addition, when the final algebraic equations are solved we obtain the nodal values u_j^e directly as opposed to parameters c_j, which often do not have any physical meaning.

Since the actual solution u is replaced by its approximation u_h^e over an element Ω^e, the left side of Eq. (3.4.1) will not be equal to zero in Ω^e. The error in the approximation of the differential equation is denoted by R^e and it is called the *residual*:

$$R^e(x, u_h^e) \equiv -\frac{d}{dx}\left(a_e \frac{du_h^e}{dx}\right) + c_e u_h^e - f_e \neq 0 \quad \text{for} \quad x_a^e < x < x_b^e$$

where a_e, c_e, and f_e are element-wise continuous functions. Since $u_h^e(x)$ is expressed as a linear combination of the unknown coefficients u_j^e, we wish to determine them by requiring the residual R^e to be zero in an integral sense. The necessary and sufficient number (n) of algebraic relations among the u_j^e can be obtained only by forcing the integral of the weighted-residual to zero (the first step of the weak-form development):

$$0 = \int_{x_a^e}^{x_b^e} w_i^e(x)\, R^e(x, u_h^e)\, dx = \int_{x_a^e}^{x_b^e} w_i^e \left[-\frac{d}{dx}\left(a_e \frac{du_h^e}{dx}\right) + c_e u_h^e - f_e\right] dx \qquad (3.4.4)$$

where $w_i^e(x)$ denotes the ith weight function from a set of n *linearly independent* functions $\{w_i^e\}$. For each choice of w_i^e, we obtain an independent algebraic equation among the unknowns $(u_1^e, u_2^e, \ldots, u_n^e)$. When ψ_i^e is selected to be the same as ψ_j^e and Eq. (3.4.4) is used to obtain the n equations, the resulting finite element model (i.e., system of algebraic equations among the nodal values) is termed the *Galerkin finite element model*.[1]

The second step is to weaken the continuity required of u_h^e (and hence of ψ_j^e) and include variables that participate in the specification of force-like boundary conditions (in addition to the displacement-like boundary conditions); thus, we trade the differentiation in the first term of Eq. (3.4.4) from u_h^e to w_i^e such that both u_h^e and w_i^e are differentiated equally – once

each in the present case. Using integration by parts [see Eq. (2.2.26)], we obtain:

$$0 = \int_{x_a^e}^{x_b^e} \left(a_e \frac{dw_i^e}{dx} \frac{du_h^e}{dx} + c_e w_i^e u_h^e - w_i^e f_e \right) dx - \left[w_i^e \, a_e \frac{du_h^e}{dx} \right]_{x_a^e}^{x_b^e} \tag{3.4.5}$$

The third and last step is to identify the so-called primary and secondary variables of the formulation. The identification is unique; examine the boundary term that appeared because of integration by parts in Eq. (3.4.5):

$$\left[w_i^e \cdot a_e \frac{du_h^e}{dx} \right]_{x_a^e}^{x_b^e}$$

First, the coefficient of the weight function w_i^e in the boundary expression, namely, $a_e(du_h^e/dx)$, is identified as the *secondary variable*, and its specification constitutes the *natural* or Neumann boundary condition. Next, examine the form of the weight function itself in the boundary expression. Whatever form w_i^e appears there, the variable of the differential equation in the same form is termed the *primary variable*. Thus, u_h^e is the primary variable, and its specification constitutes the *essential* or Dirichlet boundary condition. If the form of the weight function in the boundary expression was (dw_i^e/dx), then the primary variable would have been (du_h^e/dx). Thus, for the model equation at hand, the primary and secondary variables are u_h^e and $Q_h^e \equiv a_e(du_h^e/dx)$. This duality is unique, and it also indicates the type variables, u_h^e and Q_h^e (and only one of them at a point), involved in the specification of the boundary conditions for the model equation.

In writing the final expression of the weak form, we must denote the secondary variables evaluated at the nodes by a symbol, such as Q_h^e. For a typical line element, the end points (nodes 1 and 2) are the boundary points. At these points we assume the following boundary conditions (only one of the two conditions would be specified at a node):

$$\text{At } x = x_a^e: \quad u_h^e(x_a^e) = u_1^e \quad \text{or} \quad \left(-a_e \frac{du_h^e}{dx}\right)_{x=x_a^e} = Q_1^e$$

$$\text{At } x = x_b^e: \quad u_h^e(x_b^e) = u_2^e \quad \text{or} \quad \left(a_e \frac{du_h^e}{dx}\right)_{x=x_b^e} = Q_2^e$$

The finite element approximation should facilitate imposing either one of the conditions at a node. If we select $u_h^e(x)$ in Eq. (3.4.3) such that it automatically satisfies the end conditions $u_h^e(x_a^e) = u_1^e$ and $u_h^e(x_b^e) = u_2^e$ (these conditions will be used to derive the approximation functions), then it remains that we include the remaining conditions

$$Q_1^e = \left[-a_e \frac{du_h^e}{dx}\right]_{x_a^e}, \quad Q_2^e = \left[a_e \frac{du_h^e}{dx}\right]_{x_b^e} \tag{3.4.6}$$

in the weak form of Eq. (3.4.5). This way, one can readily impose boundary conditions on u_h^e or Q_h^e in the finite element analysis. The primary and secondary variables at the nodes are shown on the typical element in Fig. 3.4.4. With the notation in Eq. (3.4.6), the weak form now becomes

$$0 = \int_{x_a^e}^{x_b^e} \left(a_e \frac{dw_i^e}{dx}\frac{du_h^e}{dx} + c_e w_i^e u_h^e\right) dx - \int_{x_a^e}^{x_b^e} w_i^e f_e \, dx - w_i^e(x_a^e) Q_1^e - w_i^e(x_b^e) Q_2^e \tag{3.4.7}$$

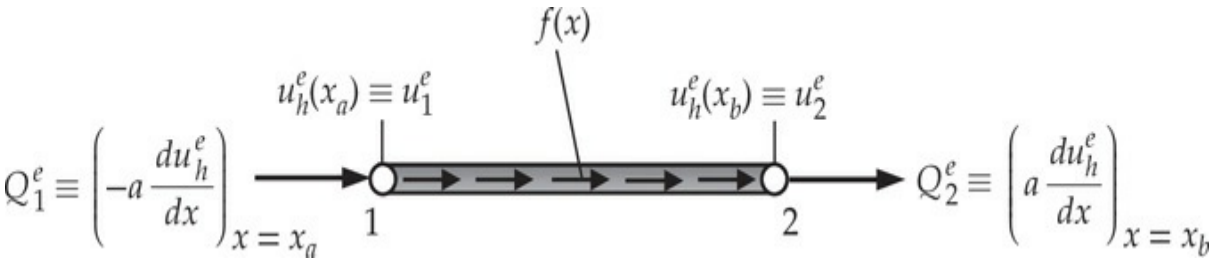

Fig. 3.4.4 A typical element, with the definition of the primary (u) and secondary (Q) variables at the element nodes.

This completes the three-step procedure of constructing the weak form of the model equation, Eq. (3.4.1). The finite element model based on the weak form in Eq. (3.4.7) is called the *Ritz finite element model* or the *weak-form Galerkin finite element model*, provided we replace w_i^e with ψ_i^e; otherwise (i.e., when $w_i^e \neq \psi_i^e$) it is termed a *weak-form Petrov–Galerkin*

finite element model. It is clear that the weak form in Eq. (3.4.7) admits approximation functions that are lower order (e.g., linear) than the weighted-residual statement in Eq. (3.4.4).

3.4.3.2 Remarks

Some remarks concerning the weak form are in order.

1. If the line element has only two nodes (and they are necessarily at the ends of the element), a lowest-order algebraic polynomial u_h^e that satisfies the end conditions $u_h^e(x_a^e) = u_1^e$ and $u_h^e(x_b^e) = u_2^e$ will be a linear polynomial. If the element has more than two nodes, they will be inside the element, and the polynomial order will increase in order to interpolate all the nodal values. The secondary variables Q_1^e and Q_n^e for an n-node element (where the nodes are numbered sequentially from the left to the right) are the only ones that are "reactions" (because the element is taken out of a continuum), and Q_i^e (for $i = 2, 3, \ldots, n-1$) at the internal nodes are necessarily known (i.e., externally applied).
2. For axial deformation of bars, u denotes the axial displacement, du/dx is the strain ε, $E\varepsilon$ is the stress σ, and $A\sigma$ denotes the force, where E is the Young's modulus and A is the area of cross section of the bar; hence, $a_e(du_h^e/dx)n_x = E_eA_e(du_h^e/dx)n_x$ (where $n_x = -1$ at the left end and $n_x = +1$ at the right end of the element) has the meaning of a force; Q_1^e is a compressive force while Q_2^e is a tensile force (algebraically both are positive, as shown in Fig. 3.4.4). For heat transfer problems, u denotes the temperature above a reference value, $u = T - T_\infty$, du/dx is the temperature gradient, $-k(du/dx)$ is the heat flux q, and Aq denotes the heat, where k is the thermal conductivity and A is the area of cross section of the bar; hence, $a_e(du_h^e/dx)n_x = k_eA_e(du_h^e/dx)n_x$ has the meaning of heat; $Q_1^e = [-k_eA_e(du_h^e/dx)]_a$ is the heat *input* at node 1, while $Q_2^e = [k_eA_e(du_h^e/dx)]_b$ denotes the heat *input* at node 2. Thus, the arrow on the second node should be reversed for heat transfer problems.
3. The weak form in Eq. (3.4.7) contains two types of expressions: those containing both w_i^e and u_h^e and those containing only w_i^e. These are denoted as

$$B^e(w_i^e, u_h^e) = \int_{x_a^e}^{x_b^e} \left(a_e \frac{dw_i^e}{dx} \frac{du_h^e}{dx} + c_e w_i^e u_h^e \right) dx \tag{3.4.8a}$$

$$\ell^e(w_i^e) = \int_{x_a^e}^{x_b^e} w_i^e f_e \, dx + w_i^e(x_a^e) Q_1^e + w_i^e(x_b^e) Q_2^e \tag{3.4.8b}$$

Clearly, $B^e(\cdot\,,\cdot)$ is linear in w_i^e and u_h^e and hence called a *bilinear form*. It is also symmetric, $B^e(w_i^e, u_h^e) = B^e(u_h^e, w_i^e)$. The expression $\ell^e(\cdot)$ is linear in w_i^e and it is called a *linear form*. The weak form in Eq. (3.4.7) can be expressed as

$$B^e(w_i^e, u_h^e) = \ell^e(w_i^e), \quad i = 1, 2, \ldots, n \tag{3.4.9}$$

which is called the *variational problem* associated with Eq. (3.4.1). As will be seen later, the bilinear form results directly in the element coefficient matrix, and the linear form leads to the right-hand-side column vector of the finite element equations. Derivation of the variational problem of the type in Eq. (3.4.9) is possible for all problems described by differential equations. However, in general, the bilinear form $B^e(w_i^e, u_h^e)$ may not be linear in u_h^e and it may not be symmetric in its arguments w_i^e and u_h^e.

4. Those who have a background in applied mathematics or solid and structural mechanics will appreciate the fact that the variational problem in Eq. (3.4.9), when $B^e(w_i^e, u_h^e)$ is symmetric $B^e(w_i^e, u_h^e) = B^e(u_h^e, w_i^e)$ and $\ell^e(w_i^e)$ is linear in w_i^e, is the same as the statement of the minimum of the quadratic functional $I^e(u_h^e)$, $\delta I^e = 0$, where

$$\begin{aligned} I^e(u_h^e) &= \frac{1}{2} B^e(u_h^e, u_h^e) - \ell^e(u_h^e) \\ &= \frac{1}{2} \int_{x_a^e}^{x_b^e} \left[a_e \left(\frac{du_h^e}{dx} \right)^2 + c(u_h^e)^2 \right] dx \\ &\quad - \int_{x_a^e}^{x_b^e} u_h^e f \, dx - u_h^e(x_a^e) Q_1^e - u_h^e(x_b^e) Q_2^e \end{aligned} \tag{3.4.10}$$

Thus, the relationship between the weak form and the minimum of quadratic functional I^e is obvious [$w_i^e = \delta u_h^e$; see Eq. (3.4.9)]:

$$0 = \delta I^e = B^e(\delta u_h^e, u_h^e) - \ell^e(\delta u_h^e) \qquad (3.4.11)$$

5. The statement $\delta I^e = 0$ in solid and structural mechanics is also known as the *principle of minimum total potential energy* or the principle of virtual displacements (see Section 2.3). When Eq. (3.4.1) describes the axial deformation of a bar, $\frac{1}{2}B^e(u,u)$ represents the elastic strain energy stored in the bar element, $\ell^e(u)$ represents the work done by applied forces, and $I^e(u)$ is the total potential energy (Π^e) of the bar element. Thus, the finite element model can be developed using either the statement of the principle of minimum total potential energy ($\delta I^e = 0$) of an element or the weak form of the governing equations of an element. However, this choice is restricted to those problems which admit minimum of a quadratic functional $I^e(u)$ that corresponds to the governing equations. On the other hand, one can always construct a weak form of any set of differential equations, linear or not, of order 2 and higher. Finite element formulations do not require the existence of the functional $I^e(u)$; they only need weighted-integral statements or weak forms. However, when the functional $I^e(u)$ exists with an extremum (i.e., minimum or maximum principle), existence and uniqueness of solution to the variational problem and its discrete analog can be established. In all problems discussed in this book, the variational problem is derivable from a quadratic functional.

3.4.3.3 Approximation functions

Recall that in the traditional variational methods, approximate solutions are sought over the total domain $\Omega = (0, L)$ at once. Consequently, the approximate solution $[u(x) \approx u_n(x) = \sum_{j=1}^{n} c_j \phi_j(x) + \phi_0(x)]$ is required to satisfy the boundary conditions of the problem. This places severe restrictions on the derivation of the approximation functions $\varphi_j(x)$ and $\varphi_0(x)$, especially when discontinuities exist in the geometry, material properties, and/or loading of the problem. The finite element method overcomes this shortcoming by seeking an approximate solution in the form of Eq. (3.4.3) over each element. Obviously, geometry of the element should be simpler than that of the whole domain and it should allow a systematic and unique derivation of the approximation functions.

To put the elements back together into their original positions, we require the primary variables to be the same at an interface (in 1-D

problems, at the nodes) common to elements. Therefore, we identify the end points of each line element as the *element nodes*, which play the role of interpolation points in constructing the approximation functions over an element.

Since the weak form over an element is equivalent to the differential equation and the natural boundary conditions in Eq. (3.4.6) of the problem for a typical element (i.e., conditions on Q_i^e of the element), the approximate solution u_h^e of Eq. (3.4.3) is required to satisfy only the end conditions $u_h^e(x_a^e) = u_1^e$ and $u_h^e(x_b^e) = u_2^e$ of the element. That way, we can include all possible boundary conditions that Eq. (3.4.1) admits [boundary conditions in Eq. (3.4.2) are the most general type that Eq. (3.4.1) will require].

We seek the approximate solution in the form of algebraic polynomials, although this is not a requirement of the finite element method. The reason for this choice is twofold: first, the interpolation theory of numerical analysis can be used to derive the approximation functions systematically over an element; second, numerical evaluation of integrals of algebraic polynomials is easy.

As in classical variational methods, the approximate solution u_h^e must fulfill certain conditions in order that it be convergent to the actual solution u as the number of elements or the degree of the polynomial is increased. These are:

1. The approximate solution $u_h^e(x)$ should be continuous over the element, and sufficiently differentiable, as required by the weak form.
2. The solution $u_h^e(x)$ should be a *complete* polynomial, that is, include all lower-order terms up to the highest order desired.
3. The solution $u_h^e(x)$ should interpolate all primary variables at the nodes of the finite element (so that continuity of solution can be imposed across an inter-element boundary).

The reason for the first condition is obvious; it ensures that all terms of the weak form are nonzero. The second condition is necessary in order to capture all possible states (i.e., constant, linear, and so on) of the actual solution. For example, if a linear polynomial without the constant term is used to represent the temperature distribution in a one-dimensional system, the approximate solution can never be able to represent a uniform state of temperature in the element should such a state occur. The third condition is

necessary in order to enforce continuity of the primary variables at points common to elements.

For the weak form in Eq. (3.4.7), the minimum polynomial order of u_h^e is linear.

A complete linear polynomial is of the form

$$u_h^e(x) = c_1^e + c_2^e x \tag{3.4.12}$$

where c_1^e and c_2^e are constants. The expression in Eq. (3.4.12) meets the first two conditions of an approximation. The third condition is satisfied if

$$u_h^e(x_a^e) = c_1^e + c_2^e x_a^e \equiv u_1^e, \quad u_h^e(x_b^e) = c_1^e + c_2^e x_b^e \equiv u_2^e \tag{3.4.13}$$

Equation (3.4.13) provides two relations between (c_1^e, c_2^e) and (u_1^e, u_2^e), which can be expressed in matrix form as

$$\begin{Bmatrix} u_1^e \\ u_2^e \end{Bmatrix} = \begin{bmatrix} 1 & x_a^e \\ 1 & x_b^e \end{bmatrix} \begin{Bmatrix} c_1^e \\ c_2^e \end{Bmatrix} \quad \text{or} \quad \mathbf{u}^e = \mathbf{A}^e \mathbf{c}^e \tag{3.4.14}$$

Inverting Eq. (3.4.14), we obtain [$\mathbf{c}^e = (\mathbf{A}^e)^{-1}\,\mathbf{u}^e$]

$$\begin{Bmatrix} c_1^e \\ c_2^e \end{Bmatrix} = \frac{1}{x_b^e - x_a^e} \begin{bmatrix} x_b^e & -x_a^e \\ -1 & 1 \end{bmatrix} \begin{Bmatrix} u_1^e \\ u_2^e \end{Bmatrix}$$

Solving for c_1^e and c_2^e in terms of u_1^e and u_2^e, we obtain

$$c_1^e = \frac{1}{h_e}(u_1^e x_b^e - u_2^e x_a^e), \quad c_2^e = \frac{1}{h_e}(u_2^e - u_1^e) \tag{3.4.15}$$

where $h_e = x_b^e - x_a^e$. Substituting c_1^e and c_2^e from Eq. (3.4.15) into Eq. (3.4.12), we obtain

$$\begin{aligned} u_h^e(x) = c_1^e + c_2^e x &= \frac{1}{h_e}(u_1^e x_b^e - u_2^e x_a^e) + \frac{1}{h_e}(u_2^e - u_1^e)x \\ &= \frac{1}{h_e}(x_b^e - x)u_1^e + \frac{1}{h_e}(x - x_a^e)u_2^e \\ &\equiv \psi_1^e(x)u_1^e + \psi_2^e(x)u_2^e = \sum_{j=1}^{2} \psi_j^e(x)u_j^e \end{aligned} \tag{3.4.16}$$

where

$$\psi_1^e(x) = \frac{x_b^e - x}{h_e}, \quad \psi_2^e(x) = \frac{x - x_a^e}{h_e} \tag{3.4.17}$$

which are called the linear *finite element approximation functions*.

The approximation functions $\{\psi_i^e(x)\}$ have some interesting properties. First, note that

$$\begin{aligned} u_1^e &\equiv u_h^e(x_a) = \psi_1^e(x_a^e)u_1^e + \psi_2^e(x_a^e)u_2^e \\ u_2^e &\equiv u_h^e(x_b^e) = \psi_1^e(x_b^e)u_1^e + \psi_2^e(x_b^e)u_2^e \end{aligned} \tag{3.4.18}$$

which imply that $\psi_1^e(x_a^e) = 1, \psi_2^e(x_a^e) = 0, \psi_1^e(x_b^e) = 0$, and $\psi_2^e(x_b^e) = 1$. In other words, ψ_i^e is unity at the ith node and zero at the other node. This property is known as the *interpolation property* of $\psi_i^e(x)$ and hence they are called *interpolation functions*. When they are derived to interpolate function values only and not the derivatives of the function, they are named as the *Lagrange interpolation functions*. When the function and its derivatives are interpolated, the resulting interpolation functions are known as the *Hermite family of interpolation functions*. These will be discussed in connection with beam elements in Chapter 5.

Another property of the set $\{\psi_i^e\}$ is that their sum is unity. To see this, consider a constant state of $u_h^e = c_0^e$. Then both nodal values, u_1^e and u_2^e, should be equal to the constant c_0^e. Hence, we have

$$u_h^e(x) = \psi_1^e(x)u_1^e + \psi_2^e(x)u_2^e = c_0^e \;\rightarrow\; 1 = \psi_1^e(x) + \psi_2^e(x)$$

This property of $\{\psi_i^e\}$ is known as the *partition of unity*. In summary, we have

$$\psi_i^e(x_j^e) = \begin{cases} 0 & \text{if } i \neq j \\ 1 & \text{if } i = j \end{cases}; \quad 1 = \sum_{i=1}^{n} \psi_i^e(x) \tag{3.4.19}$$

where $x_1^e = x_a^e$ and $x_2^e = x_b^e$ are the global coordinates of the element nodes 1 and 2 [see Eq. (3.4.16)]. Plots of the functions ψ_1^e and ψ_2^e are shown in Fig. 3.4.5(a), and plot of the approximate solution $u_h^e(x)$ is shown in Fig. 3.4.5(b). Although properties in Eq. (3.4.19) are verified for the linear Lagrange interpolation functions, they hold for any degree Lagrange interpolation functions.

The element interpolation functions $\{\psi_i^e\}$ in Eq. (3.4.18) were derived in terms of the *global coordinate* x [i.e., the coordinate appearing in the

governing differential equation, Eq. (3.4.1)], but they are defined only on the element domain $\Omega^e = (x_a^e, x_b^e)$. If we choose to express them in terms of the element coordinate $\bar{x} = x - x_a^e$, shown in Fig. 3.4.5, which is convenient in evaluating integrals of ψ_i^e, we obtain

$$\psi_1^e(\bar{x}) = 1 - \frac{\bar{x}}{h_e}, \quad \psi_2^e(\bar{x}) = \frac{\bar{x}}{h_e}$$
$$\frac{d\psi_1^e}{d\bar{x}} = -\frac{1}{h_e}, \qquad \frac{d\psi_2^e}{d\bar{x}} = \frac{1}{h_e} \tag{3.4.20}$$

The coordinate $\bar{x}$ is termed the *local coordinate*.

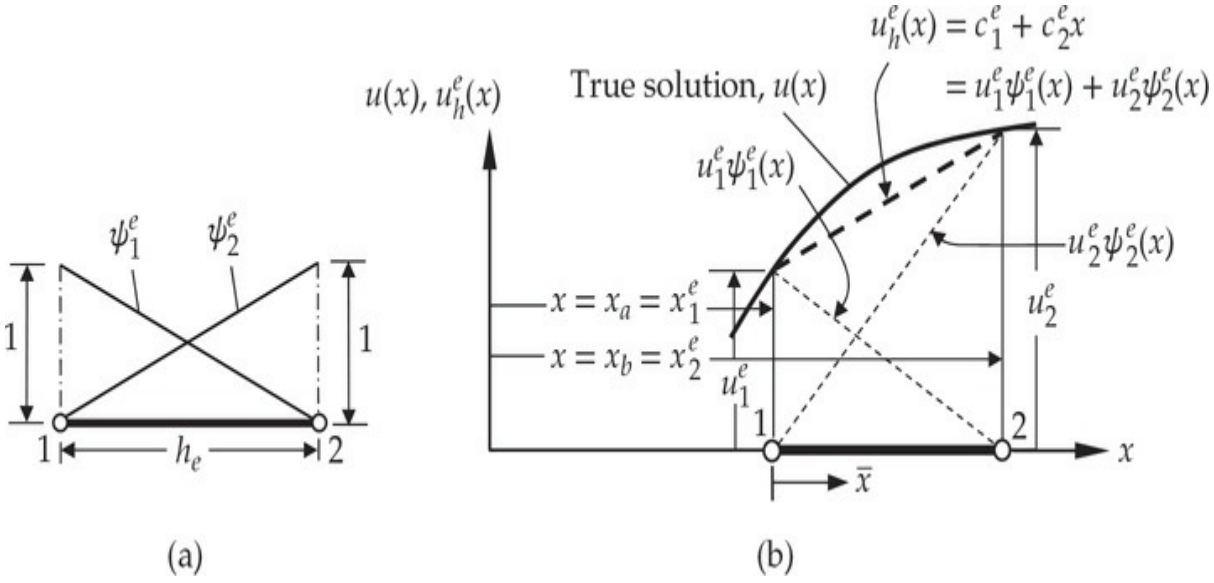

Fig. 3.4.5 (a) Linear interpolation functions. (b) Linear approximation over an element.

The interpolation functions ψ_i^e were derived systematically. We started with an assumed degree of a complete algebraic polynomial for the primary variable *u* and expressed the coefficients of the polynomial in terms of the nodal values u_j^e of *u* at the element nodes, which resulted in a linear combination of approximation functions $\psi_j^e(x)$ and the nodal values u_j^e. The nodal values u_j^e are called the *element nodal degrees of freedom*. The key point in this procedure is the use of nodal values of the primary variable as the unknowns so that the inter-element continuity may be easily imposed.

The degree (or order) of the polynomial approximation can be increased to improve the accuracy. The difference between using two

linear elements versus one quadratic element (the number of nodes is the same in both) to approximate a function is illustrated in Fig. 3.4.6.

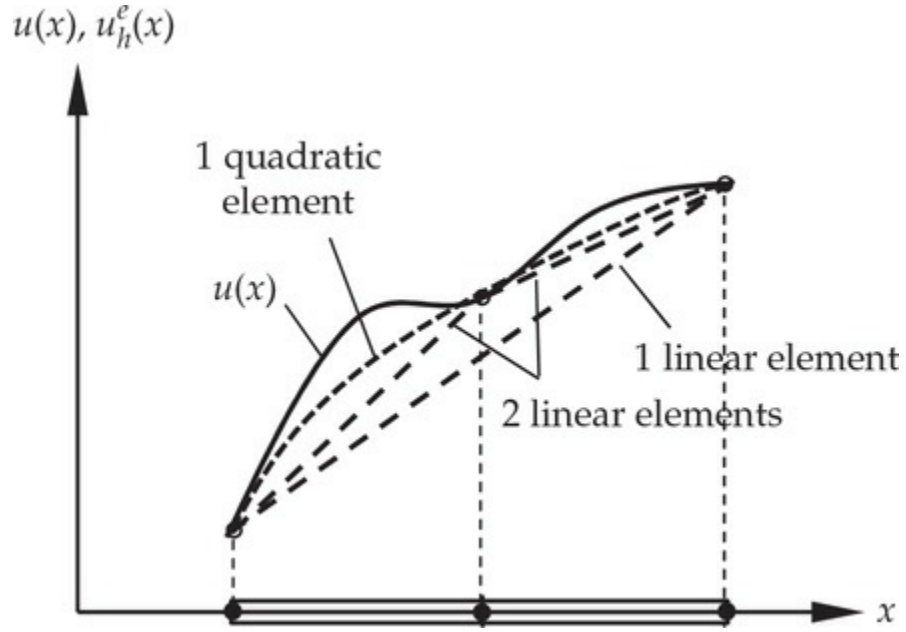

Fig. 3.4.6 Approximation of a function with linear and quadratic polynomials.

To illustrate the derivation of the interpolation functions of higher order, we consider the quadratic approximation of *u(x)*. Since the approximation is over an element, we can use a coordinate $\bar{x}$ with origin at the left end of the line element (i.e., node 1) and write

$$u_h^e(\bar{x}) = c_1^e + c_2^e \bar{x} + c_3^e \bar{x}^2 \tag{3.4.21}$$

where $\bar{x}$ is related to x by $x = \bar{x} + x_a^e$. Since there are three parameters c_i^e $(i = 1, 2, 3)$, we must identify three nodes in the element so that the three parameters can be expressed in terms of the three nodal values u_i^e $(i = 1, 2, 3)$. Two of the nodes are identified as the end points of the element to define the geometry, and the third node is taken interior to the element, as shown in Fig. 3.4.7. In theory, the third node can be placed at any interior point. However, the midpoint of the element, being equidistant from the end nodes, is the best choice. Following the procedure outlined for the linear polynomial, we eliminate c_i^e by rewriting $u_h^e(\bar{x})$ in terms of the three nodal values, (u_1^e, u_2^e, u_3^e). The three relations among c_i^e and u_i^e are

$$u_1^e \equiv u_h^e(0) = c_1^e$$
$$u_2^e \equiv u_h^e(0.5h_e) = c_1^e + c_2^e(0.5h_e) + c_3^e(0.5h_e)^2$$
$$u_3^e \equiv u_h^e(h_e) = c_1^e + c_2^e h_e + c_3^e h_e^2$$

or, in matrix form,

$$\begin{Bmatrix} u_1^e \\ u_2^e \\ u_3^e \end{Bmatrix} = \begin{bmatrix} 1 & 0 & 0 \\ 1 & 0.5h_e & 0.25h_e^2 \\ 1 & h_e & h_e^2 \end{bmatrix} \begin{Bmatrix} c_1^e \\ c_2^e \\ c_3^e \end{Bmatrix} \tag{3.4.22}$$

Inverting Eq. (3.4.22), we obtain

$$c_1^e = u_1^e, \quad c_2^e = \frac{1}{h_e}\left(-3u_1^e + 4u_2^e - u_3^e\right), \quad c_3^e = \frac{1}{h_e^2}\left(2u_1^e - 4u_2^e + 2u_3^e\right) \tag{3.4.23}$$

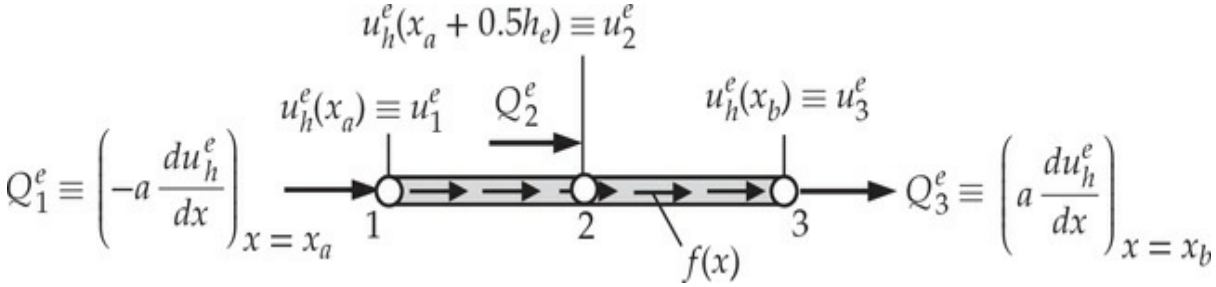

Fig. 3.4.7 A quadratic element with primary and secondary degrees of freedom at the nodes. Note that Q_2^e is a known point source applied externally at node 2.

Substituting for c_i^e from Eq. (3.4.23) into Eq. (3.4.21) and collecting the coefficients of u_1^e, u_2^e, and u_3^e separately, we obtain

$$u_h^e(x) = u_1^e + \left(-3u_1^e + 4u_2^e - u_3^e\right)\frac{\bar{x}}{h_e} + \left(2u_1^e - 4u_2^e + 2u_3^e\right)\frac{\bar{x}^2}{h_e^2}$$
$$= u_1^e\psi_1^e(x) + u_2^e\psi_2^e(x) + u_3^e\psi_3^e(x) = \sum_{j=1}^{3} u_j^e\psi_j^e(x) \tag{3.4.24}$$

where ψ_j^e are the *quadratic Lagrange interpolation functions*

$$
\begin{aligned}
\psi_1^e(\bar{x}) &= \left(1-\frac{\bar{x}}{h_e}\right)\left(1-\frac{2\bar{x}}{h_e}\right), & \frac{d\psi_1^e}{d\bar{x}} &= \frac{1}{h_e}\left(-3+4\frac{\bar{x}}{h_e}\right)\\
\psi_2^e(\bar{x}) &= 4\frac{\bar{x}}{h_e}\left(1-\frac{\bar{x}}{h_e}\right), & \frac{d\psi_2^e}{d\bar{x}} &= \frac{4}{h_e}\left(1-2\frac{\bar{x}}{h_e}\right)\\
\psi_3^e(\bar{x}) &= -\frac{\bar{x}}{h_e}\left(1-\frac{2\bar{x}}{h_e}\right), & \frac{d\psi_3^e}{d\bar{x}} &= -\frac{1}{h_e}\left(1-4\frac{\bar{x}}{h_e}\right)
\end{aligned}
\tag{3.4.25}
$$

Plots of the quadratic interpolation functions are given in Fig. 3.4.8.

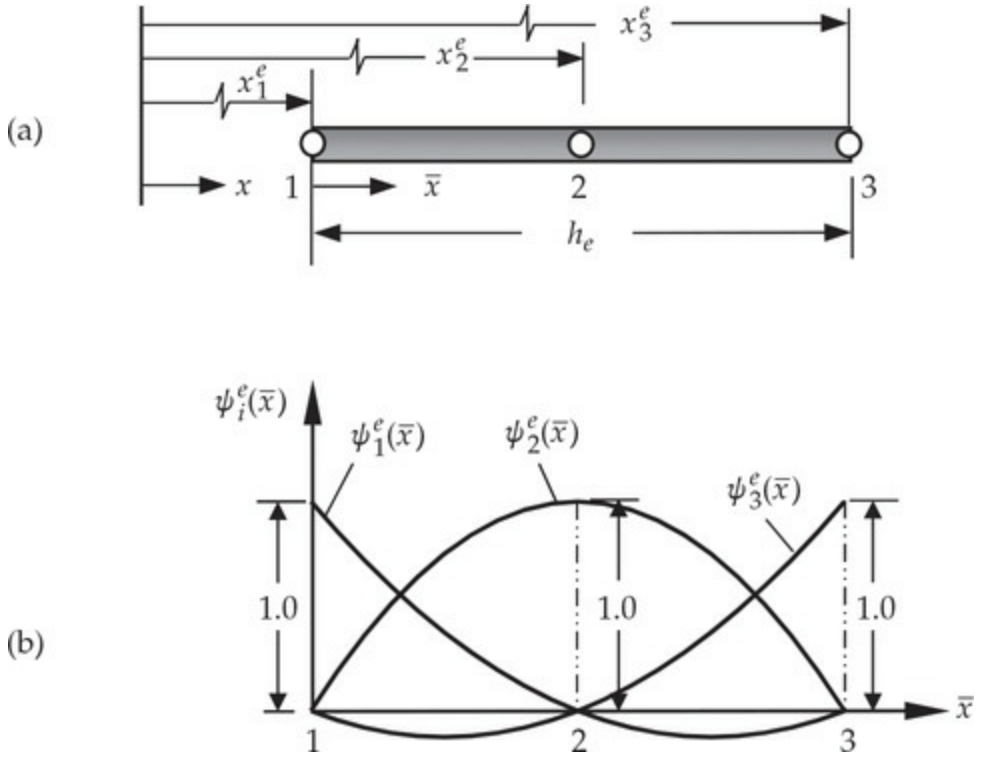

Fig. 3.4.8 One-dimensional Lagrange quadratic element and its interpolation functions: (a) geometry of the element and (b) interpolation functions.

The interpolation properties in Eq. (3.4.19) can be used to construct the Lagrange interpolation functions of any degree. For example, the quadratic interpolation functions in Eq. (3.4.25) can be derived using the interpolation property in Eq. (3.4.19). Since $\psi_1^e(\bar{x})$ must vanish at nodes 2 and 3, that is, at $\bar{x}=h_e/2$ and $\bar{x}=h_e$, $\psi_1^e(\bar{x})$ is of the form

$$
\psi_1^e(\bar{x}) = c_1^e(\bar{x}-0.5h_e)(\bar{x}-h_e) \tag{3.4.26}
$$

Then the constant c_1^e is determined such that ψ_1^e is equal to 1 at $\bar{x}=0$:

$$1 = c_1^e(0 - 0.5h_e)(0 - h_e) \quad \text{or} \quad c_1^e = 2/h_e^2 \tag{3.4.27}$$

This gives

$$\psi_1^e(\bar{x}) = \frac{2}{h_e^2}(\bar{x} - 0.5h_e)(\bar{x} - h_e) = \left(1 - \frac{\bar{x}}{h_e}\right)\left(1 - \frac{2\bar{x}}{h_e}\right)$$

which is the same as in Eq. (3.4.25). The other two interpolation functions can be derived in a similar manner.

Although a detailed discussion is presented here on how to construct the Lagrange interpolation functions for one-dimensional elements, they are readily available in books on numerical analysis, and their derivation is independent of the physics of the problem to be solved. Their derivation depends only on the geometry of the element and the number and location of the nodes. For the Lagrange elements, the number of nodes must be equal to the number of terms in the polynomial. Thus, the interpolation functions derived above are useful not only in the finite element approximation of the problem at hand, but also in all problems that admit Lagrange interpolation of the variables; that is, all problems for which the primary variables are the dependent variables and not their derivatives. Thus, the approximation of a primary variable $u(x)$ by the Lagrange element with n nodes can be expressed as

$$u(x) \approx u_h^e(x) = \sum_{j=1}^{n} u_j^e \psi_j^e(x) \tag{3.4.28}$$

where ψ_j^e are the Lagrange interpolation functions of degree $n - 1$, $n \geq 2$.

3.4.3.4 Finite element model

The weak form in Eq. (3.4.7) or (3.4.9) is equivalent to the differential equation in Eq. (3.4.1) over the element Ω^e, and it also contains the natural boundary conditions in Eq. (3.4.6). Further, the finite element approximations in Eqs. (3.4.3) and (3.4.28) are the interpolants of the solution. The substitution of Eq. (3.4.28) into Eq. (3.4.7) will give n algebraic equations among the n nodal values u_i^e and Q_i^e $(i = 1, 2, \ldots, n)$ of the element Ω^e. In order to develop the finite element model based on the weak form in Eq. (3.4.7), it is *not* necessary to decide *a priori* the degree of approximation of u_h^e. The finite element model can be developed for an arbitrary degree of interpolation. For $n > 2$, the weak form in Eq. (3.4.7) must be modified to include nonzero secondary variables, if any, at interior

nodes. This modification is discussed next.

The integration by parts in step 2 of the weak-form development for an element with n nodes should be carried out in intervals $(x_1^e, x_2^e),\ (x_2^e, x_3^e),\ \ldots,\ (x_{n-1}^e, x_n^e)$, where x_i^e is the global coordinate of the ith node of the element:

$$
\begin{aligned}
0 &= \sum_{i=1}^{n-1}\left\{\int_{x_i^e}^{x_{i+1}^e}\left(a_e\frac{dw_i^e}{dx}\frac{du_h^e}{dx}+c_e w_i^e u_h^e - w_i^e f_e\right)dx - \left[w_i^e\, a_e\frac{du_h^e}{dx}\right]_{x_i^e}^{x_{i+1}^e}\right\} \\
&= \int_{x_1^e}^{x_n^e}\left(a_e\frac{dw_i^e}{dx}\frac{du_h^e}{dx}+c_e w_i^e u_h^e - w_i^e f_e\right)dx - w_i^e(x_1^e)\left(-a_e\frac{du_h^e}{dx}\right)_{x_1^e} \\
&\quad - w_i^e(x_2^e)\left(a_e\frac{du_h^e}{dx}\right)_{x_2^e} - w_i^e(x_2^e)\left(-a_e\frac{du_h^e}{dx}\right)_{x_2^e} - w_i^e(x_3^e)\left(a_e\frac{du_h^e}{dx}\right)_{x_3^e} - \cdots \\
&\quad - w_i^e(x_{n-1}^e)\left(-a_e\frac{du_h^e}{dx}\right)_{x_{n-1}^e} - w_i^e(x_n^e)\left(a_e\frac{du_h^e}{dx}\right)_{x_n^e} \\
&= \int_{x_1^e}^{x_n^e}\left(a_e\frac{dw_i^e}{dx}\frac{du_h^e}{dx}+c_e w_i^e u_h^e - w_i^e f_e\right)dx - w_i^e(x_1^e)\left(-a_e\frac{du_h^e}{dx}\right)_{x_1^e} \\
&\quad - w_i^e(x_2^e)\left[\left(a_e\frac{du_h^e}{dx}\right)_{x_2^{e-}} + \left(-a_e\frac{du_h}{dx}\right)_{x_2^{e+}}\right] \\
&\quad - w_i^e(x_3^e)\left[\left(a_e\frac{du_h}{dx}\right)_{x_3^{e-}} + \left(-a_e\frac{du_h}{dx}\right)_{x_3^{e+}}\right] - \cdots \\
&\quad - w_i^e(x_{n-1}^e)\left[\left(a_e\frac{du_h}{dx}\right)_{x_{n-1}^{e-}} + \left(-a_e\frac{du_h^e}{dx}\right)_{x_{n-1}^{e+}}\right] - w_i^e(x_n^e)\left(a_e\frac{du_h^e}{dx}\right)_{x_n^e}
\end{aligned}
$$

$$
\begin{aligned}
0 = \int_{x_1^e}^{x_n^e}\left(a_e\frac{dw_i^e}{dx}\frac{du_h^e}{dx}+c_e w_i^e u_h^e - w_i^e f_e\right)dx - w_i^e(x_1^e)\,Q_1^e - w_i^e(x_2^e)\,Q_2^e \\
- w_i^e(x_3^e)\,Q_3^e - \cdots - w_i^e(x_{n-1}^e)\,Q_{n-1}^e - w_i^e(x_n^e)\,Q_n^e
\end{aligned}
\tag{3.4.29}
$$

where x_i^{e-} and x_i^{e+} denote the left and right sides, respectively, of x_i^e, and

$$Q_1^e = \left(-a_e \frac{du_h^e}{dx}\right)_{x_1^e}, \quad Q_2^e = \left[\left(a_e \frac{du_h^e}{dx}\right)_{x_2^{e-}} + \left(-a_e \frac{du_h^e}{dx}\right)_{x_2^{e+}}\right]$$

$$\vdots \tag{3.4.30}$$

$$Q_{n-1}^e = \left[\left(a \frac{du_h^e}{dx}\right)_{x_{n-1}^{e-}} + \left(-a_e \frac{du_h^e}{dx}\right)_{x_{n-1}^{e+}}\right], \quad Q_n^e = \left(a_e \frac{du_h^e}{dx}\right)_{x_n^e}$$

Thus, Q_i^e, $i = 2, 3, \ldots, n-1$, denotes the jump in the value of the secondary variable in going from the left to the right of the *i*th node. This value is zero if no external source is applied at the node. Thus, for an element with *n* nodes, the weak form becomes

$$0 = \int_{x_a^e}^{x_b^e} \left(a_e \frac{dw_i^e}{dx}\frac{du_h^e}{dx} + c_e w_i^e u_h^e\right) dx - \int_{x_a^e}^{x_b^e} w_i f_e \, dx - \sum_{i=1}^{n} w_i^e(x_i^e) Q_i^e \tag{3.4.31}$$

Note that $Q_1^e = Q_a^e$ and $Q_n^e = Q_b^e$ represent the unknown point sources at the end nodes, and all other Q_i^e $(i = 2, 3, \ldots, n-1)$ are the specified point sources, if any, at the interior nodes.

Next, we develop the finite element model of Eq. (3.4.1) when (n − 1)st degree Lagrange polynomials are used to approximate $u(x)$. Following the Ritz procedure developed in Section 2.5.2, we substitute Eq. (3.4.28) for u_h^e, and $w_1^e = \psi_1^e$, $w_2 = \psi_2^e$, $\ldots$, $w_n = \psi_n^e$, one at a time, into the weak form in Eq. (3.4.31) to obtain the following *n* algebraic equations (equations are numbered conveniently: the *i*th equation is obtained with $w_i^e = \psi_i^e$):

$$0 = \int_{x_a^e}^{x_b^e} \left[a_e \frac{d\psi_1^e}{dx} \left(\sum_{j=1}^{n} u_j^e \frac{d\psi_j^e}{dx} \right) + c_e \psi_1^e \left(\sum_{j=1}^{n} u_j^e \psi_j^e(x) \right) - \psi_1^e f_e \right] dx$$

$$- \sum_{j=1}^{n} \psi_1^e(x_j^e) Q_j^e \qquad \text{(1st algebraic relation among } u_1^e, u_2^e, \ldots, u_n^e, Q_1^e, Q_n^e)$$

$$0 = \int_{x_a^e}^{x_b^e} \left[a_e \frac{d\psi_2^e}{dx} \left(\sum_{j=1}^{n} u_j^e \frac{d\psi_j^e}{dx} \right) + c_e \psi_2^e \left(\sum_{j=1}^{n} u_j^e \psi_j^e(x) \right) - \psi_2^e f_e \right] dx$$

$$- \sum_{j=1}^{n} \psi_2^e(x_j^e) Q_j^e \qquad \text{(2nd algebraic relation among } u_1^e, u_2^e, \ldots, u_n^e, Q_1^e, Q_n^e)$$

$$\vdots$$

$$0 = \int_{x_a}^{x_b} \left[a_e \frac{d\psi_i^e}{dx} \left(\sum_{j=1}^{n} u_j^e \frac{d\psi_j^e}{dx} \right) + c_e \psi_i^e \left(\sum_{j=1}^{n} u_j^e \psi_j^e(x) \right) - \psi_i^e f_e \right] dx$$

$$- \sum_{j=1}^{n} \psi_i^e(x_j^e) Q_j^e \qquad (i\text{th algebraic relations among } u_1^e, u_2^e, \ldots, u_n^e, Q_1^e, Q_n^e)$$

$$\vdots$$

$$0 = \int_{x_a^e}^{x_b^e} \left[a_e \frac{d\psi_n^e}{dx} \left(\sum_{j=1}^{n} u_j^e \frac{d\psi_j^e}{dx} \right) + c_e \psi_n^e \left(\sum_{j=1}^{n} u_j^e \psi_j^e(x) \right) - \psi_n^e f_e \right] dx$$

$$- \sum_{j=1}^{n} \psi_n^e(x_j^e) Q_j^e \qquad (n\text{th algebraic relation among } u_1^e, u_2^e, \ldots, u_n^e, Q_1^e, Q_n^e)$$

Recall that $Q_2^e, Q_3^e, \ldots, Q_{n-1}^e$ are always known as specified values at nodes interior to the element. The *i*th algebraic equation of the system of *n* equations can be written as

$$0 = \sum_{j=1}^{n} K_{ij}^e u_j^e - f_i^e - Q_i^e \quad (i = 1, 2, \ldots, n) \tag{3.4.32a}$$

or in matrix form

$$\mathbf{K}^e \mathbf{u}^e = \mathbf{f}^e + \mathbf{Q}^e \equiv \mathbf{F}^e \tag{3.4.32b}$$

where $x = \bar{x} + x_a^e$ and $dx = d\bar{x}$)

$$
\begin{aligned}
K_{ij}^e &= \int_{x_a^e}^{x_b^e} \left(a_e(x) \frac{d\psi_i^e}{dx} \frac{d\psi_j^e}{dx} + c_e(x) \psi_i^e \psi_j^e \right) dx \\
&= \int_0^{h_e} \left(a_e(\bar{x}) \frac{d\psi_i^e}{d\bar{x}} \frac{d\psi_j^e}{d\bar{x}} + c_e(\bar{x}) \psi_i^e \psi_j^e \right) d\bar{x} \\
f_i^e &= \int_{x_a^e}^{x_b^e} f_e(x) \psi_i^e(x)\, dx = \int_0^{h_e} f_e(\bar{x}) \psi_i^e(\bar{x})\, d\bar{x} \\
Q_i^e &= \sum_{j=1}^{n} \psi_i^e(x_j^e) Q_j^e
\end{aligned}
\tag{3.4.33}
$$

Thus, there are n algebraic relations of the form

$$
\begin{aligned}
K_{11}^e u_1^e + K_{12}^e u_2^e + \cdots + K_{1n}^e u_n^e &= f_1^e + Q_1^e \\
K_{21}^e u_1^e + K_{22}^e u_2^e + \cdots + K_{2n}^e u_n^e &= f_2^e + Q_2^e \\
&\vdots \\
K_{n1}^e u_1^e + K_{n2}^e u_2^e + \cdots + K_{nn}^e u_n^e &= f_n^e + Q_n^e
\end{aligned}
\tag{3.4.34}
$$

The matrix $\mathbf{K}^e$ is called the *coefficient matrix*, or *stiffness matrix* in structural mechanics applications. The column vector $\mathbf{f}e$ is the *source vector*, or the *force vector* in structural mechanics problems. Note that Eq. (3.4.34) contains $n + 2$ unknowns: $(u_1^e, u_2^e, \ldots, u_n^e)$ and (Q_1^e, Q_n^e); hence, Eq. (3.4.34) cannot be solved without having additional equations. Some of these are provided by the boundary conditions and the remainder by balance of the secondary variables Q_i^e at nodes common to several elements. This balance can be implemented by putting the elements together (i.e., assembling the element equations). Upon assembly and imposition of boundary conditions, we shall obtain exactly the same number of algebraic equations as the number of unknown primary and secondary nodal degrees of freedom in the mesh of elements. The ideas underlying the assembly procedure are discussed in the next section.

The coefficient matrix $\mathbf{K}^e$, which is symmetric (i.e., $K_{ij}^e = K_{ji}^e$), and source vector $\mathbf{f}^e$ can be evaluated for a given element data (a, c, f, x_a^e, and x_b^e). Numerical evaluation of these integrals will be discussed in Chapter 8. For element-wise-constant values of a, c, and f (say, a_e, c_e, and f_e,

respectively) the coefficients K_{ij}^e and f_i^e can be expressed in terms of the local coordinate $\bar{x} = x + x_a^e$ as

$$K_{ij}^e = a_e \int_0^{h_e} \frac{d\psi_i^e}{d\bar{x}} \frac{d\psi_j^e}{d\bar{x}} d\bar{x} + c_e \int_0^{h_e} \psi_i^e \psi_j^e \, d\bar{x}, \quad f_i^e = f_e \int_0^{h_e} \psi_i^e \, d\bar{x} \tag{3.4.35}$$

We note that

$$dx = d\bar{x}, \quad \frac{d\psi_i^e}{dx} = \frac{d\psi_i^e}{d\bar{x}}$$

Next, we evaluate these integrals analytically for the linear and quadratic elements.

Linear element. For a typical linear element Ω^e [see Fig. 3.4.5(b)], the ψ_i^e and their derivatives can be expressed in terms of x as given in Eq. (3.4.20). Then we have

$$K_{11}^e = \int_0^{h_e} \left[a_e \left(-\frac{1}{h_e} \right) \left(-\frac{1}{h_e} \right) + c_e \left(1 - \frac{\bar{x}}{h_e} \right) \left(1 - \frac{\bar{x}}{h_e} \right) \right] d\bar{x} = a_e \frac{1}{h_e} + c_e \frac{h_e}{3}$$

$$K_{12}^e = \int_0^{h_e} \left[a_e \left(-\frac{1}{h_e} \right) \frac{1}{h_e} + c_e \left(1 - \frac{\bar{x}}{h_e} \right) \frac{\bar{x}}{h_e} \right] d\bar{x} = -a_e \frac{1}{h_e} + c_e \frac{h_e}{6} = K_{21}^e$$

$$K_{22}^e = \int_0^{h_e} \left(a_e \frac{1}{h_e} \frac{1}{h_e} + c_e \frac{\bar{x}}{h_e} \frac{\bar{x}}{h_e} \right) d\bar{x} = a_e \frac{1}{h_e} + c_e \frac{h_e}{3}$$

$$f_1^e = \int_0^{h_e} f_e \left(1 - \frac{\bar{x}}{h_e} \right) d\bar{x} = \frac{1}{2} f_e h_e, \quad f_2^e = \int_0^{h_e} f_e \frac{\bar{x}}{h_e} d\bar{x} = \frac{1}{2} f_e h_e$$

Thus, for constant f_e, the total source $f_e \, h_e$ is equally distributed to the two nodes. The coefficient matrix and column vector are

$$\mathbf{K}^e = \frac{a_e}{h_e} \begin{bmatrix} 1 & -1 \\ -1 & 1 \end{bmatrix} + \frac{c_e h_e}{6} \begin{bmatrix} 2 & 1 \\ 1 & 2 \end{bmatrix}, \quad \mathbf{f}^e = \frac{f_e h_e}{2} \begin{Bmatrix} 1 \\ 1 \end{Bmatrix} \tag{3.4.36}$$

If $a(x) = a_e \, x$ [or $a(\bar{x}) = a^e(x_a^e + \bar{x})$] and $c = 0$, the coefficient matrix $\mathbf{K}^e$ can be evaluated as

$$\mathbf{K}^e = \frac{a_e}{h_e} \left(\frac{x_a^e + x_b^e}{2} \right) \begin{bmatrix} 1 & -1 \\ -1 & 1 \end{bmatrix}$$

The reader should verify this. Note that when $a(x)$ is a linear function of x, this is equivalent to replacing $a(x)$ in the coefficient matrix with its average value:

$$a_{\text{avg}} = \frac{1}{2}(x_a^e + x_b^e)a_e$$

For example, consider a bar element with linearly varying cross-sectional area (see Fig. 3.4.9)

$$a(\bar{x}) = E_e A_e(\bar{x}) = E_e \left(A_a^e + \frac{A_b^e - A_a^e}{h_e} \bar{x} \right)$$

where A_a^e is the cross-sectional area at x_a^e (or $\bar{x} = 0$) and A_b^e is the cross-sectional area at $x = x_b^e$ (or $\bar{x} = h_e$). Then the stiffness matrix of such element is given by

$$\mathbf{K}^e = \frac{E_e}{h_e} \left(\frac{A_a^e + A_b^e}{2} \right) \begin{bmatrix} 1 & -1 \\ -1 & 1 \end{bmatrix} = \frac{E_e \bar{A}_e}{h_e} \begin{bmatrix} 1 & -1 \\ -1 & 1 \end{bmatrix} \tag{3.4.37}$$

which amounts to replacing the linearly varying cross-sectional area with the average area of cross section of the element. Similar arguments apply when A_e is constant and $E(x)$ varies linearly.

Quadratic element. For a quadratic element (with equally spaced nodes) of length h_e, the interpolation functions and their derivatives are given in Eq. (3.4.25). Evaluating the integrals in Eq. (3.4.35), we obtain

$$f_1^e = \int_0^{h_e} f_e \left[1 - \frac{3\bar{x}}{h_e} + 2\left(\frac{\bar{x}}{h_e}\right)^2\right] d\bar{x} = \frac{1}{6} f_e h_e$$

$$f_2^e = \int_0^{h_e} f_e \left[4\frac{\bar{x}}{h_e}\left(1 - \frac{\bar{x}}{h_e}\right)\right] d\bar{x} = \frac{4}{6} f_e h_e$$

$$f_3^e = f_1^e \quad \text{(by symmetry)}$$

$$K_{11}^e = \int_0^{h_e} \left\{ a_e \left(-\frac{3}{h_e} + \frac{4\bar{x}}{h_e^2}\right)\left(-\frac{3}{h_e} + \frac{4\bar{x}}{h_e^2}\right) + c_e \left[1 - \frac{3\bar{x}}{h_e} + 2\left(\frac{\bar{x}}{h_e}\right)^2\right]\left[1 - \frac{3\bar{x}}{h_e} + 2\left(\frac{\bar{x}}{h_e}\right)^2\right] \right\} d\bar{x}$$

$$= \frac{7}{3}\frac{a_e}{h_e} + \frac{2}{15} c_e h_e$$

$$K_{12}^e = \int_0^{h_e} \left\{ a_e \left(-\frac{3}{h_e} + \frac{4\bar{x}}{h_e^2}\right)\left(\frac{4}{h_e} - \frac{8\bar{x}}{h_e^2}\right) + c_e \left[1 - \frac{3\bar{x}}{h_e} + 2\left(\frac{\bar{x}}{h_e}\right)^2\right]\left[4\frac{\bar{x}}{h_e}\left(1 - \frac{\bar{x}}{h_e}\right)\right] \right\} d\bar{x}$$

$$= -\frac{8}{3}\frac{a_e}{h_e} + \frac{2}{30} c_e h_e = K_{21}^e$$

$$K_{22}^e = \int_0^{h_e} \left\{ a_e \left(\frac{4}{h_e} - \frac{8\bar{x}}{h_e^2}\right)\left(\frac{4}{h_e} - \frac{8\bar{x}}{h_e^2}\right) + c_e \left[4\frac{\bar{x}}{h_e}\left(1 - \frac{\bar{x}}{h_e}\right)\right]\left[4\frac{\bar{x}}{h_e}\left(1 - \frac{\bar{x}}{h_e}\right)\right] \right\} d\bar{x}$$

$$= \frac{16}{3}\frac{a_e}{h_e} + \frac{8}{15} c_e h_e$$

Similarly, other K_{ij}^e can be evaluated.

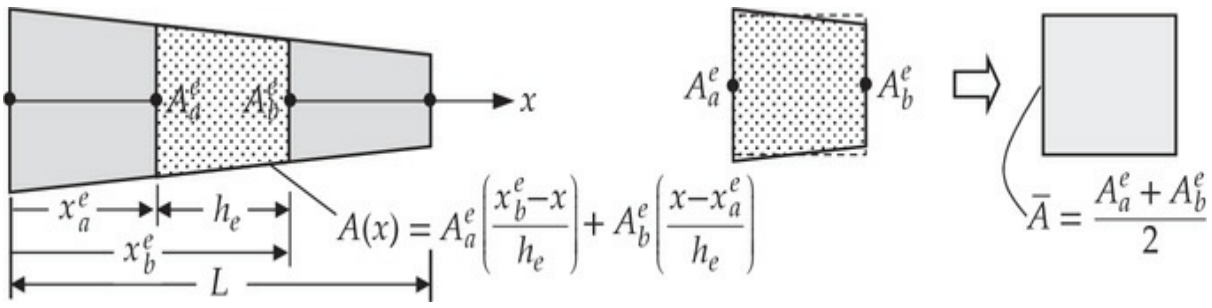

Fig. 3.4.9 Approximation of a bar element with linearly varying cross section by an equivalent element of constant cross section.

Thus, the element coefficient matrix and source vector for a quadratic element are

$$\mathbf{K}^e = \frac{a_e}{3h_e}\begin{bmatrix} 7 & -8 & 1 \\ -8 & 16 & -8 \\ 1 & -8 & 7 \end{bmatrix} + \frac{c_e h_e}{30}\begin{bmatrix} 4 & 2 & -1 \\ 2 & 16 & 2 \\ -1 & 2 & 4 \end{bmatrix}, \quad \mathbf{f}^e = \frac{f_e h_e}{6}\begin{Bmatrix} 1 \\ 4 \\ 1 \end{Bmatrix} \tag{3.4.38}$$

Note that, for quadratic elements, the total value of the source $f_e\, h_e$ is not distributed equally between the three nodes. Also, the distribution is *not* equivalent to that of two linear elements of length $\frac{1}{2}h_e$. The computation of f_i^e should be based on the interpolation functions of that element. The sum of f_i^e for *any element* should always be equal to the integral of $f(x)$ over the element:

$$\sum_{i=1}^{n} f_i^e = \int_{x_a^e}^{x_b^e} f_e(x)\, dx = \int_0^{h_e} f_e(\bar{x})\, d\bar{x}, \quad x = \bar{x} + x_a^e \tag{3.4.39}$$

In summary, for element-wise-constant values of the data a_e, c_e, and f_e, the element equations associated with model Eq. (3.4.1) for linear and quadratic elements are presented in Eqs. (3.4.40) and (3.4.41), respectively.

Linear element

$$\left(\frac{a_e}{h_e}\begin{bmatrix} 1 & -1 \\ -1 & 1 \end{bmatrix} + \frac{c_e h_e}{6}\begin{bmatrix} 2 & 1 \\ 1 & 2 \end{bmatrix}\right)\begin{Bmatrix} u_1^e \\ u_2^e \end{Bmatrix} = \frac{f_e h_e}{2}\begin{Bmatrix} 1 \\ 1 \end{Bmatrix} + \begin{Bmatrix} Q_1^e \\ Q_2^e \end{Bmatrix} \tag{3.4.40}$$

Quadratic element

$$\left(\frac{a_e}{3h_e}\begin{bmatrix} 7 & -8 & 1 \\ -8 & 16 & -8 \\ 1 & -8 & 7 \end{bmatrix} + \frac{c_e h_e}{30}\begin{bmatrix} 4 & 2 & -1 \\ 2 & 16 & 2 \\ -1 & 2 & 4 \end{bmatrix}\right)\begin{Bmatrix} u_1^e \\ u_2^e \\ u_3^e \end{Bmatrix} = \frac{f_e h_e}{6}\begin{Bmatrix} 1 \\ 4 \\ 1 \end{Bmatrix} + \begin{Bmatrix} Q_1^e \\ Q_2^e \\ Q_3^e \end{Bmatrix} \tag{3.4.41}$$

When the coefficient $c_e = 0$, the corresponding contribution to the above equations should be omitted. Similarly, when f_e is zero, we omit the column vector involving f_e. Of course, a_e is never zero.

When $a_e(x)$, $c_e(x)$, and $f_e(x)$ are polynomials, the evaluation of K_{ij}^e and f_j^e is straightforward. When they are complicated functions of x, the integrals in $\mathbf{K}^e$ and $\mathbf{f}^e$ are evaluated using numerical integration. However, in practice all data (i.e., geometry, material properties, and source term) is usually expressed as polynomials. A complete discussion of numerical integration will be presented in Chapter 8.

3.4.4 Assembly of Element Equations

In deriving the element equations, we isolated a typical element from the mesh and formulated the weak form and developed its finite element model. The finite element model of a typical element contains n equations among $n + 2$ unknowns, $(u_1^e, u_2^e, \ldots, u_n^e)$ and (Q_1^e, Q_n^e). Hence, they cannot be solved without using the equations from other elements. From a physical point of view, this makes sense because one should not be able to solve the element equations without considering the assembled set of equations and the boundary conditions of the total problem.

To obtain the finite element equations of the total problem, we must put the elements back into their original positions. In putting the elements with their nodal degrees of freedom back into their original positions, we must require that the primary variable $u(x)$ is uniquely defined (i.e., u is continuous) and the source terms Q_i^e are "balanced" at the points where elements are connected to each other. Of course, if the variable u is not continuous, we do not impose its continuity; but in all problems studied in this book, unless otherwise stated explicitly (like in the case of an internal hinge in the case of beam bending), the primary variables are required to be continuous. Thus, the assembly of elements is carried out by imposing the following two conditions:

1. If the end node i of element Ω^e is connected to the end node j of element Ω^f and the end node k of element Ω^g, the continuity of the primary variable u requires

$$u_i^{(e)} = u_j^{(f)} = u_k^{(g)}$$

When node n of element Ωe is connected to node 1 of element Ω^{e+1}

(with m nodes) in series, as shown in Fig. 3.4.10a, the continuity of u requires

$$u_n^{(e)} = u_1^{(e+1)} \tag{3.4.42}$$

2. For the same three elements, the balance of secondary variables at connecting nodes requires

$$Q_i^{(e)} + Q_j^{(f)} + Q_k^{(g)} = Q_I \tag{3.4.43}$$

where I is the global node number assigned to the nodal point that is common to the three elements, and Q_I is the value of externally applied source, if any (otherwise zero), at this node (the sign of Q_I must be consistent with the sign of Q_e in Fig. 3.4.4). For the case shown in Fig. 3.4.10, we have

$$Q_n^e + Q_1^{e+1} = \begin{cases} 0, & \text{if no external point source is applied} \\ Q_I, & \text{if an external point source of magnitude} \\ & Q_I \text{ is applied} \end{cases} \tag{3.4.44}$$

The balance of secondary variables can be interpreted as the continuity of a(du/dx) (not $a_e du_h^e/dx$ at the node (say, global node I) common to elements Ω^e and Ω^{e+1} when no change in adu/dx is imposed externally:

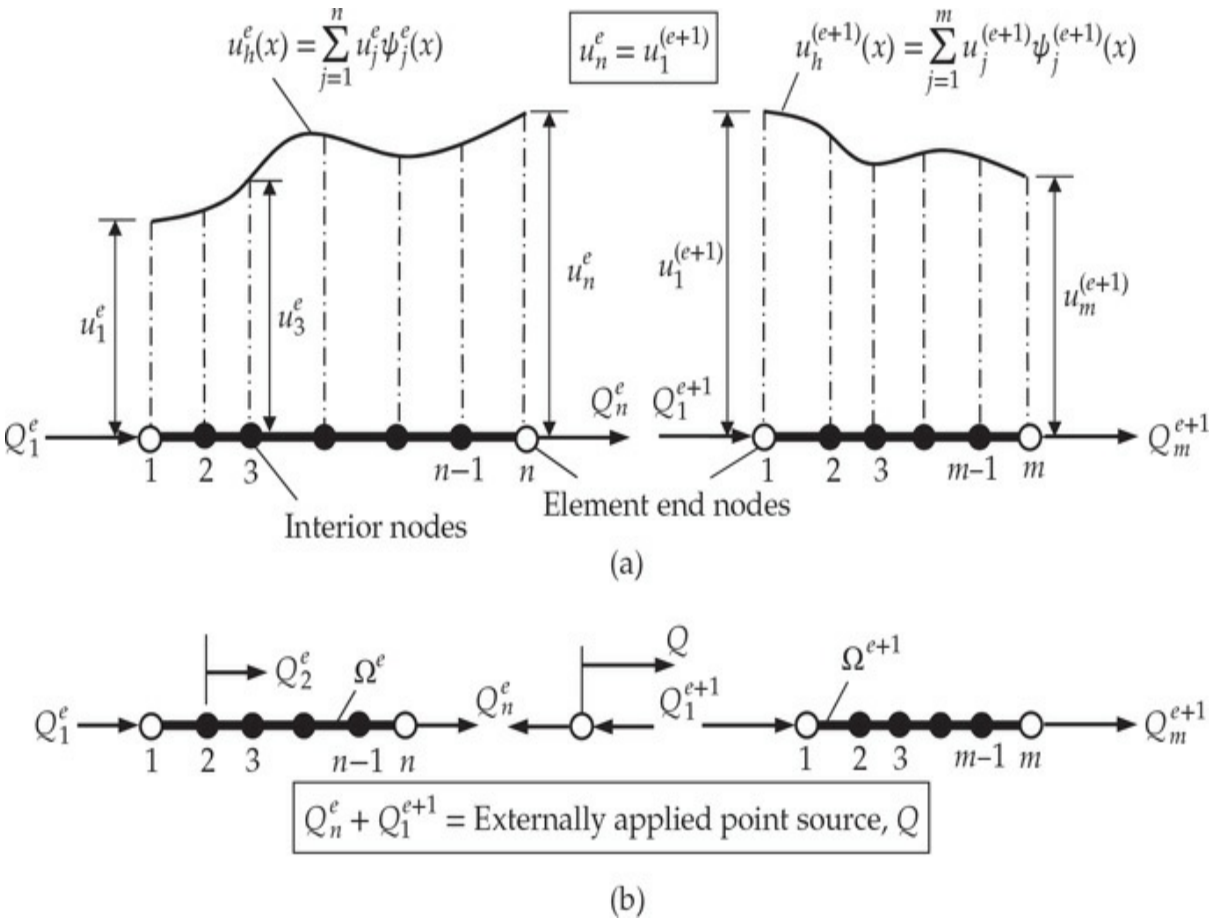

Fig. 3.4.10 Assembly of two Lagrange elements: (a) continuity of the primary variable and (b) balance of the secondary variables.

$$\left(a\frac{du}{dx}\right)_I^e = \left(a\frac{du}{dx}\right)_I^{e+1}$$

or

$$\left(a\frac{du}{dx}\right)_I^e + \left(-a\frac{du}{dx}\right)_I^{e+1} = 0 \rightarrow Q_n^e + Q_1^{e+1} = 0 \tag{3.4.45}$$

If there is a discontinuity of magnitude QI in $a\frac{du}{dx}$ in going from one side of the node to the other side (in the positive x direction), we impose

$$\left(a\frac{du}{dx}\right)_I^e + \left(-a\frac{du}{dx}\right)_I^{e+1} = Q_I \rightarrow Q_n^e + Q_1^{e+1} = Q_I \tag{3.4.46}$$

The inter-element continuity of the primary variables can be imposed by simply renaming the variables of all elements connected to the common node. For the continuity in Eq. (3.4.42), we simply use the name

$$u_i^{(e)} = u_j^{(f)} = u_k^{(g)} \equiv U_I \tag{3.4.47}$$

where I is the global node number at which the three elements are connected. For example, for a mesh of N linear finite elements ($n = 2$) connected in series (see Fig. 3.4.11), we have (superscripts on u_i denote the element number)

$$u_1^1 = U_1, \quad u_2^1 = u_1^2 = U_2, \quad u_2^2 = u_1^3 = U_3, \ldots, u_2^{N-1} = u_1^N = U_N, \quad u_2^N = U_{N+1}$$

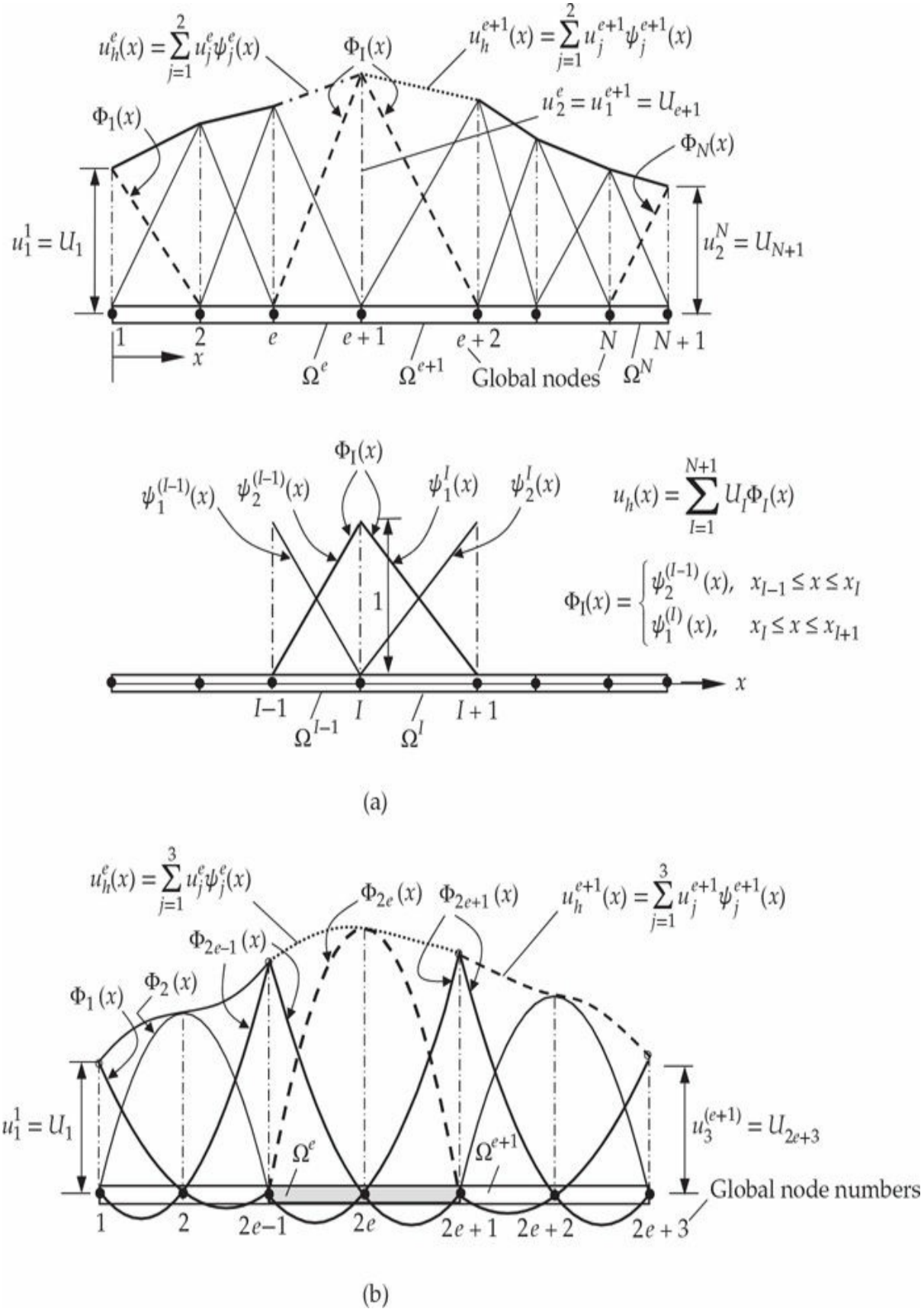

Fig. 3.4.11 Global interpolation functions for the (a) linear elements and (b) quadratic elements.

The connected linear finite element solution, u_h^e, composed of the element solutions u_h^e, is shown in Fig. 3.4.11(a). From the connected solution, we can identify the *global interpolation functions* ΦI, which can be defined in terms of the element interpolation functions ψ_i^e corresponding to the global node I, as shown in Fig. 3.4.11(a). Figure 3.4.11(b) contains global solution and global approximation functions for the quadratic case.

To enforce balance of the secondary variables, it is clear that we can set [see Eq. (3.4.45)] $Q_i^{(e)} + Q_j^{(f)} + Q_k^{(g)}$ equal to zero or to a specified value Q_I only if we have such an expression in the finite element equations. To obtain such expressions, it is clear that we must add the ith equation of the element Ω^e, the jth equation of the element Ω^f, and the kth equation of the element Ω^g together. For the case shown in Fig. 3.4.10, the nth equation of element Ω^e must be added to the first equation of the element Ω^{e+1}; that is, we add

$$\sum_{j=1}^{n} K_{nj}^e u_j^e = f_n^e + Q_n^e \quad \text{and} \quad \sum_{j=1}^{m} K_{1j}^{e+1} u_j^{e+1} = f_1^{e+1} + Q_1^{e+1}$$

to obtain

$$\sum_{j=1}^{n} \left(K_{nj}^e u_j^e + K_{1j}^{e+1} u_j^{e+1} \right) = f_n^e + f_1^{e+1} + \left(Q_n^e + Q_1^{e+1} \right) = f_n^e + f_1^{e+1} + Q_I \tag{3.4.48}$$

This process reduces the number of equations from $2N$ to $N + 1$ in a mesh of N linear elements. The first equation of the first element and the last equation of the last element will remain unchanged, except for renaming of the primary variables. The left-hand side of Eq. (3.4.48) can be written in terms of the global nodal values as

$$\begin{aligned}
&\left(K_{n1}^e \; u_1^e + K_{n2}^e u_2^e + \cdots + K_{nn}^e u_n^e \right) + \left(K_{11}^{e+1} u_1^{e+1} + K_{12}^{e+1} u_2^{e+1} + \cdots + K_{1n}^{e+1} u_n^{e+1} \right) \\
&\quad = \left(K_{n1}^e U_N + K_{n2}^e U_{N+1} + \cdots + K_{nn}^e U_{N+n-1} \right) \\
&\qquad + \left(K_{11}^{e+1} U_{N+n-1} + K_{12}^{e+1} U_{N+n} + \cdots + K_{1n}^{e+1} U_{N+2n-2} \right) \\
&\quad = K_{n1}^e U_N + K_{n2}^e U_{N+1} + \cdots + K_{n(n-1)}^e U_{N+n-2} + \left(K_{nn}^e + K_{11}^{e+1} \right) U_{N+n-1} \\
&\qquad + K_{12}^{e+1} U_{N+n} + \ldots + K_{1n}^{e+1} U_{N+2n-2}
\end{aligned} \tag{3.4.49}$$

where $N = (n - 1)e + 1$. For a mesh of N linear elements ($n = 2$), we have

$$
\begin{aligned}
K_{11}^1 U_1 + K_{12}^1 U_2 &= f_1^1 + Q_1^1 \quad \text{(unchanged)} \\
K_{21}^1 U_1 + \left(K_{22}^1 + K_{11}^2\right) U_2 + K_{12}^2 U_3 &= f_2^1 + f_1^2 + Q_2^1 + Q_1^2 \\
K_{21}^2 U_2 + \left(K_{22}^2 + K_{11}^3\right) U_3 + K_{12}^3 U_4 &= f_2^2 + f_1^3 + Q_2^2 + Q_1^3 \\
&\vdots \\
K_{21}^{N-1} U_{N-1} + \left(K_{22}^{N-1} + K_{11}^N\right) U_N + K_{12}^N U_{N+1} &= f_2^{N-1} + f_1^N + Q_2^{N-1} + Q_1^N \\
K_{21}^N U_N + K_{22}^N U_{N+1} &= f_2^N + Q_2^N \quad \text{(unchanged)}
\end{aligned}
\tag{3.4.50}
$$

These are called the *assembled equations*. Note that the numbering of the global equations corresponds to the numbering of the global primary degrees of freedom, U_I. This correspondence carries the symmetry of element matrices to the global matrix. Equations in Eq. (3.4.50) can be expressed in matrix form as

$$
\begin{bmatrix}
K_{11}^1 & K_{12}^1 & & & \\
K_{21}^1 & K_{22}^1 + K_{11}^2 & K_{12}^2 & 0 & \\
 & K_{21}^2 & K_{22}^2 + K_{11}^3 & & \\
 & \cdots\cdots & \cdots\cdots & \cdots\cdots & \\
 & 0 & & K_{22}^{N-1} + K_{11}^N & K_{12}^N \\
 & & & K_{21}^N & K_{22}^N
\end{bmatrix}
\begin{Bmatrix}
U_1 \\ U_2 \\ U_3 \\ \vdots \\ U_N \\ U_{N+1}
\end{Bmatrix}
$$

$$
= \begin{Bmatrix}
f_1^1 \\ f_2^1 + f_1^2 \\ f_2^2 + f_1^3 \\ \vdots \\ f_2^{N-1} + f_1^N \\ f_2^N
\end{Bmatrix}
+ \begin{Bmatrix}
Q_1^1 \\ Q_2^1 + Q_1^2 \\ Q_2^2 + Q_1^3 \\ \vdots \\ Q_2^{N-1} + Q_1^N \\ Q_2^N
\end{Bmatrix}
\tag{3.4.51}
$$

Note that the assembly in Eqs. (3.4.50) and (3.4.51) is based on the assumption that elements are connected in series. In general, several elements can be connected at a global node, and the elements do not have to be consecutively numbered. In that case, the coefficients coming from all elements connected at that global node will add up, as discussed in **Examples 3.3.1 and 3.3.4**. When certain primary nodal values are not required to be continuous across elements (as dictated by physics or the

variational formulation of the problem), such variables may be *condensed* out at the element level before elements are assembled.

3.4.5 Imposition of Boundary Conditions and Condensed Equations

In the weak-form finite element models, imposition of the boundary conditions is straightforward because the boundary conditions involve specifying the primary variable or the secondary variable (but not both) at a boundary node. The mixed boundary conditions (i.e., boundary conditions that involve a relation between the values of the primary and secondary variables at the node) can be handled as follows. For one-dimensional problems with one primary degree of freedom per node, the mixed boundary conditions are of the general form:

$$Q_I + \beta(U_I - U_\infty) = \hat{Q}_I \tag{3.4.52}$$

where Q_I is the secondary variable and U_I is the primary variable, and U_∞ and $\hat{Q}_I$ are specified quantities at the global node I. They arise, for example, in heat transfer when a boundary point is exposed to ambient temperature U_∞ (convection heat transfer; see **Example 3.3.5**), where ∫ denotes the convective heat transfer coefficient. In axial deformation of bars, mixed boundary conditions arise when a boundary point is spring-supported ($U_\infty = 0$), as shown in Fig. 2.5.3, where β denotes the spring constant k. In such cases, the secondary variable Q_I is replaced in terms of the primary variable U_I at that node, $Q_I = -\beta U_I + \beta U_\infty + \hat{Q}_I$, and the contribution $-\beta U_I$ is taken to the left-hand side (β adds to K_{II}) while keeping $\hat{Q}_I + \beta U_\infty$ on the right-hand side (adds to any F_I already there) of the equations.

If neither the primary variable nor the secondary variable is specified at a node, then the problem is ill-defined (or the person doing the analysis did not understand the problem). In most finite element programs, not specifying both variables at a node is taken to mean that the secondary variable is zero at that node.

As already discussed in Eqs. (3.4.45) and (3.4.46), the point sources at the nodes are included in a finite element analysis via the balance of sources at the nodes. If a point source is placed at a point other than a node, it is possible to "distribute" it to the element nodes, consistent with the finite element approximation, as follows. Let Q_0 denote a point source

at a point $\bar{x} = \bar{x}_0$, $\bar{x}_i^e \le \bar{x}_0 \le \bar{x}_n^e$, where $\bar{x}$ is the local coordinate (with origin at node 1) and $\bar{x}_i^e$ being the local coordinate of the *i*th node of the element. The point source Q_0 can be represented as a "function" with the help of the Dirac delta function as

$$f(\bar{x}) = Q_0 \delta(\bar{x} - \bar{x}_0) \tag{3.4.53}$$

where the Dirac delta function $\delta(\cdot)$ is defined by

$$\int_{-\infty}^{\infty} F(\bar{x}) \delta(\bar{x} - \bar{x}_0)\, d\bar{x} = F(\bar{x}_0) \tag{3.4.54}$$

where $F(\bar{x})$ is any function. The contribution of the function $f(\bar{x})$ to the nodes of the element $\Omega^e = (\bar{x}_1^e, \bar{x}_n^e)$ is computed using Eq. (3.4.35):

$$f_i^e = \int_0^{h_e} f_e(\bar{x}) \psi_i^e(\bar{x})\, d\bar{x} = \int_0^{h_e} Q_0 \delta(\bar{x} - \bar{x}_0) \psi_i^e(\bar{x})\, d\bar{x} = Q_0 \psi_i^e(\bar{x}_0) \tag{3.4.55}$$

where $\psi_i^e(\bar{x})$ are the interpolation functions of the element Ω^e. Thus, the point source Q_0 is distributed to the element node *i* by the value $Q_0 \psi_i^e(\bar{x}_0)$. Equation (3.4.55) holds for any element, irrespective of the degree of interpolation, the nature of the interpolation (i.e., Lagrange or Hermite polynomials), or the dimension of (i.e., one-dimensional, two-dimensional, or three-dimensional) elements. For one-dimensional linear Lagrange interpolation functions, Eq. (3.4.55) yields

$$f_1^e = Q_0 \psi_1^e(\bar{x}_0) = Q_0 \left(1 - \frac{\bar{x}_0}{h_e}\right), \quad f_2^e = Q_0 \psi_2^e(\bar{x}_0) = Q_0 \left(\frac{\bar{x}_0}{h_e}\right) \tag{3.4.56}$$

In particular, when $\bar{x}_0 = 0.5 h_e$, we have $f_1^e = f_2^e = 0.5 Q_0$, as expected.

After the boundary conditions are imposed, it is possible to partition the assembled finite element equations according to the vectors of specified and unspecified primary and secondary degrees of freedom by rewriting the assembled equations in the following form:

$$\begin{bmatrix} \mathbf{K}^{11} & \mathbf{K}^{12} \\ \mathbf{K}^{21} & \mathbf{K}^{22} \end{bmatrix} \begin{Bmatrix} \mathbf{U}^1 \\ \mathbf{U}^2 \end{Bmatrix} = \begin{Bmatrix} \mathbf{F}^1 \\ \mathbf{F}^2 \end{Bmatrix} \tag{3.4.57}$$

where $\mathbf{U}^1$ is the vector of known (i.e., specified) primary variables, $\mathbf{U}^2$ is the vector of unknown primary variables, $\mathbf{F}^1$ is the vector of unknown secondary variables, and $\mathbf{F}^2$ is the vector of known secondary variables.

Writing Eq. (3.4.57) as two matrix equations, we obtain

$$\begin{aligned} \mathbf{K}^{11}\mathbf{U}^1 + \mathbf{K}^{12}\mathbf{U}^2 &= \mathbf{F}^1 \\ \mathbf{K}^{21}\mathbf{U}^1 + \mathbf{K}^{22}\mathbf{U}^2 &= \mathbf{F}^2 \end{aligned} \tag{3.4.58}$$

From the second equation in (3.4.58), the equation for the vector of unknown primary variables is

$$\mathbf{K}^{22}\mathbf{U}^2 = \mathbf{F}^2 - \mathbf{K}^{21}\mathbf{U}^1, \quad \mathbf{U}^2 = (\mathbf{K}^{22})^{-1}\left(\mathbf{F}^2 - \mathbf{K}^{21}\mathbf{U}^1\right) \tag{3.4.59}$$

Equation (3.4.59) is termed the *condensed equations for the unknown primary variables*.

Once $\mathbf{U}^2$ is known from Eq. (3.4.59), the vector of unknown secondary variables, $\mathbf{F}^1$, can be computed using the first equation in Eq. (3.4.58):

$$\mathbf{F}^1 = \mathbf{K}^{11}\mathbf{U}^1 + \mathbf{K}^{12}\mathbf{U}^2 \tag{3.4.60}$$

Equation (3.4.60) is called the *condensed equations for the unknown secondary variables*. Note that when all specified primary variables are zero, $\mathbf{U}^1 = 0$, the condensed equations for the unknown primary variables and secondary variables take the form

$$\mathbf{U}^2 = (\mathbf{K}^{22})^{-1}\mathbf{F}^2, \quad \mathbf{F}^1 = \mathbf{K}^{12}\,\mathbf{U}^2 \tag{3.4.61}$$

Equation (3.4.59) suggests that it is sufficient to assemble element coefficients to obtain $\mathbf{K}^{22}$, $\mathbf{F}^2$, and $\mathbf{K}^{21}$ (when $\mathbf{U}^1 \neq 0$) in order to determine the vector of unknown primary variables, $\mathbf{U}^2$. We shall make use of Eqs. (3.4.59)–(3.4.61) in setting up the condensed equations for the primary and secondary variables.

3.4.6 Postprocessing of the Solution

The solution of the finite element equations in Eq. (3.4.59) gives the values of the primary variables (e.g., displacement, velocity, or temperature) at the global nodes. Once the nodal values of the primary variables are known, we can use the finite element approximation $u_h^e(x)$ to compute the desired quantities. The process of computing desired quantities in numerical form or graphical form from the known finite element solution is termed *postprocessing*; this phrase is meant to indicate that further computations are made after obtaining the solution of the finite element equations for the nodal values of the primary variables.

Postprocessing of the solution includes one or more of the following tasks:

1. Computation of the primary and secondary variables at points of interest; primary variables are known at nodal points.
2. Interpretation of the results to check whether the solution makes sense (an understanding of the physical process and experience are the guides when other solutions are not available for comparison).
3. Tabular and/or graphical presentation of the results.

To determine the solution u as a continuous function of position x, we return to the approximation in Eq. (3.4.28) over each element:

$$u(x) \approx \begin{cases} u_h^1(x) = \sum_{j=1}^{n} u_j^1 \psi_j^1(x) \\ u_h^2(x) = \sum_{j=1}^{n} u_j^2 \psi_j^2(x) \\ \vdots \\ u_h^N(x) = \sum_{j=1}^{n} u_j^N \psi_j^N(x) \end{cases} \tag{3.4.62a}$$

where N is the number of elements in the mesh. Depending on the value of x, the corresponding element equation from Eq. (3.4.62a) is used. The derivative of the solution is obtained by differentiating $u_h(x)$ in Eq. (3.4.62a):

$$\frac{du}{dx} \approx \begin{cases} \frac{du_h^1}{dx} = \sum_{j=1}^{n} u_j^1 \frac{d\psi_j^1}{dx} \\ \frac{du_h^2}{dx} = \sum_{j=1}^{n} u_j^2 \frac{d\psi_j^2}{dx} \\ \vdots \\ \frac{du_h^N}{dx} = \sum_{j=1}^{n} u_j^N \frac{d\psi_j^N}{dx} \end{cases} \tag{3.4.62b}$$

Note that the derivative du_h^e/dx of the finite element approximation u_h^e based on Lagrange interpolation is discontinuous, for any order element, at the nodes between elements because the continuity of the derivative, which is not a primary variable, at the connecting nodes is not imposed. In the case of linear elements, the derivative of the solution is constant within each element, as shown in Fig. 3.4.12(a), whereas it is linear for quadratic elements as shown in Fig. 3.4.12(b). Typically these values are interpreted to be those of the midpoint of the elements.

The secondary variables Q_j^e can be computed in two different ways: using the (1) condensed equations in Eq. (3.4.60) for the secondary variables and the (2) definitions in Eq. (3.4.6) introduced during the weak-form development. Secondary variables computed from Eq. (3.4.60) are denoted $(Q_I^e)_{\text{equil}}$ and those computed from the definitions are denoted $(Q_I^e)_{\text{def}}$. Since $(Q_I^e)_{\text{def}}$ are calculated using the approximate solution u_h^e, they are not as accurate as $(Q_I^e)_{\text{equil}}$. In most finite element computer programs, element matrices are assembled as soon as they are generated and they are not stored in the memory of the computer. Hence, element equations are not available for post-computation of the secondary variables from equilibrium. Thus, in practice, secondary variables are often computed using their definitions.

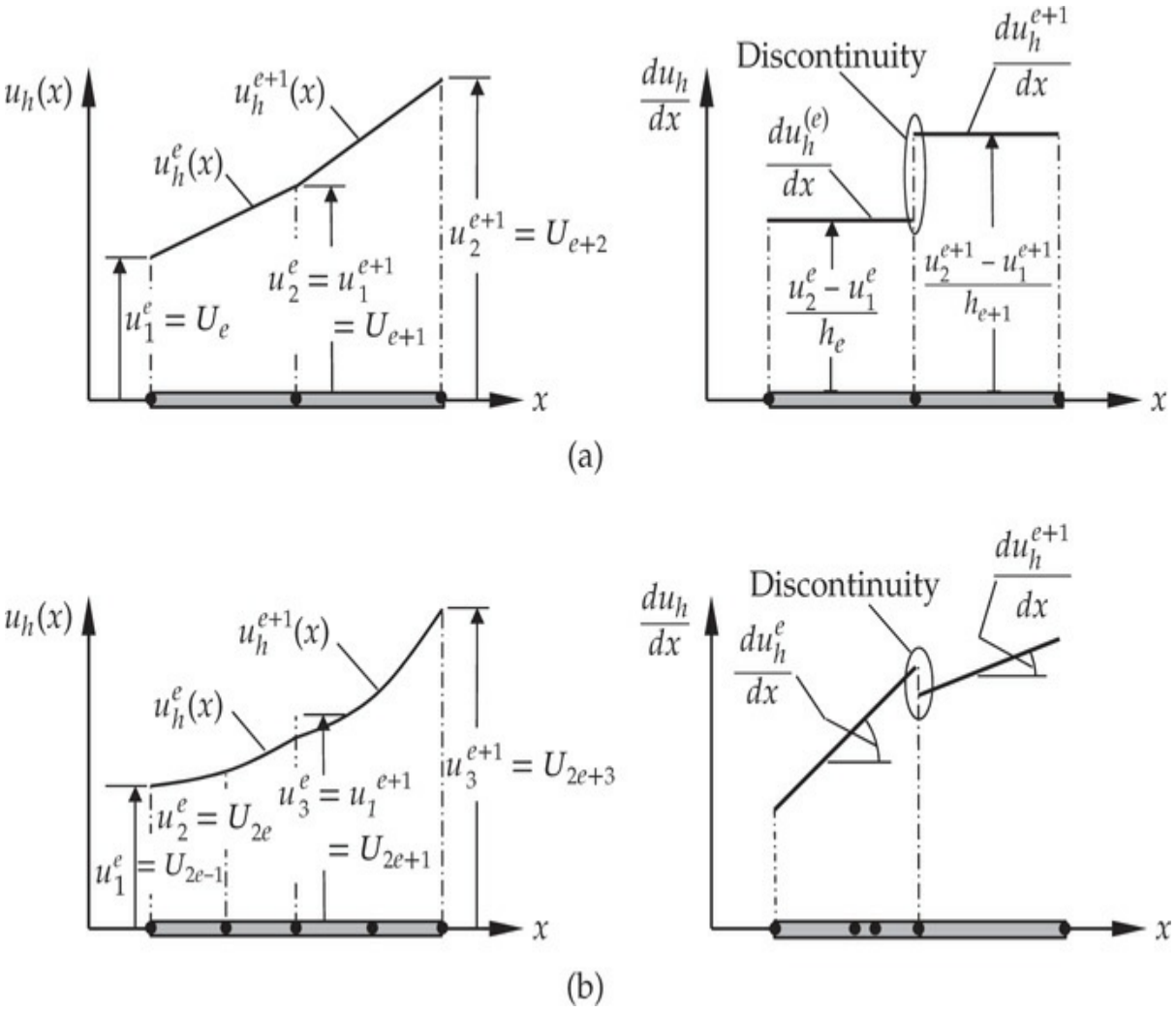

Fig. 3.4.12 Solution and the gradient of the solution using (a) linear elements and (b) quadratic elements.

This completes the basic steps involved in the finite element analysis

of the model equation in Eq. (3.4.1). We now consider an example of application of the finite element method to illustrate the steps involved in solving a differential equation which is a special case of the model equation. Additional examples of heat transfer, fluid mechanics, and solid mechanics are presented in Chapter 4.

Example 3.4.1

Use the finite element method to solve the problem described by the following differential equation and boundary conditions (see Example 2.5.1):

$$\frac{d^2u}{dx^2} + u = x^2 \quad \text{for} \quad 0 < x < 1 \tag{1}$$

$$u(0) = 0, \quad u(1) = 0 \tag{2}$$

Use (a) a uniform mesh of four linear elements and then (b) a uniform mesh of two quadratic elements (see Fig. 3.4.13) to solve the problem for the nodal values of u. Also determine the secondary variables using the definitions and equilibrium.

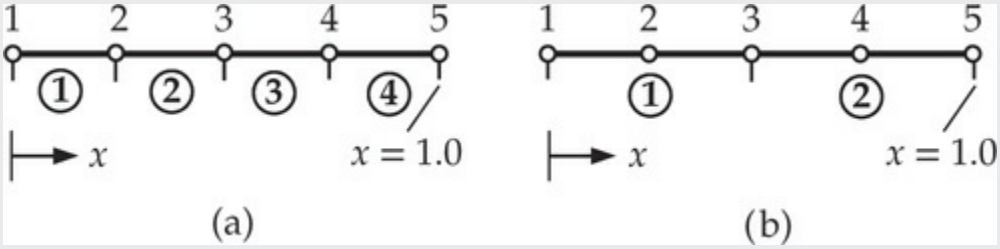

Fig. 3.4.13 Finite element meshes: (a) four linear elements and (b) two quadratic elements.

Solution: First, we note that the given differential equation in Eq. (1) is a special case of the model equation, Eq. (3.4.1), for the following data: $a = 1$, $c = -1$ and $f(x) = -x^2$. Hence, the element coefficients are defined, for any degree of interpolation, by

$$K_{ij}^e = \int_{x_a}^{x_b} \left(\frac{d\psi_i^e}{dx}\frac{d\psi_j^e}{dx} - \psi_i^e \psi_j^e \right) dx = \int_0^{h_e} \left(\frac{d\psi_i^e}{d\bar{x}}\frac{d\psi_j^e}{d\bar{x}} - \psi_i^e \psi_j^e \right) d\bar{x} \tag{3}$$

$$f_i^e = -\int_{x_a}^{x_b} (x)^2 \psi_i^e(x)\, dx = -\int_0^{h_e} (x_a + \bar{x})^2 \psi_i^e(\bar{x})\, d\bar{x} \tag{4}$$

(a) *Linear elements.* The element coefficient matrix is known from Eq. (3.4.36), with $a_e = 1$, $c = -1$, and $h_e = \frac{1}{4}$ as

$$\mathbf{K}^e = 4\begin{bmatrix} 1 & -1 \\ -1 & 1 \end{bmatrix} - \frac{1}{24}\begin{bmatrix} 2 & 1 \\ 1 & 2 \end{bmatrix} = \frac{1}{24}\begin{bmatrix} 94 & -97 \\ -97 & 94 \end{bmatrix} = \begin{bmatrix} 3.9167 & -4.0417 \\ -4.0417 & 3.9167 \end{bmatrix}$$

The coefficients f_i^e are evaluated using Eq. (4) with $\psi_1^e = 1 - \bar{x}/h_e$, $\psi_2^e = \bar{x}/h_e$, and $h_e = 1/4$:

$$\begin{aligned} f_1^e &= -\int_0^{h_e} (x_a + \bar{x})^2 \left(1 - \frac{\bar{x}}{h_e}\right) d\bar{x} = -h_e\left(\tfrac{1}{2}x_a^2 + \tfrac{1}{3}x_a h_e + \tfrac{1}{12}h_e^2\right) \\ &= -\tfrac{1}{8}x_a^2 - \tfrac{1}{48}x_a - \tfrac{1}{768} \\ f_2^e &= -\int_0^{h_e} (x_a + \bar{x})^2 \frac{\bar{x}}{h_e}\, d\bar{x} = -\left(\tfrac{1}{2}x_a^2 h_e + \tfrac{2}{3}x_a h_e^2 + \tfrac{1}{4}h_e^3\right) \\ &= -\tfrac{1}{8}x_a^2 - \tfrac{1}{24}x_a - \tfrac{1}{256} \end{aligned}$$

These can be specialized to each element as follows:

$$\begin{aligned} &\text{Element 1 } (x_a = 0): && f_1^1 = -\tfrac{1}{768} = -0.001302, \quad f_2^1 = -\tfrac{1}{256} = -0.003906 \\ &\text{Element 2 } (x_a = h_1): && f_1^2 = -\tfrac{11}{768} = -0.014323, \quad f_2^2 = \tfrac{17}{768} = -0.022135 \\ &\text{Element 3 } (x_a = h_1 + h_2): && f_1^3 = -\tfrac{33}{768} = -0.042969, \quad f_2^3 = -\tfrac{43}{768} = -0.055989 \\ &\text{Element 4 } (x_a = h_1 + h_2 + h_3): && f_1^4 = -\tfrac{67}{768} = -0.087239, \quad f_2^4 = -\tfrac{27}{256} = -0.105468 \end{aligned}$$

The balance conditions on Q_i^e for this case, where all elements are connected in series, take the form

$$Q_2^1 + Q_1^2 = 0, \quad Q_2^2 + Q_1^3 = 0, \quad Q_2^3 + Q_1^4 = 0$$

These conditions require adding the second equation of element 1 to the first equation of element 2, and so on. The first equation of element 1 and the second equation of element 4 remain unaltered. Thus the assembled set of equations is

$$\begin{bmatrix} 3.9167 & -4.0417 & 0.0000 & 0.0000 & 0.0000 \\ -4.0417 & 7.8333 & -4.0417 & 0.0000 & 0.0000 \\ 0.0000 & -4.0417 & 7.8333 & -4.0417 & 0.0000 \\ 0.0000 & 0.0000 & -4.0417 & 7.8333 & -4.0417 \\ 0.0000 & 0.0000 & 0.0000 & -4.0417 & 3.9167 \end{bmatrix} \begin{Bmatrix} U_1 \\ U_2 \\ U_3 \\ U_4 \\ U_5 \end{Bmatrix}$$

$$= -10^{-2} \begin{Bmatrix} 0.1302 \\ 1.8229 \\ 6.5104 \\ 14.3230 \\ 10.5470 \end{Bmatrix} + \begin{Bmatrix} Q_1^1 \\ Q_2^1 + Q_1^2 \\ Q_2^2 + Q_1^3 \\ Q_2^3 + Q_1^4 \\ Q_2^4 \end{Bmatrix}$$

Since U_1 and U_5 are specified, as implied by Eq. (2), we can rearrange the above assembled equations into the form in Eq. (3.4.57), with the definitions

$$\mathbf{U}^1 = \begin{Bmatrix} U_1 \\ U_5 \end{Bmatrix}, \quad \mathbf{U}^2 = \begin{Bmatrix} U_2 \\ U_3 \\ U_4 \end{Bmatrix},$$

$$\mathbf{F}^1 = \begin{Bmatrix} F_1 \\ F_5 \end{Bmatrix} = \begin{Bmatrix} -0.00130 + Q_1^1 \\ -0.10547 + Q_2^4 \end{Bmatrix}, \quad \mathbf{F}^2 = \begin{Bmatrix} F_2 \\ F_3 \\ F_4 \end{Bmatrix} = -\begin{Bmatrix} 0.01823 \\ 0.06510 \\ 0.14323 \end{Bmatrix}$$

$$\mathbf{K}^{11} = \begin{bmatrix} K_{11} & K_{15} \\ K_{51} & K_{55} \end{bmatrix} = \begin{bmatrix} 3.9167 & 0.0000 \\ 0.0000 & 3.9167 \end{bmatrix}$$

$$\mathbf{K}^{12} = \begin{bmatrix} K_{12} & K_{13} & K_{14} \\ K_{52} & K_{53} & K_{54} \end{bmatrix} = \begin{bmatrix} -4.0417 & 0 & 0.0000 \\ 0.0000 & 0 & -4.0417 \end{bmatrix}, \quad \mathbf{K}^{21} = (\mathbf{K}^{12})^{\mathrm{T}}$$

$$\mathbf{K}^{22} = \begin{bmatrix} K_{22} & K_{23} & K_{24} \\ K_{32} & K_{33} & K_{34} \\ K_{42} & K_{43} & K_{44} \end{bmatrix} = \begin{bmatrix} 7.8333 & -4.0417 & 0.0000 \\ -4.0417 & 7.8333 & -4.0417 \\ 0.0000 & -4.0417 & 7.8333 \end{bmatrix}$$

Since the specified values are zero, $\mathbf{U}^1 = 0$, the condensed equations for the primary variables are simply ($\mathbf{K}^{22}\,\mathbf{U}^2 = \mathbf{F}^2$):

$$\begin{bmatrix} 7.8333 & -4.0417 & 0.0000 \\ -4.0417 & 7.8333 & -4.0417 \\ 0.0000 & -4.0417 & 7.8333 \end{bmatrix} \begin{Bmatrix} U_2 \\ U_3 \\ U_4 \end{Bmatrix} = -\begin{Bmatrix} 0.01823 \\ 0.06510 \\ 0.14323 \end{Bmatrix}$$

The solution is (obtained using a computer)

$$U_1 = 0.0,\ U_2 = -0.02323,\ U_3 = -0.04052,\ U_4 = -0.03919,\ U_5 = 0.0 \tag{5}$$

The secondary variables can be computed using either the condensed equations for the secondary variables or from the definitions in Eq.

(3.4.6). From the condensed equations ($\mathbf{F}^1 = \mathbf{K}^{12}\,\mathbf{U}^2$), we have

$$\begin{Bmatrix} Q_1^1 \\ Q_2^4 \end{Bmatrix} = \begin{Bmatrix} 0.00130 \\ 0.10547 \end{Bmatrix} + \begin{bmatrix} -4.0417 & 0 & 0.0000 \\ 0.0000 & 0 & -4.0417 \end{bmatrix} \begin{Bmatrix} -0.02323 \\ -0.04052 \\ -0.03919 \end{Bmatrix} = \begin{Bmatrix} 0.09520 \\ 0.26386 \end{Bmatrix} \tag{6}$$

From the definitions in Eq. (3.4.6), we have

$$(Q_1^1)_{\text{def}} \equiv \left(-a\frac{du_h^1}{dx}\right)\Big|_{x=0} = -\left[a\left(u_1^1\frac{d\psi_1^1}{dx} + u_2^1\frac{d\psi_2^1}{dx}\right)\right]_{x=0}$$
$$= \frac{U_1 - U_2}{h} = 0.09293 \tag{7}$$

$$(Q_2^4)_{\text{def}} \equiv \left(a\frac{du_h^4}{dx}\right)\Big|_{x=1} = \left[a\left(u_1^4\frac{d\psi_1^4}{dx} + u_2^4\frac{d\psi_2^4}{dx}\right)\right]_{x=1}$$
$$= \frac{U_5 - U_4}{h} = 0.15676 \tag{8}$$

$$(Q_1^1)_{\text{equil}} = K_{11}^1 U_1 + K_{12}^1 U_2 - f_1^1 = 0.09520 \tag{9}$$

$$(Q_2^4)_{\text{equil}} = K_{21}^4 U_4 + K_{22}^4 U_5 - f_2^4 = 0.26386 \tag{10}$$

(b) *Quadratic elements.* The element coefficient matrix is known from Eq. (3.4.38) with $a_e = 1$, $c_e = -1$, $h_e = \frac{1}{2}$:

$$\mathbf{K}^e = \frac{2}{3}\begin{bmatrix} 7 & -8 & 1 \\ -8 & 16 & -8 \\ 1 & -8 & 7 \end{bmatrix} - \frac{1}{60}\begin{bmatrix} 4 & 2 & -1 \\ 2 & 16 & 2 \\ -1 & 2 & 4 \end{bmatrix}$$

or

$$\mathbf{K}^e = \frac{1}{60}\begin{bmatrix} 276 & -322 & 41 \\ -322 & 624 & -322 \\ 41 & -322 & 276 \end{bmatrix} = \begin{bmatrix} 4.6000 & -5.3667 & 0.6833 \\ -5.3667 & 10.4000 & -5.3667 \\ 0.6833 & -5.3667 & 4.6000 \end{bmatrix}$$

The coefficients f_i^e are evaluated using Eq. (4) with

$$\psi_1^e(\bar{x}) = \left(1 - \frac{\bar{x}}{h_e}\right)\left(1 - \frac{2\bar{x}}{h_e}\right), \quad \psi_2^e(\bar{x}) = 4\frac{\bar{x}}{h_e}\left(1 - \frac{\bar{x}}{h_e}\right), \quad \psi_3^e(\bar{x}) = -\frac{\bar{x}}{h_e}\left(1 - \frac{2\bar{x}}{h_e}\right)$$

We obtain (with $h_e = 1/2$)

$$f_1^e = -\int_0^{h_e} (x_a + \bar{x})^2 \left(1 - 3\frac{\bar{x}}{h_e} + 2\frac{\bar{x}^2}{h_e^2}\right) d\bar{x} = -\tfrac{1}{480}(-1 + 40x_a^2)$$

$$f_2^e = -4\int_0^{h_e} (x_a + \bar{x})^2 \left(\frac{\bar{x}}{h_e} - \frac{\bar{x}^2}{h_e^2}\right) d\bar{x} = -\tfrac{1}{120}(3 + 20x_a + 40x_a^2)$$

$$f_3^e = \int_0^{h_e} (x_a + \bar{x})^2 \left(\frac{\bar{x}}{h_e} - 2\frac{\bar{x}}{h_e^2}\right) d\bar{x} = -\tfrac{1}{480}(9 + 40x_a + 40x_a^2)$$

Element 1 ($h_1 = \frac{1}{2}$, $x = 0$):

$$f_1^1 = \tfrac{1}{480} = 0.00208, \quad f_2^1 = -\tfrac{1}{40} = -0.02500, \quad f_3^1 = -\tfrac{3}{160} = -0.01875$$

Element 2 ($h_2 = \frac{1}{2}, x_a = h_1 = \frac{1}{2}$):

$$f_1^2 = -\tfrac{9}{480} = -0.01875, \quad f_2^2 = -\tfrac{23}{120} = -0.19167, \quad f_3^2 = -\tfrac{39}{480} = -0.08125$$

For the mesh of two quadratic elements connected in series (i.e., end to end), the condition on Q_i^e is that $Q_3^1 + Q_1^2 = 0$. Then the assembled set of equations is

$$\begin{bmatrix} 4.6000 & -5.3667 & 0.6833 & 0.0000 & 0.0000 \\ -5.3667 & 10.4000 & -5.3667 & 0.0000 & 0.0000 \\ 0.6833 & -5.3667 & 9.2000 & -5.3667 & 0.6833 \\ 0.0000 & 0.0000 & -5.3667 & 10.4000 & -5.3667 \\ 0.0000 & 0.0000 & 0.6833 & -5.3667 & 4.6000 \end{bmatrix} \begin{Bmatrix} U_1 \\ U_2 \\ U_3 \\ U_4 \\ U_5 \end{Bmatrix}$$

$$= -\begin{Bmatrix} -0.00208 \\ 0.02500 \\ 0.03750 \\ 0.19167 \\ 0.08125 \end{Bmatrix} + \begin{Bmatrix} Q_1^1 \\ Q_2^1 \\ Q_3^1 + Q_1^2 \\ Q_2^2 \\ Q_3^2 \end{Bmatrix}$$

Again, using $U_1 = 0$ and $U_5 = 0$, the condensed equations are obtained as

$$\begin{bmatrix} 10.4000 & -5.3667 & 0.0000 \\ -5.3667 & 9.2000 & -5.3667 \\ 0.0000 & -5.3667 & 10.4000 \end{bmatrix} \begin{Bmatrix} U_2 \\ U_3 \\ U_4 \end{Bmatrix} = -\begin{Bmatrix} 0.02500 \\ 0.03750 \\ 0.19167 \end{Bmatrix}$$

The solution is

$$U_1 = 0.0, \; U_2 = -0.02345, \; U_3 = -0.04078, \; U_4 = -0.03947, \; U_5 = 0.0 \qquad (12)$$

The unknown secondary variables can be obtained from the definition as

$$(Q_1^1)_{\text{equil}} = K_{11}^1 U_1 + K_{12}^1 U_2 + K_{13}^1 U_3 - f_1^1 = 0.10006$$
$$(Q_3^2)_{\text{equil}} = K_{13}^2 U_3 + K_{23}^2 U_4 + K_{33}^2 U_5 - f_3^2 = 0.26521 \tag{13}$$

$$\begin{aligned}
(Q_1^1)_{\text{def}} &\equiv -a\frac{du_h^1}{dx}\bigg|_{x=0} = -\left[a\left(u_1^1\frac{d\psi_1^1}{dx} + u_2^1\frac{d\psi_2^1}{dx} + u_3^1\frac{d\psi_3^1}{dx}\right)\right]_{x=0} \\
&= -\left[\frac{U_1}{h}\left(-3 + 4\frac{x}{h}\right) + \frac{U_2}{h}\left(4 - 8\frac{x}{h}\right) + \frac{U_3}{h}\left(-1 + 4\frac{x}{h}\right)\right]_{x=0} \\
&= \left(\frac{3}{h}U_1 - \frac{4}{h}U_2 + \frac{1}{h}U_3\right) = 0.10602 \\
(Q_3^2)_{\text{def}} &\equiv a\frac{du_h^2}{dx}\bigg|_{x=1} = \left[a\left(u_1^2\frac{d\psi_1^2}{dx} + u_2^2\frac{d\psi_2^2}{dx} + u_3^2\frac{d\psi_3^2}{dx}\right)\right]_{x=1} \\
&= \left[\frac{U_3}{h}\left(-3 + 4\frac{\bar{x}}{h}\right) + \frac{U_4}{h}\left(4 - 8\frac{\bar{x}}{h}\right) + \frac{U_5}{h}\left(-1 + 4\frac{\bar{x}}{h}\right)\right]_{\bar{x}=h} \\
&= \left(\frac{1}{h}U_3 - \frac{4}{h}U_4 + \frac{3}{h}U_5\right) = 0.23422
\end{aligned} \tag{14}$$

Table 3.4.2 contains a comparison of the finite element solutions obtained with four and eight linear elements and two and four quadratic elements against the threeparameter Ritz solution and the exact solution (see **Example 2.5.1** and Table 2.5.1). The four linear element and two quadratic element solutions are not as accurate as the threeparameter Ritz solution. However, the solution obtained with eight linear elements or four quadratic elements are more accurate with the four quadratic element solutions being virtually the same as the exact solution. Plots of u_h^e and du_h/dx are shown in Figs. 3.4.14 and 3.4.15, respectively. Note that the finite element solutions for the derivative [post-computed from $u_h^e(x)$] are discontinuous between the elements; the value of the difference in du_h/dx between elements reduces as the mesh is refined or degree of approximation is increased.

Table 3.4.2 Comparison of the finite element results with the exact solution ($-10u$) of Eqs.

(1) and (2): $\frac{d^2u}{dx^2} - u + x^2 = 0$ for 0 > x > 1; u(0) = u(1) = 0.

	FEM solution[1]				Ritz[2]	Exact
x	4L	2Q	8L	4Q	solution	solution
0.0000	**0.0000**[3]	**0.0000**	**0.0000**	**0.0000**	0.0000	0.0000
0.0625	0.0581	0.0644	0.0595	0.0602	0.0596	0.0598
0.1250	0.1162	0.1249	**0.1190**	**0.1193**	0.1191	0.1192
0.1875	0.1743	0.1816	0.1762	0.1771	0.1776	0.1775
0.2500	**0.2323**	**0.2345**	**0.2334**	**0.2337**	0.2339	0.2337
0.3125	0.2756	0.2835	0.2837	0.2876	0.2868	0.2866
0.3750	0.3188	0.3288	**0.3334**	**0.3345**	0.3347	0.3345
0.4375	0.3620	0.3702	0.3705	0.3745	0.3757	0.3755
0.5000	**0.4052**	**0.4078**	**0.4070**	**0.4076**	0.4076	0.4076
0.5625	0.4019	0.4403	0.4207	0.4298	0.4282	0.4283
0.6250	0.3986	0.4490	**0.4343**	**0.4350**	0.4347	0.4350
0.6875	0.3952	0.4338	0.4140	0.4231	0.4244	0.4246
0.7500	**0.3919**	**0.3947**	**0.3936**	**0.3942**	0.3940	0.3942
0.8125	0.2939	0.3318	0.3261	0.3421	0.3401	0.3402
0.8750	0.1960	0.2451	**0.2587**	**0.2591**	0.2592	0.2590
0.9375	0.0980	0.1345	0.1293	0.1450	0.1472	0.1470
1.0000	**0.0000**	**0.0000**	**0.0000**	**0.0000**	0.0000	0.0000

[1] 4L = 4 linear elements; 8L = 8 linear elements; 2Q = 2 quadratic elements; 4Q = 4 quadratic elements. [2] Three-parameter Ritz solution from Example 2.5.1. [3] Numbers in bold are the nodal values; others are the interpolated values obtained using the underlying finite element approximation, $u(x) = \sum_{j=1}^{2} u_j^e \psi_j^e(x)$.

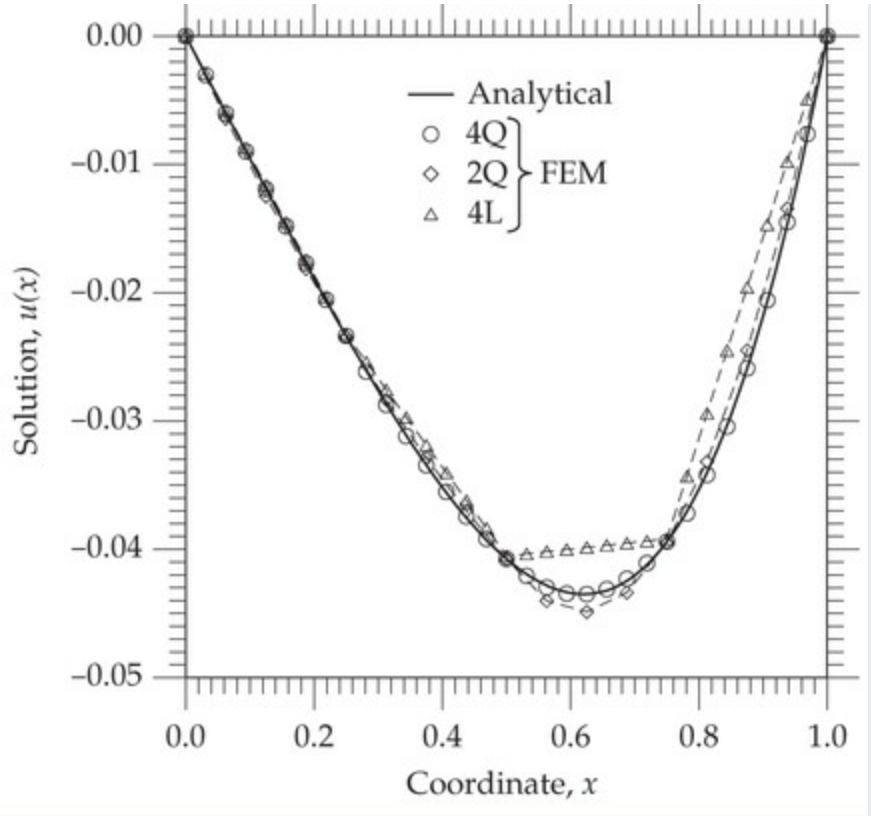

Fig. 3.4.14 Comparison of the finite element solutions $u_h^e(x)]$ with the exact and Ritz solutions.

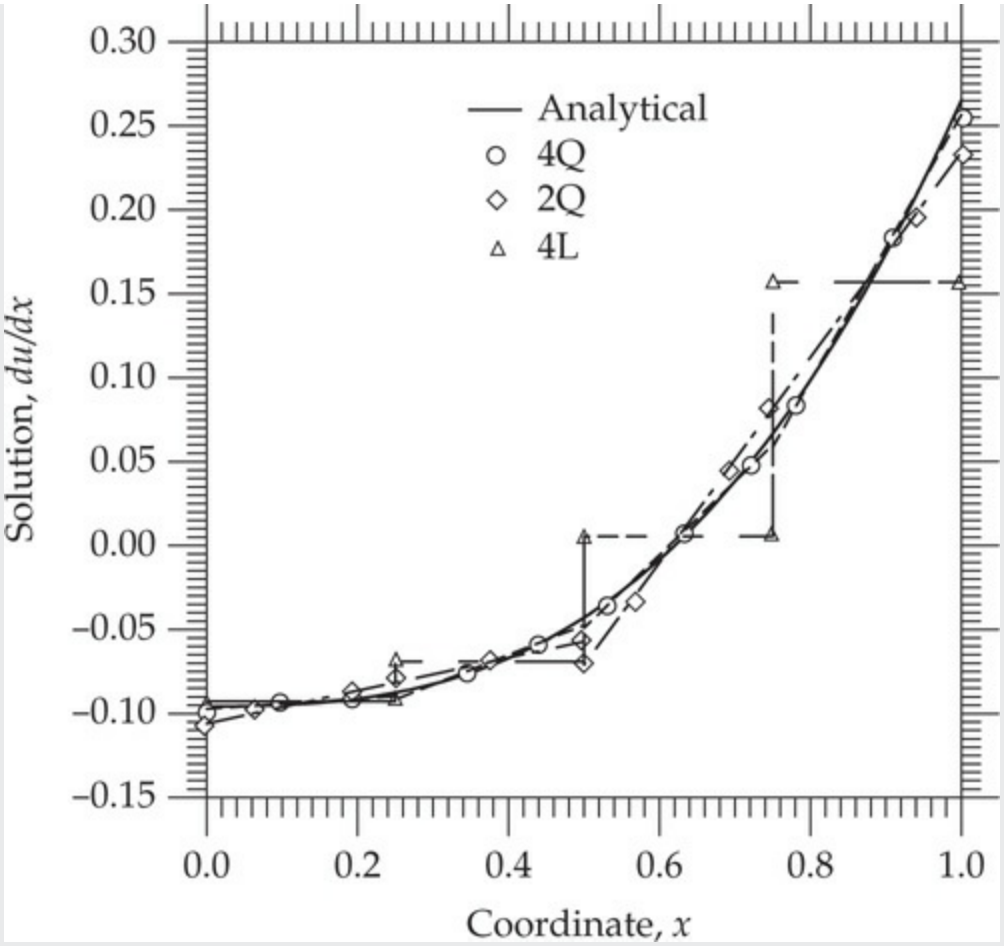

Fig. 3.4.15 Comparison of the finite element solutions du_h/dx with the exact and Ritz solutions.

3.4.7 Remarks and Observations

Some remarks and observations on the steps described for the finite element analysis of the model equation, Eq. (3.4.1), are presented here.

1. Although the Ritz method was used to set up the element equations, any other method, such as a weighted-residual (i.e., the least-squares or subdomain) method, could be used to derive the finite element equations.
2. Steps 1–6 of a finite element analysis (see Table 3.2.1) are common for any problem. The derivation of interpolation functions depends only on the element geometry and on the number and position of nodes in the element. The number of nodes in the element and the degree of approximation used are related.
3. The finite element equations (3.4.32b) are derived for the linear

operator equation

$$A(u) = f, \quad \text{where} \quad A = -\frac{d}{dx}\left(a\frac{d}{dx}\right) + c \tag{3.4.63}$$

Hence, they are valid for any physical problem that is described by the operator equation $A(u) = f$ or its special cases. One needs to interpret the quantities appropriately. Examples of problems described by this operator are listed in Table 3.4.1. Thus, a computer program written for the finite element analysis of Eq. (3.4.1) can be used to analyze any of the problems in Table 3.4.1. Also, note that the data $a = a(x)$, $c = c(x)$, and $f = f(x)$ can be different, in general, in different elements.

Table 3.4.1 Some examples of engineering problems governed by the second-order differential equation in Eq. (3.4.1).*

Field of study	Primary variable, u	Problem data			Secondary variable, Q
		a	c	f	
Heat transfer in bars	Temperature $T - T_\infty$	Thermal conductance kA	Surface convection $P\beta$	Heat generation f	Heat Q
Flow through porous medium	Fluid-head ϕ	Permeability μ	0	Infiltration f	Point source Q
Flow through pipes	Pressure p	Pipe resistance $1/R$	0	0	Volume rate of flow Q
Flow of viscous fluids	Velocity v_z	Viscosity μ	0	Pressure gradient $-dP/dx$	Shear stress $\sigma_{xz} = \tau_{xz}$
Elastic cables	Displacement u	Tension T	0	Transverse force f	Point load P
Elastic bars	Displacement u	Axial stiffness EA	Surface resistance c	Axial force f	Point force P
Torsion of bars	Angle of twist θ	Shear stiffness GJ	0	0	Torque T
Electrostatics	Electrical potential ϕ	Dielectric constant ε	0	Charge density ρ	Electric flux E

*k is thermal conductivity; β is the film conductance; P is the perimeter; T_∞ is the ambient temperature of the surrounding fluid medium; $R = 128\mu h/(\pi d^4)$ with μ being the viscosity, h being the length, and d being the diameter of the pipe; E is the Young's modulus; A is the area of cross section; J is the polar moment of inertia.

4. Integration of the element matrices in Eq. (3.4.33) can be implemented on a computer using numerical integration. When these integrals are algebraically complicated, one has no other choice but to use numerical integration, which will be discussed in Chapter 8.
5. Another interpretation of Eq. (3.4.40) for $c_e = 0$ can be given in terms of the finite difference approximation when EA is element-wise constant. The axial force at any point x is given by $P(x) = (EA\, du/dx)n_x$, where n_x takes the value of −1 at the left end and +1 at the right end of the bar (to account for the direction of the unit normal). Using the forward difference approximation at $x = x_a$ and backward difference approximation at $x = x_b$ to replace the derivative du/dx, we obtain

$$P_1^e \equiv P^e(x_a) = \left(-E_e A_e \frac{du}{dx}\right)_{x_a} \approx -E_e A_e \frac{u(x_b) - u(x_a)}{h_e} = \frac{E_e A_e}{h_e}(u_1^e - u_2^e) \quad (3.4.64)$$

$$P_2^e \equiv P^e(x_b) = \left(E_e A_e \frac{du}{dx}\right)_{x_b} \approx E_e A_e \frac{u(x_b) - u(x_a)}{h_e} = \frac{E_e A_e}{h_e}(u_2^e - u_1^e) \quad (3.4.65)$$

which are the same as Eq. (3.3.6). Note that no explicit approximation of $u(x)$ itself is assumed in writing Eqs. (3.4.64) and (3.4.65); but the fact that we used values of the function from two consecutive points to define its slope implies that we assumed a linear approximation of the function. Thus, to compute the value of u at a point other than the nodes (or mesh points), linear interpolation must be used.
6. For the model problem considered, the element matrix $\mathbf{K}^e$ in Eq. (3.4.33) is symmetric: $K_{ij}^e = K_{ji}^e$. This enables one to compute $K_{ij}^e\ (i, j = 1, 2, \ldots, n)$ for $j \le i$ only. In other words, one need compute only the diagonal terms and the upper or lower diagonal terms. Because of the symmetry of the element matrices, the assembled global matrix will also be symmetric. Thus, one need store only the upper triangle, including the diagonal, of the assembled matrix in a finite element computer program. Another property characteristic of the finite element method is the *sparseness* of the assembled matrix. Since $K_{IJ} = 0$ if global nodes I and J do not belong to the same finite element, the global coefficient matrix is *banded*; that is, all coefficients beyond a certain distance

from the diagonal are zero. The maximum of the distances between the diagonal element, including the latter, of a row and the last nonzero coefficient in that row is called the *half-bandwidth*. When a matrix is banded and symmetric, one need store only entries in the upper or lower band of the matrix. Equation solvers written for the solution of banded symmetric equations are available for use in such cases. The symmetry of the coefficient matrix depends on the type of the differential equation, its variational form, and the numbering of the finite element equations. The sparseness of the matrix is a result of the finite element interpolation functions, which have nonzero values only over an element of the domain (i.e., so-called *compactness* property of the approximation functions). Of course, when iterative solvers are used, as opposed to Gauss elimination procedures, bandwidth is not a concern.

7. There are three sources of error that may contribute to the inaccuracy of the finite element solution of a problem:

a. *Domain approximation error*, which is due to the approximation of the domain.

b. *Computational errors*, which are due to inexact evaluation of the coefficients K_{ij}^e and f_i^e, or are introduced owing to the finite arithmetic in a computer.

c. *Approximation error*, which is due to approximation of the solution by piecewise polynomials.

Since the geometry of the problem is exactly represented, and the linear approximation is able to represent the exact solution at the nodes when a is a constant, $c = 0$, and f is arbitrary (see Reddy [2], p. 403), the first and third types of errors are zero. The only error that can be introduced into the final numerical results is possibly due to the computer evaluation of the coefficients K_{ij}^e and f_i^e and the solution of algebraic equations. However, in general, computational as well as approximation errors exist even in one-dimensional problems. Additional discussion of the errors in the finite element approximation can be found in Surana and Reddy [3].

3.5 Axisymmetric Problems

3.5.1 Model Equation

Consider the second-order differential equation in vector form

$$-\nabla \cdot (\mathbf{a} \cdot \nabla u) = f(\mathbf{x}) \tag{3.5.1}$$

where ∇ is the gradient operator discussed in Section 2.2.1.3, **a** is a known second-order tensor, u is the field variable to be determined, and f is a known source. An example of Eq. (3.5.1) is provided by heat conduction equation (see Reddy [1,4]) where u is the temperature, **a** is the conductivity tensor, and f is the internal heat generation.

The equations governing physical processes in cylindrical geometries are described analytically in terms of cylindrical coordinates (r, θ, z). For isotropic material (i.e., $a_{rr} = a_{\theta\theta} = a_{zz} \equiv a$), Eq. (3.5.1) takes the form

$$-\frac{1}{r}\frac{\partial}{\partial r}\left(ra\frac{\partial u}{\partial r}\right) - \frac{1}{r}\frac{\partial}{\partial \theta}\left(\frac{a}{r}\frac{\partial u}{\partial \theta}\right) - \frac{\partial}{\partial z}\left(a\frac{\partial u}{\partial z}\right) = f(r,\theta,z) \tag{3.5.2}$$

When the geometry, loading, and boundary conditions are independent of the circumferential direction (i.e., θ-coordinate direction), the problem is said to be axisymmetric and the governing equations become two-dimensional in terms of r and z. In addition, if the problem geometry and data are independent of z, for example, when the cylinder is very long, the equations are functions of only the radial coordinate r, as shown in Fig. 1.4.6, which is reproduced in Fig. 3.5.1(a) through (c):

$$-\frac{1}{r}\frac{d}{dr}\left[ra(r)\frac{du}{dr}\right] = f(r) \quad \text{for} \quad R_i < r < R_0 \tag{3.5.3}$$

where r is the radial coordinate, a and f are known functions of r, and u is the dependent variable. Such equations arise, for example, in connection with radial heat flow in a long circular cylinder of inner radius $R_i \geq 0$ and outer radius R_0. The radially symmetric conditions require that both $a = k$ (k is the conductivity) and f (internal heat generation) be functions of only r. In this section we develop the finite element model of one-dimensional axisymmetric problems described by Eq. (3.5.3).

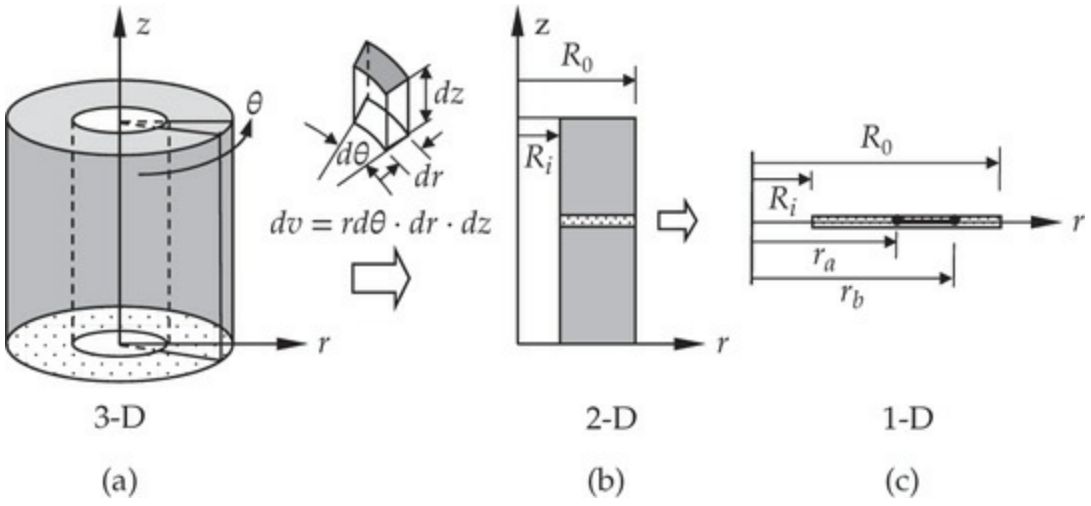

Fig. 3.5.1 Volume element and computational domain of an axisymmetric problem.

3.5.2 Weak Form

We begin with the development of the weak form, where the volume element in the weighted-integral statement is replaced by $dv = rdrd\theta dz$. Since the integrand is independent of both θ and z and considering cylinder of unit length, we obtain

$$\int_{v^e} F(r)\, dv = \int_0^1 \int_0^{2\pi} \int_{r_a}^{r_b} F(r)\, r dr\, d\theta\, dz = 2\pi \int_{r_a}^{r_b} F(r)\, r dr \tag{3.5.4}$$

where (r_a, r_b) is the domain of a typical element along the radial direction. Next, we carry out the remaining two steps of the weak formulation.

In developing the weak form of Eq. (3.5.3), we replace u with its approximation u_h^e, multiply resulting residual with a weight function $w_i^e(r)$, and integrate over the element volume of the cylinder of unit length (see Fig. 3.5.1):

$$0 = 2\pi \int_{r_a}^{r_b} w_i^e \left[-\frac{1}{r}\frac{d}{dr}\left(ra \frac{du_h}{dr} \right) - f \right] r\, dr \tag{3.5.5a}$$

$$0 = 2\pi \int_{r_a}^{r_b} \left(a \frac{dw_i}{dr}\frac{du_h}{dr} - w_i f \right) r dr - 2\pi \left[w_i^e\, ra \frac{du_h}{dr} \right]_{r_a}^{r_b}$$

$$0 = 2\pi \int_{r_a}^{r_b} \left(a \frac{dw_i}{dr}\frac{du_h}{dr} - w_i f \right) r dr - w_i^e(r_a)\, Q_1^e - w_i^e(r_b)\, Q_2^e \tag{3.5.5b}$$

$$Q_1^e \equiv -2\pi \left(ra \frac{du_h}{dr} \right) \Big|_{r_a}, \quad Q_2^e \equiv 2\pi \left(ra \frac{du_h}{dr} \right) \Big|_{r_b} \tag{3.5.5c}$$

3.5.3 Finite Element Model

The finite element model is obtained by substituting the approximation

$$u(r) \approx u_h(r) = \sum_{j=1}^{n} u_j^e \psi_j^e(r) \tag{3.5.6}$$

where $\psi_i^e(r)$ are the Lagrange interpolation functions, which were already derived for linear and quadratic elements earlier in Section 3.4.3.3; the only change is that the axial coordinate x is replaced by the radial r. For example, the linear interpolation functions are of the form ($h_e = r_b - r_a$)

$$\psi_1^e(r) = \frac{r_b - r}{h_e}, \quad \psi_2^e(r) = \frac{r - r_a}{h_e} \tag{3.5.7}$$

As before, we replace w_i^e with ψ_i^e to obtain the ith algebraic equation of the Ritz (or weak-form Galerkin) finite element model:

$$\sum_{j=1}^{n} K_{ij}^e u_j^e = f_i^e + Q_i^e \quad \text{or} \quad \mathbf{K}^e \mathbf{u}^e = \mathbf{f}^e + \mathbf{Q}^e \tag{3.5.8a}$$

$$K_{ij}^e = 2\pi \int_{r_a}^{r_b} a(r) \frac{d\psi_i^e}{dr} \frac{d\psi_j^e}{dr} \, r dr, \quad f_i^e = 2\pi \int_{r_a}^{r_b} \psi_i^e f(r) \, r \, dr \tag{3.5.8b}$$

The explicit forms of the coefficients K_{ij}^e and f_i^e for element-wise constant values of $a = a_e$ and $f = f_e$ are given below. Here r_a denotes the global coordinate of node 1 of the element.

Linear element

$$\mathbf{K}^e = \frac{2\pi a_e}{h_e} (r_a + \tfrac{1}{2} h_e) \begin{bmatrix} 1 & -1 \\ -1 & 1 \end{bmatrix}$$
$$\mathbf{f}^e = \frac{2\pi f_e h_e}{6} \begin{Bmatrix} 3r_a + h_e \\ 3r_a + 2h_e \end{Bmatrix} \tag{3.5.9}$$

Quadratic element

$$\mathbf{K}^e = \frac{2\pi a_e}{6h_e}\begin{bmatrix} 3h_e + 14r_a & -(4h_e + 16r_a) & h_e + 2r_a \\ -(4h_e + 16r_a) & 16h_e + 32r_a & -(12h_e + 16r_a) \\ h_e + 2r_a & -(12h_e + 16r_a) & 11h_e + 14r_a \end{bmatrix} \tag{3.5.10}$$

$$\mathbf{f}^e = \frac{2\pi f_e h_e}{6}\begin{Bmatrix} r_a \\ 4r_a + 2h_e \\ r_a + h_e \end{Bmatrix}$$

For example, for a solid cylinder, the first node of the first element has $r_a = 0$. Then $\mathbf{K}^1$ and $\mathbf{f}^1$ take the form

$$\mathbf{K}^1 = \frac{2\pi a_1}{6}\begin{bmatrix} 3 & -4 & 1 \\ -4 & 16 & -12 \\ 1 & -12 & 11 \end{bmatrix}, \quad \mathbf{f}^1 = \frac{2\pi f_1 h_1^2}{6}\begin{Bmatrix} 0 \\ 2 \\ 1 \end{Bmatrix} \tag{3.5.11}$$

We now consider two examples of axisymmetric problems.

Example 3.5.1

Equation (3.5.3) governs, for example, temperature distribution $u(r)$ in a *long* solid cylindrical bar of radius R and thermal conductivity k (i.e., $a(r) = k$) that is heated by the passage of electric current, which generates heat energy f_0. Heat is dissipated from the surface of the bar by convection into the surrounding medium at an ambient temperature of u_∞. Determine the temperature distribution as a function of the radial distance. The boundary conditions are

$$\frac{du}{dr} = 0 \text{ at } r = 0 \text{ (symmetry)}, \quad rk\frac{du}{dr} + r\beta(u - u_\infty) = 0 \text{ at } r = R \text{ (convection)} \tag{1}$$

Use four linear finite elements and the following data:

$$R = 0.05 \text{ m}, \quad k = 40 \text{ W/(m°C)}, \quad f = 4 \times 10^6 \text{ W/m}^3, \quad \beta = 400 \text{ W/(m}^2\text{°C)}, \quad u_\infty = 20\text{°C} \tag{2}$$

Solution: Since the cylinder is very long, it is sufficient to consider only a typical section of the cylinder (neglecting the end effects). Then due to the axisymmetry of the geometry, material, and boundary conditions, one may reduce the problem to a one-dimensional problem by simply considering heat transfer along a radial line of the cross section. For the uniform mesh of four linear elements (h = 0.0125 m), we have the following coefficient matrices and source vectors [see Eq. (3.5.9)] when

the common factor 2π is omitted in the equations.

Element 1 ($a = k = 40$, $r_a = 0$ and $r_b = h$):

$$\mathbf{K}^1 = \frac{40}{2}\begin{bmatrix} 1 & -1 \\ -1 & 1 \end{bmatrix}, \quad \mathbf{f}^1 = \frac{4\times 10^6(0.0125)^2}{6}\begin{Bmatrix} 1 \\ 2 \end{Bmatrix} = 10^2\begin{Bmatrix} 1.0417 \\ 2.0833 \end{Bmatrix}$$

Element 2 ($a = k = 40$, $r_a = h$ and $r_b = 2h$):

$$\mathbf{K}^2 = \frac{40}{2}\begin{bmatrix} 3 & -3 \\ -3 & 3 \end{bmatrix}, \quad \mathbf{f}^2 = \frac{4\times 10^6(0.0125)^2}{6}\begin{Bmatrix} 4 \\ 5 \end{Bmatrix} = 10^2\begin{Bmatrix} 4.1667 \\ 5.2083 \end{Bmatrix}$$

Element 3 ($a = k = 40$, $r_a = 2h$ and $r_b = 3h$):

$$\mathbf{K}^3 = \frac{40}{2}\begin{bmatrix} 5 & -5 \\ -5 & 5 \end{bmatrix}, \quad \mathbf{f}^3 = \frac{4\times 10^6(0.0125)^2}{6}\begin{Bmatrix} 7 \\ 8 \end{Bmatrix} = 10^2\begin{Bmatrix} 7.2917 \\ 8.3333 \end{Bmatrix}$$

Element 4 ($a = k = 40$, $r_a = 3h$ and $r_b = 4h = R$):

$$\mathbf{K}^4 = \frac{40}{2}\begin{bmatrix} 7 & -7 \\ -7 & 7 \end{bmatrix}, \quad \mathbf{f}^4 = \frac{4\times 10^6(0.0125)^2}{6}\begin{Bmatrix} 10 \\ 11 \end{Bmatrix} = 10^3\begin{Bmatrix} 1.0417 \\ 1.1458 \end{Bmatrix}$$

For this case where all elements are connected in series, the assembled equations are the same as those shown in Eq. (3.4.50) and the balance conditions on Q_i^e are the same as in Eq. (3.4.45). Therefore, the assembled equations with the balance conditions are given by

$$\begin{bmatrix} 20 & -20 & 0 & 0 & 0 \\ -20 & 80 & -60 & 0 & 0 \\ 0 & -60 & 160 & -100 & 0 \\ 0 & 0 & -100 & 240 & -140 \\ 0 & 0 & 0 & -140 & 140 \end{bmatrix}\begin{Bmatrix} U_1 \\ U_2 \\ U_3 \\ U_4 \\ U_5 \end{Bmatrix} = \alpha\begin{Bmatrix} 1 \\ 6 \\ 12 \\ 18 \\ 11 \end{Bmatrix} + \begin{Bmatrix} Q_1^1 \\ Q_2^1 + Q_1^2 = 0 \\ Q_2^2 + Q_1^3 = 0 \\ Q_2^3 + Q_1^4 = 0 \\ Q_2^4 \end{Bmatrix} \tag{3}$$

where α = 104.166. The boundary conditions require

$$Q_1^1 = 0, \quad Q_2^4 = -R\beta(U_5 - u_\infty) = -20(U_5 - 20) \tag{4}$$

The condensed equations are the same as the assembled equations with the boundary conditions imposed, as there are no specified primary variables in this problem

$$\begin{bmatrix} 20 & -20 & 0 & 0 & 0 \\ -20 & 80 & -60 & 0 & 0 \\ 0 & -60 & 160 & -100 & 0 \\ 0 & 0 & -100 & 240 & -140 \\ 0 & 0 & 0 & -140 & 160 \end{bmatrix} \begin{Bmatrix} U_1 \\ U_2 \\ U_3 \\ U_4 \\ U_5 \end{Bmatrix} = 104.166 \begin{Bmatrix} 1 \\ 6 \\ 12 \\ 18 \\ 11 \end{Bmatrix} + \begin{Bmatrix} 0 \\ 0 \\ 0 \\ 0 \\ 400 \end{Bmatrix} \tag{5}$$

The solution of these equations (with the help of a computer) is obtained as

$$U_1 = 334.68, \quad U_2 = 329.47, \quad U_3 = 317.32, \quad U_4 = 297.53, \quad U_5 = 270.00 \tag{6}$$

For the uniform mesh of two quadratic elements, the element matrices are as follows:

Element 1 ($a = k = 40$, $r_a = 0$ and $r_b = h = 0.025$):

$$\mathbf{K}^1 = 10^2 \begin{bmatrix} 0.2000 & -0.2667 & 0.0667 \\ -0.2667 & 1.0667 & -0.8000 \\ 0.0667 & -0.8000 & 0.7333 \end{bmatrix}, \quad \mathbf{f}^1 = 10^3 \begin{Bmatrix} 0.0000 \\ 0.8333 \\ 0.4167 \end{Bmatrix}$$

Element 2 ($a = k = 40$, $r_a = h$ and $r_b = 2h = 0.05$):

$$\mathbf{K}^2 = 10^2 \begin{bmatrix} 1.1333 & -1.3333 & 0.2000 \\ -1.3333 & 3.2000 & -1.8667 \\ 0.2000 & -1.8667 & 1.6667 \end{bmatrix}, \quad \mathbf{f}^2 = 10^3 \begin{Bmatrix} 0.4167 \\ 2.5000 \\ 0.8333 \end{Bmatrix}$$

The mesh of two quadratic yields the nodal values

$$U_2 = 332.50, \quad U_3 = 328.59, \quad U_3 = 316.87, \quad U_4 = 297.34, \quad U_5 = 270.00 \tag{7}$$

These nodal values coincide with the exact solution at the nodes

$$u(r) = u_\infty + \frac{f_0 R}{2\beta} + \frac{f_0 R^2}{4k}\left(1 - \frac{r^2}{R^2}\right) \tag{3.5.12}$$

The movement of particles (or molecules) of a substance from an area of high concentration of that substance to an area of lower concentration is called *diffusion* (see Reddy [1], pp. 179–181). Flow of fluid particles through a porous solid medium and flow of heat from high temperature region to a low temperature region provide examples of diffusion. The governing equation of such a process has already been discussed in Example 1.2.2 in the case of heat transfer. The transfer of molecules is governed, similar to Fourier's heat conduction law, by Fick's first law that relates the diffusion flux of a solute to the concentration gradient in a dilute solution:

$$\mathbf{q} = -D\nabla C \tag{3.5.13}$$

where C denotes concentration (the dependent unknown), D the diffusion coefficient, and $\mathbf{q}$ the diffusion flux. Mass conservation of the solutes in a tissue without any chemical reaction leads to

$$\frac{\partial C}{\partial t} - \nabla \cdot (D\nabla C) = 0 \tag{3.5.14}$$

For steady-state analysis, the time derivative term is omitted. In the next example, an application of the diffusion equation [see Eq. (3.5.3)] and its finite element solution are discussed.

Example 3.5.2

The diffusion of low-density lipoprotein (LDL) from the blood flow through the artery wall causes diseases like *atherosclerosis*. For the analysis purposes, we consider the artery wall to be composed of the *intima* near the blood flow region, called *lumen*, and the *media*, as shown in Fig. 3.5.2. The intermediate region between the intima and the media, called internal elastic lamina (IEL), the adventitia, and the region between the media and adventitia, called the external elastic layer (EEL), will be neglected in the present numerical study. Assuming that the artery is a long two-layer cylindrical shell and the diffusion of LDL (cholesterol) is axisymmetric, one can adopt a one-dimensional model. Let the lumen radius be a, the radius of the media be b, and the radial distance to the interface between the intima and the media be R. Assuming that the diffusion coefficients for LDL in the intima and the media are D_i and D_m, respectively, and the concentration at the intima surface is C_a and at the outside of the media is C_b, determine the LDL concentration as a function of the radial distance from the center of the artery. Use two quadratic finite elements and the following data [5,6]:

$$\begin{aligned} &a = 3.100\,\text{mm},\quad b = 3.310\,\text{mm},\quad R = 3.110\,\text{mm},\quad D_i = 5\times10^{-6}\,\text{mm}^2/\text{s} \\ &D_m = 5\times10^{-8}\,\text{mm}^2/\text{s},\quad C_a = 1.2\times10^{-6}\,\text{g/mm}^3,\quad C_b = 0.1\times10^{-6}\,\text{g/mm}^3 \end{aligned} \tag{1}$$

Solution: Diffusion in a cylindrical geometry is also governed by Eq. (3.5.14), which, for the present steady and axisymmetric case, reduces to

$$-\frac{1}{r}\frac{d}{dr}\left(rD\frac{dC}{dr}\right) = 0 \tag{2}$$

for both intima (layer 1) and media (layer 2). Clearly, Eq. (2) is a special case of Eq. (3.5.3), with $u = C$, $a(r) = D$, and $f(r) = 0$ (i.e., $\mathbf{f}e = 0$).

For a mesh of two quadratic elements, the element coefficients for the problem at hand are [use Eq. (3.5.10) with $a_1 = D_i = 5 \times 10^{-6}$ mm^2/s, $h_1 = R - a = 0.01$ mm, $a_2 = D_m = 5 \times 10^{-8}$ mm^2/s, and $h_2 = b - R = 0.2$ mm; omit the common factor 2π from the coefficients] presented next.

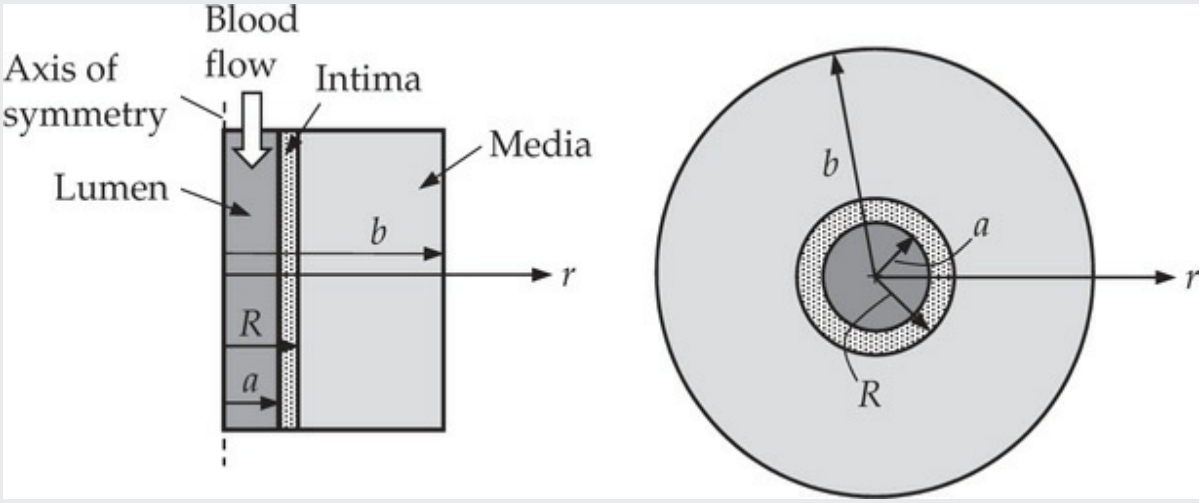

Fig. 3.5.2 Diffusion of low-density lipoprotein through two-layer artery wall.

Element 1 ($a_1 = D_i = 5 \times 10^{-6}$, $r_a = a = 3.10$, $h_1 = 0.01$):

$$\mathbf{K}^1 = \frac{5 \times 10^{-9}}{6 \times 0.01} \begin{bmatrix} 3 \times 10 + 14 \times 3100 & -(4 \times 10 + 16 \times 3100) & 10 + 2 \times 3100 \\ -(4 \times 10 + 16 \times 3100) & 16 \times 10 + 32 \times 3100 & -(12 \times 10 + 16 \times 3100) \\ 10 + 2 \times 3100 & -(12 \times 10 + 16 \times 3100) & 11 \times 10 + 14 \times 3100 \end{bmatrix}$$

$$= 10^{-2} \begin{bmatrix} 0.36192 & -0.41367 & 0.05175 \\ -0.41367 & 0.82800 & -0.41433 \\ 0.05175 & -0.41433 & 0.36258 \end{bmatrix}$$

Element 2 ($a_2 = D_m = 5 \times 10^{-8}$, $r_a = R = 3.11$, $h_2 = 0.20$):

$$\mathbf{K}^2 = \frac{5\times10^{-11}}{6\times0.2}\begin{bmatrix} 3\times200+14\times3,110 & -(4\times200+16\times3110) & 200+2\times3110 \\ -(4\times200+16\times3110) & 16\times200+32\times3110 & -(12\times200+16\times3110) \\ 200+2\times3110 & -(12\times200+16\times3110) & 11\times200+14\times3,110 \end{bmatrix}$$

$$= 10^{-5}\begin{bmatrix} 0.18392 & -0.21067 & 0.02675 \\ -0.21067 & 0.42800 & -0.21733 \\ 0.02675 & -0.21733 & 0.19058 \end{bmatrix}$$

The boundary conditions are $U_1 = C_a$ and $U_5 = C_b$. Hence the condensed equations are obtained by applying the boundary conditions, moving the known quantities to the right-hand side, and deleting the first and last rows and columns of the assembled system of equations:

$$10^{-5}\begin{bmatrix} 828.000 & -414.333 & 0.000 \\ -414.333 & 362.764 & -0.211 \\ 0.000 & -0.211 & 0.428 \end{bmatrix}\begin{Bmatrix} U_2 \\ U_3 \\ U_4 \end{Bmatrix} = 10^{-5}\begin{Bmatrix} 413.66667\,C_a \\ -51.75\,C_a - 0.2675\,C_b \\ 0.21733\,C_b \end{Bmatrix}$$

The solution of these equations yields (units: 10^{-6}g/mm^3)

$$U_2 = 1.1997,\quad U_3 = 1.1994,\quad U_5 = 0.64115 \tag{3}$$

The secondary variables computed using the definition are almost the same at all nodes and they are all equal to $Q = 0.882 \times 10^{-12}$ (g/s).

The analytical solution of Eq. (2) subjected to the boundary conditions

$$\begin{aligned} &r=a: \quad C_1 = C_a, && r=b: && C_2 = C_b \\ &r=R: \quad C_1 = C_2, && r=R: && rD_i\frac{dC_1}{dr} = rD_m\frac{dC_2}{dr} \end{aligned} \tag{4}$$

is

$$\begin{aligned} C_1(r) &= A_1\log r + B_1 \quad \text{for } a<r<R \\ C_2(r) &= A_2\log r + B_2 \quad \text{for } R<r<b \end{aligned} \tag{5}$$

where

$$\begin{aligned} &A_2 = \beta A_1,\quad A_1 = \frac{C_b - C_a}{\log\frac{R}{a} - \beta\log\frac{R}{b}},\quad \beta = \frac{D_i}{D_m} \\ &B_1 = C_a - A_1\log a,\quad B_2 = C_b - \beta A_1\log b \end{aligned} \tag{6}$$

The finite element solution in Eq. (3) matches with the exact values at the nodes:

$$u(3.105) = 1.1997, \quad u(3.110) = 1.1994, \quad u(3.210) = 0.64115 \tag{7}$$

The exact value of the diffusion flux is $Q = 0.882 \times 10^{-12}$ (g/s).

3.6 Errors in Finite Element Analysis

3.6.1 Types of Errors

As stated earlier, the errors introduced into finite element solution of a given differential equation can be attributed to three basic sources:

1. *Domain approximation error*, which is due to the approximation of the domain.
2. *Quadrature and finite arithmetic errors*, which are due to the numerical evaluation of integrals and the numerical computation on a computer.
3. *Approximation error*, which is due to the approximation of the solution:

$$u(x) \approx u_h(x) \equiv \sum_{I=1}^{N} U_I \Phi_I(x) \tag{3.6.1}$$

where U_I denotes the value of u at global node I and Φ_I denotes the global interpolation function associated with global node I (see Fig. 3.4.11).

In the one-dimensional problems, the domains considered have been straight lines. Therefore, no approximation of the domain has been necessary. In two-dimensional problems involving non-rectangular domains, domain (or boundary) approximation errors are introduced into finite element solutions. In general, these can be interpreted as errors in the specification of the data of the problem because we are now solving the given differential equation on a modified domain. As we refine the mesh, the domain is more accurately represented, and, therefore, the boundary approximation errors are expected to approach zero.

When finite element computations are performed on a computer,

round-off errors in the computation of numbers and errors due to the numerical evaluation of integrals are introduced into the solution. In most linear problems with a reasonably small number of total degrees of freedom in the system, these errors are expected to be small (or zero when only a certain decimal point accuracy is desired).

The error introduced into the finite element solution u_h^e because of the approximation of the dependent variable u in an element Ω_e is inherent to any problem

$$u(x) \approx u_h(x) = \sum_{e=1}^{N} \sum_{i=1}^{n} u_i^e \psi_i^e(x) = \sum_{I=1}^{M} U_I \Phi_I(x) \tag{3.6.2}$$

where u_h is the finite element solution over the domain ($u_h = u_h^e$ in Ω_e), N is the number of elements in the mesh, M is the total number of global nodes, and n is the number of nodes in an element. We wish to know how the error $E = u - u_h$, measured in a meaningful way, behaves as the number of elements in the mesh is increased. It can be shown that the approximation error is zero at the global nodes for the single second-order and fourth-order equations with element-wise-constant coefficients.

3.6.2 Measures of Errors

There are several ways in which one can measure the "difference" (or distance) between any two functions u and u_h. The *pointwise error* is the difference of u and u_h at each point of the domain. One can also define the difference of u and u_h to be the maximum of all absolute values of the differences of u and u_h in the domain $\Omega = (a, b)$:

$$\|u - u_h\|_\infty \equiv \max_{a \le x \le b} |u(x) - u_h(x)| \tag{3.6.3}$$

This measure of difference is called the *supmetric*. Note that the supmetric is a real number, whereas the pointwise error is a function and does not qualify as a distance or *norm* in a strict mathematical sense. The norm of a function is a non-negative real number.

More generally used measures (or norms) of the difference of two functions are the *energy norm* and the L_2 *norm* (pronounced "L-two norm"). For any squareintegrable functions u and u_h defined on the domain $\Omega = (a, b)$, the two norms are defined by

Energy norm: $$\|u-u_h\|_m=\left(\int_a^b\sum_{i=0}^{m}\left|\frac{d^iu}{dx^i}-\frac{d^iu_h}{dx^i}\right|^2dx\right)^{1/2} \tag{3.6.4}$$

L_2 norm: $$\|u-u_h\|_0=\left(\int_a^b|u-u_h|^2\,dx\right)^{1/2} \tag{3.6.5}$$

where $2m$ is the order of the differential equation being solved. The term "energy norm" is used to indicate that this norm contains the same-order derivatives as the quadratic functional (which, for most solid mechanics problems, denotes the energy) associated with the equation. Various measures of the distance between two functions are illustrated in Fig. 3.6.1. These definitions can easily be modified for two-dimensional domains.

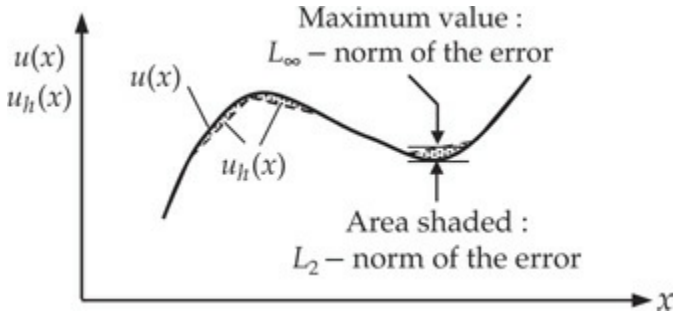

Fig. 3.6.1 Different measures of the error $E = u - u_h$ between the exact solution u and the finite element solution u_h. The maximum norm and the L_2 norms are illustrated.

3.6.3 Convergence and Accuracy of Solutions

The finite element solution u_h in Eq. (3.6.1) is said to *converge in the energy norm* to the true solution u if

$$\|u-u_h\|_m \le c\,h^p \quad \text{for} \quad p>0 \tag{3.6.6}$$

where c is a constant independent of u and u_h and h is the characteristic length of an element. The constant p is called the *rate of convergence*. Note that the convergence depends on h as well as on p; p depends on the order of the derivative of u in the weak form and the degree of the polynomials used to approximate u [see Eq. (3.6.15)]. Therefore, the error in the approximation can be reduced either by reducing the size of the elements or increasing the degree of approximation. Convergence of the

finite element solutions with mesh refinements (i.e., more of the same kind of elements are used) is termed *h-convergence*. Convergence with increasing degree of polynomials is called *p-convergence*.

Returning to the question of estimating the approximation error, we consider a 2*m*th-order differential equation in one dimension (*m* = 1, second-order equations; *m* = 2, fourth-order equations):

$$\sum_{i=1}^{m}(-1)^i \frac{d^i}{dx^i}\left(a_i \frac{d^i u}{dx^i}\right) = f \quad \text{for} \quad 0 < x < L \tag{3.6.7}$$

where the coefficients $a_1(x)$ and $a_2(x)$ are assumed to be positive. Suppose that the essential boundary conditions of the problem are

$$u(0) = u(L) = 0 \quad (m = 1, 2) \tag{3.6.8}$$

when *m* = 1 or 2 and

$$\left(\frac{du}{dx}\right)\Big|_{x=0} = \left(\frac{du}{dx}\right)\Big|_{x=L} = 0 \tag{3.6.9}$$

when *m* = 2. The variational (or weak) formulation of Eq. (3.6.7) is given by

$$0 = \int_0^L \left(\sum_{i=1}^{m} a_i \frac{d^i v}{dx^i}\frac{d^i u}{dx^i} - vf\right) dx \tag{3.6.10}$$

The quadratic functional corresponding to the variational form is

$$I(u) = \int_0^L \frac{1}{2}\left[\sum_{i=1}^{m} a_i \left(\frac{d^i u}{dx^i}\right)^2\right] dx - \int_0^L uf\, dx \tag{3.6.11}$$

Now consider a finite element discretization of the domain using *N* elements of equal length *h*. If u_h denotes the finite element solution in Eq. (3.6.1), we have, from Eq. (3.6.11),

$$I(u_h) = \int_0^L \frac{1}{2}\left[\sum_{i=1}^{m} a_i \left(\frac{d^i u_h}{dx^i}\right)^2\right] dx - \int_0^L u_h f\, dx \tag{3.6.12}$$

Next, we show that the energy *I* associated with the finite element solution approaches the true energy from above, and we then give an error estimate. We confine our discussion, for the sake of simplicity, to the second-order

equation ($m = 1$).

From Eqs. (3.6.11) and (3.6.12), and

$$f = -\frac{d}{dx}\left(a_1 \frac{du}{dx}\right)$$

we have

$$\begin{aligned} I(u_h) - I(u) &= \int_0^L \frac{1}{2}\left[a_1\left(\frac{du_h}{dx}\right)^2 - a_1\left(\frac{du}{dx}\right)^2 + 2f(u - u_h)\right] dx \\ &= \int_0^L \left[\frac{a_1}{2}\left(\frac{du_h}{dx}\right)^2 - \frac{a_1}{2}\left(\frac{du}{dx}\right)^2 - \frac{d}{dx}\left(a_1 \frac{du}{dx}\right)(u - u_h)\right] dx \\ &= \int_0^L \left\{\frac{a_1}{2}\left[\left(\frac{du_h}{dx}\right)^2 - \left(\frac{du}{dx}\right)^2\right] + a_1 \frac{du}{dx}\frac{d}{dx}(u - u_h)\right\} dx \\ &= \int_0^L \frac{a_1}{2}\left[\left(\frac{du_h}{dx}\right)^2 + \left(\frac{du}{dx}\right)^2 - 2\frac{du}{dx}\frac{du_h}{dx}\right] dx \\ &= \int_0^L \frac{a_1}{2}\left(\frac{du_h}{dx} - \frac{du}{dx}\right)^2 dx \geq 0 \end{aligned} \tag{3.6.13}$$

Thus, we have

$$I(u_h) \geq I(u) \tag{3.6.14}$$

The equality holds only for $u = u_h$. Equation (3.6.14) implies that the convergence of the energy of the finite element solution to the true energy is from above. Since the relation in Eq. (3.6.14) holds for any u_h, the inequality also indicates that the true solution u minimizes the energy. A similar relation can be established for the fourth-order equation ($m = 2$).

Now suppose that the finite element interpolation functions $\Phi_I (I = 1, 2, \ldots, M)$ are complete polynomials of degree k. Then the error in the energy norm can be shown to satisfy the inequality (see Reddy [2], p. 401)

$$\|e\|_m \equiv \|u - u_h\|_m \leq ch^p, \quad p = k + 1 - m > 0 \tag{3.6.15}$$

where c is a constant. This estimate implies that the error goes to zero as the pth power of h when h is decreased (or the number of elements is increased). In other words, the logarithm of the error in the energy norm versus the logarithm of h is a straight line whose slope is $k + 1 - m$. The

greater the degree of the interpolation functions, the more rapid the rate of convergence. Note also that the error in the energy goes to zero at the rate of $k + 1 - m$; the error in the L_2 norm will decrease even more rapidly, namely, at the rate of $k + 1$, i.e., derivatives converge more slowly than the solution itself.

Error estimates of the type in Eq. (3.6.15) are very useful because they give an idea of the accuracy of the approximate solution, whether or not we know the true solution. While the estimate gives an idea of how rapidly the finite element solution converges to the true solution, it does not tell us when to stop refining the mesh. This decision rests with the analysts, because only they know what a reasonable tolerance is for the problems they are solving.

As an example of estimating the error in the approximation, Eq. (3.6.15), we consider the linear (two-node) element for the finite element solution of a second-order equation ($m = 1$). For an element, we have

$$u_h = u_1(1 - s) + u_2 s \tag{3.6.16}$$

where $s = \bar{x}/h$ and $\bar{x}$ is the local coordinate. Since u_2 can be viewed as a function of u_1 via Eq. (3.6.16), one can expand u_2 in Taylor's series around the solution at node 1 to obtain

$$u_2 = u_1 + u_1' + \frac{1}{2}u_1'' + \cdots, \quad u' \equiv \frac{du}{ds} \tag{3.6.17}$$

Substituting this into (3.5.16), we obtain

$$u_h = u_1 + u_1' s + \frac{1}{2}u_1'' s + \cdots, \quad u'' \equiv \frac{d^2u}{ds^2} \tag{3.6.18}$$

Expanding the true solution in Taylor's series about the solution at node 1, we obtain

$$u = u_1 + u_1' s + \frac{1}{2}u_1'' s^2 + \cdots \tag{3.6.19}$$

Therefore, from Eqs. (3.6.18) and (3.6.19) we have the result:

$$|u_h - u| \le \frac{1}{2}(s - s^2) \max_{0 \le s \le 1} \left|\frac{d^2u_1}{ds^2}\right| = \tfrac{1}{2}(s - s^2)h^2 \max_{0 \le \bar{x} \le h} \left|\frac{d^2u}{d\bar{x}^2}\right| \tag{3.6.20}$$

$$\left|\frac{d}{d\bar{x}}(u_h - u)\right| \le \tfrac{1}{2}h \max_{0 \le \bar{x} \le h} \left|\frac{d^2u_1}{d\bar{x}^2}\right| \tag{3.6.21}$$

These equations lead to

$$\|u - u_h\|_0 \le c_1 h^2, \quad \|u - u_h\|_1 \le c_2 h \tag{3.6.22}$$

where the constants c_1 and c_2 depend only on the length L of the domain. The reader may carry out a similar error analysis for a fourth-order equation (which is the subject of Chapter 5).

Example 3.6.1

Consider the differential equation

$$-\frac{d^2u}{dx^2} = 2 \quad \text{for} \quad 0 < x < 1 \tag{1}$$

with

$$u(0) = u(1) = 0 \tag{2}$$

The exact solution is

$$u(x) = x(1 - x) \tag{3}$$

while the finite element solutions are, for $N = 2$,

$$u_h = \begin{cases} h^2(x/h) & \text{for } 0 \le x \le h \\ h^2(2 - x/h) & \text{for } h \le x \le 2h \end{cases} \tag{4}$$

for $N = 3$,

$$u_h = \begin{cases} 2h^2(x/h) & \text{for } 0 \le x \le h \\ 2h^2(2 - x/h) + 2h^2(x/h - 1) & \text{for } h \le x \le 2h \\ 2h^2(3 - x/h) & \text{for } 2h \le x \le 3h \end{cases} \tag{5}$$

and, for $N = 4$,

$$u_h = \begin{cases} 3h^2(x/h) & \text{for } 0 \le x \le h \\ 3h^2(2 - x/h) + 4h^2(x/h - 1) & \text{for } h \le x \le 2h \\ 4h^2(3 - x/h) + 3h^2(x/h - 2) & \text{for } 2h \le x \le 3h \\ 3h^2(4 - x/h) & \text{for } 3h \le x \le 4h \end{cases} \tag{6}$$

Verify the error estimates in Eq. (3.6.15) or (3.6.22).

Solution: For the two-element case ($h = 0.5$), the errors are given by

$$\| u - u_h \|_0^2 = \int_0^h (x - x^2 - hx)^2 dx + \int_h^{2h} (x - x^2 - 2h^2 + xh)^2 dx$$
$$= 0.002083$$
$$\left\| \frac{du}{dx} - \frac{du_h}{dx} \right\|_0^2 = \int_0^h (1 - 2x - h)^2 dx + \int_h^{2h} (1 - 2x + h)^2 dx \tag{7}$$
$$= 0.08333$$

Similar calculations can be performed for $N = 3$ and $N = 4$. The errors for $N = 2$, 3, and 4 are shown in Table 3.6.3.

Table 3.6.3 The L_2 and energy norms of the errors in the finite element solution of Eqs. (1) and (2) (**Example 3.6.1**).

h	$\log_{10} h$	$\|e\|_0$	$\log_{10} \|e\|_0$	$\|e\|_1$	$\log_{10} \|e\|_1$
$\frac{1}{2}$	−0.301	0.04564	−1.341	0.2887	−0.5396
$\frac{1}{3}$	−0.477	0.02028	−1.693	0.1925	−0.7157
$\frac{1}{4}$	−0.601	0.01141	−1.943	0.1443	−0.8406

Plots of $\|e\|_0$ and $\log\|e\|_1$ versus $\log h$ show that (see Fig. 3.6.2)

$$\log \|e\|_0 = 2 \log h + \log c_1, \quad \log \|e\|_1 = \log h + \log c_2 \tag{8}$$

In other words, the rate of convergence of the finite element solution is 2 in the L_2 norm and 1 in the energy norm, verifying the estimates in Eq. (3.6.22).

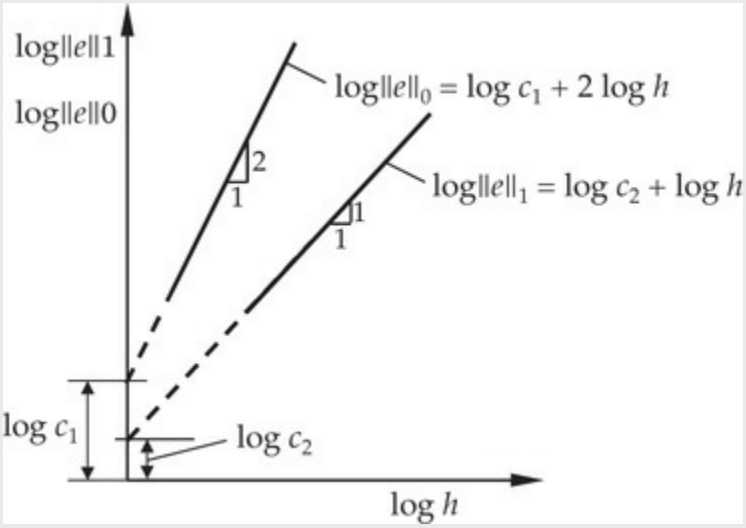

Fig. 3.6.2 Plots of the L_2 and energy norms of errors versus the mesh size. The log–log plots give the rates of convergence in the respective norms. The rates of convergence are given by the slopes of the lines (the plots shown are for linear elements).

As noted earlier, in the case of both second- and fourth-order equations in a single unknown [see Eq. (3.6.7)] and with constant coefficients ($a_1 = a$ and $a_2 = b$),

$$-\frac{d}{dx}\left(a\frac{du}{dx}\right) = f(x), \quad 0 < x < L \tag{3.6.23a}$$

$$-\frac{d^2}{dx^2}\left(b\frac{d^2u}{dx^2}\right) = f(x), \quad 0 < x < L \tag{3.6.23b}$$

the finite element solutions of the equations coincide with the exact solutions at the nodes. The proof is presented next for the second-order equation, Eq. (3.6.23a).

Consider Eq. (3.6.23a) with the boundary conditions

$$u(0) = 0 \quad u(L) = 0 \tag{3.6.24}$$

The global finite element solution is given by ($U_1 = U_N = 0$)

$$u_h = \sum_{I=2}^{N-1} U_I \Phi_I \tag{3.6.25}$$

where Φ_I are the linear global interpolation functions shown in Fig. 3.4.11. From the definition of the variational problem, we have

$$\int_0^L \left(\frac{du}{dx} - \frac{du_h}{dx} - \Phi_I \hat{f}\right) dx = 0 \quad \text{for each } I = 2, \ldots, N-1 \tag{3.6.26}$$

where $\hat{f} = f/a$. The exact solution also satisfies this equation. Hence, by subtracting the finite element equation (3.6.26) from the exact solution, we obtain

$$\int_0^L \left(\frac{du}{dx} - \frac{du_h}{dx}\right) \frac{d\Phi_I}{dx}\, dx = 0 \quad (I = 2, \ldots, N-1) \tag{3.6.27}$$

Since we have $\Phi_I = 0$ for $x \le (I+1)h$ and $x \ge (I-1)h$, and $d\Phi_I/dx = 1/h$ for $(I-1)h \le x \le Ih$ and $d\Phi_I/dx = -1/h$ for $Ih \le x \le (I+1)h$, it follows that

$$\int_{(I-1)h}^{Ih} \left(\frac{du}{dx} - \frac{du_h}{dx}\right)\frac{1}{h}dx + \int_{Ih}^{(I+1)h} \left(\frac{du}{dx} - \frac{du_h}{dx}\right)\left(-\frac{1}{h}\right)dx = 0 \qquad (3.6.28)$$

for $I = 2, 3, \ldots, N-1$. Denoting $\varepsilon(x) = u(x) - u_h(x)$, we have

$$\frac{1}{h}(\epsilon_I - \epsilon_{I-1}) + \left(-\frac{1}{h}\right)(\epsilon_{I+1} - \epsilon_I) = 0 \qquad (3.6.29)$$

or

$$\frac{1}{h}(-\epsilon_{I-1} + 2\epsilon_I - \epsilon_{I+1}) = 0 \quad (I = 2, 3, \ldots, N-1) \qquad (3.6.30)$$

where $\varepsilon_I = \varepsilon(Ih)$ (i.e., the value of ε at $x = Ih$). Since $\varepsilon_0 = \varepsilon_N = 0$ (because both u and u_h satisfy the essential boundary conditions), it follows from the above homogeneous equations that the solution is trivial: $\varepsilon_1 = \varepsilon_2 = \ldots = \varepsilon_{N-1} = 0$. Thus the finite element solution coincides with the exact solution at the nodes.

3.7 Summary

In this chapter a direct approach is used to develop finite element models of discrete systems, followed by a systematic study of the steps involved in the finite element formulation of a representative second-order differential equation in a single variable. For discrete systems, such as a network of springs or electrical circuits, no differential equations exist and, therefore, the direct approach based on laws of physics is convenient to develop finite element models. The direct approach for discrete systems is simple for the reader to get familiar with the idea of the derivation of the element equations, assembly of element equations, imposition of boundary conditions, and solution of equations for the nodal values of the primary and secondary variables. However, the direct approach cannot be used to derive higher-order finite element models where higher-order approximations of the field variables are desired.

The differential equation approach to the finite element method, which can be used for all continuum problems described by differential

equations, is described with the help of a model equation (including the axisymmetric case) that is representative of equations arising in various fields of engineering, as summarized in Table 3.4.1. The basic steps, as outlined in Table 3.2.1, of developing the weak form of the equation over an element, identification of primary and secondary variables, derivation of approximation functions, finite element model development, assembly of element equations to obtain global equations are presented in detail. Several numerical examples of typical field problems are presented to illustrate the steps in the finite element analysis of second-order differential equations. Additional examples from heat transfer, fluid mechanics, and solid mechanics are presented in Chapter 4.

A brief discussion of the errors introduced in finite element analysis is presented and illustrated through a numerical example. It was also established that for differential equations with constant coefficients [for arbitrary $f(x)$], the finite element solution coincides with the exact solution at the nodes. For additional information on error estimation, see [3, 7].

Table 3.7.1 contains a summary of 1-D linear and quadratic interpolation functions, their derivatives, and the numerical values of various integral expressions.

Table 3.7.1 Summary of one-dimensional approximation functions and their integrals.

Expression	Linear	Quadratic
ψ_i	$\psi_1(s) = 1 - \frac{s}{h},\ \psi_2(s) = \frac{s}{h}$	$\psi_1(s) = (1 - \frac{s}{h})(1 - 2\frac{s}{h})$ $\psi_2(s) = 4\frac{s}{h}(1 - \frac{s}{h})$ $\psi_3(s) = -\frac{s}{h}(1 - 2\frac{s}{h})$
$\frac{d\psi_i}{ds}$	$\frac{d\psi_1}{ds} = -\frac{1}{h},\ \frac{d\psi_2}{ds} = \frac{1}{h}$	$\frac{d\psi_1}{ds} = \frac{1}{h}(-3 + 4\frac{s}{h})$ $\frac{d\psi_2}{ds} = \frac{4}{h}(1 - 2\frac{s}{h})$ $\frac{d\psi_3}{ds} = -\frac{1}{h}(1 - 4\frac{s}{h})$
$\left\{\int_0^h \psi_i(s)\,ds\right\}$	$\frac{h}{2}\begin{Bmatrix} 1 \\ 1 \end{Bmatrix}$	$\frac{h}{6}\begin{Bmatrix} 1 \\ 4 \\ 1 \end{Bmatrix}$
$\left\{\int_0^h s\psi_i(s)\,ds\right\}$	$\frac{h^2}{6}\begin{Bmatrix} 1 \\ 2 \end{Bmatrix}$	$\frac{h^2}{6}\begin{Bmatrix} 0 \\ 2 \\ 1 \end{Bmatrix}$
$\left\{\int_0^h \frac{d\psi_i}{ds}\,ds\right\}$	$\begin{Bmatrix} -1 \\ 1 \end{Bmatrix}$	$\begin{Bmatrix} -1 \\ 0 \\ 1 \end{Bmatrix}$
$\left\{\int_0^h s\frac{d\psi_i}{ds}\,ds\right\}$	$\frac{h}{2}\begin{Bmatrix} -1 \\ 1 \end{Bmatrix}$	$\frac{h}{6}\begin{Bmatrix} -1 \\ -4 \\ 5 \end{Bmatrix}$
$\left[\int_0^h \psi_i(s)\psi_j(s)\,ds\right]$	$\frac{h}{6}\begin{bmatrix} 2 & 1 \\ 1 & 2 \end{bmatrix}$	$\frac{h}{30}\begin{bmatrix} 4 & 2 & -1 \\ 2 & 16 & 2 \\ -1 & 2 & 4 \end{bmatrix}$
$\left[\int_0^h s\psi_i(s)\psi_j(s)\,ds\right]$	$\frac{h^2}{12}\begin{bmatrix} 1 & 1 \\ 1 & 3 \end{bmatrix}$	$\frac{h^2}{60}\begin{bmatrix} 1 & 0 & -1 \\ 0 & 16 & 4 \\ -1 & 4 & 7 \end{bmatrix}$
$\left[\int_0^h \frac{d\psi_i}{ds}\frac{d\psi_j}{ds}\,ds\right]$	$\frac{1}{h}\begin{bmatrix} 1 & -1 \\ -1 & 1 \end{bmatrix}$	$\frac{1}{3h}\begin{bmatrix} 7 & -8 & 1 \\ -8 & 16 & -8 \\ 1 & -8 & 7 \end{bmatrix}$
$\left[\int_0^h s\frac{d\psi_i}{ds}\frac{d\psi_j}{ds}\,ds\right]$	$\frac{1}{2}\begin{bmatrix} 1 & -1 \\ -1 & 1 \end{bmatrix}$	$\frac{1}{6}\begin{bmatrix} 3 & -4 & 1 \\ -4 & 16 & -12 \\ 1 & -12 & 11 \end{bmatrix}$
$\left[\int_0^h \psi_i\frac{d\psi_j}{ds}\,ds\right]$	$\frac{1}{2}\begin{bmatrix} -1 & 1 \\ -1 & 1 \end{bmatrix}$	$\frac{1}{6}\begin{bmatrix} -3 & 4 & -1 \\ -4 & 0 & 4 \\ 1 & -4 & 3 \end{bmatrix}$

Problems

DISCRETE ELEMENTS

3.1 Consider the system of linear elastic springs shown in Fig. P3.1. Assemble the element equations to obtain the force-displacement relations for the entire system. Use the boundary conditions to write the condensed equations for the unknown displacements and forces.

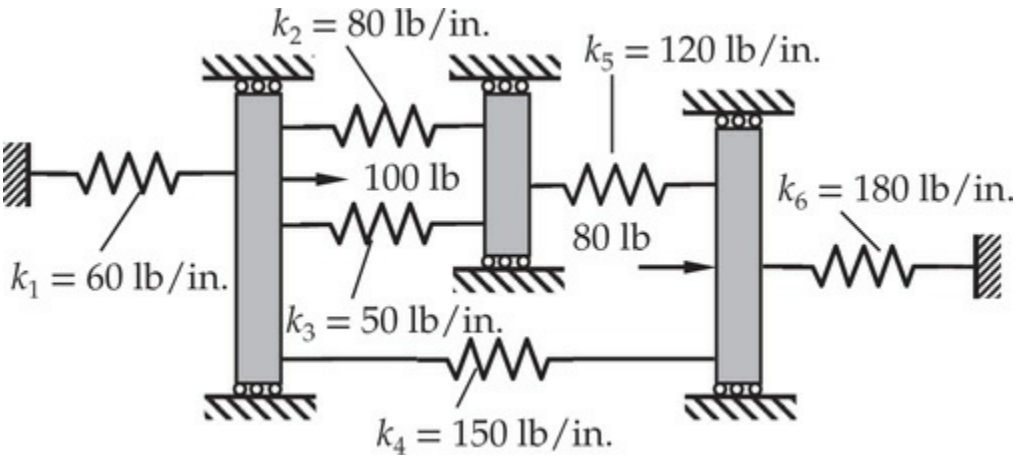

Fig. P3.1

3.2 Repeat **Problem 3.1** for the system of linear springs shown in Fig. P3.2.

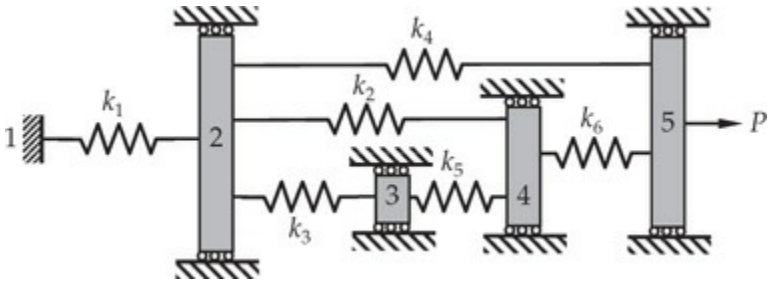

Fig. P3.2

3.3 Find the stresses and compressions in each section of the composite member shown in Fig. P3.3. Use $E_s = 30 \times 10^6$ psi, $E_a = 10^7$ psi, and the minimum number of bar elements.

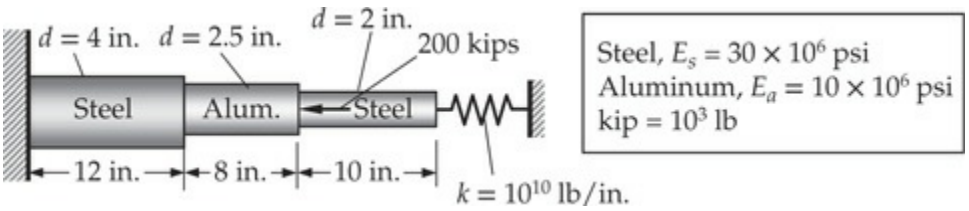

Fig. P3.3

3.4 Determine the maximum shear stresses in the solid steel (G_s = 12 msi) and aluminum (G_a = 4 msi) shafts shown in Fig. P3.4.

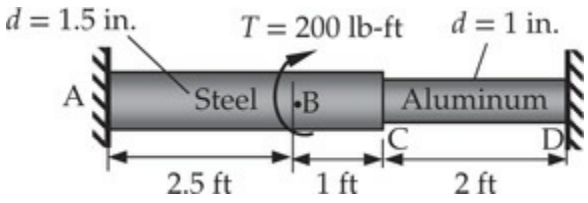

Fig. P3.4

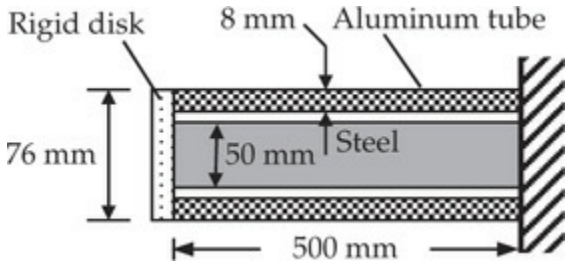

Fig. P3.5

3.5 A steel shaft and an aluminum tube are connected to a fixed support and to a rigid disk, as shown in Fig. P3.5. If the torque applied at the end is equal to T = 6,325 N · m, determine the shear stresses in the steel shaft and aluminum tube. Use G_s = 77 GPa and G_a = 27 GPa.

3.6 Consider the direct current electric network shown in Fig. P3.6. We wish to determine the voltages V and currents I in the network using the finite element method. Set up the algebraic equations (i.e., condensed equations) for the unknown voltages and currents.

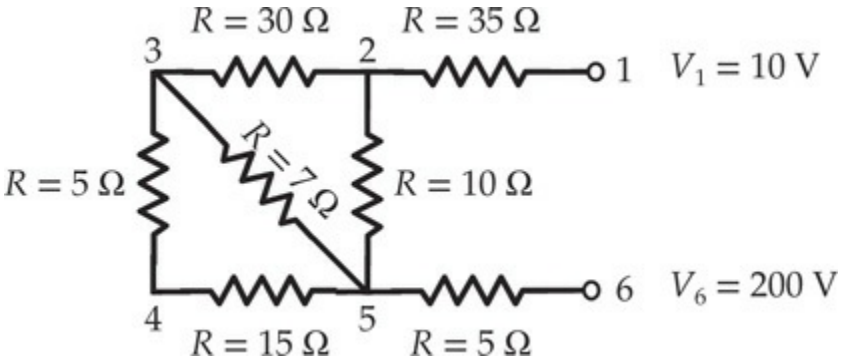

Fig. P3.6

3.7 Repeat **Problem 3.6** for the direct current electric network shown in Fig. P3.7.

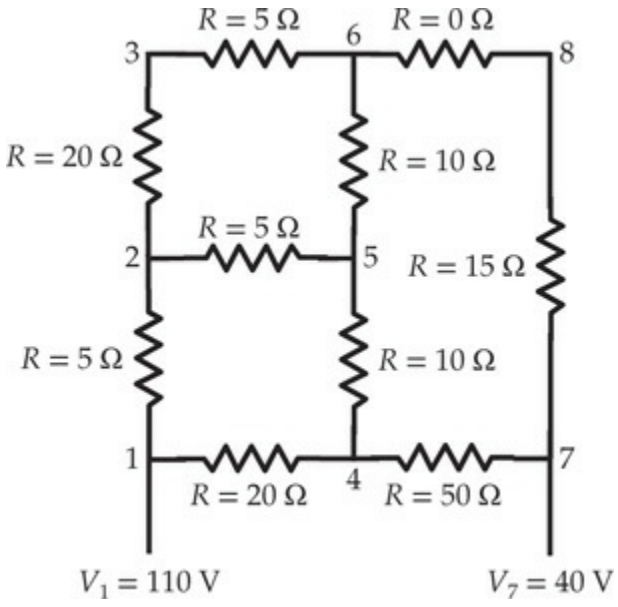

Fig. P3.7

3.8 Write the condensed equations for the unknown pressures and flows (use the minimum number of elements) for the hydraulic pipe network shown in Fig. P3.8. *Answer:* $P_1 = \frac{39}{14}Qa$, $P_2 = \frac{12}{7}Qa$, and $P_3 = \frac{15}{14}Qa$.

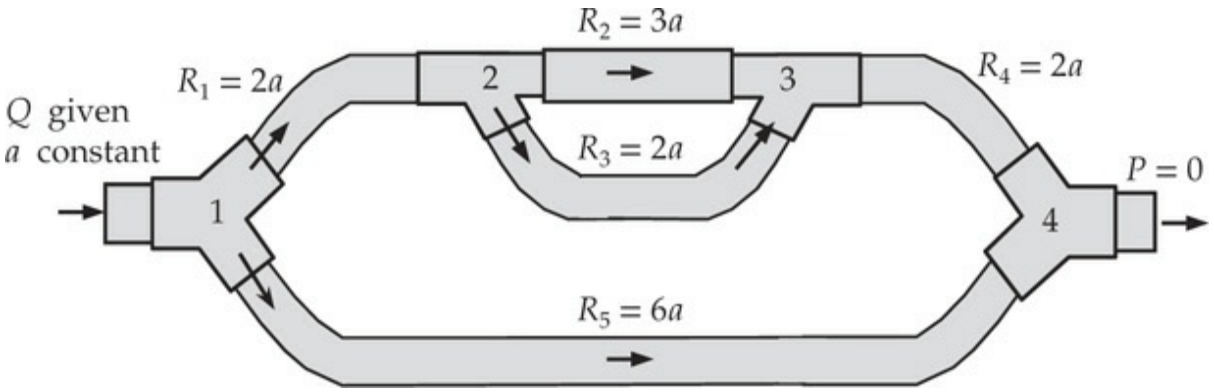

Fig. P3.8

3.9 Consider the hydraulic pipe network (the flow is assumed to be laminar) shown in Fig. P3.9. Write the condensed equations for the unknown pressures and flows.

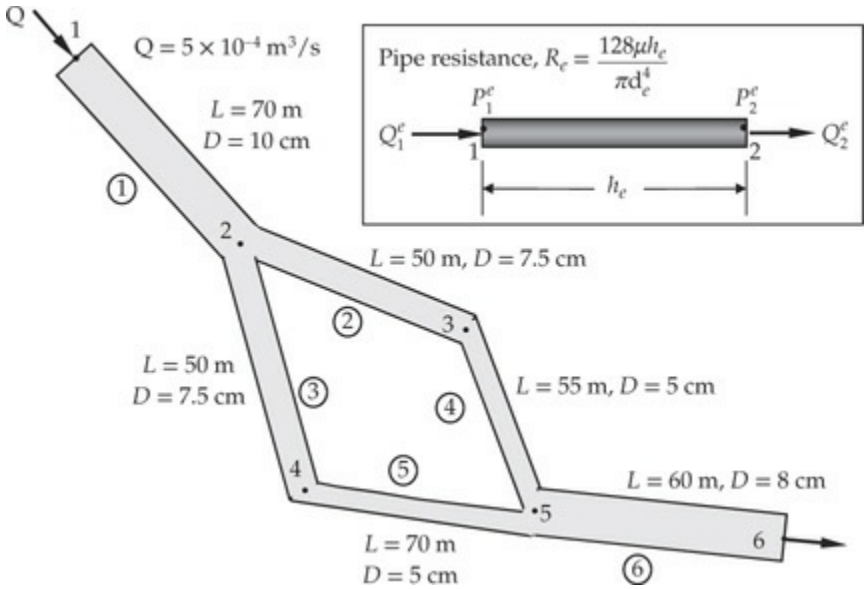

Fig. P3.9

3.10 Find the heat transfer per unit area through the composite wall shown in Fig. P3.10. Assume one-dimensional heat flow and that the walls are at the temperatures of the moving fluid.

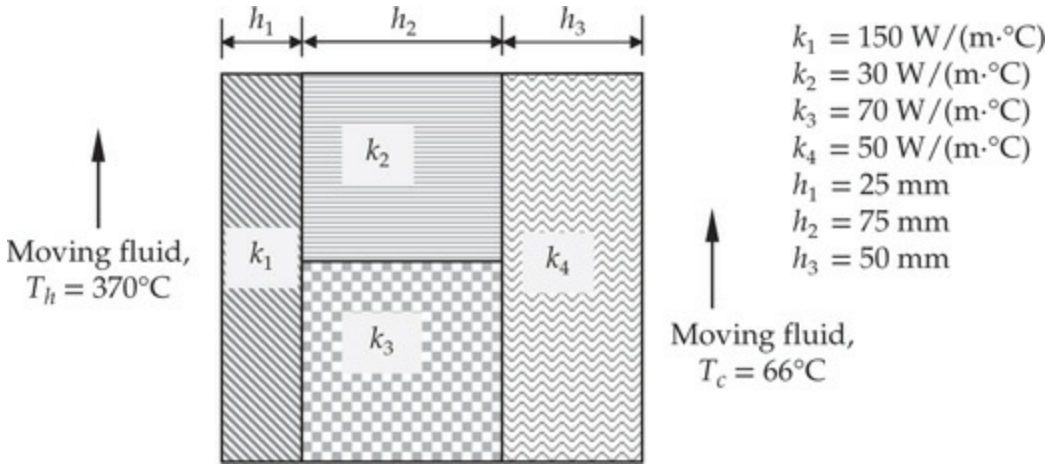

Fig. P3.10

CONTINUUM ELEMENTS

For **Problems 3.11–3.15**, carry out the following tasks:

(a) Develop the *weak forms* of the given differential equation(s) over a typical finite element Ω^e, which is a geometric subdomain located between $x = x_a$ and $x = x_b$. Note that there are no "specified" boundary conditions at the element level. Therefore, in going from step 2 to step 3 of the weak-form development, one must identify the secondary variable(s) at the two ends of the domain using some symbols like Q_1^e and Q_2^e and complete the weak form. Stopping with step 2 of the weak-form development is considered incomplete; see Example 2.4.3 for additional help.

(b) Assume an approximation(s) of the form

$$u(x) = \sum_{j=1}^{n} u_j^e \psi_j^e(x) \tag{1}$$

for each primary variable of the formulation, where $\psi_j^e(x)$ are the interpolation functions and u_j^e are the values of the primary variable(s) at the jth node of the element. Substitute the expression(s) in Eq. (1) for each primary variable and ψ_i^e for the corresponding weight function into the weak form(s) and derive the finite element model. Be sure to define, in algebraic form (no numerical values are being asked), all coefficients of the model in terms of the problem data and ψ_i^e. Note that when more than one differential equation is given, you must develop weak forms of all equations, assuming different weight function for each equation.

3.11 Develop the weak form and the finite element model of the following differential equation over an element:

$$-\frac{d}{dx}\left(a\frac{du}{dx}\right)+\frac{d^2}{dx^2}\left(b\frac{d^2u}{dx^2}\right)+cu=f \quad \text{for} \quad x_a<x<x_b$$

where a, b, c, and f are known functions of position x. Ensure that the element coefficient matrix $\mathbf{K}^e$ is symmetric. Discuss the nature (i.e., Lagrange type or Hermite type) of the admissible approximation functions for the development of the finite element model.

3.12 Construct the weak form and the finite element model of the differential equation

$$-\frac{d}{dx}\left(a\frac{du}{dx}\right)-b\frac{du}{dx}=f \quad \text{for} \quad 0<x<L$$

over a typical element $\Omega^e = (x_a, x_b)$. Here a, b, and f are known functions of x, and u is the dependent variable. The natural boundary condition should *not* involve the function $b(x)$. What type of interpolation functions may be used for u?

3.13 Consider the differential equation

$$-\frac{1}{r}\frac{d}{dr}\left(r\mu\frac{dv}{dr}\right)=f_0, \quad 0<r<R$$

where r is the radial coordinate, $v = v(r)$, and μ and f_0 are constants. Develop the weak form of the equation over an element $\Omega^e = (r_a, r_b)$ and derive the finite element model. Identify the explicit form of the element matrices for the linear and quadratic elements.

3.14 Develop the weak forms (only) of the following pair of coupled second-order differential equations over a typical element $\Omega^e = (x_a, x_b)$:

$$-\frac{d}{dx}\left[a(x)\left(u+\frac{dv}{dx}\right)\right]=f(x)$$

$$-\frac{d}{dx}\left(b(x)\frac{du}{dx}\right)+a(x)\left(u+\frac{dv}{dx}\right)=q(x)$$

where u and v are the dependent variables, a, b, f, and q are known functions of x. Also identify the primary and secondary variables of

the formulation.

3.15 Consider the second-order differential equation

$$-\frac{d}{dx}\left(\mu\frac{du}{dx}\right)=f(x), \qquad \mu=\mu_0\left(\frac{du}{dx}\right)^{n-1}$$

where $u(x)$ is the dependent unknown, $f(x)$ is a known function of position x, and μ is a function of the dependent variable u, as given in Eq. (1). Develop the weak form of the equation over a typical element $\Omega^e = (x_a, x_b)$. Attempt to derive the finite element model based on the weak form developed.

3.16 Consider the following differential equations governing bending of a beam using the Euler–Bernoulli beam theory:

$$-\frac{d^2w}{dx^2}-\frac{M}{EI}=0, \qquad -\frac{d^2M}{dx^2}+kw=q$$

where w denotes the transverse deflection, M the bending moment, q the distributed transverse load, and k the elastic foundation modulus. Develop the weak forms of the above pair of coupled second-order differential equations over a typical element (x_a, x_b). Also identify the primary and secondary variables of the formulation. *Caution:* Do not eliminate M from the equations; treat both w and M as independent unknowns; use a different weight function for different equation (e.g., v_1 for the first equation and v_2 for the second equation).

3.17 Consider the following weak forms of a pair of coupled differential equations:

$$0=\int_{x_a}^{x_b}\left(\frac{dw_1}{dx}\frac{dv}{dx}-w_1 f\right)dx-P_a w_1(x_a)-P_b w_1(x_b)$$

$$0=\int_{x_a}^{x_b}\left(\frac{dw_2}{dx}\frac{du}{dx}+c\,w_2 v-w_2 q\right)dx-Q_a w_2(x_a)-Q_b w_2(x_b)$$

where $c(x)$ is a known function, w_1 and w_2 are weight functions, u and v are dependent variables (primary variables), and P_a, P_b, Q_a, and Q_b are the secondary variables (at x_a and x_b) of the formulation. Use the finite element approximations of the form

$$u(x) = \sum_{j=1}^{m} u_j^e \psi_j^e(x)\,, \quad v(x) = \sum_{j=1}^{n} v_j^e \varphi_j^e(x)$$

and $w_1 = \psi_i$ and $w_2 = \varphi_i$ and derive the finite element equations from the weak forms. The finite element equations should be in the form

$$0 = \sum_{j=1}^{m} K_{ij}^{11} u_j^e + \sum_{j=1}^{n} K_{ij}^{12} v_j^e - F_i^1$$

$$0 = \sum_{j=1}^{m} K_{ij}^{21} u_j^e + \sum_{j=1}^{n} K_{ij}^{22} v_j^e - F_i^2$$

Define the coefficients K_{ij}^{11}, K_{ij}^{12}, K_{ij}^{21}, K_{ij}^{22}, F_i^1, and F_i^2 in terms of the interpolation functions, known data, and secondary variables.

3.18 Develop the weighted-residual finite element model (*not* weak-form finite element model) of the following pair of equations:

$$-\frac{d^2w}{dx^2} - \frac{M}{EI} = 0, \qquad -\frac{d^2M}{dx^2} + kw = q$$

Assume the following approximations of the form

$$w(x) \approx \sum_{i=1}^{m} \Delta_i \varphi_i^{(1)}(x), \quad M(x) \approx \sum_{i=1}^{n} \Lambda_i \varphi_i^{(2)}(x)$$

The finite element equations should be in the form

$$0 = \sum_{j=1}^{m} K_{ij}^{11} \Delta_j^e + \sum_{j=1}^{n} K_{ij}^{12} \Lambda_j^e - F_i^1$$

$$0 = \sum_{j=1}^{m} K_{ij}^{21} \Delta_j^e + \sum_{j=1}^{n} K_{ij}^{22} \Lambda_j^e - F_i^2$$

(a) Define the coefficients K_{ij}^{11}, K_{ij}^{12}, K_{ij}^{21}, K_{ij}^{22}, F_i^1, and F_i^2 in terms of the interpolation functions, known data, and secondary variables, and (b) comment on the choice of the interpolation functions (what type, Lagrange or Hermite, and why).

3.19 Derive the Lagrange cubic interpolation functions for a four-node (one-dimensional) element with equally spaced nodes using the alternative procedure based on interpolation properties in Eq. (3.4.19). Use the local coordinate x, with the origin at node 1, for simplicity.

3.20 Suppose that the *1-D Lagrange cubic element with equally spaced*

nodes has a source of $f(\bar{x}) = f_0\bar{x}/h$, where $\bar{x}$ is the local coordinate with origin at node 1. Compute its contribution to node 2.

3.21 Numerically evaluate the element matrices $\mathbf{K}^{11}$, $\mathbf{K}^{12}$, and $\mathbf{K}^{22}$ for the linear interpolation of $u(x)$ and $v(x)$ in **Problem 3.17**.

3.22 Evaluate the following coefficient matrices and source vector using the linear Lagrange interpolation functions:

$$K_{ij}^e = \int_{x_a}^{x_b} (a_0^e + a_1^e x)\frac{d\psi_i^e}{dx}\frac{d\psi_j^e}{dx}dx, \quad M_{ij}^e = \int_{x_a}^{x_b} (c_0^e + c_1^e x)\psi_i^e\psi_j^e dx$$

$$f_i^e = \int_{x_a}^{x_b} (f_0^e + f_1^e x)\psi_i^e dx$$

where a_0^e, a_1^e, c_0^e, c_1^e, f_0^e, and f_1^e are constants.

3.23 Consider the following differential equation and boundary conditions:

$$-\frac{d^2\theta}{dx^2} + c\theta = 0, \quad 0 < x < L$$

$$\theta(0) = \theta_0, \quad \left[k\frac{d\theta}{dx} + \beta\theta\right]_{x=L} = 0$$

where k and β are constants. For a mesh of two linear elements (of equal length), give (a) the boundary conditions on the nodal variables (primary as well as secondary variables) and (b) the final condensed finite element equations for the unknowns (both primary and secondary nodal variables). Use the following data: $\theta_0 = 100$, $L = 0.25$, $c = 256$, $\beta = 64$, and $k = 50$.

3.24 Solve the differential equation in **Example 3.4.1** for the mixed boundary conditions

$$u(0) = 0, \quad \left(\frac{du}{dx}\right)\Big|_{x=1} = 1$$

Use the uniform mesh of three linear elements. The exact solution is

$$u(x) = \frac{2\cos(1-x) - \sin x}{\cos(1)} + x^2 - 2$$

Answer: $U_2 = 0.4134$, $U_3 = 0.7958$, $U_4 = 1.1420$, $(Q_1^1)_{\text{def}} = -1.2402$.

3.25 Solve the differential equation in **Example 3.4.1** for the *natural* (or Neumann) boundary conditions

$$\left(\frac{du}{dx}\right)\Big|_{x=0} = 1, \quad \left(\frac{du}{dx}\right)\Big|_{x=1} = 0$$

Use the uniform mesh of three linear finite elements to solve the problem. Verify your solution with the analytical solution

$$u(x) = \frac{\cos(1-x) + 2\cos x}{\sin(1)} + x^2 - 2$$

Answer: $U_1 = 1.0280$, $U_2 = 1.3002$, $U_4 = 1.4447$, $U_5 = 1.4821$.

3.26 Solve the problem described by the following equations:

$$-\frac{d^2u}{dx^2} = \cos \pi x, \quad 0 < x < 1; \quad u(0) = 0, \quad u(1) = 0$$

Use the uniform mesh of three linear elements to solve the problem and compare against the exact solution

$$u(x) = \frac{1}{\pi^2}(\cos \pi x + 2x - 1)$$

3.27 Solve the differential equation in **Problem 3.26** using the mixed boundary conditions

$$u(0) = 0, \quad \left(\frac{du}{dx}\right)\Big|_{x=1} = 0$$

Use the uniform mesh of three linear elements to solve the problem and compare against the exact solution

$$u(x) = \frac{1}{\pi^2}(\cos \pi x - 1)$$

3.28 Solve the differential equation in **Problem 3.26** using the Neumann boundary conditions

$$\left(\frac{du}{dx}\right)\Big|_{x=0} = 0, \quad \left(\frac{du}{dx}\right)\Big|_{x=1} = 0$$

Use the uniform mesh of three linear elements to solve the problem and compare against the exact solution

$$u(x) = \frac{\cos \pi x}{\pi^2}$$

Note: For Neumann boundary conditions, none of the primary

dependent variables are specified, and therefore the solution can be determined within an arbitrary constant for this equation (i.e., the coefficient matrix is singular and cannot be inverted). In such cases, one of the U_i should be set equal to a constant to remove the "rigid-body" mode (i.e., to determine the arbitrary constant in the solution).

3.29 Consider a uniaxial bar element of length h, constant area of cross section A, and constant Young's modulus E. Suppose that the axial displacement $u(x)$ is expressed in terms of the displacements u_1, u_2, and u_3 at three equally spaced nodes (see Fig. 3.4.7; element label "e" is omitted here and the x coordinate has the origin at node 1):

$$u(x) = \left(1 - \frac{x}{h}\right)\left(1 - \frac{2x}{h}\right)u_1 + 4\frac{x}{h}\left(1 - \frac{x}{h}\right)u_2 - \frac{x}{h}\left(1 - \frac{2x}{h}\right)u_3 \qquad (1)$$

Determine the strain energy in terms of the displacements u_1, u_2, and u_3 and then derive the force-displacement relationships using Castigliano's theorem I. Note that the axial strain in the bar is given by

$$\varepsilon = \frac{du}{dx} = \frac{1}{h}\left(-3 + 4\frac{x}{h}\right)u_1 + \frac{4}{h}\left(1 - 2\frac{x}{h}\right)u_2 - \frac{1}{h}\left(1 - 4\frac{x}{h}\right)u_3 \qquad (2)$$

Follow the steps in **Examples 2.3.1** and **2.3.7** to obtain the required answer.

References for Additional Reading

1. J. N. Reddy, *Principles of Continuum Mechanics*, 2nd ed., Cambridge University Press, New York, NY, 2013.
2. J. N. Reddy, *Applied Functional Analysis and Variational Methods in Engineering* McGraw-Hill, New York, NY, 1986; Krieger, Melbourne, FL, 1991.
3. K. S. Surana and J. N. Reddy, *The Finite Element Method for Boundary Value Problems, Mathematics and Computations*, CRC Press, Boca Raton, FL, 2017.
4. J. N. Reddy, *An Introduction to Continuum Mechanics*, 2nd ed., Cambridge University Press, New York, NY, 2013.

5. G. Karner, and K. Perktold, “Effect of endothelial injury and increased blood pressure on albumin accumulation in the arterial wall: a numerical study,” *Journal of Biomechanics*, **22**, 709–715, 2000.
6. L. Ai and K. Vafai, “A coupling model for macromolecule transport in a stenosed arterial wall,” *International Journal of Heat and Mass Transfer*, **49**, 1568–1591, 2006.
7. K. S. Surana and J. N. Reddy, *The Finite Element Method for Initial Value Problems, Mathematics and Computations*, CRC Press, Boca Raton, FL, 2018.
8. J. N. Reddy, *Energy Principles and Variational Methods in Applied Mechanics*, 3rd ed., John Wiley & Sons, New York, NY, 2017.
9. J. N. Reddy and M. L. Rasmussen, *Advanced Engineering Analysis*, John Wiley & Sons, New York, NY, 1982; Krieger, Melbourne, FL, 1990.
10. S. G. Mikhlin, *Variational Methods in Mathematical Physics*, Pergamon Press, New York, NY, 1964.
11. S. G. Mikhlin, *The Numerical Performance of Variational Methods*, Wolters-Noordhoff, Groningen, The Netherlands, 1971.
12. J. T. Oden and J. N. Reddy, *Variational Methods in Theoretical Mechanics*, Springer-Verlag, New York, NY, 1976; 2nd ed., 1983.
13. J. N. Reddy, *An Introduction to Nonlinear Finite Element Analysis*, 2nd ed., Oxford University Press, Oxford, UK, 2015.
14. K. Rektorys, *Variational Methods in Mathematics, Science and Engineering*, Reidel, Boston, MA, 1977.

---

[1] This phrase should not be confused with the same phrase used by most authors to mean the *weak-form Galerkin finite element model*, which is reserved for that based on Eq. (3.4.7).

4 Applications to 1-D Heat Transfer and Fluid and Solid Mechanics Problems

An ounce of practice is worth more than tons of preaching (or theory).
— Mahatma Gandhi

4.1 Preliminary Comments

The objective of this chapter is to present applications of the finite element models developed in Chapter 3 to continuum problems from various fields of engineering. We will consider several examples to illustrate the steps involved in the finite element analysis of second-order differential equations arising in one-dimensional problems of heat transfer, fluid mechanics, and solid mechanics. The examples presented here make use of the element equations already developed in Chapter 3. While the notation used for the dependent variables, independent coordinates, and data of problems vary from field to field, the reader should keep the common mathematical structure in mind and not get confused with the change of notation from one problem to another.

4.2 Heat Transfer

4.2.1 Governing Equations

The equations governing three-dimensional heat transfer were reviewed in Eqs. (2.6.1)–(2.6.5), and the derivation of one-dimensional heat transfer was presented in **Example 1.2.2**. The finite element model was developed in Chapter 3. Here we briefly review the pertinent equations of one-dimensional heat transfer for our use (see [1–4] for additional details). Equations to be reviewed here are one-dimensional analogues of those listed in Eqs. (2.6.2) and (2.6.3), except for the addition of cross-sectional

area A of the system.

The Fourier heat conduction law for one-dimensional systems states that the heat flow $q(x)$ (W/m^2) is related to the temperature gradient $\partial T/\partial x$ by (with heat flow in the positive direction of x),

$$q = -k\frac{\partial T}{\partial x} \tag{4.2.1}$$

where k is the thermal conductivity of the material [W/(m · °C)] and T the temperature (°C). The negative sign in Eq. (4.2.1) indicates that heat flows downhill (i.e., from high to low) on the temperature scale. The balance of energy requires that

$$\rho cA\frac{\partial T}{\partial t} - \frac{\partial}{\partial x}\left(kA\frac{\partial T}{\partial x}\right) = Ag \tag{4.2.2}$$

where A is the cross-sectional area (m^2), g is the internal heat energy generated per unit volume (the unit of Ag is W/m), ρ is the mass density (kg/m^3), c is the specific heat of the material [J/(kg · °C)], and t is time (s). Equation (4.2.2) governs the transient heat conduction in a slab or fin (i.e., a one-dimensional system). For plane wall, we take A = 1.

In the case of radially symmetric problems with cylindrical geometries, Eq. (4.2.2) takes a different form, as already discussed in Section 3.5. Consider a long cylinder of inner radius R_i, outer radius R_o, length L, and made of isotropic material. When L is very large compared with the diameter and the boundary conditions are also axisymmetric, heat flows in the radial direction r only. The transient radially symmetric heat flow in a cylinder is governed by

$$\rho c\frac{\partial T}{\partial t} - \frac{1}{r}\frac{\partial}{\partial r}\left(kr\frac{\partial T}{\partial r}\right) = g \tag{4.2.3}$$

A cylindrical fuel element of a nuclear reactor, a current-carrying electrical wire, and a thick-walled circular tube (all are assumed to be long compared to their cross-sectional dimensions) provide examples of one-dimensional radial systems.

The boundary conditions for heat conduction involve specifying either temperature T or the heat flow Q at a point

$$T = T_0 \quad \text{or} \quad Q \equiv -kA\frac{\partial T}{\partial x} = Q_0 \tag{4.2.4}$$

It is known that when a heated surface is exposed to a cooling medium, such as air or liquid, the surface will cool faster. We say that the heat is convected away. The *convection heat transfer* between the surface and the medium in contact is governed by *Newton's law of cooling*:

$$Q = \beta A(T_s - T_\infty) \tag{4.2.5}$$

where T_s is the surface temperature, T_∞ is the temperature of the surrounding medium, called the *ambient temperature*; and β is the *convection heat transfer coefficient* or *film coefficient* [W/(m^2 · °C)]). The heat flow due to conduction and convection at a boundary point must be in balance with the applied flow Q_0:

$$n_x kA\frac{\partial T}{\partial x} + \beta A(T - T_\infty) + Q_0 = 0 \tag{4.2.6}$$

where n_x denotes the direction of the normal to the end surface and it takes the value $n_x = -1$ when the heat flow is from the fluid at T_∞ to the surface at the left end of the element, and $n_x = +1$ when the heat flow is from the fluid at T_∞ to the surface at the right end.

Convection of heat from a surface to the surrounding fluid can be increased by attaching thin strips of conducting metal to the surface. The metal strips are called *fins*. For a fin with heat flow along its length, heat can convect across the lateral surface of the fin [see Fig. 4.2.1(a)]. To account for the convection of heat through the surface, we must add the rate of heat loss by convection to the left-hand side of Eq. (4.2.2) [cf. Eq. (1.2.13)]:

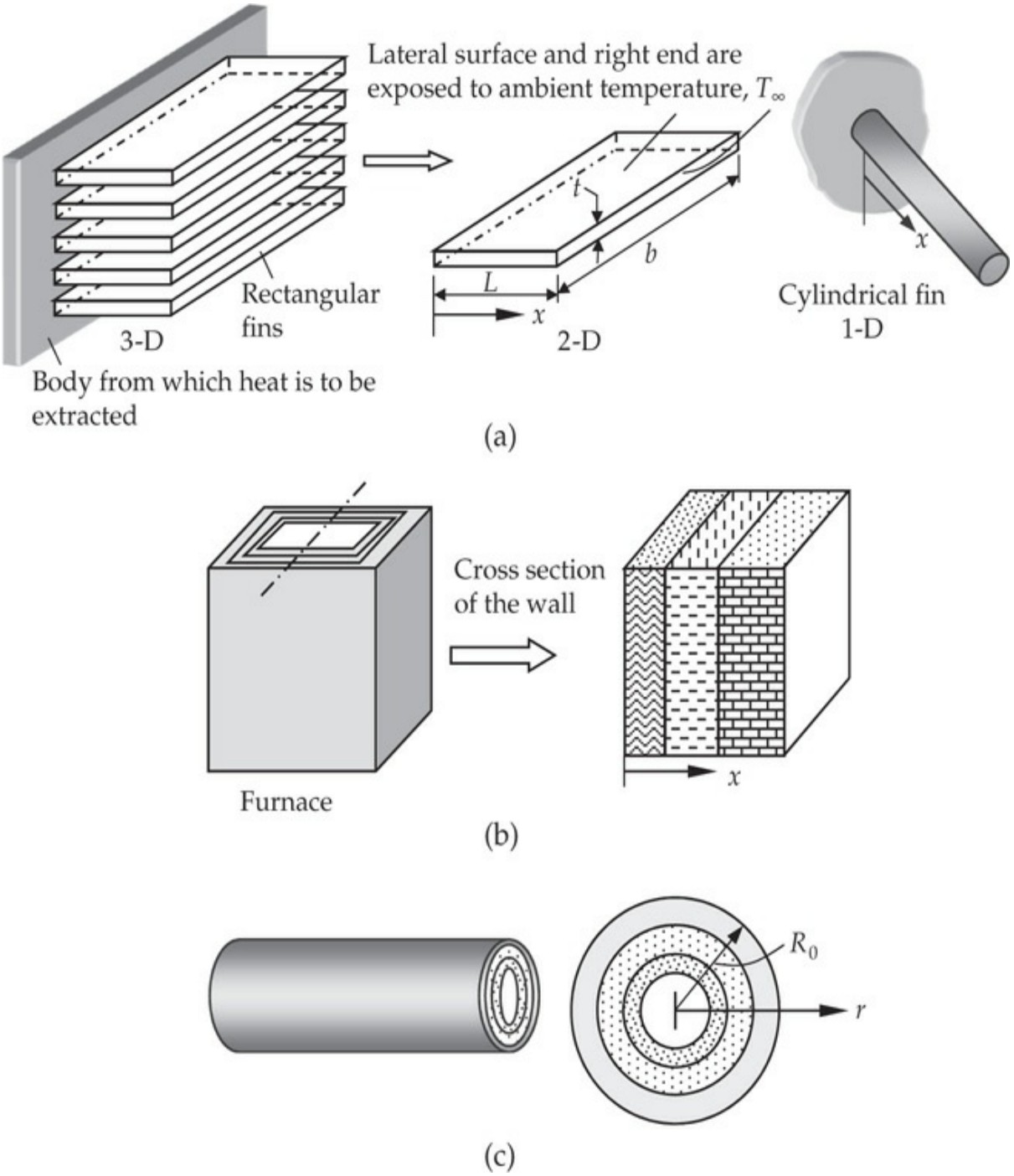

Fig. 4.2.1 Heat transfer in (a) fins, (b) plane wall, and (c) radially symmetric system.

$$\rho cA\frac{\partial T}{\partial t} - \frac{\partial}{\partial x}\left(kA\frac{\partial T}{\partial x}\right) + P\beta(T - T_\infty) = Ag \tag{4.2.7}$$

where P is the perimeter and β is the film coefficient. For the steady-state case, Eq. (4.2.7) reduces to

$$-\frac{d}{dx}\left(kA\frac{dT}{dx}\right)+P\beta T=Ag+P\beta T_\infty \tag{4.2.8}$$

The units of various quantities (in the metric system) are summarized here [1–5]:

T	°C (celsius)	k	W/(m·°C)	g	W/m^3
ρ	kg/m^3	c	J/(kg·°C)	β	$W/(m^2\cdot°C)$

The steady-state equations for various one-dimensional systems are summarized below [see Fig. 4.2.1; see Eqs. (1.2.14) and (1.2.17)].

Bar or fin:

$$-\frac{d}{dx}\left(kA\frac{dT}{dx}\right)+P\beta T=f(x),\quad f=Ag+P\beta T_\infty \tag{4.2.9}$$

Plane wall ($A = 1$ and $\beta = 0$):

$$-\frac{d}{dx}\left(k\frac{dT}{dx}\right)=g(x) \tag{4.2.10}$$

Cylindrical system ($\beta = 0$):

$$-\frac{1}{r}\frac{d}{dr}\left(rk\frac{dT}{dr}\right)=g(r) \tag{4.2.11}$$

Equation (4.2.9), which includes Eq. (4.2.10) as a special case, can be obtained from the model equation, Eq. (3.4.1), discussed in Section 3.4 by setting $u = T$, $a = kA$, $c = P\beta$, and $f = Ag + P\beta T_\infty$. Equation (4.2.11) governing an axisymmetric problem is also a special case of Eq. (3.5.3) discussed in Section 3.5. The essential and natural boundary conditions associated with Eq. (4.2.9) or Eq. (4.2.10) are of the form (only one of them can be specified at a point)

$$T=T_0,\quad n_xQ+\beta A(T-T_\infty)=Q_0 \tag{4.2.12}$$

4.2.2 Finite Element Equations

The finite element model of Eq. (4.2.9) is readily available from Eq. (3.4.33) as

$$\mathbf{K}^e\mathbf{T}^e=\mathbf{f}^e+\mathbf{Q}^e \tag{4.2.13a}$$

$$K_{ij}^e = \int_{x_a}^{x_b} \left(k_e A_e \frac{d\psi_i^e}{dx}\frac{d\psi_j^e}{dx} + P\beta\psi_i^e\psi_j^e \right) dx$$

$$f_i^e = \int_{x_a}^{x_b} \psi_i^e (A_e g_e + P_e \beta_e T_\infty^e)\, dx \qquad (4.2.13b)$$

$$Q_1^e = \left(-k_e A_e \frac{dT}{dx} \right)_{x_a}, \quad Q_2^e = \left(k_e A_e \frac{dT}{dx} \right)_{x_b}$$

where Q_1^e and Q_2^e denote heat flow *into* the element at the nodes (i.e., Q_2^e should be interpreted as heat flow in). We note that $\beta = 0$ for the case of plane wall as there is no possibility of convection heat transfer inside a wall.

When $k_e A_e$, $P_e \beta_e$, and $A_e g_e$ are element-wise constant, the finite element equations for linear and quadratic elements are available from Eqs. (3.4.40) and (3.4.41), respectively. They are recorded here for ready reference.

Linear element

$$\left(\frac{A_e k_e}{h_e} \begin{bmatrix} 1 & -1 \\ -1 & 1 \end{bmatrix} + \frac{P_e \beta_e h_e}{6} \begin{bmatrix} 2 & 1 \\ 1 & 2 \end{bmatrix} \right) \begin{Bmatrix} T_1^e \\ T_2^e \end{Bmatrix} = \frac{f_e h_e}{2} \begin{Bmatrix} 1 \\ 1 \end{Bmatrix} + \begin{Bmatrix} Q_1^e \\ Q_2^e \end{Bmatrix} \qquad (4.2.14)$$

Quadratic element

$$\left(\frac{A_e k_e}{3h_e} \begin{bmatrix} 7 & -8 & 1 \\ -8 & 16 & -8 \\ 1 & -8 & 7 \end{bmatrix} + \frac{P_e \beta_e h_e}{30} \begin{bmatrix} 4 & 2 & -1 \\ 2 & 16 & 2 \\ -1 & 2 & 4 \end{bmatrix} \right) \begin{Bmatrix} T_1^e \\ T_2^e \\ T_3^e \end{Bmatrix} = \frac{f_e h_e}{6} \begin{Bmatrix} 1 \\ 4 \\ 1 \end{Bmatrix} + \begin{Bmatrix} Q_1^e \\ Q_2^e \\ Q_3^e \end{Bmatrix} \qquad (4.2.15)$$

where $f_e = A_e g_e + P_e \beta_e T_\infty^e$.

The finite element model of Eq. (4.2.11) governing axisymmetric problems is given in Eqs. (3.5.8a) and (3.5.8b):

$$\mathbf{K}^e \mathbf{T}^e = \mathbf{f}^e + \mathbf{Q}^e \qquad (4.2.16a)$$

$$K_{ij}^e = 2\pi \int_{r_a}^{r_b} k_e \frac{d\psi_i^e}{dr}\frac{d\psi_j^e}{dr}\, r dr, \quad f_i^e = 2\pi \int_{r_a}^{r_b} \psi_i^e g_e\, r\, dr$$
$$Q_1^e \equiv -2\pi \left(rk_e \frac{dT}{dr}\right)\Big|_{r_a}, \quad Q_2^e \equiv 2\pi \left(rk_e \frac{dT}{dr}\right)\Big|_{r_b} \tag{4.2.16b}$$

The numerical values of the coefficients K_{ij}^e and f_i^e for element-wise constant values of k_e and g_e are given in Eqs. (3.5.9) and (3.5.10), respectively, and they are reproduced below for ready reference.

Linear element

$$\mathbf{K}^e = \frac{2\pi k_e}{h_e}\left(r_a + \tfrac{1}{2}h_e\right)\begin{bmatrix} 1 & -1 \\ -1 & 1 \end{bmatrix}, \quad \mathbf{f}^e = \frac{2\pi g_e h_e}{6}\begin{Bmatrix} 3r_a + h_e \\ 3r_a + 2h_e \end{Bmatrix} \tag{4.2.17}$$

Quadratic element

$$\mathbf{K}^e = \frac{2\pi k_e}{6h_e}\begin{bmatrix} 3h_e + 14r_a & -(4h_e + 16r_a) & h_e + 2r_a \\ -(4h_e + 16r_a) & 16h_e + 32r_a & -(12h_e + 16r_a) \\ h_e + 2r_a & -(12h_e + 16r_a) & 11h_e + 14r_a \end{bmatrix}$$
$$\mathbf{f}^e = \frac{2\pi g_e h_e}{6}\begin{Bmatrix} r_a \\ 4r_a + 2h_e \\ r_a + h_e \end{Bmatrix} \tag{4.2.18}$$

4.2.3 Numerical Examples

In this section a variety of example problems of one-dimensional heat transfer are presented. Axisymmetric problems as well as problems with convection boundary conditions are also considered.

Example 4.2.1

Rectangular fins are used to remove heat from a heated surface, as indicated in Fig. 4.2.1(a). The fins are exposed to ambient air at T_∞ . The heat transfer coefficient associated with fin material and the air is β. Assuming that heat is conducted along the length of the fin and uniform along the width and thickness directions, determine the temperature distribution along the fin and heat loss per fin for two different sets of

boundary conditions. The governing differential equation and boundary conditions of the problem are

$$-\frac{d}{dx}\left(kA\frac{dT}{dx}\right)+\beta P(T-T_\infty)=0, \quad 0<x<L \tag{1}$$

$$\textbf{Set 1:} \quad T(0)=T_0, \quad \left[kA\frac{dT}{dx}+\beta A(T-T_\infty)\right]_{x=L}=0 \tag{2a}$$

$$\textbf{Set 2:} \quad T(0)=T_0, \quad T(L)=T_L=T_\infty \tag{2b}$$

where T is the temperature, k is the conductivity, β is the heat transfer coefficient, P is the perimeter, and A is the area of cross section. Use a uniform mesh (i.e., elements of equal size) of (a) four linear elements and (b) two quadratic elements in the domain to analyze the problem. Use the following data (material of the fin is copper) in the numerical calculations:

$$k=385\ \text{W/m}\cdot^\circ\text{C}, \quad \beta=25\ \text{W/m}^2{}^\circ\text{C}, \quad T_0=100^\circ\text{C}, \quad T_\infty=20^\circ\text{C}$$
$$L=100\ \text{mm}, \quad t=1\ \text{mm}, \quad b=5\ \text{mm} \tag{3}$$

Solution: Let $\theta = T - T_\infty$. Then Eqs. (1), (2a), and (2b) take the form

$$-\frac{d}{dx}\left(kA\frac{d\theta}{dx}\right)+P\beta\theta=0 \tag{4}$$

$$\textbf{Set 1:} \quad \theta(0)=T_0-T_\infty=80^\circ\text{C}, \quad \left[kA\frac{d\theta}{dx}+\beta A\theta\right]_{x=L}=0 \tag{5a}$$

$$\textbf{Set 2:} \quad \theta(0)=T_0-T_\infty=80^\circ\text{C}, \quad \theta(L)=T_L-T_\infty=0^\circ\text{C} \tag{5b}$$

which is simpler than Eq. (1) because Eq. (4) has a zero right-hand side, $g = 0$. The finite element equations in (4.2.13a) are valid with $g = 0$. For the given data we have $kA = 385 \times (5 \times 10^{-6}) = 1.925 \times 10^{-3}$ (W · m), $\beta P = 25 \times (12 \times 10^{-3}) = 0.3$ (W/m°C), and $\beta A = 25 \times (5 \times 10^{-6}) = 0.125 \times 10^{-3}$ (W/°C). Since kA and $P\beta$ are constant throughout the domain, we can use the coefficients from Eqs. (4.2.14) and (4.2.15) for linear and quadratic elements, respectively. First, we set up the assembled equations for the two different meshes and then discuss the imposition of the two sets of boundary conditions on each set of assembled equations.

Assembled equations

(a) For the uniform mesh (i.e., $h_1 = h_2 = h_3 = h_4 = h = L/4$) of four linear

elements, as shown in Fig. 4.2.2, the element equations are

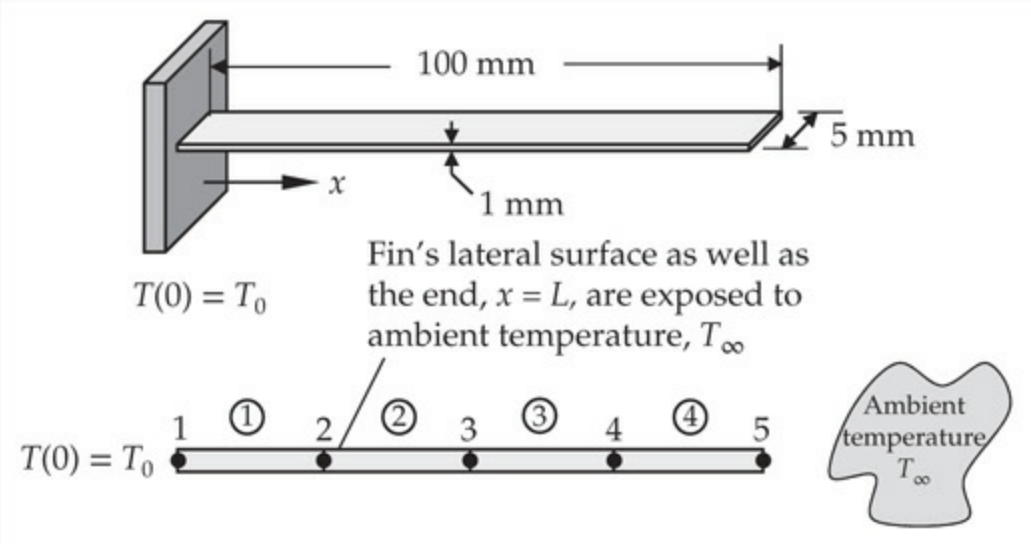

Fig. 4.2.2 Finite element mesh of a rectangular fin.

$$\left(\frac{kA}{h}\begin{bmatrix} 1 & -1 \\ -1 & 1 \end{bmatrix} + \frac{P\beta h}{6}\begin{bmatrix} 2 & 1 \\ 1 & 2 \end{bmatrix}\right)\begin{Bmatrix} \theta_1^e \\ \theta_2^e \end{Bmatrix} = \begin{Bmatrix} Q_1^e \\ Q_2^e \end{Bmatrix} \tag{6}$$

From the mesh it is clear that heat balance between elements (three interfaces) requires

$$Q_2^1 + Q_1^2 = 0, \quad Q_2^2 + Q_1^3 = 0, \quad Q_2^3 + Q_1^4 = 0 \tag{7}$$

Then the assembled system of equations is given by (U_I denotes the value of the temperature θ at the Ith global node)

$$\left(\frac{kA}{h}\begin{bmatrix} 1 & -1 & 0 & 0 & 0 \\ -1 & 2 & -1 & 0 & 0 \\ 0 & -1 & 2 & -1 & 0 \\ 0 & 0 & -1 & 2 & -1 \\ 0 & 0 & 0 & -1 & 1 \end{bmatrix} + \frac{\beta Ph}{6}\begin{bmatrix} 2 & 1 & 0 & 0 & 0 \\ 1 & 4 & 1 & 0 & 0 \\ 0 & 1 & 4 & 1 & 0 \\ 0 & 0 & 1 & 4 & 1 \\ 0 & 0 & 0 & 1 & 2 \end{bmatrix}\right)\begin{Bmatrix} U_1 \\ U_2 \\ U_3 \\ U_4 \\ U_5 \end{Bmatrix} = \begin{Bmatrix} Q_1^1 \\ 0 \\ 0 \\ 0 \\ Q_2^4 \end{Bmatrix}$$

(b) For the uniform mesh ($h_1 = h_2 = h = L/2$) of two quadratic elements, the element equations are

$$\left(\frac{kA}{3h}\begin{bmatrix} 7 & -8 & 1 \\ -8 & 16 & -8 \\ 1 & -8 & 7 \end{bmatrix} + \frac{\beta Ph}{30}\begin{bmatrix} 4 & 2 & -1 \\ 2 & 16 & 2 \\ -1 & 2 & 4 \end{bmatrix}\right)\begin{Bmatrix} \theta_1^e \\ \theta_2^e \\ \theta_3^e \end{Bmatrix} = \begin{Bmatrix} Q_1^e \\ Q_2^e \\ Q_3^e \end{Bmatrix} \tag{8}$$

The balance of heats at the interface of the two quadratic elements, that is, at global node 3, requires $Q_3^1 + Q_1^2 = 0$. Hence, the assembled equations

are

$$\left(\frac{kA}{3h}\begin{bmatrix} 7 & -8 & 1 & 0 & 0 \\ -8 & 16 & -8 & 0 & 0 \\ 1 & -8 & 7+7 & -8 & 1 \\ 0 & 0 & -8 & 16 & -8 \\ 0 & 0 & 1 & -8 & 7 \end{bmatrix} + \frac{\beta Ph}{30}\begin{bmatrix} 4 & 2 & -1 & 0 & 0 \\ 2 & 16 & 2 & 0 & 0 \\ -1 & 2 & 4+4 & 2 & -1 \\ 0 & 0 & 2 & 16 & 2 \\ 0 & 0 & -1 & 2 & 4 \end{bmatrix}\right)\begin{Bmatrix} U_1 \\ U_2 \\ U_3 \\ U_4 \\ U_5 \end{Bmatrix} = \begin{Bmatrix} Q_1^1 \\ Q_2^1 \\ 0 \\ Q_2^2 \\ Q_3^2 \end{Bmatrix}$$

The assembled equations presented above for a mesh of four linear elements and for a mesh of two quadratic elements, where both meshes consist of elements connected in series, are valid for any set of boundary conditions. Next, we modify each set of equations for the two sets of boundary conditions given in Eqs. (5a) and (5b).

Condensed equations and solutions

Set 1 Boundary Conditions. In this case we have

$$U_1 = \theta(0) = T(0) - T_\infty = T_0 - T_\infty \equiv \theta_0, \quad Q_2^N = -\beta A U_5 \tag{9}$$

To obtain the condensed equations for the unknown U's, we delete the first row of the equations and modify the rest of the equations to account for the known U_1 and Q_2^N (N being the number of elements in the mesh).

(a) For the mesh of four linear elements ($N = 4$), the condensed equations for the unknown nodal temperatures are

$$\left(\frac{kA}{h}\begin{bmatrix} 2 & -1 & 0 & 0 \\ -1 & 2 & -1 & 0 \\ 0 & -1 & 2 & -1 \\ 0 & 0 & -1 & 1 \end{bmatrix} + \frac{\beta Ph}{6}\begin{bmatrix} 4 & 1 & 0 & 0 \\ 1 & 4 & 1 & 0 \\ 0 & 1 & 4 & 1 \\ 0 & 0 & 1 & 2+\alpha \end{bmatrix}\right)\begin{Bmatrix} U_2 \\ U_3 \\ U_4 \\ U_5 \end{Bmatrix} = \begin{Bmatrix} \left(\frac{kA}{h} - \frac{\beta Ph}{6}\right)\theta_0 \\ 0 \\ 0 \\ 0 \end{Bmatrix} \tag{10}$$

where $\alpha = \beta A/(\beta Ph/6) = 6A/Ph$. The unknown heats at nodes 1 and 5 are

$$Q_1^1 = \left(\frac{kA}{h} + \frac{\beta Ph}{3}\right)\theta_0 + \left(-\frac{kA}{h} + \frac{\beta Ph}{6}\right)U_2 \qquad (11)$$
$$Q_2^4 = -\beta A U_5$$

The condensed equations for the unknown nodal temperatures become (for the given data)

$$10^{-2}\begin{bmatrix} 15.9000 & -7.5750 & 0.0000 & 0.0000 \\ -7.5750 & 15.9000 & -7.5750 & 0.0000 \\ 0.0000 & -7.5750 & 15.9000 & -7.5750 \\ 0.0000 & 0.0000 & -7.5750 & 7.9625 \end{bmatrix}\begin{Bmatrix} U_2 \\ U_3 \\ U_4 \\ U_5 \end{Bmatrix} = \begin{Bmatrix} 6.06 \\ 0.00 \\ 0.00 \\ 0.00 \end{Bmatrix} \qquad (12)$$

The solution of these equations (obtained with the help of an equation solver in a computer) is

$$U_1 = 80.0°\text{C},\ U_2 = 62.283°\text{C},\ U_3 = 50.732°\text{C},\ U_4 = 44.204°\text{C},\ U_5 = 42.053°\text{C} \qquad (13)$$

The heat input at node 1 from equilibrium is

$$(Q_1^1)_{\text{equil}} = \frac{kA}{h}(U_1 - U_2) + \frac{\beta Ph}{6}(2U_1 + U_2) = \left(\frac{kA}{h} + \frac{\beta Ph}{3}\right)U_1 + \left(-\frac{kA}{h} + \frac{\beta Ph}{6}\right)U_2$$
$$= (0.077 + 0.0025)\,80 + (-0.077 + 0.00125)\,62.283 = 1.642\ \text{W} \qquad (14)$$

whereas from the definition we have

$$(Q_1^1)_{\text{def}} = -kA\left(\frac{d\theta}{dx}\right)_{x=0} = -385 \times 5 \times 10^{-6}\left(\frac{U_2 - U_1}{0.025}\right) = 1.3642\ \text{W} \qquad (15)$$

The total heat loss from the surface of the fin can be calculated using

$$Q = \sum_{e=1}^{N=4} Q^e + \beta A\theta(L) = \sum_{e=1}^{N=4} \int_{x_a}^{x_b} P\beta\theta\, dx + \beta A\theta(L)$$
$$= \sum_{e=1}^{N=4} \int_{x_a}^{x_b} P\beta\,(\theta_1^e\psi_1^e + \theta_2^e\psi_2^e)\, dx + \beta A U_5 = \sum_{e=1}^{N=4} \beta Ph_e\left(\frac{\theta_1^e + \theta_2^e}{2}\right) + \beta A U_5$$
$$= 0.0075\,(0.5U_1 + U_2 + U_3 + U_4 + 0.5U_5) + 25 \times 5 \times 10^{-6} \times 42.053$$
$$= 1.6368 + 0.00526 = 1.642\ \text{W} \qquad (16)$$

(b) For the mesh of two quadratic elements, the condensed equations are

$$\left(\frac{kA}{3h}\begin{bmatrix}16 & -8 & 0 & 0\\ -8 & 14 & -8 & 1\\ 0 & -8 & 16 & -8\\ 0 & 1 & -8 & 7\end{bmatrix}+\frac{\beta Ph}{30}\begin{bmatrix}16 & 2 & 0 & 0\\ 2 & 8 & 2 & -1\\ 0 & 2 & 16 & 2\\ 0 & -1 & 2 & 4+\alpha\end{bmatrix}\right)\begin{Bmatrix}U_2\\ U_3\\ U_4\\ U_5\end{Bmatrix}$$

$$=\begin{Bmatrix}\left(\frac{8kA}{3h}-\frac{2\beta Ph}{30}\right)\theta_0\\ \left(-\frac{kA}{3h}+\frac{\beta Ph}{30}\right)\theta_0\\ 0\\ 0\end{Bmatrix} \tag{17}$$

where $\alpha = \beta A/(\beta Ph/30) = 30A/Ph$. Using the problem data, the condensed equations for the unknown nodal temperatures for the mesh of two quadratic elements can be expressed as

$$10^{-2}\begin{bmatrix}21.3300 & -10.1667 & 0.0000 & 0.0000\\ -10.1667 & 18.3667 & -10.1667 & 1.2333\\ 0.0000 & -10.1667 & 21.3333 & -10.1667\\ 0.0000 & 1.2333 & -10.1667 & 9.1958\end{bmatrix}\begin{Bmatrix}U_2\\ U_3\\ U_4\\ U_5\end{Bmatrix}=\begin{Bmatrix}8.1333\\ -0.9867\\ 0.0000\\ 0.0000\end{Bmatrix} \tag{18}$$

The solution of the condensed equations for the unknown temperatures is

$$U_1 = 80.0°\text{C},\quad U_2 = 62.374°\text{C},\quad U_3 = 50.884°\text{C},\quad U_4 = 44.380°\text{C},\quad U_5 = 42.240°\text{C} \tag{19}$$

The heat input at node 1 is

$$\begin{aligned}(Q_1^1)_{\text{equil}} &= \frac{kA}{3h}(7U_1 - 8U_2 + U_3) + \frac{\beta Ph}{30}(4U_1 + 2U_2 - U_3)\\ &= \frac{0.0385}{3}(7\times 80 - 8\times 62.374 + 50.884) + \frac{0.0025}{5}(4\times 80 + 2\times 62.374 - 50.884)\\ &= 1.633\ \text{W}\end{aligned} \tag{20}$$

and from the definition we have

$$(Q_1^1)_{\text{def}} = -kA\left(\frac{d\theta}{dx}\right)_{x=0} = -385\times 5\times 10^{-6}\left(\frac{-3U_1 + 4U_2 - U_3}{0.05}\right) = 1.5934\ \text{W} \tag{21}$$

The total heat loss from the surface of the fin can be calculated using

$$Q = \sum_{e=1}^{N=2} \int_{x_a}^{x_b} P\beta\,(\theta_1^e\psi_1^e + \theta_2^e\psi_2^e + \theta_3^e\psi_3^e)\,dx + \beta A U_5$$

$$= \sum_{e=1}^{N=2} \beta P h_e \left(\frac{\theta_1^e + 4\theta_2^e + \theta_3^e}{6}\right) + \beta A U_5$$

$$= \frac{\beta P h}{6}(U_1 + 4U_2 + 2U_3 + 4U_4 + U_5) + \beta A U_5 = 1.633\ \text{W} \tag{22}$$

The exact solution of Eq. (4) for the boundary conditions in Eq. (5a) is

$$\theta(x) = \theta_0 \left[\frac{\cosh m(L-x) + (\beta/mk)\sinh m(L-x)}{\cosh mL + (\beta/mk)\sinh mL}\right], \quad m^2 = \frac{\beta P}{Ak} \tag{23a}$$

$$Q(0) = -kA\frac{d\theta}{dx} = \theta_0 M \left[\frac{\sinh mL + (\beta/mk)\cosh mL}{\cosh mL + (\beta/mk)\sinh mL}\right], \quad M^2 = \beta P A k \tag{23b}$$

Evaluating the exact solution at the nodes, we obtain

$$\theta(0.025) = 62.414°\text{C},\ \theta(0.05) = 50.958°\text{C},\ \theta(0.075) = 44.505°\text{C},\ \theta(0.1) = 42.422°\text{C} \tag{24}$$

and $Q_1^1 = 1.63$ W. Clearly, the two-element mesh of quadratic elements yields more accurate solution than the four-element mesh of linear elements.

Set 2 Boundary Conditions. For set 2 boundary conditions in Eq. (5b), we have

$$U_1 = T_0 - T_\infty = 80°\text{C}, \quad U_5 = 0°\text{C} \tag{25}$$

The condensed equations for the unknown temperatures are obtained by deleting the first and fifth rows of the assembled equations and modifying the remaining equations to account for U_1 = 80°C and U_5 = 0. The condensed equations for the unknown heats are obtained from rows 1 and 5 directly.

(a) For the four-element mesh, the condensed equations are

$$\left(\frac{kA}{h}\begin{bmatrix} 2 & -1 & 0 \\ -1 & 2 & -1 \\ 0 & -1 & 2 \end{bmatrix} + \frac{\beta P h}{6}\begin{bmatrix} 4 & 1 & 0 \\ 1 & 4 & 1 \\ 0 & 1 & 4 \end{bmatrix}\right)\begin{Bmatrix} U_2 \\ U_3 \\ U_4 \end{Bmatrix} = \left(\frac{kA}{h} - \frac{\beta P h}{6}\right)\begin{Bmatrix} \theta_0 \\ 0 \\ 0 \end{Bmatrix} \tag{26}$$

and the finite element solution is

$$U_1 = 80.0°C,\ \ U_2 = 53.955°C,\ \ U_3 = 33.252°C,\ \ U_4 = 15.842°C,\ \ U_5 = 0°C \tag{27}$$

The heats at nodes 1 and 5 from equilibrium are

$$\begin{aligned}(Q_1^1)_{\text{equil}} &= \frac{kA}{h}(U_1 - U_2) + \frac{\beta Ph}{6}(2U_1 + U_2)\\ &= 0.077(80 - 53.995) + 0.00125(2 \times 80 + 53.955) = 2.270\ \text{W}\end{aligned} \tag{28a}$$

$$\begin{aligned}(Q_2^4)_{\text{equil}} &= \frac{kA}{h}(-U_4 + U_5) + \frac{\beta Ph}{6}(U_4 + 2U_5)\\ &= 0.077(-15.842 + 0) + 0.00125(15.842 + 2 \times 0) = -1.200\ \text{W}\end{aligned} \tag{28b}$$

whereas from the definitions, we obtain

$$(Q_1^1)_{\text{def}} = 2.0055\ \text{W}, \quad (Q_2^4)_{\text{def}} = -1.2198\ \text{W} \tag{29}$$

Thus the heat loss from the end of the fin is overestimated by assuming that the end $x = L$ is at the ambient temperature. The total heat loss from the lateral surface of the fin is given by

$$Q = \sum_{e=1}^{4} Q^e = 0.0075\,(0.5U_1 + U_2 + U_3 + U_4 + 0.5U_5) = 1.073\ \text{W} \tag{30}$$

(b) The condensed equations for the unknown nodal temperatures for the mesh of two quadratic elements are

$$\left(\frac{kA}{3h}\begin{bmatrix} 16 & -8 & 0 \\ -8 & 14 & -8 \\ 0 & -8 & 16 \end{bmatrix} + \frac{\beta Ph}{30}\begin{bmatrix} 16 & 2 & 0 \\ 2 & 8 & 2 \\ 0 & 2 & 16 \end{bmatrix}\right)\begin{Bmatrix} U_2 \\ U_3 \\ U_4 \end{Bmatrix} = \begin{Bmatrix} \left(\frac{8kA}{3h} - \frac{2\beta Ph}{30}\right)\theta_0 \\ \left(-\frac{kA}{3h} + \frac{\beta Ph}{30}\right)\theta_0 \\ 0 \end{Bmatrix} \tag{31}$$

whose solution is

$$U_1 = 80.0°C,\ \ U_2 = 53.995°C,\ \ U_3 = 33.301°C,\ \ U_4 = 15.870°C,\ \ U_5 = 0°C \tag{32}$$

The unknown heats at global nodes 1 and 5 are computed from

$$\begin{aligned}(Q_1^1)_{\text{equil}} &= \frac{kA}{3h}(7U_1 - 8U_2 + U_3) + \frac{\beta Ph}{30}(4U_1 + 2U_2 - U_3) = 2.268\ \text{W}\\ (Q_3^2)_{\text{equil}} &= \frac{kA}{3h}(U_3 - 8U_4 + 7U_5) + \frac{\beta Ph}{30}(-U_3 + 2U_4 + 4U_5) = -1.203\ \text{W}\end{aligned} \tag{33}$$

From the definitions, we have

$$(Q_1^1)_{\text{def}} = 2.2069\ \text{W}, \quad (Q_2^4)_{def} = -1.1619\ \text{W} \tag{34}$$

The exact solution of Eq. (4) for boundary conditions in Eq. (5b) is ($\theta_L = T_L - T_\infty$ and $\theta_0 = T_0 - T_\infty$)

$$\theta(x) = \left[\frac{\theta_L \sinh mx + \theta_0 \sinh m(L-x)}{\sinh mL}\right], \quad m^2 = \frac{\beta P}{Ak} \tag{35a}$$

$$Q(0) = -kA\frac{d\theta}{dx} = M\left[\frac{\theta_0 \cosh mL - \theta_L}{\sinh mL}\right], \quad M^2 = \beta PAk \tag{35b}$$

Evaluating the exact solution at the nodes, we obtain

$$\theta(0.025) = 54°\text{C}, \ \theta(0.05) = 33.3°\text{C}, \ \theta(0.075) = 15.87°\text{C}, \ \theta(0.1) = 0°\text{C} \tag{36}$$

and $Q_1^1 = 2.268$ W.

The next example is concerned with heat transfer in a rod and a comparison of the finite element and finite difference solutions.

Example 4.2.2

A steel rod of uniform diameter D = 0.02 m, length L = 0.05 m, and constant thermal conductivity k = 50 W/(m · °C) is exposed to ambient air at T_∞ = 20°C with a heat transfer coefficient β = 100 W/(m^2 · °C). The left end of the rod is maintained at temperature T_0 = 320°C and the other end is insulated, as shown in Fig. 4.2.3(a).

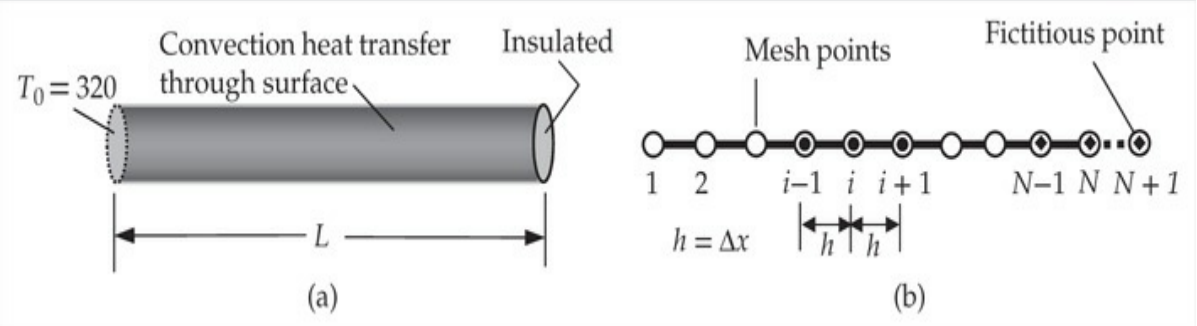

Fig. 4.2.3 (a) Heat transfer in a rod. (b) Finite difference mesh.

Determine the temperature distribution and the heat input at the left end of the rod using uniform meshes of (a) two linear elements and (b) four linear elements. For the sake of comparison, also compute a suitable finite difference solution of the problem with the same number of mesh points.

Solution: The governing equation of the problem is the same as Eq. (4) of

Example 4.2.1. We rewrite it in the form (by dividing the equation throughout with Ak)

$$-\frac{d^2\theta}{dx^2} + m^2\theta = 0 \quad \text{for} \quad 0 < x < L \tag{1}$$

where $\theta = T - T_\infty$, T being the temperature, and m^2 is given by

$$m^2 = \frac{\beta P}{Ak} = \frac{\beta \pi D}{\frac{1}{4}\pi D^2 k} = \frac{4\beta}{kD} = \frac{4 \times 100}{50 \times 0.02} = 400 \tag{2}$$

The boundary conditions of the problem become

$$\theta(0) = T(0) - T_\infty = 300°\text{C}, \quad \left(\frac{d\theta}{dx}\right)\Big|_{x=L} = 0 \tag{3}$$

The exact solution is given by

$$\theta(x) = \theta(0)\frac{\cosh m(L-x)}{\cosh mL}, \quad Q(0) = \left(-\frac{d\theta}{dx}\right)\Big|_{x=0} = m\theta(0)\frac{\sinh mL}{\cosh mL} \tag{4}$$

Finite Difference Solution

In the finite difference method (see **Example 1.3.2** for additional discussion), one may think of identifying a number of mesh points (instead of elements), including the boundary points, as shown in Fig. 4.2.3(b). Then derivatives of a function u at every mesh point, which corresponds to a fixed location, in the domain are approximated in terms of the values of u at several points including the mesh point where the derivative is evaluated. For example, the second derivative of u at the ith mesh point, whose coordinate is x_i, may be approximated in terms of the values of u at mesh points $i - 1$, i, and $i + 1$ as [see Eq. (1.3.7)]

$$\left(\frac{d^2\theta}{dx^2}\right)_i \approx \frac{1}{h^2}(\theta_{i-1} - 2\theta_i + \theta_{i+1}) \tag{5}$$

where h is the distance between two mesh points. Equation (5) is known as the centered finite difference formula, and it can be viewed as the "element equation," as shown in Fig. 4.2.3(b). We note that the coefficients in the finite difference equation (5) are real numbers (i.e., no evaluation of integrals is required). Substituting the above formula for the second derivative into Eq. (1), we arrive at

$$-\theta_{i-1} + (2 + m^2h^2)\theta_i - \theta_{i+1} = 0 \tag{6}$$

which is valid for any point where θ is not specified. By applying the formula in Eq. (6) to nodes 2, 3, . . . , N, we obtain the relations among the values of u at the mesh points. Thus, we obtain the global equations directly. Note that application of the formula to mesh point N involves mesh point $N + 1$, which is not a part of the domain, and it is called fictitious mesh point. We shall discuss how to deal with this situation in the sequel.

(a) First, we choose a mesh of three points ($h = 0.025$), two end points and one in the middle. Applying Eq. (6) at nodes 2 and 3, we obtain ($m^2 = 400$)

$$(2 + 400h^2)\,\theta_2 - \theta_3 = \theta_1, \quad -\theta_2 + (2 + 400h^2)\,\theta_3 - \theta_4 = 0 \tag{7}$$

where $\theta_1 = \theta(0) = 300°C$. Note that θ_4 is the value of θ at the fictitious node 4, which is considered to be a mirror image because of the boundary condition $d\theta/dx = 0$. To eliminate θ_4, we can use one of the following formulas:

$$\left(\frac{d\theta}{dx}\right)_{x=0} = \frac{\theta_4 - \theta_3}{h} = 0 \ \text{(forward)} \tag{8a}$$

$$\left(\frac{d\theta}{dx}\right)_{x=0} = \frac{\theta_4 - \theta_2}{2h} = 0 \ \text{(centered)} \tag{8b}$$

The latter is of order $O(h^2)$, consistent with the centered difference formula in Eq. (5). Using Eq. (8b), we set $\theta_4 = \theta_2$ in Eq. (7). Equations (7) can be written in matrix form as

$$\begin{bmatrix} 2.25 & -1 \\ -2 & 2.25 \end{bmatrix} \begin{Bmatrix} \theta_2 \\ \theta_3 \end{Bmatrix} = \begin{Bmatrix} 300 \\ 0 \end{Bmatrix} \tag{9}$$

The solution of these equations is

$$\theta_2 = 220.41°C, \quad \theta_3 = 195.92°C \tag{10}$$

The exact values are $\theta(0.025) = 219.22°C$ and $\theta(0.05) = 195.94°C$. The heat at mesh point 1 ($x = 0$) can be computed using the definition

$$Q(0) = \left(-\frac{d\theta}{dx}\right)_{x=0} = \frac{\theta_1 - \theta_2}{h} = 3{,}183.6 \text{ W} \tag{11}$$

whereas the exact value is 4,569.56 W.

(b) Next, we use a mesh of five points. Applying Eq. (6) at mesh points 2, 3, 4, and 5, and using $\theta_6 = \theta_4$, we obtain ($h = 0.0125$)

$$\begin{bmatrix} 2.0625 & -1 & 0 & 0 \\ -1 & 2.0625 & -1 & 0 \\ 0 & -1 & 2.0625 & -1 \\ 0 & 0 & -2 & 2.0625 \end{bmatrix} \begin{Bmatrix} \theta_2 \\ \theta_3 \\ \theta_4 \\ \theta_5 \end{Bmatrix} = \begin{Bmatrix} 300 \\ 0 \\ 0 \\ 0 \end{Bmatrix} \tag{12}$$

The solution of these equations is

$$\theta_2 = 251.89°\text{C}, \quad \theta_3 = 219.53°\text{C}, \quad \theta_4 = 200.89°\text{C}, \quad \theta_5 = 194.80°\text{C} \tag{13}$$

The heat at mesh point 1 ($x = 0$) is

$$Q(0) = \left(-\frac{d\theta}{dx}\right)_{x=0} = \frac{\theta_1 - \theta_2}{h} = 3,848.8 \text{ W} \tag{14}$$

Finite Element Solutions

The element equations are

$$\left(\frac{1}{h_e}\begin{bmatrix} 1 & -1 \\ -1 & 1 \end{bmatrix} + \frac{m^2 h_e}{6}\begin{bmatrix} 2 & 1 \\ 1 & 2 \end{bmatrix}\right)\begin{Bmatrix} \theta_1^e \\ \theta_2^e \end{Bmatrix} = \begin{Bmatrix} Q_1^e \\ Q_2^e \end{Bmatrix} \tag{15}$$

(a) For the choice of two linear elements ($h = h_1 = h_2 = 0.025$) connected in series, the assembled system of equations is ($1/h + m^2 h/3 = 43.333$ and $-1/h + m^2 h/6 = -38.333$)

$$\begin{bmatrix} 43.333 & -38.333 & 0.000 \\ -38.333 & 86.667 & -38.333 \\ 0.000 & -38.333 & 43.333 \end{bmatrix} \begin{Bmatrix} U_1 \\ U_2 \\ U_3 \end{Bmatrix} = \begin{Bmatrix} Q_1^{(1)} \\ Q_2^{(1)} + Q_1^{(2)} = 0 \\ Q_2^{(2)} \end{Bmatrix} \tag{16}$$

where U_I denotes the temperature $\theta(x)$ at the Ith global node. The boundary conditions are

$$U_1 = 300°\text{C}, \quad Q_2^{(2)} = 0 \tag{17}$$

Hence, the condensed equations are

$$\begin{bmatrix} 86.667 & -38.333 \\ -38.333 & 43.333 \end{bmatrix} \begin{Bmatrix} U_2 \\ U_3 \end{Bmatrix} = \begin{Bmatrix} 38.333 \times 300 \\ 0 \end{Bmatrix} \tag{18}$$

The solution of these equations is

$$U_2 = 217.98°\text{C}, \quad U_3 = 192.83°\text{C} \tag{19}$$

The heat at node 1 ($x = 0$) can be computed using the first row of the assembled equations (i.e., from equilibrium)

$$Q_1^1 = 43.333U_1 - 38.333U_2 = 4{,}644.1 \text{ W} \tag{20}$$

whereas from definition we have

$$(Q_1^1)_{def} = -\frac{U_2 - U_1}{h_1} = \frac{300 - 217.98}{0.025} = 3{,}280.8 \text{ W} \tag{21}$$

Once we have the nodal values U_1, U_2 and U_3, values at other points (intermediate to the nodes) can be computed using the approximation

$$\theta^e(\bar{x}) = \sum_{j=1}^{2} \theta_j^e \psi_j^e(\bar{x}), \quad 0 \le \bar{x} \le h_e \tag{22}$$

where $\theta_1^1 = U_1$, $\theta_2^1 = U_2 = \theta_1^2$, and $\theta_2^2 = U_3$. Such a formula is not readily available in the finite difference method; one may use mesh point data to construct an interpolation consistent with the finite difference formula used.

(b) For the choice of four linear elements, the assembled system of equations is

$$\begin{bmatrix} 81.667 & -79.167 & 0.000 & 0.000 & 0.000 \\ -79.167 & 163.333 & -79.167 & 0.000 & 0.000 \\ 0.000 & -79.167 & 163.333 & -79.167 & 0.000 \\ 0.000 & 0.000 & -79.167 & 163.333 & -79.167 \\ 0.000 & 0.000 & 0.000 & -79.167 & 81.667 \end{bmatrix} \begin{Bmatrix} U_1 \\ U_2 \\ U_3 \\ U_4 \\ U_5 \end{Bmatrix} = \begin{Bmatrix} Q_1^{(1)} \\ Q_2^{(1)} + Q_1^{(2)} \\ Q_2^{(2)} + Q_1^{(3)} \\ Q_2^{(3)} + Q_1^{(4)} \\ Q_2^{(4)} \end{Bmatrix} \tag{23}$$

The balance conditions require $Q_2^{(1)} + Q_1^{(2)} = 0$, $Q_2^{(2)} + Q_1^{(3)} = 0$, and $Q_2^{(3)} + Q_1^{(4)} = 0$; the boundary conditions are $U_1 = 300°\text{C}$ and $Q_2^{(4)} = 0$. The condensed equation is obtained by deleting the first row and column and modifying the right-hand side to account for the specified value $U_1 = \theta_0 = 300$:

$$\begin{bmatrix} 163.333 & -79.167 & 0 & 0 \\ -79.167 & 81.667 & -79.167 & 0 \\ 0 & -79.167 & 81.667 & -79.167 \\ 0 & 0 & -79.167 & 81.667 \end{bmatrix} \begin{Bmatrix} U_2 \\ U_3 \\ U_4 \\ U_5 \end{Bmatrix} = \begin{Bmatrix} 79.167 \times 300 \\ 0 \\ 0 \\ 0 \end{Bmatrix} \tag{24}$$

The solution of these equations is

$$U_2 = 251.52°\text{C}, \quad U_3 = 218.92°\text{C}, \quad U_4 = 200.16°\text{C}, \quad U_5 = 194.03°\text{C} \tag{25}$$

The heat at node 1 ($x = 0$) is

$$(Q_1^1)_{\text{equil}} = 81.667\,U_1 - 79.167\,U_2 = 4{,}587.92\ \text{W} \tag{26}$$

A comparison of the nodal values of θ obtained by the two methods with the exact values is presented in Table 4.2.1. Both finite difference and finite element solutions are in good agreement with the exact solution. We note that the finite element method adjusts the nodal values to minimize the error in the approximation over the domain in the weak-form sense. When a uniform mesh of four quadratic elements is used, we will obtain the exact solution for θ shown in Table 4.2.1.

Table 4.2.1 Comparison of finite difference and finite element solutions with the exact solution of

$$-\frac{d^2\theta}{dx^2} + 400\,\theta = 0,\ 0 < x < 0.05;\ \theta(0) = 300,\ \left.\frac{d\theta}{dx}\right|_{x=0.05} = 0$$

x	Exact solution	FEM solution			FDM solution		
		$N=2$	$N=4$	$N=8$	$N=2$	$N=4$	$N=8$
0.00000	300.00	300.00	300.00	300.00	300.00	300.00	300.00
0.00625	273.71	––	––	273.69	––	––	273.74
0.01250	251.71	––	251.52	251.66	––	251.89	251.75
0.01875	233.64	––	––	233.58	––	––	233.70
0.02500	219.23	217.98	218.92	219.15	220.41	219.53	219.30
0.03125	208.25	––	––	208.16	––	––	208.33
0.03750	200.52	––	200.16	200.43	––	200.89	200.61
0.04375	195.94	––	––	195.84	––	––	196.03
0.05000	194.42	192.83	194.03	194.32	195.92	194.80	194.51

The last example of heat transfer deals with a radially symmetric problem.

Example 4.2.3

Consider a *long*, homogeneous, solid cylinder of radius R_0 [see Fig. 4.2.1(c)] in which energy is generated at a constant rate g_0 (W/m^3). One may consider a circular disc of radius R_0 and unit thickness to analyze the problem. The boundary surface at $r = R_0$ is maintained at a constant temperature T_0 . Calculate the temperature distribution $T(r)$ and heat flux $q(r) = -kdT/dr$ (or heat $Q = -AkdT/dr$) in the disc using (a) one-element and (b) two-element meshes of linear elements. Use the following data: $R_0 = 0.01$ m, $g_0 = 2 \times 108$ W/m^3, $k = 20$ W/(m · °C), $T_0 = 100$°C.

Solution: The governing equation for this problem is given by Eq. (4.2.11) with $g = g_0$. The boundary conditions are

$$T(R_0) = T_0, \quad \left(2\pi kr\frac{dT}{dr}\right)\Big|_{r=0} = 0 \tag{1}$$

The zero-flux boundary condition at $r = 0$ is a result of the radial symmetry at $r = 0$. If the cylinder is hollow with inner radius R_i then the boundary condition at $r = R_i$ can be a specified temperature, specified heat flux, or convection boundary condition, depending on the situation.

The finite element model of the governing equation is given by Eqs. (4.2.16a) and (4.2.16b). For linear interpolation of $T(r)$, the element matrices for a typical element are given in Eq. (4.2.17).

(a) For the mesh of one linear element, we have ($r_a = 0$ and $r_2 = h_1 = R_0$)

$$\pi k\begin{bmatrix} 1 & -1 \\ -1 & 1 \end{bmatrix}\begin{Bmatrix} U_1 \\ U_2 \end{Bmatrix} = \frac{\pi g_0 R_0^2}{3}\begin{Bmatrix} 1 \\ 2 \end{Bmatrix} + \begin{Bmatrix} Q_1^1 \\ Q_2^1 \end{Bmatrix} \tag{2}$$

The boundary conditions imply $U_2 = T_0$ and $Q_1^1 = 0$. Hence the temperature at node 1 is

$$U_1 = \frac{g_0 R_0^2}{3k} + T_0 \tag{3}$$

and the heat at $r = R_0$ is

$$(Q_2^1)_{\text{equil}} = \pi k(U_2 - U_1) - \tfrac{2}{3}\pi g_0 R_0^2 = -\pi g_0 R_0^2 \tag{4}$$

The negative sign indicates that heat is removed from the body. The one-element solution as a function of the radial coordinate r is

$$T_h(r) = U_1\psi_1^1(r) + U_2\psi_2^1(r) = \frac{g_0R_0^2}{3k}\left(1 - \frac{r}{R_0}\right) + T_0 \tag{5}$$

and the heat flux is

$$q(r) \equiv -k\frac{dT_h}{dr} = \tfrac{1}{3}g_0R_0 \tag{6}$$

(b) For a mesh of two linear elements ($h_1 = h_2 = \frac{1}{2}R_0$), the assembled equations are

$$\pi k\begin{bmatrix} 1 & -1 & 0 \\ -1 & 1+3 & -3 \\ 0 & -3 & 3 \end{bmatrix}\begin{Bmatrix} U_1 \\ U_2 \\ U_3 \end{Bmatrix} = \frac{\pi g_0R_0^2}{6}\begin{Bmatrix} \frac{1}{2} \\ 1+2 \\ \frac{1}{2}+2 \end{Bmatrix} + \begin{Bmatrix} Q_1^1 \\ Q_2^1 + Q_1^2 = 0 \\ Q_2^2 \end{Bmatrix} \tag{7}$$

Imposing the boundary conditions $U_3 = T_0$ and $Q_1^1 = 0$, the condensed equations for the unknown temperatures are

$$\pi k\begin{bmatrix} 1 & -1 \\ -1 & 4 \end{bmatrix}\begin{Bmatrix} U_1 \\ U_2 \end{Bmatrix} = \frac{\pi g_0R_0^2}{12}\begin{Bmatrix} 1 \\ 6 \end{Bmatrix} + \pi k\begin{Bmatrix} 0 \\ 3T_0 \end{Bmatrix} \tag{8}$$

The nodal values are

$$U_1 = \frac{5}{18}\frac{g_0R_0^2}{k} + T_0, \quad U_2 = \frac{7}{36}\frac{g_0R_0^2}{k} + T_0 \tag{9}$$

From equilibrium, Q_2^2 is computed as

$$Q_2^2 = -\frac{5}{12}\pi g_0R_0^2 + 3\pi k(U_3 - U_2) = -\pi g_0R_0^2 \tag{10}$$

The finite element solution becomes

$$\begin{aligned} T_h(r) &= \begin{cases} U_1\psi_1^1(r) + U_2\psi_2^1(r) = \left(\frac{5}{18}\frac{g_0R_0^2}{k} + T_0\right)\left(1 - 2\frac{r}{R_0}\right) + 2\left(\frac{7}{36}\frac{g_0R_0^2}{k} + T_0\right)\frac{r}{R_0} \\ U_2\psi_1^2 + U_3\psi_2^2 = 2\left(\frac{7}{36}\frac{g_0R_0^2}{k} + T_0\right)\left(1 - \frac{r}{R_0}\right) + T_0\left(2\frac{r}{R_0} - 1\right) \end{cases} \\ &= \begin{cases} \frac{1}{18}\frac{g_0R_0^2}{k}\left(5 - 3\frac{r}{R_0}\right) + T_0, & \text{for } 0 \le r \le \frac{1}{2}R_0 \\ \frac{7}{18}\frac{g_0R_0^2}{k}\left(1 - \frac{r}{R_0}\right) + T_0, & \text{for } \frac{1}{2}R_0 \le r \le R_0 \end{cases} \end{aligned} \tag{11}$$

The exact solution of the problem is

$$T(r) = \frac{g_0 R_0^2}{4k}\left[1 - \left(\frac{r}{R_0}\right)^2\right] + T_0 \ (^\circ\text{C}) \tag{12a}$$

$$q(r) = \frac{1}{2} g_0 r \ (\text{W/m}^2), \quad Q(R_0) = -\left(2\pi k r \frac{dT}{dr}\right)\Big|_{R_0} = \pi g_0 R_0^2 \ (\text{W}) \tag{12b}$$

The temperature at the center of the cylinder according to the exact solution is $T(0) = g_0 R_0^2/4k + T_0$, whereas it is $g_0 R_0^2/3k + T_0$ and $5g_0 R_0^2/18k + T_0$ according to the one- and two-element models, respectively.

The finite element solutions obtained using one-, two-, four-, and eight-element meshes of linear elements are compared with the exact solution in Table 4.2.2. Convergence of the finite element solutions, $\bar{T} = (T - T_0)k/g_0 R_0^2$, to the exact solution with an increasing number of elements is clear (see Fig. 4.2.4). Figure 4.2.5 shows plots of $\bar{Q}(r) = Q(r)/2\pi R_0 g_0$, $Q(r) = 2\pi k r dT/dr$, versus $\bar{r} = r/R_0$, as computed in the finite element analysis and the exact solution.

Table 4.2.2 Comparison of the finite element and exact solutions for temperature in a radially symmetric circular disc.

	Finite element solution*					
$\frac{r}{R_0}$	1L element	2L elements	4L elements	8L elements	4Q elements	Exact solution
0.000	433.33	377.78	358.73	352.63	350.00	350.00
0.125	391.67	356.24	348.31	347.42	346.09	346.09
0.250	350.00	335.11	337.90	335.27	334.37	334.38
0.375	308.33	315.28	313.59	315.48	314.84	314.84
0.500	266.67	294.44	289.29	287.95	287.50	287.50
0.625	225.00	245.83	249.70	252.65	252.34	252.34
0.750	183.33	197.22	210.12	209.56	209.37	209.38
0.875	141.67	148.61	155.06	158.68	158.59	158.59
1.000	100.00	100.00	100.00	100.00	100.00	100.00

*The underlined terms are nodal values and others are interpolated values. L, linear element; Q, quadratic element.

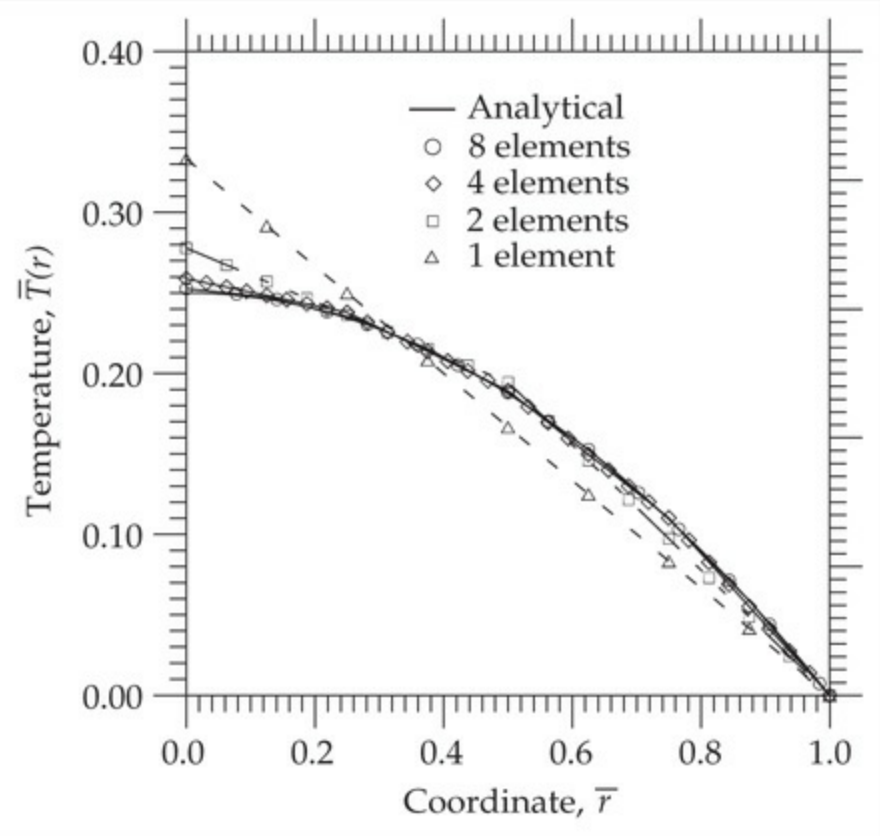

Fig. 4.2.4 Comparison of the finite element solutions with the exact solution for heat transfer in a radially symmetric problem with cylindrical geometry.

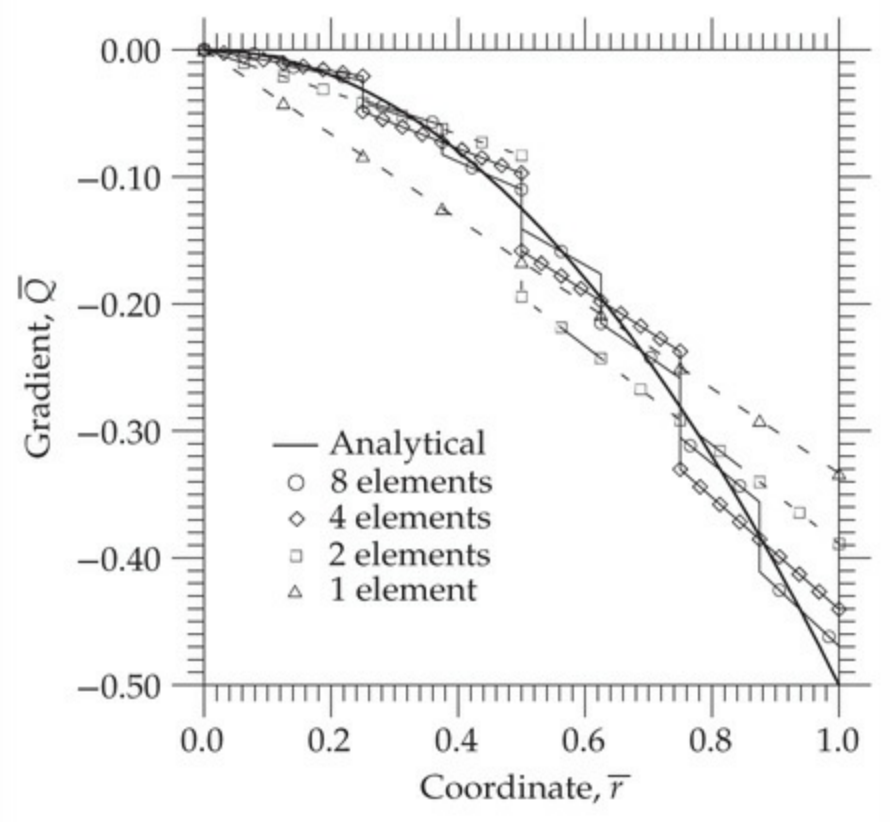

Fig. 4.2.5 Comparison of the finite element solution with the exact solution for the temperature gradient in a radially symmetric problem with cylindrical geometry.

4.3 Fluid Mechanics

4.3.1 Governing Equations

All bulk matter in nature exists in one of two forms: solid or fluid. A solid body is characterized by relative immobility of its molecules, whereas a fluid state is characterized by their relative mobility. Fluids can exist either as gases or liquids. The field of fluid mechanics is concerned with the motion of fluids and its effects on the surroundings (see [5, 6]).

The basic equations of fluid mechanics are derived from the global laws of conservation of mass, momentum, and energy, as well as constitutive relations, and the governing equations were summarized in Eqs. (2.6.6)–(2.6.10). Recall from Section 2.6.3 that the principle of conservation of mass gives the so-called continuity equation, while the conservation of linear momentum results in the equations of motion; the

principle of conservation of angular momentum yields, when no body couples exist, symmetry of the stress tensor. For additional details, see Reddy [4], Reddy and Gartling [5] and Schlichting and Gersten [6]. More details are provided in Chapter 11, which is dedicated to finite element analysis of two-dimensional flows of viscous incompressible fluids.

In this section, we consider the so-called parallel steady flow where all fluid particles are moving in one direction, that is, only one velocity component is non-zero, $v_x = u(x, y, z)$, where v_x is the velocity component along the x coordinate. We assume that there are no body forces. The z-momentum equation requires that $v_x = u(x, y)$. The conservation of mass in this case reduces to

$$\frac{\partial u}{\partial x} = 0, \quad \text{which implies that} \quad u = u(y)$$

The y-momentum equation simplifies to

$$\frac{\partial P}{\partial y} = 0, \quad \text{which implies that} \quad P = P(x)$$

where P is the pressure. The x-momentum equation simplifies to

$$-\mu \frac{d^2 u}{dy^2} = -\frac{dP}{dx} \tag{4.3.1}$$

The energy equation as applied to a viscous flow region has the form

$$\rho c u \frac{\partial T}{\partial x} - k\left(\frac{\partial^2 T}{\partial x^2} + \frac{\partial^2 T}{\partial y^2}\right) = \mu \left(\frac{du}{dy}\right)^2 \tag{4.3.2}$$

where the fluid is assumed to be isotropic and homogeneous (i.e., k is a constant). The first and last terms in the above equation couple the velocity u to the temperature T. For a given velocity field $u(y)$ [i.e., known from Eq. (4.3.1)], one can solve Eq. (4.3.2) to determine the temperature field.

4.3.2 Finite Element Model

In this section we are interested in solving Eq. (4.3.1) to determine the velocity $u(y)$ due to an applied pressure gradient, $-dP/dx$. Equation (4.3.1) is a special case of the model equation (3.4.1), with the following correspondence:

$$f = -\frac{dP}{dx} = \text{constant} \equiv f_0, \quad a = \mu = \text{constant}, \quad c = 0, \quad x = y \tag{4.3.3}$$

Therefore, the finite element equations in (3.4.32b) and (3.4.33) are valid for this problem:

$$\mathbf{K}^e\mathbf{u}^e = \mathbf{f}^e + \mathbf{Q}^e \tag{4.3.4a}$$

$$K_{ij}^e = \int_{y_a}^{y_b} \mu \frac{d\psi_i^e}{dy}\frac{d\psi_j^e}{dy}\,dy, \quad f_i^e = \int_{y_a}^{y_b} \left(-\frac{dP}{dx}\right)\psi_i^e\,dy \tag{4.3.4b}$$

$$Q_1^e = -\left(\mu\frac{du}{dy}\right)\Big|_a, \quad Q_2^e = \left(\mu\frac{du}{dy}\right)\Big|_b \tag{4.3.4c}$$

Example 4.3.1

Consider parallel flow between two long flat walls separated by a distance $2L$ [see Fig. 4.3.1(a)]. Determine the velocity distribution $u(y)$, $-L < y < L$, for a given pressure gradient $-dP/dx$ and for the following two sets of boundary conditions [see Fig. 4.3.1(b)]:

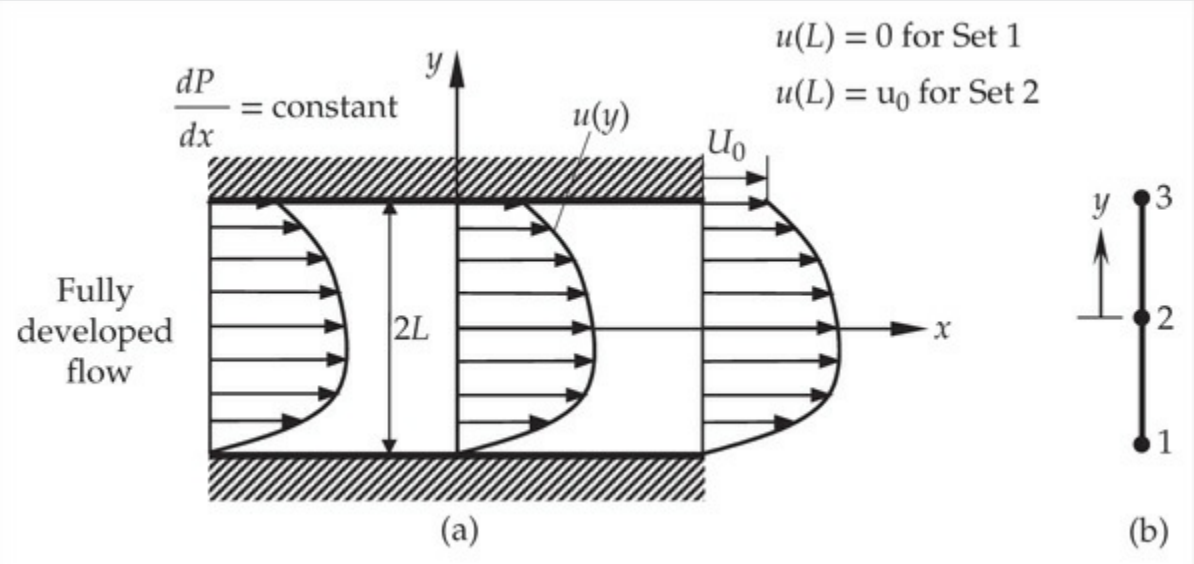

Fig. 4.3.1 (a) Flow between parallel plates. (b) Finite element mesh.

Set 1: $u(-L) = 0, \; u(L) = 0$ (two stationary walls: *Poiseuille flow*) (1)

Set 2: $u(-L) = 0, \; u(L) = U_0$ (bottom wall stationary and top wall moving: *Couette flow*) (2)

Use (a) two-element mesh of linear finite elements and (b) one-element

mesh of the quadratic element.

Solution: Here we consider the full domain for the two sets of boundary conditions.

(a) For a two-element mesh of linear elements ($h = L$), the assembled equations are

$$\frac{\mu}{h}\begin{bmatrix} 1 & -1 & 0 \\ -1 & 2 & -1 \\ 0 & -1 & 1 \end{bmatrix}\begin{Bmatrix} U_1 \\ U_2 \\ U_3 \end{Bmatrix} = \frac{f_0 h}{2}\begin{Bmatrix} 1 \\ 2 \\ 1 \end{Bmatrix} + \begin{Bmatrix} Q_1^1 \\ Q_2^1 + Q_1^2 = 0 \\ Q_2^2 \end{Bmatrix} \tag{3}$$

We note that the interpolation functions for the two elements are

$$\psi_1^1(y) = -\frac{y}{L}, \quad \psi_2^1(y) = 1 + \frac{y}{L}, \quad \psi_1^2(y) = 1 - \frac{y}{L}, \quad \psi_2^2(y) = \frac{y}{L} \tag{4}$$

For set 1 boundary conditions, $U_1 = U_3 = 0$, the finite element solution is given by

$$U_2 = \frac{f_0 L^2}{2\mu}, \quad u_h(y) = \begin{cases} \frac{f_0 L^2}{2\mu}\left(1 + \frac{y}{L}\right), & -L \le y \le 0 \\ \frac{f_0 L^2}{2\mu}\left(1 - \frac{y}{L}\right), & 0 \le y \le L \end{cases} \tag{5}$$

For set 2 boundary conditions, $U_1 = 0$ and $U_3 = U_0$, the finite element solution is

$$U_2 = \frac{f_0 L^2}{2\mu} + \frac{1}{2}U_0, \quad u_h(y) = \begin{cases} \left(\frac{f_0 L^2}{2\mu} + \frac{1}{2}U_0\right)\left(1 + \frac{y}{L}\right), & -L \le y \le 0 \\ \left(\frac{f_0 L^2}{2\mu} + \frac{1}{2}U_0\right)\left(1 - \frac{y}{L}\right) + U_0\frac{y}{L}, & 0 \le y \le L \end{cases} \tag{6}$$

(b) For a one-element mesh of the quadratic element ($h = 2L$), we have

$$\frac{\mu}{6L}\begin{bmatrix} 7 & -8 & 1 \\ -8 & 16 & -8 \\ 1 & -8 & 7 \end{bmatrix}\begin{Bmatrix} U_1 \\ U_2 \\ U_3 \end{Bmatrix} = \frac{f_0 L}{3}\begin{Bmatrix} 1 \\ 4 \\ 1 \end{Bmatrix} + \begin{Bmatrix} Q_1^1 \\ 0 \\ Q_3^1 \end{Bmatrix} \tag{7}$$

The finite element solutions for the two sets of boundary conditions are $[\psi_2^1(y) = 1 - y^2/L^2$ and $\psi_3^1(y) = 0.5(1 - y/L)(y/L)]$

Set 1: $U_2 = \frac{f_0 L^2}{2\mu}, \qquad u_h(y) = \frac{f_0 L^2}{2\mu}\left(1 - \frac{y^2}{L^2}\right)$ (8)

$$\textbf{Set 2:}\quad U_2 = \frac{f_0 L^2}{2\mu} + \frac{1}{2}U_0, \quad u_h(y) = \left(\frac{f_0 L^2}{2\mu} + \frac{1}{2}U_0\right)\left(1 - \frac{y^2}{L^2}\right) + \frac{1}{2}U_0\left(\frac{y}{L} + \frac{y^2}{L^2}\right) \tag{9}$$

Although the nodal values predicted in the linear- and quadratic-element meshes are the same, they vary linearly and quadratically between nodes of linear and quadratic elements, respectively.

The exact solutions for the two sets of boundary conditions in Eqs. (1) and (2) are ($-L \le y \le L$)

$$\textbf{Set 1:}\quad u(y) = \frac{f_0 L^2}{2\mu}\left(1 - \frac{y^2}{L^2}\right) \tag{10}$$

$$\textbf{Set 2:}\quad u(y) = U_0\frac{1}{2}\left(1 + \frac{y}{L}\right) + \frac{f_0 L^2}{2\mu}\left(1 - \frac{y^2}{L^2}\right) \tag{11}$$

Note that the finite element solutions at the nodes are exact, as expected. The quadratic-element solutions in Eqs. (8) and (9) coincide with the exact solutions in Eqs. (10) and (11), respectively.

4.4 Solid and Structural Mechanics

4.4.1 Preliminary Comments

Solid mechanics is that branch of mechanics dealing with the motion and deformation of solids (see [7–9]). The Lagrangian description of motion is used to express the global conservation laws [4]. The conservation of mass for solid bodies is trivially satisfied because of the fixed material viewpoint used in the Lagrangian description. The conservation of momentum is nothing but Newton's second law of motion. Under isothermal conditions, the energy equation uncouples from the momentum equations, and we need only consider the equations of motion or equilibrium.

Unlike in fluid mechanics, the equations governing solid bodies undergoing different forms of deformations are derived directly, without specializing the three-dimensional elasticity equations. Various types of load-carrying members are called by different names, for example, bars, beams, and plates [7]. A *bar* is a structural member that is subjected to only axial loads (see **Examples 1.2.3** and **2.3.1**), while a *beam* is a member that is subjected to loads that tend to bend it about an axis perpendicular to

the axis of the member (see **Example 2.4.2**). A *plate* is a two-dimensional flat body whose thickness is very small compared to the in-plane dimensions and subjected loads transverse to the plane, causing bending. If a plate is subjected only to in-plane forces, it is known as a plane elastic body. Thus, plane elastic body is two-dimensional version of a bar while plate is a two-dimensional version of a beam. The finite element modeling of beams will be considered in Chapter 5; plane elastic bodies will be considered in Chapter 12. In this section we consider the finite element analysis of bars and cables.

4.4.2 Finite Element Model of Bars and Cables

The average transverse deflection $u(x)$ of a cable (also termed rope or string) made of elastic material is also governed by an equation of the form:

$$-\frac{d}{dx}\left(a\frac{du}{dx}\right)=f(x) \tag{4.4.1}$$

where a is the uniform tension in the cable and f is the distributed transverse force. Equation (4.4.1) is a special case of Eq. (3.4.1), with c = 0. Therefore, the finite element equations presented in (3.4.32b) and (3.4.33) are valid (with c = 0) for cables.

For axial deformation of bars, we also consider the effect of temperature increase (from a room temperature) on the strain, while presuming that the material properties are unaffected by the temperature change. The equations governing axial deformation of a bar are (see **Example 1.2.3**)

$$\text{Equilibrium:} \quad -\frac{d(A\sigma)}{dx}=f(x) \tag{4.4.2a}$$

$$\text{Kinematics:} \quad \varepsilon=\frac{du}{dx}-\alpha T \tag{4.4.2b}$$

$$\text{Hooke's law:} \quad \sigma=E\varepsilon \tag{4.4.2c}$$

where $\sigma(x)$ denotes the axial stress (N/m^2 = Pa), $\varepsilon(x)$ (m/m) is the axial strain, $u(x)$ is the axial displacement (m), $T(x)$ is the temperature rise from a reference value (°C), $E = E(x)$ is the modulus of elasticity (Pa), $\alpha(x)$ is the thermal coefficient of expansion (1/°C), $A = A(x)$ is the area of cross section of the bar (m^2), and $f(x)$ is the body force (N/m). It should be

recalled that Eq. (4.4.2b) is derived under the assumption that the stress on any cross section is uniform.

When σ and ε are eliminated using Eqs. (4.4.2b) and (4.4.2c), Eq. (4.4.2a) can be expressed solely in terms of the displacement u as

$$-\frac{d}{dx}\left[EA\left(\frac{du}{dx}-\alpha T\right)\right]=f(x) \tag{4.4.3}$$

In deriving the weak form of Eq. (4.4.3), we must preserve the physical meaning of the secondary variable and integrate by parts the entire expression inside the square brackets:

$$0=\int_{x_a^e}^{x_b^e}\left[E_eA_e\frac{dw}{dx}\left(\frac{du^e}{dx}-\alpha_eT_e\right)-wf(x)\right]dx-Q_1^e w(x_a^e)-Q_2^e w(x_b^e) \tag{4.4.4a}$$

where Q_1^e and Q_2^e are the forces at the left and right ends of the element:

$$Q_1^e=\left[-E_eA_e\left(\frac{du_h^e}{dx}-\alpha_eT_e\right)\right]_{x_a^e},\quad Q_2^e=\left[E_eA_e\left(\frac{du_h^e}{dx}-\alpha_eT_e\right)\right]_{x_b^e} \tag{4.4.4b}$$

The finite element model is

$$\mathbf{K}^e\mathbf{u}^e=\mathbf{f}^e+\mathbf{Q}^e \tag{4.4.5a}$$

$$K_{ij}^e=\int_{x_a^e}^{x_b^e}E_eA_e\frac{d\psi_i^e}{dx}\frac{d\psi_j^e}{dx}\,dx,\quad f_i^e=\int_{x_a^e}^{x_b^e}\left(f\psi_i^e+E_eA_e\alpha_eT_e\frac{d\psi_i^e}{dx}\right)dx \tag{4.4.5b}$$

Values of various integrals presented in Table 3.7.1 facilitate the computation of the element matrices in Eq. (4.4.5b).

Next, an alternative derivation of the finite element model that is found in structural mechanics finite element books is presented here for the sake of information. The derivation makes use of matrix notation to write all equations.

The total potential energy, Π^e, of a bar element (see Eq. (3.4.10)) is

$$\Pi^e=\frac{1}{2}\int_{x_a^e}^{x_b^e}A_e(\varepsilon^e)^{\mathrm{T}}\sigma^e\,dx-\int_{x_a^e}^{x_b^e}(u^e)^{\mathrm{T}}f\,dx-\sum_i(u_i^e)^{\mathrm{T}}Q_i^e \tag{4.4.6}$$

The finite element approximation u_h^e in Eq. (3.4.28) of u^e can be expressed

(for a Lagrange finite element with n nodes) as

$$u_h^e = \sum_{j=1}^{n} \psi_j^e(x) u_j^e = \{\psi_1^e \ \psi_2^e \ \dots \ \psi_n^e\} \begin{Bmatrix} u_1^e \\ u_2^e \\ \vdots \\ u_n^e \end{Bmatrix} \equiv \boldsymbol{\Psi}^e \mathbf{u}^e \tag{4.4.7}$$

The strains in Eq. (4.4.2b) and stresses in Eq. (4.4.2c) take the form

$$\begin{aligned} \varepsilon^e &= \frac{du_h^e}{dx} - \alpha_e T_e = \frac{d}{dx}(\boldsymbol{\Psi}^e \mathbf{u}^e) - \alpha_e T_e = \frac{d\boldsymbol{\Psi}^e}{dx}\mathbf{u}^e - \alpha_e T_e \equiv \mathbf{B}^e \mathbf{u}^e - \alpha_e T_e \\ \sigma^e &= E_e \varepsilon^e = E_e(\mathbf{B}^e \mathbf{u}^e - \alpha_e T_e) \end{aligned} \tag{4.4.8}$$

and the expression for the total potential energy becomes

$$\begin{aligned} \Pi^e = \frac{1}{2}\int_{x_a^e}^{x_b^e} A_e[(\mathbf{u}^e)^{\mathrm{T}}(\mathbf{B}^e)^{\mathrm{T}} - \alpha_e T_e] E_e (\mathbf{B}^e \mathbf{u}^e - \alpha_e T_e)\, dx \\ - \int_{x_a^e}^{x_b^e} (\mathbf{u}^e)^{\mathrm{T}} (\boldsymbol{\Psi}^e)^{\mathrm{T}} f\, dx - (\mathbf{u}^e)^{\mathrm{T}} \mathbf{Q}^e \end{aligned} \tag{4.4.9}$$

Then the principle of minimum total potential energy, $\delta\Pi^e = 0$, yields:

$$0 = \left(\int_{x_a^e}^{x_b^e} (\mathbf{B}^e)^{\mathrm{T}} E_e A_e \mathbf{B}^e\, dx \right) \mathbf{u}^e - \int_{x_a^e}^{x_b^e} \left[(\boldsymbol{\Psi}^e)^{\mathrm{T}} f + (\mathbf{B}^e)^{\mathrm{T}} E_e A_e \alpha_e T_e \right] dx - \mathbf{Q}^e \tag{4.4.10}$$

where we have used $\delta(\alpha_e T_e) = 0$ (because a specified quantity cannot be varied) and that $\delta\mathbf{u}^e$ is arbitrary. The finite element model is

$$\mathbf{K}^e \mathbf{u}^e = \mathbf{f}^e + \mathbf{Q}^e \tag{4.4.11a}$$

$$\begin{aligned} \mathbf{K}^e &= \int_{x_a^e}^{x_b^e} (\mathbf{B}^e)^{\mathrm{T}} D_e \mathbf{B}^e\, dx \\ \mathbf{f}^e &= \int_{x_a^e}^{x_b^e} \left[(\boldsymbol{\Psi}^e)^{\mathrm{T}} f + (\mathbf{B}^e)^{\mathrm{T}} D_e \alpha_e T_e \right] dx \end{aligned} \tag{4.4.11b}$$

where $D_e = E_e A_e$. Equations (4.4.11a) and (4.4.11b) are just a matrix form of the equations already presented in Eqs. (4.4.5a) and (4.4.5b), except that

the present model is in a matrix form.

4.4.3 Numerical Examples

In this section we consider a number of examples of finite element analysis of bars. Some require the formulation of the problem (i.e., equations are not readily available).

Example 4.4.1

A bridge is typically supported by several concrete piers, and the geometry and loads of a typical (but idealized) pier are shown in Fig. 4.4.1. The load 20 kN/m^2 represents the weight of the bridge and an assumed distribution of the traffic on the bridge at any fixed time. The concrete weighs approximately 25 kN/m^3 and its modulus is E = 28 GPa = 28 × 10^9 N/m^2. The pier is indeed a three-dimensional structure, but you may approximate the deformation and stress fields in the pier as one-dimensional with respect to the height. Analyze the pier for displacements and stresses using meshes of linear 1-D finite elements.

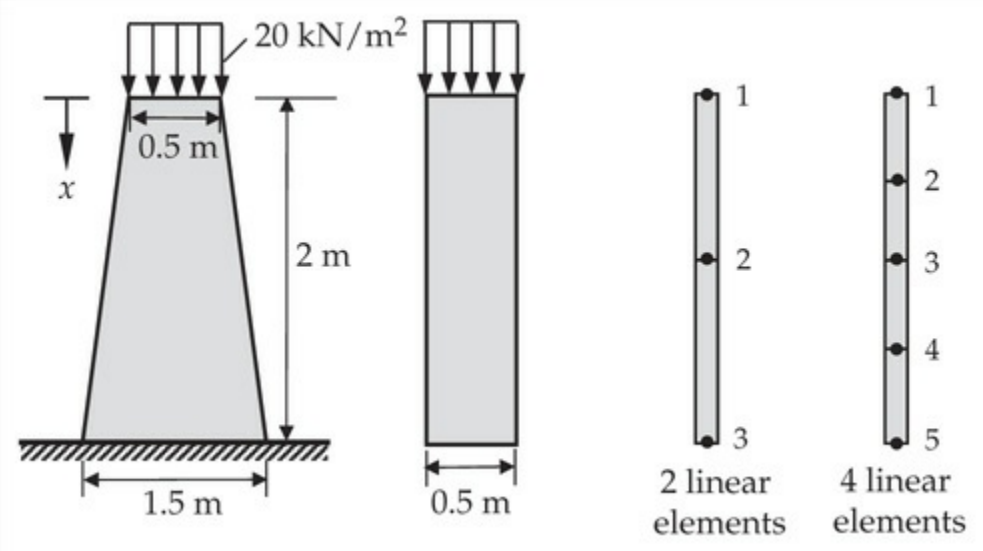

Fig. 4.4.1 The geometry and loading in the concrete pier problem of **Example 4.4.1**.

Solution: Since the pier is modeled as a one-dimensional member with respect to its height, we must represent the distributed force at the top of the pier as a point force

$$F_0 = (0.5 \times 0.5)20 = 5 \text{ kN} \tag{1}$$

The weight of the concrete may be represented as the body force per unit length. The total force at any distance x, measured from the top of the pier, is equal to the weight of the concrete above that point. Thus, the weight at a distance x is equal to the product of the volume of the body above x and the specific weight of the concrete:

$$W(x) = 0.5\frac{0.5 + (0.5 + 0.5x)}{2}x \times 25.0 = 6.25(1 + 0.5x)x \text{ kN} \tag{2}$$

The body force per unit length is computed from

$$f(x) = \frac{dW}{dx} = 6.25(1 + x) \text{ kN/m} \tag{3}$$

This completes the load representation of the problem.

The governing differential equation for the problem is given by Eq. (4.4.1), with $a = EA$, $E = 28 \times 10^6$ kN/m^2, and cross-sectional area $A(x)$ at a distance x:

$$A(x) = (0.5 + 0.5x)0.5 = \frac{1}{4}(1 + x) \text{ m}^2 \tag{4}$$

Thus, the concrete pier problem is idealized as a one-dimensional problem whose axial displacement u is governed by the equation ($E = 28 \times 10^9$ N/m^2)

$$-\frac{d}{dx}\left[\frac{1}{4}E(1 + x)\frac{du}{dx}\right] = 6250(1 + x) \tag{5a}$$

subject to the boundary conditions

$$-\left[\frac{1}{4}E(1 + x)\frac{du}{dx}\right]\Big|_{x=0} = 5000, \quad u(2) = 0 \tag{5b}$$

Equation (5a) is a special case of the model equation, Eq. (4.4.1), with the following correspondence:

$$a(x) = 7 \times 10^9 (1 + x), \quad f(x) = 6250(1 + x) \tag{6}$$

For a typical linear element, the stiffness matrix and force vector can be computed as

$$\mathbf{K}^e = \frac{7 \times 10^9}{h_e}\left[1 + \frac{1}{2}(x_a^e + x_b^e)\right]\begin{bmatrix} 1 & -1 \\ -1 & 1 \end{bmatrix} \tag{7a}$$

$$\mathbf{f}^e = 6250\frac{h_e}{2}\left(\begin{Bmatrix} 1 \\ 1 \end{Bmatrix} + \frac{1}{3}\begin{Bmatrix} x_b^e + 2x_a^e \\ 2x_b^e + x_a^e \end{Bmatrix}\right) \tag{7b}$$

where x_a^e is the global coordinate of the first node and x_b^e is the global coordinate of the second node of the eth element. Let us consider a two-element mesh with $h_1 = h_2 = 1$ m. For element 1, we have $x_a^1 = 0$ and $x_b^1 = h_1$; and for element 2, we have $x_a^2 = h_1$ and $x_b^2 = h_1 + h_2$. Thus,

$$\mathbf{K}^1 = 10^9\begin{bmatrix} 10.5 & -10.5 \\ -10.5 & 10.5 \end{bmatrix}, \quad \mathbf{f}^1 = \frac{6250}{6}\begin{Bmatrix} 3+1 \\ 3+2 \end{Bmatrix} = \begin{Bmatrix} 4167 \\ 5208 \end{Bmatrix} \tag{8a}$$

$$\mathbf{K}^2 = 10^9\begin{bmatrix} 17.5 & -17.5 \\ -17.5 & 17.5 \end{bmatrix}, \quad \mathbf{f}^2 = \frac{6250}{6}\begin{Bmatrix} 3+4 \\ 3+5 \end{Bmatrix} = \begin{Bmatrix} 7292 \\ 8333 \end{Bmatrix} \tag{8b}$$

The assembled equations of two linear elements connected in series are

$$10^9\begin{bmatrix} 10.5 & -10.5 & 0.000 \\ -10.5 & 28.0 & -17.5 \\ 0.000 & -17.5 & 17.5 \end{bmatrix}\begin{Bmatrix} U_1 \\ U_2 \\ U_3 \end{Bmatrix} = \begin{Bmatrix} 4167 \\ 12500 \\ 8333 \end{Bmatrix} + \begin{Bmatrix} Q_1^1 \\ Q_2^1 + Q_1^2 = 0 \\ Q_2^2 \end{Bmatrix} \tag{9}$$

The boundary conditions in Eq. (5b) translate to

$$Q_1^1 = F_0 = 5000 \text{ N}, \quad U_3 = 0 \tag{10}$$

The condensed equations for the unknown displacements and forces are then

$$10^9\begin{bmatrix} 10.5 & -10.5 \\ -10.5 & 28.0 \end{bmatrix}\begin{Bmatrix} U_1 \\ U_2 \end{Bmatrix} = \begin{Bmatrix} 9167 \\ 12500 \end{Bmatrix}, \quad (Q_2^2)_{\text{equil}} = -17.5 \times 10^9\, U_2 - 8333 \tag{11}$$

The solution is given by (positive displacements, because of the coordinate system used, indicate that the pier is in compression)

$$U_1 = u_h(0) = 2.1111 \times 10^{-6}\text{m}, \quad U_2 = u_h(0.5) = 1.2381 \times 10^{-6}\text{m}, \quad (Q_2^2)_{\text{equil}} = -30000 \text{ N} \tag{12}$$

Hence, the stress at the fixed end is (compressive)

$$\sigma_x = \frac{Q_2^2}{A_L} = -\frac{30000}{0.75} = -40000 \text{ N/m}^2 \tag{13}$$

Note that $(Q_2^2)_{\text{def}}$ is given by

$$(Q_2^2)_{\text{def}} = \left(EA \frac{du_h^2}{dx} \right)_{x=2} = 28 \times 10^9 \times 0.75 \left(\frac{U_3 - U_2}{1} \right) = -26000 \text{ N} \tag{14}$$

which is in considerable error for this crude mesh.

The exact solution of Eqs. (5a) and (5b) is

$$u(x) = \frac{1}{E} \left[56250 - 6250(1 + x)^2 - 7500 \ln \left(\frac{1 + x}{3} \right) \right] \tag{15}$$

The exact values of u at $x = 0$ m and $x = 1$ m and the reaction at $x = 2$ m are

$$u(0) = 2.080 \times 10^{-6} \text{m}, \quad u(1) = 1.225 \times 10^{-6} \text{m}, \quad \left[EA \frac{du}{dx} \right]_{x=2} = -30000 \text{ N} \tag{16}$$

The finite element solution at the nodes is not exact because $a = EA$ is not a constant in this problem.

The solution can be improved with refined meshes. For example, the mesh of four linear elements gives the displacements u_h (0) = 2.0877 × 10^{-6} m and u_h (0.5) = 1.2281 × 10^{-6} m, and $(Q_2^2)_{\text{def}}$ for this mesh is 27898 N. A mesh of two quadratic elements (of equal length) gives the solution: u_h (0) = 2.0797 × 10^{-6} m and u_h (0.5) = 1.2247 × 10^{-6} m; $(Q_2^2)_{\text{def}}$ for this mesh is 29949 N.

Example 4.4.2

Consider the composite bar consisting of a tapered steel bar fastened to an aluminum rod of uniform cross section, and subjected to loads as shown in Fig. 4.4.2. Determine the displacement field in the bar using (a) one linear element in each part and (b) one quadratic element in each part. Use the following data:

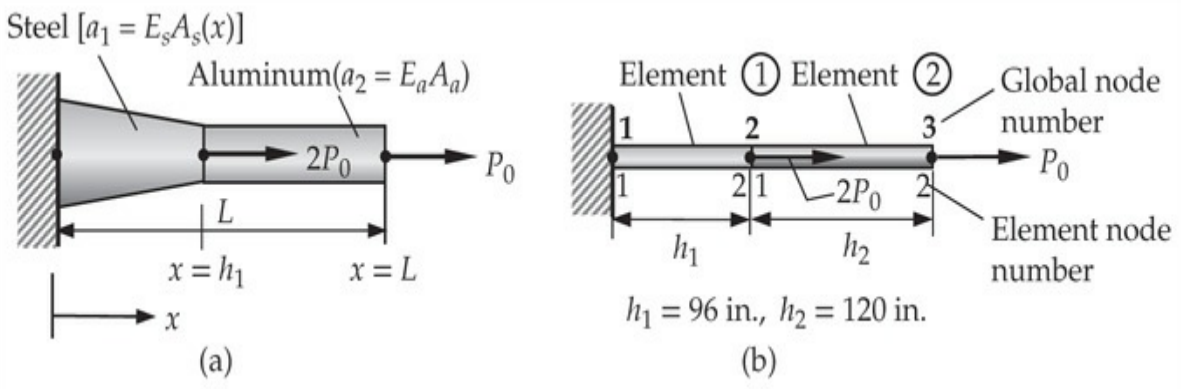

Fig. 4.4.2 Axial deformation of a composite bar. (a) Geometry and loading (b) Finite element representation with two linear elements.

$$E_s = 30 \times 10^6 \text{ psi}, A_s = \left(1.5 - \tfrac{1}{192}x\right)^2 \text{ in}^2, E_a = 10^7 \text{ psi}, \quad (1)$$
$$A_a = 1 \text{ in.}^2, \ h_1 = 96 \text{ in.}, \ h_2 = 120 \text{ in.}, \ L = 216 \text{ in.}, \ P_0 = 10000 \text{ lb}$$

where the subscript "s" refers to steel and "a" to aluminum.
Solution: The governing equations are given by

$$-\frac{d}{dx}\left(E_s A_s \frac{du_s}{dx}\right) = 0, \quad 0 < x < h_1 \quad (2a)$$

$$-\frac{d}{dx}\left(E_a A_a \frac{du_a}{dx}\right) = 0, \quad h_1 < x < h_1 + h_2 = L \quad (2b)$$

The boundary conditions are obvious from Fig. 4.4.2.

The minimum number of elements needed to solve the problem is 2. For elements in the steel portion, A_s is a function of x, and for elements in the aluminum portion, we have $A_a = 1$. Hence, we need to evaluate K_{ij}^e in steel and aluminum using the definitions (it is convenient to use the local coordinate $\bar{x}$; $x = \bar{x} + x_a$, $dx = d\bar{x}$, and $d\psi_i^e/dx = d\psi_i^e/d\bar{x}$)

$$(K_{ij}^e)_s = \int_0^{h_e} E_s \left[1.5 - \left(\frac{\bar{x} + x_a^e}{192}\right)\right]^2 \frac{d\psi_i^e}{d\bar{x}} \frac{d\psi_j^e}{d\bar{x}} d\bar{x}; \quad (K_{ij}^e)_a = \int_0^{h_e} E_a \frac{d\psi_i^e}{d\bar{x}} \frac{d\psi_j^e}{d\bar{x}} d\bar{x} \quad (3)$$

respectively. We note that $f_i^e = 0$ for both parts.

(a) *Mesh of linear elements.* First, we evaluate K_{11}^e for steel as follows:

$$K_{11}^e = \frac{E_s}{h_e^2} \int_0^{h_e} [k_1 + k_2(\bar{x} + x_a^e)]^2 d\bar{x}$$
$$= \frac{E_s}{h_e}\left\{(k_1)^2 + (k_2)^2\left[(x_a^e)^2 + \tfrac{1}{3}h_e^2 + x_a^e h_e\right] + 2k_1k_2(x_a^e + 0.5h_e)\right\} \equiv \frac{E_s \bar{A}_s}{h_e} \quad (4a)$$

where $k_1 = 1.5$, $k_2 = -1/192$, and

$$\bar{A}_s = (k_1)^2 + (k_2)^2\left[(x_a^e)^2 + \tfrac{1}{3}h_e^2 + x_a^e h_e\right] + k_1k_2(2x_a^e + h_e) \quad (4b)$$

It is obvious that $K_{22}^e = K_{11}^e$ and $K_{12}^e = K_{21}^e = -K_{11}^e$. Hence, the finite element equations of a typical element in steel and aluminum are given

by

$$\frac{E_s \bar{A}_s}{h_e}\begin{bmatrix} 1 & -1 \\ -1 & 1 \end{bmatrix}\begin{Bmatrix} u_1^e \\ u_2^e \end{Bmatrix} = \begin{Bmatrix} Q_1^e \\ Q_2^e \end{Bmatrix} \tag{5a}$$

$$\frac{E_a}{h_e}\begin{bmatrix} 1 & -1 \\ -1 & 1 \end{bmatrix}\begin{Bmatrix} u_1^e \\ u_2^e \end{Bmatrix} = \begin{Bmatrix} Q_1^e \\ Q_2^e \end{Bmatrix} \tag{5b}$$

For a mesh of two linear elements of lengths $h_1 = 96$ in. and $h_2 = 120$ in., the element stiffness matrices become ($E_s = 30 \times 10^6$, $k_1 = 1.5$, $k_2 = -1/192$, and $x_a^1 = 0$, i.e., $\bar{A}_s = 4.75/3$

for element 1, and $E_a = 10 \times 10^6$ for element 2):

$$\begin{aligned} \mathbf{K}^1 &= \frac{47.5 \times 10^6}{96}\begin{bmatrix} 1 & -1 \\ -1 & 1 \end{bmatrix} = 10^4\begin{bmatrix} 49.479 & -49.479 \\ -49.479 & 49.479 \end{bmatrix} \\ \mathbf{K}^2 &= \frac{10 \times 10^6}{120}\begin{bmatrix} 1 & -1 \\ -1 & 1 \end{bmatrix} = 10^4\begin{bmatrix} 8.333 & -8.333 \\ -8.333 & 8.333 \end{bmatrix} \end{aligned} \tag{6}$$

Since the two elements are connected in series, the assembled equations are

$$10^4\begin{bmatrix} 49.479 & -49.479 & 0.000 \\ -49.479 & 57.812 & -8.333 \\ 0.000 & -8.333 & 8.333 \end{bmatrix}\begin{Bmatrix} U_1 \\ U_2 \\ U_3 \end{Bmatrix} = \begin{Bmatrix} Q_1^1 \\ Q_2^1 + Q_1^2 = 2P_0 \\ Q_2^2 \end{Bmatrix} \tag{7}$$

The boundary conditions $u(0) = 0$ and $[E_a\,(du_a/dx)]L = P_0$ imply

$$U_1 = 0, \quad Q_2^2 = P_0 \tag{8}$$

Hence, the condensed equations are

$$10^4\begin{bmatrix} 57.812 & -8.333 \\ -8.333 & 8.333 \end{bmatrix}\begin{Bmatrix} U_2 \\ U_3 \end{Bmatrix} = \begin{Bmatrix} 2P_0 \\ P_0 \end{Bmatrix}, \quad Q_1^1 = -10^4 \times 49.479\, U_2 \tag{9}$$

whose solution is

$$U_2 = 0.06063 \text{ in.}, \quad U_3 = 0.18063 \text{ in.}, \quad (Q_1^1)_{\text{equil}} = -30000 \text{ lb} \tag{10}$$

The negative sign indicates that the reaction is acting away from the end (i.e., tensile force). The magnitude of Q_1^1 is consistent with the static equilibrium of the forces:

$$Q_1^1 + 2P_0 + P_0 = 0 \text{ or } Q_1^1 = -3P_0 = -30000 \text{ lb} \tag{11}$$

The axial displacement at any point x along the bar is given by [$\psi_1^e = (x_b^e - x)/h_e$ and $\psi_2^e = (x - x_a^e)/h_e$]

$$u_h(x) = \begin{cases} u_1^{(1)}\psi_1^{(1)}(x) + u_2^{(1)}\psi_2^{(1)}(x) = 0.00063\,x, & 0 \le x \le 96 \\ u_1^{(2)}\psi_1^{(2)}(x) + u_2^{(2)}\psi_2^{(2)}(x) = -0.03537 + 0.001x, & 96 \le x \le 216 \end{cases} \tag{12}$$

and its first derivative is given by

$$\frac{du_h}{dx} = \begin{cases} 0.00063, & 0 \le x \le 96 \\ 0.001, & 96 \le x \le 216 \end{cases} \tag{13}$$

The exact solution of Eqs. (2a,b) subject to the boundary conditions

$$u(0) = 0, \quad \left[\left(E_a \frac{du_a}{dx}\right)_{x=96^+} - \left(E_s A_s \frac{du_s}{dx}\right)_{x=96^-}\right] = 2P_0, \quad \left(E_a \frac{du_a}{dx}\right)_{x=216} = P_0 \tag{14}$$

is given by

$$u(x) = \begin{cases} 0.128[x/(288 - x)], & 0 \le x \le 96 \\ 0.001(x - 32), & 96 \le x \le 216 \end{cases}$$
$$\frac{du}{dx} = \begin{cases} 36.864/(288 - x)^2, & 0 \le x \le 96 \\ 0.001, & 96 \le x \le 216 \end{cases} \tag{15}$$

In particular, the exact solution at nodes 2 and 3 is given by

$$u(96) = 0.064 \text{ in.}, \quad u(216) = 0.1840 \text{ in.} \tag{16}$$

Thus, the two-element solution is about 1.8% off from the maximum displacement.

(b) *Mesh of quadratic elements*. For a mesh of two linear elements of lengths h_1 = 96 in. and h_2 = 120 in. the element matrices are

$$\mathbf{K}^1 = 10^4 \begin{bmatrix} 142.19 & -159.37 & 17.18 \\ -159.37 & 266.67 & -107.29 \\ 17.18 & -107.29 & 90.10 \end{bmatrix}, \quad \mathbf{K}^2 = \frac{10^7}{3 \times 120} \begin{bmatrix} 7 & -8 & 1 \\ -8 & 16 & -8 \\ 1 & -8 & 7 \end{bmatrix} \tag{17}$$

The condensed equations for the two-element mesh are

$$10^6 \begin{bmatrix} 2.6667 & -1.0729 & 0.0000 & 0.0000 \\ -1.0729 & 1.0955 & -0.2222 & 0.0278 \\ 0.0000 & -0.2222 & 0.4444 & -0.2222 \\ 0.0000 & 0.0278 & -0.2222 & 0.1944 \end{bmatrix} \begin{Bmatrix} U_2 \\ U_3 \\ U_4 \\ U_5 \end{Bmatrix} = 10^4 \begin{Bmatrix} 0 \\ 2 \\ 0 \\ 1 \end{Bmatrix} \tag{18}$$

Solving the 4 × 4 equations, we obtain

$$U_2 = 0.02572 \text{ in.}, \quad U_3 = 0.06392 \text{ in.}, \quad U_4 = 0.12392 \text{ in.}, \quad U_5 = 0.18392 \text{ in.} \tag{19}$$

The two-element solution obtained using the quadratic element is very accurate, as can be seen from a comparison of the finite element solution with the exact solution presented in Table 4.4.1.

Table 4.4.1 Comparison of the finite element solutions with the exact solution of the bar problem in **Example 4.4.2**.

x (in.)	Exact solution	Linear[1]				Quadratic[1]	
		(1, 1)	(2, 1)	(3, 2)	(6, 2)	(1, 1)	(3, 1)
16	0.00753	–	–	–	0.00752	–	0.00753
32	0.01600	–	–	0.01593	0.01598	–	0.01600
48	0.02560	–	0.02532	–	0.02557	0.02572	0.02560
64	0.03657	–	–	0.03638	0.03652	–	0.03657
80	0.04923	–	–	–	0.04916	–	0.04923
96	0.06400	0.06063	0.06309	0.06359	0.06390	0.06392	0.06400
156	0.12400	–	–	0.12359	0.12390	0.12392	0.12400
216	0.18400	0.18063	0.18309	0.18359	0.18390	0.18392	0.18400

[1] (m, n) means m elements in the interval (0, 96) and n elements in the interval (96, 216); all elements in each interval are of the same size.

Example 4.4.3

A uniform stepped rod having two different solid circular cross sections is held between rigid supports as shown in Fig. 4.4.3. If the bar is subjected to uniform temperature increase of T = 30°C, determine (a) the compressive force in the bar, and (b) the displacement at the interface of the two cross sections. Assume the following data:

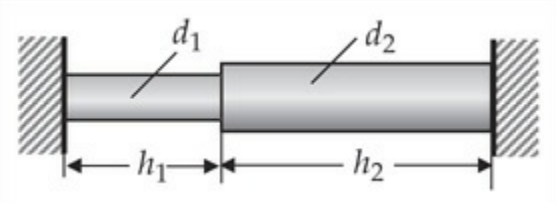

Fig. 4.4.3 A composite bar subjected to uniform temperature rise.

$$d_1 = 50 \text{ mm}, \quad d_2 = 75 \text{ mm}, \quad h_1 = 225 \text{ mm}, \quad h_2 = 300 \text{ mm}$$
$$E = 6 \times 10^9 \text{ Pa}, \quad \alpha = 100 \times 10^{-6}/^\circ\text{C} \tag{1}$$

Solution: The finite element model for this problem was formulated in Eqs. (4.4.5a) and (4.4.5b). The required results can be obtained with a mesh of two linear finite elements. First we calculate the necessary parameters:

$$k_1 = \frac{E_1 A_1}{h_1} = \frac{6 \times 10^9 \times \pi (50)^2 \times 10^{-6}}{4 \times 225 \times 10^{-3}} = 52.36 \times 10^6 \text{ N/m}$$
$$k_2 = \frac{E_2 A_2}{h_2} = \frac{6 \times 10^9 \times \pi (75)^2 \times 10^{-6}}{4 \times 300 \times 10^{-3}} = 88.36 \times 10^6 \text{ N/m} \tag{2}$$

$$A_1 E\alpha T = \frac{\pi}{4}(50)^2 \times 10^{-6} \times 6 \times 10^9 \times 100 \times 10^{-6} \times 30 = 353.43 \times 10^2 \text{ N}$$
$$A_2 E\alpha T = \frac{\pi}{4}(75)^2 \times 10^{-6} \times 6 \times 10^9 \times 100 \times 10^{-6} \times 30 = 795.22 \times 10^2 \text{ N} \tag{3}$$

Using the element equations in Eq. (4.4.5b), we obtain the following assembled equations [note that $f(x) = 0, f_1^e = -E_e A_e \alpha_e T_e$, and $f_2^e = E_e A_e \alpha_e T_e$]:

$$10^6 \begin{bmatrix} 52.36 & -52.36 & 0.00 \\ -52.36 & 140.72 & -88.36 \\ 0.00 & -88.36 & 88.36 \end{bmatrix} \begin{Bmatrix} U_1 \\ U_2 \\ U_3 \end{Bmatrix} = 10^2 \begin{Bmatrix} -353.43 \\ 353.43 - 795.22 \\ 795.22 \end{Bmatrix} + \begin{Bmatrix} Q_1^1 \\ Q_2^1 + Q_1^2 \\ Q_2^2 \end{Bmatrix} \tag{4}$$

The force balance and boundary conditions are

$$Q_2^1 + Q_1^2 = 0, \quad U_1 = 0, \quad U_3 = 0 \tag{5}$$

Hence, the condensed equation for U_2 yields

$$U_2 = \frac{353.43 - 795.22}{140.72} \times 10^{-4} = -0.31396 \times 10^{-3} \text{ m} \tag{6}$$

The negative sign indicates that the smaller section is in compression and the larger section is in tension due to the temperature change. The force $Q_1^1 = -Q_2^2$ can be computed from the first row of the assembled equations as

$$Q_1^1 = 10^6(-52.36) \times 10^{-3}(-0.31396) + 353.43 \times 10^2 = 51782 \text{ N} \tag{7}$$

The positive value indicates that the left end of the rod is in compression.

We note that Q_2^2 computed from the last row of the assembled equations will yield the same result but with a negative sign. The maximum compressive stress will occur in the smaller diameter portion and it is given by

$$\sigma = \frac{Q_1^1}{A_1} = \frac{51782}{1963.4954 \times 10^{-6}} = 26.372 \times 10^6 \text{ Pa} = 26.372 \text{ MPa} \tag{8}$$

Example 4.4.4

Consider a hollow circular cylinder with inner radius a, outer radius b, and length L. The outer surface of the hollow cylinder is assumed to be fixed and its inner surface ideally bonded to a rigid circular cylindrical core of radius a and length L, as shown in Fig. 4.4.4. Suppose that an axial force P is applied to the rigid core along its centroidal axis. Find the axial displacement δ of the rigid core by assuming that the displacement field in the hollow cylinder is of the form

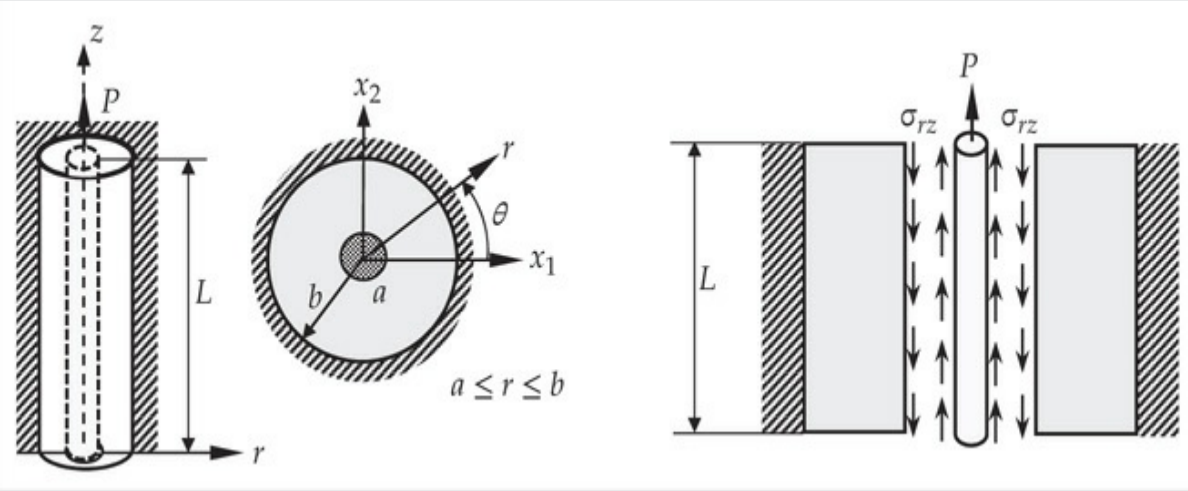

Fig. 4.4.4 Axisymmetric deformation of a hollow cylinder fixed at the outer surface and pulled by a rigid core at the inner surface.

$$u_r = u_\theta = 0, \quad u_z = U(r) \tag{1}$$

where (u_r, u_θ, u_z) are the displacements along (r, θ, z) coordinates.

Solution: The equation governing $U(r)$ can be determined as follows. We have

$$\varepsilon_{rr} = \varepsilon_{\theta\theta} = \varepsilon_{zz} = \varepsilon_{r\theta} = \varepsilon_{\theta z} = 0, \quad 2\varepsilon_{rz} = \frac{dU}{dr} \tag{2a}$$

$$\sigma_{rr} = \sigma_{\theta\theta} = \sigma_{zz} = \sigma_{\theta r} = \sigma_{\theta z} = 0; \quad \sigma_{rz} = G\frac{dU}{dr} \tag{2b}$$

where G is the shear modulus. Of the three stress-equilibrium equations in the cylindrical coordinates, the two equilibrium equations associated with r and θ directions are trivially satisfied (in the absence of body forces) by the stress field. The third equilibrium equation

$$\frac{1}{r}\left[\frac{\partial}{\partial r}(r\sigma_{rz}) + \frac{\partial \sigma_{\theta z}}{\partial \theta} + r\frac{\partial \sigma_{zz}}{\partial z}\right] = 0 \Rightarrow \frac{1}{r}\frac{d}{dr}\left(rG\frac{dU}{dr}\right) = 0 \tag{3}$$

The boundary conditions on $U(r)$ are

$$u_z(b) = 0 \rightarrow U(b) = 0; \quad -2\pi L(r\sigma_{rz})|_{r=a} = P \rightarrow -\left(rG\frac{dU}{dr}\right)_{r=a} = \frac{P}{2\pi L} \tag{4}$$

This completes the theoretical formulation of the problem. We wish to analyze the problem using the finite element method.

The finite element model in Eq. (3) [cf. Eq. (3.5.3)] is given by Eqs. (3.5.9) and (3.5.10) with $a(r) = G$ and $f = 0$. One linear element in the domain yields ($r_a = a$ and $h = b - a$)

$$\frac{2\pi G}{h}\left(r_a + \frac{1}{2}h\right)\begin{bmatrix} 1 & -1 \\ -1 & 1 \end{bmatrix}\begin{Bmatrix} U_1 \\ U_2 \end{Bmatrix} = \begin{Bmatrix} Q_1^1 \\ Q_2^1 \end{Bmatrix} \tag{5}$$

and with $U_2 = 0$ and $Q_1^1 = P/L$, we obtain

$$U_1 = \frac{P}{\pi LG}\frac{(b-a)}{(b+a)} \tag{6}$$

The exact solution of Eqs. (3) and (4) is given by

$$U(r) = -\frac{P}{2\pi LG}\log(r/b), \quad U(a) \equiv \delta = \frac{P}{2\pi LG}\log(b/a) \tag{7}$$

The one-element solution in Eq. (6) corresponds to the first term in the logarithmic series of δ [i.e., $\log(b/a)$].

Use of one quadratic element gives ($h = b - a$)

$$\frac{2\pi G}{6h}\begin{bmatrix} 3h+14a & -(4h+16a) & h+2a \\ -(4h+16a) & 16h+32a & -(12h+16a) \\ h+2a & -(12h+16a) & 11h+14a \end{bmatrix}\begin{Bmatrix} U_1 \\ U_2 \\ U_3 \end{Bmatrix}=\begin{Bmatrix} Q_1^1 \\ 0 \\ Q_3^1 \end{Bmatrix} \tag{8}$$

Using the boundary conditions $U_3 = 0$ and $Q_1^1 = P/L$, we obtain the following condensed equations in U_1 and U_2:

$$\frac{2\pi G}{6h}\begin{bmatrix} 3h+14a & -(4h+16a) \\ -(4h+16a) & 16h+32a \end{bmatrix}\begin{Bmatrix} U_1 \\ U_2 \end{Bmatrix}=\begin{Bmatrix} P/L \\ 0 \end{Bmatrix} \tag{9}$$

whose solution is

$$U_1 = \frac{3hP}{\pi GL}\frac{h+2a}{3h^2+20ah+28a^2}, \quad U_2 = \frac{3hP}{\pi GL}\frac{h+4a}{12h^2+80ah+112a^2} \tag{10}$$

The finite element solution becomes ($\bar{r} = r - a$)

$$U_h(\bar{r}) = U_1\left(1-\frac{\bar{r}}{h}\right)\left(1-2\frac{\bar{r}}{h}\right)+4U_2\frac{\bar{r}}{h}\left(1-\frac{\bar{r}}{h}\right) \tag{11}$$

A comparison of the finite element solutions obtained with linear and quadratic elements with the analytical solution is shown in Fig. 4.4.5. The four-element mesh of quadratic elements virtually gives the exact solution.

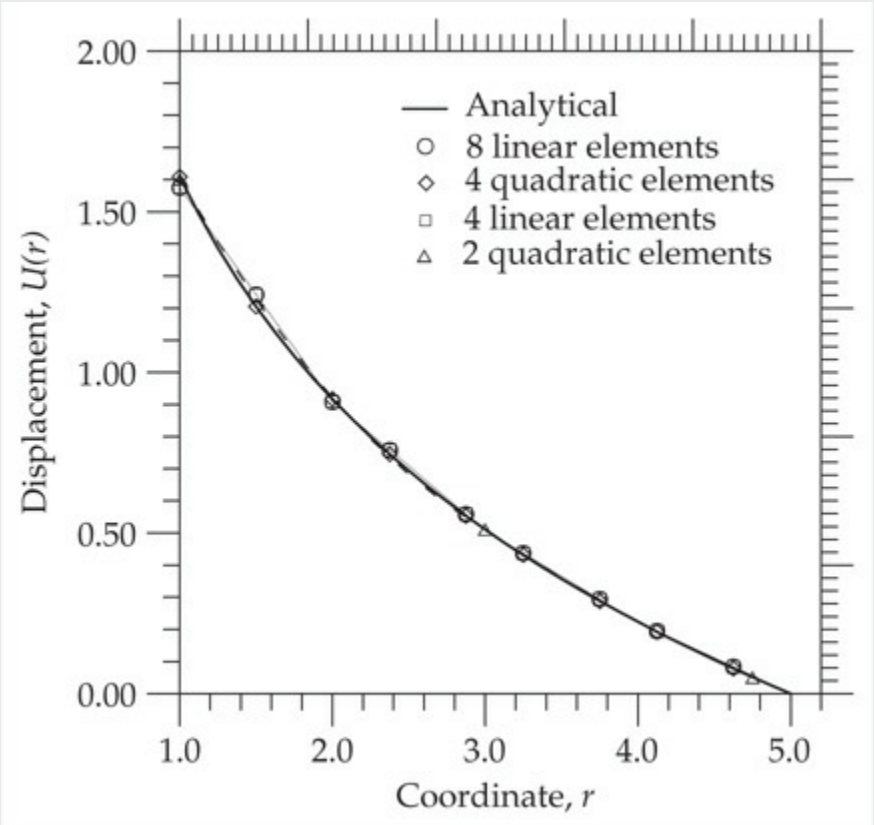

Fig. 4.4.5 Comparison of finite element solutions with the analytical solution for axisymmetric deformation of a hollow cylinder fixed at the outer surface and pulled by a rigid core at the inner surface.

4.5 Summary

In this chapter, applications of finite element models to the solution of 1-D problems of heat transfer, fluid mechanics, and solid mechanics have been presented. To aid the reader, a brief review of the basic terminology and governing equations of each of the three fields has also been given.

It has been shown that the secondary variables of a problem can be computed using either the global algebraic equations of the finite element mesh (i.e., condensed equations for the secondary variables) or their original definitions through finite element interpolation. The former method gives more accurate results, which will satisfy the equilibrium at inter-element nodes, whereas the latter gives less accurate results, and they are discontinuous at the nodes. The secondary variables computed using the linear elements are element-wise constant, while they are element-wise linear for the Lagrange quadratic elements. The values of the secondary variables post-computed using the definition at a global node can be improved by refining the mesh (*h* or *p* refinement). We note that the derivative of a primary variable in second-order equations is not always continuous across element boundaries due to the presence of an externally placed point source (secondary variable).

Problems

Many of the following problems are designed for hand calculations, while some are intended specifically for computer calculations using the program FEM1D (see Chapter 8 for details on how to use the program). The problem set should give the student deeper understanding of what is involved in the setting up of the finite element equations, imposition of boundary conditions, and identifying the condensed equations for the unknown primary and secondary variables of a given problem.

HEAT TRANSFER

4.1 Consider the equations governing conduction and convection heat transfer in bar:

$$-\frac{d}{dx}\left(a\frac{du}{dx}\right)+cu=g \quad \text{for} \quad 0<x<L$$

$$\text{EBC: specify } u, \quad \text{NBC: specify } n_x a\frac{du}{dx}+\beta(u-u_\infty)=Q$$

where $n_x = -1$ at $x = x_a$ and $n_x = 1$ at $x = x_b$. Construct the weak form to include the convective boundary conditions and develop the finite element model that accounts for the convection boundary conditions explicitly.

4.2 Consider heat transfer in a plane wall of total thickness L. The left surface is maintained at temperature T_0 and the right surface is exposed to ambient temperature T_∞ with heat transfer coefficient β. Determine the temperature distribution in the wall and heat input at the left surface of the wall for the following data: $L = 0.1$ m, $k = 0.01$ W/(m · °C), $\beta = 25$ W/(m^2 · °C), $T_0 = 50$°C, and $T_\infty = 5$°C. Solve for nodal temperatures and the heat at the left wall using (a) two linear finite elements and (b) one quadratic element. *Answer:* (a) $U_2 = 27.59$°C, $U_3 = 5.179$°C, $Q_1^1 = 4.482\ \text{W/m}^2 = -Q_2^2$.

4.3 An insulating wall is constructed of three homogeneous layers with conductivities k_1, k_2, and k_3 in intimate contact (see Fig. P4.3). Under steady-state conditions, the temperatures of the media in contact at the left and right surfaces of the wall are at ambient temperatures of T_∞^L and T_∞^R, respectively, and film coefficients β_L and β_R, respectively.

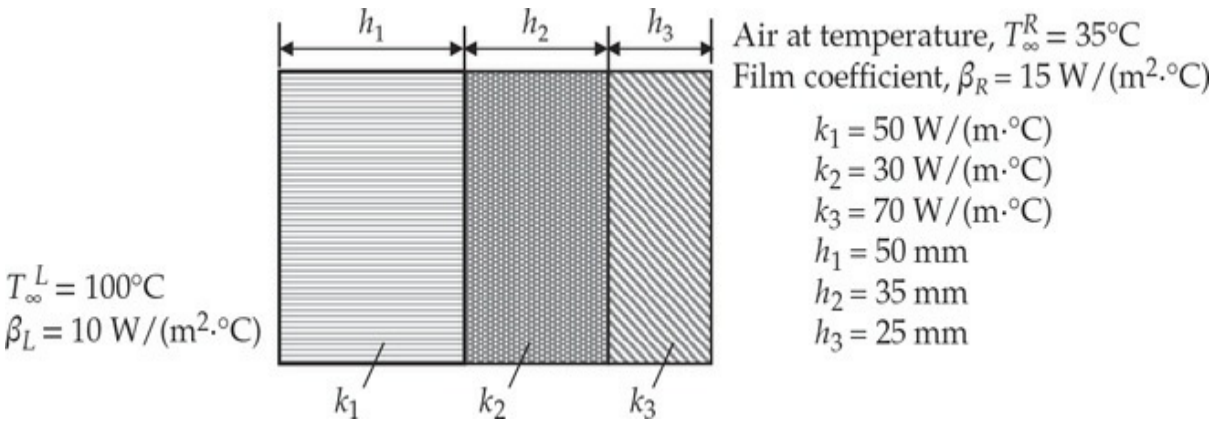

Fig. P4.3

Determine the temperatures on the left and right surfaces as well as at the interfaces. Assume that there is no internal heat generation and that the heat flow is one-dimensional ($\partial T/\partial y = 0$). *Answer:* $U_1 = 61.582°C$, $U_2 = 61.198°C$, $U_3 = 60.749°C$, $U_4 = 60.612°C$.

4.4 Repeat **Problem 4.3** for the data shown in Fig. P4.4. Assume one-dimensional heat flow.

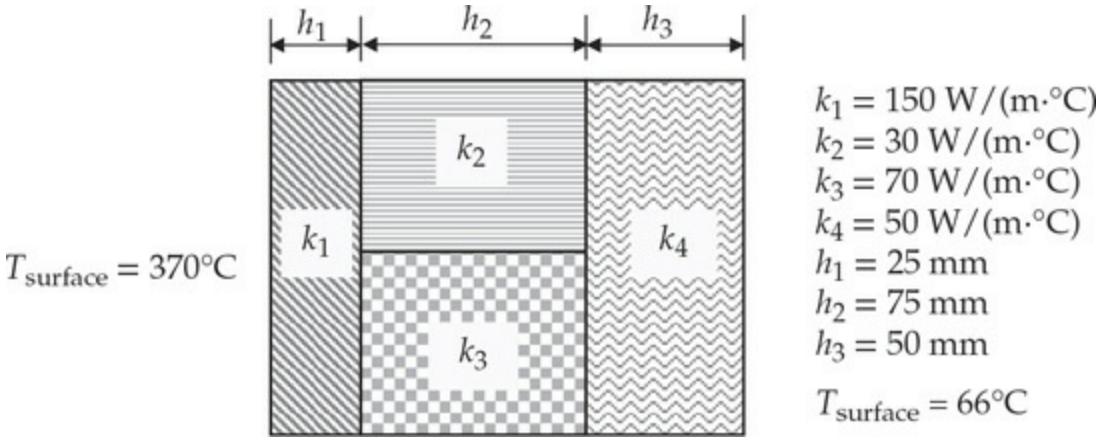

Fig. P4.4

4.5 Consider the differential equation (corresponds to heat transfer in a rod, in nondimensional form)

$$-\frac{d^2u}{dx^2} + 400u = 0 \quad \text{for} \quad 0 < x < L = 0.05$$

with the boundary conditions

$$u(0) = 300, \quad \left(\frac{du}{dx} + 2u\right)\Big|_{x=L} = 0$$

Use two linear finite elements to determine the temperatures at $x = L/2$ and $x = L$. You must at least set up the final condensed equations for the nodal unknowns.

4.6 Rectangular fins are used to remove heat from the surface of a body (at 100°C) by conduction along the fins and convection from the surface of the fins into the surroundings. The fins are 100 mm long, 5 mm wide and 1 mm thick, and made of aluminum with thermal conductivity $k = 170$ W/(m · K). The natural convection heat transfer coefficient associated with the surrounding air is $\beta = 35$ W/(m^2 · K) and the ambient temperature is $T_\infty = 20°C$. Assuming that the heat transfer is one dimensional along the length of the fins and that the

heat transfer in each fin is independent of the others, determine the temperature distribution along the fins, and the heat removed from each fin by convection. Use (a) four linear elements, and (b) two quadratic elements.

4.7 A steel rod of diameter $D = 2$ cm, length $L = 5$ cm, and thermal conductivity $k = 50$ W/(m · °C) is exposed to ambient air at $T = 20$°C with a heat transfer coefficient $\beta = 100$ W/(m^2 · °C). If the left end of the rod is maintained at temperature $T_0 = 320$°C, determine the temperatures at distances 25 mm and 50 mm from the left end, and the heat at the left end. The governing equation of the problem is

$$-\frac{d^2\theta}{dx^2} + m^2\theta = 0 \quad \text{for} \quad 0 < x < L$$

where $\theta = T - T_\infty$, T is the temperature, and $m^2 = \beta P/Ak$. The boundary conditions are

$$\theta(0) = T(0) - T_\infty = 300°\text{C}, \qquad \left(\frac{d\theta}{dx} + \frac{\beta}{k}\theta\right)\bigg|_{x=L} = 0$$

Use (a) two linear elements and (b) one quadratic element to solve the problem by the finite element method. Compare the finite element nodal temperatures against the exact values.

Answer: (a) $U_1 = 300$°C, $U_2 = 211.97$°C, $U_3 = 179.24$°C, $Q_1^1 = 3,521.1$ W/m^2 (b) $U_1 = 300$°C, $U_2 = 213.07$°C, $U_3 = 180.77$°C, $Q_1^1 = 4,569.9$ W/m^2

4.8 Find the temperature distribution in the tapered fin shown in Fig. P4.8. Assume that the temperature at the root of the fin is 250°F, the conductivity $k = 120$ Btu/(h ft °F), and the film coefficient $\beta = 15$ Btu/(h ft^2 °F), and use three linear elements. The ambient temperature at the top and bottom of the fin is $T_\infty = 75$°F. *Answer:* T_1 (tip) = 166.23°F, $T_2 = 191.1$°F, $T_3 = 218.89$°F.

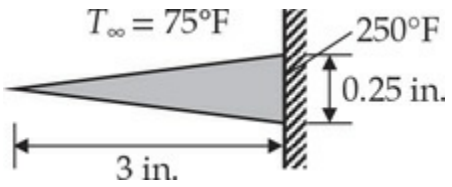

Fig. P4.8

4.9 Consider steady heat conduction in a wire of circular cross section

with an electrical heat source. Suppose that the radius of the wire is R_0, its electrical conductivity is K_e (Ω^{-1}/cm), and it is carrying an electric current density of I (A/cm^2). During the transmission of an electric current, some of the electrical energy is converted into thermal energy. The rate of heat production per unit volume is given by $g_e = I^2/K_e$. Assume that the temperature rise in the wire is sufficiently small that the dependence of the thermal or electric conductivity on temperature can be neglected. The governing equations of the problem are

$$-\frac{1}{r}\frac{d}{dr}\left(rk\frac{dT}{dr}\right)=g_e \quad \text{for} \quad 0\le r\le R_0, \quad \left(rk\frac{dT}{dr}\right)\Big|_{r=0}=0, \quad T(R_0)=T_0$$

Determine the distribution of temperature in the wire using (a) two linear elements and (b) one quadratic element, and compare the finite element solution at eight equal intervals with the exact solution

$$T(r)=T_0+\frac{g_eR_0^2}{4k}\left[1-\left(\frac{r}{R_0}\right)\right]$$

Also, determine the heat flow, $Q = -2\pi R_0\, k(dT/dr)|R_0$, at the surface using (i) the temperature field and (ii) the balance equations.

4.10 The energy equation for heat conduction in a circular disc of radius R is given by (*an axisymmetric*, one-dimensional problem)

$$-\frac{1}{r}\frac{d}{dr}\left(r\frac{d\theta}{dr}\right)=2\,, \quad 0<r<R \tag{1}$$

and the boundary conditions are

$$r\frac{d\theta}{dr}=0 \text{ at } r=0 \quad \text{and} \quad r\frac{d\theta}{dr}+\theta=1 \text{ at } r=1 \tag{2}$$

where θ is the non-dimensional temperature, r is the radial coordinate, and $R = 1$ is the radius of the disc. Use two linear finite elements of equal length to determine the unknown temperatures. It is sufficient to give the condensed equations for the unknown nodal temperatures.

4.11 Consider a nuclear fuel element of spherical form, consisting of a sphere of "fissionable" material surrounded by a spherical shell of aluminum "cladding" as shown in Fig. P4.11. Nuclear fission is a

source of thermal energy, which varies non-uniformly from the center of the sphere to the interface of the fuel element and the cladding.

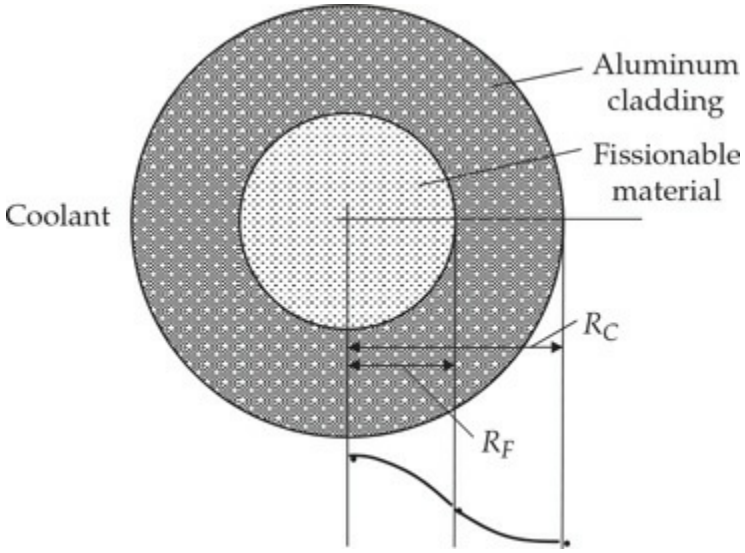

Fig. P4.11

The governing equations for the two regions are the same, with the exception that there is no heat source term for the aluminum cladding. We have

$$-\frac{1}{r^2}\frac{d}{dr}\left(r^2 k_1 \frac{dT_1}{dr}\right) = g \quad \text{for} \quad 0 \le r \le R_F$$

$$-\frac{1}{r^2}\frac{d}{dr}\left(r^2 k_2 \frac{dT_2}{dr}\right) = 0 \quad \text{for} \quad R_F \le r \le R_C$$

where subscripts 1 and 2 refer to the nuclear fuel element and cladding, respectively. The heat generation in the nuclear fuel element is assumed to be of the form

$$g_1 = g_0\left[1 + c\left(\frac{r}{R_F}\right)^2\right]$$

where g_0 and c are constants depending on the nuclear material. The boundary conditions are

$$kr^2\frac{dT_1}{dr} = 0 \quad \text{at} \quad r = 0$$

$$T_1 = T_2 \quad \text{at} \quad r = R_F, \text{ and } T_2 = T_0 \quad \text{at} \quad r = R_C$$

(a) Develop the finite element model, (b) give the *form* of the assembled equations, and (c) indicate the specified primary and secondary variables at the nodes. Use two linear elements to determine the finite element solution for the temperature distribution, and compare the nodal temperatures with the exact solution:

$$T_1 - T_0 = \frac{g_0 R_F^2}{6k_1}\left\{\left[1-\left(\frac{r}{R_F}\right)^2\right]+\frac{3}{10}c\left[1-\left(\frac{r}{R_F}\right)^4\right]\right\}+\frac{g_0 R_F^2}{3k_2}\left(1+\frac{3}{5}c\right)\left(1-\frac{R_F}{R_C}\right)$$

$$T_2 - T_0 = \frac{g_0 R_F^2}{3k_2}\left(1+\frac{3}{5}c\right)\left(\frac{R_F}{r}-\frac{R_F}{R_C}\right)$$

FLUID MECHANICS

4.12 Consider the flow of a Newtonian viscous fluid on an inclined flat surface, as shown in Fig. P4.12. Examples of such flow can be found in wetted-wall towers and the application of coatings to wallpaper rolls. The momentum equation, for a fully developed steady laminar flow along the z coordinate, is given by

$$-\mu\frac{d^2w}{dx^2} = \rho g\cos\beta$$

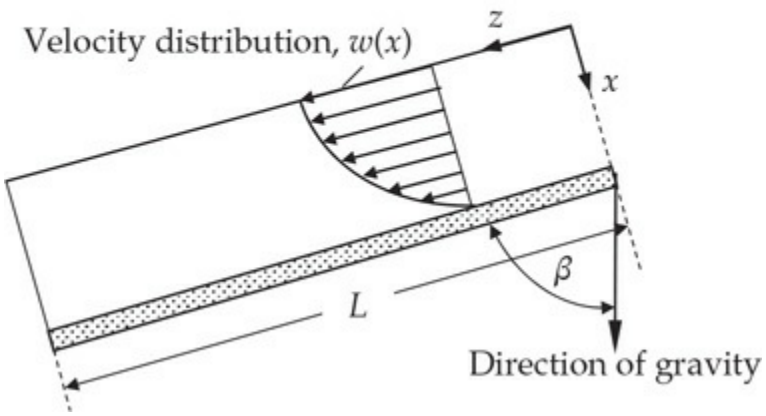

Fig. P4.12

where w is the z component of the velocity, μ is the viscosity of the fluid, ρ is the density, g is the acceleration due to gravity, and β is the angle between the inclined surface and the vertical.

The boundary conditions associated with the problem are that the shear stress is zero at $x = 0$ and the velocity is zero at $x = L$:

$$\left(\frac{dw}{dx}\right)\Big|_{x=0} = 0 \quad w(L) = 0$$

Use (a) two linear finite elements of equal length and (b) one quadratic finite element in the domain $(0, L)$ to solve the problem and compare the two finite element solutions at four points $x = 0$, $\frac{1}{4}L$, $\frac{1}{2}L$, and $\frac{3}{4}L$ of the domain with the exact solution

$$w_e = \frac{\rho g L^2 \cos\beta}{2\mu}\left[1 - \left(\frac{x}{L}\right)^2\right]$$

Evaluate the shear stress ($\tau_{xz} = -\mu\, dw/dx$) at the wall using (i) the velocity fields and (ii) the equilibrium equations, and compare with the exact value. *Answer:* (a) $U_1 = \frac{1}{2}f_0$, $U_2 = \frac{3}{8}f_0$, $f_0 = (\rho g \cos\beta)L^2/\mu$.

4.13 Consider the steady laminar flow of a viscous fluid through a long circular cylindrical tube of radius R_0. The governing equation is

$$-\frac{1}{r}\frac{d}{dr}\left(r\mu\frac{dv_x}{dr}\right) = \frac{P_0 - P_L}{L} \equiv f_0$$

where $v_x = v_x(r)$ is the axial (i.e., x) component of velocity, μ is the viscosity, f_0 is the gradient of pressure (which includes the combined effect of static pressure and gravitational force), and r is the radial coordinate. The boundary conditions are

$$\left(r\frac{dv_x}{dr}\right)\Big|_{r=0} = 0 \quad v_x(R_0) = 0$$

Using the symmetry and (a) two linear elements and (b) one quadratic element, determine the velocity field and compare with the exact solution at the nodes:

$$v_x(r) = \frac{f_0 R_0^2}{4\mu}\left[1 - \left(\frac{r}{R_0}\right)^2\right]$$

4.14 In the problem of the flow of a viscous fluid through a circular cylinder (see **Problem 4.13**), assume that the fluid slips at the cylinder wall; i.e., instead of assuming that $v_x = 0$ at $r = R_0$, use the boundary condition that

$$kv_x = -\mu\frac{dv_x}{dr} \quad \text{at} \quad r = R_0$$

in which k is the "coefficient of sliding friction." Solve the problem with a mesh of two linear elements.

4.15 Consider the steady laminar flow of a Newtonian fluid with constant density in a long annular region between two coaxial cylinders of radii R_i and R_0 (see Fig. P4.15). The differential equation for this case is given by

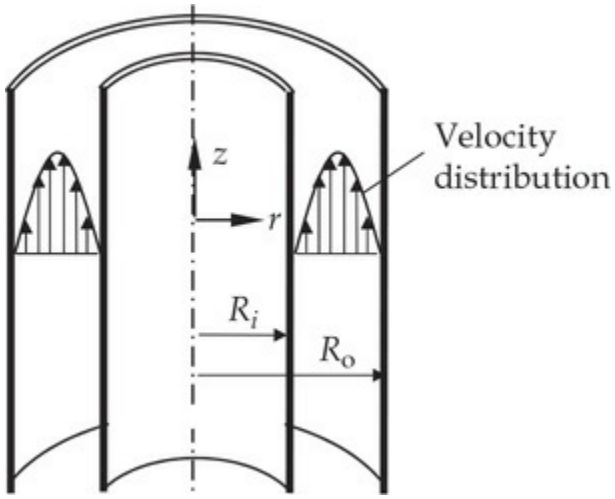

Fig. P4.15

$$-\frac{1}{r}\frac{d}{dr}\left(r\mu\frac{dw}{dr}\right)=\frac{P_1-P_2}{L}\equiv f_0$$

where w is the velocity along the cylinders (i.e., the z component of velocity), μ is the viscosity, L is the length of the region along the cylinders in which the flow is fully developed, and P_1 and P_2 are the pressures at $z = 0$ and $z = L$, respectively (P_1 and P_2 represent the combined effect of static pressure and gravitational force). The boundary conditions are

$$w=0 \quad \text{at} \quad r=R_0 \quad \text{and} \quad R_i$$

Solve the problem using (a) two linear elements and (b) one quadratic element, and compare the finite element solutions with the exact solution at the nodes:

$$w_e(r)=\frac{f_0R_0^2}{4\mu}\left[1-\left(\frac{r}{R_0}\right)^2+\frac{1-k^2}{\ln(1/k)}\ln\left(\frac{r}{R_0}\right)\right]$$

where $k = R_i/R_0$. Determine the shear stress $\tau_{rz} = -\mu\, dw/dr$ at the walls using (a) the velocity field and (b) the equilibrium equations,

and compare with the exact values. (Note that the steady laminar flow of a viscous fluid through a long cylinder or a circular tube can be obtained as a limiting case of $k \to 0$.)

4.16 Consider the steady laminar flow of two immiscible incompressible fluids in a region between two parallel stationary plates under the influence of a pressure gradient. The fluid rates are adjusted such that the lower half of the region is filled with Fluid I (the denser and more viscous fluid) and the upper half is filled with Fluid II (the less dense and less viscous fluid), as shown in Fig. P4.16. We wish to determine the velocity distributions in each region using the finite element method.

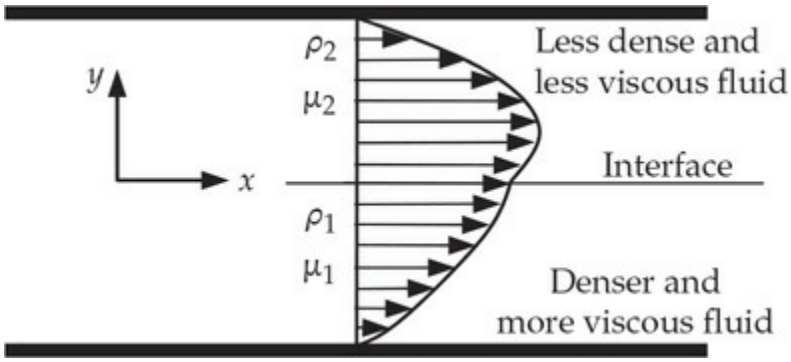

Fig. P4.16

The governing equations for the two fluids are

$$-\mu_1 \frac{d^2 u_1}{dx^2} = f_0, \quad -\mu_2 \frac{d^2 u_2}{dx^2} = f_0$$

where $f_0 = (P_0 - P_L)/L$ is the pressure gradient. The boundary conditions are

$$u_1(-b) = 0 \quad u_2(b) = 0, \quad u_1(0) = u_2(0)$$

Solve the problem using four linear elements, and compare the finite element solutions with the exact solution at the nodes

$$u_i = \frac{f_0 b^2}{2\mu_i}\left[\frac{2\mu_i}{\mu_1 + \mu_2} + \frac{\mu_1 - \mu_2}{\mu_1 + \mu_2}\frac{y}{b} - \left(\frac{y}{b}\right)^2\right] \quad (i = 1, 2)$$

4.17 The governing equation for an unconfined aquifer with flow in the radial direction is given by the differential equation

$$-\frac{1}{r}\frac{d}{dr}\left(rk\frac{du}{dr}\right)=f$$

where k is the coefficient of permeability, f the recharge, and u the piezometric head. Pumping is considered to be a negative recharge. Consider the following problem. A well penetrates an aquifer and pumping is performed at $r = 0$ at a rate $Q = 150$ m^2/h. The permeability of the aquifer is $k = 25$ m^3/h. A constant head $u_0 = 50$ m exists at a radial distance $L = 200$ m. Determine the piezometric head at radial distances of 0, 10, 20, 40, 80, and 140 m (see Fig. P4.17). You are required to set up the finite element equations for the unknowns using a nonuniform mesh of six linear elements.

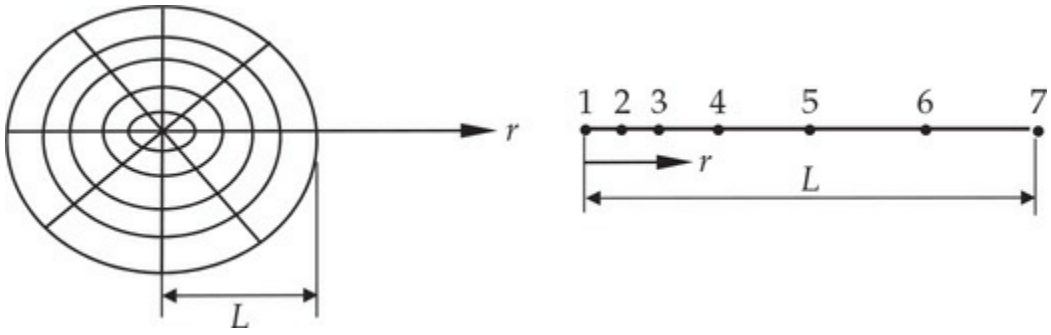

Fig. P4.17

4.18 Consider a slow, laminar flow of a viscous substance (for example, glycerin solution) through a narrow channel under controlled pressure drop of 150 Pa/m. The channel is 5 m long (flow direction), 10 cm high, and 50 cm wide. The upper wall of the channel is maintained at 50°C while the lower wall is maintained at 25°C. The viscosity and density of the substance are temperature dependent, as given in Table P4.18. Assuming that the flow is essentially one dimensional (justified by the dimensions of the channel), determine the velocity field and mass flow rate of the fluid through the channel.

Table P4.18 Properties of the viscous substance of Problem 4.18.

y (m)	Temp. (°C)	Viscosity [kg/(m· s)]	Density (kg/m^3)
0.00	50	0.10	1233
0.02	45	0.12	1238
0.04	40	0.20	1243
0.06	35	0.28	1247
0.08	30	0.40	1250
0.10	25	0.65	1253

SOLID AND STRUCTURAL MECHANICS

4.19 For the stepped bar problem shown in Fig. P4.19, use the minimum number of linear elements and give (a) the boundary conditions on the nodal variables (primary as well as secondary variables) and (b) the final condensed finite element equations for the unknowns.

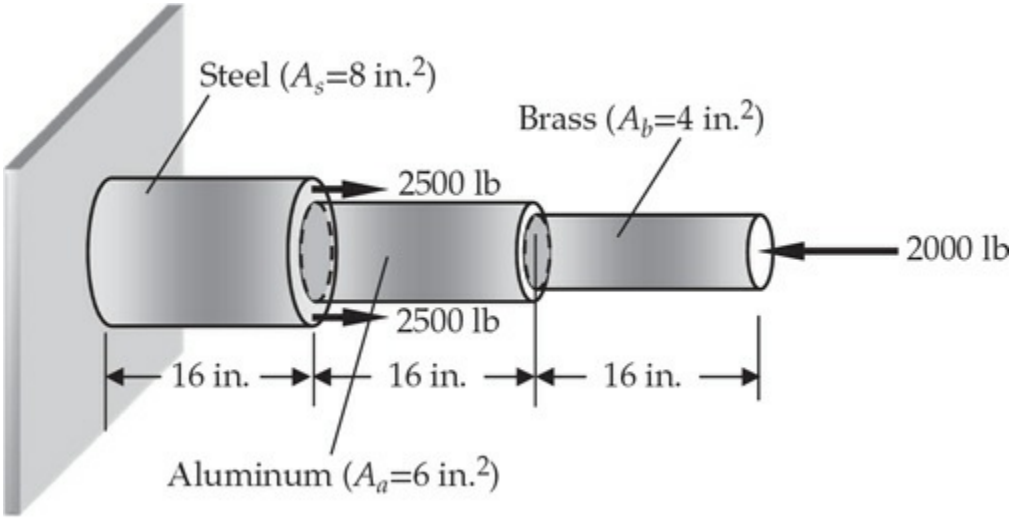

Fig. P4.19

4.20 Find the three-element finite element solution to the stepped-bar problem. See Fig. P4.20 for the geometry and data. *Hint:* Solve the problem to see if the end displacement exceeds the gap. If it does, resolve the problem with modified boundary condition at x = 24 in.

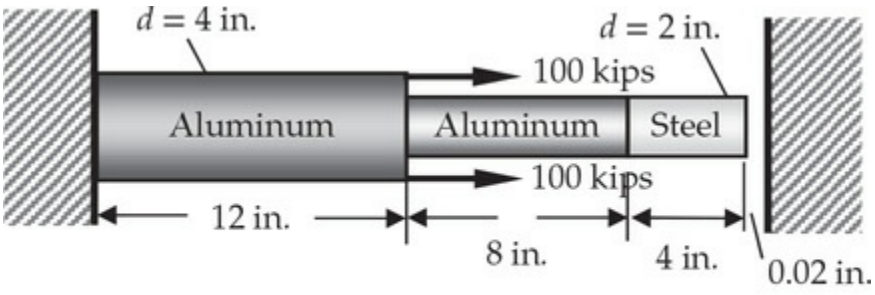

Steel, $E_s = 30 \times 10^6$ psi, Aluminum, $E_a = 10 \times 10^6$ psi

Fig. P4.20

4.21 Analyze the stepped bar with its right end supported by a linear axial spring (see Fig. P4.21). The boundary condition at $x = 24$ in. is $EA(du/dx) + ku = 0$.

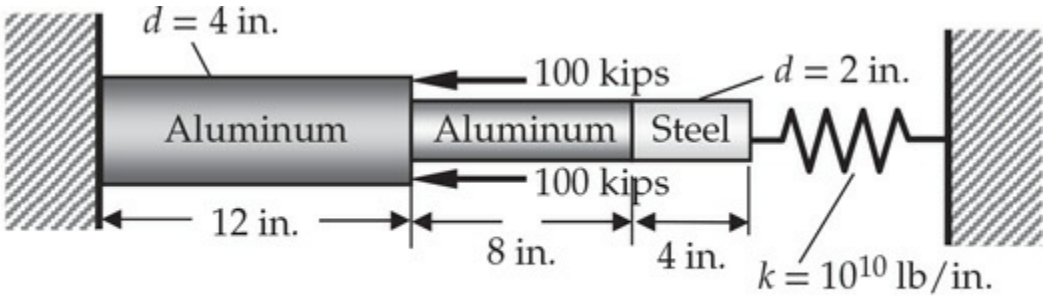

Steel, $E_s = 30 \times 10^6$ psi, Aluminum, $E_a = 10 \times 10^6$ psi

Fig. P4.21

4.22 A solid circular brass cylinder ($Eb = 15 \times 10^6$ psi, $d_s = 0.25$ in.) is encased in a hollow circular steel ($E_s = 30 \times 10^6$ psi, $d_s = 0.21$ in.). A load of $P = 1,330$ lb compresses the assembly, as shown in Fig. P4.22.

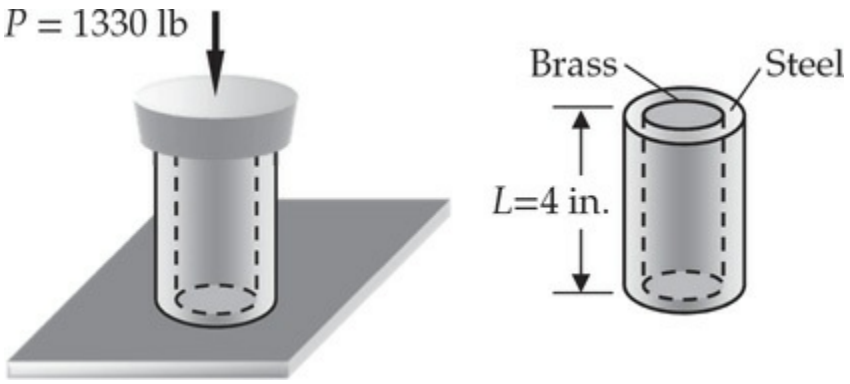

Fig. P4.22

Determine (a) the compression, and (b) compressive forces and stresses in the steel shell and brass cylinder. Use the minimum number of linear finite elements. Assume that the Poisson effect is negligible.

4.23 A rectangular steel bar ($E_s = 30 \times 10^6$ psi) of length 24 in. has a slot in the middle half of its length, as shown in Fig. 4.23. Determine the displacement of the ends due to the axial loads $P = 2,000$ lb. Use the minimum number of linear elements.

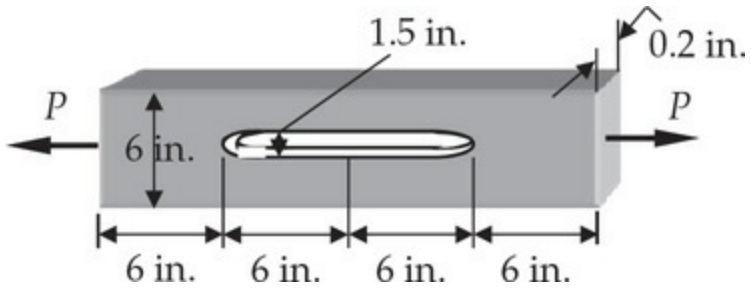

Fig. P4.23

4.24 Repeat **Problem 4.25** for the steel bar shown in Fig. P4.24.

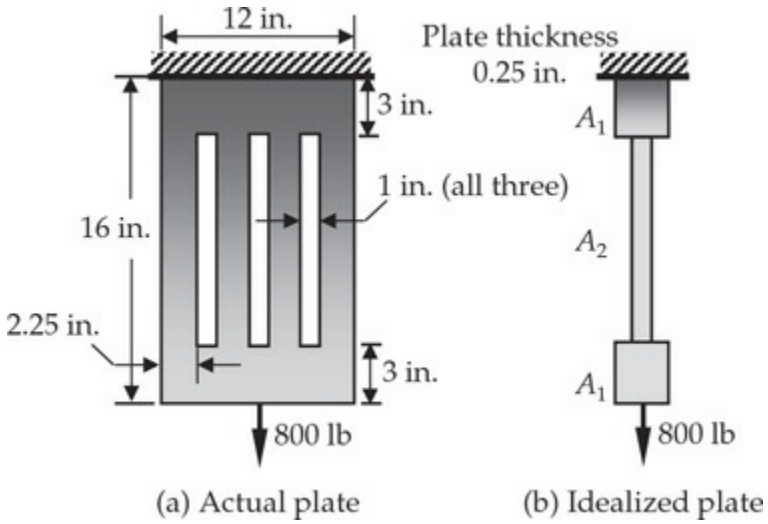

Fig. P4.24

4.25 The aluminum and steel pipes shown in Fig. P4.25 are fastened to rigid supports at ends A and B and to a rigid plate C at their junction. Determine the displacement of point C and stresses in the aluminum and steel pipes due to the net axial load of 100, 000 N. Use the minimum number of linear finite elements.

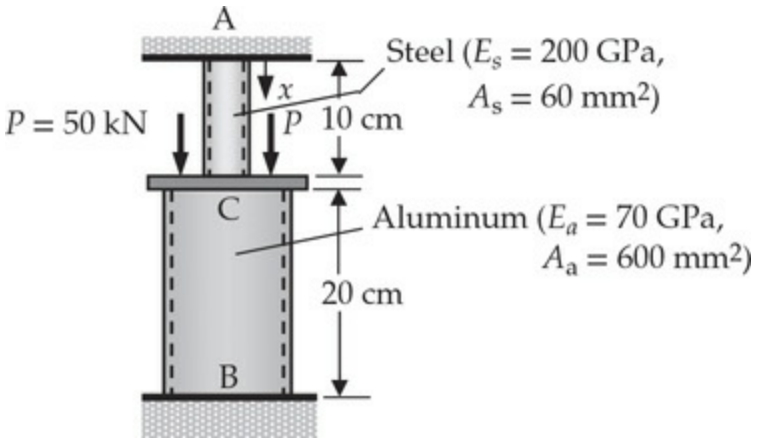

Fig. P4.25

4.26 A steel bar ABC is pin-supported at its upper end A to an immovable wall and loaded by a force F_1 at its lower end C, as shown in Fig. P4.26. A rigid horizontal beam BDE is pinned to the vertical bar at B, supported at point D, and carries a load F_2 at end E. Determine the displacements u_B and u_C at points B and C.

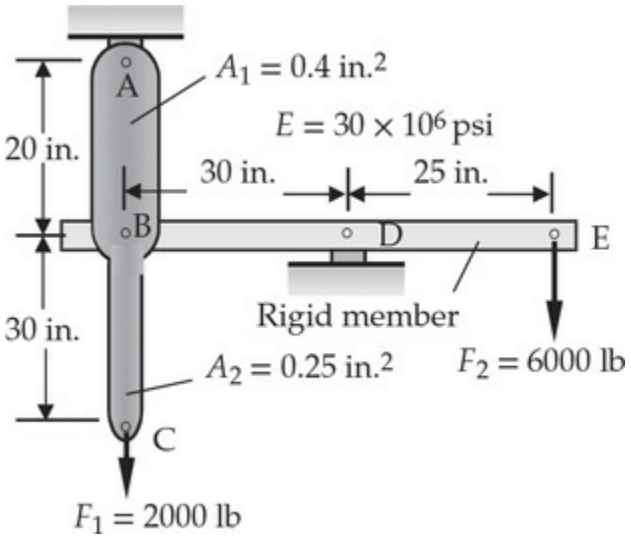

Fig. P4.26

4.27 Repeat **Problem 4.26** when point C is supported vertically by a spring (k = 1, 000 lb/in.).

4.28 Consider the steel column (a typical column in a multi-storey building structure) shown in Fig. P4.27. The loads shown are due to the loads of different floors. The modulus of elasticity is $E = 30 \times 10^6$ psi and cross-sectional area of the column is $A = 40$ in^2. Determine the vertical displacements and axial stresses in the column at various floor-column connection points.

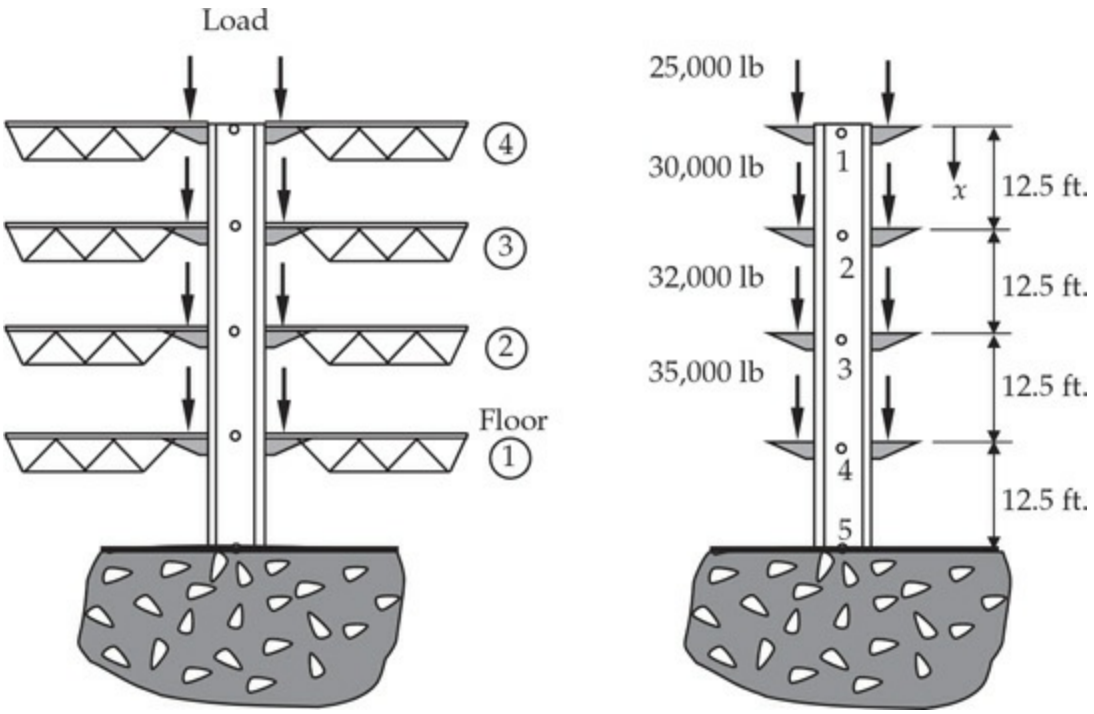

Fig. P4.27

4.29 The equation governing the axial deformation of an elastic bar in the presence of distributed mechanical load $f(x)$ and a temperature change $T(x)$ is

$$-\frac{d}{dx}\left[EA\left(\frac{du}{dx}-\alpha T\right)\right]=f \quad \text{for} \quad 0<x<L \tag{1}$$

where α is the thermal expansion coefficient, E the modulus of elasticity, and A the cross-sectional area (all of which can be functions of x). Develop the finite element model of the equation and compute the element coefficients for the case of linear approximation of $u(x)$. *Answer:* For a linear element, with constant f_e and $\alpha_e\ E_e\ A_e\ T_e$, we have

$$\frac{E_eA_e}{h_e}\begin{bmatrix}1 & -1\\ -1 & 1\end{bmatrix}\begin{Bmatrix}u_1^e\\ u_2^e\end{Bmatrix}=\frac{f_eh_e}{2}\begin{Bmatrix}1\\ 1\end{Bmatrix}+E_eA_e\alpha_eT_e\begin{Bmatrix}-1\\ 1\end{Bmatrix}+\begin{Bmatrix}Q_1^e\\ Q_2^e\end{Bmatrix} \tag{2}$$

4.30 Consider a bar element of length h_e and constant properties $E_e\ A_e$ and $\alpha_e\ T_e$. Let $\bar{x}$ be the local coordinate, with the origin at the left end. Define

$$u_1^e=u(0),\quad u_2^e=u(h_e) \tag{1}$$

$$Q_1^e = \left[-E_e A_e \left(\frac{du}{d\bar{x}} - \alpha_e T_e\right)\right]_{\bar{x}=0}, \quad Q_2^e = \left[E_e A_e \left(\frac{du}{d\bar{x}} - \alpha_e T_e\right)\right]_{\bar{x}=h_e} \tag{2}$$

Then using the homogeneous solution of Eq. (1) of **Problem 4.29**,

$$u(\bar{x}) = c_1 + c_2 \bar{x} \tag{3}$$

derive the finite element equations of the element. The answer should match that in **Problem 4.29** with $f_e = 0$. *Hint:* First express c_1 and c_2 in terms of the nodal values u_1^e and u_2^e, and then use Eq. (2) to derive the finite element model.

4.31 Consider a nonuniform rod of length 30 in., and subjected to a uniform temperature change of $T = 60°\text{F}$. Take $A(x) = 6 - \frac{1}{10}x \text{ in}^2$, $E = 30 \times 10^6 \text{ lb/in}^2$, and $\alpha = 12 \times 10^{-6}/(°\text{F})$. Determine the displacements and reactions forces when (a) the left end is fixed and the right end is free, and (b) both ends are fixed.

4.32 The bending moment (M) and transverse deflection (w) in a beam according to the Euler–Bernoulli beam theory are related by

$$-EI\frac{d^2w}{dx^2} = M(x)$$

For statically determinate beams, one can readily obtain the expression for the bending moment in terms of the applied loads. Thus, $M(x)$ is a known function of x. Determine the maximum deflection of the simply supported beam under uniform load (see Fig. P4.32) using a mesh of two linear finite elements in the half beam.

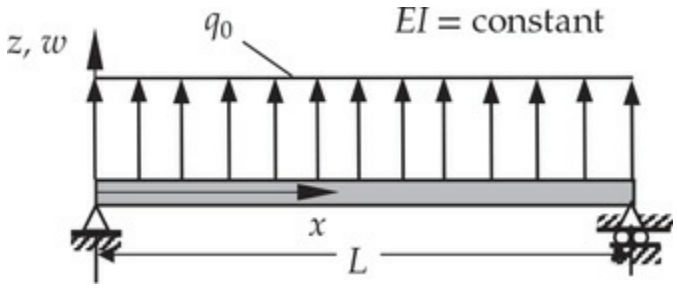

Fig. P4.32

4.33 Repeat **Problem 4.32** for the cantilever beam shown in Fig. P4.33.

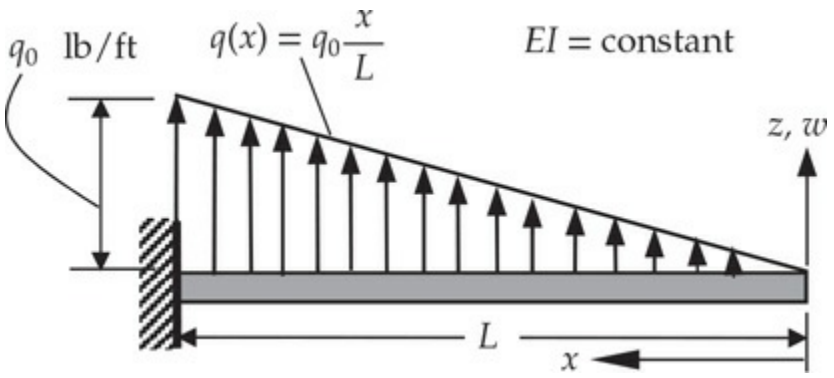

Fig. P4.33

4.34 Turbine disks are often thick near their hub and taper down to a smaller thickness at the periphery. The equation governing a variable-thickness $H = H(r)$ disk is

$$\frac{d}{dr}(H\sigma_r) + \frac{H}{r}(\sigma_r - \sigma_\theta) + H\rho\omega^2 r = 0 \tag{1}$$

where ω^2 is the angular velocity of the disk and

$$\sigma_r = c\left(\frac{du}{dr} + \nu\frac{u}{r}\right), \quad \sigma_\theta = c\left(\frac{u}{r} + \nu\frac{du}{dr}\right), \quad c = \frac{E}{1-\nu^2} \tag{2}$$

(a) Construct the weak integral form of the governing equation such that the bi-linear form is symmetric and the natural boundary condition involves specifying the quantity $tr\sigma_r$. (b) Develop the finite element model associated with the weak form derived in part (a).

4.35 Consider an isotropic, hollow circular cylinder of internal radius a and outside radius b, as shown in Fig. P4.35. The cylinder is pressurized at $r = a$ and at $r = b$, and rotating with a uniform speed of ω about its axis (z-axis). Determine the governing differential equation and construct its finite element model. *Hint:* Due to the symmetry about the z-axis, the displacement field is of the form

$$u_r = U(r), \quad u_\theta = u_z = 0, \tag{1}$$

where $U(r)$ is an unknown function to be determined. The body force vector is $\mathbf{f} = \rho\omega^2 r\hat{\mathbf{e}}_r$ and the equilibrium equation in the r-direction is

$$-\frac{1}{r}\left[\frac{d}{dr}\left(r\frac{dU}{dr}\right) - \frac{U}{r}\right] = \frac{\rho\omega^2}{(2\mu+\lambda)}r$$

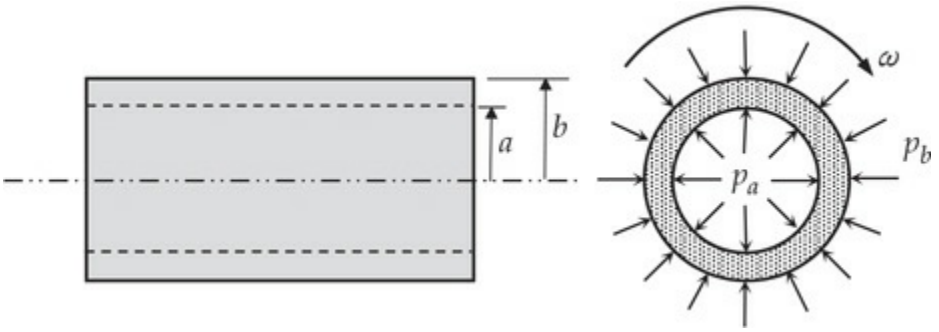

Fig. P4.35

References for Additional Reading

1. J. P. Holman, *Heat Transfer*, 10th ed., McGraw-Hill, New York, NY, 2010.
2. F. Kreith, R. M. Manglik, and M. S. Bohn, *Principles of Heat Transfer*, 7th ed., Cengage Learning, Stamford, CT, 2011.
3. M. N. Özisik, *Heat Conduction*, 2nd ed., John Wiley & Sons, New York, NY, 1993.
4. J. N. Reddy, *An Introduction to Continuum Mechanics*, 2nd ed., Cambridge University Press, New York, NY, 2013.
5. J. N. Reddy and D. K. Gartling, *The Finite Element Method in Heat Transfer and Fluid Dynamics*, 3rd ed., CRC Press, Boca Raton, FL, 2010.
6. H. Schlichting and K. Gersten, *Boundary-Layer Theory*, 8th ed., Springer-Verlag, Berlin, Germany 2000 (corrected printing 2003).
7. J. N. Reddy, *Energy Principles and Variational Methods in Applied Mechanics*, 3rd ed., John Wiley & Sons, New York, NY, 2017.
8. S. P. Timoshenko and J. N. Goodier, *Theory of Elasticity*, 2nd ed., McGraw-Hill, New York, NY, 1951 (reprinted 1970, 2001).
9. R. T. Fenner and J. N. Reddy, *Mechanics of Solids and Structures*, CRC Press, Boca Raton, FL, 2012.

5 Finite Element Analysis of Beams and Circular Plates

It is better to be roughly right than precisely wrong.

— John Maynard Keynes

5.1 Introduction

Beams are structural elements whose length is very large compared to the crosssectional dimensions, supported at few points along its length, and subjected to loads transverse to the axis of the beam that cause bending. They are studied in mechanics of materials (or deformable solids) courses in undergraduate curricula of aerospace, civil, and mechanical engineering departments. The straight line connecting all geometric centroids of a beam cross sections is termed the *centroidal axis* and it is labelled as the x-axis. The coordinate normal to the x-axis in the plane of the paper is taken to be the z-axis, as shown in Fig. 5.1.1, and all transverse loads are assumed to be applied in the xz-plane (or placed symmetrically about the xz-plane) so that there is no twisting of the beam about the x-axis. The reason for taking the z-axis as the vertical axis (as opposed to the y-axis) is that a beam is, geometrically, a one-dimensional counterpart of the plate, whose transverse normal coordinate is taken to be the z-axis (while the xy plane coincides with the midplane of the plate). Again, because of the introduction of cross-sectional area-averaged forces and moments, beam equations can be expressed in terms of only the x coordinate.

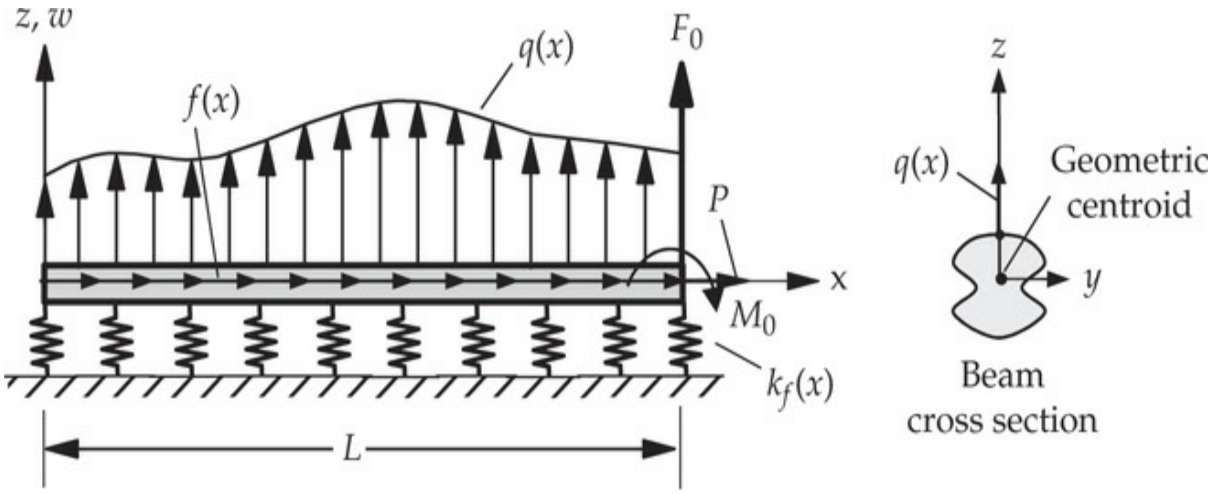

Fig. 5.1.1 Typical beam with distributed forces $f(x)$ and $q(x)$, and point forces P and F_0 and moment M_0.

Plates are structural elements whose plane-form dimensions are large compared to their thickness. The loads are applied normal to the plane of the plate. When the plane-form is a circle, we call them circular plates. In the case of circular plates, we use the cylindrical coordinate system (r, θ, z), with $r\theta$-plane being the middle plane of the plate, as shown in Fig. 5.1.2. If the geometry, material properties, loads, and boundary conditions are independent of the angular coordinate θ, the deformation is said to be axisymmetric. Consequently, axisymmetric bending of circular plates can be described in terms of (r, z) coordinates. Due to the introduction of thickness-averaged forces and moments, the governing equations of axisymmetric bending of circular plates can be described in terms of only the radial coordinate r.

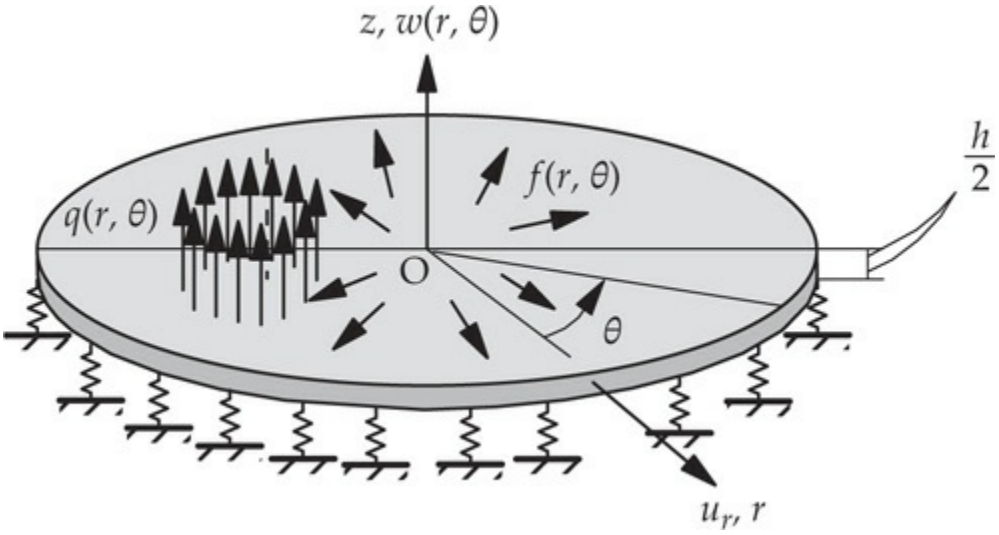

Fig. 5.1.2 Typical circular plate with distributed in-plane and transverse

loads $f(r,\theta)$ and $q(r, \theta)$, respectively.

The present study is limited to (a) straight beams with the geometric centroids of all cross sections connected by the x-axis and bending about the y-axis, and (b) axisymmetric bending of circular plates. The finite element formulations of the governing equations of these two classes of problems involve the same steps as described in Section 3.4 for a single second-order equation, but the mathematical details are somewhat different, especially in the finite element formulation of the equations.

The deformation of the axisymmetric bending of circular plates and straight beams can be represented in terms of the radial/axial displacement (u) and the transverse displacement (w) of a typical material point on the midplane. The displacement fields are different depending on the assumptions made concerning the deformation. In this chapter we consider two different structural theories that govern beam and plate bending: (1) the classical theory and (2) a first-order shear deformation theory. The classical beam theory is known as the Euler–Bernoulli beam theory, which is introduced in mechanics of materials courses, and the classical plate theory is called the Kirchhoff–Love plate theory. The shear deformation beam theory is known as the Timoshenko beam theory, while it is called the Mindlin plate theory in the case of plates.

5.2 Euler–Bernoulli Beam Element

5.2.1 Governing Equation

The Euler–Bernoulli beam theory (EBT) is based on the assumption that plane cross sections perpendicular to the axis of the beam remain plane, rigid, and perpendicular to the axis after deformation. Under the EBT hypothesis, the displacements of a point $(x, 0, z)$ in the beam along the three coordinate directions are

$$u_x = u(x) + z\theta_x(x), \quad u_y = 0, \quad u_z = w(x), \quad \theta_x \equiv -\frac{dw}{dx} \tag{5.2.1}$$

where (u_x, u_y, u_z) are the components of the displacement vector **u** referred to a rectangular Cartesian coordinate system, and (u, w) are the axial and transverse displacements (measured in meters) of a point on the x-axis (i.e., at $z = 0$). Here $\theta x\,(x) = -(dw/dx)$ denotes the (clockwise) rotation

about the *y*-axis of a straight line originally perpendicular to the *x*-axis, as shown in Fig. 5.2.1. Under the assumption of infinitesimal strains, the only nonzero strain (m/m) component is

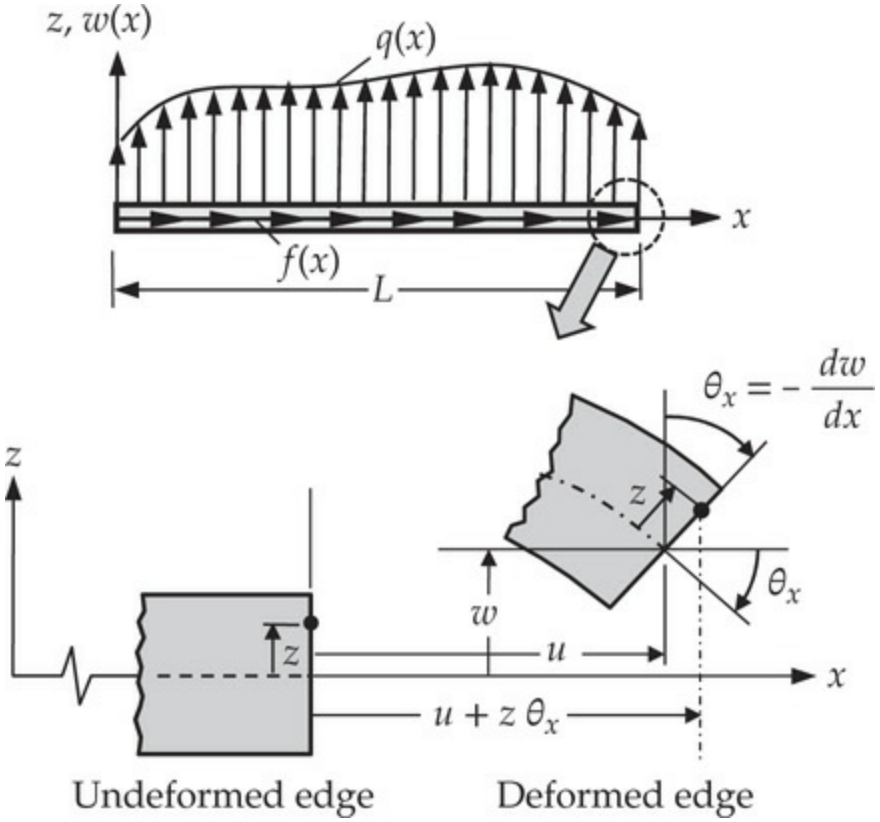

Fig. 5.2.1 Kinematics of deformation of a beam according to the Euler–Bernoulli hypothesis.

$$\varepsilon_{xx} = \frac{du}{dx} - \alpha T + z\frac{d\theta_x}{dx} = \frac{du}{dx} - \alpha T - z\frac{d^2w}{dx^2} \tag{5.2.2}$$

where α is the thermal coefficient of expansion and T is the temperature rise, both of which are assumed to be functions of x but not z. Using the uniaxial stress–strain relation, the axial stress (N/m^2) in the beam is given by

$$\sigma_{xx} = E\left(\frac{du}{dx} - \alpha T + z\frac{d\theta_x}{dx}\right) = E\left(\frac{du}{dx} - \alpha T - z\frac{d^2w}{dx^2}\right) \tag{5.2.3}$$

where $E = E(x)$ denotes the modulus of elasticity (N/m^2). For a homogeneous beam, E is a constant. We note that the shear stress σ_{xz} computed from the constitutive equation is zero because the shear strain is zero: $\gamma_{xz} = \theta_x + (dw/dx) = 0$. However, in reality the shear stress and hence

shear force cannot be zero because transverse loads induce transverse shear stresses. Therefore, the shear force is determined using the equilibrium equations.

The stresses (σ_{xx}, σ_{xz}) and the resultant normal force N (N), shear force V (N), and bending moment M (N-m), called *stress resultants*, are shown on a typical section of the beam in Fig. 5.2.2(a). The stress resultants (N, V, M) are defined as net forces and moment over the beam cross section

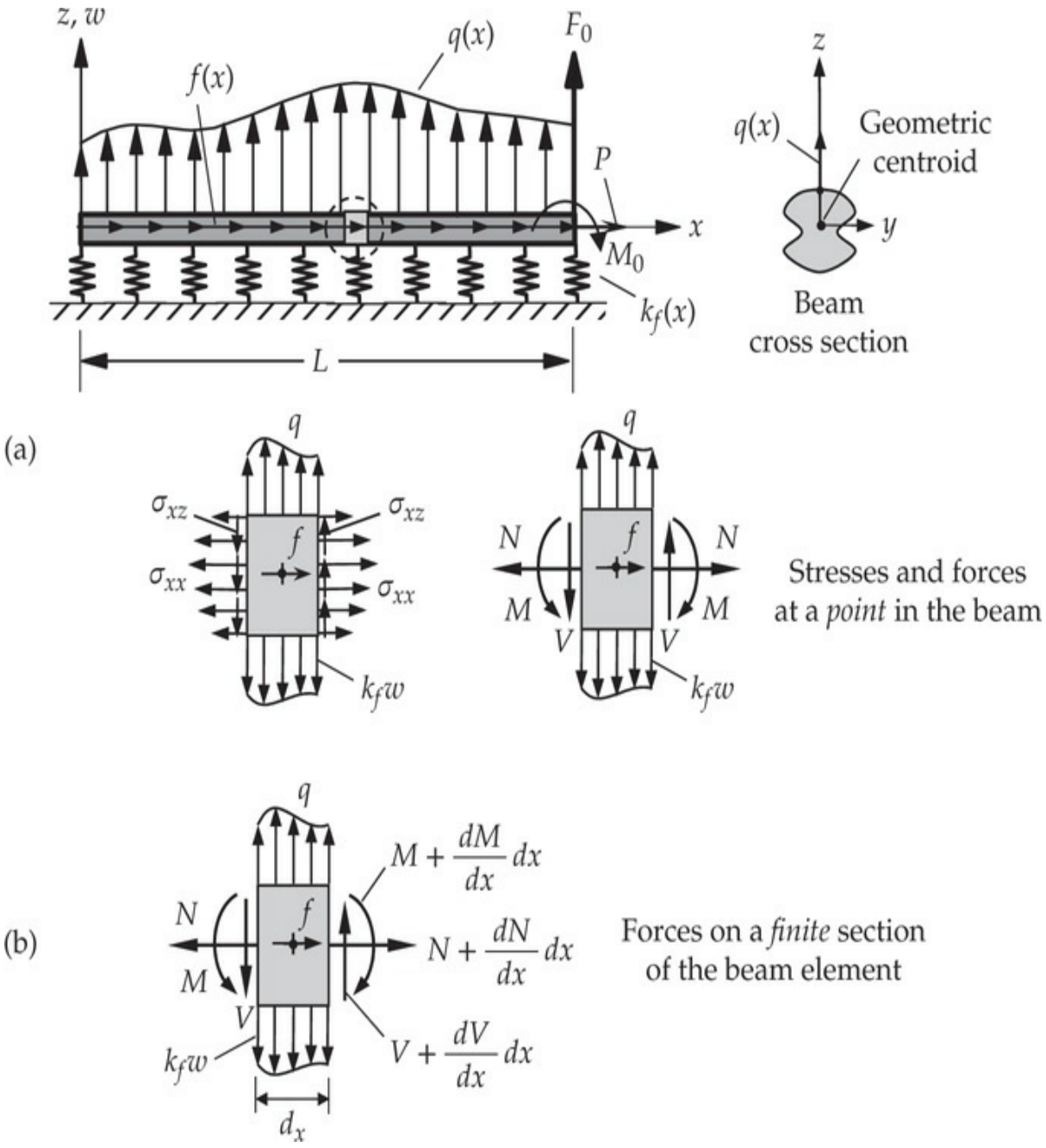

Fig. 5.2.2 (a) Stresses and stress resultants at a point in the beam element. (b) Equilibrium of a beam element of length dx.

$$N = \int_A \sigma_{xx}\, dA, \quad V = \int_A \sigma_{xz}\, dA, \quad M = \int_A z\,\sigma_{xx}\, dA \tag{5.2.4}$$

The axial force (N) and the bending moment M are related to the axial and transverse displacements (u, w) by

$$N = \int_A \sigma_{xx}\, dA = \int_A E\left(\frac{du}{dx} - \alpha T - z\frac{d^2w}{dx^2}\right) dA = EA\left(\frac{du}{dx} - \alpha T\right) \tag{5.2.5a}$$

$$M = \int_A z\,\sigma_{xx}\, dA = \int_A zE\left(\frac{du}{dx} - \alpha T - z\frac{d^2w}{dx^2}\right) dA = -EI\frac{d^2w}{dx^2} \tag{5.2.5b}$$

where $A = A(x)$ is the area of cross section (m^2) and $I = I(x)$ is the second moment of area (m^4) about the y-axis of the beam. For beams with constant cross sections, A and I are constant. In arriving at the relations in Eqs. (5.2.5a) and (5.2.5b), we have used the fact that the first moment of area is zero:

$$\int_A z\, dA = 0 \tag{5.2.6}$$

because the x-axis is taken through the geometric centroid of the beam.

Equilibrium of forces in the x and z directions and equilibrium of moments about the y-axis, shown on an element of beam in Fig. 5.2.2(b), yield

$$\frac{dN}{dx} + f = 0, \quad \frac{dV}{dx} - k_f w + q = 0, \quad V - \frac{dM}{dx} = 0 \tag{5.2.7}$$

Here, $k_f = k_f(x)$ is the modulus (N/m) of the elastic foundation, $f = f(x)$ is the distributed axial force (N/m), and $q = q(x)$ is the distributed transverse load (N/m). Note that the shear force calculated using the definition in Eq. (5.2.4) is zero because σ_{xz} is assumed to be negligible in the Euler–Bernoulli theory. Therefore, we shall calculate V from the equilibrium equation, $V = (dM/dx)$. Thus, the second and third equations in Eq. (5.2.7) can be combined into a single equation in terms of the bending moment as

$$\frac{d^2M}{dx^2} - k_f w + q = 0 \tag{5.2.8}$$

Next, we use the relations in Eqs. (5.2.5a) and (5.2.5b) to express the

first equation of Eqs. (5.2.7) and Eq. (5.2.8) in terms of the displacements (u, w):

$$-\frac{d}{dx}\left(EA\frac{du}{dx}-EA\alpha T\right)-f=0,\quad \frac{d^2}{dx^2}\left(EI\frac{d^2w}{dx^2}\right)+k_f w=q(x) \tag{5.2.9}$$

Note that temperature change that is only a function of x does not enter the bending equation. Only when the temperature is a function of z, it will cause a thermal moment about the y-axis.

Clearly, the differential equations governing displacements u and w are uncoupled, that is, solution of one equation does not depend on the other. In fact, the first equation in Eq. (5.2.9) was already considered in Chapters 3 and 4 (axial deformation of a bar). Therefore, in this section we develop the weak-form Galerkin finite element model of the equation that governs the bending deformation:

$$\frac{d^2}{dx^2}\left(EI\frac{d^2w}{dx^2}\right)+k_f w=q(x)\quad \text{for}\quad 0<x<L \tag{5.2.10}$$

5.2.2 Discretization of the Domain

The domain $\Omega = (0, L)$ of the straight beam shown in Fig. 5.2.3(a) is divided into a set of, say, N line elements, a typical element being $\Omega^e = (x_a^e, x_b^e)$, as indicated in Fig. 5.2.3(b). Although the element is geometrically the same as that used for bars, the number and form of the primary and secondary unknowns at each end point, which constitutes a node, are dictated by the weak formulation of

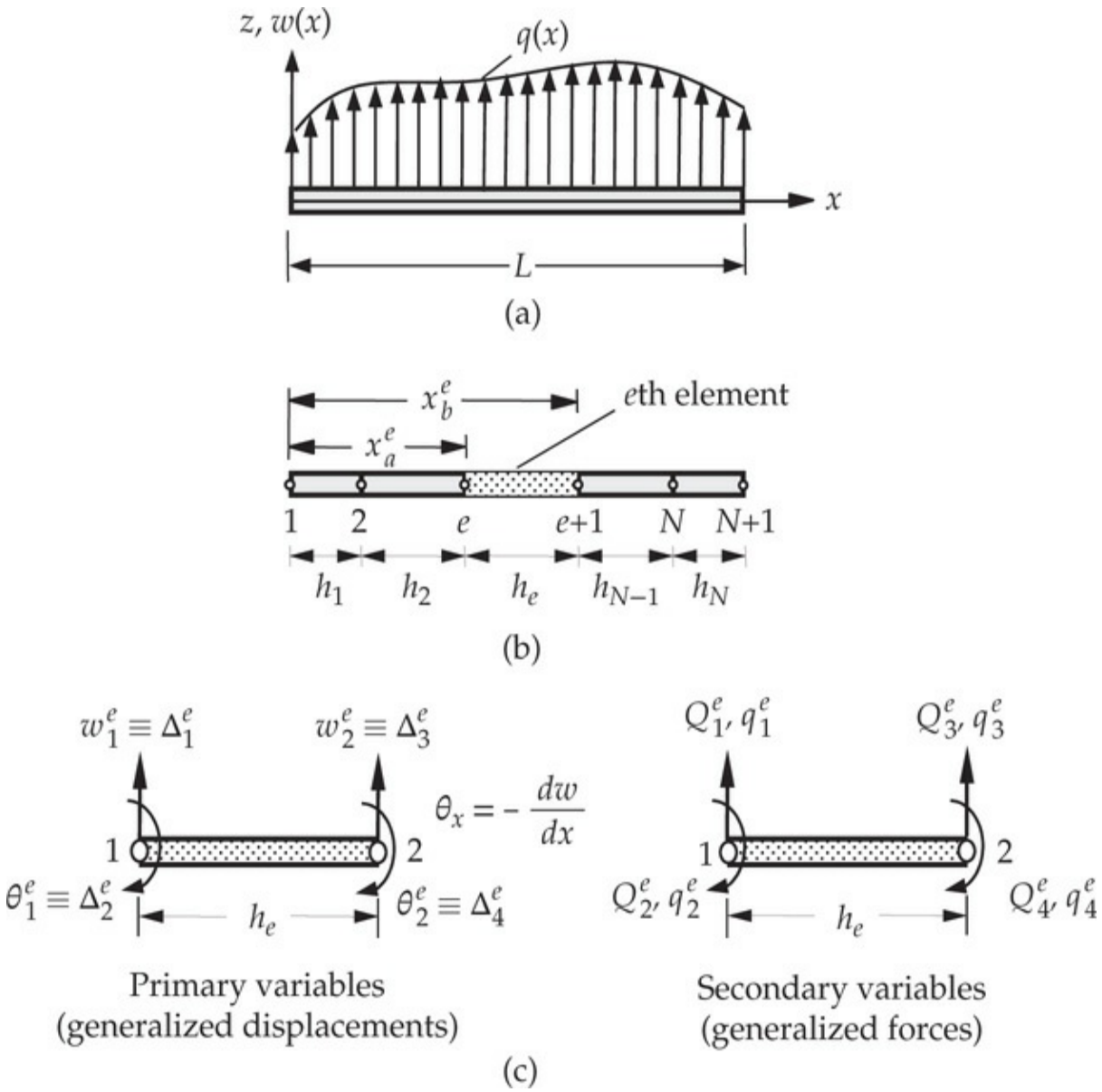

Fig. 5.2.3 (a) Geometry and typical loads on the beam. (b) Finite element discretization. (c) Generalized displacements and generalized forces on a typical element.

the differential equation, (5.2.10). We isolate a typical element $\Omega^e = (x_a^e, x_b^e)$ and construct the weak form of Eq. (5.2.10) over the element. The weak form provides the form of the primary and secondary variables of the problem. The primary variables are kinematic quantities that are required to be continuous throughout the domain, while the secondary variables are kinetic entities that are required to satisfy equilibrium conditions. When the secondary variables are physically not meaningful, the integration-by-parts step that yields them should not be carried out.

5.2.3 Weak-Form Development

The weak forms of problems in solid mechanics can be developed either from the principle of virtual work (i.e., the principle of virtual displacements or virtual forces) or from the governing differential equations. Here we start with the given differential equation, Eq. (5.2.10), and using the three-step procedure obtain the weak form. We shall also consider the principle of virtual work in the sequel.

Suppose that w_h^e is the finite element approximation of w and let v_i^e be a weight function over the element $\Omega^e = (x_a^e, x_b^e)$. Following the three-step procedure illustrated in **Example 2.4.2**, we write

$$
\begin{aligned}
0 &= \int_{x_a^e}^{x_b^e} v_i^e \left[\frac{d^2}{dx^2}\left(E_e I_e \frac{d^2 w_h^e}{dx^2} \right) + k_f^e w_h^e - q_e \right] dx \\
&= \int_{x_a^e}^{x_b^e} \left[-\frac{dv_i^e}{dx}\frac{d}{dx}\left(E_e I_e \frac{d^2 w_h^e}{dx^2} \right) + k_f^e v_i^e w_h^e - v_i^e q_e \right] dx + \left[v_i^e \frac{d}{dx}\left(E_e I_e \frac{d^2 w_h^e}{dx^2} \right) \right]_{x_a^e}^{x_b^e} \\
&= \int_{x_a^e}^{x_b^e} \left(E_e I_e \frac{d^2 v_i^e}{dx^2}\frac{d^2 w_h^e}{dx^2} + k_f^e v_i^e w_h^e - v_i^e q_e \right) dx \\
&\quad + \left[v_i^e \frac{d}{dx}\left(E_e I_e \frac{d^2 w_h^e}{dx^2} \right) - \frac{dv_i^e}{dx}\left(E_e I_e \frac{d^2 w_h^e}{dx^2} \right) \right]_{x_a^e}^{x_b^e}
\end{aligned}
\tag{5.2.11}
$$

where $\{v_i^e(x)\}$ is a set of weight functions that are twice differentiable with respect to x. Note that, in the present case, the first term of the equation is integrated twice by parts to trade two differentiations to the weight function v_i^e, while retaining two derivatives of the dependent variable, w_h^e; that is, the differentiation is distributed equally between the weight function v_i^e and the transverse deflection w_h^e. Because of the two integrations by parts, there appear two boundary expressions, which are to be evaluated at the two boundary points $x = x_a^e$ and $x = x_b^e$. Examination of the boundary terms indicates that the bending moment $M_h^e = -E_e I_e \, d^2 w_h^e / dx^2$ and shear force $V_h^e = -(d/dx)(E_e I_e \, d^2 w_h^e / dx^2)$ are the secondary variables and $(v_i^e \sim)\ w_h^e$ and slope $(dv_i^e/dx \sim)\ dw_h^e/dx$ are the primary variables. Thus, the weak form indicates that the boundary

conditions for the EBT involve specifying one element of each of the following two pairs:

$$\left(w,\ V=\frac{dM}{dx}\right),\quad \left(\theta_x\equiv-\frac{dw}{dx},\ M\right)$$

Mixed boundary conditions involve specifying a relationship between the variables of each pair:

Vertical spring: $V + k_s w = 0$; Torsional spring: $M + \mu_s \theta_x = 0$

where k_s and μ_s are the stiffness coefficients of linear and torsional springs, respectively.

We introduce the following notation for the secondary variables that is consistent with the sign convention in Fig. 5.2.2(b) $[\theta_x^e = -dw_h^e/dx]$:

$$\begin{aligned} Q_1^e &\equiv \left[\frac{d}{dx}\left(E_eI_e\frac{d^2w_h^e}{dx^2}\right)\right]_{x_a^e} = -V_h^e(x_a^e),\quad Q_2^e \equiv \left[E_eI_e\frac{d^2w_h^e}{dx^2}\right]_{x_a^e} = -M_h^e(x_a^e) \\ Q_3^e &\equiv -\left[\frac{d}{dx}\left(E_eI_e\frac{d^2w_h^e}{dx^2}\right)\right]_{x_b^e} = V_h^e(x_b),\quad Q_4^e \equiv -\left[E_eI_e\frac{d^2w_h^e}{dx^2}\right]_{x_b^e} = M_h^e(x_b^e) \end{aligned} \tag{5.2.12}$$

where V_h^e and M_h^e are the finite element approximations of the shear force V and bending moments M, respectively, and Q_1^e and Q_3^e denote the shear forces, and Q_2^e and Q_4^e denote the bending moments, as indicated in Fig. 5.2.3(c). The set $\{Q_1^e, Q_2^e, Q_3^e, Q_4^e\}$ is often referred to as the *generalized forces*. The corresponding displacements and rotations are called the *generalized displacements*. The generalized displacements are shown on a deformed beam element in Fig. 5.2.4.

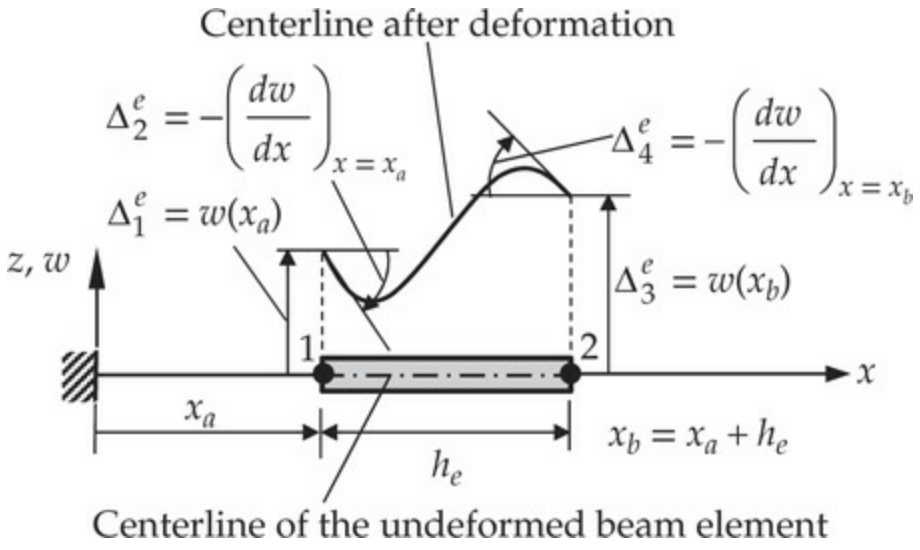

Fig. 5.2.4 Deformation of a beam element.

With the notation in Eq. (5.2.12), the weak form in Eq. (5.2.11) can be expressed as

$$0 = \int_{x_a^e}^{x_b^e} \left(E_e I_e \frac{d^2 v_i^e}{dx^2} \frac{d^2 w_h^e}{dx^2} + k_f^e v_i^e w_h^e - v_i^e q_e \right) dx$$
$$- v_i^e(x_a^e) Q_1^e - \left(-\frac{dv_i^e}{dx} \right)\Big|_{x_a^e} Q_2^e - v_i^e(x_b^e) Q_3^e - \left(-\frac{dv_i^e}{dx} \right)\Big|_{x_b^e} Q_4^e \qquad (5.2.13)$$

We can identify the bilinear and linear forms of the problem as

$$B(v_i^e, w_h^e) = \int_{x_a^e}^{x_b^e} \left(E_e I_e \frac{d^2 v_i^e}{dx^2} \frac{d^2 w_h^e}{dx^2} + k_f^e v_i^e w_h^e \right) dx \qquad (5.2.14a)$$

$$l(v_i^e) = \int_{x_a^e}^{x_b^e} v_i^e q_e \, dx + v_i^e(x_a^e) Q_1^e + \left(-\frac{dv_i^e}{dx} \right)\Big|_{x_a^e} Q_2^e$$
$$+ v_i^e(x_b^e) Q_3^e + \left(-\frac{dv_i^e}{dx} \right)\Big|_{x_b^e} Q_4^e \qquad (5.2.14b)$$

Since $B(\cdot\,, \cdot)$ is bilinear and symmetric in its arguments, we can identify the associated quadratic functional, known as the *total potential energy* of the isolated beam element, as [see Fig. 5.2.4 for the definitions of Δ_i^e; also, see Eq. (5.2.16)]

$$\Pi_e(w_h^e, \Delta_i^e) = \int_{x_a^e}^{x_b^e} \left[\frac{E_e I_e}{2} \left(\frac{d^2 w_h^e}{dx^2} \right)^2 + \frac{k_f^e}{2} (w_h^e)^2 \right] dx - \int_{x_a^e}^{x_b^e} w_h^e q_e \, dx$$
$$- \Delta_1^e Q_1^e - \Delta_3^e Q_3^e - \Delta_2^e Q_2^e - \Delta_4^e Q_4^e \equiv U^e - V^e \qquad (5.2.15)$$

The first term in the square brackets represents the elastic strain energy due to bending and the second term is the strain energy stored in the elastic foundation (the sum is the strain energy, U^e). The third term in Π^e denotes the work done by the distributed load q_e (x) and the remaining terms account for the work done by the generalized forces Q_i^e in moving through their respective generalized displacements Δ_i^e (the sum of the work done by external forces is V^e). Conversely, one may go from the total potential energy functional, Eq. (5.2.15), to the weak form, Eq. (5.2.13), by using the principle of minimum total potential energy, $\delta\Pi^e = \delta U^e - \delta V^e = 0$.

5.2.4 Approximation Functions

The weak form in Eq. (5.2.13) requires that the approximation $w_h^e(x)$ of $w(x)$ over a finite element should be such that it is twice-differentiable and satisfies the interpolation properties; that is, satisfies the following geometric "boundary conditions" of the element, as illustrated in Fig. 5.2.4:

$$w_h^e(x_a) \equiv \Delta_1^e, \quad w_h^e(x_b^e) \equiv \Delta_3^e, \quad \theta_x^e(x_a^e) \equiv \Delta_2^e, \quad \theta_x^e(x_b^e) \equiv \Delta_4^e \qquad (5.2.16)$$

Note that x_a^e and x_b^e are the global coordinates of nodes 1 and 2, respectively. In satisfying the essential (or geometric) boundary conditions in Eq. (5.2.16), the approximation automatically satisfies the continuity conditions. Hence, we pay attention to the satisfaction of the conditions in Eq. (5.2.16), which forms the basis for the derivation of the interpolation functions of the Euler–Bernoulli beam element.

Since the approximation functions to be derived are valid over the element domain, it is simpler to derive them in terms of the local coordinate $\bar{x}$ with origin at node 1, $\bar{x} = x - x_a^e$. Since there are a total of four conditions in an element (two per node), a four-parameter polynomial must be selected for w_h^e:

$$w(\bar{x}) \approx w_h^e(\bar{x}) = c_1^e + c_2^e \bar{x} + c_3^e \bar{x}^2 + c_4^e \bar{x}^3 \qquad (5.2.17)$$

Note that the minimum continuity requirement (i.e., the existence of a

nonzero second derivative of w_h^e in the element) is automatically met. In addition, the cubic approximation of w_h allows computation of the shear force, which involves the third derivative of w_h^e. Next, we express c_i^e in terms of the primary nodal variables

$$\Delta_1^e = w_h^e(0), \quad \Delta_2^e = -\left.\frac{dw_h^e}{d\bar{x}}\right|_{\bar{x}=0}, \quad \Delta_3^e = w_h^e(h_e), \quad \Delta_4^e = -\left.\frac{dw_h^e}{d\bar{x}}\right|_{\bar{x}=h_e}$$

such that the conditions (5.2.16) are satisfied:

$$\begin{aligned}
\Delta_1^e &= w_h^e(0) && = c_1^e \\
\Delta_2^e &= -\left.\frac{dw_h}{dx}\right|_{x=x_a} = -\left.\frac{dw_h^e}{d\bar{x}}\right|_{\bar{x}=0} && = -c_2^e \\
\Delta_3^e &= w_h^e(h_e) && = c_1^e + c_2^e h_e + c_3^e h_e^2 + c_4^e h_e^3 \\
\Delta_4^e &= -\left.\frac{dw_h^e}{dx}\right|_{x=x_b} = -\left.\frac{dw_h^e}{d\bar{x}}\right|_{\bar{x}=h_e} && = -c_2^e - 2c_3^e h_e - 3c_4^e h_e^2
\end{aligned} \tag{5.2.18}$$

Solving the above equations for $(c_1^e, c_2^e, c_3^e, c_4^e)$ in terms of $(\Delta_1^e, \Delta_2^e, \Delta_3^e, \Delta_4^e)$ and substituting the result into Eq. (5.2.17), we obtain (the details of this algebra are not outlined here)

$$w_h^e(\bar{x}) = \Delta_1^e \phi_1^e(\bar{x}) + \Delta_2^e \phi_2^e(\bar{x}) + \Delta_3^e \phi_3^e(\bar{x}) + \Delta_4^e \phi_4^e(\bar{x}) = \sum_{j=1}^{4} \Delta_j^e \phi_j^e(\bar{x}) \tag{5.2.19}$$

where

$$\begin{aligned}
\phi_1^e(\bar{x}) &= 1 - 3\left(\frac{\bar{x}}{h_e}\right)^2 + 2\left(\frac{\bar{x}}{h_e}\right)^3, \quad \phi_2^e(\bar{x}) = -\bar{x}\left(1 - \frac{\bar{x}}{h_e}\right)^2 \\
\phi_3^e(\bar{x}) &= 3\left(\frac{\bar{x}}{h_e}\right)^2 - 2\left(\frac{\bar{x}}{h_e}\right)^3, \qquad \phi_4^e(\bar{x}) = -\bar{x}\left[\left(\frac{\bar{x}}{h_e}\right)^2 - \frac{\bar{x}}{h_e}\right]
\end{aligned} \tag{5.2.20}$$

Note that the cubic interpolation functions in Eq. (5.2.20) are derived by interpolating w_h^e as well as its derivative $dw_h^e/dx = dw_h^e/d\bar{x}$ at the nodes. Such polynomials are known as the *Hermite family of interpolation functions*; in particular, the ϕ_i^e in Eq. (5.2.20) are called the *Hermite cubic*

interpolation functions. The functions ϕ_i^e can be expressed in terms of x by simply replacing $\bar{x}$ with $x - x_a^e$. Plots of the Hermite cubic interpolation functions are shown in Fig. 5.2.5.

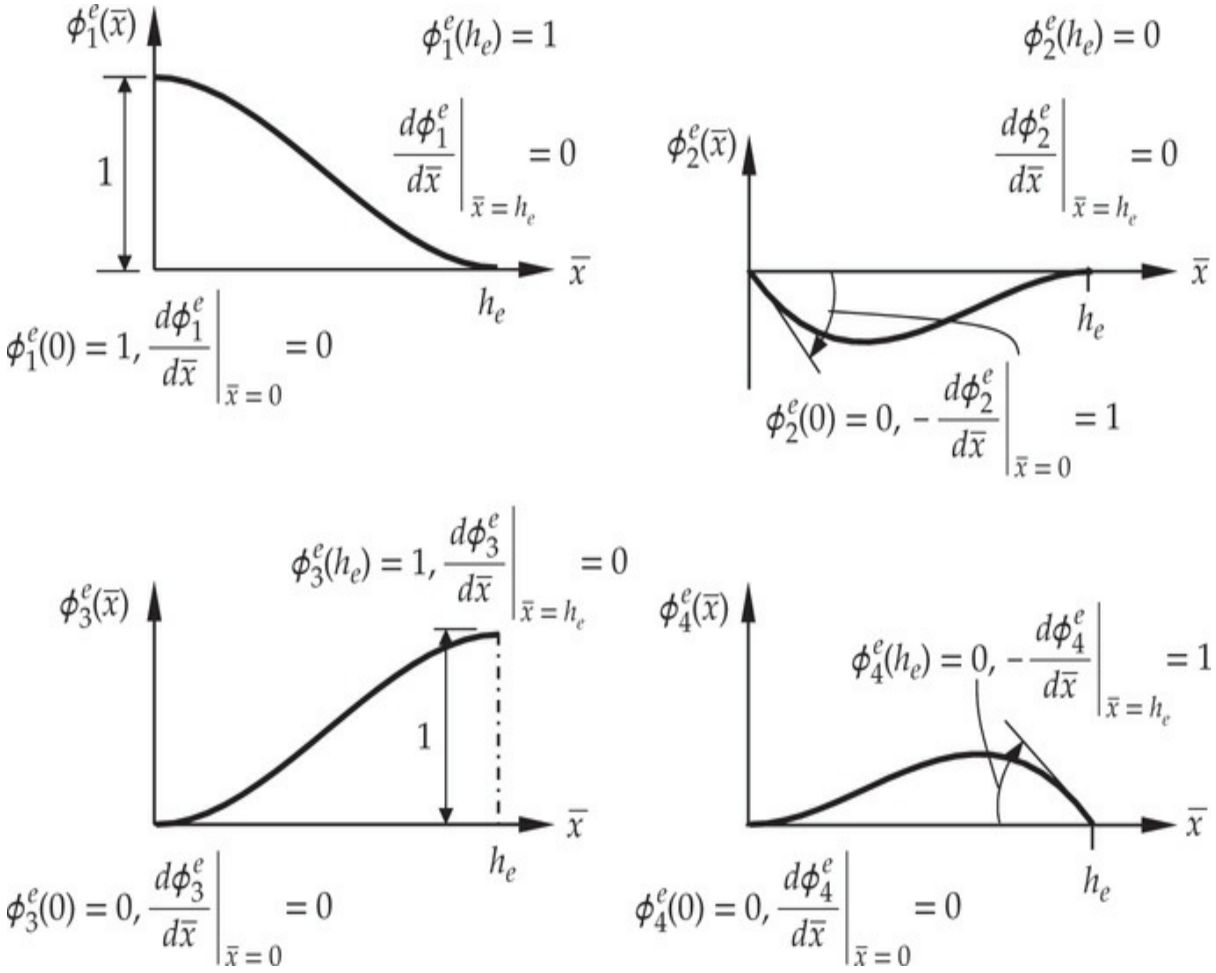

Fig. 5.2.5 Hermite cubic interpolation functions used in the Euler-Bernoulli beam element.

Recall that the Lagrange cubic interpolation functions are derived to interpolate a function, but not its derivatives, at the nodes. Hence, a Lagrange cubic element will have four nodes, with the dependent variable, not its derivative, as the nodal degree of freedom at each node. Since the derivative of w_h^e must be continuous between elements, as required by the weak form for the EBT, the Lagrange cubic approximation of w_h^e meets the continuity of w_h^e but not dw_h^e/dx, and therefore it is *not admissible* in the weak form in Eq. (5.2.13) of the EBT (see Fig. 5.2.6).

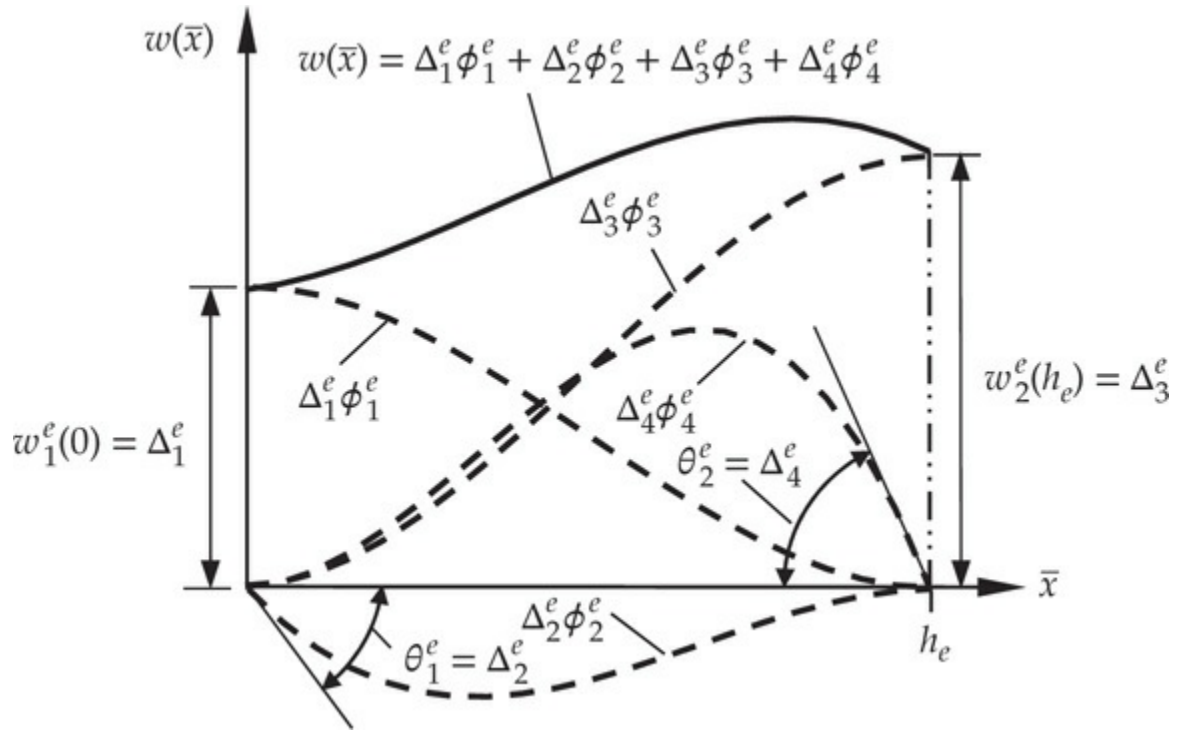

Fig. 5.2.6 Finite element solution over an element.

The first, second, and third derivatives of ϕ_i^e with respect to $\bar{x}$ (same as the derivatives with respect to x) are

$$\frac{d\phi_1^e}{d\bar{x}} = -\frac{6}{h_e}\frac{\bar{x}}{h_e}\left(1-\frac{\bar{x}}{h_e}\right), \quad \frac{d\phi_2^e}{d\bar{x}} = -\left[1+3\left(\frac{\bar{x}}{h_e}\right)^2 - 4\frac{\bar{x}}{h_e}\right]$$

$$\frac{d\phi_3^e}{d\bar{x}} = \frac{6}{h_e}\frac{\bar{x}}{h_e}\left(1-\frac{\bar{x}}{h_e}\right), \quad \frac{d\phi_4^e}{d\bar{x}} = -\frac{\bar{x}}{h_e}\left(3\frac{\bar{x}}{h_e}-2\right) \tag{5.2.21a}$$

$$\frac{d^2\phi_1^e}{d\bar{x}^2} = -\frac{6}{h_e^2}\left(1-2\frac{\bar{x}}{h_e}\right), \quad \frac{d^2\phi_2^e}{d\bar{x}^2} = -\frac{2}{h_e}\left(3\frac{\bar{x}}{h_e}-2\right)$$

$$\frac{d^2\phi_3^e}{d\bar{x}^2} = \frac{6}{h_e^2}\left(1-2\frac{\bar{x}}{h_e}\right), \quad \frac{d^2\phi_4^e}{d\bar{x}^2} = -\frac{2}{h_e}\left(3\frac{\bar{x}}{h_e}-1\right) \tag{5.2.21b}$$

$$\frac{d^3\phi_1^e}{d\bar{x}^3} = \frac{12}{h_e^3}, \quad \frac{d^3\phi_2^e}{d\bar{x}^3} = -\frac{6}{h_e^2}, \quad \frac{d^3\phi_3^e}{d\bar{x}^3} = -\frac{12}{h_e^3}, \quad \frac{d^3\phi_4^e}{d\bar{x}^3} = -\frac{6}{h_e^2} \tag{5.2.21c}$$

Plots of $d\phi_i^e/dx = d\phi^e/d\bar{x}$ are shown in Fig. 5.2.7.

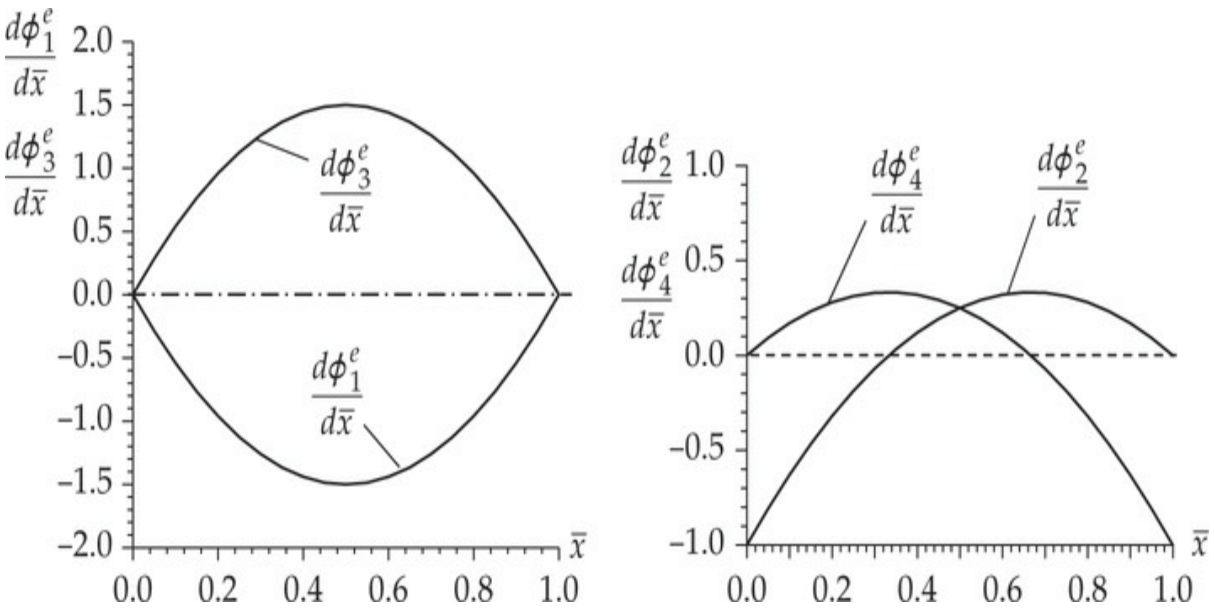

Fig. 5.2.7 Plots of the first derivatives, $d\phi_i^e/dx$, of the Hermite cubic interpolation functions.

The Hermite cubic polynomials in Eq. (5.2.20) satisfy the following interpolation properties:

$$\phi_1^e(0)=1,\quad \phi_3^e(h_e)=1,\quad \left(-\frac{d\phi_2^e}{d\bar{x}}\right)\Big|_0=1,\quad \left(-\frac{d\phi_4^e}{d\bar{x}}\right)\Big|_{h_e}=1$$

$$\phi_i^e(0)=0,\quad \phi_j^e(h_e)=0,\quad \left(-\frac{d\phi_k^e}{d\bar{x}}\right)\Big|_0=0,\quad \left(-\frac{d\phi_p^e}{d\bar{x}}\right)\Big|_{h_e}=0$$

for $i = 2, 3, 4$, $j = 1, 2, 4$, $k = 1, 3, 4$, and $p = 1, 2, 3$. These can be stated in compact form as ($i, j = 1, 2$)

$$\begin{aligned}&\phi_{2i-1}^e(\bar{x}_j)=\delta_{ij},\quad \phi_{2i}^e(\bar{x}_j)=0,\quad \sum_{i=1}^{2}\phi_{2i-1}^e=1\\ &\left(\frac{d\phi_{2i-1}^e}{d\bar{x}}\right)\Big|_{\bar{x}_j}=0,\quad \left(-\frac{d\phi_{2i}^e}{d\bar{x}}\right)\Big|_{\bar{x}_j}=\delta_{ij}\end{aligned}\tag{5.2.22}$$

where $\bar{x}_1 = 0$ and $\bar{x}_2 = h_e$ are the local coordinates of nodes 1 and 2.

It should be noted that the order of the interpolation functions derived above is the minimum required for the variational formulation in Eq. (5.2.13). If a higher-order (i.e., higher than cubic) approximation of w is desired, one must either identify additional primary unknowns at each of

the two nodes or add additional nodes with w or w and θ_x. For example, if we add d_2w/dx^2 as the primary unknown (in general, $d^2\ w/dx^2$ is not continuous between elements) at each of the two nodes, or add a third node with (w, θ_x) at each node, there will be a total of six conditions, and a fifth-order polynomial is required to interpolate the end conditions (see **Problems 5.1–5.4** for details). A fourth-degree polynomial with w and θ_x at the end nodes and w at the interior node may also be used.

5.2.5 Derivation of Element Equations (Finite Element Model)

The finite element model (i.e., algebraic equations relating the primary and secondary variables at the element nodes) of the Euler–Bernoulli beam is obtained by substituting the finite element approximation in Eq. (5.2.19) for w_h^e and the ϕ_i^e for the weight function v_i^e into the weak form in Eq. (5.2.13). The four different choices $v_1^e = \phi_1^e$, $v_2^e = \phi_2^e$, $v_3^e = \phi_3^e$, and $v_4^e = \phi_4^e$ yield a set of four algebraic equations:

$$0=\int_{x_a^e}^{x_b^e}\left[E_eI_e\frac{d^2\phi_1^e}{dx^2}\left(\sum_{j=1}^{4}\Delta_j^e\frac{d^2\phi_j^e}{dx^2}\right)+k_f^e\phi_1^e\left(\sum_{j=1}^{4}\Delta_j^e\phi_j^e\right)-\phi_1^e q_e\right]dx$$
$$-\phi_1^e(x_a^e)Q_1^e-\left(-\frac{d\phi_1^e}{dx}\right)\Big|_{x_a^e}Q_2^e-\phi_1^e(x_b^e)Q_3^e-\left(-\frac{d\phi_1^e}{dx}\right)\Big|_{x_b^e}Q_4^e$$

$$0=\int_{x_a^e}^{x_b^e}\left[E_eI_e\frac{d^2\phi_2^e}{dx^2}\left(\sum_{j=1}^{4}\Delta_j^e\frac{d^2\phi_j^e}{dx^2}\right)+k_f^e\phi_2^e\left(\sum_{j=1}^{4}\Delta_j^e\phi_j^e\right)-\phi_2^e q_e\right]dx$$
$$-\phi_2^e(x_a^e)Q_1^e-\left(-\frac{d\phi_2^e}{dx}\right)\Big|_{x_a^e}Q_2^e-\phi_2^e(x_b^e)Q_3^e-\left(-\frac{d\phi_2^e}{dx}\right)\Big|_{x_b^e}Q_4^e$$

$$0=\int_{x_a^e}^{x_b^e}\left[E_eI_e\frac{d^2\phi_3^e}{dx^2}\left(\sum_{j=1}^{4}\Delta_j^e\frac{d^2\phi_j^e}{dx^2}\right)+k_f^e\phi_3^e\left(\sum_{j=1}^{4}\Delta_j^e\phi_j^e\right)-\phi_3^e q_e\right]dx$$
$$-\phi_3^e(x_a^e)Q_1^e-\left(-\frac{d\phi_3^e}{dx}\right)\Big|_{x_a^e}Q_2^e-\phi_3^e(x_b^e)Q_3^e-\left(-\frac{d\phi_3^e}{dx}\right)\Big|_{x_b^e}Q_4^e$$

$$0=\int_{x_a^e}^{x_b^e}\left[E_eI_e\frac{d^2\phi_4^e}{dx^2}\left(\sum_{j=1}^{4}\Delta_j^e\frac{d^2\phi_j^e}{dx^2}\right)+k_f^e\phi_4^e\left(\sum_{j=1}^{4}\Delta_j^e\phi_j^e\right)-\phi_4^e q_e\right]dx$$
$$-\phi_4^e(x_a^e)Q_1^e-\left(-\frac{d\phi_4^e}{dx}\right)\Big|_{x_a^e}Q_2^e-\phi_4^e(x_b^e)Q_3^e-\left(-\frac{d\phi_4^e}{dx}\right)\Big|_{x_b^e}Q_4^e$$

The *i*th algebraic equation of the finite element model is given by

$$0=\sum_{j=1}^{4}\left[\int_{x_a^e}^{x_b^e}\left(E_eI_e\frac{d^2\phi_i^e}{dx^2}\frac{d^2\phi_j^e}{dx^2}+k_f^e\,\phi_i^e\phi_j^e\right)dx\right]\Delta_j^e-\int_{x_a^e}^{x_b^e}\phi_i^e q_e\,dx-Q_i^e$$

or

$$0=\sum_{j=1}^{4}K_{ij}^e\Delta_j^e-q_i^e-Q_i^e=0\quad\text{or}\quad\mathbf{K}^e\boldsymbol{\Delta}^e=\mathbf{q}^e+\mathbf{Q}^e\tag{5.2.23}$$

where

$$K_{ij}^e = \int_{x_a^e}^{x_b^e} \left[E_e(x) I_e(x) \frac{d^2\phi_i^e}{dx^2} \frac{d^2\phi_j^e}{dx^2} + k_f^e(x)\, \phi_i^e \phi_j^e \right] dx$$

$$= \int_0^{h_e} \left[E_e(\bar{x}) I_e(\bar{x}) \frac{d^2\phi_i^e}{d\bar{x}^2} \frac{d^2\phi_j^e}{d\bar{x}^2} + k_f^e(\bar{x})\, \phi_i^e \phi_j^e \right] d\bar{x} \qquad (5.2.24a)$$

$$q_i^e = \int_{x_a^e}^{x_b^e} \phi_i^e(x) q_e(x)\, dx = \int_0^{h_e} \phi_i^e(\bar{x}) q_e(\bar{x})\, d\bar{x} \qquad (5.2.24b)$$

Note that the coefficients K_{ij}^e are symmetric: $K_{ij}^e = K_{ji}^e$.

In matrix notation, Eq. (5.2.23) can be written explicitly as

$$\begin{bmatrix} K_{11}^e & K_{12}^e & K_{13}^e & K_{14}^e \\ K_{21}^e & K_{22}^e & K_{23}^e & K_{24}^e \\ K_{31}^e & K_{32}^e & K_{33}^e & K_{34}^e \\ K_{41}^e & K_{42}^e & K_{43}^e & K_{44}^e \end{bmatrix} \begin{Bmatrix} \Delta_1^e \\ \Delta_2^e \\ \Delta_3^e \\ \Delta_4^e \end{Bmatrix} = \begin{Bmatrix} q_1^e \\ q_2^e \\ q_3^e \\ q_4^e \end{Bmatrix} + \begin{Bmatrix} Q_1^e \\ Q_2^e \\ Q_3^e \\ Q_4^e \end{Bmatrix} \qquad (5.2.25)$$

This represents the finite element model of Eq. (5.2.10). Here $\mathbf{K}^e$ is the *stiffness matrix* and $\mathbf{F}^e \equiv \mathbf{q}^e + \mathbf{Q}^e$ is the *load vector* of a beam finite element.

For the case in which $E_e I_e$, k_f^e, and $q_e = q_0^e$ are constant over an element, the element stiffness matrix $\mathbf{K}^e$ and force vector $\mathbf{F}^e$ have the following specific forms [see Fig. 5.2.3(c) for the element-generalized displacement and force degrees of freedom; when there is no elastic foundation, set $k_f^e = 0$]:

$$\mathbf{K}^e = \frac{2E_e I_e}{h_e^3} \begin{bmatrix} 6 & -3h_e & -6 & -3h_e \\ -3h_e & 2h_e^2 & 3h_e & h_e^2 \\ -6 & 3h_e & 6 & 3h_e \\ -3h_e & h_e^2 & 3h_e & 2h_e^2 \end{bmatrix} + \frac{k_f^e h_e}{420} \begin{bmatrix} 156 & -22h_e & 54 & 13h_e \\ -22h_e & 4h_e^2 & -13h_e & -3h_e^2 \\ 54 & -13h_e & 156 & 22h_e \\ 13h_e & -3h_e^2 & 22h_e & 4h_e^2 \end{bmatrix} \qquad (5.2.26a)$$

$$\mathbf{q}^e = \frac{q_0^e h_e}{12} \begin{Bmatrix} 6 \\ -h_e \\ 6 \\ h_e \end{Bmatrix} \qquad (5.2.26b)$$

For any given distribution of the transverse load $q_e(x)$, Eq. (5.2.24b) provides a straightforward way of computing its contributions to the vector of generalized forces $\mathbf{q}^e$ at the nodes. For example, the generalized force vector in Eq. (5.2.26b) represents the "statically equivalent" forces and moments at nodes 1 and 2 due to the uniformly distributed load of intensity q_0^e over the element [see Fig. 5.2.8(a)]. Similarly, a transverse point load F_0^e applied at a point $\bar{x} = \bar{x}_0$ inside the element can be replaced by the following nodal generalized forces [see Eqs. (3.4.53)–(3.4.55)], which consist of both transverse forces (q_1^e and q_3^e) and bending moments (q_2^e and q_4^e) [see Fig. 5.2.8(b)]:

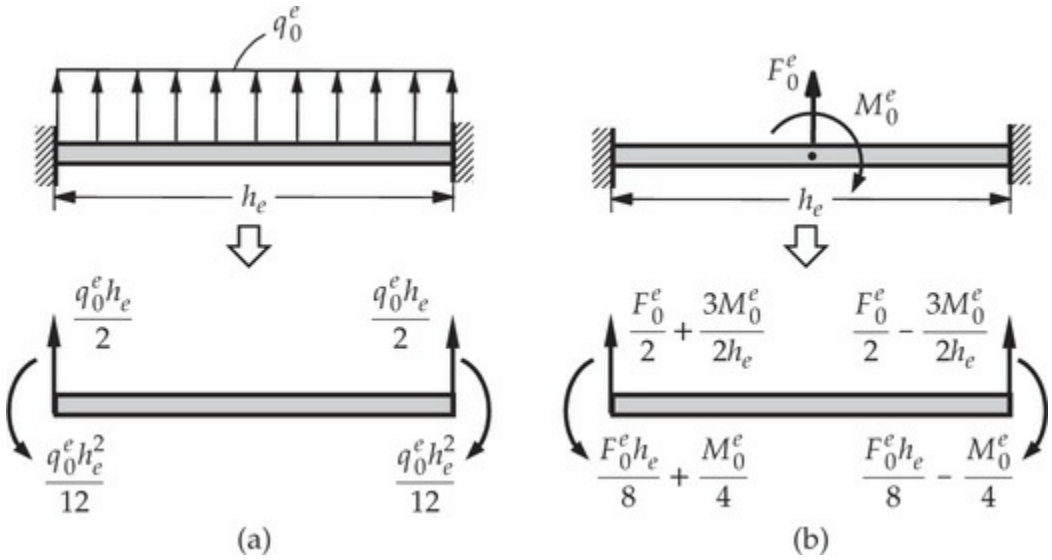

Fig. 5.2.8 Generalized nodal forces due to various applied loads.

$$q_i^e = \int_0^{h_e} \phi_i^e(\bar{x}) F_0^e \delta(\bar{x} - \bar{x}_0)\, d\bar{x} = F_0^e \phi_i^e(\bar{x}_0), \quad 0 \le \bar{x}_0 \le h_e \tag{5.2.27a}$$

$$q_1^e = F_0^e \phi_1^e(\bar{x}_0), \quad q_2^e = F_0^e \phi_2^e(\bar{x}_0), \quad q_3^e = F_0^e \phi_3^e(\bar{x}_0), \quad q_4^e = F_0^e \phi_4^e(\bar{x}_0) \tag{5.2.27b}$$

For example, when $\bar{x}_0 = 0.5h_e$, we have [using the Hermite cubic approximation functions in Eq. (5.2.20)]

$$q_1^e = F_0^e \phi_1^e(\bar{x}_0) = F_0^e \left[1 - 3\left(\frac{\bar{x}_0}{h_e}\right)^2 + 2\left(\frac{\bar{x}_0}{h_e}\right)^3\right] = 0.5F_0^e$$

$$q_2^e = F_0^e \phi_2^e(\bar{x}_0) = -F_0^e \left[\bar{x}_0\left(1 - \frac{\bar{x}_0}{h_e}\right)^2\right] = -0.125F_0^e h_e$$

$$q_3^e = F_0^e \phi_3^e(\bar{x}_0) = F_0^e \left[3\left(\frac{\bar{x}_0}{h_e}\right)^2 - 2\left(\frac{\bar{x}_0}{h_e}\right)^3\right] = 0.5F_0^e$$

$$q_4^e = F_0^e \phi_4^e(\bar{x}_0) = -F_0^e \bar{x}_0 \left[\left(\frac{\bar{x}_0}{h_e}\right)^2 - \frac{\bar{x}_0}{h_e}\right] = 0.125F_0^e h_e$$

A point moment M_0^e (clockwise) located at $\bar{x} = \bar{x}_0$ can be represented as a distributed load with the help of the derivative of the Dirac delta function (m^{-2}) as $q_e(\bar{x}) = M_0^e \delta'(\bar{x} - \bar{x}_0)$. Then we have [see Fig. 5.2.8(b)]

$$q_i^e = M_0^e \int_0^{h_e} \delta'(\bar{x} - \bar{x}_0)\phi_i^e(\bar{x})\, d\bar{x} = -M_0^e \int_0^{h_e} \delta(\bar{x} - \bar{x}_0)\phi'^e_i(\bar{x})\, d\bar{x} = -M_0^e \phi'^e_i(\bar{x}_0) \quad (5.2.28)$$

5.2.6 Assembly of Element Equations

The assembly procedure for beam elements is the same as that used for bar elements, except that we must take into account the two degrees of freedom at each node. Recall that the assembly of elements is based on (a) inter-element continuity of the primary variables (deflection and slope) and (b) inter-element equilibrium of the secondary variable (shear force and bending moment) at the nodes common to elements. To demonstrate the assembly procedure, we select a two-element model shown in Fig. 5.2.9. There are three global nodes and a total of six global generalized displacements and six generalized forces in the problem. The continuity of the primary variables implies the following relation between the element degrees of freedom Δ_i^e and the global degrees of freedom U_i (see Fig. 5.2.9):

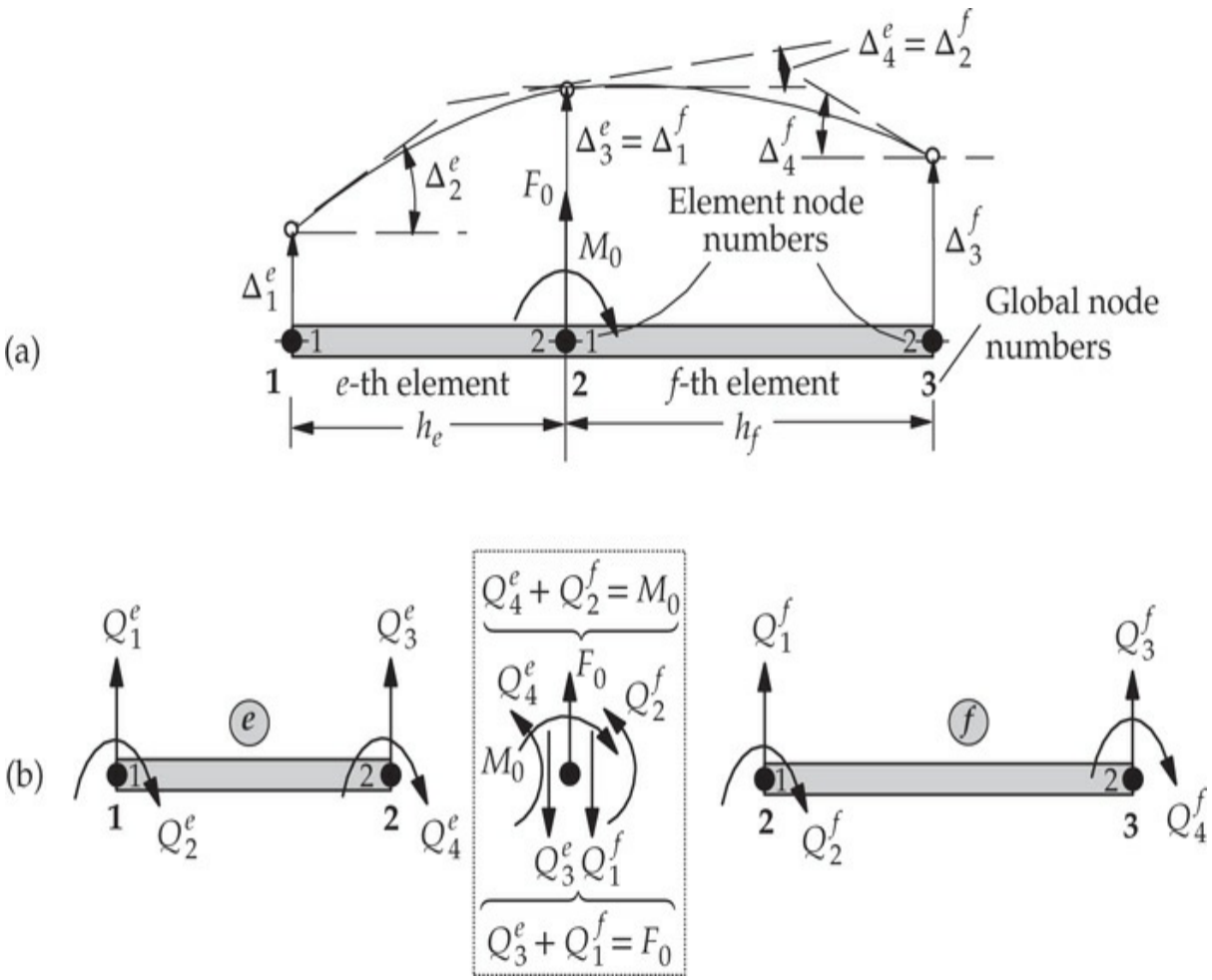

Fig. 5.2.9 Assembly of two Euler–Bernoulli beam finite elements. (a) Continuity of generalized displacements. (b) Balance of the generalized forces.

$$\begin{aligned} &\Delta_1^1 = U_1, \quad \Delta_2^1 = U_2, \quad \Delta_3^1 = \Delta_1^2 = U_3 \\ &\Delta_4^1 = \Delta_2^2 = U_4, \quad \Delta_3^2 = U_5, \quad \Delta_4^2 = U_6 \end{aligned} \tag{5.2.29}$$

In general, the equilibrium of the generalized forces at a node between two connecting elements Ω_e and Ω_f requires that

$$\begin{aligned} Q_3^e + Q_1^f &= \text{applied external point force} \\ Q_4^e + Q_2^f &= \text{applied external bending moment} \end{aligned} \tag{5.2.30}$$

If no external applied forces are given, the sum should be equated to zero. In equating the sums to the applied generalized forces (i.e., force or moment), the sign convention for the element force degrees of freedom [see Fig. 5.2.3(c)] should be followed. Forces are taken positive acting in the direction of positive z-axis and moments are taken positive when they

follow the right-hand screw rule (i.e., when thumb is along the positive *y*-axis, the four fingers show the direction of the moment). With respect to the coordinate system used in Figs. 5.2.1 and 5.2.2, *forces acting up are positive and clockwise moments are positive*.

To impose the equilibrium of forces in Eq. (5.2.30), it is necessary to add the third and fourth equations (corresponding to the second node) of element Ω^e to the first and second equations (corresponding to the first node) of element Ω^f. Consequently, the global stiffnesses K_{33}, K_{34}, K_{43}, and K_{44} associated with global node 2 are the superposition of the element stiffness coefficients:

$$K_{33} = K_{33}^1 + K_{11}^2, \quad K_{34} = K_{34}^1 + K_{12}^2, \quad K_{43} = K_{43}^1 + K_{21}^2, \quad K_{44} = K_{44}^1 + K_{22}^2 \tag{5.2.31}$$

In general, the assembled stiffness matrix and force vector *for beam elements connected in series* have the following forms:

$$\mathbf{K} = \begin{bmatrix} K_{11}^1 & K_{12}^1 & K_{13}^1 & K_{14}^1 & 0 & 0 \\ K_{21}^1 & K_{22}^1 & K_{23}^1 & K_{24}^1 & 0 & 0 \\ K_{31}^1 & K_{32}^1 & K_{33}^1 + K_{11}^2 & K_{34}^1 + K_{12}^2 & K_{13}^2 & K_{14}^2 \\ K_{41}^1 & K_{42}^1 & K_{43}^1 + K_{21}^2 & K_{44}^1 + K_{22}^2 & K_{23}^2 & K_{24}^2 \\ 0 & 0 & K_{31}^2 & K_{32}^2 & K_{33}^2 & K_{34}^2 \\ 0 & 0 & K_{41}^2 & K_{42}^2 & K_{43}^2 & K_{44}^2 \end{bmatrix}$$

$$\mathbf{F} = \begin{Bmatrix} q_1^1 \\ q_2^1 \\ q_3^1 + q_1^2 \\ q_4^1 + q_2^2 \\ q_3^2 \\ q_4^2 \end{Bmatrix} + \begin{Bmatrix} Q_1^1 \\ Q_2^1 \\ Q_3^1 + Q_1^2 \\ Q_4^1 + Q_2^2 \\ Q_3^2 \\ Q_4^2 \end{Bmatrix} \tag{5.2.32}$$

5.2.7 Imposition of Boundary Conditions and the Condensed Equations

At this step of the analysis, we must impose the particular boundary conditions of the problem being analyzed. The type of essential (also known as *geometric*) boundary conditions for a specific beam problem depends on the nature of the geometric support. Table 5.2.1 contains a list

of commonly used geometric supports for beams. The natural (also called *force*) boundary conditions involve the specification of generalized forces when the corresponding primary variables are not constrained. One must bear in mind that one and only one element of each of the following pairs must be specified at every node of the finite element mesh of a problem:

$$\left[w \text{ or } V = -\frac{d}{dx}\left(EI\frac{d^2w}{dx^2}\right)\right] \text{ and } \left[\theta_x \equiv -\frac{dw}{dx} \text{ or } M = -EI\frac{d^2w}{dx^2}\right] \tag{5.2.33}$$

At an interior node, we impose the continuity of generalized displacements and balance of generalized forces as discussed in Eqs. (5.2.29) and (5.2.30).

There are two alternative ways to include the effect of a linear elastic spring (extensional as well as torsional). (1) Include it through the boundary condition for the appropriate degree of freedom (see Table 5.2.1). (2) Include the spring as another finite element, whose element equations are given by Eq. (3.3.2). In the former case, after assembly of the element equations, the secondary variable in the direction of the spring action is replaced by the negative of the spring constant times the associated primary variable. Let V_I and M_I denote the secondary variables (transverse force and bending moment, respectively) associated with the transverse and rotational degrees of freedom and Q_0 and M_0 be their specified values at global node I. Then, we have

Table 5.2.1 Types of commonly used support conditions for beams and frames.

Type of support	Displacement boundary conditions	Force boundary conditions
Free 	None	All, as specified
Pinned 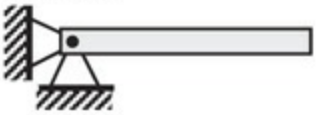	$u = w = 0$	Moment is specified
Roller (vertical) 	$u = 0$	Vertical force and moment are specified
Roller (horizontal) 	$w = 0$	Axial force and moment are specified
Fixed (or clamped) 	$u = w = \theta_x = 0$	None specified
Elastically restrained 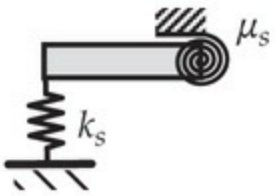	$EI\frac{d^2w}{dx^2} + \mu_s\theta_x = 0$ (mixed BC)	$\frac{d}{dx}\left(EI\frac{d^2w}{dx^2}\right) + k_s w = 0$ (mixed BC)

$$V_I + k_s w = Q_0 \quad \text{or} \quad V_I = -k_s w + Q_0 \quad \text{for vertical spring}$$
$$M_I + \mu_s \theta_x = M_0 \quad \text{or} \quad M_I = -\mu_s \theta_x + M_0 \quad \text{for torsional spring} \tag{5.2.34}$$

For example, consider the case of a beam of length L and constant bending stiffness EI, clamped at the left end and supported vertically by a linear elastic spring at the right end, and loaded by uniformly distributed force of intensity q_0, as shown in Fig. 5.2.10(a). Using one-element model of the beam, we obtain

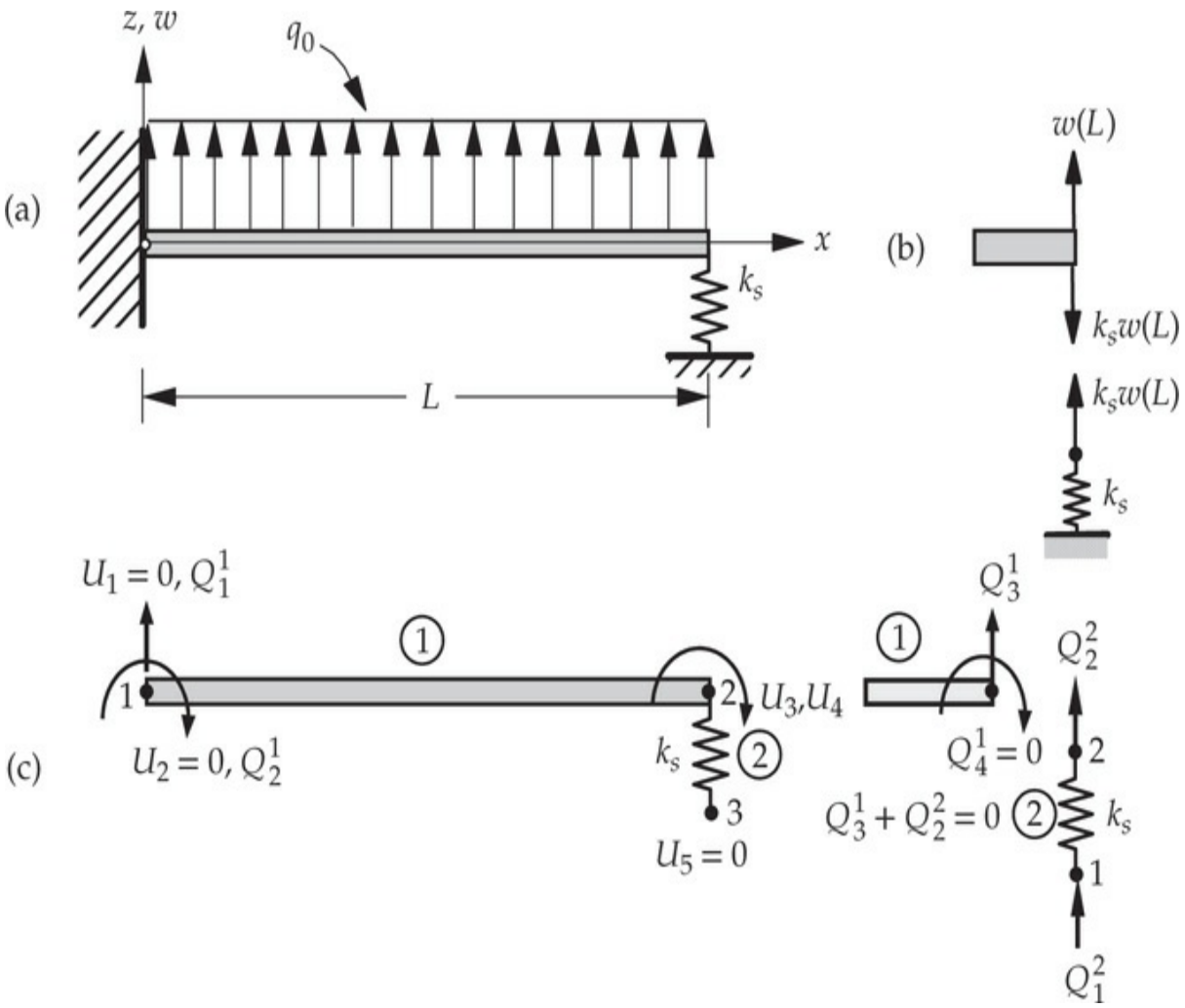

Fig. 5.2.10 (a) A spring-supported cantilever beam. (b) Spring action. (c) Finite element mesh of beam and spring elements.

$$\frac{2EI}{L^3}\begin{bmatrix} 6 & -3L & -6 & -3L \\ -3L & 2L^2 & 3L & L^2 \\ -6 & 3L & 6 & 3L \\ -3L & L^2 & 3L & 2L^2 \end{bmatrix}\begin{Bmatrix} U_1 \\ U_2 \\ U_3 \\ U_4 \end{Bmatrix} = \frac{q_0 L}{12}\begin{Bmatrix} 6 \\ -L \\ 6 \\ L \end{Bmatrix} + \begin{Bmatrix} Q_1^1 \\ Q_2^1 \\ Q_3^1 \\ Q_4^1 \end{Bmatrix} \qquad (5.2.35)$$

The boundary conditions on the primary variables (w, θ_x) are

$$w(0) = \theta_x(0) = 0 \rightarrow U_1 = U_2 = 0$$

The boundary conditions on the secondary variables (V, M) are

$$V(L) = -k_s w(L), \quad M(L) = 0 \rightarrow Q_3^1 = -k_s U_3, \quad Q_4^1 = 0$$

The spring exerts a force of $k_s\,U_3$ downward on the beam, as shown in Fig. 5.2.10(b). The direction of the spring force is solely based on the assumed direction of the vertical displacement at the point where the spring is connected. Hence, $Q_3^1 = -k_s U_3$. Imposing the boundary conditions on the finite element equations, we obtain

$$\frac{2EI}{L^3}\begin{bmatrix} 6 & -3L & -6 & -3L \\ -3L & 2L^2 & 3L & L^2 \\ -6 & 3L & 6 & 3L \\ -3L & L^2 & 3L & 2L^2 \end{bmatrix}\begin{Bmatrix} 0 \\ 0 \\ U_3 \\ U_4 \end{Bmatrix} = \frac{q_0 L}{12}\begin{Bmatrix} 6 \\ -L \\ 6 \\ L \end{Bmatrix} + \begin{Bmatrix} Q_1^1 \\ Q_2^1 \\ -k_s U_3 \\ 0 \end{Bmatrix}$$

The condensed equations for the unknown displacements U_3 (deflection) and U_4 (rotation) are

$$\begin{bmatrix} \frac{12EI}{L^3} + k_s & \frac{6EI}{L^2} \\ \frac{6EI}{L^2} & \frac{4EI}{L} \end{bmatrix}\begin{Bmatrix} U_3 \\ U_4 \end{Bmatrix} = \frac{q_0 L}{12}\begin{Bmatrix} 6 \\ L \end{Bmatrix}$$

and the condensed equations for the unknown generalized forces (i.e., reactions) are (noting that $U_1 = U_2 = 0$)

$$\begin{Bmatrix} Q_1^1 \\ Q_2^1 \end{Bmatrix} = \frac{2EI}{L^3}\begin{bmatrix} -6 & -3L \\ 3L & L^2 \end{bmatrix}\begin{Bmatrix} U_3 \\ U_4 \end{Bmatrix} - \frac{q_0 L}{12}\begin{Bmatrix} 6 \\ -L \end{Bmatrix}$$

We note that Q_1^1 and Q_2^1 can be computed only after the unknown generalized displacements are determined first. The solution of the condensed equations for the generalized displacements is

$$U_3 = w(L) = \frac{q_0 L^4}{8EI}\frac{1}{\left(1 + \frac{k_s L^3}{3E_e I_e}\right)}, \quad U_4 = \theta_x(L) = -\frac{q_0 L^3}{6EI}\frac{\left(EI - \frac{k_s L^3}{24}\right)}{\left(EI + \frac{k_s L^3}{3}\right)}$$

Note that when $k_s = 0$, we obtain the deflection $U_3 = q_0 L^4/8EI$ and rotation $U_4 = -q_0 L^3/6EI$ at the free end of a cantilever beam under uniformly distributed load of intensity q_0. When $k_s \to \infty$, we obtain the deflection $U_3 = 0$ and rotation $U_4 = -q_0 L^3/48EI$ at $x = L$ (where it is simply supported).

Alternatively, using beam (element 1) and spring (element 2) elements

connected at global node 2 and imposing the equilibrium condition $Q_3^1 + Q_2^2 = 0$, we obtain the assembled equations [see Fig. 5.2.10(c)]

$$\begin{bmatrix} \frac{12EI}{L^3} & -\frac{6EI}{L^2} & -\frac{12EI}{L^3} & -\frac{6EI}{L^2} & 0 \\ -\frac{6EI}{L^2} & \frac{4EI}{L} & \frac{6EI}{L^2} & \frac{2EI}{L} & 0 \\ -\frac{12EI}{L^3} & \frac{6EI}{L^2} & \frac{12E_eI_e}{L^3} + k_s & \frac{6EI}{L^2} & -k_s \\ -\frac{6EI}{L^2} & \frac{2EI}{L} & \frac{6EI}{L^2} & \frac{4EI}{L} & 0 \\ 0 & 0 & -k_s & 0 & k_s \end{bmatrix} \begin{Bmatrix} U_1 \\ U_2 \\ U_3 \\ U_4 \\ U_5 \end{Bmatrix} = \frac{q_0 L}{12} \begin{Bmatrix} 6 \\ -L \\ 6 \\ L \\ 0 \end{Bmatrix} + \begin{Bmatrix} Q_1^1 \\ Q_2^1 \\ 0 \\ Q_4^1 \\ Q_1^2 \end{Bmatrix}$$

Using the boundary conditions, $U_1 = U_2 = U_5 = 0$ and $Q_4^1 = 0$, we obtain the condensed equations, which are identical to those obtained earlier:

$$\begin{bmatrix} \frac{12EI}{L^3} + k_s & \frac{6EI}{L^2} \\ \frac{6EI}{L^2} & \frac{4EI}{L} \end{bmatrix} \begin{Bmatrix} U_3 \\ U_4 \end{Bmatrix} = \frac{q_0 L}{12} \begin{Bmatrix} 6 \\ L \end{Bmatrix}$$

The condensed equations for the unknown generalized forces (i.e., reactions) are (noting that $U_1 = U_2 = U_5 = 0$)

$$\begin{Bmatrix} Q_1^1 \\ Q_2^1 \\ Q_1^2 \end{Bmatrix} = \begin{bmatrix} -\frac{12EI}{L^3} & -\frac{6EI}{L^2} \\ \frac{6EI}{L^2} & \frac{2EI}{L} \\ -k_s & 0 \end{bmatrix} \begin{Bmatrix} U_3 \\ U_4 \end{Bmatrix} - \frac{q_0 L}{12} \begin{Bmatrix} 6 \\ -L \\ 0 \end{Bmatrix}$$

5.2.8 Postprocessing of the Solution

Once the boundary conditions are imposed, the resulting (condensed) equations are solved for the unknown generalized nodal displacements. The generalized forces can be computed using the condensed equations for the unknown reactions. However, this is seldom the case in practice, because the assembled equations are modified to solve for the unknown primary variables (i.e., generalized displacements). Therefore, the generalized forces are computed using the known displacement field.

The solution w_h^e and its slope θ_x^e in each element $\Omega^e = (x_a^e, x_a^e)$ are given by

$$w_h^e(\bar{x}) = \sum_{j=1}^{4} \Delta_j^e \phi_j^e(\bar{x}), \quad \theta_x^e(x) = -\frac{dw_h^e}{dx} = -\sum_{j=1}^{4} \Delta_j^e \frac{d\phi_j^e}{d\bar{x}}, \quad 0 \le \bar{x} \le h_e \tag{5.2.36}$$

The bending moment M and shear force V at any point in the element Ω^e of the beam can be post-computed from the finite element solution $w_h^e(\bar{x}),\ 0 \le \bar{x} \le h_e$, using

$$\begin{aligned} M_h^e(\bar{x}) &= -E_e I_e \frac{d^2 w_h^e}{d\bar{x}^2} \approx -E_e I_e \sum_{j=1}^{4} \Delta_j^e \frac{d^2\phi_j^e}{d\bar{x}^2} \\ V_h^e(\bar{x}) &= -\frac{d}{d\bar{x}}\left(E_e I_e \frac{d^2 w_h^e}{d\bar{x}^2}\right) \approx -\frac{d}{d\bar{x}}\left(E_e I_e \sum_{j=1}^{4} \Delta_j^e \frac{d^2\phi_j^e}{d\bar{x}^2}\right) \end{aligned} \tag{5.2.37}$$

The bending and shear stresses are given by

$$\begin{aligned} \sigma_{xx}^e(\bar{x}, z) &= -\frac{M_h^e(\bar{x}) z}{I_e} = E_e z \frac{d^2 w_h^e}{d\bar{x}^2} \approx E_e z \sum_{j=1}^{4} \Delta_j^e \frac{d^2\phi_j^e}{d\bar{x}^2} \\ \sigma_{xz}(\bar{x}, z) &= \frac{V(\bar{x}) Q(z)}{It} = -\frac{Q}{It}\frac{d}{d\bar{x}}\left(E_e I_e \frac{d^2 w}{d\bar{x}^2}\right) \approx -\frac{Q}{It}\frac{d}{d\bar{x}}\left(E_e I_e \sum_{j=1}^{4} \Delta_j^e \frac{d^2\phi_j^e}{d\bar{x}^2}\right) \end{aligned} \tag{5.2.38}$$

where t is the width of the beam at z and $Q(z)$ is the first moment of area.

Whenever the flexural rigidity $E_e I_e$ is a constant and $k_e = 0$ in each element, the finite element solution for the generalized displacements at the nodes is exact for any applied transverse load q_e. The bending moment and shear force (post-)computed using Eq. (5.2.37) are only approximate. Since the distributed load $q_e(x)$ can be represented as equivalent point loads on the element [using Eq. (5.2.24b)], the governing equation becomes a homogeneous differential equation, $E_e I_e (d^4 w^e / dx^4) = 0$, whose exact solution is a cubic polynomial, $w^e(x) = c_1^e + c_2^e x + c_3^e x^2 + c_4^e x^3$; this is the polynomial approximation assumed in the finite element approximation [see Eq. (5.2.17)]. Further, the finite element solution is exact at all points of the element if the distributed load is zero.

5.2.9 Numerical Examples

In this section we consider several examples to illustrate the application of the finite element method for the analysis of straight beams. As indicated earlier, the finite element method gives exact generalized nodal displacements and forces when $k_f = 0$ and EI is a constant (element-wise).

Example 5.2.1

Consider a cantilever beam of length L and subjected to linearly varying distributed load $q(x)$, point load F_0 and moment M_0, as shown in Fig. 5.2.11. Determine the displacement field $w(x)$ and bending moment $M(x)$ in the beam using two elements ($h_1 = h_2 = h = L/2$). Compare the finite element solution against the exact solution.

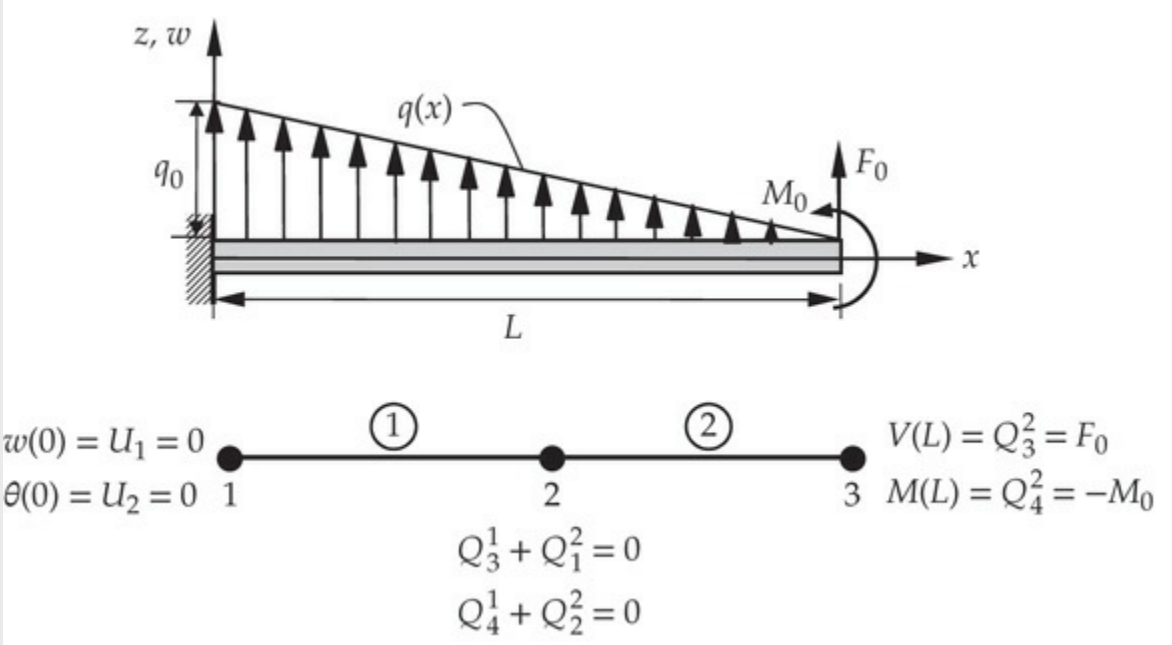

Fig. 5.2.11 The cantilever beam problem considered in **Example 5.2.1**.

Solution: First we note that $q(x) = q_0\,(1 - x/L)$. Therefore, we must evaluate its contribution to the element load vector according to Eq. (5.2.24b):

$$q_i^e = \int_{x_a^e}^{x_b^e} q_0\left(1 - \frac{x}{L}\right)\phi_i^e(x)\,dx = \int_0^{h_e} q_0\left(1 - \frac{\bar{x} + x_a^e}{L}\right)\phi_i^e(\bar{x})\,d\bar{x} \tag{1}$$

where $\phi_i^e(\bar{x})$ are given in Eq. (5.2.20). Evaluating the integrals, we obtain

$$\mathbf{q}^e = \frac{q_0 h_e}{12}\begin{Bmatrix} 6 \\ -h_e \\ 6 \\ h_e \end{Bmatrix} + \frac{q_0 h_e}{60L}\begin{Bmatrix} -(9h_e + 30x_a^e) \\ h_e(2h_e + 5x_a^e) \\ -(21h_e + 30x_a^e) \\ -h_e(3h_e + 5x_a^e) \end{Bmatrix} \tag{2}$$

and specializing the above vectors to element $1\ (x_a^1 = 0)$ and element $2\ (x_a^2 = h_1 = L/2)$, one obtains ($h_1 = h_2 = h = L/2$)

$$\mathbf{q}^1 = \frac{q_0 h}{12}\begin{Bmatrix} 6 \\ -h \\ 6 \\ h \end{Bmatrix} - \frac{q_0 h}{120}\begin{Bmatrix} 9 \\ -2h \\ 21 \\ 3h \end{Bmatrix};\quad \mathbf{q}^2 = \frac{q_0 h}{12}\begin{Bmatrix} 6 \\ -h \\ 6 \\ h \end{Bmatrix} - \frac{q_0 h}{120}\begin{Bmatrix} 39 \\ -7h \\ 51 \\ 8h \end{Bmatrix} \tag{3}$$

The equilibrium of generalized forces at global node 2 requires

$$Q_3^1 + Q_1^2 = 0, \quad Q_4^1 + Q_2^2 = 0$$

These conditions require us to add the third equation of element 1 to the first equation of element 2 and the fourth equation of element 1 to the second equation of element 2. The first two equations of element 1 and the last two equations of element 2 remain unchanged. Thus, the assembled system of equations for a uniform mesh of two elements ($h_1 = h_2 = L/2$) with constant EI and foundation modulus $k_f = 0$ is

$$\frac{2EI}{h^3}\begin{bmatrix} 6 & -3h & -6 & -3h & 0 & 0 \\ -3h & 2h^2 & 3h & h^2 & 0 & 0 \\ -6 & 3h & 6+6 & 3h-3h & -6 & -3h \\ -3h & h^2 & 3h-3h & 2h^2+2h^2 & 3h & h^2 \\ 0 & 0 & -6 & 3h & 6 & 3h \\ 0 & 0 & -3h & h^2 & 3h & 2h^2 \end{bmatrix}\begin{Bmatrix} U_1 \\ U_2 \\ U_3 \\ U_4 \\ U_5 \\ U_6 \end{Bmatrix}$$

$$= \frac{q_0 h}{12}\begin{Bmatrix} 6 \\ -h \\ 12 \\ 0 \\ 6 \\ h \end{Bmatrix} - \frac{q_0 h}{120}\begin{Bmatrix} 9 \\ -2h \\ 60 \\ -4h \\ 51 \\ 8h \end{Bmatrix} + \begin{Bmatrix} Q_1^1 \\ Q_2^1 \\ Q_3^1 + Q_1^2 = 0 \\ Q_4^1 + Q_2^2 = 0 \\ Q_3^2 \\ Q_4^2 \end{Bmatrix} \tag{4}$$

Since the beam is clamped at global node 1, the transverse displacement U_1 and slope U_2 are zero there. Hence, the corresponding generalized forces Q_1^1 and Q_2^1 (the shear force and the bending moment,

respectively) are not known. At global node 3, the shear force is given as F_0, and the bending moment as M_0 [use the sign convention for F_0 and M_0 from Fig. 5.2.3(c)]:

$$Q_3^2 = F_0, \quad Q_4^2 = -M_0$$

Hence, the assembled equations take the form ($h = L/2$)

$$\frac{4EI}{L^3}\begin{bmatrix} 24 & -6L & -24 & -6L & 0 & 0 \\ -6L & 2L^2 & 6L & L^2 & 0 & 0 \\ -24 & 6L & 48 & 0 & -24 & -6L \\ -6L & L^2 & 0 & 4L^2 & 6L & L^2 \\ 0 & 0 & -24 & 6L & 24 & 6L \\ 0 & 0 & -6L & L^2 & 6L & 2L^2 \end{bmatrix}\begin{Bmatrix} 0 \\ 0 \\ U_3 \\ U_4 \\ U_5 \\ U_6 \end{Bmatrix}$$

$$= \frac{q_0 L}{48}\begin{Bmatrix} 12 \\ -L \\ 24 \\ 0 \\ 12 \\ L \end{Bmatrix} - \frac{q_0 L}{480}\begin{Bmatrix} 18 \\ -2L \\ 120 \\ -4L \\ 102 \\ 8L \end{Bmatrix} + \begin{Bmatrix} Q_1^1 \\ Q_2^1 \\ 0 \\ 0 \\ F_0 \\ -M_0 \end{Bmatrix}$$

The condensed equations for the unknown generalized displacements are obtained by deleting the rows and columns corresponding to the known generalized displacements (i.e., rows and columns 1 and 2)

$$\frac{4EI}{L^3}\begin{bmatrix} 48 & 0 & -24 & -6L \\ 0 & 4L^2 & 6L & L^2 \\ -24 & 6L & 24 & 6L \\ -6L & L^2 & 6L & 2L^2 \end{bmatrix}\begin{Bmatrix} U_3 \\ U_4 \\ U_5 \\ U_6 \end{Bmatrix} = \frac{q_0 L}{48}\begin{Bmatrix} 24 \\ 0 \\ 12 \\ L \end{Bmatrix} - \frac{q_0 L}{480}\begin{Bmatrix} 120 \\ -4L \\ 102 \\ 8L \end{Bmatrix} + \begin{Bmatrix} 0 \\ 0 \\ F_0 \\ -M_0 \end{Bmatrix}$$

The condensed equations for the unknown generalized forces are obtained from the first two equations of the assembled system

$$\begin{Bmatrix} Q_1^1 \\ Q_2^1 \end{Bmatrix} = \frac{4EI}{L^3}\begin{bmatrix} -24 & -6L & 0 & 0 \\ 6L & L^2 & 0 & 0 \end{bmatrix}\begin{Bmatrix} U_3 \\ U_4 \\ U_5 \\ U_6 \end{Bmatrix} - \frac{q_0 L}{48}\begin{Bmatrix} 12 \\ -L \end{Bmatrix} + \frac{q_0 L}{480}\begin{Bmatrix} 18 \\ -2L \end{Bmatrix}$$

The solution of the condensed equations for the displacements yields

$$\begin{Bmatrix} U_3 \\ U_4 \\ U_5 \\ U_6 \end{Bmatrix} = \frac{L^3}{4EI}\begin{bmatrix} 48 & 0 & -24 & -6L \\ 0 & 4L^2 & 6L & L^2 \\ -24 & 6L & 24 & 6L \\ -6L & L^2 & 6L & 2L^2 \end{bmatrix}^{-1} \begin{Bmatrix} \frac{1}{4}q_0 L \\ \frac{1}{120}q_0 L^2 \\ F_0 + \frac{3}{80}q_0 L \\ -M_0 + \frac{1}{240}q_0 L^2 \end{Bmatrix}$$

$$= \frac{L}{48EI}\begin{bmatrix} 2L^2 & -6L & 5L^2 & -6L \\ -6L & 24 & -18L & 24 \\ 5L^2 & -18L & 16L^2 & -24L \\ -6L & 24 & -24L & 48 \end{bmatrix} \begin{Bmatrix} \frac{1}{4}q_0 L \\ \frac{1}{120}q_0 L^2 \\ F_0 + \frac{3}{80}q_0 L \\ -M_0 + \frac{1}{240}q_0 L^2 \end{Bmatrix}$$

$$= \frac{L}{48EI}\begin{Bmatrix} 5L^2 F_0 + 6LM_0 + \frac{49}{80}q_0 L^3 \\ -18LF_0 - 24M_0 - \frac{15}{8}q_0 L^2 \\ 16L^2 F_0 + 24LM_0 + \frac{16}{10}q_0 L^3 \\ -24LF_0 - 48M_0 - 2q_0 L^2 \end{Bmatrix} \tag{5}$$

The reactions Q_1^1 and Q_2^1 are

$$\begin{Bmatrix} Q_1^1 \\ Q_2^1 \end{Bmatrix} = \frac{4EI}{L^3}\begin{bmatrix} -24 & -6L \\ 6L & L^2 \end{bmatrix}\begin{Bmatrix} U_3 \\ U_4 \end{Bmatrix} - \frac{q_0 L}{480}\begin{Bmatrix} 102 \\ -8L \end{Bmatrix}$$

$$= \begin{Bmatrix} -\left(F_0 + \frac{1}{2}q_0 L\right) \\ L\left(F_0 + \frac{1}{6}q_0 L\right) + M_0 \end{Bmatrix} \tag{6}$$

It is clear that the reactions Q_1^1 and Q_2^1 computed above satisfy the static equilibrium equations of the beam:

$$Q_1^1 + F_0 + \frac{1}{2}q_0 L = 0, \quad Q_2^1 - \left(F_0 L + \frac{1}{6}q_0 L^2 + M_0\right) = 0$$

The reactions Q_1^1 and Q_2^1 can also be computed using the definitions in Eq. (5.2.12):

$$(Q_1^1)_{\text{def}} \equiv \frac{d}{dx}\left(EI\frac{d^2 w}{dx^2}\right)\Big|_{x=0}, \quad (Q_2^1)_{\text{def}} \equiv \left(EI\frac{d^2 w}{dx^2}\right)\Big|_{x=0}$$

From Eqs. (5.2.21b) and (5.2.21c) we note that the second derivatives of the Hermite cubic interpolation functions are linear polynomials over the element and the third derivative is constant over the element. Therefore, the bending moment and shear force computed using the definitions in

Eq. (5.2.37) are element-wise linear and constant, respectively. Further, at nodes connecting two elements, they yield discontinuous values because the second and third derivatives of w are not made continuous across the inter-element nodes. Thus, we have

$$\begin{aligned}
(Q_1^1)_{\text{def}} &= EI\left(U_3\frac{d^3\phi_3^1}{dx^3} + U_4\frac{d^3\phi_4^1}{dx^3}\right)\Big|_{x=0} \\
&= EI\left[U_3\left(-\frac{96}{L^3}\right) + U_4\left(-\frac{24}{L^2}\right)\right] \\
&= -\left(F_0 + \frac{23}{80}q_0L\right) \\
(Q_2^1)_{\text{def}} &= EI\left(U_3\frac{24}{L^2} + U_4\frac{4}{L}\right) \\
&= \left(M_0 + F_0L + \frac{3}{20}q_0L^2\right)
\end{aligned} \tag{7}$$

which are in error by $q_1^e = -\frac{17}{80}q_0L$ and $q_2^e = \frac{1}{60}q_0L^2$ compared with those computed using the condensed (i.e., equilibrium) equations.

The finite element solution as a function of position x is given by

$$w_h^e(x) = \begin{cases} U_3\phi_3^{(1)} + U_4\phi_4^{(1)} & \text{for } 0 \le x \le h \\ U_3\phi_1^{(2)} + U_4\phi_2^{(2)} + U_5\phi_3^{(2)} + U_6\phi_4^{(2)} & \text{for } h \le x \le 2h \end{cases} \tag{8}$$

$$\begin{aligned}
\phi_3^{(1)} &= 3\left(\frac{x}{h}\right)^2 - 2\left(\frac{x}{h}\right)^3, & \phi_4^{(1)} &= h\left[\left(\frac{x}{h}\right)^2 - \left(\frac{x}{h}\right)^3\right] \\
\phi_1^{(2)} &= 1 - 3\left(1 - \frac{x}{h}\right)^2 - 2\left(1 - \frac{x}{h}\right)^3, & \phi_2^{(2)} &= h\left(1 - \frac{x}{h}\right)\left(2 - \frac{x}{h}\right)^2 \\
\phi_3^{(2)} &= 3\left(1 - \frac{x}{h}\right)^2 + 2\left(1 - \frac{x}{h}\right)^3, & \phi_4^{(2)} &= h\left[\left(1 - \frac{x}{h}\right)^3 + \left(1 - \frac{x}{h}\right)^2\right]
\end{aligned} \tag{9}$$

The exact solution of the problem can be obtained by direct integration as

$$
\begin{aligned}
w(x) &= \frac{q_0 L^4}{120EI}\left[10\left(\frac{x}{L}\right)^2 - 10\left(\frac{x}{L}\right)^3 + 5\left(\frac{x}{L}\right)^4 - \left(\frac{x}{L}\right)^5\right] \\
&\quad + \frac{F_0 L^3}{6EI}\left[3\left(\frac{x}{L}\right)^2 - \left(\frac{x}{L}\right)^3\right] + \frac{M_0 L^2}{2EI}\left(\frac{x}{L}\right)^2 \\
\theta_x(x) &= -\frac{q_0 L^3}{24EI}\left[4\left(\frac{x}{L}\right) - 6\left(\frac{x}{L}\right)^2 + 4\left(\frac{x}{L}\right)^3 - \left(\frac{x}{L}\right)^4\right] \\
&\quad + \frac{F_0 L^2}{2EI}\left[-2\left(\frac{x}{L}\right) + \left(\frac{x}{L}\right)^2\right] - \frac{M_0 L}{EI}\left(\frac{x}{L}\right) \\
M(x) &= -\frac{q_0 L^2}{6}\left[1 - 3\left(\frac{x}{L}\right) + 3\left(\frac{x}{L}\right)^2 - \left(\frac{x}{L}\right)^3\right] + F_0 L\left[-1 + \left(\frac{x}{L}\right)\right] - M_0 \\
V(x) &= -\frac{q_0 L}{2}\left[-1 + 2\frac{x}{L} - \left(\frac{x}{L}\right)^2\right] + F_0
\end{aligned}
\tag{10}
$$

The finite element solution in Eq. (8) and the exact solution in Eq. (10) are compared in Table 5.2.2 for the following data: q_0 = 24 kN/m, F_0 = 60 kN, L = 3 m, M_0 = 0 kN-m, E = 200 × 10^6 kN/m^2, and I = 29 × 10^6 mm^4 (EI = 5800 kN-m^2). As expected, the finite element solutions for w and $\theta_x = -dw/dx$ coincide with the exact values at the nodes. At points other than the nodes, the difference between the finite element and exact solutions is virtually negligible.

Table 5.2.2 Comparison of the finite element solution with the exact solution of the cantilever beam of Fig. 5.2.11 (2 elements); q_0 = 24 kN/m, F_0 = 60 kN, L = 3 m, M^0 = 0 kN-m, and EI = 5800 kN-m^2.

	w (m)		dw/dx		$-M \times 10^{-6}$ (N-m)	
x (m)	FEM	Exact	FEM	Exact	FEM	Exact
0.0000	0.0000[1]	0.0000	0.0000[1]	0.0000	0.2124[2]	0.2160
0.1875	0.0006	0.0006	0.0066	0.0067	0.1973	0.1984
0.3750	0.0025	0.0025	0.0128	0.0128	0.1821	0.1816
0.5625	0.0054	0.0054	0.0184	0.0185	0.1670	0.1656
0.7500	0.0093	0.0094	0.0235	0.0235	0.1519	0.1502
0.9375	0.0142	0.0142	0.0282	0.0282	0.1367	0.1354
1.1250	0.0199	0.0199	0.0324	0.0323	0.1216	0.1213
1.3125	0.0263	0.0263	0.0361	0.0360	0.1065	0.1077
1.5000	0.0333[1]	0.0334	0.0393[1]	0.0393	0.0913[3]	0.0945
1.6875	0.0410	0.0410	0.0421	0.0421	0.0814	0.0818
1.8750	0.0491	0.0491	0.0445	0.0446	0.0696	0.0694
2.0625	0.0577	0.0577	0.0466	0.0466	0.0579	0.0574
2.2500	0.0666	0.0666	0.0483	0.0483	0.0461	0.0456
2.4375	0.0758	0.0758	0.0496	0.0496	0.0344	0.0340
2.6250	0.0852	0.0852	0.0505	0.0505	0.0226	0.0226
2.8025	0.0947	0.0947	0.0510	0.0510	0.0109	0.0113
3.0000	0.1043[1]	0.1042	0.0512[1]	0.0512	−0.0009	0.0000

[1] Nodal values; all others are computed by interpolation; [2] post-computed values using the definition; [3] 0.0932 from the second element.

Example 5.2.2

Consider an I-section composite beam made of structural steel (E = 200 GPa), fixed at the right end and spring-supported at the left end, as shown in Fig. 5.2.12(a). Assume the following discontinuous data for the moment of inertia I:

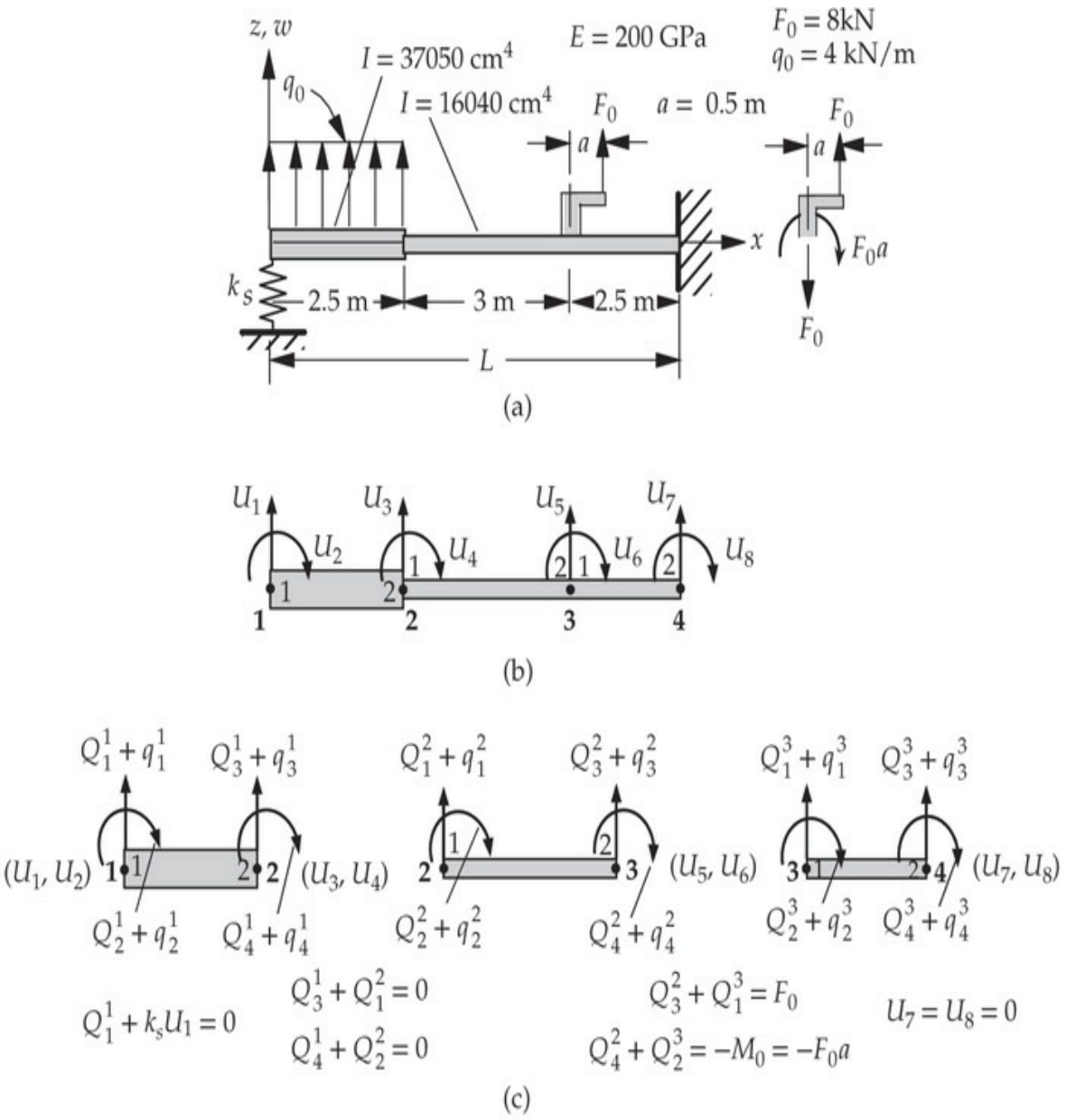

Fig. 5.2.12 (a) Physical problem. (b) Finite element mesh of three elements. (c) Equilibrium of generalized forces.

$$I = \begin{cases} 37050\ \text{cm}^4 & \text{for } 0.0 \le x \le 2.5\ \text{m} \\ 16040\ \text{cm}^4 & \text{for } 2.5\ \text{m} \le x \le 8.0\ \text{m} \end{cases}$$

and F_0 = 8 kN. The depth of the beam is h_1 = 460 mm in the first part and h_2 = 358 mm in the second part. Use the minimum number of Euler–Bernoulli beam finite elements to formulate the steps in the finite element analysis of the problem. Determine the generalized displacements at the nodes and the generalized reaction forces for the three ratios: $k_s/EI = 0$, $k_s/EI = 10^{-3}$, and $k_s/EI = 1$, where k_s is the spring constant.

Solution: We shall use three finite elements, as dictated by the problem data, to analyze the problem. There are four nodes and eight global degrees of freedom in the non-uniform mesh, as can be seen from Fig. 5.2.12(b). Since EI and q are element-wise constant, the element stiffness matrix (with $k_f = 0$) and the force vector are given by Eqs. (5.2.26a) and (5.2.26b), respectively ($q^{(1)} = 4$ kN/m and $q^{(2)} = q^{(3)} = 0$).

The equilibrium of internal forces and moments require, as indicated in Fig. 5.2.12(c),

$$Q_3^1 + Q_1^2 = 0, \quad Q_4^1 + Q_2^2 = 0, \quad Q_3^2 + Q_1^3 = F_0, \quad Q_4^2 + Q_2^3 = -aF_0$$

The assembled finite element equations of the three-element mesh are [$(EI)_1 = 74.1 \times 10^6$ N-m^2 and $(EI)_2 = 32.08 \times 10^6$ N-m^2, $F_0 = 8$ kN, $q_0 = 4$ kN/m, and $aF_0 = 4$ kN-m]:

$$10^8 \begin{bmatrix} 0.5691 & -0.7114 & -0.5691 & -0.7114 & 0.0000 & 0.0000 & 0.0000 & 0.0000 \\ -0.7114 & 1.1856 & 0.7114 & 0.5928 & 0.0000 & 0.0000 & 0.0000 & 0.0000 \\ -0.5691 & 0.7114 & 0.7117 & 0.4975 & -0.1426 & -0.2139 & 0.0000 & 0.0000 \\ -0.7114 & 0.5928 & 0.4975 & 1.6133 & 0.2139 & 0.2139 & 0.0000 & 0.0000 \\ 0.0000 & 0.0000 & -0.1426 & 0.2139 & 0.3889 & -0.0941 & -0.2464 & -0.3080 \\ 0.0000 & 0.0000 & -0.2139 & 0.2139 & -0.0941 & 0.9410 & 0.3080 & 0.2566 \\ 0.0000 & 0.0000 & 0.0000 & 0.0000 & -0.2464 & 0.3080 & 0.2464 & 0.3080 \\ 0.0000 & 0.0000 & 0.0000 & 0.0000 & -0.3080 & 0.2566 & 0.3080 & 0.5133 \end{bmatrix}$$

$$\times \begin{Bmatrix} U_1 \\ U_2 \\ U_3 \\ U_4 \\ U_5 \\ U_6 \\ U_7 \\ U_8 \end{Bmatrix} = 10^4 \begin{Bmatrix} 0.5000 \\ -0.2083 \\ 0.5000 \\ 0.2083 \\ 0.0000 \\ 0.0000 \\ 0.0000 \\ 0.0000 \end{Bmatrix} + \begin{Bmatrix} Q_1^1 \\ Q_2^1 \\ Q_3^1 + Q_1^2 = 0 \\ Q_4^1 + Q_2^2 = 0 \\ Q_3^2 + Q_1^3 = F_0 \\ Q_4^2 + Q_2^3 = -aF_0 \\ Q_3^3 \\ Q_4^3 \end{Bmatrix}$$

The boundary conditions of the problem are

$$\left[EI\frac{d^3w}{dx^3} + k_s w\right]_{x=0} = 0, \quad \left[EI\frac{d^2w}{dx^2}\right]_{x=0} = 0, \quad w(8) = 0, \quad \left[\frac{dw}{dx}\right]_{x=8} = 0$$

which translate into

$$Q_1^1 + k_s U_1 = 0, \quad Q_2^1 = 0, \quad U_7 = 0, \quad U_8 = 0$$

Note that the forces Q_1^1 and Q_3^3 and the moment Q_4^3 (the reactions at the supports) are not known.

Using the boundary and equilibrium conditions listed above, we can write the condensed equations for the unknown generalized displacements and forces. The condensed equations for the unknown generalized displacements can be obtained by deleting the last two rows and two columns, which correspond to the known generalized displacements U_7 and U_8 ($\alpha = 10^{-8}k_s$):

$$10^8 \begin{bmatrix} 0.5691+\alpha & -0.7114 & -0.5691 & -0.7114 & 0.0000 & 0.0000 \\ -0.7114 & 1.1856 & 0.7114 & 0.5928 & 0.0000 & 0.0000 \\ -0.5691 & 0.7114 & 0.7117 & 0.4975 & -0.1426 & -0.2139 \\ -0.7114 & 0.5928 & 0.4975 & 1.6133 & 0.2139 & 0.2139 \\ 0.0000 & 0.0000 & -0.1426 & 0.2139 & 0.3889 & -0.0941 \\ 0.0000 & 0.0000 & -0.2139 & 0.2139 & -0.0941 & 0.9410 \end{bmatrix} \begin{Bmatrix} U_1 \\ U_2 \\ U_3 \\ U_4 \\ U_5 \\ U_6 \end{Bmatrix}$$

$$= 10^4 \begin{Bmatrix} 0.5000 \\ -0.2083 \\ 0.5000 \\ 0.2083 \\ 0.8000 \\ -0.4000 \end{Bmatrix}$$

The reactions at the support can be computed from the last two equations of the assembled system:

$$\begin{Bmatrix} Q_3^3 \\ Q_4^3 \end{Bmatrix} = 10^8 \begin{bmatrix} -0.2464 & 0.3080 \\ -0.2464 & 0.2566 \end{bmatrix} \begin{Bmatrix} U_5 \\ U_6 \end{Bmatrix}$$

The force in the spring, Q_1^1, can be computed from $Q_1^1 = -k_s U_1$ N.

The solution (with the help of the program FEM1D discussed in Chapter 8) of the condensed equations for the generalized displacements, post-computed generalized reaction forces [the same as those obtained using the definitions, Eq. (5.2.12)], and the maximum bending stress ($\sigma = -Q_4^3 h_2/2I_2$) for various ratios of k_s to EI are:

$$
\begin{aligned}
k_s/EI = 0: \quad & U_1 = 0.0441 \text{ m},\ U_2 = 0.7466 \times 10^{-2},\ U_3 = 0.0255 \text{ m} \\
& U_4 = 0.7325 \times 10^{-2},\ U_5 = 0.0067 \text{ m},\ U_6 = 0.4754 \times 10^{-2} \\
& Q_3^3 = -18 \text{ kN},\ Q_4^3 = -83.5 \text{ kN-m},\ \sigma(8) = 93.2 \text{ MPa} \\
k_s/EI = 10^{-3}: \quad & U_1 = 0.0318 \text{ m},\ U_2 = 0.5248 \times 10^{-2},\ U_3 = 0.0186 \text{ m} \\
& U_4 = 0.5207 \times 10^{-2},\ U_5 = 0.0050 \text{ m},\ U_6 = 0.3516 \times 10^{-2} \\
& Q_3^3 = -15.65 \text{ kN},\ Q_4^3 = -64.67 \text{ kN-m},\ \sigma(8) = 72.2 \text{ MPa} \\
k_s/EI = 1: \quad & U_1 = 0.0001 \text{ m},\ U_2 = 0.4565 \times 10^{-3},\ U_3 = 0.0010 \text{ m} \\
& U_4 = 0.2425 \times 10^{-3},\ U_5 = 0.0008 \text{ m},\ U_6 = 0.3309 \times 10^{-3} \\
& Q_3^3 = -9.59 \text{ kN},\ Q_4^3 = -16.24 \text{ kN-m},\ \sigma(8) = 18.1 \text{ MPa}
\end{aligned}
$$

Example 5.2.3

Consider the indeterminate beam shown in Fig. 5.2.13. The beam is made of steel ($E = 30 \times 10^6$ psi) and the cross-sectional dimensions are 2 × 3 in. ($I = 4.5$ in.^{4}). Find the transverse deflection w and slope dw/dx using the Euler–Bernoulli beam finite elements and compare the finite element solution against the exact solution.

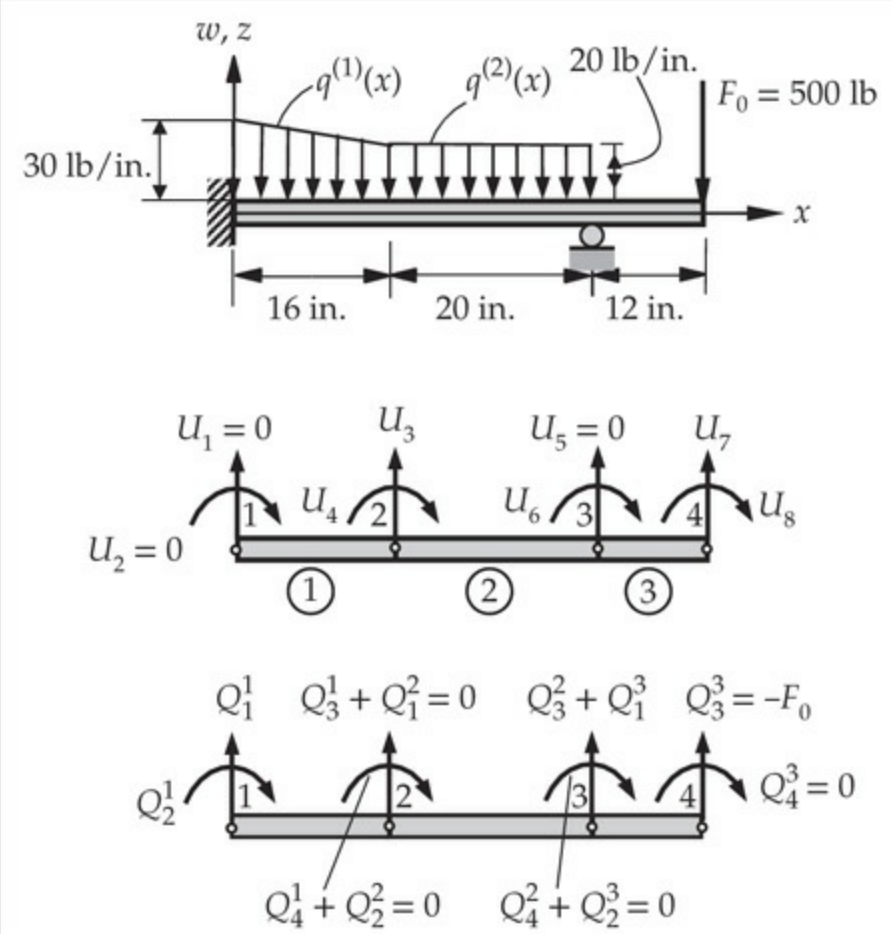

Fig. 5.2.13 Finite element modeling of an indeterminate beam (three elements).

Solution: Because of the discontinuity in loading, the beam should be divided into three elements: $\Omega^1 = (0, 16)$, $\Omega^2 = (16, 36)$, and $\Omega^3 = (36, 48)$; the element lengths are: $h_1 = 16$ in., $h_2 = 20$ in., and $h_3 = 12$ in. The load variation in each element is given by

$$q^{(1)}(x) = -\left(30 - \frac{10}{16}x\right), \quad q^{(2)}(x) = -20, \quad q^{(3)}(x) = 0$$

Using Eq. (5.2.24b), we obtain the following load vectors due to the distributed loads:

$$\mathbf{q}^1 = -\begin{Bmatrix} 216.00 \\ -554.67 \\ 184.00 \\ 512.00 \end{Bmatrix}, \quad \mathbf{q}^2 = -\begin{Bmatrix} 200.00 \\ -666.77 \\ 200.00 \\ 666.67 \end{Bmatrix}, \quad \mathbf{q}^3 = 0$$

The element stiffness matrices can be computed from Eq. (5.2.26a) by substituting appropriate values of h_e, E_e, I_e, and $k_f^e = 0$. The boundary

conditions for the problem are

$$w(0)=0\rightarrow U_1=0,\quad \frac{dw}{dx}(0)=0\rightarrow U_2=0,\quad w(36)=0\rightarrow U_5=0$$
$$Q_3^1+Q_1^2=0,\quad Q_4^1+Q_2^2=0,\quad Q_4^2+Q_2^3=0,\quad Q_3^3=-500,\quad Q_4^3=0$$

Note that Q_1^1, Q_2^1, and $Q_3^2+Q_1^3$ are the reactions that are not known and are to be calculated in the post-computation. Since the specified boundary conditions on the primary variables are homogeneous, one can delete the rows and columns corresponding to the specified displacements (i.e., delete rows and columns 1, 2, and 5) and solve the remaining five equations for U_3, U_4, U_6, U_7, and U_8 (all multiplied by 10^{-3}: U_3 = −0.3221 in., U_4 = −0.0594 in., U_6 = −0.2514 in., U_7 = −5.1497 in., and U_8 = 0.5180 in. The exact deflection in the three intervals of the beam is (after a very tedious algebra)

$$w(x)=\begin{cases} -\frac{1}{EI}\left(\frac{1}{2}a_2x^2+\frac{1}{6}a_1x^3+\frac{5}{4}x^4-\frac{1}{192}x^5\right), & 0\le x\le 16\\ -\frac{1}{EI}\left(b_4+b_3x+\frac{1}{2}b_2x^2+\frac{1}{6}b_1x^3+\frac{5}{6}x^4\right), & 16\le x\le 36\\ -\frac{1}{EI}\left(c_4+c_3x+\frac{1}{2}c_2x^2+\frac{1}{6}c_1x^3\right), & 36\le x\le 48 \end{cases}$$

where ($EI = 135\times 10^6$)

$$a_1=-\frac{201496}{729},\quad a_2=\frac{43504}{81},\quad b_1=-\frac{143176}{729},\quad b_2=\frac{8944}{81},\quad b_3=\frac{5120}{3}$$
$$b_4=-\frac{16384}{3},\quad c_1=-500,\quad c_2=24000,\quad c_3=-\frac{4554592}{9},\quad c_4=6554368$$

The exact bending moment and shear force in the three segments can be determined using the definitions [see Eq. (5.2.33)].

Figures 5.2.14 and 5.2.15 show a comparison of the generalized displacements and post-computed generalized forces, respectively, for the case of three elements in the mesh. The finite element solution for the deflection and its derivative are exact at the nodes and their variation between the nodes is also very good, as stated previously. The bending moment and shear force computed using Eq. (5.2.37) are only approximate and their values can be improved by further subdividing the beam into more elements. The finite element solutions for deflections (w), slopes (θ_x), and bending moment (M) at points other than the nodes are compared with the exact values in Table 5.2.3 for three different meshes

(finite element solution for w and θ_x coincides with the exact solution at the nodes).

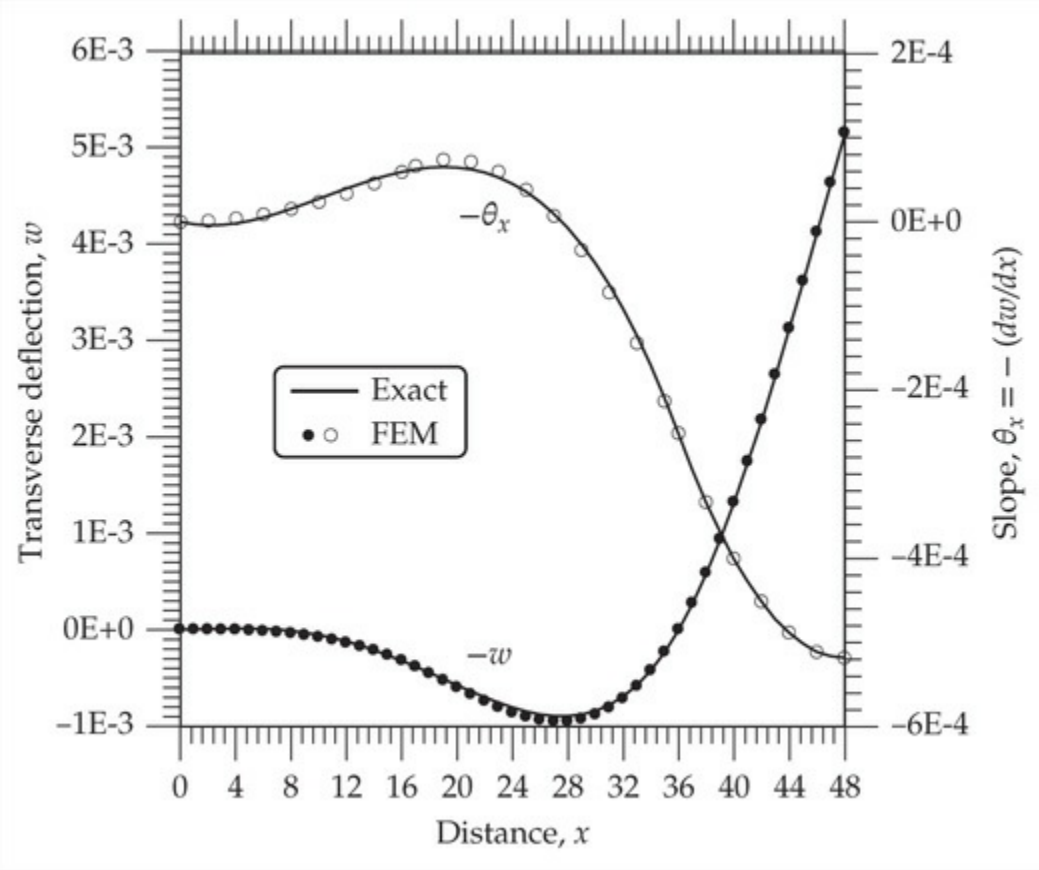

Fig. 5.2.14 A comparison of finite element results for the deflection w and slope θx with the exact values of the beam problem in **Example 5.2.3**.

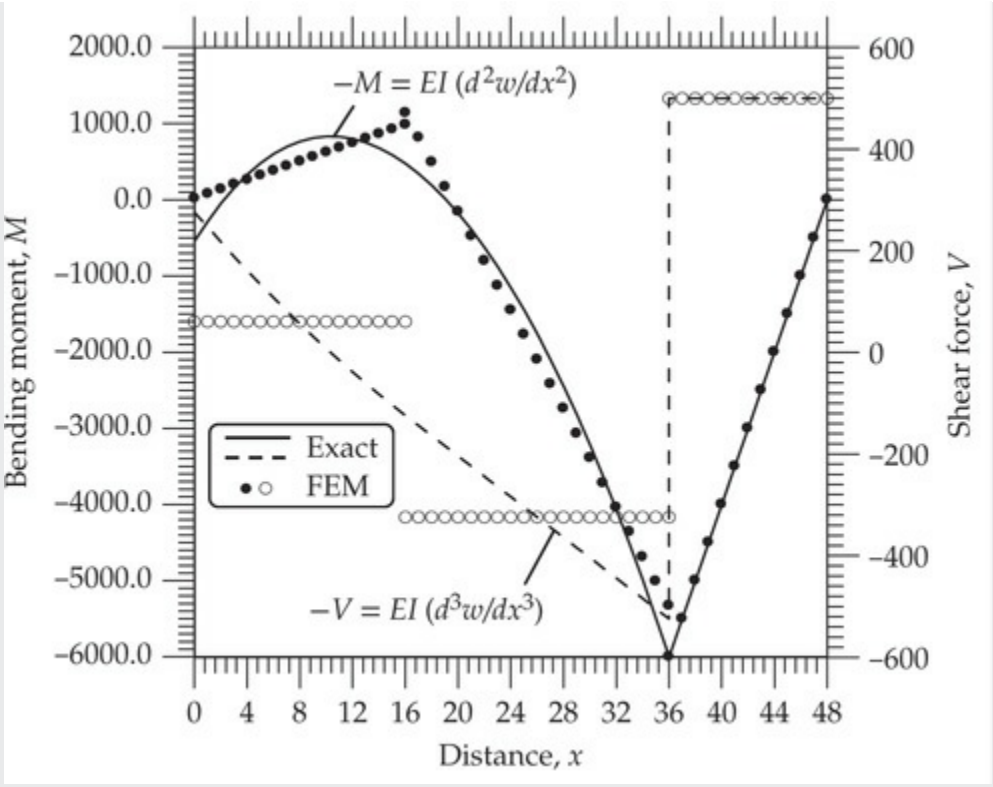

Fig. 5.2.15 A comparison of finite element results for the bending moment and shear force (post-computed) with the exact results of the beam problem in **Example 5.2.3**.

Table 5.2.3 Comparison of the finite element solution with the exact solution (units of the quantities should be obvious) of the beam problem considered in **Example 5.2.3**.

		$w \times 10^6$ (in.)		$-\frac{dw}{dx} \times 10^6$		$(M/EI) \times 10^6$	
x	N^*	FEM	Exact	FEM	Exact	FEM	Exact
	3	81.080		−23.673		−4.604	
10.0	5	54.591	53.580	−28.147	−27.478	−6.036	−6.156
	9	53.697		−27.478		−6.039	
	3	217.38		−45.669		−6.394	
14.0	5	212.50	211.51	−50.065	−50.729	−4.922	−5.025
	9	211.62		−50.729		−4.920	
	3	490.60		−72.948		−2.442	
18.5	5	480.95	478.78	−66.003	−64.846	−0.590	−0.744
	9	479.02		−64.846		−0.590	
	3	835.92		−55.194		9.543	
23.5	5	783.84	781.67	−48.250	−49.407	7.691	7.537
	9	781.91		−49.407		7.691	
	3	942.66		22.485		21.528	
28.5	5	890.58	888.41	15.540	16.698	19.676	19.522
	9	888.65		16.698		19.676	
	3	−2174.90		451.360		22.222	
42.0	5	−2174.90	−2174.90	451.360	451.360	22.222	22.222
	9	−2174.90		451.360		22.222	

* Number of elements in the mesh; $N = 3 : h_1 = 16, h_2 = 20, h_3 = 12$; $N = 5 : h_1 = 8, h_2 = 8, h_3 = 10, h_4 = 10, h_5 = 12$; $N = 9 : h_1 = h_2 = h_3 = h_4 = 4, h_5 = h_6 = h_7 = h_8 = 5, h_9 = 12$.

Example 5.2.4

The beam shown in Fig. 5.2.16 is supported at its free end by an elastic cable of cross-sectional area $A_c = 10^{-3}$ m^2 and modulus $E_c = 210$ GPa. The beam is of length $L = 3$ m, cross-sectional area $A = 2 \times 10^{-3}$ m^2, modulus $E = 210$ GPa, and moment of inertia about the axis of bending is $I = 5 \times 10^{-5}$ m^4 . A vertical load of $F = 500$ kN is applied at a distance $x = 1.5$ m along the beam. Use one-element model for the cable and the beam to determine the generalized displacements (u_1, w_1, and θ_1) at node 1.

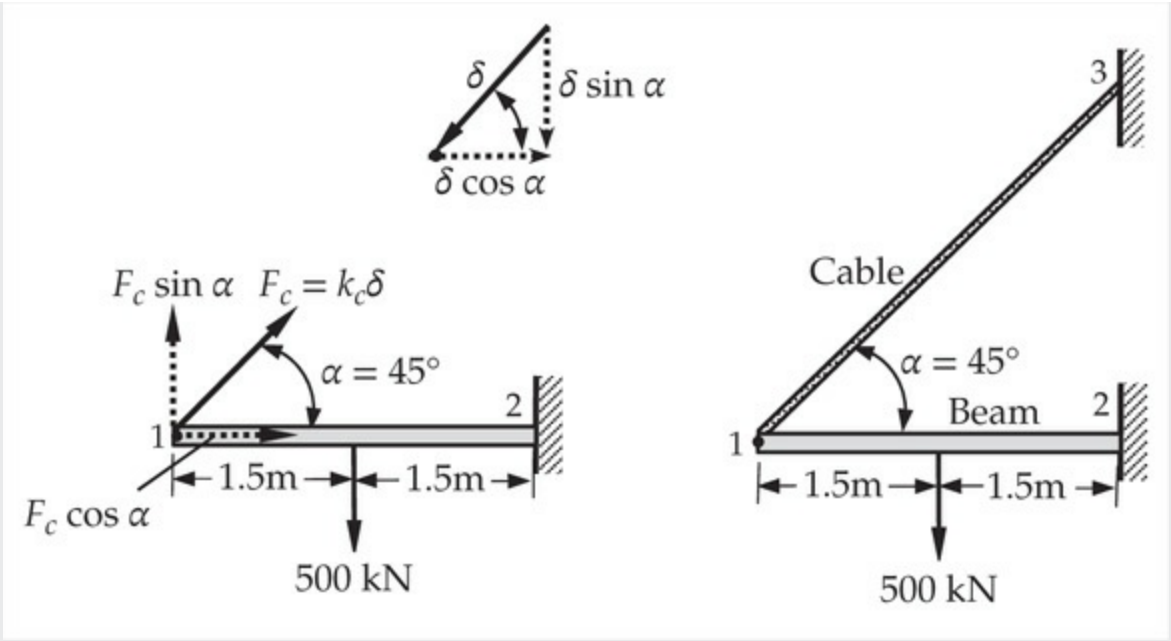

Fig. 5.2.16 A cable-supported beam.

Solution: First, we find the nodal forces statically equivalent to the applied point load F at the center of the beam using $f_i = -F\phi_i(L/2)$:

$$f_1 = -F\left(1 - \frac{3}{4} + \frac{1}{4}\right) = -0.5F = -250 \times 10^3, \qquad f_2 = F\frac{L}{2}\left(1 - \frac{1}{2}\right)^2 = 187.5 \times 10^3$$

$$f_3 = -F\left(\frac{3}{4} - \frac{1}{4}\right) = -250 \times 10^3, \qquad f_4 = F\frac{L}{2}\left(\frac{1}{4} - \frac{1}{2}\right) = -187.5 \times 10^3$$

Let F_c denote the tensile force in the cable, which is related to the elongation δ in the cable by

$$F_c = \frac{E_c A_c}{L_c}\delta \equiv k_c\delta, \quad \delta = -(u_1 \cos\alpha + w_1 \sin\alpha)$$

where $L_c = \sqrt{2}L$, and (u_1, w_1) are the axial and transverse displacements at node 1 (here we have $\alpha = 45°$). The minus sign indicates that the displacements are opposite to the assumed convention.

The horizontal and vertical forces and moment at node 1 in terms of the nodal displacements u_1 and w_1 are

$$Q_h = F_c \cos\alpha = k_c \delta \cos\alpha = -\frac{E_c A_c}{L_c} \cos\alpha\,(u_1 \cos\alpha + w_1 \sin\alpha)$$
$$= -24.75 \times 10^6 (u_1 + w_1)$$
$$Q_v = F_c \sin\alpha = k_c \delta \sin\alpha = -\frac{E_c A_c}{L_c} \sin\alpha\,(u_1 \cos\alpha + w_1 \sin\alpha)$$
$$= -24.75 \times 10^6 (u_1 + w_1)$$
$$Q_m = 0$$

The finite element equations using a single element are (i.e., superposition of the equations of bar and beam elements and noting that the generalized displacements at the second node are zero):

$$\begin{bmatrix} \frac{EA}{L} & 0 & 0 \\ 0 & \frac{12E_eI_e}{L^3} & -\frac{6E_eI_e}{L^2} \\ 0 & -\frac{6E_eI_e}{L^2} & \frac{4E_eI_e}{L} \end{bmatrix} \begin{Bmatrix} u_1 \\ w_1 \\ \theta_1 \end{Bmatrix} = 10^3 \begin{Bmatrix} 0 \\ -250.0 \\ 187.5 \end{Bmatrix} + \begin{Bmatrix} Q_h \\ Q_v \\ Q_m \end{Bmatrix}$$

or [the same equations can also be obtained by an assembly of the equations of the transformed cable (or bar) element and untransformed beam element]

$$10^6 \begin{bmatrix} 140.00 + 24.75 & 24.75 & 0 \\ 24.75 & 4.67 + 24.75 & -7.00 \\ 0 & -7.00 & 14.00 \end{bmatrix} \begin{Bmatrix} u_1 \\ w_1 \\ \theta_1 \end{Bmatrix} = 10^3 \begin{Bmatrix} 0 \\ -250.0 \\ 187.5 \end{Bmatrix}$$

Solving for $u_1 = U_1$, $w_1 = U_2$, and $\theta_1 = U_3$, we obtain

$$U_1 = 1.057 \times 10^{-3} \text{ m}, \quad U_2 = -7.039 \times 10^{-3} \text{ m}, \quad U_3 = 9.873 \times 10^{-3} \text{ rad.}$$

The elongation and the tensile force in the cable are

$$\delta = -(\cos\alpha\, u_1 + \sin\alpha\, w_1) = 4.23 \times 10^{-3} \text{ m}, \quad F_c = \frac{E_c A_c}{L_c} \delta = 209.357 \text{ kN}$$

The reaction forces are

$$R_h = -\frac{EA}{L} u_1 = -148.04 \text{ kN}$$
$$R_v = -f_3 - \frac{12E_eI_e}{L^3} U_1 + \frac{6E_eI_e}{L^2} U_2 = 351.96 \text{ kN}$$
$$M_2 = -f_4 - \frac{6E_eI_e}{L^2} U_1 + \frac{2E_eI_e}{L} U_2 = 305.89 \text{ kN-m}$$

5.2.9.1 Beams with internal hinge

It is not uncommon to find beams with an internal hinge about which the beam is free to rotate. Thus, at the hinge there cannot be any moment and the rotation is *not* continuous at a hinge between two elements (i.e., two elements connected at a hinge will have two different rotations). The assembly of element equations becomes simple if we eliminate the rotation variable at a node with a hinge.

Consider a uniform beam element of length h_e with a hinge at node 2 (but without elastic foundation, $k_f = 0$), as shown in Fig. 5.2.17(a). The element equation is given by Eq. (5.2.25), with the stiffness matrix given in Eq. (5.2.26a):

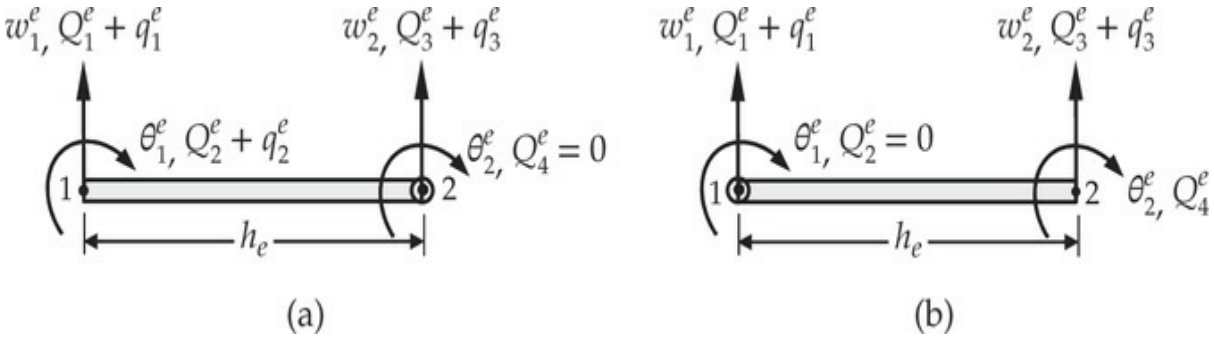

Fig. 5.2.17 (a) Beam element with a hinge at node 2. (b) Beam element with a hinge at node 1.

$$\frac{2E_eI_e}{h_e^3}\begin{bmatrix} 6 & -3h_e & -6 & -3h_e \\ -3h_e & 2h_e^2 & 3h_e & h_e^2 \\ -6 & 3h_e & 6 & 3h_e \\ -3h_e & h_e^2 & 3h_e & 2h_e^2 \end{bmatrix}\begin{Bmatrix} w_1^e \\ \theta_1^e \\ w_2^e \\ \theta_2^e \end{Bmatrix} = \begin{Bmatrix} q_1^e \\ q_2^e \\ q_3^e \\ q_4^e \end{Bmatrix} + \begin{Bmatrix} Q_1^e \\ Q_2^e \\ Q_3^e \\ Q_4^e \end{Bmatrix} \tag{5.2.39}$$

Since the moment at a hinge is zero, we have $Q_4^e = 0$. This allows us to eliminate θ_2^e (rotation at node 2) using the procedure discussed in Eqs. (3.4.57)–(3.4.61).

Comparing Eq. (5.2.39) with Eq. (3.4.57), we have the following definitions:

$$\mathbf{K}^{11} = \frac{2E_eI_e}{h_e^3}\begin{bmatrix} 6 & -3h_e & -6 \\ -3h_e & 2h_e^2 & 3h_e \\ -6 & 3h_e & 6 \end{bmatrix}, \quad \mathbf{K}^{12} = \frac{2E_eI_e}{h_e^3}\begin{Bmatrix} -3h_e \\ h_e^2 \\ 3h_e \end{Bmatrix} = (\mathbf{K}^{21})^{\mathrm{T}}$$

$$\mathbf{K}^{22} = \frac{4E_eI_e}{h_e}, \quad \mathbf{U}^1 = \begin{Bmatrix} w_1^e \\ \theta_1^e \\ w_2^2 \end{Bmatrix}, \quad \mathbf{U}^2 = \theta_2^e, \quad \mathbf{F}^1 = \begin{Bmatrix} q_1^e \\ q_2^e \\ q_3^e \end{Bmatrix} + \begin{Bmatrix} Q_1^e \\ Q_2^e \\ Q_3^e \end{Bmatrix}$$

Substituting for $\mathbf{U}^2 = \theta_2^e$ from the second equation of Eq. (3.4.59) into the first equation of (3.4.58), we obtain $\hat{\mathbf{K}}\mathbf{U}^1 = \hat{\mathbf{F}}$, where

$$\hat{\mathbf{K}} = \mathbf{K}^{11} - \mathbf{K}^{12}\left(\mathbf{K}^{22}\right)^{-1}\mathbf{K}^{21} = \frac{E_eI_e}{h_e^3}\begin{bmatrix} 12 & -6h_e & -12 \\ -6h_e & 4h_e^2 & 6h_e \\ -12 & 6h_e & 12 \end{bmatrix}$$

$$-\frac{2E_eI_e}{h_e^3}\begin{Bmatrix} -3h_e \\ h_e^2 \\ 3h_e \end{Bmatrix}\frac{h_e}{4E_eI_e}\frac{2E_eI_e}{h_e^3}\{-3h_e\ h_e^2\ 3h_e\}$$

$$= \frac{3E_eI_e}{h_e^3}\begin{bmatrix} 1 & -h_e & -1 \\ -h_e & h_e^2 & h_e \\ -1 & h_e & 1 \end{bmatrix}$$

Thus, the equations for a beam element with a hinge at node 2 can be written as

$$\frac{3E_eI_e}{h_e^3}\begin{bmatrix} 1 & -h_e & -1 \\ -h_e & h_e^2 & h_e \\ -1 & h_e & 1 \end{bmatrix}\begin{Bmatrix} w_1^e \\ \theta_1^e \\ w_2^e \end{Bmatrix} = \begin{Bmatrix} F_1^e \\ F_2^e \\ F_3^e \end{Bmatrix} \tag{5.2.40}$$

where $F_i^e = q_i^e + Q_i^e$. Similarly, we can derive the element equations for a beam element with hinge at node 1 [see Fig. 5.2.17(b)]

$$\frac{3E_eI_e}{h_e^3}\begin{bmatrix} 1 & -1 & -h_e \\ -1 & 1 & h_e \\ -h_e & h_e & h_e^2 \end{bmatrix}\begin{Bmatrix} w_1^e \\ w_2^e \\ \theta_2^e \end{Bmatrix} = \begin{Bmatrix} F_1^e \\ F_3^e \\ F_4^e \end{Bmatrix} \tag{5.2.41}$$

Example 5.2.5

Consider the beam in Fig. 5.2.18. Use a two-element mesh, with element

1 having the hinge at its node 2, while element 2 is the usual beam element. Determine the generalized displacements at the nodes.

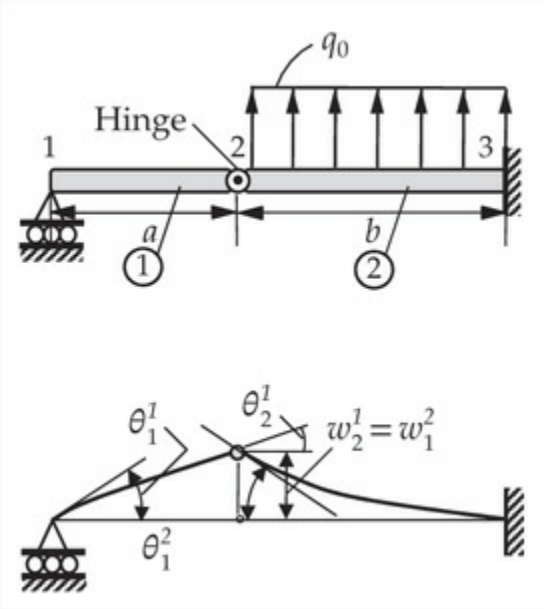

Fig. 5.2.18 Compound beam with an internal hinge.

Solution: The assembled system of equations is

$$E_e I_e \begin{bmatrix} \frac{3}{a^3} & -\frac{3}{a^2} & -\frac{3}{a^3} & 0 & 0 & 0 \\ -\frac{3}{a^2} & \frac{3}{a} & \frac{3}{a^2} & 0 & 0 & 0 \\ -\frac{3}{a^3} & \frac{3}{a^2} & \frac{3}{a^3}+\frac{12}{b^3} & -\frac{6}{b^2} & -\frac{12}{b^3} & -\frac{6}{b^2} \\ 0 & 0 & -\frac{6}{b^2} & \frac{4}{b} & \frac{6}{b^2} & \frac{2}{b} \\ 0 & 0 & -\frac{12}{b^3} & \frac{6}{b^2} & \frac{12}{b^3} & \frac{6}{b^2} \\ 0 & 0 & -\frac{6}{b^2} & \frac{2}{b} & \frac{6}{b^2} & \frac{4}{b} \end{bmatrix} \begin{Bmatrix} w_1^1 \\ \theta_1^1 \\ w_2^1 = w_1^2 \\ \theta_1^2 \\ w_2^2 \\ \theta_2^2 \end{Bmatrix}$$

$$= \begin{Bmatrix} Q_1^1 \\ Q_2^1 \\ Q_3^1 + Q_1^2 = 0 \\ Q_2^2 = 0 \\ Q_3^2 \\ Q_4^2 \end{Bmatrix} + \frac{q_0 b}{12} \begin{Bmatrix} 0 \\ 0 \\ 6 \\ -b \\ 6 \\ b \end{Bmatrix} \qquad (5.2.42)$$

Using the boundary conditions

$$w_1^1 = 0, \quad w_2^2 = 0, \quad \theta_2^2 = 0, \quad Q_2^1 = 0$$

we obtain the condensed equations

$$E_e I_e \begin{bmatrix} \frac{3}{a} & \frac{3}{a^2} & 0 \\ \frac{3}{a^2} & \frac{3}{a^3}+\frac{12}{b^3} & -\frac{6}{b^2} \\ 0 & -\frac{6}{b^2} & \frac{4}{b} \end{bmatrix} \begin{Bmatrix} \theta_1^1 \\ w_2^1 = w_1^2 \\ \theta_1^2 \end{Bmatrix} = \frac{q_0 b}{12} \begin{Bmatrix} 0 \\ 6 \\ -b \end{Bmatrix} \tag{5.2.43}$$

and the solution is given by

$$\theta_1^1 = -\frac{q_0 b^4}{8aEI}, \quad w_2^1 = w_1^2 = \frac{q_0 b^4}{8E_e I_e}, \quad \theta_2^2 = \frac{q_0 b^3}{2E_e I_e}$$

5.3 Timoshenko Beam Elements

5.3.1 Governing Equations

Recall that the Euler–Bernoulli beam theory is based on the assumption that plane cross sections remain plane and *normal* to the longitudinal axis after bending. This assumption results in zero transverse shear strain, $\gamma_{xz} = 2\varepsilon_{xz} = 0$. When the normality assumption is not used, i.e., plane sections remain plane but not necessarily normal to the longitudinal axis after deformation, the transverse shear strain γ_{xz} is not zero. We denote the rotation about the y-axis by an independent function $\phi_x(x)$. For short and thick beams (i.e., length-to-height ratio less than 20), the rotation ϕ_x is not equal to the slope θ_x, $\phi_x \neq \theta_x = -(dw/dx)$, and the difference, $\phi_x - \theta_x = \phi_x + dw/dx$, is the transverse shear strain. Beam theory based on this relaxed assumption is known as a *shear deformation beam theory*, most commonly known as the *Timoshenko beam theory* (TBT).

The total displacements of a point (x, z) in the beam along the three coordinate directions are

$$u_x = u(x) + z\phi_x(x), \quad u_y = 0, \quad u_z = w(x) \tag{5.3.1}$$

where (u, w) denote the axial and transverse displacements of a point located on the x-axis (which is taken as the centroidal axis), as shown in Fig. 5.3.1. The only nonzero strains associated with the displacement field are

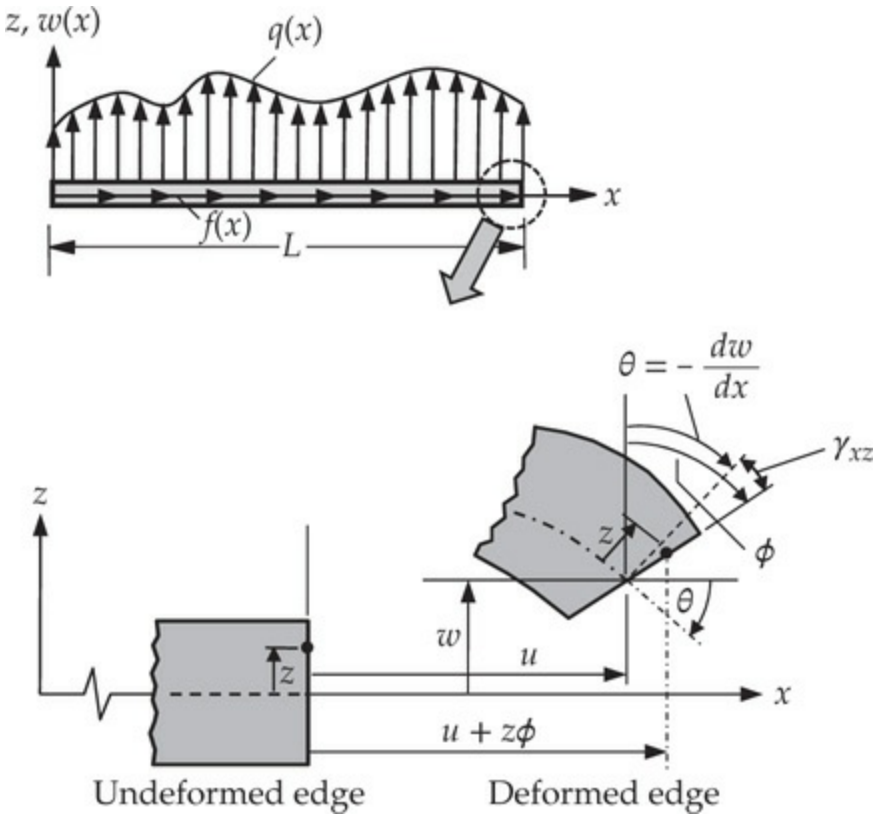

Fig. 5.3.1 Kinematics of the Timoshenko beam theory where a normal before deformation no longer remains normal after deformation.

$$\varepsilon_{xx} = \frac{du}{dx} + z\frac{d\phi_x}{dx}, \quad \gamma_{xz} = 2\varepsilon_{xz} = \phi_x(x) + \frac{dw}{dx} \tag{5.3.2}$$

The equilibrium equations of the TBT are the same as those of the EBT, since equilibrium equations are derived by considering the equilibrium of a beam element, shown in Fig. 5.2.2. Again, the equilibrium of axial forces [i.e., the first equation in Eq. (5.2.7)] is omitted because it is decoupled from the remaining two equations. We have

$$-\frac{dV}{dx} + k_f w = q, \quad -\frac{dM}{dx} + V = 0 \tag{5.3.3}$$

where k_f is the modulus of the elastic foundation (if any). The relations between the stress resultants (V, M) and the generalized displacements (w, ϕ_x) in the TBT are different from those for the EBT in Eq. (5.2.33). In the TBT, they are given by

$$M = \int_A z\,\sigma_{xx}\,dA = EI\frac{d\phi_x}{dx}$$
$$V = K_s \int_A \sigma_{xz}\,dA = GAK_s\left(\frac{dw}{dx} + \phi_x\right) \tag{5.3.4}$$

where G is the shear modulus and K_s is the *shear correction coefficient*, which is introduced to account for the difference in the constant state of shear stress in this theory and the parabolic variation of the shear stress through the beam thickness predicted by the elasticity theory (see Reddy [1, 2]). All other quantities have the same meaning as in the EBT. The two equilibrium equations in Eq. (5.3.3), expressed in terms of the deflection w and rotation ϕ_x by means of Eq. (5.3.4), take the form

$$-\frac{d}{dx}\left[GAK_s\left(\phi_x + \frac{dw}{dx}\right)\right] + k_f w = q \tag{5.3.5a}$$

$$-\frac{d}{dx}\left(EI\frac{d\phi_x}{dx}\right) + GAK_s\left(\phi_x + \frac{dw}{dx}\right) = 0 \tag{5.3.5b}$$

When the shear strain is zero (i.e., for long slender beams), substituting the second equation into the first for GAK_s ($\phi_x + dw/dx$), and replacing ϕ_x with $-dw/dx$, we obtain the governing equation, Eq. (5.2.10), of the EBT.

5.3.2 Weak Forms

Let w_h^e and ϕ_x^e denote the finite element approximations of w and ϕ_x, respectively, on a typical finite element $\Omega^e = (x_a^e, x_b^e)$. Substitution of w_h^e and ϕ_x^e for w and ϕ_x, respectively, into Eqs. (5.3.5a) and (5.3.5b) give two residual functions. The weighted integrals of these two residuals over an element Ω^e are used to develop the weak forms, as was already discussed in **Example 2.4.3**. Suppose that $\{v_{1i}^e\}$ and $\{v_{2i}^e\}$ are the independent sets of weight functions used for the two equations. The physical meaning of these functions will be clear after completing the steps of the weak-form development. At the end of the second step of the three-step procedure (i.e., after integration by parts), we obtain

$$0 = \int_{x_a^e}^{x_b^e} \left[G_e A_e K_s \frac{dv_{1i}^e}{dx} \left(\phi_x^e + \frac{dw_h^e}{dx} \right) + k_f^e v_{1i}^e w_h^e - v_{1i}^e q_e \right] dx$$
$$- \left[v_{1i}^e G_e A_e K_s \left(\phi_x^e + \frac{dw_h^e}{dx} \right) \right]_{x_a^e}^{x_b^e} \tag{5.3.6a}$$

$$0 = \int_{x_a^e}^{x_b^e} \left[E_e I_e \frac{dv_{2i}^e}{dx} \frac{d\phi_x^e}{dx} + G_e A_e K_s v_{2i}^e \left(\phi_x^e + \frac{dw_h^e}{dx} \right) \right] dx$$
$$- \left[v_{2i}^e E_e I_e \frac{d\phi_h^e}{dx} \right]_{x_a^e}^{x_b^e} \tag{5.3.6b}$$

The coefficients of the weight functions v_{1i}^e and v_{2i}^e in the boundary expressions are

$$G_e A_e K_s \left(\phi_x^e + \frac{dw_h^e}{dx} \right) \equiv V_h^e \quad \text{and} \quad E_e I_e \frac{d\phi_x^e}{dx} \equiv M_h^e \tag{5.3.7}$$

where V_h^e is the shear force and M_h^e is the bending moment. Therefore, (V_h^e, M_h^e) constitute the secondary variables dual to the primary variables (w_h^e, ϕ_x^e) of the weak forms. Thus, the duality pairs of primary and secondary variables are

$$(w_h^e, V_h^e) \quad \text{and} \quad (\phi_x^e, M_h^e)$$

The weight functions v_{1i}^e and v_{2i}^e must have the physical interpretations that give $v_{1i}^e V_h^e$ and $v_{2i}^e M_h^e$ units of work. Therefore, v_{1i}^e must be equivalent to the transverse deflection w_h^e, and v_{2i}^e must be equivalent to the rotation function ϕ_x^e. This interpretation helps us in identifying the proper functions for v_{1i}^e and v_{2i}^e when the weak-form Galerkin finite element model is developed. More specifically, to obtain the *i*th equation of each set, v_{1i}^e will be replaced with the *i*th function from the set of approximations used to represent w_h^e and v_{2i}^e will be replaced with the *i*th function from the set of approximations used to represent ϕ_x^e.

Let us denote the shear forces and bending moments at the end points of the element by [cf. Eq. (5.2.12)]

$$
\begin{aligned}
Q_1^e &\equiv -\left[G_e A_e K_s\left(\phi_x^e + \frac{dw_h^e}{dx}\right)\right]\Big|_{x_a^e} = -V_h^e(x_a^e)\\
Q_2^e &\equiv -\left[E_e I_e \frac{d\phi_x^e}{dx}\right]_{x_a^e} = -M_h^e(x_a^e)\\
Q_3^e &\equiv \left[G_e A_e K_s\left(\phi_x^e + \frac{dw_h^e}{dx}\right)\right]_{x_b^e} = V_h^e(x_b^e)\\
Q_4^e &\equiv \left[E_e I_e \frac{d\phi_x^e}{dx}\right]_{x_b^e} = M_h^e(x_b^e)
\end{aligned}
\tag{5.3.8}
$$

We note that Q_i^e have the same meaning as well as the sense as in the EBT.

Substituting the definitions from Eq. (5.3.8) into Eq. (5.3.6a) and (5.3.6b), we obtain the weak forms

$$
\begin{aligned}
0 = &\int_{x_a^e}^{x_b^e}\left[G_e A_e K_s \frac{dv_{1i}^e}{dx}\left(\phi_x^e + \frac{dw_h^e}{dx}\right) + k_f^e v_{1i}^e w_h^e - v_{1i}^e q_e\right]dx\\
&- v_{1i}^e(x_a^e)Q_1^e - v_{1i}^e(x_b^e)Q_3^e
\end{aligned}
\tag{5.3.9a}
$$

$$
\begin{aligned}
0 = &\int_{x_a^e}^{x_b^e}\left[E_e I_e \frac{dv_{2i}^e}{dx}\frac{d\phi_x^e}{dx} + G_e A_e K_s v_{2i}^e\left(\phi_x^e + \frac{dw_h^e}{dx}\right)\right]dx\\
&- v_{2i}^e(x_a^e)Q_2^e - v_{2i}^e(x_b^e)Q_4^e
\end{aligned}
\tag{5.3.9b}
$$

Equations (5.3.9a) and (5.3.9b) are equivalent to the statement of the principle of virtual displacements for the TBT.

Identifying the bilinear and linear forms for the case where there is more than one weak form is not easy. Each element of the bilinear form in this case is a pair $\mathbf{v}_i^e = (v_{1i}^e, v_{2i}^e)$ and $\mathbf{u}_h^e = (w_h^e, \phi_x^e)$. We identify bilinear form to be one that contains all four elements $(w_h^e, \phi_x^e, v_{1i}^e, v_{2i}^e)$ and linear form to be one that contains only (v_{1i}^e, v_{2i}^e):

$$
\begin{aligned}
B(\mathbf{v}_i^e, \mathbf{u}_h^e) = &\int_{x_a^e}^{x_b^e}\left[GAK_s\left(\frac{dv_{1i}^e}{dx} + v_{2i}^e\right)\left(\phi_x^e + \frac{dw_h^e}{dx}\right) + E_e I_e \frac{dv_{2i}^e}{dx}\frac{d\phi_x^e}{dx}\right.\\
&\left. + k_f^e v_{1i}^e w_h^e\right]dx
\end{aligned}
\tag{5.3.10a}
$$

$$\ell(\mathbf{v}_i^e) = \int_{x_a^e}^{x_b^e} v_{1i}^e q_e \, dx + v_{1i}^e(x_a^e)\, Q_1^e + v_{2i}^e(x_a^e)\, Q_2^e + v_{1i}^e(x_b^e) Q_3^e + v_{2i}^e(x_b^e) Q_4^e$$

(5.3.10b)

Clearly, $B(\mathbf{v}_i^e, \mathbf{u}_h^e)$ is bilinear and symmetric in $\mathbf{v}_i^e$ and $\mathbf{u}_h^e$ and $\ell(\mathbf{v}_i^e)$ is linear in $\mathbf{v}_i^e$. Then the quadratic functional, or the total potential energy functional, of the isolated TBT finite element can be obtained using the formula (2.4.25) [also, see Eq. (2.4.44)]:

$$\Pi_e(\mathbf{u}_h^e) = \int_{x_a^e}^{x_b^e} \left[\frac{E_e I_e}{2} \left(\frac{d\phi_x^e}{dx} \right)^2 + \frac{G_e A_e K_s}{2} \left(\frac{dw_h^e}{dx} + \phi_x^e \right)^2 + \frac{1}{2} k_f^e (w_h^e)^2 \right] dx$$
$$- \int_{x_a^e}^{x_b^e} w_h^e q_e \, dx - w_h^e(x_a^e) Q_1^e - \phi_x^e(x_a^e) Q_2^e - w_h^e(x_b^e) Q_3^e - \phi_x^e(x_b^e) Q_4^e \quad (5.3.11)$$

The first term in the square brackets represents the elastic strain energy due to bending, the second term represents the elastic energy due to the transverse shear deformation, the third term is the strain energy stored in the elastic foundation, and the fourth term is the work done by the distributed load; the remaining terms account for the work done by the generalized forces Q_i^e in moving through their respective generalized displacements (w_h^e, ϕ_x^e). We note that the weak form contains only the first derivatives of the generalized displacements (w_h^e, ϕ_x^e), and the boundary terms involve specification of w_h^e and ϕ_x^e, and not their derivatives.

5.3.3 General Finite Element Model

A close examination of the terms in the weak forms, Eqs. (5.3.9a) and (5.3.9b), shows that only the first derivatives of w_h^e and ϕ_x^e appear, requiring at least linear approximation of w_h^e and ϕ_x^e. Also, since the list of primary variables contain only the functions w_h^e and ϕ_x^e and not their derivatives, the Lagrange interpolation of w_h^e and ϕ_x^e is admissible. Therefore, the Lagrange interpolation functions derived in Chapter 3 can be used. In general, w_h^e and ϕ_x^e can be interpolated using different degree polynomials. In fact, the definition of shear strain $\gamma_{xz}^e = \phi_x^e + dw_h^e/dx$ suggests that w_h should be represented by a polynomial of one degree higher than that used to represent ϕ_x^e.

Let us consider Lagrange approximation of w and ϕ over an element $\Omega^e = (x_a^e, x_b^e)$ in the form

$$w \approx w_h^e = \sum_{j=1}^{m} w_j^e \psi_j^{(1)}, \quad \phi_x \approx \phi_x^e = \sum_{j=1}^{n} S_j^e \psi_j^{(2)} \tag{5.3.12}$$

where $\psi_j^{(1)}$ and $\psi_j^{(2)}$ are the Lagrange interpolation functions of degree $m-1$ and $n-1$, respectively. From the discussion above, it is advisable to use $m = n + 1$ for consistency of representing the variables w and ϕ_x.

Substitution of Eq. (5.3.12) for w_h^e and ϕ_x^e, and $v_{1i}^e = \psi_i^{(1)}$ and $v_{2i}^e = \psi_i^{(2)}$ into the weak forms, Eqs. (5.3.9a) and (5.3.9b), we obtain the following finite element equations of the TBT element:

$$\begin{aligned} 0 &= \sum_{j=1}^{m} K_{ij}^{11} w_j^e + \sum_{j=1}^{n} K_{ij}^{12} S_j^e - F_i^1 \quad (i = 1, 2, \ldots, m) \\ 0 &= \sum_{j=1}^{m} K_{ij}^{21} w_j^e + \sum_{j=1}^{n} K_{ij}^{22} S_j^e - F_i^2 \quad (i = 1, 2, \ldots, n) \end{aligned} \tag{5.3.13}$$

where

$$\begin{aligned} K_{ij}^{11} &= \int_{x_a^e}^{x_b^e} \left(G_e A_e K_s \frac{d\psi_i^{(1)}}{dx} \frac{d\psi_j^{(1)}}{dx} + k_f^e \psi_i^{(1)} \psi_j^{(1)} \right) dx \\ K_{ij}^{12} &= \int_{x_a^e}^{x_b^e} G_e A_e K_s \frac{d\psi_i^{(1)}}{dx} \psi_j^{(2)} \, dx = K_{ji}^{21} \quad [\text{i.e., } \mathbf{K}^{21} = (\mathbf{K}^{12})^{\mathrm{T}}] \\ K_{ij}^{22} &= \int_{x_a^e}^{x_b^e} \left(E_e I_e \frac{d\psi_i^{(2)}}{dx} \frac{d\psi_j^{(2)}}{dx} + G_e A_e K_s \psi_i^{(2)} \psi_j^{(2)} \right) dx \\ F_i^1 &= \int_{x_a^e}^{x_b} q_e \psi_i^{(1)} \, dx + Q_{2i-1}, \quad F_i^2 = Q_{2i} \end{aligned} \tag{5.3.14}$$

In the interest of clarity, the element label e on the coefficients is omitted. Equations (5.3.14) can be written in matrix form as

$$\begin{bmatrix} \mathbf{K}^{11} & \mathbf{K}^{12} \\ \mathbf{K}^{21} & \mathbf{K}^{22} \end{bmatrix}^e \begin{Bmatrix} \mathbf{w} \\ \mathbf{S} \end{Bmatrix}^e = \begin{Bmatrix} \mathbf{F}^1 \\ \mathbf{F}^2 \end{Bmatrix}^e \quad \text{or} \quad \mathbf{K}^e\mathbf{U}^e = \mathbf{F}^e \tag{5.3.15}$$

The finite element model in Eq. (5.3.15) with the coefficients given in Eq. (5.3.14) is the most general displacement finite element model of the TBT. The size of the stiffness matrix is $(m + n) \times (m + n)$, unless the degrees of freedom associated with internal nodes are eliminated. It can be used to obtain a number of specific finite element models, as discussed next.

5.3.4 Shear Locking and Reduce Integration

When $m = n = 2$ in Eq. (5.3.12), that is, linear interpolation of both w and ϕ_x is used (see Fig. 5.3.2), the derivative of w_h^e is

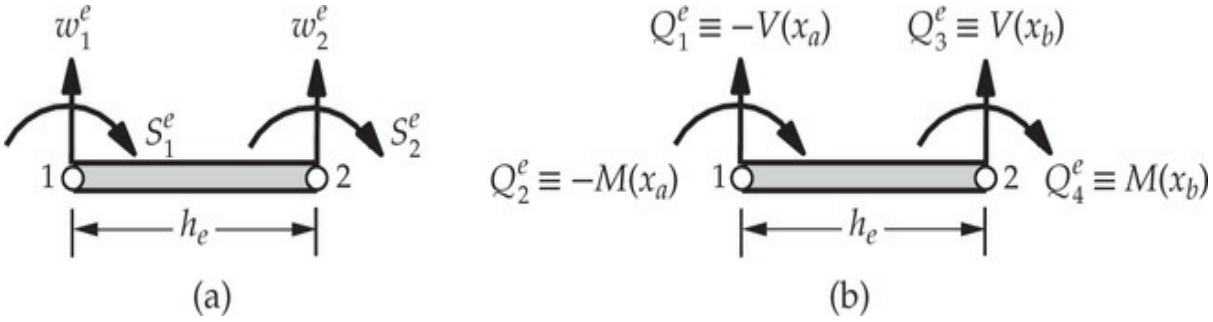

Fig. 5.3.2 Timoshenko beam finite element with linear approximation of both w and ϕ. (a) Generalized displacements. (b) Generalized forces.

$$\frac{dw_h^e}{dx} = \frac{w_2^e - w_1^e}{h_e}$$

which is an element-wise constant. For thin beams, the transverse shear deformation is negligible, implying $\phi_h^e \to -dw_h^e/dx$, which requires

$$S_1^e\left(1 - \frac{\bar{x}}{h_e}\right) + S_2^e\left(\frac{\bar{x}}{h_e}\right) = -\frac{w_2^e - w_1^e}{h_e}$$

or, equivalently (by equating like coefficients on both sides),

$$S_1^e = -\frac{w_2^e - w_1^e}{h_e}, \quad S_2^e - S_1^e = 0 \tag{5.3.16}$$

This implies that $\phi_x^e(x)$ is a constant. However, a constant state of $\phi_h^e(x)$ is

not admissible because the bending energy of the element

$$\int_{x_a^e}^{x_b^e} \frac{E_e I_e}{2} \left(\frac{d\phi_x^e}{dx} \right)^2 dx \tag{5.3.17}$$

would be zero. Thus, the element does not have any mechanism to degenerate, in thin beam limit, to the Euler–Bernoulli beam element (i.e., $\phi_x^e \rightarrow -dw_h^e/dx$). This numerical problem is known in the finite element literature as *shear locking*.

To overcome shear locking, two alternative procedures have been used in the literature:

1. *Consistent interpolation.* Use approximations of w^e and ϕ_x^e such that dw_h^e/dx and ϕ_h^e are polynomials of the same degree (i.e., $m = n + 1$). Thus a quadratic approximation of w^e and linear approximation of ϕ_x^e or a cubic approximation of w^e and quadratic approximation of ϕ_x^e are the possibilities.
2. *Reduced integration.* Represent both w_h^e and ϕ_h^e using the same degree of polynomials (i.e., $m = n$) and numerically evaluate (numerical integration will be discussed in Chapter 9) the energy due to transverse shear strain in Eq. (5.3.11) as if it is the same degree polynomial as $(dw_h^f/dx)^2$. Thus, when $G_e A_e K_s$ is a constant, the expression

$$\frac{G_e A_e K_s}{2} \int_{x_a}^{x_b} \left(\frac{dw_h^e}{dx} + \phi_h^e \right)^2 dx = \frac{G_e A_e K_s}{2} \int_0^{h_e} \left(\frac{dw_h^e}{d\bar{x}} + \phi_h^e \right)^2 d\bar{x} \tag{5.3.18}$$

is evaluated using a numerical integration rule that treats ϕ_h^e as if it is the same order polynomial as dw_h^e/dx. Thus, if w_h^e and ϕ_h^e are represented with linear polynomials (i.e., $m = n = 2$), dw_h^e/dx is a constant and ϕ_h^e is linear. In evaluating the stiffness terms associated with the shear energy in Eq. (5.3.18), one must use one-point integration, as dictated by dw_h^e/dx and not ϕ_h^e. Note that one-point integration in this case is sufficient to evaluate the integral of $(dw_h^e/dx)^2$ exactly but not the $(\phi_h^e)^2$ because it is a quadratic polynomial. Thus, using one-point integration amounts to under-integrating the term. This is known as the *reduced integration* technique. Similar discussion for $m = n = 3$ leads to the conclusion

that a two-point integration for the evaluation of the integral in Eq. (5.3.18) is a reduced integration rule.

For illustrative purposes, we take a detailed look at the expression

$$\frac{G_e A_e K_s}{2}\int_0^{h_e}\left(\frac{dw_h^e}{d\bar{x}}+\phi_h^e\right)^2 d\bar{x}\approx\frac{G_e A_e K_s}{2}\left[\left(\frac{dw_h^e}{d\bar{x}}+\phi_h^e\right)^2\Bigg|_{\bar{x}=h_e/2}\right]h_e$$

where $\bar{x}=\frac{1}{2}h_e$ is the midpoint of the element and h_e is its length. Substituting Eq. (5.3.12) into this expression (with $m = n- = 2$) and requiring it to be zero (for thin beams), we obtain:

$$\frac{G_e A_e K_s h_e}{2}\left[\frac{w_2^e-w_1^e}{h_e}+S_1^e\left(1-\frac{\bar{x}}{h_e}\right)+S_2^e\left(\frac{\bar{x}}{h_e}\right)\right]^2\Bigg|_{\bar{x}=h_e/2}=0$$

or

$$\frac{w_1^e-w_2^e}{h_e}=\frac{S_1^e+S_2^e}{2} \tag{5.3.19}$$

which is a weaker requirement than (5.3.16); that is, if Eq. (5.3.16) holds then Eq. (5.3.19) also holds, but Eq. (5.3.19) does not imply Eq. (5.3.16). We note that Eq. (5.3.16) or (5.3.19) must hold only for problems for which the transverse shear energy in Eq. (5.3.18) is negligible.

5.3.5 Consistent Interpolation Element (CIE)

We consider the case in which w_h^e is approximated as a quadratic polynomial and ϕ_x^e as a linear polynomial. That is, we select $\psi_i^{(1)}$ to be quadratic and $\psi_i^{(2)}$ to be linear in Eq. (5.3.12). Then in thin beam limit the shear strain

$$\begin{aligned}\gamma_{xz}^e&=\phi_x^e+\frac{dw_h^e}{d\bar{x}}\\&=S_1^e\left(1-\frac{\bar{x}}{h}\right)+S_2^e\frac{\bar{x}}{h}+\frac{w_1^e}{h}\left(-3+4\frac{\bar{x}}{h}\right)+\frac{4w_2^e}{h}\left(1-2\frac{\bar{x}}{h}\right)-\frac{w_3^e}{h}\left(1-4\frac{\bar{x}}{h}\right)\end{aligned}$$

must go to zero, requiring

$$S_1^e+\frac{1}{h}\left(-3w_1^e+4w_2^e-w_3^e\right)=0,\quad -S_1^e+S_2^e+\frac{4}{h}\left(w_1^e-2w_2^e+w_3^e\right)=0$$

which are *not* inconsistent relations. Hence, no shear locking occurs. For this choice of interpolation, $\mathbf{K}^{11}$ is 3 × 3, $\mathbf{K}^{12}$ is 3 × 2, and $\mathbf{K}^{22}$ is 2 × 2 [see Eq. (5.3.15)]. The explicit forms of the matrices, when E_e I_e and GAK_s are constant, are (note that some of the matrix coefficients are readily available from Chapter 3)

$$\mathbf{K}^{11} = \frac{G_e A_e K_s}{3h_e}\begin{bmatrix} 7 & -8 & 1 \\ -8 & 16 & -8 \\ 1 & -8 & 7 \end{bmatrix} + \frac{k_f^e h_e}{30}\begin{bmatrix} 4 & 2 & -1 \\ 2 & 16 & 2 \\ -1 & 2 & 4 \end{bmatrix}$$

$$\mathbf{K}^{12} = \frac{G_e A_e K_s}{6}\begin{bmatrix} -5 & -1 \\ 4 & -4 \\ 1 & 5 \end{bmatrix} = (\mathbf{K}^{21})^{\mathrm{T}} \tag{5.3.20}$$

$$\mathbf{K}^{22} = \frac{G_e A_e K_s h_e}{6}\begin{bmatrix} 2 & 1 \\ 1 & 2 \end{bmatrix} + \frac{E_e I_e}{h_e}\begin{bmatrix} 1 & -1 \\ -1 & 1 \end{bmatrix}$$

When there is no elastic foundation $k_f^e = 0$, the finite element equations in Eq. (5.3.15), for this choice of interpolation, take the form

$$\frac{G_e A_e K_s}{6h_e}\begin{bmatrix} 14 & -16 & 2 & -5h_e & -h_e \\ -16 & 32 & -16 & 4h_e & -4h_e \\ 2 & -16 & 14 & h_e & 5h_e \\ -5h_e & 4h_e & h_e & 2h_e^2\lambda_e & h_e^2\gamma_e \\ -h_e & -4h_e & 5h_e & h_e^2\gamma_e & 2h_e^2\lambda_e \end{bmatrix}\begin{Bmatrix} w_1^e \\ w_2^e \\ w_3^e \\ S_1^e \\ S_2^e \end{Bmatrix} = \begin{Bmatrix} q_1^e \\ q_c^e \\ q_2^e \\ 0 \\ 0 \end{Bmatrix} + \begin{Bmatrix} Q_1^e \\ \hat{Q}_c^e \\ Q_3^e \\ Q_2^e \\ Q_4^e \end{Bmatrix} \tag{5.3.21a}$$

$$\mu_e = \frac{E_e I_e}{G_e A_e K_s h_e^2}, \quad \lambda_e = 1 + 3\mu_e, \quad \gamma_e = 1 - 6\mu_e \tag{5.3.21b}$$

where $(Q_1^e, Q_2^e, Q_3^e, Q_4^e)$ are the generalized forces defined in Eq. (5.3.7), w_c^e and $\hat{Q}_c^e$ are the deflection and applied external load, respectively, at the center node of the quadratic element, and

$$q_i^e = \int_{x_a}^{x_b} \psi_i^{(1)} q_e \, dx, \quad (i = 1, 2, 3), \quad \psi_i^{(1)} = \text{quadratic} \tag{5.3.22}$$

This element is designated as CIE and is shown in Fig. 5.3.3.

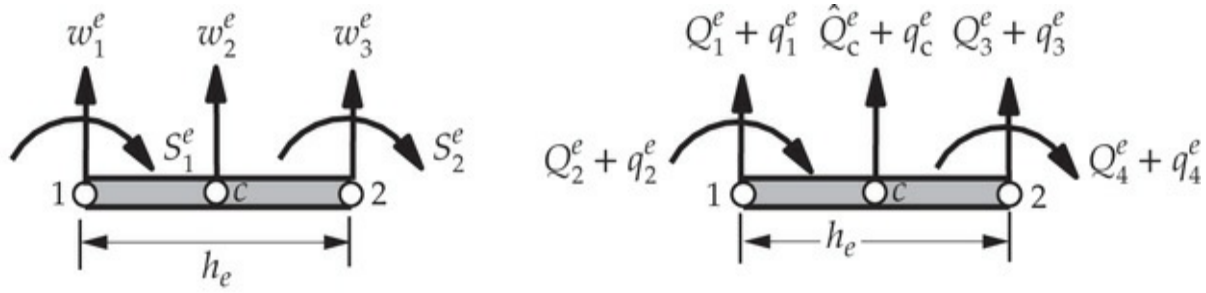

(a) Generalized displacements (b) Generalized forces

Fig. 5.3.3 Consistent interpolation Timoshenko beam element, CIE. (a) Generalized displacements. (b) Generalized forces.

Note that node *c*, which is the center node of the element, is not connected to other elements, and the only degree of freedom at this node is the transverse deflection, w_c^e . We can eliminate w_c^e (i.e., use static condensation procedure) by expressing it in terms of the degrees of freedom $(w_1^e, w_2^e, S_1^e, S_2^3)$ and known loads $(q_c^e, \hat{Q}_c^e)$:

$$w_c^e = \frac{6h_e}{32G_eA_eK_s}(q_c^e + \hat{Q}_c^e) + \left(\frac{w_1^e + w_2^e}{2}\right) + h_e\left(\frac{S_2^e - S_1^e}{8}\right) \tag{5.3.23}$$

Substituting w_c^e from Eq. (5.3.23) into the remaining equations of (5.3.21a) and rearranging the nodal variables and the equations (to keep the symmetry), we obtain

$$\left(\frac{E_eI_e}{6\mu_eh_e^3}\right)\begin{bmatrix} 6 & -3h_e & -6 & -3h_e \\ -3h_e & h_e^2(1.5+6\mu_e) & 3h_e & h_e^2(1.5-6\mu_e) \\ -6 & 3h_e & 6 & 3h_e \\ -3h_e & h_e^2(1.5-6\mu_e) & 3h_e & h_e^2(1.5+6\mu_e) \end{bmatrix}\begin{Bmatrix} w_1^e \\ S_1^e \\ w_2^e \\ S_2^e \end{Bmatrix}$$

$$= \begin{Bmatrix} q_1^e + \frac{1}{2}\hat{q}_c^e \\ -\frac{1}{8}\hat{q}_c^e h_e \\ q_2^e + \frac{1}{2}\hat{q}_c^e \\ \frac{1}{8}\hat{q}_c^e h_e \end{Bmatrix} + \begin{Bmatrix} Q_1^e \\ Q_2^e \\ Q_3^e \\ Q_4^e \end{Bmatrix} \tag{5.3.24}$$

where $\hat{q}_c^e = q_c^e + \hat{Q}_c^e$. For simplicity, but without loss of generality, we will assume that $\hat{Q}_c^e = 0$ (i.e., no external point force is placed at the center of the element) so that $\hat{q}_c^e = q_c^e$. Note that the load vector is similar to that of the Euler–Bernoulli beam element [see Eq. (5.2.24b)]. In fact, for uniform

load of intensity q_0 we have $q_1^e = q_2^e = q_0 h_e/6$ and $q_c^e = 4q_0 h_e/6$, and the load vector due to q_0 in Eq. (5.3.24) is identical to the one in Eq. (5.2.26b) (of course, this is not true in general). Thus, the CIE, for all analysis steps, is exactly the same as that shown in Fig. 5.3.2 with the element equations given by Eq. (5.3.24). However, one must keep in mind that w and q_i^e are determined by quadratic interpolation functions.

The next CIE in the sequence is one in which Lagrange cubic interpolation of $w(x)$ and quadratic interpolation of $\phi_x(x)$ are used. The element will have a 7 × 7 element stiffness matrix with seven degrees of freedom $(w_1^e, w_2^e, w_3^e, w_4^e, S_1^e, S_2^e, S_3^e)$, as shown in Fig. 5.3.4. Elimination of the internal nodal degrees of freedom will result in a 4 × 4 matrix. The element is not discussed further here.

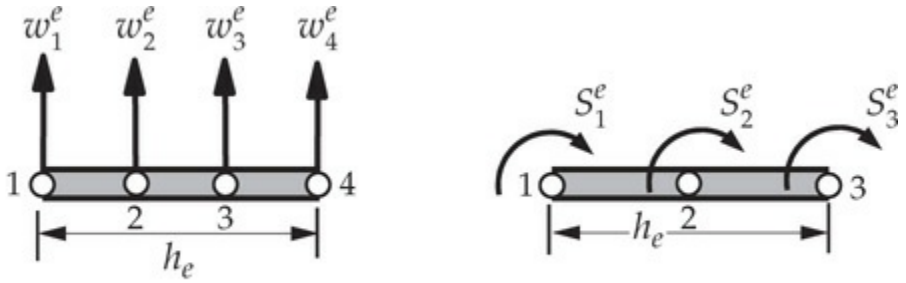

(a) Transverse displacements (b) Rotations

Fig. 5.3.4 Consistent interpolation Timoshenko beam element with (a) cubic variation of the transverse deflection w and (b) quadratic variation of the rotation ϕ_x.

5.3.6 Reduced Integration Element (RIE)

When equal interpolation of $w_h^e(x)$ and $\phi_x^e(x)$ is used ($m = n$), all sub-matrices in Eq. (5.3.15) are of the same order: $n \times n$, where n is the number of terms in the polynomial (or $n - 1$ is the degree of interpolation). The element coefficient matrices K_{ij}^{11}, K_{ij}^{12} as well as the first part of K_{ij}^{22} are evaluated exactly. The second part of K_{ij}^{22} is to be evaluated using reduced integration. For the choice of linear interpolation functions, and for element-wise constant values of $G_e A_e K_s$ and $E_e I_e$, the matrices in Eq. (5.3.15) for this case have the following explicit values (when $k_f^e = 0$):

$$\mathbf{K}^{11} = \frac{G_e A_e K_s}{h_e}\begin{bmatrix} 1 & -1 \\ -1 & 1 \end{bmatrix}, \quad \mathbf{K}^{12} = \frac{G_e A_e K_s}{2}\begin{bmatrix} -1 & -1 \\ 1 & 1 \end{bmatrix}$$
$$\mathbf{K}^{22} = \frac{E_e I_e}{h_e}\begin{bmatrix} 1 & -1 \\ -1 & 1 \end{bmatrix} + \frac{G_e A_e K_s h_e}{4}\begin{bmatrix} 1 & 1 \\ 1 & 1 \end{bmatrix} \tag{5.3.25a}$$

where one-point integration is used to evaluate the second part of $\mathbf{K}^{22}$. Note that $\mathbf{K}^{11}$, $\mathbf{K}^{12}$, and the first part of $\mathbf{K}^{22}$ can be evaluated exactly with one-point quadrature (i.e., numerical integration) when $E_e\, I_e$ and $G_e\, A_e\, K_s$ are constant because the integrands of these coefficients are constant. Hence, one-point integration for $\mathbf{K}^{\alpha\beta}$ satisfies all requirements. The resulting beam element is termed the reduced integration element (RIE). Expressing Eq. (5.3.15), with $\mathbf{K}^{\alpha\beta}$ from Eq. (5.3.25a), and rearranging the nodal vector, we obtain

$$\frac{G_e A_e K_s}{4h_e}\begin{bmatrix} 4 & -2h_e & -4 & -2h_e \\ -2h_e & h_e^2(1+4\mu_e) & 2h_e & h_e^2(1-4\mu_e) \\ -4 & 2h_e & 4 & 2h_e \\ -2h_e & h_e^2(1-4\mu_e) & 2h_e & h_e^2(1+4\mu_e) \end{bmatrix}\begin{Bmatrix} w_1^e \\ S_1^e \\ w_2^e \\ S_2^e \end{Bmatrix} = \begin{Bmatrix} q_1^e \\ 0 \\ q_2^e \\ 0 \end{Bmatrix} + \begin{Bmatrix} Q_1^e \\ Q_2^e \\ Q_3^e \\ Q_4^e \end{Bmatrix} \tag{5.3.25b}$$

where

$$\mu_e = E_e I_e / G_e A_e K_s h_e^2 \tag{5.3.25c}$$

To resemble Eq. (5.3.24), we can write the element equations of the RIE element as

$$\frac{E_e I_e}{6\mu_e h_e^3}\begin{bmatrix} 6 & -3h_e & -6 & -3h_e \\ -3h_e & h_e^2(1.5+6\mu_e) & 3h_e & h_e^2(1.5-6\mu_e) \\ -6 & 3h_e & 6 & 3h_e \\ -3h_e & h_e^2(1.5-6\mu_e) & 3h_e & h_e^2(1.5+6\mu_e) \end{bmatrix}\begin{Bmatrix} w_1^e \\ S_1^e \\ w_2^e \\ S_2^e \end{Bmatrix} = \begin{Bmatrix} q_1^e \\ 0 \\ q_2^e \\ 0 \end{Bmatrix} + \begin{Bmatrix} Q_1^e \\ Q_2^e \\ Q_3^e \\ Q_4^e \end{Bmatrix} \tag{5.3.26a}$$

$$q_i^e = \int_0^{h_e} \psi_i^e\, q_e\, d\bar{x}, \quad (i=1,2) \ (\psi_i^e \text{ are linear}) \tag{5.3.26b}$$

$$\mu_e = \frac{E_e I_e}{G_e A_e K_s h_e^2} \tag{5.3.26c}$$

It is interesting to note that the element stiffness matrix in Eq. (5.3.26a) of the linear RIE is the same as that of the CIE in Eq. (5.3.24) obtained using quadratic approximation of w and linear approximation of ϕ_x. The only difference is the load representation. In CIE, the load vector is similar

(but not the same, in general) to that of the Euler–Bernoulli beam theory, whereas in RIE it is based on Eq. (5.3.26c), which contributes only to the force degrees of freedom and not to the moment degrees of freedom.

Unlike the Euler–Bernoulli beam finite element, only certain types of TBT elements yield exact generalized displacements and forces at the nodes. Both, the RIE and the CIE, do not give exact nodal values because the exact homogeneous solution of Eqs. (5.3.5a) and (5.3.5b) for w and ϕ_x is cubic and quadratic, respectively.

5.3.7 Numerical Examples

Here we consider several examples to illustrate the accuracy of various Timoshenko beam elements developed in this section. In general, the accuracy of the results increases with increasing number of elements. To obtain a reasonably accurate solution, one needs to use four or more RIE or CIE elements in each span of any beam problem (see [3,4]).

Example 5.3.1

Consider a simply supported rectangular cross-section (width b and height H) beam of length L and subjected to (a) uniform $q = q_0$ and (b) linearly varying $q = 2q_0\, x/L$ for $0 \le x \le L/2$ and $q = 2q_0\,(1 - x/L)$ for $L/2 \le x \le L$ (pyramid load) transverse loads (one at a time). Use the following data:

$$\nu = 0.25, \quad K_s = \frac{5}{6}, \quad I = \frac{bH^3}{12}, \quad A = bH \tag{1}$$

and two different beam length-to-height ratios, $L/H = 10$ and $L/H = 100$, and half beam model to determine the finite element solution (in dimensionless form) based on the two TBT beam finite elements and the EBT element discussed in this chapter.

Solution: (a) For one RIE element in half beam ($h = 0.5L$) and uniformly distributed load (UDL) of intensity q_0, we have

$$\frac{EI}{6\mu h^3}\begin{bmatrix} 6 & -3h & -6 & -3h \\ -3h & h^2(1.5+6\mu) & 3h & h^2(1.5-6\mu) \\ -6 & 3h & 6 & 3h \\ -3h & h^2(1.5-6\mu) & 3h & h^2(1.5+6\mu) \end{bmatrix}\begin{Bmatrix} U_1 \\ U_2 \\ U_3 \\ U_4 \end{Bmatrix} = \frac{q_0 h}{2}\begin{Bmatrix} 1 \\ 0 \\ 1 \\ 0 \end{Bmatrix} + \begin{Bmatrix} Q_1 \\ Q_2 \\ Q_3 \\ Q_4 \end{Bmatrix}$$

where $\mu = EI/(GAK_s h^2) = (H/h)^2/4 = (H/L)^2$. The boundary conditions require $w(0) = U_1 = 0$, $(dw/dx)(h) = U_4 = 0$, and $Q_2 = Q_3 = 0$. Thus, the condensed equations are

$$\frac{EI}{6\mu h^3}\begin{bmatrix} h^2(1.5+6\mu) & 3h \\ 3h & 6 \end{bmatrix}\begin{Bmatrix} U_2 \\ U_3 \end{Bmatrix} = \frac{q_0 h}{2}\begin{Bmatrix} 0 \\ 1 \end{Bmatrix}$$

Hence, the TBT solution using one RIE element in half beam is given by

$$U_2 = -\frac{3q_0h^3}{EbH^3} = -\frac{3}{8}\alpha, \quad U_3 = (1.5+6\mu)\frac{q_0h^4}{EbH^3} = \left(\frac{1.5}{16}+\frac{3}{8}\mu\right)\alpha, \quad \alpha = \frac{q_0L^3}{EbH^3}$$

For one CIE element in half beam ($h = 0.5L$) and uniformly distributed load, the condensed equations for the unknown generalized displacements are

$$\frac{EI}{6\mu h^3}\begin{bmatrix} h^2(1.5+6\mu) & 3h \\ 3h & 6 \end{bmatrix}\begin{Bmatrix} U_2 \\ U_3 \end{Bmatrix} = \frac{q_0 h}{12}\begin{Bmatrix} -h \\ 6 \end{Bmatrix}$$

The TBT solution using the CIE element is given by

$$U_2 = -\frac{4q_0h^3}{EbH^3} = -\frac{1}{2}\alpha, \quad U_3 = 2(1+3\mu)\frac{q_0h^4}{EbH^3} = \left(\frac{1}{8}+\frac{3}{8}\mu\right)\alpha L$$

For one EBT element in half beam and uniformly distributed load, the condensed equations for the unknown generalized displacements are

$$\frac{2EI}{h^3}\begin{bmatrix} 2h^2 & 3h \\ 3h & 6 \end{bmatrix}\begin{Bmatrix} U_2 \\ U_3 \end{Bmatrix} = \frac{q_0 h}{12}\begin{Bmatrix} -h \\ 6 \end{Bmatrix}$$

The EBT solution using the Euler–Bernoulli element (EBE) is given by

$$U_2 = -\frac{4q_0h^3}{EbH^3} = -\frac{1}{2}\alpha, \quad U_3 = \frac{5q_0h^4}{2EbH^3} = \frac{5}{32}\alpha L, \quad \alpha = \frac{q_0L^3}{EbH^3}$$

(b) For the linearly varying load, the load vectors of the RIE, EBE, and CIE are given by

$$\{q\}^{\text{RIE}} = \frac{q_0 h}{6}\begin{Bmatrix} 1 \\ 0 \\ 2 \\ 0 \end{Bmatrix}, \quad \{q\}^{\text{CIE}} = \frac{q_0 h}{24}\begin{Bmatrix} 4 \\ -h \\ 8 \\ h \end{Bmatrix}, \quad \{q\}^{\text{EBE}} = \frac{q_0 h}{60}\begin{Bmatrix} 9 \\ -2h \\ 21 \\ 3h \end{Bmatrix}$$

and the one-element solutions are

$$\begin{Bmatrix} U_2 \\ U_3 \end{Bmatrix}^{\text{RIE}} = \alpha \begin{Bmatrix} -\frac{1}{4} \\ \frac{L}{24}(1.5+6\mu) \end{Bmatrix}, \quad \begin{Bmatrix} U_2 \\ U_3 \end{Bmatrix}^{\text{CIE}} = \alpha \begin{Bmatrix} -\frac{5}{16} \\ \frac{L}{64}(5+16\mu) \end{Bmatrix}$$

$$\begin{Bmatrix} U_2 \\ U_3 \end{Bmatrix}^{\text{EBE}} = \alpha \begin{Bmatrix} -\frac{5}{16} \\ \frac{L}{10} \end{Bmatrix}$$

Table 5.3.1 shows a comparison of the finite element solutions obtained with two, four, and eight elements in half beam with the exact beam solutions for two different types of loads, namely, uniform load and sinusoidal load.

Table 5.3.1 Comparison of the finite element solutions with the exact maximum deflection and rotation of a simply supported isotropic beam (N = number of elements used in half beam).

	$w(L/2) \times (EbH^3/q_0L^4)$			$-\phi_x(0) \times (EbH^3/q_0L^3)$		
Element	$N=2$	$N=4$	$N=8$	$N=2$	$N=4$	$N=8$
UDL ($L/H=10$)						
RIE	0.14438	0.15609	0.15902	0.46875	0.49219	0.49805
CIE	0.15219	0.15805	0.15951	0.50000	0.50000	0.50000
EBE (exact)	0.15625	0.15625	0.15625	0.50000	0.50000	0.50000
UDL($L/H=100$)						
RIE	0.14066	0.15238	0.15531	0.46875	0.49219	0.49805
CIE	0.14848	0.15433	0.15580	0.50000	0.50000	0.50000
EBE (exact)	0.15625	0.15625	0.15625	0.50000	0.50000	0.50000
Pyramid ($L/H=10$)						
RIE	0.09234	0.09991	0.10185	0.29688	0.30859	0.31152
CIE	0.09723	0.10119	0.10217	0.31250	0.31250	0.31250
EBE (exact)	0.10000	0.10000	0.10000	0.31250	0.31250	0.31250
Pyramid ($L/H=100$)						
RIE	0.08987	0.09744	0.09938	0.29688	0.30859	0.31152
CIE	0.09475	0.09872	0.09970	0.31250	0.31250	0.31250
EBE (exact)	0.10000	0.10000	0.10000	0.31250	0.31250	0.31250

The exact solutions according to EBT and TBT are as follow (for $0 \le \bar{x} \le L/2$; $\bar{x} = x/L$; $q_0 L^4/EI = 12\alpha L$):

EBT

$$w^{\mathrm{E}}(x) = 0.5\alpha L\,(\bar{x} - 2\bar{x}^3 + \bar{x}^4) \quad \textit{Uniform load} \tag{2}$$

$$w^{\mathrm{E}}(x) = \frac{\alpha L}{80}\bar{x}\,(4\bar{x}^2 - 5)^2 \quad \textit{Pyramid load} \tag{3}$$

The maximum values are $w(L/2) = (5/32)\alpha L$ and $\theta(0) = -0.5\alpha$ for the uniform load and $w(L/2) = 0.1\alpha L$ and $\theta(0) = -(5/16)\alpha$ for the pyramid load.

TBT

Uniform load

$$\begin{aligned} w^{\mathrm{T}}(\bar{x}) &= \left[w^{\mathrm{E}}(x) + \frac{1}{GAK_s}M^{\mathrm{E}}(x)\right] = 0.5\alpha L\left[\bar{x} - 2\bar{x}^3 + \bar{x}^4 + 12\Lambda\,(\bar{x} - \bar{x}^3)\right] \\ \phi_x^{\mathrm{T}}(\bar{x}) &= -\frac{dw^{\mathrm{E}}}{dx} = -0.5\alpha\,(1 - 6\bar{x}^2 + 4\bar{x}^3) \end{aligned} \tag{4}$$

The maximum values are

$$w(L/2) = 0.5\alpha L\left[\frac{5}{16} + \frac{9}{8}\frac{H^2}{L^2}\right], \quad \phi_x^{\mathrm{T}}(0) = -0.5\alpha$$

Pyramid load

$$\begin{aligned} w^{\mathrm{T}}(\bar{x}) &= \left[w^{\mathrm{E}}(x) + \frac{1}{GAK_s}M^{\mathrm{E}}(x)\right] = \frac{\alpha L}{80}\left[\bar{x}\,(4\bar{x}^2 - 5)^2 + 80\Lambda(3\bar{x} - 4\bar{x}^2)\right] \\ \phi_x^{\mathrm{T}}(\bar{x}) &= -\frac{dw^{\mathrm{E}}}{dx} = \frac{\alpha}{16}\,(-5 + 24\bar{x}^2 - 16\bar{x}^4), \quad \Lambda = \frac{EI}{GAK_sL^2} = 0.25\frac{H^2}{L^2} \end{aligned} \tag{5}$$

The maximum values are

$$w(L/2) = \frac{\alpha L}{80}\left[8 + 10\frac{H^2}{L^2}\right], \quad \phi_x^{\mathrm{T}}(0) = -\frac{5}{16}\alpha$$

The superscripts “E” and “T” refer to the EBT and TBT, respectively (see Wang, Reddy, and Lee [3] and Reddy [1] for the derivation of the relations between the Timoshenko beam deflections in terms of the Euler–Bernoulli beam deflections). Clearly, more than two elements of CIE and RIE are required to obtain acceptable solutions. The CIE gives slightly more accurate solutions compared to the RIE, but both have slow convergence especially for small ratios of H/L (i.e., thin beams).

Example 5.3.2

Consider the cantilever beam of **Example 5.2.1**. Analyze the problem using various Timoshenko beam finite elements. Take the problem data as $F_0 = 0$, and $M_0 = 0$ kN-m, and determine the generalized displacements in dimensionless form for $\nu = 0.25$, $K_s = 5/6$, and $H/L = 0.1$ and $H/L = 0.01$.

Solution: The exact solution of the problem according to the Timoshenko beam theory is given by (see Reddy [1])

$$w^{\mathrm{T}}(x) = w^{\mathrm{E}}(x) + \frac{1}{GAK_s}\left[M^{\mathrm{E}}(x) - M^{\mathrm{E}}(0)\right], \quad \phi_x(x) = -\frac{dw^{\mathrm{E}}}{dx} \tag{1}$$

where w^{E} and M^{E} are the exact solutions of the Euler–Bernoulli beam theory, and they are given in Eq. (10) of **Example 5.2.1**. The maximum values are

$$w^{\mathrm{T}}(L) = \frac{q_0 L^4}{30EI}(1 + 5\Lambda), \quad \phi_x(L) = -\frac{q_0 L^3}{24EI}, \quad \Lambda = \frac{EI}{GAK_s L^2} \tag{2}$$

The dimensionless forms are (amounts to setting $L = 1$, $q_0 = 1$, $EI = 1$, $GAK_s = 4EI/H^2 = 4/H^2$, and $H = 0.1$ and $H = 0.01$ in the numerical computations):

$$\bar{w}^{\mathrm{T}}(L) = w^{\mathrm{T}}(L)\frac{EI}{q_0 L^4} = \frac{1 + 5\Lambda}{30}, \quad \bar{\phi}_x(L) = \phi_x(L)\frac{EI}{q_0 L^3} = -\frac{1}{24}, \quad \Lambda = 0.25\left(\frac{H}{L}\right)^2 \tag{3}$$

Table 5.3.2 contains the end deflection $\bar{w}(L)$ and end rotation $\bar{\phi}_x(L)$ for two, four, and eight elements in full beam. The results converge, rather slowly, to the exact solution with an increase in number of elements.

Table 5.3.2 Comparison of the finite element solutions obtained with various types of finite elements for the cantilever beam of Fig. 5.2.11 (for the EBT, $\phi_x = \theta_x$).

	$\bar{w}(L)$			$-\bar{\phi}_x(L)$		
N	EBT	RIE	CIE	EBT	RIE	CIE
$H/L = 0.1$						
2	0.03333	0.03688	0.03036	0.04167	0.05208	0.04167
4	0.03333	0.03460	0.03289	0.04167	0.04427	0.04167
8	0.03333	0.03397	0.03353	0.04167	0.04232	0.04167
Exact	0.03333	0.03375	0.03375	0.04167	0.04167	0.04167
$H/L = 0.01$						
2	0.03333	0.03646	0.02995	0.04167	0.05208	0.04167
4	0.03333	0.03418	0.03247	0.04167	0.04427	0.04167
8	0.03333	0.03355	0.03312	0.04167	0.04232	0.04167
Exact	0.03333	0.03334	0.03334	0.04167	0.04167	0.04167

To further understand the effect of shear locking, we consider Timoshenko beam elements with equal interpolation of w and ϕ_x. Linear as well as quadratic elements with and without reduced integration are tested and the results are included in Table 5.3.3. It is clear that the full integration rules (2 × 2 for linear approximation and 3 × 3 for quadratic approximation) produce erroneous results, implying that shear locking is present. Shear locking gradually vanishes as the mesh is refined (either number of elements or the polynomial order is increased). Clearly, the quadratic elements outperform the linear elements.

Table 5.3.3 Effect of reduced integration of transverse shear coefficients on the deflections of the cantilever beam of Fig. 5.2.11.

Element	Linear			Quadratic			
Gauss rule	$N = 2$	$N = 4$	$N = 8$	Gauss rule	$N = 1$	$N = 2$	$N = 4$
$H/L = 0.1$							
2 × 1	0.03687	0.03460	0.03397	3 × 2	0.03514	0.03384	0.03376
2 × 2	0.00432	0.01150	0.02247	3 × 3	0.02306	0.03167	0.03350
Exact		0.03375				0.03375	
$H/L = 0.01$							
2 × 1	0.03646	0.03418	0.03355	3 × 2	0.03473	0.03342	0.03334
2 × 2	0.00048	0.00017	0.00064	3 × 3	0.02086	0.02997	0.03249
Exact		0.03334				0.03334	

The following general observations can be made about various finite element models of the TBT discussed here.

1. Reduced integration exhibits less locking compared with the full integration of shear stiffness coefficients.
2. Shear locking goes away with mesh refinements and with the use of higher-order elements.
3. Quadratic approximation of both w and ϕ_x and reduced integration of the shear stiffness coefficients yield the most accurate results.

5.4 Axisymmetric Bending of Circular Plates

5.4.1 Governing Equations

In this section, the finite element model of axisymmetric bending of circular plates using the classical plate theory (i.e., the theory in which transverse shear strain is assumed to be zero) is developed. We select the cylindrical coordinate system (r, θ, z) such that r is the radial coordinate outward from the center of the plate $(0 \le r \le R)$, z denotes the transverse coordinate $(-H/2 \le z \le H/2)$, where H is the total thickness of the plate, and θ is the angular coordinate $(0 \le \theta \le 2\pi)$, as shown in Fig. 5.4.1.

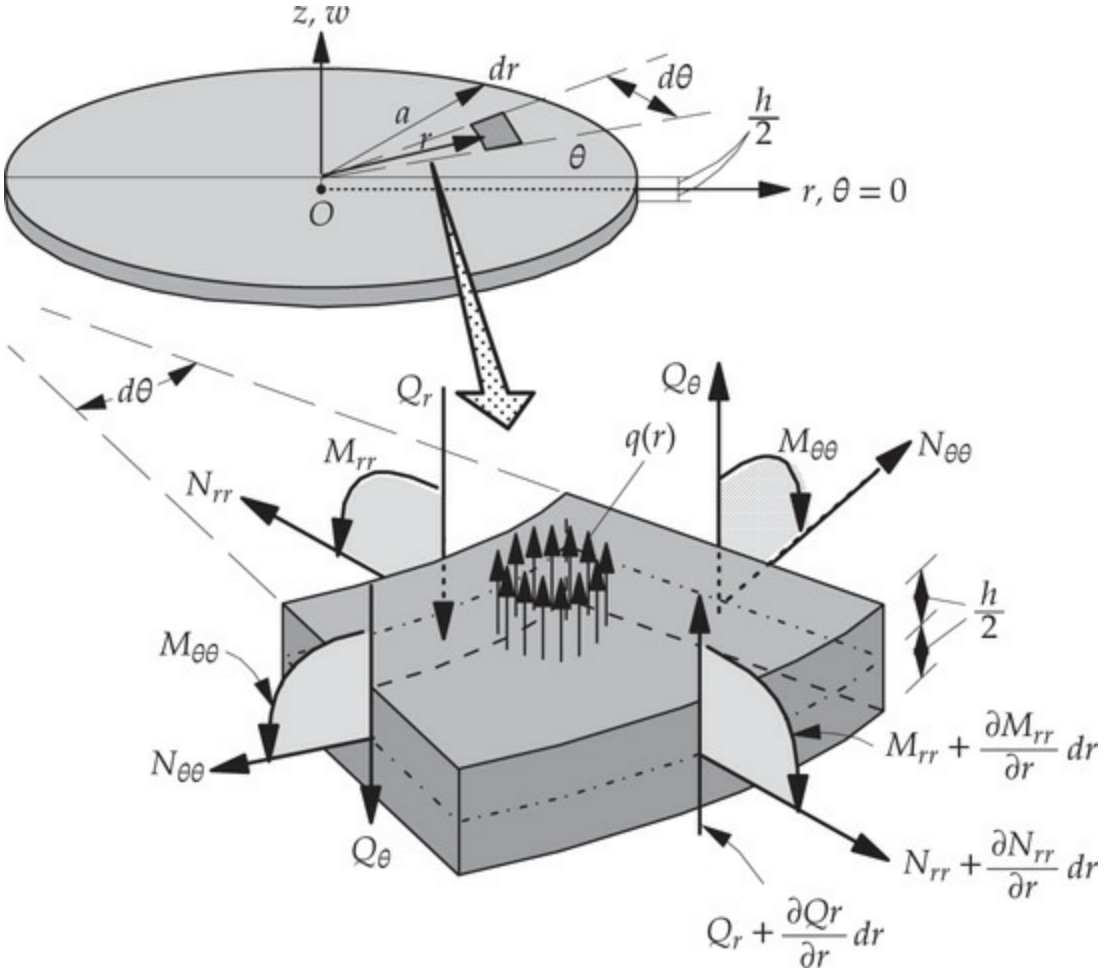

Fig. 5.4.1 A circular plate with stress resultants.

Governing equations of circular plates subjected to loads as well as boundary conditions that are independent of the angular coordinate θ can be formulated in terms of the radial coordinate r alone. Thus, the axisymmetric bending of circular plates is a one-dimensional problem, as discussed next (see Fig. 5.4.2).

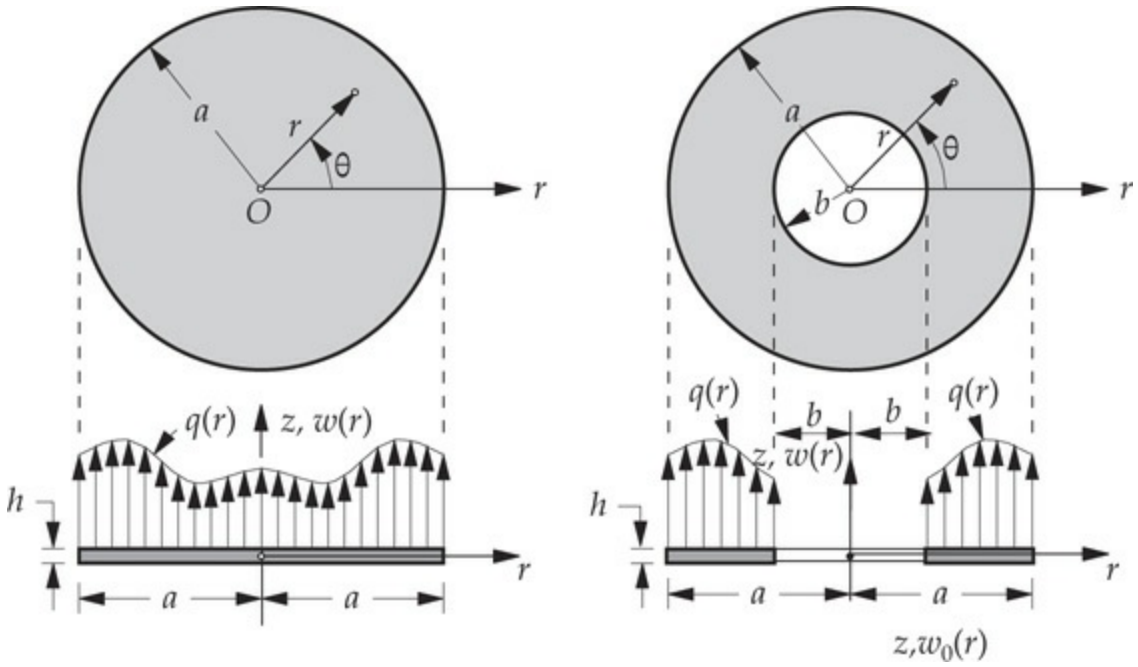

Fig. 5.4.2 Axisymmetric circular and annular plates.

The total displacements (u_r, u_θ, u_z) along the three coordinate directions (r, θ, z), as implied by the Love–Kirchhoff hypothesis for plates, which is the same as the Euler–Bernoulli hypothesis for beams, are given by

$$u_r(r,z) = -z\frac{dw}{dr}, \quad u_\theta(r,z) = 0, \quad u_z(r,z) = w(r) \tag{5.4.1}$$

where w denotes the transverse displacement of a point on the midplane of the plate. The nonzero linear strain components referred to the cylindrical coordinate system are given by (see Reddy [1, 2] and Ugural [6])

$$\varepsilon_{rr} = \frac{du_r}{dr} = -z\frac{d^2w}{dr^2}, \quad \varepsilon_{\theta\theta} = \frac{u_r}{r} = -\frac{z}{r}\frac{dw}{dr} \tag{5.4.2}$$

For an isotropic linear elastic material the stress-strain relations are

$$\begin{Bmatrix} \sigma_{rr} \\ \sigma_{\theta\theta} \\ \sigma_{r\theta} \end{Bmatrix} = \frac{E}{1-\nu^2}\begin{bmatrix} 1 & \nu & 0 \\ \nu & 1 & 0 \\ 0 & 0 & \frac{1-\nu}{2} \end{bmatrix}\begin{Bmatrix} \varepsilon_{rr} \\ \varepsilon_{\theta\theta} \\ 2\varepsilon_{r\theta} \end{Bmatrix} \tag{5.4.3}$$

where E is Young's modulus and ν is Poisson's ratio. The stress resultants on a plate element, as shown in Fig. 5.4.1, are defined by Eq. (5.4.4):

$$M_{rr} = \int_{-\frac{H}{2}}^{\frac{H}{2}} \sigma_{rr} z \, dz = -D\left(\frac{d^2w}{dr^2} + \frac{\nu}{r}\frac{dw}{dr}\right)$$
$$M_{\theta\theta} = \int_{-\frac{H}{2}}^{\frac{H}{2}} \sigma_{\theta\theta} z \, dz = -D\left(\nu\frac{d^2w}{dr^2} + \frac{1}{r}\frac{dw}{dr}\right) \tag{5.4.4}$$

where D denotes the bending stiffness

$$D = \frac{EH^3}{12(1-\nu^2)} \tag{5.4.5}$$

and H is the total thickness of the plate.

Equilibrium of forces and moments on an element of the plate yields

$$-\frac{1}{r}\frac{d}{dr}(rV_r) + k_f w = q \tag{5.4.6}$$

$$V_r - \frac{1}{r}\left[\frac{d}{dr}(rM_{rr}) - M_{\theta\theta}\right] = 0 \tag{5.4.7}$$

where k_f is the foundation modulus. Combining the above equations to eliminate the shear force V_r, we obtain

$$-\frac{1}{r}\frac{d}{dr}\left[\frac{d}{dr}(rM_{rr}) - M_{\theta\theta}\right] + k_f w - q = 0 \tag{5.4.8}$$

in which M_{rr} and $M_{\theta\theta}$ are given by Eq. (5.4.4).

5.4.2 Weak Form

The weak form of Eq. (5.4.8) over a typical element $\Omega^e = (r_a^e, r_b^e)$ is obtained using the three-step procedure. Let w_h^e be the approximation of w. Then the weightedresidual statement (step 1) and subsequent steps are carried out as for the Euler–Bernoulli beams:

$$
\begin{aligned}
0 &= \int_{r_a^e}^{r_b^e} v_i^e \left\{ -\frac{1}{r}\frac{d}{dr}\left[\frac{d}{dr}(rM_{rr}^h) - M_{\theta\theta}^h\right] + k_f^e w_h^e - q \right\} r\,dr \quad \text{(Step 1)} \\
&= \int_{r_a^e}^{r_b^e} \left\{ \frac{1}{r}\frac{dv_i^e}{dr}\left[\frac{d}{dr}(rM_{rr}^h) - M_{\theta\theta}^h\right] + k_f^e v_i^e w_h^e - v_i^e q \right\} r\,dr \\
&\quad - \left\{ v_i \left[\frac{d}{dr}(rM_{rr}^h) - M_{\theta\theta}^h\right] \right\}_{r_a^e}^{r_b^e} \\
&= \int_{r_a^e}^{r_b^e} \left[-\frac{d^2 v_i^e}{dr^2} M_{rr}^h - \frac{1}{r}\frac{dv_i^e}{dr} M_{\theta\theta}^h + k_f^e v_i^e w_h^e - v_i^e q \right] r dr \\
&\quad - \left\{ v_i^e \left[\frac{d}{dr}(rM_{rr}^h) - M_{\theta\theta}^h\right] \right\}_{r_a^e}^{r_b^e} - \left[-\frac{dv_i^e}{dr} rM_{rr}^h \right]_{r_a^e}^{r_b^e} \quad \text{(Step 2)}
\end{aligned} \tag{5.4.9}
$$

where $\{v_i^e\}$ is the set of weight functions, and M_{rr}^h and $M_{\theta\theta}^h$ are the bending moments derived from w_h according to Eq. (5.4.4). From the last expression, it is clear that

$$
\begin{aligned}
&\text{Primary variables: } w_h^e,\ -\frac{dw_h^e}{dr} \\
&\text{Secondary variables: } \left[\frac{d}{dr}(rM_{rr}^h) - M_{\theta\theta}^h\right] \equiv rV_r^h,\ rM_{rr}^h
\end{aligned} \tag{5.4.10}
$$

Thus, one element of each of the pairs (w_h^e, rV_r^h) and $(-dw_h^e/dr, rM_{rr}^h)$ must be known at any boundary point.

With the notation in Eq. (5.4.10), the final weak form is given by

$$
\begin{aligned}
0 &= \int_{r_a^e}^{r_b^e} \left[-\frac{d^2 v_i^e}{dr^2} M_{rr}^h - \frac{1}{r}\frac{dv_i^e}{dr} M_{\theta\theta}^h + k_f^e v_i^e w_h^e - v_i^e q \right] r\,dr - v_i^e(r_a^e) Q_1^e - v_i(r_b^e) Q_3^e \\
&\quad - \left(-\frac{dv_i^e}{dr}\right)_{r_a^e} Q_2^e - \left(-\frac{dv_i^e}{dr}\right)_{r_b^e} Q_4^e \quad \text{(Step 3)}
\end{aligned} \tag{5.4.11}
$$

where

$$Q_1^e = -\left[\frac{d}{dr}(rM_{rr}^h) - M_{\theta\theta}^h\right]_{r_a^e}, \quad Q_2^e = \left[-rM_{rr}^h\right]_{r_a^e}$$
$$Q_3^e = \left[\frac{d}{dr}(rM_{rr}^h) - M_{\theta\theta}^h\right]_{r_b^e}, \quad Q_4^e = \left[rM_{rr}^h\right]_{r_b^e} \tag{5.4.12}$$

Clearly, Q_1^e and Q_3^e are the shear forces and Q_2^e and Q_4^e are the bending moments. In order to express the weak form in Eq. (5.4.11) in terms of the displacement w_h, the bending moments M_{rr}^h and $M_{\theta\theta}^h$ appearing in Eq. (5.4.11) should be expressed in terms of w_h by means of Eq. (5.4.4). We have

$$\begin{aligned} 0 = \int_{r_a^e}^{r_b^e} \left[D\frac{d^2v_i}{dr^2}\left(\frac{d^2w_h}{dr^2} + \frac{\nu}{r}\frac{dw_h^e}{dr}\right) + \frac{D}{r}\frac{dv_i^e}{dr}\left(\nu\frac{d^2w_h^e}{dr^2} + \frac{1}{r}\frac{dw_h^e}{dr}\right) \right. \\ \left. + k_f^e v_i^e w_h^e - v_i^e q_e \right] r\,dr - v_i^e(r_a^e)Q_1^e - v_i^e(r_b^e)Q_3^e \\ - \left(-\frac{dv_i^e}{dr}\right)_{r_a^e} Q_2^e - \left(-\frac{dv_i^e}{dr}\right)_{r_b^e} Q_4^e \end{aligned} \tag{5.4.13}$$

5.4.3 Finite Element Model

The weak-form Galerkin (or Ritz) finite element model of axisymmetric bending of circular plates is obtained by assuming Hermite cubic approximation of $w(r)$ over a typical element $\Omega^e = (r_a^e, r_b^e)$ in the form

$$w(r) \approx w_h^e(r) = \sum_{j=1}^{4} \Delta_j^e \phi_j^e(r) \tag{5.4.14}$$

where $\phi_j^e(r)$ are the Hermite cubic polynomials given in Eq. (5.2.20) with x replaced by r (i.e., $\bar{r} = \bar{x}$ and $\bar{r} = r - r_a^e$) and Δ_j are the nodal values ($\theta = -dw/dr$)

$$\Delta_1^e = w(r_a^e), \quad \Delta_3^e = w(r_b^e), \quad \Delta_2^e = \theta(r_a^e), \quad \Delta_4^e = \theta(r_b^e)$$

Substituting Eq. (5.4.14) for w_h^e and $v_i^e = \phi_i^e$, we obtain

$$\mathbf{K}^e\boldsymbol{\Delta}^e = \mathbf{f}^e + \mathbf{Q}^e \tag{5.4.15}$$

$$K_{ij}^e = \int_{r_a^e}^{r_b^e} \left[D \frac{d^2\phi_i^e}{dr^2} \left(\frac{d^2\phi_j^e}{dr^2} + \frac{\nu}{r} \frac{d\phi_j^e}{dr} \right) + \frac{D}{r} \frac{d\phi_i^e}{dr} \left(\nu \frac{d^2\phi_j^e}{dr^2} + \frac{1}{r} \frac{d\phi_j^e}{dr} \right) + k_f^e \phi_i^e \phi_j^e \right] r\, dr$$

$$f_i^e = \int_{r_a^e}^{r_b^e} q_e \phi_i^e \, r dr, \tag{5.4.16}$$

$$Q_i^e = \phi_i^e(r_a^e) Q_1^e + \phi_i^e(r_b) Q_3^e + \left(-\frac{d\phi_i^e}{dr} \right)_{r_a^e} Q_2^e + \left(-\frac{d\phi_i}{dr} \right)_{r_b^e} Q_4^e$$

Clearly, the stiffness matrix $\mathbf{K}^e$ is symmetric and is of the order 4 × 4.

The standard boundary conditions (i.e., free, simply supported, and clamped) for axisymmetric bending of solid circular plates and annular plates are listed in Table 5.4.1. In addition, one can also have the mixed boundary conditions associated with vertical or torsional springs.

Table 5.4.1 Typical boundary conditions for solid circular and annular plates.[1]

Plate Type/Edge	Free	Hinged	Clamped
Solid Circular Plate			
$r = 0$ (for all cases)		$\frac{dw}{dr} = 0,$	$2\pi\, rQ_r = -Q_0$
$r = a$	$Q_r = Q_a$	$w = 0$	$w = 0$
	$M_{rr} = M_a$	$M_{rr} = M_a$	$\frac{dw}{dr} = 0$
Annular Plate			
$r = b$	$Q_r = Q_b$	$w = 0$	$w = 0$
	$M_{rr} = M_b$	$M_{rr} = M_b$	$\frac{dw}{dr} = 0$
$r = a$	$Q_r = Q_a$	$w = 0$	$w = 0$
	$M_{rr} = M_a$	$M_{rr} = M_a$	$\frac{dw}{dr} = 0$

[1] Q_a, Q_b, M_a, and M_b are distributed edge forces and moments and Q_0 is a concentrated force; a is the outer radius and b is the inner radius.

Example 5.4.1

Consider a circular steel plate ($E = 30 \times 10^6$ psi, $\nu = 0.29$) of radius $a = 10$ in. and thickness $H = 0.1$ in., simply supported at its rim, and subjected to a pressure load of $q_0 = 0.4$ psi. Determine the transverse deflection at the center of the plate using meshes of 2 and 4 Hermite cubic finite elements.

Solution: The bending stiffness is given by $D = EH^3/[12(1 - \nu^2)] = 2,729.6$ lb/in. For the two-element mesh, the element stiffness matrices and force vectors (evaluated using numerical integration in FEM1D) are

$$\mathbf{K}^1 = \begin{bmatrix} 0.98264E+03 & -0.81887E+03 & -0.98264E+03 & -0.24566E+04 \\ -0.81887E+03 & 0.58049E+04 & 0.81887E+03 & 0.20472E+04 \\ -0.98264E+03 & 0.81887E+03 & 0.98264E+03 & 0.24566E+04 \\ -0.24566E+04 & 0.20472E+04 & 0.24566E+04 & 0.96626E+04 \end{bmatrix}$$

$$\mathbf{K}^2 = \begin{bmatrix} 0.20541E+04 & -0.43902E+04 & -0.20541E+04 & -0.55076E+04 \\ -0.43902E+04 & 0.13160E+05 & 0.43902E+04 & 0.81228E+04 \\ -0.20541E+04 & 0.43902E+04 & 0.20541E+04 & 0.55076E+04 \\ -0.55076E+04 & 0.81228E+04 & 0.55076E+04 & 0.20113E+05 \end{bmatrix}$$

$$\mathbf{f}^1 = \begin{Bmatrix} 1.5000 \\ -1.6667 \\ 3.5000 \\ 2.5000 \end{Bmatrix}, \quad \mathbf{f}^2 = \begin{Bmatrix} 6.5000 \\ -5.8333 \\ 8.5000 \\ 6.6667 \end{Bmatrix}$$

The boundary conditions on the generalized displacements are $U_2 = U_5 = 0$. The solution of the condensed equations of the two-element mesh is

$$\mathbf{U} = \{0.0940\ 0.0000\ 0.0662\ 0.0105\ 0.0000\ 0.0142\}^{\mathrm{T}}$$

For the mesh of four elements ($U_2 = U_9 = 0$), the solution vector is given by

$$\mathbf{U} = \{0.0939\ 0.0000\ 0.0867\ 0.0057\ 0.0661\ 0.0105\ 0.0354\ 0.0136\ 0.0000\ 0.0142\}^{\mathrm{T}}$$

The analytical solution is given by (see Reddy [1, 2])

$$w(r) = \frac{q_0 a^4}{64D}\left[\left(\frac{r}{a}\right)^4 - 2\left(\frac{3+\nu}{1+\nu}\right)\left(\frac{r}{a}\right)^2 + \frac{5+\nu}{1+\nu}\right], \quad w(0) = \left(\frac{5+\nu}{1+\nu}\right)\frac{q_0 a^4}{64D} = 0.0939$$

For linearly varying (pyramid) load, $q(r) = q_0\,(1 - r/a)$, the four-element solution is given by

$$\mathbf{U} = \{0.0463\ 0.0000\ 0.0424\ 0.0030\ 0.0318\ 0.0053\ 0.0167\ 0.0065\ 0.0000\ 0.0066\}^{\mathrm{T}}$$

The analytical solution is given by (see Reddy [1, 2])

$$w(r) = \frac{q_0 a^4}{14400D}\left[\left(-64\frac{r}{a}\right)^5 + 255\left(\frac{r}{a}\right)^4 - \frac{710+290\nu}{1+\nu}\left(\frac{r}{a}\right)^2 + \frac{549+129\nu}{1+\nu}\right]$$

$$w(0) = \left(\frac{183+43\nu}{1+\nu}\right)\frac{q_0 a^4}{4800D} = 0.0463$$

Example 5.4.2

Consider a circular steel plate ($E = 30 \times 10^6$ psi, $\nu = 0.29$) of outside radius $a = 10$ in. and thickness $H = 0.1$ in., clamped at its rim, and subjected to a pressure load of $q_0 = 1$ psi. Determine the transverse deflection at the inner rim of the plate using a mesh of four Hermite cubic finite elements.

Solution: The only difference between **Example 5.4.1** and the present one is the change in the boundary conditions. For a mesh of four elements, the boundary conditions on the generalized displacements are $U_2 = U_9 = U_{10} = 0$. The solution for U_1, U_3, U_4, U_5, U_6, U_7, and U_8 is given by

$$\mathbf{U} = \{0.05726\ 0.05032\ 0.00536\ 0.03221\ 0.00858\ 0.01096\ 0.00751\}^{\mathrm{T}}$$

The analytical solution is given by

$$w(r) = \frac{q_0 a^4}{64D}\left[\left(1-\frac{r}{a}\right)^2\right]^2, \quad w(0) = \frac{q_0 a^4}{64D} = 0.05724$$

For linearly varying load, $q(r) = q_0\,(r/a)$, the four-element solution for U_1, U_3, U_4, U_5, U_6, U_7, and U_8 is

$$\mathbf{U} = \{0.02443\ 0.02190\ 0.00200\ 0.01476\ 0.00356\ 0.00539\ 0.00353\}^{\mathrm{T}}$$

The analytical solution is given by

$$w(r) = \frac{q_0 a^4}{450D}\left[\left(2\frac{r}{a}\right)^5 - 5\left(\frac{r}{a}\right)^2 + 3\right], \quad w(0) = \frac{q_0 a^4}{150D} = 0.02442$$

The finite element model associated with the first-order shear deformation theory (i.e., the Timoshenko beam theory applied to plates) of axisymmetric bending of circular plates is not included here, but the development follows the same steps as for the classical plate theory.

Problems 5.31–5.33 are designed to formulate the finite element model of the axisymmetric bending of circular plates when the first-order shear deformation theory is used.

5.5 Summary

In this chapter, finite element models of the classical (i.e., Euler–Bernoulli) and shear deformable (i.e., Timoshenko) beam theories and axisymmetric bending of circular plates using the classical plate theory have been developed. The classical theory of beams as well as axisymmetric circular plates involve a fourth-order equation in terms of the transverse deflection, while the shear deformation theory is expressed in terms of the transverse deflection and a rotation. Numerical examples of the elements developed are presented. One may also develop finite element model based on the shear deformation theory of axisymmetric circular plates (see **Problems 5.31–5.33** for shear deformation finite elements for axisymmetric circular plates).

The classical theory of beams and axisymmetric circular plates is governed by a fourth-order differential equation, and therefore results in a weak form whose primary variables contain the transverse deflection w and its first derivative (slope) θ_x. Therefore, Hermite interpolation of the transverse deflection is required in order to impose the continuity of the deflection and slope (w, θ_x) at the nodes between elements. When bending stiffness EI is constant and the elastic foundation term is zero (i.e., $k_f = 0$), the element yields the exact solution for displacements and generalized forces at the nodes, independent of the applied loads. The finite element solution is exact everywhere when applied distributed loads are zero. This is due to the fact that the homogeneous solution to the fourth-order equation is a cubic polynomial, and a cubic polynomial is used in the finite element method to approximate the solution. Such an element is called a *superconvergent element* (see **Problem 5.24** for additional information; see also Reddy [4, 5]). When $k_f \neq 0$ the exact solution of the fourth-order equation with constant EI is a hyperbolic function and, therefore, the finite element solution based on the cubic polynomial will not give exact solution even at the nodes.

In the case of the Timoshenko beam theory, there are two coupled second-order differential equations governing the transverse deflection w and an independent rotation function ϕx . In the thin beam limit, ϕ_x

degenerates, in theory, to $\theta_x = -dw/dx$. The weak forms of the two governing equations require Lagrange interpolation of both w and ϕ_x, with a minimum degree of interpolation being linear. Since the rotation function ϕ_x is like $\theta_x = -dw/dx$, the degree of the interpolation used for ϕ_x should be one less than that used for w. Such selective interpolation of the variables is called *consistent interpolation*. When the same degree of interpolation is used to approximate the transverse deflection w and the rotation ϕ_x, especially when both are approximated by linear polynomials, the resulting stiffness matrix is often too stiff to yield good solutions. This is due to the inconsistency of interpolation of the variables, and the phenomenon is known as *shear locking*. The locking may be overcome by the use of reduced integration to evaluate the stiffness coefficients associated with transverse shear strains or by using higher-order interpolation of w and ϕx (ideally, cubic for w and quadratic for ϕx). Reduced integration elements (RIEs) and consistent interpolation elements (CIEs) with quadratic interpolation of the transverse deflection and linear interpolation of the rotation have been discussed. The RIE and CIE developed herein, being lower order than the homogeneous solution of the corresponding differential equations, do not yield exact nodal values. An element based on the analytical solution to the homogeneous solutions of the Timoshenko beam equations (for constant EI and GAK_s) yields exact nodal values (see **Problem 5.24** and Reddy [3, 4]).

Problems

EULER–BERNOULLI BEAM ELEMENT

5.1 Consider a beam element of length h_e and constant material and geometric properties E_e, A_e, and I_e. Let $\bar{x}$ be the local coordinate with origin at the left end (i.e., node 1) of the element. The homogeneous solution to the fourth-order equation governing the EBT, $E_e I_e (d^4 w/d\bar{x}^4) = q_e$, is

$$w_h^e(\bar{x}) = c_1^e + c_2^e \bar{x} + c_3^e \bar{x}^2 + c_4^e \bar{x}^3 \tag{1}$$

First, express the constants c_1^e through c_4^e in terms of the nodal generalized displacements as [see Eq. (5.2.18)]

$$\Delta_1^e = w_h^e(0), \quad \Delta_2^e = -\left.\frac{dw_h^e}{d\bar{x}}\right|_{\bar{x}=0}, \quad \Delta_3^e = w(h_e), \quad \Delta_4^e = -\left.\frac{dw_h^e}{d\bar{x}}\right|_{\bar{x}=h_e} \tag{2}$$

Next, derive the finite element equations, Eq. (5.2.35), for $q_0 = 0$ and $L = h_e$ using the definitions of the generalized forces [see Eq. (5.2.12)]

$$\begin{aligned} Q_1^e &\equiv \left[\frac{d}{d\bar{x}}\left(E_e I_e \frac{d^2 w_h^e}{d\bar{x}^2}\right)\right]_{\bar{x}=0}, \qquad Q_2^e \equiv \left[E_e I_e \frac{d^2 w_h^e}{d\bar{x}^2}\right]_{\bar{x}=0} \\ Q_3^e &\equiv -\left[\frac{d}{d\bar{x}}\left(E_e I_e \frac{d^2 w_h^e}{d\bar{x}^2}\right)\right]_{\bar{x}=h_e}, \quad Q_4^e \equiv -\left[E_e I_e \frac{d^2 w_h^e}{d\bar{x}^2}\right]_{\bar{x}=h_e} \end{aligned} \tag{3}$$

This problem illustrates that the EBT element yields the exact values of the generalized displacements at the nodes when the material and geometric properties are element-wise constant, as long as the distributed load $q(x)$ can be represented as equivalent nodal forces. Such elements are called *superconvergent element*.

5.2 Consider the fourth-order equation in (5.2.10) and its weak form (5.2.13). Suppose that a two-node element is employed, with *three* primary variables at each node: (w_h^e, θ_x^e, and κ_h^e), where $\theta_x^e = dw_h^e/dx$ (no minus sign in front of dw/dx) and $\kappa_h^e = d^2 w_h^e/dx^2$. Show that the associated Hermite interpolation functions are given by

$$\begin{aligned} \phi_1^e &= 1 - 10\frac{\bar{x}^3}{h^3} + 15\frac{\bar{x}^4}{h^4} - 6\frac{\bar{x}^5}{h^5}, \qquad \phi_2^e = \bar{x}\left(1 - 6\frac{\bar{x}^2}{h^2} + 8\frac{\bar{x}^3}{h^3} - 3\frac{\bar{x}^4}{h^4}\right) \\ \phi_3^e &= \frac{\bar{x}^2}{2}\left(1 - 3\frac{\bar{x}}{h} + 3\frac{\bar{x}^2}{h^2} - \frac{\bar{x}^3}{h^3}\right), \quad \phi_4^e = 10\frac{\bar{x}^3}{h^3} - 15\frac{\bar{x}^4}{h^4} + 6\frac{\bar{x}^5}{h^5} \\ \phi_5^e &= -\bar{x}\left(4\frac{\bar{x}^2}{h^2} - 7\frac{\bar{x}^3}{h^3} + 3\frac{\bar{x}^4}{h^4}\right), \qquad \phi_6^e = \frac{\bar{x}^2}{2}\left(\frac{\bar{x}}{h} - 2\frac{\bar{x}^2}{h^2} + \frac{\bar{x}^3}{h^3}\right) \end{aligned} \tag{1}$$

where $\bar{x}$ is the element coordinate with the origin at node 1.

5.3 Compute the following matrix and vector coefficients for the beam element of **Problem 5.2**:

$$K_{ij}^e = E_e I_e \int_0^h \frac{d^2\phi_i}{dx^2}\frac{d^2\phi_j}{dx^2}\,dx, \quad M_{ij}^e = \rho_e A_e \int_0^h \phi_i^e \phi_j^e\,dx, \quad f_i^e = q_0^e \int_0^{h_e} \phi_i^e\,dx \tag{1}$$

where E_e I_e, $\rho_e A_e$, and q_0^e are constants (have the usual meaning).

5.4 Consider the weak form in Eq. (5.2.13) of the EBT element. Use a three-node element with two degrees of freedom (w_h^e, θ_x^e), where $\theta_x^e \equiv -dw_h^e/dx$. Derive the Hermite interpolation functions for the element. Compute the element stiffness matrix and force vector. *Partial answer:*

$$\phi_1^e = 1 - 23\frac{\bar{x}^2}{h_e^2} + 66\frac{\bar{x}^3}{h_e^3} - 68\frac{\bar{x}^4}{h_e^4} + 24\frac{\bar{x}^5}{h_e^5}$$

5.5 Compute element stiffness matrix $\mathbf{K}^e$, mass matrix $\mathbf{M}^e$, and force vector (for uniform load) $\mathbf{f}^e$ (see **Problem 5.3** for the definitions of the coefficients) for the beam element of **Problem 5.4**.

5.6 Consider the following pair of differential equations:

$$-\frac{d}{dx}\left(a\frac{du}{dx} - b\frac{d^2w}{dx^2}\right) = 0, \quad -\frac{d^2}{dx^2}\left(b\frac{du}{dx} - c\frac{d^2w}{dx^2}\right) - f = 0 \tag{1}$$

where u and w are the dependent unknowns; a, b, c, and f are given functions of x.

(a) Develop the weak forms of the equations over a typical element and identify the primary and secondary variables of the formulation. Make sure that the bilinear form is symmetric (so that the element coefficient matrix is symmetric).

(b) Develop the finite element model by assuming approximation of the form

$$u(x) \approx u_h^e(x) = \sum_{j=1}^{m} u_j^e \psi_j^e(x), \quad w(x) \approx w_h^e(x) = \sum_{j=1}^{n} w_j^e \phi_j^e(x) \tag{1}$$

Hint: The weight functions v_{i1}^e and v_{2i}^e used for the two equations are like u_h^e and w_h^e, respectively.

(c) Comment on the type of interpolation functions ψ_j^e and ϕ_h^e (i.e., Lagrange type or Hermite type) and the minimum degree of approximation functions that can be used in this problem.

5.7–5.23 Use the minimum number of Euler–Bernoulli beam finite elements to analyze the beam problems shown in Figs. P5.7–P5.23. In particular, give:

(a) the assembled stiffness matrix and force vector;

(b) the specified global displacements and forces, and the equilibrium conditions;

(c) the condensed matrix equations for the unknown

generalized displacements and unknown generalized forces separately.

Exploit symmetries, if any, in analyzing the problems. The positive convention used for the generalized displacements and forces is the same as that shown in Fig. 5.2.3.

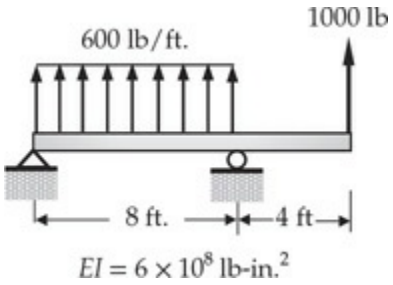

Fig. P5.7

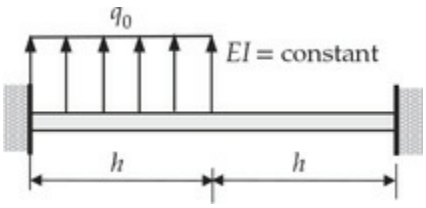

Fig. P5.8

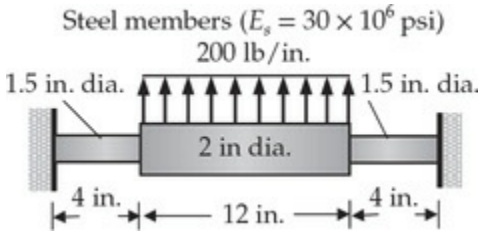

Fig. P5.9

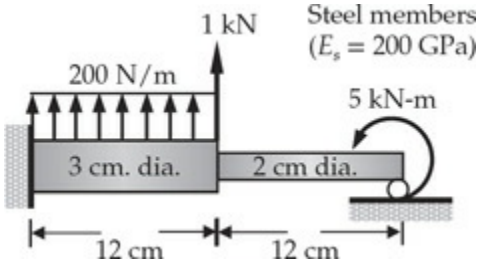

Fig. P5.10

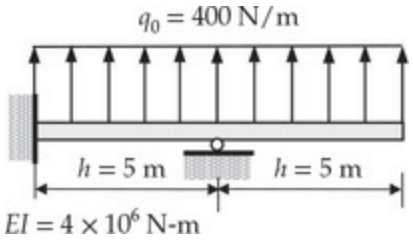

Fig. P5.11

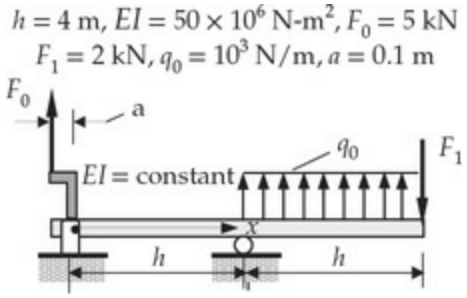

Fig. P5.12

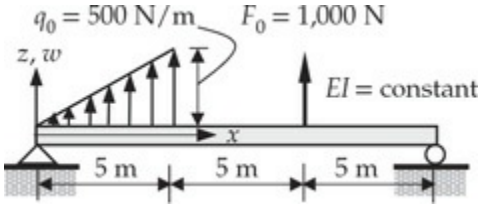

Fig. P5.13

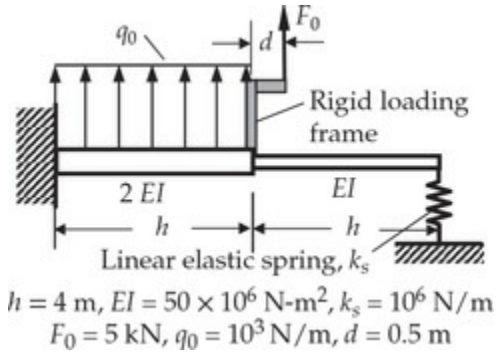

Fig. P5.14

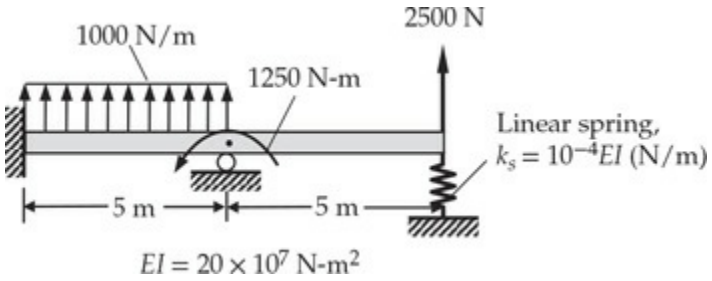

Fig. P5.15

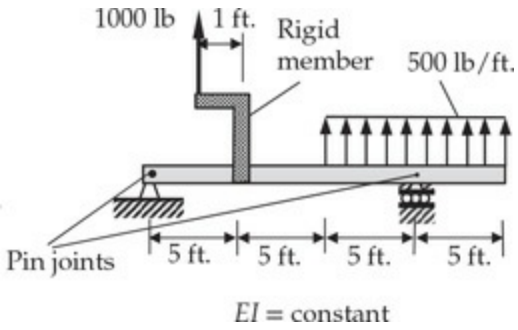

Fig. P5.16

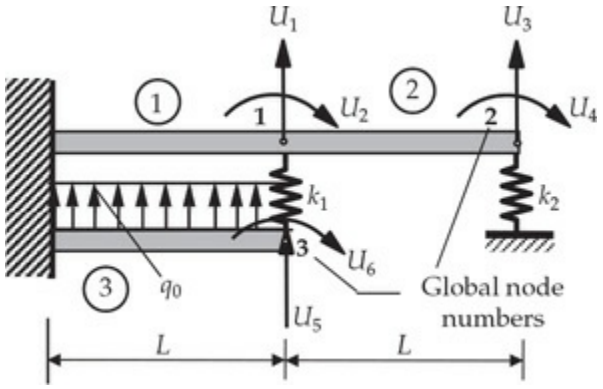

Fig. P5.17

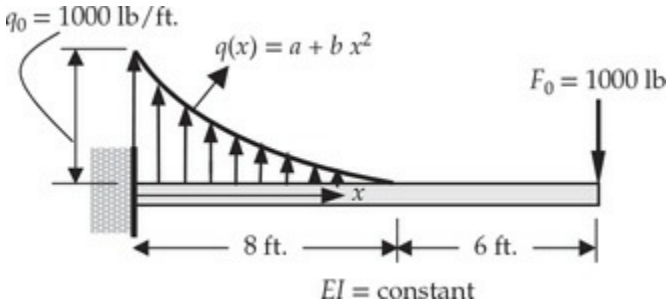

Fig. P5.18

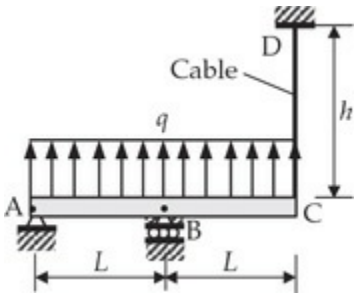

Fig. P5.19

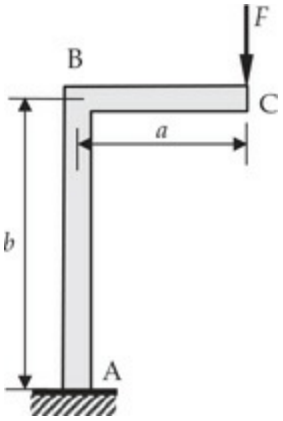

Fig. P5.20

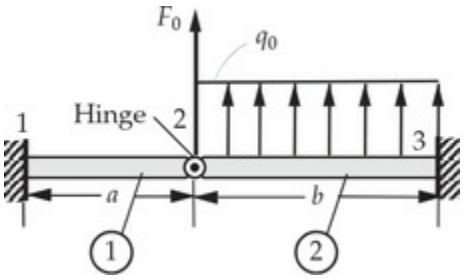

Fig. P5.21

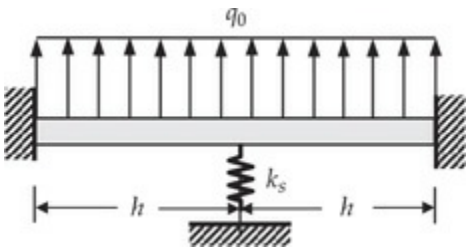

Fig. P5.22

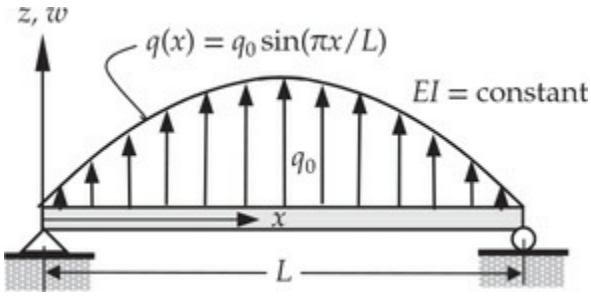

Fig. P5.23

TIMOSHENKO BEAM ELEMENT

5.24 Consider a beam element of length h_e and constant material and

geometric properties E_e, A_e, and I_e. Let x be the local coordinate with origin at the left end (i.e., node 1) of the element. (a) Show that the homogeneous solution to the following pair of equations that govern the Timoshenko beam theory (see Reddy [3, 4]):

$$-\frac{d}{dx}\left[G_eA_eK_s\left(\phi_x+\frac{dw}{dx}\right)\right]=0 \tag{1}$$

$$-\frac{d}{dx}\left(E_eI_e\frac{d\phi}{dx}\right)+G_eA_eK_s\left(\phi_x+\frac{dw}{dx}\right)=0 \tag{2}$$

is

$$w^e(x)=-\left(c_1^e\frac{x^3}{6}+c_2^e\frac{x^2}{2}+c_3^ex+c_4^e\right)+\frac{E_eI_e}{G_eA_eK_s}c_1^ex \tag{3}$$

$$\phi_x^e(x)=c_1^e\frac{x^2}{2}+c_2^ex+c_3^e \tag{4}$$

where c_i^e $(i=1,2,3,4)$ are constants of integration.

(b) Use the definitions of the generalized displacements

$$\Delta_1^e=w(0),\quad \Delta_2^e=\phi_x(0),\quad \Delta_3^e=w(h_e),\quad \Delta_4^e=\phi_x(h_e)$$

and generalized forces

$$\begin{aligned} Q_1^e&\equiv-\left[GAK_s\left(\phi_x+\frac{dw}{dx}\right)\right]_{x=0},\quad Q_2^e\equiv-\left[EI\frac{d\phi_x}{dx}\right]_{x=0}\\ Q_3^e&\equiv\left[GAK_s\left(\phi_x+\frac{dw}{dx}\right)\right]_{x=h_e},\quad Q_4^e\equiv\left[EI\frac{d\phi_x}{dx}\right]_{x=h_e}\end{aligned} \tag{5}$$

to derive the finite element model of Eqs. (1) and (2) in the form

$$\left(\frac{2E_eI_e}{\Lambda_eh_e^3}\right)\begin{bmatrix}6 & -3h_e & -6 & -3h_e\\ -3h_e & 2h_e^2\lambda_e & 3h_e & h_e^2\gamma_e\\ -6 & 3h_e & 6 & 3h_e\\ -3h_e & h_e^2\gamma_e & 3h_e & 2h_e^2\lambda_e\end{bmatrix}\begin{Bmatrix}\Delta_1^e\\ \Delta_2^e\\ \Delta_3^e\\ \Delta_4^e\end{Bmatrix}=\begin{Bmatrix}Q_1^e\\ Q_2^e\\ Q_3^e\\ Q_4^e\end{Bmatrix} \tag{6}$$

where

$$\mu_e=\frac{E_eI_e}{G_eA_eK_sh_e^2},\quad \Lambda_e=1+12\mu_e,\quad \lambda_e=1+3\mu_e,\quad \gamma_e=1-6\mu_e \tag{7}$$

5.25 Analyze the beam in Fig. P5.8 using the reduced integration

Timoshenko beam finite element (RIE). Use a value of $\frac{5}{6}$ for the shear correction factor K_s and $\nu = 0.3$.

5.26 Analyze the beam in Fig. P5.8 using the consistent interpolation Timoshenko beam element (CIE). Use a value of $\frac{5}{6}$ for the shear correction factor K_s and $\nu = 0.3$.

5.27 Analyze the problem in Fig. P5.8 using the interdependent interpolation Timoshenko beam element (IIE) of **Problem 5.24**. Use a value of $\frac{5}{6}$ for the shear correction factor K_s and $\nu = 0.3$.

5.28 Analyze the problem in Fig. P5.22 using the reduced integration Timoshenko beam finite element (RIE). Use a value of $\frac{5}{6}$ for the shear correction factor K_s and $\nu = 0.3$.

5.29 Analyze the problem in Fig. P5.22 using the consistent interpolation Timoshenko beam element (CIE). Use a value of $\frac{5}{6}$ for the shear correction factor K_s and $\nu = 0.3$.

5.30 Analyze the problem in Fig. P5.22 using the interdependent interpolation Timoshenko beam element (IIE) developed in **Problem 5.24**. Use a value of $\frac{5}{6}$ for the shear correction factor K_s and $\nu = 0.3$.

CIRCULAR PLATE ELEMENTS

5.31 The differential equations governing axisymmetric bending of circular plates according to the shear deformation plate theory are

$$-\frac{1}{r}\frac{d}{dr}(rQ_r) - q = 0 \tag{1}$$

$$-\frac{1}{r}\left[\frac{d}{dr}(rM_{rr}) - M_{\theta\theta}\right] + Q_r = 0 \tag{2}$$

where

$$M_{rr} = D\left(\frac{d\phi_r}{dr} + \nu\frac{\phi_r}{r}\right),\quad M_{\theta\theta} = D\left(\nu\frac{d\phi_r}{dr} + \frac{\phi_r}{r}\right)$$
$$Q_r = K_s GH\left(\phi_r + \frac{dw}{dr}\right) \tag{3}$$

$D = EH^3/[12(1 - \nu^2)]$ and H is the plate thickness. Develop (a) the weak form of the equations over an element, and (b) the finite element model of the equations.

5.32 The principle of minimum total potential energy for axisymmetric bending of polar orthotropic plates according to the first-order shear deformation theory requires $\delta\Pi = 0$, where

$$\delta\Pi(w^e, \phi_r^e) = 2\int_{r_a^e}^{r_b^e}\left[\left(D_{11}^e\frac{d\phi_r^e}{dr} + D_{12}^e\frac{\phi_r^e}{r}\right)\frac{d\delta\phi_r^e}{dr} + \frac{1}{r}\left(D_{12}^e\frac{d\phi_r^e}{dr} + D_{22}^e\frac{\phi_r^e}{r}\right)\delta\phi_r^e + A_{55}^e\left(\phi_r^e + \frac{dw^e}{dr}\right)\left(\delta\phi_r^e + \frac{d\delta w^e}{dr}\right) - q_e\delta w^e\right]rdr - \sum_{i=1}^{4} Q_i^e\delta\Delta_i^e \tag{1}$$

where r_a^e is the inner radius and r_b^e the outer radius of the radial element, Δ_i^e are defined by

$$\begin{aligned}\Delta_1^e &\equiv w^e(r_a^e), \quad \Delta_2^e \equiv \phi_r^e(r_a^e)\\ \Delta_3^e &\equiv w^e(r_b^e), \quad \Delta_4^e \equiv \phi_r^e(r_b^e)\end{aligned} \tag{2}$$

and Q_1^e and Q_3^e denote the shear forces (i.e., values of rQ_r) and Q_2^e and Q_4^e the bending moments (i.e., values of rM_{rr}) at the left and right ends, respectively (see **Problem 5.36** for the definition of Q_r and M_{rr}). Derive the displacement finite element model of the equations. In particular, show that the finite element model is of the form

$$\begin{bmatrix}\mathbf{K}^{11} & \mathbf{K}^{12}\\ (\mathbf{K}^{12})^{\mathrm{T}} & \mathbf{K}^{22}\end{bmatrix}^e\begin{Bmatrix}\mathbf{w}\\ \mathbf{\Phi}\end{Bmatrix}^e = \begin{Bmatrix}\mathbf{F}^1\\ \mathbf{F}^2\end{Bmatrix}^e \tag{3}$$

and define the coefficients K_{ij}^{11}, K_{ij}^{12}, K_{ij}^{22}, F_i^1, and F_i^2.

5.33 The general homogeneous solution (i.e., for the case $q = 0$) of Eqs. (1)–(3) of **Problem 5.31** that governs the shear deformation theory for axisymmetric bending of circular plates is of the form (prove to yourself)

$$w(r) = C_1 + C_2r^2 + C_3\ln r + C_4r^2\ln r \tag{1}$$

$$\phi_r(r) = -2C_2r - \frac{C_3}{r} - C_4\left[r(1 + 2\ln r) + \frac{1}{r}\Gamma\right] \tag{2}$$

where C_i are constants of integration and $\Gamma = (4D/GAK_s)$. The classical plate theory solution is obtained from (1) and (2) by setting $\Gamma = 0$.

Next, consider a finite element of length h_e located in (r_a, r_b) in a circular plate. Let the generalized displacements at nodes 1 and 2 of

the element be defined as

$$w(r_a) = \Delta_1, \quad \phi_r(r_a) \equiv \Delta_2$$
$$w(r_b) = \Delta_3, \quad \phi_r(r_b) \equiv \Delta_4 \tag{3}$$

Next, let Q_1 and Q_3 denote the shear forces (i.e., values of rQ_r) and Q_2 and Q_4 denote the bending moments (i.e., values of rM_{rr}) at nodes 1 and 2. Using Eqs. (1) and (2), relate the nodal degrees of freedom Δ_i defined in Eq. (3) to the generalized forces Q_i (i.e., determine the finite element model).

5.34 Consider a solid circular plate of radius a and thickness H. If the plate is simply supported at the outer edge and subjected to a linearly varying load q_0 (r/a), analyze the problem using a uniform mesh of four elements and compare the solution with the analytical solution:

$$w(r) = \frac{q_0 a^4}{450D}\left(\frac{r^5}{a^5} - \frac{20+5\nu}{1+\nu}\frac{r^2}{a^2} + \frac{18+3\nu}{1+\nu}\right), \quad w(0) = \frac{6+\nu}{1+\nu}\frac{q_0 a^4}{150D}$$

where $D = EH^3/12(1-\nu^2)$, E is Young's modulus, and ν is Poisson's ratio. Use $E = 30 \times 10^6$ psi, $\nu = 0.29$, $q_0 = 0.5$ psi, $H = 0.1$ in., and $a = 10.0$ in.

5.35 Consider a thin isotropic solid circular plate of radius a and thickness H. Suppose that the plate is clamped at $r = a$ and subjected to a quadratically varying transverse load of q_0 (r^2/a^2). (a) Give the boundary conditions on the primary and secondary variables when a uniform mesh of two elements is used. (b) Determine the center deflection with a uniform mesh of four elements and compare with the exact solution

$$w(r) = \frac{q_0 a^4}{576D}\left[2 - 3\left(\frac{r}{a}\right)^2 + \left(\frac{r}{a}\right)^6\right], \quad w(0) = \frac{q_0 a^4}{288D}$$

where $D = EH^3/12(1-\nu^2)$, E is Young's modulus, and ν is Poisson's ratio. Use $E = 30 \times 10^6$ psi, $\nu = 0.29$, $q_0 = 1$ psi, $H = 0.1$ in., and $a = 10.0$ in.

5.36 Consider a thin isotropic annular plate of outer radius a, inner radius b, and thickness H. Suppose that the plate is clamped at the inner edge $r = b$ and subjected to a uniformly distributed transverse load of intensity q_0 (see Fig. P5.36). If two finite elements are used in the

domain ($0 \le r \le a$), give the boundary conditions on the primary and secondary variables of the mesh.

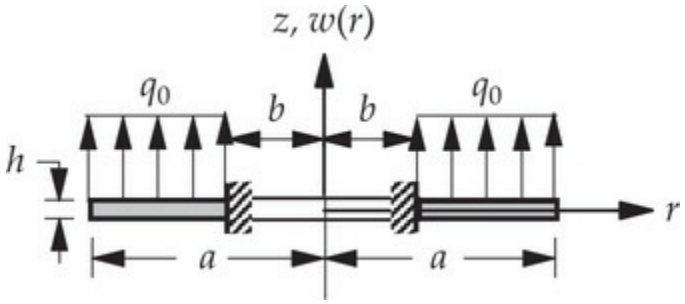

Fig. P5.36

5.37 Repeat **Problem 5.36** when the plate is clamped at the outer edge $r = a$ (and the inner edge is not clamped), subjected to a transverse line load of intensity Q_0 per unit length along the inner edge $r = b$, and a two-element mesh is used.

5.38 Repeat Part (a) of **Problem 5.35** when a two-element mesh of Timoshenko elements is used.

References for Additional Reading

1. J. N. Reddy, *Energy Principles and Variational Methods in Applied Mechanics*, 3rd ed., John Wiley & Sons, New York, NY, 2017.
2. J. N. Reddy, *Theory and Analysis of Elastic Plates and Shells*, 2nd ed., CRC Press, Boca Raton, FL, 2007.
3. C. M. Wang, J. N. Reddy, and K. H. Lee, *Shear Deformable Beams and Plates. Relationships with Classical Solutions*, Elsevier, Oxford, UK, 2000.
4. J. N. Reddy, "On locking-free shear deformable beam finite elements," *Computer Methods in Applied Mechanics and Engineering*, **149**, 113–132, 1997.
5. J. N. Reddy, "On the derivation of the superconvergent Timoshenko beam finite element," *International Journal for Computational Civil and Structural Engineering*, **1**(2), 71–84, 2000.
6. A. C. Ugural, *Plates and Shells, Theory and Analysis*, 4th ed., CRC Press, Boca Raton, FL, 2018.

6 Plane Trusses and Frames

Only those who attempt the absurd will achieve the impossible.

— M. C. Escher

6.1 Introduction

Consider a structure consisting of several bar elements, with different orientations, connected to each other by pins, as shown in Fig. 6.1.1(a). The members may rotate freely about the axis of the pin. Consequently, each member carries only axial forces. The planar structure (i.e., all members lie in the same plane) with pin-connected members is called a *plane truss*. When the members are connected rigidly, that is, welded, bonded, rivetted, or bolted [see Fig. 6.1.1(b)], bending moments will develop at the joints, in addition to forces along and transverse to the members. The planar structure with rigidly connected members is called a *plane frame*.

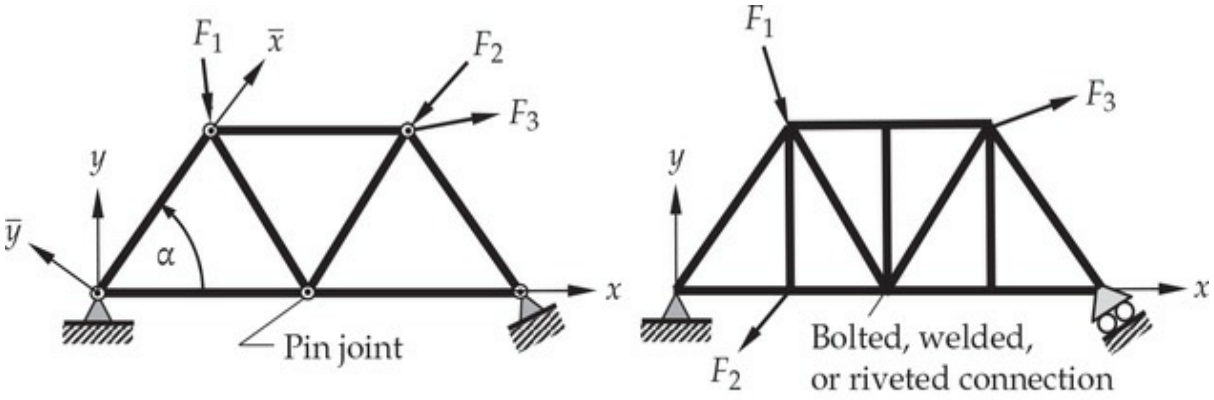

Fig. 6.1.1 (a) A plane truss structure. (b) A plane frame structure.

In a truss or a frame structure, each member is oriented differently with respect to a chosen global coordinate system (x, y). Therefore, it is necessary to transform the force–displacement relations that were derived in the element coordinate system $(\bar{x}, \bar{y})$ to the global coordinate system (x,

y) so that the force–displacement relations at the structural level can be obtained from an assembly of element equations referred to a common global coordinate system. We shall discuss these ideas next. The elements used are based on the linear approximation of the axial displacement and Hermite cubic approximation of the transverse deflection in the case of Bernoulli–Euler beam theory.

6.2 Analysis of Trusses

6.2.1 The Truss Element in the Local Coordinates

First, we consider a uniform bar element Ω^e with constant E_eA_e and oriented at an angle α_e, measured counterclockwise, from the positive x-axis. If the member coordinate system $(\bar{x}_e, \bar{y}_e)$ is taken as shown in Fig. 6.2.1(a), where $(\bar{u}_i^e, \bar{v}_i^e)$ denote the displacements and $(\bar{F}_i^e, 0)$ denote the forces along and transverse to the member at node i with respect to the member coordinate system $(\bar{x}_e, \bar{y}_e)$, the element equations (3.3.2) can be expressed as:

$$\frac{E_eA_e}{h_e}\begin{bmatrix} 1 & 0 & -1 & 0 \\ 0 & 0 & 0 & 0 \\ -1 & 0 & 1 & 0 \\ 0 & 0 & 0 & 0 \end{bmatrix}\begin{Bmatrix} \bar{u}_1^e \\ \bar{v}_1^e \\ \bar{u}_2^e \\ \bar{v}_2^e \end{Bmatrix} = \begin{Bmatrix} \bar{F}_1^e \\ 0 \\ \bar{F}_2^e \\ 0 \end{Bmatrix} \quad \text{or} \quad \bar{\mathbf{K}}^e\bar{\boldsymbol{\Delta}}^e = \bar{\mathbf{F}}^e \tag{6.2.1}$$

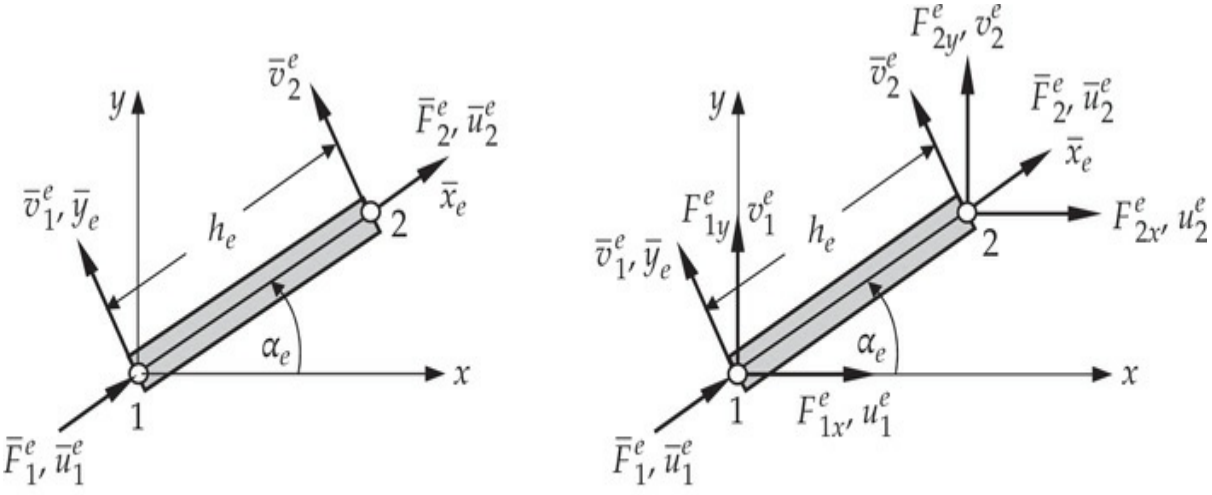

(a) Forces and displacements in the element coordinates

(b) Forces and displacements in the global coordinates

Fig. 6.2.1 A bar element oriented at an angle to the global x-coordinate.

6.2.2 The Truss Element in the Global Coordinates

We wish to write the force-deflection relations in Eq. (6.2.1) in terms of the corresponding global displacements and forces. Toward this end, we first write the transformation relations between the two sets of coordinate systems (x, y) and $(\bar{x}_e, \bar{y}_e)$ shown in Fig. 6.2.1(a) and (b):

$$\bar{x}_e = x\ \cos\alpha_e + y\ \sin\alpha_e, \qquad \bar{y}_e = -x\ \sin\alpha_e + y\ \cos\alpha_e$$
$$x = \bar{x}_e\ \cos\alpha_e - \bar{y}_e\ \sin\alpha_e, \quad y = \bar{x}_e\ \sin\alpha_e + \bar{y}_e\ \cos\alpha_e$$

or, in matrix form, we have

$$\begin{Bmatrix} \bar{x}_e \\ \bar{y}_e \end{Bmatrix} = \begin{bmatrix} \cos\alpha_e & \sin\alpha_e \\ -\sin\alpha_e & \cos\alpha_e \end{bmatrix} \begin{Bmatrix} x \\ y \end{Bmatrix}$$
$$\begin{Bmatrix} x \\ y \end{Bmatrix} = \begin{bmatrix} \cos\alpha_e & -\sin\alpha_e \\ \sin\alpha_e & \cos\alpha_e \end{bmatrix} \begin{Bmatrix} \bar{x}_e \\ \bar{y}_e \end{Bmatrix} \tag{6.2.2}$$

where α_e is the angle between the positive x-axis and positive $\bar{x}_e$-axis, measured in the counterclockwise direction. Note that all quantities with a bar over them are referred to the member (or local) coordinate system $(\bar{x}_e, \bar{y}_e)$, while the quantities without a bar refer to the global coordinates (x, y), as shown in Fig. 6.2.1(b).

The transformation in Eq. (6.2.2) also holds for the components of the displacement and force vectors in the two coordinate systems. To relate $(\bar{u}_i, \bar{v}_i)$ in the local coordinate system to (u_i, v_i) in the global coordinate system at both nodes (i = 1, 2), we write

$$\begin{Bmatrix} \bar{u}_1^e \\ \bar{v}_1^e \\ \bar{u}_2^e \\ \bar{v}_2^e \end{Bmatrix} = \begin{bmatrix} \cos\alpha_e & \sin\alpha_e & 0 & 0 \\ -\sin\alpha_e & \cos\alpha_e & 0 & 0 \\ 0 & 0 & \cos\alpha_e & \sin\alpha_e \\ 0 & 0 & -\sin\alpha_e & \cos\alpha_e \end{bmatrix} \begin{Bmatrix} u_1^e \\ v_1^e \\ u_2^e \\ v_2^e \end{Bmatrix} \tag{6.2.3a}$$

or

$$\bar{\boldsymbol{\Delta}}^e = \mathbf{T}^e \boldsymbol{\Delta}^e \tag{6.2.3b}$$

where $\bar{\boldsymbol{\Delta}}^e$ and Δ^e denote the nodal displacement vectors in the member

(local) and structure (global) coordinate systems, respectively. Similarly, we have

$$\bar{\mathbf{F}}^e = \mathbf{T}^e \mathbf{F}^e \tag{6.2.4}$$

where $\bar{\mathbf{F}}^e$ and $\mathbf{F}^e$ are the nodal force vectors in the member and structure coordinate systems, respectively [see Fig. 6.2.1(a) and (b)].

Next, we derive the relationship between the global displacements and global forces of a typical element. Using Eqs. (6.2.3b) and (6.2.4) in Eq. (6.2.1), we obtain

$$\bar{\mathbf{K}}^e \mathbf{T}^e \boldsymbol{\Delta}^e = \mathbf{T}^e \mathbf{F}^e \tag{6.2.5}$$

Pre-multiplying both sides of Eq. (6.2.5) with $(\mathbf{T}^e)^{-1}$ and noting that $(\mathbf{T}^e)^{-1} = (\mathbf{T}^e)^{\mathrm{T}}$, we obtain

$$(\mathbf{T}^e)^{\mathrm{T}} \bar{\mathbf{K}}^e \mathbf{T}^e \boldsymbol{\Delta}^e = \mathbf{F}^e \quad \text{or} \quad \mathbf{K}^e \boldsymbol{\Delta}^e = \mathbf{F}^e \tag{6.2.6}$$

where

$$\mathbf{K}^e = (\mathbf{T}^e)^{\mathrm{T}} \bar{\mathbf{K}}^e \mathbf{T}^e, \quad \mathbf{F}^e = (\mathbf{T}^e)^{\mathrm{T}} \bar{\mathbf{F}}^e \tag{6.2.7}$$

Carrying out the indicated matrix multiplications in (6.2.7), we obtain

$$\mathbf{K}^e = \frac{E_e A_e}{h_e} \begin{bmatrix} \cos^2\alpha_e & \frac{1}{2}\sin 2\alpha_e & -\cos^2\alpha_e & -\frac{1}{2}\sin 2\alpha_e \\ \frac{1}{2}\sin 2\alpha_e & \sin^2\alpha_e & -\frac{1}{2}\sin 2\alpha_e & -\sin^2\alpha_e \\ -\cos^2\alpha_e & -\frac{1}{2}\sin 2\alpha_e & \cos^2\alpha_e & \frac{1}{2}\sin 2\alpha_e \\ -\frac{1}{2}\sin 2\alpha_e & -\sin^2\alpha_e & \frac{1}{2}\sin 2\alpha_e & \sin^2\alpha_e \end{bmatrix} \tag{6.2.8}$$

$$\mathbf{F}^e = \begin{Bmatrix} F_1^e \\ F_2^e \\ F_3^e \\ F_4^e \end{Bmatrix} \equiv \begin{Bmatrix} (\bar{Q}_1^e + \bar{f}_1^e)\cos\alpha_e \\ (\bar{Q}_1^e + \bar{f}_1^e)\sin\alpha_e \\ (\bar{Q}_2^e + \bar{f}_2^e)\cos\alpha_e \\ (\bar{Q}_2^e + \bar{f}_2^e)\sin\alpha_e \end{Bmatrix} \tag{6.2.9}$$

where the forces $\bar{f}_i^e$ due to both body force $f(x)$ and temperature effect are computed using [see Eq. (4.4.11b)]

$$\bar{f}_i^e = \int_0^{h_e} f(\bar{x})\psi_i^e(\bar{x})\, d\bar{x} + \int_0^{h_e} EA\alpha_T T \frac{d\psi_i^e}{d\bar{x}}\, d\bar{x} \tag{6.2.10}$$

Here α_T is the thermal coefficient of expansion (not to be confused with α_e, the orientation of a member) and T is the temperature rise from a room temperature (at which the structure is stress free).

Equations (6.2.8) and (6.2.9) provide the means to compute the element stiffness matrix **K***e* and force vector $\mathbf{F}^e$, both referred to the global coordinate system, of a typical bar element oriented at an angle α_e. Once all element equations are expressed with respect to the global coordinate system, the assembly of elements with their stiffness matrix and force vector in the global coordinates follows the same ideas as discussed before, except that we must note that each node now has two displacement degrees of freedom. These ideas are illustrated through the following truss problem.

Example 6.2.1

Consider a three-member truss shown in Fig. 6.2.2(a). Suppose that all members of the truss have identical areas of cross section A and modulus E. The hinged supports at joints A, B and C allow free rotation of the members about the z-axis (taken positive into the plane of the page). Determine the horizontal and vertical displacements at the joint C and forces and stresses in each member of the structure. Use the following data for numerical answers: E = 200 GPa, $A = 5 \times 10^3$ mm^2, L = 5 m.

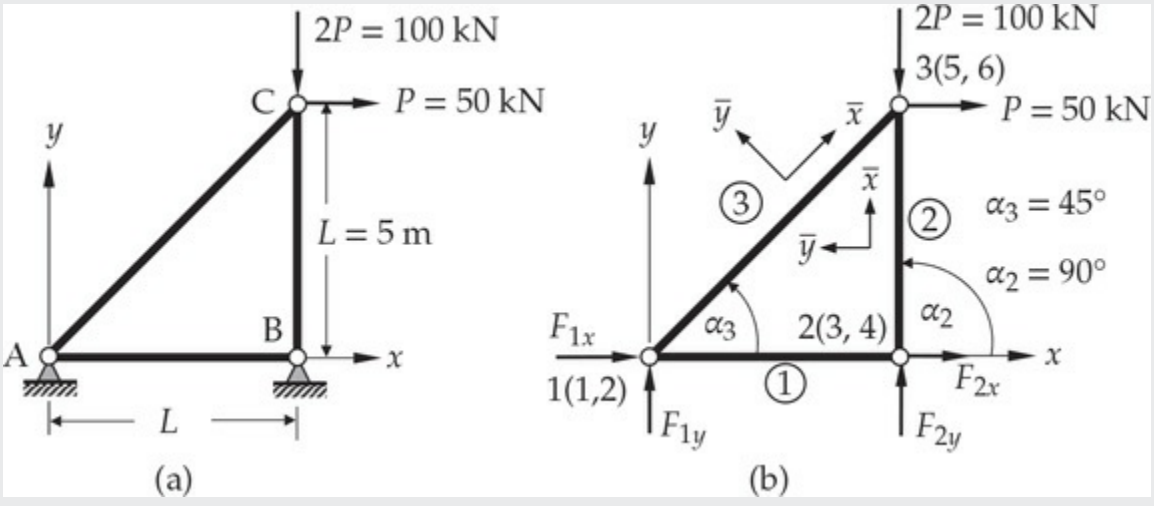

Fig. 6.2.2 Geometry and finite element representation of a plane truss. (a) Geometry and applied loads. (b) Element numbering and reaction forces.

Solution: Various steps in the finite element analysis of the problem are presented next.

Finite element mesh. We use three finite elements to model the structure (element 1 is redundant). Any further subdivision of the members does not add to the accuracy because for all truss problems the finite element solutions for displacements and forces at the nodes are exact. The global node numbers and element numbers are shown in Fig. 6.2.2(b). There are two displacement degrees of freedom, horizontal and vertical displacements, at each node of the element. The element stiffness matrix in the local coordinate system is given by Eq. (6.2.1) while the stiffness matrix and force vector (with $\bar{f}_i^e = 0$) in the global coordinate system are given by Eqs. (6.2.8) and (6.2.9), respectively. The element data and connectivity are presented in Table 6.2.1.

Table 6.2.1 Global-local connectivity.

Element number	Global nodes	Geometric properties	Material property	Orientation
1	1 2	$A,\ h_1 = L$	E	$\theta_1 = 0°$
2	2 3	$A,\ h_2 = L$	E	$\theta_2 = 90°$
3	1 3	$A,\ h_3 = \sqrt{2}L$	E	$\theta_3 = 45°$

Element matrices. The element stiffness matrices of each member are given by $[1/(2\sqrt{2}) = 0.3536]$

$$\mathbf{K}^1 = \frac{EA}{L}\begin{bmatrix} 1 & 0 & -1 & 0 \\ 0 & 0 & 0 & 0 \\ -1 & 0 & 1 & 0 \\ 0 & 0 & 0 & 0 \end{bmatrix}, \quad \mathbf{K}^2 = \frac{EA}{L}\begin{bmatrix} 0 & 0 & 0 & 0 \\ 0 & 1 & 0 & -1 \\ 0 & 0 & 0 & 0 \\ 0 & -1 & 0 & 1 \end{bmatrix} \tag{1a}$$

$$\mathbf{K}^3 = \frac{EA}{L}\begin{bmatrix} 0.3536 & 0.3536 & -0.3536 & -0.3536 \\ 0.3536 & 0.3536 & -0.3536 & -0.3536 \\ -0.3536 & -0.3536 & 0.3536 & 0.3536 \\ -0.3536 & -0.3536 & 0.3536 & 0.3536 \end{bmatrix} \tag{1b}$$

Assembly of elements. The assembled stiffness matrix can be formed by using the relationship between the global degrees of freedom and the element degrees of freedom. We obtain

$$\mathbf{K} = \begin{array}{c} \begin{matrix} 1 & 2 & 3 & 4 & 5 & 6 \end{matrix} \\ \left[\begin{array}{cccccc} K_{11}^1 + K_{11}^3 & K_{12}^1 + K_{12}^3 & K_{13}^1 & K_{14}^1 & K_{13}^3 & K_{14}^3 \\ & K_{22}^1 + K_{22}^3 & K_{23}^1 & K_{24}^1 & K_{23}^3 & K_{24}^3 \\ & & K_{33}^1 + K_{11}^2 & K_{34}^1 + K_{12}^2 & K_{13}^2 & K_{14}^2 \\ & \text{symm.} & & K_{44}^1 + K_{22}^2 & K_{23}^2 & K_{24}^2 \\ & & & & K_{33}^2 + K_{33}^3 & K_{34}^2 + K_{34}^3 \\ & & & & & K_{44}^2 + K_{44}^3 \end{array}\right] \begin{matrix} 1 \\ 2 \\ 3 \\ 4 \\ 5 \\ 6 \end{matrix} \end{array} \tag{2}$$

The element stiffness matrices of Eqs. (1a) and (1b) can be used in Eq. (2) to obtain the assembled global stiffness matrix

$$\mathbf{K} = \frac{EA}{L}\left[\begin{array}{cccc|cc} 1.3536 & 0.3536 & -1.0 & 0.0 & -0.3536 & -0.3536 \\ & 0.3536 & 0.0 & 0.0 & -0.3536 & -0.3536 \\ & & 1.0 & 0.0 & 0.0 & 0.0 \\ & & & 1.0 & 0.0 & -1.0 \\ \text{symm.} & --- & --- & --- & ---- & ---- \\ & & & & 0.3536 & 0.3536 \\ & & & & & 1.3536 \end{array}\right] \tag{3}$$

The displacement continuity conditions are

$$\begin{aligned} u_1^1 &= u_1^3 = U_1, \quad & v_1^1 &= v_1^3 = V_1 \\ u_2^1 &= u_1^2 = U_2, \quad & v_2^1 &= v_1^2 = V_2 \\ u_2^2 &= u_2^3 = U_3, \quad & v_2^2 &= v_2^3 = V_3 \end{aligned} \tag{4}$$

and the force equilibrium conditions are

$$\begin{aligned} F_1^1 + F_1^3 &= F_x^1, \quad & F_2^1 + F_2^3 &= F_y^1 \\ F_3^1 + F_1^2 &= F_x^2, \quad & F_4^1 + F_2^2 &= F_y^2 \\ F_3^2 + F_3^3 &= F_x^3, \quad & F_4^2 + F_4^3 &= F_y^3 \end{aligned} \tag{5}$$

can be used to write the global displacement and force vectors as

$$\mathbf{\Delta} = \begin{Bmatrix} U_1 \\ V_1 \\ U_2 \\ V_2 \\ U_3 \\ V_3 \end{Bmatrix}, \quad \mathbf{F} = \begin{Bmatrix} F_1^1 + F_1^3 \\ F_2^1 + F_2^3 \\ F_3^1 + F_1^2 \\ F_4^1 + F_2^2 \\ F_3^2 + F_3^3 \\ F_4^2 + F_4^3 \end{Bmatrix} = \begin{Bmatrix} F_x^1 \\ F_y^1 \\ F_x^2 \\ F_y^2 \\ F_x^3 \\ F_y^3 \end{Bmatrix} \tag{6}$$

where (U_I, V_I) and (F_x^I, F_y^I) denote the x and y components of the

displacement and external forces, respectively, at the global node *I*.

Boundary conditions. The specified global displacement and force degrees of freedom are

$$U_1 = V_1 = U_2 = V_2 = 0, \quad F_x^3 = P, \quad F_y^3 = -2P \tag{7}$$

The first two boundary conditions correspond to the horizontal and vertical displacements at node 1, the next two correspond to the horizontal and vertical displacements at node 2, and the last correspond to the force boundary conditions at node 3. The unknowns are: the displacements (U_3, V_3) of node 3 and forces (F_x^1, F_y^1) at node 1 and forces (F_x^2, F_y^2) at node 2.

Condensed equations. The condensed equations for the unknown displacements (U_3, V_3) are obtained from the last two equations of the system, as indicated by the dotted lines in Eq. (3):

$$\frac{EA}{L}\begin{bmatrix} 0.3536 & 0.3536 \\ 0.3536 & 1.3536 \end{bmatrix}\begin{Bmatrix} U_3 \\ V_3 \end{Bmatrix} = \begin{Bmatrix} P \\ -2P \end{Bmatrix} \tag{8}$$

and the condensed equations for the unknown reactions are (from the first four equations of the system)

$$\begin{Bmatrix} F_x^1 \\ F_y^1 \\ F_x^2 \\ F_y^2 \end{Bmatrix} = \frac{EA}{L}\begin{bmatrix} -0.3536 & -0.3536 \\ -0.3536 & -0.3536 \\ 0.0000 & 0.0000 \\ 0.0000 & -1.0000 \end{bmatrix}\begin{Bmatrix} U_3 \\ V_3 \end{Bmatrix} \tag{9}$$

Solution of the finite element equations. Solving Eq. (8) for U_5 and U_6, we obtain

$$U_3 = (3 + 2\sqrt{2})\frac{PL}{EA} = 5.828\,\frac{PL}{EA} = 1.457\ \text{mm}, \quad V_3 = -\frac{3PL}{EA} = -0.75\ \text{mm} \tag{10}$$

and the reaction forces are computed using Eq. (9):

$$F_x^1 = -P, \quad F_y^1 = -P, \quad F_x^2 = 0.0, \quad F_y^2 = 3P \tag{11}$$

Post-computation. The stress in each member can be computed from the relation

$$\sigma^e = -\frac{\bar{Q}_1^e}{A_e} = \frac{\bar{Q}_2^e}{A_e} \tag{12}$$

where $\bar{Q}_1^e$ and $\bar{Q}_2^e$ can be determined from the element equations

$$\begin{Bmatrix} \bar{Q}_1^e \\ \bar{Q}_2^e \end{Bmatrix} = \frac{A_e E_e}{h_e} \begin{bmatrix} 1 & -1 \\ -1 & 1 \end{bmatrix} \begin{Bmatrix} \bar{u}_1^e \\ \bar{u}_2^e \end{Bmatrix} \tag{13}$$

and the element displacements $(\bar{u}_1^e, \bar{u}_2^e)$ are determined from the transformation relation in Eq. (6.2.3a):

$$\begin{Bmatrix} \bar{u}_1^e \\ \bar{v}_1^e \\ \bar{u}_2^e \\ \bar{v}_2^e \end{Bmatrix} = \begin{bmatrix} \cos\alpha_e & \sin\alpha_e & 0 & 0 \\ -\sin\alpha_e & \cos\alpha_e & 0 & 0 \\ 0 & 0 & \cos\alpha_e & \sin\alpha_e \\ 0 & 0 & -\sin\alpha_e & \cos\alpha_e \end{bmatrix} \begin{Bmatrix} u_1^e \\ v_1^e \\ u_2^e \\ v_2^e \end{Bmatrix} \tag{14}$$

By definition [see Eq. (4)] we have

$$\begin{aligned} &u_1^1 = v_1^1 = u_2^1 = v_2^1 = 0, \quad u_1^2 = v_1^2 = u_1^3 = v_1^3 = 0 \\ &u_2^2 = u_2^3 = U_3 = (3 + 2\sqrt{2})\frac{PL}{EA}, \quad v_2^2 = v_2^3 = V_3 = -\frac{3PL}{EA} \end{aligned} \tag{15}$$

Hence, Eqs. (12)–(15) give

$$\sigma^e = \frac{E_e}{h_e}(\bar{u}_2^e - \bar{u}_1^e) \tag{16}$$

$$\begin{aligned} \bar{u}_1^1 &= u_1^1 \cos\alpha_1 + v_1^1 \sin\alpha_1 = 0 \\ \bar{u}_2^1 &= u_2^1 \cos\alpha_1 + v_2^1 \sin\alpha_1 = 0 \\ \bar{u}_1^2 &= u_1^2 \cos\alpha_2 + v_1^2 \sin\alpha_2 = 0 \\ \bar{u}_2^2 &= U_3 \cos\alpha_2 + V_3 \sin\alpha_2 = V_3 = -\frac{3PL}{EA} \\ \bar{u}_1^3 &= u_1^3 \cos\alpha_3 + v_1^3 \sin\alpha_3 = 0 \\ \bar{u}_2^3 &= U_3 \cos\alpha_3 + V_3 \sin\alpha_3 = \frac{1}{\sqrt{2}}(U_3 + V_3) = \frac{2PL}{EA} \end{aligned} \tag{17}$$

Thus, the member forces are

$$\bar{Q}_1^1 = -\bar{Q}_2^1 = 0, \quad \bar{Q}_1^2 = -\bar{Q}_2^2 = 3P, \quad \bar{Q}_1^3 = -\bar{Q}_2^3 = -\sqrt{2}P \tag{18}$$

The axial stresses in the members are

$$\sigma^{(1)} = 0, \quad \sigma^{(2)} = -\frac{3P}{A} = -30 \text{ MPa}, \quad \sigma^{(3)} = \sqrt{2}\,\frac{P}{A} = 14.142 \text{ MPa} \tag{19}$$

Interpretation and verification of the results. An examination of the structure and the sense of loads applied indicate that the displacements (U_3, V_3) are qualitatively correct (positive U_3 and negative V_3). Also, the geometry of the structure indicates that it has relatively more stiffness in the vertical direction (member 2 takes much of the load directly) compared to the horizontal direction, which explains the relatively large displacement in the horizontal direction. Also member 1 is redundant, taking no load (because both ends of the member are fixed).

The forces in Eq. (11) can be verified by applying the method of sections to the freebody diagram in Fig. 6.2.3. Sections AA, BB, and CC yield the relations

$$\frac{1}{\sqrt{2}}(F_{1x} + F_{1y}) + R = 0, \quad \frac{1}{\sqrt{2}}R + F_{1y} = 0, \quad F_{1x} + H + \frac{1}{\sqrt{2}}R = 0 \tag{20a}$$

$$F_{2x} - H = 0, \quad F_{2y} + Q = 0, \quad -\frac{1}{\sqrt{2}}R + P = 0, \quad \frac{1}{\sqrt{2}}R + Q + 2P = 0 \tag{20b}$$

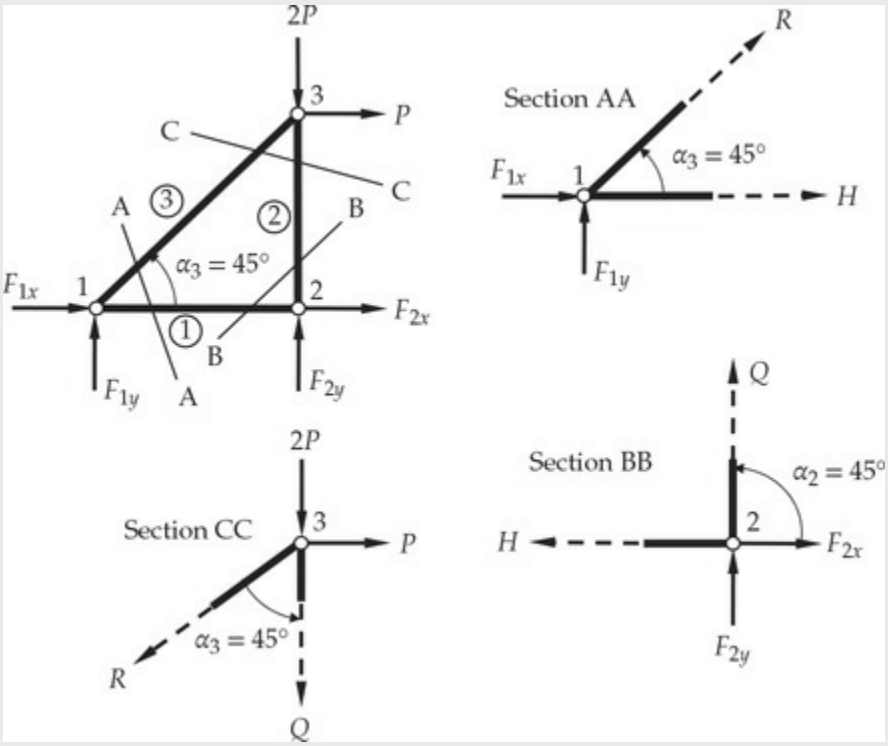

Fig. 6.2.3 Method of sections to determine the member forces.

which yield

$$Q = -3P,\quad R = \sqrt{2}P,\quad F_{2y} = 3P,\quad F_{1y} = -P,\quad F_{1x} = -P,\quad H = F_{2x} = 0 \qquad (20c)$$

Note that the member forces computed using the method of sections agree with those computed in the finite element method ($\bar{Q}_1^1 = H,\quad \bar{Q}_1^2 = -Q$, and $\bar{Q}_1^3 = -R$). It should be noted that this exercise is only for checking purposes, and the finite element method can be used to determine the member forces *Q*, *R*, and *H*, as discussed in the post-computation. This completes the example.

6.3 Analysis of Plane Frame Structures

6.3.1 Introductory Comments

Recall from Section 6.1 that a *bar* element, from the analysis point of view, is one that has axial stiffness *EA* and carries only axial (tensile or compressive) loads. When it is oriented arbitrarily in space is called a *truss* element. A plane truss element contains two nodes and two degrees of freedom per node, namely, a horizontal displacement (*u*) and vertical displacement (*w*), with respect to the global coordinates (*x*, *z*), *x* being taken as the horizontal and *z* being the vertical coordinates. The element has an axial displacement $(\bar{u})$ and transverse displacement $(\bar{w} = 0)$ with respect to the element coordinates $(\bar{x}_e, \bar{y}_e, \bar{z}_e)$, where $\bar{x}_e$ is along and $\bar{z}_e$ is transverse to the length of the element, and the $\bar{y}_e = y$-axis is into the plane of the paper to form a right-handed rectangular cartesian system. The global displacements (*u*, *w*) along the *x* and *z* axes, in general, are nonzero $(\bar{v} = v = 0)$.

In Chapter 5 the *beam* element is introduced as a "pure" bending element (i.e., without the extensional degree of freedom) that can carry loads transverse to the element, which can bend the element about the *y*-axis and shear through its cross section. A superposition of the bar and pure beam degrees of freedom gives a general beam finite element that is called a *frame* element, as illustrated in Fig. 6.3.1. Thus, a frame element can take loads along the length of the beam as well as transverse to it, and bending moments about an axis (i.e., *y*) perpendicular to the plane of the element. Members of a frame structure are connected by rigid connections (riveted or welded), and therefore axial and transverse forces and bending moments are developed in such members. The objective of this section is to formulate a plane frame finite element, with the help of the

developments from Sections 4.4, 5.2, 5.3, and 6.2.

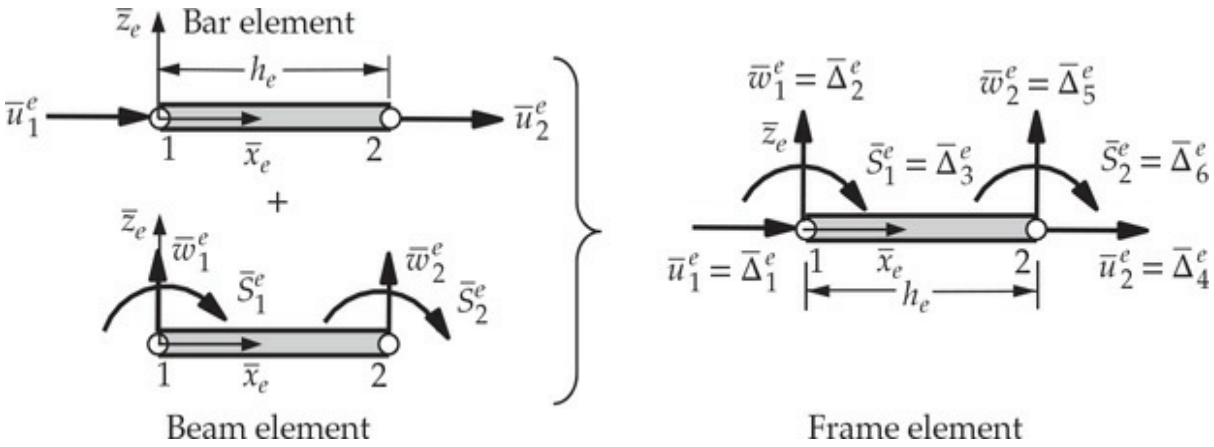

Fig. 6.3.1 Superposition of bar and beam elements to obtain a frame element [degrees of freedom are referred to the element coordinate system $(\bar{x}_e, \bar{y}_e, \bar{z}_e)$; the $\bar{y}_e = y$ axis is positive into the plane of the page].

6.3.2 General Formulation

In many truss and frame structures, the bar and beam elements are found in many different orientations [see, e.g., Fig. 6.1.1(b)]. Analysis of such structures for displacements and stresses requires the setting up of a global coordinate system and referencing all quantities (i.e., displacements, forces, and stiffness) of individual elements to the common (global) coordinate system in order to assemble the elements and impose boundary conditions on the whole structure.

A superposition of the bar element of Section 4.4 with the Euler–Bernoulli beam element (EBE) of Section 5.2 or the Timoshenko element (RIE or CIE) of Section 5.3 gives a frame element with three primary degrees of freedom (u, w, S) per node, where S denotes the rotation [i.e., $S = \theta_x = -(dw/dx)$ in the EBT and $S = \varphi_x$ in the TBT]; note that the transverse displacement v of Section 6.2 is denoted by w to be consistent with Sections 5.2 and 5.3. When the axial stiffness EA and bending stiffness EI are element-wise constant, the superposition of the linear bar element with any of the beam elements with two nodes and two degrees of freedom per node give the associated frame elements with two nodes and three degrees of freedom per node. A typical finite element equation of a frame element in element coordinate system is of the form

$$\bar{\mathbf{K}}^e \bar{\boldsymbol{\Delta}}^e = \bar{\mathbf{F}}^e \tag{6.3.1}$$

where

$$\bar{\Delta}_1^e = \bar{u}_1^e,\quad \bar{\Delta}_2^e = \bar{w}_1^e,\quad \bar{\Delta}_3^e = \bar{S}_1^e,\quad \bar{\Delta}_4^e = \bar{u}_2^e,\quad \bar{\Delta}_5^e = \bar{w}_2^e,\quad \bar{\Delta}_6^e = \bar{S}_2^e \tag{6.3.2}$$

In the following paragraphs, we develop transformation relations to express the element equations, Eq. (6.3.1), in the global coordinate system. The local coordinate system $(\bar{x}_e, \bar{y}_e, \bar{z}_e)$ of an element Ω^e is obtained by rotating the global coordinate system about the $\bar{y}_e = y$ axis in the counterclockwise direction by an angle α_e. Therefore, the local coordinates $(\bar{x}_e, \bar{y}_e, \bar{z}_e)$ are related to the global coordinates (x, y, z) by (the order of the transformation relations is changed to match the order of the generalized displacements: $\bar{u}^e, \bar{w}^e, \bar{S}^e$)

$$\begin{Bmatrix} \bar{x}_e \\ \bar{z}_e \\ \bar{y}_e \end{Bmatrix}^e = \begin{bmatrix} \cos\alpha_e & \sin\alpha_e & 0 \\ -\sin\alpha_e & \cos\alpha_e & 0 \\ 0 & 0 & 1 \end{bmatrix} \begin{Bmatrix} x \\ z \\ y \end{Bmatrix} \tag{6.3.3}$$

where the angle α_e is measured counterclockwise from the global x-axis to the element $\bar{x}_e$-axis. Note that the y and $\bar{y}_e$ coordinates are parallel to each other, and they are *into* the plane of the paper (see Fig. 6.3.2). The same transformation relations hold for displacements (u, w) along the global coordinates (x, z) and displacements $(\bar{u}^e, \bar{w}^e)$ in the local coordinates $(\bar{x}_e, \bar{z}_e)$. Because of the planar nature of the structure (i.e., all applied loads are only in the xy-plane), we have $\bar{v}_i^e = 0$. However, there is a rotation about the y-axis and it remains the same in both coordinate systems, because $y = \bar{y}_e$. Hence, the relationship between (u, w, S) and (u_i^e, w_i^e, S_i^e) can be written as

$$\begin{Bmatrix} \bar{u}^e \\ \bar{w}^e \\ \bar{S}^e \end{Bmatrix} = \begin{bmatrix} \cos\alpha_e & \sin\alpha_e & 0 \\ -\sin\alpha_e & \cos\alpha_e & 0 \\ 0 & 0 & 1 \end{bmatrix} \begin{Bmatrix} u^e \\ w^e \\ S^e \end{Bmatrix} \tag{6.3.4}$$

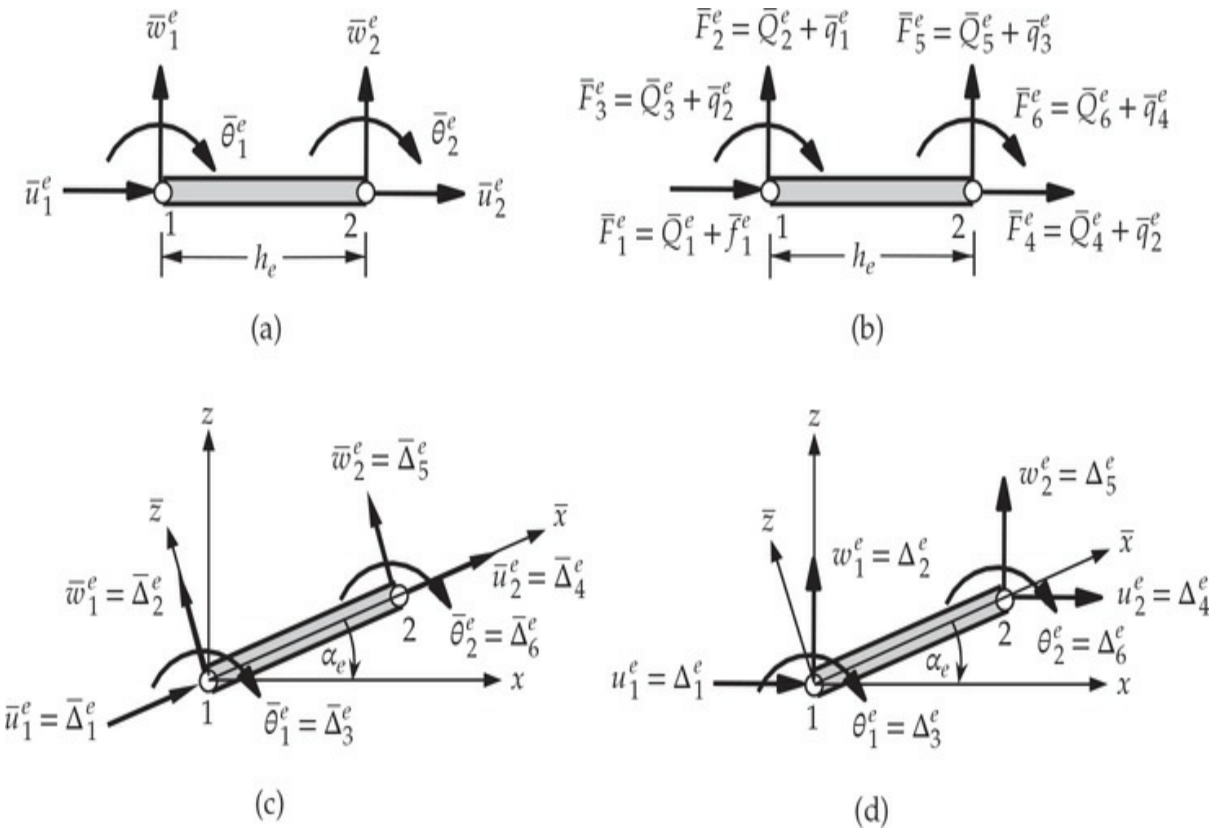

Fig. 6.3.2 (a) Generalized displacements. (b) Generalized forces in the element coordinates. Generalized displacements in the (c) local coordinates and (d) global coordinates.

Therefore, the three nodal degrees of freedom $(\bar{u}_i^e, \bar{w}_i^e, \bar{S}_i^e)$ at the *i*th node (*i* = 1, 2) in the $(\bar{x}_e, \bar{z}_e, \bar{y}_e)$ system are related to the three degrees of freedom (u_i^e, w_i^e, S_i^e) in the (*x*, *z*, *y*) coordinate system by

$$\begin{Bmatrix} \bar{u}_1^e \\ \bar{w}_1^e \\ \bar{S}_1^e \\ \bar{u}_2 \\ \bar{w}_2 \\ \bar{S}_2 \end{Bmatrix} = \begin{bmatrix} \cos\alpha_e & \sin\alpha_e & 0 & 0 & 0 & 0 \\ -\sin\alpha_e & \cos\alpha_e & 0 & 0 & 0 & 0 \\ 0 & 0 & 1 & 0 & 0 & 0 \\ 0 & 0 & 0 & \cos\alpha_e & \sin\alpha_e & 0 \\ 0 & 0 & 0 & -\sin\alpha_e & \cos\alpha_e & 0 \\ 0 & 0 & 0 & 0 & 0 & 1 \end{bmatrix} \begin{Bmatrix} u_1^e \\ w_1^e \\ S_1^e \\ u_2^e \\ w_2^e \\ S_2^e \end{Bmatrix} \tag{6.3.5a}$$

or

$$\bar{\boldsymbol{\Delta}}^e = \mathbf{T}^e \boldsymbol{\Delta}^e \tag{6.3.5b}$$

Analogously, the element force vectors in the local and global coordinate systems are related according to

$$\bar{\mathbf{F}}^e = \mathbf{T}^e \mathbf{F}^e \tag{6.3.6}$$

We note that $(\mathbf{T}^e)^{\mathrm{T}} = (\mathbf{T}^e)^{-1}$. Substituting the transformation equations (6.3.5b) and (6.3.6) into Eq. (6.3.1), we obtain

$$\bar{\mathbf{K}}^e \mathbf{T}^e \boldsymbol{\Delta}^e = \mathbf{T}^e \mathbf{F}^e \tag{6.3.7}$$

Premultiplying both sides with $(\mathbf{T}^e)^{-1} = (\mathbf{T}^e)^{\mathrm{T}}$, we obtain

$$(\mathbf{T}^e)^{\mathrm{T}} \bar{\mathbf{K}}^e \mathbf{T}^e \boldsymbol{\Delta}^e = \mathbf{F}^e \quad \text{or} \quad \mathbf{K}^e \boldsymbol{\Delta}^e = \mathbf{F}^e \tag{6.3.8}$$

where

$$\mathbf{K}^e = (\mathbf{T}^e)^{\mathrm{T}} \bar{\mathbf{K}}^e \mathbf{T}^e, \quad \mathbf{F}^e = (\mathbf{T}^e)^{\mathrm{T}} \bar{\mathbf{F}}^e \tag{6.3.9}$$

Thus, if we know the element matrices $\bar{\mathbf{K}}^e$ and $\bar{\mathbf{F}}^e$ of an element Ω^e in the local coordinate system $(\bar{x}_e, \bar{y}_e, \bar{z}_e)$, the element matrices $\mathbf{K}^e$ and $\mathbf{F}^e$ in the global coordinate system are obtained using Eq. (6.3.9).

6.3.3 Euler–Bernoulli Frame Element

For the Euler–Bernoulli beam element, the stiffness matrix $\bar{\mathbf{K}}^e$ and load vector $\bar{\mathbf{F}}^e$, when $k_f^e = 0$ and $E_e A_e$ and $E_e A_e$ are element-wise constant, are

$$\bar{\mathbf{K}}^e = \frac{2E_e I_e}{h_e^3} \begin{bmatrix} \kappa_e & 0 & 0 & -\kappa_e & 0 & 0 \\ 0 & 6 & -3h_e & 0 & -6 & -3h_e \\ 0 & -3h_e & 2h_e^2 & 0 & 3h_e & h_e^2 \\ -\kappa_e & 0 & 0 & \kappa_e & 0 & 0 \\ 0 & -6 & 3h_e & 0 & 6 & 3h_e \\ 0 & -3h_e & h_e^2 & 0 & 3h_e & 2h_e^2 \end{bmatrix}, \quad \kappa_e = \frac{A_e h_e^2}{2I_e}$$

$$\bar{\mathbf{F}}^e = \begin{Bmatrix} \bar{f}_1^e \\ \bar{q}_1^e \\ \bar{q}_2^e \\ \bar{f}_2^e \\ \bar{q}_3^e \\ \bar{q}_4^e \end{Bmatrix} + \begin{Bmatrix} \bar{Q}_1^e \\ \bar{Q}_2^e \\ \bar{Q}_3^e \\ \bar{Q}_4^e \\ \bar{Q}_5^e \\ \bar{Q}_6^e \end{Bmatrix}, \quad \bar{\boldsymbol{\Delta}} = \begin{Bmatrix} \bar{u}_1^e = \bar{\Delta}_1^e \\ \bar{w}_1^e = \bar{\Delta}_2^e \\ \bar{\theta}_1^e = \bar{\Delta}_3^e \\ \bar{u}_2^e = \bar{\Delta}_4^e \\ \bar{w}_2^e = \bar{\Delta}_5^e \\ \bar{\theta}_2^e = \bar{\Delta}_6^e \end{Bmatrix} \tag{6.3.10}$$

where Q_i^e are the generalized forces at $\bar{x}_e = 0, h_e$:

$$\bar{Q}_1^e \equiv \left[-E_e A_e \frac{d\bar{u}^e}{d\bar{x}}\right]_0 = -\bar{N}^e(0), \quad \bar{Q}_2^e \equiv \left[\frac{d}{d\bar{x}}\left(E_e I_e \frac{d^2\bar{w}_h^e}{d\bar{x}^2}\right)\right]_0 = -\bar{V}_h^e(0)$$

$$\bar{Q}_3^e \equiv \left[E_e I_e \frac{d^2\bar{w}_h^e}{d\bar{x}^2}\right]_0 = -\bar{M}_h^e(0), \quad \bar{Q}_4^e \equiv \left[E_e A_e \frac{d\bar{u}^e}{d\bar{x}}\right]_{h_e} = \bar{N}^e(h_e) \tag{6.3.11}$$

$$Q_5^e \equiv -\left[\frac{d}{d\bar{x}}\left(E_e I_e \frac{d^2\bar{w}_h^e}{d\bar{x}^2}\right)\right]_{h_e} = \bar{V}_h^e(h_e), \quad \bar{Q}_6^e \equiv -\left[E_e I_e \frac{d^2\bar{w}_h^e}{d\bar{x}^2}\right]_{h_e} = \bar{M}_h^e(h_e)$$

and

$$\bar{f}_i^e = \int_0^{h_e} \left[f(\bar{x})\,\psi_i^e(\bar{x}) + EA\alpha T\right] d\bar{x}, \quad \bar{q}_i^e = \int_0^{h_e} q(\bar{x})\,\phi_i^e(\bar{x})\,d\bar{x} \tag{6.3.12}$$

Here ψ_i^e are the linear Lagrange polynomials, ϕ_i^e are the Hermite cubic polynomials, α is the coefficient of thermal expansion, and T is the temperature rise, the latter two variables assumed to be a function of only x, not z.

Substituting the expressions for $\bar{\mathbf{K}}^e$ and $\bar{\mathbf{F}}^e$ from Eq. (6.3.10) into Eq. (6.3.9) and carrying out the indicated matrix multiplication, we obtain

$$\mathbf{K}^e = \frac{2E_eI_e}{h_e^3}\begin{bmatrix} \kappa_e\cos^2\alpha_e + 6\sin^2\alpha_e & (\kappa_e-6)\cos\alpha_e\sin\alpha_e & 3h_e\sin\alpha_e \\ (\kappa_e-6)\cos\alpha_e\sin\alpha_e & \kappa_e\sin^2\alpha_e + 6\cos^2\alpha_e & -3h_e\cos\alpha_e \\ 3h_e\sin\alpha_e & -3h_e\cos\alpha_e & 2h_e^2 \\ -(\kappa_e\cos^2\alpha_e + 6\sin^2\alpha_e) & -(\kappa_e-6)\sin\alpha_e\cos\alpha_e & -3h_e\sin\alpha_e \\ -(\kappa_e-6)\cos\alpha_e\sin\alpha_e & -(\kappa_e\sin^2\alpha_e + 6\cos^2\alpha_e) & 3h_e\cos\alpha_e \\ 3h_e\sin\alpha_e & -3h_e\cos\alpha_e & h_e^2 \end{bmatrix}$$

$$\begin{bmatrix} -(\kappa_e\cos^2\alpha_e + 6\sin^2\alpha_e) & -(\kappa_e-6)\cos\alpha_e\sin\alpha_e & 3h_e\sin\alpha_e \\ -(\kappa_e-6)\cos\alpha_e\sin\alpha_e & -(\kappa_e\sin^2\alpha_e + 6\cos^2\alpha_e) & -3h_e\cos\alpha_e \\ -3h_e\sin\alpha_e & 3h_e\cos\alpha_e & h_e^2 \\ \kappa_e\cos^2\alpha_e + 6\sin^2\alpha_e & (\kappa_e-6)\cos\alpha_e\sin\alpha_e & -3h_e\sin\alpha_e \\ (\kappa_e-6)\cos\alpha_e\sin\alpha_e & \kappa_e\sin^2\alpha_e + 6\cos^2\alpha_e & 3h_e\cos\alpha_e \\ -3h_e\sin\alpha_e & 3h_e\cos\alpha_e & 2h_e^2 \end{bmatrix} \tag{6.3.13}$$

$$\mathbf{F}^e = \begin{Bmatrix} \bar{F}_1^e\cos\alpha_e - \bar{F}_2^e\sin\alpha_e \\ \bar{F}_1^e\sin\alpha_e + \bar{F}_2^e\cos\alpha_e \\ \bar{F}_3^e \\ \bar{F}_4^e\cos\alpha_e - \bar{F}_5^e\sin\alpha_e \\ \bar{F}_4^e\sin\alpha_e + \bar{F}_5^e\cos\alpha_e \\ \bar{F}_6^e \end{Bmatrix}, \qquad \kappa_e = \frac{A_eh_e^2}{2I_e}$$

6.3.4 Timoshenko Frame Element Based on CIE

The element equations of the CIE Timoshenko frame element in the element coordinates are given by [see Eq. (5.3.24)]

$$\frac{E_e I_e}{6\mu_e h_e^3}\begin{bmatrix} \kappa_e & 0 & 0 & -\kappa_e & 0 & 0 \\ 0 & 6 & -3h_e & 0 & -6 & -3h_e \\ 0 & -3h_e & h_e^2(1.5+6\mu_e) & 0 & 3h_e & h_e^2(1.5-6\mu_e) \\ -\kappa_e & 0 & 0 & \kappa_e & 0 & 0 \\ 0 & -6 & 3h_e & 0 & 6 & 3h_e \\ 0 & -3h_e & h_e^2(1.5-6\mu_e) & 0 & 3h_e & h_e^2(1.5+6\mu_e) \end{bmatrix}\begin{Bmatrix} \bar{u}_1^e = \bar{\Delta}_1^e \\ \bar{w}_1^e = \bar{\Delta}_2^e \\ \bar{\phi}_1^e = \bar{\Delta}_3^e \\ \bar{u}_2^e = \bar{\Delta}_4^e \\ \bar{w}_2^e = \bar{\Delta}_5^e \\ \bar{\phi}_2^e = \bar{\Delta}_6^e \end{Bmatrix}$$

$$= \begin{Bmatrix} \bar{F}_1^e \\ \bar{F}_2^e \\ \bar{F}_3^e \\ \bar{F}_4^e \\ \bar{F}_5^e \\ \bar{F}_6^e \end{Bmatrix}^e \equiv \begin{Bmatrix} \bar{f}_1^e \\ \bar{q}_1^e + \frac{1}{2}\bar{q}_c^e \\ -\frac{h_e}{8}\bar{q}_c^e \\ \bar{f}_2 \\ \bar{q}_2^e + \frac{1}{2}\bar{q}_c^e \\ \frac{h_e}{8}\bar{q}_c^e \end{Bmatrix}^e + \begin{Bmatrix} \bar{Q}_1^e \\ \bar{Q}_2^e \\ \bar{Q}_3^e \\ \bar{Q}_4^e \\ \bar{Q}_5^e \\ \bar{Q}_6^e \end{Bmatrix}^e \tag{6.3.14}$$

where

$$\bar{f}_i = \int_0^{h_e} f^e(\bar{x})\psi_i^e(\bar{x})\,d\bar{x}\ \ (i=1,2),\quad \bar{q}_i = \int_0^{h_e} q^e(\bar{x})\psi_i^e(\bar{x})\,d\bar{x}\ \ (i=1,2,c) \tag{6.3.15}$$

and

$$\begin{aligned}
\bar{Q}_1^e &\equiv \left[-E_e A_e \frac{d\bar{u}^e}{d\bar{x}}\right]_{\bar{x}=0} = -\bar{N}_h^e(0) \\
\bar{Q}_2^e &\equiv -\left[G_e A_e K_s\left(\bar{\phi}_h^e + \frac{d\bar{w}_h^e}{d\bar{x}}\right)\right]_{\bar{x}=0} = -\bar{V}_h^e(0) \\
\bar{Q}_3^e &\equiv -\left[E_e I_e \frac{d\bar{\phi}_h^e}{d\bar{x}}\right]_{\bar{x}=0} = -\bar{M}_h^e(0) \\
\bar{Q}_4^e &\equiv \left[E_e A_e \frac{d\bar{u}^e}{d\bar{x}}\right]_{\bar{x}=h_e} = \bar{N}_h^e(h_e) \\
\bar{Q}_5^e &\equiv \left[G_e A_e K_s\left(\bar{\phi}_h^e + \frac{d\bar{w}_h^e}{d\bar{x}}\right)\right]_{\bar{x}=h_e} = \bar{V}_h^e(h_e) \\
\bar{Q}_6^e &\equiv \left[E_e I_e \frac{d\bar{\phi}_h^e}{d\bar{x}}\right]_{\bar{x}=h_e} = \bar{M}_h^e(h_e)
\end{aligned} \tag{6.3.16}$$

and

$$\kappa_e = \frac{6A_e\mu_e h_e^2}{I_e}, \qquad \mu_e = \frac{E_e I_e}{G_e A_e K_s h_e^2} \tag{6.3.17}$$

The frame element stiffness matrix in the global coordinate system is

$$\mathbf{K}^e = \frac{E_e I_e}{6\mu_e h_e^3}\begin{bmatrix} \kappa_e\cos^2\alpha_e + 6\sin^2\alpha_e & (\kappa_e-6)\cos\alpha_e\sin\alpha_e & 3h_e\sin\alpha_e \\ (\kappa_e-6)\cos\alpha_e\sin\alpha_e & \kappa_e\sin^2\alpha_e + 6\cos^2\alpha_e & -3h_e\cos\alpha_e \\ 3h_e\sin\alpha_e & -3h_e\cos\alpha_e & h_e^2(1.5+6\mu_e) \\ -(\kappa_e\cos^2\alpha_e + 6\sin^2\alpha_e) & -(\kappa_e-6)\sin\alpha_e\cos\alpha_e & -3h_e\sin\alpha_e \\ -(\kappa_e-6)\cos\alpha_e\sin\alpha_e & -(\kappa_e\sin^2\alpha_e + 6\cos^2\alpha_e) & 3h_e\cos\alpha_e \\ 3h_e\sin\alpha_e & -3h_e\cos\alpha_e & h_e^2(1.5-6\mu_e) \end{bmatrix}$$

$$\begin{bmatrix} -(\kappa_e\cos^2\alpha_e + 6\sin^2\alpha_e) & -(\kappa_e-6)\cos\alpha_e\sin\alpha_e & 3h_e\sin\alpha_e \\ -(\kappa_e-6)\sin\alpha_e\cos\alpha_e & -(\kappa_e\sin^2\alpha_e + 6\cos^2\alpha_e) & -3h_e\cos\alpha_e \\ -3h_e\sin\alpha_e & 3h_e\cos\alpha_e & h_e^2(1.5-6\mu_e) \\ (\kappa_e\cos^2\alpha_e + 6\sin^2\alpha_e) & (\kappa_e-6)\cos\alpha_e\sin\alpha_e & -3h_e\sin\alpha_e \\ (\kappa_e-6)\cos\alpha_e\sin\alpha_e & \kappa_e\sin^2\alpha_e + 6\cos^2\alpha_e & 3h_e\cos\alpha_e \\ -3h_e\sin\alpha_e & 3h_e\cos\alpha_e & h_e^2(1.5+6\mu_e) \end{bmatrix} \tag{6.3.18}$$

The form of the element force vector in the global coordinate system is the same as that in Eq. (6.3.13) with $\mathbf{F}^e$ given by Eq. (6.3.15).

6.3.5 Timoshenko Frame Element Based on RIE

Since the element stiffness matrix of the RIE is the same as the CIE, the element stiffness matrix in the global coordinates as given in Eq. (6.3.18) is valid for the frame element based on the RIE. The contributions of the axial and transverse distributed forces to the nodes are given by

$$\bar{f}_i^e = \int_0^{h_e} f(\bar{x})\,\psi_i^e(\bar{x})\,d\bar{x}, \qquad \bar{q}_i^e = \int_0^{h_e} q(\bar{x})\,\psi_i^e(\bar{x})\,d\bar{x} \tag{6.3.19}$$

where ψ_i^e are the linear interpolation functions. Then the element force vector for the RIE frame element is given by

$$\mathbf{F}^e = \begin{Bmatrix} \bar{F}_1^e \cos\alpha_e - \bar{F}_2^e \sin\alpha_e \\ \bar{F}_1^e \sin\alpha_e + \bar{F}_2^e \cos\alpha_e \\ \bar{F}_3^e \\ \bar{F}_4^e \cos\alpha_e - \bar{F}_5^e \sin\alpha_e \\ \bar{F}_4^e \sin\alpha_e + \bar{F}_5^e \cos\alpha_e \\ \bar{F}_6^e \end{Bmatrix}, \quad \begin{Bmatrix} \bar{F}_1^e \\ \bar{F}_2^e \\ \bar{F}_3^e \\ \bar{F}_4^e \\ \bar{F}_5^e \\ \bar{F}_6^e \end{Bmatrix} = \begin{Bmatrix} \bar{f}_1^e \\ \bar{q}_1^e \\ 0 \\ \bar{f}_2^e \\ \bar{q}_2^e \\ 0 \end{Bmatrix} + \begin{Bmatrix} \bar{Q}_1^e \\ \bar{Q}_2^e \\ \bar{Q}_3^e \\ \bar{Q}_4^e \\ \bar{Q}_5^e \\ \bar{Q}_6^e \end{Bmatrix} \tag{6.3.20}$$

Example 6.3.1

Consider the frame structure shown in Fig. 6.3.3. Analyze the structure for displacements and forces using (a) the Euler–Bernoulli frame element, (b) the Timoshenko frame element based on the CIE, and (c) the Timoshenko frame element based on the RIE. Both members of the structure are made of the same material (E) and have the same geometric properties (A, I).

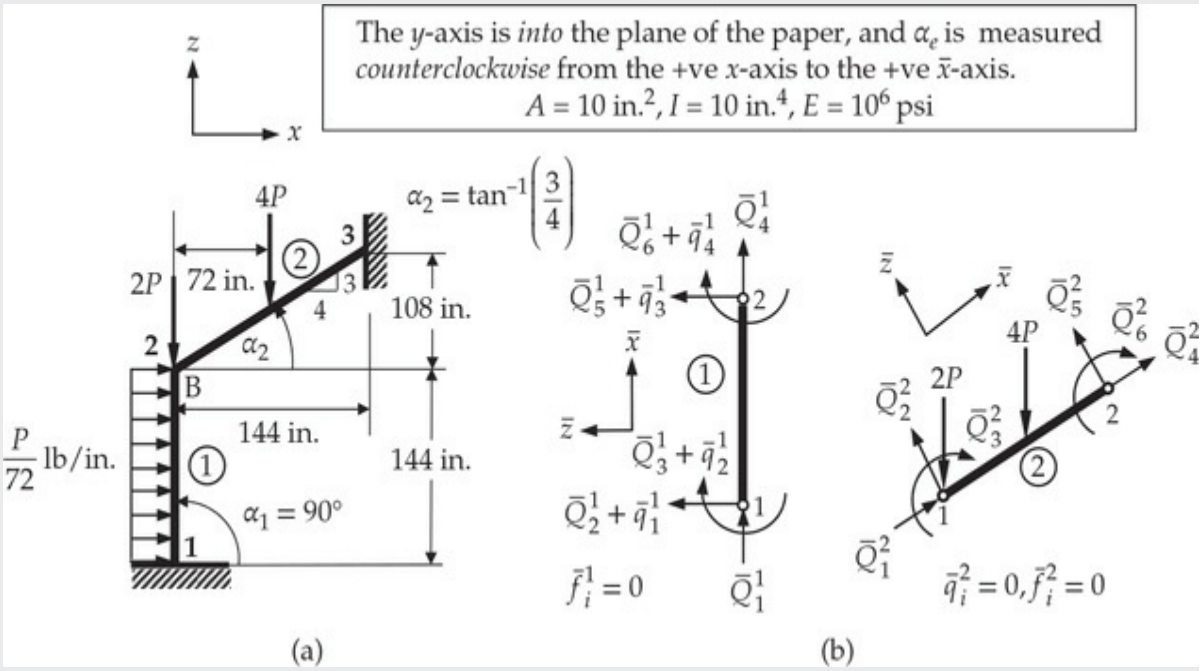

Fig. 6.3.3 (a) Geometry and loading, and (b) member forces in the plane frame structure of Example 6.3.1.

Solution: The element stiffness matrices and force vectors in the global coordinate system (x, y, z) can be computed from Eqs. (6.3.13) to (6.3.20), depending on the type of element. The geometric and material properties of each element are as follows ($f = 0$ is the distributed axial

force and q is the distributed transverse load).

Element 1

$$L = 144 \text{ in.}, \quad A = 10 \text{ in.}^2, \quad I = 10 \text{ in.}^4, \quad E = 10^6 \text{ psi}, \quad \cos\alpha_1 = 0.0, \quad \sin\alpha_1 = 1.0$$

$$q^{(1)} = -P/72 \text{ lb/in.}, \quad EA/L = 69.444 \times 10^3, \quad EI/L^2 = 482.253, \quad EI/L^3 = 3.349$$

$$q_1^1 = q_3^1 = \frac{q^{(1)} \times 144}{2} = -P, \quad q_2^1 = -\frac{q^{(1)} \times (144)^2}{12} = 24P, \quad q_4^1 = -q_2^1 = -24P$$

Element 2 The load $F_0 = -4P$ at the center of element 2 (in the global z direction) is distributed to the element nodes according to Eq. (5.2.27b) [see Fig. 5.2.8(b)].

$$L = 180 \text{ in.}, \quad A = 10 \text{ in.}^2, \quad I = 10 \text{ in.}^4, \quad E = 10^6 \text{ psi}, \quad \cos\alpha_2 = 0.8, \quad \sin\alpha_2 = 0.6$$

$$q^{(2)} = 0, \quad EA/L = 55.555 \times 10^3, \quad EI/L^2 = 308.642, \quad EI/L^3 = 1.715$$

$$q_1^1 = q_3^1 = -2P, \quad q_2^1 = \frac{4P \times (144)}{8} = 72P, \quad q_4^1 = -q_2^1 = -72P$$

The load $2P$ at global node 2 is included through equilibrium of nodal forces there.

(a) *Euler–Bernoulli frame element, EBE*. The element stiffness matrices and load vectors are

$$\mathbf{K}^1 = 10^3 \begin{bmatrix} 0.4019E2 & 0.0000E0 & 0.2894E4 & -0.4019E2 & 0.0000E0 & 0.2894E4 \\ 0.0000E0 & 0.6944E5 & 0.0000E0 & 0.0000E0 & -0.6944E5 & 0.0000E0 \\ 0.2894E4 & 0.0000E0 & 0.2778E6 & -0.2894E4 & 0.0000E0 & 0.1389E6 \\ -0.4019E2 & 0.0000E0 & -0.2894E4 & 0.4019E2 & 0.0000E0 & -0.2894E4 \\ 0.0000E0 & -0.6944E5 & 0.0000E0 & 0.0000E0 & 0.6944E5 & 0.0000E0 \\ 0.2894E4 & 0.0000E0 & 0.1389E6 & -0.2894E4 & 0.0000E0 & 0.2778E6 \end{bmatrix}$$

$$\mathbf{f}^1 = P\{\ 1.0 \quad 0.0 \quad 24.0 \quad 1.0 \quad 0.0 \quad -24.0\ \}^{\mathrm{T}}$$

$$\mathbf{K}^2 = 10^3 \begin{bmatrix} 0.3556E5 & 0.2667E5 & 0.1111E4 & -0.3556E5 & -0.2667E5 & 0.1111E4 \\ 0.2667E5 & 0.2001E5 & -0.1482E4 & -0.2667E5 & -0.2001E5 & -0.1482E4 \\ 0.1111E4 & -0.1482E4 & 0.2222E6 & -0.1111E4 & 0.1482E4 & 0.1111E6 \\ -0.3556E5 & -0.2667E5 & -0.1111E4 & 0.3556E5 & 0.2667E5 & -0.1111E4 \\ -0.2667E5 & -0.2001E5 & 0.1482E4 & 0.2667E5 & 0.2001E5 & 0.1482E4 \\ 0.1111E4 & -0.1482E4 & 0.1111E6 & -0.1111E4 & 0.1482E4 & 0.2222E6 \end{bmatrix}$$

$$\mathbf{f}^2 = P\{\ 0.0 \quad -2.0 \quad 72.0 \quad 0.0 \quad -2.0 \quad -72.0\ \}^{\mathrm{T}}$$

The balance of generalized forces at global node 2 are

$$Q_4^1 + Q_1^2 = 0, \quad Q_5^1 + Q_2^2 = -2P, \quad Q_6^1 + Q_3^2 = 0$$

Therefore, the condensed equations for the unknown displacements are obtained by superposing the last three rows and columns (i.e., 4, 5, and 6) of element 1 to the first three rows and columns (i.e., 1, 2, and 3) of element 2; that is, the 3 × 3 submatrix associated with rows and columns 4, 5, and 6 of element 1, and the 3 × 3 submatrix associated with rows and columns 1, 2, and 3 of element 2 overlap in the global stiffness matrix.

The known geometric boundary conditions are

$$U_1 = 0,\ U_2 = 0,\ U_3 = 0,\ U_7 = 0,\ U_8 = 0,\ U_9 = 0$$

Since all specified values of the primary variables are zero, the condensed equations for the unknown generalized displacement degrees of freedom are

$$10^3 \begin{bmatrix} 0.3560 & 0.2666 & -0.0178 \\ 0.2666 & 0.8946 & -0.0148 \\ -0.0178 & -0.0148 & 5.0000 \end{bmatrix} \begin{Bmatrix} U_4 \\ U_5 \\ U_6 \end{Bmatrix} = P \begin{Bmatrix} 1.0 \\ -4.0 \\ 48.0 \end{Bmatrix}$$

The solution is

$$U_4 = 0.8390 \times 10^{-4} P \text{ (in.)}, \quad U_5 = -0.6812 \times 10^{-4} P \text{ (in.)}, \quad U_6 = 0.9610 \times 10^{-4} P \text{ (rad)}$$

The reactions and forces in each member in the global coordinates can be computed from the element equations

$$\mathbf{Q}^e = \mathbf{K}^e \mathbf{u}^e - \mathbf{f}^e$$

The forces Q_i^e can be transformed to those in the element coordinate system by means of Eq. (6.3.6):

$$\bar{\mathbf{Q}}^e = \mathbf{T}^e \mathbf{Q}^e$$

We obtain

$$\bar{\mathbf{Q}}^1 = \begin{Bmatrix} 4.731 \\ 0.725 \\ -10.900 \\ -4.731 \\ 1.275 \\ 50.450 \end{Bmatrix} P, \quad \bar{\mathbf{Q}}^2 = \begin{Bmatrix} 2.658 \\ 1.420 \\ -50.450 \\ -0.258 \\ 1.780 \\ 82.870 \end{Bmatrix} P$$

(b) *Timoshenko frame element, RIE*. The element stiffness matrices and load vectors are

$$\mathbf{K}^1 = 10^3 \begin{bmatrix} 0.2226E2 & 0.0000E0 & 0.1603E4 & -0.2226E2 & 0.0000E0 & 0.1603E4 \\ 0.0000E0 & 0.6944E2 & 0.0000E0 & 0.0000E0 & -0.6944E2 & 0.0000E0 \\ 0.1603E4 & 0.0000E0 & 0.1155E6 & -0.1603E4 & 0.0000E0 & 0.1153E6 \\ -0.2226E2 & 0.0000E0 & -0.1603E4 & 0.2226E2 & 0.0000E0 & -0.1603E4 \\ 0.0000E0 & -0.6944E2 & 0.0000E0 & 0.0000E0 & 0.6944E2 & 0.0000E0 \\ 0.1603E4 & 0.0000E0 & 0.1153E6 & -0.1603E4 & 0.0000E0 & 0.1155E6 \end{bmatrix}$$

$$\mathbf{f}^1 = P\{\ 1.0 \quad 0.0 \quad 0.0 \quad 1.0 \quad 0.0 \quad 0.0\ \}^T$$

$$\mathbf{K}^2 = 10^3 \begin{bmatrix} 0.4197E2 & 0.1812E2 & 0.9615E3 & -0.4197E2 & -0.1812E2 & 0.9615E3 \\ 0.1812E2 & 0.3140E2 & -0.1282E4 & -0.1812E2 & -0.3140E2 & -0.1282E4 \\ 0.9615E3 & -0.1282E4 & 0.1443E6 & -0.9615E3 & 0.1282E4 & 0.1442E6 \\ -0.4197E2 & -0.1812E2 & -0.9615E3 & 0.4197E2 & 0.1812E2 & -0.9615E3 \\ -0.1812E2 & -0.3140E2 & 0.1282E4 & 0.1812E2 & 0.3140E2 & 0.1282E4 \\ 0.9615E4 & -0.1282E4 & 0.1442E6 & -0.9615E3 & 0.1282E4 & 0.1443E6 \end{bmatrix}$$

$$\mathbf{f}^2 = P\{\ 0.0 \quad -2.0 \quad 72.0 \quad 0.0 \quad -2.0 \quad -72.0\ \}^T$$

Table 6.3.1 contains the displacements obtained by various types of elements at point B. As noted earlier, one EBE per member of a structure gives exact displacements, whereas at least four RIEs or CIEs per member are needed to obtain acceptable results. The forces in each element are included in Table 6.3.2. The forces calculated from the element equations are also exact for the EBE.

Table 6.3.1 Comparison of the generalized displacements [$\bar{v} = (v/P) \times 10^4$ where v is a typical displacement] at global node 2 of the frame structure shown in Fig. 6.3.3.

Displ.	RIE			CIE			EBE†
	1*	2	4	1	2	4	
$\bar{u}_B$	0.2709	0.8477	0.8411	0.2844	0.8415	0.8396	0.8390
$-\bar{w}_B$	0.4661	0.6806	0.6811	0.4432	0.6808	0.6811	0.6812
$\bar{\phi}_B$	−0.0016	0.8665	0.9450	0.0004	0.7703	0.9164	0.9610

* Number of elements per member.
† Values independent of the number of elements (and coincide with the exact values predicated by the respective beam theories).

Table 6.3.2 Comparison of the generalized forces in the local coordinates (divided by P) in each member of the frame structure.

Element*	$\bar{Q}_1$	$-\bar{Q}_2$	$-\bar{Q}_3$	$\bar{Q}_4$	$-\bar{Q}_5$	$-\bar{Q}_6$
RIE (1)	3.237	1.865	−62.24	−3.237	0.136	−62.26
	0.850	0.908	62.26	1.550	2.292	62.28
RIE (2)	4.723	0.671	−0.332	−4.723	1.329	47.70
	2.699	1.384	−47.70	−0.299	1.816	86.67
RIE (4)	4.730	0.713	−8.362	−4.730	1.288	49.76
	2.668	1.411	−49.76	−0.268	1.789	83.74
CIE (1)	3.077	1.575	−65.39	−3.077	0.425	−17.38
	0.987	0.607	17.38	1.413	2.593	161.4
CIE (2)	4.728	0.708	−8.328	−4.728	1.292	50.37
	2.670	1.407	−50.37	−0.270	1.793	85.07
CIE (4)	4.730	0.721	−10.30	−4.730	1.279	50.43
	2.661	1.417	−50.43	−0.261	1.783	83.39
EBE†	4.731	0.725	−10.90	−4.731	1.275	50.45
	2.658	1.420	−50.45	−0.258	1.780	82.87

* Number within the parentheses denotes the number of elements per member, and the two rows correspond to the two members of the structure.
† Values independent of the number of elements (and coincide with the exact values predicated by the respective beam theories).

6.4 Inclusion of Constraint Conditions

6.4.1 Introduction

It is not uncommon in structural systems to find that the displacement components at a point are related. For example, when the plane of a roller support is at an angle to the global coordinate system (see Fig. 6.4.1), the boundary conditions on displacements and forces at the roller are known only in terms of the normal (to the support) component of the displacement and the tangential component of the force

$$u_n^e = 0, \quad Q_t^e = Q_0 \tag{6.4.1}$$

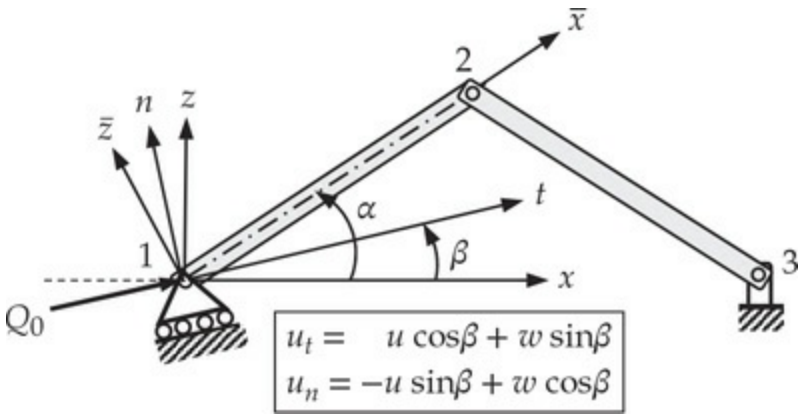

Fig. 6.4.1 Transformation of specified boundary conditions from a local coordinate system to the global coordinate system (for an inclined support).

where u_n^e is the normal component of displacement and Q_t^e is the tangential component of the force at node 1 of the element Ω^e (see Fig. 6.4.1); Q_0 is the specified value of the tangential force. These conditions, when expressed in terms of the global components of displacements and forces by means of the transformations in Eq. (6.2.2), become

$$u_n^e = -u_1^e \sin\beta + u_2^e \cos\beta = 0 \tag{6.4.2a}$$

$$Q_t^e = Q_1^e \cos\beta + Q_2^e \sin\beta = Q_0 \tag{6.4.2b}$$

where $(u_1^e = u^e, u_2^e = w^e)$ and (Q_1^e, Q_2^e) are the x and z components of the displacements and forces, respectively, at the support. Equations in Eq. (6.4.2a) can be viewed as constraint conditions among the global displacements, which have a companion relation among the associated forces, namely Eq. (6.4.2b). In this section we study ways to incorporate algebraic constraint conditions into the solution procedure. There are two alternative methods: (1) Lagrange multiplier method and (2) the penalty function method. The basic ideas of these two methods are explained by considering the following algebraic problem with a constraint: *minimize the function* $f(x, y)$ *subject to the constraint* $G(x, y) = 0$. In the coming sections the basic ideas behind the penalty and Lagrange multiplier methods are presented.

6.4.2 Lagrange Multiplier Method

In the Lagrange multiplier method the problem is reformulated as one of determining the stationary (or critical) points of the modified function F_L

(x, y),

$$F_L(x,y) = f(x,y) + \lambda\, G(x,y) \tag{6.4.3}$$

subject to no constraints. Here λ (a number) denotes the Lagrange multiplier. The solution to the problem is obtained by setting partial derivatives of F_L with respect to x, y, and λ to zero:

$$\begin{aligned} \frac{\partial F_L}{\partial x} &= \frac{\partial f}{\partial x} + \lambda \frac{\partial G}{\partial x} = 0 \\ \frac{\partial F_L}{\partial y} &= \frac{\partial f}{\partial y} + \lambda \frac{\partial G}{\partial y} = 0 \\ \frac{\partial F_L}{\partial \lambda} &= G(x,y) = 0 \end{aligned} \tag{6.4.4}$$

Thus, there are three equations in three unknowns (x, y, λ). In the Lagrange multiplier method a new variable, Lagrange multiplier, is introduced with each constraint equation.

6.4.3 Penalty Function Approach

The penalty function method allows us to reformulate a problem with constraints as one without constraints. In the penalty function method, the problem is reformulated as one of finding the minimum of the modified function F_P :

$$F_P(x,y) = f(x,y) + \frac{\gamma}{2}[G(x,y)]^2 \tag{6.4.5}$$

where γ is a preassigned weight parameter, called the penalty parameter. The factor $\frac{1}{2}$ in Eq. (6.4.5) is used for convenience: when F_p is differentiated with respect to its arguments, the factor will be cancelled by the power on $G(x, y)$. The solution to the modified problem is given by the following two equations:

$$\begin{aligned} \frac{\partial F_P}{\partial x} &= \frac{\partial f}{\partial x} + \gamma G \frac{\partial G}{\partial x} = 0 \\ \frac{\partial F_P}{\partial y} &= \frac{\partial f}{\partial y} + \gamma G \frac{\partial G}{\partial y} = 0 \end{aligned} \tag{6.4.6a}$$

The solution (x_γ, y_γ) of Eq. (6.4.6a) will be a function of the penalty parameter γ. The larger the value of γ, the more exactly the constraint is satisfied (in a least-square sense), and (x_γ, y_γ) approaches the actual solution (x, y) as $\gamma \to \infty$. An approximation to the Lagrange multiplier is computed from the equation [compare Eq. (6.4.6a) with the first two equations of Eq. (6.4.4)]

$$\lambda_\gamma = \gamma G(x_\gamma, y_\gamma) \tag{6.4.6b}$$

We consider a specific example to illustrate the ideas presented above.

Example 6.4.1

Minimize the quadratic function

$$f(x, y) = 4x^2 - 3y^2 + 2xy + 6x - 3y + 5 \tag{1}$$

subject to the constraint

$$G(x, y) \equiv 2x + 3y = 0 \tag{2}$$

Solution: Geometrically, we seek the inflection point of the surface $f(x, y)$ that is on the line $2x + 3y = 0$. We solve the problem using the Lagrange multiplier method and the penalty function method.

Lagrange Multiplier Method. The modified functional is

$$F_L(x, y) = f(x, y) + \lambda(2x + 3y) \tag{3}$$

where λ is the Lagrange multiplier to be determined. We have

$$\begin{aligned} \frac{\partial F_L}{\partial x} &= 8x + 2y + 6 + 2\lambda = 0 \\ \frac{\partial F_L}{\partial y} &= -6y + 2x - 3 + 3\lambda = 0 \\ \frac{\partial F_L}{\partial \lambda} &= 2x + 3y = 0 \end{aligned} \tag{4}$$

Solving the three algebraic equations, we obtain

$$x = -3, \quad y = 2, \quad \lambda = 7 \tag{5}$$

Penalty Function Method. The modified functional is

$$F_P(x,y) = f(x,y) + \frac{\gamma}{2}(2x+3y)^2 \tag{6}$$

and we have

$$\begin{aligned} \frac{\partial F_P}{\partial x} &= 8x + 2y + 6 + 2\gamma(2x+3y) = 0 \\ \frac{\partial F_P}{\partial y} &= -6y + 2x - 3 + 3\gamma(2x+3y) = 0 \end{aligned} \tag{7}$$

The solution of these equations is

$$x_\gamma = \frac{15 - 36\gamma}{-26 + 12\gamma}, \; y_\gamma = \frac{18 + 24\gamma}{-26 + 12\gamma} \tag{8}$$

The Lagrange multiplier is given by

$$\lambda_\gamma = \gamma G(x_\gamma, y_\gamma) = \frac{84\gamma}{-26 + 12\gamma} \tag{9}$$

Clearly, in the limit $\gamma \to \infty$, the penalty function solution approaches the exact solution:

$$\lim_{\gamma\to\infty} x_\gamma = -3, \quad \lim_{\gamma\to\infty} y_\gamma = 2, \quad \lim_{\gamma\to\infty} \lambda_\gamma = 7 \tag{10}$$

An approximate solution to the problem can be obtained, within a desired accuracy, by selecting a finite value of the penalty parameter (see Table 6.4.3).

Table 6.4.3 Convergence of penalty function solution with increasing penalty parameter.

γ	x_γ	y_γ	λ_γ	$G_\gamma = 2x_\gamma + 3y_\gamma$
0	−0.5769	−0.6923	0.0000	−3.2308
1	1.5000	−3.0000	−6.0000	−6.0000
10	−3.6702	2.7447	8.9362	0.8936
100	−3.0537	2.0596	7.1550	0.0716
1000	−3.0053	2.0058	7.0152	0.0068
10000	−3.0005	2.0006	7.0015	0.0008
∞	−3.0000	2.0000	7.0000	0.0000

Next, we turn our attention to constraint equations of the type in Eq.

(6.4.2a) that arise in connection with truss and frame structures. Consider the following constraint relation among two displacement components at a node (no sum on repeated indices is implied):

$$\beta_m u_m + \beta_n u_n = \beta_{mn} \tag{6.4.7}$$

where βm, βn, and βmn are known constants and u_m and u_n are the mth and nth displacement degrees of freedom in the mesh. The functional that must be minimized subject to the constraint in Eq. (6.4.7) in this case is the total potential energy of the system [see Eq. (4.4.9)]

$$\Pi = \frac{1}{2}\int_\Omega [A\,\mathbf{u}^{\mathrm{T}}\mathbf{B}^{\mathrm{T}}E\,\mathbf{B}\mathbf{u} + EA(\alpha T)^2]\,dx - \int_\Omega \mathbf{u}^{\mathrm{T}}\left(\mathbf{\Psi}^{\mathrm{T}}f + \mathbf{B}^{\mathrm{T}}EA\alpha T\right)dx - \mathbf{u}^{\mathrm{T}}\mathbf{Q} \tag{6.4.8}$$

where α is the thermal coefficient of expansion and T is the temperature increase. The penalty functional is given by

$$\Pi_p = \frac{1}{2}\int_\Omega [A\,\mathbf{u}^{\mathrm{T}}\mathbf{B}^{\mathrm{T}}E\,\mathbf{B}\mathbf{u} + EA(\alpha T)^2]\,dx - \int_\Omega \mathbf{u}^{\mathrm{T}}\left(\mathbf{\Psi}^{\mathrm{T}}f + \mathbf{B}^{\mathrm{T}}EA\alpha T\right)dx - \mathbf{u}^{\mathrm{T}}\mathbf{Q} + \frac{\gamma}{2}(\beta_m u_m + \beta_n u_n - \beta_{mn})^2 \tag{6.4.9}$$

The functional Π_p attains a minimum only when $\beta_m\, u_m + \beta_n\, u_n - \beta_{mn}$ is very small, that is, approximately satisfying the constraint in Eq. (6.4.7). Setting $\delta\Pi_p = 0$ yields

$$\left(\mathbf{K} + \mathbf{K}_p\right)\mathbf{u} = \mathbf{f} + \mathbf{Q} + \mathbf{Q}_p \tag{6.4.10a}$$

where

$$\mathbf{K} = \int_\Omega A\,\mathbf{B}^{\mathrm{T}}E\,\mathbf{B}\,dx, \quad \mathbf{K}_p = \begin{bmatrix} \cdots & \cdots & \cdots & \cdots \\ \cdots\gamma\beta_m^2 & \cdots & \gamma\beta_m\beta_n & \cdots \\ \cdots & \cdots & \cdots & \cdots \\ \cdots\gamma\beta_m\beta_n & \cdots & \gamma\beta_n^2 & \cdots \\ \cdots & \cdots & \cdots & \cdots \end{bmatrix}$$

$$\mathbf{f} = \int_\Omega \left(\mathbf{\Psi}^{\mathrm{T}}f + \mathbf{B}^{\mathrm{T}}EA\alpha T\right)dx, \quad \mathbf{Q}_p = \begin{Bmatrix} \cdots \\ \gamma\beta_{mn}\beta_m \\ \cdots \\ \gamma\beta_{mn}\beta_n \\ \cdots \end{Bmatrix} \tag{6.4.10b}$$

Thus, a modification of the stiffness and force coefficients associated with the constrained degrees of freedom will provide the desired solution to the constrained problem. As illustrated in **Example 6.4.1**, the value of the penalty parameter γ dictates the degree to which the constraint condition in Eq. (6.4.7) is met. An analysis of the discrete problem shows that the following value of γ may be used:

$$\gamma = \max|K_{ij}| \times 10^4, \quad 1 \le i, j \le N \tag{6.4.11}$$

where N is the order of the global coefficient matrix. The reaction forces associated with the constrained displacement degrees of freedom are obtained from

$$\begin{aligned} F_{mp} &= -\gamma\beta_m(\beta_m u_m + \beta_n u_n - \beta_{mn}) \\ F_{np} &= -\gamma\beta_n(\beta_m u_m + \beta_n u_n - \beta_{mn}) \end{aligned} \tag{6.4.12}$$

Because of the large magnitudes of the penalty terms, it is necessary to carry out computations in double precision (hand calculations may not be accurate).

Example 6.4.2

Consider the structure shown in Fig. 6.4.2(a). The rigid bar ABE is supported by deformable bars AC and BD. Bar AC is made of aluminum (E_a = 70 GPa) and has cross-sectional area of A_a = 500 mm^2; bar BD is made of steel (E_s = 200 GPa) and has a cross-sectional area of A_s = 600 mm^2. The rigid bar carries a load of F_2 = 30 kN at point E. Determine the displacements of points A, B, and E and the stresses in the aluminum and steel bars when (a) end O is subjected to a load of F_1 = 10 kN, and (b) end O is pin-connected to a rigid support [see Fig. 6.4.2(d)].

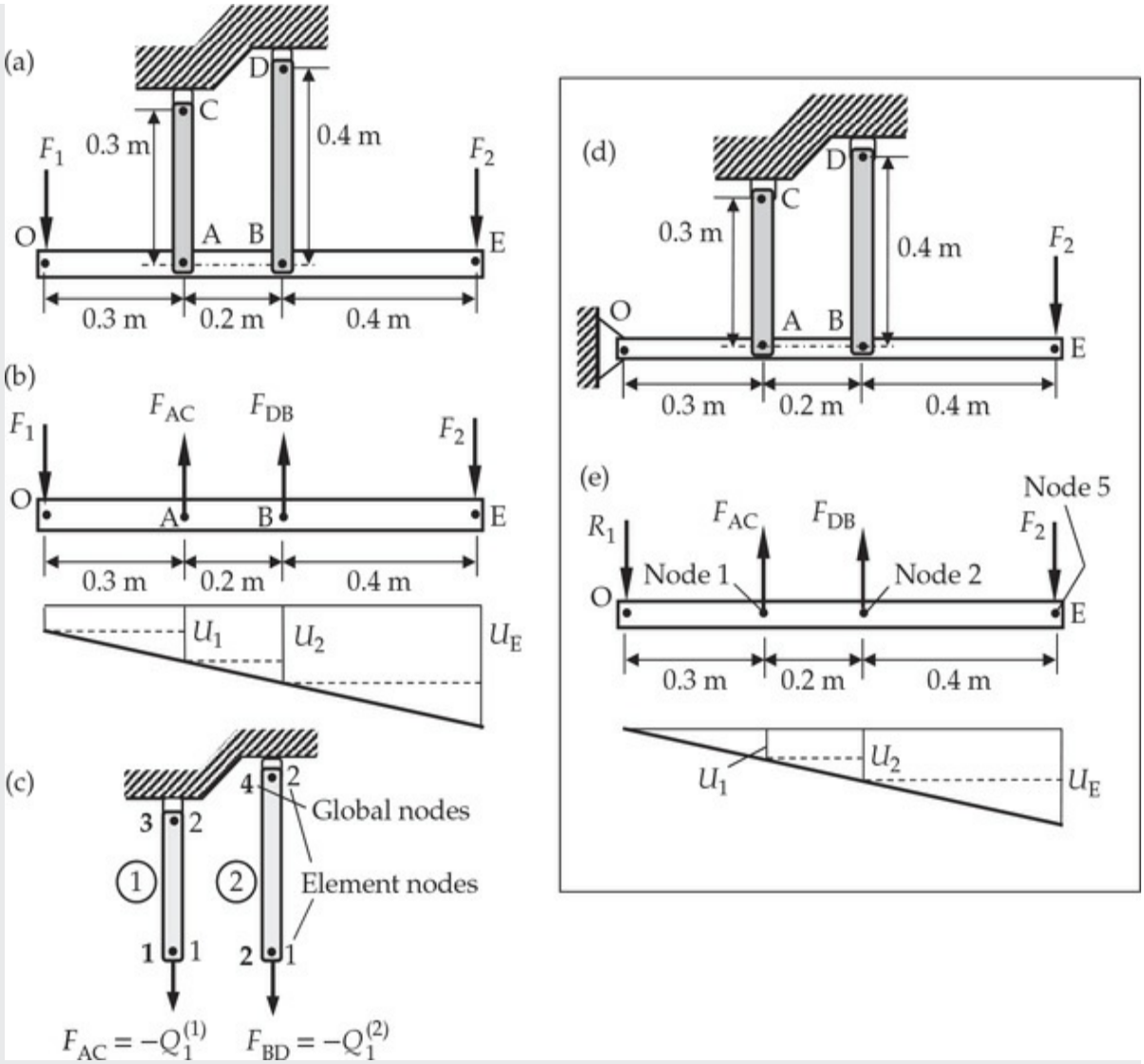

Fig. 6.4.2 (a) Given structure. (b) Free-body diagram. (c) Finite element mesh. (d) Modified structure. (e) Free-body diagram of the modified structure.

Solution: (a) One may note that this is a statically determinate problem; that is, the forces at points A and B can be readily determined from statics. Using the free-body diagram of the rigid bar ABE [see Fig. 6.4.2(b)], we obtain

$$F_{AC} + F_{BD} = F_1 + F_2, \quad 0.3F_{AC} + 0.5F_{BD} - 0.9F_2 = 0 \tag{1}$$

which yield the values

$$F_{AC} = 2.5F_1 - 2F_2 = -35\text{kN}, \quad F_{BD} = -1.5F_1 + 3F_2 = 75\ \text{kN} \tag{2}$$

Let

$$k_1 = \frac{E_a A_a}{h_1} = 116.6667 \times 10^6 \text{ N/m}, \quad k_2 = \frac{E_s A_s}{h_2} = 300 \times 10^6 \text{ N/m} \tag{3}$$

If we use a single linear finite element to represent bars AC and BD, the assembled matrix of the structure is given by [see Fig. 6.4.2(c)]

$$\begin{bmatrix} k_1 & 0 & -k_1 & 0 \\ 0 & k_2 & 0 & -k_2 \\ -k_1 & 0 & k_1 & 0 \\ 0 & -k_2 & 0 & k_2 \end{bmatrix} \begin{Bmatrix} U_1 \\ U_2 \\ U_3 \\ U_4 \end{Bmatrix} = \begin{Bmatrix} Q_1^1 \\ Q_1^2 \\ Q_2^1 \\ Q_2^2 \end{Bmatrix} \tag{4}$$

The boundary conditions of the problem are

$$U_3 = U_4 = 0; \quad Q_1^1 = -F_{AC} = 35 \text{ kN}, \quad Q_1^2 = -F_{BD} = -75 \text{ kN}$$

Hence, the condensed equations are given by

$$\begin{bmatrix} k_1 & 0 \\ 0 & k_2 \end{bmatrix} \begin{Bmatrix} U_1 \\ U_2 \end{Bmatrix} = 10^3 \begin{Bmatrix} 35 \\ -75 \end{Bmatrix}$$

whose solution is

$$U_1 = 0.30 \times 10^{-3} \text{ (m)} = 0.30 \text{ (mm)}, \; U_2 = -0.25 \times 10^{-3} \text{ (m)} = -0.25 \text{ (mm)}$$

By similarity of triangles, we can determine the displacement of point E. We have

$$\frac{U_E - U_1}{0.6} = \frac{U_2 - U_1}{0.2} \quad \rightarrow \quad U_E = 3U_2 - 2U_1 = -1.35 \text{ (mm)}$$

Thus, end A of the bar AC moves up by 0.3 mm, end B of BD moves down by 0.25 mm, and point E moves down by 1.35 mm. The stresses in bars AC and BD are

$$\sigma_{AC} = \frac{F_{AC}}{A_a} = -\frac{35}{500 \times 10^{-6}} = -70 \text{ MPa}, \quad \sigma_{BD} = \frac{F_{BD}}{A_s} = \frac{75}{600 \times 10^{-6}} = -125 \text{ MPa}$$

(b) Next, consider the case in which point O is pin-connected to a fixed, immovable part, as shown in Fig. 6.4.2(d). Then the problem becomes statically indeterminate one. Of course, the finite element method can still be used to solve the problem. The assembled equations in Eq. (6) are still valid for this case. However, forces Q_1^1 and Q_1^2 are not known (because we cannot solve for F_{AC} and F_{BD}). In addition, points A and B are constrained to move as the rigid member ABE is rotated about point O.

This geometric constraint is equivalent to the following conditions among the displacements U_1, U_2, and U_5 :

$$\frac{U_1}{0.3} = \frac{U_5}{0.9} \rightarrow 3U_1 - U_5 = 0, \quad \frac{U_2}{0.5} = \frac{U_5}{0.9} \rightarrow 1.8U_2 - U_5 = 0 \tag{5}$$

Here, we have $\beta_1 = 3$, $\beta_5 = -1$, $\beta_{15} = 0$, $\beta_2 = 1.8$, and $\beta_{25} = 0$. These constraints bring in an additional degree of freedom, namely U_5, into the equations. Hence, we must add a column and row corresponding to U_5 to be able to include the constraints.

Using the procedure developed in this section, we can include the constraints of Eq. (5) into assembled equations. The value of the penalty parameter is selected to be $\gamma = k_2 \times 10^4 = (300 \times 10^6)10^4$. The stiffness additions due to the two constraints are

$$\begin{array}{c} \\ 1 \\ 5 \end{array} \begin{array}{c} \begin{array}{cc} 1 & 5 \end{array} \\ \begin{bmatrix} (3)^2\gamma & 3(-1)\gamma \\ (-1)3\gamma & (-1)^2\gamma \end{bmatrix} \end{array} = 10^{10} \begin{bmatrix} 2700 & -900 \\ -900 & 300 \end{bmatrix}$$

$$\begin{array}{c} \\ 2 \\ 5 \end{array} \begin{array}{c} \begin{array}{cc} 2 & 5 \end{array} \\ \begin{bmatrix} (1.8)^2\gamma & (-1)1.8\gamma \\ (-1)1.8\gamma & (-1)^2\gamma \end{bmatrix} \end{array} = 10^{10} \begin{bmatrix} 972 & -540 \\ -540 & 300 \end{bmatrix} \tag{6}$$

The force additions are zero (i.e., $\mathbf{Q}_p = 0$) on account of $\beta_{15} = \beta_{25} = 0$. Hence, the modified finite element equations become

$$\begin{bmatrix} 27\times10^{12}+k_1 & 0 & -k_1 & 0 & -9\times10^{12} \\ 0 & 9.72\times10^{12}+k_2 & 0 & -k_2 & -5.4\times10^{12} \\ -k_1 & 0 & k_1 & 0 & 0 \\ 0 & -k_2 & 0 & k_2 & 0 \\ -9\times10^{12} & -5.4\times10^{12} & 0 & 0 & 6\times10^{12} \end{bmatrix} \begin{Bmatrix} U_1 \\ U_2 \\ U_3 \\ U_4 \\ U_5 \end{Bmatrix} = \begin{Bmatrix} Q_1^1 \\ Q_1^2 \\ Q_2^1 \\ Q_2^2 \\ F_2 \end{Bmatrix} \tag{7}$$

The condensed equations are

$$\begin{bmatrix} 27\times10^{12}+k_1 & 0 & -9\times10^{12} \\ 0 & 9.72\times10^{12}+k_2 & -5.4\times10^{12} \\ -9\times10^{12} & -5.4\times10^{12} & 6\times10^{12} \end{bmatrix} \begin{Bmatrix} U_1 \\ U_2 \\ U_5 \end{Bmatrix} = 30\times10^3 \begin{Bmatrix} 0 \\ 0 \\ 1 \end{Bmatrix} \tag{8}$$

whose solution is (deflections are in the direction of the forces)

$$U_1 = 0.947390478948\times10^{-4}\ (\text{m}), \quad U_2 = 0.157894222157\times10^{-3}\ (\text{m})$$
$$U_5 = 0.284218371783\times10^{-3}\ (\text{m}) \tag{9}$$

The forces in the bars AC and BD can be calculated using Eq. (4):

$$\begin{Bmatrix} Q_1^1 \\ Q_1^2 \end{Bmatrix} = \begin{bmatrix} k_1 & 0 \\ 0 & k_2 \end{bmatrix} \begin{Bmatrix} U_1 \\ U_2 \end{Bmatrix} = 10^3 \begin{Bmatrix} 11.053 \\ 47.368 \end{Bmatrix} \text{N} \tag{10}$$

Alternatively, from Eq. (6.4.12) we have

$$(Q_1^1)_p = -3\gamma\,(3U_1 - U_5) = 11.053 \text{ kN}$$
$$(Q_1^2)_p = -1.8\gamma\,(1.8U_2 - U_5) = 47.368 \text{ kN}$$

The stresses are $\sigma_{AC} = 22.11$ MPa and $\sigma_{BD} = 79$ MPa.

Next, we consider a plane truss with an inclined support.

Example 6.4.3

Consider the truss shown in Fig. 6.4.3(a). Determine the unknown displacements of nodes 2 and 3 and the reactions associated with these displacements.

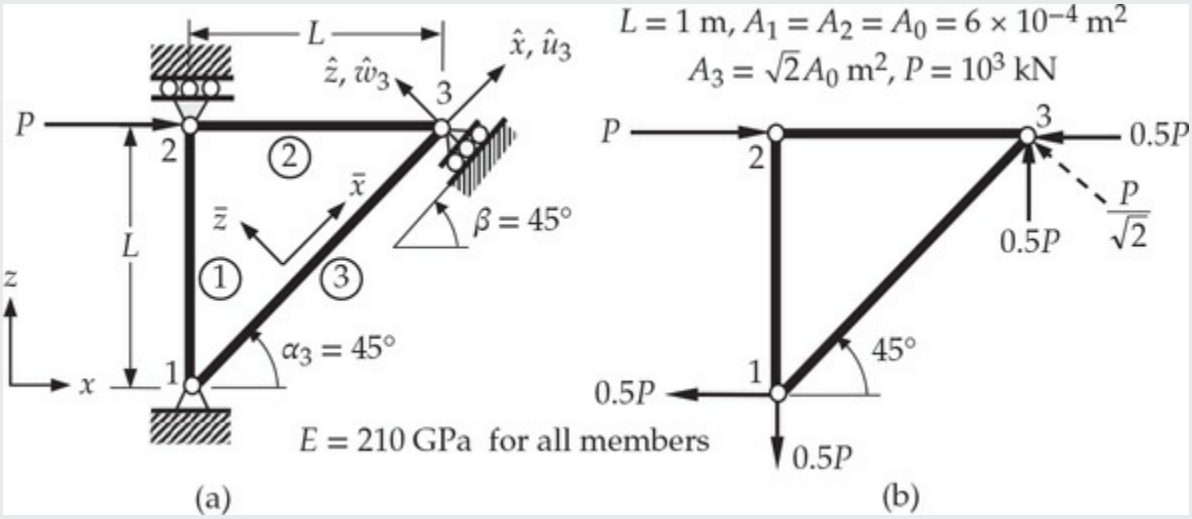

Fig. 6.4.3 (a) Given structure. (b) Reaction forces.

Solution: The element stiffness matrices are

$$\mathbf{K}^1 = 10^9 \begin{bmatrix} 0.000 & 0.000 & 0.000 & 0.000 \\ 0.000 & 0.126 & 0.000 & -0.126 \\ 0.000 & 0.000 & 0.000 & 0.000 \\ 0.000 & -0.126 & 0.000 & 0.126 \end{bmatrix}$$

$$\mathbf{K}^2 = 10^9 \begin{bmatrix} 0.126 & 0.000 & -0.126 & 0.000 \\ 0.000 & 0.000 & 0.000 & 0.000 \\ -0.126 & 0.000 & 0.126 & 0.000 \\ 0.000 & 0.000 & 0.000 & 0.000 \end{bmatrix}$$

$$\mathbf{K}^3 = 0.63 \times 10^8 \begin{bmatrix} 1.0 & 1.0 & -1.0 & -1.0 \\ 1.0 & 1.0 & -1.0 & -1.0 \\ -1.0 & -1.0 & 1.0 & 1.0 \\ -1.0 & -1.0 & 1.0 & 1.0 \end{bmatrix}$$

The assembled equations before including the constraint conditions are

$$10^8 \begin{bmatrix} 0.63 & 0.63 & 0.00 & 0.00 & -0.63 & -0.63 \\ 0.63 & 1.89 & 0.00 & -1.26 & -0.63 & -0.63 \\ 0.00 & 0.00 & 1.26 & 0.00 & -1.26 & 0.00 \\ 0.00 & -1.26 & 0.00 & 1.26 & 0.00 & 0.00 \\ -0.63 & -0.63 & -1.26 & 0.00 & 1.89 & 0.63 \\ -0.63 & -0.63 & 0.00 & 0.00 & 0.63 & 0.63 \end{bmatrix} \begin{Bmatrix} U_1 \\ U_2 \\ U_3 \\ U_4 \\ U_5 \\ U_6 \end{Bmatrix} = \begin{Bmatrix} Q_1^1 + Q_1^3 \\ Q_2^1 + Q_2^3 \\ Q_3^1 + Q_3^2 \\ Q_4^1 + Q_4^2 \\ Q_3^2 + Q_3^3 \\ Q_4^2 + Q_4^3 \end{Bmatrix} \quad (1)$$

The constraint condition at node 3 is

$$u_n \equiv -u \sin\alpha + w \cos\alpha = 0 \rightarrow -0.7071\, u + 0.7071\, w = 0 \quad (2)$$

Comparing this constraint equation to the general constraint equation, Eq. (6.4.7), we find that $\beta_1 = -0.7071$, $\beta_2 = 0.7071$ and $\beta_0 = 0$.

The value of the penalty parameter is selected to be $\gamma = (1.89 \times 10^8)10^4$. The stiffness additions due to the constraint are

$$\begin{matrix} & 5 & 6 \\ 5 \\ 6 \end{matrix} \gamma \begin{bmatrix} (-0.7071)^2 & -(0.7071)^2 \\ -(0.7071)^2 & (0.7071)^2 \end{bmatrix} = 1.89 \times 10^{12} \begin{bmatrix} 0.5 & -0.5 \\ -0.5 & 0.5 \end{bmatrix} \quad (3)$$

The assembled equations after including the constraint conditions are (the numbers shown are truncated but more accurate numbers are used in actual computation in a computer):

$$10^8\begin{bmatrix} 0.63 & 0.63 & 0.00 & 0.00 & -0.63 & -0.63 \\ 0.63 & 1.89 & 0.00 & -1.26 & -0.63 & -0.63 \\ 0.00 & 0.00 & 1.26 & 0.00 & -1.26 & 0.00 \\ 0.00 & -1.26 & 0.00 & 1.26 & 0.00 & 0.00 \\ -0.63 & -0.63 & -1.26 & 0.00 & 6301.80 & 6299.20 \\ -0.63 & -0.63 & 0.00 & 0.00 & 6299.20 & 6300.50 \end{bmatrix}\begin{Bmatrix} U_1 \\ U_2 \\ U_3 \\ U_4 \\ U_5 \\ U_6 \end{Bmatrix} = \begin{Bmatrix} Q_1^1 + Q_1^3 \\ Q_2^1 + Q_2^3 \\ Q_3^1 + Q_1^2 \\ Q_4^1 + Q_2^2 \\ Q_3^2 + Q_3^3 \\ Q_4^2 + Q_4^3 \end{Bmatrix} \tag{4}$$

Imposing the boundary and force equilibrium conditions $U_1 = U_2 = U_4 = 0$ and $Q_3^1 + Q_1^2 = P$, we obtain the condensed equations

$$10^8\begin{bmatrix} 1.26 & -1.26 & 0.00 \\ -1.26 & 6301.80 & 6299.20 \\ 0.00 & 6299.20 & 6300.50 \end{bmatrix}\begin{Bmatrix} U_3 \\ U_5 \\ U_6 \end{Bmatrix} = \begin{Bmatrix} P \\ 0 \\ 0 \end{Bmatrix} \tag{5}$$

The solution to these equations (as computed in double precision in a computer) is

$$U_3 = 11.905 \times 10^{-3}\ \text{m},\ U_5 = 3.9688 \times 10^{-3}\ \text{m},\ U_6 = 3.9681 \times 10^{-3}\ \text{m}$$

and the reactions at node 3 are obtained using Eq. (1) as

$$F_{3x} = -500\ \text{kN},\ F_{3y} = 500\ \text{kN}$$

The reactions of the whole structure are shown in Fig. 6.4.3(b).

6.4.4 A Direct Approach

Here, we present an exact method by which constraint equations of the type in Eqs. (6.4.2a) and (6.4.2b) can be included in the assembled equations for the unknowns. The method involves expressing the global displacement degrees of freedom at the node with a constraint in terms of the local displacement degrees of freedom so that the boundary conditions can be readily imposed.

Recall from Eq. (6.2.3a) that the displacements $(\hat{u}, \hat{w})$ referred to the local coordinate system $(\hat{x}, \hat{z})$ at a point are related to the displacements (u, w) referred to the global coordinates (x, z) by

$$\begin{Bmatrix} \hat{u} \\ \hat{w} \end{Bmatrix}_c = \begin{bmatrix} \cos\beta & \sin\beta \\ -\sin\beta & \cos\beta \end{bmatrix}\begin{Bmatrix} u \\ w \end{Bmatrix}_c \quad \rightarrow \quad \hat{\mathbf{u}}_c = \mathbf{A}\mathbf{u}_c \tag{6.4.13a}$$

and the inverse relation is given by

$$\mathbf{u}_c = \mathbf{A}^{\mathrm{T}}\hat{\mathbf{u}}_c, \quad \text{where} \quad \mathbf{A} = \begin{bmatrix} \cos\beta & \sin\beta \\ -\sin\beta & \cos\beta \end{bmatrix} \tag{6.4.13b}$$

where the subscript "c" refers to the constrained degrees of freedom. Since we wish to express the global displacements at a given node in terms of the local displacements at a specific node, we construct the transformation of the whole (global) system as

$$\mathbf{T} = \begin{bmatrix} \mathbf{I} & 0 & 0 \\ 0 & \mathbf{A}^{\mathrm{T}} & 0 \\ 0 & 0 & \mathbf{I} \end{bmatrix} \tag{6.4.14}$$

Thus, all displacement degrees of freedom that are not constrained are unaffected and only global displacements that are constrained are transformed to the local displacements. Further, note that the transformation matrix [**A**] is placed in [**T**] in such a way that only the constrained degrees of freedom are transformed. We have

$$\begin{Bmatrix} \boldsymbol{\Delta}^1 \\ \mathbf{u}_c \\ \boldsymbol{\Delta}^2 \end{Bmatrix} = \begin{bmatrix} \mathbf{I} & 0 & 0 \\ 0 & \mathbf{A}^{\mathrm{T}} & 0 \\ 0 & 0 & \mathbf{I} \end{bmatrix} \begin{Bmatrix} \boldsymbol{\Delta}^1 \\ \hat{\mathbf{u}}_c \\ \boldsymbol{\Delta}^2 \end{Bmatrix} \quad \text{or} \quad \boldsymbol{\Delta} = \mathbf{T}\hat{\boldsymbol{\Delta}} \tag{6.4.15}$$

where $\boldsymbol{\Delta}^1$ and $\boldsymbol{\Delta}^2$ denote the global displacement components ahead and behind (in terms of numbering) the constrained displacement degrees of freedom **u***c* in the mesh. We also note that the transformed displacement vector $\hat{\boldsymbol{\Delta}}$ contains the global displacement vectors $\boldsymbol{\Delta}^1$ and $\boldsymbol{\Delta}^2$ and the local (constrained) displacement vector $\hat{\mathbf{u}}_c$.

The remaining steps of the procedure is the same as that described in Sections 6.2.2 and 6.3.2. Thus, we obtain

$$\hat{\mathbf{K}}\hat{\boldsymbol{\Delta}} = \hat{\mathbf{F}} \tag{6.4.16}$$

where the transformed global stiffness matrix $\hat{\mathbf{K}}$ and global force vector $\hat{\mathbf{F}}$ are known in terms of the assembled global stiffness matrix **K** and force vector **F** as [see Eq. (6.2.7)]

$$\hat{\mathbf{K}} = \mathbf{T}^{\mathrm{T}}\mathbf{K}\mathbf{T}, \quad \hat{\mathbf{F}} = \mathbf{T}^{\mathrm{T}}\mathbf{F} \tag{6.4.17}$$

Since the constrained displacements are a part of the global system of equations, one may impose the boundary conditions on them directly (such as $\hat{u}_n = \hat{w} = 0$ at an inclined roller support, where *n* denotes the coordinate normal to the roller).

In summary, one may introduce a transformation of the displacements that facilitates the imposition of boundary conditions or inclusion of constraints on the displacements. Once the transformation **T** is identified, one may use Eq. (6.4.17) to obtain the modified equations that have the desired effect. We revisit the problems of **Examples 6.4.2** and **6.4.3** to illustrate the ideas described here.

Example 6.4.4

Use the direct approach to solve the problem of **Example 6.4.2** [see Fig. 6.4.2(d)].

Solution: First we note that the geometric constraint between the displacements U_1 and U_2 is

$$\frac{U_1}{0.3} = \frac{U_2}{0.5} \rightarrow U_1 = 0.6U_2 \tag{1}$$

The assembled equations are

$$10^3 \begin{bmatrix} 116.67 & 0.00 & -116.67 & 0.00 \\ 0.00 & 300.00 & 0.00 & -300.00 \\ -116.67 & 0.00 & 116.67 & 0.00 \\ 0.00 & -300.00 & 0.00 & 300.00 \end{bmatrix} \begin{Bmatrix} U_1 \\ U_2 \\ U_3 \\ U_4 \end{Bmatrix} = \begin{Bmatrix} Q_1^1 \\ Q_1^2 \\ Q_2^1 \\ Q_2^2 \end{Bmatrix} \tag{2}$$

In this case, we can introduce a transformation **T** between (U_1, U_2, U_3, U_4) and (U_2, U_3, U_4) (i.e., eliminate U_1 by means of the constraint equation $U_1 = 0.6U_2$) as

$$\begin{Bmatrix} U_1 \\ U_2 \\ U_3 \\ U_4 \end{Bmatrix} = \begin{bmatrix} 0.6 & 0.0 & 0.0 \\ 1.0 & 0.0 & 0.0 \\ 0.0 & 1.0 & 0.0 \\ 0.0 & 0.0 & 1.0 \end{bmatrix} \begin{Bmatrix} U_2 \\ U_3 \\ U_4 \end{Bmatrix} \quad \text{or} \quad \boldsymbol{\Delta} = \mathbf{T}\hat{\boldsymbol{\Delta}} \tag{3}$$

where

$$\boldsymbol{\Delta} = \begin{Bmatrix} U_1 \\ U_2 \\ U_3 \\ U_4 \end{Bmatrix}, \quad \hat{\boldsymbol{\Delta}} = \begin{Bmatrix} U_2 \\ U_3 \\ U_4 \end{Bmatrix} \tag{4}$$

The transformed equations ($\hat{\mathbf{K}}\hat{\boldsymbol{\Delta}} = \hat{\mathbf{F}}$) in explicit form are

$$10^3\begin{bmatrix} 342 & -70.00 & -300 \\ -70 & 116.67 & 0 \\ -300 & 0.00 & 300 \end{bmatrix}\begin{Bmatrix} U_2 \\ U_3 \\ U_4 \end{Bmatrix}=\begin{Bmatrix} 0.6Q_1^1+Q_1^2 \\ Q_2^1 \\ Q_2^2 \end{Bmatrix} \tag{5}$$

From the free-body diagram of bar OABE, we find that $0.6F_{AC}+F_{BD}=1.8F_2$ or $0.6Q_1^1+Q_1^2=1.8F_2=54$ kN. The condensed equation for the unknown U_2 is

$$342U_2=54,\quad U_2=0.15789\ (\text{mm}),\quad U_1=0.6U_2=0.09474\ (\text{mm}) \tag{6}$$

The forces and stresses in the bars AC and BD can be calculated as in **Example 6.4.2**.

Example 6.4.5

Consider the truss in Fig. 6.4.3(a). Use the direct approach to solve the problem.

Solution: The assembled global equations are given in **Example 6.4.3**. The transformation between the global degrees of freedom ($U_1 = u_1$, $U_2 = w_1$, $U_3 = u_2$, $U_4 = w_2$, $U_5 = u_3$, $U_6 = w_3$) and ($U_1 = u_1$, $U_2 = w_1$, $U_3 = u_2$, $U_4 = w_2$, $u_t = \hat{u}_3$, $u_n = \hat{w}_3$) is given by [i.e., Eq. (6.4.15) for the problem at hand takes the form]

$$\begin{Bmatrix} U_1 \\ U_2 \\ U_3 \\ U_4 \\ U_5 \\ U_6 \end{Bmatrix}=\begin{bmatrix} 1 & 0 & 0 & 0 & 0 & 0 \\ 0 & 1 & 0 & 0 & 0 & 0 \\ 0 & 0 & 1 & 0 & 0 & 0 \\ 0 & 0 & 0 & 1 & 0 & 0 \\ 0 & 0 & 0 & 0 & \cos\beta & -\sin\beta \\ 0 & 0 & 0 & 0 & \sin\beta & \cos\beta \end{bmatrix}\begin{Bmatrix} U_1 \\ U_2 \\ U_3 \\ U_4 \\ \hat{u}_3 \\ \hat{w}_3 \end{Bmatrix} \tag{1}$$

where $\beta = 45°$. Using Eq. (6.4.17), we obtain the transformed equations

$$10^8\begin{bmatrix} 0.630 & 0.630 & 0.000 & 0.000 & -0.891 & 0.000 \\ 0.630 & 1.890 & 0.000 & -1.260 & -0.891 & 0.000 \\ 0.000 & 0.000 & 1.260 & 0.000 & -0.891 & 0.891 \\ 0.000 & -1.260 & 0.000 & 1.260 & 0.000 & 0.000 \\ -0.891 & -0.891 & -0.891 & 0.000 & 1.890 & -0.630 \\ 0.000 & 0.000 & 0.891 & 0.000 & -0.630 & 0.630 \end{bmatrix}\begin{Bmatrix} U_1 \\ U_2 \\ U_3 \\ U_4 \\ \hat{u}_3 \\ \hat{w}_3 \end{Bmatrix}=\begin{Bmatrix} Q_1^1+Q_1^3 \\ Q_2^1+Q_2^3 \\ Q_3^1+Q_1^2 \\ Q_4^1+Q_2^2 \\ \hat{F}_{3t} \\ \hat{F}_{3n} \end{Bmatrix}$$

Here $\hat{F}_{3t}$ and $\hat{F}_{3n}$ are the reaction forces at node 3 in the tangential and normal directions, respectively.

Applying the boundary conditions ($u_n = \hat{w}_3$ and $u_t = \hat{u}_3$)

$$U_1 = U_2 = U_4 = \hat{w}_3 = 0, \quad Q_3^1 + Q_1^2 = P = 10^6, \quad \hat{F}_{3t} = 0 \tag{2}$$

we obtain the following condensed equations:

$$10^8 \begin{bmatrix} 1.26000 & -0.89095 \\ -0.89095 & 1.88990 \end{bmatrix} \begin{Bmatrix} U_3 \\ \hat{u}_3 \end{Bmatrix} = 10^6 \begin{Bmatrix} 1 \\ 0 \end{Bmatrix} \tag{3}$$

The horizontal displacement at node 2 and the tangential displacement at node 3 are

$$U_3 = 11.905 \times 10^{-3} \text{ m}, \quad \hat{u}_3 = 5.6122 \times 10^{-3} \text{ m} \tag{4}$$

The unknown reactions can be calculated as

$$F_{1x} = -500 \text{ kN}, \quad F_{1y} = -500 \text{ kN}, \quad F_{2y} = 0 \text{ kN}, \quad F_{3n} = 707.1 \text{ kN} \tag{5}$$

These results are the same as those obtained by the penalty method in **Example 6.4.3**.

6.5 Summary

This chapter is dedicated to the development of plane truss and plane frame finite elements and the inclusion of constraint conditions into the element equations. The force–displacement equations of a plane truss element, which can only carry axial loads, are developed by transforming the bar element equations from the local (bar) coordinate system $(\bar{x}, \bar{z})$ to a global (structure) coordinate system (x, z) to which all members are referred. The plane frame element in the local coordinate system is a superposition of the bar element and pure beam element. Once again, using the transformation of element equations to the global coordinates, equations of a plane frame in the global coordinate system are obtained. The plane frame elements based on the Euler–Bernoulli beam element and the reduced integration element (RIE) and consistent interpolation element (CIE) of the Timoshenko beam theory are developed. Example problems are presented to illustrate the use of the truss elements and frame elements (use of FEM1D becomes necessary to actually solve the problems for displacements and forces).

Inclusion of constraint relations between primary variables (i.e., displacement degrees of freedom) by two different methods is also

discussed to facilitate the imposition of boundary conditions associated with inclined supports in truss and frame problems as well as to include any kinematic constraints. Several numerical examples are presented to illustrate the solution of truss problems with constraints. Even those not interested in structural mechanics should find Section 6.4 on the inclusion of constraints into finite element equations very useful.

Problems

PLANE TRUSS PROBLEMS

6.1–6.8 For the plane truss structures shown in Figs. P6.1–P6.8, give (a) the transformed element matrices, (b) the assembled element matrices, and (c) the condensed matrix equations for the unknown displacements and forces (kip = 10^3 lb).

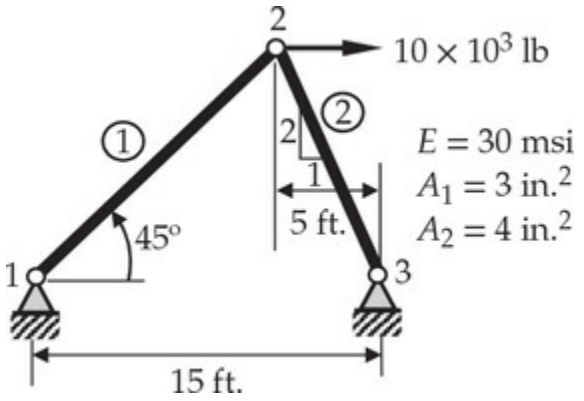

Fig. P6.1

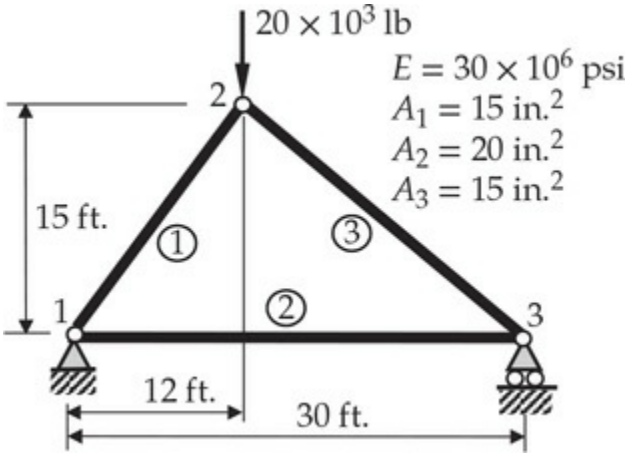

Fig. P6.2

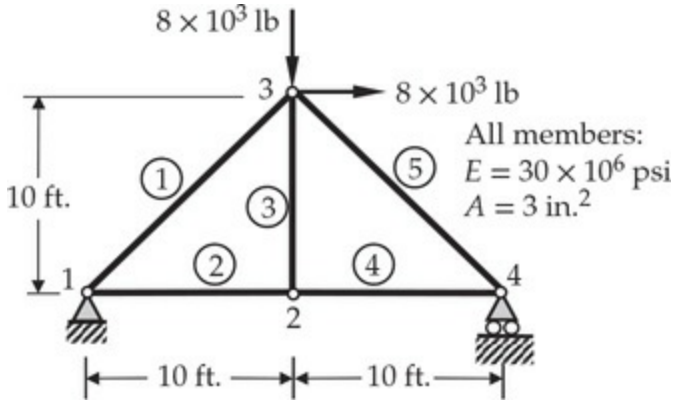

Fig. P6.3

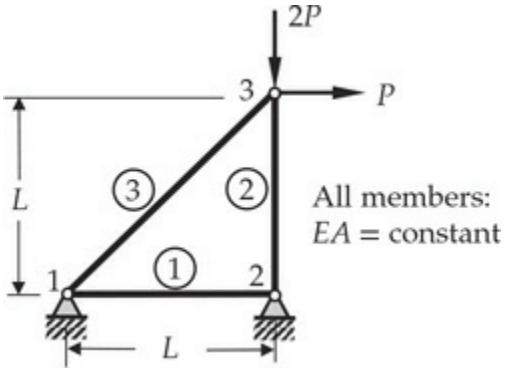

Fig. P6.4

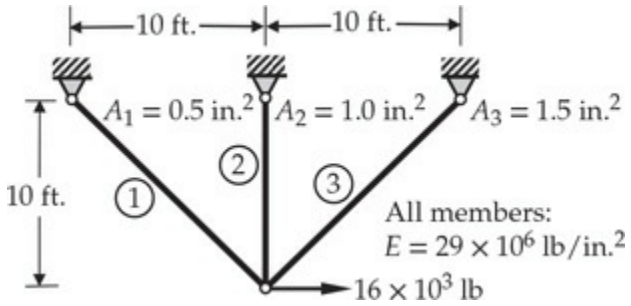

Fig. P6.5

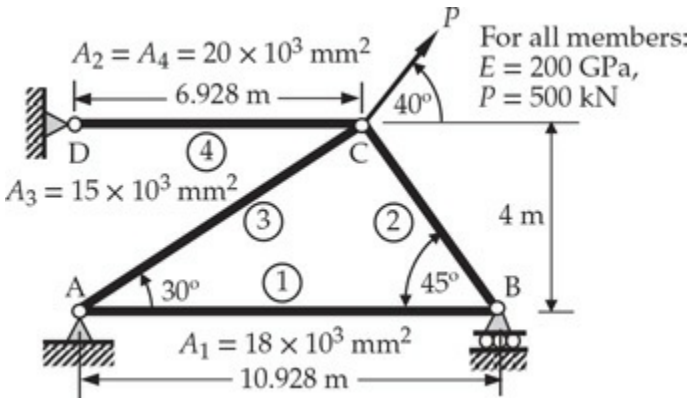

Fig. P6.6

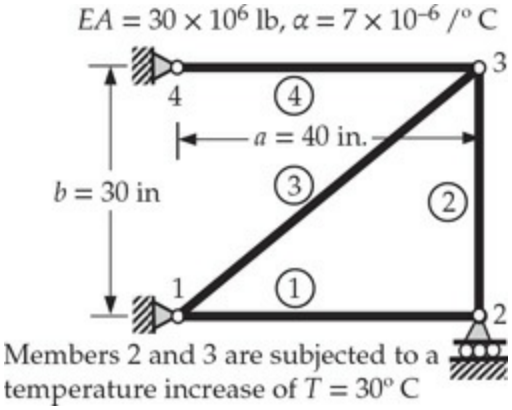

Fig. P6.7

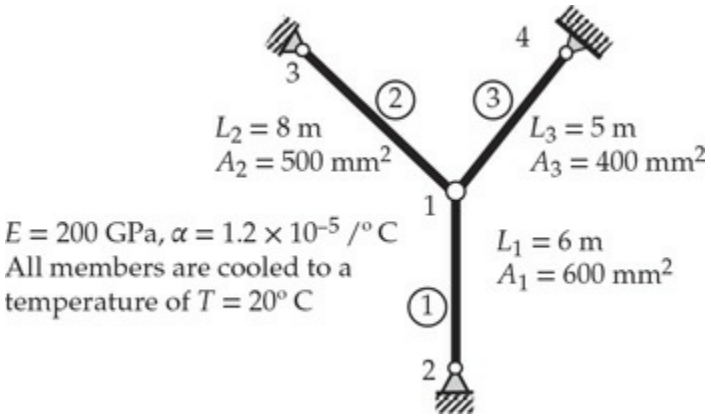

Fig. P6.8

6.9 Determine the forces and displacements of node 2 of the structure shown in Fig. P6.9.

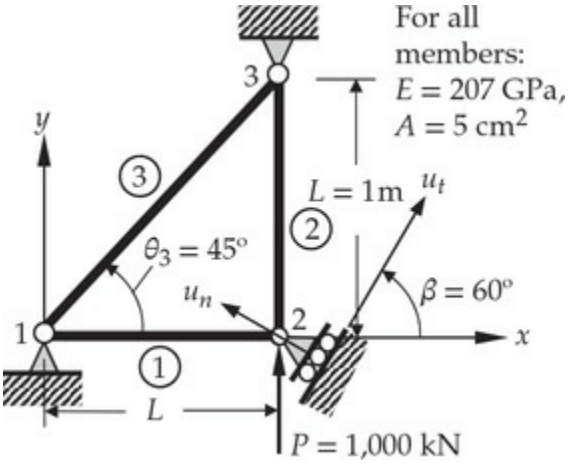

Fig. P6.9

6.10 Determine the forces and displacements of points B and C of the structure shown in Fig. P6.10.

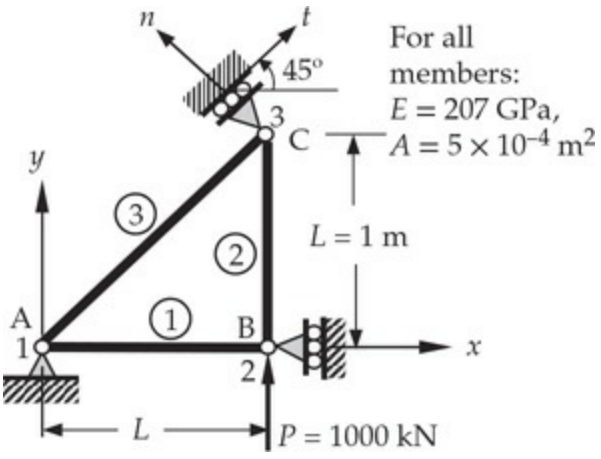

Fig. P6.10

6.11 Determine the forces and elongations of each bar in the structure shown in Fig. P6.11. Also, determine the vertical displacements of points A and D.

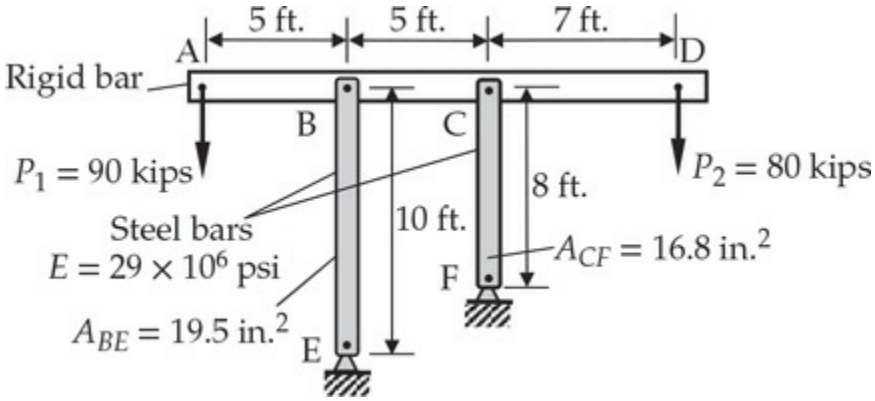

Fig. P6.11

6.12 Determine the forces and elongations of each bar in the structure shown in Fig. P6.11 when end A is pinned to a rigid wall (and P_1 is removed).

PLANE FRAME PROBLEMS

6.13–6.20 For frame problems shown in Figs. P6.13–P6.20, give (a) the transformed element matrices; (b) the assembled element matrices; (c) the condensed matrix equations for the unknown generalized displacements and forces. Use the sign conventions shown in the figure below for global and element displacement (and force) degrees of freedom. The angle between the +ve x-axis and +ve x-axis is measured in the counterclockwise sense.

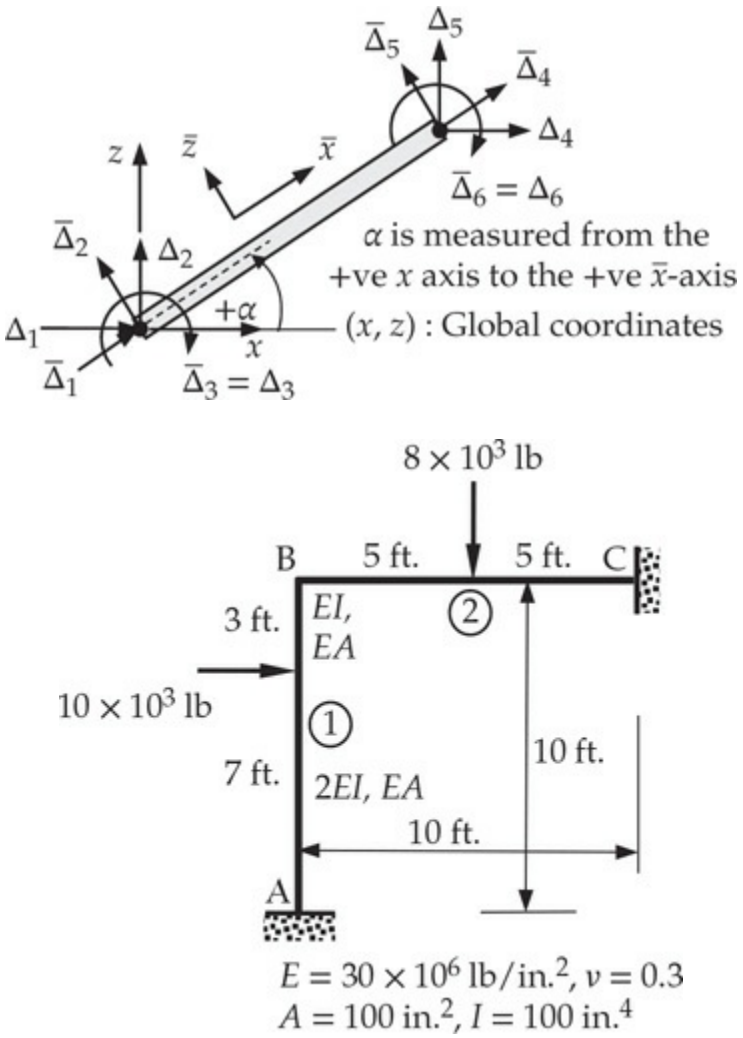

Fig. P6.13

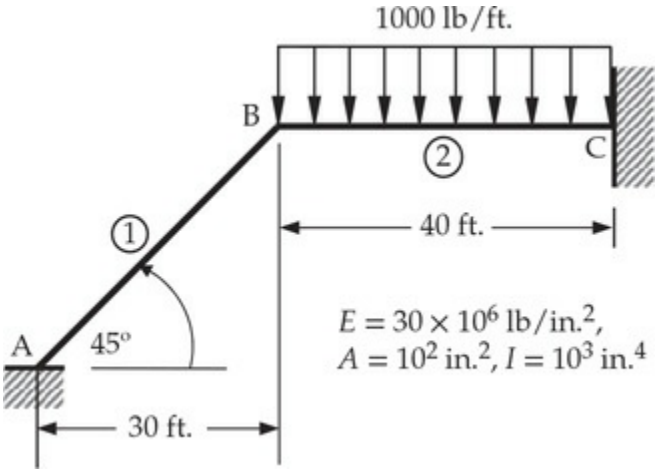

Fig. P6.14

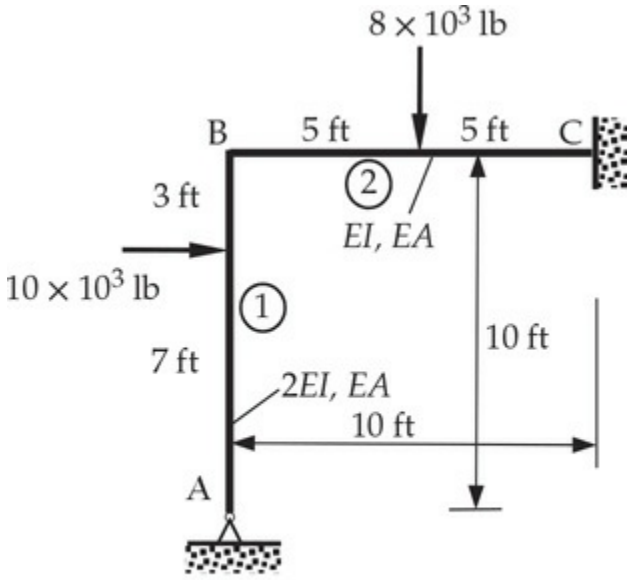

$E = 30 \times 10^6$ lb/in.^{2}, $\nu = 0.3$
$A = 10^2$ in.^{2}, $I = 10^2$ in.^{4}

Fig. P6.15

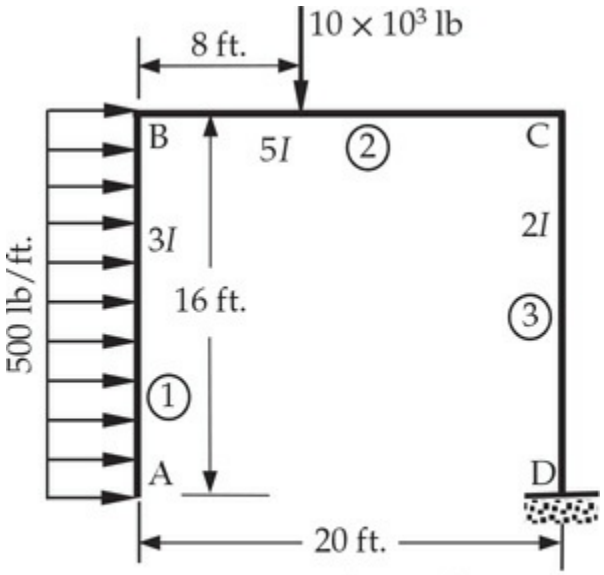

$E = 30 \times 10^6$ lb/in.^{2},
$A = 100$ in.^{2}, $I = 200$ in.^{4}

Fig. P6.16

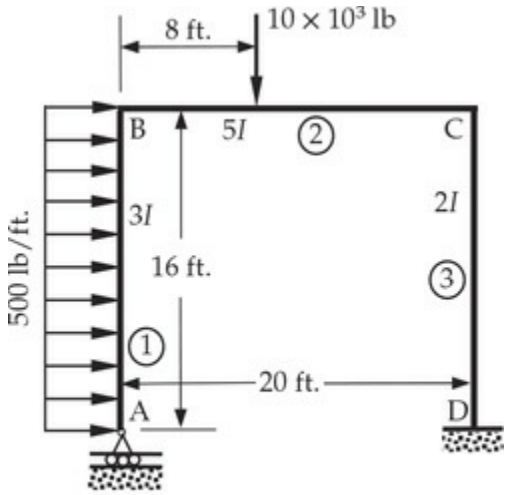

Fig. P6.17

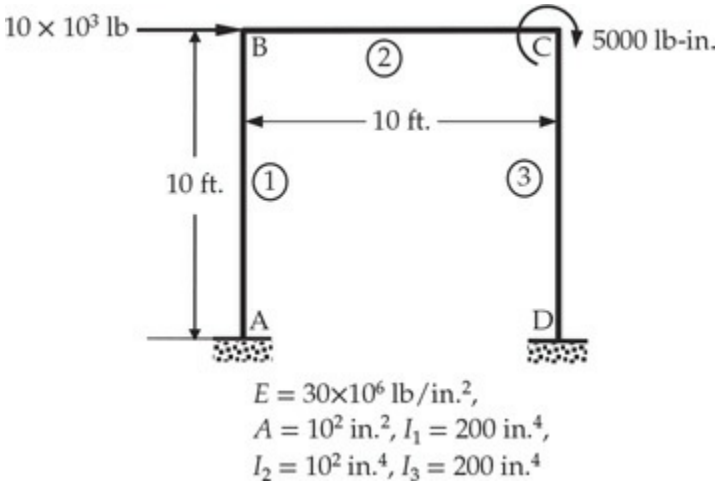

Fig. P6.18

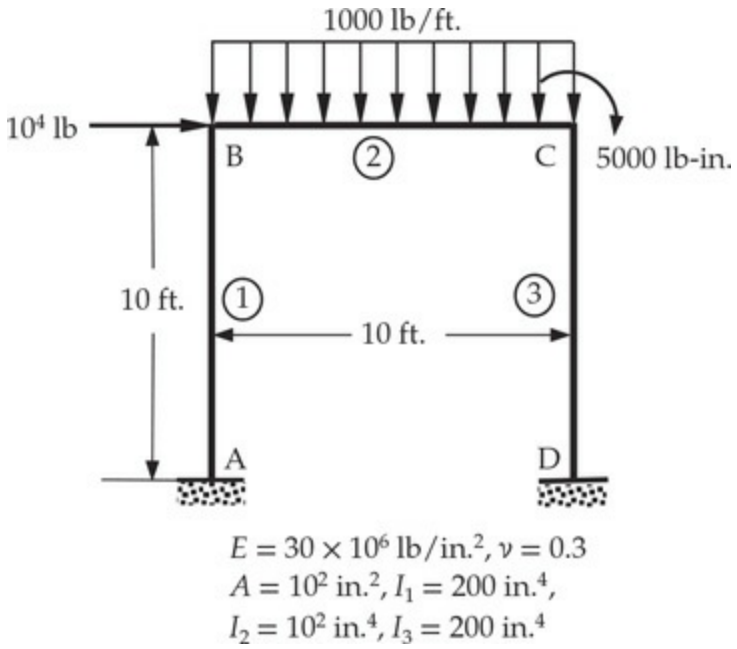

Fig. P6.19

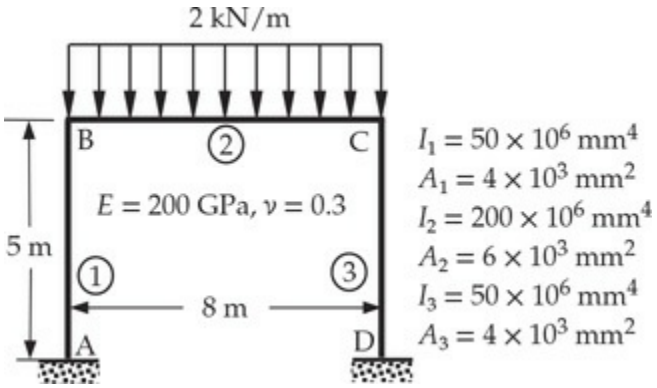

Fig. P6.20

References for Additional Reading

1. J. N. Reddy, *Energy Principles and Variational Methods in Applied Mechanics*, 3rd ed., John Wiley & Sons, New York, 2017.
2. J. N. Reddy, *Theory and Analysis of Elastic Plates and Shells*, 2nd ed., CRC Press, Boca Raton, FL, 2007.
3. W. McGuire, R. H. Gallagher, and R. D. Ziemian, *Matrix Structural Analysis*, 2nd ed., John Wiley & Sons, New York, NY, 2000.
4. C.-K. Wang and C. G. Salmon, *Introductory Structural Analysis*, Prentice-Hall, Englewood Cliffs, NJ, 1984.

5. N. Willems and W. M. Lucas, Jr., *Structural Analysis for Engineers*, McGraw-Hill, New York, NY, 1978.

7 Eigenvalue and Time-Dependent Problems in 1-D

I can calculate the motion of heavenly bodies but not the madness of people.

— Isaac Newton

7.1 Introduction

All phenomena in nature are time-dependent. When the external stimuli causing the motion is independent of time, the phenomena may attain a steady-state (i.e., the response does not change with time) at some point in time. Otherwise, the response of the system continues to change with time (i.e., unsteady response). The governing equations of an unsteady response are obtained using an appropriate physical principle. For example, in the case of heat transfer the principle is the balance of energy and in the case of fluid mechanics and solid mechanics, the principle is the balance of linear momentum. When the motion is periodic or decay type, the time-dependent equations can be reduced to a special kind of steady-state equations, called *eigenvalue problems*. In addition, certain problems can be formulated directly as eigenvalue problems, for example, buckling of beam-columns under compressive loads. A detailed discussion of eigenvalue problems is presented in Section 7.3.

This chapter is dedicated to finite element formulations of equations governing both eigenvalue problems and time-dependent problems. The finite element models of eigenvalue problems can also be obtained from the finite element models of time-dependent problems under the assumption of periodic motion or motion of decay type, as discussed in Section 7.3. The general scheme of finite element model development is shown in the flowchart of Fig. 7.2.1. We begin with a summary of the time-dependent versions of the steady-state (or equilibrium) equations already introduced in Chapters 3 through 5.

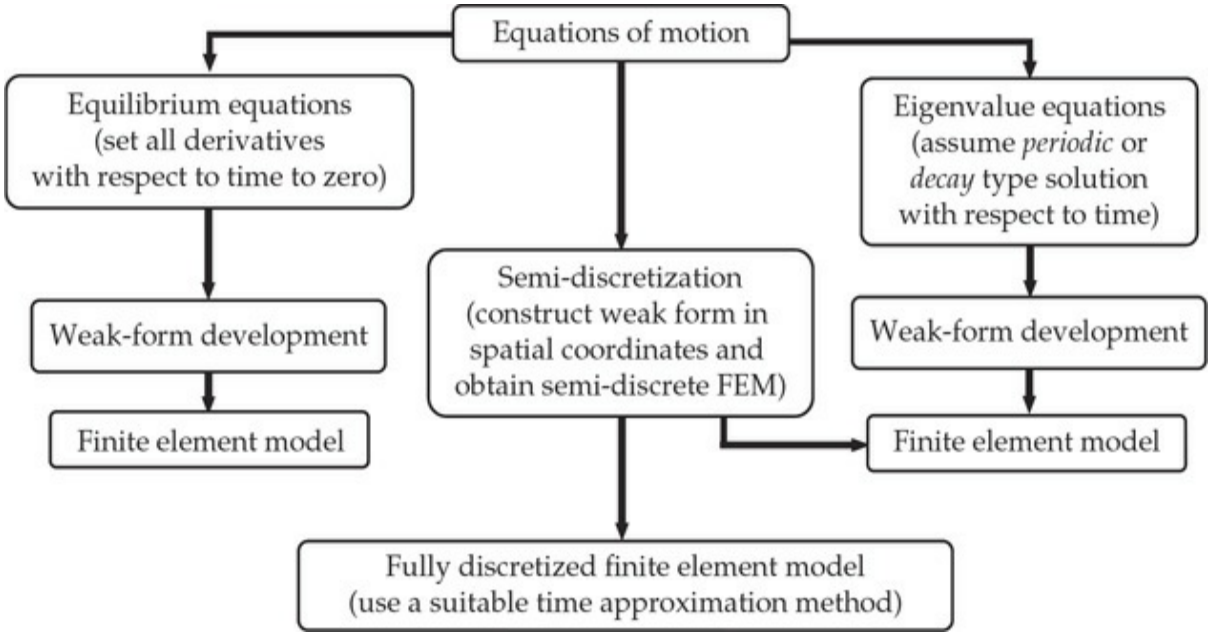

Fig. 7.2.1 Flowchart showing the finite element model development.

7.2 Equations of Motion

7.2.1 One-Dimensional Heat Flow

The principle of balance of energy, which can be stated as the time-rate of change of internal energy of a system is equal to the heat input to the system, for a one-dimensional heat flow (e.g., in a plane wall or a fin) results in the equation

$$c_1 \frac{\partial u}{\partial t} - \frac{\partial}{\partial x}\left(kA\frac{\partial u}{\partial x}\right) = f(x,t), \quad 0 < x < L, \quad t > 0 \tag{7.2.1}$$

where u denotes the temperature above a reference temperature ($u = T - T_0$), $c_1 = c_v \rho A$, k denotes the thermal conductivity, ρ is the mass density, A is the cross-sectional area, c_v is the specific heat at constant volume, and f is the internal heat generation per unit length, all of which can be, in general, known functions of position x and time t.

7.2.2 Axial Deformation of Bars

The following equation of motion arises in connection with the axial motion of a bar:

$$c_2\frac{\partial^2 u}{\partial t^2}-\frac{\partial}{\partial x}\left(EA\frac{\partial u}{\partial x}\right)=f(x,t),\quad 0<x<L,\quad t>0 \tag{7.2.2}$$

where u denotes the axial displacement, $c_2 = \rho A$, E is the modulus of elasticity, A is the area of cross section, ρ is the mass density, and f is the axial force per unit length.

7.2.3 Bending of Beams: The Euler–Bernoulli Beam Theory

The equation of motion of bending of beams using the Euler–Bernoulli beam theory is given by (see **Examples 2.3.5** and **2.3.6** and the textbook by Reddy [1], pp. 73–76 for the development of the EBT)

$$c_2\frac{\partial^2 w}{\partial t^2}-c_3\frac{\partial^4 w}{\partial t^2\partial x^2}+\frac{\partial^2}{\partial x^2}\left(EI\frac{\partial^2 w}{\partial x^2}\right)=q(x,t),\quad 0<x<L,\quad t>0 \tag{7.2.3}$$

where $c_2 = \rho A$ and $c_3 = \rho I$; ρ denotes the mass density per unit length, A the area of cross section, E the modulus, and I the moment of inertia.

7.2.4 Bending of Beams: The Timoshenko Beam Theory

The equations of motion of the Timoshenko beam theory are (see **Example 2.4.3** and Reddy [1], pp. 76–78 for the development of the TBT)

$$c_2\frac{\partial^2 w}{\partial t^2}-\frac{\partial}{\partial x}\left[GAK_s\left(\frac{\partial w}{\partial x}+\phi_x\right)\right]=q(x,t) \tag{7.2.4a}$$

$$c_3\frac{\partial^2 \phi}{\partial t^2}-\frac{\partial}{\partial x}\left(EI\frac{\partial \phi_x}{\partial x}\right)+GAK_s\left(\frac{\partial w}{\partial x}+\phi_x\right)=0 \tag{7.2.4b}$$

for $0 < x < L$, $t > 0$, where G is the shear modulus ($G = E/[2(1 + \nu)]$) and K_s is the shear correction factor (a typical value is $K_s = 5/6$); all other parameters have the same meaning as in Eq. (7.2.3).

Thus, almost all linear physical systems of engineering and applied science are described, in general, by operator equations of the type (here u is a generic dependent variable)

$$A_t u + A_{xt} u + A_x u = f(\mathbf{x}, t) \text{ in } \Omega \tag{7.2.5}$$

where A_t is a linear differential operator in time t, A_x is a linear differential operator in the spatial coordinates $\mathbf{x}$, A_{xt} is a linear differential operator in

both t and $\mathbf{x}$, f is a "forcing" function of position $\mathbf{x}$ and time t. Examples of the operator equation Eq. (7.2.5) are provided by Eqs. (7.2.1)–(7.2.4b), where operators A_t, A_{xt}, and A_x can be readily identified [$A_{xt} \neq 0$ only in Eq. (7.2.3)].

Equations containing first-order time derivatives are called *parabolic equations* while those containing second-order time derivatives are termed *hyperbolic equations*. The operator equations that describe the steady-state response can be obtained by setting the time-dependent parts to zero. Analysis of the time-dependent problems to determine their time-dependent solution $u(\mathbf{x}, t)$ is known as the *transient analysis* and $u(\mathbf{x}, t)$ is called the *transient response*, and it is presented in Section 7.4. The eigenvalue problem associated with a time-dependent problem can be derived from the governing equations of motion by assuming a suitable (i.e., decaying or periodic type) solution form. Details are presented in the next section.

7.3 Eigenvalue Problems

7.3.1 General Comments

An *eigenvalue problem* is defined to be one in which we seek the values of the parameter λ and function $u(\mathbf{x})$ such that the equation

$$Au = \lambda Bu \tag{7.3.1}$$

is satisfied for all nontrivial values of $u = u(\mathbf{x})$. Here A and B denote either matrix operators or differential operators and u is either a vector or a function to be determined along with λ. The values of λ for which Eq. (7.3.1) is satisfied are called *eigenvalues*, and for each value of λ there is a nonzero vector u for which Eq. (7.3.1) holds is called *eigenvector* or *eigenfunction*. Equation (2.5.41) provides an example of the eigenvalue problems, where operators A and B are given by

$$Au = -\frac{d}{dx}\left(EA\frac{du}{dx}\right), \quad Bu = \rho A\, u \tag{7.3.2}$$

and $\lambda = \omega^2$, ω being the natural frequency of axial vibration of a bar.

In general, the determination of the eigenvalues is of engineering as well as mathematical importance. In structural problems, eigenvalues denote either (the square of) the natural frequencies or buckling loads. In

fluid mechanics and heat transfer, eigenvalue problems arise in connection with the determination of the homogeneous parts of the transient solution, as will be shown shortly. In these cases, eigenvalues often denote amplitudes of the Fourier components making up the solution. Eigenvalues are also useful in determining the stability characteristics of time-approximation schemes, as will be discussed in Section 7.4.

7.3.2 Physical Meaning of Eigenvalues

In this section, analytical solutions of one-dimensional problems are discussed to show the physical meaning of the eigenvalues and how they enter the representation of the solution. This is particularly useful in the case of heat transfer problems, where eigenvalues are more mathematical in nature than in structural mechanics, where eigenvalues represent (a) the square of the frequencies of natural vibration or (b) buckling loads.

Consider Eq. (7.2.1) governing one-dimensional heat flow in a bar. The homogenous solution (i.e., the solution when $f = 0$) of Eq. (7.2.1) is often sought in the form of a product of a function of x and a function of t (i.e., through the *separation of variables* technique):

$$u^h(x,t) = U(x)\,T(t) \tag{7.3.3}$$

Substitution of this assumed form of solution into the homogeneous form of Eq. (7.2.1) gives

$$c_1 U \frac{dT}{dt} - \frac{d}{dx}\left(kA\frac{dU}{dx}\right)T = 0 \tag{7.3.4}$$

Separating variables of t and x (i.e., dividing throughout by $c_1\,UT$), we arrive at the equations

$$\frac{1}{T}\frac{dT}{dt} = \frac{1}{c_1}\frac{1}{U}\left[\frac{d}{dx}\left(kA\frac{dU}{dx}\right)\right] \tag{7.3.5}$$

Note that the left-hand side of this equation is a function of t only while the right-hand side is a function of x only. For two expressions to be equal for all values of the independent parameters x and t, both expressions must be equal to the same constant, say $-\lambda$ ($\lambda > 0$), and we obtain

$$\frac{1}{T}\frac{dT}{dt} = \frac{1}{c_1}\frac{1}{U}\left[\frac{d}{dx}\left(kA\frac{dU}{dx}\right)\right] = -\lambda \tag{7.3.6}$$

or

$$\frac{dT}{dt} = -\lambda T \tag{7.3.7}$$

$$-\frac{d}{dx}\left(kA\frac{dU}{dx}\right) = \lambda c_1 U \tag{7.3.8}$$

The negative sign of the constant λ is based on the physical requirement that the solution $U(x)$ be harmonic in x while $T(t)$ be a decaying function with increasing t. The problem of solving Eqs. (7.3.7) and (7.3.8) for λ and $U(x)$ will lead to an eigenvalue problem. With $T(t)$ and $U(x)$ known, we have the complete homogeneous solution (7.3.3) of Eq. (7.2.1).

The solution of Eq. (7.3.7) is

$$T(t) = Be^{-\lambda t} \tag{7.3.9}$$

where B is a constant of integration. When k, A, and $c_1 = \rho A c_v$ are constants, the solution of Eq. (7.3.8) is

$$U(x) = C\sin\alpha x + D\cos\alpha x, \quad \alpha^2 = \frac{\rho c_v}{k}\lambda \tag{7.3.10}$$

where C and D are constants of integration, which are determined using the boundary conditions of the problem. Suppose that the bar is subject to the boundary conditions (e.g., a fin with specified temperature at $x = 0$ and insulated at $x = L$)

$$U(0) = 0, \quad \left[kA\frac{dU}{dx}\right]_{x=L} = 0 \tag{7.3.11}$$

Using the boundary conditions in Eq. (7.3.11), we obtain

$$0 = C\cdot 0 + D\cdot 1, \quad 0 = \alpha(C\cos\alpha L - D\sin\alpha L) \Rightarrow C\alpha\cos\alpha L = 0 \tag{7.3.12}$$

For nontrivial solution (i.e., not both C and D are zero) and since α cannot be zero, we have

$$\cos\alpha L = 0 \;\rightarrow\; \alpha_n L = \frac{(2n-1)\pi}{2}, \quad n = 1, 2, \ldots, \infty \tag{7.3.13}$$

Hence, the homogeneous solution becomes [note that the constant B of Eq. (7.3.9) is absorbed into C_n]

$$u^h(x,t)=\sum_{n=1}^{\infty} C_n e^{-\lambda_n t}\sin\alpha_n x,\quad \lambda_n=\alpha_n^2\left(\frac{k}{\rho c_v}\right),\quad \alpha_n=\frac{(2n-1)\pi}{2L} \tag{7.3.14}$$

The constants C_n are determined using the initial condition of the problem. The complete solution of Eq. (7.2.1) is given by the sum of homogeneous solution and particular solution $u(x, t) = u^h(x, t) + u^p(x, t)$. Thus, the need for determining eigenvalues (λ_n) in the context of finding the transient response of a parabolic equation is clear.

Next, we consider the transient response of a bar, whose motion is described by Eq. (7.2.2). Again, the solution of Eq. (7.2.2) consists of two parts: homogeneous solution u^h (i.e., when $f = 0$) and particular solution u^p. The homogenous solution of Eq. (7.2.2) is assumed to be of the same form as in Eq. (7.3.3). Substitution of Eq. (7.3.3) into the homogeneous form of Eq. (7.2.2) gives

$$\rho AU\frac{d^2T}{dt^2}-\frac{d}{dx}\left(EA\frac{dU}{dx}\right)T=0 \tag{7.3.15}$$

Assuming that ρA and EA are functions of x only, we arrive at

$$\frac{1}{T}\frac{d^2T}{dt^2}=\frac{1}{\rho A}\frac{1}{U}\frac{d}{dx}\left(EA\frac{dU}{dx}\right)=-\lambda^2 \tag{7.3.16}$$

or

$$\frac{d^2T}{dt^2}+\lambda^2T=0 \tag{7.3.17}$$

$$-\frac{d}{dx}\left(EA\frac{dU}{dx}\right)-\lambda^2\rho AU=0 \tag{7.3.18}$$

The negative sign of the constant λ is based on the physical requirement that the solution $u(x, t)$ be harmonic in x and t.

The solution of Eq. (7.3.17) is

$$T(t)=B_1\cos\lambda t+B_2\sin\lambda t \tag{7.3.19}$$

where B_1 and B_2 are constants of integration. The solution of Eq. (7.3.18), when E, A, and ρ are constants, is

$$U(x)=C\sin\alpha x+D\cos\alpha x,\quad \alpha^2=\frac{\rho}{E}\lambda^2 \tag{7.3.20}$$

where C and D are constants of integration. In the process of determining the constants C and D using the boundary conditions of the problem, once again we are required to solve an eigenvalue problem. For example, for a bar fixed at the left end and free (for the homogeneous solution) at the right end, the boundary conditions take the same form as in Eq. (7.3.11) (with k replaced by E). Hence we obtain $D = 0$ and $C\alpha \cos \alpha L = 0$, giving the same result as in Eq. (7.3.13). The homogeneous solution becomes (C is absorbed into constants B_{1n} and B_{2n}):

$$u^h(x,t) = \sum_{n=1}^{\infty} (B_{1n} \cos \lambda_n t + B_{2n} \sin \lambda_n t) \sin \alpha_n x$$
$$\lambda_n = \alpha_n \sqrt{E/\rho}, \quad \alpha_n = \frac{(2n-1)\pi}{2L} \tag{7.3.21}$$

The constants B_{1n} and B_{2n} are determined using the initial conditions on u and its time derivative.

Unlike in the case of heat conduction problem, the eigenvalues λ_n in the case of bars have direct physical meaning, namely, natural frequencies of the system (as will be seen shortly). Thus, in structural mechanics one may be interested in determining only the natural frequencies of the system but not the transient response.

7.3.3 Reduction of the Equations of Motion to Eigenvalue Equations

7.3.3.1 Parabolic equations: Heat transfer and like problems

The eigenvalue problems associated with homogeneous parabolic equations of the type in Eq. (7.2.1) are obtained by assuming solution of the form

$$u(x,t) = U(x)e^{-\lambda t} \tag{7.3.22}$$

where we wish to determine both U and λ. Substitution of Eq. (7.3.22) into Eq. (7.2.1) (with $f = 0$) yields

$$e^{-\lambda t}\left[-c_1 \lambda U - \frac{d}{dx}\left(kA\frac{dU}{dx}\right)\right] = 0, \quad 0 < x < L, \quad t > 0 \tag{7.3.23}$$

Since $e^{-\lambda t} \neq 0$, we have the eigenvalue problem

$$-\frac{d}{dx}\left(kA\frac{dU}{dx}\right)-c_1\lambda U=0,\quad 0<x<L \tag{7.3.24}$$

7.3.3.2 Hyperbolic equations: Bars

Consider the homogeneous [i.e., $f = 0$ in Eq. (7.2.2)] equation governing the axial motion of bars. Assume solution of the periodic type

$$u(x,t)=U(x)e^{-i\omega t},\quad i=\sqrt{-1} \tag{7.3.25}$$

where ω denotes the frequency of the periodic motion (the period of oscillation is given by $T = 2\pi/\omega$). Substituting Eq. (7.3.25) into Eq. (7.2.2), we obtain

$$\left[-c_2\omega^2U-\frac{d}{dx}\left(EA\frac{dU}{dx}\right)\right]e^{-i\omega t}=0,\quad 0<x<L,\quad t>0 \tag{7.3.26}$$

Since $e^{-i\omega t} \neq 0$, we have the eigenvalue problem

$$-\frac{d}{dx}\left(EA\frac{dU}{dx}\right)-c_2\lambda U=0,\quad 0<x<L,\quad \lambda=\omega^2 \tag{7.3.27}$$

7.3.3.3 Hyperbolic equations: Euler–Bernoulli beams

For the Euler–Bernoulli beam theory, the homogeneous equation of motion [i.e., set $q = 0$ in Eq. (7.2.3)] is reduced to the eigenvalue problem by substituting $w(x, t) = W(x)e^{-i\omega t}$:

$$\frac{d^2}{dx^2}\left(EI\frac{d^2W}{dx^2}\right)-\omega^2\rho\left(AW-I\frac{d^2W}{dx^2}\right)=0 \tag{7.3.28}$$

We wish to determine the natural frequencies ω and the associated mode shapes

7.3.3.4 Hyperbolic equations: Timoshenko beams

Following the same procedure as in the case of the Euler–Bernoulli beam theory, the homogeneous form of the equations of motion of the Timoshenko beam theory, Eqs. (7.2.4a) and (7.2.4b), can be reduced to eigenvalue equations by assuming periodic motion of the form

$$w(x,t)=W(x)e^{-i\omega t},\quad \phi_x(x,t)=S(x)e^{-i\omega t} \tag{7.3.29}$$

We obtain the following differential equations governing natural vibration of beams according to the Timoshenko beam theory:

$$-\frac{d}{dx}\left[GAK_s\left(\frac{dW}{dx}+S\right)\right]-\omega^2\rho AW=0 \tag{7.3.30a}$$

$$-\frac{d}{dx}\left(EI\frac{dS}{dx}\right)+GAK_s\left(\frac{dW}{dx}+S\right)-\omega^2\rho I\,S=0 \tag{7.3.30b}$$

We wish to determine the natural frequency ω and the mode shape (W, S).

7.3.4 Eigenvalue Problem: Buckling of Beams

7.3.4.1 Euler–Bernoulli beam theory

The study of buckling (also called stability) of beam-columns also leads to an eigenvalue problem. For example, equation governing the onset of buckling of a column subjected to an axial compressive force N^0 (see Fig. 7.3.1) according to the Euler–Bernoulli beam theory is (see Reddy [1,2])

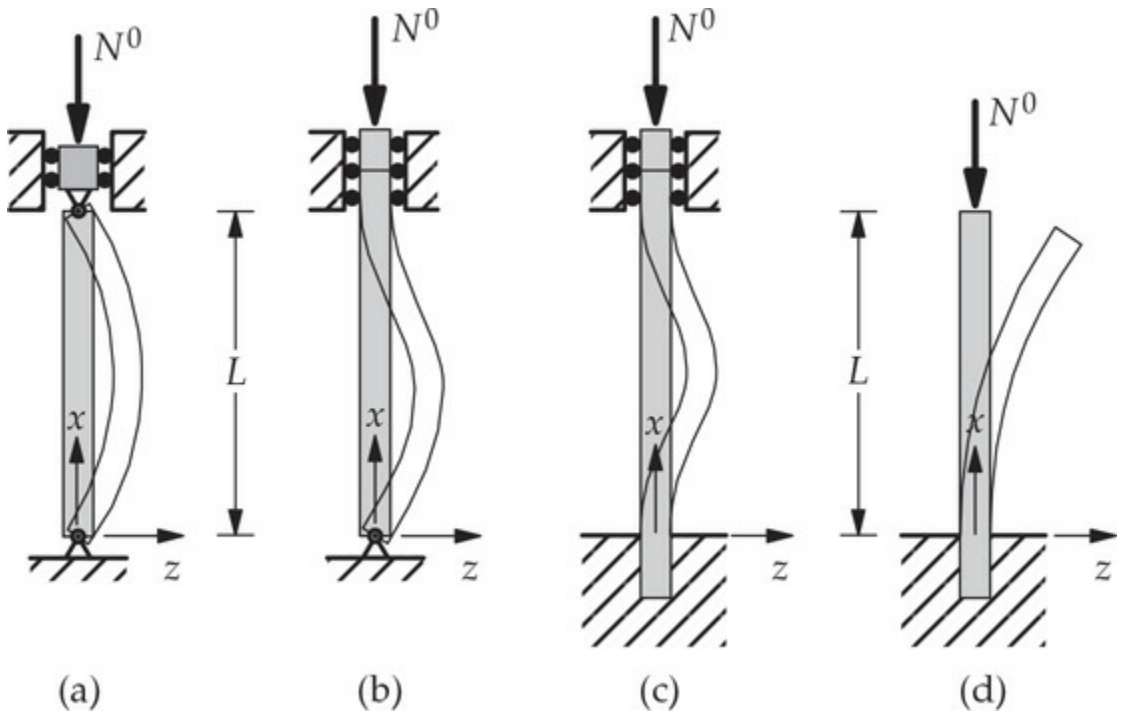

Fig. 7.3.1 Columns with different boundary conditions and subjected to axial compressive load, N^0. (a) Hinged–hinged. (b) Hinged–clamped. (c) Clamped–clamped. (d) Clamped–free.

$$\frac{d^2}{dx^2}\left(EI\frac{d^2W}{dx^2}\right)+N^0\frac{d^2W}{dx^2}=0 \tag{7.3.31}$$

where $W(x)$ is the lateral deflection at the onset of buckling. Equation (7.3.31) describes an eigenvalue problem with $\lambda = N^0$. The smallest value

of N^0 is called the *critical buckling load*.

7.3.4.2 Timoshenko beam theory

For the Timoshenko beam theory, the equations governing buckling of beams are given by

$$-\frac{d}{dx}\left[GAK_s\left(\frac{dW}{dx}+S\right)\right]+N^0\frac{d^2W}{dx^2}=0 \tag{7.3.32a}$$

$$-\frac{d}{dx}\left(EI\frac{dS}{dx}\right)+GAK_s\left(\frac{dW}{dx}+S\right)=0 \tag{7.3.32b}$$

Here $W(x)$ and $S(x)$ denote the transverse deflection and rotation, respectively, at the onset of buckling. Equations (7.3.32a) and (7.3.32b) together define an eigenvalue problem of finding the buckling load N^0 (eigenvalue) and the associated mode shape defined by $W(x)$ and $S(x)$ (eigenvector).

This completes the descriptions of the types of eigenvalue problems that will be treated in this chapter. The task of determining natural frequencies and mode shapes of a structure undergoing free (or natural) vibration is termed *modal analysis*. In addition, we also study buckling of beam-columns. In the following sections, we develop weak forms and finite element models of the eigenvalue problems described here. Numerical examples will be presented to illustrate the procedure of determining eigenvalues and eigenvectors, although this exercise may be familiar to the readers from other courses (e.g., a course on vibrations).

7.3.5 Finite Element Models

In this section, we develop finite element models of eigenvalue problems described by differential equations of heat transfer, bars, and beams. In view of the close similarity between the differential equations governing eigenvalue and boundary value problems, the steps involved in the construction of their finite element models are entirely analogous. The eigenvalue problems described by differential equations are reduced to algebraic eigenvalue problems by means of finite element approximations. The methods of solution of algebraic eigenvalue problems are then used to solve for the eigenvalues λ and eigenvectors.

We note that a continuous system has an infinite number of eigenvalues while a discrete system has only a finite number of

eigenvalues. The number of eigenvalues is equal to the number of unconstrained primary degrees of freedom in the mesh. The number of eigenvalues will increase with a mesh refinement, and the newly added eigenvalues will be larger in magnitude.

7.3.5.1 Heat transfer and bar-like problems (second-order equations)

Governing equation. The eigenvalue problem associated with one-dimensional heat flow and straight bars both share the same type of governing equation:

$$-\frac{d}{dx}\left(a\frac{dU}{dx}\right)+c_0U-c\lambda U=0,\quad 0<x<L \tag{7.3.33}$$

Here a, c_0 and c are known parameters (data) that depend on the physical problem, λ is the eigenvalue, and U is the eigenfunction. Special cases of Eq. (7.3.33) are given below.

$$\text{Heat transfer:}\quad a=kA,\quad c_0=P\beta,\quad c=\rho c_v A \tag{7.3.34}$$

$$\text{Bars:}\quad a=EA,\quad c_0=0,\quad c=c_2=\rho A \tag{7.3.35}$$

Weak form. In view of the discussion of Chapters 3 and 4, the weak form of Eq. (7.3.33) over $\Omega^e=(x_a^e,x_b^e)$ can be readily obtained as

$$0=\int_{x_a^e}^{x_b^e}\left(a\frac{dw_i}{dx}\frac{dU_h}{dx}+c_0w_iU_h-\lambda cw_iU_h\right)dx-Q_1^e w_i(x_a^e)-Q_n^e w_i(x_b^e) \tag{7.3.36}$$

where U_h is an approximation of U, w_i is the ith weight function (which will be replaced with ψ_i^e in deriving the finite element model), and Q_1^e and Q_n^e are the secondary variables at the first and last nodes, respectively, of a finite element with n nodes (for eigenvalue problems, we take $Q_i^e=0$ for $1<i<n$):

$$Q_1^e=-\left[a\frac{dU_h}{dx}\right]_{x_a^e},\quad Q_n^e=\left[a\frac{dU_h}{dx}\right]_{x_b^e} \tag{7.3.37}$$

Finite element model. Over a typical element $\Omega^e=(x_a^e,x_b^e)$, we seek a finite element approximation U_h as

$$U_h(x) = \sum_{j=1}^{n} u_j^e \psi_j^e(x) \tag{7.3.38}$$

Substitution of the finite element approximation (7.3.38) for U_h and $w_i = \psi_i^e$ into the weak form gives the weak-form Galerkin finite element model:

$$(\mathbf{K}^e - \lambda \mathbf{M}^e)\mathbf{u}^e = \mathbf{Q}^e \tag{7.3.39}$$

where

$$K_{ij}^e = \int_{x_a^e}^{x_b^e} \left(a \frac{d\psi_i^e}{dx} \frac{d\psi_j^e}{dx} + c_0 \psi_i^e \psi_j^e \right) dx, \quad M_{ij}^e = \int_{x_a^e}^{x_b^e} c \psi_i^e \psi_j^e \, dx \tag{7.3.40}$$

When a, c_0, and c are element-wise constant, the numerical values of $\mathbf{K}^e$ and $\mathbf{M}^e$ for linear and quadratic elements are available from Eqs. (3.4.36) and (3.4.38), respectively.

The assembly of element equations and imposition of boundary conditions on the assembled equations remain the same as in the static problems of Chapter 3. The condensed finite element equations of an eigenvalue problem are the following general form:

$$(\mathbf{K}_c - \lambda \mathbf{M}_c)\mathbf{U}_c = 0 \tag{7.3.41}$$

where the subscript c on $\mathbf{K}_c$ and $\mathbf{M}_c$ indicates that they are the condensed matrices and $\mathbf{U}_c$ denotes the global nodal degrees of freedom that are not specified. The solution of the condensed equations for λ and $\mathbf{U}_c$ constitutes the algebraic eigenvalue problem. There are several numerical methods of solving eigenvalue problems and they will not be discussed here, in the same way that no attempt has been made in this book to discuss numerical solution of linear algebraic equations (see Hildebrand [3]).

The analytical method of solving an eigenvalue problem involves setting the determinant of the coefficient matrix to zero (see Hildebrand [3], Reddy [1, 2], and Surana and Reddy [4]):

$$|\mathbf{K}_c - \lambda \mathbf{M}_c| = 0 \tag{7.3.42}$$

which yields an Nth degree algebraic polynomial in λ, known as the *characteristic equation*, where N denotes the number of unknown nodal values (i.e., the size of $\mathbf{U}_c$ is $N \times 1$ and that of $\mathbf{K}_c$ and $\mathbf{M}_c$ is $N \times N$). The

roots of the polynomial, known as the *eigenvalues* or *characteristic values*, are denoted as $\lambda_1, \lambda_2, \ldots, \lambda_N$.

In most problems of engineering interest, especially the undamped systems considered in this book, matrices $\mathbf{K}_c$ and $\mathbf{M}_c$ are real (i.e., not complex) and symmetric, and $\mathbf{M}_c$ is nonsingular. It can be shown that all eigenvalues and eigenvectors of real symmetric matrices are real. In addition, the eigenvectors of two different eigenvalues are orthogonal with respect to $\mathbf{M}_c$ in the sense:

$$(\mathbf{U}^{(i)})^{\mathrm{T}}\mathbf{M}_c\mathbf{U}^{(j)} = 0 \quad \text{for } i \neq j \tag{7.3.43}$$

When both $\mathbf{K}_c$ and $\mathbf{M}_c$ are positive definite, the eigenvalues determined from Eq. (7.3.42) are all positive (see Hildebrand [3] for the details).

There exists at least one eigenvector (or modal vector) $\mathbf{U}^{(i)}$ associated with each eigenvalue λ_i, which is determined within an arbitrary multiplicative constant from

$$(\mathbf{K}_c - \lambda_i\mathbf{M}_c)\mathbf{U}_c^{(i)} = 0 \tag{7.3.44}$$

which provides $N - 1$ relations among the N components $U_n^{(i)}$, $n = 1, 2, \ldots, N$. Therefore, one of the components, say $U_1^{(i)}$, is set to unity and the remaining are determined with respect to that component.

It is often convenient to "normalize" the eigenvectors $\mathbf{U}^{(k)}$ associated with the kth eigenvalue with respect to $\mathbf{M}_c$ such that each is a unit vector:

$$\hat{\mathbf{U}}^{(k)} = \frac{\mathbf{U}^{(k)}}{\|\mathbf{U}^{(k)}\|_M}, \quad \|\mathbf{U}^{(k)}\|_M^2 = \sum_{i,j=1}^{N} m_{ij}U_i^{(k)}U_j^{(k)} \tag{7.3.45}$$

If the components $U_i^{(k)}$ are dimensionally different from each other, they all should be expressed in dimensionless form before the normalization is used. The eigenfunction $U_h^{(k)}(x)$ is then determined using the expression in Eq. (7.3.38) in each element.

Let us define an orthonormal *modal matrix* $\mathbf{\Phi}$, associated with Eq. (7.3.41), as the matrix whose kth column is the kth normalized eigenvector $\hat{\mathbf{U}}^{(k)}$. Then, since

$$\mathbf{K}_c\hat{\mathbf{U}}^{(i)} = \lambda_i\mathbf{M}_c\hat{\mathbf{U}}^{(i)} \quad (i = 1, 2, \ldots, N) \tag{7.3.46}$$

there follows

$$\mathbf{K}_c\boldsymbol{\Phi} = \mathbf{M}_c\boldsymbol{\Phi}\begin{bmatrix} \lambda_1 & 0 & \cdots & 0 \\ 0 & \lambda_2 & \cdots & 0 \\ \cdots & \cdots & \cdots & \cdots \\ 0 & 0 & \cdots & \lambda_N \end{bmatrix} \equiv \mathbf{M}_c\boldsymbol{\Phi}\boldsymbol{\Lambda} \tag{7.3.47}$$

Also, in view of Eq. (7.3.43), we have

$$\boldsymbol{\Phi}^{\mathrm{T}}\mathbf{M}_c\boldsymbol{\Phi} = \mathbf{I} \tag{7.3.48}$$

where **I** is the unit matrix of order $N \times N$. Then from Eqs. (7.3.47) and (7.3.48), we have

$$\boldsymbol{\Phi}^{\mathrm{T}}\mathbf{K}_c\boldsymbol{\Phi} = \boldsymbol{\Phi}^{\mathrm{T}}\mathbf{M}_c\boldsymbol{\Phi}\boldsymbol{\Lambda} = \mathbf{I}\boldsymbol{\Lambda} = \boldsymbol{\Lambda}\mathbf{I} \tag{7.3.49}$$

Example 7.3.1

A plane wall with constant properties, initially at a uniform temperature T_0, has both surfaces suddenly exposed to a fluid at temperature T_∞. The governing differential equation is

$$k\frac{\partial^2 T}{\partial x^2} = \rho c_v \frac{\partial T}{\partial t} \tag{1}$$

where k is the thermal conductivity, ρ the density, and c_v the specific heat at constant volume. Equation (1) is also known as the *diffusion equation* with diffusion coefficient $\alpha = k/\rho c_v$. Use the finite element method to determine the eigenvalues for the following two sets of boundary conditions, each representative of a different scenario for $x = L$:

Set 1. If the heat transfer coefficient at the surfaces of the wall is assumed to be infinite, the boundary conditions can be expressed as

$$T(0,t) = T_\infty, \quad T(L,t) = T_\infty \quad \text{for } t > 0 \tag{2}$$

Set 2. If we assume that the wall at $x = L$ is subjected to ambient temperature, we have

$$T(0,t) = T_\infty, \quad \left[k\frac{\partial T}{\partial x} + \beta(T - T_\infty)\right]_{x=L} = 0 \tag{3}$$

Use a mesh of two linear elements to determine the eigenvalues and the eigenfunctions and compare the results with those obtained with a single quadratic element. As discussed in Section 7.3.2, the eigenvalues and

eigenfunctions are useful in constructing the transient solution.

Solution: Equations (1)–(3) can be cast in a dimensionless form (not a necessary requirement). Let

$$\alpha = \frac{k}{\rho c_v}, \quad \xi = \frac{x}{L}, \quad \tau = \frac{\alpha t}{L^2}, \quad \theta(\xi,\tau) = \frac{T(\xi,\tau) - T_\infty}{T_0 - T_\infty} \tag{4}$$

Then Eqs. (1)–(3) become

$$-\frac{\partial^2\theta}{\partial\xi^2} + \frac{\partial\theta}{\partial\tau} = 0 \tag{5}$$

Set 1: $\theta(0,\tau) = 0, \quad \theta(1,\tau) = 0$ (6)

Set 2: $\theta(0,\tau) = 0, \quad \left(\frac{\partial\theta}{\partial\xi} + H\theta\right)\Big|_{\xi=1} = 0, \quad H = \frac{\beta L}{k}$ (7)

We note that the complete solution to the time-dependent problem in Eqs. (5)–(7) is a linear combination of the mode shapes U_n and temporal terms $e^{-\lambda_n\tau}$:

$$\theta(\xi,\tau) = \sum_{n=1}^{\infty} k_n U_n(\xi) e^{-\lambda_n\tau} \tag{8}$$

where k_n are constants that are determined using the initial condition (if we were to find the transient solution). In an approximate solution, the number of terms in the series (8) is finite (i.e., n is finite) and it is equal to the number of unconstrained (i.e., unspecified) nodal degrees of freedom in the mesh.

We set out to determine $U_n(\xi)$ and λ_n by converting the problem to an eigenvalue problem. To begin with assume solution of the form (i.e., decay type) $\theta(\xi, \tau) = U(\xi)e^{-\lambda\tau}$ (the subscript n is omitted for now and will be added when the number of eigenvalues of the system are greater than 1) and substitute in Eq. (5) and obtain the equation

$$-\frac{d^2U}{d\xi^2} - \lambda U = 0 \tag{9}$$

subjected to the boundary conditions

Set 1: $U(0) = 0, \quad U(1) = 0$ (10)

$$\textbf{Set 2:}\quad U(0)=0,\quad \left(\frac{dU}{d\xi}+HU\right)\Big|_{\xi=1}=0 \tag{11}$$

Equation (9) is a special case of Eq. (7.3.33) with $a = 1$, $c = 1$, and $c_0 = 0$. Therefore, the finite element model in Eqs. (7.3.39) and (7.3.40) is valid here.

For a mesh of linear finite elements, the element equations (7.3.39) have the explicit form [see Eq. (3.4.36) with $c_e = 0$ for element matrices]

$$\left(\frac{1}{h_e}\begin{bmatrix}1 & -1\\ -1 & 1\end{bmatrix}-\lambda\frac{h_e}{6}\begin{bmatrix}2 & 1\\ 1 & 2\end{bmatrix}\right)\begin{Bmatrix}u_1^e\\ u_2^e\end{Bmatrix}=\begin{Bmatrix}Q_1^e\\ Q_2^e\end{Bmatrix} \tag{12}$$

For a mesh of two linear elements, with $h_1 = h_2 = 0.5$, the assembled equations (based on the requirement $Q_2^1 + Q_1^2 = 0$) are

$$\left(2\begin{bmatrix}1 & -1 & 0\\ -1 & 2 & -1\\ 0 & -1 & 1\end{bmatrix}-\frac{\lambda}{12}\begin{bmatrix}2 & 1 & 0\\ 1 & 4 & 1\\ 0 & 1 & 2\end{bmatrix}\right)\begin{Bmatrix}U_1\\ U_2\\ U_3\end{Bmatrix}=\begin{Bmatrix}Q_1^1\\ Q_2^1+Q_1^2=0\\ Q_2^2\end{Bmatrix} \tag{13}$$

For a mesh of one quadratic finite element ($h = 1$), the element equations (7.3.39) have the form [see Eq. (3.4.38) for element matrices]

$$\left(\frac{1}{3}\begin{bmatrix}7 & -8 & 1\\ -8 & 16 & -8\\ 1 & -8 & 7\end{bmatrix}-\frac{\lambda}{30}\begin{bmatrix}4 & 2 & -1\\ 2 & 16 & 2\\ -1 & 2 & 4\end{bmatrix}\right)\begin{Bmatrix}u_1^1\\ u_2^1\\ u_3^1\end{Bmatrix}=\begin{Bmatrix}Q_1^1\\ 0\\ Q_3^1\end{Bmatrix} \tag{14}$$

Solution for **set 1** *boundary conditions*

The boundary conditions $U(0) = 0$ and $U(1) = 0$ reduce to $U_1 = U_3 = 0$. For the mesh of two linear elements, the condensed equations are obtained by deleting the first and last rows and columns of the matrix equation in Eq. (13). Thus, we obtain the single equation

$$\left(4-\lambda\frac{4}{12}\right)U_2=0,$$

which can be solved for λ as

$$\lambda_1 = 12 \text{ because } U_2 \neq 0$$

The value of U_2 is arbitrary (a nonzero value); we take $U_2 = 1$. Hence, the

mode shape $U_h(\xi)$ is given by

$$U_h(\xi) = \begin{cases} U_1\psi_1^{(1)}(\xi) + U_2\psi_2^{(1)}(\xi) = U_2\dfrac{\xi}{h} = 2\xi & 0 \le \xi \le 0.5 \\ U_2\psi_1^{(2)}(\xi) + U_3\psi_2^{(2)}(\xi) = U_2\left(2 - \dfrac{\xi}{h}\right) = 2(1-\xi) & 0.5 \le \xi \le 1.0 \end{cases}$$

For a mesh of one quadratic element, Eq. (14) is all we consider. The condensed equation is

$$\frac{16}{3} - \lambda\frac{16}{30} = 0 \quad \text{or} \quad \lambda_1 = 10, \;\; U_2 \neq 0$$

The corresponding eigenfunction is (for $U_2 = 1$)

$$U_h(\xi) = U_1\psi_1^{(1)} + U_2\psi_2^{(1)} + U_3\psi_3^{(1)} = U_2\psi_2^{(1)} = 4\frac{\xi}{h}\left(1 - \frac{\xi}{h}\right), \;\; 0 \le \xi \le 1.0$$

Hence, the finite element approximation of $U(\xi)$ is

$$U_h(\xi) = \begin{cases} 2\xi & 0 \le \xi \le 0.5 \\ 2(1-\xi) & 0.5 \le \xi \le 1.0 \end{cases} \quad \text{for the mesh of two linear elements}$$

$$U_h(\xi) = 4\xi(1-\xi) \quad 0 \le \xi \le 1.0, \;\; \text{for the mesh of one quadratic element}$$

The analytical solution of Eq. (9) with boundary conditions in Eq. (10) is

$$\theta(\xi,\tau) = \sum_{n=1}^{\infty} k_n U_n(\xi) e^{-\lambda_n \tau} = \sum_{n=1}^{\infty} k_n \sin n\pi\xi \; e^{-(n\pi)^2\tau}, \quad \lambda_n = (n\pi)^2 \qquad (15)$$

where k_n are constants to be determined using the initial condition of the problem. Thus the exact eigenfunctions for set 1 boundary conditions are $U_n(\xi) = \sin n\pi\xi$. The one-term solution is

$$\theta(\xi,\tau) = k_1 \sin \pi\xi \, e^{-\pi^2\tau}$$

Clearly, one quadratic element mesh gives more accurate solution than the mesh of two linear elements when compared with the one-term analytical solution ($\pi^2 \approx 9.87$).

Solution for **set 2** *boundary conditions*

The set 2 boundary conditions translate into $U_1 = 0$ and $Q_2^2 + HU_3 = 0$ (or

$Q_3^1 + HU_3 = 0$). For a mesh of two linear elements, the condensed equations are obtained by deleting the first row and column of the assembled equations (13) and replacing $Q_2^2 = -HU_3$:

$$\left(\frac{1}{h}\begin{bmatrix} 2 & -1 \\ -1 & 1 \end{bmatrix} - \lambda\frac{h}{6}\begin{bmatrix} 4 & 1 \\ 1 & 2 \end{bmatrix}\right)\begin{Bmatrix} U_2 \\ U_3 \end{Bmatrix} = \begin{Bmatrix} 0 \\ -HU_3 \end{Bmatrix}$$

or

$$\left(\begin{bmatrix} 4 & -2 \\ -2 & 2+H \end{bmatrix} - \frac{\lambda}{12}\begin{bmatrix} 4 & 1 \\ 1 & 2 \end{bmatrix}\right)\begin{Bmatrix} U_2 \\ U_3 \end{Bmatrix} = \begin{Bmatrix} 0 \\ 0 \end{Bmatrix}$$

For a nontrivial solution (i.e., not both U_2 and U_3 are zero), the determinant of the coefficient matrix should be set to zero [see Eq. (7.3.42)]:

$$\begin{vmatrix} 4-4\bar{\lambda} & -(2+\bar{\lambda}) \\ -(2+\bar{\lambda}) & 2+H-2\bar{\lambda} \end{vmatrix} = 0, \quad \bar{\lambda} = \frac{\lambda}{12}$$

or

$$7\bar{\lambda}^2 - 4(5+H)\bar{\lambda} + 4(1+H) = 0$$

The above equation is known as the *characteristic equation* of the eigenvalue problem. The two roots of this quadratic equation for $H = 1$ are

$$\bar{\lambda}_{1,2} = \frac{12 \pm \sqrt{(12)^2 - 7\times 8}}{7} \rightarrow \bar{\lambda}_1 = 0.3742, \quad \bar{\lambda}_2 = 3.0544$$

and the eigenvalues are ($\lambda_i = 12\bar{\lambda}_i$) $\lambda_1 = 4.4899$ and $\lambda_2 = 36.6528$. The eigenvectors associated with each eigenvalue can be computed from the equations

$$\begin{bmatrix} 4-4\bar{\lambda}_i & -(2+\bar{\lambda}_i) \\ -(2+\bar{\lambda}_i) & 3-2\bar{\lambda}_i \end{bmatrix}\begin{Bmatrix} U_2 \\ U_3 \end{Bmatrix}^{(i)} = \begin{Bmatrix} 0 \\ 0 \end{Bmatrix}, \quad i = 1,2$$

For example, for $\bar{\lambda}_1 = 0.3742$, we have

$$2.5034U_2^{(1)} - 2.3742U_3^{(1)} = 0$$

Taking $U_2^{(1)} = 1$, we obtain

$$\mathbf{U}^{(1)} = \begin{Bmatrix} U_2^{(1)} \\ U_3^{(1)} \end{Bmatrix} = \begin{Bmatrix} 1.0000 \\ 1.0544 \end{Bmatrix}$$

On the other hand, we can normalize the components with respect to $\mathbf{M}_c$. To this end first calculate the square of the length of the vector $\mathbf{U}^{(1)}$ with respect to $\mathbf{M}_c$:

$$e_1^2 = (\mathbf{U}^{(1)})^{\mathrm{T}} \mathbf{M}_c \mathbf{U}^{(1)} = \{1.0 \;\; 1.0544\} \begin{bmatrix} 4 & 1 \\ 1 & 2 \end{bmatrix} \begin{Bmatrix} 1.0000 \\ 1.0544 \end{Bmatrix} = 8.3323$$

Then the normalized vector is ($\hat{U}_2^{(1)} = U_2^{(1)}/\sqrt{8.3323}$ and $\hat{U}_3^{(1)} = U_3^{(1)}/\sqrt{8.3323}$)

$$\hat{\mathbf{U}}^{(1)} = \begin{Bmatrix} \hat{U}_2^{(1)} \\ \hat{U}_3^{(1)} \end{Bmatrix} = \begin{Bmatrix} 0.34643 \\ 0.36528 \end{Bmatrix}$$

Thus, we obtain a mode shape whose amplitude is unique only within a multiplicative constant. Hence, the eigenfunction corresponding to λ_1 = 4.4899 is

$$U_h^{(1)}(\xi) = \begin{cases} 0.34643\,(2\xi) & \text{for } 0 \le \xi \le 0.5 \\ 0.34643\,(2-2\xi) + 0.36528(2\xi - 1) & \text{for } 0.5 \le \xi \le 1.0 \end{cases}$$

Similarly, the normalized eigenvector corresponding to λ_2 = 36.6528 is

$$\hat{\mathbf{U}}^{(2)} = \begin{Bmatrix} \hat{U}_2^{(2)} \\ \hat{U}_3^{(2)} \end{Bmatrix} = \begin{Bmatrix} 0.40706 \\ -0.66182 \end{Bmatrix}$$

The corresponding eigenfunction is given by

$$U_h^{(2)}(\xi) = \begin{cases} 0.40706\xi & \text{for } 0 \le \xi \le 0.5 \\ 0.40706(2-2\xi) - 0.66182(2\xi - 1) & \text{for } 0.5 \le x \le 1.0 \end{cases}$$

For a mesh of one quadratic element, the condensed equations are

$$\left(\frac{1}{3} \begin{bmatrix} 16 & -8 \\ -8 & 7+3H \end{bmatrix} - \lambda \frac{1}{30} \begin{bmatrix} 16 & 2 \\ 2 & 4 \end{bmatrix} \right) \begin{Bmatrix} U_2 \\ U_3 \end{Bmatrix} = \begin{Bmatrix} 0 \\ 0 \end{Bmatrix}$$

and the characteristic equation is

$$15\bar{\lambda}^2 - 4(13+3H)\bar{\lambda} + 12(1+H) = 0, \quad \bar{\lambda} = \frac{\lambda}{10}$$

The two roots of this quadratic equation for $H = 1$ are

$$\bar{\lambda}_{1,2} = \frac{32 \pm \sqrt{(32)^2 - 15 \times 24}}{15} \rightarrow \bar{\lambda}_1 = 0.4155, \quad \bar{\lambda}_2 = 3.8512$$

and the eigenvalues are $((\lambda_i = 10\bar{\lambda}_i)\ \lambda_1 = 4.1545)$ and $\lambda_2 = 38.5121$. The corresponding eigenvector are (not normalized)

$$\mathbf{U}^{(1)} = \begin{Bmatrix} U_2^{(1)} \\ U_3^{(1)} \end{Bmatrix} = \begin{Bmatrix} 1.0000 \\ 1.0591 \end{Bmatrix}, \quad \mathbf{U}^{(2)} = \begin{Bmatrix} U_2^{(2)} \\ U_3^{(2)} \end{Bmatrix} = \begin{Bmatrix} 1.0000 \\ -2.9052 \end{Bmatrix}$$

The eigenfunctions are given by ($h = 1$)

$$U_h^{(1)}(\xi) = U_2^{(1)}\psi_2(\xi) + U_3^{(1)}\psi_3(\xi) = 4\frac{\xi}{h}\left(1 - \frac{\xi}{h}\right) + 1.0591\,\frac{\xi}{h}\left(2\frac{\xi}{h} - 1\right)$$

$$U_h^{(2)}(\xi) = U_2^{(2)}\psi_2(\xi) + U_3^{(2)}\psi_3(\xi) = 4\frac{\xi}{h}\left(1 - \frac{\xi}{h}\right) - 2.9052\,\frac{\xi}{h}\left(2\frac{\xi}{h} - 1\right)$$

The analytical solution $U_n(\xi)$ for set 2 boundary conditions is

$$U_n(\xi) = \sin\sqrt{\lambda_n}\xi \tag{16}$$

where the eigenvalues λ_n are computed from the equation

$$H\sin\sqrt{\lambda_n} + \sqrt{\lambda_n}\cos\sqrt{\lambda_n} = 0$$

The first two roots of this transcendental equation are (for $H = 1$)

$$\sqrt{\lambda_1} = 2.0288 \rightarrow \lambda_1 = 4.1160; \quad \sqrt{\lambda_2} = 4.9132 \rightarrow \lambda_2 = 24.1393$$

Thus, the analytical solution for the two eigenfunctions is

$$U_1(\xi) = \sin 2.0288\,\xi, \quad U_2(\xi) = \sin 4.9132\,\xi \tag{17}$$

A comparison of the eigenvalues obtained using various meshes of linear elements and quadratic elements with the exact values is presented in Table 7.3.1. Note that the number of eigenvalues obtained in the finite element method is always equal to the number of unknown nodal values. As the mesh is refined, not only do we increase the number of eigenvalues but also improve the accuracy of the preceding eigenvalues. Note also that the convergence of the numerical eigenvalues to the exact

ones is from the above, that is, the finite element solution provides an upper bound to the exact eigenvalues. The first three mode shapes of the system are shown in Figs. 7.3.2 and 7.3.3 for set 1 and set 2 boundary conditions, respectively.

Table 7.3.1 Eigenvalues of the heat conduction equation (9) for the two sets of boundary conditions in Eqs. (10) and (11). For each mesh, the first row corresponds to set 1 boundary conditions and the second row to set 2 boundary conditions.

Mesh	λ_1	λ_2	λ_3	λ_4	λ_5	λ_6	λ_7
2L	12.0000						
	4.4900	36.6529					
4L	10.3866	48.0000	126.756				
	4.2054	27.3318	85.7864	177.604			
8L	9.9971	41.5466	99.4855	192.000	328.291	507.025	686.512
	4.1380	24.9088	69.1036	143.530	257.580	417.706	607.018
1Q	10.000						
	4.1545	38.5121					
2Q	9.9439	40.0000	128.723				
	4.1196	24.8995	81.4446	207.654			
4Q	9.8747	39.7754	91.7847	160.000	308.253	514.891	794.794
	4.1161	24.2040	64.7704	129.261	240.540	405.254	658.133
Exact-1	9.8696	39.4784	88.8264	157.914	246.740	355.306	483.611
Exact-2	4.1160	24.1393	63.6597	122.889	201.851	300.550	418.987

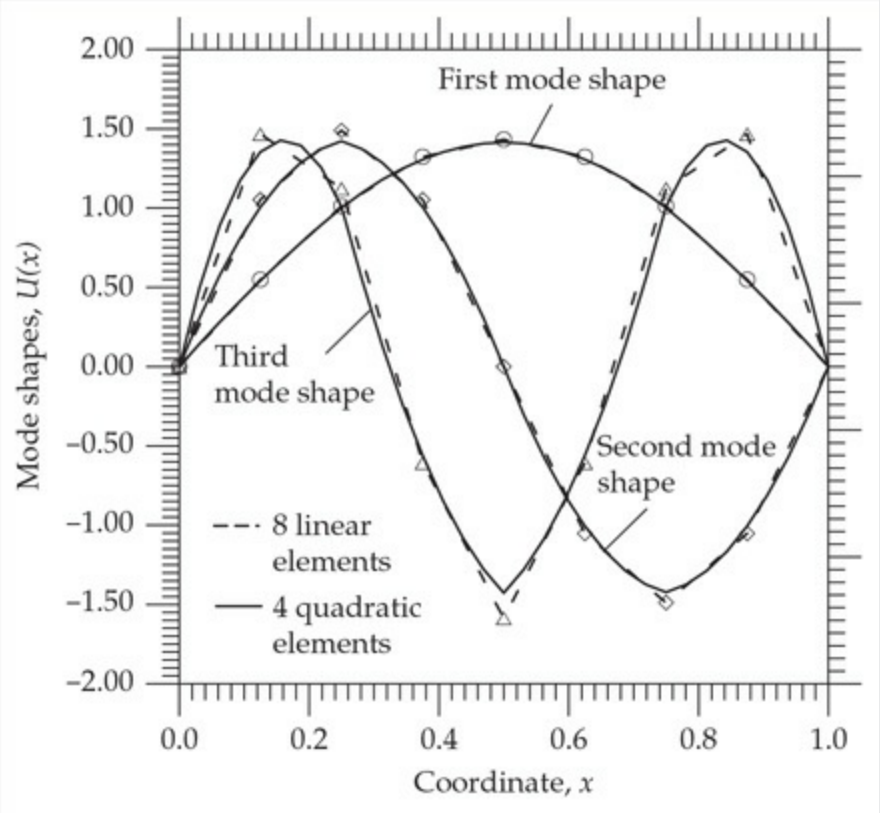

Fig. 7.3.2 The first three mode shapes as predicted by mesh of eight linear elements and a mesh of four quadratic elements for the heat transfer problem of **Example 7.3.1** (set 1 boundary conditions).

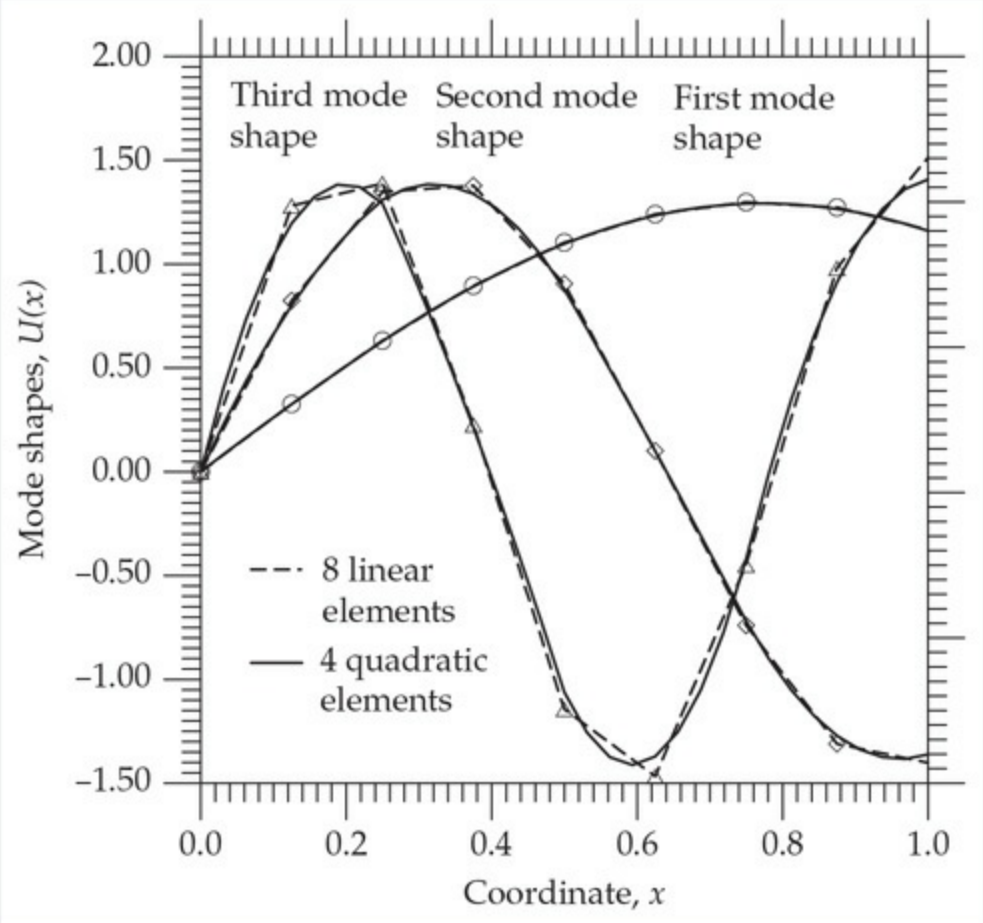

Fig. 7.3.3 The first three mode shapes of the heat transfer problem of **Example 7.3.1** (set 2 boundary conditions).

In view of the similarity of Eqs. (7.3.24) and (7.3.27), the eigenvalue problem described by Eqs. (9)–(11) can also be interpreted as those arising in connection with the axial vibrations of a constant cross-section member of length L and axial stiffness EA for the two sets of boundary conditions: (1) fixed at both ends and (2) fixed at the left end and connected to a linear elastic spring at the right end (see Fig. 7.3.4). We only need to use the following correspondence (U being the displacement mode shape and $\xi = x/L$):

$$\lambda = \omega^2 L^2 \frac{\rho}{E}, \quad H = \frac{kL}{EA}$$

Thus, the eigenvalues presented in Table 7.3.1 can be interpreted as $\omega^2 L^2 \rho/E$ of a uniform bar for the two different boundary conditions shown in Fig. 7.3.4. According to the principle of minimum total potential energy,

any approximate displacement field would over estimate the total potential energy of the system. This is equivalent to approximating the stiffness of the system with a larger value than the actual one. A stiffer system will have larger eigenvalues (or frequencies). As the number of elements is increased the stiffness is represented more closely to the actual stiffness, with the approximate stiffness always being larger than the exact.

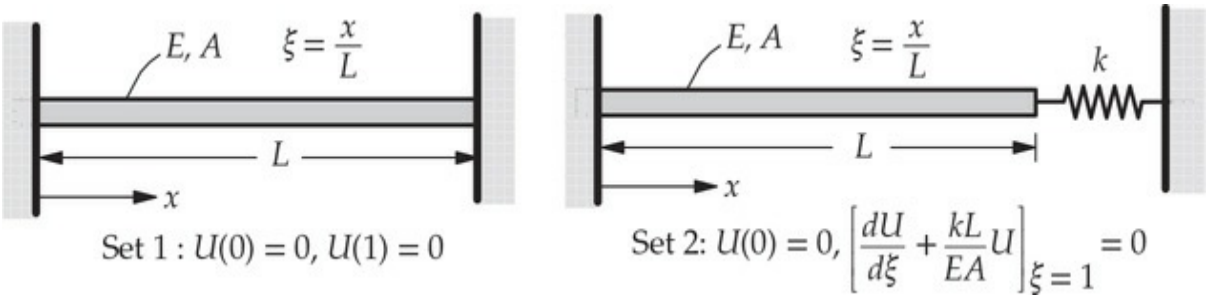

Fig. 7.3.4 Uniform bar with two sets of boundary conditions.

7.3.5.2 Natural vibration of Euler–Bernoulli beams

Weak form. The weak form of Eq. (7.3.28) is obtained by the same three-step procedure that was used in Chapter 5. In the present case, we must also integrate by parts the rotatory inertia term. We obtain

$$0 = \int_{x_a^e}^{x_b^e} \left[EI \frac{d^2 v_i}{dx^2} \frac{d^2 W_h}{dx^2} - \omega^2 \left(\rho A\, v_i W_h + \rho I \frac{dv_i}{dx} \frac{dW_h}{dx} \right) \right] dx$$
$$- v_i(x_a) Q_1^e - v_i(x_b) Q_3^e - \left(-\frac{dv_i}{dx} \right)_{x_a} Q_2^e - \left(-\frac{dv_i}{dx} \right)_{x_b} Q_4^e \qquad (7.3.50)$$

where W_h is the finite element approximation of W, v_i is the ith weight function, and

$$Q_1^e \equiv \left[\frac{d}{dx} \left(EI \frac{d^2 W_h}{dx^2} \right) + \omega^2 \rho I \frac{dW_h}{dx} \right]_{x_a^e}, \qquad Q_2^e \equiv \left[EI \frac{d^2 W_h}{dx^2} \right]_{x_a^e}$$
$$Q_3^e \equiv -\left[\frac{d}{dx} \left(EI \frac{d^2 W_h}{dx^2} \right) + \omega^2 \rho I \frac{dW_h}{dx} \right]_{x_b^e}, \quad Q_4^e \equiv -\left[EI \frac{d^2 W_h}{dx^2} \right]_{x_b^e} \qquad (7.3.51)$$

Note that the rotary inertia term contributes to the shear force term, giving rise to an effective shear force that must be known at a boundary point where the deflection is unknown. The typical boundary conditions for

natural vibration of the Euler–Bernoulli beams involve specifying one element of each of the following two pairs:

$$(W, V), \quad \left(-\frac{dW}{dx}, M\right) \tag{7.3.52}$$

Mixed boundary conditions involve specifying a relationship between the elements of each pair:

$$\begin{aligned} \text{Vertical spring:} \quad & V + kW = 0 \\ \text{Torsional spring:} \quad & M - \mu \frac{dW}{dx} = 0 \\ \text{Attached mass, } M_0\text{:} \quad & V - M_0 \omega^2 W = 0 \end{aligned} \tag{7.3.53}$$

where k and μ are the stiffness parameters of extensional and torsional springs, respectively, and M_0 is the attached mass.

Finite element model. To develop the weak-form Galerkin (or Ritz) finite element model of Eq. (7.3.28), we seek approximation of the form

$$W(x) \approx W_h(x) = \sum_{j=1}^{4} \Delta_j^e \phi_j^e(x) \tag{7.3.54}$$

where ϕ_i^e are the Hermite cubic polynomials [see Eq. (5.2.20) and Fig. 5.2.5] and Δ_i^e $(i = 1, 2, 3, 4)$ denote the nodal values of W_h and $-dW_h/dx$ at the two nodes. Substituting Eq. (7.3.54) for W_h and $v_i = \phi_i$, into Eq. (7.3.50), we obtain

$$\left(\mathbf{K}^e - \omega^2 \mathbf{M}^e\right) \boldsymbol{\Delta}^e = \mathbf{Q}^e \tag{7.3.55}$$

where

$$K_{ij}^e = \int_{x_a^e}^{x_b^e} EI \frac{d^2\phi_i^e}{dx^2} \frac{d^2\phi_j^e}{dx^2}\, dx, \quad M_{ij}^e = \int_{x_a^e}^{x_b^e} \left(\rho A\, \phi_i^e \phi_j^e + \rho I \frac{d\phi_i^e}{dx} \frac{d\phi_j^e}{dx}\right) dx \tag{7.3.56}$$

For element-wise constant values of E, ρ, A, and I, the stiffness matrix $\mathbf{K}^e$ and mass matrix $\mathbf{M}^e$ without the rotary inertia are

$$\mathbf{K}^e = \frac{2E_eI_e}{h_e^3}\begin{bmatrix} 6 & -3h_e & -6 & -3h_e \\ -3h_e & 2h_e^2 & 3h_e & h_e^2 \\ -6 & 3h_e & 6 & 3h_e \\ -3h_e & h_e^2 & 3h_e & 2h_e^2 \end{bmatrix}$$

$$\mathbf{M}^e = \frac{\rho_e A_e h_e}{420}\begin{bmatrix} 156 & -22h_e & 54 & 13h_e \\ -22h_e & 4h_e^2 & -13h_e & -3h_e^2 \\ 54 & -13h_e & 156 & 22h_e \\ 13h_e & -3h_e^2 & 22h_e & 4h_e^2 \end{bmatrix} \tag{7.3.57}$$

If the rotary inertia is included, the mass matrix should be appended with the following matrix:

$$\frac{\rho_e I_e}{30h_e}\begin{bmatrix} 36 & -3h_e & -36 & -3h_e \\ -3h_e & 4h_e^2 & 3h_e & -h_e^2 \\ -36 & 3h_e & 36 & 3h_e \\ -3h_e & -h_e^2 & 3h_e & 4h_e^2 \end{bmatrix} \tag{7.3.58}$$

7.3.5.3 Natural vibration of Timoshenko beams

Weak form. The equations governing natural vibration of beams according to the Timoshenko beam theory are given by Eqs. (7.3.30a) and (7.3.30b). The weak forms of these equations are [see Eqs. (5.3.9a) and (5.3.9b)]

$$0 = \int_{x_a^e}^{x_b^e} \left[GAK_s \frac{dv_{1i}}{dx}\left(S_h + \frac{dW_h}{dx}\right) - \omega^2 \rho A\, v_{1i} W_h \right] dx - v_{1i}(x_a^e)Q_1^e - v_{1i}(x_b^e)Q_3^e \tag{7.3.59a}$$

$$0 = \int_{x_a^e}^{x_b^e} \left[EI \frac{dv_{2i}}{dx}\frac{dS_h}{dx} + GAK_s\, v_{2i}\left(S_h + \frac{dW_h}{dx}\right) - \omega^2 \rho I\, v_{2i} S_h \right] dx - v_{2i}(x_a^e)Q_2^e - v_{2i}(x_b^e)Q_4^e \tag{7.3.59b}$$

where

$$Q_1^e \equiv -\left[GAK_s\left(S_h + \frac{dW_h}{dx}\right)\right]_{x_a^e}, \quad Q_2^e \equiv -\left[EI\frac{dS_h}{dx}\right]_{x_a^e}$$
$$Q_3^e \equiv \left[GAK_s\left(S_h + \frac{dW_h}{dx}\right)\right]_{x_b^e}, \quad Q_4^e \equiv \left[EI\frac{dS_h}{dx}\right]_{x_b^e} \tag{7.3.59c}$$

Finite element model. For equal interpolation of $W(x)$ and $S(x)$

$$W_h(x) = \sum_{j=1}^{n} W_j^e \psi_j^e(x), \quad S_h(x) = \sum_{j=1}^{n} S_j^e \psi_j^e(x) \tag{7.3.60}$$

where ψ_i^e are the $(n-1)$st order Lagrange polynomials, the finite element model is given by

$$\left(\begin{bmatrix} \mathbf{K}^{11} & \mathbf{K}^{12} \\ \mathbf{K}^{21} & \mathbf{K}^{22} \end{bmatrix} - \omega^2 \begin{bmatrix} \mathbf{M}^{11} & 0 \\ 0 & \mathbf{M}^{22} \end{bmatrix}\right) \begin{Bmatrix} \mathbf{W} \\ \mathbf{S} \end{Bmatrix} = \begin{Bmatrix} \mathbf{F}^1 \\ \mathbf{F}^2 \end{Bmatrix}$$
$$\text{or} \quad (\mathbf{K}^e - \omega^2 \mathbf{M}^e)\boldsymbol{\Delta}^e = \mathbf{F}^e \tag{7.3.61}$$

where $\mathbf{K}^e$ is the stiffness matrix, $\mathbf{M}^e$ is the mass matrix, and $\mathbf{F}^e$ is the vector of reaction forces; the stiffness, mass, and force coefficients of Eq. (7.3.61) are defined as

$$K_{ij}^{11} = \int_{x_a^e}^{x_b^e} \left(GAK_s \frac{d\psi_i^e}{dx}\frac{d\psi_j^e}{dx}\right) dx$$
$$K_{ij}^{12} = \int_{x_a^e}^{x_b^e} GAK_s \frac{d\psi_i^e}{dx}\psi_j^e \, dx = K_{ji}^{21}$$
$$K_{ij}^{22} = \int_{x_a^e}^{x_b^e} \left(EI\frac{d\psi_i^e}{dx}\frac{d\psi_j^e}{dx} + GAK_s \psi_i^e \psi_j^e\right) dx \tag{7.3.62}$$
$$M_{ij}^{11} = \int_{x_a^e}^{x_b} \rho A \, \psi_i^e \psi_j^e \, dx, \quad M_{ij}^{22} = \int_{x_a^e}^{x_b} \rho I \, \psi_i^e \psi_j^e \, dx$$
$$F_i^1 = Q_{2i-1}, \quad F_i^2 = Q_{2i}$$

For the choice of linear interpolation functions ψ_i^e, evaluations of the shear stiffness coefficients with reduced integration, and neglecting the rotary inertia, the element stiffness and mass matrices Eq. (7.3.61) have

the form [see Eqs. (5.3.26a)–(5.3.26c)]

$$\mathbf{K}^e = \frac{E_e I_e}{6\mu_e h_e^3}\begin{bmatrix} 6 & -3h_e & -6 & -3h_e \\ -3h_e & h_e^2(1.5+6\mu_e) & 3h_e & h_e^2(1.5-6\mu_e) \\ -6 & 3h_e & 6 & 3h_e \\ -3h_e & h_e^2(1.5-6\mu_e) & 3h_e & h_e^2(1.5+6\mu_e) \end{bmatrix} \tag{7.3.63a}$$

$$\mathbf{M}^e = \frac{\rho_e A_e h_e}{6}\begin{bmatrix} 2 & 0 & 1 & 0 \\ 0 & 2r_e & 0 & r_e \\ 1 & 0 & 2 & 0 \\ 0 & r_e & 0 & 2r_e \end{bmatrix}, \quad \mu_e = \frac{E_e I_e}{G_e A_e K_s h_e^2}, \quad r_e = \frac{I_e}{A_e} \tag{7.3.63b}$$

When the rotatory inertia is neglected, $\mathbf{M}^e$ will have zeros on the diagonal.

Example 7.3.2

Consider a uniform linear elastic beam (EI) of length L and rectangular cross section ($B \times H$) fixed at $x = 0$ and supported vertically at $x = L$ by a short linear elastic post (length $L0$ and stiffness $E_0 A_0$). Determine the first four natural frequencies of the beam using (a) the Euler–Bernoulli beam element and (b) the RIE of the Timoshenko beam theory.

Solution: The elastic support is equivalent to an elastic spring with the spring constant equal to $k_0 = E_0 A_0/L_0$.

(a) The boundary conditions of the beam in the Euler–Bernoulli beam theory are

$$W(0) = 0, \quad \left.\frac{dW}{dx}\right|_{x=0} = 0, \quad \left[EI\frac{d^2W}{dx^2}\right]_{x=L} = 0, \quad \left[EI\frac{d^3W}{dx^3} + k_0 W\right]_{x=L} = 0 \tag{1}$$

The number of natural frequencies we wish to determine dictates the minimum number of elements to be used to analyze the beam. Since two primary degrees of freedom are specified ($U_1 = U_2 = 0$), a one-element mesh will have only two unknown degrees of freedom (U_3 and U_4) and therefore we obtain only two eigenvalues. A two-element mesh will have a total of three nodes or six primary degrees of freedom, of which two are specified. Hence, we obtain four eigenvalues. Thus, a minimum of two Euler–Bernoulli beam elements are required to determine four natural frequencies.

For illustrative purpose, first we consider the one-element mesh (i.e.,

$h = L$) of the Euler–Bernoulli beam element. We have

$$\left(\frac{2EI}{L^3} \begin{bmatrix} 6 & -3L & -6 & -3L \\ -3L & 2L^2 & 3L & L^2 \\ -6 & 3L & 6 & 3L \\ -3L & L^2 & 3L & 2L^2 \end{bmatrix} - \omega^2 \frac{\rho AL}{420} \begin{bmatrix} 156 & -22L & 54 & 13L \\ -22L & 4L^2 & -13L & -3L^2 \\ 54 & -13L & 156 & 22L \\ 13L & -3L^2 & 22L & 4L^2 \end{bmatrix} \right.$$

$$\left. - \omega^2 \frac{\rho I}{30L} \begin{bmatrix} 36 & -3L & -36 & -3L \\ -3L & 4L^2 & 3L & -L^2 \\ -36 & 3L & 36 & 3L \\ -3L & -L^2 & 3L & 4L^2 \end{bmatrix} \right) \begin{Bmatrix} U_1 \\ U_2 \\ U_3 \\ U_4 \end{Bmatrix} = \begin{Bmatrix} Q_1 \\ Q_2 \\ Q_3 \\ Q_4 \end{Bmatrix} \tag{2}$$

The specified generalized displacement degrees of freedom are $U_1 = 0$ and $U_2 = 0$; the known generalized nodal forces are $Q_3 = -k_0 U_3$ and $Q_4 = 0$. Hence, the condensed equations are

$$\left(\frac{EI}{L^3} \begin{bmatrix} 12 + \alpha & 6L \\ 6L & 4L^2 \end{bmatrix} - \omega^2 \frac{\rho AL}{420} \begin{bmatrix} 156 & 22L \\ 22L & 4L^2 \end{bmatrix} - \omega^2 \frac{\rho I}{30L} \begin{bmatrix} 36 & 3L \\ 3L & 4L^2 \end{bmatrix} \right) \begin{Bmatrix} U_3 \\ U_4 \end{Bmatrix} = \begin{Bmatrix} 0 \\ 0 \end{Bmatrix} \tag{3}$$

where $\alpha = k_0 L^3/EI$. Setting the determinant of the coefficient matrix in the above equation to zero, we obtain a quadratic polynomial in ω^2 : $a\omega^4 - b\omega^2 + c = 0$, where the coefficients a, b, and c are known in terms of E, k_0 , ρ, L, A, and I.

First, consider the case in which the rotary inertia is neglected and $\alpha = 2$ (i.e., $k_0 = 2EI/L^3$). We have

$$\left(\begin{bmatrix} 14 & 6L \\ 6L & 4L^2 \end{bmatrix} - \omega^2 \frac{\rho AL^4}{420EI} \begin{bmatrix} 156 & 22L \\ 22L & 4L^2 \end{bmatrix} \right) \begin{Bmatrix} U_3 \\ U_4 \end{Bmatrix} = \begin{Bmatrix} 0 \\ 0 \end{Bmatrix} \tag{4}$$

Then the quadratic polynomial in $\lambda = (\rho AL^4/420EI)\omega^2$ is given by setting the determinant of the coefficient matrix in the above equation to zero:

$$35\lambda^2 - 104\lambda + 5 = 0, \quad \lambda = \frac{\rho AL^4}{420EI}\omega^2$$

whose roots are [$2a\lambda_{1,2} = b \pm \sqrt{b^2 - 4ac}$ and $(\omega_i)^2 = (420EI/\rho AL^4)\lambda_i$]$\lambda_1 = 0.04888$ and $\lambda_2 = 2.92255$. Hence the frequencies are

$$\omega_1 = \frac{1}{L^2}\sqrt{\frac{420EI\lambda_1}{\rho A}} = 4.531\,\beta, \quad \omega_2 = \frac{1}{L^2}\sqrt{\frac{420EI\lambda_2}{\rho A}} = 35.035\,\beta \tag{5}$$

where $\beta = \sqrt{EI/\rho A}/L^2$. For $\alpha = 0$ (i.e., for a cantilever beam), the frequencies are

$$\omega_1 = 3.533\,\beta, \quad \omega_2 = 34.80,\beta, \quad \beta = \frac{1}{L^2}\sqrt{\frac{EI}{\rho A}} \tag{6}$$

The eigenvector components for each eigenvalue (for the $\alpha = 0$ case) can be computed from the condensed equations:

$$\left(\begin{bmatrix} 6 & 3L \\ 3L & 2L^2 \end{bmatrix} - \lambda_i \begin{bmatrix} 78 & 11L \\ 11L & 2L^2 \end{bmatrix}\right)\begin{Bmatrix} U_3 \\ U_4 \end{Bmatrix}^{(i)} = \begin{Bmatrix} 0 \\ 0 \end{Bmatrix}, \quad \lambda_i = \frac{\rho A L^4}{420EI}\omega^2$$

The first of the two equations above can be written as

$$U_3^{(i)} = -L\left(\frac{3 - 11\lambda_i}{6 - 78\lambda_i}\right)U_4^{(i)}, \quad i = 1,2$$

If we select $U_4 = 1$ (components are not normalized), the two eigenvectors are

$$\begin{Bmatrix} U_3 \\ U_4 \end{Bmatrix}^{(1)} = \begin{Bmatrix} -0.7259L \\ 1.0000 \end{Bmatrix}, \quad \begin{Bmatrix} U_3 \\ U_4 \end{Bmatrix}^{(2)} = \begin{Bmatrix} -0.1312L \\ 1.0000 \end{Bmatrix}$$

If we use the normalization $(U_3/L)^2 + (U_4)^2 = 1$, the two eigenvectors are

$$\begin{Bmatrix} \hat{U}_3 \\ \hat{U}_4 \end{Bmatrix}^{(1)} = \begin{Bmatrix} -0.5874L \\ 0.8093 \end{Bmatrix}, \quad \begin{Bmatrix} \hat{U}_3 \\ \hat{U}_4 \end{Bmatrix}^{(2)} = \begin{Bmatrix} -0.1301L \\ 0.9915 \end{Bmatrix}$$

The normalized mode shape corresponding to the eigenvalue λ_i is

$$\begin{aligned} \hat{W}_h^{(i)}(x) &= \hat{U}_3^{(i)}\phi_3(x) + \hat{U}_4^{(i)}\phi_4(x) = \hat{U}_3^{(i)}\left[3\left(\frac{x}{L}\right)^2 - 2\left(\frac{x}{L}\right)^3\right] - \hat{U}_4^{(i)}x\left[\left(\frac{x}{L}\right)^2 - \frac{x}{L}\right] \\ &= \left(3\hat{U}_3^{(i)} + L\hat{U}_4^{(i)}\right)\left(\frac{x}{L}\right)^2 - \left(2\hat{U}_3^{(i)} + L\hat{U}_4^{(i)}\right)\left(\frac{x}{L}\right)^3 \end{aligned} \tag{7}$$

In particular, the mode shapes associated with the natural frequencies are

$$\begin{aligned} \hat{W}_h^{(1)}(x) &= L\left[-0.9529\left(\frac{x}{L}\right)^2 + 0.3655\left(\frac{x}{L}\right)^3\right] \\ \hat{W}_h^{(2)}(x) &= L\left[0.6012\left(\frac{x}{L}\right)^2 - 0.7313\left(\frac{x}{L}\right)^3\right] \end{aligned} \tag{8}$$

For the case in which rotary inertia is included, we write $\rho I = \rho A$

(H_2/12) and take $H/L = 0.01$, where H is the beam height. The eigenvalues for the case $\alpha = 0$ are

$$\lambda_1 = 12.4801, \quad \lambda_2 = 1211.51, \quad \text{or} \quad \omega_1 = 3.533\beta, \quad \omega_2 = 34.807\beta$$

The effect of the rotary inertia is to decrease the natural frequencies. Clearly, the rotary inertia has negligible effect on the frequencies.

Next, consider two-element mesh of the Euler–Bernoulli beam element without rotary inertia. The assembled equations are ($h = 0.5L$)

$$\left(\frac{2EI}{h^3} \begin{bmatrix} 6 & -3h & -6 & -3h & 0 & 0 \\ -3h & 2h^2 & 3h & h^2 & 0 & 0 \\ -6 & 3h & 6+6 & 3h-3h & -6 & -3h \\ -3h & h^2 & 3h-3h & 2h^2+2h^2 & 3h & h^2 \\ 0 & 0 & -6 & 3h & 6 & 3h \\ 0 & 0 & -3h & h^2 & 3h & 2h^2 \end{bmatrix} - \omega^2 \frac{\rho Ah}{420} \begin{bmatrix} 156 & -22h & 54 & 13h & 0 & 0 \\ -22h & 4h^2 & -13h & -3h^2 & 0 & 0 \\ 54 & -13h & 156+156 & 22h-22h & 54 & 13h \\ 13h & -3h^2 & 22h-22h & 4h^2+4h^2 & -13h & -3h^2 \\ 0 & 0 & 54 & -13h & 156 & 22h \\ 0 & 0 & 13h & -3h^2 & 22h & 4h^2 \end{bmatrix} \right) \begin{Bmatrix} U_1 \\ U_2 \\ U_3 \\ U_4 \\ U_5 \\ U_6 \end{Bmatrix} = \begin{Bmatrix} Q_1^1 \\ Q_2^1 \\ Q_3^1 + Q_1^2 = 0 \\ Q_4^1 + Q_2^2 = 0 \\ Q_3^2 \\ Q_4^2 \end{Bmatrix} \tag{9}$$

The condensed equations are ($U_1 = U_2 = Q_4^2 = 0$ and $Q_3^2 = -k_0 U_5$)

$$\left(\frac{16EI}{L^3} \begin{bmatrix} 12 & 0 & -6 & -1.5L \\ 0 & L^2 & 1.5L & 0.25L^2 \\ -6 & 1.5L & 6+(\alpha/16) & 1.5L \\ -1.5L & 0.25L^2 & 1.5L & 0.5L^2 \end{bmatrix} - \omega^2 \frac{\rho AL}{840} \begin{bmatrix} 312 & 0 & 54 & 6.5L \\ 0 & 2L^2 & -6.5L & -0.75L^2 \\ 54 & -6.5L & 156 & 11L \\ 6.5L & -0.75L^2 & 11L & L^2 \end{bmatrix} \right) \begin{Bmatrix} U_3 \\ U_4 \\ U_5 \\ U_6 \end{Bmatrix} = \begin{Bmatrix} 0 \\ 0 \\ 0 \\ 0 \end{Bmatrix}$$

where $\alpha = k_0 L^3/EI$, as before. Setting the determinant of the 4 × 4 coefficient matrix to zero gives a 4th degree polynomial in ω^2. The roots

of the polynomial are (computed using the FEM1D program discussed in Chapter 8)

$$\alpha = 0: \quad \omega_1 = 3.518\,\beta, \quad \omega_2 = 22.221\,\beta, \quad \omega_3 = 75.157\,\beta, \quad \omega_4 = 218.14\,\beta$$
$$\alpha = 2: \quad \omega_1 = 4.498\,\beta, \quad \omega_2 = 22.407\,\beta, \quad \omega_3 = 75.224\,\beta, \quad \omega_4 = 218.20\,\beta$$

where $\beta = \sqrt{EI/\rho A}/L^2$. The first four frequencies obtained using a four-element mesh are

$$\alpha = 0: \quad \omega_1 = 3.516\,\beta, \quad \omega_2 = 22.060\,\beta, \quad \omega_3 = 62.175\,\beta, \quad \omega_4 = 122.66\,\beta$$
$$\alpha = 2: \quad \omega_1 = 4.495\,\beta, \quad \omega_2 = 22.244\,\beta, \quad \omega_3 = 62.241\,\beta, \quad \omega_4 = 122.69\,\beta$$

The exact frequencies of the cantilever beam according to the Euler–Bernoulli beam theory, including rotary inertia but without the elastic support (i.e., $\alpha = 0$), can be computed from the transcendental equation (see Reddy [2], pp. 135–139)

$$\cos \mu L \cosh \mu L + 1 = 0 \tag{7.3.64}$$

and the mode shape is given by

$$W_h(x) = \frac{\sin \mu x - \sinh \mu x}{\sin \mu L - \sinh \mu L} - \frac{\cos \mu x - \cosh \mu x}{\cos \mu L + \cosh \mu L} \tag{7.3.65}$$

where $\omega = \mu^2 \sqrt{\frac{EI}{\rho A}} \sqrt{\frac{12}{12 + H^2\mu^2}}$, with rotary inertia; $\omega = \mu^2 \sqrt{\frac{EI}{\rho A}}$, without rotary inertia; and H is the height of the beam. The first four roots of the transcendental equation are

$$\mu_1 L = 1.875, \quad \mu_2 L = 4.694, \quad \mu_3 L = 7.855, \quad \mu_4 L = 10.9955$$

Hence, the first four natural frequencies are

$$\omega_1 = 3.5156\,\beta, \quad \omega_2 = 22.0336\,\beta, \quad \omega_3 = 61.701\,\beta, \quad \omega_4 = 120.90\,\beta$$

when the rotary inertia is neglected, and

$$\omega_1 = 3.5155\,\beta, \quad \omega_2 = 22.0316\,\beta, \quad \omega_3 = 61.685\,\beta, \quad \omega_4 = 120.839\,\beta$$

when the rotary inertia is included ($H/L = 0.01$). When the rotary inertia is neglected, the first frequency predicted by one element model is in less than 0.5% error and the second frequency is in 57% error. The second frequency predicted by the two-element mesh is in less than 1% error.

With increasing number of elements in the mesh, additional frequencies are obtained while refining the frequencies obtained with fewer elements.

(b) The boundary conditions for the Timoshenko beam theory are

$$W(0)=0,\quad S(0)=0,\quad \left[EI\frac{dS}{dx}\right]_{x=L}=0,\quad \left[GAK_s\left(\frac{dW}{dx}+S\right)k_0W\right]_{x=L}=0 \qquad (10)$$

If we use the reduced integration Timoshenko beam element, a mesh of two linear elements can only represent the first two mode shapes of the cantilever beam (see Fig. 7.3.5) because there are only two independent deflection degrees of freedom that are unspecified. In order to represent the first four mode shapes using the RIE, we must use at least four linear elements or two quadratic elements.

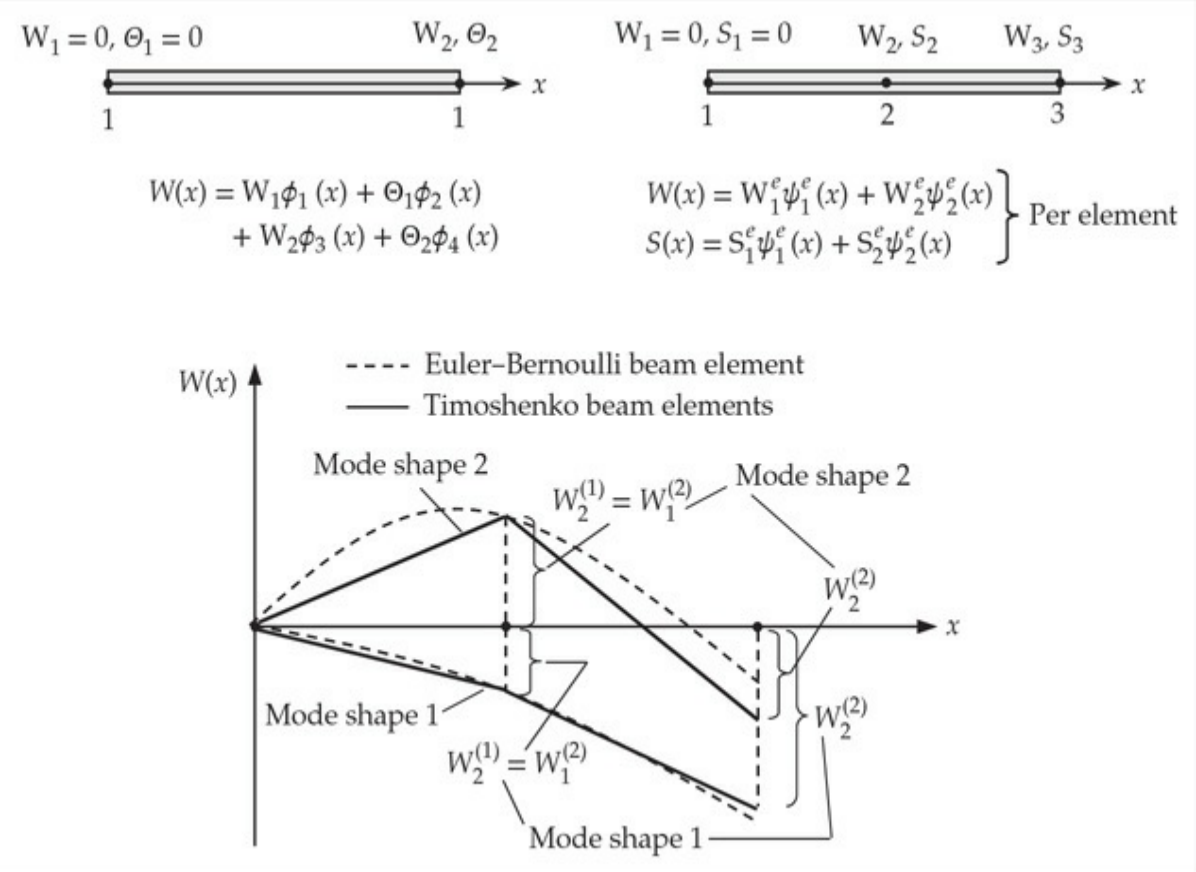

Fig. 7.3.5 Two possible nonzero mode shapes of a cantilever beam that can be represented by a mesh of two linear Timoshenko beam elements (or one Euler–Bernoulli beam element).

First, we consider the one-element mesh ($h = L$) of the reduced-integration Timoshenko beam element (for illustrative purposes):

$$\left(\frac{EI}{6\mu L^3}\begin{bmatrix} 6 & -3L & -6 & -3L \\ -3L & L^2(1.5+6\mu) & 3L & L^2(1.5-6\mu) \\ -6 & 3L & 6 & 3L \\ -3L & L^2(1.5-6\mu) & 3L & L^2(1.5+6\mu) \end{bmatrix} - \omega^2\frac{\rho AL}{6}\begin{bmatrix} 2 & 0 & 1 & 0 \\ 0 & 2r & 0 & r \\ 1 & 0 & 2 & 0 \\ 0 & r & 0 & 2r \end{bmatrix}\right)\begin{Bmatrix} W_1 \\ S_1 \\ W_2 \\ S_2 \end{Bmatrix} = \begin{Bmatrix} Q_1 \\ Q_2 \\ Q_3 \\ Q_4 \end{Bmatrix} \tag{11a}$$

where $K_s = 5/6$, $r = I/A = H^2/12$, and

$$\mu = \frac{EI}{GAK_sL^2} = \frac{1+\nu}{5}\frac{H^2}{L^2} \tag{11b}$$

The specified generalized displacement and force degrees of freedom are $W_1 = 0$, $S_1 = 0$, $Q_3 = -k_0 W_2$ and $Q_4 = 0$. The condensed equations are

$$\left(\frac{EI}{6\mu L^3}\begin{bmatrix} 6(1+\mu\alpha) & 3L \\ 3L & 1.5L^2(1+4\mu) \end{bmatrix} - \omega^2\frac{\rho AL}{6}\begin{bmatrix} 2 & 0 \\ 0 & 2r \end{bmatrix}\right)\begin{Bmatrix} W_2 \\ S_2 \end{Bmatrix} = \begin{Bmatrix} 0 \\ 0 \end{Bmatrix}$$

Neglecting the rotatory inertia (i.e., $r = 0$), the characteristic equation becomes linear in $\lambda = (\rho AL^4\,\mu/EI)\omega^2$ (we cannot set $r = 0$ in a computer program because it makes the mass matrix singular):

$$\lambda = \frac{12\mu}{(1+4\mu)} + 3\mu\alpha \Rightarrow \omega^2 = \lambda\frac{EI}{\mu\rho AL^4} = \left[\frac{12}{(1+4\mu)} + 3\alpha\right]\frac{EI}{\rho AL^4}$$

Clearly, α has the effect of increasing the frequency (because it stiffens the structure) and $\mu \neq 0$ (depends on the ratio, H^2/L^2—the effect of shear deformation) tends to reduce the frequency. Since the frequencies are normalized, $\bar{\omega} = \omega L^2\sqrt{(\rho A/EI)}$, it is necessary only to select the values of ν and L/H. We also note that (for $\nu = 0.25$)

$$GAK_s = \frac{E}{2(1+\nu)}BH\frac{5}{6} = \frac{4EI}{H^2}, \quad m_2 = \rho I = \rho\frac{BH^3}{12} = \rho\frac{AH^2}{12}$$

where B and H are the width and height, respectively, of the beam cross section ($A = BH$).

To further simplify the expressions, we assume $\nu = 0.25$ ($4\mu = H^2/L^2$) and obtain

$$\omega^2 = \left[\frac{12}{(1+H^2/L^2)} + 3\alpha\right]\beta^2; \quad \beta^2 = \frac{EI}{\rho AL^4}$$

For two different side-to-thickness ratios (that characterize thin and thick beams), we obtain

$$\alpha = 0.0: \quad \frac{L}{H} = 100: \quad \omega = 3.4639\,\beta; \quad \frac{L}{H} = 10: \quad \omega = 3.4469\,\beta$$
$$\alpha = 2.0: \quad \frac{L}{H} = 100: \quad \omega = 4.2425\,\beta, \quad \frac{L}{H} = 10: \quad \omega = 4.2286\,\beta$$

The exact frequency for $\alpha = 0$ is $\bar{\omega} = 3.5158$ for $L/H = 100$ and $\bar{\omega} = 3.5092$ for $L/H = 10$, where $\bar{\omega}_i = \omega_i/\beta$.

If the rotary inertia is included (calculations are not shown here), we obtain

$$\frac{L}{H} = 100: \quad \omega = 3.4639\,\beta; \quad \frac{L}{H} = 10: \quad \omega = 3.4413\,\beta; \quad \beta = \frac{1}{L^2}\sqrt{\frac{EI}{\rho A}}$$

The frequencies obtained by the Timoshenko beam elements (RIEs) with rotary inertia are shown in Table 7.3.2 for two different values of the length-to-height ratio L/H. For comparison, the frequencies obtained with the Euler–Bernoulli beam elements are also listed. For thin beams (i.e., $L/H = 100$), the effect of shear deformation is negligible, and we obtain essentially the same result as in the Euler–Bernoulli beam theory. The effect of rotary inertia is not significant in lower modes.

Table 7.3.2 Natural frequencies of a cantilever beam according to Timoshenko beam theory (TBT) and Euler–Bernoulli beam theory (EBT) $[\bar{\omega} = \omega L^2(\rho A/EI)^{1/2}]$.

	$L/H = 100$				$L/H = 10$			
Mesh	$\bar{\omega}_1$	$\bar{\omega}_2$	$\bar{\omega}_3$	$\bar{\omega}_4$	$\bar{\omega}_1$	$\bar{\omega}_2$	$\bar{\omega}_3$	$\bar{\omega}_4$
4L‡	3.5406	25.6726	98.3953	417.1262	3.5137	24.1345	80.2244	189.929
8L	3.5223	22.8850	68.8936	151.8435	3.4956	21.7003	60.6296	119.280
16L	3.5174	22.2350	63.3412	127.5438	3.4908	21.1257	56.4715	104.680
2Q	3.5214	23.3226	78.3114	328.3247	3.4947	22.0762	67.0884	181.068
4Q	3.5161	22.1054	63.3269	133.9823	3.4895	21.0103	56.4572	108.606
8Q	3.5158	22.0279	61.7323	121.4459	3.4892	20.9421	55.2405	100.750
TBT†	3.5158	22.0309	61.7523	121.5184	3.4958	21.1956	56.580	104.4120
EBT‡	3.5160	22.0333	61.7148	121.1005	3.5092	21.7442	59.8359	114.530
EBT†	3.5160	22.0363	61.7347	121.1727	3.5160	22.0363	61.7347	121.173

† Rotary inertia is neglected (used $\rho I_2 = 10^{-15}$ for the TBT and $\rho I_2 = 0$ for the EBT).

‡ Rotary inertia is included. The results for the EBT are independent of the ratio L/H when the rotary inertia is neglected (eight quadratic elements for the TBT and eight Hermite cubic elements for the EBT are used).

We note from Table 7.3.2 that the finite element results converge with the *h*-refinement (i.e., when more of the same kind of elements are used) as well as with the *p*-refinement (i.e., when higher-order elements are used). The *p*-refinement shows more rapid convergence of the fundamental (i.e., lowest) frequency. We also note that the effect of shear deformation is to reduce the magnitude of natural frequency when compared to the Euler–Bernoulli beam theory. In other words, the assumed infinite shear rigidity makes the Euler–Bernoulli beam theory over predict the magnitude of frequencies. The first four mode shapes of the cantilever beam, as obtained using the 16-element mesh of linear elements, are shown in Fig. 7.3.6.

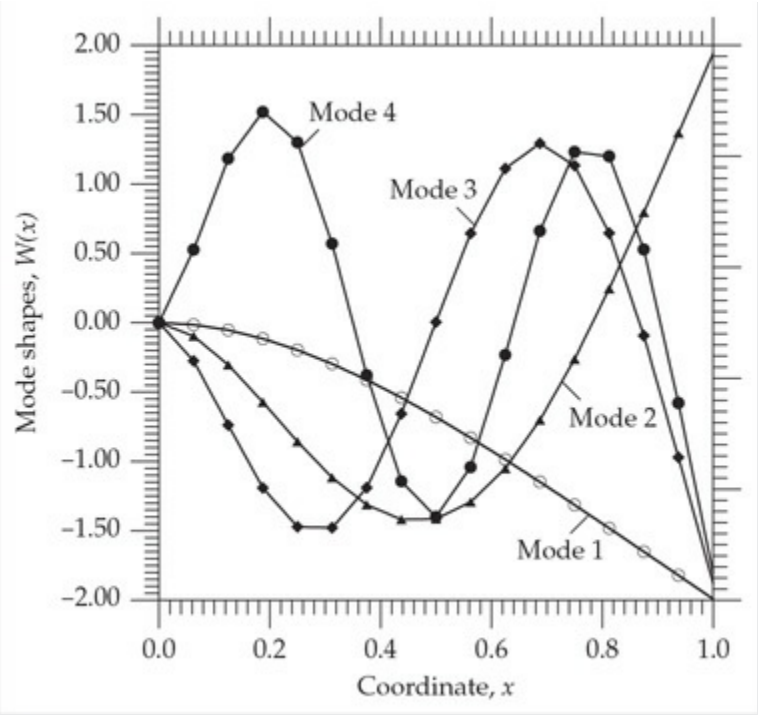

Fig. 7.3.6 First four natural mode shapes of a cantilever beam, as predicted using a 16-element mesh of linear Timoshenko beam elements *(L/H* = 10).

In closing the discussion on natural vibration, it is noted that when symmetry of the system is used to model the problem, only symmetric modes are predicted. It is necessary to model the whole system in order to obtain all modes of vibration.

7.3.6 Buckling of Beams

7.3.6.1 Weak form of EBT

The weak form of the equation governing the EBT, Eq. (7.3.31), is given by

$$0 = \int_{x_a^e}^{x_b^e} \left(EI \frac{d^2v}{dx^2} \frac{d^2W}{dx^2} - N^0 \frac{dv}{dx} \frac{dW}{dx} \right) dx$$
$$- v(x_a^e) Q_1^e - \left(-\frac{dv}{dx} \right)_{x_a^e} Q_2^e - v(x_b^e) Q_3^e - \left(-\frac{dv}{dx} \right)_{x_b^e} Q_4^e \qquad (7.3.66a)$$

where v is the weight function and

$$Q_1^e = \left[\frac{d}{dx}\left(EI\frac{d^2W}{dx^2}\right) + N^0\frac{dW}{dx}\right]_{x_a^e}, \quad Q_2^e = \left(EI\frac{d^2W}{dx^2}\right)_{x_a^e}$$
$$Q_3^e = \left[-\frac{d}{dx}\left(EI\frac{d^2W}{dx^2}\right) - N^0\frac{dW}{dx}\right]_{x_b^e}, \quad Q_4^e = \left(-EI\frac{d^2W}{dx^2}\right)_{x_b^e} \tag{7.3.66b}$$

Clearly, the duality pairs of the weak form are (W, V) and ($-dW/dx$,M). We note that for the buckling problem, the buckling load is a part of the shear forces Q_1^e and Q_3^e because it contributes to the reaction forces.

7.3.6.2 Finite element model of EBT

The finite element model is obtained by approximating $W(x)$ such that both W and its derivative $(-dW/dx)$ are interpolated at the nodes of the element. As already discussed in Chapter 5 (see Section 5.2.4), the minimum degree of interpolation of W is cubic:

$$W(x) \approx \sum_{j=1}^{4} \Delta_j^e \phi_j^e(x) \tag{7.3.67}$$

where $\phi_j(x)$ are the Hermite cubic polynomials given in Eq. (5.2.20). Substituting Eq. (7.3.67) into the weak form (7.3.66a), we obtain the finite element model

$$\mathbf{K}^e\boldsymbol{\Delta}^e - N^0\mathbf{G}^e\boldsymbol{\Delta}^e = \mathbf{Q}^e \tag{7.3.68a}$$

where $\boldsymbol{\Delta}^e$ and $\mathbf{Q}^e$ are the columns of generalized displacement and force degrees of freedom at the two ends of the Euler–Bernoulli beam element:

$$\boldsymbol{\Delta}^e = \begin{Bmatrix} W(x_a^e) \\ \left(-\frac{dW}{dx}\right)_{x_a^e} \\ W(x_b^e) \\ \left(-\frac{dW}{dx}\right)_{x_b^e} \end{Bmatrix}, \quad \mathbf{Q}^e = \begin{Bmatrix} Q_1^e \\ Q_2^e \\ Q_3^e \\ Q_4^e \end{Bmatrix} \tag{7.3.68b}$$

The coefficients of the stiffness matrix $\mathbf{K}^e$ and the *stability matrix* $\mathbf{G}^e$ are defined by

$$K_{ij}^e = \int_{x_a}^{x_b} EI \frac{d^2\phi_i^e}{dx^2}\frac{d^2\phi_j^e}{dx^2}\,dx, \quad G_{ij}^e = \int_{x_a}^{x_b} \frac{d\phi_i^e}{dx}\frac{d\phi_j^e}{dx}\,dx \tag{7.3.68c}$$

where ϕ_i^e are the Hermite cubic interpolation functions. The explicit form of $\mathbf{K}^e$ is given by Eq. (5.2.26a) with $k_f^e = 0$ for element-wise constant value of E_eI_e. The element equations for buckling of a beam-column according to the Euler–Bernoulli beam theory (for the case $k_f^e = 0$) are

$$\left(\frac{2E_eI_e}{h_e^3}\begin{bmatrix} 6 & -3h_e & -6 & -3h_e \\ -3h_e & 2h_e^2 & 3h_e & h_e^2 \\ -6 & 3h_e & 6 & 3h_e \\ -3h_e & h_e^2 & 3h_e & 2h_e^2 \end{bmatrix} - N^0\frac{1}{30h_e}\begin{bmatrix} 36 & -3h_e & -36 & -3h_e \\ -3h_e & 4h_e^2 & 3h_e & -h_e^2 \\ -36 & 3h_e & 36 & 3h_e \\ -3h_e & -h_e^2 & 3h_e & 4h_e^2 \end{bmatrix}\right)\begin{Bmatrix} \Delta_1^e \\ \Delta_2^e \\ \Delta_3^e \\ \Delta_4^e \end{Bmatrix} = \begin{Bmatrix} Q_1^e \\ Q_2^e \\ Q_3^e \\ Q_4^e \end{Bmatrix} \tag{7.3.69}$$

The mode shape in the element is given by Eq. (7.3.67).

7.3.6.3 Finite element model of TBT

The equations governing buckling of beams according to the Timoshenko beam theory are given by Eqs. (7.3.32a) and (7.3.32b). The finite element model [based on the RIE stiffness matrix in Eq. (5.3.26a)] of these equations is given by (details are omitted)

$$\left(\frac{E_eI_e}{6\mu_e h_e^3}\begin{bmatrix} 6 & -3h_e & -6 & -3h_e \\ -3h_e & h_e^2(1.5+6\mu_e) & 3h_e & h_e^2(1.5-6\mu_e) \\ -6 & 3h_e & 6 & 3h_e \\ -3h_e & h_e^2(1.5-6\mu_e) & 3h_e & h_e^2(1.5+6\mu_e) \end{bmatrix} - N^0\frac{1}{h_e}\begin{bmatrix} 1 & 0 & -1 & 0 \\ 0 & 0 & 0 & 0 \\ -1 & 0 & 1 & 0 \\ 0 & 0 & 0 & 0 \end{bmatrix}\right)\begin{Bmatrix} \Delta_1^e \\ \Delta_2^e \\ \Delta_3^e \\ \Delta_4^e \end{Bmatrix} = \begin{Bmatrix} Q_1^e \\ Q_2^e \\ Q_3^e \\ Q_4^e \end{Bmatrix} \tag{7.3.70a}$$

where (K_s = 5/6 and $h = L$)

$$\mu_e = \frac{E_e I_e}{G_e A_e K_s h_e^2} = \frac{1+\nu}{5}\frac{H^2}{h^2} = \frac{1+\nu}{5}\frac{4H^2}{L^2} \qquad (7.3.70b)$$

Since zeros appear on the diagonal of the stability matrix, special eigenvalue solvers are needed.

Example 7.3.3

Consider a uniform column (L, A, I, E, and ν) fixed at one end and pinned at the other, as shown in Fig. 7.3.7. Determine the critical buckling load using two (a) EBT elements and (b) TBT elements.

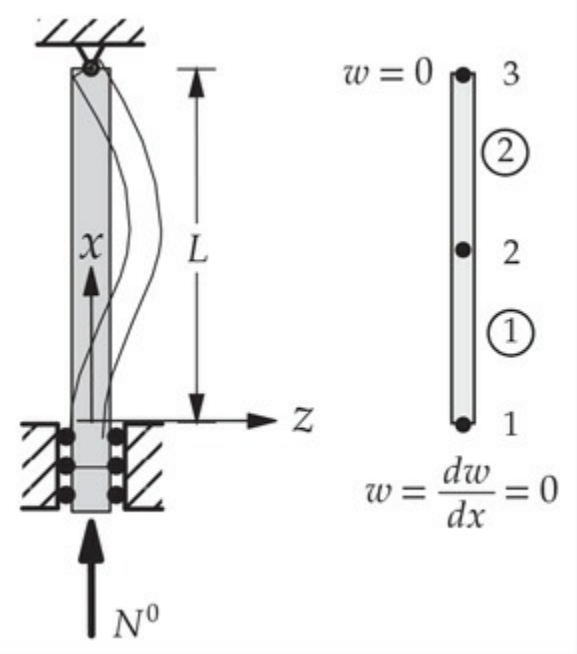

Fig. 7.3.7 A column fixed at $x = 0$ and hinged at $x = L$, and subjected to axial compressive load N^0.

Solution: (a) Let us first consider a mesh of two Euler–Bernoulli beam elements. The geometric supports and equilibrium conditions of the column require that

$$U_1 = U_2 = U_5 = 0, \quad Q_3^1 + Q_1^2 = 0, \quad Q_4^1 + Q_2^2 = 0, \quad Q_4^2 = 0$$

Since 3 of the 6 primary degrees of freedom are specified, there will be only 3 eigenvalues in the problem.

The assembled system of finite element equations is ($h = L/2$)

$$\left(\frac{2EI}{h^3}\begin{bmatrix} 6 & -3h & -6 & -3h & 0 & 0 \\ -3h & 2h^2 & 3h & h^2 & 0 & 0 \\ -6 & 3h & 6+6 & 3h-3h & -6 & -3h \\ -3h & h^2 & 3h-3h & 2h^2+2h^2 & 3h & h^2 \\ 0 & 0 & -6 & 3h & 6 & 3h \\ 0 & 0 & -3h & h^2 & 3h & 2h^2 \end{bmatrix}\right.$$

$$\left. -\frac{N^0}{30h}\begin{bmatrix} 36 & -3h & -36 & -3h & 0 & 0 \\ -3h & 4h^2 & 3h & -h^2 & 0 & 0 \\ -36 & 3h & 36+36 & 3h-3h & -36 & -3h \\ -3h & -h^2 & 3h-3h & 4h^2+4h^2 & 3h & -h^2 \\ 0 & 0 & -36 & 3h & 36 & 3h \\ 0 & 0 & -3h & -h^2 & 3h & 4h^2 \end{bmatrix}\right)\begin{Bmatrix} U_1 \\ U_2 \\ U_3 \\ U_4 \\ U_5 \\ U_6 \end{Bmatrix} = \begin{Bmatrix} Q_1^1 \\ Q_2^1 \\ 0 \\ 0 \\ Q_3^2 \\ 0 \end{Bmatrix}$$

where U_I denote the generalized displacements of the global nodes. The condensed equations are (obtained by deleting rows and columns 1, 2, and 5)

$$\left(\frac{2EI}{h^3}\begin{bmatrix} 12 & 0 & -3h \\ 0 & 4h^2 & h^2 \\ -3h & h^2 & 2h^2 \end{bmatrix} - \frac{N^0}{30h}\begin{bmatrix} 72 & 0 & -3h \\ 0 & 8h^2 & -h^2 \\ -3h & -h^2 & 4h^2 \end{bmatrix}\right)\begin{Bmatrix} U_3 \\ U_4 \\ U_6 \end{Bmatrix} = \begin{Bmatrix} 0 \\ 0 \\ 0 \end{Bmatrix}$$

which defines the eigenvalue problem for the determination of N^0 and U_I.

Setting the determinant of the coefficient matrix to zero, we obtain a cubic equation for N^0. The smallest value of N^0 is the critical buckling load, which is (obtained using FEM1D)

$$N^0_{\text{crit}} = 20.7088\frac{EI}{L^2}$$

whereas the exact solution is 20.187 EI/L^2 (see Reddy [2], pp. 130–135). (b) Next, we consider a two-element mesh ($h = L/2$) of the RIE [see Eq. (5.3.26a)]. The assembled equations are

$$\left(\frac{EI}{6\mu h^3}\begin{bmatrix} 6 & -3h & -6 & -3h & 0 & 0 \\ -3h & h^2(1.5+6\mu) & 3h & h^2(1.5-6\mu) & 0 & 0 \\ -6 & 3h & 12 & 0 & -6 & -3h \\ -3h & h^2(1.5-6\mu) & 0 & 2h^2(1.5+6\mu) & 3h & h^2(1.5-6\mu) \\ 0 & 0 & -6 & 3h & 6 & 3h \\ 0 & 0 & -3h & h^2(1.5-6\mu) & 3h & h^2(1.5+6\mu) \end{bmatrix}\right.$$

$$\left. -\frac{N^0}{h}\begin{bmatrix} 1 & 0 & -1 & 0 & 0 & 0 \\ 0 & 0 & 0 & 0 & 0 & 0 \\ -1 & 0 & 2 & 0 & -1 & 0 \\ 0 & 0 & 0 & 0 & 0 & 0 \\ 0 & 0 & -1 & 0 & 1 & 0 \\ 0 & 0 & 0 & 0 & 0 & 0 \end{bmatrix}\right)\begin{Bmatrix} U_1 \\ U_2 \\ U_3 \\ U_4 \\ U_5 \\ U_6 \end{Bmatrix} = \begin{Bmatrix} Q_1^1 \\ Q_2^1 \\ Q_3^1 + Q_1^2 = 0 \\ Q_4^1 + Q_2^2 = 0 \\ Q_3^2 \\ Q_4^2 = 0 \end{Bmatrix}$$

The condensed equations are ($U_1 = U_2 = U_5 = 0$)

$$\frac{EI}{6\mu h^3}\begin{bmatrix} 12+\hat{N}^0 & 0 & -3h \\ 0 & 2h^2(1.5+6\mu) & h^2(1.5-6\mu) \\ -3h & h^2(1.5-6\mu) & h^2(1.5+6\mu) \end{bmatrix}\begin{Bmatrix} U_3 \\ U_4 \\ U_6 \end{Bmatrix} = \begin{Bmatrix} 0 \\ 0 \\ 0 \end{Bmatrix}$$

where $\hat{N}^0 = (12\mu h^2/EI)N^0$. Because of the zero diagonal elements in the stability matrix, we obtain a linear equation for N^0($\nu = 0.25$ and $\mu = H^2/L^2$)

$$N^0 = \frac{180 + 144\mu}{2.25 + 54\mu + 36\mu^2}\frac{EI}{L^2}$$

which is almost four times the correct value! A mesh of 8 linear RIEs yields 21.348 EI/L^2 and 4 quadratic elements yields 20.267 EI/L^2 for $L/H = 100$. Clearly, the RIE element has a slow convergence rate for buckling problems.

Table 7.3.3 contains the critical buckling loads computed using the Euler–Bernoulli beam element for various boundary conditions and meshes (in full beam) and Fig. 7.3.8 shows the fundamental buckling mode shapes $W(x)$. The numerical results were computed using the FEM1D program. Analytical solutions are also included for comparison. It is clear that the critical buckling loads converge to the analytical solutions as the mesh is refined. The rate of convergence depends on the type of boundary conditions (indeterminate beams exhibit slower convergence).

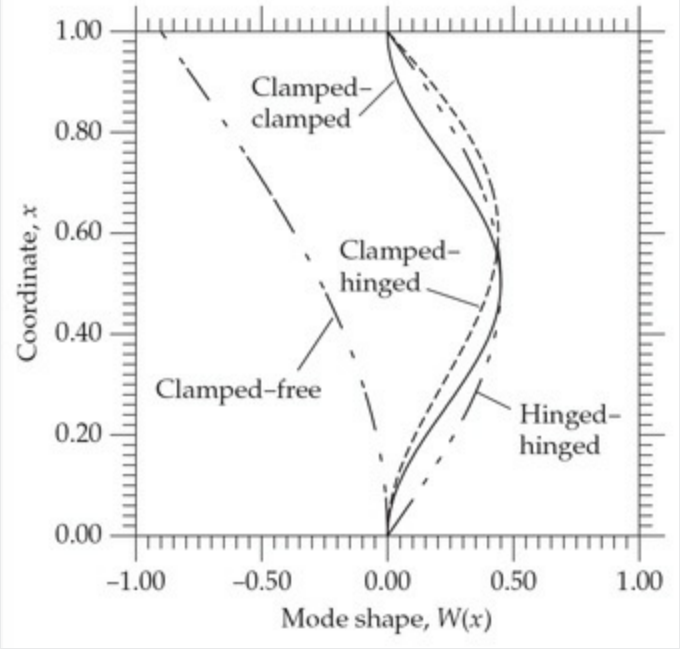

Fig. 7.3.8 Fundamental buckling mode shapes for various boundary conditions.

Table 7.3.3 Critical buckling loads of a beam fixed at one end and pinned at the other using the Euler–Bernoulli beam theory (EBT) ($\bar{N}^0 = N^0 L^2/EI$).

Boundary conditions	2	4	8	16	Exact [2]
Hinged–hinged	9.9438	9.8747	9.8699	9.8696	9.8696
Clamped–free	2.4687	2.4675	2.4674	2.4674	2.4674
Clamped–hinged	20.7088	20.2322	20.1935	20.1909	20.1870
Clamped–clamped	40.0000	39.7754	39.4986	39.4797	39.4784

We close this section with a note that eigenvalue problems (for natural vibration and buckling analysis) of frame structures can be formulated using the ideas discussed in Chapter 6. The transformed element equations are of the form

$$(\mathbf{K}^e - \omega^2 \mathbf{M}^e)\boldsymbol{\Delta}^e = \mathbf{Q}^e, \quad (\mathbf{K}^e - N^0 \mathbf{G}^e)\boldsymbol{\Delta}^e = \mathbf{Q}^e$$
$$\mathbf{K}^e = (\mathbf{T}^e)^{\mathrm{T}} \bar{\mathbf{K}}^e \mathbf{T}^e, \quad \mathbf{M}^e = (\mathbf{T}^e)^{\mathrm{T}} \bar{\mathbf{M}}^e \mathbf{T}^e, \quad \mathbf{G}^e = (\mathbf{T}^e)^{\mathrm{T}} \bar{\mathbf{G}}^e \mathbf{T}^e \tag{7.3.71}$$

7.4 Transient Analysis

7.4.1 Introduction

In this section, we develop the finite element models for the transient response of time-dependent problems and describe time approximation schemes to convert ordinary differential equations in time to algebraic equations. We consider finite element models of the equations presented in Section 7.2.

Finite element models of time-dependent problems can be developed in two alternative ways (see Surana and Reddy [4]): (a) coupled formulation in which the time t is treated as an additional coordinate along with the spatial coordinate x and (b) decoupled formulation where time and spatial variations are assumed to be separable. Thus, the finite element approximation in the two formulations takes the form:

$$u(x,t) \approx u_h^e(x,t) = \sum_{j=1}^{n} \hat{u}_j^e \hat{\psi}_j^e(x,t) \quad \text{(coupled formulation)} \tag{7.4.1a}$$

$$u(x,t) \approx u_h^e(x,t) = \sum_{j=1}^{n} u_j^e(t) \psi_j^e(x) \quad \text{(decoupled formulation)} \tag{7.4.1b}$$

where $\hat{\psi}_j^e(x,t)$ are time-space (two-dimensional) interpolation functions and $\hat{u}_j$ are the nodal values that are independent of x and t, whereas $\psi_i^e(x)$ are the usual one-dimensional interpolation functions in spatial coordinate x only and the nodal values $u_j^e(t)$ are functions of time t only. Derivation of the interpolation functions in two dimensions will be discussed in Chapter 9 in connection with the finite element analysis of two-dimensional problems. Space-time coupled finite element formulations are not commonly used, and they have remained as a topic of research. Although the assumption that space and time variations are separable is not valid in general, especially in wave propagation in solids, with sufficiently small time steps, it is possible to obtain accurate solutions to even those problems for which the solution is not separable in time and space. In this book, we consider the space-time decoupled formulation only.

The space-time decoupled finite element formulation of time-dependent problems involves two major steps:

1. *Spatial approximation* (*semidiscretization*), where the solution u of the equation under consideration is approximated by expressions of

the form in Eq. (7.4.1b), and the spatial finite element model of the equation is developed using the procedures of static or steady-state problems, while carrying all time-dependent terms in the formulation. This step results in a set of ordinary differential equations (i.e., a semidiscrete system of differential equations) in time for the nodal variables $u_j^e(t)$ of the element.

2. *Temporal approximation*, where the system of ordinary differential equations in time are further approximated, often using finite difference formulae for the time derivatives. This step allows conversion of the system of ordinary differential equations into a set of algebraic equations among u_j^e at time t_{s+1} [= $(s + 1)\Delta t$, when uniform time increment Δt is used]. Here s denotes the time step number.

All time approximation schemes seek to find the vector of nodal values **u** at time t_{s+1} using the known values of **u** from the previous times:

$$\text{compute } \mathbf{u}_{s+1} \text{ using } \mathbf{u}_s, \mathbf{u}_{s-1}, \ldots$$

Thus, at the end of the two-stage approximation, one has a continuous spatial solution but only at discrete intervals of time:

$$u(x, t_s) \approx u_h^e(x, t_s) = \sum_{j=1}^{n} u_j^e(t_s)\psi_j^e(x) \quad (s = 0, 1, \ldots) \tag{7.4.2}$$

Note that the approximate solution in Eq. (7.4.2) has the same form as that in separation of variables technique used to solve time-dependent problems (see Section 7.3.2). By taking nodal values to be functions of time, we presume that the nodes have different values of the variable at different times, as illustrated in Fig. 7.4.1.

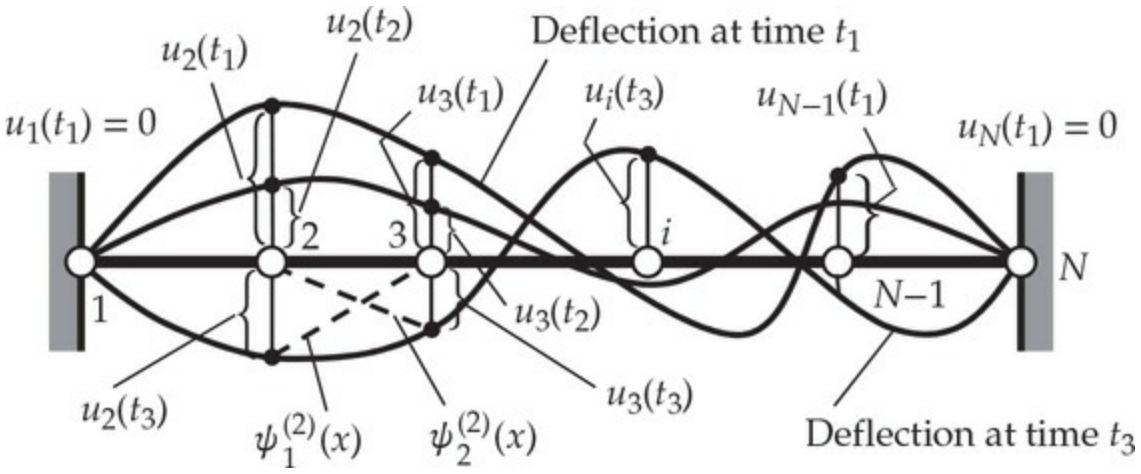

Fig. 7.4.1 Deflections of a cable at different times.

In Section 7.4.2 we study the details of the two steps by considering a model differential equation that contains three different model equations, namely, Eqs. (7.2.1)–(7.2.3). The Timoshenko beam equations are considered in Section 7.4.3.

7.4.2 Semidiscrete Finite Element Model of a Single Model Equation

7.4.2.1 Governing equation

We consider the following general model differential equation that contains Eqs. (7.2.1)–(7.2.3) as special cases:

$$-\frac{\partial}{\partial x}\left(a\frac{\partial u}{\partial x}\right)+\frac{\partial^2}{\partial x^2}\left(b\frac{\partial^2 u}{\partial x^2}\right)+c_0u+c_1\frac{\partial u}{\partial t}+c_2\frac{\partial^2 u}{\partial t^2}-c_3\frac{\partial^2}{\partial t^2}\left(\frac{\partial^2 u}{\partial x^2}\right)=f(x,t) \quad (7.4.3)$$

There may not exist any physical problem for which all terms in the differential equation are nonzero. Equation (7.4.3) contains the following model equations as special cases:

1. Heat transfer and fluid flow: $a \neq 0$, $b = 0$, $c_0 \neq 0$, $c_1 \neq 0$, $c_2 = 0$, $c_3 = 0$.
2. Transverse motion of cables and axial motion of bars: $a = T$ or EA, $b = 0$, $c_0 = 0$, $c_1 = 0$ (damping is not considered), $c_2 = \rho A$, $c_3 = 0$.
3. The transverse motion of beams using the Euler–Bernoulli beam theory: $a = 0$, $b = EI$, $c_0 = k_f$, $c_1 = 0$, $c_2 = \rho A$, $c_2 = \rho I$.

Once the finite element formulation of Eq. (7.4.3) is completed, the

results can be specialized to any model equation considered in Chapters 3, 4, and 5.

Equation (7.4.3) is subject to appropriate boundary conditions (depending on the problem). The initial conditions involve specifying

$$u(x,0) \quad \text{or} \quad u(x,0) \text{ and } \dot{u}(x,0) \quad (\dot{u} \equiv \partial u/\partial t) \tag{7.4.4}$$

7.4.2.2 Weak form

We begin with the development of the weak form of Eq. (7.4.3) over an element for any arbitrary time, followed by the derivation of the semidiscrete finite element model using the approximation of the form in Eq. (7.4.1b). Following the three-step procedure of constructing the weak form of a differential equation (all of the terms in the differential equation have already been considered previously), we obtain

$$\begin{aligned} 0 &= \int_{x_a^e}^{x_b^e} \left[a\frac{dw}{dx}\frac{\partial u}{\partial x} + b\frac{d^2w}{dx^2}\frac{\partial^2 u}{\partial x^2} + c_3\frac{dw}{dx}\frac{\partial^3 u}{\partial x \partial t^2} + w\left(c_0 u + c_1\frac{\partial u}{\partial t} + c_2\frac{\partial^2 u}{\partial t^2} - f\right)\right] dx \\ &\quad + \left[w\left(-a\frac{\partial u}{\partial x} + \frac{\partial}{\partial x}\left(b\frac{\partial^2 u}{\partial x^2}\right) - c_3\frac{\partial^3 u}{\partial x \partial t^2}\right) + \frac{dw}{dx}\left(-b\frac{\partial^2 u}{\partial x^2}\right)\right]_{x_a^e}^{x_b^e} \\ &= \int_{x_a^e}^{x_b^e} \left[a\frac{dw}{dx}\frac{\partial u}{\partial x} + b\frac{d^2w}{dx^2}\frac{\partial^2 u}{\partial x^2} + c_3\frac{dw}{dx}\frac{\partial^3 u}{\partial x \partial t^2} + w\left(c_0 u + c_1\frac{\partial u}{\partial t} + c_2\frac{\partial^2 u}{\partial t^2} - f\right)\right] dx \\ &\quad - Q_1^e w(x_a^e) - Q_3^e w(x_b^e) - Q_2^e \left(-\frac{dw}{dx}\right)\Big|_{x_a^e} - Q_4^e \left(-\frac{dw}{dx}\right)\Big|_{x_b^e} \end{aligned} \tag{7.4.5a}$$

where $w(x)$ is the weight function and

$$\begin{aligned} Q_1^e &= \left[-a\frac{\partial u}{\partial x} + \frac{\partial}{\partial x}\left(b\frac{\partial^2 u}{\partial x^2}\right) - c_3\frac{\partial^3 u}{\partial x \partial t^2}\right]_{x_a^e}, \quad Q_2^e = \left[b\frac{\partial^2 u}{\partial x^2}\right]_{x_a^e} \\ Q_3^e &= -\left[-a\frac{\partial u}{\partial x} + \frac{\partial}{\partial x}\left(b\frac{\partial^2 u}{\partial x^2}\right) - c_3\frac{\partial^3 u}{\partial x \partial t^2}\right]_{x_b^e}, \quad Q_4^e = -\left[b\frac{\partial^2 u}{\partial x^2}\right]_{x_b^e} \end{aligned} \tag{7.4.5b}$$

We note that the primary variables are u and $\partial u/\partial x$. Therefore, the finite element approximation of $u(x, t)$ is necessarily based on the Hermite cubic polynomials.

7.4.2.3 Semidiscrete finite element model

Next, we assume that u is interpolated by an expression of the form in Eq. (7.4.1b). The finite element solution that we obtain at the end of the analysis is continuous in space but not in time. We obtain the finite element solution in the form

$$u(x,t_s)=\sum_{j=1}^{n}u_j^e(t_s)\psi_j^e(x)=\sum_{j=1}^{n}(u_j^s)^e\psi_j^e(x)\quad(s=1,2,\ldots)$$

where $(u_j^s)^e$ is the value of $u(x, t)$ at time $t = t_s$ and node j of the element Ω_e. As already noted earlier, ψ_i^e are the Hermite cubic polynomials when $b \neq 0$ (i.e., when the fourth-order term is present); otherwise, they are Lagrange interpolation functions of a desired degree.

Substituting $w = \psi_i(x)$ (to obtain the ith equation of the system) and Eq. (7.4.1b) into Eq. (7.4.5a), we obtain (the element label "e" is omitted for brevity)

$$\begin{aligned}0=&\sum_{j=1}^{n}u_j\int_{x_a}^{x_b}\left(a\frac{d\psi_i}{dx}\frac{d\psi_j}{dx}+b\frac{d^2\psi_i}{dx^2}\frac{d^2\psi_j}{dx^2}+c_0\psi_i\psi_j\right)dx\\&+\sum_{j=1}^{n}\frac{du_j}{dt}\int_{x_a}^{x_b}c_1\psi_i\psi_j\,dx+\sum_{j=1}^{n}\frac{d^2u_j}{dt^2}\int_{x_a}^{x_b}\left(c_2\psi_i\psi_j+c_3\frac{d\psi_i}{dx}\frac{d\psi_j}{dx}\right)dx\\&-\left[\int_{x_a}^{x_b}\psi_i f\,dx+Q_1\psi_i(x_a)+Q_3\psi_i(x_b)+Q_2\left(-\frac{d\psi_i}{dx}\right)\Big|_{x_a}+Q_4\left(-\frac{d\psi_i}{dx}\right)\Big|_{x_b}\right]\\=&\sum_{j=1}^{n}\left(K_{ij}u_j+C_{ij}\frac{du_j}{dt}+M_{ij}\frac{d^2u_j}{dt^2}\right)-F_i\end{aligned}\qquad(7.4.6a)$$

In matrix form, Eq. (7.4.6a) takes the form

$$\mathbf{Ku}+\mathbf{C}\dot{\mathbf{u}}+\mathbf{M}\ddot{\mathbf{u}}=\mathbf{F}\qquad(7.4.6b)$$

where $\mathbf{F} = \mathbf{f} + \mathbf{Q}$, and

$$K_{ij} = \int_{x_a}^{x_b} \left(a \frac{d\psi_i}{dx}\frac{d\psi_j}{dx} + b \frac{d^2\psi_i}{dx^2}\frac{d^2\psi_j}{dx^2} + c_0 \psi_i \psi_j \right) dx, \quad f_i = \int_{x_a}^{x_b} \psi_i f \, dx$$

$$C_{ij} = \int_{x_a}^{x_b} c_1 \psi_i \psi_j \, dx, \quad M_{ij} = \int_{x_a}^{x_b} \left(c_2 \psi_i \psi_j + c_3 \frac{d\psi_i}{dx}\frac{d\psi_j}{dx} \right) dx \tag{7.4.6c}$$

$$Q_i = Q_1 \psi_i(x_a) + Q_3 \psi_i(x_b) + Q_2 \left[-\frac{d\psi_i}{dx} \right]_{x_a} + Q_4 \left[-\frac{d\psi_i}{dx} \right]_{x_b}$$

7.4.3 The Timoshenko Beam Theory

7.4.3.1 Weak forms

The governing equations of motion of the Timoshenko beam theory are given by Eqs. (7.2.4a) and (7.2.4b). Their weak forms are given by Eqs. (5.3.9a) and (5.3.9b) with the addition of the inertia terms (where v^e_{1i} and v^e_{2i} denote the weight functions):

$$0 = \int_{x_a^e}^{x_b^e} \left[c_2 v^e_{1i} \frac{\partial^2 w}{\partial t^2} + G_e A_e K_s \frac{dv^e_{1i}}{dx} \left(\phi^e_x + \frac{dw^e_h}{dx} \right) + k^e_f v^e_{1i} w^e_h - v^e_{1i} q_e \right] dx$$
$$- v^e_{1i}(x^e_a) Q^e_1 - v^e_{1i}(x^e_b) Q^e_3 \tag{7.4.7a}$$

$$0 = \int_{x_a^e}^{x_b^e} \left[c_3 v^e_{2i} \frac{\partial^2 \phi^e_x}{\partial t^2} + E_e I_e \frac{dv^e_{2i}}{dx}\frac{d\phi^e_x}{dx} + G_e A_e K_s v^e_{2i} \left(\phi^e_x + \frac{dw^e_h}{dx} \right) \right] dx$$
$$- v^e_{2i}(x^e_a) Q^e_2 - v^e_{2i}(x^e_b) Q^e_4 \tag{7.4.7b}$$

where

$$
\begin{aligned}
Q_1^e &\equiv -\left[G_e A_e K_s \left(\phi_x^e + \frac{dw_h^e}{dx}\right)\right]\Big|_{x_a^e} \\
Q_2^e &\equiv -\left[E_e I_e \frac{d\phi_x^e}{dx}\right]_{x_a^e} \\
Q_3^e &\equiv \left[G_e A_e K_s \left(\phi_x^e + \frac{dw_h^e}{dx}\right)\right]_{x_b^e} \\
Q_4^e &\equiv \left[E_e I_e \frac{d\phi_x^e}{dx}\right]_{x_b^e}
\end{aligned}
\tag{7.4.7c}
$$

7.4.3.2 Semidiscrete finite element model

The finite element model of the Timoshenko beam theory is derived by assuming approximation of the form [see Eq. (5.3.12)]

$$
w \approx w_h^e = \sum_{j=1}^{m} w_j^e(t)\psi_j^{(1)}(x), \quad \phi_x \approx \phi_x^e = \sum_{j=1}^{n} S_j^e(t)\psi_j^{(2)}(x) \tag{7.4.8}
$$

Substituting these approximations into the weak forms in Eqs. (7.4.7a) and (7.4.7b), we arrive at the semidiscrete finite element model [see Eq. (5.3.15)]

$$
\begin{bmatrix} \mathbf{M}^{11} & 0 \\ 0 & \mathbf{M}^{22} \end{bmatrix}^e \begin{Bmatrix} \ddot{\mathbf{w}} \\ \ddot{\mathbf{s}} \end{Bmatrix} + \begin{bmatrix} \mathbf{K}^{11} & \mathbf{K}^{12} \\ \mathbf{K}^{21} & \mathbf{K}^{22} \end{bmatrix} \begin{Bmatrix} \mathbf{w} \\ \mathbf{s} \end{Bmatrix} = \begin{Bmatrix} \mathbf{F}^1 \\ \mathbf{F}^2 \end{Bmatrix} \tag{7.4.9a}
$$

where $K_{ij}^{\alpha\beta}$ and F_i^{α} are defined in Eq. (5.3.14), and

$$
M_{ij}^{11} = \int_{x_a^e}^{x_b^e} c_2 \psi_i^{(1)} \psi_j^{(1)}\, dx, \quad M_{ij}^{22} = \int_{x_a^e}^{x_b^e} c_3 \psi_i^{(2)} \psi_j^{(2)}\, dx \tag{7.4.9b}
$$

In the standard matrix form, Eq. (7.4.9a) can be expressed as

$$
\mathbf{K}^e \boldsymbol{\Delta}^e + \mathbf{M}^e \ddot{\boldsymbol{\Delta}}^e = \mathbf{F}^e \tag{7.4.10}
$$

Equations (7.4.6b) and (7.4.10) are hyperbolic equations. The time approximation of parabolic and hyperbolic equations to derive the fully discretized (i.e., algebraic) equations will be considered separately because

methods used are different for these two types of equations.

7.4.4 Parabolic Equations

7.4.4.1 Time approximations

The time approximation is discussed with the help of a single first-order differential equation for u_i, and then we generalize for a vector of unknowns, **u**. Suppose that we wish to determine $u_i(t)$ for $t > 0$ such that $u_i(t)$ satisfies

$$a\frac{du_i}{dt} + bu_i = f_i(t), \quad 0 < t < T \quad \text{and} \quad u_i(0) = u_i^0 \tag{7.4.11}$$

where $a \neq 0$, b, and u_i^0 are constants and f_i is a function of time t. The exact solution of the problem consists of two parts: the homogeneous and particular solutions. The homogeneous solution is

$$u_i^h(t) = Ae^{-kt}, \quad k = \frac{b}{a}$$

where A is a constant of integration. The particular solution is given by

$$u_i^p(t) = \frac{1}{a}e^{-kt}\left(\int_0^t e^{k\tau} f_i(\tau)\, d\tau\right)$$

The complete solution is given by

$$u_i(t) = e^{-kt}\left(A + \frac{1}{a}\int_0^t e^{k\tau} f_i(\tau)\, d\tau\right)$$

Finite difference approximations. The finite difference methods are based on truncated (using the desired degree of accuracy) Taylor's series expansions. For example, Taylor's series expansions of function $F(t)$ about $t = t_s$ and $t = t_{s+1}$ are given by

$$F(t) = F(t_s) + (t - t_s)\dot{F}(t_s) + \frac{1}{2!}(t - t_s)^2\ddot{F}(t_s) + \cdots \tag{7.4.12a}$$

$$F(t) = F(t_{s+1}) + (t - t_{s+1})\dot{F}(t_{s+1}) + \frac{1}{2!}(t - t_{s+1})^2\ddot{F}(t_{s+1}) + \cdots \tag{7.4.12b}$$

In particular, for $t = t_{s+1}$ in Eq. (7.4.12a), we have

$$F(t_{s+1}) = F(t_s) + (t_{s+1} - t_s)\dot{F}(t_s) + \frac{1}{2!}(t_{s+1} - t_s)^2\ddot{F}(t_s) + \frac{1}{3!}(t_{s+1} - t_s)^3\dddot{F}(t_s) + \cdots$$

If we truncate the series after the second term and solve for $\dot{F}(t_s)$, we obtain

$$\dot{F}(t_s) = \frac{F(t_{s+1}) - F(t_s)}{t_{s+1} - t_s} + O(\Delta t_{s+1}) \tag{7.4.13a}$$

The order of accuracy of the approximation is said to be of the order $O(\Delta t_{s+1})$, where $\Delta t_{s+1} = t_{s+1} - t_s$. Thus we have

$$\dot{F}(t_s) \approx \frac{F(t_{s+1}) - F(t_s)}{t_{s+1} - t_s} \quad \text{or} \quad \dot{F}^s \approx \frac{F^{s+1} - F^s}{\Delta t_{s+1}} \tag{7.4.13b}$$

which is known as the *forward difference* or *Euler's* scheme. The name forward difference indicates that the slope at time $t = t_s$ is obtained using the difference in the value of F at the next (forward) time $t = t_{s+1}$ and the current $t = t_s$ (see Fig. 7.4.2). Next let $t = t_s$ in Eq. (7.4.12b). We arrive at

$$\dot{F}(t_{s+1}) \approx \frac{F(t_{s+1}) - F(t_s)}{t_{s+1} - t_s} \quad \text{or} \quad \dot{F}^{s+1} \approx \frac{F^{s+1} - F^s}{\Delta t_{s+1}} \tag{7.4.13c}$$

which is known, for the obvious reason, as the *backward difference* scheme (see Fig. 7.4.2).

The forward and backward difference schemes can be put into a single scheme with the help of a parameter, α, $0 \le \alpha \le 1$. First, we change the variable $F(t)$ to our original variable $u_i(t)$ used in Eq. (7.4.11). Then the two schemes in Eqs. (7.4.13b) and (7.4.13c) can be expressed in a single equation as

$$(1 - \alpha)\dot{u}_i^s + \alpha\,\dot{u}_i^{s+1} = \frac{u_i^{s+1} - u_i^s}{\Delta t_{s+1}} \quad \text{for } 0 \le \alpha \le 1 \tag{7.4.14}$$

where u_i^s denotes the value of $u_i(t)$ at time $t = t_s = \sum_{i=1}^{s} \Delta t_i$, and $\Delta t_{s+1} = t_{s+1} - t_s$ is the $(s + 1)$st time increment. The scheme in Eq. (7.4.14) is known as the *α-family of approximation*, in which a weighted average of the time derivatives of u_i at two consecutive time steps is approximated by linear

interpolation of the values of the variable at the two different times (see Fig. 7.4.2). When we set $\alpha = 0$ in Eq. (7.4.14), we obtain the forward difference scheme and when $\alpha = 1$, we obtain the backward difference scheme. For $\alpha = 1/2$, the scheme in Eq. (7.4.14) is known as the *Crank–Nicolson scheme*. If the total time $(0, T]$ is divided into equal time steps, say Δt, then $t_s = s\Delta t$. In the rest of the book, we assume that the time steps are of uniform size.

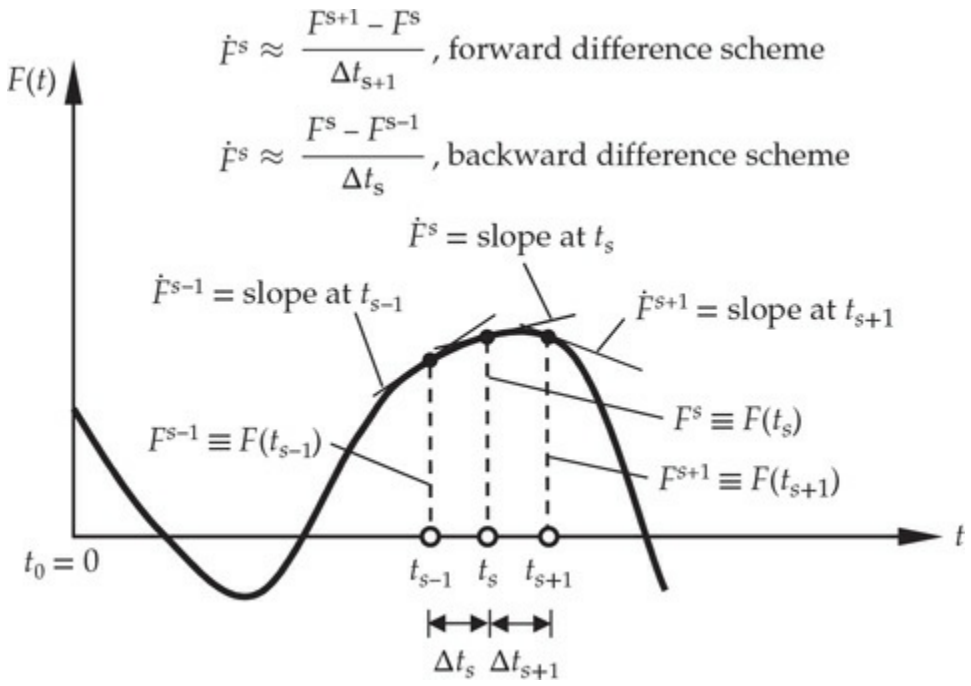

Fig. 7.4.2 Approximation of the time derivative of a function.

Equation (7.4.14) can be expressed as

$$u_i^{s+1} = u_i^s + \Delta t\left[(1-\alpha)\dot{u}_i^s + \alpha\,\dot{u}_i^{s+1}\right], \quad \text{for } 0 \le \alpha \le 1 \tag{7.4.15}$$

Returning to Eq. (7.4.11), we note that it is valid for all times $t > 0$. In particular, it is valid at times $t = t_s$ and $t = t_{s+1}$. Hence, from Eq. (7.4.11) we have

$$\dot{u}_i^s = \frac{1}{a}\left(f_i^s - bu_i^s\right), \quad \dot{u}_i^{s+1} = \frac{1}{a}\left(f_i^{s+1} - bu_i^{s+1}\right) \tag{7.4.16}$$

Substituting the expressions from Eq. (7.4.16) into Eq. (7.4.15), we arrive at

$$(1-\alpha)\left(f_i^s - bu_i^s\right) + \alpha\left(f_i^{s+1} - bu_i^{s+1}\right) = a\left(\frac{u_i^{s+1} - u_i^s}{\Delta t}\right)$$

Solving for u_i^{s+1}, we obtain

$$[a + \alpha\,\Delta t\, b]\, u_i^{s+1} = [a - (1-\alpha)\,\Delta t\, b]\, u_i^s + \Delta t\left[\alpha f_i^{s+1} + (1-\alpha) f_i^s\right] \tag{7.4.17a}$$

or

$$u_i^{s+1} = \frac{a - (1-\alpha)\,\Delta t\, b}{a + \alpha\,\Delta t\, b}\, u_i^s + \Delta t \frac{\alpha f_i^{s+1} + (1-\alpha) f_i^s}{a + \alpha\,\Delta t\, b} \tag{7.4.17b}$$

Thus, Eq. (7.4.17b) can be used repeatedly (i.e., march in time) to obtain the solution at times $t = t_{s+1}, t_{s+2}, \ldots, t_N$, where N is the number of time steps required to reach the final time T (or solution reaches steady state). At the very beginning, that is when $s = 0$, the solution u_i^1 is calculated using the initial value u_i^0:

$$u_i^1 = \frac{a - (1-\alpha)\,\Delta t\, b}{a + \alpha\,\Delta t\, b}\, u_i^0 + \Delta t\, \frac{\alpha f_i^1 + (1-\alpha) f_i^0}{a + \alpha\,\Delta t\, b} \tag{7.4.18}$$

Finite element approximations. One may also develop a time approximation scheme using the finite element method with the Galerkin method of approximation. We divide the time domain into a finite set of intervals (time finite elements), the domain of a typical element being $[t_s, t_{s+1}]$. The weighted-residual form of Eq. (7.4.11) over the time finite element (t_s, t_{s+1}) is

$$0 = \int_{t_s}^{t_{s+1}} v(t)\left(a\frac{du_i}{dt} + bu_i - f_i\right) dt \tag{7.4.19}$$

where v is the weight function. Assuming solution of the form

$$u_i(t) \approx \sum_{k=1}^{n} u_{ki}\, \psi_k(t) \tag{7.4.20}$$

where $\psi_k(t)$ are interpolation functions of order $(n-1)$. The Galerkin finite element model is obtained by substituting the expression in Eq. (7.4.20) for u_i and $v = \psi_j$ into Eq. (7.4.19). We obtain

$$\mathbf{A}\mathbf{u}_i = \mathbf{F}_i \tag{7.4.21a}$$

where

$$A_{jk} = \int_{t_s}^{t_{s+1}} \psi_j(t)\left(a\frac{d\psi_k}{dt} + b\psi_k\right)dt, \quad F_{ji} = \int_{t_s}^{t_{s+1}} \psi_j(t) f_i(t)\, dt \tag{7.4.21b}$$

Equation (7.4.21b) is valid in the time interval (t_s, t_{s+1}), and it represents a relationship between the values $u_{1i}, u_{2i}, \ldots, u_{ni}$, which are the values of u_i at time $t_s, t_{s+\Delta t/(n-1)}, t_{s+2\Delta t/(n-1)}, \ldots, t_{s+1}$, respectively. This would yield, for $n > 2$, a multi-step approximation scheme.

To obtain a single-step approximation scheme, that is, write u_i^{s+1} in terms of u_i^s only, we assume linear approximation (i.e., $n = 2$)

$$u_i(t) = u_i^s \psi_1(t) + u_i^{s+1}\psi_2(t); \quad \psi_1(t) = \frac{t_{s+1} - t}{\Delta t}, \quad \psi_2(t) = \frac{t - t_s}{\Delta t} \tag{7.4.22a}$$

In the same fashion, $f_i(t)$ can be represented in terms of its values at t_s and t_{s+1}:

$$f_i(t) = f_i^s\, \psi_1(t) + f_i^{(s+1)}\, \psi_2(t) \tag{7.4.22b}$$

For this choice of approximation, Eq. (7.4.21a) becomes (see Table 3.7.1)

$$\left(\frac{a}{2}\begin{bmatrix} -1 & 1 \\ -1 & 1 \end{bmatrix} + \frac{b\Delta t}{6}\begin{bmatrix} 2 & 1 \\ 1 & 2 \end{bmatrix}\right)\begin{Bmatrix} u_i^s \\ u_i^{s+1} \end{Bmatrix} = \frac{\Delta t}{6}\begin{bmatrix} 2 & 1 \\ 1 & 2 \end{bmatrix}\begin{Bmatrix} f_i^s \\ f_i^{s+1} \end{Bmatrix} \tag{7.4.22c}$$

Assuming that u_i^s is known, we solve for u_i^{s+1} from the second equation in Eq. (7.4.22c):

$$\left(a + \frac{2}{3}\Delta t\, b\right)u_i^{s+1} = \left(a - \frac{1}{3}\Delta t\, b\right)u_i^s + \Delta t\left(\frac{1}{3}f_i^s + \frac{2}{3}f_i^{s+1}\right) \tag{7.4.22d}$$

Comparing Eq. (7.4.22d) with Eq. (7.4.17a), we find that the Galerkin finite element scheme of Eq. (7.4.22d) is a special case of the α-family of approximation for $\alpha = 2/3$.

7.4.4.2 Numerical stability

Since the time-marching scheme in Eq. (7.4.17b) uses the previous time step solution u_i^s, which itself is an approximate solution, there is a

possibility that the error introduced in u_i^s may be amplified when u_i^{s+1} is computed and may grow unboundedly with time. When the error grows without bounds, the underlying scheme is said to be *unstable*. Here we wish to determine the conditions under which the error remains bounded.

Consider Eq.(7.4.17b) in operator form

$$u_i^{s+1} = Bu_i^s + \bar{F}^{s,s+1} \tag{7.4.23a}$$

where

$$B = \frac{a - (1-\alpha)\,\Delta t\, b}{a + \alpha\,\Delta t\, b}, \quad \bar{F}_{s,s+1} = \Delta t\, \frac{\alpha f_{s+1} + (1-\alpha) f_s}{a + \alpha\,\Delta t\, b} \tag{7.4.23b}$$

If the magnitude of the operator B, known as the *amplification operator*, is greater than 1, $|B| > 1$, the error will be amplified during each time step. On the other hand, if the magnitude is equal to or less than unity, the error will not grow with time. Therefore, in order for the scheme to be stable it is necessary that $|B| \leq 1$:

$$|B| = \left| \frac{a - (1-\alpha)\,\Delta t\, b}{a + \alpha\,\Delta t\, b} \right| \leq 1 \tag{7.4.24}$$

The above equation places a restriction on the magnitude of the time step for certain values of α. When the error remains bounded for any time step [i.e., condition (7.4.24) is trivially satisfied for any value of Δt], it is known as a *stable* scheme. If the error remains bounded only when the time step remains below certain value [in order to satisfy (7.4.24)], it is said to be *conditionally stable* scheme. In the finite element method, the coefficients a and b appearing in Eq. (7.4.24) depend on problem material parameters (which cannot be changed) and the element length (which can be selected). Hence, for a given mesh there is a value of Δt that makes the scheme conditionally stable (more details on this topic can be found in the book by Surana and Reddy [4]).

7.4.4.3 Consistency and accuracy

In addition to the truncation error introduced in approximating the time derivative, round-off errors can be introduced because of the finite arithmetic used in the computations. The numerical scheme (7.4.23a) is said to be *consistent* with the continuous problem (7.4.6b) if the round-off and truncation errors go to zero as $\Delta t \to 0$. *Accuracy* of a numerical scheme is a measure of the closeness between the approximate solution

and the exact solution, whereas stability of a solution is a measure of the boundedness of the approximate solution with time. As one might expect, the size of the time step as well as the mesh can influence both accuracy and stability. When we construct an approximate solution, we like it to converge to the true solution when the number of elements or the degree of approximation is increased and the time step Δt is decreased. A time-approximation scheme is said to be *convergent* if, for fixed t_s and Δt, the numerical value $\mathbf{u}_s$ converges to its true value $\mathbf{u}(t_s)$ as the mesh size h goes to zero. Accuracy is measured in terms of the rate at which the approximate solution converges. If a numerical scheme is both stable and consistent, it is also convergent.

7.4.4.4 Fully discretized finite element equations

We now have the tools necessary to convert a set of ordinary differential equations such as those in Eq. (7.4.6b) for the case in which $\mathbf{M} = 0$, to a set of algebraic equations, much the same way a single differential equation (7.4.11) was converted to the algebraic equation (7.4.17a). We begin with the parabolic equation

$$\mathbf{C}\dot{\mathbf{u}} + \mathbf{K}\mathbf{u} = \mathbf{F} \tag{7.4.25a}$$

subject to the initial conditions

$$\mathbf{u}(0) = \mathbf{u}^0 \tag{7.4.25b}$$

where $\mathbf{u}(0)$ denotes the vector of nodal values of $\mathbf{u}(x, t)$ at time $t = 0$, whereas $\mathbf{u}^0$ denotes the column of nodal values u_j^0. The eigenvalue problem associated with Eq. (7.4.25a) is (set $f = 0$, $\mathbf{u} = \mathbf{u}_0 e^{-\lambda t}$, and $\mathbf{F} = \mathbf{Q} = \mathbf{Q}_0 e^{-\lambda t}$)

$$(-\lambda \mathbf{C} + \mathbf{K})\,\mathbf{u}_0 = \mathbf{Q}_0 \tag{7.4.25c}$$

As applied to a vector of time derivatives of the nodal values, the α-family of approximation in Eq. (7.4.15) takes the form

$$\mathbf{u}^{s+1} = \mathbf{u}^s + a_2\dot{\mathbf{u}}^s + a_1\dot{\mathbf{u}}^{s+1} \quad \text{for } 0 \le \alpha \le 1 \tag{7.4.26a}$$

$$a_1 = \alpha\,\Delta t, \quad a_2 = (1-\alpha)\Delta t \tag{7.4.26b}$$

Evaluating Eq. (7.4.25a) for times $t = t_s$ and $t = t_{s+1}$, we have

$$\mathbf{C}\dot{\mathbf{u}}^s + \mathbf{K}\mathbf{u}^s = \mathbf{F}^s \tag{7.4.27a}$$

$$\mathbf{C}\dot{\mathbf{u}}^{s+1} + \mathbf{K}\mathbf{u}^{s+1} = \mathbf{F}^{s+1} \tag{7.4.27b}$$

where it is assumed that the matrices **C** and **M** are independent of time. Premultiplying both sides of Eq. (7.4.26a) with **C**, we obtain

$$\mathbf{C}(\mathbf{u}^{s+1} - \mathbf{u}^{s}) = a_1\mathbf{C}\dot{\mathbf{u}}^{s+1} + a_2\mathbf{C}\dot{\mathbf{u}}^{s} \tag{7.4.27c}$$

Substituting for $\mathbf{C}\dot{\mathbf{u}}^{s}$ and $\mathbf{C}\dot{\mathbf{u}}^{s+1}$ from Eqs. (7.4.27a) and (7.4.27b), respectively, we arrive at

$$\mathbf{C}(\mathbf{u}^{s+1} - \mathbf{u}^{s}) = a_1\left(\mathbf{F}^{s+1} - \mathbf{K}\mathbf{u}^{s+1}\right) + a_2\left(\mathbf{F}^{s} - \mathbf{K}\mathbf{u}^{s}\right) \tag{7.4.28}$$

Solving for the vector $\mathbf{u}^{s+1}$, we obtain the recursive relation (i.e., a relation between solutions at two consecutive time steps)

$$\hat{\mathbf{K}}\mathbf{u}^{s+1} = \bar{\mathbf{K}}\mathbf{u}^{s} + \bar{\mathbf{F}}^{s,s+1} \equiv \hat{\mathbf{F}}^{s,s+1} \tag{7.4.29a}$$

where

$$\hat{\mathbf{K}} = \mathbf{C} + a_1\mathbf{K}, \quad \bar{\mathbf{K}} = \mathbf{C} - a_2\mathbf{K}$$
$$\bar{\mathbf{F}}^{s,s+1} = \left(a_1\mathbf{F}^{s+1} + a_2\mathbf{F}^{s}\right) \tag{7.4.29b}$$

Equations (7.4.29a) and (7.4.29b) are valid for a typical finite element. Equations (7.4.29a) and (7.4.29b) hold for any problem, independent of the dimension and method of spatial approximation, as long as the end result is Eq. (7.4.25a). The assembly, imposition of boundary conditions, and solution of the assembled equations are the same as described before for steady-state problems. Calculation of $\hat{\mathbf{K}}$ and $\bar{\mathbf{F}}$ at time $t = 0$ requires knowledge of the initial conditions $\mathbf{u}^0$ and the time variation of **F**.

All numerical schemes with $\alpha \geq \frac{1}{2}$ (e.g., backward difference, Crank–Nicolson, and Galerkin schemes) are stable independent of the mesh. Numerical schemes obtained with $\alpha < \frac{1}{2}$ (e.g., the forward difference method) are stable only if the time step satisfies the following (stability) condition (see Surana and Reddy [4] for details):

$$\Delta t < \Delta t_{cr} \equiv \frac{2}{(1-2\alpha)\lambda_{\max}}, \quad \alpha < \frac{1}{2} \tag{7.4.30}$$

where $\lambda_{\max}$ is the largest eigenvalue of the eigenvalue problem in Eq. (7.4.25c).

The stability and accuracy characteristics of the following well-known time-approximation schemes should be noted:

$$\alpha = \begin{cases} 0, & \text{the forward difference (or Euler) scheme (conditionally stable);} \\ & \text{order of accuracy} = O(\Delta t) \\ \frac{1}{2}, & \text{the Crank–Nicolson scheme (stable);} \\ & \text{order of accuracy} = O(\Delta t)^2 \\ \frac{2}{3}, & \text{the Galerkin method (stable);} \\ & \text{order of accuracy} = O(\Delta t)^2 \\ 1, & \text{the backward difference scheme (stable);} \\ & \text{order of accuracy} = O(\Delta t) \end{cases} \tag{7.4.31}$$

Of these schemes, the Crank–Nicolson scheme ($\alpha = 0.5$) is the most commonly used stable scheme.

7.4.5 Hyperbolic Equations

7.4.5.1 Equations of structural dynamics

Consider matrix equations of the form

$$\mathbf{M}\ddot{\mathbf{u}} + \mathbf{C}\dot{\mathbf{u}} + \mathbf{K}\mathbf{u} = \mathbf{F} \tag{7.4.32a}$$

subjected to initial conditions

$$\mathbf{u}(0) = \mathbf{u}_0, \quad \dot{\mathbf{u}}(0) = \mathbf{v}_0 \tag{7.4.32b}$$

Such equations arise in structural dynamics, where **M** is the mass matrix, **C** is the damping matrix, and **K** is the stiffness matrix. The damping matrix **C** is often taken to be a linear combination of the mass and stiffness matrices, $\mathbf{C} = c_1\,\mathbf{M} + c_2\,\mathbf{K}$, where c_1 and c_2 are determined from physical experiments. In the present study, we will not consider damping (i.e., **C** = 0) in the numerical examples, although the theoretical developments will account for it. Transient analysis of both bars and beams lead to equations of the type given in Eqs. (7.4.32a) and (7.4.32b). The mass and stiffness matrices for bars and beams can be found in Eqs. (7.3.40), (7.3.57), (7.3.63a), and (7.3.63b). The eigenvalue problem associated with Eq. (7.4.32a) (with **C** = 0) is

$$(-\lambda\mathbf{M} + \mathbf{K})\,\mathbf{u}_0 = \mathbf{Q}_0, \quad \lambda = \omega^2 \tag{7.4.32c}$$

There are several numerical methods available to approximate the secondorder time derivatives and convert differential equations in time to

algebraic equations (see Surana and Reddy [4] for different order Runge–Kutta methods, the Newmark family of methods, Wilson's θ method, and Houbolt's method). Recently, Kim and Reddy [5–8] have developed a number of timeapproximation schemes based on weighted-residual and least-squares concepts [similar to the Galerkin scheme discussed in Eqs. (7.4.19)–(7.4.22d)]. In the interest of simplicity and wide use, we only consider the Newmark family of time approximations and the central difference scheme.

7.4.5.2 Fully discretized equations

Let us consider the following (α, γ)-*family of approximation*, where the function and its first time derivative are approximated as [following the truncated Taylor's series notation of Eq. (7.4.15)]

$$\mathbf{u}^{s+1} \approx \mathbf{u}^s + \Delta t\, \dot{\mathbf{u}}^s + \frac{1}{2}(\Delta t)^2 \left[(1-\gamma)\ddot{\mathbf{u}}^s + \gamma \ddot{\mathbf{u}}^{s+1}\right] \tag{7.4.33}$$

$$\dot{\mathbf{u}}^{s+1} \approx \dot{\mathbf{u}}^s + a_2 \ddot{\mathbf{u}}^s + a_1 \ddot{\mathbf{u}}^{s+1} \tag{7.4.34}$$

Here α and γ are parameters that determine the stability and accuracy of the scheme. Equations (7.4.33) and (7.4.34) are Taylor's series expansions of $\mathbf{u}^{s+1}$ and $\dot{\mathbf{u}}^{s+1}$, respectively, about $t = t_s$.

The fully discretized form of Eq. (7.4.32a) is obtained using the approximations introduced in Eqs. (7.4.33) and (7.4.34). First, we eliminate $\ddot{\mathbf{u}}^{s+1}$ from Eqs. (7.4.33) and (7.4.34) and write the result for $\dot{\mathbf{u}}^{s+1}$:

$$\dot{\mathbf{u}}^{s+1} = a_6\left(\mathbf{u}^{s+1} - \mathbf{u}^s\right) - a_7 \dot{\mathbf{u}}^s - a_8 \ddot{\mathbf{u}}^s \tag{7.4.35a}$$

$$a_6 = \frac{2\alpha}{\gamma \Delta t}, \quad a_7 = \frac{2\alpha}{\gamma} - 1, \quad a_8 = \left(\frac{\alpha}{\gamma} - 1\right)\Delta t \tag{7.4.35b}$$

Now pre-multiplying Eq. (7.4.33) with $\mathbf{M}$ and substituting for $\mathbf{M}\ddot{\mathbf{u}}^{s+1}$ from Eq. (7.4.32a), we obtain

$$\left(\mathbf{M} + \frac{\gamma(\Delta t)^2}{2}\mathbf{K}\right)\mathbf{u}^{s+1} = \mathbf{M}\mathbf{b}^s + \frac{\gamma(\Delta t)^2}{2}\mathbf{F}^{s+1} - \frac{\gamma(\Delta t)^2}{2}\mathbf{C}\dot{\mathbf{u}}^{s+1} \tag{7.4.36a}$$

where

$$\mathbf{b}^s = \mathbf{u}^s + \Delta t\, \dot{\mathbf{u}}^s + \frac{1}{2}(1-\gamma)(\Delta t)^2 \ddot{\mathbf{u}}^s \tag{7.4.36b}$$

Now, multiplying throughout with $2/[\gamma(\Delta t)^2]$ we arrive at

$$\left(\frac{2}{\gamma(\Delta t)^2}\mathbf{M}+\mathbf{K}\right)\mathbf{u}^{s+1}=\frac{2}{\gamma(\Delta t)^2}\mathbf{M}\mathbf{b}_s+\mathbf{F}^{s+1}-\mathbf{C}\dot{\mathbf{u}}^{s+1} \tag{7.4.36c}$$

Using Eq. (7.4.35a) for $\dot{\mathbf{u}}^{s+1}$ in Eq. (7.4.36c) and collecting terms, we obtain the recursive relation:

$$\hat{\mathbf{K}}\mathbf{u}^{s+1}=\hat{\mathbf{F}}^{s,s+1} \tag{7.4.37a}$$

where

$$\begin{aligned}
&\hat{\mathbf{K}}=\mathbf{K}+a_3\mathbf{M}+a_6\mathbf{C},\quad \hat{\mathbf{F}}^{s,s+1}=\mathbf{F}^{s+1}+\mathbf{M}\bar{\mathbf{u}}^s+\mathbf{C}\hat{\mathbf{u}}^s\\
&\bar{\mathbf{u}}^s=a_3\mathbf{u}^s+a_4\dot{\mathbf{u}}^s+a_5\ddot{\mathbf{u}}^s,\quad \hat{\mathbf{u}}^s=a_6\mathbf{u}^s+a_7\dot{\mathbf{u}}^s+a_8\ddot{\mathbf{u}}^s\\
&a_3=\frac{2}{\gamma(\Delta t)^2},\quad a_4=a_3\Delta t,\quad a_5=\frac{1}{\gamma}-1
\end{aligned} \tag{7.4.37b}$$

The two special cases of the (α, γ)-family of approximation are: (1) constant-average acceleration method ($\alpha = \gamma = 1/2$), which is known as the *Newmark scheme*, and (2) linear acceleration method ($\alpha = 1/2$ and $\gamma = 1/3$). For these two cases, the fully discretized equations in (7.4.37a) take the following explicit forms:

Constant-average acceleration scheme ($\alpha = \gamma = 1/2$):

$$\begin{aligned}
\left(\frac{4}{(\Delta t)^2}\mathbf{M}+\frac{2}{\Delta t}\mathbf{C}+\mathbf{K}\right)\mathbf{u}^{s+1}=\mathbf{F}^{s+1}&+\left(\frac{4}{(\Delta t)^2}\mathbf{M}+\frac{2}{\Delta t}\mathbf{C}\right)\mathbf{u}^s\\
&+\left(\frac{4}{\Delta t}\mathbf{M}+\mathbf{C}\right)\dot{\mathbf{u}}^s+\mathbf{M}\ddot{\mathbf{u}}^s
\end{aligned} \tag{7.4.38}$$

Linear acceleration scheme ($\alpha = 1/2$ and $\gamma = 1/3$):

$$\begin{aligned}
\left(\frac{6}{(\Delta t)^2}\mathbf{M}+\frac{3}{\Delta t}\mathbf{C}+\mathbf{K}\right)\mathbf{u}^{s+1}=\mathbf{F}^{s+1}&+\left(\frac{6}{(\Delta t)^2}\mathbf{M}+\frac{3}{\Delta t}\mathbf{C}\right)\mathbf{u}^s\\
&+\left(\frac{6}{\Delta t}\mathbf{M}+2\mathbf{C}\right)\dot{\mathbf{u}}^s+\left(2\mathbf{M}+\frac{\Delta t}{2}\mathbf{C}\right)\ddot{\mathbf{u}}^s
\end{aligned} \tag{7.4.39}$$

7.4.5.3 Fully discretized equations using central difference scheme

The central difference scheme can be derived using Taylor's series expansion of $\mathbf{u}(t_s + \Delta t) \equiv \mathbf{u}^{s+1}$ and $\mathbf{u}(t_s - \Delta t) \equiv \mathbf{u}^{s-1}$ about its value at t_s:

$$\mathbf{u}^{s+1}=\mathbf{u}^s+\Delta t\,\dot{\mathbf{u}}^s+\frac{(\Delta t)^2}{2}\ddot{\mathbf{u}}^s+O(\Delta t)^3 \tag{7.4.40a}$$

$$\mathbf{u}^{s-1} = \mathbf{u}^s - \Delta t\,\dot{\mathbf{u}}^s + \frac{(\Delta t)^2}{2}\ddot{\mathbf{u}}^s + O(\Delta t)^3 \tag{7.4.40b}$$

Subtracting Eq. (7.4.40b) from Eq. (7.4.40a), truncating the series after the linear terms in Δt, and solving for $\dot{\mathbf{u}}^s$, we obtain

$$\dot{\mathbf{u}}^s = \frac{1}{2\Delta t}\left(\mathbf{u}^{s+1} - \mathbf{u}^{s-1}\right) + O(\Delta t)^2 \tag{7.4.41a}$$

Adding Eq. (7.4.40a) to Eq. (7.4.40b), truncating the series after the quadratic terms in Δt, and solving for $\ddot{\mathbf{u}}^s$, we arrive at

$$\ddot{\mathbf{u}}^s = \frac{1}{(\Delta t)^2}\left(\mathbf{u}^{s+1} - 2\mathbf{u}^s + \mathbf{u}^{s-1}\right) + O(\Delta t) \tag{7.4.41b}$$

Substituting the approximations from Eqs. (7.4.41a) and (7.4.41b) into Eq. (7.4.32a) evaluated at $t = t_s$, we obtain the fully discretized equations of the central difference scheme:

$$\left(\frac{1}{(\Delta t)^2}\mathbf{M} + \frac{1}{2\Delta t}\mathbf{C}\right)\mathbf{u}^{s+1} = \mathbf{F}^s + \left(\frac{2}{(\Delta t)^2}\mathbf{M} - \mathbf{K}\right)\mathbf{u}^s - \left(\frac{1}{(\Delta t)^2}\mathbf{M} - \frac{1}{2\Delta t}\mathbf{C}\right)\mathbf{u}^{s-1} \tag{7.4.42}$$

7.4.5.4 Numerical stability

For all schemes in which $\gamma \geq \alpha \geq 1/2$ are stable; for $\alpha \geq \frac{1}{2}$ and $\gamma < \alpha$, the stability requirement (for the case in which $\mathbf{C} = 0$) is

$$\Delta t \leq \Delta t_{cr} = \left[\frac{1}{2}\omega_{\max}^2(\alpha - \gamma)\right]^{-1/2} \tag{7.4.43}$$

where $\omega_{\max}^2 = \lambda_{\max}$ is the maximum eigenvalue of the undamped system in Eq. (7.4.32c). The stability characteristics of various schemes are as follows:

- $\alpha = \frac{1}{2}$, $\gamma = \frac{1}{2}$, the constant-average acceleration method (stable)
- $\alpha = \frac{1}{2}$, $\gamma = \frac{1}{3}$, the linear acceleration method (conditionally stable)
- the central difference method (conditionally stable)

(7.4.44)

7.4.5.5 Starting of the time-marching algorithm

Note that the calculation of $\hat{\mathbf{F}}$ requires the knowledge of the initial conditions $\mathbf{u}^0$, $\dot{\mathbf{u}}^0$, and $\ddot{\mathbf{u}}^0$. Mathematically, a second-order equation requires only two initial conditions, namely, the displacement $\mathbf{u}^0$ and velocity $\dot{\mathbf{u}}^0$; one does not know $\ddot{\mathbf{u}}^0$ but is required by the recursive scheme to march forward in time. Thus, the (α, γ)-family as well as the central difference schemes are not self-starting schemes, and they are called implicit schemes. They all require $\mathbf{u}^{s-1}$ and $\mathbf{u}^s$ to calculate $\mathbf{u}^{s+1}$. Here we discuss ways to overcome this difficulty.

As an approximation, $\ddot{\mathbf{u}}^0$ can be calculated from Eq. (7.4.32a) (we often assume that the applied force is zero at $t = 0$, $\mathbf{F}^0 = 0$):

$$\ddot{\mathbf{u}}^0 = \mathbf{M}^{-1}\left(\mathbf{F}_0 - \mathbf{K}\mathbf{u}^0 - \mathbf{C}\dot{\mathbf{u}}^0\right) \tag{7.4.45}$$

At the end of each time step, the new velocity vector $\dot{\mathbf{u}}_{s+1}$ and acceleration vector $\ddot{\mathbf{u}}_{s+1}$ are computed using the equations [from Eqs. (7.4.33) and (7.4.34)]

$$\ddot{\mathbf{u}}^{s+1} = a_3\left(\mathbf{u}^{s+1} - \mathbf{u}^s\right) - a_4\dot{\mathbf{u}}^s - a_5\ddot{\mathbf{u}}^s \tag{7.4.46a}$$

$$\dot{\mathbf{u}}^{s+1} = \dot{\mathbf{u}}^s + a_2\ddot{\mathbf{u}}^s + a_1\ddot{\mathbf{u}}^{s+1} \tag{7.4.46b}$$

where a_1 through a_5 are defined in Eqs. (7.4.26b) and (7.4.37b).

For the central difference scheme, $\mathbf{u}^{s-1}$ at $s = 0$ is computed as follows. First note that the vectors $\mathbf{u}^0$, $\dot{\mathbf{u}}^0$, and $\ddot{\mathbf{u}}^0$ are known from the initial conditions in Eq. (7.4. 32b) and Eq. (7.4.45). Then from Eq. (7.4.40b), it follows that (set $s = 0$)

$$\mathbf{u}^{(-1)} = \mathbf{u}^0 - \Delta t\,\dot{\mathbf{u}}^0 + \frac{(\Delta t)^2}{2}\ddot{\mathbf{u}}^0 \tag{7.4.47}$$

7.4.6 Explicit and Implicit Formulations and Mass Lumping

The solution of the fully discretized equations of parabolic equations and hyperbolic equations (after assembly and imposition of boundary and initial conditions) require the inversion of $\hat{\mathbf{K}}$ appearing in Eqs. (7.4.29a) and (7.4.37a) to march forward in time and find the solution at different times. This can be an enormous computational expense, depending on the size of the mesh and the number of time steps. For example, if one needs to solve these equations for 1,000 time steps, the cost is equivalent to solving 1,000 static problems. Thus, it is of practical interest to find ways to reduce the computational cost. It is clear that if the element $\hat{\mathbf{K}}^e$ were a

diagonal matrix, then the assembled or global coefficient matrix $\hat{\mathbf{K}}$ would be diagonal, and there is no inversion required to solve for u_i^{s+1} (i.e., simply divide each equation with the diagonal element):

$$U_i^{s+1} = \frac{1}{\hat{K}_{(ii)}} \left(\sum_{j=1}^{NEQ} \bar{K}_{ij} U_j^s + \bar{F}_i^{s,s+1} \right) \quad \text{(no sum on } i\text{)} \tag{7.4.48}$$

Formulations that require the inversion of $\hat{\mathbf{K}}$ (because it is not diagonal) are termed *implicit formulations* and those in which no inversion is required are called *explicit formulations*.

In the finite element method, no time-approximation scheme results in a diagonal matrix $\hat{\mathbf{K}}$ because matrices **C** and/or **M** appearing in $\hat{\mathbf{K}}$ are not diagonal matrices. A matrix (**C** or **M**) computed according to the definition is called a *consistent (mass) matrix*, and it is *not* diagonal unless the approximation functions ψ_i are orthogonal over the element domain. In real-world problems where hundreds of thousands of degrees of freedom are involved, the cost of computation precludes the inversion of large systems of equations. Thus, one needs to pick a scheme that eliminates **K** from $\hat{\mathbf{K}}$ (because, it would be a gross approximation to diagonalize **K**) and then diagonalize **C** and/or **M** to have an explicit formulation.

For example, the forward difference scheme (i.e., $\alpha = 0$) results in the following time-marching scheme [see Eq. (7.4.29a)]:

$$\mathbf{C}\mathbf{U}^{s+1} = (\mathbf{C} - \Delta t\, \mathbf{K})\mathbf{U}^s + \Delta t\, \mathbf{F}^s \tag{7.4.49}$$

If the matrix **C** is diagonal then the assembled equations can be solved directly (i.e., without inverting a matrix). Similarly, the central difference scheme for an undamped system (i.e., **C** = 0) is [see Eq. (7.4.42)]

$$\mathbf{M}\mathbf{U}^{s+1} = (\Delta t)^2 \mathbf{F}^{s+1} + \left(2\mathbf{M} - (\Delta t)^2 \mathbf{K}\right)\mathbf{U}^s - \mathbf{M}\dot{\mathbf{U}}^s \tag{7.4.50}$$

which requires diagonalization of **M** (and **C**, in the case of a damped system) in order for the central difference formulation to be explicit. The explicit nature of Eq. (7.4.48) motivated analysts to find rational ways of making **C** and/or **M** diagonal. There are several ways of constructing diagonal mass matrices by lumping the mass at the nodes, while preserving the total mass. Two such approaches are discussed next.

7.4.6.1 Row-sum lumping

The sum of the elements of each row of the consistent (mass) matrix is

used as the diagonal element and setting the off-diagonal elements to zero [(*ii*) means no sum on *i*]:

$$M^e_{(ii)} = \sum_{j=1}^{n} \int_{x_a^e}^{x_b^e} \rho \psi_i^e \psi_j^e \, dx = \int_{x_a^e}^{x_b^e} \rho \psi_i^e \, dx \tag{7.4.51}$$

where the property $\sum_{j=1}^{n} \psi_j^e = 1$ of the interpolation functions is used.

When ρ_e is element-wise constant, the consistent matrices associated with the linear and quadratic 1-D elements are

$$\mathbf{M}^e_C = \frac{\rho_e A_e h_e}{6} \begin{bmatrix} 2 & 1 \\ 1 & 2 \end{bmatrix}, \quad \mathbf{M}^e_C = \frac{\rho_e A_e h_e}{30} \begin{bmatrix} 4 & 2 & -1 \\ 2 & 16 & 2 \\ -1 & 2 & 4 \end{bmatrix} \tag{7.4.52a}$$

As per Eq. (7.4.51), the associated diagonal matrices for the linear and quadratic elements are

$$\mathbf{M}^e_L = \frac{\rho_e A_e h_e}{2} \begin{bmatrix} 1 & 0 \\ 0 & 1 \end{bmatrix}, \quad \mathbf{M}^e_L = \frac{\rho_e A_e h_e}{6} \begin{bmatrix} 1 & 0 & 0 \\ 0 & 4 & 0 \\ 0 & 0 & 1 \end{bmatrix} \tag{7.4.52b}$$

Here subscripts *L* and *C* refer to lumped and consistent mass matrices, respectively.

The consistent mass matrix for the Euler–Bernoulli beam is given in Eq. (7.3.57). The row-sum diagonal mass matrix is obtained in two ways: (a) neglecting the terms corresponding to the rotational degrees of freedom in each row and (b) neglecting the terms corresponding to the rotational degrees of freedom in rows 1 and 3 and neglecting the terms associated with the translational degrees of freedom in rows in 2 and 4:

$$\mathbf{M}^e_L = \frac{\rho_e A_e h_e}{2} \begin{bmatrix} 1 & 0 & 0 & 0 \\ 0 & 0 & 0 & 0 \\ 0 & 0 & 1 & 0 \\ 0 & 0 & 0 & 0 \end{bmatrix}, \quad \hat{\mathbf{M}}^e_L = \frac{\rho_e A_e h_e}{420} \begin{bmatrix} 210 & 0 & 0 & 0 \\ 0 & h_e^2 & 0 & 0 \\ 0 & 0 & 210 & 0 \\ 0 & 0 & 0 & h_e^2 \end{bmatrix} \tag{7.4.53a}$$

The consistent mass matrix of the Timoshenko beam theory is given in Eq. (7.3.63b). The lumped mass matrices for the Timoshenko beam are

$$\mathbf{M}_L^e = \frac{\rho_e A_e h_e}{2}\begin{bmatrix} 1 & 0 & 0 & 0 \\ 0 & 0 & 0 & 0 \\ 0 & 0 & 1 & 0 \\ 0 & 0 & 0 & 0 \end{bmatrix}, \quad \hat{\mathbf{M}}_L^e = \frac{\rho_e A_e h_e}{2}\begin{bmatrix} 1 & 0 & 0 & 0 \\ 0 & r_e & 0 & 0 \\ 0 & 0 & 1 & 0 \\ 0 & 0 & 0 & r_e \end{bmatrix}, \quad r_e = \frac{I_e}{A_e} \tag{7.4.53b}$$

7.4.6.2 Proportional lumping

Here the diagonal elements of the lumped matrix are computed to be proportional to the diagonal elements of the consistent matrix while conserving the total mass of the element [(*ii*) means no sum on *i*]:

$$M_{(ii)}^e = \alpha^e \int_{x_a^e}^{x_b^e} m_e \psi_i^e \psi_i^e \, dx, \quad \alpha^e = \frac{\int_{x_a^e}^{x_b^e} m_e \, dx}{\sum_{i=1}^{n} \int_{x_a^e}^{x_b^e} m_e \psi_i^e \psi_i^e \, dx} \tag{7.4.54}$$

where m_e is the mass per unit length ($m_e = \rho_e A_e$). For constant m_e, in the case of linear element we have

$$\alpha^e = \frac{m_e h_e}{\left(\frac{m_e h_e}{2} + \frac{m_e h_e}{2}\right)} = 1; \quad M_{11}^e = M_{22}^e = \frac{\rho_e A_e h_e}{2}$$

Thus, the proportional lumping gives the same lumped mass matrices as those obtained in the row-sum technique.

7.4.6.3 Comparison of critical time steps using consistent and lumped mass matrices

Here we illustrate through numerical examples that the eigenvalues computed using the lumped mass matrix are smaller than those computed using the consistent mass matrix. Consequently, the critical time step size for explicit formulations will be larger.

First consider a one linear element model of heat transfer in a uniform bar of length *L*, with left end maintained at zero temperature and the right end insulated. The eigenvalue problem with a consistent mass matrix is (*h* = *L*)

$$\left(\frac{kA}{L}\begin{bmatrix} 1 & -1 \\ -1 & 1 \end{bmatrix} - \lambda_C \frac{\rho c_v AL}{6}\begin{bmatrix} 2 & 1 \\ 1 & 2 \end{bmatrix}\right)\begin{Bmatrix} U_1 \\ U_2 \end{Bmatrix} = \begin{Bmatrix} Q_1^1 \\ Q_2^1 \end{Bmatrix}$$

Since $U_1 = 0$ and $Q_2^1 = 0$, we have from the second equation

$$\lambda_C = \frac{kA}{L}\frac{3}{\rho c_v AL} = \frac{3k}{L^2 \rho c_v}$$

Substituting this into the critical time step relation in Eq. (7.4.30) with $\alpha = 0$, we have

$$(\Delta t_{\text{cr}})_C = \frac{2}{\lambda} = \frac{2L^2 \rho c_v}{3k}$$

If we use the lumped matrix, we have

$$\left(\frac{kA}{L}\begin{bmatrix} 1 & -1 \\ -1 & 1 \end{bmatrix} - \lambda_L \frac{\rho c_v AL}{2}\begin{bmatrix} 1 & 0 \\ 0 & 1 \end{bmatrix}\right)\begin{Bmatrix} U_1 \\ U_2 \end{Bmatrix} = \begin{Bmatrix} Q_1^1 \\ Q_2^1 \end{Bmatrix}$$

Then λ_L is given by

$$\lambda_L = \frac{2k}{L^2 \rho c_v} < \lambda_C$$

and the critical time step is

$$(\Delta t_{\text{cr}})_L = \frac{L^2 \rho c_v}{k} > (\Delta t_{\text{cr}})_C$$

The aforementioned finite element model can be interpreted as one for the axial deformation of a uniform bar of modulus E. We have

$$\lambda_C = \omega_C^2 = \frac{3E}{L^2 \rho}$$

Substituting this into the critical time step relation in Eq. (7.4.43) with $\alpha = 1/2$ and $\gamma = 1/3$ we have

$$(\Delta t_{\text{cr}})_C = \left[\frac{1}{12}\omega_C^2\right]^{-\frac{1}{2}} = 2L\left(\frac{\rho}{E}\right)^{\frac{1}{2}}$$

whereas with the lumped mass matrix, we have $\lambda_L = \omega_L^2 = 2E/L^2\rho < \lambda_C$ and the critical time step is

$$(\Delta t_{\text{cr}})_L = \left[\frac{1}{12}\omega_L^2\right]^{-\frac{1}{2}} = 2L\left(\frac{3\rho}{2E}\right)^{\frac{1}{2}} > (\Delta t_{\text{cr}})_C$$

Next, we consider a one Euler–Bernoulli beam element without rotary inertia and with lumped mass matrix for a cantilever beam of length L, bending stiffness EA, and mass per unit length ρA (see **Example 7.3.2**). When we use $\mathbf{M}_L$ we obtain

$$\left(\begin{bmatrix} 12 & 6L \\ 6L & 4L^2 \end{bmatrix} - \omega_L^2 \frac{\rho A L^4}{2EI}\begin{bmatrix} 1 & 0 \\ 0 & 0 \end{bmatrix}\right)\begin{Bmatrix} U_3 \\ U_4 \end{Bmatrix} = \begin{Bmatrix} 0 \\ 0 \end{Bmatrix}$$

By setting the determinant of the coefficient matrix in the above equation to zero, we obtain

$$\frac{\rho A L^4}{2EI}\omega_L^2 = 3 \;\Rightarrow\; \omega_L = 2.4495\,\beta, \quad \beta = \frac{1}{L^2}\sqrt{\frac{EI}{\rho A}}$$

If we use the lumped mass matrix $\hat{\mathbf{M}}_L$, we obtain $\omega_L = 2.4364\,\beta$. Recall from **Example 7.3.2** that the one element model with the consistent mass matrix gave $\omega_C = 3.533\,\beta$, which is greater than that obtained with the diagonal mass matrices. Consequently, the critical time step for conditionally stable schemes is larger with the lumped mass than with the consistent mass.

In summary, the use of a lumped mass matrix in transient analysis can save computational time in two ways. First, for forward difference and central difference schemes, lumped (mass) matrices result in explicit algebraic equations, not requiring matrix inversions. Second, the critical time step required with the lumped matrix is larger than that required with the consistent matrix.

7.4.7 Examples

Example 7.4.1

Consider the transient heat conduction problem described by the differential equation

$$\frac{\partial u}{\partial t} - \frac{\partial^2 u}{\partial x^2} = 0 \quad \text{for } 0 < x < 1 \tag{1a}$$

subjected to the boundary conditions

$$u(0,t)=0, \quad \frac{\partial u}{\partial x}(1,t)=0 \tag{1b}$$

and initial condition

$$u(x,0)=1.0 \tag{1c}$$

where u is the dimensionless temperature. Determine the transient response.

Solution: The problem at hand is a special case of Eq. (7.4.3) with $a = 1$, $b = 0$, $c_0 = 0$, $c_1 = 1$, $c_2 = 0$, $c_3 = 0$, and $f = 0$ [or Eq. (7.2.1) with $kA = 1$, $c_1 = c_v \rho A = 1$, and $f = 0$]. The finite element model is given by

$$\mathbf{M}^e\dot{\mathbf{u}}^e + \mathbf{K}^e\mathbf{u}^e = \mathbf{Q}^e \tag{2a}$$

where

$$M_{ij}^e = \int_{x_a^e}^{x_b^e} \psi_i^e \psi_j^e \, dx, \quad K_{ij}^e = \int_{x_a^e}^{x_b^e} \frac{d\psi_i^e}{dx}\frac{d\psi_j^e}{dx} \, dx \tag{2b}$$

For the choice of linear interpolation functions, the semidiscrete equations of a typical element are

$$\frac{h_e}{6}\begin{bmatrix} 2 & 1 \\ 1 & 2 \end{bmatrix}\begin{Bmatrix} \dot{u}_1^e \\ \dot{u}_2^e \end{Bmatrix} + \frac{1}{h_e}\begin{bmatrix} 1 & -1 \\ -1 & 1 \end{bmatrix}\begin{Bmatrix} u_1^e \\ u_2^e \end{Bmatrix} = \begin{Bmatrix} Q_1^e \\ Q_2^e \end{Bmatrix} \tag{3}$$

where h_e is the length of the element. Use of the α-family of approximation, with time step Δt, results in the equation [see Eqs. (7.4.29a) and (7.4.29b)]

$$(\mathbf{M} + \Delta t\, \alpha\mathbf{K})\mathbf{u}^{s+1} = (\mathbf{M} - \Delta t(1-\alpha)\mathbf{K})\mathbf{u}^s + \Delta t(\alpha\mathbf{Q}^{s+1} + (1-\alpha)\mathbf{Q}^s) \tag{4}$$

First, consider a one-element mesh ($h = 1$). Then we have

$$\begin{bmatrix} \frac{1}{3}+\alpha\Delta t & \frac{1}{6}-\alpha\Delta t \\ \frac{1}{6}-\alpha\Delta t & \frac{1}{3}+\alpha\Delta t \end{bmatrix}\begin{Bmatrix} U_1 \\ U_2 \end{Bmatrix}^{s+1}$$
$$= \begin{bmatrix} \frac{1}{3}-(1-\alpha)\Delta t & \frac{1}{6}+(1-\alpha)\Delta t \\ \frac{1}{6}+(1-\alpha)\Delta t & \frac{1}{3}-(1-\alpha)\Delta t \end{bmatrix}\begin{Bmatrix} U_1 \\ U_2 \end{Bmatrix}^{s} + \Delta t\begin{Bmatrix} \bar{Q}_1 \\ \bar{Q}_2 \end{Bmatrix} \tag{5}$$

where $\bar{Q}_i = \alpha(Q_i^1)^{s+1} + (1-\alpha)(Q_i^1)^s$. The boundary conditions of the problem require

$$U_1^s = 0, \quad (Q_2^1)^s = 0 \quad \text{for all } s > 0 \text{ (i.e., } t > 0) \tag{6}$$

However, the initial condition in Eq. (1c) requires $U_1(0)\psi_1(x) + U_2(0)\psi 2(x) = 1$. Since the initial condition should be consistent with the boundary conditions, we take $U_1^0 = 0$. Then it follows that $U_2^0 = 1$.

Using the boundary conditions, we can write for the one-element model ($h = 1.0$)

$$\left(\frac{1}{3} + \alpha\Delta t\right)U_2^{s+1} = \left[\frac{1}{3} - (1-\alpha)\Delta t\right]U_2^s \tag{7}$$

which can be solved repeatedly for U_2^{s+1} at different times, $s = 0, 1, \ldots$.

Repeated use of Eq. (4) can cause the temporal approximation error to grow with time, depending on the value of α. As noted earlier, the forward difference scheme ($\alpha = 0$) is a conditionally stable scheme. To determine the critical time step for conditionally stable scheme using the one-element mesh, we calculate the maximum eigenvalue of the associated system first (using the consistent mass matrix because that is what is used in the transient analysis). Since there is only one free degree freedom in the mesh, we obtain only one eigenvalue:

$$\left(-\frac{\lambda}{6}\begin{bmatrix} 2 & 1 \\ 1 & 2 \end{bmatrix} + \begin{bmatrix} 1 & -1 \\ -1 & 1 \end{bmatrix}\right)\begin{Bmatrix} U_1 \\ U_2 \end{Bmatrix} = \begin{Bmatrix} Q_1^1 \\ Q_2^1 \end{Bmatrix}, \quad U_1 = 0, \quad Q_2^1 = 0 \tag{8}$$

The eigenvalue is

$$\left(-\frac{1}{3}\lambda + 1\right)U_2 = 0, \quad \text{or} \quad \lambda = 3 \tag{9}$$

Hence, from Eq. (7.4.30) we have $\Delta t_{cr} = 2/\lambda = 0.66667$. Thus, in order for the forward difference approximation [from Eq. (7)]

$$\frac{1}{3}U_2^{s+1} = \left(\frac{1}{3} - \Delta t\right)U_2^s \tag{10}$$

to be stable, the time step should be smaller than $\Delta t_{cr} = 0.6667$; otherwise, the solution will be unstable, as shown in Fig. 7.4.3. For a two-element mesh we have ($h_1 = h_2 = h = 0.5$), the condensed equations of the time-marching scheme are given by

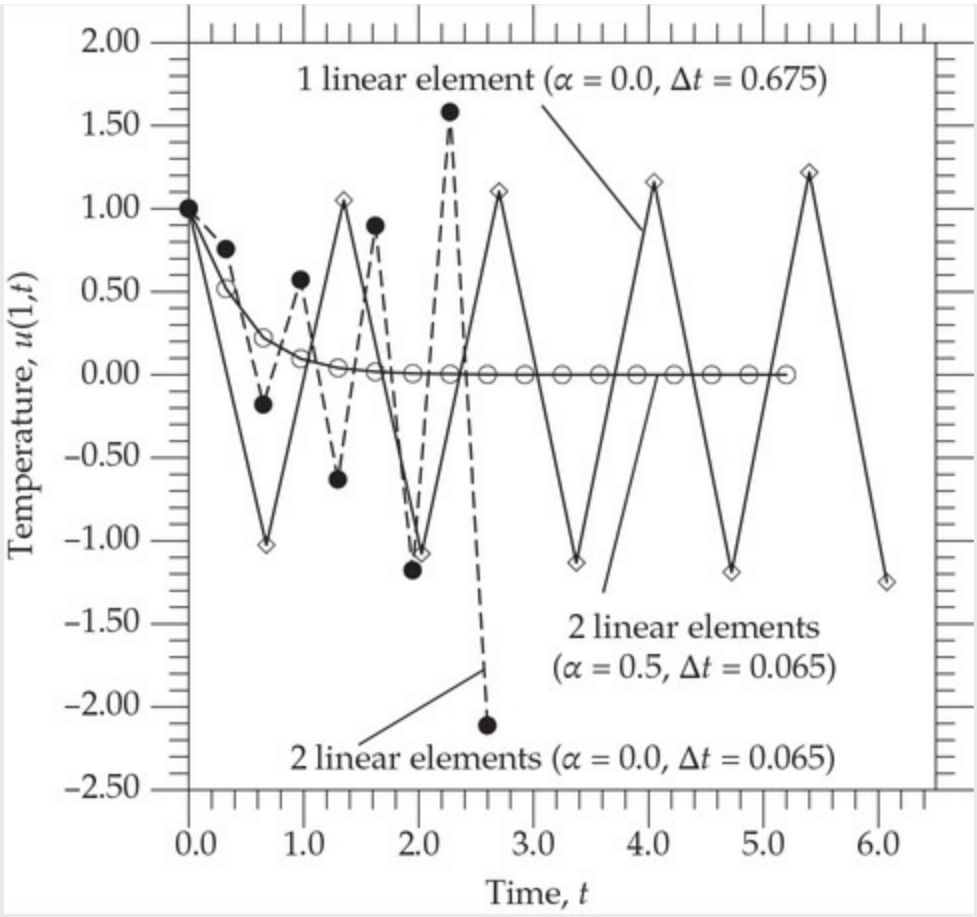

Fig. 7.4.3 Stability of the forward difference ($\alpha = 0.0$) and Crank–Nicolson ($\alpha = 0.5$) schemes as applied to a parabolic equation.

$$\begin{bmatrix} \frac{2}{3}h + 2\alpha\frac{\Delta t}{h} & \frac{1}{6}h - \alpha\frac{\Delta t}{h} \\ \frac{1}{6}h - \alpha\frac{\Delta t}{h} & \frac{1}{3}h + \alpha\frac{\Delta t}{h} \end{bmatrix} \begin{Bmatrix} U_2 \\ U_3 \end{Bmatrix}^{s+1}$$
$$= \begin{bmatrix} \frac{2}{3}h - 2(1-\alpha)\frac{\Delta t}{h} & \frac{1}{6}h + (1-\alpha)\frac{\Delta t}{h} \\ \frac{1}{6}h + (1-\alpha)\frac{\Delta t}{h} & \frac{1}{3}h - (1-\alpha)\frac{\Delta t}{h} \end{bmatrix} \begin{Bmatrix} U_2 \\ U_3 \end{Bmatrix}^{s} \tag{11}$$

with initial values U_0 and U_0 known. The forward difference scheme ($\alpha = 0$) yields

$$\frac{h}{6}\begin{bmatrix} 4 & 1 \\ 1 & 2 \end{bmatrix} \begin{Bmatrix} U_2 \\ U_3 \end{Bmatrix}^{s+1} = \frac{h}{6}\begin{bmatrix} 4-2\mu & 1+\mu \\ 1+\mu & 2-\mu \end{bmatrix} \begin{Bmatrix} U_2 \\ U_3 \end{Bmatrix}^{s}, \quad \mu = \frac{6\Delta t}{h^2} \tag{12}$$

The associated eigenvalue problem is

$$\left(-\lambda\frac{h}{6}\begin{bmatrix} 4 & 1 \\ 1 & 2 \end{bmatrix} + \frac{1}{h}\begin{bmatrix} 2 & -1 \\ -1 & 1 \end{bmatrix}\right) \begin{Bmatrix} U_2 \\ U_3 \end{Bmatrix} = \begin{Bmatrix} 0 \\ 0 \end{Bmatrix} \tag{13}$$

The characteristic equation is ($\bar{\lambda} = \lambda h^2/6$)

$$7\bar{\lambda}^2 - 10\bar{\lambda} + 1 = 0, \quad \bar{\lambda}_{1,2} = \frac{5 \mp \sqrt{18}}{7} \tag{14}$$

Thus, we have $\lambda_1 = 2.5967$ and $\lambda_2 = 31.6891$. Hence, the critical time step becomes $\Delta t_{cr} = 2/31.6891 = 0.0631$. For example, a time step of $\Delta t = 0.065$ results in an unstable solution, as shown in Fig. 7.4.3.

For unconditionally stable schemes ($\alpha \geq \frac{1}{2}$), there is no restriction on the time step. For example, the Crank–Nicolson method with two linear elements and $\Delta t = 0.065$ yields very smooth and stable solution, as shown in Fig. 7.4.3. However, to obtain a sufficiently accurate solution, even when the solution is stable, the time step must be taken as a fraction of Δt_{cr}. Of course, the accuracy of the solution also depends on the mesh size h. When the number of elements is increased, the maximum eigenvalue of the system increases and Δt_{cr} decreases.

Plots of $u(1, t)$ versus time for $\alpha = 0$ and $\alpha = 0.5$ with $\Delta t = 0.05$ are shown in Fig. 7.4.4. Solutions predicted by meshes of one and two linear elements (L) and the mesh of one quadratic element (Q) are compared. The convergence of the solution with increasing number of elements is clear. The finite element solutions obtained with different methods, time steps, and meshes are compared with the exact solution in Table 7.4.1.

Table 7.4.1 A comparison of the finite element solutions obtained using various time approximation schemes and meshes with the analytical solution of a parabolic equation ($\Delta t = 0.05$).

t	$\alpha = 0$	$\alpha = 1$	$\alpha = 0.5$							
	1L	1L	1L	2L	4L	8L	1Q	2Q	4Q	Exact
0.00	1.000	1.000	1.000	1.000	1.000	1.000	1.000	1.000	1.000	1.000
0.05	0.850	0.870	0.861	1.036	0.995	0.993	1.087	0.994	0.993	0.997
0.10	0.723	0.756	0.740	0.928	0.959	0.955	0.982	0.955	0.955	0.949
0.15	0.614	0.658	0.637	0.817	0.864	0.871	0.869	0.883	0.873	0.864
0.20	0.522	0.572	0.548	0.718	0.756	0.769	0.768	0.763	0.773	0.772
0.25	0.444	0.497	0.472	0.630	0.676	0.682	0.678	0.693	0.686	0.685
0.30	0.377	0.432	0.406	0.553	0.591	0.604	0.599	0.601	0.607	0.607
0.35	0.321	0.376	0.349	0.486	0.525	0.533	0.529	0.539	0.536	0.537
0.40	0.273	0.327	0.301	0.427	0.461	0.471	0.467	0.471	0.474	0.475
0.45	0.232	0.284	0.259	0.375	0.408	0.416	0.412	0.420	0.419	0.419
0.50	0.197	0.247	0.223	0.329	0.359	0.368	0.364	0.369	0.370	0.371
0.55	0.167	0.215	0.191	0.289	0.318	0.325	0.321	0.328	0.327	0.328
0.60	0.142	0.187	0.165	0.254	0.280	0.289	0.284	0.288	0.289	0.290
0.65	0.121	0.163	0.142	0.223	0.247	0.254	0.251	0.256	0.256	0.256
0.70	0.103	0.141	0.122	0.196	0.218	0.224	0.221	0.225	0.226	0.226
0.75	0.087	0.123	0.105	0.172	0.192	0.198	0.195	0.200	0.200	0.200
0.80	0.074	0.107	0.090	0.151	0.170	0.175	0.173	0.176	0.176	0.177
0.85	0.063	0.093	0.078	0.132	0.150	0.154	0.152	0.156	0.156	0.156
0.90	0.054	0.081	0.067	0.116	0.132	0.136	0.135	0.138	0.138	0.138
0.95	0.046	0.070	0.058	0.102	0.117	0.121	0.119	0.122	0.122	0.122
1.00	0.039	0.061	0.050	0.090	0.103	0.107	0.105	0.107	0.108	0.108

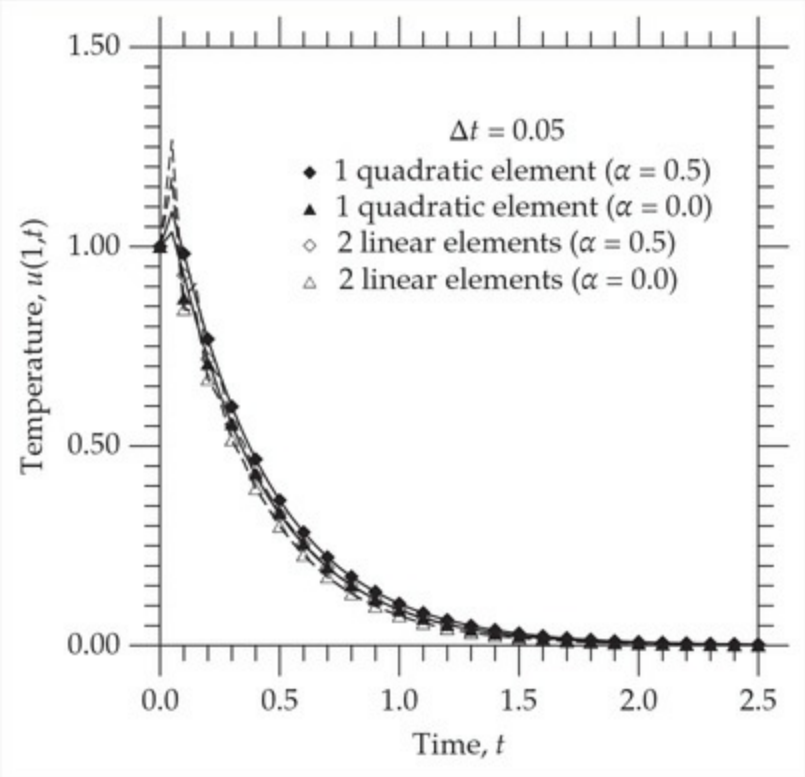

Fig. 7.4.4 Transient solution of a parabolic equation according to linear and quadratic finite elements.

Example 7.4.2

Determine the transverse motion of a beam clamped at both ends and subjected to initial conditions given in Eq. (1). Assume constant material and geometric properties, neglect rotary inertia, and assume $\rho A = 1$ and $EI = 1$, and $L = 1$ (amounts to using dimensionless deflection and time). Investigate various time approximation schemes to analyze the problem using the Euler–Bernoulli beam theory (EBT). Also, determine the critical time step for conditionally stable schemes. Assume the following initial conditions:

$$w(x,0) = \sin \pi x - \pi x(1-x), \quad \frac{\partial w}{\partial t}(x,0) = 0 \tag{1}$$

Solution: The dimensionless form of the governing equations according to the EBT are

$$\frac{\partial^2 w}{\partial t^2} + \frac{\partial^4 w}{\partial x^4} = 0 \quad \text{for } 0 < x < 1 \tag{2}$$

$$w(0,t)=0, \quad \frac{\partial w}{\partial x}(0,t)=0, \quad w(1,t)=0, \quad \frac{\partial w}{\partial x}(1,t)=0 \tag{3}$$

Note that the initial deflection of the beam is consistent with the boundary conditions. The initial slope is given by

$$\theta(x,0)=-\left(\frac{\partial w}{\partial x}\right)_{t=0}=-\pi\cos\pi x+\pi(1-2x) \tag{4}$$

Because of symmetry about $x = 0.5$ (center of the beam), we consider only half span of the beam for finite element modeling. Here we use the first half of the beam, $0 \le x \le 0.5$, as the computational domain. The boundary condition at $x = 0.5$ is $\theta(0.5, t) = -(\partial w/\partial x)(0.5, t) = 0$.

We begin with a one-element mesh with the Euler–Bernoulli beam element to illustrate the procedure and then present solutions for various meshes of the EBT and TBT elements.

The semidiscretized model for a one-element mesh ($h = 0.5L = 0.5$) is

$$\frac{h}{420}\begin{bmatrix} 156 & -22h & 54 & 13h \\ -22h & 4h^2 & -13h & -3h^2 \\ 54 & -13h & 156 & 22h \\ 13h & -3h^2 & 22h & 4h^2 \end{bmatrix}\begin{Bmatrix} \ddot{U}_1 \\ \ddot{U}_2 \\ \ddot{U}_3 \\ \ddot{U}_4 \end{Bmatrix} + \frac{2}{h^3}\begin{bmatrix} 6 & -3h & -6 & -3h \\ -3h & 2h^2 & 3h & h^2 \\ -6 & 3h & 6 & 3h \\ -3h & h^2 & 3h & 2h^2 \end{bmatrix}\begin{Bmatrix} U_1 \\ U_2 \\ U_3 \\ U_4 \end{Bmatrix} = \begin{Bmatrix} Q_1^1 \\ Q_2^1 \\ Q_3^1 \\ Q_4^1 \end{Bmatrix} \tag{5}$$

The boundary conditions for the one-element model translate into

$$U_1=0, \quad U_2=0, \quad U_4=0, \quad Q_3^1=0 \quad \text{for all } t>0 \tag{6}$$

The initial conditions can be computed from Eqs. (3) and (4):

$$\left.\begin{array}{llll} U_1=0, & U_2=0, & U_3=0.2146, & U_4=0 \\ \dot{U}_1=0, & \dot{U}_2=0, & \dot{U}_3=0 & \dot{U}_4=0 \end{array}\right\} \quad \text{for } t=0 \tag{7}$$

The condensed equation of the time-marching scheme for this case takes the form

$$(K_{33}+a_3M_{33})U_3^{s+1}=\hat{F}_3^{s,s+1}\equiv M_{33}(a_3U_3^s+a_4\dot{U}_3^s+a_5\ddot{U}_3^s), \quad s=0,1,\ldots \tag{8}$$

where a_3, a_4, and a_5 are defined in Eq. (7.4.37b). The second derivative $\ddot{U}_3^0$ for time $t = 0$ is computed from the equation of motion:

$$\ddot{U}_3^0 = -\frac{K_{33}U_3^0}{M_{33}} = -\left(\frac{12}{h^3} \times 0.2146\right)\frac{420}{156h} = -110.9317 \tag{9}$$

For $\gamma < 1/2$, we must compute the critical time step Δt_{cr}, which depends on the square of maximum natural frequency of the beam [see Eq. (7.4.43)]. For the present model, ω_{max} is computed from the eigenvalue problem

$$(K_{33} - \omega^2 M_{33})U_3 = 0 \quad \text{or } \omega^2 = K_{33}/M_{33} = 516.923 \tag{10}$$

Hence, the critical time step for $\alpha = 0.5$ and $\gamma = 1/3$ (i.e., the linear acceleration scheme) is

$$\Delta t_{cr} = \sqrt{12}/\omega_{max} = 0.15236 \tag{11}$$

Although there is no restriction on time integration schemes with $\alpha = 0.5$ and $\alpha \geq 0.5$, the critical time step provides an estimate of the time step to be used to obtain the transient solution.

Figure 7.4.5 shows plots of $w(0.5, t)$ versus time for the scheme with $\alpha = 0.5$ and $\gamma = 1/3$. Three different time steps, $\Delta t = 0.175$, 0.150, and 0.05, are used to illustrate the accuracy. For $\Delta t = 0.175 > \Delta t_{cri}$, the solution is unstable, whereas for $\Delta t < \Delta t_{cri}$, it is stable but inaccurate. The period of the solution is given by

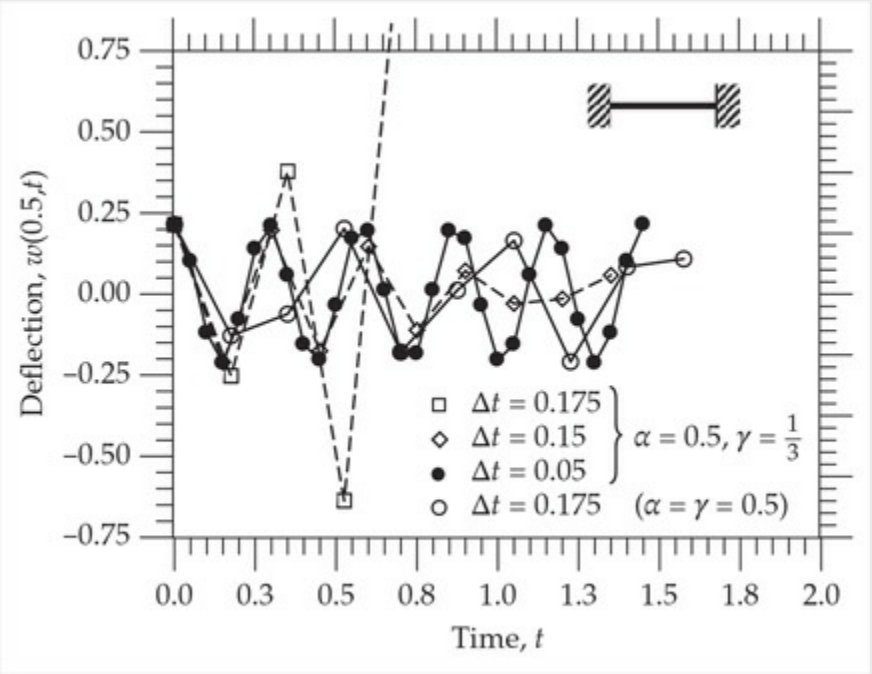

Fig. 7.4.5 Center deflection *w(0.5,t)* versus time *t* for a clamped beam.

$$T = 2\pi/\omega = 0.27635$$

For two- and four-element meshes of Euler–Bernoulli elements, the critical time steps are (details are not presented here)

$$(\Delta t_{\text{cr}})_2 = 0.00897, \quad (\Delta t_{\text{cr}})_4 = 0.00135 \tag{12}$$

where the subscripts refer to the number of elements in the mesh. The transverse deflection obtained with the one and two Euler–Bernoulli elements ($\Delta t = 0.005$) in half beam for a complete period (0, 0.28) are shown in Fig. 7.4.6.

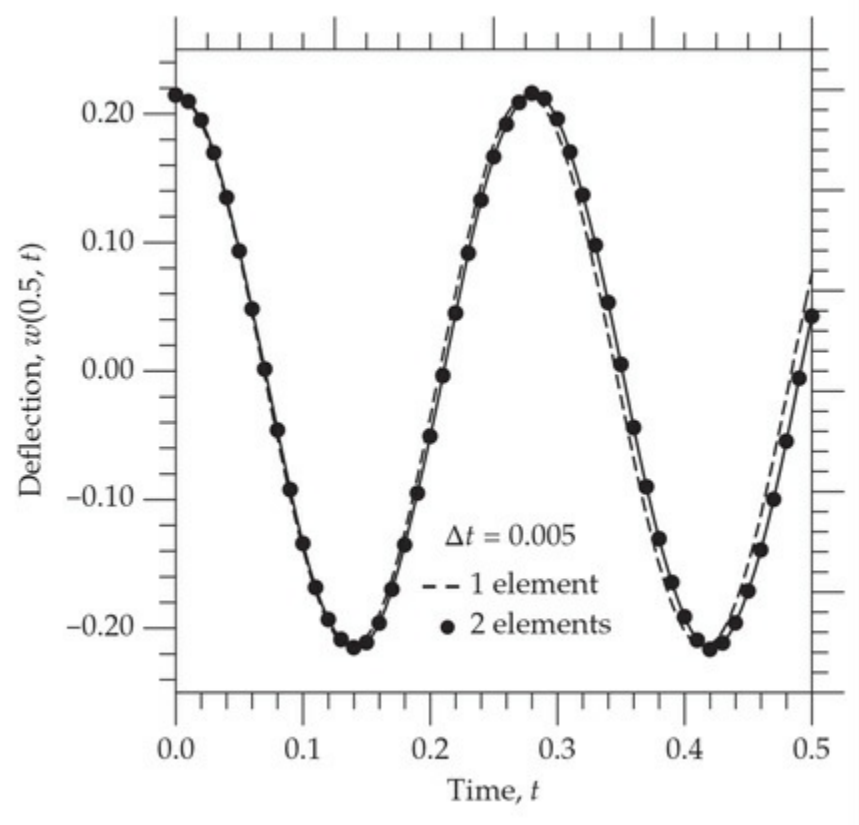

Fig. 7.4.6 Center transverse deflection versus time for a clamped beam subjected to an initial transverse deflection ($\Delta t = 0.005$, $\alpha = 0.5$,and $\gamma = 0.5$).

The problem can also be analyzed using the Timoshenko beam theory (TBT), with the stiffness matrix **K** and mass matrix **M** of Eq. (7.4.10) given by Eqs. (7.3.63a) and (7.3.63b), respectively. In writing the governing equations [see Eqs. (7.2.4a) and (7.2.4b)] of the TBT as applied to the present problem, we first identify the coefficients GAK_s and $c_3 = \rho I$ consistent with those (i.e., ρA and EI) in the Euler-Bernoulli beam equation. We can relate GAK_s to EI and beam height Has

$$GAK_s = \frac{E}{2(1+\nu)} BHK_s = \frac{EI}{2(1+\nu)} \frac{12}{H^2} \frac{5}{6} = \frac{4}{H^2} EI \tag{13}$$

where B is the width and H the height of the beam and $I = BH^3/12$; $\nu = 0.25$ and $K_s = \frac{5}{6}$ are used in arriving at the last expression. Similarly,

$$\rho I = \rho \frac{1}{12} BH^3 = \frac{1}{12} \rho AH^2 = \frac{H^2}{12} \rho A \tag{14}$$

In summary, when using the TBT to analyze the given problem, we use the following data:

$$EI = 1, \quad GAK_s = \frac{4}{H^2}, \quad \rho A = 1, \quad \rho I = \frac{H^2}{12} \tag{15}$$

To neglect the rotary inertia in the TBT, we set $\rho I = 10{-}15$.

The values of $w(0.5, t)$ as obtained using the EBT and TBT elements (both elements include the rotary inertia) for various numbers of elements are presented in Table 7.4.2. The time step is taken to be $\Delta t = 0.005$, which is smaller than the critical time step of the two-element mesh of the EBT beam element when $\gamma = \frac{1}{3}$. Plots of $w(0.5, t)$ obtained with two and four linear TBT elements, two quadratic Timoshenko beam elements for $L/H = 100$ (since $L = 1.0$, we take $H = 0.01$; for $L/H = 100$ the effect of shear deformation is negligible) along with the two-element solution of the Euler–Bernoulli beam element are shown in Fig. 7.4.7. The two-element mesh of linear TBT beam elements predicts transient response that differs significantly from the EBT solution, and the TBT solution converges to the EBT solution as the number of elements or the degree of approximation is increased. Should we use conditionally stable schemes, it can be shown that the Timoshenko beam element requires larger Δt_{cri} than the Euler–Bernoulli beam element. This is because, as L/H is decreased, the $\omega_{\max}$ predicted by the TBT is smaller than that predicted by the EBT.

Table 7.4.2 Effect of mesh on the transverse deflection $w(0.5,t) \times 10$ of a beam clamped at both ends ($\Delta t = 0.005$, $L/H = 100$, $EI = 1$, and $\rho A = 1$).

	EBT elements[1]					TBT elements[2]		
	$\alpha = 0.5, \gamma = 1/3$		$\alpha = 0.5, \gamma = 0.5$			$\alpha = 0.5, \gamma = 0.5$		
t	1	2	1	2	4	2L	4L	2Q
0.00	2.146	2.146	2.146	2.146	2.146	2.146	2.146	2.146
0.01	2.091	2.098	2.091	2.098	2.098	2.083	2.097	2.100
0.02	1.928	1.951	1.928	1.951	1.951	1.890	1.955	1.953
0.03	1.666	1.696	1.667	1.696	1.698	1.556	1.665	1.695
0.04	1.319	1.346	1.320	1.348	1.350	1.079	1.244	1.342
0.05	0.904	0.930	0.905	0.931	0.935	0.483	0.832	0.929
0.06	0.442	0.481	0.443	0.482	0.483	−0.180	0.388	0.484
0.07	−0.043	0.014	−0.041	0.014	0.018	−0.836	−0.151	0.016
0.08	−0.525	−0.462	−0.523	−0.459	−0.455	−1.408	−0.672	−0.469
0.09	−0.980	−0.926	−0.978	−0.923	−0.916	−1.837	−1.120	−0.937
0.10	−1.385	−1.345	−1.383	−1.342	−1.336	−2.094	−1.500	−1.349
0.11	−1.719	−1.685	−1.717	−1.685	−1.682	−2.180	−1.809	−1.680
0.12	−1.964	−1.933	−1.963	−1.933	−1.932	−2.117	−2.069	−1.931
0.13	−2.108	−2.088	−2.108	−2.088	−2.087	−1.928	−2.185	−2.100
0.14	−2.144	−2.153	−2.144	−2.150	−2.148	−1.628	−2.117	−2.168
0.15	−2.070	−2.113	−2.071	−2.112	−2.111	−1.220	−1.994	−2.116

[1] Hermite cubic elements. [2] RIEs; 2L = two linear elements; 4L = four linear elements; 2Q = two quadratic elements.

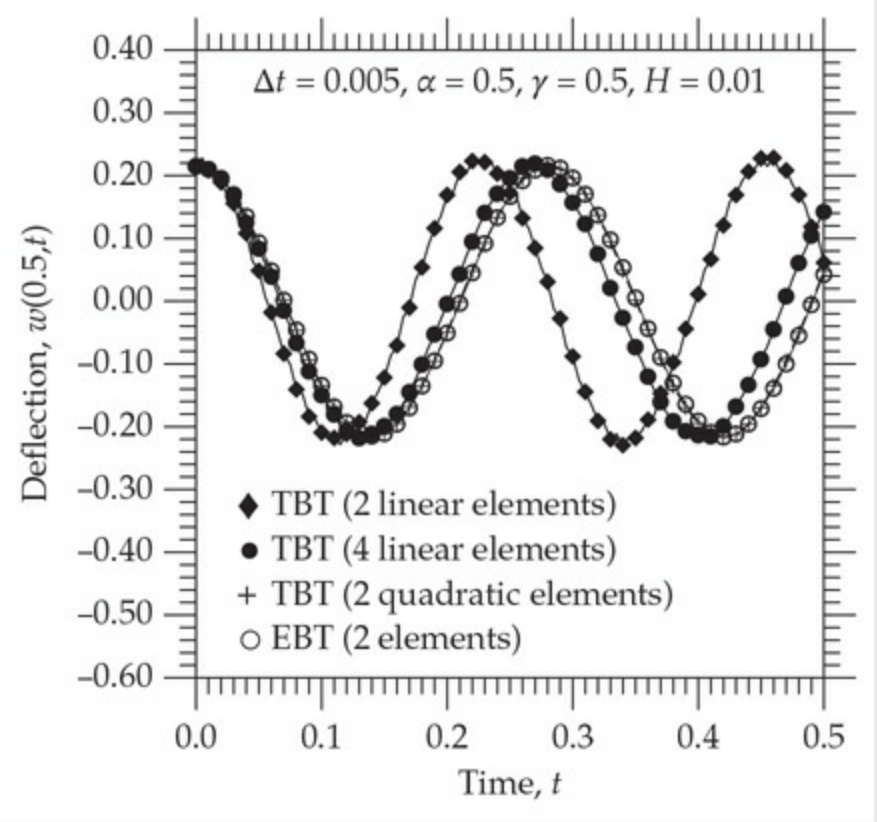

Fig. 7.4.7 Transient response of a beam clamped at both ends, according to the TBT and EBT ($EI = 1$, $\rho A = 1$, $H = 0.01$, $\Delta t = 0.005$, $\alpha = 0.5$, and $\gamma = 0.5$).

7.5 Summary

In this chapter, finite element formulations of eigenvalue problems and time-dependent problems are developed. One-dimensional, second- and fourthorder equations (beams) are discussed. The eigenvalue problems studied include problems of heat transfer (and the like), bars, and beams. In the case of bars and beams, the eigenvalue problems arise in connection with natural vibrations and buckling of columns. Except for the solution procedure, the finite element formulation of eigenvalue problems is entirely analogous to boundary value problems.

Finite element models of time-dependent problems described by parabolic and hyperbolic equations have also been presented. A two-step procedure to derive finite element models from differential equations has been described. In the first step, we seek spatial approximations of the dependent variables of the problem as linear combinations of nodal values

that are functions of time and of interpolation functions that are functions of space. This procedure is entirely analogous to the finite element formulation presented for boundary value problems in Chapters 3–5. The end result of this step is a set of ordinary differential equations (in time) among the nodal values. In the second step, the ordinary differential equations are further approximated using the finite difference approximation of the time derivatives. The resulting algebraic equations can be solved for repeatedly, marching in time. Examples of both transient heat transfer and beam bending are presented.

Problems

Most problems are formulative in nature. For eigenvalue problems one needs to write the final characteristic equations for the eigenvalues.

EIGENVALUE PROBLEMS

7.1 Determine the first two eigenvalues associated with the heat transfer problem, whose governing equations and boundary conditions are given by (see Fig. P7.1)

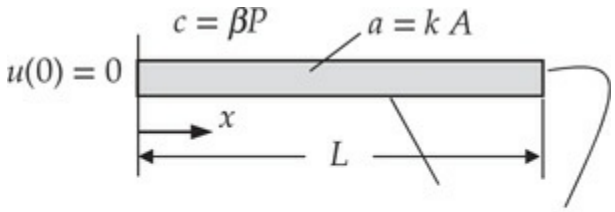

Fin's lateral surface as well as the end $x = L$ are exposed to ambient temperature

Fig. P7.1

$$-\frac{\partial}{\partial x}\left(a\frac{\partial u}{\partial x}\right)+b\frac{\partial u}{\partial t}+cu=0 \quad \text{for } 0<x<L$$

$$u(0)=0, \quad \left(a\frac{\partial u}{\partial x}+\beta u\right)\Big|_{x=L}=0$$

where a, b, c, and β are constants. Use (a) two linear finite elements and (b) one quadratic element in the domain to solve the problem.

7.2 Determine the first two longitudinal frequencies of a rod (with Young's modulus E, area of cross section A, and length L) that is fixed at one end (say, at $x = 0$) and supported axially at the other end (at $x = L$) by a linear elastic spring (with spring constant k), as shown in Fig. P7.2:

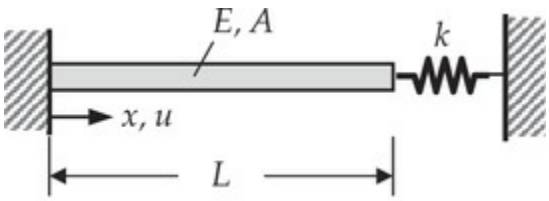

Fig. P7.2

$$-EA\frac{\partial^2 u}{\partial x^2} + \rho A\frac{\partial^2 u}{\partial t^2} = 0 \quad \text{for } 0 < x < L$$

$$u(0) = 0, \quad \left(EA\frac{du}{dx} + ku\right)\Big|_{x=L} = 0$$

Use (a) two linear finite elements, and (b) one quadratic element in the domain to solve the problem. *Answer:* (a) The characteristic equation is $7\lambda^2 - (10 + 4c)\lambda + (1 + 2c) = 0$, $c = kL/2EA$, $\lambda = (\rho h^2/6E)\omega^2$.

7.3 The natural vibration of a beam under applied axial compressive load N^0 is governed by the differential equation

$$\frac{d^2}{dx^2}\left(EI\frac{d^2w}{dx^2}\right) + N_0\frac{d^2w}{dx^2} = \rho A\omega^2 w$$

where ω denotes non-dimensional frequency of natural vibration, EI is the bending stiffness, and ρA is the mass per unit length of the beam. Develop (a) the weak form and (b) finite element model of the equation.

7.4 Determine the smallest natural frequency of a beam with clamped ends, and of constant EA and EI and length L. Use the symmetry and two Euler–Bernoulli beam elements in the half beam.

7.5 Re-solve **Problem 7.4** with two reduced-integration Timoshenko beam elements (RIEs) in the half-beam.

7.6 Consider a beam shear stiffness GAK_s, bending stiffness EI, and length L. The right end ($x = L$) is clamped and its left end ($x = 0$) is supported vertically by a linear elastic spring (see Fig. P7.6). Determine the fundamental natural frequency using (a) one Euler–

Bernoulli beam element and (b) one Timoshenko beam element (IIE). Use the same mass matrix in both elements.

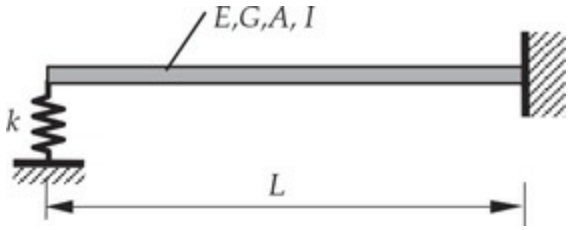

Fig. P7.6

7.7 Consider a simply supported beam (of Young's modulus E, mass density ρ, area of cross section A, second moment of area about the axis of bending I, and length L) with an elastic support at the center of the beam (see Fig. P7.7). Determine the fundamental natural frequency using the minimum number of Euler–Bernoulli beam elements. *Answer:* The characteristic polynomial is $455\lambda^2 - 2(129 + c)\lambda + 3 + 2c = 0$.

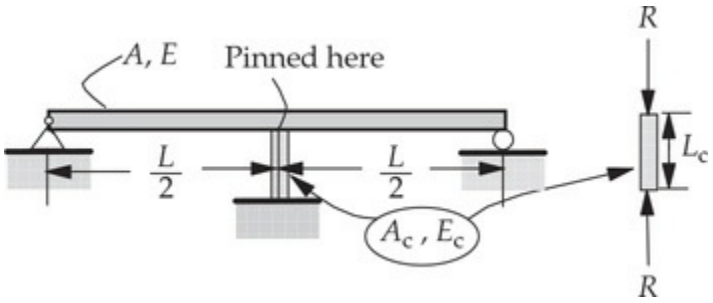

Fig. P7.7

7.8 The natural vibration of a beam under applied axial compressive load N^0 is governed by the differential equation

$$EI\frac{d^4w}{dx^4} + N^0\frac{d^2w}{dx^2} = \lambda w$$

where λ denotes the non-dimensional frequency of natural vibration and EI is the flexural stiffness of the beam. Determine the fundamental (i.e., smallest) natural frequency ω of a cantilever beam (i.e., fixed at one end and free at the other end) of length L with axial compressive load N_0 using one beam element. You are required to give the final characteristic equation.

7.9 Determine the fundamental natural frequency of the truss shown in Fig. P7.9 (you are required only to formulate the problem).

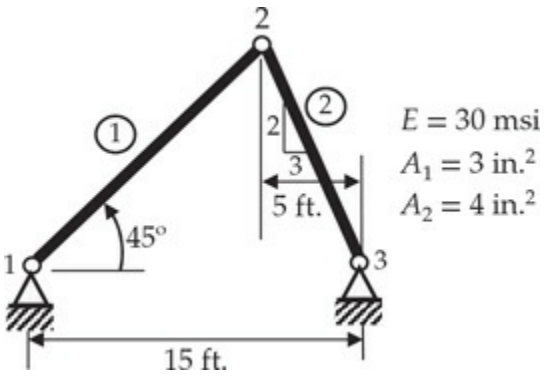

Fig. P7.9

7.10 Determine the fundamental natural frequency of the frame shown in Fig. P7.10 (you are required only to formulate the problem).

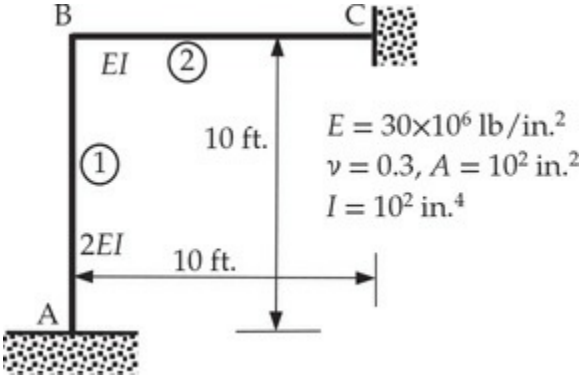

Fig. P7.10

7.11 Determine the first two longitudinal natural frequencies of a rod (A, E, L, m), fixed at one end and with an attached mass m_2 at the other. Use two linear elements. *Hint:* Note that the boundary conditions for the problem are $u(0) = 0$ and $(EA\,\partial u/\partial x + m_2\,\partial^2 u/\partial t^2)|_{x=L} = 0$.

7.12 The equation governing torsional vibration of a circular rod is

$$-GJ\frac{\partial^2\phi}{\partial x^2} + mJ\frac{\partial^2\phi}{\partial t^2} = 0$$

where ϕ is the angular displacement, J the moment of inertia, G the shear modulus, and m the density. Determine the fundamental torsional frequency of a rod with disk (J_1) attached at each end. Use the symmetry and (a) two linear elements, (b) one quadratic element.

7.13 The equations governing the motion of a beam according to the Timoshenko beam theory can be reduced to the single equation

$$a^2\frac{\partial^4 w}{\partial x^4}+\frac{\partial^2 w}{\partial t^2}-b^2\left(1+\frac{E}{K_sG}\right)\frac{\partial^4 w}{\partial x^2\partial t^2}+\frac{b^2 m}{K_s}\frac{\partial^4 w}{\partial t^4}=0$$

where $a^2 = EI/mA$ and $b^2 = I/A$. Here E is the Young's modulus, G is the shear modulus, m is the mass per unit volume, A is the area of cross section, I is the moment of inertia, and K_s is a correction factor. Assuming that $(b^2m/K_sG) << 1$ (i.e., neglect the last term in the governing equation), formulate the finite element model of the (a) eigenvalue problem for the determination of natural frequencies, and (b) fully discretized problem for the determination of the transient response.

7.14 Use the finite element model of **Problem 7.13** to determine the fundamental frequency of a simply supported beam.

7.15 Determine the critical buckling load of a cantilever beam (A, I, L, E) using (a) one Euler–Bernoulli beam element and (b) one Timoshenko beam element [see Fig. 7.3.1(d)].

7.16 Find the critical buckling load P_{cr} of a **clamped beam** [see Fig. 7.3.1(c)] by determining the eigenvalue (P_{cr}) of the equation

$$EI\frac{d^4 w}{dx^4}+P_{cr}\frac{d^2 w}{dx^2}=0 \tag{1}$$

with the boundary conditions

$$w(0)=0\,,\ w(L)=0\,,\ \frac{dw}{dx}(0)=0\,,\ \frac{dw}{dx}(L)=0 \tag{2}$$

(a) Use symmetry and **one** Euler–Bernoulli beam element in **half beam**. (b) Use two Euler–Bernoulli beam elements in the full beam.

7.17 Find the critical buckling load $P_{\rm cr}$ by determining the eigenvalues of the equation

$$EI\frac{d^4 w}{dx^4}+P_{\rm cr}\frac{d^2 w}{dx^2}=0 \quad \text{for } 0<x<L$$

$$w(0)=w(L)=0, \qquad \left(EI\frac{d^2 w}{dx^2}\right)\bigg|_{x=0}=\left(EI\frac{d^2 w}{dx^2}\right)\bigg|_{x=L}=0$$

Use one Euler–Bernoulli element in the half-beam. *Answer:* $P_{\rm cr} = 9.9439EI/L^2$.

TIME-DEPENDENT PROBLEMS

7.18 Consider the partial differential equation arising in connection with unsteady heat transfer in an insulated rod:

$$\frac{\partial u}{\partial t} - \frac{\partial}{\partial x}\left(a\frac{\partial u}{\partial x}\right) = f \quad \text{for } 0 < x < L$$

$$u(0,t) = 0, \quad u(x,0) = u_0, \quad \left[a\frac{\partial u}{\partial x} + \beta(u - u_\infty) + \hat{q}\right]\Big|_{x=L} = 0$$

Following the procedure outlined in Section 7.4, derive the semidiscrete variational form, the semidiscrete finite element model, and the fully discretized finite element equations for a typical element.

7.19 Using a two-element (linear) model and the semidiscrete finite element equations derived in **Problem 7.18**, determine the nodal temperatures as functions of time for the case in which $a = 1$, $f = 0$, $u_0 = 1$, and $\hat{q} = 0$. Use the Laplace transform technique (see Reddy [2]) to solve the ordinary differential equations in time.

7.20 Consider a uniform bar of cross-sectional area A, modulus of elasticity E, mass density m, and length L. The axial displacement under the action of time-dependent axial forces is governed by the wave equation

$$\frac{\partial^2 u}{\partial t^2} = a^2\frac{\partial^2 u}{\partial x^2}, \quad a = \left(\frac{E}{m}\right)^{1/2}$$

Determine the transient response [i.e., find $u(x, t)$] of the bar when the end $x = 0$ is fixed and the end $x = L$ is subjected to a force P_0. Assume zero initial conditions. Use one linear element to approximate the spatial variation of the solution, and solve the resulting ordinary differential equation in time exactly to obtain

$$u_2(x,t) = \frac{P_0 L}{AE}\frac{x}{L}(1 - \cos\alpha t), \quad \alpha = \sqrt{3}\frac{a}{L}$$

7.21 Re-solve **Problem 7.20** with a mesh of two linear elements. Use the Laplace transform method to solve the two ordinary differential equations in time.

7.22 Solve **Problem 7.20** when the right end is subjected to an axial force F_0 and supported by an axial spring of stiffness k. *Answer:*

$$u_2(t) = c(1 - \cos\beta t), \quad c = \frac{3F_0}{mAL\beta^2}, \quad \beta = \sqrt{3}\frac{E}{L}\left(1 + \frac{kL}{EA}\right)^{1/2}$$

7.23 A bar of length L moving with velocity v_0 strikes a spring of stiffness k. Determine the motion $u(x, t)$ from the instant when the end $x = 0$ strikes the spring. Use one linear element.

7.24 A uniform rod of length L and mass m is fixed at $x = 0$ and loaded with a mass M at $x = L$. Determine the motion $u(x, t)$ of the system when the mass M is subjected to a force P_0. Use one linear element.

Answer:

$$u_2(t) = c(1 - \cos\lambda t), \quad c = \frac{P_0 L}{AE}, \quad \lambda = \sqrt{3}\frac{a}{L}\left(\frac{3M}{AL} + m\right)^{-1}$$

7.25 The flow of liquid in a pipe, subjected to a surge-of-pressure wave (i.e., a water hammer), experiences a surge pressure p, which is governed by the equation

$$\frac{\partial^2 p}{\partial t^2} - c^2\frac{\partial^2 p}{\partial x^2} = 0, \quad c^2 = \frac{1}{m}\left(\frac{1}{k} + \frac{D}{bE}\right)^{-1}$$

where m is the mass density and k the bulk modulus of the fluid, D is the diameter and b the thickness of the pipe, and E is the modulus of elasticity of the pipe material. Determine the pressure $p(x, t)$ using one linear finite element for the following boundary and initial conditions:

$$p(0, t) = 0, \quad \frac{\partial p}{\partial x}(L, t) = 0, \quad p(x, 0) = p_0, \quad \dot{p}(x, 0) = 0$$

7.26 Consider the problem of determining the temperature distribution of a solid cylinder, initially at a uniform temperature T_0 and cooled in a medium of zero temperature (i.e., $T_\infty = 0$). The governing equation of the problem is

$$\rho c\frac{\partial T}{\partial t} - \frac{1}{r}\frac{\partial}{\partial r}\left(rk\frac{\partial T}{\partial r}\right) = 0$$

The boundary conditions are

$$\frac{\partial T}{\partial r}(0, t) = 0, \quad \left(rk\frac{\partial T}{\partial r} + \beta T\right)\Big|_{r=R} = 0$$

The initial condition is $T(r, 0) = T_0$. Determine the temperature distribution $T(r, t)$ using one linear element. Take $R = 2.5$ cm, $T_0 = 130°C$, $k = 215$ W/(m · °C), $\beta = 525$ W/(m · °C), $\rho = 2700$ kg/m^2, and $c = 0.9$ kJ/(kg°C). What is the heat loss at the surface? Formulate the problem.

7.27 Determine the non-dimensional temperature $\theta(r, t)$ in the region bounded by two long cylindrical surfaces of radii R_1 and R_2. The dimensionless heat conduction equation is

$$-\frac{1}{r}\frac{\partial}{\partial r}\left(r\frac{\partial \theta}{\partial r}\right) + \frac{\partial \theta}{\partial t} = 0$$

with boundary and initial conditions

$$\frac{\partial \theta}{\partial r}(R_1, t) = 0, \quad \theta(R_2, t) = 1, \quad \theta(r, 0) = 0$$

7.28 Show that Eqs. (7.4.32a) and (7.4.32b) can be expressed in the alternative form to Eqs. (7.4.37a) and (7.4.37b) using the (α, γ)-family of approximation in Eqs. (7.4.33) and (7.4.34) as

$$\mathbf{H}^{s+1}\ddot{\mathbf{u}}^{s+1} = \tilde{\mathbf{F}}$$

and define $\mathbf{H}^{s+1}$ and $\tilde{\mathbf{F}}$.

7.29 Use the Galerkin method with quadratic approximation to convert Eqs. (7.4.32a) and (7.4.32b) into fully discretized equations.

7.30 A uniform cantilever beam of length L, moment of inertia I, modulus of elasticity E, and mass m begins to vibrate with initial displacement

$$w(x, 0) = \frac{w^0 x^2}{L^2}$$

and zero initial velocity. Formulate equations for the unknown generalized displacements. Use one (a) Euler–Bernoulli beam element and (b) Timoshenko beam element to determine the solution.

References for Additional Reading

1. J.N. Reddy, *Energy Principles and Variational Methods in Applied*

Mechanics, 3rd ed., John Wiley, New York, NY 2017.

2. J.N. Reddy, *Theory and Analysis of Elastic Plates and Shells*, 2nd ed., CR C Press, Boac Raton, FL, 2007.
3. F.B. Hildebrand, *Methods of Applied Mathematics*, 2nd ed., Prentice–Hall, Englewood Cliffs, NJ, 1965.
4. K.S. Surana and J.N. Reddy, *The Finite Element Method for Initial Value Problems, Mathematics and Computations*, CRC Press, Boca Raton, FL, 2018.
5. Wooram Kim and J.N. Reddy, "Nonconventional finite element models for nonlinear analysis of beams," *International Journal of Computational Methods*, **8**(3), 349–368, 2011.
6. Wooram Kim, Sang-Shin Park, and J.N. Reddy, "A cross weighted-residual time integration scheme for structural dynamics," *International Journal of Structural Stability and Dynamics*, **14** (6), 1450023-1 to 1450023-20, Aug 2014.
7. Wooram Kim and J.N. Reddy, "A New Family of Higher-Order Time Integration Algorithms for the Analysis of Structural Dynamics," *Journal of Applied Mechanics*, **84**, 071008-1 to 071008-17, July 2017.
8. Wooram Kim and J.N. Reddy, "Effective higher-order time integration algorithms for the analysis of linear structural dynamics," *Journal of Applied Mechanics*, **84**, 071009-1 to 071009-13, July 2017.
9. J.H. Argyris and O.W. Scharpf, "Finite elements in time and space," *Aeronautical Journal of the Royal Society*, **73**, 1041–1044, 1969.
10. J.C. Houbolt, "A recurrence matrix solution for the dynamic response of elastic aircraft," *Journal of Aeronautical Science*, **17**, 540–550, 1950.
11. N.M. Newmark, "A method of computation for structural dynamics," *Journal of Engineering Mechanics Division, ASCE*, **85**, 67–94, 1959.
12. R.E., Nickell, "On the stability of approximation operators in problems of structural dynamics," *International Journal of Solids and Structures*, **7**, 301–319, 1971.
13. G.L. Goudreau and R.L. Taylor, "Evaluation of numerical integration methods in elastodynamics," *Journal of Computer Methods in Applied Mechanics and Engineering*, **2**(1), 69–97, 1973.
14. K.J. Bathe and W.L. Wilson, "Stability and accuracy analysis of

direct integration methods," *International Journal of Earthquake Engineering and Structural Dynamics*, **1**, 283–291, 1973.

15. H.M. Hilber, "Analysis and design of numerical integration methods in structural dynamics," EERC Report no. 77–29, Earthquake Engineering Research Center, University of California, Berkeley, California, November 1976.
16. H.M. Hilber, T.J. R. Hughes, and R.L. Taylor, "Improved numerical dissipation for time integration algorithms in structural dynamics," *Earthquake Engineering and Structural Dynamics*, **5**, 283–292, 1977.
17. W.L. Wood, "Control of Crank–Nicolson noise in the numerical solution of the heat conduction equation," *International Journal for Numerical Methods in Engineering*, **11**, 1059–1065, 1977.
18. T. Belytschko, "An overview of semidiscretization and time integration procedures," in *Computational Methods for Transient Analysis*, T. Belytschko and T.J.R. Hughes (eds), 1–65, North-Holland, Amsterdam, 1983.
19. J. Chung and G.M. Hulbert, "A time integration algorithm for structural dynamics with improved numerical dissipation: The generalized-alpha method," *Journal of Applied Mechanics*, **60**, 271–275, 1993.
20. G.M. Hulbert, "A unified set of single-step asymptotic annihilation algorithms for structural dynamics," *Computer Methods in Applied Mechanics and Engineering*, **113**(1), 1–9, 1994.
21. T.C. Fung, "Unconditionally stable higher-order accurate Hermitian time finite elements," *International Journal for Numerical Methods in Engineering*, **39**(20), 3475–3495, 1996.
22. S.J. Kim, J.Y. Cho, and W.D. Kim, "From the trapezoidal rule to higher-order accurate and unconditionally stable time-integration method for structural dynamics," *Computer Methods in Applied Mechanics and Engineering*, **149**(1), 73–88, 1997.
23. M.M.I. Baig and K.J. Bathe, "On direct time integration in large deformation dynamic analysis," *3rd MIT Conference on Computational Fluid and Solid Mechanics*, 1044–1047, 2005.
24. A.V. Idesman, "A new high-order accurate continuous Galerkin method for linear elastodynamics problems," *Computational Mechanics*, **40**(2), 261–279, 2007.

8 Numerical Integration and Computer Implementation

You cannot depend on your eyes when your imagination is out of focus.

— Mark Twain

8.1 Introduction

The finite element method, like most approximation methods, converts a continuum problem to a discrete one (i.e., an infinite number of degrees of freedom system is transformed into one with finite number of degrees of freedom), in which algebraic relations between the primary and secondary variables are set up (this is what we termed as the finite element model). Chapters 3–7 were devoted to the finite element formulations of the following two *classes* of boundary and initial value problems in one dimension:

1. Second-order differential equations (e.g., heat transfer, fluid mechanics, 1-D elasticity, bars, and the Timoshenko beam theory).
2. Fourth-order differential equations governing the Euler–Bernoulli beam theory.

The truss and frame elements, which are extensions of bars and beams to two dimensions, were discussed in Chapter 6.

By now, it should be clear to the reader that the steps involved in the finite element analysis of a general class of problems (e.g., single second-order, single fourth-order, and a pair of second-order equations) are systematic, and once the finite element model development is completed the finite element analysis steps can be implemented on a digital computer. For example, if we develop a general computer program to solve equations of the form

$$c_1\frac{\partial u}{\partial t}+c_2\frac{\partial^2 u}{\partial t^2}-c_3\frac{\partial^4 u}{\partial x^2\partial t^2}-\frac{\partial}{\partial x}\left(a\frac{\partial u}{\partial x}\right)+\frac{\partial^2}{\partial x^2}\left(b\frac{\partial^2 u}{\partial x^2}\right)+cu=f \qquad (8.1.1)$$

then all physical problems described by Eqs. (3.4.1), (3.5.3), (5.2.10), (5.4.8) [with (5.4.4)], and (7.2.1)–(7.2.4b) can be solved for any compatible boundary and initial conditions. A particular class of problems described by the model equation of the class can be solved by simply supplying the required input data (i.e., c_1, c_2, c_3, a, b, c, and f) to the program. Indeed, the success of the finite element method is largely due to the ease with which the analysis of a class of problems, without regard to the specific data, geometry, boundary conditions, and the degree of approximation, can be implemented on a digital computer.

The finite element model of any system ultimately represents a set of algebraic relations among the values of the primary and secondary variables (i.e., duality pairs) of the system at the nodes of an element Ω^e. For example, for a static problem, we have

$$\begin{aligned} K^e_{11}u^e_1 + K^e_{12}u^e_2 + \cdots + K^e_{1n}u^e_n &= F^e_1 \\ K^e_{21}u^e_1 + K^e_{22}u^e_2 + \cdots + K^e_{2n}u^e_n &= F^e_2 \\ \cdots\cdots\cdots\cdots\cdots\cdots\cdots\cdots\cdots\cdots\cdots\cdots & \\ K^e_{n1}u^e_1 + K^e_{n2}u^e_2 + \cdots + K^e_{nn}u^e_n &= F^e_n \end{aligned} \tag{8.1.2}$$

The coefficients $K^e_{ij}\ (i,j=1,2,\cdots,n)$ are typically integrals of the approximation functions ψ^e_i multiplied by the data (a, b, and c) of the problem [see Eq. (8.1.1) with time derivative terms set to zero]

$$K^e_{ij} = \int_{x^e_a}^{x^e_b} \left[a(x)\frac{d\psi^e_i}{dx}\frac{d\psi^e_j}{dx} + b(x)\frac{d^2\psi^e_i}{dx^2}\frac{d^2\psi^e_j}{dx^2} + c(x)\psi^e_i\psi^e_j \right] dx \tag{8.1.3}$$

Exact evaluation of these integrals is not always possible because of the algebraic complexity of the data $a(x)$, $b(x)$, and $c(x)$ in the mathematical model. In such cases, it is natural to seek numerical evaluation of these integrals. Numerical evaluation of the coefficient matrices is also useful in problems with constraints, where reduced integration techniques are used (e.g., the reduced integration element of the Timoshenko beam theory in Section 5.3).

This chapter is devoted to two topics: (1) numerical integration and (2) computer implementation of the finite element models developed in the preceding chapters. The computer implementation of the class of problems described by Eq. (8.1.1) as well as those of the Timoshenko beam theory, trusses, and frames is discussed here.

8.2 Numerical Integration

8.2.1 Preliminary Comments

Numerical evaluation of integrals, called *numerical integration* or *numerical quadrature*, involves approximation of the integrand by a polynomial of sufficient degree, because the integral of a polynomial can be evaluated exactly. The integrals are generally expressed in terms of the coordinate appearing in the problem description (like x or r). We shall call x and r as the *problem coordinates* or global coordinates. Since the finite element approximation (or interpolation) functions are derived over an element, it is convenient to use a local (i.e., element) coordinate, such as $\bar{x}$ used earlier.

For example, consider the integral,

$$I_e = \int_{x_a^e}^{x_b^e} F_e(x)\, dx = \int_0^{h_e} F^e(\bar{x})\, d\bar{x} \tag{8.2.1}$$

where F^e is a function of $x = x_a^e + \bar{x}$, and $h_e = x_b^e - x_a^e$. We approximate the function $F^e(\bar{x})$ in Ω^e by a polynomial

$$F^e(\bar{x}) \approx \sum_{I=1}^{N} F_I^e \psi_I^e(\bar{x}) \tag{8.2.2}$$

where F_I^e denotes the value of $F^e(\bar{x})$ at the Ith point $\bar{x}_I$ of the interval $[0, h_e]$ and $\psi_I^e(\bar{x})$ are polynomials of degree $N-1$ in the interval. The representation can be viewed as the finite element interpolation of $F^e(\bar{x})$, where F_I^e is the value of the function at the Ith node. The interpolation functions $\psi_I^e(\bar{x})$ can be of the Lagrange type or the Hermite type.

Substitution of Eq. (8.2.2) into Eq. (8.2.1) and evaluation of the integral give an approximate value of the integral I_e. For example, suppose that we choose linear interpolation of $F^e(\bar{x})$, as shown in Fig. 8.2.1. For $N = 2$, we have

$$\psi_1^e = 1 - \frac{\bar{x}}{h_e}, \quad \psi_2^e = \frac{\bar{x}}{h_e}, \quad \int_0^{h_e} \psi_I^e(\bar{x})\, d\bar{x} = \frac{h_e}{2} \ \ (I = 1, 2) \tag{8.2.3a}$$

and

$$I_e = \frac{h_e}{2}\left(F_1^e + F_2^e\right), \quad F_1^e = F^e(0), \quad F_2^e = F^e(h_e) \tag{8.2.3b}$$

Thus, the value of the integral is given by the area of a trapezoid used to approximate the area under the function $F^e(\bar{x})$ (see Fig. 8.2.1). Equation (8.2.3b) is known as the *trapezoidal rule* of numerical integration.

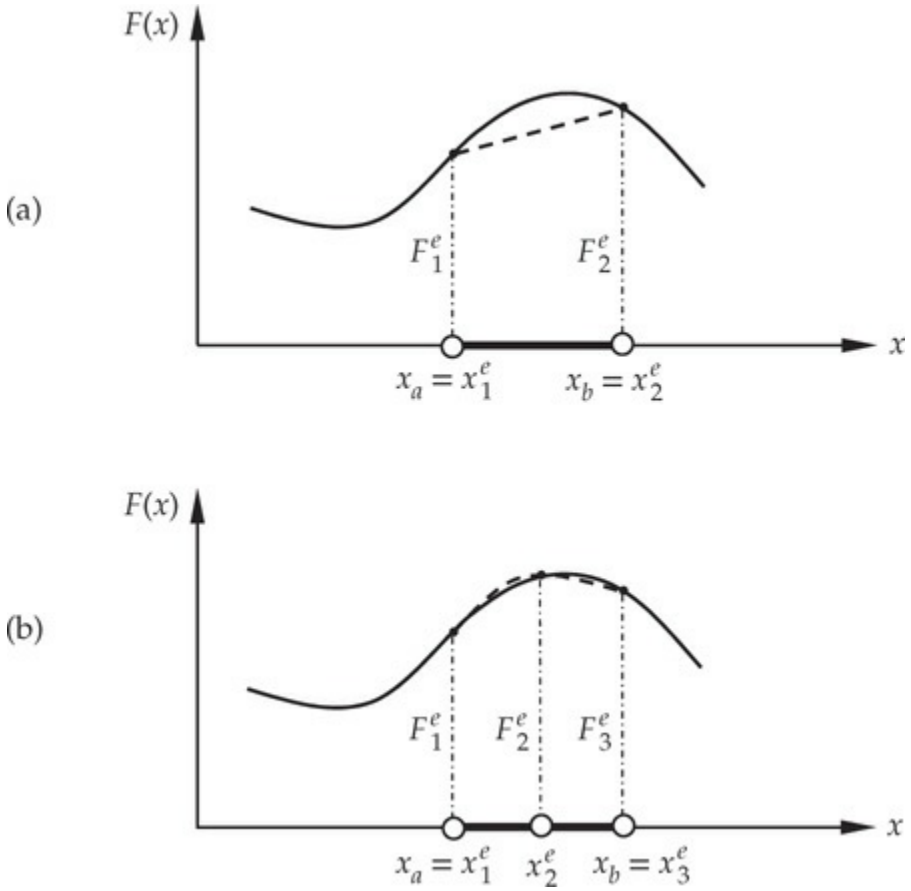

Fig. 8.2.1 Approximate evaluation of an integral using the trapezoidal rule: (a) two-point formula; (b) three-point formula.

If we use the quadratic interpolation of $F^e(\bar{x})$, with

$$\psi_1^e(\bar{x}) = \left(1 - \frac{\bar{x}}{h_e}\right)\left(1 - \frac{2\bar{x}}{h_e}\right), \quad \psi_2^e(\bar{x}) = 4\frac{\bar{x}}{h_e}\left(1 - \frac{\bar{x}}{h_e}\right), \quad \psi_3^e(\bar{x}) = -\frac{\bar{x}}{h_e}\left(1 - \frac{2\bar{x}}{h_e}\right) \tag{8.2.4a}$$

and

$$\int_0^{h_e} \psi_1^e(\bar{x})\, d\bar{x} = \frac{h_e}{6}, \quad \int_0^{h_e} \psi_2^e(\bar{x})\, d\bar{x} = \frac{4h_e}{6}, \quad \int_0^{h_e} \psi_3^e(\bar{x})\, d\bar{x} = \frac{h_e}{6} \tag{8.2.4b}$$

we obtain

$$I_e = \frac{h_e}{6}(F_1^e + 4F_2^e + F_3^e) \tag{8.2.4c}$$

where

$$F_1^e = F^e(\bar{x}_1) = F^e(0), \quad F_2^e = F^e(\bar{x}_2) = F^e(0.5h_e), \quad F_3^e = F^e(\bar{x}_3) = F^e(h_e) \tag{8.2.4d}$$

Equation (8.2.4c) is known as *Simpson's one-third rule*.

Equations (8.2.3b) and (8.2.4c) represent the form of numerical quadrature formulae. In general, they have the following general form:

$$I_e = \int_{x_a^e}^{x_b^e} F^e(x)\,dx \approx \sum_{I=1}^{r} F^e(x_I) W_I \tag{8.2.5}$$

where x_I are called the *quadrature points*, W_I are the *quadrature weights*, and r is the number of quadrature points. These formulae require functional evaluations, multiplications, and additions to obtain the numerical value of the integral. They yield exact values of the integral whenever $F_e(x)$ is a polynomial of order $r - 1$.

In this section, we describe several numerical integration schemes and formulations in which the geometry as well as the dependent variables are approximated using different degrees of polynomials. We begin with the discussion of a local coordinate system that is needed in the numerical integration by the Gauss–Legendre rule.

8.2.2 Natural Coordinates

Of all the quadrature formulae, the Gauss–Legendre quadrature is the most commonly used. The details of the method itself will be discussed shortly. The quadrature formula requires the integral to be cast as one to be evaluated over the interval (element) $\hat{\Omega}^e \equiv [-1, 1]$. This requires the transformation of the problem coordinate x (i.e., the coordinate used to describe the governing equation) to the element coordinate ξ such that the integrals are posed on $[-1, 1]$ (see Fig. 8.2.2). Thus, the relationship between x and ξ is linear and it can be established with the help of the conditions

$$\text{when } x = x_a^e, \ \xi = -1; \ \text{and when } x = x_b^e, \ \xi = 1 \tag{8.2.6a}$$

This transformation between x and ξ can be represented by the linear

"stretch" mapping

$$x = a^e + b^e \xi \quad \text{for} \quad x \text{ in } \bar{\Omega}^e = [x_a^e, x_b^e] \tag{8.2.6b}$$

where a^e and b^e are constants to be determined such that conditions in Eq. (8.2.6a) hold:

$$x_a^e = a^e + b^e \cdot (-1), \quad x_b^e = a^e + b^e \cdot (1)$$

Solving for a^e and b^e, we obtain

$$b^e = \tfrac{1}{2}(x_b^e - x_a^e) = \tfrac{1}{2}h_e, \quad a^e = \tfrac{1}{2}(x_b^e + x_a^e) = x_a^e + \tfrac{1}{2}h_e$$

Hence the transformation between x and ξ becomes

$$x(\xi) = \tfrac{1}{2}(x_b^e + x_a^e) + \tfrac{1}{2}(x_b^e - x_a^e)\xi = x_a^e \tfrac{1}{2}(1-\xi) x_b^e \tfrac{1}{2}(1+\xi) = x_a^e + \tfrac{1}{2}h_e(1+\xi) \tag{8.2.7}$$

where x_a^e and x_b^e denote the global coordinates of the left end and the right end, respectively, of the element $\bar{\Omega}^e$ and h_e is the element length (see Fig. 8.2.2).

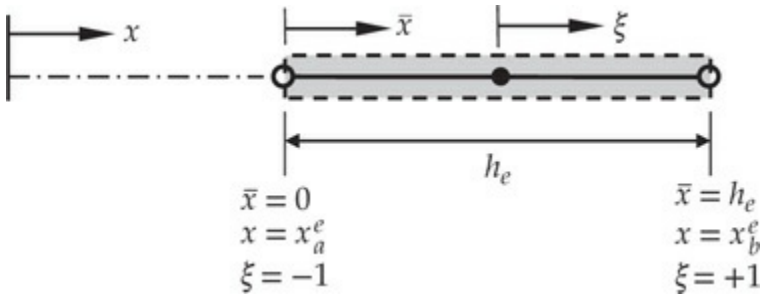

Fig. 8.2.2 Global (problem) coordinate x, local (element) coordinate $\bar{x}$, and normalized local coordinate ξ.

The local coordinate ξ is called the *normal coordinate* or *natural coordinate*, and its values always lie between −1 and 1, with its origin at the center of the 1-D element. The local coordinate ξ is useful in two ways: it is (1) convenient in constructing the interpolation functions and (2) required in the numerical integration based on the Gauss–Legendre quadrature.

The derivation of the Lagrange family of interpolation functions in terms of the natural coordinate ξ is made easy by the following interpolation property of the approximation functions:

$$\psi_i^e(\xi_j) = \begin{cases} 1 & \text{if } i = j \\ 0 & \text{if } i \neq j \end{cases} \tag{8.2.8}$$

where ξ_j is the ξ-coordinate of the jth node in the element. For an element with n nodes, the Lagrange interpolation functions ψ_i^e $(i = 1, 2, \ldots, n)$ are polynomials of degree $n - 1$. To construct ψ_i^e satisfying the properties in Eq. (8.2.8), we proceed as follows. For each ψ_i^e, we form the product of $n - 1$ linear functions $\xi - \xi_j$ ($j = 1, 2, \ldots, i - 1, i + 1, \ldots, n$ and $j \neq i$):

$$\psi_i^e = c_i(\xi - \xi_1)(\xi - \xi_2)\cdots(\xi - \xi_{i-1})(\xi - \xi_{i+1})\cdots(\xi - \xi_n)$$

Note that ψ_i^e is zero at all nodes except the ith. Next we determine the constant c_i such that $\psi_i^e = 1$ at $\xi - \xi_i$:

$$c_i = [(\xi_i - \xi_1)(\xi_i - \xi_2)\cdots(\xi_i - \xi_{i-1})(\xi_i - \xi_{i+1})\cdots(\xi_i - \xi_n)]^{-1}$$

Thus, the interpolation function associated with node i is

$$\psi_i^e(\xi) = \frac{(\xi - \xi_1)(\xi - \xi_2)\cdots(\xi - \xi_{i-1})(\xi - \xi_{i+1})\cdots(\xi - \xi_n)}{(\xi_i - \xi_1)(\xi_i - \xi_2)\cdots(\xi_i - \xi_{i-1})(\xi_i - \xi_{i+1})\cdots(\xi_i - \xi_n)} \tag{8.2.9}$$

The linear, quadratic, and cubic Lagrange interpolation functions (which were already derived in terms of x in Chapter 3) in terms of the natural coordinate (for equally spaced nodes) are shown in Fig. 8.2.3.

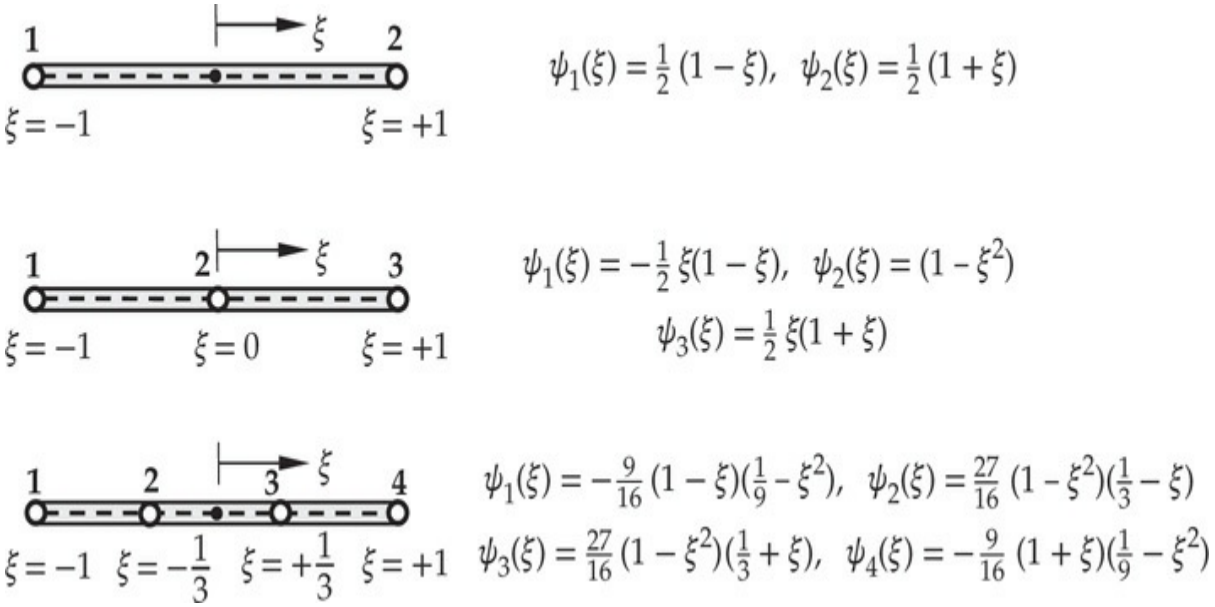

Fig. 8.2.3 Lagrange family of one-dimensional interpolation functions in terms of the normalized coordinate.

8.2.3 Approximation of Geometry

We wish to use the Gauss quadrature to numerically evaluate all integrals in finite element method. The Gauss quadrature requires us to express the integral in terms of ξ over the interval −1 to +1. We assume a relation (or transformation) between the problem coordinate x and natural coordinate ξ in the form

$$x = f(\xi) \tag{8.2.10}$$

where f is assumed to be a one-to-one transformation. An example of $f(\xi)$ is provided by Eq. (8.2.7), where $n = 2$:

$$f(\xi) = x_a^e + \frac{1}{2} h_e (1 + \xi)$$

In this case, $f(\xi)$ is a linear function of ξ. Hence, a straight line is transformed into a straight line.

It is natural to think of approximating the geometry in the same way as we approximated a dependent variable. In other words, the transformation $x = f(\xi)$ can be written as

$$x = \sum_{i=1}^{m} x_i^e \hat{\psi}_i^e(\xi), \tag{8.2.11}$$

where x_i^e is the global coordinate of the ith node of the element Ω_e and $\hat{\psi}_i^e$ are the Lagrange interpolation functions of degree $m - 1$. When $m = 2$ we have a linear transformation and Eq. (8.2.11) is exactly the same as Eq. (8.2.7). When $m = 3$, Eq. (8.2.11) expresses a quadratic relation between x and ξ. The functions $\hat{\psi}_i^e$ are called *shape functions* because they are used to express the geometry or shape of the element. When the element is a straight line, the mapping is linear because the two end points, x_1^e and x_n^e, are sufficient to define a line.

The transformation in Eq. (8.2.11) allows us to rewrite integrals involving x as those in terms of ξ:

$$\int_{x_a^e}^{x_b^e} F(x)\, dx = \int_{-1}^{1} \hat{F}(\xi)\, d\xi, \quad \hat{F}(\xi)\, d\xi = F(x(\xi))\, dx \tag{8.2.12}$$

so that the Gauss quadrature can be used to evaluate the integral over [−1, 1]. The differential element dx in the global coordinate system x is related

to the differential element $d\xi$ in the natural coordinate system ξ by

$$dx = \frac{dx}{d\xi} d\xi = J_e \, d\xi \tag{8.2.13}$$

where J_e is called the *Jacobian* of the transformation. We have

$$J_e = \frac{dx}{d\xi} = \frac{d}{d\xi}\left(\sum_{i=1}^{m} x_i^e \hat{\psi}_i^e\right) = \sum_{i=1}^{m} x_i^e \frac{d\hat{\psi}_i^e}{d\xi} \tag{8.2.14}$$

For a linear transformation [i.e., when $m = 2$ in Eq. (8.2.11)], we have

$$\begin{aligned} \hat{\psi}_1^e &= \tfrac{1}{2}(1-\xi), \quad \hat{\psi}_2^e = \tfrac{1}{2}(1+\xi) \\ J_e &= x_1^e\left(-\tfrac{1}{2}\right) + x_2^e\left(\tfrac{1}{2}\right) = \tfrac{1}{2}(x_2^e - x_1^e) = \tfrac{1}{2}h_e \end{aligned} \tag{8.2.15}$$

It can be shown that $J_e = \frac{1}{2}h_e$, whenever the element is a straight line, irrespective of the degree of interpolation used in the transformation in Eq. (8.2.11).

8.2.4 Parametric Formulations

Recall that a dependent variable u is approximated in an element Ω_e by expressions of the form

$$u(x) = \sum_{j=1}^{n} u_j^e \psi_j^e(x) \tag{8.2.16}$$

In general, the degree of approximation used to describe the coordinate transformation in Eq. (8.2.11) is not equal to the degree of approximation in Eq. (8.2.16) used to represent a dependable variable, $\hat{\psi}_i^e \neq \psi_i^e$. In other words, two independent meshes of elements may be used in the finite element formulation of a problem: one for the approximation of the geometry x and the other for the interpolation of the dependent variable u. Depending on the relationship between the degree of approximation used for the coordinate transformation and that used for the dependent variable, the finite element formulations are classified into three categories:

1. Subparametric formulations: $m < n$
2. Isoparametric formulations: $m = n$

3. Superparametric formulations: $m > n$

In subparametric formulations, the geometry is represented by lower-order elements than those used to approximate the dependent variable. An example of this category is provided by the Euler–Bernoulli beam element, where the Hermite cubic functions are used to approximate the deflection $w(x)$ and linear interpolation can be used, when straight beams are analyzed, to represent the geometry. In isoparametric formulations (which are the most common in practice), the same element is used to approximate the geometry as well as the dependent unknowns: $\psi_i^e(x) = \hat{\psi}_i^e(\xi)$. In the superparametric formulations, the geometry is represented with higher-order elements than those used to approximate the dependent variables. The superparametric formulation is seldom used in practice. It is not correct to say "isoparametric element" because an element is what it is (i.e., linear, quadratic, and so on).

8.2.5 Numerical Integration

As discussed in the introduction, the evaluation of integrals of the form

$$\int_a^b F(x)\,dx \tag{8.2.17}$$

by exact means is either difficult or impossible owing to the complicated form of the integrand F. Numerical integration is also required when the integrand is to be evaluated inexactly (as in the Timoshenko beam element) or when the integrand is known only at discrete points (e.g., experimentally obtained data).

The basic idea behind all numerical integration techniques is to find a function $P(x)$, often a polynomial, that is both a suitable approximation of $F(x)$ and simple to integrate. The interpolating polynomials of degree n, denoted by P_n, which interpolate the integrand at $n + 1$ points of the interval $[a, b]$, often produce a suitable approximation and possess the desired property of simple integrability. An illustration of the approximation of the function $F(x)$ by the polynomial $P_4(x)$ that exactly matches the function $F(x)$ at the indicated base points is given in Fig. 8.2.4(a). The exact value of the integral in Eq. (8.2.17) is given by the area under the solid curve, while the approximate value

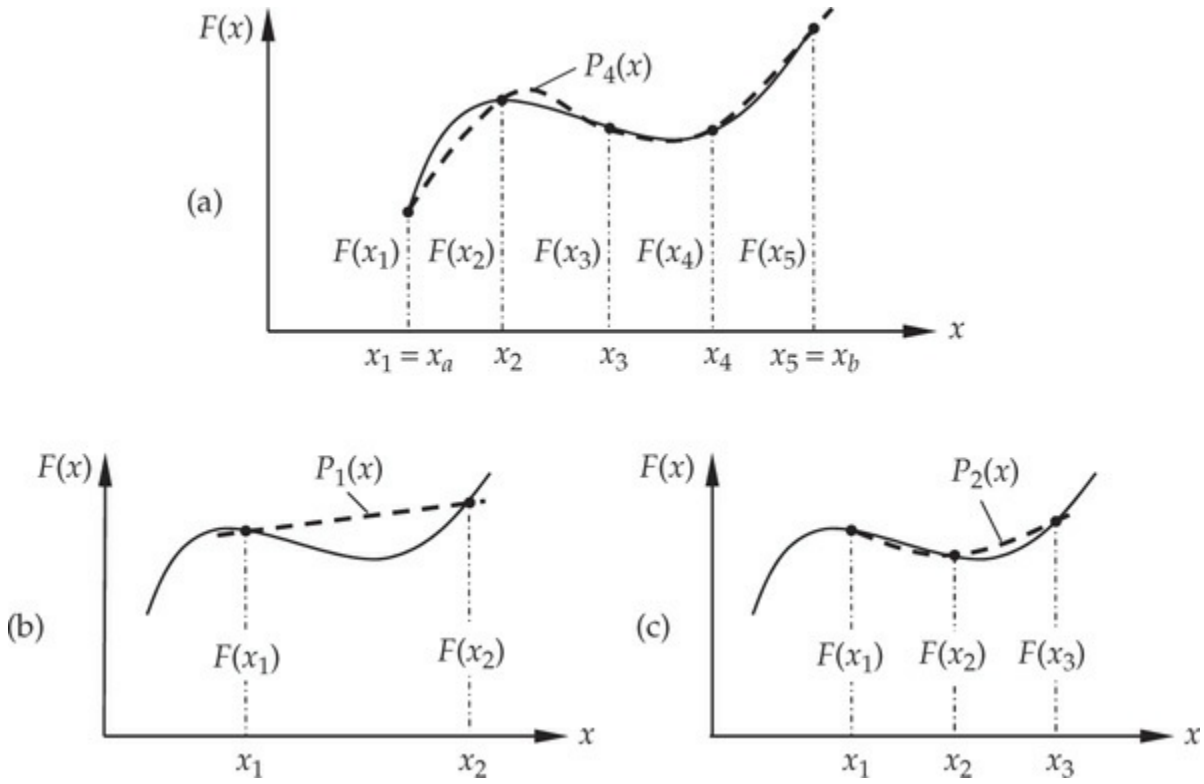

Fig. 8.2.4 Numerical integration by the Newton–Cotes quadrature: (a) approximation of a function by P_4 (x); (b) the trapezoidal rule; (c) Simpson's rule.

$$\int_a^b P_4(x)\,dx$$

is given by the area under the dashed curve. It should be noted that the difference (i.e., the error in the approximation) $E = F(x) - P_4(x)$ is not always of the same sign, and therefore the overall integration error may be small (because positive errors in one part may cancel negative errors in other parts), even when P_4 is not a good approximation of F.

The commonly used numerical integration methods can be classified into two groups:

1. The Newton–Cotes formulae that employ values of the function at equally spaced points.
2. The Gauss quadrature formula that employs unequally spaced points.

These two methods are described next.

8.2.5.1 The Newton–Cotes Quadrature

For r equally spaced base points, the *Newton–Cotes closed integration formula* is given by

$$\int_a^b F(x)\,dx = (b-a)\sum_{I=1}^{r} F(x_I)w_I \tag{8.2.18}$$

where w_I are the *weighting coefficients*, x_I are the *base points* that are equally spaced, and r is the number of base points (or $r-1$ is the number of intervals). Note that $r = 1$ is a special case in which the number of base points as well as the number of intervals are the same; in this case Eq. (8.2.18) gives the rectangle formula. For $r = 2$, it gives the familiar *trapezoidal rule*, in which the required area under the solid curve in Fig. 8.2.4(b) is approximated by the area under the dotted straight line [i.e., $F(x)$ is approximated by $P_1(x)$]:

$$\int_{a=x_1}^{b=x_2} F(x)\,dx = \frac{b-a}{2}[F(x_1)+F(x_2)],\quad E=O(h^3),\quad h=b-a \tag{8.2.19}$$

where E denotes the error in the approximation and h is the uniform spacing between two base points. The notation $O(h)$, read as "order of h", is used to indicate the order of the error in terms of the spacing h. For $r = 3$ (i.e., two intervals), Eq. (8.2.17) gives the familiar *Simpson's one-third rule* [see Fig. 8.2.4(c)]:

$$\int_{a=x_1}^{b=x_3} F(x)\,dx = \frac{b-a}{6}[F(x_1)+4F(x_2)+F(x_3)],\quad E=O(h^5),\quad h=0.5(b-a) \tag{8.2.20}$$

The weighting coefficients for $r = 1, 2,...,7$ are given in Table 8.2.1. Note that $\sum_{I=1}^{r} w_I = 1$. The base point location for $r = 1$ is $x_1 = a + \frac{1}{2}(b-a) = \frac{1}{2}(a+b)$. For $r > 1$, the base point locations are

Table 8.2.1 Weighting coefficients for the Newton–Cotes formula.

r	w_1	w_2	w_3	w_4	w_5	w_6	w_7
1	1						
2	$\frac{1}{2}$	$\frac{1}{2}$					
3	$\frac{1}{6}$	$\frac{4}{6}$	$\frac{1}{6}$				
4	$\frac{1}{8}$	$\frac{3}{8}$	$\frac{3}{8}$	$\frac{1}{8}$			
5	$\frac{7}{90}$	$\frac{32}{90}$	$\frac{12}{90}$	$\frac{32}{90}$	$\frac{7}{90}$		
6	$\frac{19}{288}$	$\frac{75}{288}$	$\frac{50}{288}$	$\frac{50}{288}$	$\frac{75}{288}$	$\frac{19}{288}$	
7	$\frac{41}{840}$	$\frac{216}{840}$	$\frac{27}{840}$	$\frac{272}{840}$	$\frac{27}{840}$	$\frac{216}{840}$	$\frac{41}{840}$

$$x_1 = a, \quad x_2 = a + \Delta x, \ \ldots, \ x_r = a + (r-1)\Delta x = b$$

and $\Delta x = (b - a)/(r - 1)$. We note that when $r - 1$ is *even* (i.e., when there is an even number of intervals or an odd number of base points), the formula is exact when $F(x)$ is a polynomial of degree r or less; when $r - 1$ is *odd*, the formula is exact for a polynomial of degree $r - 1$ or less. Odd-point formulae are frequently used because of their high order of accuracy (see Carnahan, Luther, and Wilkes [1]).

Example 8.2.1

Evaluate the integral of the following polynomial using the trapezoidal and Simpson's rules.

$$f(x) = 5 + 3x + 2x^2 - x^3, \quad -1 \le x \le 1 \tag{1}$$

Solution: The exact value of the integral of $f(x)$ is

$$\int_{-1}^{1} f(x)\,dx = \int_{-1}^{1} (5 + 3x + 2x^2 - x^3)dx = \left[5x + \frac{3x^2}{2} + \frac{2x^3}{3} - \frac{x^4}{4}\right]_{-1}^{1} = \frac{34}{3} \tag{2}$$

Using the trapezoidal rule in Eq. (8.2.19), we obtain ($h = 2$, $x_1 = -1$, $x_2 = 1$, $f(x_1) = 5$, and $f(x_2) = 9$)

$$\int_{-1}^{1} f(x)\,dx = \frac{h}{2}\left[f(x_1) + f(x_2)\right] = \frac{2}{2}(5 + 9) = 14 \tag{3}$$

Using Simpson's rule in Eq. (8.2.20), we obtain ($h = 1$, $x_1 = -1$, $x_2 = 0$, $x_3 = 1$, $f(x_1) = 5$, $f(x_2) = 5$, and $f(x_3) = 9$)

$$\int_{-1}^{1} f(x)\,dx = \frac{h}{3}\left[f(x_1) + 4f(x_2) + f(x_3)\right] = \frac{1}{3}(5 + 4 \times 5 + 9) = \frac{34}{3} \tag{4}$$

which coincides with the exact value.

8.2.5.2 The Gauss Quadrature

In the Newton–Cotes quadrature, the base point locations have been specified. If the x_I are not specified then there will be $2r$ undetermined parameters, r weights w_I and r base points x_I, which define a polynomial of degree $2r - 1$. The Gauss–Legendre quadrature is based on the idea that the base points xI and the weights w_I can be chosen so that the sum of the r appropriately weighted values of the function yields the integral exactly when $F(x)$ is a polynomial of degree $2r - 1$ or less. The Gauss–Legendre quadrature formula is given by

$$\int_a^b F(x)\,dx = \int_{-1}^{1} \hat{F}(\xi)\,d\xi \approx \sum_{I=1}^{r} \hat{F}(\xi_I) w_I \tag{8.2.21}$$

where w_I are the weight factors (or simply weights), ξ_I are the base points [roots of the Legendre polynomial $P_r(\xi)$], and $\hat{F}$ is the transformed integrand

$$\hat{F}(\xi) = F(x(\xi))J(\xi), \quad dx = J\,d\xi \tag{8.2.22}$$

Here J is the Jacobian of the transformation between the global coordinate x and the local coordinate ξ. In 2-D and 3-D problems, Eq. (8.2.22) is a matrix equation with the Jacobian of the transformation being a matrix $[J]$ and its determinant being J. The weights and Gauss points for the Gauss–Legendre quadrature (or simply Gauss quadrature) in Eq. (8.2.21) are given for $r = 1, 2, \ldots, 10$ in Table 8.2.2.

Table 8.2.2 Weights (positive) and Gauss points for the Gauss quadrature (included 15 significant figures*).

$$\int_{-1}^{1} F(\xi)d\xi = \sum_{i=1}^{r} F(\xi_i)w_i$$

ξ_i	r	w_i
0.00000 00000 00000	One-point formula	2.00000 00000 00000
± 0.57735 02691 89626	Two-point formula	1.00000 00000 00000
± 0.77459 66692 41483	Three-point formula	0.55555 55555 55556
0.00000 00000 00000		0.88888 88888 88889
± 0.86113 63115 94053	Four-point formula	0.34785 48451 37454
± 0.33998 10435 84856		0.65214 51548 62546
± 0.90617 98459 38664	Five-point formula	0.23692 68850 56189
± 0.53846 93101 05683		0.47862 86704 99366
0.00000 00000 00000		0.56888 88888 88889
± 0.93246 95142 03152	Six-point formula	0.17132 44923 79170
± 0.66120 93864 66265		0.36076 15730 48139
± 0.23861 91860 83197		0.46791 39345 72691
± 0.94910 79123 42759	Seven-point formula	0.12948 49661 68870
± 0.74153 11855 99394		0.27970 53914 89277
± 0.40584 51513 77397		0.38183 00505 05119
0.00000 00000 00000		0.41795 91836 73469
± 0.96028 98564 97536	Eight-point formula	0.10122 85362 90376
± 0.79666 64774 13627		0.22238 10344 53374
± 0.52553 24099 16329		0.31370 66458 77887
± 0.18343 46424 95650		0.36268 37833 78362
± 0.96816 02395 07626	Nine-point formula	0.08127 43883 61574
± 0.83603 11073 26636		0.18064 81606 94857
± 0.61337 14327 00590		0.26061 06964 02935
± 0.32425 34234 03809		0.31234 70770 40003
0.00000 00000 00000		0.33023 93550 01260
± 0.97390 65285 17172	Ten-point formula	0.06667 13443 08688
± 0.86506 33666 88985		0.14945 13491 50581
± 0.67940 95682 99024		0.21908 63625 15982
± 0.43339 53941 29247		0.26926 67193 09996
± 0.14887 43389 81631		0.29552 42247 14753

*Note that $0.57735... = 1/\sqrt{3}$, $0.77459... = \sqrt{3/5}$, $0.888... = 8/9$, $0.555... = 5/9$.

The Gauss–Legendre quadrature is more frequently used than the Newton– Cotes quadrature because it requires fewer base points to achieve the same degree of accuracy. The error in the approximation is zero if the

(2r + 2)th derivative of the integrand vanishes. In other words, a polynomial of degree p is integrated exactly by employing r Gauss points, where:

$$r = \left[\tfrac{1}{2}(p+1)\right] \quad \text{(when } p+1 \text{ is odd, pick the nearest larger integer)} \qquad (8.2.23)$$

In other words, N Gauss points are needed to evaluate a polynomial of degree $2N - 1$.

Example 8.2.2

Evaluate the integral of the following polynomial using the Gauss quadrature.

$$f(\xi) = 5 + 3\xi + 2\xi^2 - \xi^3 - 4\xi^4 \qquad -1 \le \xi \le 1 \qquad (1)$$

Solution: The exact value of the integral is

$$\int_{-1}^{1} f(\xi)\,d\xi = \int_{-1}^{1} (5 + 3\xi + 2\xi^2 - \xi^3 - 4\xi^4)\,d\xi = \left[5\xi + \frac{3\xi^2}{2} + \frac{2\xi^3}{3} - \frac{\xi^4}{4} - \frac{4\xi^5}{5}\right]_{-1}^{1} = \frac{146}{15} \qquad (2)$$

We expect to obtain the exact value of the integral when the number of Gauss points is $N = [(p + 1)/2] = (4 + 1)/2 = 2.5 \rightarrow 3$. First we evaluate $f(\xi)$ at various Gauss points [$f(0) = 5$] (see Fig. 8.2.5):

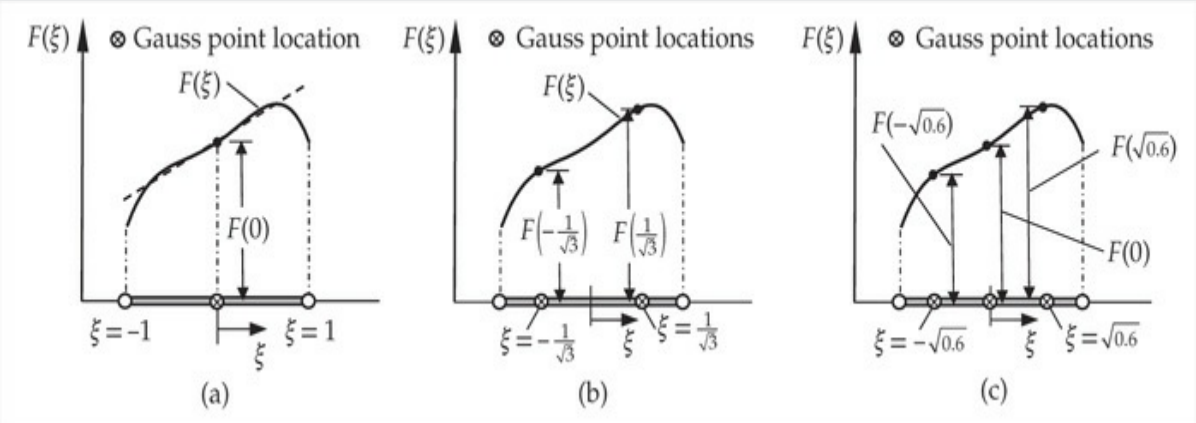

Fig. 8.2.5 One-, two-, and three-point Gauss quadrature.

$$
\begin{aligned}
f\left(-1/\sqrt{3}\right) &= 5 + 3\left(-1/\sqrt{3}\right) + 2\left(-1/\sqrt{3}\right)^2 - \left(-1/\sqrt{3}\right)^3 - 4\left(-1/\sqrt{3}\right)^4 \\
&= \frac{17}{3} - \frac{4}{9} - \frac{8}{3\sqrt{3}} \\
f\left(1/\sqrt{3}\right) &= 5 + 3\left(1/\sqrt{3}\right) + 2\left(1/\sqrt{3}\right)^2 - \left(1/\sqrt{3}\right)^3 - 4\left(1/\sqrt{3}\right)^4 \\
&= \frac{17}{3} - \frac{4}{9} + \frac{8}{3\sqrt{3}} \\
f\left(-\sqrt{3/5}\right) &= 5 + 3\left(-\sqrt{3/5}\right) + 2\left(-\sqrt{3/5}\right)^2 - \left(-\sqrt{3/5}\right)^3 - 4\left(-\sqrt{3/5}\right)^4 \\
&= \frac{155}{25} - \frac{36}{25} - 12\sqrt{\frac{3}{5}} \\
f\left(\sqrt{3/5}\right) &= 5 + 3\left(\sqrt{3/5}\right) + 2\left(\sqrt{3/5}\right)^2 - \left(\sqrt{3/5}\right)^3 - 4\left(\sqrt{3/5}\right)^4 \\
&= \frac{31}{5} - \frac{36}{25} + 12\sqrt{\frac{3}{5}}
\end{aligned} \tag{3}
$$

Using the one-point Gauss rule [$\xi_1 = 0.0$, $w_1 = 2$, and $f(\xi_1) = 5$], we obtain:

$$
\int_{-1}^{1} f(x)\,dx = f(\xi_1)w_1 = 10 \quad (2.74\% \text{ error}) \tag{4}
$$

The two-point Gauss rule
$[\xi_1 = -1/\sqrt{3}, w_1 = 1, \xi_2 = 1/\sqrt{3}, w_2 = 1, f(\xi_1) = (47/9) - 8/3\sqrt{3},$ and $f(\xi_2) = (47/9) + 8/3\sqrt{3}]$ gives

$$
\int_{-1}^{1} f(\xi)\,d\xi = f(\xi_1)w_1 + f(\xi_2)w_2 = \frac{94}{9} \quad (7.31\% \text{ error}) \tag{5}
$$

The three-point Gauss rule
$(\xi_1 = -\sqrt{0.6}, w_1 = 5/9, \xi_2 = 0.0, w_2 = 8/9, \xi_3 = \sqrt{0.6},$ and $w_3 = 5/9)$ gives the exact result:

$$
\begin{aligned}
\int_{-1}^{1} f(\xi)\,d\xi &= f(\xi_1)w_1 + f(\xi_2)w_2 + f(\xi_3)w_3 \\
&= \left(\frac{119}{25} - 12\sqrt{\frac{3}{5}}\right)\frac{5}{9} + 5 \times \frac{8}{9} + \left(\frac{119}{25} + 12\sqrt{\frac{3}{5}}\right)\frac{5}{9} = \frac{146}{15}
\end{aligned} \tag{6}
$$

In finite element formulations, we encounter integrals whose integrands F are functions of the global coordinate x and ψ_i^e (which are derived in terms of ξ) and derivatives of ψ_i^e with respect to x. For the Gauss–Legendre quadrature, we must transform $F(x)dx$ to $\hat{F}(\xi)\,d\xi$ in order to use the formula in Eq. (8.2.21). For example, consider the integral

$$K_{ij}^e = \int_{x_a^e}^{x_b^e} a(x)\frac{d\psi_i^e}{dx}\frac{d\psi_j^e}{dx}\,dx \tag{8.2.24}$$

Using the chain rule of differentiation, we have

$$\frac{d\psi_i^e(\xi)}{dx} = \frac{d\psi_i^e(\xi)}{d\xi}\frac{d\xi}{dx} = J^{-1}\frac{d\psi_i^e(\xi)}{d\xi} \tag{8.2.25}$$

Therefore, the integral in Eq. (8.2.24) can be written, with the help of Eq. (8.2.11), as

$$K_{ij}^e = \int_{-1}^{1} a(x(\xi))\frac{1}{J}\frac{d\psi_i^e}{d\xi}\frac{1}{J}\frac{d\psi_j^e}{d\xi}\,J\,d\xi \approx \sum_{I=1}^{r}\hat{F}_{ij}^e(\xi_I)w_I \tag{8.2.26}$$

where

$$\hat{F}_{ij}^e = a\frac{1}{J}\frac{d\psi_i^e}{d\xi}\frac{d\psi_j^e}{d\xi}, \quad J = \sum_{i=1}^{m} x_i^e\frac{d\hat{\psi}_i^e}{d\xi} \tag{8.2.27}$$

For the isoparametric formulation, we take $\psi_i^e = \hat{\psi}_i^e$. As noted earlier, the Jacobian matrix will be the same $(J_e = \frac{1}{2}h_e)$ when the element is a straight line with equally spaced nodes, even if the coordinate transformation is quadratic or cubic. However, when the element is curved, the Jacobian is a function of ξ for transformations other than linear. The transformation from x to ξ is not required in the Newton–Cotes quadrature.

It is possible to determine the exact number of Gauss points required to evaluate the following element coefficients over straight-line intervals (i.e., J is a constant), for different variations of the coefficients $a(x)$, $c(x)$, and $f(x)$ when linear, quadratic, and cubic interpolation functions are used:

$$K_{ij}^e = \int_{x_a^e}^{x_b^e} a(x) \frac{d\psi_i^e}{dx} \frac{d\psi_j^e}{dx} dx$$

$$= \int_{-1}^{+1} a(x(\xi)) \frac{d\psi_i^e}{d\xi} \frac{d\psi_j^e}{d\xi} (J)^{-2} J \, d\xi \equiv \sum_{I=1}^{N^K} G_{ij}^K(\xi_I) W_I \tag{8.2.28a}$$

$$f_i^e = \int_{x_a}^{x_b} f(x) \psi_i^e \, dx = \int_{-1}^{+1} f(x(\xi)) \psi_i^e(\xi) J \, d\xi \equiv \sum_{I=1}^{N^F} G_i^F(\xi_I) W_I \tag{8.2.28b}$$

$$M_{ij}^e = \int_{x_a}^{x_b} c(x) \psi_i^e \psi_j^e \, dx$$

$$= \int_{-1}^{+1} c(x(\xi)) \psi_i^e(\xi) \psi_j^e(\xi) J \, d\xi \equiv \sum_{I=1}^{N^M} G_{ij}^M(\xi_I) W_I \tag{8.2.28c}$$

For constant values of $a(x)$, $f(x)$, and $c(x)$, the integrands of K_{ij}^e, f_i^e, and M_{ij}^e are of the polynomial degree $p_K = 2(p - 1)$, $p_F = p$, and $p_M = 2p$, respectively, where p is polynomial degree of the interpolation functions, $\psi_i^e(x)$ ($p = 1$ for linear, $p = 2$ for quadratic, and $p = 3$ for cubic).

The number of Gauss points required to evaluate K_{ij}^e, f_i^e, and M_{ij}^e exactly for different polynomial expansions of $a(x)$, $f(x)$, and $c(x)$ are presented in Table 8.2.3, where p_a, p_f, and p_c denote the polynomial degrees of the coefficients $a(x)$, $f(x)$, and $c(x)$, respectively. In estimating the number of Gauss points, the Jacobian J is assumed to be a constant, which holds true when the element is a straight line. We note that $p_K = 2(p - 1) + p_a$, $p_F = p + p_f$, and $p_M = 2p + p_c$. In summary, for a cubic variation of $a(x)$, quadratic variation of $f(x)$, and linear variation of $c(x)$ (i.e., $p_a = 3$, $p_f = 2$, and $p_c = 1$), all three coefficients K_{ij}^e, f_i^e, and M_{ij}^e are evaluated exactly by using two-point, three-point, and four-point Gauss rules for linear, quadratic, and cubic elements, respectively.

Table 8.2.3 The number of Gauss quadrature points (N^K, N^F, N^M) required to evaluate K_{ij}^e, f_i^e, and M_{ij}^e of Eqs. (8.2.28a)–(8.2.28c) exactly for various elements with different polynomial variations of $a(x)$, $f(x)$, and $c(x)$.

Element type	N^K p_a				N^F p_f				N^M p_c			
	0	1	2	3	0	1	2	3	0	1	2	3
Linear	1	1	2	**2**	1	2	**2**	3	2	**2**	3	3
Quadratic	2	2	3	**3**	2	2	**3**	3	3	**3**	4	4
Cubic	3	3	4	**4**	2	3	**3**	4	4	**4**	5	5

8.3 Computer Implementation

8.3.1 Introductory Comments

The purpose of this section is to discuss the basic steps involved in the development of a finite element computer program for the solution of the model second- and fourth-order one-dimensional differential equations studied in the preceding chapters. The ideas presented here are used in the development of the model program **FEM1D**, and they are meant to be illustrative of the steps used in a typical finite element analysis (after the weak form is developed). One can make use of the ideas presented here and modify **FEM1D** to develop a program of one's own. Importance is given here to finite element computations, and no attempt is made to discuss Gauss elimination procedure used to solve the resulting system of algebraic equations (a solver is provided with **FEM1D**).

8.3.2 General Outline

A typical finite element program consists of three basic units (see Fig. 8.3.1):

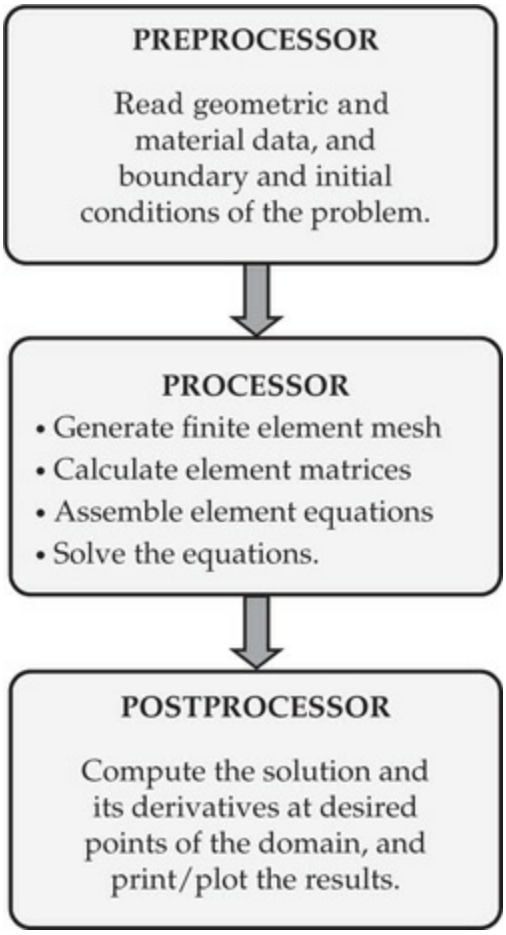

Fig. 8.3.1 The three main functional units of a finite element program.

1. Preprocessor
2. Processor
3. Postprocessor

In the preprocessor part of the program, the input data of the problem are read in and/or generated. This includes the geometry (e.g., length of the domain and boundary conditions), the data of the problem (e.g., coefficients in the differential equation), finite element mesh information (e.g., element type, number of elements, element length, coordinates of the nodes, and connectivity matrix), and indicators for various options (e.g., print, no print, type of field problem analyzed, static analysis, eigenvalue analysis, transient analysis, and degree of interpolation).

In the processor part, all steps of the finite element analysis discussed in the preceding chapters, except for postprocessing, are performed. The major steps of the processor are:

1. Generation of the element matrices using numerical integration.

2. Assembly of element equations.
3. Imposition of the boundary conditions.
4. Solution of the algebraic equations for the nodal values of the primary variables.

In the postprocessor part of the program, the solution is computed at points other than nodes by interpolation and the secondary variables are computed using their definitions. The preprocessors and postprocessors can be a few Fortran statements to read and print pertinent information to complex subroutines to generate meshes of complex geometric shapes and sophisticated graphical presentation of the input and output information.

A flowchart of the computer program **FEM1D** is presented in Fig. 8.3.2. The objective of each of the main subroutines listed in the flowchart is described below.

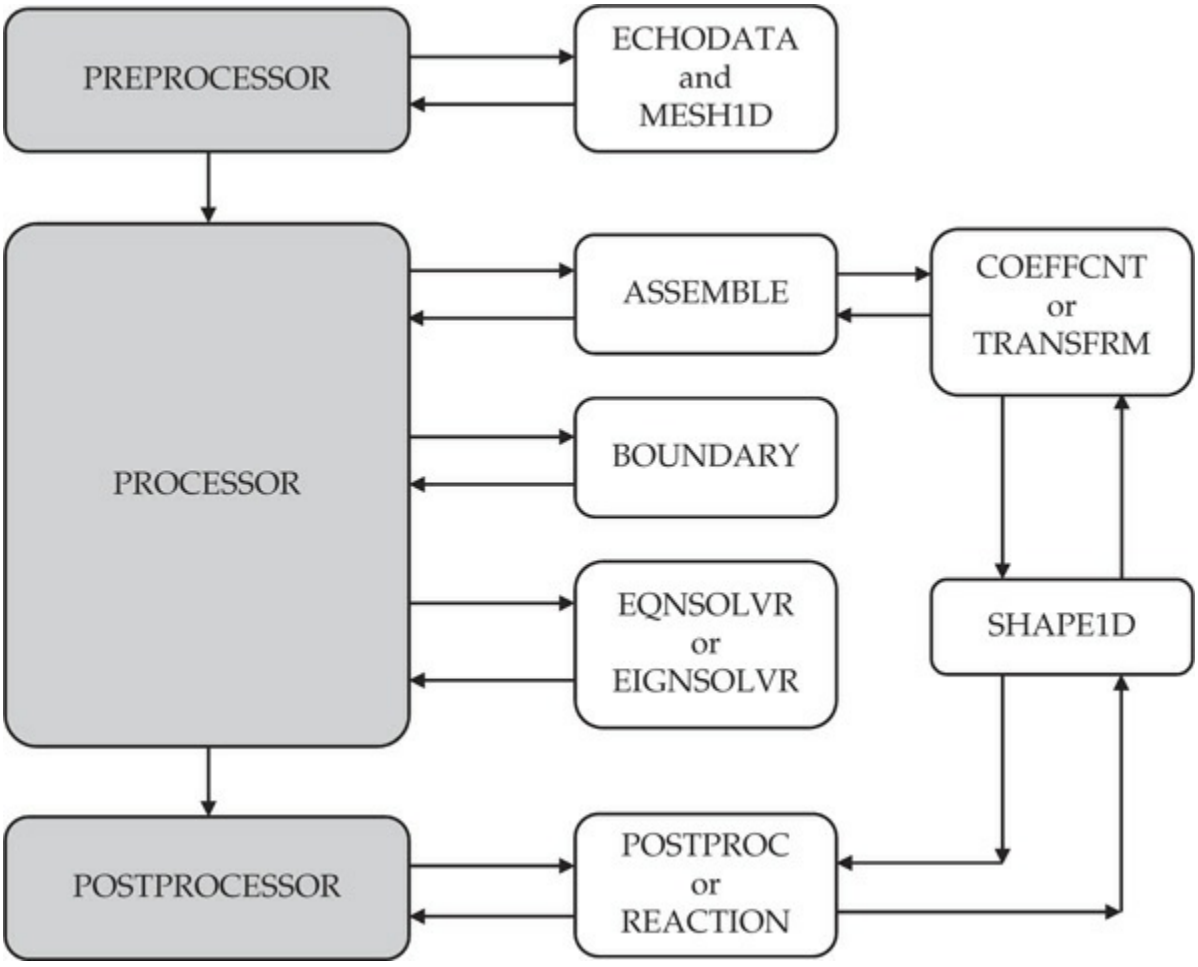

Fig. 8.3.2 Flowchart of the computer program **FEM1D**.

- **ASSEMBLE:** This subroutine is used for the assembly of element equations. The equations are assembled in upper-banded form for

static and transient problems, and in full matrix form for eigenvalue problems.

- **BOUNDARY:** The subroutine is for the imposition of specified boundary conditions. More discussion is presented in Section 8.3.6.
- **COEFFCNT:** The subroutine is dedicated to the computation of element matrices $\mathbf{K}^e$, $\mathbf{M}^e$, and $\mathbf{f}^e$ for all model problems, except for truss and frame elements.
- **ECHODATA:** The subroutine is written to echo the input to the program (so that the user knows what was input and to check if there was any error in the input data).
- **EIGNSLVR:** The subroutine written for the solution of eigenvalue problems, $\mathbf{AX} = \lambda\mathbf{BX}$.
- **EQNSOLVR:** The subroutine is developed for solving banded symmetric system of algebraic equations, $\mathbf{AX} = \mathbf{B}$.
- **MESH1D:** The subroutine is written to generate the finite element mesh (coordinates of the global nodes and the connectivity array).
- **POSTPROC:** The subroutine is written to postprocess the solution for all model problems except for truss and frame elements, that is, compute $\mathbf{u}^e$ and $\mathbf{Q}^e_{\text{def}}$ at various points in the element.
- **REACTION:** In this subroutine the element reaction forces are calculated for truss and frame elements, $\mathbf{Q}^e = \mathbf{K}e\,\mathbf{u}^e - \mathbf{f}$.
- **SHAPE1D**: The subroutine contains the approximation functions and their derivatives, that is arrays, **SF** and **DSF**.
- **TRANSFRM:** The Subroutine to compute element stiffness matrix and force vector for truss and frame elements: $\mathbf{K} = \mathbf{T}^{\mathrm{T}}\,\mathbf{KT}$, $\mathbf{F} = \mathbf{T}^{\mathrm{T}}\,\mathbf{F}$.

In the following sections, a discussion of the basic components of a typical finite element program is presented, and then the ideas are illustrated via FORTRAN statements.

8.3.3 Preprocessor

The preprocessor unit consists of reading input data and generating finite element mesh, and printing the data and mesh information. The input data to a finite element program consist of element type, IELEM (i.e., Lagrange element or Hermite element), number of elements in the mesh (NEM), specified boundary conditions on primary and secondary variables (number of boundary conditions, global node number and degree of

freedom, and specified values of the degrees of freedom), the global coordinates of global nodes, and element properties [e.g., coefficients $a(x)$, $b(x)$, $c(x)$, $f(x)$, etc.] If a uniform mesh is used, the length of the domain should be read in, and global coordinates of the nodes can be generated in the program.

The preprocessor portion that deals with the generation of finite element mesh information (when not supplied by the user) can be separated into a subroutine (**MESH1D**), depending on the convenience and complexity of the program. Mesh generation includes computation of the global coordinates X_I and the connectivity array NOD ($=B_{ij}$). Recall that the connectivity matrix describes the relationship between element nodes to global nodes:

$$\text{NOD}(n, j) = \textit{Global node number} \text{ corresponding to the } j\text{th (local) node of element } n$$

This array is used in the assembly procedure as well as to transfer information from element to the global system and vice versa. For example, to extract the vector ELX of global coordinates of element nodes from the vector GLX of global coordinates of global nodes, we can use the matrix NOD as follows. The global coordinate $x_i^{(n)}$ of the ith node of the nth element is the same as the global coordinate X_I of the global node I, where $I = \text{NOD}(n, i)$:

$$\{x_i^{(n)}\} = \{X_I\}, \quad I = \text{NOD}(n, i) \rightarrow \text{ELX}(i) = \text{GLX}(\text{NOD}(n, i)) \tag{8.3.1}$$

8.3.4 Calculation of Element Matrices (Processor)

The processor, where typically large amounts of computing time are spent, can consist of several subroutines, each having a special purpose (e.g., a subroutine for the calculation of element matrices, a subroutine for the imposition of boundary conditions, and a subroutine for the solution of equations). The degree of sophistication and the complexity of a finite element program depend on the general class of problems being programmed, the generality of the data in the equation, and the intended user of the program.

The most significant part of a processor is where we generate element matrices. The element matrices are computed in various subroutines (**COEFFCNT** and **TRANSFRM**), depending on the type of problem being solved. These subroutines typically involve numerical evaluations of

the element matrices $\mathbf{K}^e$ and $\mathbf{M}^e$ (the corresponding program variables are ELK and ELM) and the element vector $\mathbf{f}^e$ (program variable ELF) for various field problems. The Gauss quadrature described in Section 8.2.5 is used to evaluate element matrices and vectors, and the arrays are assembled as soon as they are computed. Thus, a loop on the number of elements in the mesh (NEM) is used to compute element matrices and assemble them (in subroutine **ASSEMBLE**). It is here that the connectivity array NOD plays a crucial role.

Element matrices for different model equations (MODEL) and type of problem (NTYPE) are generated by assigning values as discussed next. The variables used have the following meaning: H = thickness of the beam/plate; B = width of a beam; E = Young's modulus; $G = E/[2(1 + \nu)]$ = shear modulus; ν = Poisson's ratio; D = bending stiffness ($D = EI = EBH3/12$ for beams and $D = EH^3/[12(1 - \nu^2)]$) for plates; A = cross-sectional area; K_s = shear correction factor; and c_f foundation modulus.

1. **MODEL=0, NTYPE=0:** All problems that admit discrete elements (see Section 3.3; only static analysis).
2. **MODEL=1, NTYPE=0:** All field problems described by Eqs. (3.4.1) and (3.5.3) including radially symmetric heat-transfer-type problems described by Eq. (3.5.3); c_t takes different meaning for different problems:

$$c_1\frac{\partial u}{\partial t} + c_t\frac{\partial^2 u}{\partial t^2} - \frac{\partial}{\partial x}\left(a\frac{\partial u}{\partial x}\right) + cu - f = 0 \tag{8.3.2a}$$

$$c_1 = \rho c_v, \quad AX = a(x), \quad CX = c(x), \quad FX = f \tag{8.3.2b}$$

$$c_1\frac{\partial u}{\partial t} + c_t\frac{\partial^2 u}{\partial t^2} - \frac{1}{r}\frac{\partial}{\partial r}\left(ra\frac{\partial u}{\partial r}\right) + cu - f = 0 \tag{8.3.3a}$$

$$c_1 = \rho c_v, \quad AX = ra(r), \quad CX = rc(r), \quad FX = rf(r) \tag{8.3.3b}$$

3. **MODEL=1, NTYPE=1:** Radially symmetric deformation of polar orthotropic disks of thickness H (see **Problem 4.34**); a plane stress problem:

$$c_1\frac{\partial^2 u}{\partial t^2} - \frac{1}{r}\frac{\partial}{\partial r}\left[H\left(c_{11}r\frac{\partial u}{\partial r} + c_{12}u\right)\right] + \frac{H}{r}\left(c_{22}\frac{u}{r} + c_{12}\frac{\partial u}{\partial r}\right) = f \tag{8.3.4a}$$

$$c_1 = \rho H, \quad c_{11} = \frac{E_1}{1-\nu_{12}\nu_{21}}, \quad c_{12} = \frac{\nu_{12}E_2}{1-\nu_{12}\nu_{21}}, \quad c_{22} = \frac{E_2}{1-\nu_{12}\nu_{21}} \tag{8.3.4b}$$

where $f(r, t)$ is the distributed force per unit volume [i.e., $Hf(r) = \hat{f}$ is the distributed force per unit area]. For the isotropic case, we have $E_1 = E_2 = E$ and $\nu_{12} = \nu_{21} = \nu$.

4. **MODEL=1, NTYPE=2:** Radially symmetric deformation of cylinders (a plane strain problem):

$$c_1 \frac{\partial^2 u}{\partial t^2} - \frac{1}{r}\frac{\partial}{\partial r}\left\{c\left[(1-\nu)r\frac{\partial u}{\partial r} + \nu u\right]\right\} + \frac{c}{r}\left[(1-\nu)\frac{u}{r} + \nu\frac{\partial u}{\partial r}\right] = f \tag{8.3.5a}$$

$$c_1 = \rho, \quad c = \frac{E}{(1+\nu)(1-2\nu)} \tag{8.3.5b}$$

5. **MODEL=2, NTYPE=0 (RIE) or MODEL=2, NTYPE=2 (CIE):** Bending of straight beams using the Timoshenko beam theory ($\phi_x \rightarrow \Psi$):

$$c_1 \frac{\partial^2 w}{\partial t^2} - \frac{\partial}{\partial x}\left[GAK_s\left(\Psi + \frac{\partial w}{\partial x}\right)\right] + k_f w = q \tag{8.3.6a}$$

$$c_2 \frac{\partial^2 \Psi}{\partial t^2} - \frac{\partial}{\partial x}\left(EI\frac{\partial \Psi}{\partial x}\right) + GAK_s\left(\Psi + \frac{\partial w}{\partial x}\right) = 0 \tag{8.3.6b}$$

$$c_1 = \rho A, \quad c_2 = \rho I, \quad AX = GAK_s, \quad CX = k_f, \quad FX = q(x,t), \quad BX = EI \tag{8.3.6c}$$

6. **MODEL=2, NTYPE=1 (RIE) or MODEL=2, NTYPE=3 (CIE):** Axisymmetric bending of circular plates using the shear deformation plate theory:

$$c_1 \frac{\partial^2 w}{\partial t^2} - \frac{1}{r}\left[\frac{\partial}{\partial r}(rM_{rr}) - M_{\theta\theta}\right] + Q_r = 0 \tag{8.3.7a}$$

$$c_2 \frac{\partial^2 \Psi}{\partial t^2} - \frac{1}{r}\frac{\partial}{\partial r}(rQ_r) - q = 0 \tag{8.3.7b}$$

$$M_{rr} = D\left(\frac{\partial \Psi}{\partial r} + \nu\frac{\Psi}{r}\right), \quad M_{\theta\theta} = D\left(\nu\frac{\partial \Psi}{\partial r} + \frac{\Psi}{r}\right), \quad Q_r = K_s Gh\left(\Psi + \frac{\partial w}{\partial r}\right) \tag{8.3.7c}$$

7. **MODEL=3, NTYPE=0:** Bending of straight beams using the Euler–Bernoulli beam theory:

$$c_1\frac{\partial^2 w}{\partial t^2} - c_2\frac{\partial}{\partial x}\frac{\partial^3 w}{\partial x \partial t^2} + \frac{\partial^2}{\partial x^2}\left(EI\frac{\partial^2 w}{\partial x^2}\right) + k_f w = q, \tag{8.3.8a}$$

$$c_1 = \rho A,\ \ c_2 = \rho I,\ \ BX = EI,\ CX = k_f,\ FX = q \tag{8.3.8b}$$

8. **MODEL=3, NTYPE=1:** Axisymmetric bending of circular plates using the classical plate theory:

$$c_1\frac{\partial^2 w}{\partial t^2} - \frac{c_2}{r}\frac{\partial}{\partial r}\left(r\frac{\partial^3 w}{\partial r \partial t^2}\right) + \frac{D}{r}\frac{\partial}{\partial r}\left\{r\frac{\partial}{\partial r}\left[\frac{1}{r}\frac{\partial}{\partial r}\left(r\frac{\partial w}{\partial r}\right)\right]\right\} + c_f w = q \tag{8.3.9a}$$

$$c_1 = \rho H,\ \ c_2 = \frac{\rho H^3}{12},\ \ D = \frac{EH^3}{12} \tag{8.3.9b}$$

9. **MODEL=4, NTYPE=0:** Two-node truss element.
10. **MODEL=4, NTYPE=1:** Two-node Euler–Bernoulli frame element.
11. **MODEL=4, NTYPE=2:** Two-node Timoshenko frame element, RIE.
12. **MODEL=4, NTYPE=3:** Two-node Timoshenko frame element, CIE.

The element matrices are evaluated using the Gauss quadrature, except for MODEL=4, where the explicit forms of element coefficients are programmed in the interest of computational efficiency.

The element shape functions SF and their derivatives GDSF are evaluated at the Gauss points in subroutine **SHAPE1D**. The Gaussian weights and points associated with two-, three-, four-, and five-point integration rules are stored in arrays GAUSWT and GAUSPT, respectively. The *n*th column of GAUSWT, for example, contains the weights corresponding to the *n*-point Gauss quadrature rule:

GAUSPT (*i*, *n*) = *i*th Gauss point corresponding to the *n*-point Gauss rule

If the same number of Gauss points is used to evaluate all of the element coefficients (i.e., a single do-loop on Gauss quadrature is used to evaluate K_{ij}^e, f_i^e, and M_{ij}^e), the number of Gauss points is obviously dictated by the polynomial degree of the integrand of M_{ij}^e. The variable NGP is used to denote the number of Gauss points. If IELEM is the element type,

$$\text{IELEM} = \begin{cases} 1, & \text{linear} \\ 2, & \text{quadratic} \\ 3, & \text{cubic} \end{cases} \quad \text{(Lagrange elements)}$$

then NGP = IELEM+1 would evaluate K_{ij}^e, M_{ij}^e, and f_i^e [see Eqs. (8.2.28a)–(8.2.28c)] exactly when $c(x)$ is linear, $f(x)$ is quadratic, and $a(x)$ is cubic polynomial (see Table 8.2.3).

The Hermite cubic element is identified with IELEM = 0. The coefficients

$$\int_{x_a^e}^{x_b^e} c(x)\phi_i\phi_j\,dx$$

are evaluated exactly with NGP = 4, when $c(x)$ is at most linear in x. With NGP = 4, the coefficients

$$\int_{x_a^e}^{x_b^e} b(x)\frac{d^2\phi_i}{dx^2}\frac{d^2\phi_j}{dx^2}\,dx$$

are evaluated exactly when $b(x)$ is a polynomial of degree 5 or less!

The coefficients $a(x)$ = AX, $b(x)$ = BX, and $c(x)$ = CX, together with $f(x)$ = FX in the differential equation (8.1.1) are assumed to vary with x as follows (so that the NGP selected in the aforementioned paragraph is sufficient):

AX=AX0+AX1*X+AX2*X*X+AX3*X*X*X, $(a = a_0 + a_1x + a_2x^2 + a_3x^3)$

BX=BX0+BX1*X+BX2*X*X+BX3*X*X*X, $(b = b_0 + b_1x + b_2x^2 + b_3x^3)$

CX=CX0+CX1*X, $(c = c_0 + c_1x)$

CT=CT0, $(c_1 = c_0)$ other than beams

CT0 and CT1, $(c_1 = CT0,\ c_2 = CT1)$ for beams

FX=FX0+FX1*X+FX2*X*X, $(f = f_0 + f_1x + f_2x^2)$

For radially symmetric elasticity problems, (AX0, AX1) for circular discs and (BX0, BX1) for circular plates are used to input Young's modulus E and Poisson's ratio v; other coefficients are read as zeros.

The Gauss quadrature formula in Eq. (8.2.21) can be implemented in a computer as follows. Consider K_{ij}^e of the form

$$K_{ij}^e = \int_{x_a}^{x_b} \left[a(x) \frac{d\psi_i^e}{dx} \frac{d\psi_j^e}{dx} + c(x) \psi_i^e \psi_j^e \right] dx \tag{8.3.10}$$

We use the following program variables for the quantities in Eq. (8.3.10):

$$\text{ELK(I,J)} = K_{ij}^e, \quad \text{SF(I)} = \psi_i^e, \quad \text{GDSF(I)} = \frac{d\psi_i^e}{dx}$$

$$\text{AX} = a(x), \quad \text{CX} = c(x), \quad \text{ELX(I)} = x_i^e$$

$$\text{NPE} = n, \quad \text{the number of nodes in the element}$$

After transforming x to ξ

$$x = \sum_{i=1}^{n} x_i^e \psi_i^e(\xi) \tag{8.3.11}$$

the coefficients K_{ij}^e in Eq. (8.3.10) can be written as

$$K_{ij}^e = \int_{-1}^{1} \left[a(\xi) \frac{1}{J} \frac{d\psi_i^e}{d\xi} \frac{1}{J} \frac{d\psi_j^e}{d\xi} + c(\xi) \psi_i^e \psi_j^e \right] J \, d\xi \equiv \int_{-1}^{1} F_{ij}^e(\xi) J \, d\xi$$

$$= \sum_{I=1}^{\text{NGP}} F_{ij}^e(\xi_I) J W_I \tag{8.3.12}$$

where F_{ij}^e denotes the expression in the square brackets in Eq. (8.3.12), J is the Jacobian, and ξ_I and W_I are the Ith Gauss point and Gauss weight, respectively.

Examination of Eq. (8.3.12) shows that there are three indices: i, j, and I. We take the Gauss-point loop on I as the outermost one. Inside this loop, we evaluate F_{ij}^e at the Gauss point ξ_I for each i and j, multiply with the Jacobian $J = \frac{1}{2} h_e$ and the weights W_I, and sum over the range of I:

$$\text{ELK}(i,j) = \text{ELK}(i,j) + F_{ij}^e(\xi_I) J W_I \tag{8.3.13}$$

Since $\mathbf{K}^e$, $\mathbf{M}^e$, $\mathbf{f}^e$ are evaluated for e = 1, 2, …, NEM, where NEM denotes the number of elements in the mesh, we must initialize all arrays that are being evaluated using the Gauss quadrature. The initialization must be made outside of the Gauss quadrature loop.

The computation of coefficients K_{ij}^e in Eq. (8.3.12) requires evaluation

of a, c, ψ_i, and $d\psi_i/d\xi$ at the Gauss point ξ_I. Hence, inside the loop on I, we call subroutine **SHAPE1D** to evaluate ψ_i, $d\psi_i/dx = (d\psi_i/d\xi)/J$ at the Gauss points. Fortran statements to evaluate $\mathbf{K}^e$ and $\mathbf{f}^e$ are given in Box 8.3.1.

In the same way, all other coefficients (e.g., M_{ij}^e and f_i^e) can be evaluated. Recall that the element properties (i.e., K_{ij}^e, M_{ij}^e, and f_i^e) are calculated by calling a suitable subroutine (**COEFFCNT** or **TRANSFRM**) for the field problem being analyzed within a loop on number of elements in the mesh (NEM).

8.3.5 Assembly of Element Equations (Processor)

The assembly of element equations should be carried out as soon as the element matrices are computed, rather than waiting till element coefficients of all elements are computed. The latter requires storage of the element coefficients of all elements. In the former case, we can perform the assembly in the same loop in which a subroutine is called to calculate element matrices.

A feature of the finite element equations that enables us to save storage and computing time is the assembly of element matrices in upper-banded form. When element matrices are symmetric, the resulting global (or assembled) matrix is also symmetric, with many zeros away from the main diagonal.

Box 8.3.1: Fortran statements to compute element matrices.

```
C
C     DO-LOOP on number of Gauss points begins here
C
          DO 100 NI=1,NGP
          XI = GAUSPT(NI,NGP)
C
C  Call subroutine SHAPE1D to evaluate interpolation functions
C       and their global derivatives at the Gauss point XI
C
          CALL SHAPE1D(H,IELEM,NPE,XI)
          CONST = GJ*GAUSWT(NI,NGP)
          DO 30 J=1,NPE
   30          X = X + SF(J)*ELX(J)
C
C  Compute coefficient matrices for MODEL = 1 and NTYPE = 0
C
          CX=CX0+CX1*X
          FX=FX0+FX1*X+FX2*X*X
          AX=AX0+AX1*X+AX2*X*X+AX3*X*X*X
          DO 50 J = 1, NPE
             ELF(J) = ELF(J) + CONST*SF(J)*FX
             DO 50 I = 1,NPE
                AIJ = CONST*GDSF(I)*GDSF(J)
                CIJ = CONST*SF(I)*SF(J)
   50           ELK(I,J)=ELK(I,J) + AX*AIJ + CX*CIJ
  100        CONTINUE
```

Therefore, it is sufficient to store only the upper *half-band* of the assembled matrix. The half bandwidth of a matrix is defined as follows. Let N_i be the number of matrix elements between the diagonal element and the last nonzero element in the ith row, after which all elements in that row are zero; the half-bandwidth is the maximum of $(N_i + 1)$

$$b_I = \max_{1 \le i \le n} (N_i + 1)$$

where n is the number of rows in the matrix (or equations in the problem). General-purpose equation solvers are available for such banded systems of equations.

The half-bandwidth NHBW of the assembled (i.e., global) finite element matrix can be determined in the finite element program itself. The local nature of the finite element interpolation functions (i.e., ψ_i^e are defined to be nonzero only over the element Ω^e) is responsible for the

banded character of the assembled matrix. If two global nodes do not belong to the same element then the corresponding entries in the global matrix are zeros:

$$K_{IJ} = 0, \quad \text{if global nodes } I \text{ and } J \text{ do not correspond to local nodes of the same element}$$

This property enables us to determine the half-bandwidth (NHBW) of the assembled matrix:

$$\text{NHBW} = \max_{\substack{1 \le N \le \text{NEM} \\ 1 \le I,\, J, \le \text{NPE}}} \{\text{abs}[\text{NOD}(N,\, I) - \text{NOD}(N,\, J)] + 1\} \times \text{NDF} \qquad (8.3.14a)$$

where

$$\begin{aligned} \text{NEM} &= \underline{\text{N}}\text{umber of } \underline{\text{E}}\text{lements in the } \underline{\text{M}}\text{esh} \\ \text{NPE} &= \underline{\text{N}}\text{umber of nodes } \underline{\text{P}}\text{er } \underline{\text{E}}\text{lement} \\ \text{NDF} &= \underline{\text{N}}\text{umber of } \underline{\text{D}}\text{egrees of } \underline{\text{F}}\text{reedom per element} \end{aligned} \qquad (8.3.14b)$$

For example, for one-dimensional problems with elements connected in series and global nodes numbered sequentially, the maximum difference between nodes of an element is equal to NPE − 1. Hence,

$$\text{NHBW} = [(\text{NPE} - 1) + 1] \times \text{NDF} = \text{NPE} \times \text{NDF} \qquad (8.3.15)$$

Of course, NHBW is always less than or equal to the number of primary degrees of freedom in the mesh (i.e., the Number of EQuations in the mesh, NEQ).

The logic for assembling the element matrices K_{ij}^{e} into the upper-banded form of the global coefficients K_{ij} is that the assembly can be skipped whenever $J < I$ and $J >$NHBW. The main diagonal, $I = J$, of the assembled square matrix (i.e., full storage form) becomes the first column of the assembled banded matrix (i.e., banded storage form), as shown in Fig. 8.3.3. The upper diagonals (parallel to the main diagonal) take the position of respective columns in the banded matrix. Thus, the banded matrix has the dimension NEQ × NHBW.

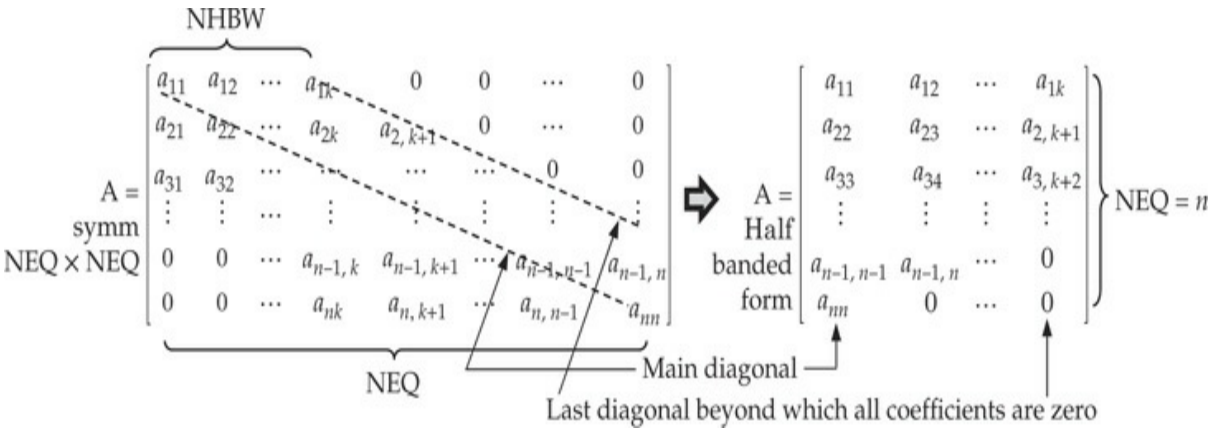

Fig. 8.3.3 Finite element coefficient matrix storage in upper-half-banded form.

The element coefficients K_{ij}^e and f_i^e of a typical element Ω^e are to be assembled into the global coefficients matrix **K** and source vector **F**, respectively. If the *i*th node of the element is equal to the *I*th global node, and the *j*th node of the element is equal to the *J*th global node, we have

$$K_{IJ} = K_{IJ} + K_{ij}^e, \quad F_I = F_I + F_i^e \quad \text{(for NDF=1)} \tag{8.3.16a}$$

The values of *I* and *J* can be obtained with the help of array NOD:

$$I = \text{NOD}(e, i), \quad J = \text{NOD}(e, j) \tag{8.3.16b}$$

where *e* is the element number. Recall that it is possible that the same *I* and *J* may correspond to a pair of *i* and *j* of some other element Ω^m. In that case, K_{ij}^m will be added to existing coefficients K_{IJ} during the assembly. For NDF>1, the logic still holds, with the change

$$K_{(\text{NR})(\text{NC})} = K^e_{((i-1)*NDF+p)((j-1)*NDF+q)} \quad (p, q = 1, 2, \ldots, \text{NDF}) \tag{8.3.17a}$$

where

$$\text{NR} = (I-1) \times \text{NDF} + p, \quad \text{NC} = (J-1) \times \text{NDF} + q \tag{8.3.17b}$$

and *I* and *J* are related to *i* and *j* by Eq. (8.3.16b). These ideas are implemented in subroutine **ASSEMBLE**.

8.3.6 Imposition of Boundary Conditions (Processor)

Imposition of boundary conditions on the primary and secondary global degrees of freedom can be carried out through a subroutine

(**BOUNDARY**), which remains unchanged for two-dimensional or three-dimensional problems. There are three types of boundary conditions for any problem:

1. Essential boundary conditions, that is, boundary conditions on primary variables (Dirichlet boundary conditions).
2. Natural boundary conditions, that is, boundary conditions on secondary variables (Neumann boundary conditions).
3. Mixed (or Newton) boundary conditions (i.e., boundary conditions that relate the primary and secondary variables at a node).

The imposition of these three types of boundary conditions in a computational scheme is discussed next.

8.3.6.1 Specified primary variables

The procedure for implementing the boundary conditions on the primary variables involves modifying the assembled coefficient matrix (GLK) and right-hand-column vector (GLF) by three operations:

1. Moving the known products in each row to the right-hand side.
2. Replacing the columns and rows of GLK corresponding to the known primary variable by zeros, and setting the coefficient on the main diagonal to unity.
3. Replacing the corresponding component of the right-hand column by the specified value of the variable.

To illustrate the procedure, we consider the following N algebraic equations in full matrix form:

$$\begin{bmatrix} K_{11} & K_{12} & K_{13} & \cdots & K_{1N} \\ K_{21} & K_{22} & K_{23} & \cdots & K_{2N} \\ K_{31} & K_{32} & K_{33} & \cdots & K_{3N} \\ \cdots & \cdots & \cdots & \cdots & \cdots \\ K_{N1} & K_{N2} & K_{N3} & \cdots & K_{NN} \end{bmatrix} \begin{Bmatrix} U_1 \\ U_2 \\ U_3 \\ \vdots \\ U_N \end{Bmatrix} = \begin{Bmatrix} F_1 \\ F_2 \\ F_3 \\ \vdots \\ F_N \end{Bmatrix} + \begin{Bmatrix} Q_1 \\ Q_2 \\ Q_3 \\ \vdots \\ Q_N \end{Bmatrix}$$

where U_I are the global primary variables, F_I are the global source values due to the source term (f or q) in the governing equation, Q_I are the global secondary variables[1], and K_{IJ} are the assembled coefficients. Suppose that $U_P = \hat{U}_P$ is specified (note that the corresponding secondary degree of

freedom Q is unknown). Set $KPP = 1$ and $F_P = \hat{U}_P$; further, set $K_{PI} = K_{IP} = 0$ for $I = 1, 2, \ldots, N$ for $I \neq P$ (after modifying the right-hand side). In particular, for $P = 2$, the modified equations are

$$\begin{bmatrix} K_{11} & 0 & K_{13} & K_{14} & \cdots & K_{1N} \\ 0 & 1 & 0 & 0 & \cdots & 0 \\ K_{31} & 0 & K_{33} & K_{34} & \cdots & K_{3n} \\ \vdots & \vdots & \vdots & \vdots & & \vdots \\ K_{n1} & 0 & K_{n3} & K_{n4} & \cdots & K_{nn} \end{bmatrix} \begin{Bmatrix} U_1 \\ U_2 \\ U_3 \\ \vdots \\ U_n \end{Bmatrix} = \begin{Bmatrix} \hat{F}_1 \\ \hat{U}_2 \\ \hat{F}_3 \\ \vdots \\ \hat{F}_n \end{Bmatrix}$$

where

$$\hat{F}_I = F_I - K_{I2}\hat{U}_2 \quad (I = 1, 3, 4, 5, \ldots, N;\ I \neq 2)$$

Thus, in general, if $U_P = \hat{U}_P$ is known, we have

$$K_{PP} = 1, \quad F_P = \hat{U}_P; \quad \hat{F}_I = F_I - K_{IP}\hat{U}_P; \quad K_{PI} = K_{IP} = 0, \quad I \neq P$$

for $I = 1, 2, \ldots, P - 1, P + 1, \ldots, N$ ($I \neq P$). This procedure is repeated for every specified primary degree of freedom. It enables us to retain the original order of the matrix (including its symmetry, if any), and the specified boundary conditions on the primary degrees of freedom are printed as part of the global solution vector. Of course, this logic should be implemented for a banded system of equations.

8.3.6.2 Specified secondary variables

The specified secondary degrees of freedom in the Ith equation are implemented directly by adding their specified value of the source Q_I to the value F_I due to the distributed source. Suppose that the specified point source corresponding to the Ith global equation is $\hat{Q}_I$. Then

$$F_I \leftarrow \hat{Q}_I + F_I \quad \text{(i.e., replace } F_I \text{ with } \hat{Q}_I + F_I\text{)}$$

where F_I is the contribution due to the distributed source (F_I is computed as a part of the element computations and is assembled).

8.3.6.3 Mixed boundary conditions

Mixed-type boundary conditions for Model 1, for example, are of the form

$$a\frac{du}{dx} + \beta(u - \bar{u}) = 0 \quad (\beta \text{ and } \bar{u} \text{ are given parameters}) \tag{8.3.18}$$

which contains both the primary variable u and the secondary variable $a\,du/dx$. Thus $a\,du/dx$ in the Ith global equation is replaced by $-\beta_I(U_I - \bar{U}_I)$:

$$Q_I = -\beta_I(U_I - \bar{U}_I)$$

This amounts to modifying the diagonal element K_{II} by adding β_I to its existing value,

$$K_{II} \leftarrow K_{II} + \beta_I$$

and adding $\beta_I\bar{U}_I$ to F_I,

$$F_I \leftarrow F_I + \beta_I\bar{U}_I \text{ (i.e., add } \beta_I\bar{U}_I \text{ to existing } F_I)$$

All three types of boundary conditions are implemented in subroutine **BOUNDARY** for boundary, initial, and eigenvalue problems. The following variables are used in the **BOUNDARY** subroutine:

NSPV	Number of Specified Primary Variables
NSSV	Number of Specified Secondary Variables
NNBC	Number of Newton Boundary Conditions
VSPV	Column of the Values of Specified Primary Variables, $\hat{\mathbf{U}}$
VSSV	Column of the Values of the Specified Secondary Variables, $\hat{\mathbf{F}}$
VNBC	Column of the specified Values of the Newton Boundary Conditions, $\boldsymbol{\beta}$
UREF	Column of the reference values, $\bar{\mathbf{U}}$
ISPV	Array of the global node, ISPV(I,1), and local degree of freedom, ISPV(I,2), that is specified

Similar definitions are used for ISSV and INBC arrays.

8.3.7 Solution of Equations and Postprocessing

Subroutine **EQNSOLVR** is used to solve a banded system of equations, and the solution vector is returned in array GLF (which is the global right-hand-side vector going into the subroutine **EQNSOLVR**). The program

performs the Gaussian elimination and back-substitution to compute the solution. For a discussion of the Gaussian elimination used to solve a set of linear algebraic equations, the reader is referred to the book by Carnahan, Luther, and Wilkes [1].

Postprocessing involves computation of the solution and its gradient at preselected points of the domain. The preselected points are the end points of the element, the midpoint, and three evenly spaced points between the end points and the midpoint. One can choose other points (e.g., the Gauss points). Subroutine **POSTPROC** is used to evaluate the solution and its derivatives at a preselected point x_0 of an element:

$$u^e(x_0) = \sum_{j=1}^{n} u_j^e \psi_j^e(x_0), \quad \left(\frac{du^e}{dx}\right)\Big|_{x_0} = \sum_{j=1}^{n} u_j^e \left(\frac{d\psi_j^e}{dx}\right)\Big|_{x_0} \tag{8.3.19}$$

for a Lagrange element and

$$w^e(x_0) = \sum_{j=1}^{4} u_j^e \phi_j^e(x_0), \quad \left(\frac{d^m w^e}{dx^m}\right)\Big|_{x_0} = \sum_{j=1}^{4} u_j^e \left(\frac{d^m \phi_j^e}{dx^m}\right)\Big|_{x_0} \quad (m = 1, 2, 3) \tag{8.3.20}$$

for a Hermite cubic element. The second- and third-order derivatives in the case of the Hermite cubic elements are needed to compute the bending moment and shear forces. The nodal values u_j^e of the element Ω_e are deduced from the global nodal values *UI* as follows:

$$u_j^e = U_I, \quad I = \text{NOD}(e, j), \quad \text{when NDF} = 1 \tag{8.3.21a}$$

For NDF > 1, *I* is given by *I* = [NOD(*e*, *j*) − 1]× NDF and

$$u^e_{(j-1)*NDF+p} = U_{I+p} \quad (p = 1, 2, \ldots, \text{NDF}) \tag{8.3.21b}$$

The values computed using the derivatives of the solution are often inaccurate because the derivatives of the approximate solution become increasingly inaccurate with increasing order of differentiation. For example, the shear force post-computed in the Euler–Bernoulli beam theory from the definition

$$V(x_0) = \frac{d}{dx}\left(EI\frac{d^2 w}{dx^2}\right)\Big|_{x_0} = \sum_{j=1}^{n} u_j^e \left[\frac{d}{dx}\left(EI\frac{d^2 \phi_j^e}{dx^2}\right)\right]_{x_0} \tag{8.3.22}$$

will be in considerable error, in addition to being discontinuous across the elements. The accuracy increases, rather slowly, with mesh refinement and higher-order elements. The physical variables computed using Eq. (8.3.22) are more accurate if they are computed at the Gauss points. When accurate values of the secondary variables are desired at the nodes, it is recommended that they be computed from the element equations:

$$Q_i^e = \sum_{j=1}^{n} K_{ij}^e u_j^e - f_i^e \quad (i = 1, 2, \ldots, n) \tag{8.3.23}$$

However, this requires re-computation or saving of element coefficients K_{ij}^e and f_i^e. Recall that the nodal values of generalized forces are exact at the nodes when computed using Eq. (8.3.23).

8.4 Applications of Program FEM1D

8.4.1 General Comments

The computer program **FEM1D**, which embodies the ideas presented in the previous section is intended to illustrate the use of the finite element models developed in Chapters 3–7 to a variety of one-dimensional field problems; some of them are not discussed in detail in this book but listed as part of the model equations. The program **FEM1D** is developed as a learning finite element program for students of a first course on the finite element method (see the website **https://mechanics.tamu.edu** for the source and executable versions of the program). In the interest of simplicity and ease of understanding, only the model equations discussed in this book and their immediate extensions are included in the program. The program can be modified to extend and made efficient for personal use (thousands of students and researchers have already done so since the first edition appeared in 1984).

Table 8.4.1 contains a summary of the definitions of coefficients of various model problems and their corresponding program variables. The table can be used as a ready reference to select proper values of AX0, AX1, and so on for different problems [higher-order terms for $a(x)$ and $b(x)$ are not included in the table]. The variable NTHER is also read to ascertain if the temperature effect is considered (NTHER = 0, no; NTHER ≠ 0, yes) (see Table 8.4.2). The discrete elements can be used with

MODEL = 0 and NTYPE = 0.

Table 8.4.1 Meaning of the program variables for various model problems.

Field problem	MODEL CX0	NTYPE CX1	ITEM† FX0	AX0 FX1	AX1 FX2	BX0 CT0‡	BX1 CT1‡
1. Plane wall	1 0	0 0	1 f_0	k_0 f_1	k_1 f_2	0 ρ_0	0 ρ_1
2. Heat flow in a fin	1 $(\rho c_v)_1$	0 $(\rho c_v)_2$	1 f_0	$(kA)_0$ f_1	$(kA)_1$ f_2	0 ρ_0	0 ρ_1
3. Radially symmetric heat transfer	1 0	0 0	1 f_1	0 f_2	k_1 0	0 ρ_1	0 0
4. Viscous flow through channels	1 0	0 0	1 f_0	μ_0 f_1	μ_1 f_2	0 ρ_0	0 ρ_1
5. Viscous flow through pipes	1 0	0 0	1 f_1	0 f_2	μ_1 0	0 ρ_1	0
6. Unidirectional seepage	1 0	0 0	1 f_0	μ_0 f_1	μ_1 f_2	0 ρ_0	0 ρ_1
7. Radially symmetric seepage (groundwater flow)	1 0	0 0	1 f_1	0 f_2	μ_1 0	0 ρ_1	0 0

8. Axial deformation of a bar	1 $(\rho A)_1$	0 $(\rho A)_2$	2 f_0	$(AE)_0$ f_1	$(AE)_1$ f_2	0 $(\rho A)_0$	0 0
9. Radially symmetric deformation of a disk	1 $(\rho H)_1$	1 $(\rho H)_2$	2 f_0	E_1 f_1	E_2 f_2	ν_{12} $(\rho A)_0$	H 0
10. Radially symmetric deformation of a cylinder	1 $(\rho)_1$	2 $(\rho)_2$	2 f_0	E_1 f_1	E_2 f_2	ν_{12} $(\rho A)_0$	H 0
11. Euler–Bernoulli beam theory	3 ρA	0 ρI	2 f_0	0 f_1	0 f_2	$(EI)_0$ ρA	$(EI)_1$ ρI
12. Euler–Bernoulli theory for circular plates	3 $(\rho H)_1$	1 $(\rho H)_2$	2 f_0	E_1 f_1	E_2 f_2	ν_{12} ρH	H $\rho H^3/12$
13. Timoshenko beam theory (RIE)*	2 $(\rho A)_1$	0 $(\rho A)_2$	2 f_0	$(SK)_0$ f_1	$(SK)_1$ f_2	$(EI)_0$ ρA	$(EI)_1$ ρI
14. Timoshenko beam theory (CIE)*	2 $(\rho A)_1$	2 $(\rho A)_2$	2 f_0	$(SK)_0$ f_1	$(SK)_1$ f_2	$(EI)_0$ ρA	$(EI)_1$ ρI
15. Timoshenko theory of circular plates (RIE)	2 c_0	1 c_1	2 f_0	E_1 f_1	E_2 K_sG_{13}	ν_{12} ρH	H $\rho H^3/12$
16. Timoshenko theory of circular plates (CIE)	2 c_0	3 c_1	2 f_0	E_1 f_1	E_2 K_sG_{13}	ν_{12} ρH	H $\rho H^3/12$
17. Plane truss[1]	4	0	0	0	0	0	0
18. The Euler–Bernoulli frame element	4	1	0	0	0	0	0
19. The Timoshenko RIE frame element	4	2	0	0	0	0	0
20. The Timoshenko CIE frame element	4	3	0	0	0	0	0

†For time-dependent problems only; when steady-state solution is required, set ITEM = 0.
‡For transient analysis only; transient analysis option is not available in FEM1D for truss and frame problems.
*$S = GA$ and K_s is the shear correction factor ($K_s = 5/6$).
[1]For field problems 17–19, the remaining parameters (CX0, CX1, FX0, FX1, FX2, CT0, CT1) are not read; A = SA, L = SL, and so on are read for each member of the structure: SE = modulus E, SA = cross-sectional area A, SI = moment of inertia I, CN = $\cos\alpha$, SN = $\sin\alpha$, and so on (see Table 8.4.2).

8.4.2 Illustrative Examples

Here we revisit some of the example problems considered earlier to illustrate the use of **FEM1D** in their solution. Only certain key observations concerning the input data are made, but complete listings of input files for each problem are given. In the interest of brevity, the complete output files for most problems are not included.

A description of the input variables to program **FEM1D** is presented in Table 8.4.2. In Table 8.4.2, "skip" means that the input data is omitted (i.e., no data is required). In the "free format" used here, variables of each "data line" (we shall use this terminology to imply an input sequence in a single instruction) are read from the same line; if the values are not found on the same line, the computer will look for them on the next line(s). However, data read in different data lines cannot be put on single line; each data card must start with a new line. The space available after typing required data on a given line may be used to include any comments. For example, one may list the variable names on that line for ready reference but only after all of the required data are listed. When the data input is incomplete or the format is wrong (e.g., a real number is encountered in place of an integer), the computer may return partial output file. In some cases, depending on the Fortran compiler used, a message like "end of unit 5" (means not enough input data is provided) may appear on the screen.

Table 8.4.2 Description of the input variables to the program **FEM1D**.

- **Input 1:** *TITLE* (Title of the problem being solved – one line only)
- **Input 2:** *MODEL NTYPE ITEM NTHER*

MODEL and NTYPE refer to the model equation and type of analysis, as described below:
MODEL = 0, NTYPE = 0 A problem that can use the discrete elements
MODEL = 1, NTYPE = 0 A problem of model equation in Eqs. (7.2.1) or (7.2.2)
MODEL = 1, NTYPE = 1 A radially axisymmetric circular

disc (plane stress) problem
MODEL = 1, NTYPE > 1 A radially axisymmetric circular disc (plane strain) problem
MODEL = 2, NTYPE = 0 A Timoshenko beam (RIE) problem
MODEL = 2, NTYPE = 1 A Timoshenko circular plate (RIE) problem
MODEL = 2, NTYPE = 2 A Timoshenko beam (CIE) problem
MODEL = 2, NTYPE > 2 A Timoshenko circular plate (CIE) problem
MODEL = 3, NTYPE = 0 An Euler–Bernoulli beam problem
MODEL = 3, NTYPE > 0 An Euler–Bernoulli circular plate problem
MODEL = 4, NTYPE = 0 A plane truss problem
MODEL = 4, NTYPE = 1 An Euler–Bernoulli frame problem
MODEL = 4, NTYPE = 2 A Timoshenko (RIE) frame problem
MODEL = 4, NTYPE = 3 A Timoshenko (CIE) frame problem

ITEM = Indicator for transient analysis:
ITEM = 0 Steady-state solution
ITEM = 1 Transient analysis of parabolic equations
ITEM = 2 Transient analysis of hyperbolic equations
ITEM = 3 Eigenvalue analysis
ITEM = 4 Buckling analysis
NTHER = Indicator for including thermal effects

- **Input 3:** *IELEM NEM*

IELEM is indicator of the type of finite element:

IELEM = 1 Linear Lagrange finite element
IELEM = 2 Quadratic Lagrange finite element
IELEM = 3 Hermite cubic finite element
NEM is the Number of Elements in the Mesh

- **Input 4:** *ICONT NPRNT*

ICONT is the indicator for continuity of data for the problem
ICONT = 1 Data (AX, BX, CX, FX and mesh) is continuous
ICONT = 0 Data is element dependent
NPRNT is the indicator for printing of element/global matrices
NPRNT = 0 Not to print element or global matrices but postprocess the solution and print
NPRNT = 1 Print element 1 coefficient matrices only but postprocess the solution and print
NPRNT = 2 Print element 1 and global matrices but not postprocess the solution
NPRNT > 2 Not to print element or global matrices and not postprocess the solution

Skip Inputs 5–17 for truss and frame problems (MODEL = 4), and read Inputs 5–17 only if MODEL > 0 and < 4.

- **Input 5:** *DX(I)* (Array of element lengths; DX(1) denotes the global coordinate of node 1 of the mesh; DX(I) (I = 2, NEM1) denotes the length of the (I – 1)st element, where NEM1 = NEM + 1 and NEM denotes the number of elements in the mesh)

Inputs 6–9 define the coefficients in the model equations. All coefficients are expressed in terms of global coordinate *x*. See Table 8.4.1 for the meaning of the coefficients.

- **Input 6:** *AX0 AX1 AX2 AX3* (coefficients of the constant,

linear, quadratic, and cubic terms of the polynomial $a(x) = a_0 + a_1 x + a_2 x^2 + a_3 x^3$)

- **Input 7:** *BX0 BX1 BX2 BX3* (coefficients of the constant, linear, quadratic, and cubic terms of the polynomial $b(x) = b_0 + b_1 x + b_2 x^2 + b_3 x^3$)

- **Input 8:** *CX0 CX1* (coefficients of the constant and linear terms of the polynomial $c(x) = c_0 + c_1 x$) Skip Input 9 for eigenvalue problems (i.e., when ITEM = 3)

- **Input 9:** *FX0 FX1 FX2* (coefficients of the constant, linear, and quadratic terms of the polynomial $f(x) = f_0 + f_1 x + f_2 x^2$)

Skip Input 10 if NTHER = 0.

- **Input 10:** *CTE TEMP* (coefficients of thermal expansion and temperature rise)

Skip Inputs 11–15 if data is continuous (ICONT ≠ 0). Inputs 11–15 are read for each element (i.e., NEM times). All coefficients are with respect to the local coordinate x.

- **Input 11:** *DCAX(I)* (coefficients of $a(x)$)
- **Input 12:** *DCBX(I)* (coefficients of $b(x)$)
- **Input 13:** *DCCX(I)* (coefficients of $c(x)$)
- **Input 14:** *DCFX(I)* (coefficients of $f(x)$)
- **Input 15:** *DCTE(I) DTEMP(I)* (when NTHER not zero)

Read Inputs 16 and 17 only for MODEL = 0 and NTYPE = 0 (discrete elements)

- **Input 16:** *NNM* (Number of global Nodes in the Mesh)

- **Input 17:** *ES(N)* (*NOD(N,I)*, I = 1,2) (ES(N) = Equivalent "stiffness" of element N; NOD(N,I) = global node number corresponding to the Ith node of element N (I = 1, NPE)

Read Inputs 18–21 only for frame problems (MODEL = 4 and NTYPE > 0)

- **Input 18:** *NNM* (number of nodes in the finite element mesh)

- **Input 19:** Read the following variables for each element:

PR – Poisson's ratio of the material (not used in EBT)
SE – Young's modulus of the material; *SL*–Length of the element
SA – Cross-sectional area of the element; *SI*–Moment of inertia of the element
CS – Cosine of the angle of orientation of the element
SN – Sine of the angle of orientation of the element; the angle is measured counterclockwise from the global *x*-axis

- **Input 20:** Read the following variables for each element:

HF – Intensity of the horizontal distributed force
VF – Intensity of the transversely distributed force
PF – Point load on the element
XB – Distance from node 1, along the length of the element, to the point of load application
CNT – Cosine of the angle of orientation of the load PF
SNT – Sine of the angle of orientation of the load PF; the angle is measured counterclockwise from the element *x*-axis.

- **Input 21:** *NOD* (connectivity of the element: NOD(N,I) = global node number corresponding to the Ith node of element N (I = 1,NPE)

Read Inputs 22 and 23 only for truss problems (MODEL = 4

and NTYPE = 0)

- **Input 22:** Read the following variables for each element:

SE – Young's modulus of the material; *SL* – Length of the element
SA – Cross-sectional area of the element
CS – Cosine of the angle of orientation of the element
SN – Sine of the angle of orientation of the element; the angle is measured counterclockwise from the *x*-axis
HF – Intensity of the horizontal distributed force

- **Input 23:** *NOD(N,I)* connectivity of the element:

NOD(N,I) = global node number corresponding to the Ith node of element N (I = 1,NPE)

- **Input 24:** *NCON* (number of inclined support conditions)

Skip Line 25 if no inclined support conditions are specified (NCON=0).

- **Input 25:** Read the following variables for I = 1 to NCON:

ICON(I) – Global node number of the support
VCON(I) – Angle (in degrees) between the normal and the global *x*-axis

- **Input 26:** *NSPV* (number of specified primary degrees of freedom (DOF)

Skip card 27 if no primary variable (PV) is specified (NSPV=0).

- **Input 27:** Read the following variables for I = 1 to NSPV:

ISPV(I,1) – Node number at which the PV is specified
ISPV(I,2) – Specified local primary DOF at the node
VSPV(I) – Specified value of the PV (will not be read for

eigenvalue problems)
Skip card 28 for eigenvalue problems (i.e., when ITEM = 3)

- **Input 28:** *NSSV* (number of specified *nonzero* secondary variables, SV)

Skip card 29 if no SV is specified (NSSV=0).

- **Input 29:** Read the following variables for I = 1 to NSSV:

ISSV(I,1) – Node number at which the SV is specified
ISSV(I,2) – Specified local secondary DOF at the node
VSSV(I) – Specified value of the SV

- **Input 30** *NNBC* (number of the Newton or mixed boundary conditions)

Skip Input 31 if no mixed boundary condition is specified (NNBC = 0). The mixed boundary condition is assumed to be of the form: SV + VNBC *(PV − UREF) = 0.

- **Input 31:** Read the following variables for I = 1 to NNBC

INBC(I,1) – Node number at which the mixed BC is specified
INBC(I,2) – Local DOF of the PV and SV at the node
VNBC(I) – Value of the coefficient of the PV in the BC
UREF(I) – Reference value of the PV

- **Input 32:** *NMPC* (number of multi-point constraints)

Skip Input 33 if no multi-point conditions are specified (i.e., NMPC = 0). The multi-point conditions are assumed to be of the form [see Eqs. (6.4.2a,b) and (6.4.7)]:
VMPC(· ,1)*PV1 + VMPC(· ,2)*PV2 = VMPC(· ,3)
VMPC(· ,2)*SV1 VMPC(· ,1)*SV2 = VMPC(· ,4)

- **Input 33:** Read the following variables for I = 1 to NMPC:

IMC1(I,1) – Node number associated with PV1
IMC1(I,2) – Local DOF of PV1
IMC2(I,1) – Node number associated with PV2
IMC2(I,2) – Local DOF of PV2
VMPC(·,I) – Values of the coefficients in the constraint equation
VMPC(·,4) – Value of the force applied at the node of PV1 or PV2

Skip Inputs 34 and 35 if ITEM = 0 (read only for time-dependent or eigenvalue problems)

- **Input 34:** *CT0* (for MODEL = 1)
- **Input 35:** *CT0 CT2* (for MODEL > 1; principal and rotary inertias)

Skip remaining inputs if steady-state or eigenvalue analysis is to be performed (ITEM = 0 or ITEM = 3)

- **Input 36:** *DT ALFA* (read only when ITEM = 1)
- **Input 37:** *DT ALFA GAMA* (read only when ITEM = 2)

DT, Time increment, which is assumed to be uniform
ALFA, Parameter in the time approximation scheme
GAMA, Parameter in the time approximation scheme

- **Input 38:** *INCOND* (indicator for initial conditions) *NTIME INTRVL*

INCOND = 0, Homogeneous (zero) initial conditions
INCOND > 0, Nonhomogeneous initial conditions
NTIME, Number of time steps for which solution is sought
INTRVL, Time step intervals at which solution is to be

printed

Skip Inputs 39 and 40 if initial conditions are zero (INCOND = 0)

- **Input 39:** *GUO(I)* (array of initial values of the primary variables)

Skip card 40 for parabolic equations (ITEM = 1).

- **Input 40:** *GU1(I)* (array of initial values of the first time derivatives of the primary variables)

In the remainder of this chapter we present a number of examples, mostly examples from Chapters 3 through 7, to illustrate the use of the program **FEM1D** in analyzing them.

Example 8.4.1

Consider the heat transfer problem of **Example 4.2.2**. The problem is governed by the equations

$$-\frac{d^2\theta}{dx^2} + m^2\theta = 0 \quad \text{for} \quad 0 < x < L; \quad \theta(0) = \theta_0, \quad \left(\frac{d\theta}{dx}\right)\Big|_{x=L} = 0 \tag{1}$$

where $\theta = T - T_\infty$ is the temperature above the reference temperature T_∞ and L, m^2, θ_0, β, and k are

$$\begin{aligned} &L = 0.05\ \text{m}, \quad m^2 = 400/\text{m}^2, \quad \theta_0 = 300°\text{C} \\ &\beta = 100\text{W}/(\text{m}^2\cdot°\text{C}), \quad k = 50\ \text{W}/(\text{m}\cdot°\text{C}) \end{aligned} \tag{2}$$

For this problem, we have MODEL = 1, NTYPE = 0, ITEM = 0 (for a steady-state solution), and NTHER = 0 (no temperature change). Since $a = 1.0$ and $c = m^2 = P\beta/Ak = 400$ are the same for all elements, we set ICONT = 1, AX0 = 1.0, and CX0 = 400. All other coefficients are zero [in addition to $b = 0$ and $q = 0$] for this problem. For a uniform mesh of four quadratic elements (NEM = 4, IELEM = 2), the increments of the array DX(I) [DX(1) is always the x-coordinate of node 1 (see Fig. 8.4.1) and $h = L/4 = 0.05/4 = 0.0125$] are: DX = {0.0, 0.0125, 0.0125, 0.0125, 0.0125}.

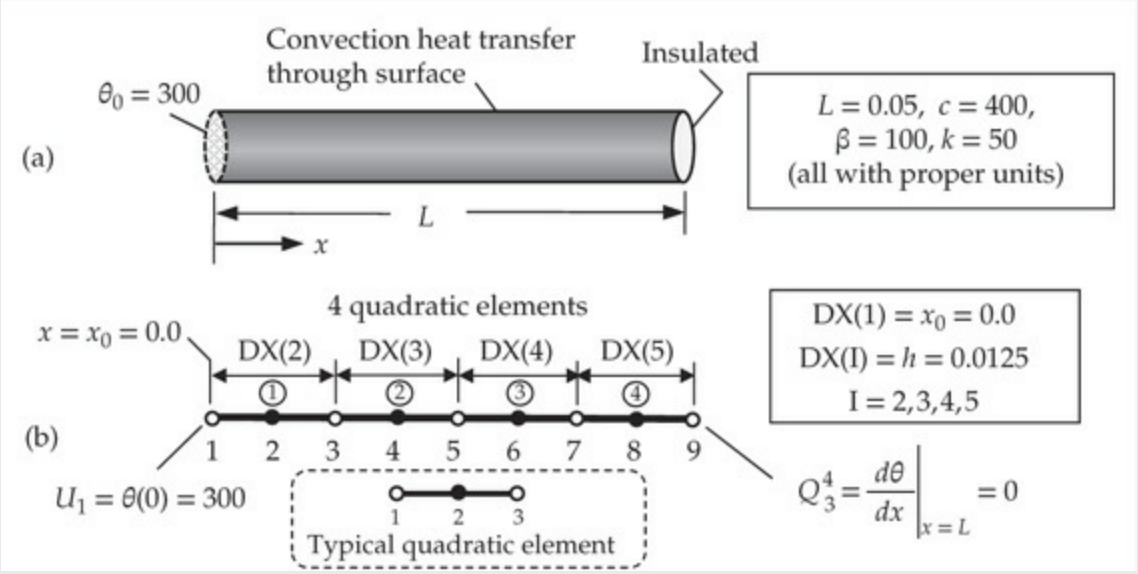

Fig. 8.4.1 Finite element mesh of a rectangular fin.

The boundary conditions of the problem reduce to $U_1 = 0$ and $Q_3^4 = 0$. There is one specified boundary condition (BC) on the primary variable (NSPV = 1), and the degree of freedom (DOF) (for heat transfer problems, there is only one degree of freedom) at node 1 is: ISPV(1,1) = 1 and ISPV(1,2) = 1. The specified value is VSPV(1) = 300. Since the natural boundary condition $(Q_3^4 = 0)$ is homogenous, there is no need to add a zero to the corresponding entry of the source vector (i.e., NSSV = 0). There are no mixed (i.e., convection) boundary conditions (NNBC = 0) or multi-point constraints (NMPC = 0) in this problem. The complete input data required to analyze the problem using **FEM1D** are presented in Box 8.4.1 and the edited output file is presented in Box 8.4.2.

Box 8.4.1: Input file from **FEM1D** for the problem in **Example 8.4.1**.

```
Example 4-2-2: Heat transfer in a rectangular fin (4Q)
  1  0  0  0                      MODEL, NTYPE, ITEM, NTHER
  2  4                            IELEM, NEM
  1  1                            ICONT, NPRNT
  0.0 0.0125 0.0125 0.0125 0.0125  DX(1)=X0; DX(2), etc.
  1.0  0.0  0.0  0.0               AX0, AX1, AX2, AX3
  0.0  0.0  0.0  0.0               BX0, BX1, BX2, BX3
 400.0      0.0                   CX0, CX1
  0.0   0.0  0.0                   FX0, FX1, FX2
  1                                NSPV
  1    1   300.0                  ISPV(1,1), ISPV(1,2), VSPV(1)
  0                                NSSV
  0                                NNBC
  0                                NMPC
```

Box 8.4.2: Edited output from **FEM1D** for the problem in **Example 8.4.1**.

```
SOLUTION (values of PVs) at the NODES:
     0.30000E+03    0.27371E+03    0.25171E+03    0.23364E+03
     0.21923E+03    0.20825E+03    0.20052E+03    0.19594E+03
     0.19442E+03
          x             PV (U)        SV (a*DU)
     0.00000E+00    0.30000E+03   -0.45487E+04
     0.25000E-01    0.21923E+03   -0.20133E+04
     0.25000E-01    0.21923E+03   -0.20179E+04
     0.50000E-01    0.19442E+03    0.20336E+01
```

Example 8.4.2

Here we consider the composite bar problem of **Example 4.4.2**. This is a problem with *discontinuous data* (ICONT = 0) because *EA* is discontinuous (as well as $h_1 \neq h_2$). The twoelement mesh of linear elements is shown in Fig. 8.4.2 and the input data and edited output for a mesh of two quadratic elements are given in Box 8.4.3.

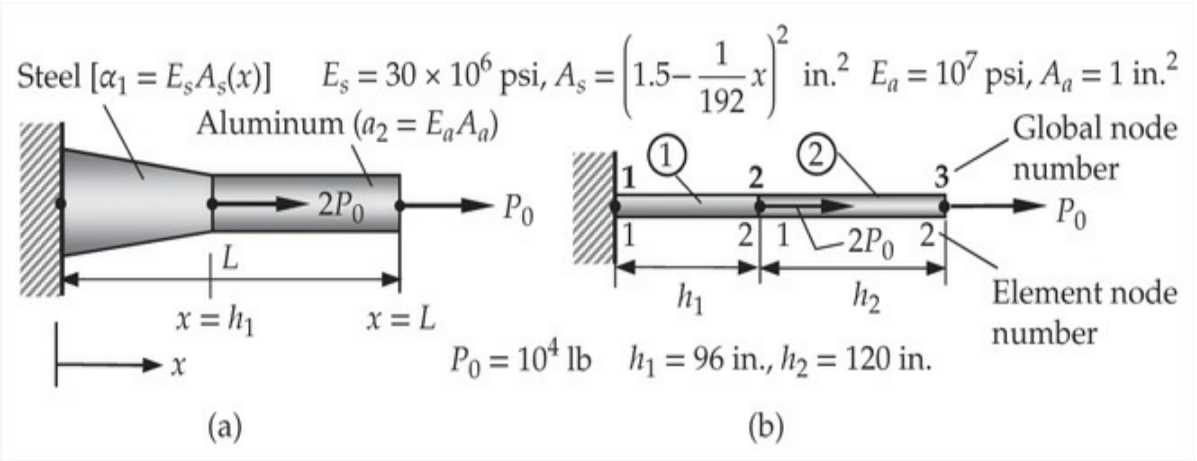

Fig. 8.4.2 Axial deformation of a composite bar. (a) Geometry and loading. (b) Finite element representation.

Box 8.4.3: Input and partial output using quadratic elements for **Example 8.4.2**.

```
Example 4-4-2: Axial deformation of a composite bar
  1  0  0  0                      MODEL, NTYPE, ITEM, NTHER
  2  2                            IELEM, NEM
  0  1                            ICONT, NPRNT
  0.0  96.0  120.0                DX(I)
67.5E6 -4687.5E2 8.138E2 0.0     AX0, AX1, AX2, AX3
  0.0  0.0  0.0  0.0              BX0, BX1, BX2, BX3
  0.0  0.0                        CX0, CX1
  0.0  0.0  0.0                   FX0, FX1, FX2
 10.E6 0.0  0.0  0.0              AX0, AX1, AX2, AX3
  0.0  0.0  0.0  0.0              BX0, BX1, BX2, BX3
  0.0  0.0                        CX0, CX1
  0.0  0.0  0.0                   FX0, FX1, FX2
  1                               NSPV
  1    1    0.0                   ISPV(1,1), ISPV(1,2), VSPV(1)
  2                               NSSV
  3    1    2.0E4                 ISPV(2,1), ISPV(2,2), VSPV(2)
  5    1    1.0E4                 ISPV(3,1), ISPV(3,2), VSPV(3)
  0                               NNBC
  0                               NMPC

SOLUTION (values of PVs) at the NODES:

     0.00000E+00    0.25717E-01    0.63917E-01    0.12392E+00
     0.18392E+00
          x            PV (U)        SV (a*DU)
     0.00000E+00    0.00000E+00    0.27386E+05
     0.96000E+02    0.63917E-01    0.10000E+05
     0.21600E+03    0.18392E+00    0.10000E+05
```

Example 8.4.3

We wish to determine the deformation and stresses in a rotating (at an angular velocity of ω) disk of radius R_0 and constant thickness H, and made of homogeneous and isotropic material (E, ν). The governing equation of the problem is (see **Problem 4.34**)

$$-\frac{1}{r}\frac{d}{dr}\left[c\left(r\frac{du}{dr}+\nu u\right)\right]+\frac{c}{r}\left(\frac{u}{r}+\nu\frac{du}{dr}\right)=\rho\omega^2 r,\quad 0<r<R_0 \tag{1}$$

$$c=\frac{E}{1-\nu^2} \tag{2}$$

For this case (plane stress), we have MODEL = 1, NTYPE = 1, ITEM =

0, and NTHER = 0. For a mesh of two quadratic elements (see Fig. 8.4.3; IELEM = 2 and NEM = 2), we use ICONT = 1 and

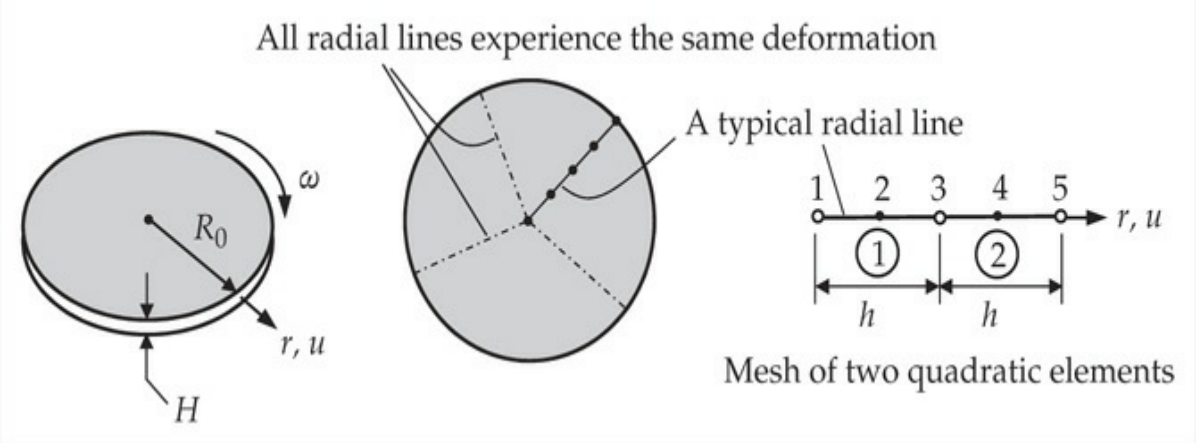

Fig. 8.4.3 The rotating disk of **Example 8.4.3**.

$$\{DX\} = \{0.0, 0.5R_0, 0.5R_0\}$$

where R_0 is the radius of the disk. Since we are seeking results in dimensionless form, we take (E_1 is the modulus along the radial direction and E_2 is the modulus in the circumferential direction)

$$R_0 = 1.0, \quad H = 1.0, \quad E_1 = E_2 = E = 1.0, \quad \nu_{12} = \nu = 0.3, \quad \rho\omega^2 = 1 \tag{3}$$

This information is supplied to the program through the following variables:

$$AX0(=E_1) = 1.0, \quad AX1(=E_2) = 1.0, \quad BX0(=\nu_{12}) = 0.3, \quad BX1(=H) = 1.0$$

$$CX0 = 0.0, \quad CX1 = 0.0, \quad FX0 = 0.0, \quad FX1 = 1.0, \quad FX2 = 0.0$$

The boundary conditions are

$$u(0) = 0 \text{ (by symmetry)}, \quad Q_1^1 = -(rH\sigma_r) = 0 \text{ at } r = R_0 \text{ (stress-free)} \tag{4}$$

Since the secondary variable is homogeneous, there is no need to include it in the data (NSSV=0). We have NSPV = 1 and NNBC = 0 with

$$ISPV(1,1) = 1, \quad ISPV(1,2) = 1, \quad VSPV(1) = 0.0$$

The input data and modified output for this problem are presented in Boxes 8.4.4 and 8.4.5, respectively.

Box 8.4.4: Input data for a mesh of two quadratic elements (**Example**

8.4.3).

```
Problem 4.34: Deformation of a rotating disk (dimensionless)
  1   1   0   0                MODEL, NTYPE, ITEM, NTHER
  2   2                        IELEM, NEM
  1   0                        ICONT, NPRNT
  0.0   0.5   0.5              DX(1)=X0; DX(2), DX(3)
  1.0   1.0   0.0   0.0        AX0, AX1, AX2, AX3
  0.3   1.0   0.0   0.0        BX0, BX1, BX2, BX3
  0.0   0.0                    CX0, CX1
  0.0   1.0   0.0              FX0, FX1, FX2
  1                            NSPV
  1     1     0.0              ISPV(1,1), ISPV(1,2), VSPV(1)
  0                            NSSV
  0                            NNBC
  0                            NMPC
```

Box 8.4.5: Output (typical from FEM1D) of the problem in **Example 8.4.3**.

```
- - - - - - - - - - - - - - - - - - - - - - - - - - - - - - - - - - - - - - - -

       OUTPUT from program   FEM1D   by J N REDDY

- - - - - - - - - - - - - - - - - - - - - - - - - - - - - - - - - - - - - - - -

Problem 4.34: Deformation of a rotating disk (dimensionless)

   *** ANALYSIS OF MODEL 1, AND TYPE 1 PROBLEM ***
             (see the code below)

   MODEL=0, NTYPE=0: A problem of discrete elements
   MODEL=1, NTYPE=0: A problem described by MODEL EQ. 1
   MODEL=1, NTYPE=1: A circular DISK (PLANE STRESS)
   MODEL=1, NTYPE>1: A circular DISK (PLANE STRAIN)
   MODEL=2, NTYPE=0: A Timoshenko BEAM (RIE) problem
   MODEL=2, NTYPE=1: A Timoshenko PLATE (RIE) problem
   MODEL=2, NTYPE=2: A Timoshenko BEAM (CIE) problem
   MODEL=2, NTYPE>2: A Timoshenko PLATE (CIE) problem
   MODEL=3, NTYPE=0: A Euler-Bernoulli BEAM problem
   MODEL=3, NTYPE>0: A Euler-Bernoulli Circular plate
   MODEL=4, NTYPE=0: A plane TRUSS problem
   MODEL=4, NTYPE=1: A Euler-Bernoulli FRAME problem
   MODEL=4, NTYPE=2: A Timoshenko (RIE) FRAME problem
   MODEL=4, NTYPE=3: A Timoshenko (CIE) FRAME problem

       Element type (1&2, Lagrange; 3, Hermite)=   2
       No. of deg. of freedom per node, NDF....=   1
       No. of elements in the mesh, NEM........=   2
       No. of total DOF in the model, NEQ......=   5
       Half bandwidth of matrix [GLK], NHBW ...=   3
       No. of specified primary DOF, NSPV......=   1
       No. of specified secondary DOF, NSSV....=   0
       No. of specified Newton B. C.: NNBC.....=   0
       No. of speci. multi-pt. cond.: NMPC.....=   0
```

```
  Boundary information on primary variables:

       1    1    0.00000E+00

  Global coordinates of the nodes, {GLX}:

     0.00000E+00    0.25000E+00    0.50000E+00    0.75000E+00
     0.10000E+01

  Coefficients of the differential equation:

   AX0 = 0.1000E+01  AX1 = 0.1000E+01  AX2 = 0.0000E+00  AX3 = 0.0000E+00
   BX0 = 0.3000E+00  BX1 = 0.1000E+01  BX2 = 0.0000E+00  BX3 = 0.0000E+00
   CX0 = 0.0000E+00  CX1 = 0.0000E+00
   FX0 = 0.0000E+00  FX1 = 0.1000E+01  FX2 = 0.0000E+00

SOLUTION (values of PVs) at the NODES:

     0.00000E+00    0.70706E-01    0.13004E+00    0.16875E+00
     0.17500E+00

           x        Displacement  Radial Stress   Hoop Stress
     0.00000E+00    0.00000E+00    0.30558E+00
     0.62500E-01    0.18743E-01    0.42216E+00    0.42654E+00
     0.12500E+00    0.36775E-01    0.40779E+00    0.41654E+00
     0.18750E+00    0.54096E-01    0.39341E+00    0.40654E+00
     0.25000E+00    0.70706E-01    0.37904E+00    0.39654E+00
     0.31250E+00    0.86606E-01    0.36466E+00    0.38654E+00
     0.37500E+00    0.10179E+00    0.35029E+00    0.37654E+00
     0.43750E+00    0.11627E+00    0.33591E+00    0.36654E+00
     0.50000E+00    0.13004E+00    0.32154E+00    0.35654E+00
     0.50000E+00    0.13004E+00    0.32727E+00    0.35826E+00
     0.56250E+00    0.14276E+00    0.28952E+00    0.34065E+00
     0.62500E+00    0.15345E+00    0.25111E+00    0.32086E+00
     0.68750E+00    0.16212E+00    0.21223E+00    0.29948E+00
     0.75000E+00    0.16875E+00    0.17299E+00    0.27690E+00
     0.81250E+00    0.17336E+00    0.13348E+00    0.25341E+00
     0.87500E+00    0.17593E+00    0.93750E-01    0.22919E+00
     0.93750E+00    0.17648E+00    0.53846E-01    0.20440E+00
     0.10000E+01    0.17500E+00    0.13802E-01    0.17914E+00
```

The exact displacement and stresses in the disc are given by

$$u(r) = \frac{(1-\nu)R_0^3}{8E}\left[(3+\nu)\frac{r}{R_0} - (1+\nu)\left(\frac{r}{R_0}\right)^3\right]\rho\omega^2$$

$$\sigma_{rr}(r) = \frac{(3+\nu)R_0^2}{8}\left[1 - \left(\frac{r}{R_0}\right)^3\right]\rho\omega^2 \tag{5}$$

$$\sigma_{\theta\theta}(r) = \frac{(3+\nu)R_0^2}{8}\left[1 - \frac{1+3\nu}{3+\nu}\left(\frac{r}{R_0}\right)^3\right]\rho\omega^2$$

The exact displacements at $x = 0.25$, $x = 0.5$, $x = 0.75$, and $x = 1.0$ are 0.0704, 0.1302, 0.1686, and 0.1750, respectively. The maximum values of stresses occur at $r = 0$ and they are $\sigma_{rr}(0) = \sigma_{\theta\theta}(0) = 0.4125$. The displacements obtained with two quadratic elements are in good agreement with the analytical solution. The post-computed stresses at $r = 0$ are not accurate because of the singularity there:

$$\sigma_{rr} = \frac{E}{1-\nu^2}\left(\frac{du}{dr} + \nu\frac{u}{r}\right), \quad \sigma_{\theta\theta} = \frac{E}{1-\nu^2}\left(\nu\frac{du}{dr} + \frac{u}{r}\right) \tag{6}$$

Example 8.4.4

Consider the cantilever beam problem of **Example 5.2.1** with $M_0 = 0$ (see Fig. 8.4.4). We wish to determine the solution using FEM1D. The input file and the modified output from FEM1D are presented in Box 8.4.6 and Box 8.4.7.

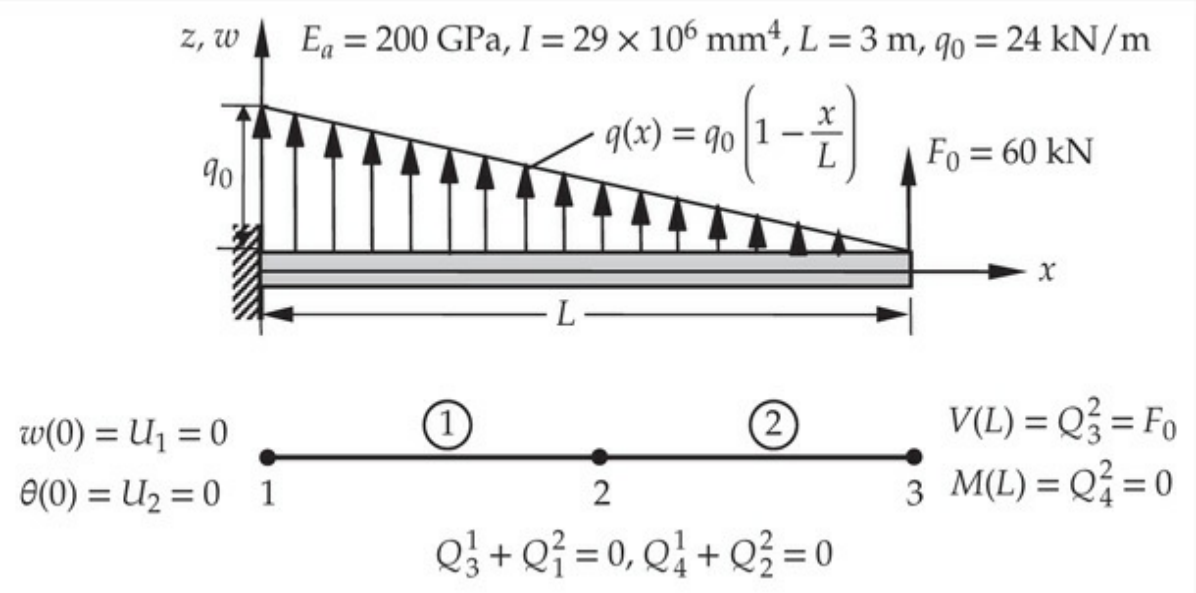

Fig. 8.4.4 The cantilever beam problem considered in **Example 8.4.4**.

Box 8.4.6: Input file for the cantilever beam problem of **Example 8.4.4**.

```
Example 5-2-1: Cantilever beam (linearly varying load, EBT)
  3   0   0   0                    MODEL, NTYPE, ITEM, NTHER
  3   2                            IELEM, NEM
  1   1                            ICONT, NPRNT
  0.0     1.5    1.5               DX(I)
  0.0     0.0    0.0   0.0         AX0, AX1, AX2, AX3
  5.8E6   0.0    0.0   0.0         BX0, BX1, BX2, BX3
  0.0     0.0                      CX0, CX1
 24.0E3 -8.0E3 0.0                 FX0, FX1, FX2
  2                                NSPV
  1   1    0.0                     ISPV(1,1), ISPV(1,2), VSPV(1)
  1   2    0.0                     ISPV(2,1), ISPV(2,2), VSPV(2)
  1                                NSSV
  3   1   60.0E3                   ISSV(2,1), ISSV(2,2), VSSV(2)
  0                                NNBC
  0                                NMPC
```

Box 8.4.7: Edited output for the cantilever beam problem of **Example 8.4.4**.

```
 Example 5-2-1: Cantilever beam (linearly varying load, EBT)
    *** ANALYSIS OF MODEL 3, AND TYPE 0 PROBLEM ***

         Element type (1&2, Lagrange; 3, Hermite)=   3
         No. of deg. of freedom per node, NDF....=   2
         No. of elements in the mesh, NEM........=   2
         No. of total DOF in the model, NEQ......=   6
         Half bandwidth of matrix [GLK], NHBW ...=   4
         No. of specified primary DOF, NSPV......=   2
         No. of specified secondary DOF, NSSV....=   1
         No. of specified Newton B. C.: NNBC.....=   0
         No. of speci. multi-pt. cond.: NMPC.....=   0

    Boundary information on primary variables:
          1    1    0.00000E+00
          1    2    0.00000E+00

    Boundary information on secondary variables:
          3    1    0.60000E+05

    Global coordinates of the nodes, {GLX}:
       0.00000E+00    0.15000E+01    0.30000E+01

    Coefficients of the differential equation:
AX0 = 0.0000E+00 AX1 = 0.0000E+00 AX2 = 0.0000E+00 AX3 =  0.0000E+00
BX0 = 0.5800E+07 BX1 = 0.0000E+00 BX2 = 0.0000E+00 BX3 =  0.0000E+00
CX0 = 0.0000E+00 CX1 = 0.0000E+00
FX0 = 0.2400E+05 FX1 = -0.8000E+04 FX2 = 0.0000E+00

 SOLUTION (values of PVs) at the NODES:
      0.00000E+00    0.00000E+00    0.33372E-01   -0.39278E-01
      0.10428E+00   -0.51207E-01

     x           Deflect.      Rotation      B. Moment      Shear Force
0.00000E+00   0.00000E+00   0.00000E+00   -0.21240E+06   0.80700E+05
0.18750E+00   0.62844E-03   -0.66218E-02  -0.19727E+06   0.80700E+05
0.37500E+00   0.24526E-02   -0.12754E-01  -0.18214E+06   0.80700E+05
0.56250E+00   0.53808E-02   -0.18398E-01  -0.16701E+06   0.80700E+05
0.75000E+00   0.93213E-02   -0.23552E-01  -0.15187E+06   0.80700E+05
0.93750E+00   0.14182E-01   -0.28217E-01  -0.13674E+06   0.80700E+05
0.11250E+01   0.19872E-01   -0.32393E-01  -0.12161E+06   0.80700E+05
0.13125E+01   0.26299E-01   -0.36080E-01  -0.10648E+06   0.80700E+05
0.15000E+01   0.33372E-01   -0.39278E-01  -0.91350E+05   0.80700E+05
0.15000E+01   0.33372E-01   -0.39278E-01  -0.93150E+05   0.62700E+05
0.16875E+01   0.41007E-01   -0.42099E-01  -0.81394E+05   0.62700E+05
0.18750E+01   0.49135E-01   -0.44541E-01  -0.69637E+05   0.62700E+05
0.20625E+01   0.57686E-01   -0.46602E-01  -0.57881E+05   0.62700E+05
0.22500E+01   0.66587E-01   -0.48283E-01  -0.46125E+05   0.62700E+05
0.24375E+01   0.75768E-01   -0.49584E-01  -0.34369E+05   0.62700E+05
0.26250E+01   0.85157E-01   -0.50505E-01  -0.22613E+05   0.62700E+05
0.28125E+01   0.94684E-01   -0.51046E-01  -0.10856E+05   0.62700E+05
0.30000E+01   0.10428E+00   -0.51207E-01   0.90000E+03   0.62700E+05
```

Example 8.4.5

Consider the beam problem with discontinuous data of **Example 5.2.3** (see Fig. 8.4.5). We wish to determine the solution using FEM1D. The input file and the modified output from FEM1D are presented in Box 8.4.8 and Box 8.4.9.

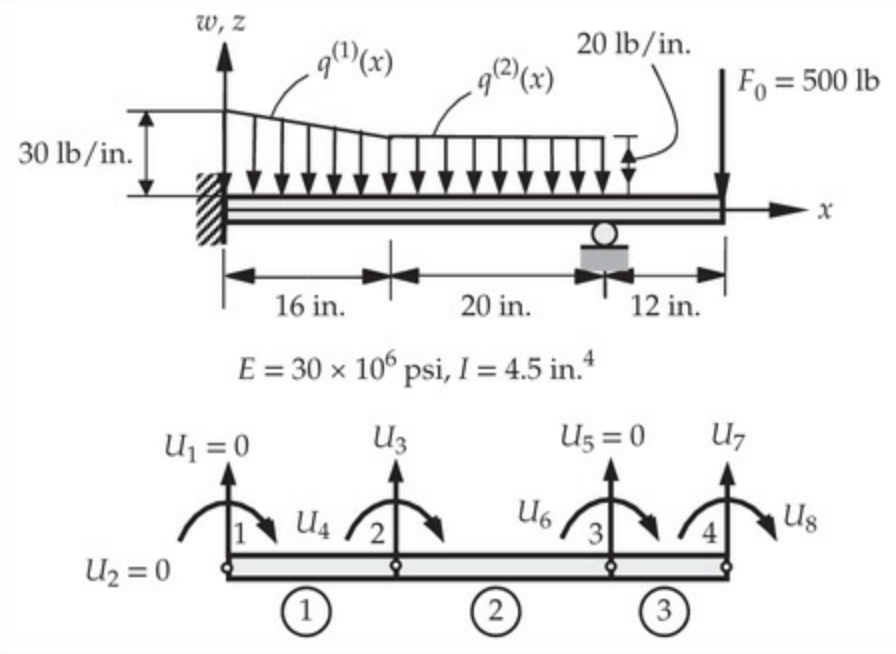

Fig. 8.4.5 Finite element modeling of an indeterminate beam (three elements).

Box 8.4.8: Input file for the beam problem of **Example 8.4.5**.

```
Example 5-2-3: A composite beam; varying transverse load (EBT)
    3   0   0   0                MODEL, NTYPE, ITEM, NTHER
    3   3                        IELEM, NEM
    0   1                        ICONT, NPRNT
   0.0   16.0   20.0 12.0        DX(I)

   0.0     0.0    0.0   0.0     AX0, AX1, AX2, AX3
 135.0E6   0.0    0.0   0.0     BX0, BX1, BX2, BX3
   0.0     0.0                  CX0, CX1
 -30.0     0.625  0.0           FX0, FX1, FX2

   0.0     0.0    0.0   0.0     AX0, AX1, AX2, AX3
 135.0E6   0.0    0.0   0.0     BX0, BX1, BX2, BX3
   0.0     0.0                  CX0, CX1
 -20.0     0.0    0.0           FX0, FX1, FX2

   0.0     0.0    0.0   0.0     AX0, AX1, AX2, AX3
 135.0E6   0.0    0.0   0.0     BX0, BX1, BX2, BX3
   0.0     0.0                  CX0, CX1
   0.0     0.0    0.0           FX0, FX1, FX2

    3                           NSPV
    1     1     0.0             ISPV(1,1), ISPV(1,2), VSPV(1)
    1     2     0.0             ISPV(2,1), ISPV(2,2), VSPV(2)
    3     1     0.0             ISPV(3,1), ISPV(3,2), VSPV(3)
    1                           NSSV
    4     1     -5.0E2          ISPV(1,1), ISPV(1,2), VSPV(1)
    0                           NNBC
    0                           NMPC
```

Box 8.4.9: Edited output file for the beam problem of **Example 8.4.5**.

```
Example 5-2-3: A composite beam; varying transverse load (EBT)
   *** ANALYSIS OF MODEL 3, AND TYPE 0 PROBLEM ***

        Element type (3, Hermite; 1&2, Lagrange)=   3
        No. of deg. of freedom per node, NDF....=   2
        No. of elements in the mesh, NEM........=   3
        No. of total DOF in the model, NEQ......=   8
        Half bandwidth of matrix [GLK], NHBW ...=   4
        No. of specified primary DOF, NSPV......=   3
        No. of specified secondary DOF, NSSV....=   1
        No. of specified Newton B. C.: NNBC.....=   0
        No. of speci. multi-pt. cond.: NMPC.....=   0

  Boundary information on primary variables:
        1    1    0.00000E+00
        1    2    0.00000E+00
        3    1    0.00000E+00

  Boundary information on secondary variables:
        4    1   -0.50000E+03

  Global coordinates of the nodes, {GLX}:
     0.00000E+00    0.16000E+02    0.36000E+02    0.48000E+02

 SOLUTION (values of PVs) at the NODES:
     0.00000E+00    0.00000E+00    0.32210E-03   -0.59352E-04
     0.00000E+00    0.25136E-03   -0.51497E-02    0.51803E-03
```

x	Deflect.	Rotation	B. Moment	Shear Force
0.00000E+00	0.00000E+00	0.00000E+00	-0.17580E+02	-0.60401E+02
0.40000E+01	0.58142E-05	-0.41002E-05	-0.25918E+03	-0.60401E+02
0.80000E+01	0.42346E-04	-0.15359E-04	-0.50078E+03	-0.60401E+02
0.10000E+02	0.81080E-04	-0.23673E-04	-0.62159E+03	-0.60401E+02
0.12000E+02	0.13823E-03	-0.33776E-04	-0.74239E+03	-0.60401E+02
0.14000E+02	0.21738E-03	-0.45669E-04	-0.86319E+03	-0.60401E+02
0.16000E+02	0.32210E-03	-0.59352E-04	-0.98399E+03	-0.60401E+02
0.16000E+02	0.32210E-03	-0.59352E-04	-0.11387E+04	0.32360E+03
0.18500E+02	0.49060E-03	-0.72948E-04	-0.32966E+03	0.32360E+03
0.21000E+02	0.67436E-03	-0.71562E-04	0.47934E+03	0.32360E+03
0.23500E+02	0.83592E-03	-0.55194E-04	0.12883E+04	0.32360E+03
0.26000E+02	0.93784E-03	-0.23845E-04	0.20973E+04	0.32360E+03
0.28500E+02	0.94266E-03	0.22485E-04	0.29063E+04	0.32360E+03
0.31000E+02	0.81293E-03	0.83797E-04	0.37153E+04	0.32360E+03
0.36000E+02	0.00000E+00	0.25136E-03	0.53333E+04	0.32360E+03
0.36000E+02	0.00000E+00	0.25136E-03	0.60000E+04	-0.50000E+03
0.37500E+02	-0.42496E-03	0.31386E-03	0.52500E+04	-0.50000E+03
0.39000E+02	-0.93743E-03	0.36803E-03	0.45000E+04	-0.50000E+03
0.42000E+02	-0.21749E-02	0.45136E-03	0.30000E+04	-0.50000E+03
0.45000E+02	-0.36123E-02	0.50136E-03	0.15000E+04	-0.50000E+03
0.48000E+02	-0.51497E-02	0.51803E-03	0.44924E-05	-0.50000E+03

The next example deals with the use of the Timoshenko beam finite elements to solve the cantilever beam problem of **Example 8.4.4**.

Example 8.4.6

Consider the cantilever beam of **Example 5.3.2** (see Fig. 8.4.4). We wish to determine the solution using four quadratic RIE (Timoshenko) beam elements. Unlike in **Example 5.3.2**, the results are presented in dimensional form (for $L/H = 100$). The input file and the modified output from FEM1D are presented in Box 8.4.10 and Box 8.4.11.

Box 8.4.10: Input file for the beam problem of **Example 8.4.6**.

```
Example 5-3-2: Cantilever beam with linearly varying load (RIE)
   2  0  0  0                    MODEL, NTYPE, ITEM, NTHER
   2  4                          IELEM, NEM
   1  0                          ICONT, NPRNT
 0.0 0.75 0.75 0.75 0.75  DX(I)
 2.57777778E10 0.0  0.0  0.0    AX0, AX1, AX2, AX3 (GAK=4EI/H^2)
 5.8E6  0.0    0.0  0.0         BX0, BX1, BX2, BX3  (EI)
 0.0    0.0                    CX0, CX1
24.0E3 -8.0E3  0.0              FX0, FX1, FX2
 2                              NSPV
 1  1   0.0                    ISPV(1,1), ISPV(1,2), VSPV(1)
 1  2   0.0                    ISPV(2,1), ISPV(2,2), VSPV(2)
 1                              NSSV
 9  1  60.0E3                   ISSV(1,1), ISSV(1,2), VSSV(1)
   0                            NNBC
   0                            NMPC
```

Box 8.4.11: Edited output file for the beam problem of **Example 8.4.6**.

```
Example 5-3-2: Cantilever beam with linearly varying load (RIE)
    *** ANALYSIS OF MODEL 2, AND TYPE 0 PROBLEM ***
 SOLUTION (values of PVs) at the NODES:
      0.00000E+00    0.00000E+00    0.24750E-02   -0.12838E-01
      0.93652E-02   -0.23549E-01    0.19897E-01   -0.32313E-01
      0.33377E-01   -0.39278E-01    0.49149E-01   -0.44570E-01
      0.66609E-01   -0.48279E-01    0.85173E-01   -0.50480E-01
      0.10429E+00   -0.51207E-01

     x          Deflect.      Rotation       B. Moment    Shear Force
0.00000E+00  0.00000E+00   0.00000E+00  -0.21502E+06   0.18377E+08
0.37500E+00  0.24750E-02  -0.12838E-01  -0.18211E+06  -0.90529E+07
0.75000E+00  0.93652E-02  -0.23549E-01  -0.14920E+06   0.18361E+08
0.75000E+00  0.93652E-02  -0.23549E-01  -0.14948E+06   0.15549E+08
0.11250E+01  0.19897E-01  -0.32313E-01  -0.12164E+06  -0.76601E+07
0.15000E+01  0.33377E-01  -0.39278E-01  -0.93797E+05   0.15537E+08
0.15000E+01  0.33377E-01  -0.39278E-01  -0.94078E+05   0.13662E+08
0.18750E+01  0.49149E-01  -0.44570E-01  -0.69609E+05  -0.67316E+07
0.20625E+01  0.57668E-01  -0.46622E-01  -0.57375E+05  -0.16357E+07
0.22500E+01  0.66609E-01  -0.48279E-01  -0.45141E+05   0.13656E+08
0.22500E+01  0.66609E-01  -0.48279E-01  -0.45422E+05   0.12718E+08
0.26250E+01  0.85173E-01  -0.50480E-01  -0.22641E+05  -0.62674E+07
0.28125E+01  0.94661E-01  -0.51027E-01  -0.11250E+05  -0.15218E+07
0.30000E+01  0.10429E+00  -0.51207E-01   0.14062E+03   0.12716E+08
```

Example 8.4.7

Consider the circular plate problem of **Example 5.4.1** with uniform load, $q(r) = q_0$. We wish to determine the solution using FEM1D. The input file and the modified output from FEM1D are presented in Box 8.4.12 and Box 8.4.13.

Box 8.4.12: Input file for the axisymmetric bending of circular plate.

```
Example 5-4-1: Axisym. bending of a SS circular plate (UDL, EBE)
    3   1   0   0                    MODEL, NTYPE, ITEM, NTHER
    3   4                            IELEM, NEM
    1   1                            ICONT, NPRNT
   0.0     2.5    2.5   2.5   2.5    DX(I)
  30.0E6  30.0E6  0.0   0.0          AX0,AX1,AX2,AX3 (AX0=E1,AX1=E2)
   0.29    0.1    0.0   0.0          BX0,BX1,BX2,BX3 (BX0=nu12,BX1=H)
   0.0     0.0                       CX0,CX1
   0.4     0.0    0.0                FX0,FX1,FX2
    2                                NSPV
    1     2     0.0                  ISPV(1,1),ISPV(1,2),VSPV(1)
    5     1     0.0                  ISPV(2,1),ISPV(2,2),VSPV(2)
    0                                NSSV
    0                                NNBC
    0                                NMPC
```

Box 8.4.13: Edited output file for the circular plate problem of **Example 8.4.7**.

```
 SOLUTION (values of PVs) at the NODES:
      0.93905E-01    0.00000E+00    0.86691E-01    0.56951E-02
      0.66132E-01    0.10534E-01    0.35447E-01    0.13655E-01
      0.00000E+00    0.14200E-01

     x       Deflect.      Rotation     Moment, Mr    Moment, Mt  Shear Force
0.00000E+0 0.93905E-01  0.00000E+00  0.00000E+00  0.00000E+00
0.62500E+0 0.93446E-01  0.14667E-02  0.51254E+01  0.51532E+01 -0.18750E+00
0.12500E+1 0.92078E-01  0.29048E-02  0.10072E+02  0.10183E+02 -0.37500E+00
0.18750E+1 0.89821E-01  0.43143E-02  0.14840E+02  0.15089E+02 -0.56250E+00
0.25000E+1 0.86691E-01  0.56951E-02  0.19428E+02  0.19872E+02 -0.75000E+00
0.25000E+1 0.86691E-01  0.56951E-02  0.19500E+02  0.19893E+02 -0.16484E+01
0.31250E+1 0.82711E-01  0.70274E-02  0.23187E+02  0.24293E+02 -0.22819E+01
0.37500E+1 0.77924E-01  0.82779E-02  0.26364E+02  0.28341E+02 -0.28827E+01
0.43750E+1 0.72381E-01  0.94468E-02  0.29031E+02  0.32036E+02 -0.34646E+01
0.50000E+1 0.66132E-01  0.10534E-01  0.31187E+02  0.35379E+02 -0.40349E+01
0.50000E+1 0.66132E-01  0.10534E-01  0.31267E+02  0.35402E+02 -0.58773E+01
0.56250E+1 0.59235E-01  0.11517E-01  0.31598E+02  0.37955E+02 -0.68933E+01
0.62500E+1 0.51765E-01  0.12364E-01  0.31085E+02  0.39925E+02 -0.78828E+01
0.68750E+1 0.43807E-01  0.13077E-01  0.29729E+02  0.41314E+02 -0.88530E+01
0.75000E+1 0.35447E-01  0.13655E-01  0.27530E+02  0.42121E+02 -0.98088E+01
0.75000E+1 0.35447E-01  0.13655E-01  0.27610E+02  0.42144E+02 -0.12600E+02
0.81250E+1 0.26772E-01  0.14074E-01  0.22658E+02  0.41755E+02 -0.14004E+02
0.87500E+1 0.17894E-01  0.14304E-01  0.16529E+02  0.40554E+02 -0.15383E+02
0.93750E+1 0.89305E-02  0.14346E-01  0.92229E+01  0.38540E+02 -0.16743E+02
0.10000E+2 0.00000E+00  0.14200E-01  0.73943E+00  0.35714E+02 -0.18087E+02
```

The next two examples deal with plane truss and frame problems.

Example 8.4.8

Here, we consider the three-member plane truss shown in Fig. 8.4.6 (see **Example 6.2.1**). We wish to determine the solution using FEM1D. A plane truss problem falls into MODEL = 4 and NTYPE = 0. The data used is: E = 200 GPa, L = 5 m, $A = 5 \times 10^{-3}$ m^2, and P = 50 kN. To run a dimensionless case, set all quantities to unity. The data are discontinuous (ICONT = 0). The element material and geometric properties are presented in Table 6.2.1.

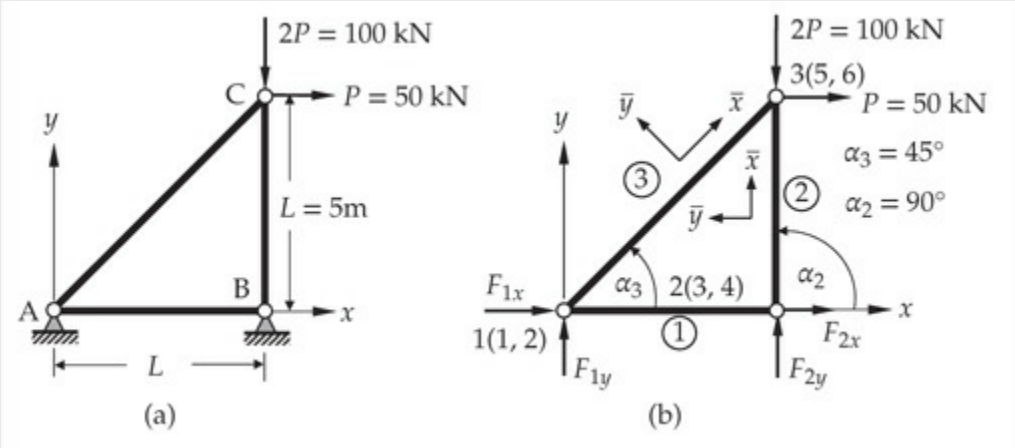

Fig. 8.4.6 The plane truss problem of **Example 6.2.1**.

The input and edited partial output are presented in Box 8.4.14 and Box 8.4.15, respectively. The axial stresses in the members are

$$\sigma^{(1)} = 0, \quad \sigma^{(2)} = -\frac{150 \times 10^3}{5 \times 10^{-3}} = -30 \text{ MPa}, \quad \sigma^{(3)} = \frac{70.71 \times 10^3}{5 \times 10^{-3}} = 14.142 \text{ MPa}$$

Box 8.4.14: Input file for the plane truss problem of **Example 8.4.8**.

```
Example 6-2-1: ANALYSIS OF A PLANE TRUSS
   4  0  0  0                          MODEL,NTYPE,ITEM,NTHER
   0  3                                IELEM,NEM
   0  1                                ICONT,NPRNT
   3                                   NNM
   2.0E11 5.0 5.0E-3 1.0 0.0 0.0       SE, SL, SA, CS, SN, HF
   1  2                                NOD(1,I)
   2.0E11 5.0 5.0E-3 0.0 1.0 0.0
   2  3                                NOD(2,I)
   2.0E11 7.0710678  5.0E-3 0.70710678  0.70710678 0.0
   1  3                                NOD(3,I)
      0                                NCON
      4                                NSPV
      1    1    0.0          <---
      1    2    0.0               | ISPV,VSPV
      2    1    0.0               |
      2    2    0.0          <---
      2                             NSSV
      3    1    5.0E4              ISSV,VSSV
      3    2   -1.0E5              ISSV,VSSV
      0                             NNBC
      0                             NMPC
```

Box 8.4.15: Edited output file for the plane truss problem of **Example 8.4.8**.

```
Example 6-2-1: ANALYSIS OF A PLANE TRUSS
    *** ANALYSIS OF MODEL 4, AND TYPE 0 PROBLEM ***
 SOLUTION (values of PVs) at the NODES:
      0.00000E+00    0.00000E+00    0.00000E+00    0.00000E+00
      0.14571E-02   -0.75000E-03

        Generalized internal forces in members
 (second line gives the results in the global coordinates)

   Ele  Force, H1   Force, V1   Force, H2  Force, V2
    1  0.0000E+00  0.0000E+00  0.0000E+00  0.0000E+00
       0.0000E+00  0.0000E+00  0.0000E+00  0.0000E+00
    2  0.1500E+06  0.0000E+00 -0.1500E+06  0.0000E+00
       0.0000E+00  0.1500E+06  0.0000E+00 -0.1500E+06
    3 -0.7071E+05  0.0000E+00  0.7071E+05  0.0000E+00
      -0.5000E+05 -0.5000E+05  0.5000E+05  0.5000E+05
```

Example 8.4.9

This example deals with the two-member frame structure shown in Fig. 8.4.7 (see **Example 6.3.1**). We shall analyze the frame for displacements and member forces using the Euler–Bernoulli frame element (MODEL = 4, NTYPE = 1). The input file of the problem using two (one element per member) Euler–Bernoulli elements is presented in Box 8.4.16 and the edited output is included in Box 8.4.17 (the displacements and forces should be multiplied with *P*). The same data is valid for multiple elements per member, except that the member lengths change. The data is also valid for the RIE Timoshenko frame element, except that MODEL = 4 and NTYPE = 2.

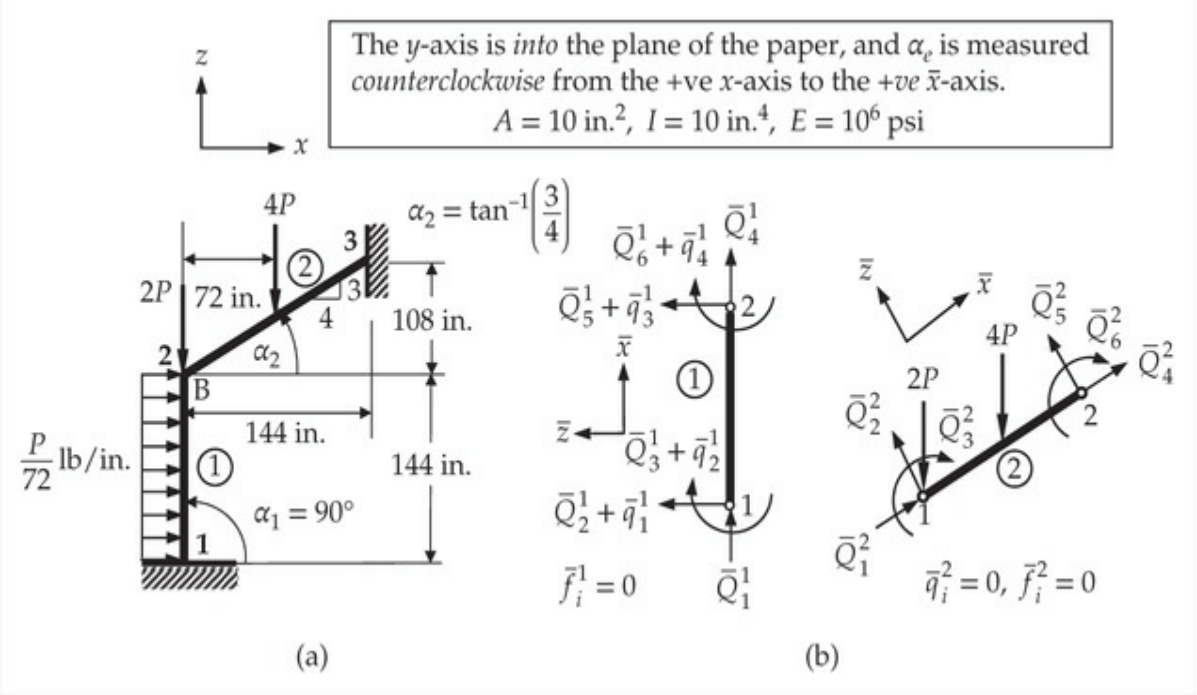

Fig. 8.4.7 The plane frame problem of **Example 8.4.9**.

Box 8.4.16: Input file for the plane frame problem of **Example 8.4.9**.

```
Example 6-2-1: ANALYSIS OF A PLANE FRAME (EBE)
    4  1  0  0                        MODEL, NTYPE, ITEM, NTHER
    3  2                              IELEM, NEM
    0  1                              ICONT, NPRNT
    3                                 NNM
0.3 1.0E6 144.0 10.0 10.0 0.0 1.0     PR, SE, SL, SA, SI, CS, SN
0.0 -0.01388888  0.0  0.0 0.0 0.0     HF, VF, PF, XB, CST, SNT
    1  2                              NOD(1,J)
0.3 1.0E6 180.0 10.0 10.0 0.8 0.6
0.0 0.0    -4.0 90.0  0.6 0.8
    2   3
    0                                 NCON
      6                               NSPV
      1     1    0.0                  ISPV, VSPV
      1     2    0.0
      1     3    0.0
      3     1    0.0
      3     2    0.0
      3     3    0.0
      1                               NSSV
      2     2   -2.0                  ISSV, VSSV
      0                               NNBC
      0                               NMPC
```

Box 8.4.17: Edited output file for the plane frame problem of **Example 8.4.9**.

```
 SOLUTION (values of PVs) at the NODES:
      0.00000E+00    0.00000E+00    0.00000E+00    0.83905E-04
     -0.68125E-04    0.96097E-04    0.00000E+00    0.00000E+00
      0.00000E+00

          Generalized internal forces in members
 (second line gives the results in the global coordinates)
Ele  Force, H1   Force, V1  Moment, M1  Force, H2   Force, V2  Moment, M2

 1  0.4731E+01  0.7253E+00 -0.1090E+02 -0.4731E+01  0.1275E+01  0.5045E+02
   -0.7253E+00  0.4731E+01 -0.1090E+02 -0.1275E+01 -0.4731E+01  0.5045E+02

 2  0.2658E+01  0.1420E+01 -0.5045E+02 -0.2583E+00  0.1780E+01  0.8287E+02
    0.1275E+01  0.2731E+01 -0.5045E+02 -0.1275E+01  0.1269E+01  0.8287E+02
```

The next two examples deal with problems involving constraint

conditions.

Example 8.4.10

A rigid bar AB of length L = 1.6 m is hinged to a support at A and supported by two vertical bars attached at points C and D, as shown in Fig. 8.4.8. Both bars have the same cross-sectional area (A = 16 mm^2) and are made of the same material with modulus E = 200 GPa. The lengths of the bars and the horizontal distances are shown in the figure. We wish to determine the elongations as well as tensile stresses in the bars. We wish to determine the solution using FEM1D.

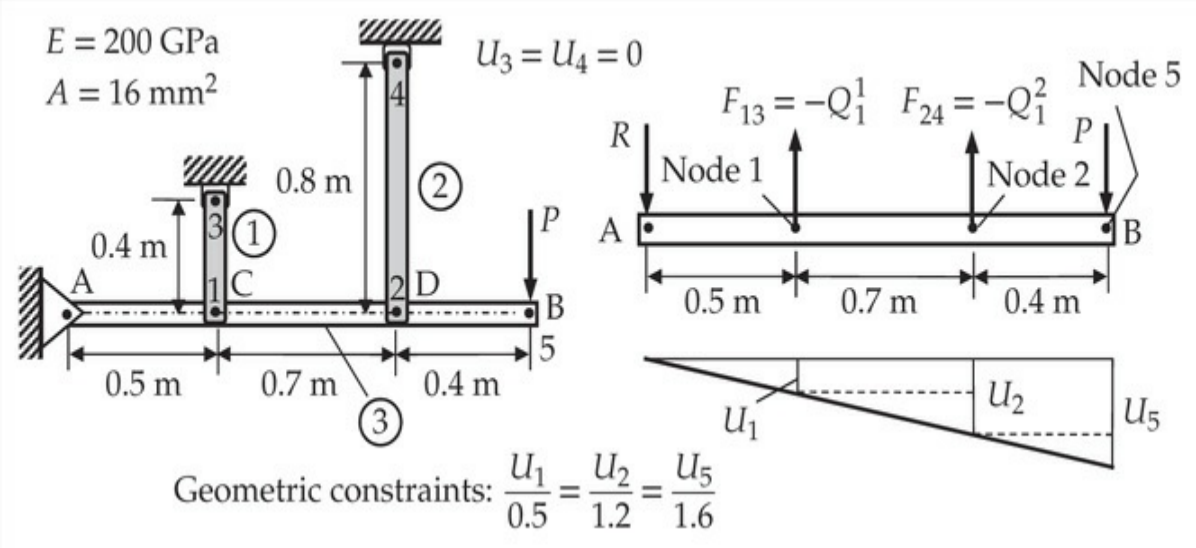

Fig. 8.4.8 A rigid member supported by cables.

The problem should be solved using the discrete elements (MODEL = 0, NTYPE = 0) because the structure does not qualify as a typical bar or truss problem where elements are all connected. The following two geometric constraints must be respected:

$$\frac{U_1}{0.5} = \frac{U_5}{1.6} \rightarrow 3.2U_1 - U_5 = 0, \quad \frac{U_2}{1.2} = \frac{U_5}{1.6} \rightarrow 1.333U_2 - U_5 = 0$$

Thus we have (see Eq. (6.4.7)]: β_1 = 3.2, β_5 = -1, and β_{15} =0; β_2 = 1.333, β_5 = -1, and β_{25} = 0.

In order to include the load P in the analysis, we introduce a node at point B. Thus, we have NEM = 3 and NNM = 5 with EA = 3.2 × 10^6 N for the bar elements and EA = 0 for the third (fictitious) element. Thus, the constraint data is (see Eq. 6.4.12]: NMPC = 2, VMPC(1,1) = β_1 = 3.2,

VMPC(1,2) = β_5 = −1.0, VMPC(1,3) = β_{15} = 0, VMPC(1,4) = 0; VMPC(2,1) = β_2 = 1.333, VMPC(2,2) = β_5 = -1.0, VMPC(2,3) = β_{25} = 0, and VMPC(2,4) = P = 970 N. The input file and modified output of the problem are presented in Box 8.4.18 and Box 8.4.19, respectively.

Box 8.4.18: Input file for the problem of **Example 8.4.10.**

```
Example 8.4.10: DEFORMATION OF A CONSTRAINED STRUCTURE
   0   0   0   0            MODEL, NTYPE, ITEM, NTHER
   1   3                    IELEM, NEM
   0   1                    ICONT, NPRNT
   5                        NNM
   8.0E6   1   3            ES(1) NOD(1,I)
   4.0E6   2   4            ES(2) NOD(2,I)
   0.0     1   5            ES(3) NOD(3,I)
    2                       NSPV
    3 1    0.0              ISPV(1,1),ISPV(1,2),VSPV(1)
    4 1    0.0              ISPV(2,1),ISPV(2,2),VSPV(2)
    0                       NSSV
    0                       NNBC
    2                       NMPC
    1   1    5   1   3.2       -1.0   0.0     0.0
    2   1    5   1   1.33333   -1.0   0.0   970.0
                    IMC1(1,1),IMC1(1,2),IMC2(1,1),
                          IMC2(1,2),(VMPC(1,I), I=1 to 4)
```

Box 8.4.19: Edited output file for the problem of **Example 8.4.10**.

```
Example 8.4.10: DEFORMATION OF A CONSTRAINED STRUCTURE
    *** ANALYSIS OF MODEL 0, AND TYPE 0 PROBLEM ***

   Multi-point constraint information:
         1    1      5    1
         0.32000E+01   -0.10000E+01    0.00000E+00    0.00000E+00
         2    1      5    1
         0.13333E+01   -0.10000E+01    0.00000E+00    0.97000E+03

    Values of the spring constants:
              0.8000E+07     0.4000E+07     0.0000E+00

 SOLUTION (values of PVs) at the NODES:
      0.10000E-03    0.24000E-03    0.00000E+00    0.00000E+00
      0.32001E-03

 Forces at the constrained points:
      0.80001E+03    0.95999E+03
     -0.25000E+03   -0.72000E+03
```

The displacements are $U_1 = 0.1$ mm, $U_2 = 0.24$ mm, and $U_5 = 0.32$ mm. The stresses are $\sigma_1 = 10^6$ (800/16) = 50 MPa and $\sigma_2 = 10^6$ (960/16) = 60 MPa.

Example 8.4.11

Consider the truss shown in Fig. 8.4.9 (see **Example 6.4.3**). We wish to determine the unknown displacements of nodes 2 and 3 and the reactions associated with these displacements using FEM1D.

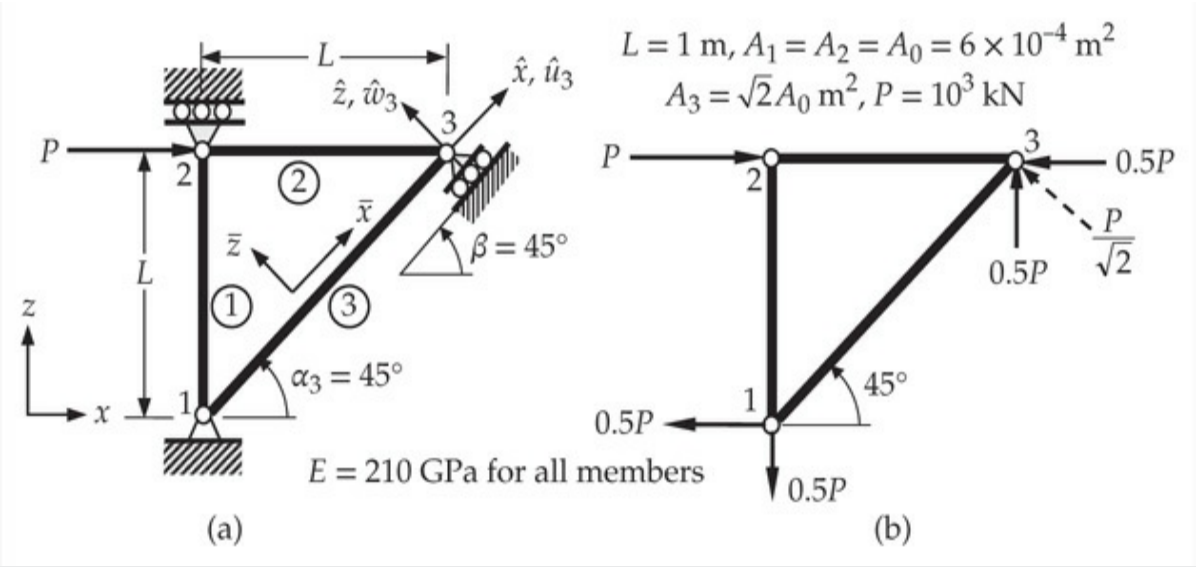

Fig. 8.4.9 (a) Given structure. (b) Reaction forces.

The constraint condition at node 3 is

$$u_n \equiv -u \sin\beta + w \cos\beta = 0 \rightarrow -0.7071\, u + 0.7071\, w = 0$$

We have [see Eq. 6.4.7] $\beta_5 = -0.7071$, $\beta_6 = 0.7071$ and $\beta_{56} = 0$. Internal to the program, the penalty parameter is assigned a value of $\gamma = (1.89 \times 10^8)10^4$ (the largest stiffness coefficient times 10^4). The input and edited files are presented in Box 8.4.20 and Box 8.4.21.

Box 8.4.20: Input file for the problem of **Example 8.4.11**.

```
Example 6.4.3: ANALYSIS OF A PLANE TRUSS WITH INCLINED SUPPORT
    4  0  0  0                    MODEL, NTYPE, ITEM, NTHER
    1  3                          IELEM, NEM
    0  2                          ICONT, NPRNT
       3                          NNM
210.0E9 1.0 0.6E-03 0.0 1.0 0.0   SE, SL, SA, CS, SN, HF
    1  2                          NOD(1,I)
210.0E9 1.0 0.6E-03 1.0 0.0 0.0   SE, SL, SA, CS, SN, HF
    2  3                          NOD(2,I)
210.0E9 1.41421 0.8485E-03 0.707107 0.707107 0.0 SE, SL, SA, CS, SN, HF
    1  3                          NOD(3,I)
    0                             NCON
    3                             NSPV
    1  1  0.0                     ISPV(1,1),ISPV(1,2),VSPV(1)
    1  2  0.0                     ISPV(2,1),ISPV(2,2),VSPV(2)
    2  2  0.0                     ISPV(3,1),ISPV(3,2),VSPV(3)
    1                             NSSV
    2  1  1.0E6                   ISSV(1,1),ISSV(1,2),VSSV(1)
    0                             NNBC
    1                             NMPC
 3 1  3 2  -0.707107  0.707107 0.0 0.0
```

Box 8.4.21: Output file for the problem of **Example 8.4.11**.

```
Example 6.4.3: ANALYSIS OF A PLANE TRUSS WITH INCLINED SUPPORT
    *** ANALYSIS OF MODEL 4, AND TYPE 0 PROBLEM ***
   Multi-point constraint information:
         3    1      3    2
    -0.70711E+00    0.70711E+00    0.00000E+00    0.00000E+00
 SOLUTION (values of PVs) at the NODES:
      0.00000E+00    0.00000E+00    0.11905E-01    0.00000E+00
      0.39688E-02    0.39680E-02

 Forces at the constrained points:
     -0.50000E+06
      0.50000E+06
```

The next several examples deal with the use of **FEM1D** for the solution of eigenvalue and time-dependent problems from Chapter 7.

Example 8.4.12

Here we consider heat transfer-like problem described in **Example 7.3.1**. In particular, we wish to determine the eigenvalues associated with the equation

$$k\frac{\partial^2 T}{\partial x^2} = \rho c_v \frac{\partial T}{\partial t},\ 0 < x < L; \quad T(0,t) = T_\infty, \quad \left[k\frac{\partial T}{\partial x} + \beta(T - T_\infty)\right]_{x=L} = 0 \qquad (1)$$

using FEMID.

The problem becomes one of solving the following dimensionless eigenvalue problem:

$$-\frac{d^2U}{d\xi^2} - \lambda U = 0,\ 0 < \xi < 1; \quad U(0) = 0, \quad \left(\frac{dU}{d\xi} + HU\right)\Big|_{\xi=1} = 0 \qquad (2)$$

For eigenvalue analysis, we set MODEL = 1, NTYPE = 0, ITEM = 3, and NTHER = 0. For four quadratic elements there are nine nodes and one specified value resulting in eight eigenvalues. The input file is presented in Box 8.4.22. The smallest five eigenvalues λ and the nodal values of the associated eigenvectors U are presented in Box 8.4.23.

Box 8.4.22: Input file for the problem of **Example 8.4.12**.

```
Example 7.3.1: Eigenvalues of heat transfer like problems (Set 2)
    1  0  3   0                          MODEL, NTYPE, ITEM, NTHER
    2  4                                 IELEM, NEM
    1  0                                 ICONT, NPRNT
      0.0    0.25  0.25  0.25  0.25      DX(I)
      1.0    0.0    0.0    0.0          AX0, AX1, AX2, AX3
      0.0    0.0    0.0    0.0          BX0, BX1, BX2, BX3
      0.0    0.0                        CX0, CX1
    1                                   NSPV
    1  1                                ISPV(1,J)
    1                                   NNBC
    9  1  1.0  0.0                      INBC(1,I), VNBC(1)
    0                                   NMPC
    1.0                                 CT0
```

Box 8.4.23: Input file for the problem of **Example 8.4.12**.

```
Example 7.3.1B: Eigenvalues of a heat transfer and like problems

     EIGENVALUE(4) = 0.2405398E+03  SQRT(EGNVAL) = 0.15509345E+02
     EIGENVECTOR:
      0.11357E+01   -0.83100E+00   -0.93930E+00    0.15183E+01
      0.58052E+00   -0.19431E+01   -0.12137E+00    0.20319E+01

     EIGENVALUE(5) = 0.1292608E+03  SQRT(EGNVAL) = 0.11369291E+02
     EIGENVECTOR:
      0.15205E+01    0.48606E+00   -0.13096E+01   -0.90471E+00
      0.91708E+00    0.11979E+01   -0.39736E+00   -0.13249E+01

     EIGENVALUE(6) = 0.6477040E+02  SQRT(EGNVAL) = 0.80480058E+01
     EIGENVECTOR:
     -0.11964E+01   -0.12933E+01   -0.21408E+00    0.10618E+01
      0.13722E+01    0.42142E+00   -0.91255E+00   -0.14079E+01

     EIGENVALUE(7) = 0.2420401E+02  SQRT(EGNVAL) = 0.49197572E+01
     EIGENVECTOR:
     -0.80058E+00   -0.13094E+01   -0.13385E+01   -0.87990E+00
     -0.98906E-01    0.71813E+00    0.12721E+01    0.13625E+01

     EIGENVALUE(8) = 0.4116107E+01  SQRT(EGNVAL) = 0.20288191E+01
     EIGENVECTOR:
      0.32451E+00    0.62828E+00    0.89183E+00    0.10984E+01
      0.12346E+01    0.12919E+01    0.12666E+01    0.11602E+01
```

Example 8.4.13

Here we consider natural vibrations of a uniform linear elastic beam (EI) fixed at $x = 0$ and supported vertically at $x = L$ by a short linear elastic post (length L^0 and stiffness $E_0 A_0$); see **Example 7.3.2**. The governing equation according to the EBT is

$$\frac{d^2}{dx^2}\left(EI\frac{d^2W}{dx^2}\right) - \omega^2\rho\left(AW - I\frac{d^2W}{dx^2}\right) = 0 \qquad (1)$$

subjected to the boundary conditions ($k_0 \equiv E_0 A_0/L^0$)

$$W(0) = 0, \quad \left.\frac{dW}{dx}\right|_{x=0} = 0, \quad \left[EI\frac{d^2W}{dx^2}\right]_{x=L} = 0, \quad \left[EI\frac{d^3W}{dx^3} + k_0 W\right]_{x=L} = 0 \qquad (2)$$

The input data for two-element mesh of the EBT elements with rotary inertia (for $H/L = 0.01$) and $k_0 = 2EI/L^3$ is presented in Box 8.4.24; and the four natural frequencies $(\sqrt{\lambda})$ and the nodal values of the associated mode shapes W are presented in Box 8.4.25.

Box 8.4.24: Input file for the problem of **Example 8.4.13**.

```
Example 7.3.2: NATURAL VIBRATIONS OF A CANTILEVER BEAM
   3  0  3  0                MODEL, NTYPE, ITEM, NTHER
   3  2                      IELEM, NEM
   1  0                      ICONT, NPRNT
   0.0   0.5  0.5            DX(I)
   0.0   0.0  0.0  0.0       AX0, AX1, AX2, AX3
   1.0   0.0  0.0  0.0       BX0, BX1, BX2, BX3
   0.0   0.0                 CX0, CX1
   2                         NSPV
   1  1                      ISPV(1,J)
   1  2                      ISPV(2,J)
   1                         NNBC
   3  1  2.0  0.0            INBC(1,I), VNBC(1)
   0                         NMPC
   1.0  8.333333E-6          CT0, CT2  (rotary)
```

Box 8.4.25: Edited output file for the problem of **Example 8.4.13**.

```
   Example 7.3.2: NATURAL VIBRATIONS OF A CANTILEVER BEAM
      *** ANALYSIS OF MODEL 3, AND TYPE 0 PROBLEM ***

    EIGENVALUE(1) = 0.4748468E+05  SQRT(EGNVAL) = 0.21790980E+03
    EIGENVECTOR:
     0.95382E+00   -0.19610E+02    0.37670E+01   -0.72811E+02

    EIGENVALUE(2) = 0.5654368E+04  SQRT(EGNVAL) = 0.75195533E+02
    EIGENVECTOR:
    -0.22691E+00   -0.17173E+02   -0.22504E+01    0.21651E+02

    EIGENVALUE(3) = 0.5019273E+03  SQRT(EGNVAL) = 0.22403733E+02
    EIGENVECTOR:
     0.14468E+01    0.94001E+00   -0.20473E+01    0.97051E+01

    EIGENVALUE(4) = 0.2023494E+02  SQRT(EGNVAL) = 0.44983266E+01
    EIGENVECTOR:
     0.70334E+00   -0.23341E+01    0.19631E+01   -0.25359E+01
```

Example 8.4.14

Consider a uniform column of constant geometric and material parameters, fixed at one end and pinned at the other (see Fig. 8.4.10). We wish to determine the critical buckling load using eight EBT elements (see **Example 7.3.3**). The input data and edited output for P_{cr} and U_j are presented in Box 8.4.26.

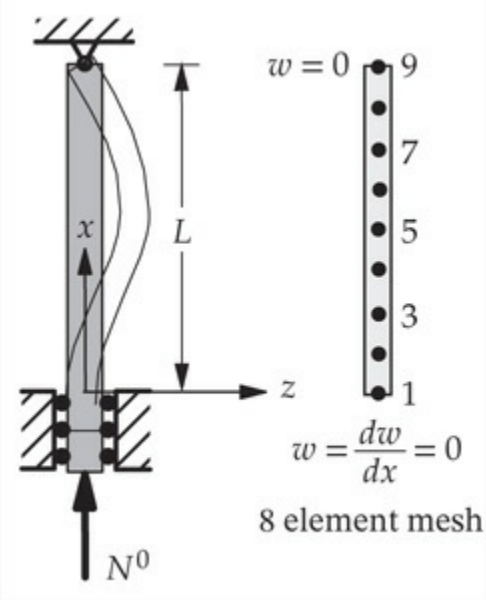

Fig. 8.4.10 A column fixed at $x = 0$ and hinged at $x = L$, and subjected to axial compressive load N^0.

Box 8.4.26: Input file for the problem of **Example 8.4.14**.

```
Example 7.3.3: Buckling of Euler-Bernoulli beams (C-H)
 3   0   4    0                    MODEL,NTYPE,ITEM,NTHER
 3   8                             IELEM,NEM
 1   0                             ICONT,NPRNT
0.0 0.125 0.125 0.125 0.125
    0.125 0.125 0.125 0.125        DX(I)
0.0 0.0    0.0   0.0               AX0,AX1,AX2,AX3
1.0 0.0    0.0   0.0               BX0,BX1,BX2,BX3
0.0 0.0                           CX0,CX1
 3                                NSPV
 1   1                            ISPV(1,J)
 1   2                            ISPV(2,J)
 9   1                            ISPV(3,J)
 0                                NNBC
 0                                NMPC

Example 7.3.3: Buckling of Euler-Bernoulli beams (C-H)
    *** ANALYSIS OF MODEL 3, AND TYPE 0 PROBLEM ***

Buckling load(15) =   0.2019347E+02
EIGENVECTOR:
  0.46324E-01  -0.70496E+00   0.16305E+00  -0.10966E+01
  0.30221E+00  -0.10545E+01   0.40896E+00  -0.59173E+00
  0.43841E+00   0.14961E+00   0.36942E+00   0.94170E+00
  0.21110E+00   0.15412E+01   0.17638E+01
```

Example 8.4.15

Consider the transient heat conduction problem describe by the equations (see **Example**

$$\frac{\partial u}{\partial t} - \frac{\partial^2 u}{\partial x^2} = 0 \text{ for } 0 < x < 1: \quad u(0,t) = 0, \quad \frac{\partial u}{\partial x}(1,t) = 0; \; u(x,0) = 1.0 \qquad (1)$$

where u is the dimensionless temperature. We wish to determine the transient response using FEM1D. The input data and edited (the output is rather large) output for $u(x, t)$ for selected times t are presented in Box 8.4.27 and Box 8.4.28, respectively.

Box 8.4.27: Input file for the problem of **Example 8.4.15**.

```
Example 7.4.1: TRANSIENT HEAT CONDUCTION
    1  0  1  0                    MODEL,NTYPE,ITEM,NTHER
    2  4                          IELEM,NEM
    1  0                          ICONT,NPRNT
    0.0  0.25 0.25 0.25 0.25      DX(I)
    1.0  0.0  0.0  0.0            AX0,AX1,AX2,AX3
    0.0  0.0  0.0  0.0            BX0,BX1,BX2,BX3
    0.0  0.0                      CX0,CX1
    0.0  0.0  0.0                 FX0,FX1,FX2
    1                             NSPV
    1  1 0.0                      ISPV(I,J), VSPV(I)
    0                             NSSV
    0                             NNBC
    0                             NMPC
    1.0   0.0                     CT0, CT1
    0.05  0.5                     DT, ALFA
    1 51  1                       INCOND, NTIME, INTVL
    0.0 1.0 1.0 1.0 1.0 1.0 1.0 1.0 1.0  GU0(I)
```

Box 8.4.28: Edited output file for the problem of **Example 8.4.15**.

```
        OUTPUT from program    FEM1D    by J N REDDY

Example 7.4.1: TRANSIENT HEAT CONDUCTION
*** ANALYSIS OF MODEL 1, AND TYPE 0 PROBLEM ***
   TIME-DEPENDENT (TRANSIENT) ANALYSIS: 1

   Coefficient, CT0 of CT=CT0..............= 0.1000E+01
   Parameter, ALFA.........................= 0.5000E+00
   Time increment, DT......................= 0.5000E-01
   No. of time steps, NTIME................= 51
   Time-step interval to print soln, INTVL =  1

Initial conditions on the primary variables:
   0.00000E+00  0.10000E+01  0.10000E+01  0.10000E+01
   0.10000E+01  0.10000E+01  0.10000E+01  0.10000E+01
   0.10000E+01

Boundary information on primary variables:
        1    1    0.00000E+00

TIME =  0.5000E-01     Time step number =  1
SOLUTION (values of PVs) at the NODES:
     0.00000E+00    0.49195E-01    0.59785E+00    0.81787E+00
     0.91647E+00    0.96192E+00    0.98197E+00    0.99055E+00
     0.99283E+00

TIME =  0.1000E+00     Time step number =  2
SOLUTION (values of PVs) at the NODES:
     0.00000E+00    0.34702E+00    0.32653E+00    0.54926E+00
     0.73054E+00    0.84563E+00    0.91197E+00    0.94502E+00
     0.95487E+00

TIME =  0.2000E+00     Time step number =  4
SOLUTION (values of PVs) at the NODES:
     0.00000E+00    0.21249E+00    0.22733E+00    0.43264E+00
     0.55980E+00    0.64898E+00    0.71559E+00    0.75835E+00
     0.77314E+00

TIME =  0.4000E+00     Time step number =  8
SOLUTION (values of PVs) at the NODES:
     0.00000E+00    0.11233E+00    0.14339E+00    0.27303E+00
     0.33283E+00    0.39251E+00    0.43766E+00    0.46501E+00
     0.47410E+00

TIME =  0.8000E+00     Time step number = 16
SOLUTION (values of PVs) at the NODES:
     0.00000E+00    0.38844E-01    0.56347E-01    0.10298E+00
     0.11975E+00    0.14728E+00    0.16272E+00    0.17295E+00
     0.17639E+00

TIME =  0.1000E+01     Time step number = 20
SOLUTION (values of PVs) at the NODES:
     0.00000E+00    0.23370E-01    0.34791E-01    0.62957E-01
     0.72281E-01    0.90280E-01    0.98883E-01    0.10554E+00
     0.10761E+00

TIME =  0.1500E+01     Time step number = 30
SOLUTION (values of PVs) at the NODES:
     0.00000E+00    0.66965E-02    0.10203E-01    0.18395E-01
     0.20572E-01    0.26527E-01    0.28364E-01    0.30785E-01
     0.31141E-01

TIME =  0.2000E+01     Time step number = 40
SOLUTION (values of PVs) at the NODES:
     0.00000E+00    0.19457E-02    0.29378E-02    0.53875E-02
     0.58524E-02    0.77930E-02    0.80996E-02    0.90126E-02
     0.89386E-02

TIME =  0.2500E+01     Time step number = 50
SOLUTION (values of PVs) at the NODES:
     0.00000E+00    0.56979E-03    0.83411E-03    0.15834E-02
     0.16547E-02    0.22942E-02    0.22967E-02    0.26492E-02
     0.25421E-02
```

Example 8.4.16

We wish to determine the transverse motion of a beam clamped at both ends and subjected to initial deflection (see **Example 7.4.2**). We shall use a mesh of four EBT elements in half beam with DT = 0.005, ALFA = 0.5, and BETA = 0.5.

The input data and edited output for $w(x, t)$ for selected times t are presented in Box 8.4.29 and Box 8.4.30, respectively.

Box 8.4.29: Input file for the problem of **Example 8.4.16**.

```
Example 7.4.2: TRANSIENT RESPONSE OF A CLAMPED BEAM (EBT)
    3  0  2  0                      MODEL,NTYPE,ITEM,NTHER
    3  4                            IELEM,NEM
    1  0                            ICONT,NPRNT
   0.0 0.125 0.125 0.125 0.125      DX(I)
   0.0 0.0   0.0   0.0              AX0,AX1,AX2,AX3
   1.0 0.0   0.0   0.0              BX0,BX1,BX2,BX3
   0.0 0.0                          CX0,CX1
   0.0 0.0   0.0                    FX0,FX1,FX2
    3                               NSPV
    1  1     0.0                    ISPV(1,J), VSPV(1)
    1  2     0.0                    ISPV(2,J), VSPV(2)
    5  2     0.0                    ISPV(3,J), VSPV(3)
    0                               NSSV
    0                               NNBC
    0                               NMPC
    1.0      8.3333333E-6           CT0,CT2
    0.005    0.5  0.5                DT,ALFA,GAMA
    1 31  1                         INCOND, NTIME, INTVL
   0.0 0.0   0.039072 -0.5462586
   0.11810  -0.65060   0.1875687
  -0.416837  0.21460   0.0          GU0(I)
   0.0 0.0 0.0 0.0 0.0 0.0
   0.0 0.0 0.0 0.0                  GU1(I)
```

Box 8.4.30: Edited output file for the problem of **Example 8.4.16**.

```
Example 7.4.2: TRANSIENT RESPONSE OF A CLAMPED BEAM (EBT)
    *** ANALYSIS OF MODEL 3, AND TYPE 0 PROBLEM ***
    TIME-DEPENDENT (TRANSIENT) ANALYSIS: 2
        Coefficient, CT0 of C1=CT0 ..............=  0.1000E+01
        Coefficient, CT2.of C2=CT2 ..............=  0.8333E-05
        Parameter, ALFA..........................=  0.5000E+00
        Parameter, GAMA..........................=  0.5000E+00
        Time increment, DT.......................=  0.5000E-02
        No. of time steps, NTIME.................=  31
        Time-step interval to print soln., INTVL=   1

   Initial conditions on the primary variables:
      0.00000E+00    0.00000E+00    0.39072E-01   -0.54626E+00
      0.11810E+00   -0.65060E+00    0.18757E+00   -0.41684E+00
      0.21460E+00    0.00000E+00

 TIME =  0.5000E-02     Time step number =  1
 SOLUTION (values of PVs) at the NODES:
      0.00000E+00    0.00000E+00    0.38665E-01   -0.54232E+00
      0.11721E+00   -0.64792E+00    0.18646E+00   -0.41502E+00
      0.21338E+00    0.00000E+00

 TIME =  0.1000E-01     Time step number =  2
 SOLUTION (values of PVs) at the NODES:
      0.00000E+00    0.00000E+00    0.37550E-01   -0.52839E+00
      0.11462E+00   -0.63888E+00    0.18308E+00   -0.41134E+00
      0.20974E+00    0.00000E+00

 TIME =  0.2000E-01     Time step number =  4
 SOLUTION (values of PVs) at the NODES:
      0.00000E+00    0.00000E+00    0.34018E-01   -0.48151E+00
      0.10493E+00   -0.59454E+00    0.16945E+00   -0.39291E+00
      0.19509E+00    0.00000E+00

 TIME =  0.4000E-01     Time step number =  8
 SOLUTION (values of PVs) at the NODES:
      0.00000E+00    0.00000E+00    0.23928E-01   -0.33771E+00
      0.73365E-01   -0.41179E+00    0.11763E+00   -0.26654E+00
      0.13496E+00    0.00000E+00

 TIME =  0.5000E-01     Time step number = 10
 SOLUTION (values of PVs) at the NODES:
      0.00000E+00    0.00000E+00    0.17497E-01   -0.24288E+00
      0.52174E-01   -0.28217E+00    0.82030E-01   -0.17758E+00
      0.93522E-01    0.00000E+00

 TIME =  0.8000E-01     Time step number = 16
 SOLUTION (values of PVs) at the NODES:
      0.00000E+00    0.00000E+00   -0.90058E-02    0.12366E+00
     -0.26216E-01    0.13638E+00   -0.40289E-01    0.81270E-01
     -0.45476E-01    0.00000E+00

 TIME =  0.1000E+00     Time step number = 20
 SOLUTION (values of PVs) at the NODES:
      0.00000E+00    0.00000E+00   -0.23036E-01    0.32702E+00
     -0.71560E-01    0.40861E+00   -0.11592E+00    0.27029E+00
     -0.13352E+00    0.00000E+00

 TIME =  0.1200E+00     Time step number = 24
 SOLUTION (values of PVs) at the NODES:
      0.00000E+00    0.00000E+00   -0.34226E-01    0.48332E+00
     -0.10499E+00    0.58911E+00   -0.16835E+00    0.38187E+00
     -0.19315E+00    0.00000E+00

 TIME =  0.1500E+00     Time step number = 30
 SOLUTION (values of PVs) at the NODES:
      0.00000E+00    0.00000E+00   -0.37133E-01    0.52454E+00
     -0.11420E+00    0.64390E+00   -0.18370E+00    0.42078E+00
     -0.21109E+00    0.00000E+00
```

8.5 Summary

In this chapter three main items have been discussed: (1) numerical integration of finite element coefficient matrices and vectors, (2) numerical implementation of a typical finite element program and their contents, and (3) applications of the finite element program **FEM1D** to various types of problems discussed in Chapters 3 through 7. The numerical evaluation of the coefficients is required because of (a) variable coefficients of the differential equations modelled and (b) special evaluation of the coefficients, as was required for the Timoshenko beam element with equal interpolation. The Newton–Cotes and Gauss–Legendre integration rules have been discussed. The integration rules require transformation of the integral expressions from the global coordinate system to a local coordinate system and interpolation of the global coordinate x. Depending on the relative degrees of interpolation of the geometry and the dependent variables, the formulations are classified as subparametric, isoparametric, and superparametric formulations.

The three logical units—preprocessor, processor, and postprocessor—of a typical computer program have been discussed. The contents of processor, where most finite element calculations are carried out, have been considered in detail. Computer implementation for numerical evaluation of integral expressions, assembly of element coefficients, and imposition of boundary conditions have been discussed. A description of the input variables to the finite element computer program **FEM1D** has been presented, and application of **FEM1D** to problems involving steady-state, eigenvalue, and transient analysis has been discussed. Applications to heat transfer and solid and structural mechanics are presented. Flows of inviscid fluids are similar in mathematical structure to heat transfer problems and hence not discussed in this chapter.

Problems

In **Problems 8.1–8.4**, use the appropriate number of integration points, and verify the results with those obtained by the exact integration.

NUMERICAL INTEGRATION

8.1 Evaluate the following integrals using the Newton–Cotes formula and Gauss–Legendre quadrature:

$$K_{12} = \int_{x_a}^{x_b} (x_0 + x) \frac{d\psi_1}{dx} \frac{d\psi_2}{dx}\, dx, \quad G_{12} = \int_{x_a}^{x_b} (x_0 + x)\psi_1\psi_2\, dx$$

where ψ_i are the quadratic interpolation functions

$$\psi_1 = \left(1 - \frac{x - x_a}{x_b - x_a}\right)\left(1 - 2\frac{x - x_a}{x_b - x_a}\right) = -\frac{1}{2}\xi(1 - \xi)$$
$$\psi_2 = 4\left(\frac{x - x_a}{x_b - x_a}\right)\left(1 - \frac{x - x_a}{x_b - x_a}\right) = (1 - \xi^2)$$
$$\psi_3 = -\frac{x - x_a}{x_b - x_a}\left(1 - 2\frac{x - x_a}{x_b - x_a}\right) = \frac{1}{2}\xi(1 + \xi)$$

8.2 Use Newton–Cotes integration formula to evaluate

$$K_{11} = \int_{x_a}^{x_b} \left(\frac{d^2\phi_1}{dx^2}\right)^2 dx, \quad G_{11} = \int_{x_a}^{x_b} (\phi_1)^2\, dx$$

where ϕ_i are the Hermite cubic interpolation functions [see Eqs. (5.2.20), (5.2.21*a*), and (5.2.21*b*)]. *Answer:* $r = 2 : K_{11} = 12/h^3$ (exact), $G_{11} = 0.398148h$.

8.3 Use the Gauss–Legendre quadrature to evaluate the integrals of **Problem 8.2** for the case in which the interpolation functions ϕi are the fifth-order Hermite polynomials of **Problem 5.2**. *Answer:* $K_{11} = \frac{120}{7}h^3$, $G_{11} = \frac{181}{462}h$ (exact).

8.4 Repeat **Problem 8.3** for the case in which the interpolation functions ϕi are the fifth-order Hermite polynomials of **Problem 5.4**. *Answer:* $K_{11} = \frac{5092}{35h_e^3}$, $G_{11} = \frac{523h_e}{3465}$ (exact).

COMPUTER PROBLEMS

8.5 Consider 1-D heat flow in a plane wall described by the equations

$$-\frac{d}{dx}\left(k\frac{dT}{dx}\right)=g_0$$

$$\left(-k\frac{dT}{dx}\right)_{x=0}=Q_0,\quad \left[k\frac{dT}{dx}+\beta(T-T_\infty)\right]_{x=L}=0$$

Analyze the problem using (a) four linear and (b) two quadratic elements. Compare the results with the exact solution. Use the following data: L = 0.02 m, k = 20 W/(m · °C), g_0 = 106 W/m^2, Q_0 = 102 W, T_∞ = 50°C, β = 500 W/(m · °C).

8.6 Solve **Problem 8.5** using (a) eight linear and (b) four quadratic elements.

8.7 Solve the heat transfer problem in **Example 4.2.1** (set 1) using (a) four linear elements and (b) two quadratic elements.

8.8 Solve the axisymmetric problem in **Example 4.2.3** using four quadratic elements and compare the solution with that obtained using eight linear elements and the exact solution of Table 4.2.2.

8.9 Solve the one-dimensional flow problem of **Example 4.3.1** (set 1), for $dP/dx = -24$, using eight linear elements (see Fig. 4.3.1). Compare the finite element results with the exact solution from Eq. (10) of **Example 4.3.1**.

8.10 Solve the Couette flow problem in **Example 4.3.1** (set 2), for $dP/dx = -24$ and $U_0 = 1$, using four quadratic elements.

Compare the finite element solution with the exact solution in Eq. (11) of **Example 4.3.1**.

8.11 Solve **Problem 4.3** (heat flow in a composite wall) using the minimum number linear finite elements.

8.12 Solve **Problem 4.17** (axisymmetric problem of unconfined aquifer) using six linear finite elements (nonuniform mesh).

8.13 Analyze the stepped bar in **Problem 4.19** using the minimum number of linear finite elements.

8.14 Analyze the composite bar in **Problem 4.21** using the minimum number of linear finite elements.

8.15 Solve **Problem 4.31** using two linear elements.

8.16 Determine the forces and elongations in the wires AB and CD shown in Fig. P8.16 when P = 700 lb. Each wire has a cross-sectional area of A = 0.03 in.^{2} and modulus of elasticity E = 30 × 10^6 psi.

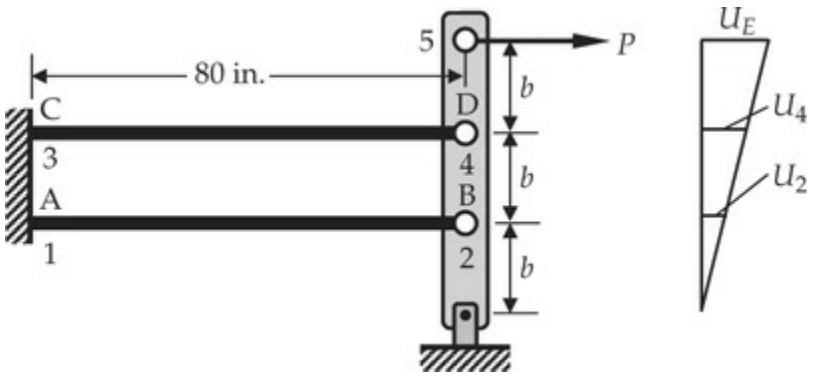

Fig. P8.16

8.17 Solve the problem of axisymmetric deformation of a rotating circular disk using (a) four quadratic and (b) eight linear elements (see **Example 8.4.3**).

8.18–8.25 Solve **Problems 5.7–5.14** using the minimum number of Euler–Bernoulli beam elements (*Note:* Numerous other beam problems can be found in books on mechanics of deformable solids).

8.26 Analyze **Problem 8.22** (same as **Problem 5.11**) using the RIE Timoshenko element. Assume $\nu = 0.25$, $K_s = 5/6$, and $H = 0.1$ m (beam height). Use 4, 8, and 16 linear elements and equivalent meshes of quadratic elements to see the convergence characteristics of the RIE.

8.27 Repeat **Problem 8.26** using 4, 8, and 16 CIE Timoshenko beam elements.

8.28 Analyze a clamped circular plate of radius a (in.), thickness $H = 0.1a$ (in.), and modulus $E = 10^7$ (psi) under a uniformly distributed transverse load using the Euler–Bernoulli plate element. Investigate the convergence using two, four, and eight elements by comparing with the exact solution (from Reddy [6])

$$w(r) = \frac{q_0 a^4}{64D}\left[1 - \left(\frac{r}{a}\right)^2\right]^2$$

where $D = EH^3/12(1 - \nu^2)$, q_0 is the intensity of the distributed load, and ν is Poisson's ratio ($\nu = 0.25$). Tabulate the center deflection.

8.29 Repeat **Problem 8.28** with the RIE Timoshenko plate element for $a/H = 10$. Use four and eight linear elements and two and

four quadratic elements and tabulate the center deflection. Take $E = 10^7$, $\nu = 0.25$, and $K_s = 5/6$. The exact solution is (see Reddy [6])

$$w(r) = \frac{q_0 a^4}{64D}\left[1 - \left(\frac{r}{a}\right)^2\right]^2 + \frac{q_0 a^2}{4K_s GH}\left[1 - \left(\frac{r}{a}\right)^2\right]$$

8.30 Repeat **Problem 8.29** with the Timoshenko plate element (CIE) (and linear elements) for $a/H = 10$.

8.31 Consider an annular plate of outer radius a, inner radius b, and thickness H. If the plate is simply supported at the outer edge and subjected to a uniformly distributed load q_0 (see Fig. P8.31), analyze the problem using the Euler–Bernoulli plate element. Compare the four-element solution with the analytical solution (from Reddy [6])

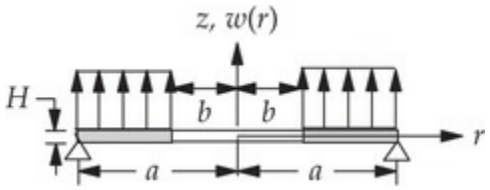

Fig. P8.31

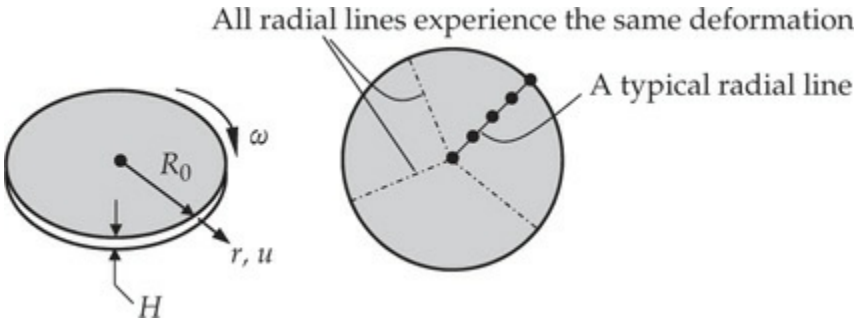

Fig. P8.17

$$w = \frac{q_0 a^4}{64D}\left\{-1 + \left(\frac{r}{a}\right)^4 + \frac{2\alpha_1}{1+\nu}\left[1 - \left(\frac{r}{a}\right)^2\right] - \frac{4\alpha_2\beta^2}{1-\nu}\log\left(\frac{r}{a}\right)\right\}$$

$$\alpha_1 = (3+\nu)(1-\beta^2) - 4(1+\nu)\beta^2\kappa, \quad \alpha_2 = (3+\nu) + 4(1+\nu)\kappa$$

$$\kappa = \frac{\beta^2}{1-\beta^2}\log\beta, \quad \beta = \frac{b}{a}, \quad D = \frac{EH^3}{12(1-\nu^2)}$$

where E is the modulus of elasticity, H the thickness, and ν Poisson's ratio. Take $E = 10^7$, $\nu = 0.3$, and $b/a = 0.25$.

8.32 Repeat **Problem 8.31** with (a) four linear elements and (b) two quadratic Timoshenko (RIE) elements for $a/H = 10$.

8.33–8.42 Analyze the truss problems in Figs. P6.1–P6.10 using FEM1D.

8.43–8.50 Analyze the frame problems in Figs. P6.13–P6.20 using FEM1D.

8.51 Consider the following dimensionless form differential equation governing the plane wall transient:

$$-\frac{\partial^2 T}{\partial x^2} + \frac{\partial T}{\partial t} = 0 \quad \text{for } 0 < x < 1$$

with boundary conditions $T(0, t) = 1$ and $T(1, t) = 0$, and initial condition $T(x, 0) = 0$. Solve the problem using eight linear elements. Determine the critical time step; solve the problem using the Crank–Nicholson method and $\Delta t = 0.002$ s.

8.52 Consider the axial motion of an elastic bar, governed by the second-order equation

$$EA\frac{\partial^2 u}{\partial x^2} = \rho A\frac{\partial^2 u}{\partial t^2} \quad \text{for } 0 < x < L$$

with the following data: length of bar $L = 500$ mm, cross-sectional area $A = 1$ mm^2, modulus of elasticity $E = 20,000$ N/mm^2, density $\rho = 0.008$ kg/mm^3, $\gamma = 0.5$, and $\gamma = 0.5$. The boundary conditions are

$$u(0, t) = 0, \quad EA\frac{\partial u}{\partial x}(L, t) = 1 \text{ N}$$

Assume zero initial conditions. Using 20 linear elements and (a) $\Delta t = 0.002$ s and (b) $\Delta t = 0.0005$ s determine the axial displacement $u(x, t)$. Plot the displacement obtained with two different time steps as a function of position x for $t = 0.1$ s and $t = 0.2$ s and as a function of time t for $x = L$ m. Use newtons (N) and meters (m) in your input ($EA = 20 \times 10_3$ N and $\rho A = 8$ kg/m).

8.53 Consider a cantilevered beam of length $L = 30$ in., square cross section of 0.5 in. by 0.5 in., modulus $E = 30 \times 10^6$ psi, and density $\rho = 733 \times 10^{-6}$ lb/in.^{3}. A point load of $P_0 = 1000$ lb is applied at its free end (see Fig. P8.53). Find the finite element solution for the transverse deflection using eight Euler–

Bernoulli beam elements and $\Delta t = 10^{-6}$ s.

Fig. P8.53

8.54 Repeat **Problem 8.53** using four quadratic Timoshenko beam elements. Use $\nu = 0.3$.

8.55 Repeat **Problem 8.53** for a clamped beam with the load at the midspan (see Fig. P8.55). Use the same data as in **Problem 8.53**.

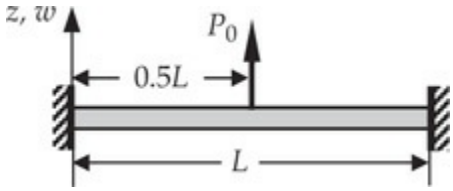

Fig. P8.55

8.56 Repeat **Problem 8.55** using four quadratic Timoshenko beam elements. Use $\nu = 0.3$.

References for Additional Reading

1. B. Carnahan, H.A. Luther, and J.O. Wilkes, *Applied Numerical Methods*, John Wiley, New York, 1969.
2. A.N. Loxan, N. Davids, and A. Levenson, "Table of the Zeros of the Legendre Polynomials of Order 1–16 and the Weight Coefficients for Gauss' Quadrature Formula," *Bulletin of the American Mathematical Society*, **48**, 739–743, 1942.
3. A.H. Stroud and D. Secrest, *Gaussian Quadrature Formulas*, Prentice–Hall, Englewood Cliffs, NJ, 1966.
4. S. Eskinazi, *Principles of Fluid Mechanics*, Allyn and Bacon, Boston, MA, 1962.
5. M.E. Harr, *Ground Water and Seepage*, McGraw–Hill, New York, NY, 1962.

6. A. Nadai, *Theory of Flow and Fracture of Solids*, vol. II, McGraw–Hill, New York, NY, 1963.
7. H. Schlichting, *Boundary-Layer Theory* (translated by J. Kestin), 7th ed., McGraw–Hill, New York, NY, 1979.
8. H.S. Carslaw and J.C. Jaeger, *Conduction of Heat in Solids*, Clarendon Press, Oxford, 1959.
9. J.P. Holoman, *Heat Transfer*, 6th ed., McGraw-Hill, New York, NY, 1986.
10. F. Kreith, *Principles of Heat Transfer*, 3rd ed., Harper & Row, New York, NY, 1973.
11. G.G. Myers, *Analytical Methods in Conduction Heat Transfer*, McGraw–Hill, New York, NY, 1972.
12. R.G. Budynas, *Advanced Strength and Applied Stress Analysis*, McGraw–Hill, New York, NY, 1977.
13. C.M. Harris and C.E. Crede, *Shock and Vibration Handbook*, Vol. 1, McGraw–Hill, New York, NY, 1961.
14. J.N. Reddy, *Energy Principles and Variational Methods in Applied Mechanics*, 3rd ed., John Wiley, New York, NY, 2018.
15. A.C. Ugural and S.K. Fenster, *Advanced Strength and Applied Elasticity*, Elsevier, New York, NY, 1975.

---

[1] In reality, the column vector of *Q*s does not exist in the computer; only when a particular *Q* is known (and the corresponding *U* will not be known), we add its specified value to the column of *F*s.

9 Single-Variable Problems in Two Dimensions

Research is to see what everybody else has seen, and to think what nobody else has thought.

— Albert Szent-Gyoergi

9.1 Introduction

Finite element analysis of two-dimensional problems involves the same basic steps as those described for one-dimensional problems discussed in Chapter 3. The analysis is somewhat complicated by the fact that two-dimensional problems are described by partial differential equations over geometrically complex regions. The boundary Γ of a two-dimensional domain Ω is, in general, a curve. Therefore, finite elements are simple two-dimensional geometric shapes that allow approximation of a given two-dimensional domain as well as the solution over it. Thus, in two-dimensional problems we not only seek an approximate solution to a given problem on a domain, but we also approximate the domain by a suitable finite element mesh. Consequently, we will have approximation errors due to the approximation of the solution as well as discretization errors due to the approximation of the domain in the finite element analysis of two-dimensional problems. The finite element mesh (discretization) consists of simple two-dimensional elements, such as triangles, rectangles, and/or quadrilaterals, that allow unique derivation of the interpolation functions. The elements are connected to each other at nodal points on the boundaries of the elements. The ability to represent domains with irregular geometries by a collection of finite elements makes the method a valuable practical tool for the solution of boundary, initial, and eigenvalue problems arising in various fields of engineering.

The objective of this chapter is to extend the basic steps discussed earlier for one-dimensional problems to two-dimensional boundary-value problems involving a single dependent variable. Once again, we describe the basic steps of the finite element analysis with a model second-order

partial differential equation, namely the Poisson equation, governing a single variable. This equation arises in a number of fields including electrostatics, heat transfer, fluid mechanics, and solid mechanics (see Table 9.1.1).

Table 9.1.1 Some examples of the Poisson equation $-\nabla \cdot (k\nabla u) = f$ in Ω.

Natural boundary condition: $k\dfrac{\partial u}{\partial n} + \beta(u - u_\infty) = q$ on Γ_q

Essential boundary condition: $u = \hat{u}$ on Γ_u

Field of application	Primary variable u	Material constant k	Source variable f	Secondary variables $\frac{\partial u}{\partial x}, \frac{\partial u}{\partial y}$
1. Heat transfer	Temperature T	Conductivity k	Heat source g	Heat flow due to conduction $k\frac{\partial T}{\partial n}$ convection $h(T - T_\infty)$
2. Irrotational flow of an ideal fluid	Stream function ψ	Density ρ	Mass production σ	Velocities $\frac{\partial \psi}{\partial x} = -v, \frac{\partial \psi}{\partial y} = u$
	Velocity potential ϕ	Density ρ	Mass production σ	$\frac{\partial \phi}{\partial x} = u, \frac{\partial \phi}{\partial y} = v$
3. Groundwater flow	Piezometric head ϕ	Permeability k	Recharge f (pumping, $-f$)	Seepage $q = k\frac{\partial \phi}{\partial n}$ Velocities $u = -k\frac{\partial \phi}{\partial x}, v = -k\frac{\partial \phi}{\partial y}$
4. Torsion of cylindrical members	Stress function Ψ	$k = 1$ G = shear modulus	$f = 2$ θ = angle of twist per unit length	$G\theta\frac{\partial \Psi}{\partial x} = -\sigma_{yz}$ $G\theta\frac{\partial \Psi}{\partial y} = \sigma_{xz}$
5. Electrostatics	Scalar potential ϕ	Dielectric constant ϵ	Charge density ρ	Displacement flux density D_n
6. Magnetostatics	Magnetic potential ϕ	Permeability μ	Charge density ρ	Magnetic flux density B_n
7. Membranes	Transverse deflection u	Tension in membrane T	Transversely distributed load	Normal force q

9.2 Boundary Value Problems

9.2.1 The Model Equation

Consider the problem of finding the solution $u(x, y)$ of the second-order partial differential equation

$$-\frac{\partial}{\partial x}\left(a_{11}\frac{\partial u}{\partial x}+a_{12}\frac{\partial u}{\partial y}\right)-\frac{\partial}{\partial y}\left(a_{21}\frac{\partial u}{\partial x}+a_{22}\frac{\partial u}{\partial y}\right)+a_{00}u-f=0 \tag{9.2.1}$$

for given data a_{ij} $(i, j = 1, 2)$, a_{00} and f, and specified boundary conditions. The form of the boundary conditions will be apparent from the weak formulation. As a special case, we can obtain the Poisson equation from (9.2.1) by setting $a_{11} = a_{22} = k(x, y)$ and $a_{12} = a_{21} = a_{00} = 0$:

$$-\nabla\cdot(k\nabla u)=f(x,y) \quad \text{in } \Omega \tag{9.2.2}$$

where ∇ is the gradient operator. If $\hat{\mathbf{e}}_x$ and $\hat{\mathbf{e}}_y$ denote the unit vectors directed along the x and y axes, respectively, the gradient operator in two dimensions can be expressed as [see Eq. (2.2.8)]

$$\nabla=\hat{\mathbf{e}}_x\frac{\partial}{\partial x}+\hat{\mathbf{e}}_y\frac{\partial}{\partial y}$$

and Eq. (9.2.2) in the Cartesian coordinate system takes the form

$$-\frac{\partial}{\partial x}\left(k\frac{\partial u}{\partial x}\right)-\frac{\partial}{\partial y}\left(k\frac{\partial u}{\partial y}\right)=f(x,y) \tag{9.2.3}$$

In the following, we shall develop the weak-form Galerkin finite element model of Eq. (9.2.1). The major steps are as follows:

1. Discretization of the domain into a set of finite elements.
2. Weak (or weighted-integral) formulation of the governing differential equation.
3. Derivation of finite element interpolation functions.
4. Development of the finite element model using the weak form.
5. Assembly of finite elements to obtain the global system of algebraic equations.
6. Imposition of boundary conditions.
7. Solution of equations.
8. Post-computation of solution and quantities of interest.

Steps 6 and 7 remain unchanged from one-dimensional finite element analysis because at the end of Step 5 we have a set of algebraic equations

whose form is independent of the dimension of the domain or nature of the problem. In the following sections, we discuss each step in detail.

9.2.2 Finite Element Discretization

In two dimensions there is more than one simple geometric shape that can be used as a finite element (see Fig. 9.2.1). As we shall see shortly, the interpolation functions depend not only on the number of nodes in the element and the number of unknowns per node, but also on the shape of the element. The shape of the element must be such that its geometry is uniquely defined by a set of points, which serve as the element nodes in the development of the interpolation functions. As will be discussed later in this section, a triangle is the simplest geometric shape, followed by a rectangle.

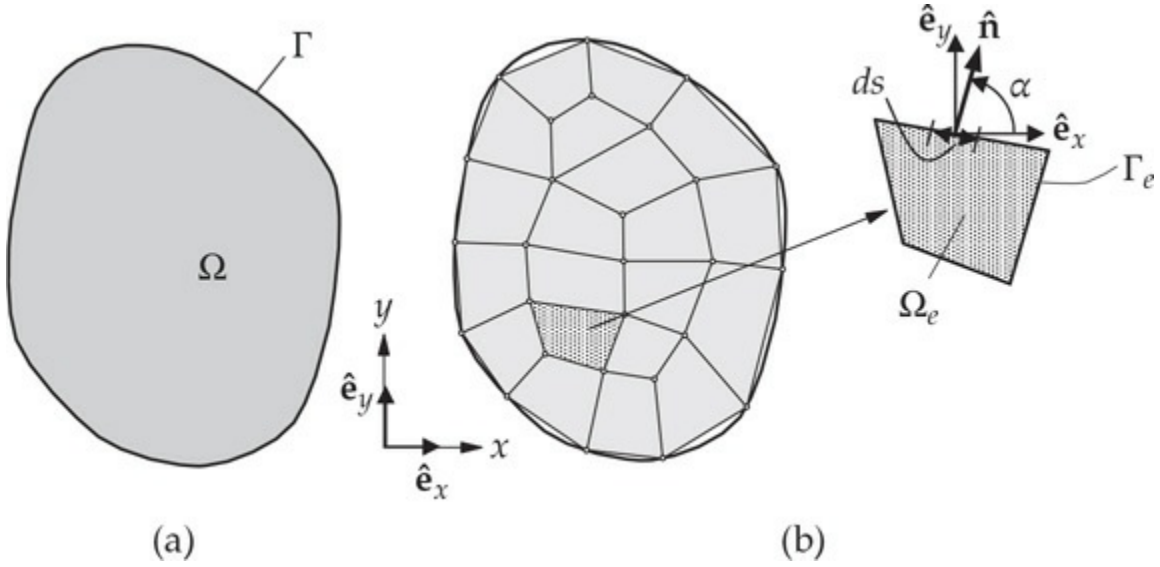

Fig. 9.2.1 Finite element discretization of an irregular domain. (a) Given domain Ω with boundary Γ. (b) Discretization of a domain by quadrilateral elements and a typical quadrilateral element Ω_e (with the unit normal $\hat{\mathbf{n}}$ on the boundary Γ_e of the element).

The representation of a given region by a set of elements (i.e., discretization or *mesh generation*) is an important step in finite element analysis. The choice of element type, number of elements, and density of elements depends on the geometry of the domain, the problem to be analyzed, and the degree of accuracy desired. Of course, there are no specific formulae to obtain this information. In general, the analyst is guided by his or her technical background, insight into the physics of the

problem being modeled (e.g., a qualitative understanding of the solution), and experience with finite element modeling. The general rules of mesh generation for finite element formulations include:

1. Select elements that characterize the governing equations of the problem.
2. The number, shape, and type (i.e., linear or quadratic) of elements should be such that the geometry of the domain is represented as accurately as desired.
3. The density of elements should be such that regions of large gradients of the solution are adequately modeled (i.e., use more elements or higher-order elements in regions of large gradients).
4. Mesh refinements should vary gradually from high-density regions to low-density regions. If *transition elements* are used, they should be used away from critical regions (i.e., regions of large gradients). Transition elements are those which connect lower-order elements to higher-order elements (e.g., linear to quadratic).

9.2.3 Weak Form

In the development of the weak form we need only consider a typical element. We assume that Ω_e is a typical element, whether triangular or quadrilateral, of the finite element mesh, and we develop the finite element model of Eq. (9.2.1) over Ω_e. Various two-dimensional elements will be discussed in the sequel.

Following the three-step procedure presented in Chapters 2 and 3, we develop the weak form of Eq. (9.2.1) over the typical element Ω_e. The first step is to multiply Eq. (9.2.1) with a weight function w, which is assumed to be differentiable once with respect to x and y, and then integrate the equation over the element domain Ω_e:

$$0 = \int_{\Omega_e} w \left[-\frac{\partial}{\partial x}(F_1) - \frac{\partial}{\partial y}(F_2) + a_{00}u - f \right] dx\, dy \tag{9.2.4a}$$

where

$$F_1 = a_{11}\frac{\partial u}{\partial x} + a_{12}\frac{\partial u}{\partial y}, \quad F_2 = a_{21}\frac{\partial u}{\partial x} + a_{22}\frac{\partial u}{\partial y} \tag{9.2.4b}$$

In the second step we distribute the differentiation among u and w equally.

To achieve this we integrate the first two terms in (9.2.4*a*) by parts. First we note the identities

$$\frac{\partial}{\partial x}(wF_1) = \frac{\partial w}{\partial x}F_1 + w\frac{\partial F_1}{\partial x} \quad \text{or} \quad -w\frac{\partial F_1}{\partial x} = \frac{\partial w}{\partial x}F_1 - \frac{\partial}{\partial x}(wF_1) \tag{9.2.5a}$$

$$\frac{\partial}{\partial y}(wF_2) = \frac{\partial w}{\partial y}F_2 + w\frac{\partial F_2}{\partial y} \quad \text{or} \quad -w\frac{\partial F_2}{\partial y} = \frac{\partial w}{\partial y}F_2 - \frac{\partial}{\partial y}(wF_2) \tag{9.2.5b}$$

Next, we use the component form of the gradient (or divergence) theorem

$$\int_{\Omega_e} \frac{\partial}{\partial x}(wF_1)dx\,dy = \oint_{\Gamma_e} wF_1 n_x\,ds \tag{9.2.6a}$$

$$\int_{\Omega_e} \frac{\partial}{\partial y}(wF_2)dx\,dy = \oint_{\Gamma_e} wF_2 n_y\,ds \tag{9.2.6b}$$

where n_x and n_y are the components (i.e., the direction cosines) of the unit normal vector

$$\hat{\mathbf{n}} = n_x\hat{\mathbf{e}}_x + n_y\hat{\mathbf{e}}_y = \cos\,\alpha\hat{\mathbf{e}}_x + \sin\,\alpha\hat{\mathbf{e}}_y \tag{9.2.7}$$

on the boundary Γ_e, and ds is the length of an infinitesimal line element along the boundary [see Fig. 9.2.1(b)]. Using Eqs. (9.2.5a), (9.2.5b), (9.2.6a) and (9.2.6b) in Eq. (9.2.4a), we obtain

$$\begin{aligned} 0 = &\int_{\Omega_e} \left[\frac{\partial w}{\partial x}\left(a_{11}\frac{\partial u}{\partial x} + a_{12}\frac{\partial u}{\partial y}\right) + \frac{\partial w}{\partial y}\left(a_{21}\frac{\partial u}{\partial x} + a_{22}\frac{\partial u}{\partial y}\right) + a_{00}wu - wf\right]dx\,dy \\ &- \oint_{\Gamma_e} w\left[n_x\left(a_{11}\frac{\partial u}{\partial x} + a_{12}\frac{\partial u}{\partial y}\right) + n_y\left(a_{21}\frac{\partial u}{\partial x} + a_{22}\frac{\partial u}{\partial y}\right)\right]ds \end{aligned} \tag{9.2.8}$$

From an inspection of the boundary integral in Eq. (9.2.8), we note that the coefficient of the weight function in the boundary expression is

$$q_n \equiv n_x\left(a_{11}\frac{\partial u}{\partial x} + a_{12}\frac{\partial u}{\partial y}\right) + n_y\left(a_{21}\frac{\partial u}{\partial x} + a_{22}\frac{\partial u}{\partial y}\right) \tag{9.2.9a}$$

Hence, q_n is the secondary variable and its specification constitutes the natural boundary condition. Mathematically, q_n is the projection of the flux vector **q**

along the unit normal vector $\hat{\mathbf{n}} = \hat{\mathbf{e}}_x n_x + \hat{\mathbf{e}}_y n_y$:

$$q_n = \hat{\mathbf{n}} \cdot \mathbf{q}, \quad \mathbf{q} = \hat{\mathbf{e}}_x \left(a_{11} \frac{\partial u}{\partial x} + a_{12} \frac{\partial u}{\partial y} \right) + \hat{\mathbf{e}}_y \left(a_{21} \frac{\partial u}{\partial x} + a_{22} \frac{\partial u}{\partial y} \right) \tag{9.2.9b}$$

Thus, q_n is the flux normal to the boundary ($q_n\, ds$ is the heat). By definition, q_n is taken positive outward (because $\hat{\mathbf{n}}$ is positive outward as we move in the counter-clockwise direction along the boundary Γ_e.) In most problems, the secondary variable q_n is of physical interest. For example, in the case of heat transfer through an anisotropic medium, a_{ij} are the conductivities of the medium and q_n is the negative of the heat flux (because of the Fourier heat conduction law) normal to the boundary of the element. The primary variable that is dual to $q_n\, ds$ (heat) is the temperature u, whose specification constitutes the essential boundary condition.

The third and last step of the formulation is to use the definition in Eq. (9.2.9a) to rewrite Eq. (9.2.8) as

$$0 = \int_{\Omega_e} \left[\frac{\partial w}{\partial x} \left(a_{11} \frac{\partial u}{\partial x} + a_{12} \frac{\partial u}{\partial y} \right) + \frac{\partial w}{\partial y} \left(a_{21} \frac{\partial u}{\partial x} + a_{22} \frac{\partial u}{\partial y} \right) + a_{00} w u - w f \right] dx\, dy - \oint_{\Gamma_e} w q_n\, ds \tag{9.2.10}$$

or

$$B^e(w, u) = l^e(w) \tag{9.2.11a}$$

where the bilinear form $B^e(\cdot\,, \cdot)$ and linear form $l^e(\cdot)$ are

$$B^e(w, u) = \int_{\Omega_e} \left[\frac{\partial w}{\partial x} \left(a_{11} \frac{\partial u}{\partial x} + a_{12} \frac{\partial u}{\partial y} \right) + \frac{\partial w}{\partial y} \left(a_{21} \frac{\partial u}{\partial x} + a_{22} \frac{\partial u}{\partial y} \right) + a_{00} w u \right] dx\, dy$$

$$l^e(w) = \int_{\Omega_e} w f\, dx\, dy + \oint_{\Gamma_e} w q_n\, ds \tag{9.2.11b}$$

The weak form (or *weighted-integral statement*) in Eq. (9.2.10) is the basis of the finite element model of Eq. (9.2.1).

Whenever $B^e(w, u)$ is symmetric in its arguments w and u [i.e., $B^e(w, u) = B^e(u, w)$], the quadratic functional associated with the variational problem (9.2.11a) can be obtained from [see Eq. (2.4.25)]

$$I^e(w) = \frac{1}{2} B^e(w, w) - l^e(w) \tag{9.2.12a}$$

The bilinear form in Eq. (9.2.11b) is symmetric if and only if $a_{12} = a_{21}$. Then the functional is given by

$$I^e(w) = \frac{1}{2} \int_{\Omega_e} \left[a_{11} \left(\frac{\partial u}{\partial x} \right)^2 + 2a_{12} \frac{\partial u}{\partial x} \frac{\partial u}{\partial y} + a_{22} \left(\frac{\partial u}{\partial y} \right)^2 + a_{00} u^2 \right] dxdy$$
$$- \int_{\Omega_e} uf dxdy - \oint_{\Gamma_e} uq_n \, ds \tag{9.2.12b}$$

9.2.4 Vector Form of the Variational Problem

It is common, especially in structural mechanics literature, to express finite element formulations in vector notation (i.e., in terms of matrices). While the vector/matrix notation is concise, it is not as transparent as the explicit form that has been used throughout the book. However, for the sake of completeness, the vector form of the variational (or weak) problem described by Eqs. (9.2.11a) and (9.2.11b) is presented here. We shall use bold face letters for matrices of different order, including 1 × 1 matrix and row and column matrices (see Section 2.2.4).

We begin with Eq. (9.2.11a), which can be written as

$$B^e(\mathbf{w}, \mathbf{u}) = l^e(\mathbf{w}) \tag{9.2.13}$$

where, in the present case, **w** is simply w and **u** is u. Next, we express $B^e(\cdot\,, \cdot)$ and

$$\mathbf{C} = \begin{bmatrix} a_{11} & a_{12} & 0 \\ a_{12} & a_{22} & 0 \\ 0 & 0 & a_{00} \end{bmatrix}, \quad \mathbf{D} = \begin{Bmatrix} \dfrac{\partial}{\partial x} \\ \dfrac{\partial}{\partial y} \\ 1 \end{Bmatrix} \tag{9.2.14}$$

Then B^e and l^e of Eq. (9.2.11b) can be expressed as

$$B^e(w, u) = \int_{\Omega_e} \begin{Bmatrix} \dfrac{\partial w}{\partial x} \\ \dfrac{\partial w}{\partial y} \\ w \end{Bmatrix}^{\mathrm{T}} \begin{bmatrix} a_{11} & a_{12} & 0 \\ a_{12} & a_{22} & 0 \\ 0 & 0 & a_{00} \end{bmatrix} \begin{Bmatrix} \dfrac{\partial u}{\partial x} \\ \dfrac{\partial u}{\partial y} \\ u \end{Bmatrix} dxdy \tag{9.2.15a}$$

$$l^e(w) = \int_{\Omega_e} \{w\}^{\mathrm{T}}\{f\}\, dxdy + \oint_{\Gamma_e} \{w\}^{\mathrm{T}}\{q_n\}\, ds \tag{9.2.15b}$$

or, simply

$$B^e(\mathbf{w},\mathbf{u}) = \int_{\Omega_e} (\mathbf{Dw})^{\mathrm{T}}\mathbf{CDu}\, dxdy, \quad l^e(\mathbf{w}) = \int_{\Omega_e} \mathbf{w}^{\mathrm{T}}\mathbf{f}\, dxdy + \int_{\Gamma_e} \mathbf{w}^{\mathrm{T}}\mathbf{q}\, ds \tag{9.2.15c}$$

9.2.5 Finite Element Model

The weak form in Eq. (9.2.10) requires that the approximation chosen for u should be at least linear in both x and y so that there are no terms in Eq. (9.2.10) which are identically zero. Since the primary variable is simply the function itself, the Lagrange family of interpolation functions is admissible.

Suppose that u is approximated over a typical finite element Ω_e by the expression

$$u(x,y) \approx u_h^e(x,y) = \sum_{j=1}^{n} u_j^e \psi_j^e(x,y) \quad \text{or} \quad u_h^e(x,y) = (\mathbf{\Psi}^e)^{\mathrm{T}}\mathbf{u}^e \tag{9.2.16a}$$

where $\mathbf{u}^e$ and $\mathbf{\Psi}^e$ are $n \times 1$ vectors

$$\mathbf{u}^e = \{u_1^e\ u_2^e\ u_3^e \ldots\ u_n^e\}^{\mathrm{T}}, \quad \mathbf{\Psi}^e = \{\psi_1^e\ \psi_2^e\ \psi_3^e \ldots\ \psi_n^e\}^{\mathrm{T}} \tag{9.2.16b}$$

and u_j^e is the value of u_h^e at the jth node (x_j, y_j) of the element and ψ_j^e are the Lagrange interpolation functions, with the property

$$\psi_i^e(x_j, y_j) = \delta_{ij} \quad (i,j = 1,2,\ldots,n) \tag{9.2.17}$$

In deriving the finite element equations in algebraic terms, we need not know the shape of the element Ω_e or the form of ψ_i^e. The specific form of ψ_i^e will be developed for triangular and rectangular geometries of the element Ω_e in Section 9.2.6 and higher-order interpolation functions will be presented in Chapter 10.

Substituting the finite element approximation in Eq. (9.2.16a) for u into the weak form (9.2.10) or (9.2.13), we obtain

$$0=\int_{\Omega_e}\left[\frac{\partial w}{\partial x}\left(a_{11}\sum_{j=1}^{n}u_j^e\frac{\partial\psi_j^e}{\partial x}+a_{12}\sum_{j=1}^{n}u_j^e\frac{\partial\psi_j^e}{\partial y}\right)+\frac{\partial w}{\partial y}\left(a_{21}\sum_{j=1}^{n}u_j^e\frac{\partial\psi_j^e}{\partial x}+a_{22}\sum_{j=1}^{n}u_j^e\frac{\partial\psi_j^e}{\partial y}\right)+a_{00}w\sum_{j=1}^{n}u_j^e\psi_j^e-wf\right]dx\,dy-\oint_{\Gamma_e}wq_n\,ds \tag{9.2.18a}$$

or

$$0=\int_{\Omega_e}(\mathbf{Dw})^{\mathrm{T}}\mathbf{CD}\left(\mathbf{\Psi}^{\mathrm{T}}\mathbf{u}^e\right)dxdy-\int_{\Omega_e}\mathbf{w}^{\mathrm{T}}\mathbf{f}\,dxdy-\oint_{\Gamma_e}\mathbf{w}^{\mathrm{T}}\mathbf{q}\,ds \tag{9.2.18b}$$

This equation must hold for every admissible choice of weight function w. Since we need n independent algebraic equations to solve for the n unknowns, $u_1^e, u_2^e, \ldots, u_n^e$, we choose n linearly independent functions for w: $w=\psi_1^e,\psi_2^e,\ldots,\psi_n^e$ (or, $\mathbf{w}=\{\psi_1^e\ \psi_2^e\ \ldots\ \psi_n^e\}=\mathbf{\Psi}^{\mathrm{T}}$). This particular choice of weight function is a natural one when the weight function is viewed as a virtual variation of the dependent unknown (i.e., $w=\delta u\approx\sum_{i=1}^{n}\delta u_i\psi_i$), and the resulting finite element model is known as the *weak-form Galerkin finite element model* or *Ritz finite element model*.

For each choice of w we obtain an algebraic relation among $(u_1^e, u_2^e, \ldots, u_n^e)$. We label the algebraic equation resulting from substitution of ψ_1^e for w into Eq. (9.2.18a) as the first algebraic equation, that resulting from $w=\psi_2^e$ as the second equation, and so on. Thus, the ith algebraic equation is obtained by substituting $w=\psi_i^e$ into Eq. (9.2.18a):

$$0=\sum_{j=1}^{n}\left\{\int_{\Omega_e}\left[\frac{\partial\psi_i^e}{\partial x}\left(a_{11}\frac{\partial\psi_j^e}{\partial x}+a_{12}\frac{\partial\psi_j^e}{\partial y}\right)+\frac{\partial\psi_i^e}{\partial y}\left(a_{21}\frac{\partial\psi_j^e}{\partial x}+a_{22}\frac{\partial\psi_j^e}{\partial y}\right)+a_{00}\psi_i^e\psi_j^e\right]dx\,dy\right\}u_j^e-\int_{\Omega_e}f\psi_i^e\,dx\,dy-\oint_{\Gamma_e}\psi_i^e q_n\,ds$$

or

$$\sum_{j=1}^{n}K_{ij}^e u_j^e=f_i^e+Q_i^e\quad(i=1,2,\ldots,n) \tag{9.2.19a}$$

where

$$K_{ij}^e = \int_{\Omega_e} \left[\frac{\partial \psi_i^e}{\partial x} \left(a_{11} \frac{\partial \psi_j^e}{\partial x} + a_{12} \frac{\partial \psi_j^e}{\partial y} \right) + \frac{\partial \psi_i^e}{\partial y} \left(a_{21} \frac{\partial \psi_j^e}{\partial x} + a_{22} \frac{\partial \psi_j^e}{\partial y} \right) + a_{00} \psi_i^e \psi_j^e \right] dx\, dy \tag{9.2.19b}$$

$$f_i^e = \int_{\Omega_e} f \psi_i^e \, dx\, dy, \quad Q_i^e = \oint_{\Gamma_e} q_n \psi_i^e \, ds \tag{9.2.19c}$$

In matrix notation, Eq. (9.2.19a) takes the form

$$\mathbf{K}^e \mathbf{u}^e = \mathbf{f}^e + \mathbf{Q}^e \tag{9.2.20a}$$

where

$$\mathbf{K}^e = \int_{\Omega_e} \mathbf{B}^{\mathrm{T}} \mathbf{C} \mathbf{B} \, dx dy, \quad \mathbf{f}^e = \int_{\Omega_e} \boldsymbol{\Psi} \mathbf{f} \, ds, \quad \mathbf{Q}^e = \int_{\Gamma_e} \boldsymbol{\Psi} \mathbf{q} \, ds$$

$$\mathbf{B} = \mathbf{D} \boldsymbol{\Psi}^{\mathrm{T}} = \begin{bmatrix} \psi_{1,x}^e & \psi_{2,x}^e & \cdots & \psi_{n,x}^e \\ \psi_{1,y}^e & \psi_{2,y}^e & \cdots & \psi_{n,y}^e \\ \psi_1^e & \psi_2^e & \cdots & \psi_n^e \end{bmatrix} \tag{9.2.20b}$$

Note that $K_{ij}^e = K_{ji}^e$ (i.e., $[K^e]$ is a symmetric matrix of order $n \times n$) only when $a_{12} = a_{21}$. Equations (9.2.20a) and (9.2.20b) represent the finite element model of Eq. (9.2.1). This completes the finite element model development. Before we discuss assembly of element equations, it is informative to consider the derivation of the interpolations ψ_i^e for certain basic elements and the evaluation of the element matrices in Eq. (9.2.19b) and force vectors in Eq. (9.2.19c).

9.2.6 Derivation of Interpolation Functions

Approximation functions (also termed *interpolation functions* because they satisfy the interpolation property) are derived only for the so-called "master elements" associated with arbitrary triangles and quadrilaterals. It is important to note that we cannot derive approximation functions explicitly for an arbitrary quadrilateral element. The master elements are the ones where the element coefficients K_{ij}^e and f_i^e are evaluated by

rewriting them in terms of the local coordinates used in the master elements. That is, the integral expressions K_{ij}^e and f_i^e that are defined over actual geometries of triangles and quadrilaterals will be transformed to those posed on the master elements and then a numerical integration rule, such as the Gauss quadrature discussed in Chapter 7, is used to evaluate them. Thus, in reality, we only need to develop interpolation functions for the master elements. Details will be presented in Chapter 10. The derivations of ψ_i^e presented in this chapter for an arbitrary triangle and a specific rectangle are only to illustrate the procedure of deriving them (which will be extended to the master elements).

The finite element approximation $u_h^e(x, y)$ over an element Ω_e must satisfy the following conditions in order for the approximate solution to be convergent to the true solution:

1. The primary variable u_h^e must be continuous as required in the weak form of the problem (i.e., all terms in the weak form are represented as nonzero values).
2. The polynomials used to represent u_h^e must be complete (i.e., all terms, beginning with a constant term up to the highest-order used in the polynomial, should be included in u_h^e).
3. All terms in the polynomial should be such that both x and y are represented in the same form and be linearly independent.

The number of linearly independent terms in the representation of u_h^e dictates the shape and number of degrees of freedom of the element. Here, we present interpolation functions for a linear triangle and a linear rectangle.

9.2.6.1 Triangular element

An examination of the weak form in Eq. (9.2.10) and the finite element matrices in Eq. (9.2.19b) shows that ψ_i^e should be at least linear functions of x and y. The complete linear polynomial in x and y in Ω_e is of the form

$$u_h^e(x, y) = c_1^e + c_2^e x + c_3^e y \tag{9.2.21}$$

where c_i^e are constants. The set $\{1, x, y\}$ is linearly independent and complete. Equation (9.2.21) defines a unique plane for fixed c_i^e. Thus, if $u(x, y)$ is a curved surface, $u_h^e(x, y)$ approximates the surface by a plane (see Fig. 9.2.2). In particular, $u_h^e(x, y)$ is uniquely defined on a triangle by

the three nodal values of $u_h^e(x, y)$; three nodes are placed at the vertices of the triangle so that the geometry of the triangle is uniquely defined, and the nodes are *numbered in counterclockwise direction*, as shown in Fig. 9.2.2, so that the unit normal always points upward from the domain. Let

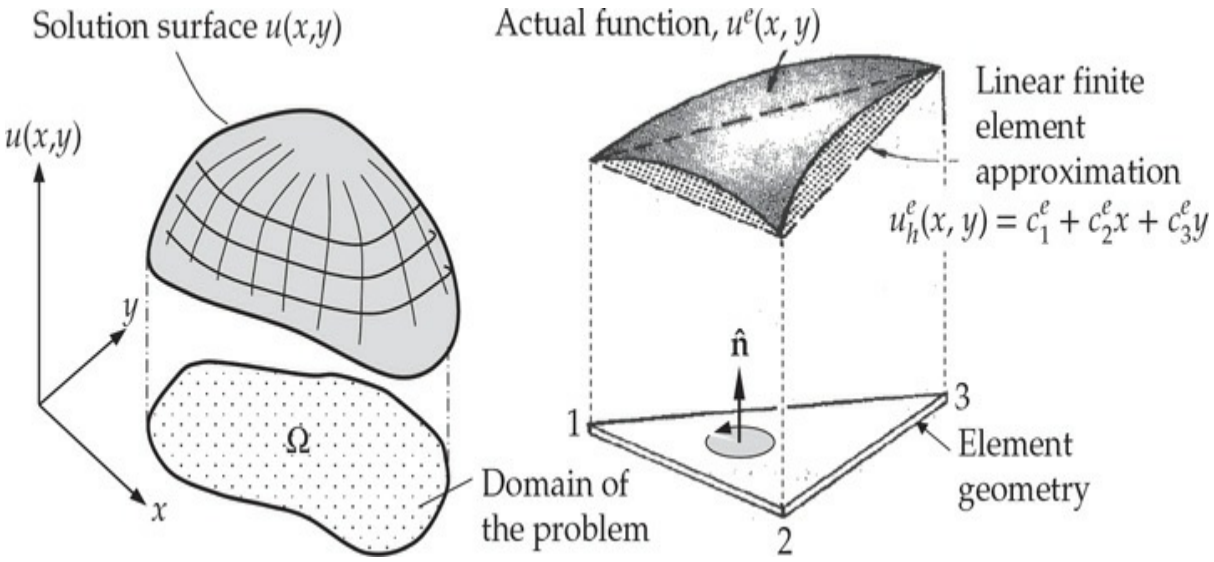

Fig. 9.2.2 Approximation of a curved surface over a triangle by a plane.

$$u_h^e(x_1, y_1) = u_1^e, \quad u_h^e(x_2, y_2) = u_2^e, \quad u_h^e(x_3, y_3) = u_3^e \tag{9.2.22}$$

where (x_i, y_i) denote the coordinates of the ith vertex of the triangle. Note that the triangle is uniquely defined by the three pairs of coordinates (x_i, y_i).

The three constants $c_i^e (i = 1, 2, 3)$ in Eq. (9.2.21) can be expressed in terms of three nodal values $u_i^e (i = 1, 2, 3)$. Thus, the polynomial in Eq. (9.2.21) is associated with a triangular element and there are three nodes identified, namely, the vertices of the triangle. Equations in (9.2.22) have the explicit form

$$\begin{aligned} u_1 &\equiv u_h(x_1, y_1) = c_1 + c_2 x_1 + c_3 y_1 \\ u_2 &\equiv u_h(x_2, y_2) = c_1 + c_2 x_2 + c_3 y_2 \\ u_3 &\equiv u_h(x_3, y_3) = c_1 + c_2 x_3 + c_3 y_3 \end{aligned}$$

where the element label e is omitted for simplicity. In matrix form, we have

$$\begin{Bmatrix} u_1 \\ u_2 \\ u_3 \end{Bmatrix} = \begin{bmatrix} 1 & x_1 & y_1 \\ 1 & x_2 & y_2 \\ 1 & x_3 & y_3 \end{bmatrix} \begin{Bmatrix} c_1 \\ c_2 \\ c_3 \end{Bmatrix} \quad \text{or} \quad \mathbf{u} = \mathbf{A}\mathbf{c} \tag{9.2.23}$$

Solution of Eq. (9.2.23) for c_i (i = 1, 2, 3) requires the inversion of the coefficient matrix **A** in Eq. (9.2.23). The inverse ceases to exist whenever any two rows or columns are the same. Two rows or columns of the coefficient matrix in Eq. (9.2.23) will be the same only when any two nodes have the same coordinates. Thus, in theory, as long as the three vertices of the triangle are distinct and do not lie on a line, the coefficient matrix is invertible. However, in actual computations, if any two of the three nodes are *very close* to each other or the three nodes are almost on a line, the coefficient matrix can be *nearly singular* and numerically non-invertible. Hence one should avoid elements with narrow geometries (see Fig. 9.2.3) in finite element meshes.

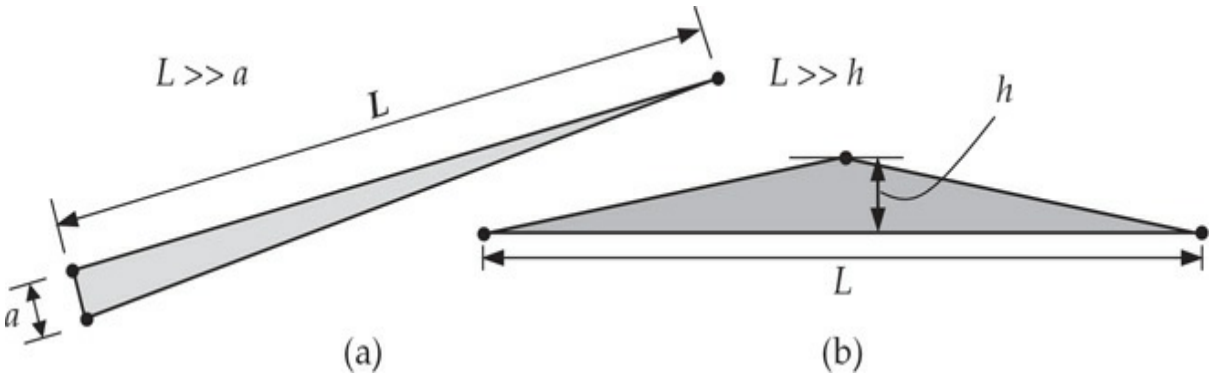

Fig. 9.2.3 Triangular geometries that should be avoided in finite element meshes.

The inverse of the coefficient matrix **A** of Eq. (9.2.23) is of the form

$$\mathbf{A}^{-1} = \frac{1}{2A}\begin{bmatrix} \alpha_1 & \alpha_2 & \alpha_3 \\ \beta_1 & \beta_2 & \beta_3 \\ \gamma_1 & \gamma_2 & \gamma_3 \end{bmatrix}, \quad 2A = \alpha_1 + \alpha_2 + \alpha_3 \tag{9.2.24a}$$

where 2A is the determinant of the matrix **A**, A being the area of the triangle whose three vertices are at (x_i, y_i) (i = 1, 2, 3), and α_i, β_i, and γ_i are constants which depend only on the global coordinates of element nodes (x_i, y_i):

$$\left.\begin{aligned}\alpha_i &= x_j y_k - x_k y_j \\ \beta_i &= y_j - y_k \\ \gamma_i &= -(x_j - x_k)\end{aligned}\right\} \quad (i \neq j \neq k;\ i, j \text{ and } k \text{ permute in a natural order}) \qquad (9.2.24b)$$

Solving Eq. (9.2.23) for **c** (i.e., $\mathbf{c} = \mathbf{A}^{-1}\,\mathbf{u}$), we obtain

$$\begin{aligned} c_1 &= \frac{1}{2A}(\alpha_1 u_1 + \alpha_2 u_2 + \alpha_3 u_3) \\ c_2 &= \frac{1}{2A}(\beta_1 u_1 + \beta_2 u_2 + \beta_3 u_3) \\ c_3 &= \frac{1}{2A}(\gamma_1 u_1 + \gamma_2 u_2 + \gamma_3 u_3) \end{aligned} \qquad (9.2.24c)$$

Substituting for c_i from Eq. (9.2.24c) into Eq. (9.2.21), we obtain

$$\begin{aligned} u_h^e(x,y) = \frac{1}{2A}[&(u_1\alpha_1 + u_2\alpha_2 + u_3\alpha_3) + (u_1\beta_1 + u_2\beta_2 + u_3\beta_3)x \\ &+ (\gamma_1 u_1 + \gamma_2 u_2 + \gamma_3 u_3)y] = \sum_{i=1}^{3} u_i^e \psi_i^e(x,y) \end{aligned} \qquad (9.2.25a)$$

where ψ_i^e are the linear interpolation functions for the triangular element

$$\psi_i^e = \frac{1}{2A_e}(\alpha_i^e + \beta_i^e x + \gamma_i^e y) \quad (i = 1, 2, 3) \qquad (9.2.25b)$$

and α_i^e, β_i^e, and γ_i^e are the constants defined in Eq. (9.2.24b). The linear interpolation functions ψ_i^e are shown in Fig. 9.2.4.

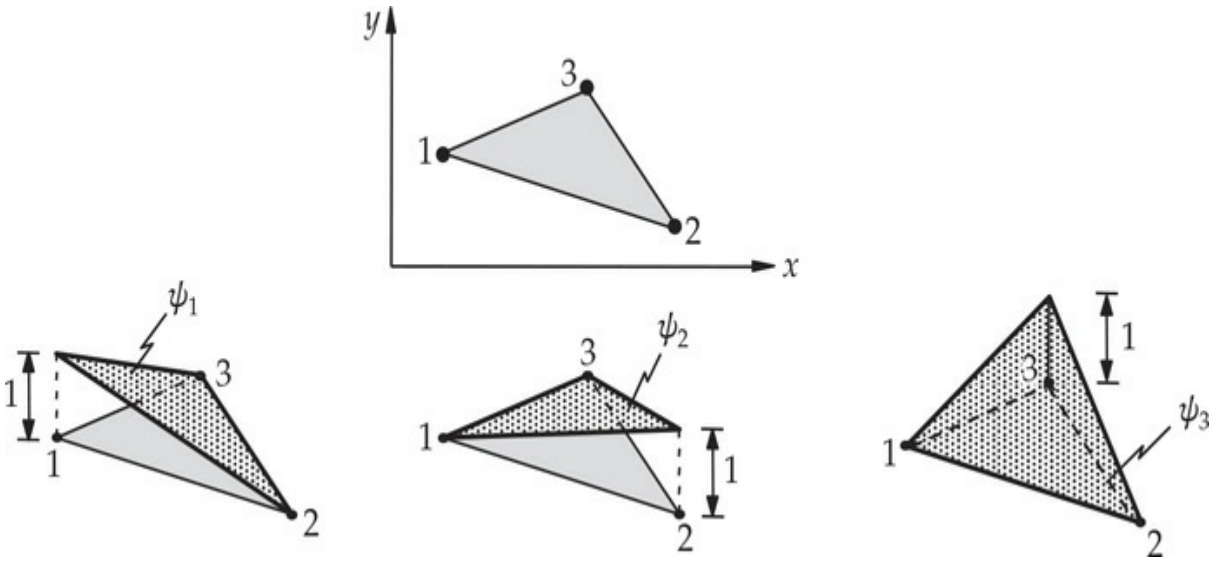

Fig. 9.2.4 Interpolation functions for the three-node triangle.

The interpolation functions ψ_i^e have the properties

$$\psi_i^e(x_j^e, y_j^e) = \delta_{ij} \quad (i,j=1,2,3) \tag{9.2.26a}$$

$$\sum_{i=1}^{3} \psi_i^e = 1, \quad \sum_{i=1}^{3} \frac{\partial \psi_i^e}{\partial x} = 0, \quad \sum_{i=1}^{3} \frac{\partial \psi_i^e}{\partial y} = 0 \tag{9.2.26b}$$

Note that Eq. (9.2.25a) determines a plane surface passing through u_1, u_2, and u_3. Hence, use of the linear interpolation functions ψ_i^e of a triangle will result in the approximation of the curved surface $u(x, y)$ by a planar function $u_h^e = \sum_{i=1}^{3} u_i^e \psi_i^e$ as shown in Fig. 9.2.5. We consider an example of computing ψ_i^e.

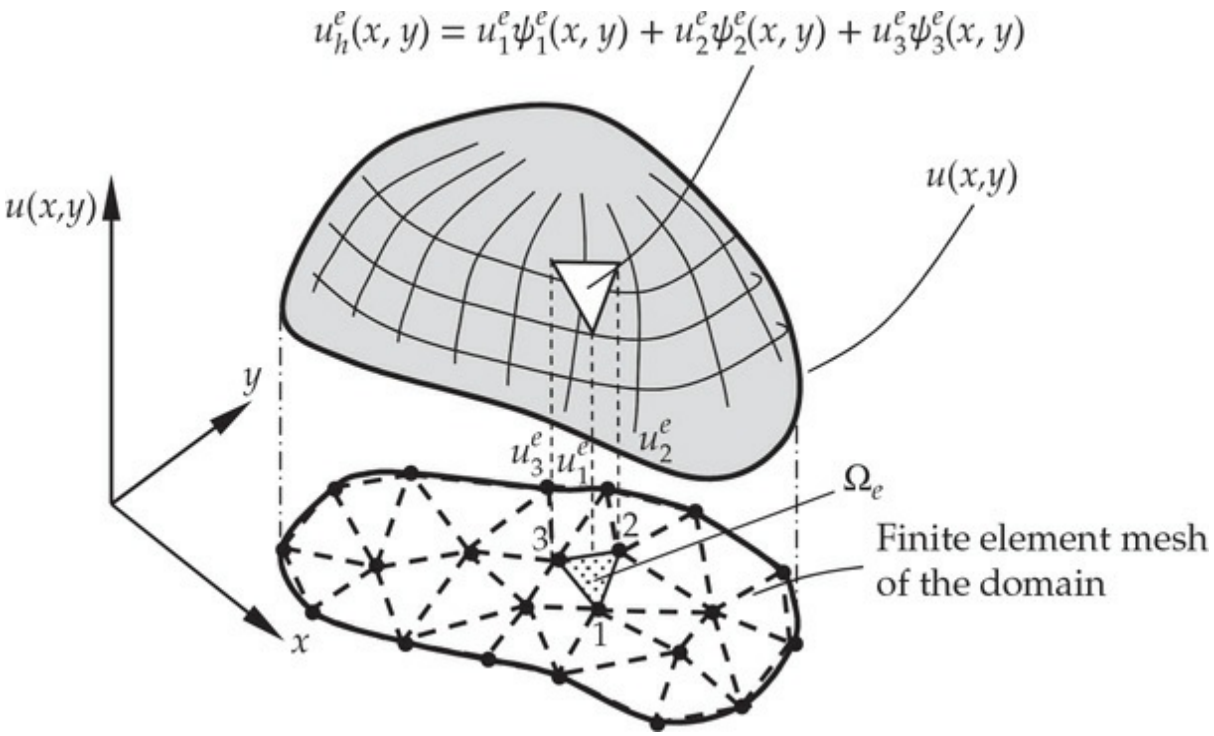

Fig. 9.2.5 Representation of a continuous function $u(x,y)$ by linear interpolation functions of three-node triangular elements.

Example 9.2.1

Consider the triangular element shown in Fig. 9.2.6. Determine the linear approximation functions.

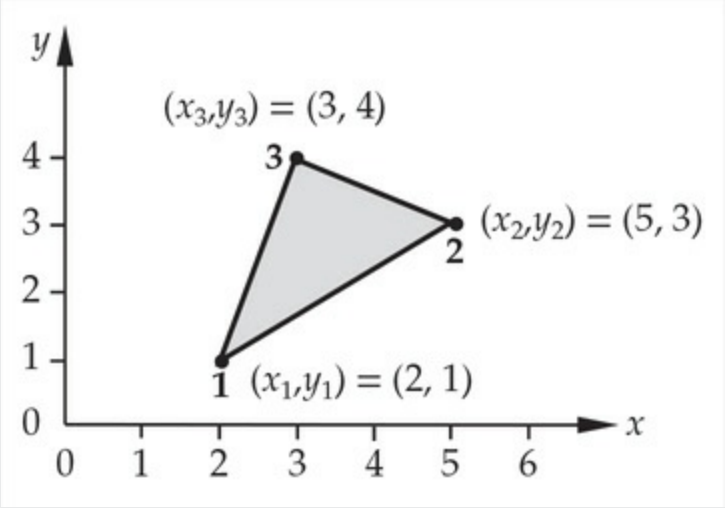

Fig. 9.2.6 The triangular element of **Example 9.2.1**.

Solution: We begin with

$$u_h(x, y) = c_1 + c_2x + c_3y$$

Evaluating this polynomial at nodes 1, 2 and 3, we obtain the equations

$$\begin{Bmatrix} u_1 \\ u_2 \\ u_3 \end{Bmatrix} = \begin{bmatrix} 1 & 2 & 1 \\ 1 & 5 & 3 \\ 1 & 3 & 4 \end{bmatrix} \begin{Bmatrix} c_1 \\ c_2 \\ c_3 \end{Bmatrix}, \quad \begin{Bmatrix} c_1 \\ c_2 \\ c_3 \end{Bmatrix} = [A]^{-1} \begin{Bmatrix} u_1 \\ u_2 \\ u_3 \end{Bmatrix}$$

where

$$[A]^{-1} = \begin{bmatrix} 1 & 2 & 1 \\ 1 & 5 & 3 \\ 1 & 3 & 4 \end{bmatrix}^{-1} = \frac{1}{7} \begin{bmatrix} 11 & -5 & 1 \\ -1 & 3 & -2 \\ -2 & -1 & 3 \end{bmatrix}$$

Substituting the last expression into u_h, we obtain

$$u_h(x,y) = \{1 \;\; x \;\; y\} \begin{Bmatrix} c_1 \\ c_2 \\ c_3 \end{Bmatrix} = \{ \; 1 \;\; x \;\; y \; \} [A]^{-1} \begin{Bmatrix} u_1 \\ u_2 \\ u_3 \end{Bmatrix}$$

$$= \frac{1}{7} \{11 - x - 2y, \;\; -5 + 3x - y, \;\; 1 - 2x + 3y\} \begin{Bmatrix} u_1 \\ u_2 \\ u_3 \end{Bmatrix}$$

$$\equiv \{ \; \psi_1^e \;\; \psi_2^e \;\; \psi_3^e \; \} \begin{Bmatrix} u_1 \\ u_2 \\ u_3 \end{Bmatrix} = \sum_{i=1}^{3} \psi_i^e u_i^e$$

where

$$\psi_1^e = \tfrac{1}{7}(11 - x - 2y), \quad \psi_2^e = \tfrac{1}{7}(-5 + 3x - y), \quad \psi_3^e = \tfrac{1}{7}(1 - 2x + 3y)$$

Alternatively, from definitions in Eq. (9.2.24b), we have

$$\alpha_1 = 5 \times 4 - 3 \times 3 = 11, \quad \alpha_2 = 3 \times 1 - 2 \times 4 = -5, \quad \alpha_3 = 2 \times 3 - 5 \times 1 = 1$$

$$\beta_1 = 3 - 4 = -1, \quad \beta_2 = 4 - 1 = 3, \quad \beta_3 = 1 - 3 = -2$$

$$\gamma_1 = -(5 - 3) = -2, \quad \gamma_2 = -(3 - 2) = -1, \quad \gamma_3 = -(2 - 5) = 3$$

$$2A = \alpha_1 + \alpha_2 + \alpha_3 = 7$$

The interpolation functions are

$$\psi_1^e = \frac{1}{7}(11 - x - 2y), \quad \psi_2^e = \frac{1}{7}(-5 + 3x - y), \quad \psi_3^e = \frac{1}{7}(1 - 2x + 3y)$$

which are the same as those obtained earlier.

9.2.6.2 Linear rectangular element

Next, consider the complete polynomial

$$u_h^e(x, y) = c_1^e + c_2^e x + c_3^e y + c_4^e xy \tag{9.2.27}$$

which contains four linearly independent terms, and is linear in x and y, with a bilinear term in x and y. This polynomial requires an element with four nodes. There are two possible geometric shapes: a triangle with the fourth node at the center (or centroid) of the triangle, or a rectangle with the nodes at the vertices. A triangle with a fourth node at the center does not provide a single-valued variation of u at interelement boundaries, resulting in *incompatible* variation of u at interelement boundaries, and is therefore not admissible (see Fig. 9.2.7). The linear rectangular element is a compatible element because on any side u_h^e varies only linearly and there are two nodes to uniquely define it.

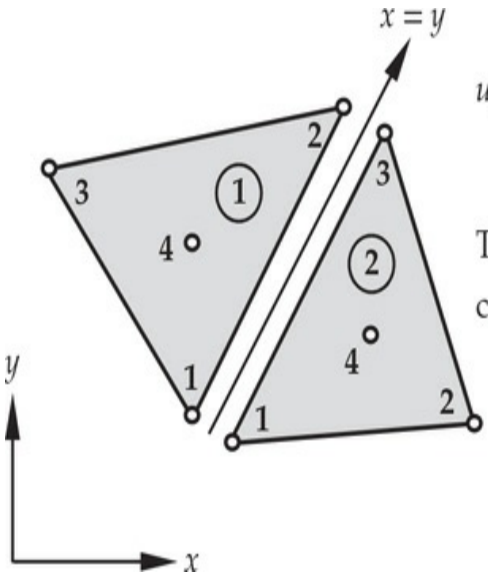

$$u_h(x, y) = c_1^{(e)} + c_2^{(e)}x + c_3^{(e)}y + c_4^{(e)}xy$$
$$= c_1^{(e)} + (c_2^{(e)} + c_3^{(e)})x + c_4^{(e)}x^2 \quad (e = 1,2)$$

Thus, the quadratic variation of u_h along $x = y$ cannot be defined uniquely with only two nodal values.

Fig. 9.2.7 Incompatible four-node triangular elements.

Here we consider an approximation of the form Eq. (9.2.27) and use a rectangular element with sides *a* and *b* [see Fig. 9.2.8(a)]. For the sake of convenience, we choose a local coordinate system $(\bar{x}, \bar{y})$ to derive the interpolation functions. We assume that (element label is omitted)

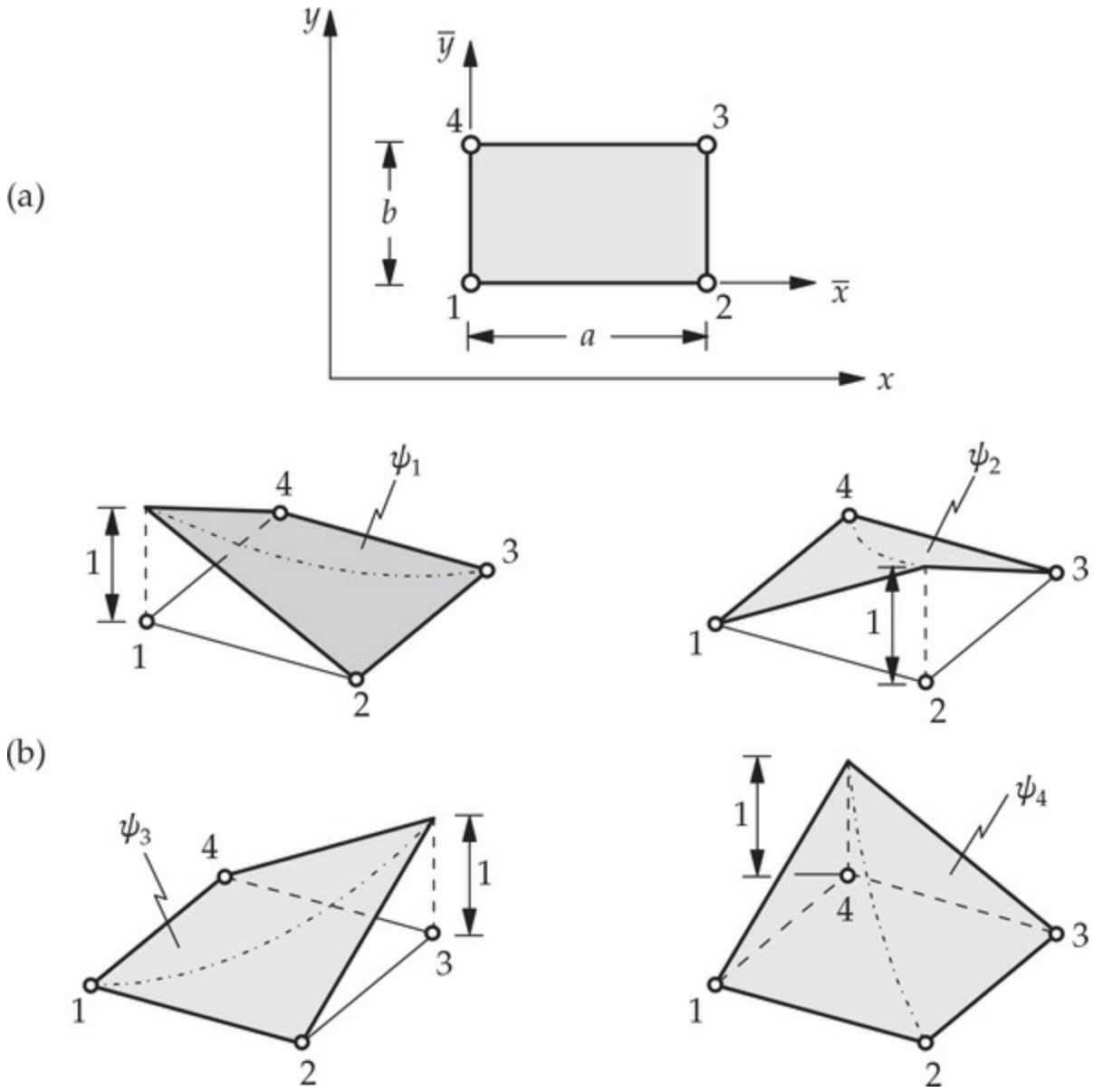

Fig. 9.2.8 Linear rectangular element and its interpolation functions.

$$u_h(\bar{x},\bar{y}) = c_1 + c_2\bar{x} + c_3\bar{y} + c_4\bar{x}\bar{y} \tag{9.2.28}$$

and require

$$\begin{aligned} u_1 &= u_h(0,0) = c_1 \\ u_2 &= u_h(a,0) = c_1 + c_2 a \\ u_3 &= u_h(a,b) = c_1 + c_2 a + c_3 b + c_4 ab \\ u_4 &= u_h(0,b) = c_1 + c_3 b \end{aligned} \tag{9.2.29}$$

Solving for c_i (i = 1,..., 4), we obtain

$$c_1 = u_1, \qquad c_2 = \frac{u_2 - u_1}{a}$$
$$c_3 = \frac{u_4 - u_1}{b}, \qquad c_4 = \frac{u_3 - u_4 + u_1 - u_2}{ab} \tag{9.2.30}$$

Substituting Eq. (9.2.30) into Eq. (9.2.28), we obtain

$$u_h(\bar{x}, \bar{y}) = u_1\left(1 - \frac{\bar{x}}{a} - \frac{\bar{y}}{b} + \frac{\bar{x}}{a}\frac{\bar{y}}{b}\right) + u_2\left(\frac{\bar{x}}{a} - \frac{\bar{x}}{a}\frac{\bar{y}}{b}\right) + u_3\frac{\bar{x}}{a}\frac{\bar{y}}{b} + u_4\left(\frac{\bar{y}}{b} - \frac{\bar{x}}{a}\frac{\bar{y}}{b}\right)$$

or

$$u_h(\bar{x}, \bar{y}) = u_1^e\psi_1^e + u_2^e\psi_2^e + u_3^e\psi_3^e + u_4^e\psi_4^e = \sum_{i=1}^{4} u_i^e\psi_i^e \tag{9.2.31}$$

where

$$\psi_1^e = \left(1 - \frac{\bar{x}}{a}\right)\left(1 - \frac{\bar{y}}{b}\right), \quad \psi_2^e = \frac{\bar{x}}{a}\left(1 - \frac{\bar{y}}{b}\right)$$
$$\psi_3^e = \frac{\bar{x}}{a}\frac{\bar{y}}{b}, \quad \psi_4^e = \left(1 - \frac{\bar{x}}{a}\right)\frac{\bar{y}}{b} \tag{9.2.32a}$$

or, in concise form,

$$\psi_i^e(\bar{x}, \bar{y}) = (-1)^{i+1}\left(1 - \frac{\bar{x} + \bar{x}_i}{a}\right)\left(1 - \frac{\bar{y} + \bar{y}_i}{b}\right) \tag{9.2.32b}$$

where $(\bar{x}_i, \bar{y}_i)$ are the $(\bar{x}, \bar{y})$ coordinates of node i. The interpolation functions are shown in Fig. 9.2.8(b). Once again, we have

$$\psi_i^e(\bar{x}_j, \bar{y}_j) = \delta_{ij} \quad (i, j = 1, \ldots, 4), \quad \sum_{i=1}^{4} \psi_i^e = 1 \tag{9.2.33}$$

Alternatively, the interpolation functions for rectangular element can also be obtained by taking the tensor product of the corresponding one-dimensional interpolation functions. To obtain the linear interpolation functions of a rectangular element, we take the “tensor product” of the one-dimensional linear interpolation functions in Eq. (3.4.20) associated with sides 1–2 and 1–3:

$$\begin{Bmatrix} 1-\dfrac{\bar{x}}{a} \\ \dfrac{\bar{x}}{a} \end{Bmatrix}\begin{Bmatrix} 1-\dfrac{\bar{y}}{b} \\ \dfrac{\bar{y}}{b} \end{Bmatrix}^{\mathrm{T}} = \begin{bmatrix} \psi_1 & \psi_4 \\ \psi_2 & \psi_3 \end{bmatrix} \tag{9.2.34}$$

The alternative procedure that makes use of the interpolation properties in Eq. (9.2.33) can also be used. Here we illustrate the alternative procedure for the four-node rectangular element. Property in Eq. (9.2.33) requires that

$$\psi_1^e(\bar{x}_i, \bar{y}_i) = 0 \quad (i = 2, 3, 4), \qquad \psi_1^e(\bar{x}_1, \bar{y}_1) = 1$$

That is, ψ_i^e is identically zero on lines $\bar{x} = a$ and $\bar{y} = b$. Hence, $\psi_1^e(\bar{x}, \bar{y})$ must be of the form

$$\psi_1^e(\bar{x}, \bar{y}) = c_1(a - \bar{x})(b - \bar{y}) \quad \text{for any } c_1 \neq 0$$

Using the condition $\psi_1^e(\bar{x}_1, \bar{y}_1) = \psi_1^e(0, 0) = 1$, we obtain $c_1 = 1/ab$. Hence,

$$\psi_1^e(\bar{x}, \bar{y}) = \frac{1}{ab}(a - \bar{x})(b - \bar{y}) = \left(1 - \frac{\bar{x}}{a}\right)\left(1 - \frac{\bar{y}}{b}\right)$$

Likewise, we can obtain the remaining three interpolation functions.

9.2.6.3 Quadratic elements

A quadratic triangular element must have three nodes per side in order to define a unique quadratic variation along that side. Thus, there are a total of six nodes in a quadratic triangular element [see Fig. 9.2.9(a)]. A six-term complete polynomial that includes both x and y is

$$u_h^e(x, y) = c_1 + c_2 x + c_3 y + c_4 xy + c_5 x^2 + c_6 y^2 \tag{9.2.35}$$

The constants may be expressed in terms of the six nodal values by the procedure outlined for the three-node triangular element and four-node rectangular element. However, in practice the interpolation functions of higher-order elements are derived using an alternative procedure to be outlined in Chapter 10.

Similarly, a quadratic rectangular element has three nodes per side, resulting in an eight-node rectangular element [see Fig. 9.2.9(b)]. The eight-term polynomial is

$$u_h^e(x, y) = c_1 + c_2 x + c_3 y + c_4 xy + c_5 x^2 + c_6 y^2 + c_7 xy^2 + c_8 yx^2 \tag{9.2.36}$$

The interpolation functions of this element cannot be generated by the tensor product of one-dimensional quadratic functions in Eq. (3.4.25). Indeed, the two-dimensional interpolation functions associated with the tensor product of one-dimensional quadratic functions correspond to the nine-node rectangular element shown in Fig. 9.2.9(c). The nine-term polynomial is given by

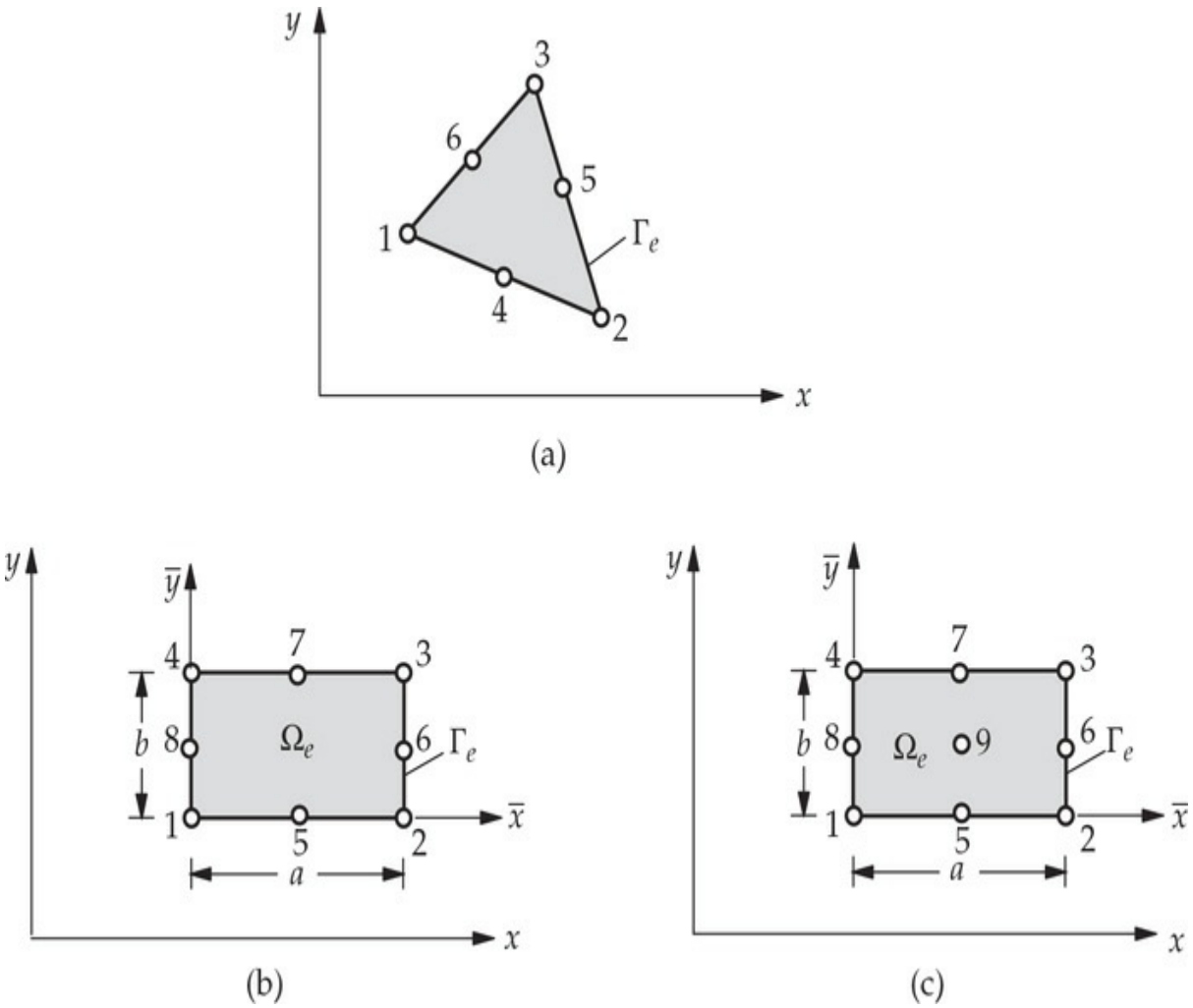

Fig. 9.2.9 (a) Quadratic triangular element. (b) Eight-node quadratic rectangular element. (c) Nine-node quadratic rectangular element.

$$u_h^e(x,y) = c_1 + c_2x + c_3y + c_4xy + c_5x^2 + c_6y^2 + c_7xy^2 + c_8yx^2 + c_9x^2y^2 \qquad (9.2.37)$$

Additional discussion on the derivation of element interpolation functions is presented in Chapter 10.

9.2.7 Evaluation of Element Matrices and Vectors

The exact evaluation of the element matrices $\mathbf{K}^e$ and $\mathbf{f}^e$ in Eqs. (9.2.19b)

and (9.2.19c) is, in general, not easy. In general, they are evaluated using numerical integration techniques described in Section 10.3. However, when a_{ij}, a_{00}, and f are element-wise constant, it is possible to evaluate the integrals exactly over the linear triangular and rectangular elements discussed in the previous section. The boundary integral in $\{Q^e\}$ of Eq. (9.2.19c) can be evaluated whenever q_n is known. For an interior element (i.e., an element that does not have any of its sides on the boundary of the problem), the contribution from the boundary integral cancels with similar contributions from adjoining elements of the mesh (analogous to the Q_i^e in the one-dimensional problems). A more detailed discussion is given below.

For the sake of brevity, we rewrite $\mathbf{K}^e$ in Eq. (9.2.19b) as the sum of five basic matrices $\mathbf{S}^{\alpha\beta}$ ($\alpha, \beta = 0, 1, 2$):

$$\mathbf{K}^e = a_{00}\mathbf{S}^{00} + a_{11}\mathbf{S}^{11} + a_{12}\mathbf{S}^{12} + a_{21}(\mathbf{S}^{12})^T + a_{22}\mathbf{S}^{22} \tag{9.2.38}$$

where $[\,\cdot\,]^T$ denotes the transpose of the enclosed matrix, and

$$S_{ij}^{\alpha\beta} = \int_{\Omega_e} \psi_{i,\alpha}\psi_{j,\beta}\, dxdy \tag{9.2.39}$$

with $\psi_{i,\alpha} \equiv \partial\psi_i/\partial x_\alpha$, $x_1 = x$, and $x_2 = y$; $\psi_{i,0} = \psi_i$. For example, we have

$$S_{ij}^{00} = \int_{\Omega_e} \psi_{i,0}\psi_{j,0}\, dxdy = \int_{\Omega_e} \psi_i\psi_j dxdy$$

$$S_{ij}^{12} = \int_{\Omega_e} \psi_{i,1}\psi_{j,2}\, dxdy = \int_{\Omega_e} \frac{\partial\psi_i}{\partial x}\frac{\partial\psi_j}{\partial y} dxdy$$

All the matrices in Eq. (9.2.38) and interpolation functions in Eq. (9.2.39) are understood to be defined over an element, that is, all expressions and quantities should have the element label e, but it is omitted in the interest of brevity. We now proceed to compute the matrices in Eq. (9.2.38) using the linear interpolation functions derived in the previous section.

9.2.7.1 Element matrices of a linear triangular element

First, we note that integrals of polynomials over arbitrary shaped triangular domains can be evaluated exactly. To this end, let I_{mn} denote the integral of the expression $x^m y^n$ over an arbitrary triangle Δ:

$$I_{mn} \equiv \int_{\Delta} x^m y^n \, dx \, dy \tag{9.2.40}$$

Then, it can be shown that

$$\begin{aligned}
I_{00} &= \int_{\Delta} x^0 y^0 \, dx \, dy = \int_{\Delta} 1 \cdot dx \, dy = A \quad \text{area of the triangle} \\
I_{10} &= \int_{\Delta} x^1 y^0 \, dx \, dy = \int_{\Delta} x \, dx \, dy = A\hat{x}, \quad \hat{x} = \frac{1}{3}\sum_{i=1}^{3} x_i \\
I_{01} &= \int_{\Delta} x^0 y^1 \, dx \, dy = \int_{\Delta} y \, dx \, dy = A\hat{y}, \quad \hat{y} = \frac{1}{3}\sum_{i=1}^{3} y_i \\
I_{11} &= \int_{\Delta} xy \, dx \, dy = \frac{A}{12}\left(\sum_{i=1}^{3} x_i y_i + 9\hat{x}\hat{y}\right) \\
I_{20} &= \int_{\Delta} x^2 \, dx \, dy = \frac{A}{12}\left(\sum_{i=1}^{3} x_i^2 + 9\hat{x}^2\right) \\
I_{02} &= \int_{\Delta} y^2 \, dx \, dy = \frac{A}{12}\left(\sum_{i=1}^{3} y_i^2 + 9\hat{y}^2\right)
\end{aligned} \tag{9.2.41}$$

where (x_i, y_i) are the coordinates of the vertices of the triangle. We can use the above results to evaluate integrals defined over triangular elements.

Next, we evaluate $\mathbf{K}^e$ and $\mathbf{f}^e$ for linear triangular element under the assumption that a_{ij} and f are element-wise constant. Also, note that (see **Problem 9.1**)

$$\sum_{i=1}^{3} \alpha_i^e = 2A_e, \quad \sum_{i=1}^{3} \beta_i^e = 0, \quad \sum_{i=1}^{3} \gamma_i^e = 0 \tag{9.2.42a}$$

$$\alpha_i^e + \beta_i^e \hat{x}_e + \gamma_i^e \hat{y}_e = \frac{2}{3} A_e \tag{9.2.42b}$$

$$\frac{\partial \psi_i}{\partial x} = \frac{\beta_i^e}{2A_e}, \quad \frac{\partial \psi_i}{\partial y} = \frac{\gamma_i^e}{2A_e} \tag{9.2.43}$$

we obtain

$$S_{ij}^{11} = \frac{1}{4A}\beta_i\beta_j, \quad S_{ij}^{12} = \frac{1}{4A}\beta_i\gamma_j, \quad S_{ij}^{22} = \frac{1}{4A}\gamma_i\gamma_j$$

$$S_{ij}^{00} = \frac{1}{4A}\left\{\left[\alpha_i\alpha_j + \left(\alpha_i\beta_j + \alpha_j\beta_i\right)\hat{x} + \left(\alpha_i\gamma_j + \alpha_j\gamma_i\right)\hat{y}\right]\right. \tag{9.2.44}$$

$$\left. + \frac{1}{A}\left[I_{20}\beta_i\beta_j + I_{11}\left(\gamma_i\beta_j + \gamma_j\beta_i\right) + I_{02}\gamma_i\gamma_j\right]\right\}$$

In view of the identity Eq. (9.2.42b) and for an element-wise constant value of $f = f_e$, we have

$$f_i^e = \int_{\Delta_e} f_e\psi_i^e(x,y)\,dxdy = \frac{f_e}{2A_e}\int_{\Delta_e}\left(\alpha_i^e + \beta_i^e x + \gamma_i^e y\right)dx\,dy$$

$$= \frac{f_e}{2A_e}\left(\alpha_i^e I_{00} + \beta_i^e I_{10} + \gamma_i^e I_{01}\right)$$

$$= \frac{f_e}{2A_e}\left(\alpha_i^e A_e + \beta_i^e A_e\hat{x}_e + \gamma_i^e A_e\hat{y}_e\right)$$

$$= \frac{1}{2}f_e\left(\alpha_i^e + \beta_i^e\hat{x}_e + \gamma_i^e\hat{y}_e\right) = \frac{1}{3}f_e A_e \tag{9.2.45}$$

The result in Eq. (9.2.45) should be obvious because for a constant source f_e the total magnitude of the source (say, heat) on the element is equal to $f_e A_e$, which is then distributed equally among the three nodes, giving a nodal value of $f_e\, A_e/3$.

Once the coordinates of the element nodes are known, one can compute α_i^e, β_i^e, and γ_i^e from Eq. (9.2.24b) and substitute into Eq. (9.2.44) to obtain the element matrices, which in turn can be used in Eq. (9.2.38) to obtain the element matrix $\mathbf{K}^e$. In particular, when a_{12}, a_{21} and a_{00} are zero and a_{11} and a_{22} are element-wise constant, Eq. (9.2.1) becomes

$$-\left(a_{11}\frac{\partial^2 u}{\partial x^2} + a_{22}\frac{\partial^2 u}{\partial y^2}\right) - f = 0 \ \text{ in } \ \Omega_e \tag{9.2.46}$$

and the associated element coefficient matrix for a linear triangular element is

$$K_{ij}^e = \frac{1}{4A_e}\left(a_{11}^e \beta_i^e \beta_j^e + a_{22}^e \gamma_i^e \gamma_j^e\right) \tag{9.2.47}$$

Example 9.2.2

Consider the right-angle triangle shown in Fig. 9.2.10(a). Determine the coefficients of Eqs. (9.2.45) and (9.2.47) associated with the Poisson equation (9.2.46).

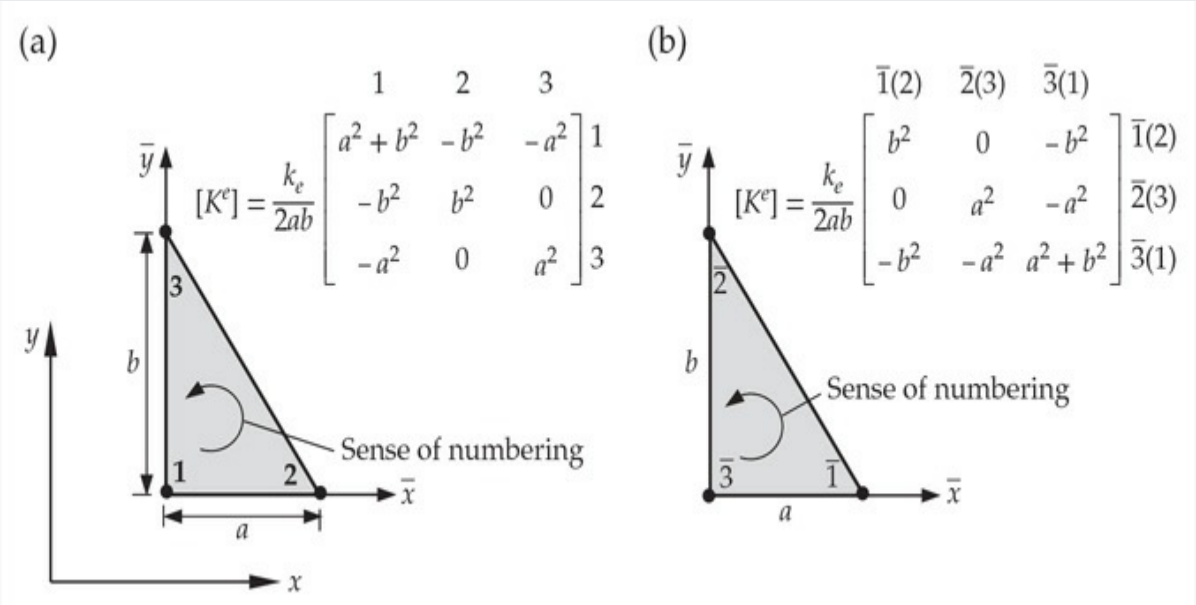

Fig. 9.2.10 The right-angle linear triangular element of **Example 9.2.2**.

Solution: It is simple to use a local (i.e., element) coordinate system to evaluate K_{ij}^e and f_i^e. We choose the local coordinate system $(\bar{x}, \bar{y})$ to compute A, α, β, and γ for the element. We have

$$\alpha_1 = ab,\ \alpha_2 = 0,\ \alpha_3 = 0,\ \beta_1 = -b,\ \beta_2 = b,\ \beta_3 = 0,\ \gamma_1 = -a,\ \gamma_2 = 0,\ \gamma_3 = a$$

$$2A = \alpha_1 + \alpha_2 + \alpha_3 = ab,\ \psi_1 = 1 - \frac{\bar{x}}{a} - \frac{\bar{y}}{b},\ \psi_2 = \frac{\bar{x}}{a},\ \psi_3 = \frac{\bar{y}}{b}$$

and

$$\mathbf{K}^e = \frac{a_{11}^e}{2ab}\begin{bmatrix} b^2 & -b^2 & 0 \\ -b^2 & b^2 & 0 \\ 0 & 0 & 0 \end{bmatrix} + \frac{a_{22}^e}{2ab}\begin{bmatrix} a^2 & 0 & -a^2 \\ 0 & 0 & 0 \\ -a^2 & 0 & a^2 \end{bmatrix},\ \{f^e\} = \frac{f_e ab}{6}\begin{Bmatrix} 1 \\ 1 \\ 1 \end{Bmatrix} \tag{9.2.48}$$

Note that the coefficient matrix is a function of element aspect ratios a/b and b/a. Therefore, elements with very large aspect ratios should not be used as they will result in an ill-conditioned matrix (i.e., very large

numbers are added to very small numbers).

If $a^e_{11} = a^e_{22} = k_e$, for the numbering system shown in Fig. 9.2.10(a) we have

$$\mathbf{K}^e = \frac{k_e}{2ab}\begin{bmatrix} b^2+a^2 & -b^2 & -a^2 \\ -b^2 & b^2 & 0 \\ -a^2 & 0 & a^2 \end{bmatrix}, \quad \mathbf{f}^e = \frac{f_e ab}{6}\begin{Bmatrix} 1 \\ 1 \\ 1 \end{Bmatrix} \tag{9.2.49}$$

In addition, if $a = b$, we have

$$\mathbf{K}^e = \frac{k_e}{2}\begin{bmatrix} 2 & -1 & -1 \\ -1 & 1 & 0 \\ -1 & 0 & 1 \end{bmatrix}, \quad \mathbf{f}^e = \frac{f_e a^2}{6}\begin{Bmatrix} 1 \\ 1 \\ 1 \end{Bmatrix} \tag{9.2.50}$$

We note that contents of $\mathbf{K}^e$ depend, even for the same geometry, on the node numbering scheme, as shown in Fig. 9.2.10(a) and (b). For the same element, if the node numbering is changed, the element coefficients will change accordingly. For example, if we renumber the element nodes of the element in Fig. 9.2.10(a) to be those in Fig. 9.2.10(b), then $\mathbf{K}^e$ for the element in Fig. 9.2.10(b) is obtained from Eq. (9.2.49) by moving rows and columns:

$$\frac{k_e}{2ab}\begin{bmatrix} b^2+a^2 & -b^2 & -a^2 \\ -b^2 & b^2 & 0 \\ -a^2 & 0 & a^2 \end{bmatrix} \rightarrow \frac{k_e}{2ab}\begin{bmatrix} b^2 & 0 & -b^2 \\ 0 & a^2 & -a^2 \\ -b^2 & -a^2 & b^2+a^2 \end{bmatrix}$$

In addition, all elements with the same geometry and node numbering, irrespective of their orientation (i.e., rigid body rotation about an axis perpendicular to the plane of the element), have the same coefficient matrix. Elements with the same coefficient matrix are listed in Fig. 9.2.11.

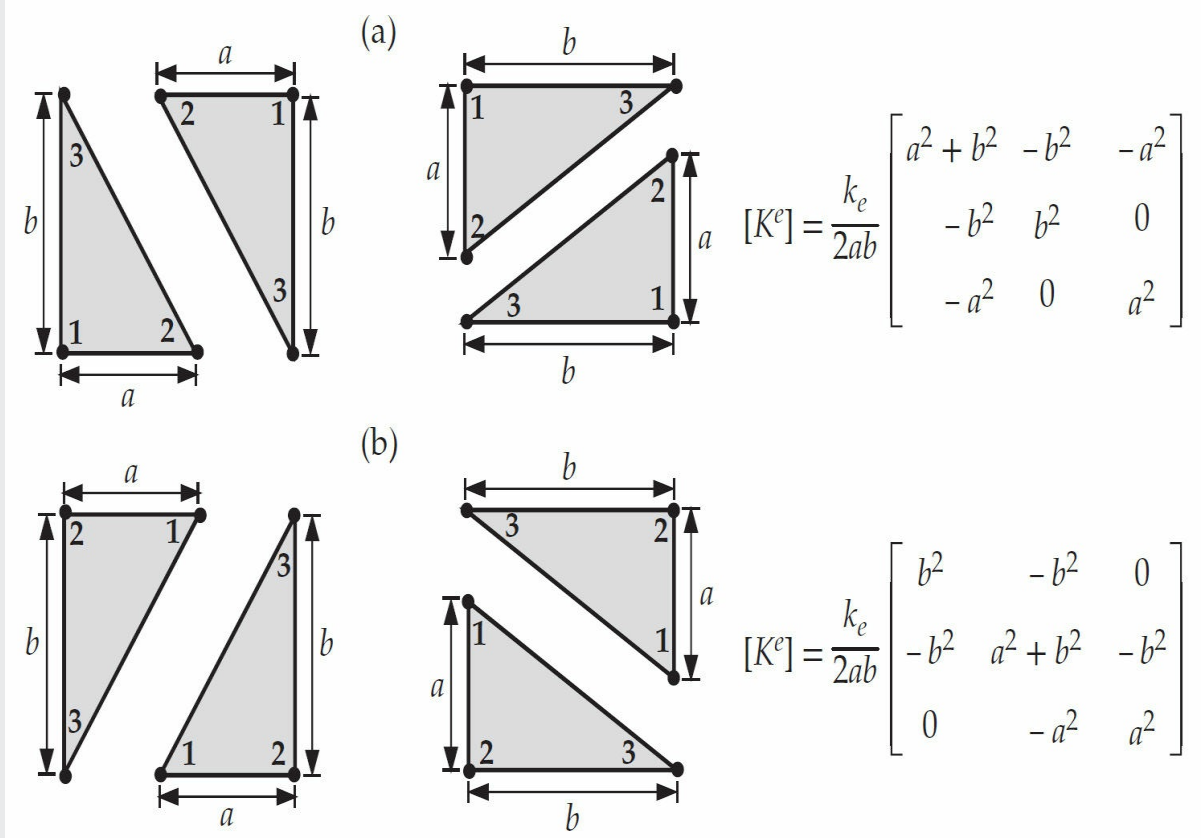

Fig. 9.2.11 Coefficient matrices associated with Eq. (9.2.46) with $a^e_{11} = a^e_{22} = k_e$ for two different element node numbers of linear right-angle triangular elements.

9.2.7.2 Element matrices of a linear rectangular element

When the data a_{ij} ($i, j = 0, 1, 2$) and f of the problem are not functions of x and y, we can use the interpolation functions in Eq. (9.2.32a), expressed in the local coordinates $(\bar{x}, \bar{y})$ that are mere translation of (x, y) (see Fig. 9.2.12), to evaluate $S^{\alpha\beta}_{ij}$ of Eq. (9.2.39). Since the integration with respect to $\bar{x}$ and $\bar{y}$ can be carried out independent of each other, integration over a rectangular element becomes the evaluation of line integrals of the type

$$\int_0^a \left(1 - \frac{s}{a}\right) ds = \frac{a}{2}, \quad \int_0^a \frac{s}{a}\, ds = \frac{a}{2}$$

$$\int_0^a \left(1 - \frac{s}{a}\right)^2 ds = \frac{a}{3}, \quad \int_0^a \frac{s}{a}\left(1 - \frac{s}{a}\right) ds = \frac{a}{6}, \quad \int_0^a \left(\frac{s}{a}\right)^2 ds = \frac{a}{3} \tag{9.2.51}$$

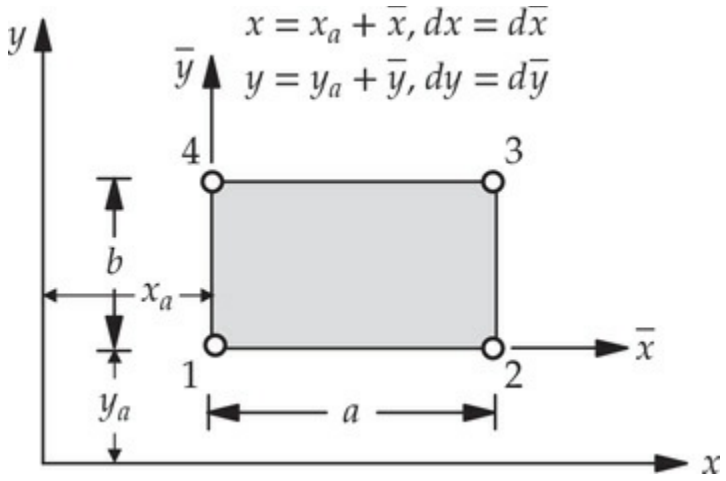

Fig. 9.2.12 A rectangular element with the global and local coordinate systems.

For example, we have

$$S_{11}^{00} = \int_0^a \int_0^b \psi_1 \psi_1 \, d\bar{x} \, d\bar{y} = \int_0^a \int_0^b \left(1 - \frac{\bar{x}}{a}\right)\left(1 - \frac{\bar{y}}{b}\right)\left(1 - \frac{\bar{x}}{a}\right)\left(1 - \frac{\bar{y}}{b}\right) d\bar{x} \, d\bar{y}$$
$$= \int_0^a \left(1 - \frac{\bar{x}}{a}\right)^2 d\bar{x} \int_0^b \left(1 - \frac{\bar{y}}{b}\right)^2 d\bar{y} = \frac{a}{3}\frac{b}{3} = \frac{ab}{9}$$

In summary, the element matrices $\mathbf{S}^{\alpha\beta}$ for a rectangular element are

$$\mathbf{S}^{11} = \frac{b}{6a}\begin{bmatrix} 2 & -2 & -1 & 1 \\ -2 & 2 & 1 & -1 \\ -1 & 1 & 2 & -2 \\ 1 & -1 & -2 & 2 \end{bmatrix}, \quad \mathbf{S}^{12} = \frac{1}{4}\begin{bmatrix} 1 & 1 & -1 & -1 \\ -1 & -1 & 1 & 1 \\ -1 & -1 & 1 & 1 \\ 1 & 1 & -1 & -1 \end{bmatrix} \tag{9.2.52}$$

$$\mathbf{S}^{22} = \frac{a}{6b}\begin{bmatrix} 2 & 1 & -1 & -2 \\ 1 & 2 & -2 & -1 \\ -1 & -2 & 2 & 1 \\ -2 & -1 & 1 & 2 \end{bmatrix}, \quad \mathbf{S}^{00} = \frac{ab}{36}\begin{bmatrix} 4 & 2 & 1 & 2 \\ 2 & 4 & 2 & 1 \\ 1 & 2 & 4 & 2 \\ 2 & 1 & 2 & 4 \end{bmatrix}$$

$$\mathbf{f} = \frac{1}{4} f_e ab \{ 1 \quad 1 \quad 1 \quad 1 \}^{\mathrm{T}}$$

Example 9.2.3

Determine the element coefficient matrix $\mathbf{K}^e$ associated with the Poisson

equation (9.2.46) over a linear rectangular element.

Solution: We have $\mathbf{K}^e = a_{11}^e \mathbf{S}^{11} + a_{22}^e \mathbf{S}^{22}$ or

$$\mathbf{K}^e = \frac{a_{11}^e b}{6a}\begin{bmatrix} 2 & -2 & -1 & 1 \\ -2 & 2 & 1 & -1 \\ -1 & 1 & 2 & -2 \\ 1 & -1 & -2 & 2 \end{bmatrix} + \frac{a_{22}^e a}{6b}\begin{bmatrix} 2 & 1 & -1 & -2 \\ 1 & 2 & -2 & -1 \\ -1 & -2 & 2 & 1 \\ -2 & -1 & 1 & 2 \end{bmatrix} \tag{9.2.53}$$

As in the case of triangular elements, the coefficient matrix is a function of the aspect ratios a/b and b/a. Therefore, rectangular elements with very large aspect ratios should not be used because either $\mathbf{S}^{11}$ or $\mathbf{S}^{22}$ will dominate the element matrix, independent of the given values of a_{11}^e and a_{22}^e.

For $a_{11}^e = a_{22}^e = k_e$, the element coefficient matrix becomes

$$\mathbf{K}^e = \frac{k_e}{6ab}\begin{bmatrix} 2(a^2+b^2) & a^2-2b^2 & -(a^2+b^2) & b^2-2a^2 \\ a^2-2b^2 & 2(a^2+b^2) & b^2-2a^2 & -(a^2+b^2) \\ -(a^2+b^2) & b^2-2a^2 & 2(a^2+b^2) & a^2-2b^2 \\ b^2-2a^2 & -(a^2+b^2) & a^2-2b^2 & 2(a^2+b^2) \end{bmatrix} \tag{9.2.54}$$

When the element aspect ratio is $a/b = 1$, the coefficient matrix in Eq. (9.2.54) becomes

$$\mathbf{K}^e = \frac{k_e}{6}\begin{bmatrix} 4 & -1 & -2 & -1 \\ -1 & 4 & -1 & -2 \\ -2 & -1 & 4 & -1 \\ -1 & -2 & -1 & 4 \end{bmatrix} \tag{9.2.55}$$

9.2.7.3 Evaluation of boundary integrals

Here, we consider the evaluation of boundary integrals of the type [see Eq. (9.2.19c)]

$$Q_i^e = \oint_{\Gamma_e} q_n^e \psi_i^e(s)\, ds \tag{9.2.56}$$

where q_n^e is a *known* function of the distance s along the boundary Γ_e, which is a set of lines or curves. It is only necessary to compute such integrals when at least a portion of Γ_e falls on the portion of the boundary Γ of the total domain Ω [see Fig. 9.2.13(a)] on which q_n^e is specified. On portions of Γ_e that are in the interior of the domain Ω, q_n^e on side (i, j) of

element Ω_e cancels with q_n^f on side (p, q) of element Ω_f when sides (i, j) of element Ω_e and (p, q) of element Ω_f are

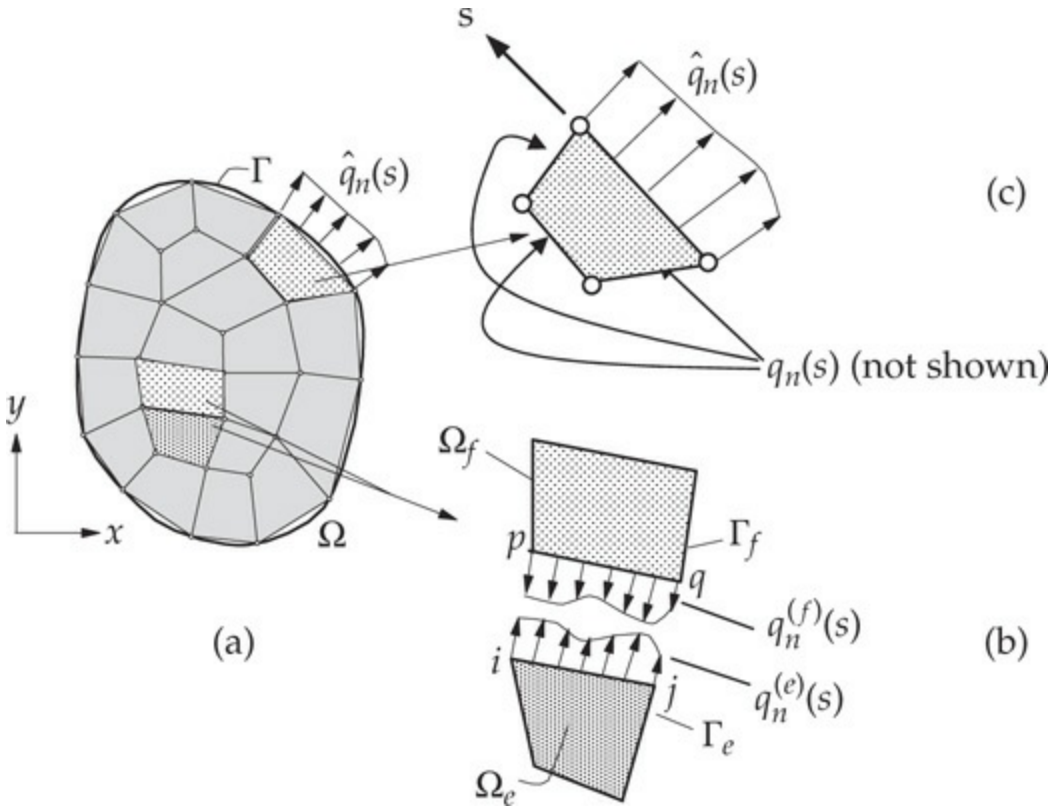

Fig. 9.2.13 (a) Finite element discretization. (b) Equilibrium of fluxes at element interfaces. (c) Computation of forces on the boundary of the total domain.

the same (i.e., at the interface of elements Ω_e and Ω_f). This can be viewed as the balance of the internal "flux" [see Fig. 9.2.13(b)]. When Γ_e falls on the boundary of the domain Ω and q_n is unknown (hence, the corresponding primary variable is known there), it is determined in the post-computation [see Fig. 9.2.13(c)].

The boundary Γ_e of a two-dimensional finite element are line segments and they can be treated as one-dimensional finite elements when evaluating the boundary integrals. Thus, the evaluation of the boundary integrals on two-dimensional problems amounts to evaluating line integrals. It should not be surprising that when two-dimensional interpolation functions are evaluated on the boundary of an element, we obtain the corresponding one-dimensional interpolation functions.

In general, the integral (9.2.56) over the boundary of a linear triangular element can be expressed as

$$Q_i^e = \int_{1-2} \psi_i(s) q_n(s)\, ds + \int_{2-3} \psi_i(s) q_n(s)\, ds + \int_{3-1} \psi_i(s) q_n(s)\, ds$$
$$\equiv Q_{i1}^e + Q_{i2}^e + Q_{i3}^e \tag{9.2.57}$$

where $\int_{i-j}$ denotes integral over the line connecting node i to node j, the s-coordinate is taken from node i to node j, with origin at node i (see Fig. 9.2.14), and Q_{ij}^e is defined to be the contribution of q_n on side J of element Ω_e to Q_i^e:

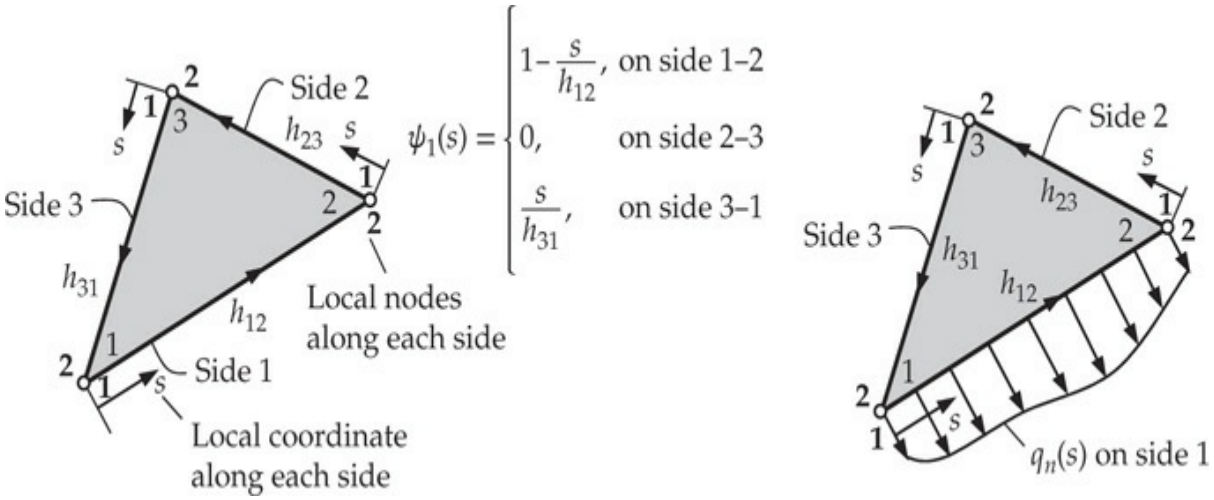

Fig. 9.2.14 Computation of the boundary integral (9.2.56) over a linear triangular element.

$$Q_{ij}^e = \int_{\text{side } J} \psi_i q_n\, ds \tag{9.2.58}$$

where i refers to the ith node of the element, and J refers to the Jth side of the element. For example, we have

$$Q_1^e = \oint_{\Gamma_e} q_n \psi_1(s)\, ds = \int_{1-2} (q_n)_{1-2} \psi_1\, ds + 0 + \int_{3-1} (q_n)_{3-1} \psi_1\, ds$$

The contribution from side 2–3 is zero because ψ_1 is zero on side 2–3 of a triangular element. For a rectangular element Q_1^e has four parts but only contributions from sides 1–2 and 4–1 are nonzero because ψ_1 is zero on sides 2–3 and 3–4.

Example 9.2.4

Evaluate the boundary integral Q_i^e in Eq. (9.2.56) for the four cases of $q(s)$ and finite element meshes shown in Fig. 9.2.15. For each case you must use the $q(s)$ and the interpolation functions associated with the type of boundary element (i.e., linear or quadratic). On element sides on which q_n is not shown, assume that it is zero.

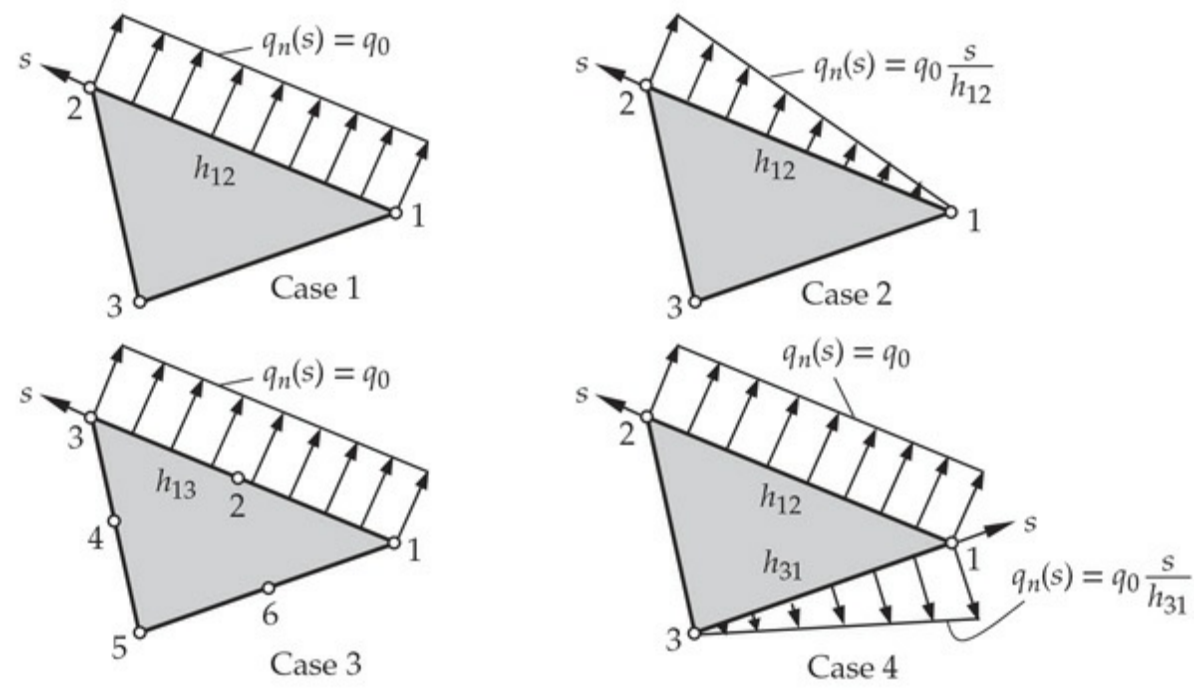

Fig. 9.2.15 Evaluation of boundary integrals in the finite element analysis (**Example 9.2.4**).

Solution:

Case 1. $q(s) = q_0$ = constant, linear element. Clearly, q_0 will contribute to the nodal values at element nodes 1 and 2. The contribution to node 3 is zero ($Q_3^e = 0$) as there is no specified flux on sides 2–3 and 3–1. We have

$$Q_1^e = \oint_{\Gamma_e} q_n(s)\psi_1(s)\,ds = \int_0^{h_{12}} q_0(\psi_1)_{12}\,ds + \int_0^{h_{31}} (0)(\psi_1)_{31}\,ds = Q_{11}^e = \frac{1}{2}q_0 h_{12}$$

$$Q_2^e = \oint_{\Gamma_e} q_n(s)\psi_2(s)\,ds = \int_0^{h_{12}} q_0(\psi_2)_{12}\,ds + \int_0^{h_{23}} (0)(\psi_2)_{23}\,ds = Q_{21}^e = \frac{1}{2}q_0 h_{12}$$

where

$$(\psi_1)_{12} = 1 - \frac{s}{h_{12}}, \quad (\psi_2)_{12} = \frac{s}{h_{12}}$$

Case 2. $q(s) = q_0 s/h_{12}$ (linear variation), linear element. The equations are the same as above except that the flux is linear. We have

$$Q_1^e = \oint_{\Gamma_e} q_n(s)\psi_1(s)\,ds = \int_0^{h_{12}} \left(q_0 \frac{s}{h_{12}}\right)(\psi_1)_{12}\,ds + \int_0^{h_{31}} (0)(\psi_1)_{31}\,ds$$

$$= Q_{11}^e = \frac{1}{6} q_0 h_{12}$$

$$Q_2^e = \oint_{\Gamma_e} q_n(s)\psi_2(s)\,ds = \int_0^{h_{12}} \left(q_0 \frac{s}{h_{12}}\right)(\psi_2)_{12}\,ds + \int_0^{h_{23}} (0)(\psi_2)_{23}\,ds$$

$$= Q_{21}^e = \frac{1}{3} q_0 h_{12}$$

Case 3. $q(s) = q_0$ = constant, quadratic triangular element. In this case, quadratic interpolation functions on side 123 must be used. We have $(Q_4^e = Q_5^e = Q_6^e = 0)$

$$Q_1^e = \oint_{\Gamma_e} q_n(s)\psi_1(s)\,ds = \int_0^{h_{13}} q_0(\psi_1)_{123}\,ds = Q_{11}^e = \frac{1}{6} q_0 h_{13}$$

$$Q_2^e = \oint_{\Gamma_e} q_n(s)\psi_2(s)\,ds = \int_0^{h_{13}} q_0(\psi_2)_{123}\,ds = Q_{21}^e = \frac{4}{6} q_0 h_{13}$$

$$Q_3^e = \oint_{\Gamma_e} q_n(s)\psi_3(s)\,ds = \int_0^{h_{13}} q_0(\psi_3)_{123}\,ds = Q_{31}^e = \frac{1}{6} q_0 h_{13}$$

where

$$(\psi_1)_{123} = \left(1 - \frac{s}{h_{13}}\right)\left(1 - \frac{2s}{h_{13}}\right), \quad (\psi_2)_{123} = 4\frac{s}{h_{13}}\left(1 - \frac{s}{h_{13}}\right)$$

$$(\psi_3)_{123} = -\frac{s}{h_{13}}\left(1 - \frac{2s}{h_{13}}\right)$$

Case 4. Two sides have nonzero $q(s)$, as shown in Fig. 9.2.15, on a linear element. In this case, all three nodes will have nonzero contributions. We have

$$Q_1^e = \oint_{\Gamma_e} q_n(s)\psi_1(s)\,ds = \int_0^{h_{12}} q_0(\psi_1)_{12}\,ds + \int_0^{h_{31}} \left(q_0 \frac{s}{h_{31}}\right)(\psi_1)_{31}\,ds$$

$$= Q_{11}^e + Q_{13}^e = q_0\left(\frac{h_{12}}{2} + \frac{h_{31}}{3}\right)$$

$$Q_2^e = \oint_{\Gamma_e} q_n(s)\psi_2(s)\,ds = \int_0^{h_{12}} q_0(\psi_2)_{12}\,ds + \int_0^{h_{31}} \left(q_0 \frac{s}{h_{31}}\right)(0)\,ds = Q_{21}^e = \frac{1}{2}q_0 h_{12}$$

$$Q_3^e = \oint_{\Gamma_e} q_n(s)\psi_3(s)\,ds = \int_0^{h_{12}} q_0(0)\,ds + \int_0^{h_{31}} \left(q_0 \frac{s}{h_{31}}\right)(\psi_3)_{31}\,ds = Q_{33}^e = \frac{1}{6}q_0 h_{31}$$

9.2.8 Assembly of Element Equations

The assembly of finite element equations is based on the same two principles that were used in one-dimensional problems:

1. Continuity of primary variables
2. "Equilibrium" (or "balance") of secondary variables

We illustrate the procedure by considering a finite element mesh consisting of a triangular element and a quadrilateral element [see Fig. 9.2.16(a)]. Let $K_{ij}^1 (i,j=1,2,3)$ denote the coefficient matrix corresponding to the triangular element, and let $K_{ij}^2 \ (i,j=1,\ldots,4)$ denote the coefficient matrix corresponding to the quadrilateral element. From the finite element mesh shown in Fig. 9.2.16(a), we note the following correspondence (i.e., connectivity relations) between the global and element nodes:

$$\mathbf{B} = \begin{bmatrix} 1 & 2 & 3 & \times \\ 2 & 4 & 5 & 3 \end{bmatrix} \tag{9.2.59}$$

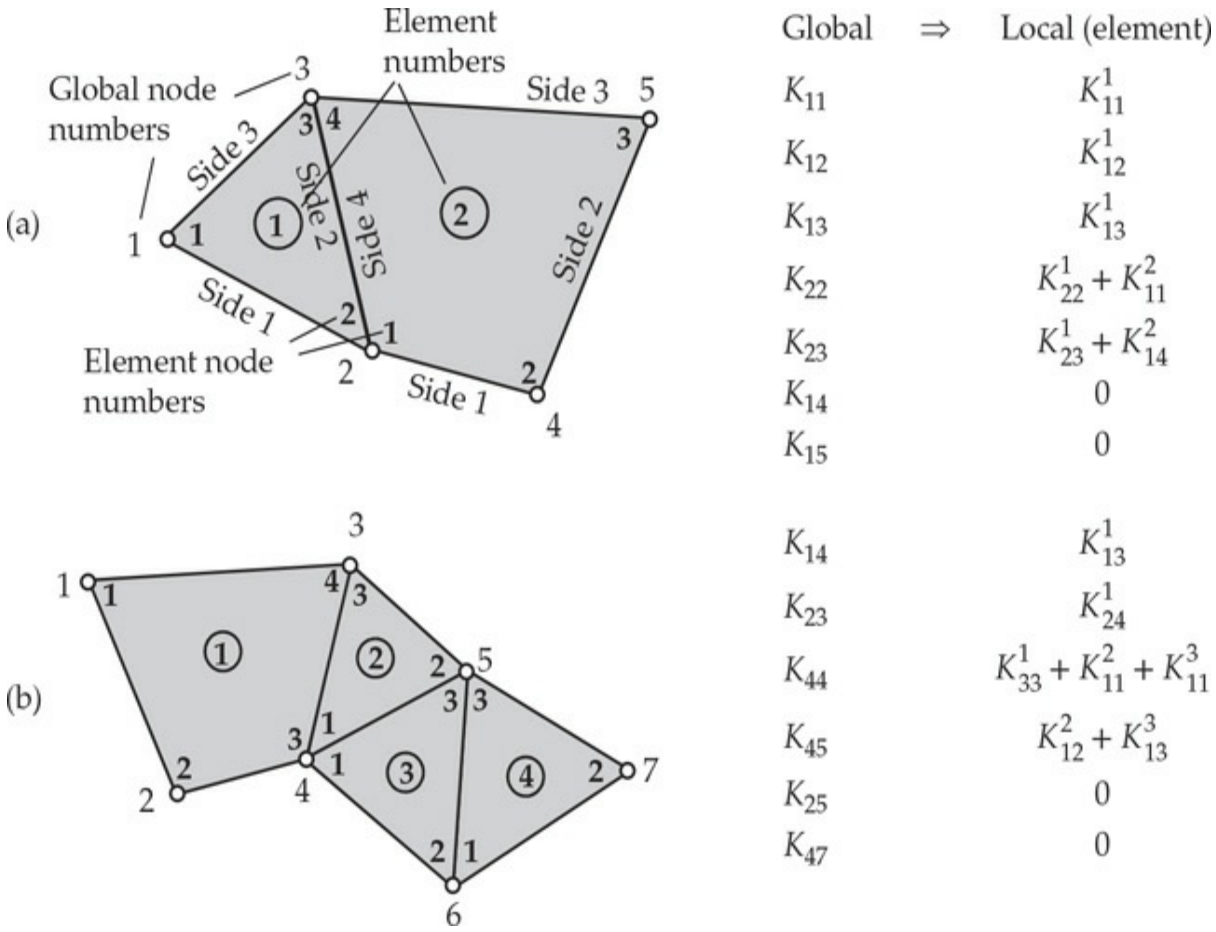

Fig. 9.2.16 Assembly of finite element coefficient matrices using the correspondence between global and element nodes (one unknown per node): (a) assembly of two elements; and (b) assembly of several elements.

where × indicates that there is no entry. The correspondence between the local and global nodal values is [see Fig. 9.2.16(a)]

$$u_1^1 = U_1, \quad u_2^1 = u_1^2 = U_2, \quad u_3^1 = u_4^2 = U_3, \quad u_2^2 = U_4, \quad u_3^2 = U_5 \tag{9.2.60}$$

which amounts to imposing the continuity of the primary variables at the nodes common to elements 1 and 2.

Note that the continuity of the primary variables at the interelement nodes guarantees the continuity of the primary variable along the entire interelement boundary. For the case in Fig. 9.2.16(a), the requirement $u_2^1 = u_1^2$ and $u_3^1 = u_4^2$ guarantees $u_h^1(s) = u_h^2(s)$ on the side connecting global nodes 2 and 3. This can be shown as follows. The solution $u_h^1(s)$ along the line connecting global nodes 2 and 3 is linear, and it is given by

$$u_h^1(s) = u_2^1\left(1 - \frac{s}{h}\right) + u_3^1\frac{s}{h}$$

where s is the local coordinate with its origin at global node 2 and h is the length of the side 2–3 (or side 2). Similarly, the finite element solution along the same line but from element 2 is

$$u_h^2(s) = u_1^2\left(1 - \frac{s}{h}\right) + u_4^2\frac{s}{h}$$

Since $u_1^2 = u_2^1$ and $u_4^2 = u_3^1$, it follows that $u_h^1(s) = u_h^2(s)$ for every value of s along the interface of the two elements.

Next we use the balance of secondary variables. At the interface between the two elements, the flux from the two elements should be equal in magnitude and opposite in sign. For the two elements in Fig. 9.2.16(a), the interface is along the side connecting global nodes 2 and 3. Hence, the internal flux q_n^1 on side 2–3 of element 1 should balance the flux q_n^2 on side 4–1 of element 2 (recall the sign convention on q_n^e):

$$(q_n^1)_{23} = (q_n^2)_{41} \quad \text{or} \quad (q_n^1)_{23} = (-q_n^2)_{14} \tag{9.2.61}$$

In the finite element method we impose the above relation in a weighted-integral sense:

$$\int_{h_{23}^1} q_n^1\psi_2^1\,ds = -\int_{h_{14}^2} q_n^2\psi_1^2\,ds, \quad \int_{h_{23}^1} q_n^1\psi_3^1\,ds = -\int_{h_{14}^2} q_n^2\psi_4^2\,ds \tag{9.2.62a}$$

where h_{pq}^e denotes length of the side connecting node p to node q of element Ω_e.

The above equations can be written in the form

$$\int_{h_{23}^1} q_n^1\psi_2^1\,ds + \int_{h_{14}^2} q_n^2\psi_1^2\,ds = 0, \quad \int_{h_{23}^1} q_n^1\psi_3^1\,ds + \int_{h_{14}^2} q_n^2\psi_4^2\,ds = 0 \tag{9.2.62b}$$

or

$$Q_{22}^1 + Q_{14}^2 = 0, \quad Q_{32}^1 + Q_{44}^2 = 0 \tag{9.2.62c}$$

where Q_{iJ}^e denotes the part of Q_i^e that comes from side J of element e [see Eq. (9.2.58)]. The sides of triangular and quadrilateral elements are numbered as shown in Fig. 9.2.16(a). These balance relations must be imposed in assembling the element equations. We note that Q_{iJ}^e is only a portion of Q_i^e [see Eqs. (9.2.57) and (9.2.58)].

The element equations of the two-element mesh shown in Fig. 9.2.16(a) are written first. For the model problem at hand, there is only one primary degree of freedom (NDF = 1) per node. For the triangular element, the element equations are of the form

$$\begin{aligned} K^1_{11}u^1_1 + K^1_{12}u^1_2 + K^1_{13}u^1_3 &= f^1_1 + Q^1_1 \\ K^1_{21}u^1_1 + K^1_{22}u^1_2 + K^1_{23}u^1_3 &= f^1_2 + Q^1_2 \\ K^1_{31}u^1_1 + K^1_{32}u^1_2 + K^1_{33}u^1_3 &= f^1_3 + Q^1_3 \end{aligned} \tag{9.2.63}$$

For the quadrilateral element the element equations are given by

$$\begin{aligned} K^2_{11}u^2_1 + K^2_{12}u^2_2 + K^2_{13}u^2_3 + K^2_{14}u^2_4 &= f^2_1 + Q^2_1 \\ K^2_{21}u^2_1 + K^2_{22}u^2_2 + K^2_{23}u^2_3 + K^2_{24}u^2_4 &= f^2_2 + Q^2_2 \\ K^2_{31}u^2_1 + K^2_{32}u^2_2 + K^2_{33}u^2_3 + K^2_{34}u^2_4 &= f^2_3 + Q^2_3 \\ K^2_{41}u^2_1 + K^2_{42}u^2_2 + K^2_{43}u^2_3 + K^2_{44}u^2_4 &= f^2_4 + Q^2_4 \end{aligned} \tag{9.2.64}$$

In order to impose the balance of secondary variables in Eq. (9.2.62c), it is required that we add the second equation of element 1 to the first equation of element 2, and also add the third equation of element 1 to the fourth equation of element 2:

$$\begin{aligned} &(K^1_{21}u^1_1 + K^1_{22}u^1_2 + K^1_{23}u^1_3) + (K^2_{11}u^2_1 + K^2_{12}u^2_2 + K^2_{13}u^2_3 + K^2_{14}u^2_4) \\ &\quad = (f^1_2 + Q^1_2) + (f^2_1 + Q^2_1) \\ &(K^1_{31}u^1_1 + K^1_{32}u^1_2 + K^1_{33}u^1_3) + (K^2_{41}u^2_1 + K^2_{42}u^2_2 + K^2_{43}u^2_3 + K^2_{44}u^2_4) \\ &\quad = (f^1_3 + Q^1_3) + (f^2_4 + Q^2_4) \end{aligned}$$

Using the global-variable notation in Eq. (9.2.60), we can rewrite the above equations as [which amounts to imposing continuity of the primary variables in Eq. (9.2.60)]:

$$\begin{aligned} &K^1_{21}U_1 + (K^1_{22} + K^2_{11})U_2 + (K^1_{23} + K^2_{14})U_3 + K^2_{12}U_4 + K^2_{13}U_5 \\ &\quad = f^1_2 + f^2_1 + (Q^1_2 + Q^2_1) \\ &K^1_{31}U_1 + (K^1_{32} + K^2_{41})U_2 + (K^1_{33} + K^2_{44})U_3 + K^2_{42}U_4 + K^2_{43}U_5 \\ &\quad = f^1_3 + f^2_4 + (Q^1_3 + Q^2_4) \end{aligned}$$

Now we can impose the conditions in Eq. (9.2.62c) by setting appropriate

portions of the expressions within parentheses on the right-hand side of the above equations to zero:

$$\begin{aligned} Q_2^1 + Q_1^2 &= (Q_{21}^1 + Q_{22}^1 + Q_{23}^1) + (Q_{11}^2 + Q_{12}^2 + Q_{13}^2 + Q_{14}^2) \\ &= Q_{21}^1 + Q_{23}^1 + \underline{(Q_{22}^1 + Q_{14}^2)} + Q_{11}^2 + Q_{12}^2 + Q_{13}^2 \\ Q_3^1 + Q_4^2 &= (Q_{31}^1 + Q_{32}^1 + Q_{33}^1) + (Q_{41}^2 + Q_{42}^2 + Q_{43}^2 + Q_{44}^2) \\ &= Q_{31}^1 + Q_{33}^1 + \underline{(Q_{32}^1 + Q_{44}^2)} + Q_{41}^2 + Q_{42}^2 + Q_{43}^2 \end{aligned} \tag{9.2.65}$$

The underlined terms are zero by the balance requirement in Eq. (9.2.62c). The remaining terms of each equation will be either known because q_n is known on the boundary or remain unknown because the primary variable is specified on the boundary.

In general, when several elements are connected, the assembly of the elements is carried out by putting element coefficients K_{ij}^e, f_i^e and Q_i^e into proper locations of the global coefficient matrix and right-hand-column vectors. This is done by means of the connectivity relations, i.e., correspondence of the local node number to the global node number. For example, if global node number 3 corresponds to node 3 of element 1 and node 4 of element 2, then we have

$$F_3 = F_3^1 + F_4^2 \equiv f_3^1 + f_4^2 + Q_3^1 + Q_4^2, \quad K_{33} = K_{33}^1 + K_{44}^2$$

If global node numbers 2 and 3 correspond, respectively, to nodes 2 and 3 of element 1 and nodes 1 and 4 of element 2, then global coefficients K_{22}, K_{23}, K_{33} are given by

$$K_{22} = K_{22}^1 + K_{11}^2, \quad K_{23} = K_{23}^1 + K_{14}^2, \quad K_{33} = K_{33}^1 + K_{44}^2$$

Similarly, the source components of global nodes 2 and 3 are added:

$$F_2 = F_2^1 + F_1^2, \quad F_3 = F_3^1 + F_4^2$$

For the two-element mesh shown in Fig. 9.2.16(a), the assembled equations are given by

$$\begin{bmatrix} K_{11}^1 & K_{12}^1 & K_{13}^1 & 0 & 0 \\ K_{21}^1 & K_{22}^1 + K_{11}^2 & K_{23}^1 + K_{14}^2 & K_{12}^2 & K_{13}^2 \\ K_{31}^1 & K_{32}^1 + K_{41}^2 & K_{33}^1 + K_{44}^2 & K_{42}^2 & K_{43}^2 \\ 0 & K_{21}^2 & K_{24}^2 & K_{22}^2 & K_{23}^2 \\ 0 & K_{31}^2 & K_{34}^2 & K_{32}^2 & K_{33}^2 \end{bmatrix} \begin{Bmatrix} U_1 \\ U_2 \\ U_3 \\ U_4 \\ U_5 \end{Bmatrix} = \begin{Bmatrix} F_1^1 \\ F_2^1 + F_1^2 \\ F_3^1 + F_4^2 \\ F_2^2 \\ F_3^2 \end{Bmatrix} \tag{9.2.66}$$

The assembly procedure described above can be used to assemble elements of any shape and type. The procedure can be implemented in a computer, as described for one-dimensional problems, with the help of the array **B** (program variable is NOD). For hand calculations, the readers are required to use the procedure described above. For example, consider the finite element mesh shown in Fig. 9.2.16(b). Location (4,4) of the global coefficient matrix contains $K_{33}^1 + K_{11}^2 + K_{11}^3$. Location 4 in the assembled column vector contains $F_3^1 + F_1^2 + F_1^3$. Locations (1,5), (1,6), (1,7), (2,5), (2,6), (2,7), (3,6), (3,7), and (4,7) of the global matrix contain zeros because $K_{IJ} = 0$ when global nodes I and J do not correspond to nodes of the same element in the mesh.

This completes the first five steps in the finite element modeling of the model equation (9.2.1). The next two steps of the analysis, namely, the imposition of boundary conditions and solution of equations, will remain the same as for one-dimensional problems. The postprocessing of the solution for two-dimensional problems is discussed next.

9.2.9 Post-computations

The finite element solution at any point (x, y) in an element Ω_e is given by

$$u_h^e(x, y) = \sum_{j=1}^{n} u_j^e \psi_j^e(x, y) \tag{9.2.67}$$

and its derivatives are computed from Eq. (9.2.67) as

$$\frac{\partial u_h^e}{\partial x} = \sum_{j=1}^{n} u_j^e \frac{\partial \psi_j^e}{\partial x}, \quad \frac{\partial u_h^e}{\partial y} = \sum_{j=1}^{n} u_j^e \frac{\partial \psi_j^e}{\partial y} \tag{9.2.68}$$

Equations (9.2.67) and (9.2.68) can be used to compute the solution and its derivatives at any point (x, y) in the element. It is useful to generate, by

interpolation of Eq. (9.2.67), information needed to plot contours of u_h^e and its gradient.

The derivatives of u_h^e will not be continuous at interelement boundaries because continuity of the derivatives is not imposed during the assembly procedure. The weak form of the equations suggests that the primary variable is u, which is to be carried as the nodal variable. If additional variables, such as higher-order derivatives of the dependent unknown, are carried as nodal variables in the interest of making them continuous across interelement boundaries, the degree of interpolation (or order of the element) increases. In addition, the continuity of higher-order derivatives that are not identified as the primary variables may violate the physical principles of the problem. For example, making $\partial u/\partial x$ continuous will violate the requirement that q_x (= $a_{11}\,\partial u/\partial x$) be continuous at the interface of two dissimilar materials because a_{11} is different for the two materials at the interface.

For the linear triangular element, the derivatives are constants within each element:

$$\psi_j^e = \frac{1}{2A_e}(\alpha_j + \beta_j x + \gamma_j y), \quad \frac{\partial \psi_j^e}{\partial x} = \frac{1}{2A_e}\beta_j, \quad \frac{\partial \psi_j^e}{\partial y} = \frac{1}{2A_e}\gamma_j$$

$$\frac{\partial u_h^e}{\partial x} = \sum_{j=1}^{n} \frac{u_j^e \beta_j}{2A_e}, \qquad \frac{\partial u_h^e}{\partial y} = \sum_{j=1}^{n} \frac{u_j^e \gamma_j}{2A_e} \tag{9.2.69}$$

For linear rectangular elements, $\partial u_h^e/\partial x$ is linear in $\bar{y}$ and $\partial u_h^e/\partial y$ is linear in $\bar{x}$ [see Eq. (9.2.32b)]:

$$\frac{\partial \psi_j^e}{\partial \bar{x}} = -\frac{(-1)^j}{a}\left(1 - \frac{\bar{y} + \bar{y}_j}{b}\right), \quad \frac{\partial \psi_j^e}{\partial \bar{y}} = \frac{(-1)^j}{b}\left(1 - \frac{\bar{x} + \bar{x}_j}{a}\right) \tag{9.2.70a}$$

$$\frac{\partial u_h^e}{\partial \bar{x}} = +\frac{1}{a}\sum_{j=1}^{n}(-1)^j u_j^e \left(1 - \frac{\bar{y} + \bar{y}_j}{b}\right), \quad \frac{\partial u_h^e}{\partial \bar{y}} = +\frac{1}{b}\sum_{j=1}^{n}(-1)^j u_j^e \left(1 - \frac{\bar{x} + \bar{x}_j}{a}\right) \tag{9.2.70b}$$

where $\bar{x}$ and $\bar{y}$ are the local coordinates [see Fig. 9.2.8(a)]. Although $\partial u_h^e/\partial \bar{x}$ and $\partial u_h^e/\partial \bar{y}$ are linear functions of y and x, respectively, in each element, they are discontinuous at inter-element boundaries. Consequently, quantities computed using derivatives of the finite element solution u_h^e are discontinuous at interelement boundaries. For example, if one computes $q_x^e = a_{11}^e \partial u_h^e/\partial x$ at node shared by three different elements, three different

values of q_x^e are expected. The difference between the three values will diminish as the mesh is refined. Some commercial finite element software give a single value of q_x at the node by averaging the values obtained from various elements connected at the node.

9.2.10 Axisymmetric Problems

In studying problems involving cylindrical geometries, it is convenient to use the cylindrical coordinate system (r, θ, z) to formulate the problem. If the geometry, boundary conditions and loading (or source) of the problem are independent of the angular coordinate θ, the problem solution will also be independent of θ. Consequently, a three-dimensional problem is reduced to a two-dimensional one in (r, z) coordinates (see Fig. 9.2.17). Here we consider a model axisymmetric problem, develop its weak form, and formulate the finite element model.

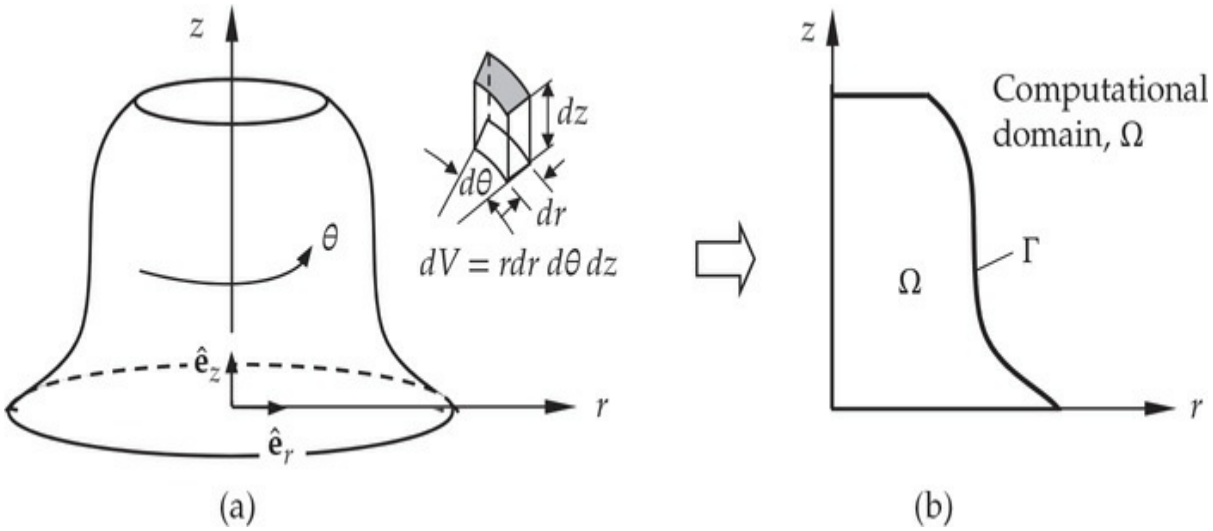

Fig. 9.2.17 (a) A 3-D axisymmetric domain. (b) 2-D axisymmetric computational domain in the r-z plane.

9.2.10.1 Model equation

Consider the partial differential equation,

$$-\frac{1}{r}\frac{\partial}{\partial r}\left(r\hat{a}_{11}\frac{\partial u}{\partial r}\right)-\frac{\partial}{\partial z}\left(\hat{a}_{22}\frac{\partial u}{\partial z}\right)+\hat{a}_{00}u=\hat{f}(r,z) \qquad (9.2.71)$$

where $\hat{a}_{00}$, $\hat{a}_{11}$, $\hat{a}_{22}$ and $\hat{f}$ are given functions of r and z. The equation arises in the study of heat transfer and other phenomena in axisymmetric geometries like the one shown in Fig. 9.2.17. In this section we formulate

the finite element model of Eq. (9.2.71) based on its weak form.

9.2.10.2 Weak form

Following the three-step procedure, we develop the weak form of Eq. (9.2.71):

$$\text{i.}\quad 0=\int_{\Omega_e} w\left[-\frac{1}{r}\frac{\partial}{\partial r}\left(r\hat{a}_{11}\frac{\partial u}{\partial r}\right)-\frac{\partial}{\partial z}\left(\hat{a}_{22}\frac{\partial u}{\partial z}\right)+\hat{a}_{00}u-\hat{f}\right]r\,dr\,dz$$

$$\text{ii.}\quad 0=\int_{\Omega_e}\left(\frac{\partial w}{\partial r}\hat{a}_{11}\frac{\partial u}{\partial r}+\frac{\partial w}{\partial z}\hat{a}_{22}\frac{\partial u}{\partial z}+w\hat{a}_{00}u-w\hat{f}\right)r\,dr\,dz$$

$$-\oint_{\Gamma_e} w\left(\hat{a}_{11}\frac{\partial u}{\partial r}n_r+\hat{a}_{22}\frac{\partial u}{\partial z}n_z\right)ds$$

$$\text{iii.}\quad 0=\int_{\Omega_e}\left(\hat{a}_{11}\frac{\partial w}{\partial r}\frac{\partial u}{\partial r}+\hat{a}_{22}\frac{\partial w}{\partial z}\frac{\partial u}{\partial z}+\hat{a}_{00}wu-w\hat{f}\right)r\,dr\,dz-\oint_{\Gamma_e} wq_n\,r\,ds \qquad (9.2.72)$$

where w is the weight function and q_n is the normal flux

$$q_n=\left(\hat{a}_{11}\frac{\partial u}{\partial r}n_r+\hat{a}_{22}\frac{\partial u}{\partial z}n_z\right) \qquad (9.2.73)$$

Note that the weak form in Eq. (9.2.72) does not differ significantly from that developed for model equation in Eq. (9.2.1) when $a_{12} = a_{21} = 0$. The only difference is the presence of r in the integrand. Consequently, Eq. (9.2.72) can be obtained as a special case of Eq. (9.2.10) for $a_{00}=\hat{a}_{00}x$, $a_{11}=\hat{a}_{11}x$, $a_{22}=\hat{a}_{22}x$, and $f=\hat{f}x$; the coordinates r and z are treated like x and y, respectively.

9.2.10.3 Finite element model

Let us assume that $u(r, z)$ is approximated by the finite element interpolation u_h^e over the element Ω_e:

$$u\approx u_h^e(r,z)=\sum_{j=1}^{n}u_j^e\psi_j^e(r,z) \qquad (9.2.74)$$

The interpolation functions $\psi_j^e(r,z)$ are the same as those developed in

Eqs. (9.2.25b) and (9.2.32a) for linear triangular and rectangular elements, respectively, with $x = r$ and $y = z$. Substitution of Eq. (9.2.74) for u and ψ_i^e for w into the weak form gives the ith equation of the finite element model

$$0 = \sum_{j=1}^{n} \left[\int_{\Omega_e} \left(\hat{a}_{11} \frac{\partial \psi_i^e}{\partial r} \frac{\partial \psi_j^e}{\partial r} + \hat{a}_{22} \frac{\partial \psi_i^e}{\partial z} \frac{\partial \psi_j^e}{\partial z} + \hat{a}_{00} \psi_i^e \psi_j^e \right) r \, dr \, dz \right] u_j^e$$

$$- \int_{\Omega_e} \psi_i^e \hat{f} r \, dr \, dz - \oint_{\Gamma_e} \psi_i^e r \, q_n \, ds \tag{9.2.75a}$$

$$0 = \sum_{j=1}^{n} K_{ij}^e u_j^e - f_i^e - Q_i^e \tag{9.2.75b}$$

where

$$K_{ij}^e = \int_{\Omega_e} \left(\hat{a}_{11} \frac{\partial \psi_i^e}{\partial r} \frac{\partial \psi_j^e}{\partial r} + \hat{a}_{22} \frac{\partial \psi_i^e}{\partial z} \frac{\partial \psi_j^e}{\partial z} + \hat{a}_{00} \psi_i^e \psi_j^e \right) r \, dr \, dz \tag{9.2.76a}$$

$$f_i^e = \int_{\Omega_e} \psi_i^e \hat{f} r \, dr \, dz, \quad Q_i^e = \oint_{\Gamma_e} \psi_i^e r \, q_n \, ds \tag{9.2.76b}$$

This completes the development of finite element model of 2-D axisymmetric problems.

For linear triangular and rectangular elements, K_{ij}^e and f_i^e can be easily evaluated analytically as before (see Section 9.2.7) for element-wise constant values of $\hat{a}_{11}^e$, $\hat{a}_{22}^e$, $\hat{a}_{00}^e$, and $\hat{f}_e$. However, in general, these coefficients are evaluated numerically using the numerical integration methods discussed in Chapter 8 for one-dimensional cases (see Section 8.2.5) and in Chapter 10 for two-dimensional problems (see Section 10.3). In the **FEM2D** computer program (to be discussed in Chapter 10), the element coefficients are evaluated using the Gauss quadrature.

Some modeling issues are discussed in the next section before a variety of applications from different fields are discussed in Section 9.4 (also see Section 10.4). The numerical results presented herein are obtained with the help of the FEM2D computer program discussed in Section 10.5.

9.3 Modeling Considerations

9.3.1 Exploitation of Solution Symmetries

First and foremost consideration, from the point of view of saving computational time and resources, is to identify any solution symmetry in the problem. A problem possesses solution symmetry about a line (or plane) only when the problem has symmetry with respect to (a) geometry, (b) material properties, (c) source term, and (d) boundary conditions (on both primary and secondary variables) about the same line (or plane). For example, if the material, the body source term (e.g., internal heat generation in a heat transfer problem), or boundary conditions of the axisymmetric geometry shown in Fig. 9.2.17 depend on (or vary with) the circumferential direction (i.e., a function of θ), then we cannot use the *rz*-plane as the computational domain because the solution is three dimensional [i.e., $u = u(r, \theta, z)$]. Whenever a portion of the domain is modeled to exploit symmetries available in the problem, the lines (or planes) of symmetries become a portion of the boundary of the domain modeled. In the case of Fig. 9.2.17 (assuming that the solution is independent of θ), the planes θ = constant are the planes of symmetry. On a plane of symmetry we must know either u or q_n. In general, on a plane of symmetry, the derivative of the solution with respect to the coordinate normal to the plane of symmetry (or, equivalently, the flux normal to the plane) is zero, requiring $q_n = 0$ on a θ = constant plane. This is not difficult to see because if $q_n \neq 0$ then there is a flow either into or out of the plane, violating the symmetry.

Another example is provided by the heat transfer in a thin orthotropic plate, with the domain and boundary conditions shown in Fig. 9.3.1(a). The governing equation is

$$-\left[\frac{\partial}{\partial x}\left(k_x\frac{\partial T}{\partial x}\right)+\frac{\partial}{\partial y}\left(k_y\frac{\partial T}{\partial y}\right)\right]=g(x,y) \text{ in } \Omega \qquad (9.3.1)$$

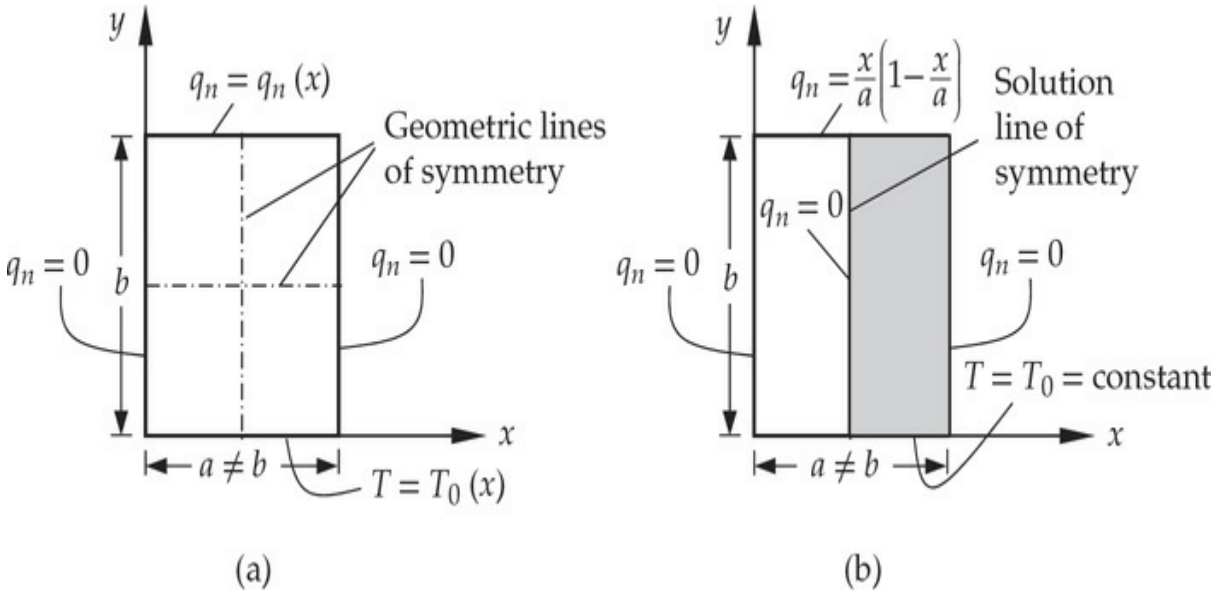

Fig. 9.3.1 (a) Given domain with boundary conditions. (b) Computational domain.

where k_x and k_y are conductivities in the x and y directions, respectively, and $g(x, y)$ is internal heat generation. From the geometric consideration, the domain has two lines of symmetry, namely $x = 0.5a$ and $y = 0.5b$. If the conductivities are constant, they too have the same lines of symmetry as the geometry. However, if the plate is orthotropic but inhomogeneous in such a way that k_x or k_y is a nonsymmetric function with respect to x or y, we have no symmetry at all. Similarly, if the internal heat generation g is a nonsymmetric function of x and y, we have no line of symmetry. From the boundary conditions it is clear that the problem has no line of symmetry if the specified temperature or boundary flux distributions are nonsymmetric. If k_x, k_y, g, T_0, and q_n are constant, then $x = 0.5a$ is a line of symmetry, and one can use the domain either on the left or on the right of the line of symmetry as the computational domain with $q_n = 0$ along the line of symmetry, as shown in Fig. 9.3.1(b). Also, when k_x, k_y, and g are constant and T_0 and q_n are symmetric functions about the $x = 0.5a$ line, we again have the solution symmetry about the $x = 0.5a$ line.

9.3.2 Choice of a Mesh and Mesh Refinement

The representation of a given computational domain by a collection of finite elements (finite element mesh) requires engineering judgement on the part of the finite element practitioner. The number, type (e.g., linear, quadratic), shape (e.g., triangular, rectangular), and density of elements

(i.e., mesh refinement) used in a given problem depend on a number of considerations. The first consideration is to discretize the domain as exactly as possible with elements that are admissible. Next consideration is an accurate representation of sources (or loads) and material and geometric discontinuities (i.e., rapid or sudden changes), including a reentrant corner. The discretization should include, for example, nodes at point sources (so that a point source is accurately lumped at the node), although it is possible to distribute a point source inside an element to the element nodes [see Eqs. (3.4.53)–(3.4.55)].

The representation of point or rapidly changing loads and material and geometric discontinuities require sufficiently small elements in the region of the rapid changes so that steep gradients of the solution are accurately represented. The engineering judgement should come from both a qualitative understanding of the behavior of the solution and an estimate of the computational costs involved in the mesh refinement (i.e., either reducing the size of the elements or increasing the order of the element; they are called *h* and *p* refinements, respectively). For example, consider the inviscid flow around a cylinder in a channel. The flow entering the channel at the left goes around the cylinder and exits the channel at the right [see Fig. 9.3.2(a)]. Since the section at the cylinder is smaller than the inlet section, it is expected that the flow accelerates in the vicinity of the cylinder. On the other hand, the velocity field far from the cylinder (e.g., at the inlet) is essentially uniform. Such knowledge of the qualitative behavior of the flow allows us to employ a coarse mesh (i.e., elements that are relatively large in size) at sites sufficiently far from the cylinder and a fine one at closer distances to the cylinder [see Fig. 9.3.2(b)]. Another reason for using a refined mesh near the cylinder is to accurately represent the curved boundary of the domain there. In general, a refined mesh is required in places where acute changes in geometry, boundary conditions, loading, or material properties occur.

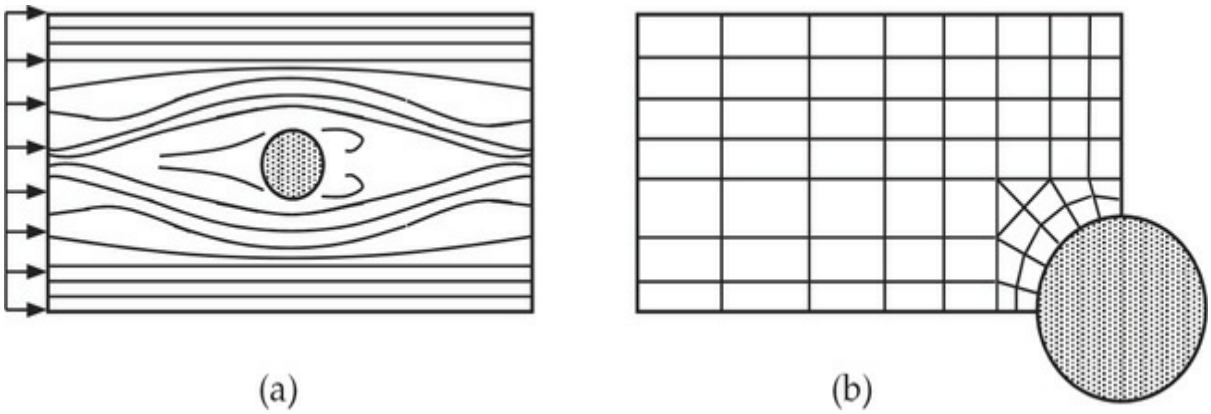

Fig. 9.3.2 (a) Flow of an inviscid fluid around a cylinder (streamlines). (b) A typical mesh for a quadrant of the domain.

A mesh refinement should meet three conditions: (1) all previous meshes should be contained in the current refined mesh; (2) every point in the body can be included within an arbitrarily small element at any stage of the mesh refinement; and (3) the same order of approximation for the solution should be retained through all stages of the refinement process. The last requirement eliminates comparison of two different approximations in two different meshes.

When a mesh is refined, care should be taken to avoid elements with very large aspect ratios (i.e., the ratio of one side of an element to the other) or small angles. When the aspect ratios are very large, the resulting coefficient matrices are ill-conditioned (i.e., numerically not invertible) and some of the physical features of the mathematical model may be lost. Although the safe lower and upper limits on aspect ratios are 0.1 to 10, the actual values are much more extreme and they depend on the nature of physical phenomenon being modeled.

The words “coarse” and “fine” are relative. In any given problem, one begins with a finite element mesh that is believed to be adequate (based on experience and engineering judgement) to solve the problem at hand. Then, as a second choice, one selects a mesh that consists of a larger number of elements (and includes the first one as a subset) to solve the problem once again. If there is a significant difference between the two solutions, one sees the benefit of mesh refinement and further mesh refinement may be warranted. If the difference is negligibly small, further mesh refinements are not necessary.

Four different meshes of rectangular elements are shown in Fig. 9.3.3. Each of the meshes contains the previous mesh as a subset. The meshes shown in Fig. 9.3.3(b) and (c) are nonuniform while those in Fig. 9.3.3(a) and (d) are uniform.

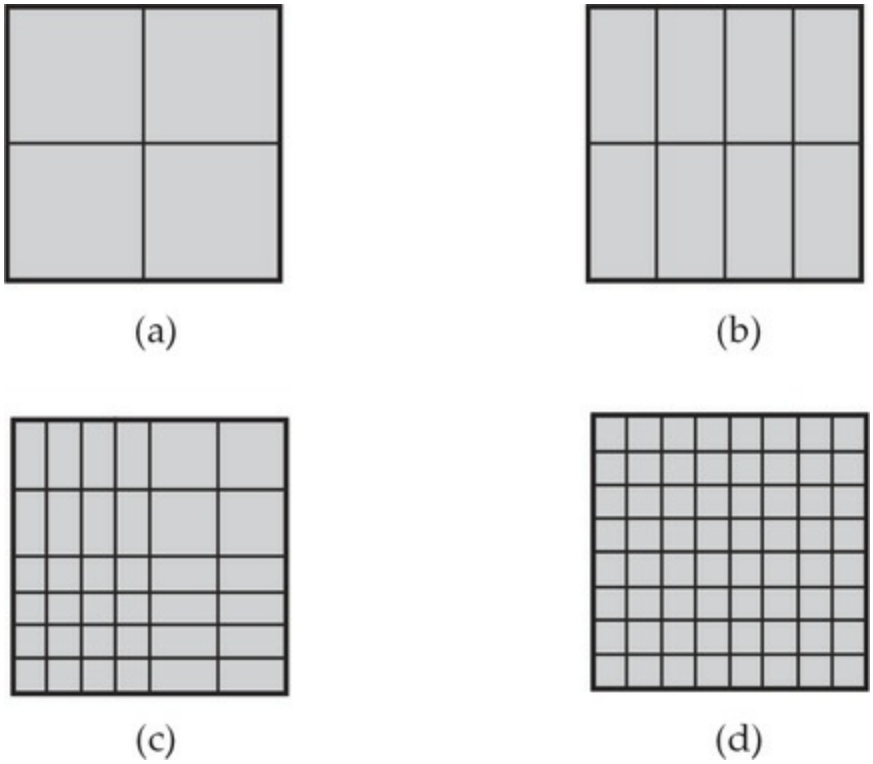

Fig. 9.3.3 (a) 2 × 2 mesh; (b) 4 × 2 mesh; (c) 6 × 6 mesh; and (d) 8 × 8 mesh. Here a *m* × *n* mesh means *m* number of elements in the *x* direction and *n* number of elements in the *y* direction. Meshes in (a) and (d) are uniform; meshes in (b) and (c) are nonuniform.

9.3.3 Imposition of Boundary Conditions

When it comes to the imposition of boundary conditions, the most important thing is to know the duality pairs (i.e., primary and secondary variables) of the problem. Then one should also know that *only one element of the duality pair can be specified at any node of the finite element mesh*, unless there is a relation linking the two (like in the the case of spring support or inclined support). In some problems of interest one encounters situations where both elements of the duality pair may appear to be known. Such points are called *singular points*. As a rule, when both elements of a duality pair are known, one should impose the boundary condition on the primary variable and let the secondary variable take its value (which is calculated in the post-computation). The reason for this is that boundary conditions on primary variables are often maintained in practice more strictly than those on the secondary variables. Of course, if the true situation in a problem is that the secondary variable are imposed and the primary variable is a result of it, then consideration must be given to the former one.

Another type of singularity one encounters is the specification of two different values of a primary or secondary variable at the same point. An example of such cases is provided by the problem in Fig. 9.3.4, where u is specified to be zero on the boundary defined by the line $x = 0$, and it is specified to be unity on the boundary defined by the line $y = 1$. Consequently, at $x = 0$ and $y = 1$, u has two different values. The analyst must make a choice between the two values. In either case, the true boundary condition is replaced by an approximate condition. Often, the larger value is used to obtain a conservative design. The closeness of the approximate boundary condition to the true one depends on the size of the element containing the point (see Fig. 9.3.4). A mesh refinement in the vicinity of the singular point often yields an acceptable solution.

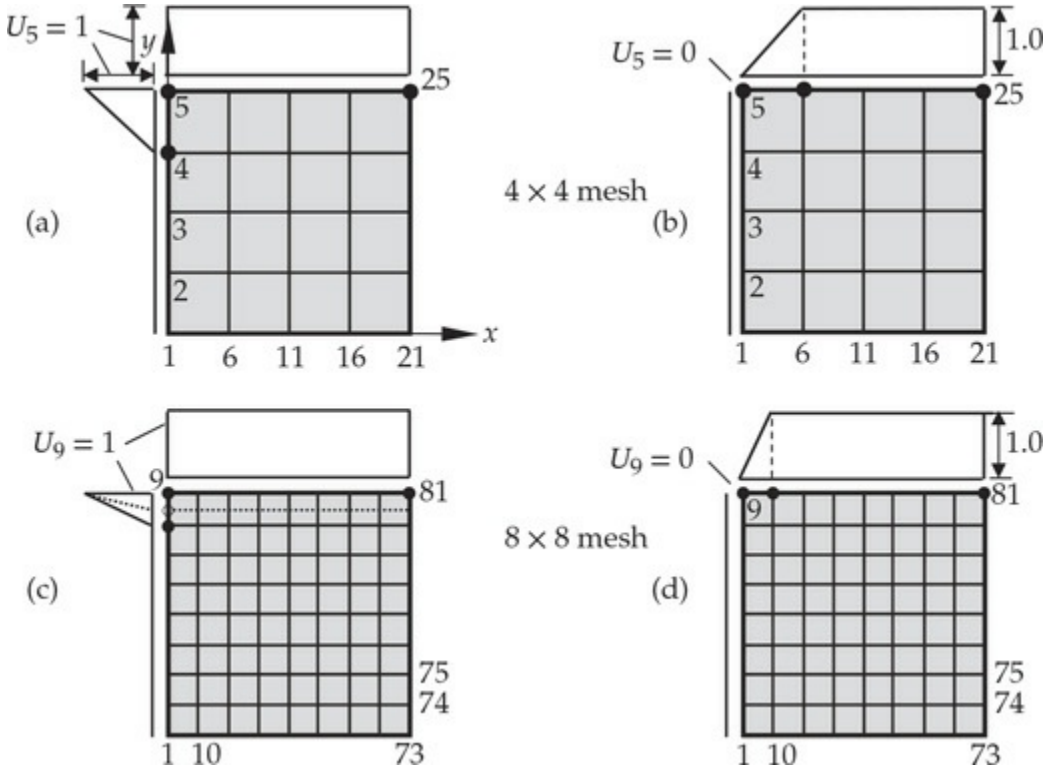

Fig. 9.3.4 Effect of specifying two values of a primary variable at a node [node 5 in (a) and (b) and node 9 in (c) and (d)]. The domain is unit square.

9.4 Numerical Examples

9.4.1 General Field Problems

An application of the finite element model developed in Sections

9.2.2–9.2.9 to problems governed by the Poisson equation is discussed here. This example is designed to illustrate selection of the computational domain, choice of elements and mesh, assembly of element equations, imposition of boundary conditions, and postprocessing. The physical background of the problem is not discussed here but Table 9.1.1 provides a list of problems in which the equation arises. All of the actual computations were carried out using the FEM2D program, which will be discussed in detail in Chapter 10.

Example 9.4.1

Consider a problem described by the Poisson equation

$$-k\nabla^2 u = f_0 \quad \text{or} \quad -k\left(\frac{\partial^2 u}{\partial x^2} + \frac{\partial^2 u}{\partial y^2}\right) = f_0 \quad \text{in } \Omega \tag{1}$$

in a square region [see Fig. 9.4.1(a)]

$$\Omega = \{(x, y) : -A < x < A,\ -A < y < A\}$$

where $u(x, y)$ is the dependent variable (temperature) to be determined, k is a material constant (thermal conductivity), and f_0 is the uniformly distributed source (internal heat generation). Consider the following boundary condition for the problem:

$$u = 0 \ \text{ on the entire boundary } \Gamma \tag{2}$$

Use the finite element method to determine $u(x, y)$ everywhere in Ω.
Solution: A number of important issues in solving the partial differential equation (heat conduction equation) by the finite element method are discussed in the following pages.

Selection of the Computational Domain

When the given domain Ω exhibits solution symmetries, it is sufficient to solve the problem on a portion of Ω that provides the solution on the entire domain. The problem at hand has the geometric symmetry about the $x = 0$ and $y = 0$ lines as well as about $x = y$ and $x = -y$ lines (i.e., diagonals); since the coefficient describing the material behavior, k, and the source term f_0 are constant, they have infinite number of planes of symmetry (i.e., they are independent of any plane). Lastly, the boundary conditions are symmetric with respect to the same four lines of symmetry

as the geometry. Thus, the solution is symmetric about to the four lines: $x = 0$, $y = 0$, $x = y$, and $x = -y$. Hence, an octant of the domain can be used as the computational domain [see Fig. 9.4.1(b)], if a mesh of triangles is used. For a mesh of rectangles (only), one can only use the quadrant as the computational domain [see Fig. 9.4.1(c)]. While it is possible to mix triangular and rectangular elements to represent the computational domain as well as the solution, in the actual solution of problems discussed in this book (and in FEM2D), we shall use only one type of element at a time.

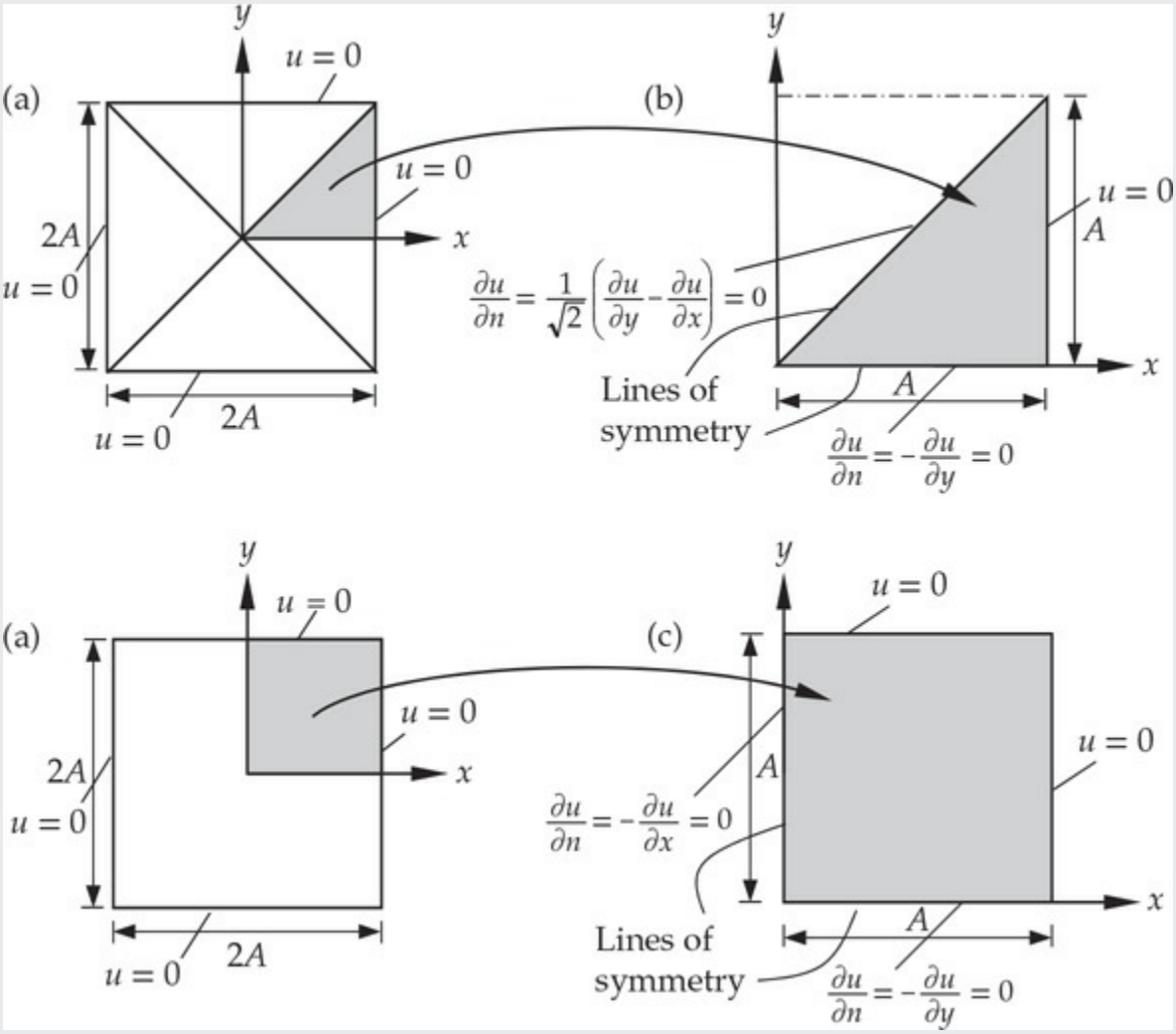

Fig. 9.4.1 (a) Geometry of the actual domain with boundary conditions. (b) Computational domain based on biaxial and diagonal symmetry. (c) Computational domain based on biaxial symmetry.

On lines of symmetry, the normal derivative of the solution (i.e., derivative of the solution with respect to the coordinate normal to the line of symmetry) is zero, giving:

$$q_n = k\frac{\partial u}{\partial n} = k\left(\frac{\partial u}{\partial x}n_x + \frac{\partial u}{\partial y}n_y\right) = 0 \tag{3}$$

Solution by Linear Triangular Elements

Due to the symmetry along the diagonal $x = y$, we model the triangular domain shown in Fig. 9.4.1(b). As a first choice we use a uniform mesh of four linear triangular elements, as shown in Fig. 9.4.2(a), to represent the domain (Mesh T1), and then use the refined mesh (Mesh T2) shown in Fig. 9.4.2(b) to compare the solutions. In the present case, there is no discretization error involved because the geometry is exactly represented.

Elements 1, 3, and 4 are identical in orientation as well as geometry. Element 2 is geometrically identical to element 1, except that it is oriented differently. If we number the local nodes of element 2 to match those of element 1, then all four elements have the same element matrices, and it is necessary to compute them only for element 1. When the element matrices are computed on a computer, such considerations are not taken into account. In solving the problem by hand, we use the similarity between element 1 and the other elements in the mesh to avoid unnecessary computations.

We consider element 1 as the typical element. The element is exactly the same as the one shown in Fig. 9.2.11(b). Hence, the element coefficient matrix and source vector are

$$\mathbf{K}^1 = \frac{k}{2ab}\begin{bmatrix} b^2 & -b^2 & 0 \\ -b^2 & a^2+b^2 & -a^2 \\ 0 & -a^2 & a^2 \end{bmatrix}, \quad \mathbf{f}^1 = \frac{f_0 ab}{6}\begin{Bmatrix} 1 \\ 1 \\ 1 \end{Bmatrix} \tag{4}$$

where, in the present case, $a = b = A/2 = 0.5$.

The element matrix in Eq. (4) is valid for the Laplace operator $-\nabla^2$ on any right-angle triangle with sides a and b in which the right angle is at node 2, and the diagonal line of the triangle connects node 3 to node 1. Note that the off-diagonal coefficient associated with the nodes on the diagonal line is zero for a right-angled triangle. In summary, for the mesh shown in Fig. 9.4.2(a), we have

$$\mathbf{K}^1 = \mathbf{K}^2 = \mathbf{K}^3 = \mathbf{K}^4, \quad \mathbf{f}^1 = \mathbf{f}^2 = \mathbf{f}^3 = \mathbf{f}^4$$

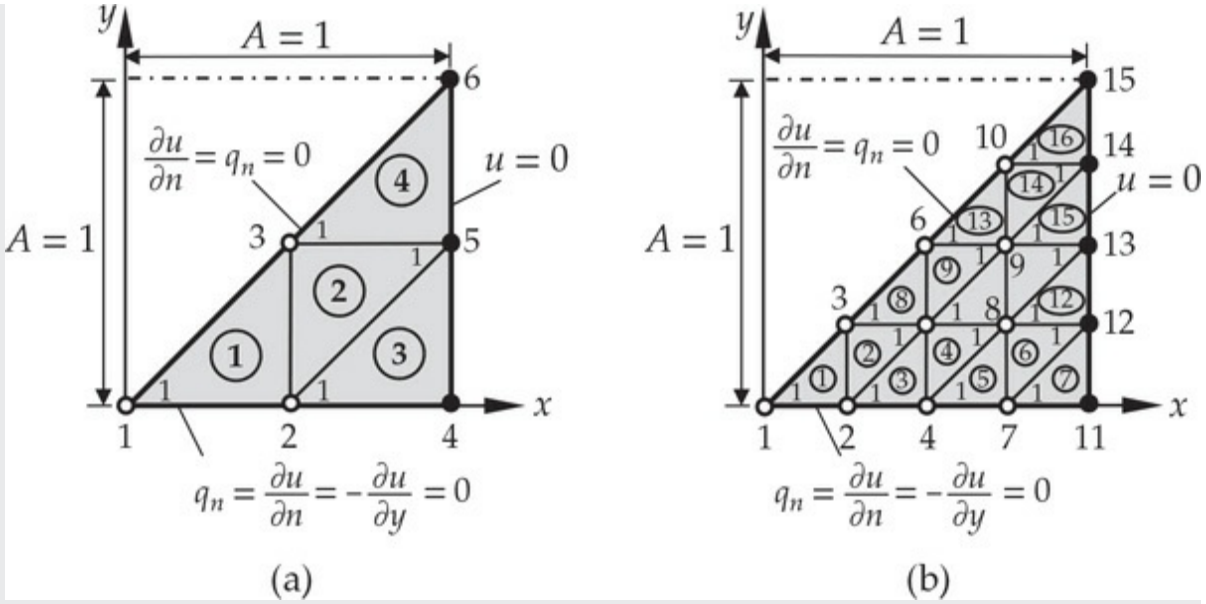

Fig. 9.4.2 (a) Mesh T1 of triangular elements. (b) Mesh T2 of triangular elements.

with

$$\mathbf{K}^e = \frac{k}{2}\begin{bmatrix} 1 & -1 & 0 \\ -1 & 2 & -1 \\ 0 & -1 & 1 \end{bmatrix}, \quad \mathbf{f}^e = \frac{f_0}{24}\begin{Bmatrix} 1 \\ 1 \\ 1 \end{Bmatrix} \tag{5}$$

The assembled coefficient matrix for the finite element mesh is 6 × 6, because there are six global nodes with one unknown per node. The assembled matrix can be obtained directly by using the correspondence between the global nodes and the local nodes, expressed through the connectivity matrix,

$$\mathbf{B} = \begin{bmatrix} 1 & 2 & 3 \\ 5 & 3 & 2 \\ 2 & 4 & 5 \\ 3 & 5 & 6 \end{bmatrix} \tag{6}$$

Few representative global coefficients in terms of the element coefficients are given below.

$$K_{11} = K_{11}^1 = \frac{k}{2},\ K_{12} = K_{12}^1 = -\frac{k}{2},\ K_{22} = K_{22}^1 + K_{33}^2 + K_{11}^3 = \frac{2k}{2} + \frac{k}{2} + \frac{k}{2}$$

$$K_{13} = K_{13}^1 = 0,\ K_{14} = 0,\ K_{15} = 0,\ K_{16} = 0,\ K_{23} = K_{23}^1 + K_{32}^2 = -\frac{k}{2} - \frac{k}{2}$$

$$K_{33} = K_{33}^1 + K_{22}^2 + K_{11}^4 = \frac{k}{2} + \frac{2k}{2} + \frac{k}{2},\ F_1 = F_1^1 = Q_1^1 + f_1^1 \tag{7}$$

$$F_2 = (Q_2^1 + Q_3^2 + Q_1^3) + (f_2^1 + f_3^2 + f_1^3),\ F_3 = (Q_3^1 + Q_2^2 + Q_1^4) + (f_3^1 + f_2^2 + f_1^4)$$

$$F_4 = F_2^3 = Q_2^3 + f_2^3,\ F_5 = (Q_1^2 + Q_3^3 + Q_2^4) + (f_1^2 + f_3^3 + f_2^4),\ F_6 = F_3^4 = Q_3^4 + f_3^4$$

The assembled system of equations associated with Mesh T1 are

$$\frac{k}{2}\begin{bmatrix} 1 & -1 & 0 & 0 & 0 & 0 \\ -1 & 4 & -2 & -1 & 0 & 0 \\ 0 & -2 & 4 & 0 & -2 & 0 \\ 0 & -1 & 0 & 2 & -1 & 0 \\ 0 & 0 & -2 & -1 & 4 & -1 \\ 0 & 0 & 0 & 0 & -1 & 1 \end{bmatrix} \begin{Bmatrix} U_1 \\ U_2 \\ U_3 \\ U_4 \\ U_5 \\ U_6 \end{Bmatrix} = \frac{f_0}{24} \begin{Bmatrix} 1 \\ 3 \\ 3 \\ 1 \\ 3 \\ 1 \end{Bmatrix} + \begin{Bmatrix} Q_1^1 \\ Q_2^1 + Q_3^2 + Q_1^3 \\ Q_3^1 + Q_2^2 + Q_1^4 \\ Q_2^3 \\ Q_1^2 + Q_3^3 + Q_2^4 \\ Q_3^4 \end{Bmatrix} \tag{8}$$

Note that at nodes 4 and 6, we have both u and q_n specified (a type of singularity in the specified data). However, we shall give priority to the primary variable over the secondary variable. Thus, we assume that

$$U_4 = U_5 = U_6 = 0 \tag{9}$$

and Q_4, Q_5, and Q_6, assumed to be unknown, are determined in the post-computation. The specified secondary degrees of freedom are (all due to symmetry)

$$Q_1 = Q_1^1 = 0, \quad Q_2 = Q_2^1 + Q_3^2 + Q_1^3 = 0, \quad Q_3 = Q_3^1 + Q_2^2 + Q_1^4 = 0 \tag{10}$$

For example, consider the sum

$$\begin{aligned} Q_2^1 + Q_3^2 + Q_1^3 &= (Q_{21}^1 + Q_{22}^1) + (Q_{32}^2 + Q_{33}^2) + (Q_{11}^3 + Q_{13}^3) \\ &= Q_{21}^1 + (Q_{22}^1 + Q_{32}^2) + (Q_{33}^2 + Q_{13}^3) + Q_{11}^3 = 0 + 0 + 0 + 0 \end{aligned}$$

where Q_{21}^1 and Q_{11}^3 are zero because of $q_n = 0$ and $Q_{22}^1 + Q_{32}^2$ and $Q_{33}^2 + Q_{13}^3$ are zero because of balance of fluxes between neighboring elements.

Since the only unknown primary variables for Mesh T1 are (U_1, U_2 and U_3), the condensed equations for the primary unknowns can be

obtained by deleting rows and columns 4, 5 and 6 from the system (7). In retrospect, it would have been sufficient to write the element equations associated with the global nodes 1, 2, and 3:

$$\begin{aligned} K_{11}U_1 + K_{12}U_2 + K_{13}U_3 &= F_1 \\ K_{21}U_1 + K_{22}U_2 + K_{23}U_3 + K_{24}U_4 + K_{25}U_5 &= F_2 \\ K_{31}U_1 + K_{32}U_2 + K_{33}U_3 + K_{35}U_5 + K_{36}U_6 &= F_3 \end{aligned}$$

Noting that $U_4 = U_5 = U_6 = 0$, we can write the above equations in terms of the element coefficients:

$$\begin{bmatrix} K_{11}^1 & K_{12}^1 & K_{13}^1 \\ K_{21}^1 & K_{22}^1 + K_{33}^2 + K_{11}^3 & K_{23}^1 + K_{32}^2 \\ K_{31}^1 & K_{32}^1 + K_{23}^2 & K_{33}^1 + K_{22}^2 + K_{11}^4 \end{bmatrix} \begin{Bmatrix} U_1 \\ U_2 \\ U_3 \end{Bmatrix} = \begin{Bmatrix} f_1^1 \\ f_2^1 + f_3^2 + f_1^3 \\ f_3^1 + f_2^2 + f_1^4 \end{Bmatrix} \tag{11}$$

The unknown secondary variables Q_4, Q_5 and Q_6 can be computed from the element equations

$$\begin{Bmatrix} Q_4 \\ Q_5 \\ Q_6 \end{Bmatrix} = -\begin{Bmatrix} f_2^3 \\ f_1^2 + f_3^3 + f_2^4 \\ f_3^4 \end{Bmatrix} + \begin{bmatrix} 0 & K_{21}^3 & 0 \\ 0 & K_{13}^2 + K_{31}^3 & K_{12}^2 + K_{21}^4 \\ 0 & 0 & K_{31}^4 \end{bmatrix} \begin{Bmatrix} U_1 \\ U_2 \\ U_3 \end{Bmatrix} \tag{12}$$

For example, we have

$$\begin{aligned} Q_4 = Q_2^3 &= Q_{21}^3 + Q_{22}^3 + Q_{23}^3 \\ &= \int_{1-2} q_n^3 \psi_2^3 \, dx + \int_{2-3} q_n^3 \psi_2^3 \, dy + \int_{3-1} q_n^3 \psi_2^3 \, ds \end{aligned} \tag{13a}$$

where

$$\begin{aligned} (q_n^3)_{1-2} &= \left(\frac{\partial u}{\partial x} n_x + \frac{\partial u}{\partial y} n_y \right)_{1-2} = 0 \quad \left(n_x = 0, \quad \frac{\partial u}{\partial y} = 0 \right) \\ (q_n^3)_{2-3} &= \left(\frac{\partial u}{\partial x} n_x + \frac{\partial u}{\partial y} n_y \right)_{2-3} = \frac{\partial u}{\partial x} \quad (n_x = 1, \quad n_y = 0) \\ (\psi_2^3)_{2-3} &= 1 - \frac{y}{h_{23}}, \quad (\psi_2^3)_{3-1} = 0 \end{aligned} \tag{13b}$$

Thus, we have

$$Q_4 = Q_{22}^3 = \int_0^{h_{23}} \frac{\partial u}{\partial x}\left(1 - \frac{y}{h_{23}}\right) dy$$

where $\partial u/\partial x$ is calculated using $\partial u_h/\partial x$ from the finite element interpolation

$$\frac{\partial u_h}{\partial x} = \sum_{j=1}^{3} u_j^3 \frac{\beta_j^3}{2A_3}$$

We obtain ($h_{23} = a = 0.5$, $\beta_1^3 = -a = -0.5$, $2A_3 = a^2 = 0.25$, $U_4 = U_5 = 0$),

$$Q_4 = \frac{h_{23}}{4A_3}\sum_{j=1}^{3} u_j^3 \beta_j^3 = \frac{h_{23}}{4A_3}(\beta_1^3 U_2 + \beta_2^3 U_4 + \beta_3^3 U_5) = -0.5U_2 \tag{13c}$$

Using the numerical values of the coefficients K_{ij}^e and f_i^e, with $k = 1$ and $f_0 = 1$, we write the condensed equations for U_1, U_2 and U_3 as

$$\begin{bmatrix} 0.5 & -0.5 & 0.0 \\ -0.5 & 2.0 & -1.0 \\ 0.0 & -1.0 & 2.0 \end{bmatrix} \begin{Bmatrix} U_1 \\ U_2 \\ U_3 \end{Bmatrix} = \frac{1}{24}\begin{Bmatrix} 1 \\ 3 \\ 3 \end{Bmatrix} \tag{14}$$

Solving Eq. (14) for U_i ($i = 1, 2, 3$), we obtain

$$\begin{Bmatrix} U_1 \\ U_2 \\ U_3 \end{Bmatrix} = \frac{1}{24}\begin{bmatrix} 3 & 1 & 0.5 \\ 1 & 1 & 0.5 \\ 0.5 & 0.5 & 0.75 \end{bmatrix} \begin{Bmatrix} 1 \\ 3 \\ 3 \end{Bmatrix} = \frac{1}{24}\begin{Bmatrix} 7.5 \\ 5.5 \\ 4.25 \end{Bmatrix} = \begin{Bmatrix} 0.31250 \\ 0.22917 \\ 0.17708 \end{Bmatrix} \tag{15}$$

and, from (12), we have

$$\begin{Bmatrix} Q_{22}^3 \\ Q_{32}^3 + Q_{22}^4 \\ Q_{32}^4 \end{Bmatrix} = -\frac{f_0}{24}\begin{Bmatrix} 1 \\ 3 \\ 1 \end{Bmatrix} + k\begin{bmatrix} 0 & -0.5 & 0 \\ 0 & 0 & -1 \\ 0 & 0 & 0 \end{bmatrix} \begin{Bmatrix} U_1 \\ U_2 \\ U_3 \end{Bmatrix} = \begin{Bmatrix} -0.197917 \\ -0.302083 \\ -0.041667 \end{Bmatrix} \tag{16}$$

By interpolation, $Q_4 = Q_{22}^3$, for example, is equal to $-0.5U_2$, and it differs from Q_{22}^3 computed from equilibrium by the amount, $f_2^3 \left(= \frac{1}{24}\right)$.

Solution by Linear Rectangular Elements

We use a 2 × 2 (2 elements in the x-direction and 2 elements in the y-direction) uniform mesh (Mesh R1) of four linear rectangular elements [see Fig. 9.4.3(a)] to discretize a quadrant of the domain. The 4 × 4 mesh (Mesh R2) [see Fig. 9.4.3(b)] will be used for comparison. Once again, no

discretization error is introduced in the present case.

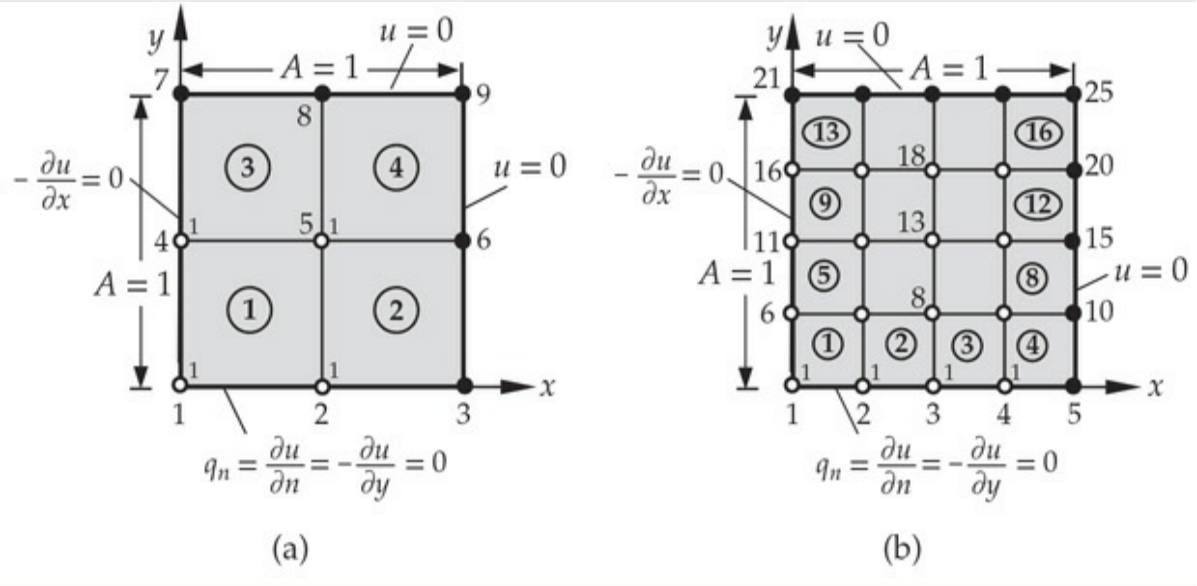

Fig. 9.4.3 (a) Mesh R1 (2 × 2) of rectangular elements. (b) Mesh R2 (4 × 4) of rectangular elements.

Since all elements in the mesh are identical, we need to compute the element coefficient matrices for only one element, say element 1. The element coefficient matrix is available from **Example 9.2.3** with $a = b$. We have

$$[K^e] = \frac{k}{6}\begin{bmatrix} 4 & -1 & -2 & -1 \\ -1 & 4 & -1 & -2 \\ -2 & -1 & 4 & -1 \\ -1 & -2 & -1 & 4 \end{bmatrix}, \quad \{f^e\} = \frac{f_0 a^2}{4}\begin{Bmatrix} 1 \\ 1 \\ 1 \\ 1 \end{Bmatrix} \tag{18}$$

The coefficient matrix of the condensed equations for the primary unknowns in Mesh R1 can be directly assembled. There are four unknowns (at nodes 1, 2, 4 and 5). The element equations associated with the four unknowns are (noting that $U_3 = U_6 = U_7 = U_8 = U_9 = 0$)

$$\begin{aligned} K_{11}U_1 + K_{12}U_2 + K_{14}U_4 + K_{15}U_5 &= F_1 \\ K_{21}U_1 + K_{22}U_2 + K_{24}U_4 + K_{25}U_5 &= F_2 \\ K_{41}U_1 + K_{42}U_2 + K_{44}U_4 + K_{45}U_5 &= F_4 \\ K_{51}U_1 + K_{52}U_2 + K_{54}U_4 + K_{55}U_5 &= F_5 \end{aligned} \tag{19a}$$

where K_{IJ} and F_I are the global coefficients, which can be written in terms of the element coefficients as

$$
\begin{aligned}
&K_{11}=K_{11}^1, \quad K_{12}=K_{12}^1, \quad K_{14}=K_{14}^1, \quad K_{15}=K_{13}^1\\
&K_{22}=K_{22}^1+K_{11}^2, \quad K_{24}=K_{24}^1, \quad K_{25}=K_{23}^1+K_{14}^2\\
&K_{44}=K_{44}^1+K_{11}^3, \quad K_{45}=K_{43}^1+K_{12}^3, \quad K_{55}=K_{33}^1+K_{44}^2+K_{11}^4+K_{22}^3\\
&F_1=f_1^1+Q_1^1, \quad F_2=f_2^1+f_1^2+Q_2^1+Q_1^2, \quad F_4=f_4^1+f_1^3+Q_4^1+Q_1^3\\
&F_5=f_3^1+f_4^2+f_1^4+f_2^3+Q_3^1+Q_4^2+Q_1^4+Q_2^3
\end{aligned}
\tag{19b}
$$

The boundary conditions on the secondary variables are

$$
Q_1^1=0, \quad Q_2^1+Q_1^2=0, \quad Q_4^1+Q_1^3=0 \tag{20a}
$$

and the balance of secondary variables at global node 5 requires

$$
Q_3^1+Q_4^2+Q_2^3+Q_1^4=0 \tag{20b}
$$

Thus the condensed equations for the primary unknowns are (for $f_0 = 1$ and $a = 0.5$)

$$
\frac{k}{6}\begin{bmatrix} 4 & -1 & -1 & -2 \\ -1 & 8 & -2 & -2 \\ -1 & -2 & 8 & -2 \\ -2 & -2 & -2 & 16 \end{bmatrix}\begin{Bmatrix} U_1 \\ U_2 \\ U_4 \\ U_5 \end{Bmatrix}=\frac{f_0}{16}\begin{Bmatrix} 1 \\ 2 \\ 2 \\ 4 \end{Bmatrix} \tag{21}
$$

The solution of these equations is (for $k = 1$ and $f_0 = 1$)

$$
U_1=0.31071, \quad U_2=0.24107, \quad U_4=0.24107, \quad U_5=0.19286 \tag{22}
$$

The secondary variables $Q_3 = Q_7$, $Q_6 = Q_8$, and Q_9 at nodes 3 (7), 6 (8) and 9, respectively (by symmetry), can be computed from the equations ($Q_3=Q_2^2,\ Q_6=Q_3^2+Q_2^4, Q_9=Q_3^4$)

$$
\begin{Bmatrix} Q_3 \\ Q_6 \\ Q_9 \end{Bmatrix}=-\begin{Bmatrix} f_2^2 \\ f_3^2+f_2^4 \\ f_3^4 \end{Bmatrix}+\begin{bmatrix} K_{31} & K_{32} & K_{34} & K_{35} \\ K_{61} & K_{62} & K_{64} & K_{65} \\ K_{91} & K_{92} & K_{94} & K_{95} \end{bmatrix}\begin{Bmatrix} U_1 \\ U_2 \\ U_4 \\ U_5 \end{Bmatrix} \tag{23a}
$$

where

$$
\begin{aligned}
&K_{31}=0, \quad K_{32}=K_{21}^2, \quad K_{34}=0, \quad K_{35}=K_{24}^2\\
&K_{61}=0, \quad K_{62}=K_{31}^2, \quad K_{64}=0, \quad K_{65}=K_{34}^2+K_{21}^4\\
&K_{91}=0, \quad K_{92}=0, \quad K_{94}=0, \quad K_{95}=K_{31}^4
\end{aligned}
\tag{23b}
$$

Substituting the numerical values, we obtain

$$\begin{Bmatrix} Q_3 \\ Q_6 \\ Q_9 \end{Bmatrix} = -\frac{1}{16}\begin{Bmatrix} 1 \\ 2 \\ 1 \end{Bmatrix} + \frac{1}{6}\begin{bmatrix} 0 & -1 & 0 & -2 \\ 0 & -2 & 0 & -2 \\ 0 & 0 & 0 & -2 \end{bmatrix}\begin{Bmatrix} U_1 \\ U_2 \\ U_4 \\ U_5 \end{Bmatrix} = -\begin{Bmatrix} 0.16697 \\ 0.26964 \\ 0.12679 \end{Bmatrix} \tag{24}$$

The finite element solutions obtained by two different meshes of triangular elements and two different meshes of rectangular elements are compared in Table 9.4.1 with the 50-term series solution (at $x = 0$ for varying y) in Eq. (2.5.40) (set $k = 1$, $g_0 = f_0 = 1$) and the one-parameter Ritz solution in Eq. (2.5.39); see also Fig. 9.4.4. The finite element solution obtained by 16 triangular elements (in an octant) is the most accurate when compared to the series solution. The accuracy of the triangular element mesh is due to the large number of elements it has compared to the number of elements in the rectangular element mesh for the same size of the domain.

Table 9.4.1 Comparison of the finite element solutions $u(0, y)$ with the series solution and the Ritz solution of Example 9.4.1.

	Triangular elem.		Rectangular elem.		Ritz solution	Series solution
y	Mesh T1	Mesh T2	Mesh R1	Mesh R2	(2.5.39)	(2.5.40)
0.00	0.3125	0.3013	0.3107	0.2984	0.3125	0.2947
0.25	0.2708[1]	0.2805	0.2759[1]	0.2824	0.2930	0.2789
0.50	0.2292	0.2292	0.2411	0.2322	0.2344	0.2293
0.75	0.1146[1]	0.1393	0.1205[1]	0.1414	0.1367	0.1397
1.00	0.0000	0.0000	0.0000	0.0000	0.0000	0.0000

[1]Interpolated values.

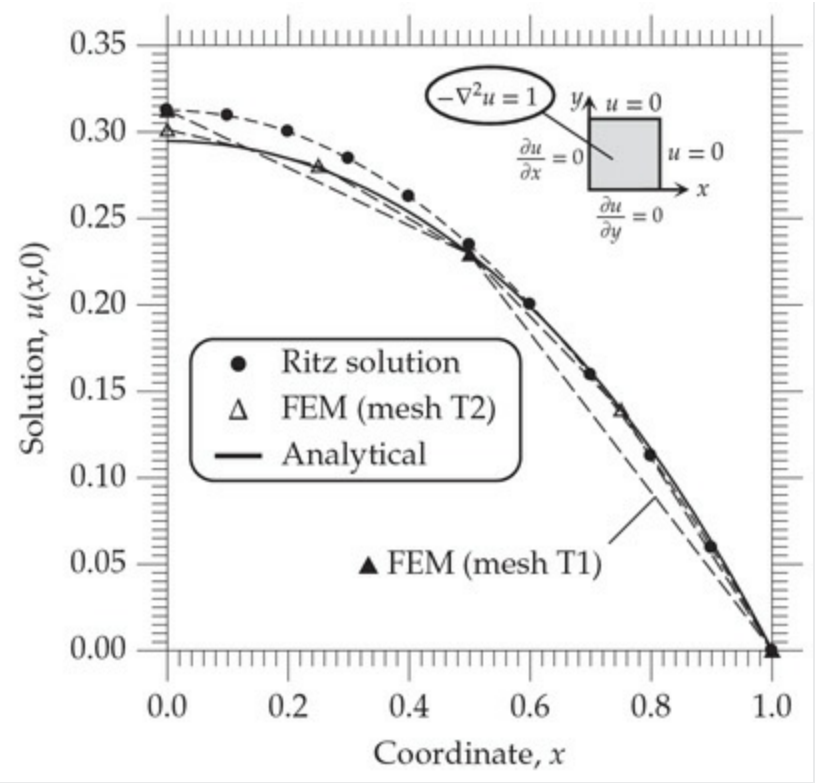

Fig. 9.4.4 Comparison of the finite element solution with the two-parameter Ritz solution and the analytical (series) solution.

The solution u and components of flux (q_x, q_y) can be computed at any interior point of the domain. For a point (x, y) in element Ω_e, we have ($k = 1$)

$$u_h^e(x,y) = \sum_{j=1}^{n} u_j^e \psi_j^e(x,y)$$

$$q_y^e(x,y) = -k\frac{\partial u_h^e}{\partial y} = -\sum_{i=1}^{n} u_i^e \frac{\partial \psi_i^e}{\partial y} \tag{25}$$

$$q_x^e(x,y) = -k\frac{\partial u_h^e}{\partial x} = -\sum_{i=1}^{n} u_i^e \frac{\partial \psi_i^e}{\partial x}$$

The negative sign in the definition of fluxes is dictated by the physics of the problem. Here we interpreted the problem at hand to be one of heat transfer. Note that for a linear triangular element q_x and q_y are constants over an entire element, whereas q_x is linear in y and q_y is linear in x for a linear rectangular element. For example, consider element 1 of mesh T1 of triangular elements

$$q_x^1(x,y) = -\frac{k}{2A_1}\sum_{i=1}^{3} u_i^1 \beta_i^1 = -2(U_2 - U_1) = 0.16667$$

$$q_y^1(x,y) = -\frac{k}{2A_1}\sum_{i=1}^{3} u_i^1 \gamma_i^1 = -2(U_3 - U_2) = 0.10417 \qquad (26a)$$

Clearly, the gradients (and hence the components of flux) are constant.
Rectangular elements (four elements)

$$q_x^1(x,y) = -k\sum_{i=1}^{4} u_i^1 \frac{\partial \psi_i^1}{\partial x} = 2U_1(1-2y) - 2U_2(1-2y) - 4yU_5 + 4yU_4$$

$$q_y^1(x,y) = -k\sum_{i=1}^{4} u_i^1 \frac{\partial \psi_i^1}{\partial y} = 2U_1(1-2x) + 4xU_2 - 4xU_5 - 2U_4(1-2x) \qquad (26b)$$

$$q_x^1(0.25, 0.25) = 0.11785, \quad q_y^1(0.25, 0.25) = 0.11785$$

Plots of q_x, obtained by mesh T1 (4 elements) and mesh T2 (16 elements) of linear triangular elements as a function of x (for $y = 0.0$) are shown in Fig. 9.4.5.

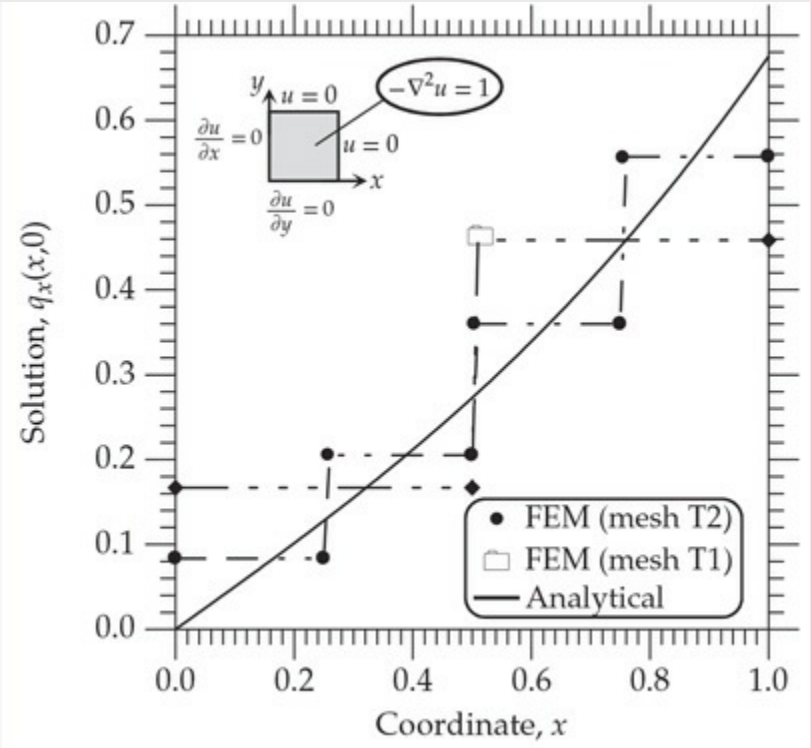

Fig. 9.4.5 Comparison of the finite element solution with the analytical (series) solution of q_x $(x,0)$. Note that, in theory, $q_y = 0$ on line $y = 0$.

Isolines

The computation of *isolines*, i.e., lines of constant u, for linear finite elements is straightforward but more complicated for higher order elements. Here we discuss the procedure for linear elements only. Suppose that we wish to find $u = u_0$ (constant) isoline. On a side of a linear triangle or rectangular element, the solution u varies according to the equation

$$u_h^e(s) = u_1^e + \frac{u_2^e - u_1^e}{h} s$$

where s is the local coordinate with its origin at node 1 of the side, (u_1^e, u_2^e) are the nodal values (see Fig. 9.4.6), and h is the length of the side. Then, if $u \equiv u_0$ lies on the line (i.e., $u_1^e < u_0 < u_2^e$ or $u_2^e < u_0 < u_1^e$), the point s_0 at which $U^e(s_0) = u_0$ is

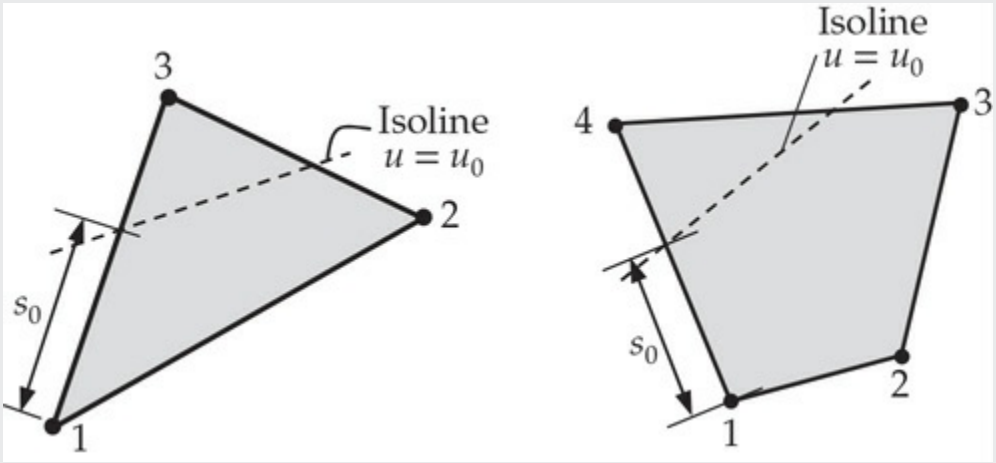

Fig. 9.4.6 Isolines for linear triangular and quadrilateral elements.

given by

$$s_0 = \frac{(u_0 - u_1^e)h}{(u_2^e - u_1^e)} \tag{27}$$

Similar equations apply for other sides of the element. Since the solution varies linearly between any two points of linear elements, the isoline is determined by joining two points on any two sides of the element for which Eq. (27) gives a positive value.

For quadratic elements, isolines are determined by finding three points s_i in the element at which $u_h^e(s_i) = u_0$ ($i = 1, 2,$ and 3):

$$\frac{s_0}{h} = \frac{-b \pm \sqrt{b^2 - 4ac}}{2a} > 0 \tag{28a}$$

$$c = u_1^e - u_0, \quad b = -3u_1^e + 4u_2^e - u_3^e, \quad a = 2(u_1^e - 2u_2^e + u_3^e) \tag{28b}$$

Equation (28a) is to be applied on any three lines in the element until three different values $h > s_0 > 0$ are found.

Triangles versus Rectangles

The accuracy of the finite element solution can also depend on the choice of the finite element mesh. For instance, if the mesh selected violates the symmetry present in the problem, the resulting solution will be less accurate than one obtained using a mesh that agrees with the physical symmetry present in the problem. Geometrically, a triangular element has fewer (or no) lines of symmetry when compared to a rectangular element, and therefore one should use meshes of triangular elements with care (e.g., select a mesh that does not contradict the mathematical symmetry present in the problem).

The effect of linear triangular element meshes shown in Fig. 9.4.7 on the solution is investigated. The finite element solutions obtained by the three meshes are compared with the series solution in Table 9.4.2. Clearly, the solution obtained using mesh 3 is less accurate. This is expected because mesh 3 is symmetric about the diagonal line connecting node 3 to node 7, whereas the mathematical symmetry is about the diagonal line connecting node 1 to node 9 (see Fig. 9.4.7). Mesh 1 is the most desirable of the three because it does not contradict the mathematical symmetry of the problem.

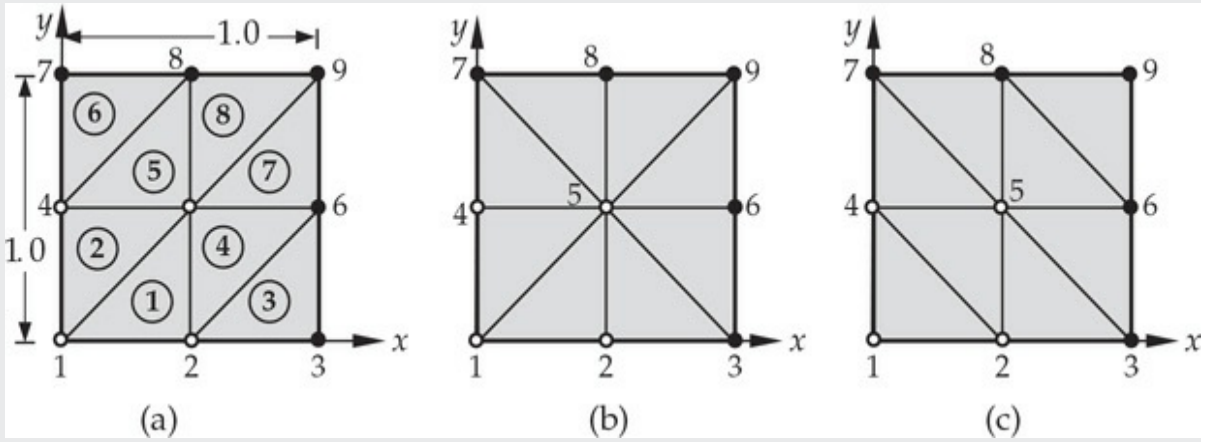

Fig. 9.4.7 Various types of triangular-element meshes for the domain of **Example 9.4.1**: (a) mesh 1; (b) mesh 2; and (c) mesh 3.

Table 9.4.2 Comparison of the finite element solutions obtained using various linear triangular-element meshes[1] with the series solution of the problem in **Example 9.4.1**.

	Finite element solution			
Node	Mesh 1	Mesh 2	Mesh 3	Series solution
1	0.31250	0.29167	0.25000	0.29469
2	0.22917	0.20833	0.20833	0.22934
3	0.22917	0.20833	0.20833	0.22934
4	0.17708	0.18750	0.16667	0.18114

[1]See Fig. 9.4.7 for the finite element meshes.

Next, the effect of mesh refinement with rectangular elements is investigated. Four different meshes of rectangular elements are shown in Fig. 9.3.3. Each of the meshes contains the previous mesh as a subset. The mesh shown in Fig. 9.3.3(c) is nonuniform; it is obtained by subdividing the first two rows and columns of elements of the mesh shown in Fig. 9.4.3(b). The finite element solutions obtained by these meshes are compared in Table 9.4.3. The numerical convergence of the finite element solution of the refined meshes to the series solution is apparent from the results presented.

Table 9.4.3 Convergence of the finite element solution (with mesh refinement)[1] of the problem in **Example 9.4.1**.

Location		Finite element solution				Series solution
x	y	2×2	4×4	6×6	8×8	
0.000	0.000	0.31071	0.29839	0.29641	0.29560	0.29469
0.125	0.000	—	—	0.29248	0.29167	0.29077
0.250	0.000	—	0.28239	0.28055	0.27975	0.27888
0.375	0.000	—	—	0.26022	0.24943	0.25863
0.500	0.000	0.24107	0.23220	0.23081	0.23005	0.22934
0.625	0.000	—	—	—	0.19067	0.19009
0.750	0.000	—	0.14137	0.14064	0.14014	0.13973
0.875	0.000	—	—	—	0.07709	0.07687
0.125	0.125	—	—	0.28862	0.28781	0.28692
0.250	0.250	—	0.26752	0.26580	0.26498	0.26415
0.375	0.375	—	—	0.22960	0.22873	0.22799
0.500	0.500	0.19286	0.18381	0.18282	0.18179	0.18114
0.625	0.625	—	—	—	0.12813	0.12757
0.750	0.750	—	0.07506	0.07481	0.07332	0.07282
0.875	0.875	—	—	—	0.02561	0.02510

[1]See Fig. 9.4.3 for the 2×2 and 4×4 finite element meshes.

9.4.2 Conduction and Convection Heat Transfer

For convection heat transfer, that is, when heat is transferred from one medium to the surrounding medium (often, a fluid) by convection, the finite element model developed earlier requires some modification. The reason for this modification is that in two-dimensional problems, the convective boundary is a curve as opposed to a point in one-dimensional problems. Therefore, the contribution of the convection (or Newton's type) boundary condition to the coefficient matrix and source vector is to be computed by evaluating boundary integrals with convection contributions. The model to be presented allows the computation of the additional contributions to the coefficient matrix and source vector whenever the element has the convection boundary condition. Radiative heat transfer boundary conditions are nonlinear and therefore are not considered here (see Holman [1]).

9.4.2.1 Plane systems

The governing equation for steady-state heat transfer in plane systems is

given by

$$-\frac{\partial}{\partial x}\left(k_x\frac{\partial T}{\partial x}\right)-\frac{\partial}{\partial y}\left(k_y\frac{\partial T}{\partial y}\right)=f(x,y) \tag{9.4.1}$$

where f is the internal heat generation per unit volume (in W/m^3). For a convection boundary, the natural boundary condition is a balance of energy transfer across the boundary due to conduction *and/or* convection (i.e., Newton's law of cooling):

$$k_x\frac{\partial T}{\partial x}n_x+k_y\frac{\partial T}{\partial y}n_y+\beta(T-T_\infty)=q_n \tag{9.4.2}$$

where β is the convective conductance (or the convective heat transfer coefficient) [in W/(m^2 · °C)], T_∞ is the (ambient) temperature of the surrounding fluid medium, and q_n is the specified heat flow (appears only when the element boundary coincides with the actual boundary). The first expression accounts for heat transfer by conduction, the second by convection, and the third accounts for the specified heat flux, if any. It is the presence of the term $\beta(T-T_\infty)$ that requires some modification of the weak form in Eq. (9.2.10).

The weak form of Eq. (9.4.1) can be obtained from Eq. (9.2.10) by setting $a_{11}=k_x$, $a_{22}=k_y$, $a_{12}=a_{21}=a_{00}=0$, $u=T$, and replacing the boundary expression with $q_n-\beta(T-T_\infty)$:

$$0=\int_{\Omega_e}\left(k_x\frac{\partial w}{\partial x}\frac{\partial T}{\partial x}+k_y\frac{\partial w}{\partial y}\frac{\partial T}{\partial y}-wf\right)dxdy-\oint_{\Gamma_e}w\left(k_x\frac{\partial T}{\partial x}n_x+k_y\frac{\partial T}{\partial y}n_y\right)ds$$

$$0=\int_{\Omega_e}\left(k_x\frac{\partial w}{\partial x}\frac{\partial T}{\partial x}+k_y\frac{\partial w}{\partial y}\frac{\partial T}{\partial y}-wf\right)dxdy-\oint_{\Gamma_e}w\left[q_n-\beta(T-T_\infty)\right]ds$$

$$0\equiv B(w,T)-l(T) \tag{9.4.3}$$

where w is the weight function, and $B(\cdot\,,\,\cdot)$ and $l(\cdot)$ are the bilinear and linear forms,

$$B(w,T)=\int_{\Omega_e}\left(k_x\frac{\partial w}{\partial x}\frac{\partial T}{\partial x}+k_y\frac{\partial w}{\partial y}\frac{\partial T}{\partial y}\right)dx\,dy+\oint_{\Gamma_e}\beta wT\,ds \tag{9.4.4a}$$

$$l(T)=\int_{\Omega_e}wf\,dx\,dy+\oint_{\Gamma_e}\beta wT_\infty\,ds+\oint_{\Gamma_e}wq_n\,ds \tag{9.4.4b}$$

The finite element model is obtained by substituting the finite element approximation,

$$T = \sum_{j=1}^{n} T_j^e \psi_j^e(x, y) \tag{9.4.5}$$

for T and ψ_i^e for w into Eq. (9.4.3), we obtain

$$\sum_{j=1}^{n} (K_{ij}^e + H_{ij}^e) T_j^e = f_i^e + Q_i^e + P_i^e \tag{9.4.6a}$$

where

$$\begin{aligned} K_{ij}^e &= \int_{\Omega_e} \left(k_x \frac{\partial \psi_i^e}{\partial x} \frac{\partial \psi_j^e}{\partial x} + k_y \frac{\partial \psi_i^e}{\partial y} \frac{\partial \psi_j^e}{\partial y} \right) dx dy, \quad f_i^e = \int_{\Omega_e} f \psi_i^e \, dx \, dy \\ Q_i^e &= \oint_{\Gamma_e} q_n^e \psi_i^e \, ds, \quad H_{ij}^e = \beta^e \oint_{\Gamma_e} \psi_i^e \psi_j^e \, ds, \quad P_i^e = \beta^e \oint_{\Gamma_e} \psi_i^e T_\infty \, ds \end{aligned} \tag{9.4.6b}$$

Note that by setting the heat transfer coefficient β to zero, we obtain the heat conduction model that accounts for no convection.

The additional coefficients H_{ij}^e $(n \times n)$ and P_i^e $(n \times 1)$ (n is the number of nodes in the element) due to convection can be determined by evaluating boundary integrals. These coefficients must be evaluated only on boundary segments of the element that are subjected to a convection boundary condition. The computation of the coefficients for the linear and quadratic triangular and quadrilateral elements is presented in the following paragraphs.

The coefficients H_{ij}^e and P_i^e for an element with m sides are defined by

$$\begin{aligned} H_{ij}^e &= \beta_{12}^e \int_0^{h_{12}^e} \psi_i^e \psi_j^e \, ds + \beta_{23}^e \int_0^{h_{23}^e} \psi_i^e \psi_j^e \, ds + \cdots + \beta_{m1}^e \int_0^{h_{m1}^e} \psi_i^e \psi_j^e \, ds \\ P_i^e &= \beta_{12}^e T_\infty^{12} \int_0^{h_{12}^e} \psi_i^e \, ds + \beta_{23}^e T_\infty^{23} \int_0^{h_{23}^e} \psi_i^e \, ds + \cdots + \beta_{m1}^e T_\infty^{m1} \int_0^{h_{m1}^e} \psi_i^e \, ds \end{aligned} \tag{9.4.7}$$

where β_{ij}^e is the film coefficient (assumed to be constant) for the side connecting nodes i and j of element Ω_e, T_∞^{ij} is the ambient temperature on

the side, h_{ij}^e is the length of the side, and m is the number of sides of the element.

Only those line integrals that have a convection boundary condition need to be evaluated. The boundary integrals are line integrals involving the interpolation functions. The local coordinate s is taken along the side, with its origin at the first node of the side (see Fig. 9.4.8). As noted earlier, 2-D interpolation functions restricted to any side become 1-D interpolation functions. Indeed, the line integrals appearing in Eq. (9.4.7) have been evaluated in Chapter 3 in connection with mass matrix and source vector for linear and quadratic line elements (see also Table 3.7.1).

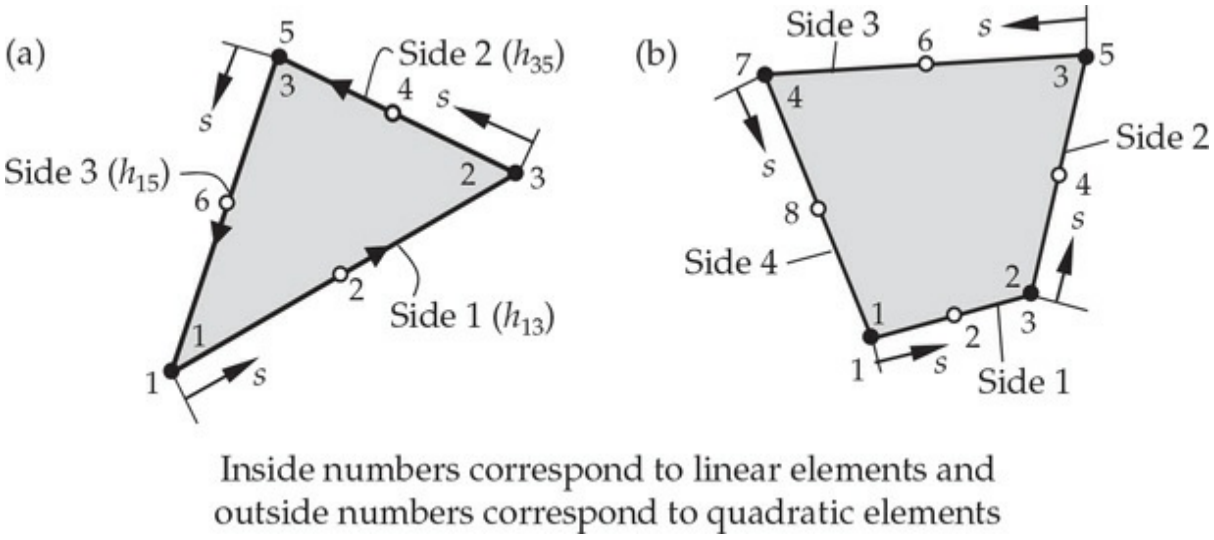

Fig. 9.4.8 Triangular and quadrilateral elements, with node and side numbers and local coordinates for the evaluation of the boundary integrals.

Also, finite element representation of a flux on a curved boundary by linear elements will necessarily result in an approximation of the boundary data (see Fig. 9.4.9). Quadratic elements will have better accuray in representing a curved boundary and hence the flux applied there.

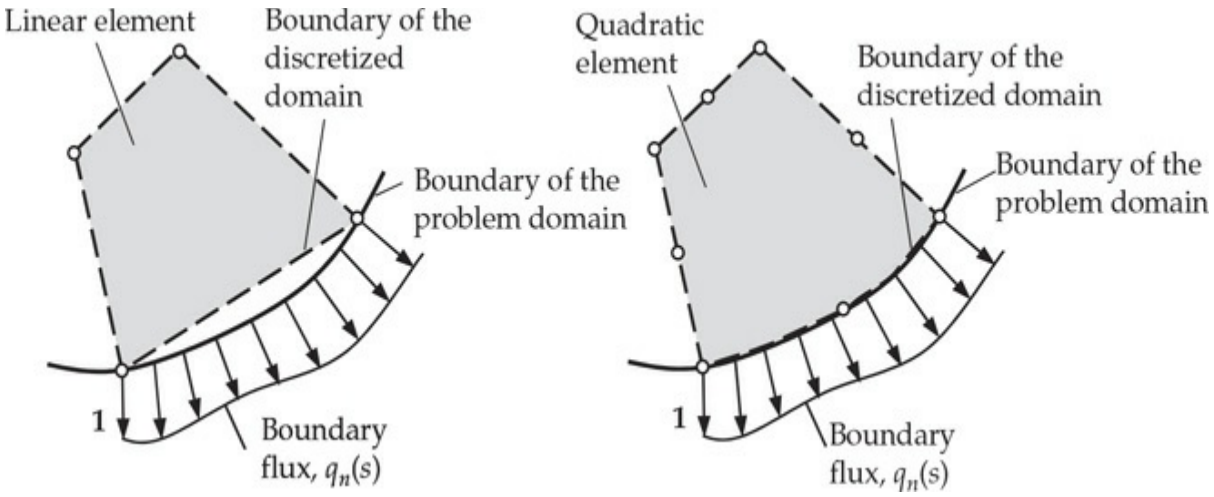

Fig. 9.4.9 Approximation of flux on a curved boundary by linear and quadratic elements.

Let $\mu_{ij}^e = \beta_{ij}^e h_{ij}^e$ and $\lambda_{ij}^e = \beta_{ij}^e h_{ij}^e T_\infty^{ij}$ in the following expressions.

Linear Triangular Element (n = 3 and m = 3)

$$\mathbf{H}^e = \frac{\mu_{12}^e}{6}\begin{bmatrix} 2 & 1 & 0 \\ 1 & 2 & 0 \\ 0 & 0 & 0 \end{bmatrix} + \frac{\mu_{23}^e}{6}\begin{bmatrix} 0 & 0 & 0 \\ 0 & 2 & 1 \\ 0 & 1 & 2 \end{bmatrix} + \frac{\mu_{31}^e}{6}\begin{bmatrix} 2 & 0 & 1 \\ 0 & 0 & 0 \\ 1 & 0 & 2 \end{bmatrix} \tag{9.4.8a}$$

$$\mathbf{P}^e = \frac{\lambda_{12}^e}{2}\begin{Bmatrix} 1 \\ 1 \\ 0 \end{Bmatrix} + \frac{\lambda_{23}^e}{2}\begin{Bmatrix} 0 \\ 1 \\ 1 \end{Bmatrix} + \frac{\lambda_{31}^e}{2}\begin{Bmatrix} 1 \\ 0 \\ 1 \end{Bmatrix} \tag{9.4.8b}$$

Quadratic Triangular Element (n = 6 and m = 3)

$$\mathbf{H}^e = \frac{\mu_{13}^e}{30}\begin{bmatrix} 4 & 2 & -1 & 0 & 0 & 0 \\ 2 & 16 & 2 & 0 & 0 & 0 \\ -1 & 2 & 4 & 0 & 0 & 0 \\ 0 & 0 & 0 & 0 & 0 & 0 \\ 0 & 0 & 0 & 0 & 0 & 0 \\ 0 & 0 & 0 & 0 & 0 & 0 \end{bmatrix} + \frac{\mu_{35}^e}{30}\begin{bmatrix} 0 & 0 & 0 & 0 & 0 & 0 \\ 0 & 0 & 0 & 0 & 0 & 0 \\ 0 & 0 & 4 & 2 & -1 & 0 \\ 0 & 0 & 2 & 16 & 2 & 0 \\ 0 & 0 & -1 & 2 & 4 & 0 \\ 0 & 0 & 0 & 0 & 0 & 0 \end{bmatrix}$$

$$+ \frac{\mu_{51}}{30}\begin{bmatrix} 4 & 0 & 0 & 0 & -1 & 2 \\ 0 & 0 & 0 & 0 & 0 & 0 \\ 0 & 0 & 0 & 0 & 0 & 0 \\ 0 & 0 & 0 & 0 & 0 & 0 \\ -1 & 0 & 0 & 0 & 4 & 2 \\ 2 & 0 & 0 & 0 & 2 & 16 \end{bmatrix} \tag{9.4.9a}$$

$$\mathbf{P}^e = \frac{\lambda_{13}^e}{6}\begin{Bmatrix}1\\4\\1\\0\\0\\0\end{Bmatrix} + \frac{\lambda_{35}^e}{6}\begin{Bmatrix}0\\0\\1\\4\\1\\0\end{Bmatrix} + \frac{\lambda_{51}^e}{6}\begin{Bmatrix}1\\0\\0\\0\\1\\4\end{Bmatrix} \tag{9.4.9b}$$

Linear Quadrilateral Element ($n = 4$ and $m = 4$)

$$\mathbf{H}^e = \frac{\mu_{12}^e}{6}\begin{bmatrix}2&1&0&0\\1&2&0&0\\0&0&0&0\\0&0&0&0\end{bmatrix} + \frac{\mu_{23}^e}{6}\begin{bmatrix}0&0&0&0\\0&2&1&0\\0&1&2&0\\0&0&0&0\end{bmatrix} + \frac{\mu_{34}^e}{6}\begin{bmatrix}0&0&0&0\\0&0&0&0\\0&0&2&1\\0&0&1&2\end{bmatrix} + \frac{\mu_{41}^e}{6}\begin{bmatrix}2&0&0&1\\0&0&0&0\\0&0&0&0\\1&0&0&2\end{bmatrix} \tag{9.4.10a}$$

$$\mathbf{P}^e = \frac{\lambda_{12}^e}{2}\begin{Bmatrix}1\\1\\0\\0\end{Bmatrix} + \frac{\lambda_{23}^e}{2}\begin{Bmatrix}0\\1\\1\\0\end{Bmatrix} + \frac{\lambda_{34}^e}{2}\begin{Bmatrix}0\\0\\1\\1\end{Bmatrix} + \frac{\lambda_{41}^e}{2}\begin{Bmatrix}1\\0\\0\\1\end{Bmatrix} \tag{9.4.10b}$$

Quadratic Quadrilateral Element ($n = 8$ and $m = 4$)

$$\mathbf{H}^e = \frac{\mu_{13}^e}{30}\begin{bmatrix}4&2&-1&&0\\2&16&2&0&\\-1&2&4&&\\&0&&0&\end{bmatrix} + \frac{\mu_{35}^e}{30}\begin{bmatrix}&&0&&\\0&4&2&-1&0\\0&2&16&2&0\\&-1&2&4&\\&&0&&\end{bmatrix} + \frac{\mu_{57}^e}{30}\begin{bmatrix}0&&0&&0\\&4&2&-1&\\0&2&16&2&0\\&-1&2&4&\\0&&0&&0\end{bmatrix} + \frac{\mu_{71}^e}{30}\begin{bmatrix}4&0&-1&2\\&0&&\\-1&0&4&2\\2&0&2&16\end{bmatrix} \tag{9.4.11a}$$

$$\mathbf{P}^e = \frac{\lambda_{13}^e}{6}\begin{Bmatrix}1\\4\\1\\0\\0\\0\\0\\0\end{Bmatrix} + \frac{\lambda_{35}^e}{6}\begin{Bmatrix}0\\0\\1\\4\\1\\0\\0\\0\end{Bmatrix} + \frac{\lambda_{57}^e}{6}\begin{Bmatrix}0\\0\\0\\0\\1\\4\\1\\0\end{Bmatrix} + \frac{\lambda_{71}^e}{6}\begin{Bmatrix}1\\0\\0\\0\\0\\0\\1\\4\end{Bmatrix} \tag{9.4.11b}$$

Example 9.4.2

Consider steady-state heat conduction in an isotropic ($k_x = k_y = k$) homogeneous rectangular region of dimensions $3a \times 2a$ [see Fig. 9.4.10(a)]. The origin of the x and y coordinates is taken at the lower left corner such that x is parallel to the side $3a$ and y is parallel to side $2a$. The boundaries $x = 0$ and $y = 0$ are insulated, the boundary $x = 3a$ is maintained at zero temperature, and the boundary $y = 2a$ is maintained at a temperature $T = T_0 \cos(\pi x/6a)$. Determine the temperature distribution using the finite element method in the region and the heat required at boundary $x = 3a$ to maintain it at zero temperature.

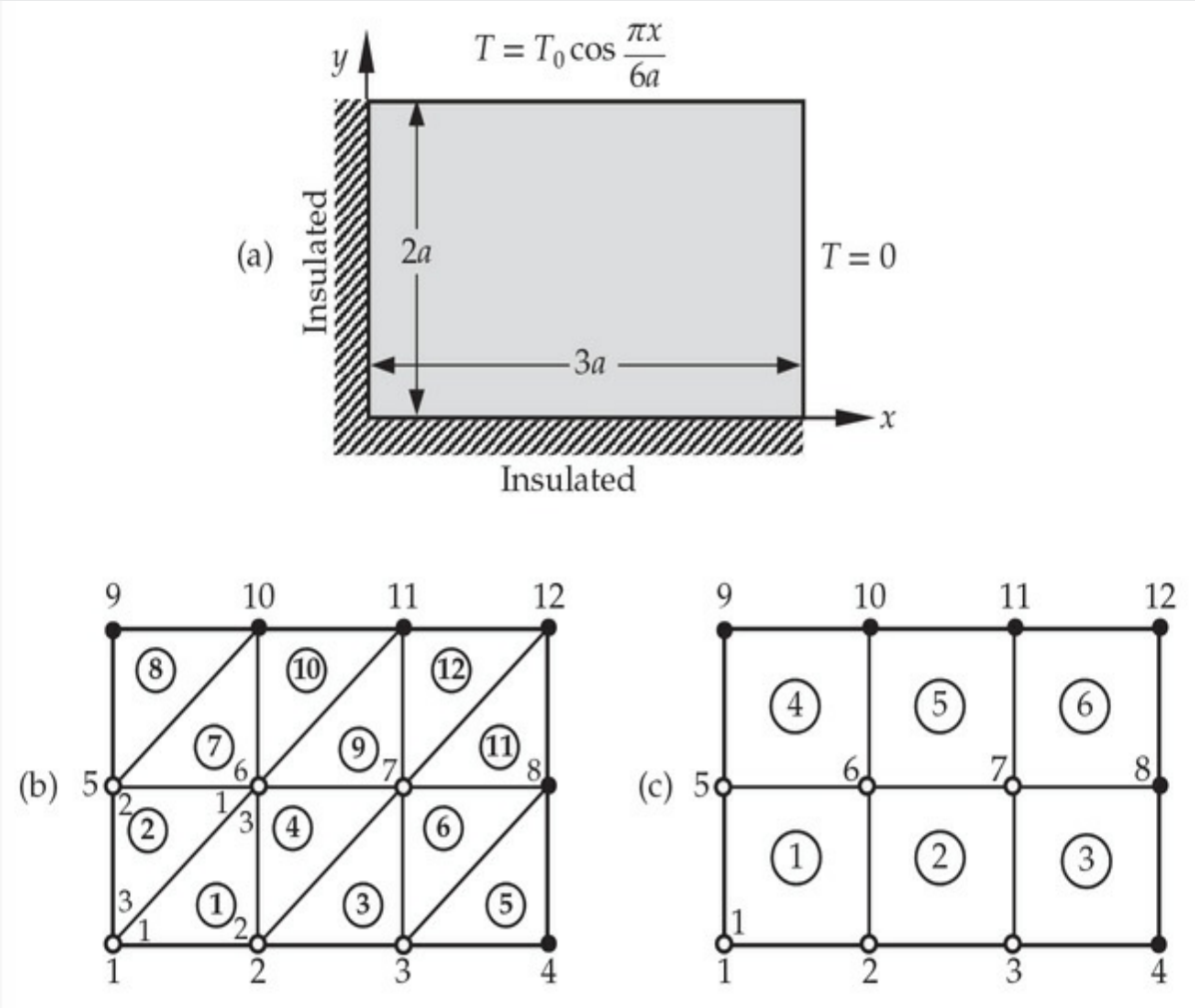

Fig. 9.4.10 Finite element analysis of a heat conduction problem over a rectangular domain: (a) domain; (b) mesh of linear triangular elements; and (c) mesh of linear rectangular elements.

Solution: To analyze the problem, first we note that the problem is

governed by Eq. (9.4.1) with zero internal heat generation, $f = 0$ $a_{12} = a_{21} = a_{00} = 0$, and no convection boundary conditions:

$$-k\nabla^2 T = 0 \tag{1}$$

Suppose that we use a 3 × 2 mesh (i.e., 3 subdivisions along the *x*-axis and 2 subdivisions along the *y*-axis) of linear triangular elements and then with a 3 × 2 mesh of linear rectangular elements, as shown in Fig. 9.4.10(b) and (c). Both meshes have the same number of global nodes (12) but differing numbers of elements.

Triangular Element Mesh (*12 Elements*)

The global node numbers, element numbers, and element node numbers are shown in Fig. 9.4.10(b). The element node numbering scheme should be the one that is used in the development of element interpolation functions. In the present study a counterclockwise numbering system was adopted (see Fig. 9.2.4). By a suitable numbering of the element nodes, all similar elements can be made to have the same element coefficient matrix (recall the discussion from **Example 9.2.2**). Such considerations are important only when hand calculations are carried out.

For a typical element of the mesh of triangles in Fig. 9.4.10(b), the element coefficient matrix is given by [set $a = b$ in Eq. (4) of **Example 9.4.1**]

$$\mathbf{K}^e = \frac{k}{2}\begin{bmatrix} 1 & -1 & 0 \\ -1 & 2 & -1 \\ 0 & -1 & 1 \end{bmatrix} \tag{2}$$

where k is the conductivity of the medium. Note that the element matrix is independent of the size of the element, as long as the element is a right-angle triangle with its base equal to its height.

The assembly of the elements follows the logic discussed earlier. For example, we have

$$\begin{aligned} &K_{11} = K_{11}^1 + K_{33}^2 = \frac{k}{2}(1+1), \quad K_{12} = K_{12}^1 = \frac{k}{2}(-1), \quad K_{13} = 0 \\ &K_{15} = K_{32}^2 = \frac{k}{2}(-1), \quad K_{16} = K_{13}^1 + K_{31}^2 = 0 + 0, \quad \text{etc.} \\ &F_1 = Q_1^1 + Q_3^2, \quad F_6 = Q_3^1 + Q_1^2 + Q_2^4 + Q_2^7 + Q_1^9 + Q_3^{10}, \quad \text{etc.} \end{aligned} \tag{3}$$

The boundary conditions require that

$$U_4 = U_8 = U_{12} = 0, \quad U_9 = T_0, \quad U_{10} = \frac{\sqrt{3}}{2} T_0, \quad U_{11} = \frac{T_0}{2} \tag{4}$$

$$F_1 = F_2 = F_3 = F_5 = 0 \quad \text{(zero heat flow due to insulated boundary)} \tag{5}$$

and the balance of internal heat flow requires that

$$F_6 = F_7 = 0 \tag{6}$$

Thus the unknown primary variables and secondary variables of the problem are

$$U_1,\ U_2,\ U_3,\ U_5,\ U_6,\ U_7;\quad F_4,\ F_8,\ F_9,\ F_{10},\ F_{11},\ F_{12}$$

We first write the six finite element equations for the six unknown primary variables (i.e., obtain the condensed equations directly for the unknown *U*s). These equations come from rows 1, 2, 3, 5, 6, and 7 (corresponding to the same global nodes):

$$\begin{aligned} K_{11}U_1 + K_{12}U_2 + \cdots + K_{1(12)}U_{12} &= F_1 = (Q_1^1 + Q_3^2) = 0 \\ K_{21}U_1 + K_{22}U_2 + \cdots + K_{2(12)}U_{12} &= F_2 = (Q_2^1 + Q_1^3 + Q_3^4) = 0 \\ &\vdots \\ K_{71}U_1 + K_{72}U_2 + \cdots + K_{7(12)}U_{12} &= F_7 = (Q_3^3 + Q_1^4 + Q_2^6 + Q_2^9 + Q_1^{11} + Q_3^{12}) = 0 \end{aligned} \tag{8}$$

Using the boundary conditions and the values of K_{IJ}, we obtain

$$\begin{aligned} k(U_1 - \tfrac{1}{2}U_2 - \tfrac{1}{2}U_5) &= 0 \\ k(-\tfrac{1}{2}U_1 + 2U_2 - \tfrac{1}{2}U_3 - U_6) &= 0 \\ k(-\tfrac{1}{2}U_2 + 2U_3 - U_7) &= 0 \\ k(-\tfrac{1}{2}U_1 + 2U_5 - U_6 - \tfrac{1}{2}U_9) &= 0 \quad (U_9 = T_0) \\ k(-U_2 - U_5 + 4U_6 - U_7 - U_{10}) &= 0 \quad (U_{10} = \tfrac{\sqrt{3}}{2}T_0) \\ k(-U_3 - U_6 + 4U_7 - U_{11}) &= 0 \quad (U_{11} = \tfrac{1}{2}T_0) \end{aligned} \tag{9}$$

In matrix form we have

$$\frac{k}{2}\begin{bmatrix} 2 & -1 & 0 & -1 & 0 & 0 \\ -1 & 4 & -1 & 0 & -2 & 0 \\ 0 & -1 & 4 & 0 & 0 & -2 \\ -1 & 0 & 0 & 4 & -2 & 0 \\ 0 & -2 & 0 & -2 & 8 & -2 \\ 0 & 0 & -2 & 0 & -2 & 8 \end{bmatrix}\begin{Bmatrix} U_1 \\ U_2 \\ U_3 \\ U_5 \\ U_6 \\ U_7 \end{Bmatrix} = \frac{k}{2}\begin{Bmatrix} 0 \\ 0 \\ 0 \\ T_0 \\ \sqrt{3}T_0 \\ T_0 \end{Bmatrix} \tag{10}$$

The solution of these equations is (in °C)

$$\begin{aligned} U_1 &= 0.6362T_0, \quad U_2 = 0.5510T_0, \quad U_3 = 0.3181T_0 \\ U_5 &= 0.7214T_0, \quad U_6 = 0.6248T_0, \quad U_7 = 0.3607T_0 \end{aligned} \tag{11}$$

The exact solution of Eq. (1) for the boundary conditions shown in Fig. 9.4.10(a) is

$$T(x,y) = T_0 \frac{\cosh(\pi y/6a)\cos(\pi x/6a)}{\cosh(\pi/3)} \tag{12}$$

Evaluating the exact solution at the nodes, we have (in °C)

$$\begin{aligned} T_1 &= 0.6249T_0, \quad T_2 = 0.5412T_0, \quad T_3 = 0.3124T_0 \\ T_5 &= 0.7125T_0, \quad T_6 = 0.6171T_0, \quad T_7 = 0.3563T_0 \end{aligned} \tag{13}$$

The heat at node 4, for example, can be computed from the 4th finite element equation

$$\begin{aligned} F_4 = Q_2^5 = K_{41}U_1 + K_{42}U_2 + K_{43}U_3 + K_{44}U_4 + K_{45}U_5 \\ + K_{46}U_6 + K_{47}U_7 + K_{48}U_8 + \cdots \end{aligned} \tag{15}$$

Noting that $K_{41} = K_{42} = K_{45} = \ldots = K_{4(12)} = 0$ and $U_4 = U_8 = 0$, we obtain

$$Q_2^5 = -\frac{1}{2}kU_3 = -0.1591kT_0 \text{ (in W)} \tag{16}$$

Rectangular Element Mesh (*Six Elements*)
For a 3 × 2 mesh of linear rectangular elements [see Fig. 9.4.10(c)], the element coefficient matrix is given by Eq. (9.2.55)

$$\mathbf{K}^e = \frac{k}{6}\begin{bmatrix} 4 & -1 & -2 & -1 \\ -1 & 4 & -1 & -2 \\ -2 & 1 & 4 & -1 \\ -1 & -2 & -1 & 4 \end{bmatrix}, \quad \mathbf{f}^e = 0 \tag{17}$$

The present mesh of rectangular elements is node-wise equivalent to the triangular element mesh considered in Fig. 9.4.10(b). Hence the boundary

conditions in (4)–(6) are valid for the present case. The six finite element equations for the unknowns U_1, U_2, U_3, U_5, U_6, and U_7 again have the same form as those in Eq. (8), with

$$K_{11} = K_{11}^1, \quad K_{12} = K_{12}^1, \quad K_{15} = K_{14}^1, \quad K_{16} = K_{13}^1$$
$$K_{22} = K_{22}^1 + K_{11}^2, \quad K_{23} = K_{12}^2, \quad K_{25} = K_{24}^1$$
$$K_{26} = K_{23}^1 + K_{14}^2, \quad K_{27} = K_{13}^2, \quad \text{and so on}$$
$$F_1 = Q_1^1, \quad F_2 = Q_2^1 + Q_1^2, \quad F_3 = Q_2^2 + Q_1^3, \quad F_4 = Q_2^3, \quad \text{and so on}$$

The equations for the unknown temperatures (i.e., condensed equations for the unknown primary variables) are

$$\frac{k}{6}\begin{bmatrix} 4 & -1 & 0 & -1 & -2 & 0 \\ -1 & 8 & -1 & -2 & -2 & -2 \\ 0 & -1 & 8 & 0 & -2 & -2 \\ -1 & -2 & 0 & 8 & -2 & 0 \\ -2 & -2 & -2 & -2 & 16 & -2 \\ 0 & -2 & -2 & 0 & -2 & 16 \end{bmatrix} \begin{Bmatrix} U_1 \\ U_2 \\ U_3 \\ U_5 \\ U_6 \\ U_7 \end{Bmatrix} = \frac{k}{6} \begin{Bmatrix} 0 \\ 0 \\ 0 \\ T_0 + \sqrt{3}T_0 \\ 2T_0 + \sqrt{3}T_0 + T_0 \\ \sqrt{3}T_0 + T_0 \end{Bmatrix} \tag{18}$$

The solution of these equations is

$$U_1 = 0.6128\,T_0, \quad U_2 = 0.5307\,T_0, \quad U_3 = 0.3064\,,T_0$$
$$U_5 = 0.7030\,T_0, \quad U_6 = 0.6088\,T_0, \quad U_7 = 0.3515\,T_0 \tag{19}$$

The value of the heat at node 4 is given by

$$Q_2^3 = K_{43}U_3 + K_{47}U_7 = -\frac{k}{6}U_3 - \frac{2k}{6}U_7 = -0.1682\,kT_0 \text{ (in W)} \tag{20}$$

We note that the results obtained using the 3 × 2 mesh of rectangular elements is not as accurate as that obtained with the 3 × 2 mesh of triangular elements. This is due to the fact that there are only half as many elements in the former case when compared to the latter. Table 9.4.4 contains a comparison of the finite element solutions with the analytical solution in Eq. (12) for two different meshes of linear triangular and rectangular elements.

Table 9.4.4 Comparison of the nodal temperatures $T\,(x, y)/T_0$, obtained using various finite element meshes[1] with the analytical solution in Eq. (12).

		Triangles		Rectangles		
x	y	3×2	6×4	3×2	6×4	Exact solution
0.0	0.0	0.6362	0.6278	0.6128	0.6219	0.6249
0.5	0.0	—	0.6064	—	0.6007	0.6036
1.0	0.0	0.5510	0.5437	0.5307	0.5386	0.5412
1.5	0.0	—	0.4439	—	0.4398	0.4419
2.0	0.0	0.3181	0.3139	0.3064	0.3110	0.3124
2.5	0.0	—	0.1625	—	0.1610	0.1617
0.0	1.0	0.7214	0.7148	0.7030	0.7102	0.7125
0.5	1.0	—	0.6904	—	0.6860	0.6882
1.0	1.0	0.6248	0.6190	0.6088	0.6150	0.6171
1.5	1.0	—	0.5054	—	0.5022	0.5038
2.0	1.0	0.3607	0.3574	0.3515	0.3551	0.3563
2.5	1.0	—	0.1850	—	0.1838	0.1844

[1]See Fig. 9.4.10 for the geometry and the finite element meshes 3×2.

Example 9.4.3

Consider heat transfer in a rectangular region of dimensions a by b, subjected to the boundary conditions shown in Fig. 9.4.11(a). Write the finite element algebraic equations for the unknown nodal temperatures and heats. Assume that the medium is orthotropic, with conductivities k_x and k_y in the x and y directions, respectively and no internal heat generation. Use a 4×2 mesh of rectangular elements shown in Fig. 9.4.11(b).

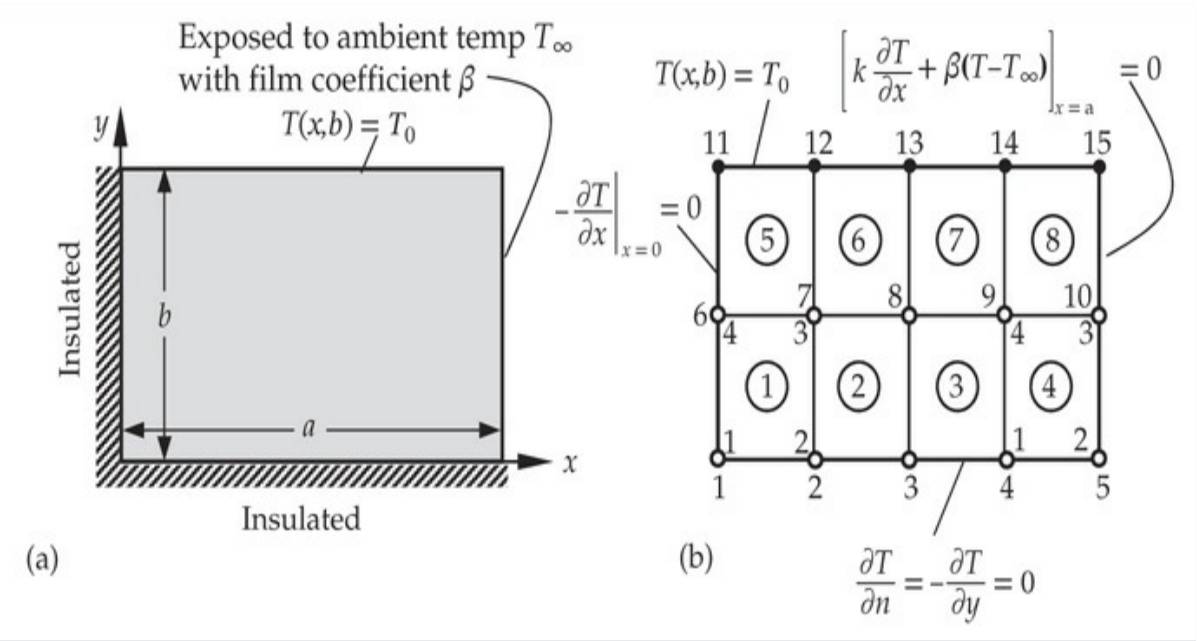

Fig. 9.4.11 Domain and boundary conditions for convective heat transfer in a rectangular domain. A mesh of linear rectangular elements is also shown.

Solution: The heat transfer in the region is governed by Eq. (9.4.1) with $f = 0$. The finite element model is given by

$$(\mathbf{K}^e + \mathbf{H}^e)\mathbf{T}^e = \mathbf{Q}^e + \mathbf{P}^e \quad (\mathbf{f}^e = 0) \tag{1}$$

where $\mathbf{T}^e$ is the vector of nodal temperatures of element Ω_e. We note that $\mathbf{H}^e$ and $\mathbf{P}^e$ must be calculated only for elements 4 and 8, which have boundaries with convection.

The element matrices for the problem at hand are given by

$$\mathbf{K}^e = \frac{k_x\mu}{6}\begin{bmatrix} 2 & -2 & -1 & 1 \\ -2 & 2 & 1 & -1 \\ -1 & 1 & 2 & -2 \\ 1 & -1 & -2 & 2 \end{bmatrix} + \frac{k_y}{6\mu}\begin{bmatrix} 2 & 1 & -1 & -2 \\ 1 & 2 & -2 & -1 \\ -1 & -2 & 2 & 1 \\ -2 & -1 & 1 & 2 \end{bmatrix} \quad (e = 1,2,\cdots,8)$$

$$\mathbf{H}^e = \frac{\beta_{23}^e h_{23}^e}{6}\begin{bmatrix} 0 & 0 & 0 & 0 \\ 0 & 2 & 1 & 0 \\ 0 & 1 & 2 & 0 \\ 0 & 0 & 0 & 0 \end{bmatrix}, \quad \mathbf{P}^e = \frac{\beta_{23}^e T_\infty^{23} h_{23}^e}{2}\begin{Bmatrix} 0 \\ 1 \\ 1 \\ 0 \end{Bmatrix} \quad (\text{for } e = 4,8)$$

where μ is the aspect ratio

$$\mu = (b/2)/(a/4) = 2b/a$$

There are ten nodal temperatures that are to be determined, and heats at

all nodes except nodes 6, 7, 8 and 9 are to be computed. To illustrate the procedure, we write algebraic equations for only representative temperatures and heats.

Node 1 (for Temperatures)

$$K_{11}^1 U_1 + K_{12}^1 U_2 + K_{14}^1 U_6 + K_{13}^1 U_7 = Q_1^1 = 0$$

Node 2 (for Temperatures)

$$K_{21}^1 U_1 + (K_{22}^1 + K_{11}^2) U_2 + K_{12}^2 U_3 + K_{24}^1 U_6 + (K_{23}^1 + K_{14}^2) U_7 + K_{13}^2 U_8 = Q_2^1 + Q_1^2 = 0$$

Node 5 (for Temperatures)

$$K_{21}^4 U_4 + (K_{22}^4 + H_{22}^4) U_5 + K_{24}^4 U_9 + (K_{23}^4 + H_{23}^4) U_{10} = Q_2^4 + P_2^4 \quad \text{(known)}$$

Node 10 (for Temperatures)

$$K_{31}^4 U_4 + (K_{32}^4 + H_{32}^4) U_5 + (K_{34}^4 + K_{21}^8) U_9 + (K_{33}^4 + H_{33}^4 + K_{22}^8 + H_{22}^8) U_{10} + K_{24}^8 U_{14} + (K_{23}^8 + H_{23}^8) U_{15} = (Q_3^4 + P_3^4) + (Q_2^8 + P_2^8) = P_3^4 + P_2^8 \text{ (known)}$$

Node 14 (for Heat Q_{14})

$$Q_{14} \equiv Q_3^7 + Q_4^8 = K_{31}^7 U_8 + (K_{32}^7 + K_{41}^8) U_9 + K_{42}^8 U_{10} + K_{34}^7 U_{13} + (K_{33}^7 + K_{44}^8) U_{14} + K_{43}^8 U_{15}$$

From the boundary conditions, temperatures at nodes 11 through 15 (i.e., U_{11}, U_{12}, …, U_{15}) are known. Substituting the values of K_{ij}^e, H_{ij}^e, and P_i^e we obtain explicit form of the algebraic equations. For example, the algebraic equation corresponding to node 10 is

$$-\frac{1}{6}\left(k_x\mu + \frac{k_y}{\mu}\right)U_4 + \left[\frac{1}{6}\left(k_x\mu - \frac{2k_y}{\mu}\right) + \frac{1}{12}\beta b\right]U_5 + \frac{1}{6}\left[\left(-2k_x\mu + \frac{k_y}{\mu}\right) + \left(-2k_x\mu + \frac{k_y}{\mu}\right)\right]U_9 + \frac{2}{3}\left[\left(k_x\mu + \frac{k_y}{\mu}\right) + \frac{\beta b}{2}\right]U_{10} - \frac{1}{6}\left(k_x\mu + \frac{k_y}{\mu}\right)U_{14} + \frac{1}{6}\left[k_x\mu - \frac{2k_y}{\mu} + \frac{\beta b}{2}\right]U_{15} = \frac{1}{2}\beta b T_\infty$$

Example 9.4.4

Consider heat transfer in a homogeneous, isotropic medium. The governing equation is given by

$$-k\nabla^2 T = f_0 \text{ in } \Omega$$

over the domain shown in Fig. 9.4.12.

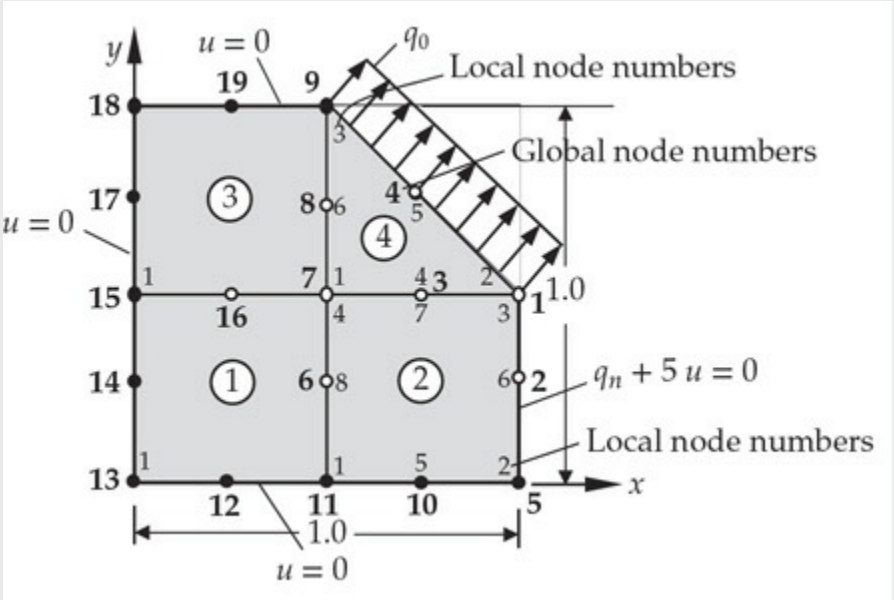

Fig. 9.4.12 Domain with finite element mesh and boundary conditions for a heat transfer problem discussed in **Example 9.4.4**.

- **a.** Write the finite element equation associated with global node 1 in terms of element coefficients.
- **b.** Compute the contribution of the flux q_0 to global nodes 1 and 4.
- **c.** Compute the contribution of the boundary condition $q_n + 5u = 0$ to the finite element equation at node 1.

(a) The finite element equation associated with global node 1 is

$$K_{11}U_1 + K_{12}U_2 + K_{13}U_3 + K_{14}U_4 + K_{16}U_6 + K_{17}U_7 + K_{18}U_8 = F_1$$

Writing the global coefficients in terms of the element coefficients, we obtain

$$\left(K_{33}^{(2)} + K_{22}^{(4)} + H_{33}^{(2)}\right)U_1 + \left(K_{36}^{(2)} + H_{36}^{(2)}\right)U_2 + \left(K_{37}^{(2)} + K_{24}^{(4)}\right)U_3$$
$$+K_{25}^{(4)}U_4 + K_{38}^{(2)}U_6 + \left(K_{34}^{(2)} + K_{21}^{(4)}\right)U_7 + K_{26}^{(4)}U_8 = F_3^{(2)} + P_3^{(2)} + F_2^{(4)}$$

Explicit form of H_{ij}^e ($P_i^e = 0$ because $u_\infty = 0$) will be given in part (c).

(b) The contributions of uniform flux q_0 to global nodes 1, 4, and 9 are readily known from one-dimensional quadratic element [see Eq.

(3.4.38)]. It can be calculated as follows:

$$Q_2^4 = \int_0^L q_0 \psi_2^4(s)\, ds = q_0 \int_0^L \left(1 - \frac{s}{L}\right)\left(1 - \frac{2s}{L}\right) ds$$
$$= q_0 \int_0^L \left(1 - 3\frac{s}{L} + \frac{2s^2}{L^2}\right) ds = q_0\left(L - 3\frac{L}{2} + \frac{2L}{3}\right) = \frac{q_0 L}{6} = Q_3^4$$

where $L = 1/\sqrt{2} = 0.7071$. Similarly, contribution to global node 4 is

$$Q_5^4 = \int_0^L q_0 \psi_5^4(s)\, ds = q_0 \int_0^L 4\frac{s}{L}\left(1 - \frac{s}{L}\right) ds$$
$$= 4q_0 \int_0^L \left(\frac{s}{L} - \frac{s^2}{L^2}\right) ds = 4q_0\left(\frac{L}{2} - \frac{L}{3}\right) = \frac{4q_0 L}{6}$$

(c) The contribution of the boundary condition $q_n + 5u = 0$ to the finite element equation associated with node 1 is

$$Q_3^2 = -\left(H_{33}^{(2)} U_1 + H_{36}^{(2)} U_2\right)$$
$$= -\frac{1}{3} U_1 - \frac{1}{6} U_2$$

9.4.3 Axisymmetric Systems

For symmetric heat transfer about the z-axis (i.e., independent of the circumferential coordinate θ), the governing equation is given by Eq. (9.2.71) with $u = T$, $\hat{a}_{11} = k_r$, $\hat{a}_{22} = k_z$, $\hat{a}_{00} = 0$, and $\hat{f} = f$. The finite element model in Eq. (9.2.75b) is now modified to account for the convective heat transfer boundary condition

$$\left(k_r \frac{\partial T}{\partial r} n_r + k_z \frac{\partial T}{\partial z} n_z\right) + \beta(T - T_\infty) = q_n \tag{9.4.12}$$

where n_r and n_z are the direction cosines of the unit normal $\hat{\mathbf{n}}$

$$\hat{\mathbf{n}} = n_r \hat{\mathbf{e}}_r + n_z \hat{\mathbf{e}}_z \tag{9.4.13}$$

and $\hat{\mathbf{e}}_r$ and $\hat{\mathbf{e}}_z$ are the unit vectors along the r and z coordinates.

The weak form is given by (integration with respect to θ gives 2π, which is retained for the sake of completeness)

$$0 = 2\pi \int_{\Omega_e} \left(k_r \frac{\partial w}{\partial r}\frac{\partial T}{\partial r} + k_z \frac{\partial w}{\partial z}\frac{\partial T}{\partial z} - wf \right) r\,dr\,dz$$
$$- 2\pi \oint_{\Gamma_e} w\left[-\beta(T - T_\infty) + q_n\right] ds \tag{9.4.14}$$

and the finite element model is

$$(\mathbf{K}^e + \mathbf{H}^e)\mathbf{T}^e = \mathbf{f}^e + \mathbf{P}^e + \mathbf{Q}^e \tag{9.4.15a}$$

where

$$K_{ij}^e = 2\pi \int_{\Omega_e} \left(k_r \frac{\partial \psi_i^e}{\partial r}\frac{\partial \psi_j^e}{\partial r} + k_z \frac{\partial \psi_i^e}{\partial z}\frac{\partial \psi_j^e}{\partial z} \right) r\,dr\,dz$$
$$H_{ij}^e = 2\pi \oint_{\Gamma_e} \beta^e \psi_i^e \psi_j^e\, ds, \quad f_i^e = 2\pi \int_{\Omega_e} \psi_i^e f(r,z)\, r\,dr\,dz \tag{9.4.15b}$$
$$Q_i^e = 2\pi \oint_{\Gamma_e} q_n \psi_i^e\, ds, \quad P_i^e = 2\pi \oint_{\Gamma_e} \beta^e T_\infty^e \psi_i^e\, ds$$

We will not consider a numerical example here because the procedure remains the same as for non-axisymmetric problems; only difference is in the values of the coefficients.

9.4.4 Fluid Mechanics

Here, we consider the equations governing flows of an ideal fluid. An *ideal fluid* is one that has zero viscosity and is incompressible. A fluid is said to be *incompressible* if the volume change is zero

$$\nabla \cdot \mathbf{v} = 0 \tag{9.4.16}$$

where **v** is the velocity vector. A fluid is termed *inviscid* if the viscosity is zero, $\mu = 0$. A flow with negligible angular velocity is called *irrotational*,

$$\nabla \times \mathbf{v} = 0 \tag{9.4.17}$$

The irrotational flow of an ideal fluid (i.e., ρ = constant and $\mu = 0$) is called a *potential flow*.

For an ideal fluid ($\mu = 0$ and ρ is constant), the continuity and the momentum equations can be written as

$$\nabla \cdot \mathbf{v} = 0 \tag{9.4.18a}$$

and

$$\frac{1}{2}\rho\nabla(\mathbf{v}\cdot\mathbf{v}) - \rho[\mathbf{v}\times(\nabla\times\mathbf{v})] = -\nabla\hat{P} \tag{9.4.18b}$$

where $\nabla\hat{P} = \nabla P - \mathbf{f}$. For irrotational flow the velocity field $\mathbf{v}$ satisfies Eq. (9.4.17). For two-dimensional irrotational flows, these equations have the form

$$\frac{\partial v_x}{\partial x} + \frac{\partial v_y}{\partial y} = 0 \tag{9.4.18c}$$

$$\frac{1}{2}\rho(v_x^2 + v_y^2) + \hat{P} = \text{constant} \tag{9.4.18d}$$

$$\frac{\partial v_x}{\partial y} - \frac{\partial v_y}{\partial x} = 0 \tag{9.4.18e}$$

These three equations are used to determine v_x, v_y, and $\hat{P}$.

The problem of determining v_x, v_y, and $\hat{P}$ is simplified by introducing a function $\psi(x, y)$ such that the continuity equation is identically satisfied:

$$v_x = \frac{\partial\psi}{\partial y}, \quad v_y = -\frac{\partial\psi}{\partial x} \tag{9.4.19}$$

Then the irrotational flow condition in terms of ψ takes the form

$$\frac{\partial^2\psi}{\partial y^2} + \frac{\partial^2\psi}{\partial x^2} \equiv \nabla^2\psi = 0 \tag{9.4.20}$$

Equation (9.4.20) is used to determine ψ; then velocities v_x and v_y are determined from Eq. (9.4.19) and $\hat{P}$ from Eq. (9.4.18d).

The function ψ has the physical significance that lines of constant ψ are lines across which there is no flow, i.e., they are streamlines of the flow. Hence, $\psi(x, y)$ is called the *stream function*.

In the cylindrical coordinates, the continuity equation takes the form

$$\frac{\partial v_r}{\partial r} + \frac{1}{r}\frac{\partial v_\theta}{\partial\theta} = 0 \tag{9.4.21}$$

where v_r and v_θ are the radial and circumferential velocity components. The stream function $\psi(r, \theta)$ is defined as

$$v_r = \frac{1}{r}\frac{\partial \psi}{\partial \theta}, \quad v_\theta = -\frac{\partial \psi}{\partial r} \tag{9.4.22}$$

and Eq. (9.4.20) takes the form

$$\nabla^2 \psi \equiv \frac{\partial^2 \psi}{\partial r^2} + \frac{1}{r}\frac{\partial \psi}{\partial r} + \frac{1}{r^2}\frac{\partial^2 \psi}{\partial \theta^2} = 0 \tag{9.4.23}$$

There exists an alternative formulation of the potential flow equations (9.4.18a) and (9.4.18b). Introduce the function $\phi(x, y)$, called the *velocity potential*, such that the condition of irrotational flow is identically satisfied:

$$v_x = -\frac{\partial \phi}{\partial x}, \quad v_y = -\frac{\partial \phi}{\partial y} \tag{9.4.24}$$

Then the continuity equation in terms of the velocity potential takes the form

$$-\nabla^2 \phi = 0 \tag{9.4.25}$$

Comparing Eq.(9.4.19) with Eq. (9.4.24), we note that

$$-\frac{\partial \phi}{\partial x} = \frac{\partial \psi}{\partial y}, \quad -\frac{\partial \phi}{\partial y} = -\frac{\partial \psi}{\partial x} \tag{9.4.26}$$

The velocity potential has the physical significance that lines of constant ϕ are lines along which there is no change in velocity. The equipotential lines and streamlines intersect at right angles (see Schlichting [2]).

Although both ψ and ϕ are governed by the Laplace equation, the boundary conditions are different in a flow problem, as should be evident by the definitions in Eqs. (9.4.19) and (9.4.24). In this section, we consider applications of the finite element method to potential flows, that is, the solution of Eqs. (9.4.23) and (9.4.25).

We consider two examples of fluid flow. The first one deals with a groundwater flow problem and the second with the flow around a cylindrical body. In discussing these problems, emphasis is placed on certain modeling aspects, data generation, postprocessing of solutions, and interpretation of the results. Evaluation of element matrices and assembly

is amply illustrated in previous examples and will not be discussed as it takes substantial space to write the assembled equations even for crude meshes used in these examples. These problems were solved using **FEM2D**.

Example 9.4.5

The governing differential equation for a homogeneous acquifer, with flow in the *xy* plane, is given by

$$-\frac{\partial}{\partial x}\left(a_{11}\frac{\partial \phi}{\partial x}\right)-\frac{\partial}{\partial y}\left(a_{22}\frac{\partial \phi}{\partial y}\right)=f \text{ in } \Omega \tag{1}$$

where a_{11} and a_{22} are the coefficients of permeability (in $m^3/day/m^2$) along the x and y directions, respectively, ϕ is the piezometric head (in m), measured from a reference level (usually the bottom of the aquifer), and f is the rate of pumping (in $m^3/day/m^3$). From the previous discussions it is clear that the primary variable is ϕ and the secondary variable is

$$q_n = a_{11}\frac{\partial \phi}{\partial x}n_x + a_{22}\frac{\partial \phi}{\partial y}n_y \tag{2}$$

Find the lines of constant potential ϕ (equipotential lines) in a 3000 m × 1500 m rectangular aquifer (see Fig. 9.4.13) bounded on the long sides by an impermeable material (i.e., $q_n = 0$) and on the short sides by a constant head of $\phi = 200$ m. In addition, suppose that a river is passing through the aquifer, infiltrating the aquifer at a rate of $q_0 = 0.24$ $m^3/day/m$, and that there are two pumps located at (830, 1000) and (600, 1900), with pumping rates of $Q_1 = 1200$ m^3/day and $Q_2 = 2400$ m^3/day, respectively. Use a mesh of 64 triangular elements and 45 nodes shown in Fig. 9.4.14(a).

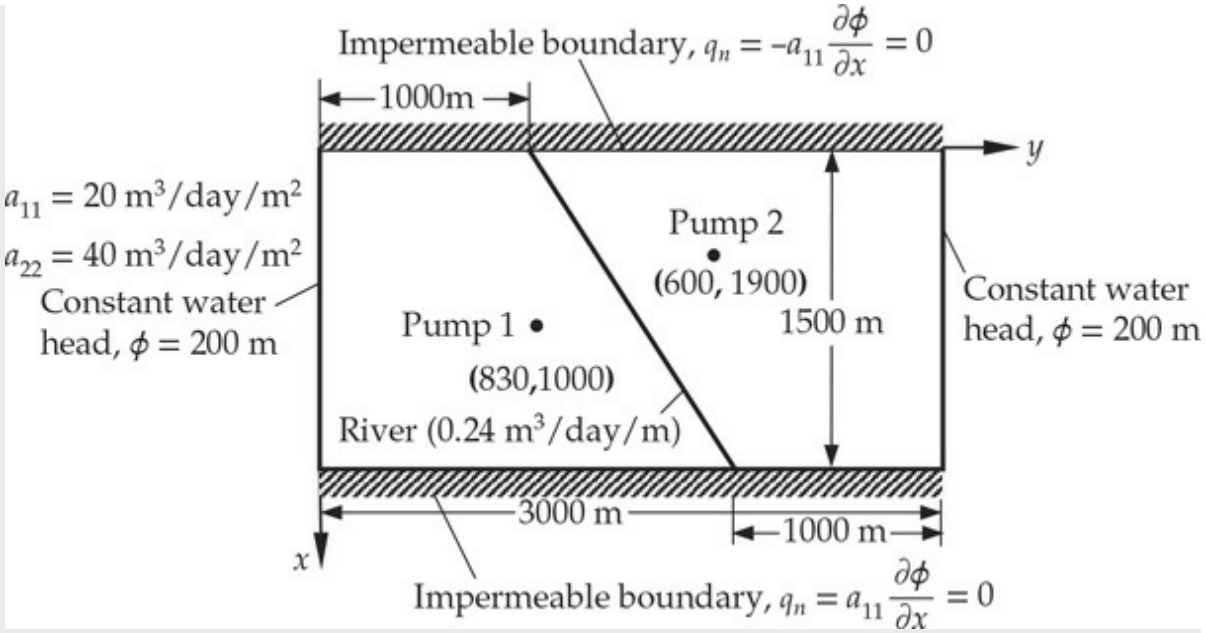

Fig. 9.4.13 Domain and boundary conditions for a groundwater flow problem discussed in **Example 9.4.5**.

Solution: The river forms the interelement boundary between elements (26, 28, 30, 32) and (33, 35, 37, 39). In the mesh selected, neither pump is located at a node. This is done intentionally for the purpose of illustrating the calculation of the generalized forces due to a point source within an element. If the pumps are located at a node, then the rate of pumping Q_0 is input as the specified secondary variable of the node. When a source (or sink) is located at a point other than a node, we must calculate its contribution to the nodes. Similarly, the source components due to the distributed line source (i.e., the river) should be computed.

First, consider the line source. We can view the river as a line source of constant intensity, $q_0 = 0.24$ m^3/day/m. Since the length of the river is equally divided by nodes 21 through 25 (into four parts), we can compute the contribution of the infiltration of the river at each of the nodes by evaluating the integrals [see Fig. 9.4.14(b)]:

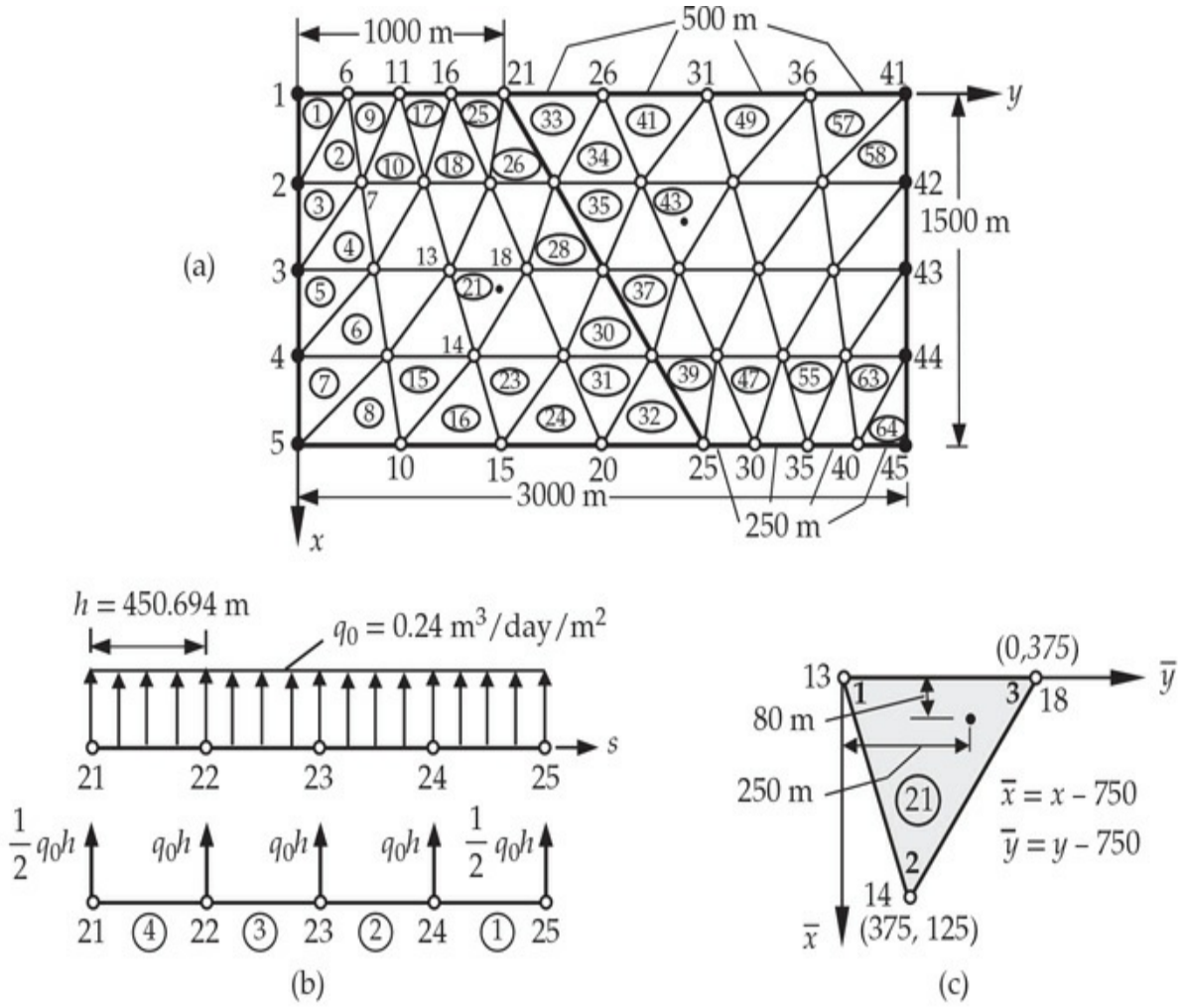

Fig. 9.4.14 (a) Finite element mesh of triangular elements (45 nodes and 64 elements), (b) computation of global forces due to the infiltration of the river, and (c) computation of global forces for pump 1 located inside element 21 for the groundwater flow problem of **Example 9.4.5**.

$$
\begin{aligned}
&\text{Node 25:} && \int_0^h (0.24)\psi_1^1\, ds \\
&\text{Node 24:} && \int_0^h (0.24)\psi_2^1\, ds + \int_0^h (0.24)\psi_1^2\, ds \\
&\text{Node 23:} && \int_0^h (0.24)\psi_2^2\, ds + \int_0^h (0.24)\psi_1^3\, ds \\
&\text{Node 22:} && \int_0^h (0.24)\psi_2^3\, ds + \int_0^h (0.24)\psi_1^4\, ds \\
&\text{Node 21:} && \int_0^h (0.24)\psi_2^4\, ds
\end{aligned} \tag{3}
$$

For constant intensity q_0 and the linear interpolation functions $\psi_1^e(s) = 1 - s/h$ and $\psi_2^e(s) = s/h$, the contribution of these integrals is well known:

$$
\int_0^h q_0 \psi_i^e\, ds = \frac{1}{2} q_0 h, \quad h = \frac{1}{4}[(1000)^2 + (1500)^2]^{\frac{1}{2}}, \quad q_0 = 0.24 \tag{4}
$$

Hence, we have

$$
F_{21} = \frac{1}{2} q_0 h, \quad F_{22} = F_{23} = F_{24} = q_0 h, \quad F_{25} = q_0 h \frac{1}{2} \tag{5}
$$

Next, we consider the contribution of the point sources. Since the point sources are located inside an element, we distribute the source to the nodes of the element by interpolation [see Fig. 9.4.14(c)]:

$$
f_i^e = \int_{\Omega_e} Q_0 \delta(x - x_0, y - y_0) \psi_i^e(x, y)\, dx\, dy = Q_0 \psi_i^e(x_0, y_0) \tag{6}
$$

For example, the source at pump 1 (located at x_0 = 830 m, y_0 = 1000 m) can be expressed as (pumping is considered to be a negative point source)

$$
Q_1(x, y) = -1200\, \delta(x - 830, y - 1000) \text{ or } Q_1(\bar{x}, \bar{y}) = -1200\, \delta(\bar{x} - 80, \bar{y} - 250) \tag{7}
$$

where $\delta(\cdot)$ is the Dirac delta function [see Eqs. (3.4.53)–(3.4.55)]. The interpolation functions ψ_i^e for element 21 are [in terms of the local coordinates $\bar{x}$ and $\bar{y}$; see Fig. 9.4.14(c)]

$$\psi_i(\bar{x},\bar{y}) = \frac{1}{2A}(\alpha_i + \beta_i\bar{x} + \gamma_i\bar{y}), \quad (i = 1,2,3) \tag{8a}$$

where

$$\begin{aligned} &\alpha_1 = (375)^2,\ \alpha_2 = 0,\ \alpha_3 = 0,\ 2A = \alpha_1 + \alpha_2 + \alpha_3 = (375)^2 \\ &\beta_1 = -250,\ \beta_2 = 375,\ \beta_3 = -125,\ \gamma_1 = -375,\ \gamma_2 = 0,\ \gamma_3 = 375 \end{aligned} \tag{8b}$$

and $\bar{x} = x - 750$, $\bar{y} = y - 750$. Therefore, we have

$$\psi_1(80,250) = 0.1911, \quad \psi_2(80,250) = 0.5956, \quad \psi_3(80,250) = 0.2133 \tag{9}$$

Similar computations can be carried out for pump 2 (see **Problem 9.8**).

In summary, primary variables and nonzero secondary variables are

$$\begin{aligned} &U_1 = U_2 = U_3 = U_4 = U_5 = U_{41} = U_{42} = U_{43} = U_{44} = U_{45} = 200.0 \\ &F_{21} = 54.0833,\ F_{22} = F_{23} = F_{24} = 108.1666,\ F_{25} = 54.0833 \\ &F_{13} = -229.33,\ F_{14} = -256.0,\ F_{18} = -714.67,\ F_{27} = -411.429 \\ &F_{28} = -1440.0,\ F_{32} = -548.571 \end{aligned} \tag{10}$$

The secondary variables at nodes 6–12, 15–17, 19, 20, 26, 29, 30, 31, and 33–40 are zero. This completes the input data generation for the problem.

The assembled equations are solved, after imposing the specified boundary conditions, for the values of ϕ at the nodes. The equipotential lines can be determined using Eq. (27) of **Example 9.4.1**. The lines of constant ϕ are shown in Fig. 9.4.15(a).

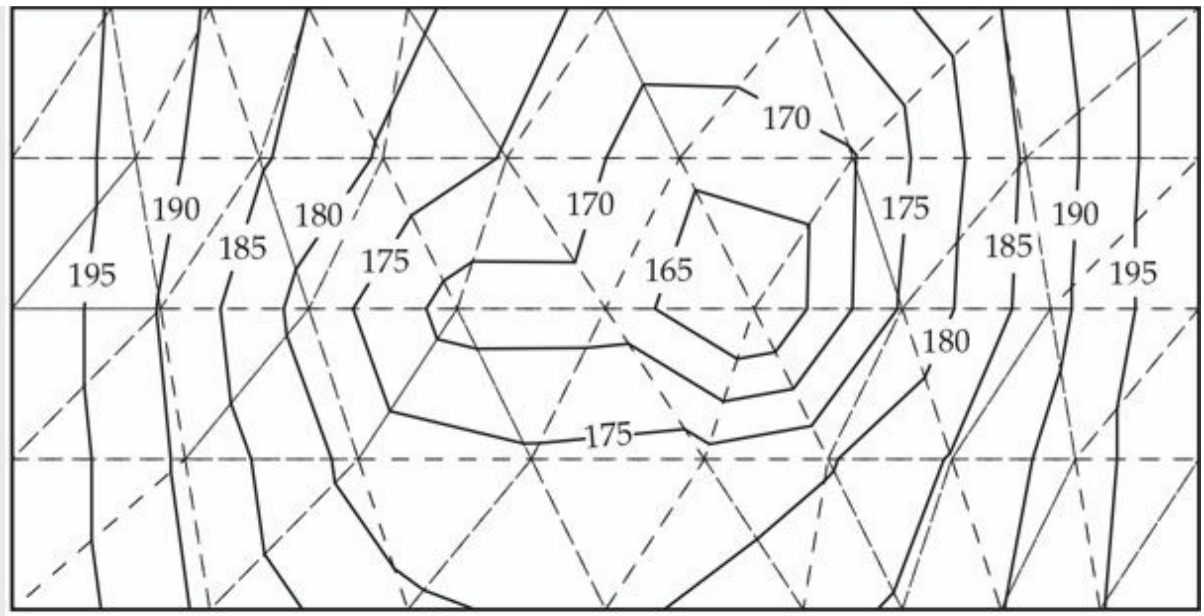

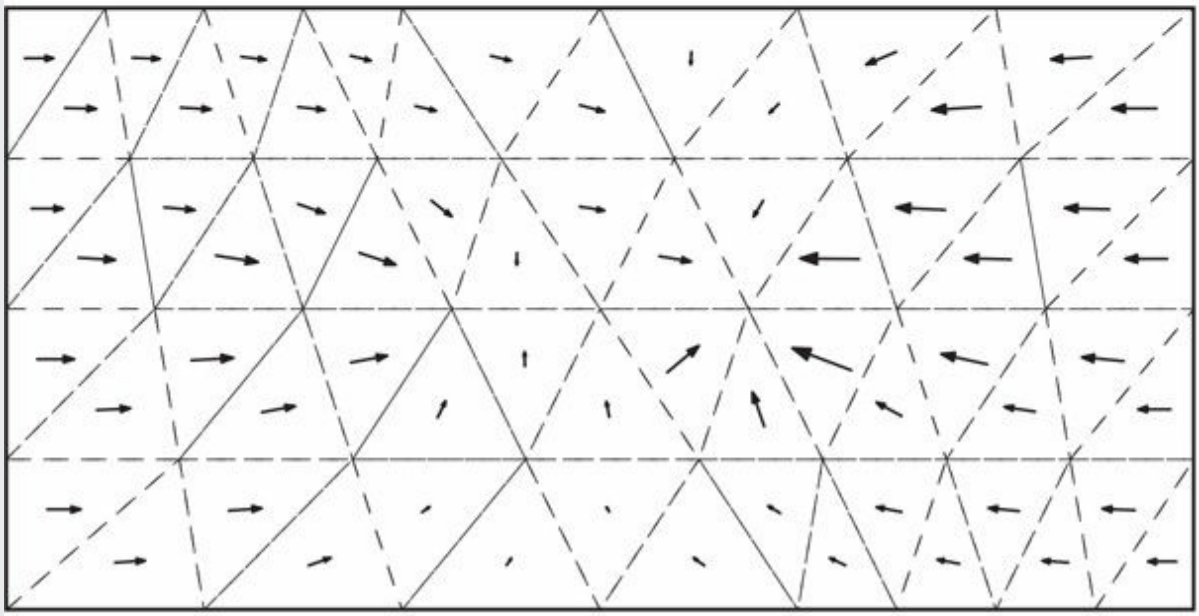

Fig. 9.4.15 Plots of constant piezometric head and velocity vector for the groundwater flow: (a) lines of constant ϕ and (b) plot of velocity vectors for **Example 9.4.5**.

The velocity components are determined in the post-computation using the definition in Eq. (9.4.24) and the velocity vector is given by

$$\mathbf{v} = v_x\hat{\mathbf{i}} + v_y\hat{\mathbf{j}}, \quad |\mathbf{v}| = \sqrt{v_x^2 + v_y^2}, \quad \theta = \tan^{-1}\frac{v_y}{v_x} \tag{11}$$

where θ is the angle, measured in the counterclockwise direction, of the velocity vector from the +ve x axis. The velocity vectors for the problem at hand are shown in Fig. 9.4.15(b).

The evaluation of the results should be based on a qualitative understanding of the problem. The first thing to check is if the boundary conditions are reflected in the solution. Since the top and bottom boundaries are assumed to be impermeable, there should be no flow across these boundaries (i.e., the velocity vectors should not cross these boundaries). Next, the obvious thing to check is if the velocity vectors are heading toward the wells (because water is drawn out) and not toward the stream. The greatest drawdown of water occurs at node 28, which has the largest portion of discharge from pump 2.

Next, we consider an example of irrotational flows of an ideal fluid (i.e., a nonviscous fluid). Examples of physical problems that can be approximated by such flows are provided by flow around bodies such as weirs, airfoils, buildings, and so on, and by flow of water through the earth and dams. Laplace equations (9.4.20) and (9.4.25) governing these flows are a special case of the model equation (9.2.1).

Example 9.4.6

The irrotational flow of an ideal fluid about a circular cylinder, placed with its axis perpendicular to the plane of the flow between two *long* horizontal walls (see Fig. 9.4.16) is governed by

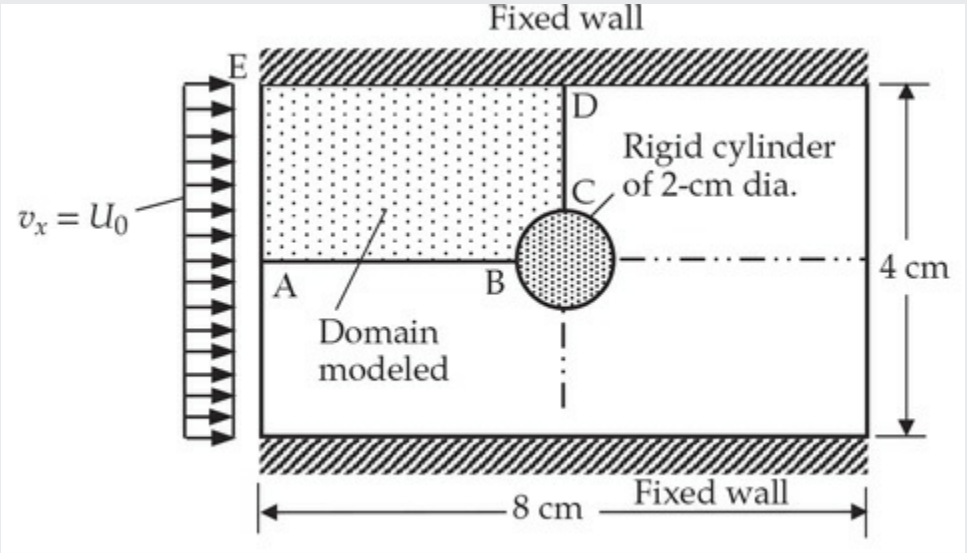

Fig. 9.4.16 Domain and boundary conditions for the stream function and

velocity potential formulations of irrotational flow about a cylinder.

$$-\nabla^2 u = 0 \quad \text{in } \Omega \tag{1}$$

where u is either (a) the stream function ψ or (b) the velocity potential ϕ. Analyze the problem using the finite element method.

Solution: We analyze the problem using both stream function and velocity potential formulations. For both formulations, symmetry of solutions ψ and ϕ exists about the horizontal and vertical center lines (note that the velocity field **v** is symmetric about the horizontal center line but not symmetric about the vertical centerline). Therefore, only a quadrant of the flow region (say, ABCDE in Fig. 9.4.17) is used as the computational domain for the chosen formulations. To determine the constant state of the solution, which does not affect the velocity field, we arbitrarily set the functions ψ and ϕ to zero (or a constant) on appropriate boundary lines.

(a) *Stream Function Formulation*

In the stream function formulation, the velocity components $\mathbf{v} = (v_x, v_y)$ of the flow field are given by

$$v_x = \frac{\partial \psi}{\partial y}, \quad v_y = -\frac{\partial \psi}{\partial x} \tag{2}$$

The boundary conditions on the stream function ψ can be determined as follows. Streamlines have the property that flow perpendicular to a streamline is zero. Therefore, the fixed walls correspond to streamlines. Note that for inviscid flows, fluid particles do not stick to rigid walls. The fact that the velocity component perpendicular to the horizontal line of symmetry is equal to zero allows us to use that line as a streamline. Since the velocity field depends on the relative difference of two streamlines, we take the value of the stream function that coincides with the horizontal axis of symmetry (i.e., on ABC) to be zero, and then determine the value of ψ on the upper wall from the condition

$$\frac{\partial \psi}{\partial y} = U_0 \tag{3}$$

where U_0 is the inlet horizontal velocity of the field. We determine the value of the stream function on the boundary $x = 0$ by integrating the above equation with respect to y:

$$\int_0^y \frac{d\psi}{dy}\,dy = \int_0^y U_0\,dy + \psi_A = U_0 y \qquad (4)$$

because $\psi_A = 0$ by the previous discussion. This gives the boundary condition on AE. Since the line ED is a streamline and its value at point E is $2U_0$, it follows that $\psi = 2U_0$ on line ED. Lastly, on the CD we assume the vertical velocity component is zero (i.e., $v_y = 0$); hence $\partial\psi/\partial x = 0$ on CD. The boundary conditions are shown on the computational domain in Fig. 9.4.17.

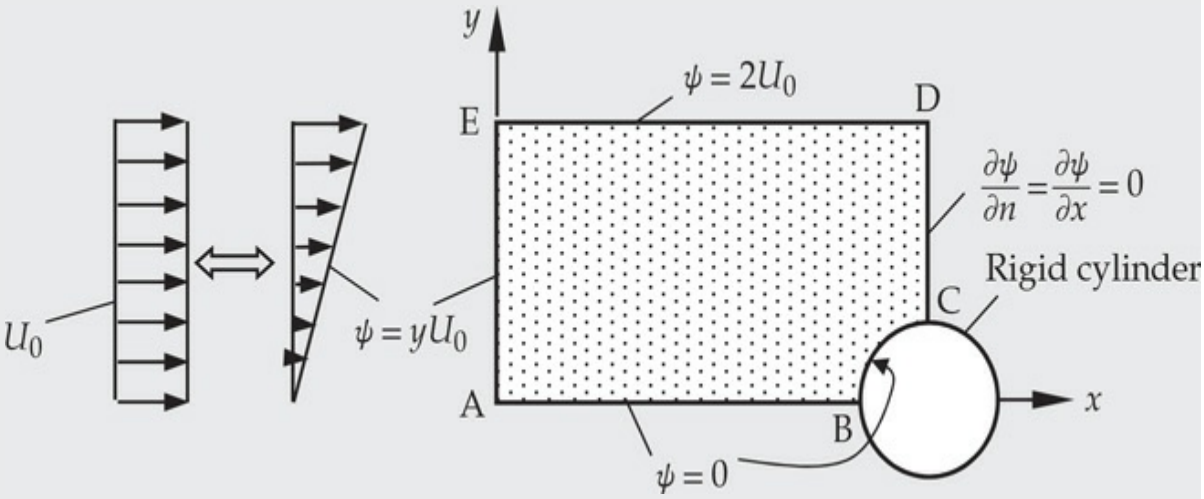

Fig. 9.4.17 Computational domain and boundary conditions for the stream function formulation of inviscid flow around a cylinder.

In selecting a mesh, we should note that the velocity field is uniform (i.e., streamlines are horizontal) at the inlet, and it takes a parabolic profile at the exit (along CD). Therefore, the mesh at the inlet should be uniform, and the mesh close to the cylinder should be relatively more refined to be able to model the curved boundary and capture the rapid change in ψ. Two coarse finite element meshes are used to discuss the boundary conditions, and results for refined meshes will be discussed subsequently. Mesh T1 consists of 60 triangular elements and mesh Q1 consists of 30 quadrilateral elements. Both meshes contain the same 42 nodes (see Fig. 9.4.18). The mesh with solid lines in Fig. 9.4.18 corresponds to mesh Q1, and the mesh with solid and dashed lines correspond to mesh T1. It should be noted that the discretization error is not zero for this case because of the cylinder geometry.

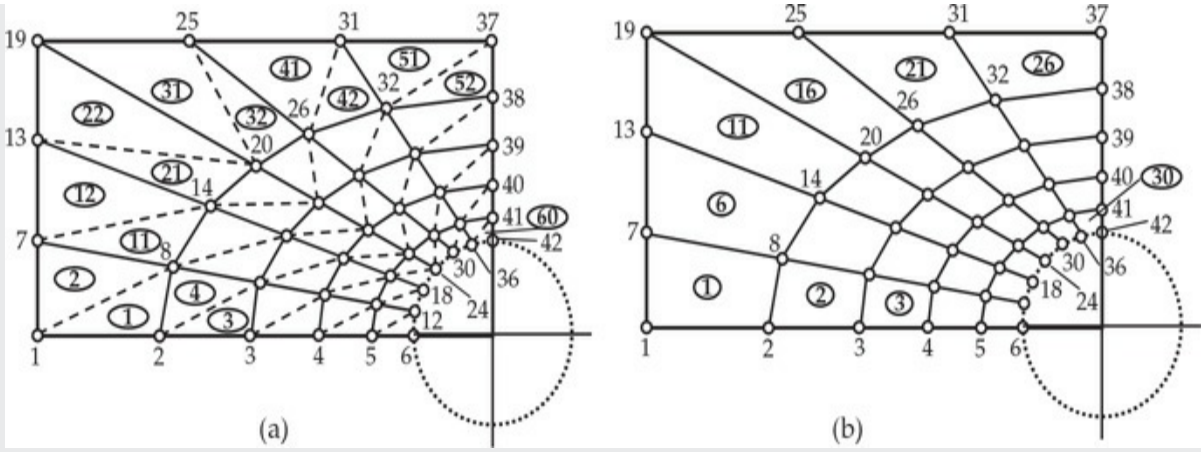

Fig. 9.4.18 Meshes used for inviscid flow around a cylinder. (a) Mesh of linear triangles (T1). (b) Mesh of linear quadrilaterals (Q1).

The specified primary degrees of freedom (i.e., nodal values of ψ) for the two meshes are

$$U_1 = U_2 = \cdots = U_6 = U_{12} = U_{18} = U_{24} = U_{30} = U_{36} = U_{42} = 0.0$$

$$U_7 = 0.6667, \quad U_{13} = 1.3333, \quad U_{19} = U_{25} = U_{31} = U_{37} = 2.0 \tag{5}$$

There are no nonzero specified secondary variables; the secondary variables are specified to be zero at the nodes on line CD:

$$F_{38} = F_{39} = F_{40} = F_{41} = 0 \tag{6}$$

Although the secondary variable is specified to be zero at nodes 37 and 42, where the primary variable is also specified, we choose to impose the boundary conditions on the primary variable over the secondary variables.

(b) *Velocity Potential Formulation*

In the velocity potential formulation, the velocity components are computed from

$$v_x = -\frac{\partial \phi}{\partial x}, \quad v_y = -\frac{\partial \phi}{\partial y} \tag{7}$$

The boundary conditions on the velocity potential ϕ can be derived as follows (see Fig. 9.4.19). The fact that $v_y = -(\partial\phi/\partial y)$ is zero (no penetration) on the upper wall as well as on the horizontal line of symmetry gives the boundary conditions on the secondary variable, $(\partial\phi/$

∂n) there. Along AE, the velocity $v_x = -(\partial\phi/\partial x)$ is specified to be U_0. On the surface of the cylinder the normal velocity $v_n = -(\partial\phi/\partial n)$ is zero. Thus all boundary conditions, so far, are of the flux type (i.e., on the secondary variable). On the boundary CD we must know either ϕ or $\partial\phi/\partial n = \partial\phi/\partial x$. It is clear that $-\partial\phi/\partial x = v_x$ is not known on CD. Therefore, we assume that ϕ is known there (necessary to eliminate "rigid body" motion), and set it equal to a constant. Since the constant does not contribute to the velocity field, we take it to be zero on CD.

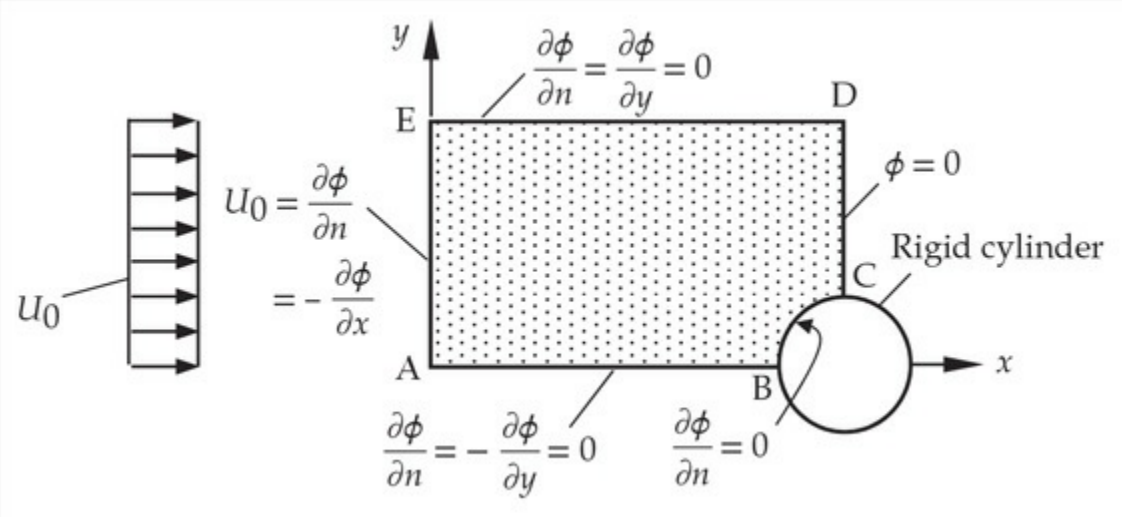

Fig. 9.4.19 Computational domain and boundary conditions for the velocity potential formulation of inviscid flow around a cylinder.

The mathematical boundary conditions of the problem must be translated into the finite element data. The boundary conditions on the primary variables come from the boundary CD. We have

$$U_{37} = U_{38} = U_{39} = U_{40} = U_{41} = U_{42} = 0.0 \tag{8}$$

The only nonzero boundary conditions on the secondary variables come from the boundary AE. There we must evaluate the boundary integral

$$\int_{\Gamma_e} \frac{\partial\phi}{\partial n}\psi_i \, ds = U_0 \int_{AE} \psi_i(y)\, dy \tag{9}$$

for each node i on AE. We obtain ($h = 2/3 = 0.66667$)

$$
\begin{aligned}
Q_1 &= U_0 \int_0^h \left(1 - \frac{\bar{y}}{h}\right) d\bar{y} = 0.33333 U_0 \\
Q_7 &= U_0 \int_0^h \frac{\bar{y}}{h} d\bar{y} + U_0 \int_0^h \left(1 - \frac{\bar{y}}{h}\right) d\bar{y} = 0.66667 U_0 \\
Q_{13} &= U_0 \int_0^h \frac{\bar{y}}{h} d\bar{y} + U_0 \int_0^h \left(1 - \frac{\bar{y}}{h}\right) d\bar{y} = 0.66667 U_0 \\
Q_{19} &= U_0 \int_0^h \frac{\bar{y}}{h} d\bar{y} = \frac{h U_0}{2} = 0.3333 U_0
\end{aligned}
\tag{10}
$$

Table 9.4.5 contains the values of the stream function and its derivative $(\partial\psi/\partial y)(= v_x)$ at selected points of the meshes. The finite element program **FEM2D** is used in the analysis. The stream function values obtained with mesh T1 and mesh Q1 are very close to each other. Recall that the derivative $\partial\psi/\partial y$ is constant in a linear triangular element, whereas it varies linearly with x in a linear rectangular element. Therefore, mesh T1 and mesh Q1 results will not be the same. The velocities included in Table 9.4.5 correspond to elements closest to the symmetry line (i.e., $y = 0$ line) and surface of the cylinder.

Table 9.4.5 Finite element results from the stream function and velocity potential formulations of inviscid flow around a cylinder (**Example 9.4.6**).

		Stream function		$v_x = \frac{\partial \psi}{\partial y}$		$v_x = -\frac{\partial \phi}{\partial x}$	
x	y	Mesh T1	Mesh Q1	Mesh T1	Mesh Q1	Mesh T1	Mesh Q1
1.3921	0.9631	0.9274	0.9375	0.995 (1)[1]	0.998 (1)	0.998 (1)	0.999 (1)
2.1817	0.7532	0.6419	0.6530	0.983 (3)	0.993 (2)	0.992 (3)	0.996 (2)
1.4627	1.4257	1.3950	1.4086	0.952 (5)	0.978 (3)	0.976 (5)	0.984 (3)
2.2923	1.1000	0.9652	0.9902	0.954 (7)	0.912 (4)	0.923 (7)	0.933 (4)
1.5416	1.8910	1.8833	1.8880	0.000 (9)	0.516 (5)	0.686 (9)	0.611 (5)
1.8624	1.7231	1.6906	1.7012	0.136 (19)	0.648 (10)	0.783 (19)	0.750 (10)
2.2958	1.4963	1.3925	1.4092	0.430 (29)	0.877 (15)	0.980 (29)	0.985 (15)
2.8416	1.2106	0.8906	0.9165	1.396 (40)	1.313 (20)	1.530 (40)	1.253 (20)
3.4147	1.2801	0.7603	0.7701	1.746 (50)	1.747 (25)	2.129 (50)	1.615 (25
4.0000	1.9039	1.8305	1.8195	2.006 (58)	1.724 (28)	1.835 (58)	1.643 (28)
4.0000	1.7558	1.5628	1.5405	2.187 (59)	1.866 (29)	1.817 (59)	1.764 (29)
4.0000	1.5558	1.1865	1.1590	2.242 (60)	2.166 (30)	2.400 (60)	2.057 (30)

[1] Denotes element number; the derivatives of ψ and ϕ are evaluated at the center of this element.

The tangential velocity v_t on the cylinder surface can be computed from the relation

$$v_t(\theta) = v_x \sin\theta + v_y \cos\theta = \frac{\partial \psi}{\partial y}\sin\theta - \frac{\partial \psi}{\partial x}\cos\theta \tag{11}$$

Contour plots of streamlines, velocity potential, and velocity vectors obtained with mesh Q1 are shown in Fig. 9.4.20 (a)–(c). We note from Table 9.4.5 that there is a difference between the velocities obtained with the two formulations (for either mesh). This is primarily due to the nature of the boundary-value problems in the two formulations. In the stream function formulation (SFF) there are more boundary conditions on the primary variable than in the velocity potential formulation (VPF) and they are exactly not the same.

A plot of the variation of the tangential velocity with the angular distance along the cylinder surface is shown in Fig. 9.4.21, along with the analytical potential solution

$$v_t = U_0(1 + R^2/r^2)\sin\theta \tag{12}$$

valid on the cylinder surface. The finite element solution of a refined mesh, mesh Q2 (not shown), is also included in the figure. The angle θ,

radial distance r, and tangential velocity v_t can be computed from the relations

$$\theta = \tan^{-1}\left(\frac{y}{4-x}\right), \quad r = \sqrt{(4-x)^2 + y^2}, \quad v_t = v_x \sin\theta + v_y \cos\theta \tag{13}$$

The finite element solution is in agreement with the potential solution of the problem. However, the finite element solution is not expected to agree closely because v_t is evaluated at a radial distance $r > R$, whereas the analytical potential solution is evaluated at $r = R$ only.

9.4.5 Solid Mechanics

In this section we consider two-dimensional boundary-value problems of solid mechanics that are cast in terms of a single dependent unknown. These problems include torsion of cylindrical members and transverse deflection of membranes. This study is restricted to small deformations.

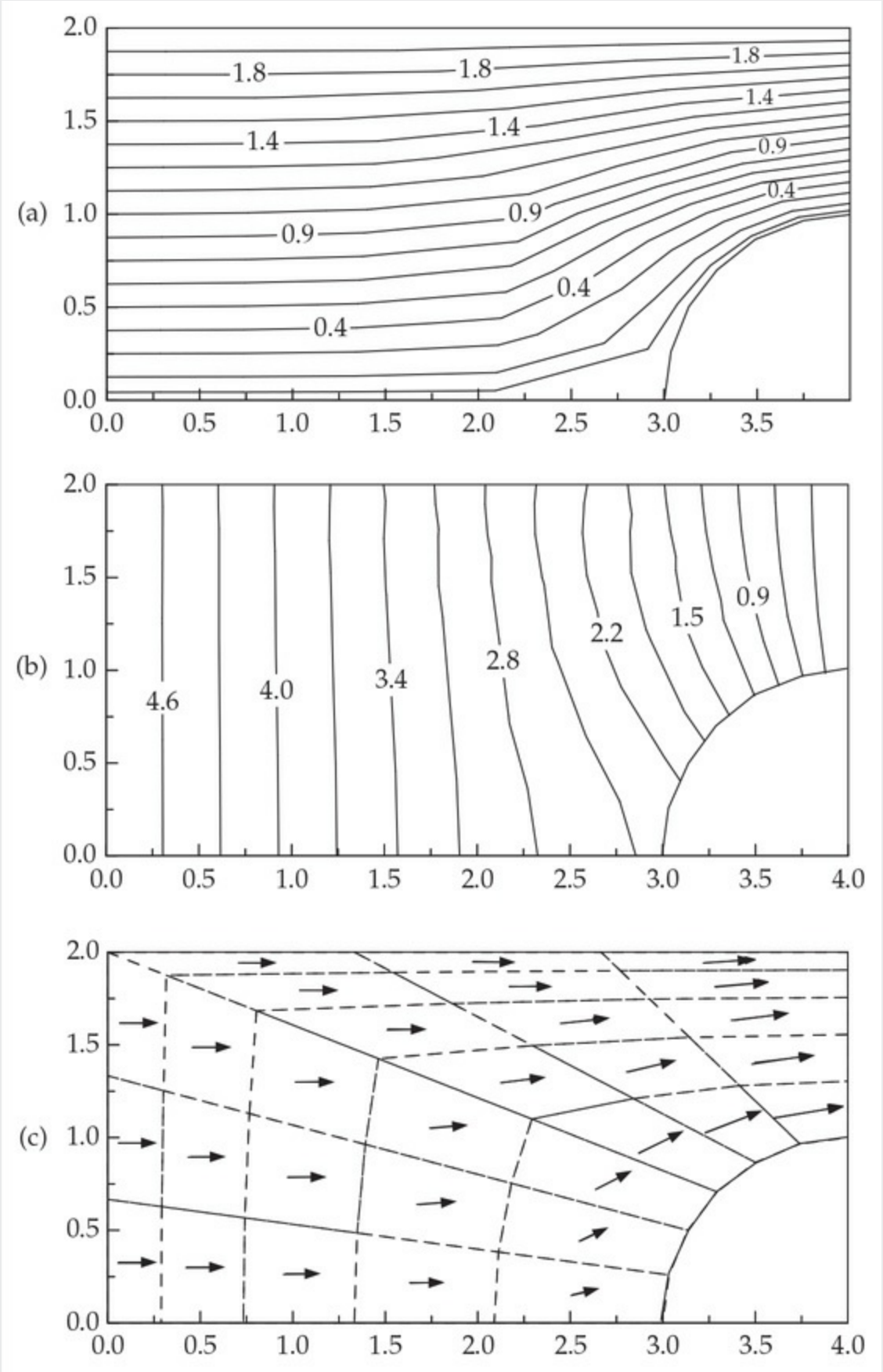

Fig. 9.4.20 Contours of (a) stream function, (b) velocity potential, and (c) velocity vectors

(from the velocity potential formulation), as obtained using mesh Q1.

9.4.5.1 Torsion of cylindrical members

Consider a cylindrical bar (i.e., a long, uniform cross-section member), fixed at one end and twisted by a couple (i.e., moment or torque) of magnitude M_z which is directed along the axis (z) of the bar, as shown in Fig. 9.4.22(a). We wish to determine the amount of twist and the associated stress field in the bar. To this end, we first derive the governing equations and then analyze the equation using the finite element method.

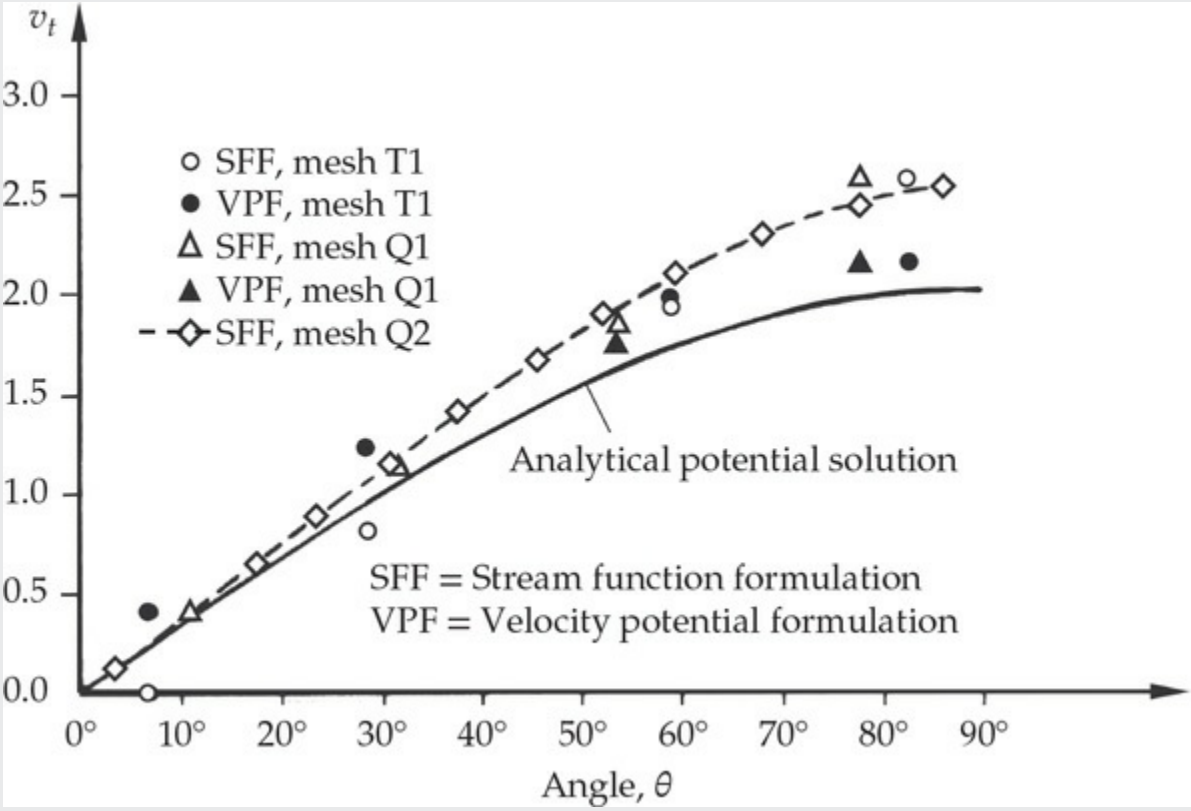

Fig. 9.4.21 Variation of the tangential velocity along the cylinder surface: comparison of the finite element results with the potential theory solution (mesh Q2 contains 96 elements and 117 nodes).

In general, a non-circular cross-section member subjected to torsional moment experiences warping at any section. We assume that all cross-sections warp in the same way (which holds true for small twisting moments and deformation). This assumption allows us to assume that the displacements (u, v, w) along the coordinates (x, y, z) are of the form [see Fig. 9.4.22(b)]

$$u = -\theta z y, \quad v = \theta z x, \quad w = \theta \phi(x, y) \tag{9.4.27}$$

where $\phi(x,y)$ is a function to be determined, and θ is the angle of twist per unit length of the bar.

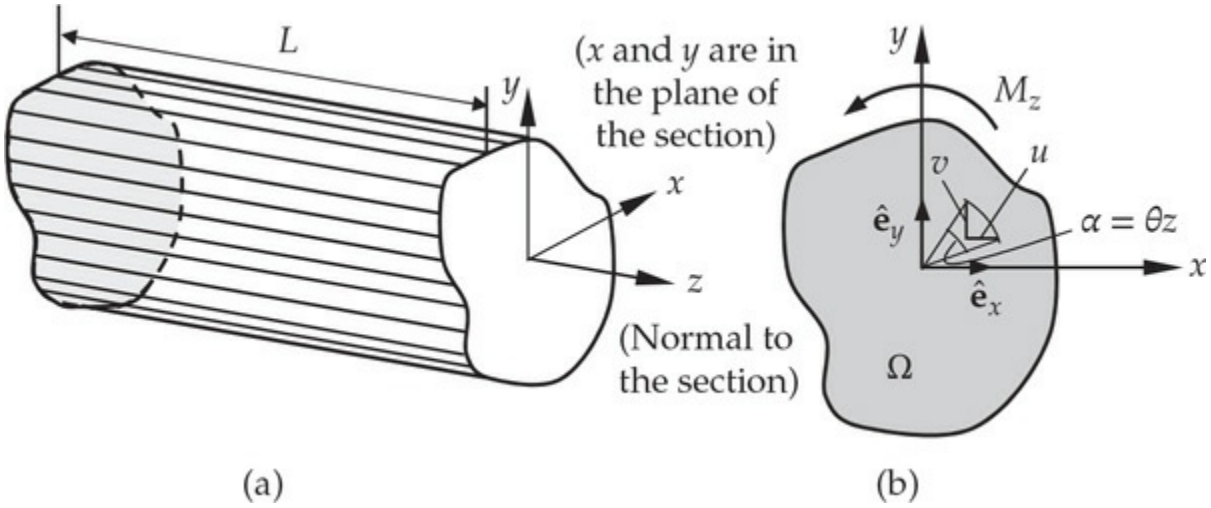

Fig. 9.4.22 Torsion of cylindrical members: (a) a cylindrical member and (b) domain of analysis.

The displacement field in Eq. (9.4.27) can be used to compute the strains, and stresses are computed using an assumed constitutive law. The stresses thus computed must satisfy the three-dimensional equations of stress equilibrium:

$$\begin{aligned} \frac{\partial \sigma_x}{\partial x} + \frac{\partial \sigma_{xy}}{\partial y} + \frac{\partial \sigma_{xz}}{\partial z} &= 0 \\ \frac{\partial \sigma_{xy}}{\partial x} + \frac{\partial \sigma_y}{\partial y} + \frac{\partial \sigma_{yz}}{\partial z} &= 0 \\ \frac{\partial \sigma_{xz}}{\partial x} + \frac{\partial \sigma_{yz}}{\partial y} + \frac{\partial \sigma_z}{\partial z} &= 0 \end{aligned} \tag{9.4.28}$$

and the stress boundary conditions on the lateral surface and at the end of the cylindrical bar. Calculation of strains and then stresses using the generalized Hooke's law gives the expressions

$$\sigma_{xz} = G\theta\left(\frac{\partial \phi}{\partial x} - y\right), \quad \sigma_{yz} = G\theta\left(\frac{\partial \phi}{\partial y} + x\right) \tag{9.4.29}$$

and all other stresses are identically zero. Here G denotes the shear

modulus of the material of the bar. Substitution of these stresses into Eq. (9.4.28) yields [the first two equations in Eq. (9.4.28) are identically satisfied and the third one leads to the following equation]:

$$\frac{\partial}{\partial x}\left(G\theta\frac{\partial\phi}{\partial x}\right)+\frac{\partial}{\partial y}\left(G\theta\frac{\partial\phi}{\partial y}\right)=0 \tag{9.4.30}$$

throughout the cross section Ω of the cylinder. The boundary conditions on the lateral surfaces Γ require that $\sigma_{xz}\, n_x + \sigma_{yz}\, n_y = 0$:

$$\left(\frac{\partial\phi}{\partial x}-y\right)n_x+\left(\frac{\partial\phi}{\partial y}+x\right)n_y=0 \Rightarrow \frac{\partial\phi}{\partial n}=yn_x-xn_y \tag{9.4.31}$$

Here (n_x, n_y) denote the direction cosines of the unit normal at a point on Γ.

In summary, the torsion of a cylindrical bar is governed by Eqs. (9.4.30) and (9.4.31). The function $\phi(x, y)$ is called the *torsion function* or *warping function*. Since the boundary condition in Eq. (9.4.31) is of the flux type, the function can be determined within an additive constant. The stresses in Eq. (9.4.29), however, are independent of this constant. The additive constant has the meaning of rigid body movement of the cylinder as a whole in the *z*-direction. For additional discussion of the topic, the reader is referred to Timoshenko and Goodier [3].

The Laplace equation (9.4.30) and the Neumann boundary condition (9.4.31) governing ϕ is not convenient in the analysis because of the nature and form of the boundary condition, especially for irregular cross-section members. The theory of analytic functions can be used to rewrite these equations in terms of the *stress function* $\Psi(x, y)$, which is related to the warping function $\phi(x, y)$ by the equations

$$\frac{\partial\Psi}{\partial x}=-\frac{\partial\phi}{\partial y}-x, \quad \frac{\partial\Psi}{\partial y}=\frac{\partial\phi}{\partial x}-y \tag{9.4.32}$$

Eliminating ϕ from Eqs. (9.4.30) and (9.4.31) gives, respectively, the results

$$-\left(\frac{\partial^2\Psi}{\partial x^2}+\frac{\partial^2\Psi}{\partial y^2}\right)=2 \text{ in } \Omega; \quad \frac{\partial\Psi}{\partial y}n_x-\frac{\partial\Psi}{\partial x}n_y=0 \text{ on } \Gamma \tag{9.4.33}$$

The boundary condition in Eq. (9.4.33) is nothing but the tangential derivative $d\Psi/ds$, and $d\Psi/ds = 0$ implies that

$$\Psi = \text{constant} \quad \text{on } \Gamma \tag{9.4.34}$$

Since the constant part of Ψ does not contribute to the stress field

$$\sigma_{xz} = G\theta \frac{\partial \Psi}{\partial y}, \quad \sigma_{yz} = -G\theta \frac{\partial \Psi}{\partial x} \tag{9.4.35}$$

we can take $\Psi = 0$ on the boundary Γ.

In summary, the torsion problem can be stated as one of determining the stress function Ψ such that

$$-\nabla^2 \Psi = 2 \text{ in } \Omega, \quad \Psi = 0 \text{ on } \Gamma \tag{9.4.36}$$

Once Ψ is determined, the stresses can be computed from Eq. (9.4.35) for a given angle of twist per unit length (θ) and shear modulus (G).

The finite element model of Eq. (9.4.36) follows immediately from that of Eq. (9.2.1):

$$\mathbf{K}^e \boldsymbol{\Psi}^e = \mathbf{f}^e + \mathbf{Q}^e \tag{9.4.37a}$$

where Ψ_i^e (not to be confused with the interpolation functions ψ_i) is the value of Ψ at the ith node of Ω_e and

$$K_{ij}^e = \int_{\Omega_e} \left(\frac{\partial \psi_i}{\partial x}\frac{\partial \psi_j}{\partial x} + \frac{\partial \psi_i}{\partial y}\frac{\partial \psi_j}{\partial y} \right) dxdy$$
$$f_i^e = \int_{\Omega_e} 2\psi_i \, dxdy, \quad Q_i^e = \oint_{\Gamma_e} \frac{\partial \Psi}{\partial n} \psi_i \, ds \tag{9.4.37b}$$

Example 9.4.7

Consider the torsion of a rectangular cross-section (side $2a \times 2b$) member made of isotropic material (G, shear modulus) subjected to angle of twist θ. Determine the shear stresses σ_{xz} and σ_{yz} using the finite element model developed. Take the origin of the coordinate system at the center of the cross section [see Fig. 9.4.23(a)]. Exploit symmetries available in the problem.

Solution: We note that the problem is antisymmetric as far as the load (angle of twist) and stress distribution are concerned; however, the stress function Ψ, being a scalar function governed by the Poisson equation (9.4.36), is symmetric about the x and y axes (as well as the diagonal lines

for $a = b$). Figure 9.4.23(b) shows 4 × 4 mesh of four-node elements for the case $a = b$. The biaxial symmetry about the x and y axes requires imposition of the following boundary conditions along the lines of symmetry:

$$\frac{\partial \Psi}{\partial x} = 0 \text{ on the line } x = 0, \quad \frac{\partial \Psi}{\partial y} = 0 \text{ on the line } y = 0 \tag{1}$$

In addition, we have the condition $\Psi = 0$ on lines $x = 0.5a$ and $y = 0.5b$.

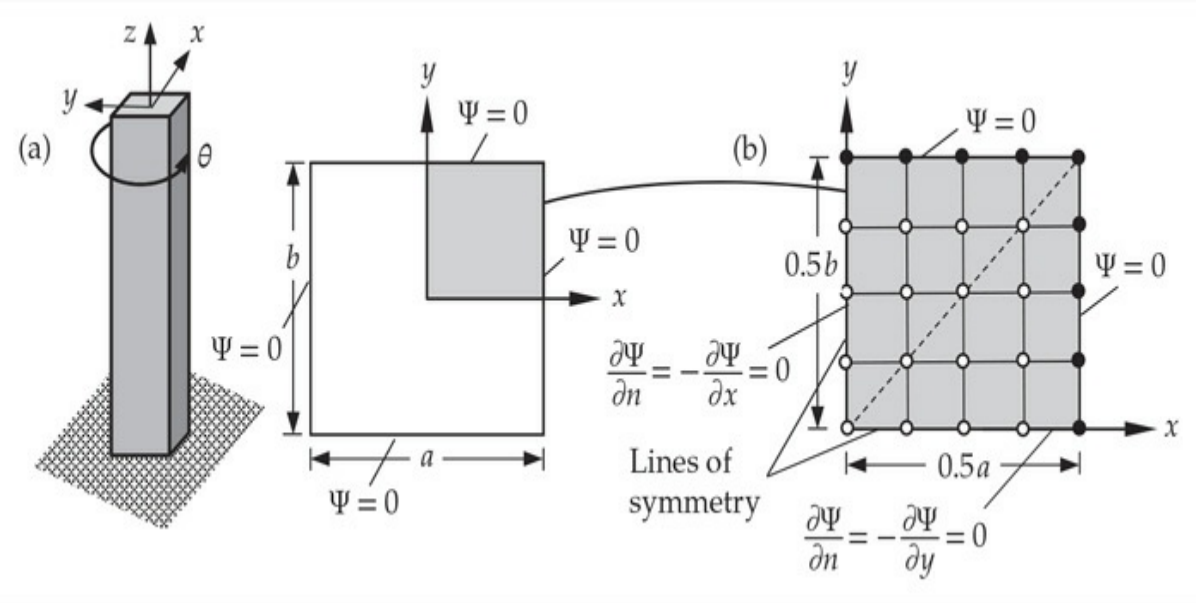

Fig. 9.4.23 Torsion of square section bar: (a) actual domain and (b) domain of analysis with a 4 × 4 mesh of linear rectangular elements.

The problem is analyzed using various meshes of four-node and nine-node rectangular elements in the quadrant of the domain. The contour lines of the surface $\Psi(x,y)$ and contour lines of the vector $\mathbf{v} = \bar{\sigma}_{xz}\hat{\mathbf{e}}_x + \bar{\sigma}_{yz}\hat{\mathbf{e}}_y$ are shown in Fig. 9.4.24. The analytical solutions for the problem are given by (see Kantorovich and Krylov [4] and Reddy [5])

$$\Psi(x,y) = \frac{a^2}{4} - x^2 + \frac{8a^2}{\pi^3} \sum_{n=1,2,3,\ldots}^{\infty} \frac{(-1)^n}{(2n-1)^3} \frac{\cosh(k_n y)\,\cos(k_n x)}{\cosh(k_n b/2)} \tag{2a}$$

$$\bar{\sigma}_{xz} = \frac{8a}{\pi^2} \sum_{n=1,2,3,\ldots}^{\infty} \frac{(-1)^n}{(2n-1)^2} \frac{\sinh(k_n y)\,\cos(k_n x)}{\cosh(k_n b/2)} \tag{2b}$$

$$\bar{\sigma}_{yz} = \left[2x + \frac{8a}{\pi^2} \sum_{n=1,2,3,\ldots}^{\infty} \frac{(-1)^n}{(2n-1)^2} \frac{\cosh(k_n y)\,\sin(k_n x)}{\cosh(k_n b/2)} \right] \tag{2c}$$

where $k_n = (2n - 1)\pi/a$. The finite element solutions for the stress function Ψ and shear stress $\bar{\sigma}_{yz} = \sigma_{yz}/G\theta$ (evaluated at the center of the element) are presented in

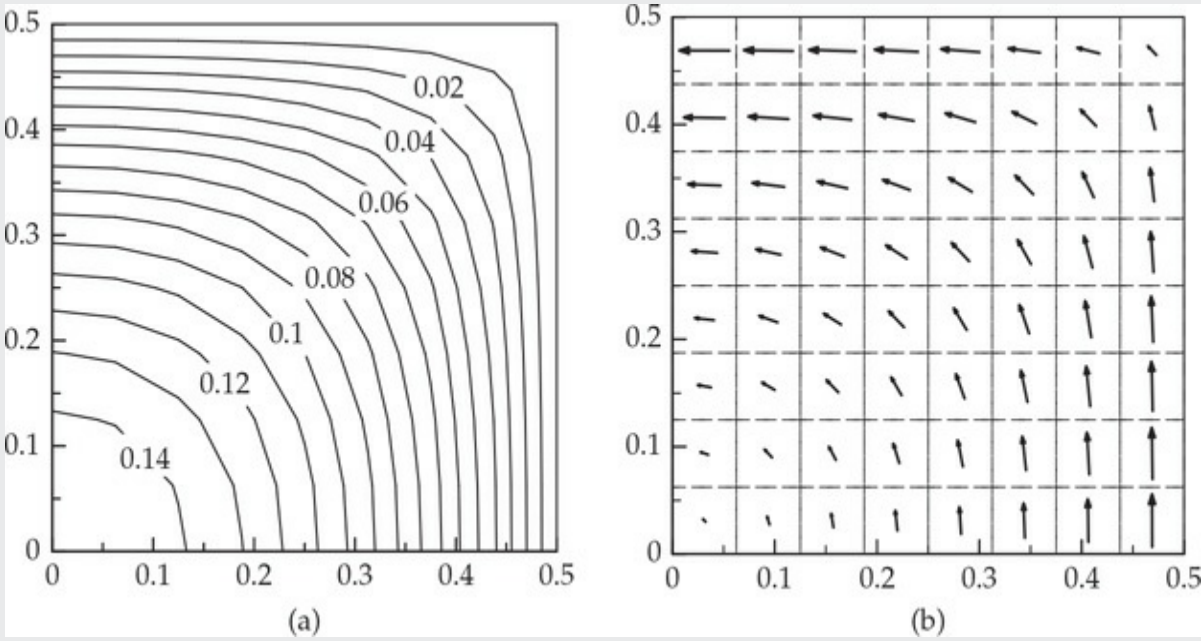

Fig. 9.4.24 (a) Contour plot of the stress function Ψ (b) plot of the vector of shear stresses, $\mathbf{v} = \bar{\sigma}_{xz}\hat{\mathbf{e}}_x + \bar{\sigma}_{yz}\hat{\mathbf{e}}_y$; results were obtained using the 8 × 8 mesh of linear rectangular elements in a quadrant of square cross section.

Tables 9.4.6 and 9.4.7, respectively (for the case $a = b = 1.0$) along with the analytical solutions (using the first 10 terms of the series). Because of the biaxial symmetry for the square cross section, we have $\bar{\sigma}_{xz}(x, y) = -\bar{\sigma}_{yz}(y, x)$. The finite element results converge, as the mesh is refined, to the analytical results. In particular, the 4 × 4 mesh of nine-node quadratic elements is in excellent agreement with the analytical solution.

Table 9.4.6 Convergence of the finite element solutions for Ψ using linear and quadratic rectangular elements (four-node and nine-node elements).

		Linear elements			Quadratic elements		
x	y	2×2	4×4	8×8	1×1	2×2	$(4\times4)^1$
0.0000	0.0000	0.15536	0.14920	0.14780	0.14744	0.14730	0.14734
0.0625	0.0000	—	—	0.14583	—	—	0.14538
0.1250	0.0000	—	0.14120	0.13987	—	0.13941	0.13944
0.1875	0.0000	—	—	0.12972	—	—	0.12931
0.2500	0.0000	0.12054	0.11610	0.11502	0.11378	0.11463	0.11467
0.3125	0.0000	—	—	0.09534	—	—	0.09505
0.3750	0.0000	—	0.07069	0.07007	—	0.069873	0.06986
0.4375	0.0000	—	—	0.03854	—	—	0.03844
0.0625	0.0625	—	—	0.14390	—	—	0.14346
0.1250	0.1250	—	0.13376	0.13249	—	0.13207	0.13207
0.1875	0.1875	—	—	0.11436	—	—	0.11399
0.2500	0.1250	—	0.11031	0.10925	—	0.10887	0.10890
0.2500	0.2500	0.09643	0.09191	0.09090	0.09095	0.09056	0.09057
0.3125	0.3125	—	—	0.06407	—	—	0.06379
0.3750	0.2500	—	0.05729	0.05660	—	0.05626	0.05636
0.3750	0.3750	—	0.03753	0.03666	—	0.03652	0.03641
0.4375	0.4375	—	—	0.01281	—	—	0.01258

[1]The solution coincides with the analytical solution to five significant decimal places.

Table 9.4.7 Comparison of finite element solutions for the shear stress $\bar{\sigma}_{yz}(x, y)$, computed using various meshes, with the analytical solution.

		Mesh of linear elements			
x	y	2×2	4×4	8×8	Analytical solution
0.03125	0.03125	—	—	0.0312	0.0312
0.09375	0.03125	—	—	0.0946	0.0946
0.15625	0.03125	—	—	0.1612	0.1611
0.21875	0.03125	—	—	0.2332	0.2331
0.28125	0.03125	—	—	0.0313	0.3124
0.34375	0.03125	—	—	0.4015	0.4011
0.40625	0.03125	—	—	0.5013	0.5008
0.46875	0.03125	—	—	0.6135	0.6128
0.06250	0.06250	—	0.0618	—	0.0618
0.18750	0.06250	—	0.1942	—	0.1939
0.31250	0.06250	—	0.3529	—	0.3516
0.43750	0.06250	—	0.5528	—	0.5504
0.12500	0.12500	0.1179	—	—	0.1193
0.37500	0.12500	0.4339	—	—	0.4272

9.4.5.2 Transverse deflections of membranes

Suppose that a membrane, with fixed edges, occupies the region Ω in the (x, y) plane. Initially the membrane is stretched so that the tension T in the membrane is uniform and that T is so large that it is not appreciably altered when the membrane is deflected by a distributed transverse force, $f(x, y)$. The equation governing the transverse deflection u of the membrane is given by

$$-T\left(\frac{\partial^2 u}{\partial x^2}+\frac{\partial^2 u}{\partial y^2}\right)=f(x,y) \quad \text{in } \Omega \tag{9.4.38a}$$

subjected to the boundary condition

$$u=0 \quad \text{on } \Gamma \tag{9.4.38b}$$

The finite element model of the equation is obvious because Eq. (9.4.38a) is a special case of the model equation (9.2.1) [also see Eqs. (9.2.3), (9.2.46), (9.4.1), and (9.4.36)]. In view of the close analogy between this problem and the torsion of cylindrical bars, we will not consider any numerical examples here.

9.5 Eigenvalue and Time-Dependent Problems

9.5.1 Finite Element Formulation

This section deals with the finite element analysis of two-dimensional eigenvalue and time-dependent problems involving a single variable. We use the results of Chapter 7 to develop finite element equations of two-dimensional time-dependent problems. Since the weak form and time approximations were already discussed in detail in Chapter 7, attention is focussed here on how to go from the given model equations to the final equations.

9.5.1.1 Model equation

Consider the following partial differential equation in a two-dimensional region Ω with total boundary Γ,

$$c_1\frac{\partial u}{\partial t}+c_2\frac{\partial^2 u}{\partial t^2}-\frac{\partial}{\partial x}\left(a_{11}\frac{\partial u}{\partial x}\right)-\frac{\partial}{\partial y}\left(a_{22}\frac{\partial u}{\partial y}\right)=f(x,y,t),\quad (x,y)\text{ in }\Omega\text{ for }t>0 \tag{9.5.1}$$

Here t denotes time, and c_1, c_2, a_{11}, a_{22} and f are known functions of position (i.e., data). In the present discussions, we assume that only the source term is a function of time. When time derivative terms are omitted, Eq. (9.5.1) reduces to Eq. (9.2.1). When $c_2 = 0$, Eq. (9.5.1) corresponds to transient heat transfer problems, with $c_1 = \rho c_v$, ρ being the mass per unit area and c_v the specific heat at constant volume. For structural problems like motion of membranes, c_1 represents the damping coefficient (we will not consider it in this book, $c_1 = 0$) and c_2 is the mass per unit area, ρ. Thus, in the examples we consider, we have either c_1 or c_2 as nonzero (but not both).

The boundary conditions (on different parts of Γ)

$$u=\hat{u}\text{ or }\ q_n^{\text{cnd}}+q_n^{\text{cnv}}=q_n\ \ (\text{for } t\geq 0) \tag{9.5.2a}$$

where q_n^{cnd} is the (conductive) flux normal to the boundary

$$q_n^{\text{cnd}}=a_{11}\frac{\partial u}{\partial x}n_x+a_{22}\frac{\partial u}{\partial y}n_y \tag{9.5.2b}$$

and q_n^{cnv} is the (convective) flux normal to the boundary

$$q_n^{\text{cnv}} = \beta(u - u_\infty) \tag{9.5.2c}$$

and q_n is the external flux on the boundary. Here β and u_∞ parameters have the meaning of, using heat transfer terminology, the film coefficient and reference value of the surrounding medium. For solid mechanics problems, q_n^{cnv} can be viewed as some type of interaction between the domain and the surroundings.

Since Eq. (9.5.1) involves time derivatives, it is expected that the initial state of the system (i.e., at $t = 0$) on u and $\dot{u} = \partial u/\partial t$ (when $c_2 \neq 0$ only) is required. The initial conditions are of the form

$$u(x, y, 0) = u_0(x, y), \quad \dot{u}(x, y, 0) = v_0(x, y) \quad \text{in } \Omega \tag{9.5.3}$$

where u_0 and v_0 are initial values of u and its time derivative (which must be known).

9.5.1.2 Weak form

The weak form of Eq. (9.5.1) over an element Ω_e is obtained by the standard procedure: multiply Eq. (9.5.1) with a weight function $w(x, y)$ and integrate over the element Ω_e (not in time), integrate-by-parts (only with respect to x and y) those terms which involve higher-order derivatives, and replace the coefficient of the weight function (namely, the secondary variable, q_n) in the boundary integral with $q_n = \hat{q}_n - \beta(u - u_\infty)$. We obtain

$$0 = \int_{\Omega_e} \left[w\left(c_1 \frac{\partial u}{\partial t} + c_2 \frac{\partial^2 u}{\partial t^2} - f \right) + a_{11} \frac{\partial w}{\partial x} \frac{\partial u}{\partial x} + a_{22} \frac{\partial w}{\partial y} \frac{\partial u}{\partial y} \right] dx\, dy$$
$$+ \oint_{\Gamma_e} \beta u w\, ds - \oint_{\Gamma_e} (\beta u_\infty + \hat{q}_n)\, w\, ds \tag{9.5.4}$$

We note that the procedure to obtain the weak form for time-dependent problems is not much different from that used for steady-state problems. The difference is that no integration by parts with respect to time is used (as the integration is only on the spatial domain) and the weight function w is only a function of (x, y).

9.5.1.3 Semidiscrete finite element model

The *semidiscrete* finite element model is obtained from Eq. (9.5.4) by substituting a finite element approximation for the dependent variable, u

[see Eq. (9.2.16a)]. In selecting the approximation for u, once again we assume that the nodal values are time dependent (i.e., separation of time from space):

$$u(x,y,t) \approx u_h(x,y,t) = \sum_{j=1}^{n} u_j^e(t)\psi_j^e(x,y) \tag{9.5.5}$$

where u_j^e denotes the value of $u(x, y, t)$ at the nodal location (x_j^e, y_j^e) in the element at time t. The ith differential equation (in time) of the finite element model is obtained by substituting $w = \psi_i^e(x,y)$ and substituting for u from Eq. (9.5.5) into Eq. (9.5.4):

$$0 = \sum_{j=1}^{n} \left(C_{ij}^e \frac{du_j^e}{dt} + M_{ij}^e \frac{d^2u_j^e}{dt^2} + \left(K_{ij}^e + H_{ij}^e\right) u_j^e \right) - f_i^e - Q_i^e - P_i^e \tag{9.5.6a}$$

or, in matrix form

$$\mathbf{C}^e\dot{\mathbf{u}} + \mathbf{M}^e\ddot{\mathbf{u}}^e + (\mathbf{K}^e + \mathbf{H}^e)\,\mathbf{u}^e = \mathbf{f}^e + \mathbf{Q}^e + \mathbf{P}^e \tag{9.5.6b}$$

where superposed dots on u denote derivatives with respect to time and

$$\begin{aligned}
C_{ij}^e &= \int_{\Omega_e} c_1 \psi_i^e \psi_j^e \, dxdy, \quad M_{ij}^e = \int_{\Omega_e} c\psi_i^e\psi_j^e \, dx\, dy \\
K_{ij}^e &= \int_{\Omega_e} \left(a_{11}\frac{\partial\psi_i^e}{\partial x}\frac{\partial\psi_j^e}{\partial x} + a_{22}\frac{\partial\psi_i^e}{\partial y}\frac{\partial\psi_j^e}{\partial y} \right) dxdy, \quad H_{ij}^e = \oint_{\Gamma_e} \beta\psi_i^e\psi_j^e \, ds \\
f_i^e &= \int_{\Omega_e} f\psi_i^e \, dxdy, \quad Q_i^e = \oint_{\Gamma_e} \hat{q}_n\psi_i^e \, ds, \quad P_i^e = \oint_{\Gamma_e} \beta u_\infty \psi_i^e \, ds
\end{aligned} \tag{9.5.6c}$$

We note that $\hat{q}_n$ now denotes the external flux normal to the element boundary. This completes the semidiscretization step. We now specialize the results to parablic and hyperbolic equations to discuss eigenvalue and transient analysis steps.

9.5.2 Parabolic Equations

Here we consider the semidiscrete model

$$\mathbf{C}^e\dot{\mathbf{u}} + (\mathbf{K}^e + \mathbf{H}^e)\,\mathbf{u}^e = \mathbf{f}^e + \mathbf{Q}^e + \mathbf{P}^e \tag{9.5.7}$$

and discuss the associated eigenvalue problem and fully discretized finite element model for transient analysis. As discussed in Chapter 7, eigenvalues in the case of heat transfer and similar problems are not commonly studied, but we consider them here for the sake of completeness as well as for determining the critical time step required for conditionally stable time approximation schemes. In view of the detailed discussion of the eigenvalue and transient analyses presented in Sections 7.3 and 7.4, it is easy to follow the developments presented here.

9.5.2.1 Eigenvalue analysis

The problem of finding

$$u_j^e(t) = u_{0j}^e\, e^{-\lambda t} \quad [\text{which implies } Q_j^e(t) = Q_{0j}^e\, e^{-\lambda t}] \tag{9.5.8a}$$

such that Eq. (9.5.1) holds for homogeneous boundary conditions (i.e., $\hat{u} = 0, \hat{q}_n = 0$, and $u_\infty = 0$) and $f = 0$ is called an *eigenvalue problem* (see Section 7.3). Here u_{0j}^e denote the nodal values (independent of time and space) which define the mode shape

$$u_0^e(x,y) = \sum_{j=1}^{n} u_{0j}^e \psi_j^e(x,y) \quad \left[\text{or} \quad u(x,y,t) \approx \sum_{j=1}^{n} u_{0j}^e \psi_j^e(x,y)\, e^{-\lambda t}\right] \tag{9.5.8b}$$

Substituting for $u_j^e(t)$ into Eq. (9.5.7), we obtain

$$(-\lambda \mathbf{C}^e + \bar{\mathbf{K}}^e)\mathbf{u}_0^e = \mathbf{Q}_0^e, \quad \bar{\mathbf{K}}^e = \mathbf{K}^e + \mathbf{H}^e \tag{9.5.9}$$

Upon assembly of the element equations, we obtain the global eigenvalue problem

$$(\bar{\mathbf{K}} - \lambda \mathbf{C})\,\mathbf{U} = \mathbf{Q} \tag{9.5.10}$$

After imposition of the homogeneous boundary conditions, the order of the global matrix equations is $N \times N$, where N is the number of nodes at which the nodal values of the primary variable u are not known. A nontrivial solution to Eq. (9.5.10) exists only if the determinant of the coefficient matrix is zero:

$$|\bar{\mathbf{K}}_c - \lambda \mathbf{C}_c| = 0 \tag{9.5.11}$$

where $\bar{\mathbf{K}}_c$ and $\mathbf{C}_c$ are the matrices of the condensed equations for the primary unknowns. Upon expansion, Eq. (9.5.11) results in a Nth-degree

polynomial of λ. The N roots λ_j ($j = 1, 2, \ldots, N$) of this polynomial give the first N eigenvalues of the discretized system (the continuous system, in general, has an infinite number of eigenvalues). There exist standard eigenvalue routines to solve Eq. (9.5.10), which give N eigenvalues and eigenvectors.

Example 9.5.1

Consider the following dimensionless form of the homogeneous model equation (e.g., governing a heat transfer problem):

$$\frac{\partial u}{\partial t} - \left(\frac{\partial^2 u}{\partial x^2} + \frac{\partial^2 u}{\partial y^2}\right) = 0 \tag{1}$$

in a unit square [see Fig. 9.5.1(a)], subjected to the homogeneous boundary conditions

$$\frac{\partial u}{\partial x}(0, y, t) = 0, \quad \frac{\partial u}{\partial y}(x, 0, t) = 0, \quad u(x, 1, t) = 0, \quad u(1, y, t) = 0 \tag{2}$$

and homogeneous initial condition

$$u(x, y, 0) = 0 \tag{3}$$

Determine the eigenvalues using various meshes of triangular and rectangular finite elements.

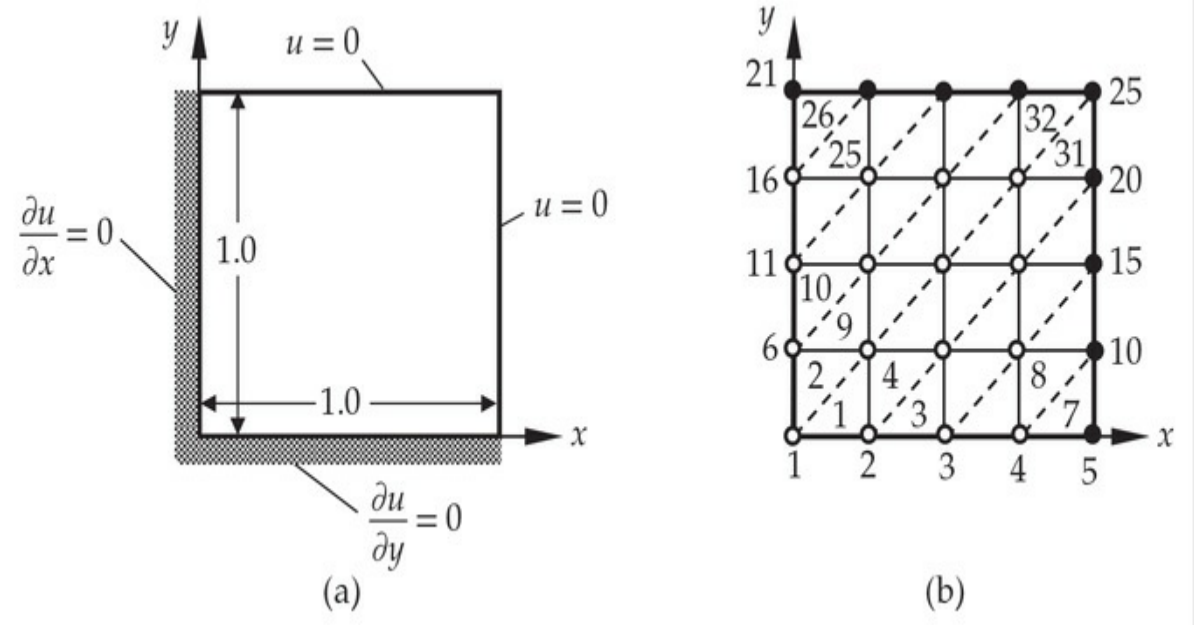

Fig. 9.5.1 (a) Domain, boundary conditions, and (b) a typical 4 × 4 finite element mesh of linear triangles (with broken lines) or linear rectangles (without the broken lines) for the eigenvalue analysis.

Solution: First we note that the problem can be viewed as one posed on a domain of 2 units square with $u = 0$ on all sides. Then by biaxial symmetry, we have the domain shown in Fig. 9.5.1(a).

As a first choice we may choose a 1 × 1 mesh of two triangular elements. Alternatively, for the choice of triangles, we can use the diagonal symmetry and model the domain with one triangular element (exploiting the diagonal symmetry); they are equivalent because in both meshes there is only one unspecified nodal value U_1 at $(x, y) = (0, 0)$. The element matrices for a right-angle triangle (with local node 1 coinciding with global node 1) are [use $a = b = 1.0$ in part (b) of Fig. 9.2.11]:

$$\mathbf{K}^e = \frac{1}{2}\begin{bmatrix} 1 & -1 & 0 \\ -1 & 2 & -1 \\ 0 & -1 & 1 \end{bmatrix}, \quad \mathbf{C}^e = \frac{1}{24}\begin{bmatrix} 2 & 1 & 1 \\ 1 & 2 & 1 \\ 1 & 1 & 2 \end{bmatrix} \tag{4}$$

The eigenvalue problem becomes

$$\left(-\frac{\lambda}{24}\begin{bmatrix} 2 & 1 & 1 \\ 1 & 2 & 1 \\ 1 & 1 & 2 \end{bmatrix} + \frac{1}{2}\begin{bmatrix} 1 & -1 & 0 \\ -1 & 2 & -1 \\ 0 & -1 & 1 \end{bmatrix}\right)\begin{Bmatrix} U_1 \\ U_2 \\ U_3 \end{Bmatrix} = \begin{Bmatrix} 0 \\ 0 \\ 0 \end{Bmatrix} \tag{5}$$

The boundary conditions require $U_2 = U_3 = 0$. Hence, we have

$$\left(-\frac{\lambda}{12} + \frac{1}{2}\right)U_1 = 0 \quad \text{or} \quad \lambda = 6 \tag{6}$$

The eigenfunction (or mode shape) becomes (we can arbitrarily set U_1 to unity)

$$U(x, y) = U_1\psi_1(x, y) = (1 - x) \tag{7}$$

which is defined over the domain below the diagonal line. For the whole domain, by symmetry the mode shape becomes $U(x, y) = (1 - x)(1 - y)$.

For a mesh of one rectangular element with $a = b = 1.0$ in the whole domain, we have

$$\mathbf{K}^e = \frac{1}{6}\begin{bmatrix} 4 & -1 & -2 & -1 \\ -1 & 4 & -1 & 2 \\ -2 & -1 & 4 & -1 \\ -1 & -2 & -1 & 4 \end{bmatrix}, \quad \mathbf{C}^e = \frac{1}{36}\begin{bmatrix} 4 & 2 & 1 & 2 \\ 2 & 4 & 2 & 1 \\ 1 & 2 & 4 & 2 \\ 2 & 1 & 2 & 4 \end{bmatrix} \tag{8}$$

and

$$\left(-\frac{\lambda}{36}\begin{bmatrix} 4 & 2 & 1 & 2 \\ 2 & 4 & 2 & 1 \\ 1 & 2 & 4 & 2 \\ 2 & 1 & 2 & 4 \end{bmatrix} + \frac{1}{6}\begin{bmatrix} 4 & -1 & -2 & -1 \\ -1 & 4 & -1 & 2 \\ -2 & -1 & 4 & -1 \\ -1 & -2 & -1 & 4 \end{bmatrix}\right)\begin{Bmatrix} U_1 \\ U_2 \\ U_3 \\ U_4 \end{Bmatrix} = \begin{Bmatrix} 0 \\ 0 \\ 0 \\ 0 \end{Bmatrix} \tag{9}$$

Using the boundary conditions $U_2 = U_3 = U_4 = 0$, we obtain

$$\left(-\frac{\lambda}{36} \times 4 + \frac{4}{6}\right)U_1 = 0, \quad \text{or } \lambda = 6 \tag{10}$$

The eigenfunction over the quadrant of the domain is given by

$$U(x, y) = U_1\psi_1(x, y) = (1 - x)(1 - y) \tag{11}$$

For this problem, the one-element mesh of triangles in half of the domain gives the same solution as the one-element mesh of rectangular elements in the whole domain.

Table 9.5.1 contains lowest five (including symmetric) eigenvalues obtained with various meshes of triangular and rectangular elements (a typical 4 × 4 mesh of linear elements is shown in Fig. 9.5.1), along with the analytical solution of the problem. Meshes of triangles, being unsymmetric, do not yield exactly the same symmetric eigenvalues (i.e., $\lambda_{mn} \neq \lambda_{nm}$). As the mesh is refined they tend to give almost the same symmetric eigenvalues. It is clear that the convergence of the lower eigenvalues obtained with the finite element method to the analytical value is rapid compared to the convergence of the higher eigenvalues. Also, the minimum eigenvalue converges faster with mesh refinements.

Table 9.5.1 Comparison of finite element solutions for eigenvalues, obtained using various meshes,[1] with the analytical solution.

	Triangles				Rectangles				
	Linear		Quadratic		Linear		Quadratic		
λ_{mn}	4×4	8×8	2×2	4×4	4×4	8×8	2×2	4×4	Exact[2]
λ_{11}	5.068	4.969	4.957	4.936	4.999	4.951	4.937	4.935	4.935
λ_{13}	27.251	25.343	25.984	24.760	27.371	25.331	25.415	24.730	24.674
λ_{31}	28.917	25.735	26.339	24.790	27.371	25.331	25.415	24.730	24.674
λ_{33}	58.216	48.076	53.201	45.097	49.744	45.712	45.892	44.524	44.413
λ_{15}	85.351	69.777	74.793	65.481	84.572	69.255	79.532	65.220	64.152
λ_{51}	86.788	69.825	75.656	65.497	84.572	69.255	79.532	65.220	64.152

[1]The maximum eigenvalues predicted by these meshes are: 386.426, 1619.05, 471.681, 1999.64, 343.256, 1492.56, 397.397, 1825.9, respectively.

[2]The exact eigenvalues are $\lambda_{mn} = \frac{1}{4}\pi^2(m^2 + n^2)$ $(m, n = 1, 3, 5, \ldots)$.

9.5.2.2 Transient analysis

We note that, symbolically, Eq. (9.5.7) is the same as the parabolic equation, Eq. (7.4.25a) discussed in Section 7.4 (with $\mathbf{K}$ replaced with $\bar{\mathbf{K}}$ because of the convective contribution). Whether a problem is one-dimensional, two-dimensional, or three-dimensional, the form of the semidiscrete finite element model is the same. Therefore, the time approximation schemes discussed in Section 7.4 for parabolic equations can be readily applied.

Using the α-family of approximation

$$\mathbf{u}^{s+1} = \mathbf{u}^s + a_2\dot{\mathbf{u}}^s + a_1\dot{\mathbf{u}}^{s+1} \quad \text{for } 0 \le \alpha \le 1 \tag{9.5.12a}$$

$$a_1 = \alpha\,\Delta t, \quad a_2 = (1-\alpha)\Delta t \tag{9.5.12b}$$

we can transform Eq. (9.5.7) into a set of algebraic equations at time t_{s+1}:

$$\hat{\mathbf{K}}\mathbf{u}^{s+1} = \hat{\mathbf{F}}^{s,s+1} \tag{9.5.13a}$$

where

$$\begin{aligned} \hat{\mathbf{K}} &= \mathbf{C} + a_1\bar{\mathbf{K}}, \\ \hat{\mathbf{F}}^{s,s+1} &= \left(\mathbf{C} - a_2\bar{\mathbf{K}}\right)\mathbf{u}^s + \left(a_1\mathbf{F}^{s+1} + a_2\mathbf{F}^s\right) \end{aligned} \tag{9.5.13b}$$

Equation (9.5.13a), after assembly and imposition of boundary conditions,

is solved at each time step for the nodal values u_j^{s+1} at time $t_{s+1} = (s + 1)\Delta t$. At time $t = 0$ (i.e., $s = 0$), $\hat{\mathbf{F}}$ is computed using the initial values $\mathbf{u}^0$ and the known source vectors $\mathbf{f}$ and $\mathbf{P}$, and known flux vector $\mathbf{Q}$.

As stated in Chapter 7, all numerical schemes with $\alpha \geq \frac{1}{2}$ (e.g., backward difference, Crank–Nicolson, and Galerkin schemes) are stable independent of the mesh. Numerical schemes obtained with $\alpha < \frac{1}{2}$ (e.g., the forward difference method) are stable only if the time step satisfies the following (stability) condition:

$$\Delta t < \Delta t_{cr} \equiv \frac{2}{(1 - 2\alpha)\lambda_{\max}}, \quad \alpha < \frac{1}{2} \tag{9.5.14}$$

where $\lambda_{\max}$ is the largest eigenvalue of the eigenvalue problem in Eq. (9.5.10).

Example 9.5.2

Use the finite element method to determine the transient response of the dimensionless transient heat conduction problem described by the equation

$$\frac{\partial \theta}{\partial t} - \left(\frac{\partial^2 \theta}{\partial x^2} + \frac{\partial^2 \theta}{\partial y^2} \right) = 1 \tag{1}$$

subject to the boundary conditions, for $t \geq 0$,

$$\begin{aligned} &\frac{\partial \theta}{\partial x}(0, y, t) = 0, \quad \frac{\partial \theta}{\partial y}(x, 0, t) = 0 \\ &\theta(1, y, t) = 0, \quad \theta(x, 1, t) = 0 \end{aligned} \tag{2}$$

and initial condition

$$\theta(x, y, 0) = 0 \quad \text{for all } (x, y) \text{ in } \Omega \tag{3}$$

Figure 9.5.1(a) with u replaced by θ shows the domain and boundary conditions.

Solution: First we investigate the stability and accuracy of the forward difference scheme ($\alpha = 0.0$) and the accuracy of the Crank–Nicolson method (i.e., $\alpha = 0.5$). Since the Crank–Nicolson method is unconditionally stable, one can choose any value of Δt but its accuracy

will depend on the choice of Δt (i.e., for large values of Δt the solution may not be accurate). The forward difference scheme is conditionally stable [i.e., it is stable if $\Delta t < \Delta t_{cr}$, where Δt_{cr} satisfies the condition in Eq. (9.5.14)]. For example, for one linear triangular element in the diagonally half domain or one linear rectangular element in full domain, we have $\lambda_{max} = 6$. Hence the critical time step is

$$\Delta t_{cr} = \frac{2}{\lambda_{max}} = \frac{2}{6} = 0.333333 \tag{4}$$

If a 4 × 4 mesh of linear triangles is used, we have $\lambda_{max} = 386.426$ (see Table 9.5.1) and the critical time step becomes

$$\Delta t_{cr} = \frac{2}{\lambda_{max}} = \frac{2}{386.426} = 0.00518 \tag{5}$$

whereas for 4 × 4 mesh of linear rectangles the critical time step is $\Delta t_{cr} = 2/343.256 = 0.00583$.

The boundary conditions on the primary variable for the 4 × 4 mesh of linear triangles or linear rectangles in the full domain are

$$U_5 = U_{10} = U_{15} = U_{20} = U_{21} = U_{22} = U_{23} = U_{24} = U_{25} = 0.0 \tag{6}$$

Beginning with the initial conditions $U_i = 0$ ($i = 1, 2, \ldots, 25$), we solve the assembled set of equations associated with Eq. (9.5.13a). All numerical results presented herein are obtained with the 4 × 4 mesh of linear triangles shown in Fig. 9.5.1(b).

The forward difference scheme would be unstable, for example, for $\Delta t > 0.00518$ when 4 × 4 mesh of triangles is used. To illustrate this point, the equations are solved using $\alpha = 0$, $\Delta t = 0.01 > \Delta t_{cr} = 0.00518$ and $\alpha = 0.5$, $\Delta t = 0.01$. The Crank–Nicolson method gives a stable solution, while the forward difference scheme yields an unstable solution (i.e., the solution error grows unboundedly with time), as can be seen from Fig. 9.5.2. For $\Delta t = 0.005$ the forward difference scheme yields a stable solution.

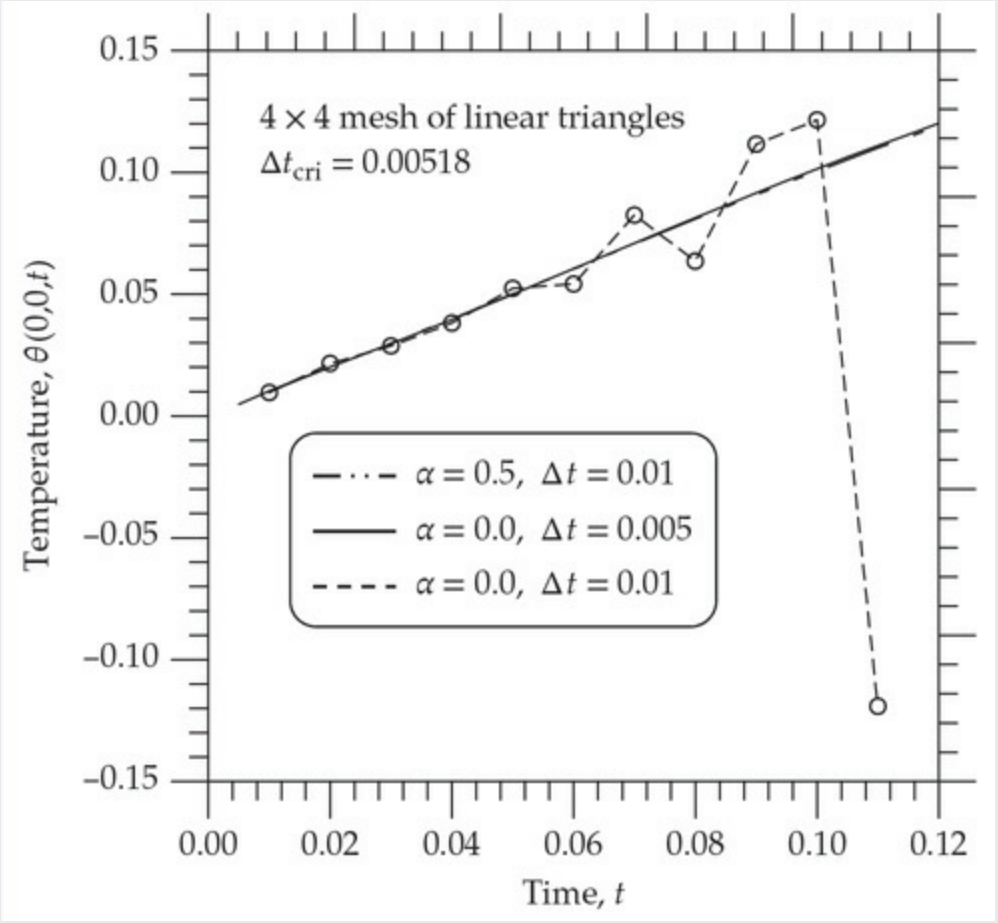

Fig. 9.5.2 Stability of the transient solutions θ(0,0,t) of the heat conduction problem in **Example 9.5.2** analyzed using a 4 × 4 mesh of linear triangles (see Fig. 9.5.1) and the Crank–Nicolson (α = 0.5) and forward difference (α = 0.0) time integration schemes.

The Crank–Nicolson method gives a stable and accurate solution for even $\Delta t = 0.05$. The temperature $\theta(x, 0, t)$ versus x for various values of time are shown in Fig. 9.5.3(a). The steady state is reached at time $t = 1.0$ (a tolerance of $\varepsilon = 10^{-3}$ is used to check the difference between two consecutive time step solutions). The temperature $\theta(0, 0, t)$ versus time, predicted by the Crank–Nicolson method, is shown in Fig. 9.5.3(b), which indicates the evolution of the temperature from zero to the steady state. A comparison of the transient solution at $t = 1.0$ is presented in Table 9.5.2 with the steady-state finite element, the finite difference, and the analytical solutions. Table 9.5.3 contains the finite element solutions for temperature predicted by 4 × 4 meshes of triangles and rectangles and various values of Δt and $\alpha = 0.5$.

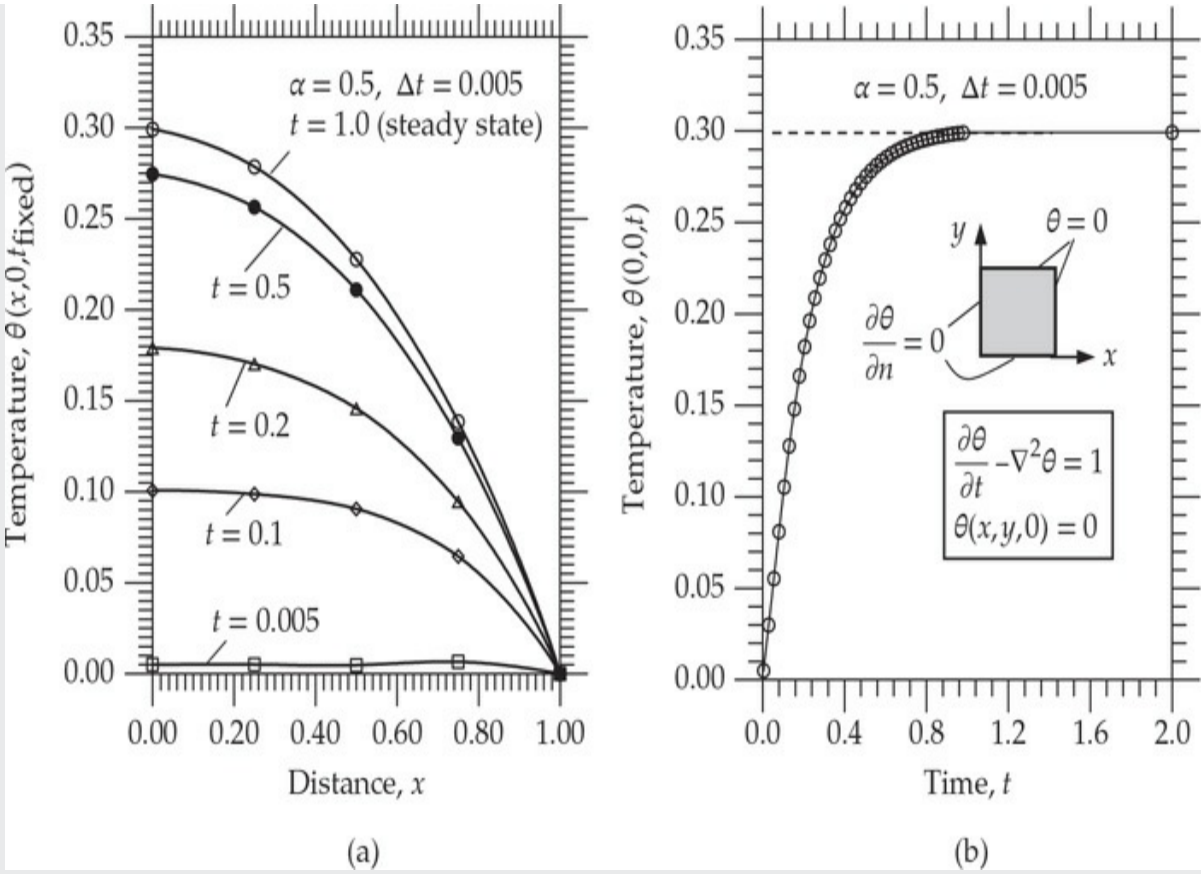

Fig. 9.5.3 (a) Variation of the temperature θ(*x*,0,*t*) as a function of position *x* and time *t* and (b) variation of the temperature θ(0,0,*t*) as a function of time *t* for the transient heat conduction problem of **Example 9.5.2** (4 × 4 mesh of linear triangles).

Table 9.5.2 Comparison of the solutions by the finite difference method (FDM) and finite element method (FEM) with the exact solution of the heat conduction problem.

Node	Exact (steady)	FDM (steady)	Error	FEM (steady)	Error	FEM[1] at $t = 1.0$
1	0.2947	0.2911	0.0036	0.3013	−0.0066	0.2993
2	0.2789	0.2755	0.0034	0.2805	−0.0016	0.2786
3	0.2293	0.2266	0.0027	0.2292	0.0001	0.2278
4	0.1397	0.1381	0.0016	0.1392	0.0005	0.1385
5	0.0000	0.0000	0.0000	0.0000	0.0000	0.0000
7	0.2642	0.2609	0.0033	0.2645	−0.0003	0.2628
8	0.2178	0.2151	0.0027	0.2172	0.0006	0.2159
9	0.1333	0.1317	0.0016	0.1327	0.0006	0.1320
10	0.0000	0.0000	0.0000	0.0000	0.0000	0.0000
13	0.1811	0.1787	0.0024	0.1801	0.0010	0.1791
14	0.1127	0.1110	0.0017	0.1117	0.0010	0.1111
15	0.0000	0.0000	0.0000	0.0000	0.0000	0.0000
19	0.0728	0.0711	0.0017	0.0715	0.0013	0.0712
20	0.0000	0.0000	0.0000	0.0000	0.0000	0.0000
25	0.0000	0.0000	0.0000	0.0000	0.0000	0.0000

[1]Obtained with the Crank–Nicolson scheme with 4×4 mesh of linear triangles and $\Delta t = 0.005$.

Table 9.5.3 Comparison of transient solutions obtained using meshes of triangular and rectangular elements.

Time	Element[1]	Temperature along the line $y = 0$: $\theta(x, 0, t) \times 10$			
t		$x = 0.0$	$x = 0.25$	$x = 0.5$	$x = 0.75$
0.1	T1	0.9758	0.9610	0.9063	0.7104
	R1	0.9684	0.9556	0.8956	0.6887
	T2	0.9928	0.9798	0.9168	0.6415
	R2	0.9841	0.9718	0.9020	0.6323
0.2	T1	1.8003	1.7238	1.4891	0.9321
	R1	1.7723	1.7216	1.4829	0.9367
	T2	1.7979	1.7060	1.4644	0.9462
	R2	1.7681	1.6990	1.4626	0.9469
0.3	T1	2.3130	2.1671	1.7961	1.1466
	R1	2.2747	2.1650	1.8084	1.1499
	T2	2.2829	2.1448	1.7943	1.1249
	R2	2.2479	2.1432	1.8018	1.1319
1.0	T1	2.9960	2.7871	2.2804	1.3843
	R1	2.9648	2.8053	2.3090	1.4059
	T2	2.9925	2.7862	2.2776	1.3849
	R2	2.9621	2.8037	2.3065	1.4053

[1]T1, triangular element mesh with $\Delta t = 0.1$; T2, triangular element mesh with $\Delta t = 0.05$; R1, rectangular element mesh with $\Delta t = 0.1$; R2, rectangular element mesh with $\Delta t = 0.05$. In all cases, $\alpha = 0.5$ and 4×4 mesh of linear elements are used.

9.5.3 Hyperbolic Equations

Here we consider the semidiscrete model

$$\mathbf{M}^e\ddot{\mathbf{u}}^e + \mathbf{K}^e\mathbf{u}^e = \mathbf{f}^e + \mathbf{Q}^e \tag{9.5.15}$$

and discuss the associated eigenvalue problem and fully discretized finite element model for transient analysis. Equations of the type (9.5.15) arise in structural dynamics, where $\mathbf{M}^e$ is the mass matrix and $\mathbf{K}^e$ is the stiffness matrix (convective contributions $\mathbf{H}^e$ and $\mathbf{P}^e$ are omitted here without the loss of generality). An example is provided by the equation governing transverse motion of a membrane, where u denotes the transverse deflection and f is the transversely distributed force. Equation (9.5.15) is classified mathematically as a hyperbolic equation.

9.5.3.1 Eigenvalue analysis

Hyperbolic problems are more typical structural dynamics, where eigenvalue problem associated with Eq. (9.5.15) corresponds to finding natural frequencies of the structure (for homogeneous boundary conditions and $f = 0$). For natural vibration, we assume periodic motion of the form

$$u_j^e(t) = u_{0j}^e e^{-i\omega t}, \quad Q_j^e(t) = Q_{0j}^e e^{-i\omega t} \tag{9.5.16a}$$

and the mode shape is

$$u_0^e(x,y) = \sum_{j=1}^{n} u_{0j}^e \psi_j^e(x,y) \tag{9.5.16b}$$

Substituting Eq. (9.5.16a) into Eq. (9.5.15), we obtain

$$(-\omega^2 \mathbf{M}^e + \mathbf{K}^e)\mathbf{u}_0^e = \mathbf{Q}_0^e \tag{9.5.17}$$

Upon assembly of the element equations, we obtain the global eigenvalue problem

$$(\mathbf{K} - \lambda \mathbf{M})\,\mathbf{U} = \mathbf{Q}, \quad \lambda = \omega^2 \tag{9.5.18}$$

The eigenvalues $\lambda = \omega^2$ and eigenfunctions $\sum_j^n u_{0j}^e \psi_j^e(x,y)$ are determined from the assembled equations associated with Eq. (9.5.18), after imposing the homogeneous boundary conditions. For a membrane problem, ω denotes the frequency of natural vibration. The number of eigenvalues of the discrete system in Eq. (9.5.18) of the problem is equal to the number of unspecified nodal values of U in the mesh.

Example 9.5.3

Consider a homogeneous-material rectangular membrane of dimensions a by b (in ft) (see Fig. 9.5.4), material density ρ (in slugs/ft^2), and fixed on all its edges (i.e., $u = 0$ on Γ). Determine the natural frequencies using finite element meshes of triangles and rectangles.

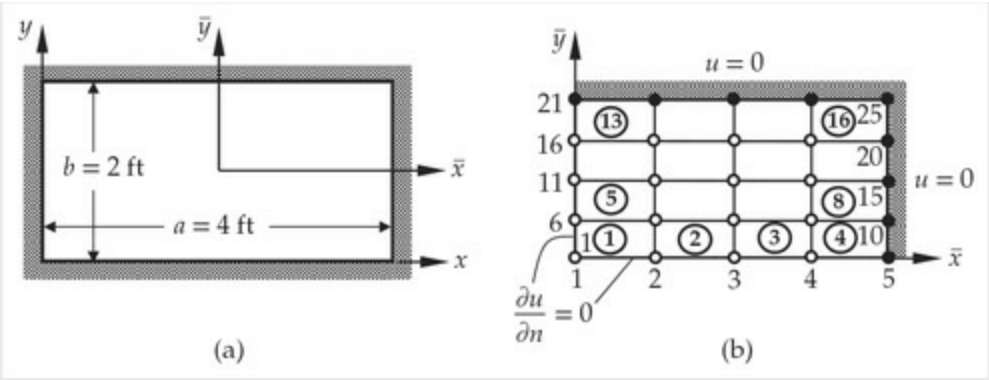

Fig. 9.5.4 Analysis of a rectangular membrane: (a) actual geometry; (b) quadrant domain with finite element mesh of rectangular elements and boundary conditions (a mesh of triangles is obtained by joining local nodes 1 and 3 of the rectangular elements).

Solution: Although the problem has biaxial symmetry [see Fig. 9.5.4(a)], use of any symmetry in the finite element analysis will eliminate the unsymmetric modes of vibration of the membrane. For example, if we consider a quadrant of the domain [see Fig. 9.5.4(b)] in the finite element analysis, the frequencies ω_{mn} ($m, n \neq 1, 3, 5, \ldots$) and associated eigenfunctions will be missed in the results [i.e., we can only obtain ω_{mn}, ($m, n = 1, 3, 5, \ldots$)]. By considering the full domain, the first N frequencies allowed by the mesh can be computed, where N is the number of unspecified nodal displacements in the mesh. To obtain all frequencies, the full domain is modeled.

If only the first eigenvalue ω_{11} is of interest or only symmetric frequencies are required, one can use a quadrant of the domain in the analysis. Indeed, results of **Example 9.5.1** are applicable here, with $\lambda_{mn} = \omega_{mn}^2$. The results presented in Table 9.5.1 can be interpreted as the squares of the symmetric natural frequencies of a square $a = b = 2$ membrane with $\rho = 1$ and $a_{11} = a_{22} \equiv T = 1$. The exact natural frequencies of a rectangular membrane of dimension a by b, with tensions $a_{11} = a_{22} = T$ and density ρ are

$$\omega_{mn} = \pi \sqrt{\frac{T}{\rho}} \sqrt{\frac{m^2}{a^2} + \frac{n^2}{b^2}} \quad (m, n = 1, 2, \ldots) \tag{1}$$

Table 9.5.4 contains the first nine frequencies of a rectangular membrane ($a = 4$ ft, $b = 2$ ft, $T = 12.5$ lb/ft, and $\rho = 2.5$ slugs/ft^2), as computed using various meshes of linear and quadratic triangular and

rectangular elements in the *total* domain. The convergence of the finite element results to the analytical solution is clear. The meshes of linear rectangular elements yield more accurate results compared with meshes of linear triangular elements. The mode shapes corresponding to the lowest four frequencies obtained with a 4 × 4 mesh of nine-node quadratic elements are shown in Fig. 9.5.5.

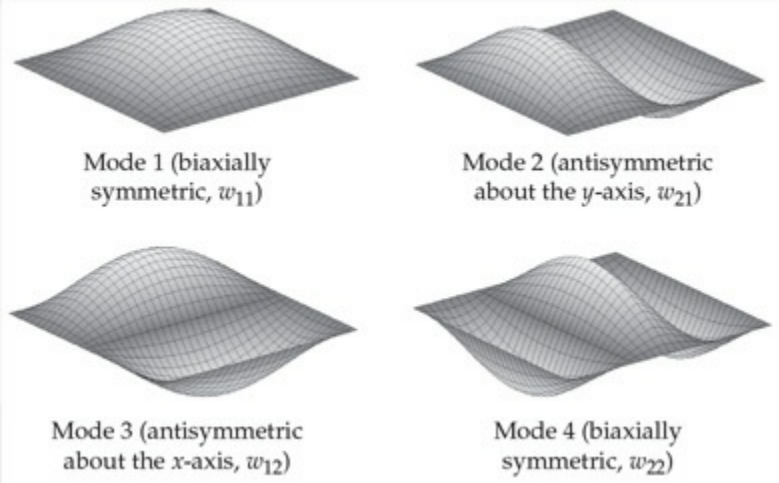

Fig. 9.5.5 Mode shapes corresponding to the lowest four natural frequencies.

Table 9.5.4 Comparison of natural frequencies computed using various meshes of linear (L) and quadratic (Q) triangular and rectangular elements with the exact solution.

	Triangles			Rectangles			
ω_{mn}	4 × 4L	8 × 8L	4 × 4Q	4 × 4L	8 × 8L	4 × 4Q	Exact
ω_{11}	4.2266	4.0025	3.9335	4.0285	3.9523	3.9280	3.9270
ω_{21}	5.9083	5.2068	5.0089	5.2899	5.0477	4.9773	4.9673
ω_{31}	9.2391	6.8788	6.4953	7.2522	6.6020	6.4052	6.3321
ω_{12}	9.3577	7.5271	7.2945	7.9527	7.4201	7.2667	7.2410
ω_{22}	10.0619	8.4565	8.0130	9.6603	8.0571	7.8835	7.8540
ω_{41}	12.1021	8.8856	8.1560	9.9805	8.5145	7.8958	7.8540
ω_{32}	13.2012	9.9280	9.2022	12.7158	9.1117	8.8545	8.7810
ω_{51}	14.6943	11.1191	10.5405	13.1699	10.5799	9.9859	9.4574
ω_{42}	15.8118	11.4426	10.8757	14.0733	10.7279	10.8543	9.9346

9.5.3.2 Transient analysis

The hyperbolic equation (9.5.15) can be reduced to a system of algebraic equations using the (α, γ)-family of approximation (see Section 7.4.5):

$$\mathbf{u}^{s+1} \approx \mathbf{u}^s + \Delta t\, \dot{\mathbf{u}}^s + \frac{1}{2}(\Delta t)^2 \left[(1-\gamma)\ddot{\mathbf{u}}^s + \gamma \ddot{\mathbf{u}}^{s+1}\right] \tag{9.5.19}$$

$$\dot{\mathbf{u}}^{s+1} \approx \dot{\mathbf{u}}^s + a_2 \ddot{\mathbf{u}}^s + a_1 \ddot{\mathbf{u}}^{s+1} \tag{9.5.20}$$

where α and γ are parameters that determine the stability and accuracy of the scheme [see Eq. (7.4.43)], and $a_1 = \alpha\Delta t$ and $a_2 = (1 - \alpha)\Delta t$. As derived in Section 7.4.5, we obtain the following fully discretized equations:

$$\hat{\mathbf{K}}\mathbf{u}^{s+1} = \hat{\mathbf{F}}^{s,s+1} \tag{9.5.21a}$$

where

$$\hat{\mathbf{K}} = \mathbf{K} + a_3\mathbf{M}, \quad \hat{\mathbf{F}}^{s,s+1} = \mathbf{F}^{s+1} + \mathbf{M}\bar{\mathbf{u}}^s \tag{9.5.21b}$$

$$\bar{\mathbf{u}}^s = a_3\mathbf{u}^s + a_4\dot{\mathbf{u}}^s + a_5\ddot{\mathbf{u}}^s, \tag{9.5.21c}$$

$$a_3 = \frac{2}{\gamma(\Delta t)^2}, \quad a_4 = a_3\Delta t, \quad a_5 = \frac{1}{\gamma} - 1$$

The two special cases of the (α, γ)-family of approximation are (1) constant-average acceleration method (α = γ = 1/2), which is known as the Newmark scheme, and (2) linear acceleration method (α = 1/2 and γ = 1/3). The fully discretized equations based on the central difference scheme are [see Eq. (7.4.42) with **C** = 0]

$$\frac{1}{(\Delta t)^2}\mathbf{M}\mathbf{u}^{s+1} = \mathbf{F}^s + \left(\frac{2}{(\Delta t)^2}\mathbf{M} - \mathbf{K}\right)\mathbf{u}^s - \frac{1}{(\Delta t)^2}\mathbf{M}\mathbf{u}^{s-1} \tag{9.5.22}$$

The stability characteristics of various schemes are as follows:

- $\alpha = \frac{1}{2}, \gamma = \frac{1}{2}$, the constant-average acceleration method (stable)
- $\alpha = \frac{1}{2}, \gamma = \frac{1}{3}$, the linear acceleration method (conditionally stable)
- the central difference method (conditionally stable)

In general, all schemes in which γ ≥ α ≥ 1/2 are stable. For $\alpha \geq \frac{1}{2}$ and γ < α,

and for the central difference scheme, the stability requirement is

$$\Delta t \le \Delta t_{cr} = \left[\frac{1}{2}\omega_{\max}^2(\alpha - \gamma)\right]^{-1/2} \tag{9.5.23}$$

where $\omega_{\max}^2 = \lambda_{\max}$ is the maximum eigenvalue of the undamped system in Eq. (9.5.18). We note that a more refined mesh will yield a higher maximum eigenvalue and hence a smaller Δt_{cr}.

As discussed in Section 7.4.5, the (α, γ)-family as well as the central difference schemes are not self-starting (implicit schemes). Equations (7.4.45) and (7.4.47) provide ways to compute $\ddot{\mathbf{u}}^0$ (for Newmark's scheme) and $\mathbf{u}^{(-1)}$ (for the central difference scheme) and they are summarized here for ready reference:

$$\ddot{\mathbf{u}}^0 = \mathbf{M}^{-1}\left(\mathbf{F}_0 - \mathbf{K}\mathbf{u}^0\right) \tag{9.5.24a}$$

$$\mathbf{u}^{(-1)} = \mathbf{u}^0 - \Delta t\,\dot{\mathbf{u}}^0 + \frac{(\Delta t)^2}{2}\ddot{\mathbf{u}}^0 \tag{9.5.24b}$$

Once $\mathbf{u}^{s+1}$ is known from the fully discretized equations (9.5.21a), the velocity vector $\dot{\mathbf{u}}_{s+1}$ and acceleration vector $\ddot{\mathbf{u}}_{s+1}$ are computed using the equations

$$\ddot{\mathbf{u}}^{s+1} = a_3\left(\mathbf{u}^{s+1} - \mathbf{u}^s\right) - a_4\dot{\mathbf{u}}^s - a_5\ddot{\mathbf{u}}^s \tag{9.5.25a}$$

$$\dot{\mathbf{u}}^{s+1} = \dot{\mathbf{u}}^s + a_2\ddot{\mathbf{u}}^s + a_1\ddot{\mathbf{u}}^{s+1} \tag{9.5.25b}$$

where a_1 through a_5 are defined in Eq. (9.5.21c).

Example 9.5.4

Consider a homogeneous rectangular membrane of sides a = 4 ft and b = 2 ft fixed on all its four edges (see **Example 9.5.3**). Assume that the tension in the membrane is 12.5 lb/ft (i.e., $a_{11} = a_{22} = 12.5$) and the density is $\rho = c = 2.5$ slugs/ft^2. The initial deflection of the membrane is assumed to be

$$u_0(x, y) = 0.1(4x - x^2)(2y - y^2) \tag{1}$$

and the initial velocity is $v_0 = 0$. Determine the deflection $u(x, y, t)$ of the membrane as a function of time using the finite element method. The analytical solution of this problem is (see Kreyszig [6], p. 684)

$$u(x,y,t) = \frac{409.6}{\pi^6} \sum_{m,n=1,3,\ldots} \frac{1}{m^3 n^3} \cos\ \omega_{mn} t\ \sin \frac{m\pi x}{4} \sin \frac{n\pi y}{2} \tag{2a}$$

$$\omega_{mn} = \frac{\pi}{4}\sqrt{5(m^2 + 4n^2)} \tag{2b}$$

where the origin of the (x, y) coordinate system is located at the lower corner of the domain [see Fig. 9.5.4(a)].

Solution: In the finite element analysis, we can utilize the biaxial symmetry of the problem and model one quadrant of the domain [see Fig. 9.5.4(b)]. We set up a new coordinate system $(\bar{x}, \bar{y})$ for the computational domain. The initial displacement in the new coordinates is given by Eq. (1) with x and y replaced in terms of $\bar{x}$ and $\bar{y}$: $x = \bar{x} + 2, \quad y = \bar{y} + 1$. The initial values of u are calculated using Eq. (9.5.24a) with $\mathbf{F}_0 = 0$ and $\mathbf{u}_0$ as given in (1) by $u_0\,(x, y)$. At $\bar{x} = 2$ and $\bar{y} = 1$ all nodal values of u and its time derivatives are zero.

As for the critical time step, we calculate λ_{max} from the solution of Eq. (9.5.18) using the same mesh as that is used for the transient analysis and then use Eq. (9.5.23) to compute Δt_{cr}. Of course, for $\alpha = \frac{1}{2}$ and $\gamma = \frac{1}{2}$, there is no restriction on the time step because the scheme is stable. For a 4×4 mesh of linear rectangular elements in a quadrant, the maximum eigenvalue is found to be $\lambda_{max} = 1072.68$, which yields $\Delta t_{cr} = 0.1058$ for the linear acceleration scheme $\left(\alpha = 0.5, \gamma = \frac{1}{3}\right)$.

Stability characteristics of the solutions computed using the constant-average acceleration ($\alpha = 0.5$, $\gamma = 0.5$) and linear acceleration $\left(\alpha = 0.5, \gamma = \frac{1}{3}\right)$ schemes for $\Delta t = 0.125 > \Delta t_{cr}$ are shown in Fig. 9.5.6. Plots of the center deflection $u(0, 0, t)$ versus time t are shown in Fig. 9.5.7. The finite element solutions are in good agreement with the analytical solution (2a) and (2b).

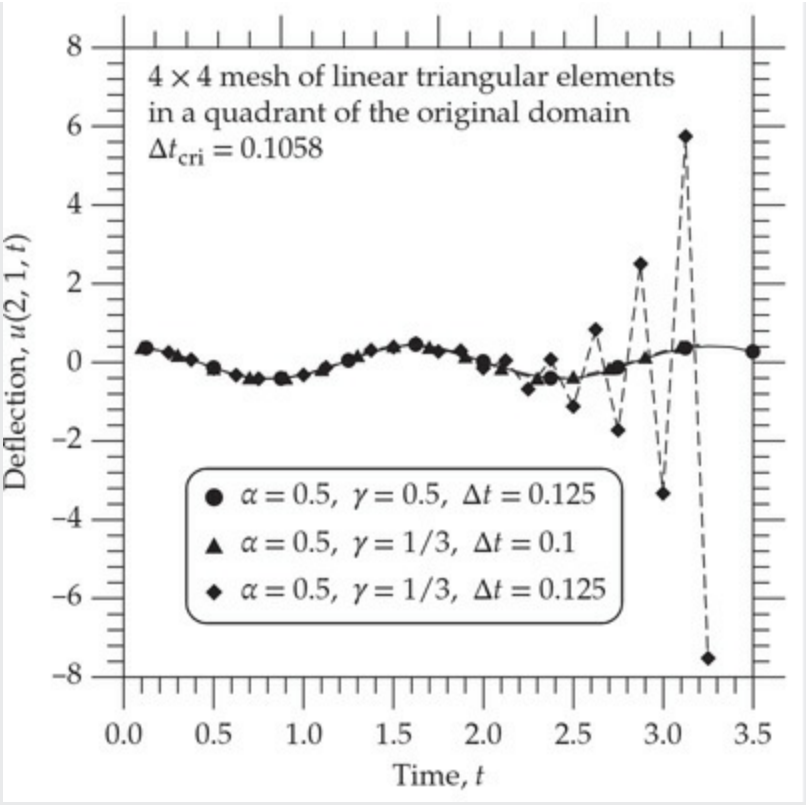

Fig. 9.5.6 Stability characteristics of the constant-average acceleration and linear acceleration schemes (a 4 × 4 mesh of linear rectangular elements is used in a quadrant of the domain).

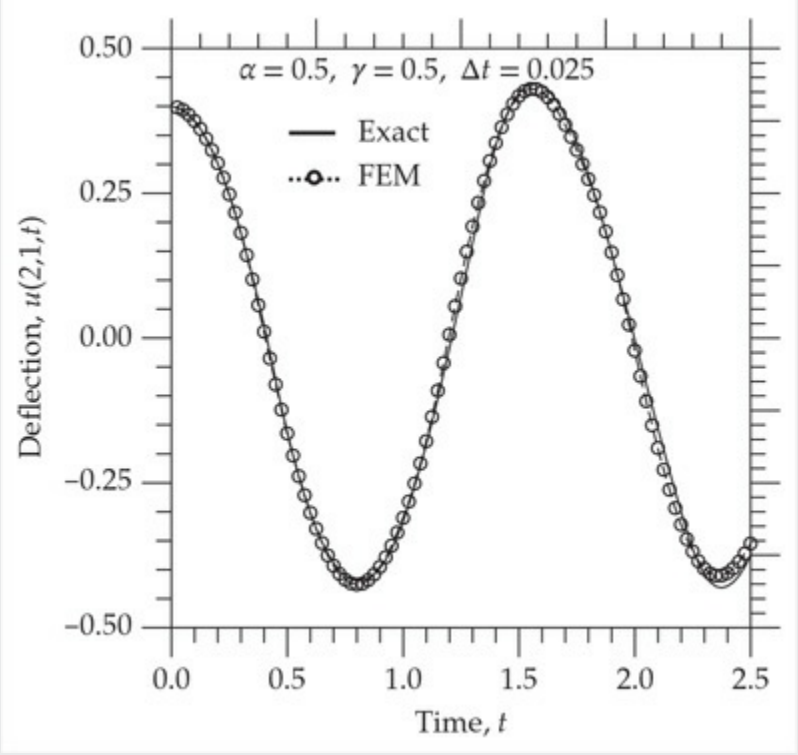

Fig. 9.5.7 Comparison of the center deflection obtained using various

meshes with the analytical solution of a rectangular membrane with initial deflection.

We close this section with a comment that there are many other approximation schemes that can be used to convert parabolic and hyperbolic equations of the type in Eqs. (9.5.7) and (9.5.15), respectively, to algebraic equations. A more complete discussion on this topic can be found in the book by Surana and Reddy [7]. As discussed in Chapter 7, explicit formulations can be developed using lumping of mass and damping matrices [e.g., Eq. (9.5.22) can be made explicit.].

9.6 Summary

In this chapter a step-by-step procedure for finite element formulation of a model second-order differential equation in two dimensions with a single dependent variable is presented. The steps include weak formulation of the equation, finite element model development, derivation of the interpolation functions for linear triangular and rectangular elements, evaluation of element matrices and vectors, assembly of element equations, solution of equations, and post-computation of the gradient of the solution. A number of illustrative problems of heat transfer (conduction and convection), fluid mechanics, and solid mechanics are discussed. Finally, finite element models of time-dependent problems are discussed and eigenvalue and fully discretized finite element models of parabolic and hyperbolic problems are also discussed and several examples are presented. This chapter is the heart of the book and paves the way for the development of finite element models of plane elasticity and flows of viscous fluids in the coming chapters.

Problems

Note: Most problems require some formulative effort (sketching a mesh when it is not given, calculations of element matrices and source vectors in some cases, assembling equations, identifying the boundary conditions in terms of the nodal variables, writing condensed equations, and so on). In some cases, complete solution is required. When the problem size is large,

essential steps of setting up the problem are required. Many of these problems can be solved using **FEM2D**, which is discussed in Chapter 10.

GENERAL FIELD PROBLEMS

In **Problems 9.1–9.4**, use the appropriate number of integration points, and verify the results with those obtained by the exact integration.

9.1 For a linear triangular element, show that

$$\sum_{i=1}^{3} \alpha_i^e = 2A_e, \quad \sum_{i=1}^{3} \beta_i^e = 0, \quad \sum_{i=1}^{3} \gamma_i^e = 0 \tag{1}$$

$$\alpha_i^e + \beta_i^e \hat{x}^e + \gamma_i^e \hat{y}^e = \frac{2}{3} A_e \quad \text{for any } i \tag{2}$$

where

$$\hat{x}^e = \frac{1}{3} \sum_{i=1}^{3} x_i^e, \quad \hat{y}^e = \frac{1}{3} \sum_{i=1}^{3} y_i^e \tag{3}$$

and (x_i^e, y_i^e) are the coordinates of the ith node of the element (i = 1, 2, 3).

9.2 Consider the partial differential equation over a typical element Ω_e with boundary Γ_e

$$-\nabla^2 u + cu = 0 \quad \text{in } \Omega_e, \qquad \text{with} \quad \frac{\partial u}{\partial n} + \beta u = q_n \quad \text{on } \Gamma_e$$

Develop the weak-form and finite element model of the equation over an element Ωe.

9.3 Assuming that c and β are constant in **Problem 9.2**, write the element coefficient matrix and source vector for a linear (a) rectangular element and (b) triangular element.

9.4 Calculate the linear interpolation functions for the linear (a) triangular and (b) rectangular elements shown in Fig. P9.4. *Answer:* (a) $\psi_1 = (12.25 - 2.5x - 1.5y)/9.25$.

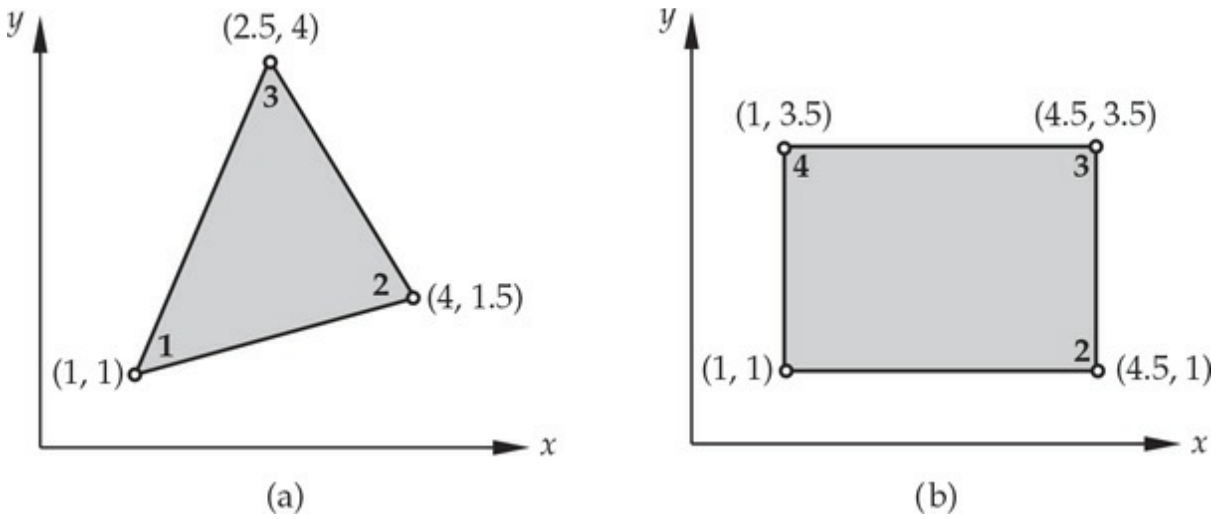

Fig. P9.4

9.5 The nodal values of a triangular element in the finite element analysis of a field problem, $-\nabla^2 u = f_0$ are

$$u_1 = 389.79, \quad u_2 = 337.19, \quad u_3 = 395.08$$

The interpolation functions of the element are given by

$$\psi_1 = \frac{1}{9.25}(12.25 - 2.5x - 1.5y), \; \psi_2 = \frac{1}{9.25}(-1.5 + 3x - 1.5y)$$

$$\psi_3 = \frac{1}{9.25}(-2.5 - 0.5x + 3y)$$

(a) Find the component of the flux in the direction of the vector $4\hat{\mathbf{e}}_x + 3\hat{\mathbf{e}}_y$ at $x = 3$ and $y = 2$.

(b) A point source of magnitude Q_0 is located at point $(x_0, y_0) = (3,2)$ inside the triangular element. Determine the contribution of the point source to the element source vector. Express your answer in terms of Q_0.

9.6 The nodal values of an element in the finite-element analysis of a field problem $-\nabla^2 u = f_0$ are $u_1 = 389.79$, $u_2 = 337.19$, and $u_3 = 395.08$ (see Fig. P9.6). (a) Find the gradient of the solution, and (b) determine where the 392 isoline intersects the boundary of the element in Fig. P9.6. *Answer:* $\nabla u_h = 10.58\hat{\mathbf{e}}_x - 105.2\hat{\mathbf{e}}_y$.

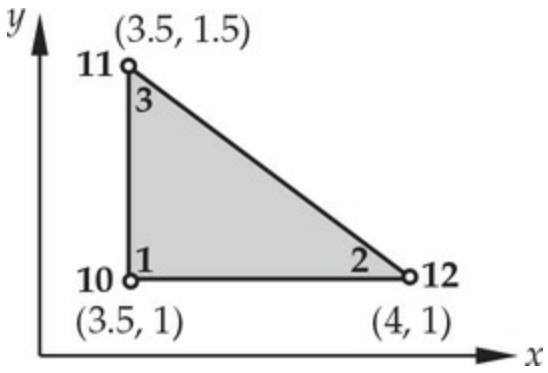

Fig. P9.6

9.7 If the nodal values of the elements shown in Fig. P9.7 are $u_1 = 0.2645$, $u_2 = 0.2172$, $u_3 = 0.1800$ for the triangular element and $u_1 = 0.2173$, $u_3 = 0.1870$, $u_2 = u_4 = 0.2232$ for the rectangular element, compute u, $\partial u/\partial x$, and $\partial u/\partial y$ at the point $(x, y) = (0.375, 0.375)$.

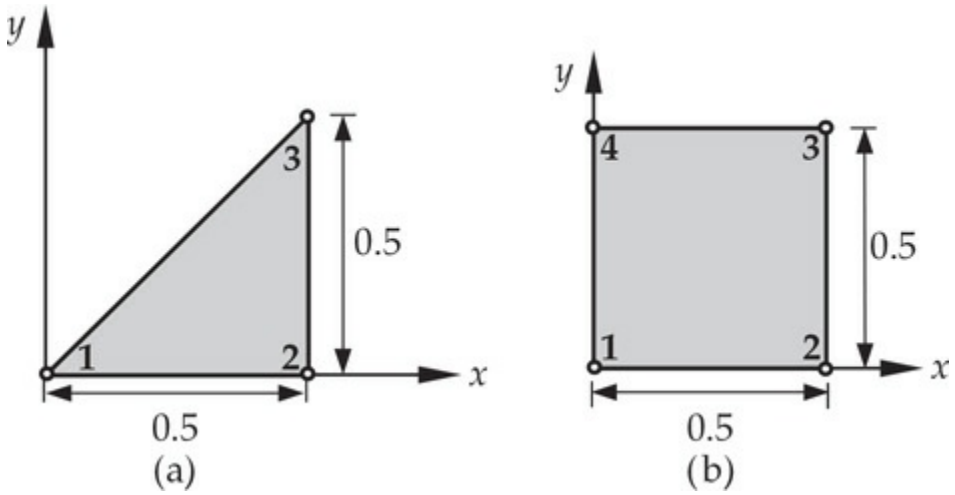

Fig. P9.7

9.8 Compute the contribution of the pump 2 discharge to the nodes of element 43 in the groundwater flow problem of **Example 9.4.5**.

9.9 Find the coefficient matrix associated with the Laplace operator when the rectangular element in Fig. P9.9(a) is divided into two triangles by joining node 1 to node 3 [see Fig. P9.9(b)]. Compare the resulting matrix with that of the rectangular element in Eq. (9.2.54).

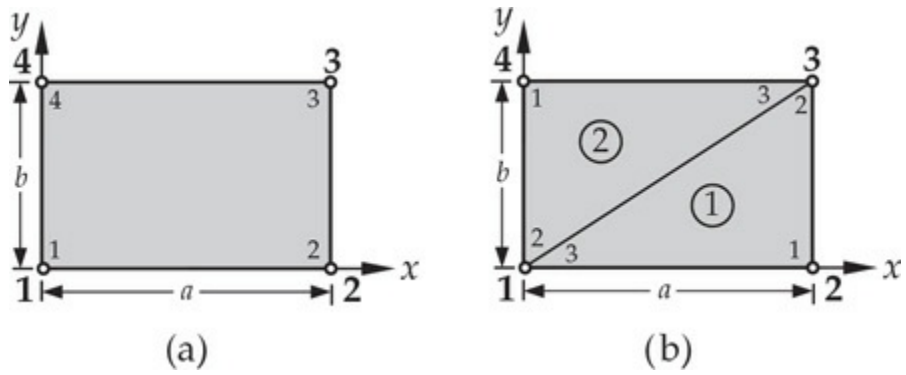

Fig. P9.9

9.10 Evaluate the following element matrices exactly:

$$S_{ij}^{01} = \int_0^a \int_0^b \psi_i \frac{d\psi_j}{dx}\, dxdy, \quad S_{ij}^{02} = \int_0^a \int_0^b \psi_i \frac{d\psi_j}{dy}\, dxdy$$

where $\psi_i\,(x, y)$ are the linear interpolation functions of a rectangular element with sides a and b.

9.11 Give the assembled coefficient matrix **K** and column vector **F** for the finite element meshes shown in Figs. P9.11(a) and P9.11(b). Assume single degree of freedom per node, and let $\mathbf{K}^e$ and $\mathbf{F}^e$ denote the element coefficients for the eth element. Your answer should be in terms of element coefficients K_{ij}^e and F_i^e.

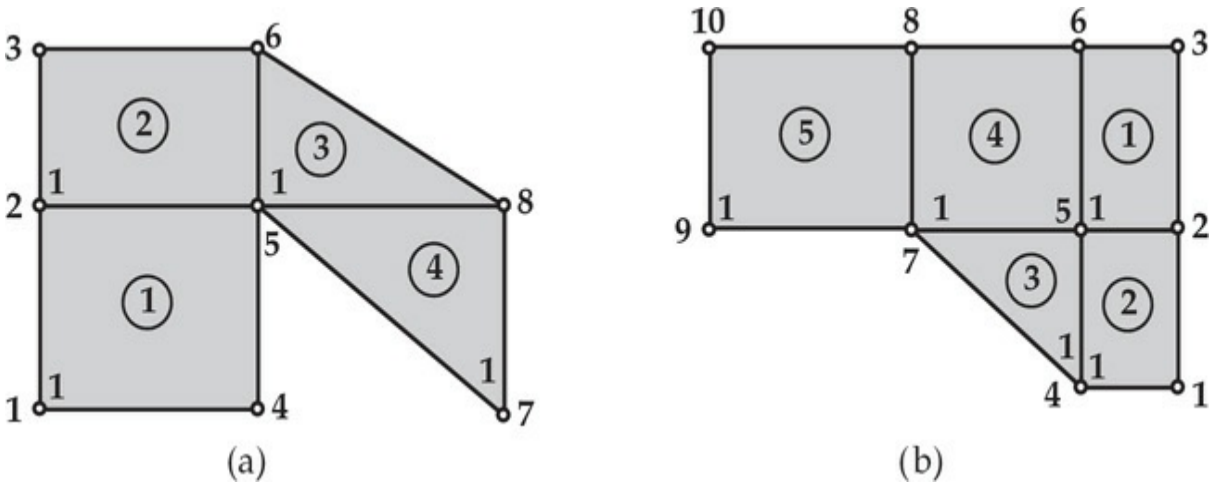

Fig. P9.11

9.12 Repeat **Problem 9.11** for the mesh shown in Fig. P9.12.

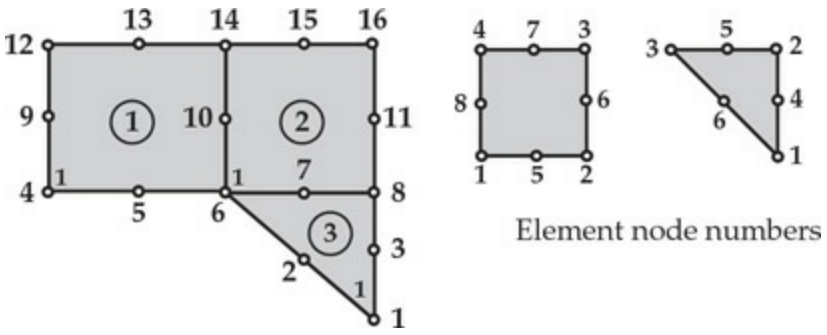

Fig. P9.12

9.13 Compute the global source vector corresponding to the nonzero specified boundary flux for the finite element mesh of linear elements shown in Fig. P9.13.

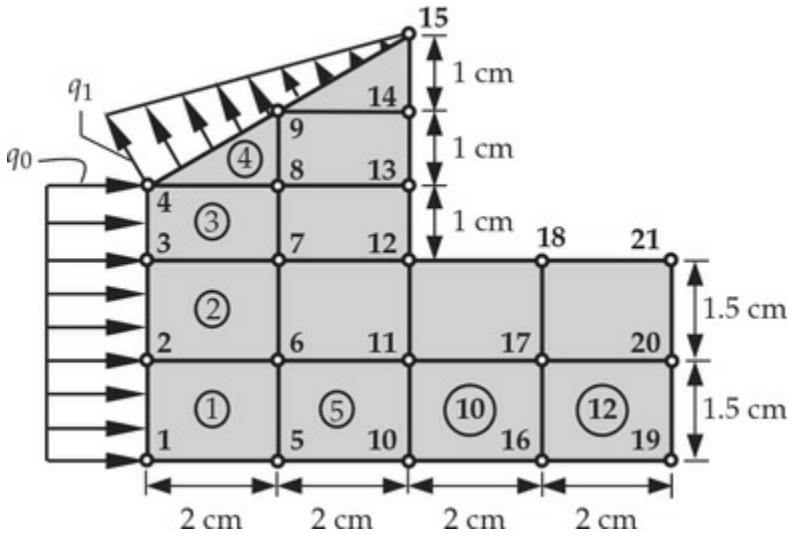

Fig. P9.13

9.14 Repeat **Problem 9.13** for the finite element mesh of quadratic elements shown in Fig. P9.14.

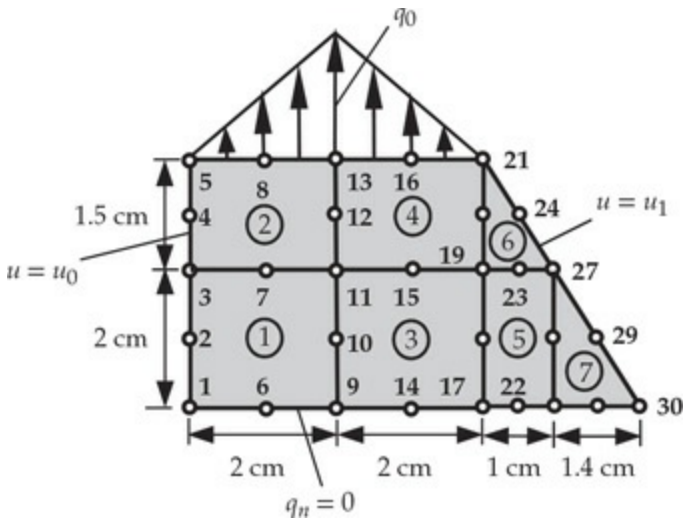

Fig. P9.14

9.15 A line source of intensity q_0 is located across the triangular element shown in Fig. P9.15. Compute the element source vector.

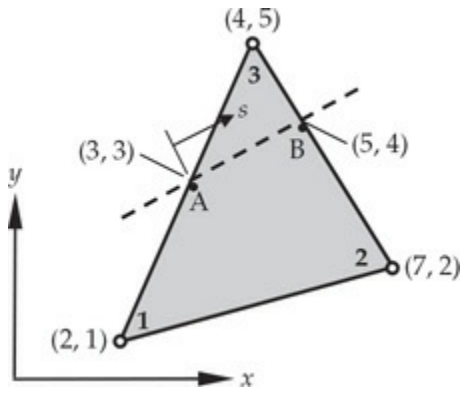

Fig. P9.15

9.16 Repeat **Problem 9.15** when the line source is $q(s) = q_0\, s/L$, where L is the distance between points A and B and s is the coordinate along the line connecting point A to point B.

9.17 Consider the following partial differential equation governing the variable u:

$$c\frac{\partial u}{\partial t} - \frac{\partial}{\partial x}\left(a\frac{\partial u}{\partial x}\right) - \frac{\partial}{\partial y}\left(b\frac{\partial u}{\partial y}\right) - f_0 = 0 \tag{1}$$

where c, a, b, and f_0 are constants. Assume approximation of the form

$$u_h(x, y, t) = (1 - x)yu_1(t) + x(1 - y)u_2(t) \tag{2}$$

where u_1 and u_2 are nodal values of u at time t.

(a) Develop the fully discretized finite element model of the equation.

(b) Evaluate the element coefficient matrices and source vector for a square element of dimension 1 unit by 1 unit (so that the evaluation of the integrals is made easy).

Note: You should not be concerned with this nonconventional approximation of the dependent unknown but just use it as given to answer the question.

9.18 Solve the Laplace equation

$$-\left(\frac{\partial^2 u}{\partial x^2}+\frac{\partial^2 u}{\partial y^2}\right)=0 \quad \text{in } \Omega \tag{1}$$

on a rectangle, when $u(0, y) = u(a, y) = u(x, 0) = 0$ and $u(x, b) = u_0(x)$. Use the symmetry and (a) a mesh of 2 × 2 triangular elements and (b) a mesh of 2 × 2 rectangular elements (see Fig. P9.18). Compare the finite element solution with the exact solution

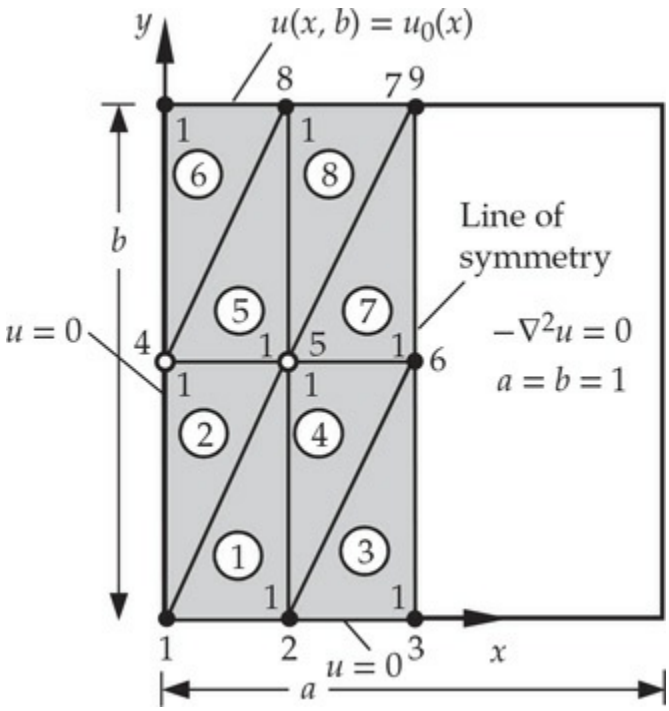

Fig. P9.18

$$u(x,y)=\sum_{n=1}^{\infty} A_n \sin\frac{n\pi x}{a}\sinh\frac{n\pi y}{b} \tag{2}$$

where

$$A_n = \frac{2}{a \sinh(n\pi b/a)} \int_0^a u_0(x) \sin \frac{n\pi x}{a}\, dx \tag{3}$$

Take $a = b = 1$, and $u_0(x) = \sin \pi x$ in the computations. For this case, the exact solution becomes

$$u(x, y) = \frac{\sin \pi x \sinh \pi y}{\sinh \pi} \tag{4}$$

Answer: For a 2 × 2 mesh of triangles, $U_4 = 0.23025$ and $U_5 = 0.16281$; for a 2 × 2 mesh of rectangles, $U_4 = 0.1520$ and $U_5 = 0.1075$.

9.19 Solve **Problem 9.18** when $u_0(x) = 1$. The analytical solution is given by

$$u(x, y) = \frac{4}{\pi} \sum_{n=0}^{\infty} \frac{\sin(2n+1)\pi x \sinh(2n+1)\pi y}{(2n+1)\sinh(2n+1)\pi}$$

Answer: (a) $U_5 = 0.2059$ and $U_6 = 0.2647$. (b) $U_5 = 0.26821$ and $U_6 = 0.33775$.

9.20 Solve **Problem 9.18** when $u_0(x) = 4(x - x^2)$. *Answer:* (a) $U_5 = 0.1691$ and $U_6 = 0.2353$; (b) $U_5 = 0.1068$ and $U_6 = 0.1623$

9.21 Solve the Laplace equation for the unit square domain and boundary conditions given in Fig. P9.21. Use one rectangular element.

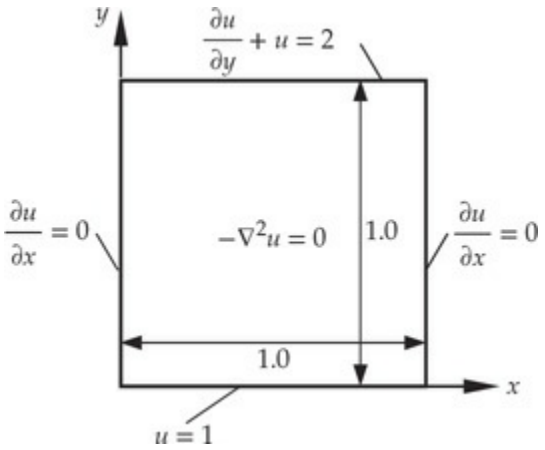

Fig. P9.21

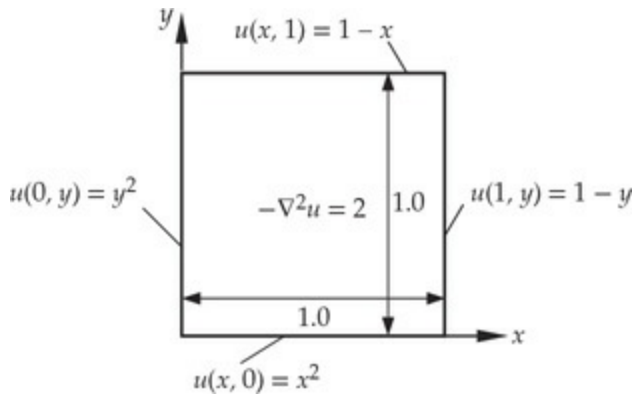

Fig. P9.22

9.22 Consider the Poisson equation (governs heat transfer and other phenomena) in a square region shown in Fig. P9.22:

$$-\frac{\partial}{\partial x}\left(k\frac{\partial u}{\partial x}\right)-\frac{\partial}{\partial y}\left(k\frac{\partial u}{\partial y}\right)=f_0 \tag{1}$$

The boundary conditions for the problem are shown in Fig. P9.22. Assuming $k = 1$ and $f_0 = 2$, determine the unknown nodal value of u using the uniform 2×2 mesh of linear rectangular elements. *Answer:* $U_5 = 0.625$.

9.23 Use two triangular elements to solve the problem in Fig. P9.21. Use the mesh obtained by joining points (1,0) and (0,1).

9.24 Solve **Problem 9.22** using the mesh of a linear rectangle and two linear triangles, as shown in Fig. P9.24. *Answer:* $U_5 = 0.675$.

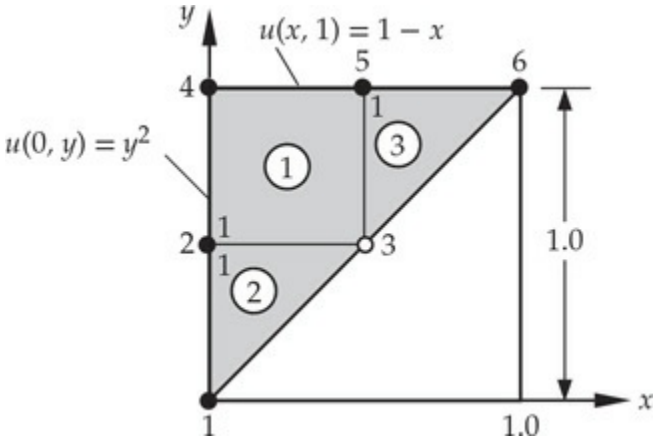

Fig. P9.24

9.25 Solve the Poisson equation $-\nabla^2 u = 2$ in Ω with $u = 0$ on Γ_1 and $-u/-n = 0$ on Γ_2, where Ω is the first quadrant bounded by the parabola

$y = 1 - x^2$ and the coordinate axes (see Fig. P9.25), and Γ_1 and Γ_2 are the boundaries shown in Fig. P9.25.

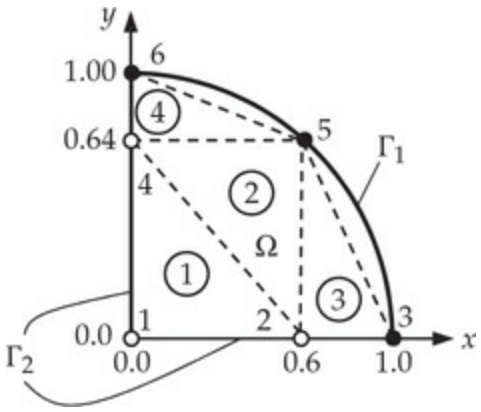

Fig. P9.25

HEAT TRANSFER PROBLEMS

9.26 Solve the axisymmetric field problem shown in Fig. P9.26 for the mesh shown there. Note that the problem has symmetry about any z = constant line. Hence, the problem is essentially onedimensional. You are only required to determine the element matrix and source vector for element 1 and give the known boundary conditions on the primary and secondary variables.

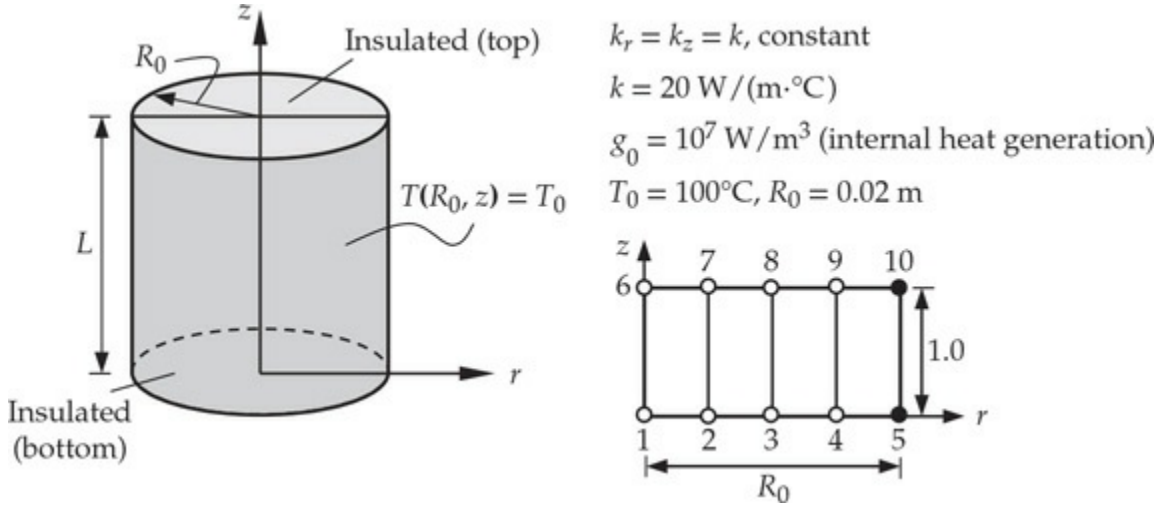

Fig. P9.26

9.27 Formulate the axisymmetric field problem shown in Fig. P9.27 for the mesh shown. You are only required to give the known boundary conditions on the primary and secondary variables and algebraic

expressions for the secondary variable at $r = R_0/2$ using equilibrium and the definition.

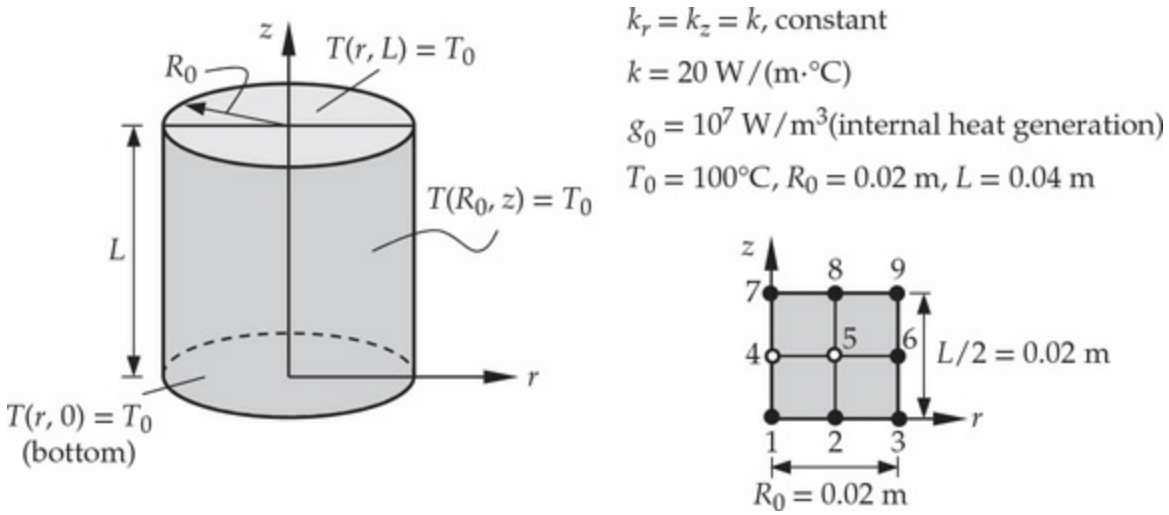

Fig. P9.27

9.28 A series of heating cables have been placed in a conducting medium, as shown in Fig. P9.28. The medium has conductivities of kx = 10 W/(cm·^{0} C) and k_y = 15 W/(cm·^{0} C), the upper surface is exposed to a temperature of -5°C [β = 5 W/(cm^2·K)], and the lower surface is bounded by an insulating medium. Assume that each cable is a point source of 250 W/em. Use a 8 × 8 mesh of linear rectangular (or triangular) elements in the

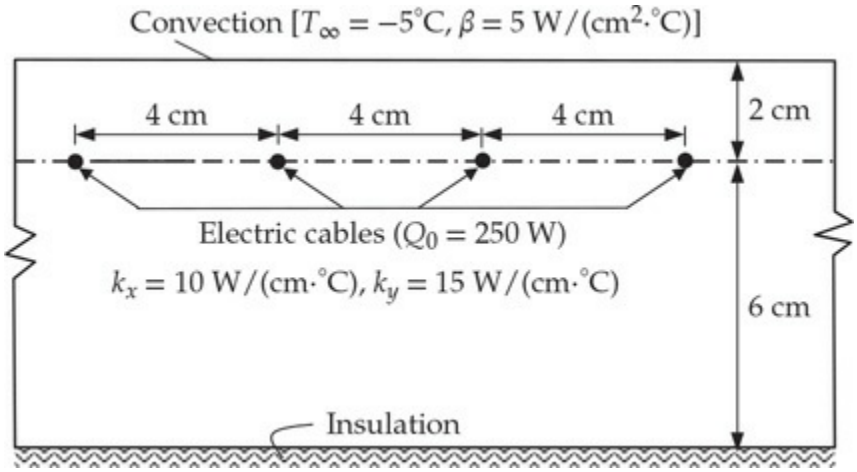

Fig. P9.28

computational domain (exploit the symmetry available in the problem), and formulate the problem (i.e., give element matrices for a typical element, give boundary conditions on primary and

secondary variables, and compute convection boundary contributions).

9.29 Formulate the finite element analysis information to determine the temperature distribution in the molded asbestos insulation shown in Fig. P9.29. Use the symmetry to identify a computational domain and give the specified boundary conditions at the nodes of the mesh. What is the connectivity of matrix for the mesh shown?

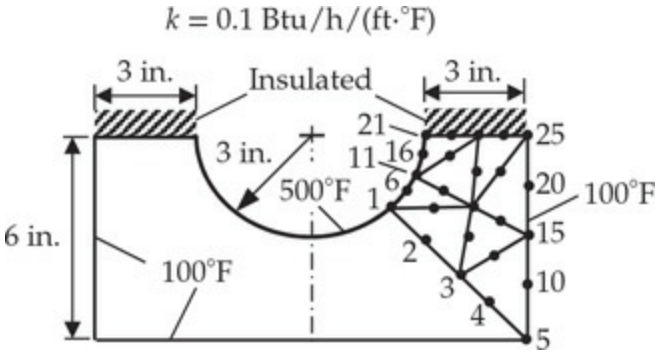

Fig. P9.29

9.30 Consider steady-state heat conduction in a square region of side $2a$. Assume that the medium has conductivity of k W/(m°C) and uniform heat (energy) generation of g_0 W/m^3. For the boundary conditions and mesh shown in Fig. P9.30, write the finite element algebraic equations for nodes 1, 3, and 7.

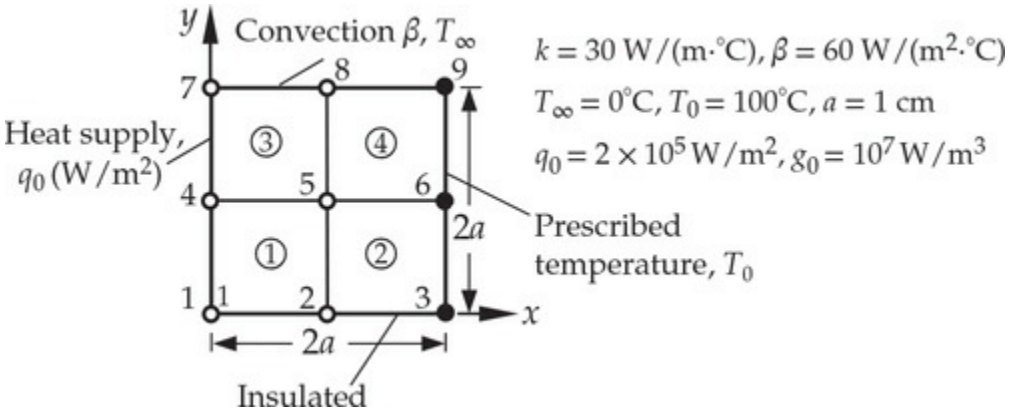

Fig. P9.30

9.31 For the convection heat transfer problem shown in Fig. P9.31, write the four finite element equations for the unknown temperatures. Assume that the thermal conductivity of the material is k = 5 W/(m °C), the convection heat transfer coefficient on the left surface is β = 28 W/(m^2 °C), and the internal heat generation is zero. Compute

the heats at nodes 2, 4 and 9 using (a) equilibrium and (b) definition.

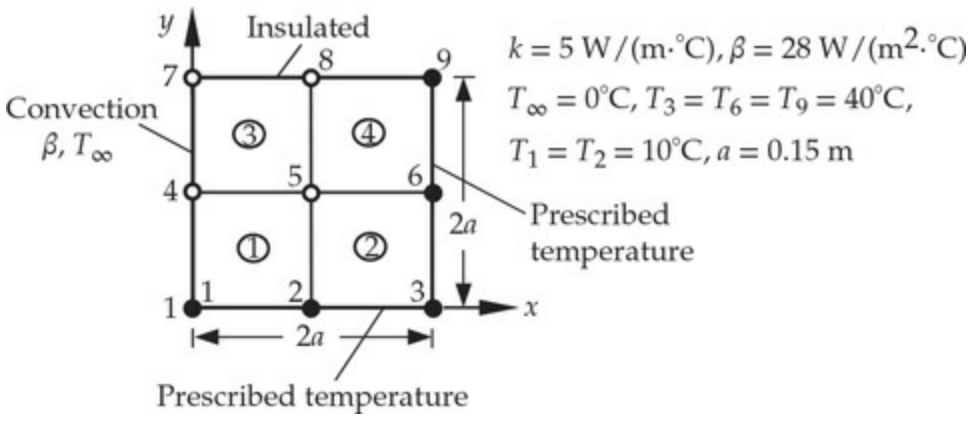

Fig. P9.31

9.32 Write the finite element equations for the unknown temperatures of the problem shown in Fig. P9.32.

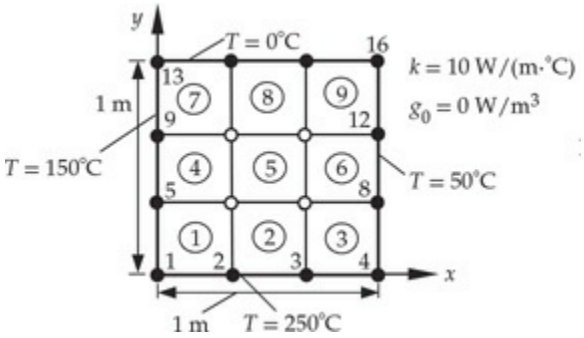

Fig. P9.32

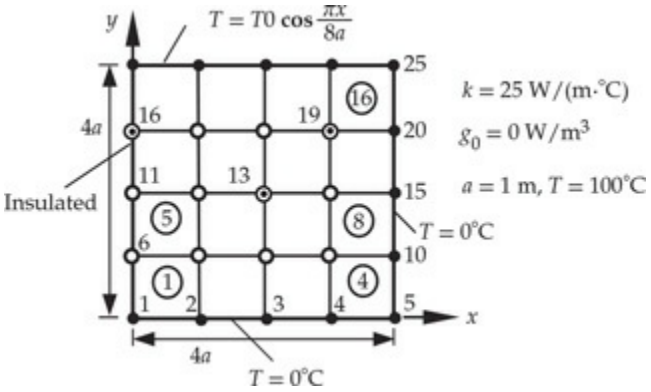

Fig. P9.33

9.33 Write the finite element equations associated with nodes 13, 16, and 19 for the problem shown in Fig. P9.33.

9.34 Write the finite element equations for the heats at nodes 1 and 13 of **Problem 9.32**. The answer should be in terms of the nodal temperatures T_1, T_2,..., T_{16}.

9.35 The fin shown in Fig. P9.35 has its base maintained at 300'C and exposed to convection on its remaining boundary. Write the finite element equations at nodes 7 and 10.

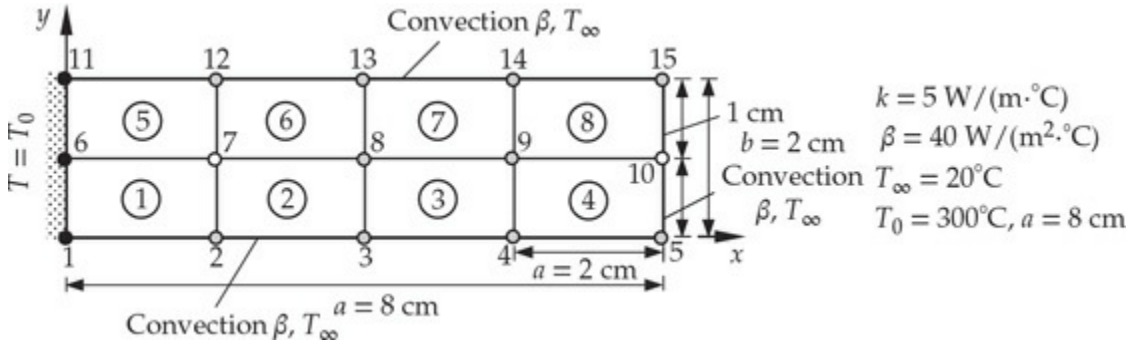

Fig. P9.35

9.36 Compute the heat loss at nodes 10 and 13 of **Problem 9.35**.

FLOW PROBLEMS

9.37 Consider the problem of the flow of groundwater beneath a coffer dam (see Fig. P9.37). For the velocity potential formulation, give the boundary conditions.

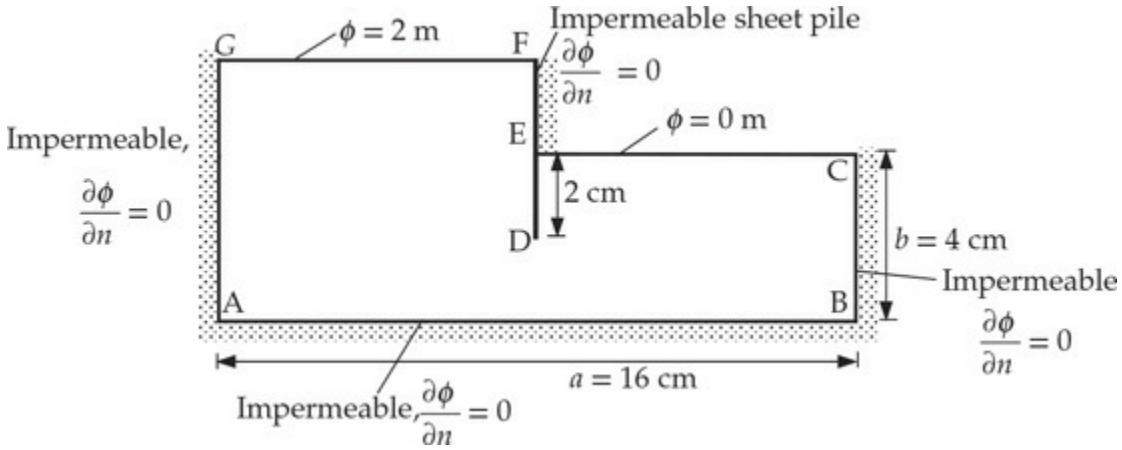

Fig. P9.37

9.38 For the groundwater flow problem of the domain shown in Fig. P9.38, give the boundary conditions and input data for finite element a nalysis. The pump is located at (x,y) = (550, 400) m.

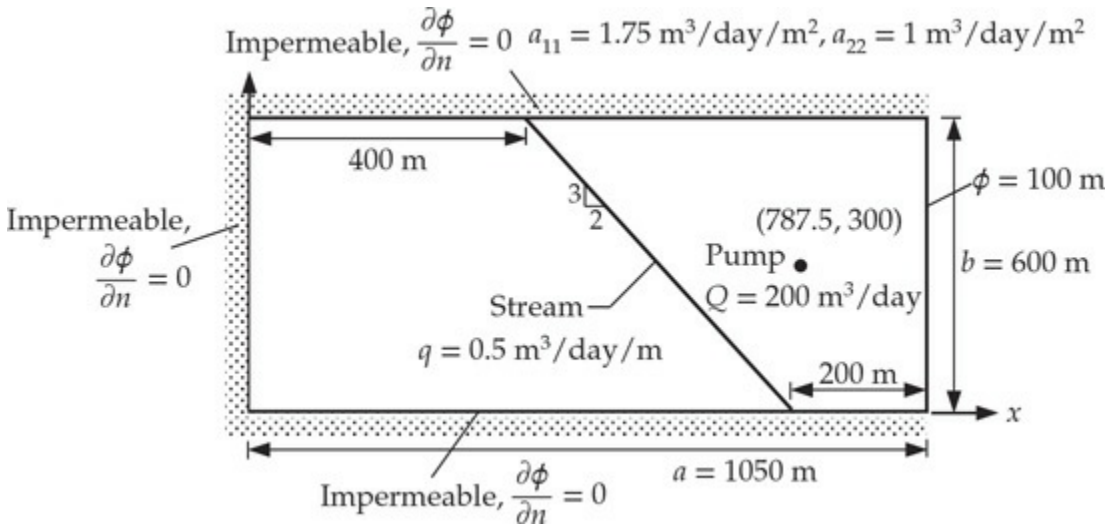

Fig. P9.38

9.39 Repeat **Problem 9.38** for the domain shown in Fig. P9.39.

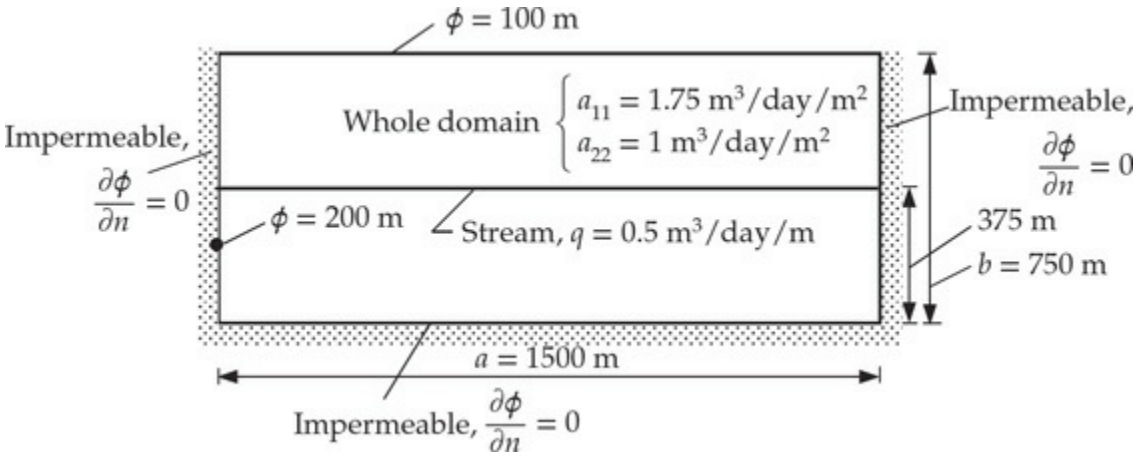

Fig. P9.39

9.40 Consider the steady confined flow through the foundation soil of a dam (see Fig. P9.40). Assuming that the soil is isotropic ($k_x = k_y$), formulate the problem for finite element

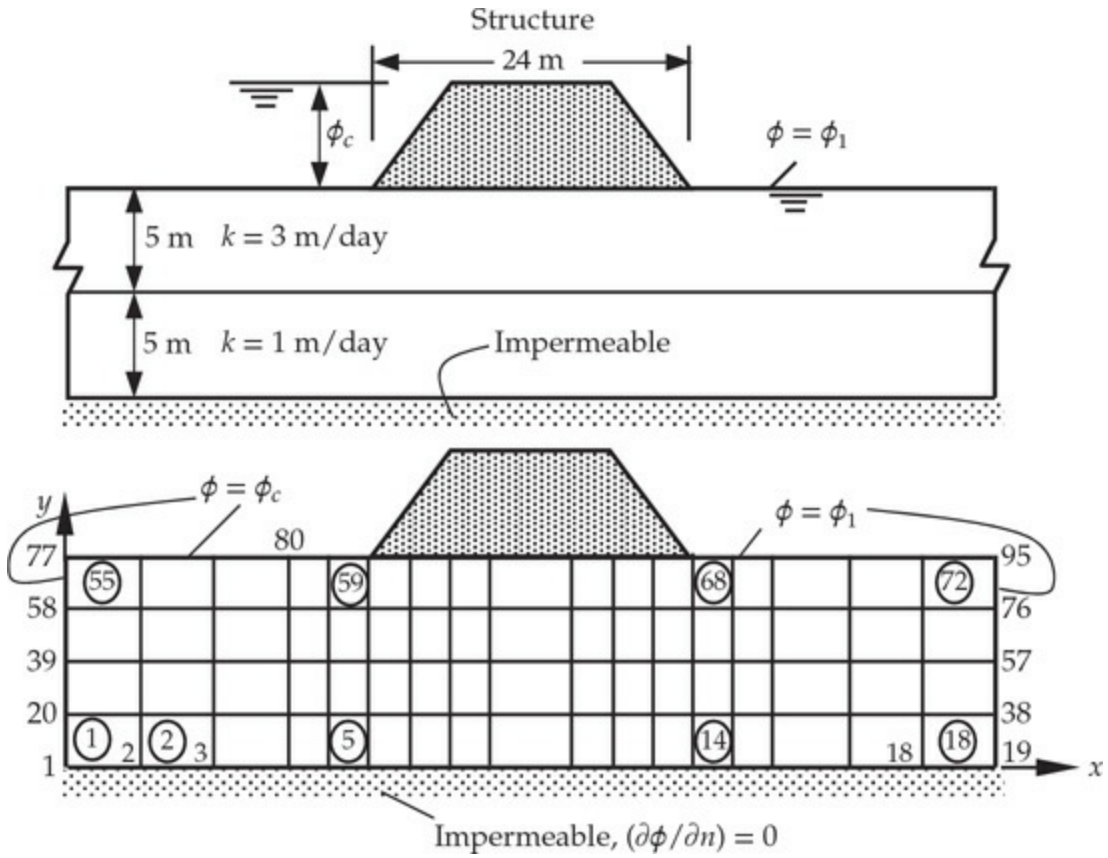

Fig. P9.40

analysis (i.e., identify the specified primary and secondary variables and their contribution to the nodes). In addition, write the finite element equations at nodes 8 and 11. Write the finite element equations for the horizontal velocity component in 5th and 10th elements.

9.41 Formulate the problem of the flow about an elliptical cylinder using the (a) stream function and (b) velocity potential. The geometry and boundary conditions are shown in Fig. P9.41.

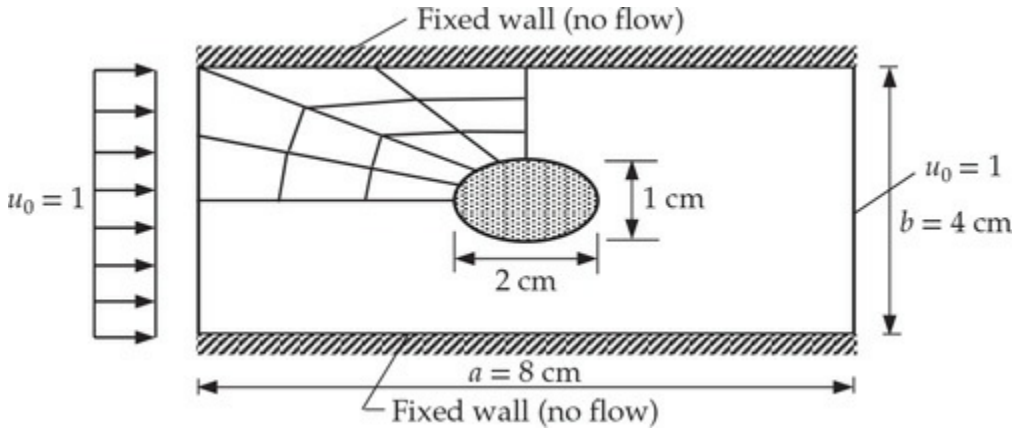

Fig. P9.41

9.42 Repeat **Problem 9.41** for the domain shown in Fig. P9.42.

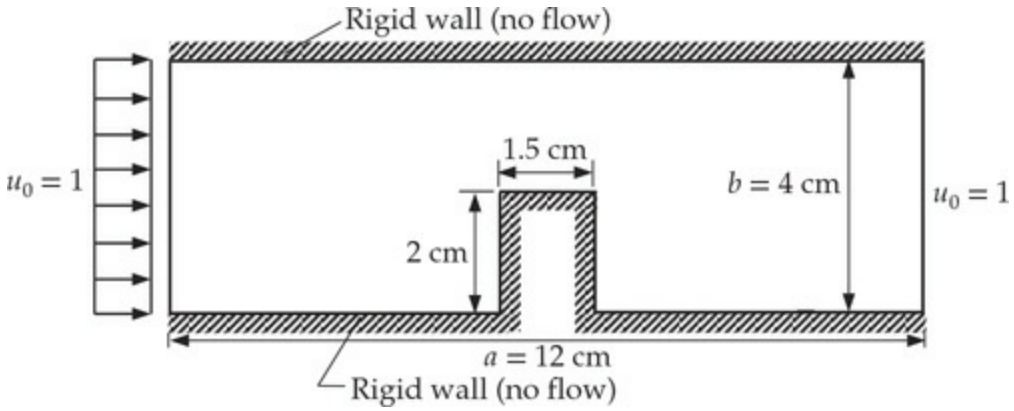

Fig. P9.42

SOLID MECHANICS PROBLEMS

9.43 The Prandtl theory of torsion of a cylindrical member leads to

$$-\nabla^2 u = 2G\theta \text{ in } \Omega;\ u = 0 \text{ on } \Gamma$$

where Ω is the cross section of the cylindrical member being twisted, Γ is the boundary of Ω, G is the shear modulus of the material of the member, θ is the angle of twist, and u is the stress function. Solve the equation for the case in which Ω is a circular section (see Fig. P9.43) using the mesh of linear triangular elements. Compare the finite-element solution with the exact solution (valid for elliptical sections with axes a and b):

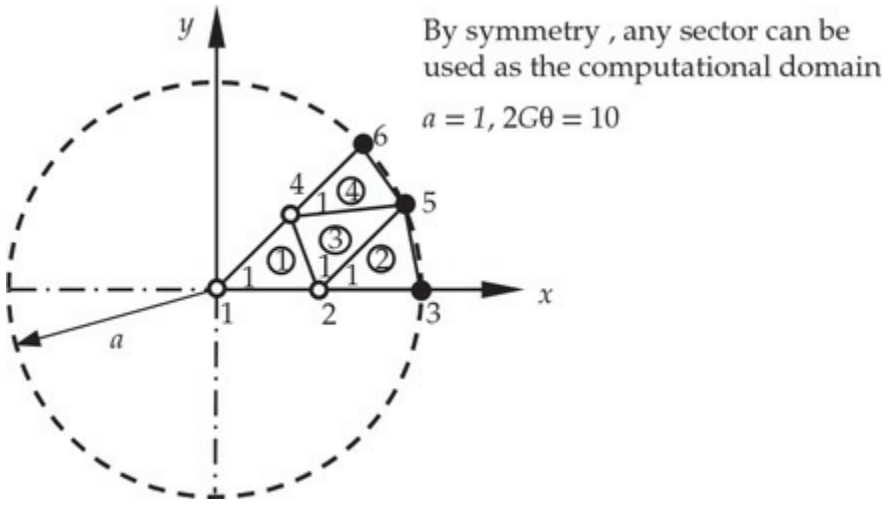

Fig. P9.43

$$u = \frac{G\theta a^2 b^2}{a^2 + b^2}\left(1 - \frac{x^2}{a^2} - \frac{y^2}{b^2}\right)$$

Use $a = 1$, $b = 1$, and $f_0 = 2G\theta = 10$.

9.44 Repeat **Problem 9.43** for an elliptical section member (see Fig. P9.44). Use $a = 1$ and $b = 1.5$.

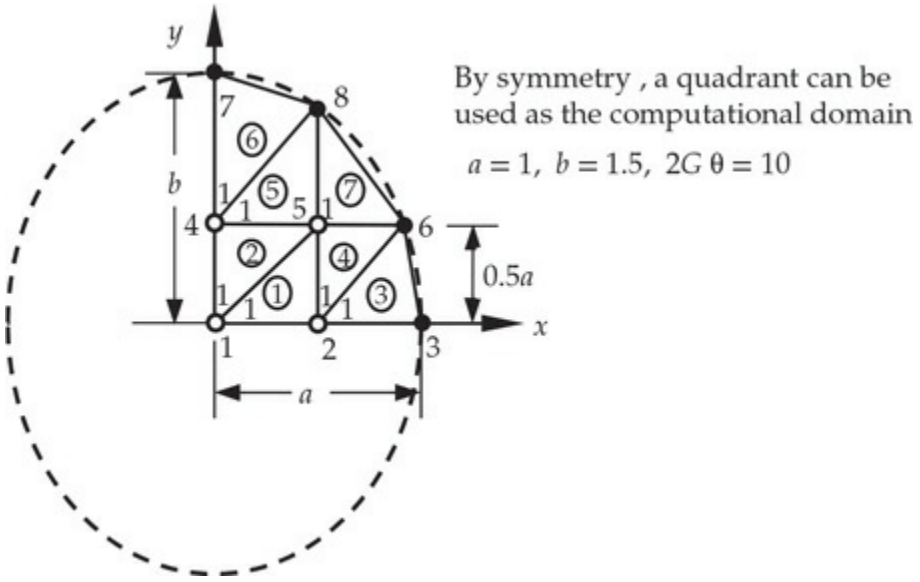

Fig. P9.44

9.45 Repeat **Problem 9.43** for the case in which Ω is an equilateral triangle (see Fig. P9.45). The exact solution is given by

$$u = -G\theta\left[\frac{1}{2}(x^2 + y^2) - \frac{1}{2}a(x^3 - 3xy^2) - \frac{2}{27}a^2\right]$$

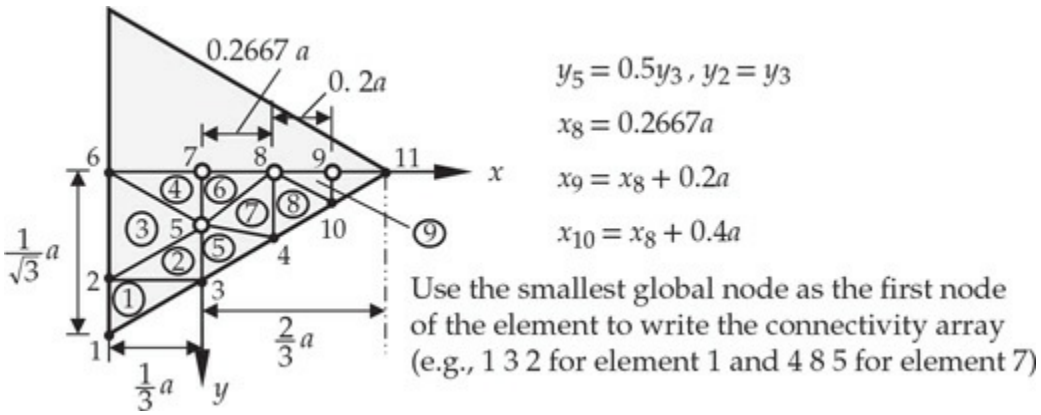

Fig. P9.45

Take $a = 1$ and $f_0 = 2G\theta = 10$. Give the finite element equation for

node 5.

Use the smallest global node as the first node of the element to write the connectivity array (e.g., 1 3 2 for element 1 and 4 8 5 for element 7)

9.46 Consider the torsion of a hollow square cross-section member. The stress function Ψ is required to satisfy the Poisson equation (9.4.36) and the following boundary conditions:

$$\Psi = 0 \quad \text{on the outer boundary;} \quad \Psi = 2r^2 \quad \text{on the inner boundary}$$

where r is the ratio of the outside dimension to the inside dimension, $r = 6a/2a$. Formulate the problem for finite element analysis using the mesh shown in Fig. P9.46.

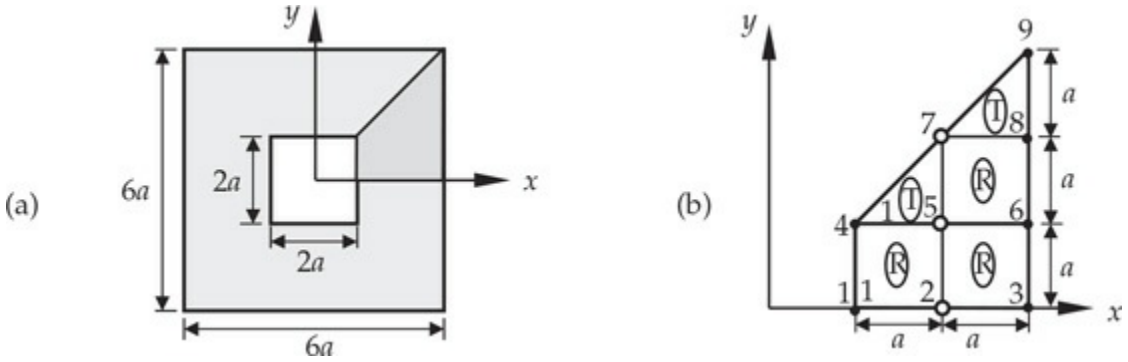

Fig. P9.46

9.47 Repeat **Problem 9.46** with the mesh of linear triangles [join nodes 1 and 5, 2 and 6, and 5 and 8 in Fig. P9.46(b)].

9.48 The membrane shown in Fig. P9.48 is subjected to uniformly distributed transverse load of intensity f_0 (in N/m^2). Write the condensed equations for the unknown displacements.

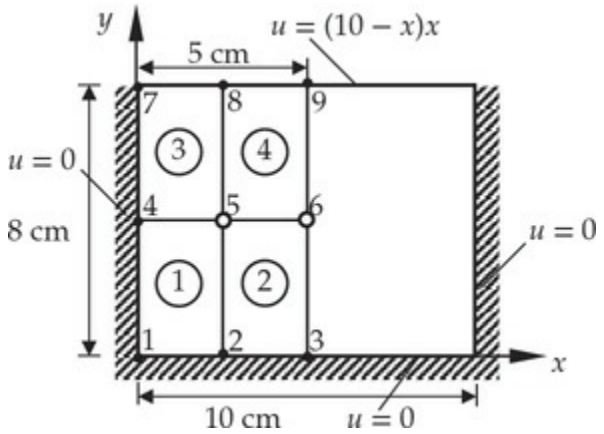

Fig. P9.48

9.49 The circular membrane shown in Fig. P9.49 is subjected to uniformly distributed transverse load of intensity f_0 (in N/m2). Write the condensed equations for the unknown displacements.

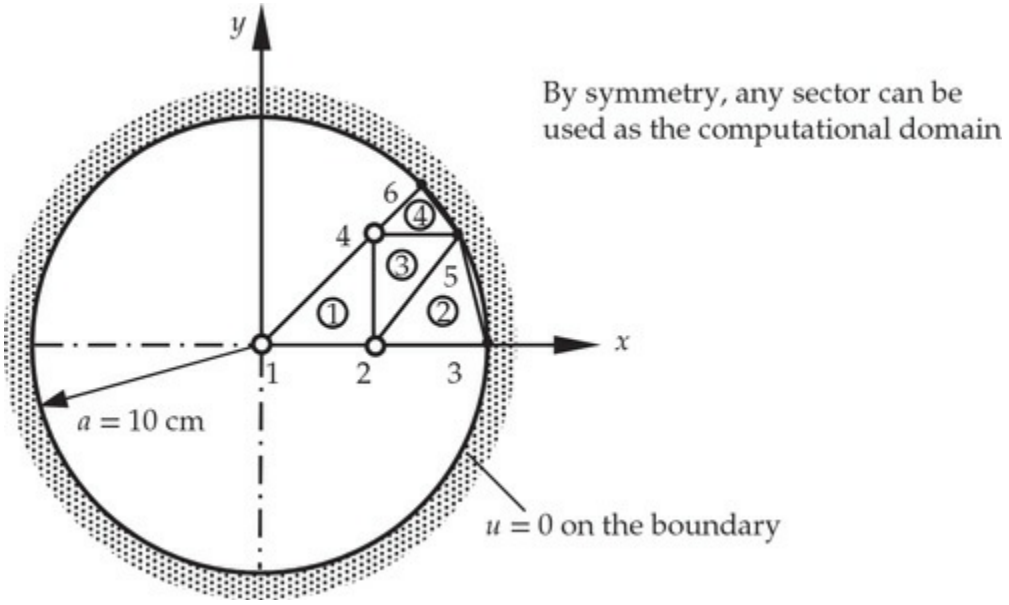

Fig. P9.49

EIGENVALUE AND TRANSIENT PROBLEMS

9.50 Determine the critical time step for the transient analysis (with $\alpha \leq \frac{1}{2}$) of the problem

$$\frac{\partial u}{\partial t} - \nabla^2 u = 1 \quad \text{in } \Omega; \quad u = 0 \quad \text{in } \Omega \text{ at } t = 0 \tag{1}$$

by determining the maximum eigenvalue of the problem

$$-\nabla^2 u = \lambda u \quad \text{in } \Omega; \quad u = 0 \quad \text{on } \Gamma \tag{2}$$

The domain is a square of 1 unit. Use (a) one triangular element in the octant, (b) four linear triangular elements in the octant [see Fig. P9.50(b)], and (c) a 2 × 2 mesh of linear rectangular elements in a quadrant [see Fig. P9.50(c)]. Determine the critical time step for the forward difference scheme. *Answer:* (a) $\lambda = 24$. (b) $\lambda_{max} = 305.549$.

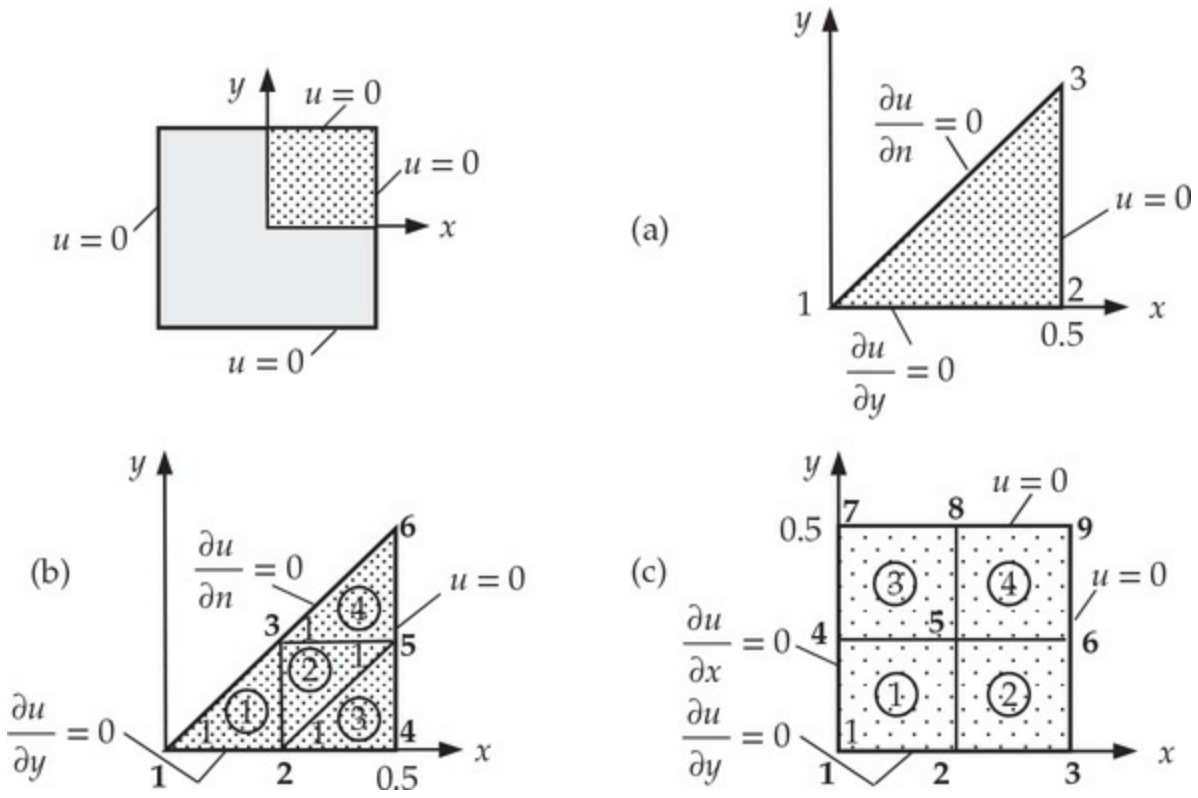

Fig. P9.50

9.51 Set up the condensed equations for the transient problem in **Problem 9.50** for the α-family of approximation. Use the mesh shown in Fig. P9.50(b).

9.52 Set up the condensed equations for the time-dependent analysis of the circular membrane in **Problem 9.49**.

9.53 Determine the fundamental natural frequency of the rectangular membrane in **Problem 9.48**.

9.54 Determine the critical time step based on the forward difference scheme for the timedependent analysis of the circular membrane in **Problem 9.49**.

9.55 (*Space-time element*) Consider the differential equation

$$c\frac{\partial u}{\partial t} - \frac{\partial}{\partial x}\left(a\frac{\partial u}{\partial x}\right) = f \quad \text{for } 0 < x < L, \quad 0 \le t \le T \tag{1}$$

with

$$u(0,t) = u(L,t) = 0 \quad \text{for } 0 \le t \le T \quad u(x,0) = u_0(x) \quad \text{for } 0 < x < L \tag{2}$$

where $c = c(x)$, $a = a(x)$, $f = f(x, t)$, and u_0 are given functions. Consider the rectangular domain defined by

$$\Omega = \{(x,t) : 0 < x < L, \quad 0 \le t \le T\} \tag{3}$$

A finite-element discretization of Ω by rectangles is a time-space rectangular element (with *y* replaced by *t*). Give a finite-element formulation of the equation over a time-space element, and discuss the *mathematical/practical* limitations of such a formulation. Compute the element matrices for a linear element.

9.56 (*Space-time finite element*) Consider the time-dependent problem

$$\frac{\partial^2 u}{\partial x^2} = c\frac{\partial u}{\partial t}, \quad \text{for } 0 < x < 1, \quad t > 0 \tag{1}$$

$$u(0,t) = 0, \quad \frac{\partial u}{\partial x}(1,t) = 1, \quad u(x,0) = x \tag{2}$$

Use linear rectangular elements in the (*x*, *t*)-plane to model the problem. Note that the finiteelement model is given by $[K^e]\{u^e\} = \{Q^e\}$, where

$$K_{ij}^e = \int_0^{\Delta t} \int_{x_a}^{x_b} \left(\frac{\partial \psi_i^e}{\partial x}\frac{\partial \psi_j^e}{\partial x} + c\psi_i^e \frac{\partial \psi_j^e}{\partial t} \right) dx\, dt \tag{3}$$

$$Q_1^e = -\left(-\int_0^{\Delta t} \frac{\partial u}{\partial x}\, dt \right)\Bigg|_{x=x_a}, \quad Q_2^e = \left(\int_0^{\Delta t} \frac{\partial u}{\partial x}\, dt \right)\Bigg|_{x=x_b} \tag{4}$$

9.57 The collocation time approximation methods are defined by the following relations:

$$\{\ddot{u}\}_{n+\alpha} = (1-\alpha)\{\ddot{u}\}_n + \alpha\{\ddot{u}\}_{n+1} \tag{1}$$

$$\{\dot{u}\}_{n+\alpha} = \{\dot{u}\}_n + \alpha\Delta t[(1-\gamma)\{\ddot{u}\}_n + \gamma\{\ddot{u}\}_{n+\alpha}] \tag{2}$$

$$\{u\}_{n+\alpha} = \{u\}_n + \alpha\Delta t\{\dot{u}\}_n + \frac{\alpha(\Delta t)^2}{2}[(1-2\beta)\{\ddot{u}\}_n + 2\beta\{\ddot{u}\}_{n+\alpha}] \tag{3}$$

The collocation scheme contains two of the well-known schemes: $\psi = 1$ gives the Newmark's scheme; $\beta = \frac{1}{6}$ and $\gamma = \frac{1}{2}$ gives the Wilson scheme. The collocation scheme is unconditionally stable, second-order accurate for the following values of the parameters:

$$\alpha \ge 1, \quad \gamma = \frac{1}{2}, \quad \frac{\alpha}{2(1+\alpha)} \ge \beta \ge \frac{2\alpha^2 - 1}{4(2\alpha^3 - 1)} \tag{4}$$

Formulate the algebraic equations associated with the matrix

differential equation

$$\mathbf{M\ddot{u} + C\dot{u} + Ku = F} \tag{5}$$

using the collocation scheme.

9.58 Consider the following pair of coupled partial differential equations:

$$-\frac{\partial}{\partial x}\left(a\frac{\partial u}{\partial x}\right) - \frac{\partial}{\partial y}\left[b\left(\frac{\partial u}{\partial y} + \frac{\partial v}{\partial x}\right)\right] + \frac{\partial u}{\partial t} - f_x = 0 \tag{1}$$

$$-\frac{\partial}{\partial x}\left[b\left(\frac{\partial u}{\partial y} + \frac{\partial v}{\partial x}\right)\right] - \frac{\partial}{\partial y}\left(c\frac{\partial v}{\partial y}\right) + \frac{\partial v}{\partial t} - f_y = 0 \tag{2}$$

where u and v are the dependent variables (unknown functions), a, b and c are known functions of x and y, and f_x and f_y are known functions of position (x, y) and time t.

(a) Use the three-step procedure on each equation with a different weight function for each equation (say, w_1 and w_2) to develop the (semidiscrete) weak form.

(b) Assume finite element approximation of (u, v) in the following form

$$u(x,y) = \sum_{j=1}^{n} \psi_j(x,y)U_j(t)\,, \quad v(x,y) = \sum_{j=1}^{n} \psi_j(x,y)V_j(t) \tag{3}$$

and develop the (semidiscrete) finite element model in the form

$$\begin{aligned} 0 &= \sum_{j=1}^{n} M_{ij}^{11}\dot{U}_j + \sum_{j=1}^{n} K_{ij}^{11}U_j + \sum_{j=1}^{n} K_{ij}^{12}V_j - F_i^1 \\ 0 &= \sum_{j=1}^{n} M_{ij}^{22}\dot{V}_j + \sum_{j=1}^{n} K_{ij}^{21}U_j + \sum_{j=1}^{n} K_{ij}^{22}V_j - F_i^2 \end{aligned} \tag{4}$$

You must define the algebraic form of the element coefficients K_{ij}^{11}, K_{ij}^{12}, F_i^1 etc.

(c) Give the fully discretized finite element model of the model (in the standard form; you are not required to derive it).

References for Additional Reading

1. J. P. Holman, *Heat Transfer*, 10th ed, McGraw–Hill, New York, NY,

2010.

2. H. Schlichting, *Boundary-Layer Theory* (translated by J. Kestin), 7th ed., McGraw–Hill, New York, NY, 1979.
3. S. P. Timoshenko and J. N. Goodier, *Theory of Elasticity*, 3rd ed, McGraw–Hill, New York, NY, 1970.
4. L. V. Kantorovich and V. I. Krylov, *Approximate Methods of Higher Analysis*, P. Noordhoff, Groningen, The Netherlands, 1958.
5. J. N. Reddy, *Energy Principles and Variational Methods in Applied Mechanics*, 3rd ed, John Wiley & Sons, New York, NY, 2017.
6. E. Kreyszig, *Advanced Engineering Mathematics*, 6th ed, John Wiley & Sons, New York, NY, 1988.
7. K. S. Surana and J. N. Reddy, *The Finite Element Method for Initial Value Problems, Mathematics and Computations*, CRC Press, Boca Raton, FL, 2018.
8. S. Eskinazi, *Principles of Fluid Mechanics*, Allyn and Bacon, Boston, MA, 1962.
9. S. G. Mikhlin, *The Numerical Performance of Variational Methods*, (translated from the Russian by R. S. Anderssen), Wolters–Noordhoff, The Netherlands, 1971.
10. M. N. Özisik, *Heat Transfer A Basic Approach*, McGraw–Hill, New York, NY, 1985.
11. J. N. Reddy, *Applied Functional Analysis and Variational Methods in Engineering*, McGraw–Hill, New York, NY, 1986; reprinted by Krieger, Melbourne, FL, 1991.
12. J. N. Reddy and M. L. Rasmussen, *Advanced Engineering Analysis*, John Wiley, New York, NY, 1982; reprinted by Krieger, Melbourne, FL, 1990.
13. K. Rektorys, *Variational Methods in Mathematics, Science and Engineering*, D. Reidel Publishing Co., Boston, MA, 1980.
14. A. C. Ugural and S. K. Fenster, *Advanced Mechanics of Materials and Applied Elasticity*, 5th ed., Pearson Education, Boston, MA, 2012.

10 2-D Interpolation Functions, Numerical Integration, and Computer Implementation

In questions of science, the authority of a thousand is not worth the humble reasoning of a single individual.

— Galileo Galilei

10.1 Introduction

10.1.1 Interpolation Functions

In the previous chapter we considered finite element analysis of a typical second-order differential equation involving one dependent unknown (u) on a two-dimensional domain (Ω) with closed boundary (Γ). The domain was divided into a set of finite elements (Ω_e) that allowed us to construct, rather uniquely, polynomial approximation functions in such a way that they interpolate u at certain points (nodes) of the element. We found that the geometry of the element, number and location of the nodes, and degree of the interpolation functions are all related. For example, a simplest linear polynomial in two dimensions has three parameters [$p(x, y) = c_1 + c_2x + c_3y$], and in order to express the three parameters (c_1, c_2, c_3) in terms of the values of u at three points of an element (u_1, u_2, u_3), we identified three nodes to be the vertices of a triangle, thus defining the geometry of the triangle. The need for writing c_i in terms of u_i comes from the requirement that the variable $u(x, y)$ must be continuous across the elements. This can be accomplished by simply equating the values of u_i from two elements at the common nodes (which cannot be done with the parameters c_i). It is also found that there are only two geometries, namely, triangles and quadrilaterals, that qualify as finite elements in two dimensions. The key aspect is the inter-element compatibility, that is, when two elements are connected side-to-side, the function u must be uniquely defined in terms of

the values of the function at the nodes common to the two elements. For example, when an element (say, triangle) with three nodes on its side is connected to another element (say a quadrilateral) with three nodes, the function u is uniquely defined (i.e., single-valued) along the common side because the nodal values from the two elements are equal. The number of terms in the polynomial expansion of $u(x, y)$ is the same as the number of nodes in the Lagrange family of finite elements (i.e., elements in which only the function values, not their derivatives, are interpolated), which are admissible for second-order problems. In addition to defining the geometry, the nodes provide higher-order variation of the solution (and geometry). The number of nodes on an edge of an element define the polynomial degree of interpolation.

Finite element approximations are local, that is, a function u defined over Ω is approximated as a collection of local approximations $u^e(x, y)$ defined on the element domain Ω_e, which are put together to define $u(x, y)$. It is important to note that the elements and their interpolation functions are independent of the physics being modeled. As such the interpolation functions are derived based on the geometry and the number of nodes in the element. For example, the Lagrange family of finite elements are useful in all finite element models that admit them in the approximation of the primary variables of the weak formulation. In other words, if a library of interpolation functions (the Lagrange or Hermite type) is available, then one can select admissible functions from the library to represent the finite element approximation of any problem. Therefore, one of the objectives of this chapter is to develop a library of two-dimensional triangular and rectangular elements of the Lagrange family.

10.1.2 Numerical Integration

As discussed in Chapter 8, the evaluation of finite element coefficients (i.e., K_{ij}^e, M_{ij}^e, and f_i^e) is carried out using numerical integration techniques. Since the integration is over an element and interpolation functions are defined over an element, they can be derived in a convenient coordinate system that aids numerical evaluation of the integrals. We shall use the *natural coordinate system*, which is a local coordinate system with normalized coordinates (i.e., the coordinates have no units, only values) to derive the interpolation functions. The *master elements*, for which interpolation functions are developed herein, can be used for numerical evaluation of integrals defined on irregularly shaped elements. Of course,

this requires a transformation of the geometry from the actual element shape to the shape of the associated master element.

10.1.3 Program FEM2D

In Chapter 8, we discussed some basic ideas concerning the development of a typical finite element program, and the use of **FEM1D** in the solution of one-dimensional problems was illustrated via many example problems. Most of the ideas presented there are also valid for two-dimensional problems. In this chapter we focus attention on the use of a model program **FEM2D** to solve problems from not only Chapter 9 but also from the forthcoming chapters on plane elasticity and two-dimensional flows of viscous fluids. The program **FEM2D** contains linear and quadratic triangular and quadrilateral elements, and it can be used for the solution of heat conduction and convection problems, laminar flows of viscous incompressible fluids using the penalty function formulation, plane elasticity problems, and plate bending problems using classical and shear deformation plate theories.

10.2 2-D Element Library

10.2.1 Pascal's Triangle for Triangular Elements

The linear (three-node) triangular element was developed in Section 9.2.6. Higher-order triangular elements (i.e., triangular elements with interpolation functions of higher degree) can be systematically developed with the help of the so-called *Pascal's triangle*, which contains the terms of polynomials of various degrees in the two coordinates ξ and η, as shown in Table 10.2.1. Here ξ and η denote some local coordinates; they do not, in general, represent the global coordinates of the problem. One can view the position of the terms as the nodes of the triangle, with the constant term and the first and last terms of a given row being the vertices of the triangle. Of course, the shape of the triangle is arbitrary—not necessarily an equilateral triangle, as might appear from Table 10.2.1.

Table 10.2.1 Top six rows of Pascal's triangle for the derivation of the Lagrange family of triangular elements.

Pascal's triangle	Degree of the complete polynomial	Number of terms in the polynomial	Element with nodes
1	0	1	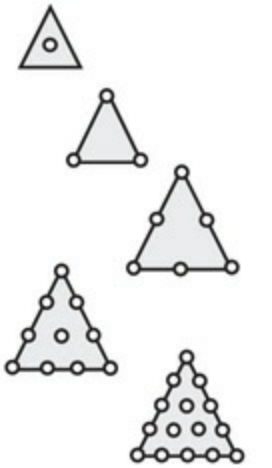
$\xi \quad \eta$	1	3	
$\xi^2 \quad \xi\eta \quad \eta^2$	2	6	
$\xi^3 \quad \xi^2\eta \quad \xi\eta^2 \quad \eta^3$	3	10	
$\xi^4 \quad \xi^3\eta \quad \xi^2\eta^2 \quad \xi\eta^3 \quad \eta^4$	4	15	
$\xi^5 \quad \xi^4\eta \quad \xi^3\eta^2 \quad \xi^2\eta^3 \quad \xi\eta^4 \quad \eta^5$	5	21	(Figure not shown)

For example, a triangular element of order 1 (i.e., linear polynomial) contains three nodes, as can be seen from the top two rows of Pascal's triangle [see Fig. 10.2.1(a)]. A triangular element of order 2 (i.e., the degree of the polynomial is 2) contains six nodes, as can be seen from the top three rows of Pascal's triangle. The position of the six nodes in the triangle is at the three vertices and at the midpoints of the three sides [see Fig. 10.2.1(b)]. The polynomial involves six constants (c_i), which can be expressed in terms of the six nodal values (u_i) of a variable u:

$$u(\xi,\eta) = c_1 + c_2\xi + c_3\eta + c_4\xi\eta + c_5\xi^2 + c_6\eta^2 = \sum_{i=1}^{6} u_i\psi_i(\xi,\eta) \qquad (10.2.1)$$

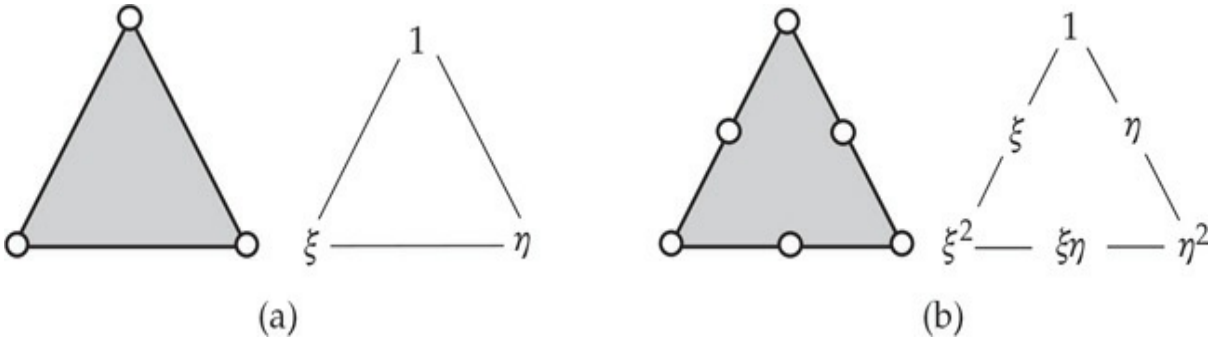

Fig. 10.2.1 Correspondence between the terms in Pascal's triangle to the nodes in the element.

where ψ_i are the quadratic interpolation functions obtained using the same procedure as that used for the linear element in Section 9.2.6.

In general, a *p*th order triangular element has a number of *n* nodes

$$n = \frac{1}{2}(p+1)(p+2) \tag{10.2.2}$$

and a complete polynomial of the *p*th degree is given by

$$u(\xi,\eta) = \sum_{i=1}^{n} a_i \xi^r \eta^s = \sum_{j=1}^{n} u_j \psi_j(\xi,\eta), \qquad r+s \le p \tag{10.2.3}$$

It can be easily seen that the *p*th-degree polynomial associated with the *p*th-order Lagrange element, when evaluated on the boundary of the element, yields a *p*th-degree polynomial in the boundary coordinate.

10.2.2 Interpolation Functions for Triangular Elements Using Area Coordinates

Recall from Eqs. (9.2.21)–(9.2.25b) that the procedure presented there for deriving the interpolation functions involves the inversion of a $n \times n$ matrix, where n is the number of terms in the polynomial used to approximate u. When $n > 3$, this procedure is algebraically very tedious, and therefore one should devise an alternative way of developing the interpolation functions.

The alternative derivation of the interpolation functions for the higher-order Lagrange family of triangular elements is simplified by the use of *area coordinates* or *barycentric coordinates*, denoted by L_i. Consider an arbitrary linear triangular element (i.e., triangle with three nodes and three straight sides), and let the side opposite to node i (i = 1, 2, 3) be labelled as side i (see Fig. 10.2.2). Now consider an arbitrary point P: (x, y) inside the element and connect it with straight lines to the nodes of the element. Then there are three triangles inside the original triangle. The area of the triangle with side i is denoted as A_i (i = 1, 2, 3). Obviously, the value of A_i will depend on the coordinates (x_i, y_i) of the nodes as well as on x and y. The area of the triangle is $A = A_1 + A_2 + A_3$, which is independent of x and y (i.e., A only depends on the coordinates of the nodes). We now introduce the dimensionless coordinates L_i(i = 1, 2, 3) as the ratio

$$L_i(x,y)=\frac{A_i}{A}, \quad A=\sum_{i=1}^{3} A_i \tag{10.2.4}$$

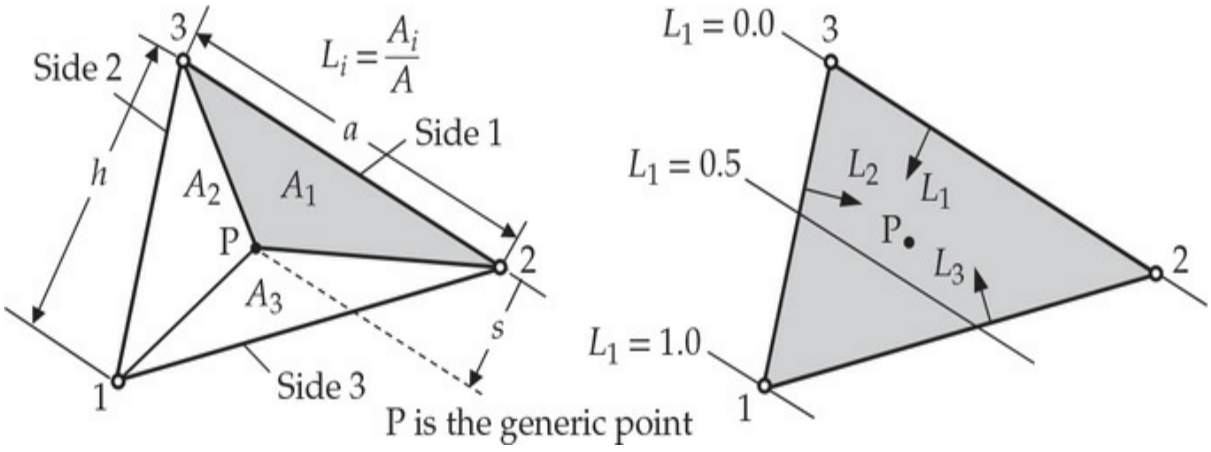

Fig. 10.2.2 Definition of the area coordinates of a triangular element.

We can also express L_i in terms of any other coordinates we choose. Suppose that the perpendicular distance from side 1 connecting nodes 2 and 3 to point P is s. Then we have $A_1 = (1/2)as$ and $A = (1/2)ah$. Hence, $L_1 = A_1/A = s/h$. Clearly, L_1 is zero on side 1 (hence, zero at nodes 2 and 3) and has a value of unity at node 1. Thus, L_1 is the interpolation function associated with node 1. Similarlft L_2 and L_3 are the interpolation functions associated with nodes 2 and 3, respectively. Therefore, we have

$$\psi_i(x,y)=L_i(x,y) \tag{10.2.5}$$

for a linear triangular element. We can use L_i to construct interpolation functions for higher-order triangular elements.

We consider a higher-order element with k, equally spaced, nodes per side (see Fig. 10.2.3). Then the total number of nodes in the element is given by

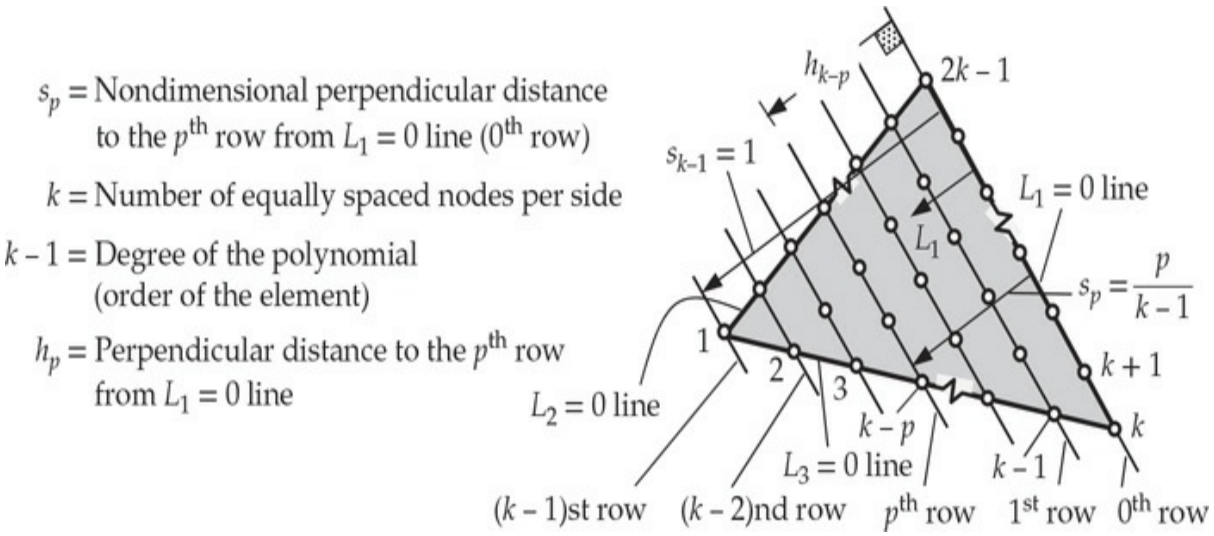

Fig. 10.2.3 Construction of the element interpolation functions of the Lagrange triangular elements for an arbitrary $(k-1)$th order element.

$$n = \sum_{i=0}^{k-1}(k-i) = k + (k-1) + \cdots + 1 = \frac{1}{2}k(k+1) \tag{10.2.6}$$

and the degree of the interpolation functions is equal to $k-1$. For example, for the quadratic element ($k = 3$), we have $k-1 = 2$ and $n = 6$. Let s denote the dimensionless local coordinate normal to side 1 (opposite to node 1) and h_1 be the perpendicular distance from side 1 to $(k-1)$st row (in general h_{k-p} is the perpendicular distance from side 1 to pth row). Then the dimensionless distance s_p to the pth row of nodes parallel to side 1 (under the assumption that the nodes are equally spaced along the sides and the rows) is given by

$$s_p = \frac{p}{k-1} \tag{10.2.7}$$

Obviously, $s_0 = 0$ and $s_{k-1} = 1$. The interpolation function ψ_1 should be zero at the nodes on rows 0, 1, 2, ... , $k-2$; in other words, ψ_1 should be zero at $L_1 = s_p$, where $s_p = p/(k-1)$ for $p = 0, 1, 2, \ldots, k-2$; and ψ_1 should be equal to 1 at $L_1 = s_{k-1} = 1$. Thus we have the necessary information for constructing the interpolation function ψ_1:

$$\psi_1 = \frac{(L_1 - s_0)(L_1 - s_1)(L_1 - s_2)\cdots(L_1 - s_{k-2})}{(s_{k-1} - s_0)(s_{k-1} - s_1)\cdots(s_{k-1} - s_{k-2})} = \prod_{p=0}^{k-2}\frac{L_1 - s_p}{s_{k-1} - s_p} \tag{10.2.8}$$

Similar expressions can be derived for nodes located at other vertices as well as for nodes at locations other than vertices. In general, ψ_i for node i is given by

$$\psi_i = \prod_{j=1}^{k-1} \frac{f_j}{f_j^i} \tag{10.2.9}$$

where f_j are functions of L_1, L_2 and L_3, and f_j^i is the value of f_j at node i. The functions f_j are derived from the equations of $k-1$ lines which pass through all the nodes except node i. The procedure is illustrated in the next example.

Example 10.2.1

Derive the quadratic and cubic interpolation functions in terms of the area coordinates for a triangular element.

Solution: First, consider the triangular element that has two nodes per side [i.e., $k = 2$; see Fig. 10.2.4(a)]. This is the linear triangular element with the total number of nodes equal to 3 ($n = 3$). For node 1 [see Fig. 10.2.4(a)], we have $k - 2 = 0$ and

$$s_0 = 0, \quad s_1 = 1, \quad \psi_1 = \frac{L_1 - s_0}{s_1 - s_0} = L_1 \tag{1}$$

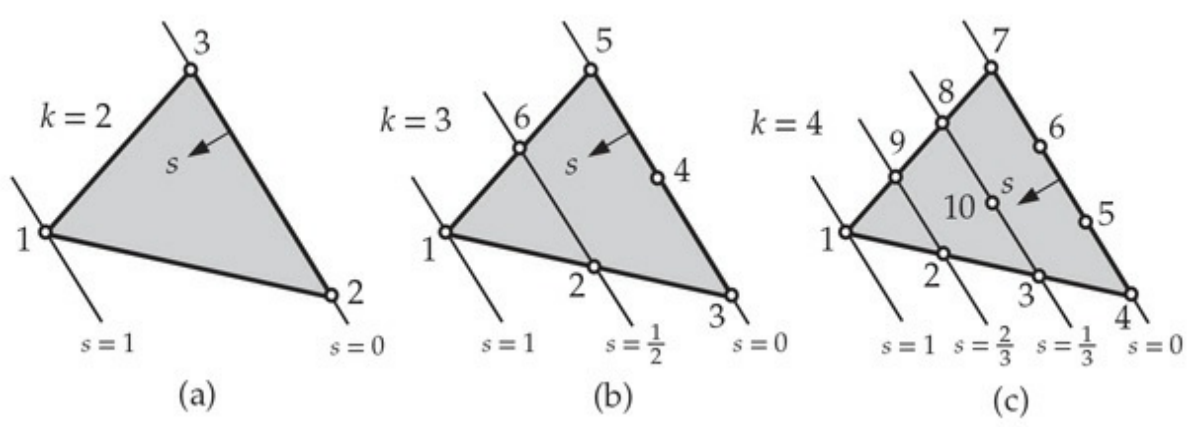

Fig. 10.2.4 Construction of the element interpolation functions of the Lagrange triangular elements: (a) linear element, (b) quadratic element, and (c) cubic element.

Similarly, for ψ_2 and ψ_3, we obtain

$$\psi_2 = L_2, \quad \psi_3 = L_3 \tag{2}$$

Next, consider the triangular element with three nodes per side ($k = 3$) [see Fig. 10.2.4(b)]. The total number of nodes is equal to 6. For node 1, we have

$$\begin{gathered} s_0 = 0, \quad s_1 = \frac{1}{2}, \quad s_2 = 1 \\ \psi_1 = \frac{L_1 - s_0}{s_2 - s_0}\frac{L_1 - s_1}{s_2 - s_1} = L_1(2L_1 - 1) \end{gathered} \tag{3}$$

The function ψ_2 [see Fig. 10.2.4(b)] should vanish at nodes 1, 3, 4, 5, and 6, and should be equal to 1 at node 2. Equivalently, ψ_2 should vanish along the lines connecting nodes 1 and 5, and 3 and 5. These two lines are given in terms of L_1 and L_2 (note that the subscripts of L refer to the nodes in the three-node triangular element) as $L_2 = 0$ and $L_1 = 0$. Hence, we have

$$\psi_2 = \frac{L_2 - s_0}{s_1 - s_0}\frac{L_1 - s_0}{s_1 - s_0} = \frac{L_2 - 0}{\frac{1}{2}}\frac{L_1 - 0}{\frac{1}{2}} = 4L_1L_2$$

Similarly,

$$\psi_3 = L_2(2L_2 - 1), \quad \psi_4 = 4L_2L_3, \qquad \psi_5 = L_3(2L_3 - 1), \quad \psi_6 = 4L_1L_3$$

Thus, the interpolation functions for an arbitrary quadratic triangular element are

$$\begin{gathered} \psi_1 = L_1(2L_1 - 1), \quad \psi_2 = 4L_1L_2, \quad \psi_3 = L_2(2L_2 - 1) \\ \psi_4 = 4L_2L_3, \quad \psi_5 = L_3(2L_3 - 1), \quad \psi_6 = 4L_1L_3 \end{gathered} \tag{10.2.10}$$

Finally, consider the cubic element [i.e., $k - 1 = 3$; see Fig. 10.2.4(c)]. For ψ_1 we note that it must vanish along lines $L_1 = 0$, $L_1 = \frac{1}{3}$, and $L_1 = \frac{2}{3}$. Therefore, we have

$$\psi_1 = \frac{L_1 - 0}{1 - 0}\frac{L_1 - \frac{1}{3}}{1 - \frac{1}{3}}\frac{L_1 - \frac{2}{3}}{1 - \frac{2}{3}} = \tfrac{1}{2}L_1(3L_1 - 1)(3L_1 - 2)$$

The function ψ_2 must vanish along lines $L_1 = 0$, $L_2 = 0$, and $L_1 = 1/3$ (and node 2 is located at $L_1 = 2/3$ and $L_2 = 1/3$):

$$\psi_2 = \frac{L_1 - 0}{\frac{2}{3} - 0}\frac{L_2 - 0}{\frac{1}{3} - 0}\frac{L_1 - \frac{1}{3}}{\frac{2}{3} - \frac{1}{3}} = \tfrac{9}{2}L_2L_1(3L_1 - 1)$$

Similarly, we can derive other functions. Thus, we have

$$\begin{aligned}
&\psi_1 = \tfrac{1}{2}L_1(3L_1 - 1)(3L_1 - 2), && \psi_2 = \tfrac{9}{2}L_2L_1(3L_1 - 1)\\
&\psi_3 = \tfrac{9}{2}L_1L_2(3L_2 - 1), && \psi_4 = \tfrac{1}{2}L_2(3L_2 - 1)(3L_2 - 2)\\
&\psi_5 = \tfrac{9}{2}L_2L_3(3L_2 - 1), && \psi_6 = \tfrac{9}{2}L_2L_3(3L_3 - 1)\\
&\psi_7 = \tfrac{1}{2}L_3(3L_3 - 1)(3L_3 - 2), && \psi_8 = \tfrac{9}{2}L_3L_1(3L_3 - 1)\\
&\psi_9 = \tfrac{9}{2}L_1L_3(3L_1 - 1), && \psi_{10} = 27L_1L_2L_3
\end{aligned} \tag{10.2.11}$$

We note that the area coordinates L_i facilitate not only the construction of the interpolation functions for higher-order elements but also the evaluation of integrals of functions of L_i over lines and areas. The following exact integration formulas prove to be useful:

$$\begin{aligned}
&\int_a^b L_1^m L_2^n ds = \frac{m!\,n!}{(m+n+1)!}(b-a)\\
&\int\int_{\text{area}} L_1^m L_2^n L_3^p dA = \frac{m!\,n!\,p!}{(m+n+p+2)!}2A
\end{aligned} \tag{10.2.12}$$

where m, n, and p are arbitrary (positive) integers, A is the area of the domain of integration, and $m!$ denotes the factorial of m ($0! = 1$). Of course, we should transform the integrals from the x and y coordinates to L_i coordinates using the transformation ($L_i = \psi_i$ and ψ_i are known in terms of L_1, L_2, and L_3),

$$x = \sum_{i=1}^{n} x_i L_i \qquad y = \sum_{i=1}^{n} y_i L_i \tag{10.2.13}$$

where (x_i, y_i) are the global coordinates of the ith node of the element.

10.2.3 Interpolation Functions Using Natural Coordinates

10.2.3.1 Triangular elements

Here we consider two different geometries of triangular elements which qualify as the master elements and determine their interpolation functions in terms of the local normalized coordinates ξ and η. Consider the linear triangular elements in Fig. 10.2.5(a) and (b). We determine the linear interpolation functions ψ_i and L_i in terms of the natural coordinates (ξ, η).

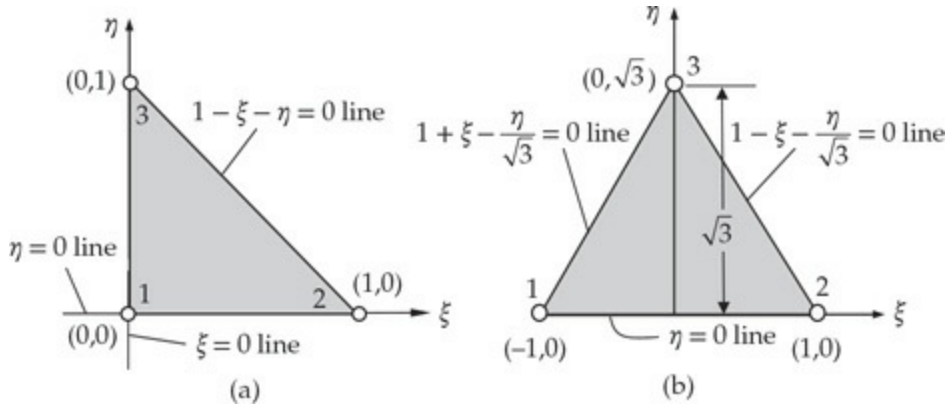

Fig. 10.2.5 (a) Master linear triangular element 1. (b) Master linear triangular element 2.

The interpolation function ψ_1 for master element 1 must vanish at nodes 2 and 3 and be unity at node 1. Since ψ_1 is zero at nodes 2 and 3, it must be also zero on the line connecting the nodes. Thus, ψ_1 is equal to $\psi_1 = 1 - \xi - \eta$. Similarly, ψ_2 must vanish at nodes 1 and 3 and on the line connecting them. Thus, $\psi_2 = \xi$. Finally,
ψ_3 must be zero at nodes 1 and 2 and on the line connecting them. Therefore, $\psi_3 = \eta$. Thus, we have

$$\psi_1(\xi,\eta) = 1 - \xi - \eta, \quad \psi_2(\xi,\eta) = \xi, \quad \psi_3(\xi,\eta) = \eta \tag{10.2.14}$$

They clearly satisfy the interpolation properties (for $n = 3$)

$$\psi_i(\xi_j,\eta_j) = \delta_{ij} \;\; (i,j = 1,2,\ldots,n); \quad \sum_{j=1}^{n} \psi_i(\xi,\eta) = 1 \tag{10.2.15}$$

To determine the area coordinates L_i, we consider an arbitrary point (ξ, η) inside the element. Then the perpendicular distance from line 3 to the point is η. Hence $L_3 = \eta/h$, where h is the perpendicular distance from line 3 to node 3, which is $h = 1$. Hence, $L_3 = \eta$. Similarly, $L_2 = \xi$. Then $L_1 = 1 - L_2 - L_3 = 1 - \xi - \eta$. Thus, we have $L_i = \psi_i$ $(i = 1, 2, 3)$.

Following the procedure used for the master element in Fig. 10.2.5(a) for the master element in Fig. 10.2.5(b), we require ψ_1 to vanish on the line connecting nodes 2 and 3, ψ_2 to vanish on the line connecting nodes 1 and 3, and ψ_3 to vanish on the line connecting nodes 1 and 2. The equations of the respective lines define the interpolation functions:

$$\psi_1(\xi,\eta)=\tfrac{1}{2}\left(1-\xi-\frac{1}{\sqrt{3}}\eta\right),\quad \psi_2(\xi,\eta)=\tfrac{1}{2}\left(1+\xi-\frac{1}{\sqrt{3}}\eta\right),\quad \psi_3(\xi,\eta)=\frac{1}{\sqrt{3}}\eta \tag{10.2.16}$$

One can verify that these functions satisfy the interpolation properties in Eq. (10.2.15).

To determine the area coordinates, we pick an arbitrary point (ξ, η). Then $L_3 = \eta/h$, where h is the perpendicular distance from side 3 to node 3, which is $h=\sqrt{3}$, giving $L_3=\eta/\sqrt{3}$. To determine L_1 and L_2, we first note that $L_1(\xi, \eta) = L_2(-\xi, \eta)$. Hence, $L_1 = a + b\xi + c\eta$ and $L_2 = a - b\xi + c\eta$. Since $L_1+L_2=1-L_3=1-\eta/\sqrt{3}$, we have $2a = 1$ and $2c=-1/\sqrt{3}$. Also, $L_1(-1, 0) = 1$ gives $b = a - 1 = -1/2$. Thus, we have

$$L_1(\xi,\eta)=\tfrac{1}{2}\left(1-\xi-\frac{1}{\sqrt{3}}\eta\right),\quad L_2(\xi,\eta)=\tfrac{1}{2}\left(1+\xi-\frac{1}{\sqrt{3}}\eta\right),\quad L_3(\xi,\eta)=\frac{1}{\sqrt{3}}\eta$$

Next we consider an example of determining interpolation functions for master quadratic triangular elements.

Example 10.2.2

Consider the quadratic triangular elements in Fig. 10.2.6(a) and (b). Determine the quadratic interpolation functions ψ_i in terms of the natural coordinates (ξ, η).

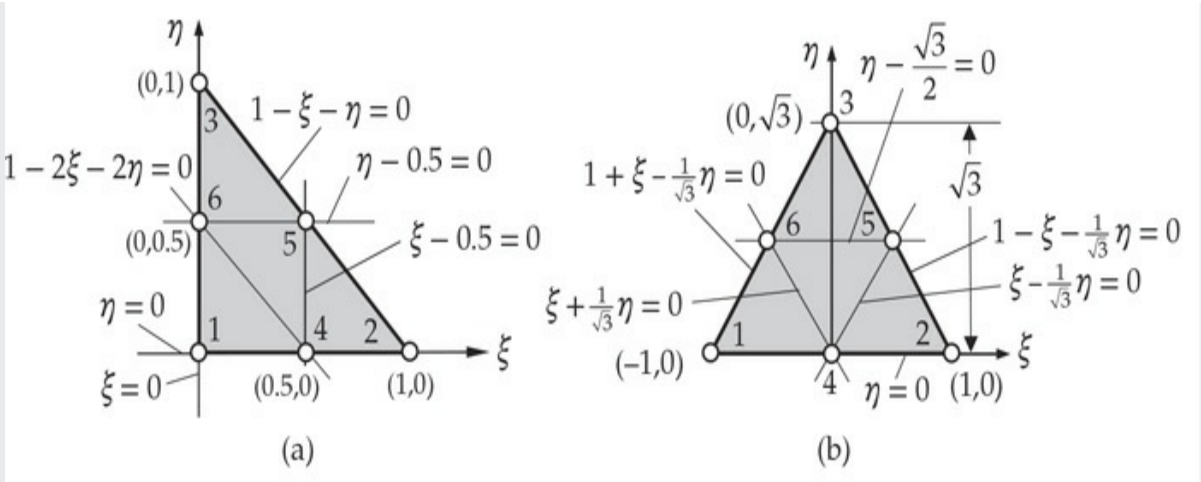

Fig. 10.2.6 (a) Master quadratic triangular element 1. (b) Master quadratic triangular element 2.

Solution: (a) The interpolation function ψ_1 for the master element in Fig. 10.2.6(a) must vanish on lines $1 - \xi - \eta = 0$ and $1 - 2\xi - 2\eta = 0$ and be unity at node 1. Thus, we have $\psi_1 = (1 - \xi - \eta)(1 - 2\xi - 2\eta)$. Also, ψ_2 must vanish on lines $\xi = 0$ and $\xi - 0.5 = 0$, giving $\psi_2 = \xi(2\xi - 1)$. Similarly, we obtain $\psi_3 = \eta(2\eta - 1)$. For nodes 4 and 6, we have $\psi 4 = 4\xi(1 - \xi - \eta)$ and $\psi_6 = 4\eta(1 - \xi - \eta)$. Finally, ψ_5 is given as $\psi_5 = 4\xi\eta$. Thus, the interpolation functions associated with the master element in Fig. 10.2.6(a) are

$$\psi_1 = (1 - \xi - \eta)(1 - 2\xi - 2\eta), \quad \psi_2 = \xi(2\xi - 1), \quad \psi_3 = \eta(2\eta - 1)$$
$$\psi_4 = 4\xi(1 - \xi - \eta), \quad \psi_5 = 4\xi\eta, \quad \psi_6 = 4\eta(1 - \xi - \eta) \tag{10.2.17}$$

For the master element in Fig. 10.2.6(b), we use the equations of various lines to construct the interpolation functions. We obtain

$$\psi_1 = \tfrac{1}{2}\left(1 - \xi - \tfrac{1}{\sqrt{3}}\eta\right)\left(\xi - \tfrac{1}{\sqrt{3}}\eta\right), \quad \psi_2 = \tfrac{1}{2}\left(1 + \xi - \tfrac{1}{\sqrt{3}}\eta\right)\left(\xi + \tfrac{1}{\sqrt{3}}\eta\right), \quad \psi_3 = \tfrac{1}{3}\eta\,(2\eta - \sqrt{3})$$
$$\psi_4 = \left(1 - \tfrac{1}{\sqrt{3}}\eta\right)^2 - \xi^2, \quad \psi_5 = \tfrac{2}{\sqrt{3}}\left(1 + \xi - \tfrac{1}{\sqrt{3}}\eta\right)\eta, \quad \psi_6 = \tfrac{2}{\sqrt{3}}\left(1 - \xi - \tfrac{1}{\sqrt{3}}\eta\right)\eta \tag{10.2.18}$$

Once again, we can check that the functions in Eqs. (10.2.17) and (10.2.18) satisfy the interpolation properties of Eq. (10.2.15).

10.2.3.2 Rectangular elements

Analogous to the Lagrange family of triangular elements, the Lagrange

family of rectangular (square) elements can be developed from Pascal's triangle shown in Table 10.2.1, which is modified to show rectangular elements (see Table 10.2.2). Since a linear rectangular element has four corners (hence, four nodes), the polynomial should have the first four terms 1, ξ, η, and $\xi\eta$ (which form a parallelogram in Pascal's triangle as shown in Table 10.2.2). The coordinates (ξ, η) are usually taken to be the element natural coordinates. In general, a pth-order Lagrange rectangular element has $n = (p + 1)^2$ nodes ($p = 0, 1, \ldots$), and the associated polynomial contains the terms from the pth parallelogram or the pth rectangle. The pth-order Lagrange rectangular element has interpolation functions which are pth-degree polynomials:

$$\psi_i(\xi,\eta)=\sum_{i=1}^{n} a_i\xi^j\eta^k \quad (j+k\le p+1;\ j,k\le p) \tag{10.2.19}$$

Table 10.2.2 Top six rows of Pascal's triangle for the derivation of the Lagrange family of rectangular elements.

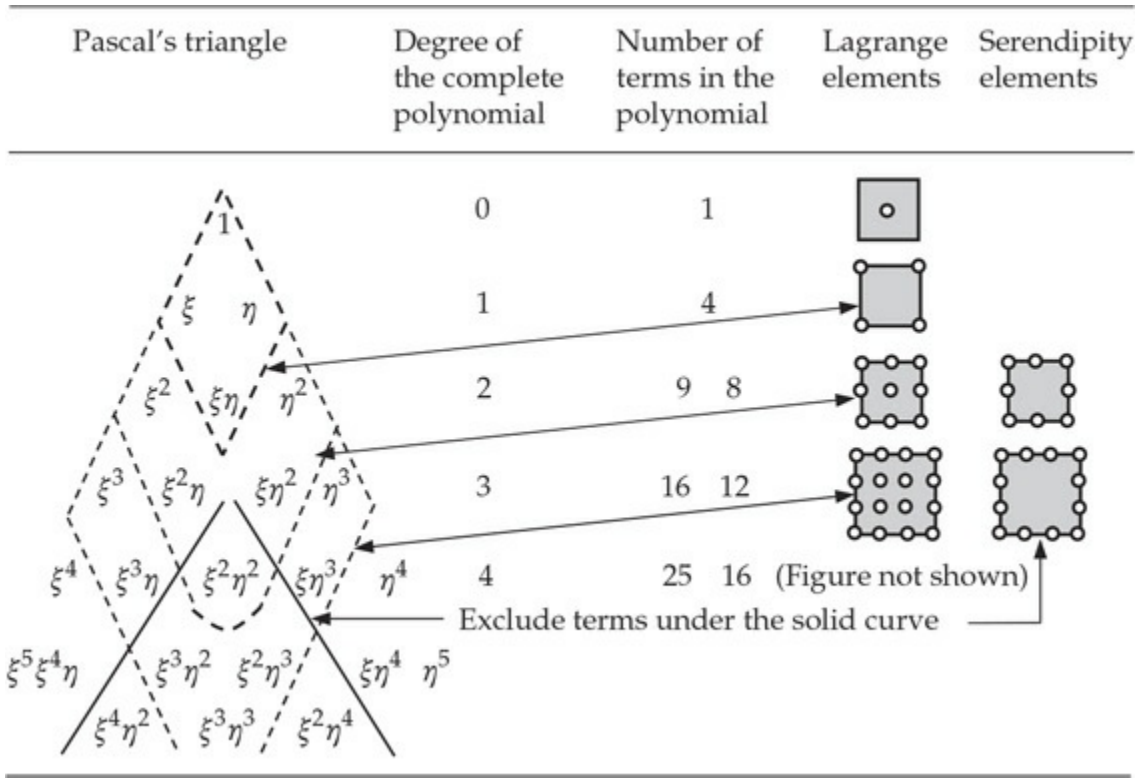

When $p = 0$, it is understood (as in triangular elements) that the node is at the center of the element (i.e., the variable is a constant on the entire element). The Lagrange linear element has four nodes which define the geometry of the element and the interpolation functions are four-term

polynomials of the form $a_1 + a_2\xi + a_3\eta + a_4\xi\eta$. The quadratic rectangular element has nine nodes, and the associated interpolation functions are of the form (strictly speaking a_1 through a_9 should have a superscript i to indicate that they correspond to the ith interpolation function):

$$\psi_i(\xi,\eta) = a_1 + a_2\xi + a_3\eta + a_4\xi\eta + a_5\xi^2 + a_6\eta^2 + a_7\xi^2\eta + a_8\xi\eta^2 + a_9\xi^2\eta^2 \tag{10.2.20}$$

The terms included in the previous expression come from the (tensor) product of the column vector $\{1\ \xi\ \xi^2\}^T$ and the row vector $\{1\ \eta\ \eta^2\}$. The polynomial contains the second degree terms, the combined third-degree terms $\xi^2\eta$ and $\xi\eta^2$, and the $\xi^2\eta^2$ term. Four of the nine nodes are placed at the four corners, four at the midpoints of the sides, and one at the center of the element. The polynomial is uniquely determined by specifying its values at each of the nine nodes. Moreover, along the sides of the element the polynomial is quadratic (with three terms—as can be seen by setting, for example, $\eta = 0$ or $\eta = 1$ to obtain quadratic polynomial in ξ), and is determined by its values at the three nodes on that side. If two quadratic elements share a side and the polynomial is required to have the same values from both elements at the three nodes of the elements, then u is uniquely defined along the entire side (shared by the two elements).

The interpolation functions for the master Lagrange family of rectangular (actually they are 2 × 2 unit squares) elements can be readily obtained using the tensor products of one-dimensional Lagrange interpolation functions. The linear, quadratic, and cubic interpolation functions for line elements (with equally spaced nodes) are given in Fig. 8.2.3 and presented here for convenience:

Linear:

$$\psi_1^{\xi} = \tfrac{1}{2}(1-\xi),\quad \psi_2^{\xi} = \tfrac{1}{2}(1+\xi) \tag{10.2.21}$$

Quadratic:

$$\psi_1^{\xi} = -\tfrac{1}{2}\xi(1-\xi),\quad \psi_2^{\xi} = (1-\xi^2),\quad \psi_3^{\xi} = \tfrac{1}{2}\xi(1+\xi) \tag{10.2.22}$$

Cubic:

$$\psi_1^{\xi} = -\frac{9}{16}(1-\xi)\left(\frac{1}{9}-\xi^2\right), \quad \psi_2^{\xi} = \frac{27}{16}(1-\xi^2)\left(\frac{1}{3}-\xi\right)$$
$$\psi_3^{\xi} = \frac{27}{16}(1-\xi^2)\left(\frac{1}{3}+\xi\right), \quad \psi_4^{\xi} = -\frac{9}{16}(1+\xi)\left(\frac{1}{9}-\xi^2\right) \qquad (10.2.23)$$

The interpolation functions for the rectangular elements are presented as tensor products of the one-dimensional functions next. The element node numbers as well as the functions corresponding to linear, quadratic, and cubic elements are shown in Fig. 10.2.7.

(a)

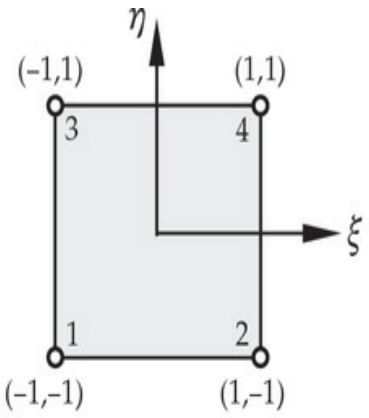

$$\psi_1 = \frac{1}{4}(1-\xi)(1-\eta)$$
$$\psi_2 = \frac{1}{4}(1+\xi)(1-\eta)$$
$$\psi_3 = \frac{1}{4}(1-\xi)(1+\eta)$$
$$\psi_4 = \frac{1}{4}(1+\xi)(1+\eta)$$

(b)

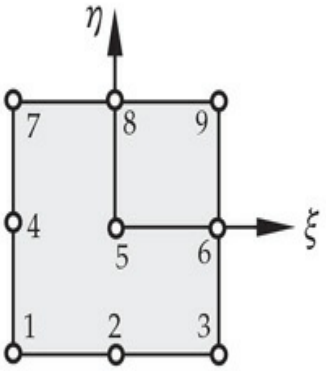

$$\psi_1 = \frac{1}{4}(\xi^2-\xi)(\eta^2-\eta), \quad \psi_2 = \frac{1}{2}(1-\xi^2)(\eta^2-\eta)$$
$$\psi_3 = \frac{1}{4}(\xi^2+\xi)(\eta^2-\eta), \quad \psi_4 = \frac{1}{2}(\xi^2-\xi)(1-\eta^2)$$
$$\psi_5 = (1-\xi^2)(1-\eta^2), \quad \psi_6 = \frac{1}{2}(\xi^2+\xi)(1-\eta^2)$$
$$\psi_7 = \frac{1}{4}(\xi^2-\xi)(\eta^2+\eta), \quad \psi_8 = \frac{1}{2}(1-\xi^2)(\eta^2+\eta)$$
$$\psi_9 = \frac{1}{4}(\xi^2+\xi)(\eta^2+\eta)$$

(c)

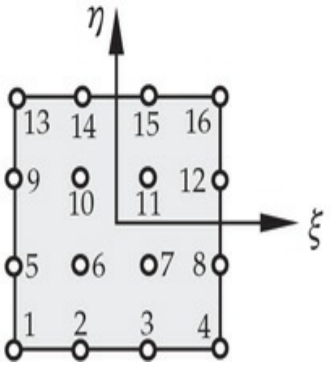

See Eq. (10.2.26)

Fig. 10.2.7 Node numbers and interpolation functions for the rectangular elements of the Lagrange family.

Linear element ($p = 1$)

$$\begin{Bmatrix} \psi_1^\xi \\ \psi_2^\xi \end{Bmatrix} \begin{Bmatrix} \psi_1^\eta & \psi_2^\eta \end{Bmatrix} = \begin{bmatrix} \psi_1^\xi \psi_1^\eta & \psi_1^\xi \psi_2^\eta \\ \psi_2^\xi \psi_1^\eta & \psi_2^\xi \psi_2^\eta \end{bmatrix} \equiv \begin{bmatrix} \psi_1 & \psi_3 \\ \psi_2 & \psi_4 \end{bmatrix}$$

$$= \frac{1}{4} \begin{bmatrix} (1-\xi)(1-\eta) & (1-\xi)(1+\eta) \\ (1+\xi)(1-\eta) & (1+\xi)(1+\eta) \end{bmatrix} \tag{10.2.24}$$

Quadratic element ($p = 2$)

$$\begin{Bmatrix} \psi_1^\xi \\ \psi_2^\xi \\ \psi_3^\xi \end{Bmatrix} \begin{Bmatrix} \psi_1^\eta & \psi_2^\eta & \psi_3^\eta \end{Bmatrix} = \begin{bmatrix} \psi_1^\xi \psi_1^\eta & \psi_1^\xi \psi_2^\eta & \psi_1^\xi \psi_3^\eta \\ \psi_2^\xi \psi_1^\eta & \psi_2^\xi \psi_2^\eta & \psi_2^\xi \psi_3^\eta \\ \psi_3^\xi \psi_1^\eta & \psi_3^\xi \psi_2^\eta & \psi_3^\xi \psi_3^\eta \end{bmatrix}$$

$$\equiv \begin{bmatrix} \psi_1 & \psi_4 & \psi_7 \\ \psi_2 & \psi_5 & \psi_8 \\ \psi_3 & \psi_6 & \psi_9 \end{bmatrix}$$

where

$$\begin{aligned} \psi_1 &= \tfrac{1}{4}(\xi - \xi^2)(\eta - \eta^2), & \psi_5 &= (1-\xi^2)(1-\eta^2) \\ \psi_2 &= -\tfrac{1}{2}(1-\xi^2)(\eta - \eta^2), & \psi_6 &= \tfrac{1}{2}(\xi + \xi^2)(1-\eta^2) \\ \psi_3 &= -\tfrac{1}{4}(\xi + \xi^2)(\eta - \eta^2), & \psi_7 &= -\tfrac{1}{4}(\xi - \xi^2)(\eta + \eta^2) \\ \psi_4 &= -\tfrac{1}{2}(\xi - \xi^2)(1-\eta^2), & \psi_8 &= \tfrac{1}{2}(1-\xi^2)(\eta + \eta^2) \\ \psi_9 &= \tfrac{1}{4}(\xi + \xi^2)(\eta + \eta^2) \end{aligned} \tag{10.2.25}$$

Cubic element ($p = 3$)

$$\left\{\begin{array}{c}\psi_1^{\xi}\\ \psi_2^{\xi}\\ \psi_3^{\xi}\\ \psi_4^{\xi}\end{array}\right\}\left\{\begin{array}{cccc}\psi_1^{\eta} & \psi_2^{\eta} & \psi_3^{\eta} & \psi_4^{\eta}\end{array}\right\}=\left[\begin{array}{cccc}\psi_1^{\xi}\psi_1^{\eta} & \psi_1^{\xi}\psi_2^{\eta} & \psi_1^{\xi}\psi_3^{\eta} & \psi_1^{\xi}\psi_4^{\eta}\\ \psi_2^{\xi}\psi_1^{\eta} & \psi_2^{\xi}\psi_2^{\eta} & \psi_2^{\xi}\psi_3^{\eta} & \psi_2^{\xi}\psi_4^{\eta}\\ \psi_3^{\xi}\psi_1^{\eta} & \psi_3^{\xi}\psi_2^{\eta} & \psi_3^{\xi}\psi_3^{\eta} & \psi_3^{\xi}\psi_4^{\eta}\\ \psi_4^{\xi}\psi_1^{\eta} & \psi_4^{\xi}\psi_2^{\eta} & \psi_4^{\xi}\psi_3^{\eta} & \psi_4^{\xi}\psi_4^{\eta}\end{array}\right]$$

$$\equiv\left[\begin{array}{cccc}\psi_1 & \psi_5 & \psi_9 & \psi_{13}\\ \psi_2 & \psi_6 & \psi_{10} & \psi_{14}\\ \psi_3 & \psi_7 & \psi_{11} & \psi_{15}\\ \psi_4 & \psi_8 & \psi_{12} & \psi_{16}\end{array}\right]$$

where ψ_i are the cubic interpolation functions presented in Eq. (10.2.26).

$$
\begin{aligned}
\psi_1 &= \tfrac{81}{256}(1-\xi)\left(\tfrac{1}{9}-\xi^2\right)(1-\eta)\left(\tfrac{1}{9}-\eta^2\right)\\
\psi_2 &= -\tfrac{243}{256}(1-\xi^2)\left(\tfrac{1}{3}-\xi\right)(1-\eta)\left(\tfrac{1}{9}-\eta^2\right)\\
\psi_3 &= -\tfrac{243}{256}(1-\xi^2)\left(\tfrac{1}{3}+\xi\right)(1-\eta)\left(\tfrac{1}{9}-\eta^2\right)\\
\psi_4 &= \tfrac{81}{256}(1+\xi)\left(\tfrac{1}{9}-\xi^2\right)(1-\eta)\left(\tfrac{1}{9}-\eta^2\right)\\
\psi_5 &= -\tfrac{243}{256}(1-\xi)\left(\tfrac{1}{9}-\xi^2\right)(1-\eta^2)\left(\tfrac{1}{3}-\eta\right)\\
\psi_6 &= \tfrac{729}{256}(1-\xi^2)\left(\tfrac{1}{3}-\xi\right)(1-\eta^2)\left(\tfrac{1}{3}-\eta\right)\\
\psi_7 &= \tfrac{729}{256}(1-\xi^2)\left(\tfrac{1}{3}+\xi\right)(1-\eta^2)\left(\tfrac{1}{3}-\eta\right)\\
\psi_8 &= -\tfrac{243}{256}(1+\xi)\left(\tfrac{1}{9}-\xi^2\right)(1-\eta^2)\left(\tfrac{1}{3}-\eta\right)\\
\psi_9 &= -\tfrac{243}{256}(1-\xi)\left(\tfrac{1}{9}-\xi^2\right)(1-\eta^2)\left(\tfrac{1}{3}+\eta\right)\\
\psi_{10} &= \tfrac{729}{256}(1-\xi^2)\left(\tfrac{1}{3}-\xi\right)(1-\eta^2)\left(\tfrac{1}{3}+\eta\right)\\
\psi_{11} &= \tfrac{729}{256}(1-\xi^2)\left(\tfrac{1}{3}+\xi\right)(1-\eta^2)\left(\tfrac{1}{3}+\eta\right)\\
\psi_{12} &= -\tfrac{243}{256}(1+\xi)\left(\tfrac{1}{9}-\xi^2\right)(1-\eta^2)\left(\tfrac{1}{3}+\eta\right)\\
\psi_{13} &= \tfrac{81}{256}(1-\xi)\left(\tfrac{1}{9}-\xi^2\right)(1+\eta)\left(\tfrac{1}{9}-\eta^2\right)\\
\psi_{14} &= -\tfrac{243}{256}(1-\xi^2)\left(\tfrac{1}{3}-\xi\right)(1+\eta)\left(\tfrac{1}{9}-\eta^2\right)\\
\psi_{15} &= -\tfrac{243}{256}(1-\xi^2)\left(\tfrac{1}{3}+\xi\right)(1+\eta)\left(\tfrac{1}{9}-\eta^2\right)\\
\psi_{16} &= \tfrac{81}{256}(1+\xi)\left(\tfrac{1}{9}-\xi^2\right)(1+\eta)\left(\tfrac{1}{9}-\eta^2\right)
\end{aligned}
\qquad (10.2.26)
$$

***p*th-order element** [$k = (p+1)p+1$ and $n = (p+1)^2$]

$$
\begin{Bmatrix} f_1(\xi)\\ f_2(\xi)\\ \vdots\\ f_{p+1}(\xi)\end{Bmatrix}\begin{Bmatrix} g_1(\eta)\\ g_2(\eta)\\ \vdots\\ g_{p+1}(\eta)\end{Bmatrix}^T = \begin{bmatrix} \psi_1 & \psi_{p+2} & \cdots & \psi_k\\ \psi_2 & & & \\ \vdots & \ddots & & \vdots\\ \psi_p & & \ddots & \\ \psi_{p+1} & \psi_{2p+2} & \cdots & \psi_n\end{bmatrix} \qquad (10.2.27a)
$$

where $f_i(\xi)$ and $g_i(\eta)$ are the pth order interpolants in ξ and η, respectively. For example, the polynomial

$$f_i(\xi) = \frac{(\xi - \xi_1)(\xi - \xi_2)\cdots(\xi - \xi_{i-1})(\xi - \xi_{i+1})\cdots(\xi - \xi_{p+1})}{(\xi_i - \xi_1)(\xi_i - \xi_2)\cdots(\xi_i - \xi_{i-1})(\xi_i - \xi_{i+1})\cdots(\xi_i - \xi_{p+1})} \qquad (10.2.27b)$$

(where ξ_i is the ξ coordinate of node i) is the pth-degree interpolation polynomial in ξ that vanishes at points $\xi_1, \xi_2,\ldots,\xi_{i-1}, \xi_{i+1},\ldots,\xi_{p+1}$. Similar expressions are valid for g_i in terms of η. One should be reminded that the subscripts of ψ_i refer to the node numbering used in Fig. 10.2.7. For any renumbering of the nodes, the subscripts of the interpolation functions should be changed accordingly. Plots of ψ_1, ψ_2 and ψ_5 (the node numbers correspond to those in Fig. 10.2.7) of the nine-node rectangular element are shown in Fig. 10.2.8.

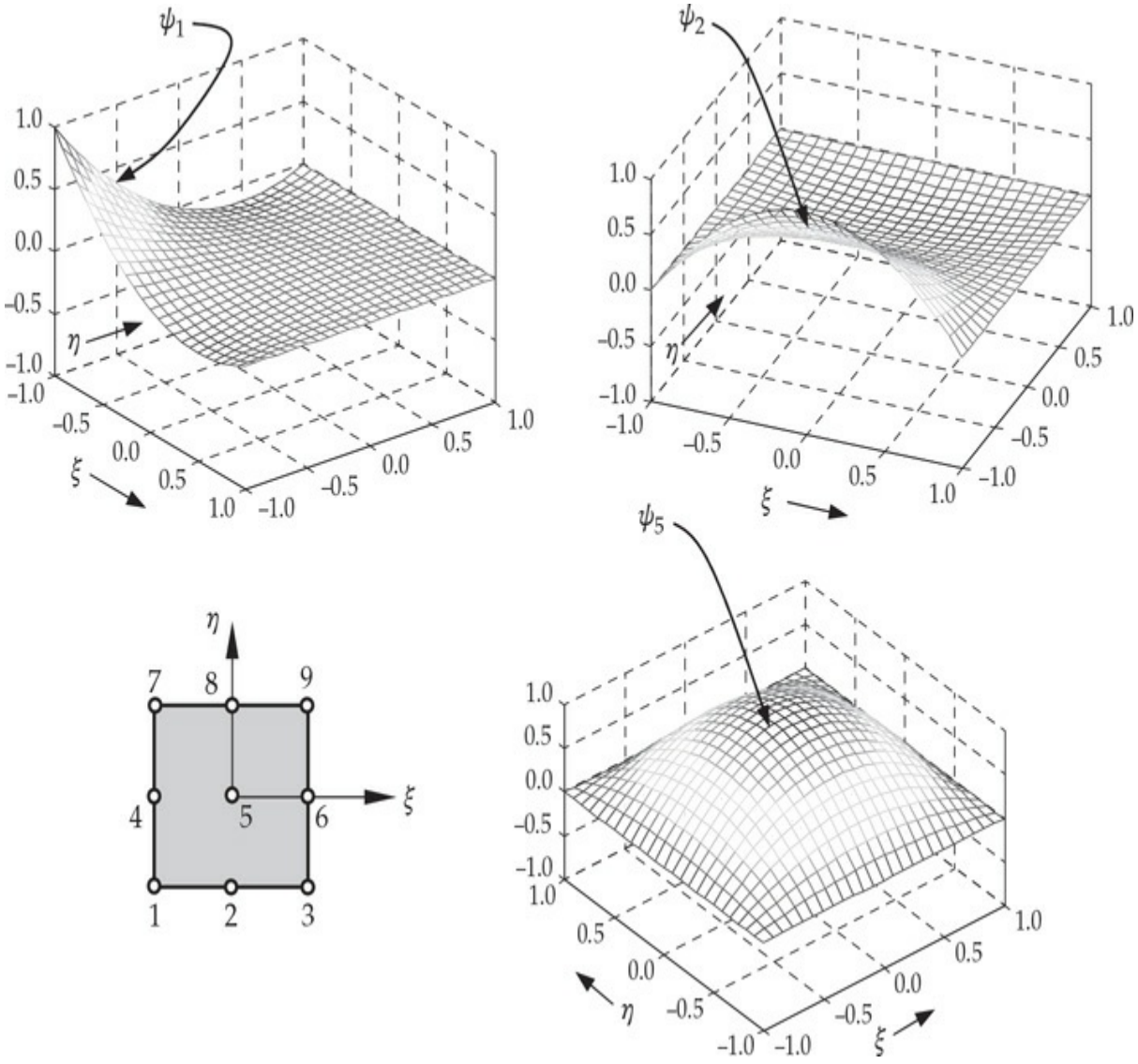

Fig. 10.2.8 Geometric variation of the Lagrange interpolation functions at nodes 1, 2, and 5 of the nine-node quadratic element.

10.2.4 The Serendipity Elements

Since the internal nodes of the higher-order elements of the Lagrange family do not contribute to the interelement connectivity, they can be condensed out at the element level so that the size of the element matrices is reduced. Alternatively, one can use the so-called serendipity elements to avoid the internal nodes in the Lagrange elements (i.e., the serendipity elements are those rectangular elements which have nodes only on the edges). The interpolation functions for serendipity elements cannot be obtained using tensor products of one-dimensional interpolation functions. Instead, an alternative procedure (similar to the one used for master triangular elements) that uses the interpolation properties in Eq. (10.2.15) is used. Here we illustrate how to construct the interpolation functions for the eight-node quadratic (first serendipity) master element [see Fig. 10.2.9(a)].

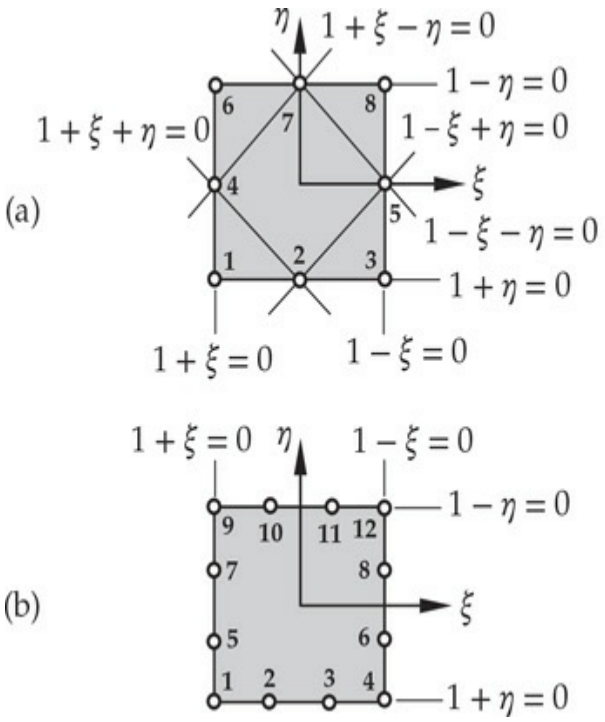

$$\psi_1 = -\tfrac{1}{4}(1-\xi)(1-\eta)(1+\xi+\eta)$$
$$\psi_2 = \tfrac{1}{2}(1-\xi^2)(1-\eta)$$
$$\psi_3 = -\tfrac{1}{4}(1+\xi)(1-\eta)(1-\xi+\eta)$$
$$\psi_4 = \tfrac{1}{2}(1-\xi)(1-\eta^2),\ \psi_5 = \tfrac{1}{2}(1+\xi)(1-\eta^2)$$
$$\psi_6 = -\tfrac{1}{4}(1-\xi)(1+\eta)(1+\xi-\eta)$$
$$\psi_7 = \tfrac{1}{2}(1-\xi^2)(1+\eta)$$
$$\psi_8 = -\tfrac{1}{4}(1+\xi)(1+\eta)(1-\xi-\eta)$$

See Eq. (10.2.32) for the interpolation functions

Fig. 10.2.9 Node numbers and interpolation functions associated with the serendipity family of elements. (a) Eight-node element. (b) Twelve-node element.

The interpolation function for node 1 should vanish on the lines defined by the equations $1 - \xi = 0$, $1 - \eta = 0$, and $1 + \xi + \eta = 0$ [see Fig. 10.2.9(a)]. Therefore ψ_1 is of the form

$$\psi_1(\xi,\eta) = c_1(1-\xi)(1-\eta)(1+\xi+\eta)$$

where c_1 is a constant which should be determined so as to yield $\psi_1(-_1, -_1) = 1$. We obtain $c_1 = -\frac{1}{4}$, and therefore

$$\psi_1(\xi,\eta) = -\frac{1}{4}(1-\xi)(1-\eta)(1+\xi+\eta)$$

Next we construct interpolation function for node 2. It should vanish on the lines $1-\xi=0$, $1+\xi=0$, and $1-\eta=0$. Hence, we have

$$\psi_2(\xi,\eta) = c_2(1-\xi)(1+\xi)(1-\eta)$$

Requiring $\psi_2(0,-1)=1$, we obtain $c_2 = 1/2$. Similarly, for node 4, we have

$$\psi_4(\xi,\eta) = c_4(1-\xi)(1-\eta)(1+\eta), \quad c_4 = \frac{1}{2}$$

Thus, all of the interpolation functions for the eight-node rectangular element are

$$\begin{aligned}
\psi_1 &= -\tfrac{1}{4}(1-\xi)(1-\eta)(1+\xi+\eta), & \psi_2 &= \tfrac{1}{2}(1-\xi^2)(1-\eta)\\
\psi_3 &= \tfrac{1}{4}(1+\xi)(1-\eta)(-1+\xi-\eta), & \psi_4 &= \tfrac{1}{2}(1-\xi)(1-\eta^2)\\
\psi_5 &= \tfrac{1}{2}(1+\xi)(1-\eta^2), & \psi_6 &= \tfrac{1}{4}(1-\xi)(1+\eta)(-1-\xi+\eta)\\
\psi_7 &= \tfrac{1}{2}(1-\xi^2)(1+\eta), & \psi_8 &= \tfrac{1}{4}(1+\xi)(1+\eta)(-1+\xi+\eta)
\end{aligned} \tag{10.2.28}$$

Note that all the ψ_i for the eight-node element have the form

$$\psi_i = c_1 + c_2\xi + c_3\eta + c_4\xi\eta + c_5\xi^2 + c_6\eta^2 + c_7\xi^2\eta + c_8\xi\eta^2 \tag{10.2.29}$$

The ψ_i for the nine-node element contains an extra term, namely, $c_9\xi^2\eta^2$. Plots of ψ_1 and ψ_2 [the node numbers correspond to those in Fig. 10.2.9(a)] for the eight-node serendipity element are shown in Fig. 10.2.10. We note that ψ_2, for example, of the nine-node element is zero at the element center ($\xi = \eta = 0$), whereas ψ_2 of the eight-node element is nonzero there.

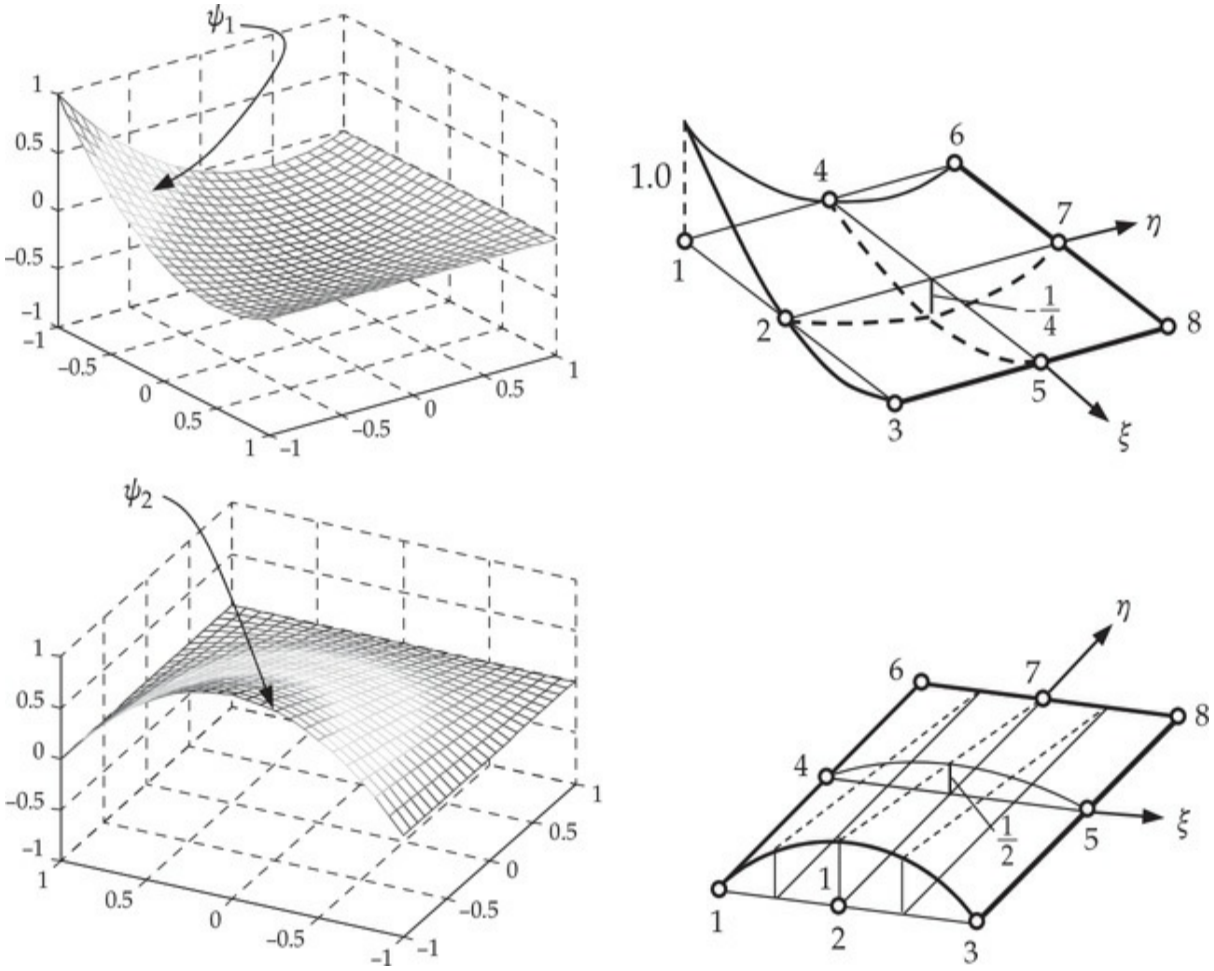

Fig. 10.2.10 Graphical representation of the interpolation functions associated with nodes 1 and 2 of the eight-node serendipity element.

The interpolation functions ψ_i for the 12-node element are of the form

$$\psi_i = \text{terms of the form in Eq. (10.2.29)} + c_9\xi^3 + c_{10}\eta^3 + c_{11}\xi^3\eta + c_{12}\xi\eta^3 \tag{10.2.30}$$

Following the same procedure as that used for the 8-node element, we can derive the interpolation functions for the 12-node serendipity element [see Fig. 10.2.9(b)]. For example, ψ_1 (ξ, η) must vanish on lines $1 - \xi = 0$ and $1 - \eta = 0$ and at points $(\xi = \pm 1/3, \eta = -1)$ and $(\xi = -1, \eta = \pm 1/3)$. Hence, ψ_1 is of the form

$$\psi_1(\xi, \eta) = c_1(1 - \xi)(1 - \eta)(a + b\xi^2 + c\eta^2)$$

First we determine a, b, and c such that $a + b\xi^2 + c\eta^2 = 0$ at $(\xi = \pm 1/3, \eta = -1)$ and $(\xi = -1, \eta = \pm 1/3)$. This gives $a = -(10/9)b$ and $c = b$. Hence (absorbing $b/9$ into c_1) we have

$$\psi_1(\xi,\eta) = c_1(1-\xi)(1-\eta)(-10+9\xi^2+9\eta^2)$$

Then setting $\psi_1(-1, -1) = 1$ gives $c_1 = 1/32$. Thus, we have

$$\psi_1 = \tfrac{1}{32}(1-\xi)(1-\eta)[-10+9(\xi^2+\eta^2)] \qquad (10.2.31a)$$

Similar procedure can be used to determine ψ_i for the corner nodes (i = 4, 9, 12). For a node on the interior of the sides, for example, node 2, we require ψ_2 to be zero on sides defined by equations $1 - \xi = 0$, $1 + \xi = 0$, and $1 - \eta = 0$, and zero at node 3 (i.e., at $\xi = 1/3$ and $\eta = -1$). Thus, ψ_2 is of the form

$$\psi_2 = c_2(1-\xi^2)(1-\eta)(1-3\xi)$$

The constant c_2 is determined by setting $\psi_2(-1/3, -1) = 1$. We obtain $c_2 = 9/32$. Thus,

$$\psi_2 = \tfrac{9}{32}(1-\xi^2)(1-\eta)(1-3\xi) \qquad (10.2.31b)$$

In summary, the interpolation functions of the cubic serendipity element are

$$\psi_1 = \tfrac{1}{32}(1-\xi)(1-\eta)[-10+9(\xi^2+\eta^2)], \quad \psi_2 = \tfrac{9}{32}(1-\eta)(1-\xi^2)(1-3\xi)$$

$$\psi_3 = \tfrac{9}{32}(1-\eta)(1-\xi^2)(1+3\xi), \quad \psi_4 = \tfrac{1}{32}(1+\xi)(1-\eta)[-10+9(\xi^2+\eta^2)]$$

$$\psi_5 = \tfrac{9}{32}(1-\xi)(1-\eta^2)(1-3\eta), \quad \psi_6 = \tfrac{9}{32}(1+\xi)(1-\eta^2)(1-3\eta)$$

$$\psi_7 = \tfrac{9}{32}(1-\xi)(1-\eta^2)(1+3\eta), \quad \psi_8 = \tfrac{9}{32}(1+\xi)(1-\eta^2)(1+3\eta)$$

$$\psi_9 = \tfrac{1}{32}(1-\xi)(1+\eta)[-10+9(\xi^2+\eta^2)], \quad \psi_{10} = \tfrac{9}{32}(1+\eta)(1-\xi^2)(1-3\xi)$$

$$\psi_{11} = \tfrac{9}{32}(1+\eta)(1-\xi^2)(1+3\xi), \quad \psi_{12} = \tfrac{1}{32}(1+\xi)(1+\eta)[-10+9(\xi^2+\eta^2)] \qquad (10.2.32)$$

10.2.4.1 Hermite cubic interpolation functions for rectangular elements

In the previous discussion, we developed only the Lagrange interpolation functions for triangular and rectangular elements. The Hermite family of interpolation functions, which interpolate the function and its derivatives (e.g., the Euler–Bernoulli beam element), are useful in connection with

finite element models of higher-order (i.e., fourth-order) equations. For the sake of completeness, while not presenting the details of the derivation, the Hermite cubic interpolation functions for two rectangular elements are summarized in Table 10.2.3. The first element is based on the interpolation of (u, $\partial u/\partial x$, $\partial u/\partial y$, $\partial^2 u/\partial x \partial y$) at each node and the second one is based on the interpolation of (u, $\partial u/\partial x$, $\partial u/\partial y$) at each node, where u is the dependent variable of a fourth-order differential equation whose weak form contains (u, $\partial u/\partial x$, $\partial u/\partial y$) as the primary variables. The node numbering system in Table 10.2.3 refers to that used in Fig. 10.2.11. The notation used in Table 10.2.3 and Fig. 10.2.11 is also followed in the computer program **FEM2D**.

Table 10.2.3 Interpolation functions for the linear and quadratic Lagrange rectangular elements, quadratic serendipity element, and Hermite cubic rectangular elements.[1]

Element type	Interpolation functions
Lagrange element	
Linear	
Nodes $i = 1, 2, 3, 4$	$\frac{1}{4}(1 + \xi\xi_i)(1 + \eta\eta_i)$
Quadratic	
Corner node i	$\psi_i = \frac{1}{4}\xi\xi_i(1 + \xi\xi_i)\,\eta\eta_i(1 + \eta\eta_i)$
Side node i, $\xi_i = 0$	$\psi_i = \frac{1}{2}\eta\eta_i(1 + \eta\eta_i)(1 - \xi^2)$
Side node i, $\eta_i = 0$	$\psi_i = \frac{1}{2}\xi\xi_i(1 + \xi\xi_i)(1 - \eta^2)$
Interior node i	$\psi_i = (1 - \xi^2)(1 - \eta^2)$
Quadratic serendipity element	
Corner node i	$\psi_i = \frac{1}{4}(1 + \xi\xi_i)(1 + \eta\eta_i)(\xi\xi_i + \eta\eta_i - 1)$
Side node i, $\xi_i = 0$	$\psi_i = \frac{1}{2}(1 - \xi^2)(1 + \eta\eta_i)$
Side node i, $\eta_i = 0$	$\psi_i = \frac{1}{2}(1 + \xi\xi_i)(1 - \eta^2)$
Hermite cubic element[2]	
Conforming element	$[I = 4(i - 1) + 1,\ i = 1, 2, 3, 4]$
$(u, \frac{\partial u}{\partial x}, \frac{\partial u}{\partial y}, \frac{\partial^2 u}{\partial x \partial y})$	$\varphi_I = \frac{1}{16}(\xi + \xi_i)^2(2 - \xi_0)(\eta + \eta_i)^2(2 - \eta_0)$
	$\varphi_{I+1} = -\frac{a}{16}\xi_i(\xi + \xi_i)^2(1 - \xi_0)(\eta + \eta_i)^2(2 - \eta_0)$
	$\varphi_{I+2} = -\frac{b}{16}(\xi + \xi_i)^2(2 - \xi_0)\eta_i(\eta + \eta_i)^2(1 - \eta_0)$
	$\varphi_{I+3} = \frac{ab}{16}\xi_i(\xi + \xi_i)^2(1 - \xi_0)\eta_i(\eta + \eta_i)^2(1 - \eta_0)$
Nonconforming element	$[I = 3(i - 1) + 1,\ i = 1, 2, 3, 4]$
$(u, \frac{\partial u}{\partial x}, \frac{\partial u}{\partial y})$	$\varphi_I = \frac{1}{8}(1 + \xi_0)(1 + \eta_0)(2 + \xi_0 + \eta_0 - \xi^2 - \eta^2)$
	$\varphi_{I+1} = \frac{a}{8}\xi_i(\xi_0 + 1)^2(\xi_0 - 1)(\eta_0 + 1)$
	$\varphi_{I+2} = \frac{b}{8}\eta_i(\xi_0 + 1)(\eta_0 + 1)^2(\eta_0 - 1)$

[1]See Fig. 10.2.11 for the coordinate system; (ξ_i, η_i) denote the natural coordinates of the ith node of the element; (x_c, y_c) are the global coordinates of the center of the element; and $2a$ and $2b$ are the sides of the rectangular element.

[2] $\xi = (x - x_c)/a,\ \ \eta = (y - y_c)/b,\ \ \xi_0 = \xi\xi_i,\ \ \eta_0 = \eta\eta_i.$

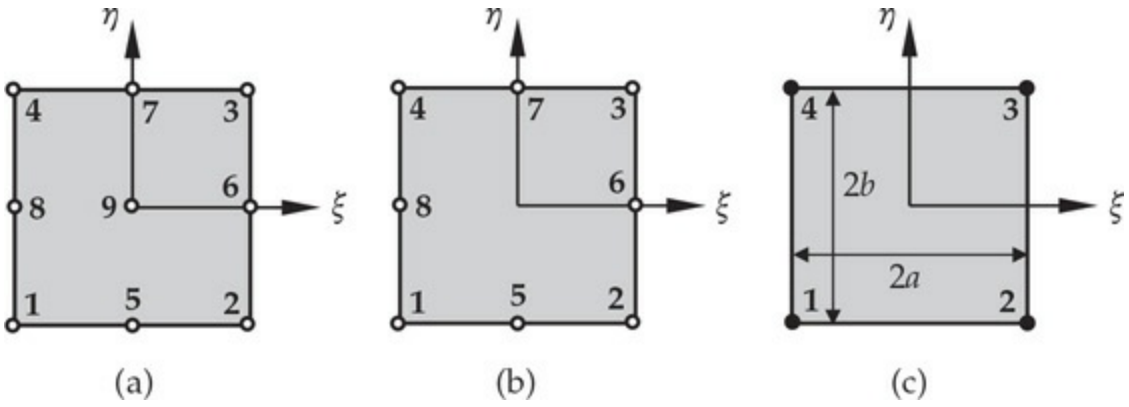

Fig. 10.2.11 Rectangular elements with the standard node numbering system: (a) linear and nine-node quadratic element; (b) quadratic serendipity element; and (c) Hermite cubic element.

10.3 Numerical Integration

10.3.1 Preliminary Comments

An accurate representation of irregular domains (e.g., domains with curved boundaries) can be accomplished by the use of refined meshes and/or higher-order elements. For example, a region with curved boundary cannot be represented exactly using linear elements; however, it can be represented, to a desired accuracy, using higher-order elements. Since it is simple to derive the interpolation functions for master triangular and rectangular elements of various orders and it is easy to evaluate integrals over these geometries using Gauss quadrature, we transform the integral expressions defined over arbitrary triangular and quadrilaterals to expressions defined over the master triangular and rectangular elements. Although the transformation of the variable coefficients of the differential equation from the problem coordinates (x, y) to the natural coordinates (ξ, η) results in algebraically complex integrands in terms of the natural coordinates (or area coordinates), only their evaluation at selected points is required to determine the values of the integrals.

Numerical integration schemes, such as the Gauss–Legendre numerical integration scheme, require the integral to be evaluated on a specific geometry and with respect to a specific coordinate system. The master triangular and rectangular elements with the natural coordinate system (ξ, η) allow us to use, for example, Gauss quadrature to evaluate element coefficients K_{ij}^e and f_i^e (which contain integrals of the interpolation

functions and their derivatives). Thus, the transformation of a given integral expression defined over a typical element Ω_e to one on the domain of the master element $\hat{\Omega}$ facilitates the numerical evaluation of the coefficients. Each element of the finite element mesh is transformed to $\hat{\Omega}$, only for the purpose of numerically evaluating the integrals. Once the numerical values of K_{ij}^e and f_i^e are determined through a quadrature rule, they are valid on the original element domain.

The transformation between Ω_e and $\hat{\Omega}$ [or equivalently, between (x, y) and (ξ, η)] is accomplished by a coordinate transformation of the form

$$x = \sum_{j=1}^{m} x_j^e \hat{\psi}_j^e(\xi, \eta), \quad y = \sum_{j=1}^{m} y_j^e \hat{\psi}_j^e(\xi, \eta) \tag{10.3.1}$$

where $\hat{\psi}_j^e$ are the finite element interpolation functions of the master element $\hat{\Omega}$. Although the Lagrange interpolation of the geometry is implied by Eq. (10.3.1), one can also use Hermite interpolation. Consider, as an example, the master element shown in Fig. 10.3.1. The coordinates in the master element are chosen to be the natural coordinates (ξ, η) such that $-1 \le (\xi, \eta) \le 1$. For this case, the $\hat{\psi}_j^e$ denote the interpolation functions of the four-node rectangular element shown in Fig. 10.2.7(a) (i.e., $m = 4$). The transformation in Eq. (10.3.1) maps a point (ξ, η) in the master element $\hat{\Omega}$ into a point (x, y) in element Ω_e, and vice versa if the Jacobian of the transformation is positive-definite. The transformation maps the line $\xi = 1$ in $\hat{\Omega}$ to a line in Ω_e defined parametrically by

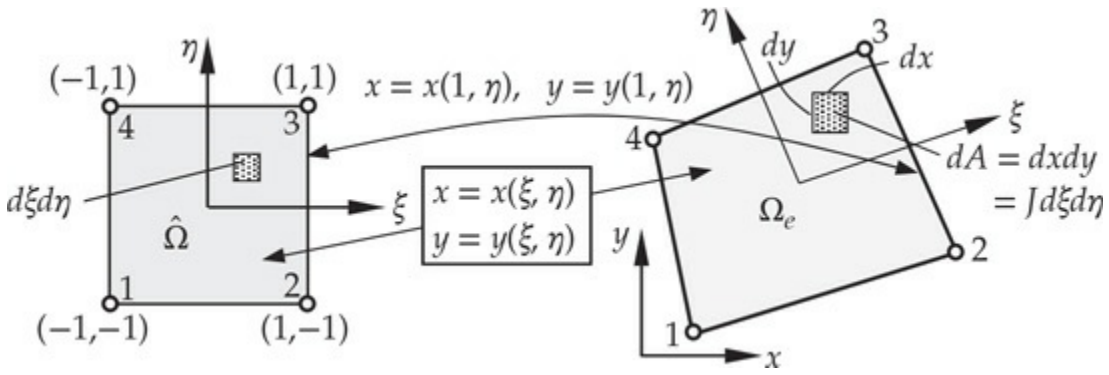

Fig. 10.3.1 Transformation of an arbitrary quadrilateral element to the master element.

$$x(1,\eta)=\sum_{i=1}^{4} x_i\hat{\psi}_i(1,\eta)=\tfrac{1}{2}(x_2+x_3)+\tfrac{1}{2}(x_3-x_2)\eta$$
$$y(1,\eta)=\sum_{i=1}^{4} y_i\hat{\psi}_i(1,\eta)=\tfrac{1}{2}(y_2+y_3)+\tfrac{1}{2}(y_3-y_2)\eta \qquad (10.3.2)$$

Similarly, the lines $\xi = -1$ and $\eta = \pm 1$ are mapped into straight lines in the element Ω_e (see Fig. 10.3.1). Thus, under the linear transformation the master element $\hat{\Omega}$ is mapped into a quadrilateral element in the (x, y) plane. Conversely, every quadrilateral element of a mesh can be mapped into the same master element $\hat{\Omega}$ in the (ξ, η) plane (see Fig. 10.3.2).

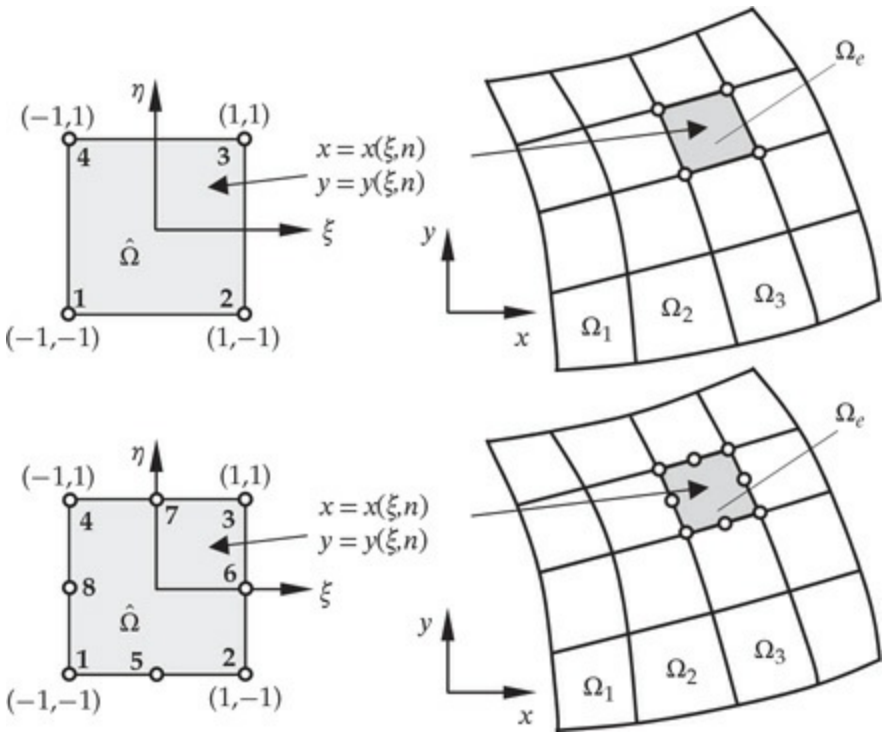

Fig. 10.3.2 Mapping of linear and quadratic quadrilateral elements of a finite element mesh to the respective master elements.

In general, the dependent variable(s) of the problem are approximated by expressions of the form

$$u(x,y)=\sum_{j=1}^{n} u_j^e\psi_j^e(x,y) \qquad (10.3.3)$$

The interpolation functions ψ_j^e used for the approximation of the dependent variable are, in general, different from $\hat{\psi}_j^e$ used in the approximation of the

geometry. Depending on the relative degree of approximations used for the geometry [see Eq. (10.3.1)] and the dependent variable(s) [see Eq. (10.3.3)], the finite element formulations are classified into three categories.

1. *Superparametric* ($m > n$): The approximation used for the geometry is higher order than that used for the dependent variable.
2. *Isoparametric* ($m = n$): Equal degree of approximation is used for both geometry and dependent variables.
3. *Subparametric* ($m < n$): Higher-order approximation of the dependent variable is used.

For example, in the finite element analysis of the Euler–Bernoulli beams, we used linear Lagrange interpolation of the geometry,

$$x = \sum_{j=1}^{2} x_j^e \hat{\psi}_j^e(\xi) \tag{10.3.4}$$

whereas the Hermite cubic interpolation was used to approximate the transverse deflection w. Such formulation falls into subparametric category. Since the axial displacement is approximated by the linear Lagrange interpolation functions, it can be said that isoparametric formulation is used for the axial displacement. Superparametric formulations are rarely used. Also, the approximation of geometry by Hermite family of interpolation functions is not common.

10.3.2 Coordinate Transformations

Once again we note that the transformation of a quadrilateral element of a mesh to the master element $\hat{\Omega}$ is solely for the purpose of numerically evaluating the integrals appearing in K_{ij}^e and f_i^e inside a computer program. Thus, in a finite element analysis there is *no transformation of the physical domain or the finite element mesh* involved. The resulting algebraic equations of the finite element formulation are always among the nodal values of the duality pairs (e.g., displacements and forces) of the problem. Element coefficients of different elements of the finite element mesh can be evaluated using the same master element. Master elements of different order define different transformations. For example, a cubic-order master rectangular element can be used to generate a mesh of cubic curvilinear quadrilateral elements. Thus, with the help of an appropriate master

element, any arbitrary element of a mesh can be generated. However, the transformations of a master element should be such that there exist no spurious gaps and element overlaps between adjacent elements. The elements in Figs. 10.2.5 and 10.2.7 can be used as master elements for generating meshes of triangular and quadrilateral elements.

When a typical element of the finite element mesh is transformed to its master element for the purpose of numerically evaluating integrals, the integrand of these integrals must be expressed in terms of the coordinates (ξ, η) of the master element. For example, consider the element coefficients

$$K_{ij}^e = \int_{\Omega^e} \left[a_{11}^e(x,y) \frac{\partial \psi_i^e}{\partial x} \frac{\partial \psi_j^e}{\partial x} + a_{22}^e(x,y) \frac{\partial \psi_i^e}{\partial y} \frac{\partial \psi_j^e}{\partial y} + a_{00}^e(x,y) \psi_i^e \psi_j^e \right] dx dy \qquad (10.3.5)$$

The integrand (i.e., the expression in the square brackets under the integral) is a function of the global coordinates x and y. We must rewrite it in terms of ξ and η using the transformation (10.3.1). Note that the integrand contains not only functions but also derivatives with respect to the global coordinates (x, y). Therefore, we must relate $\partial \psi_i^e / \partial x$ and $\partial \psi_i^e / \partial y$ to $\partial \psi_i^e / \partial \xi$ and $\partial \psi_i^e / \partial \eta$ using the transformation (10.3.1).

The functions $\psi_i^e(x, y)$ can be expressed in terms of the local coordinates ξ and η by means of Eq. (10.3.1): $\psi_i^e(x(\xi, \eta), y(\xi, \eta))$. By the chain rule of partial differentiation, we have

$$\frac{\partial \psi_i^e}{\partial \xi} = \frac{\partial \psi_i^e}{\partial x} \frac{\partial x}{\partial \xi} + \frac{\partial \psi_i^e}{\partial y} \frac{\partial y}{\partial \xi}$$
$$\frac{\partial \psi_i^e}{\partial \eta} = \frac{\partial \psi_i^e}{\partial x} \frac{\partial x}{\partial \eta} + \frac{\partial \psi_i^e}{\partial y} \frac{\partial y}{\partial \eta}$$

or, in matrix notation

$$\begin{Bmatrix} \frac{\partial \psi_i^e}{\partial \xi} \\ \frac{\partial \psi_i^e}{\partial \eta} \end{Bmatrix} = \begin{bmatrix} \frac{\partial x}{\partial \xi} & \frac{\partial y}{\partial \xi} \\ \frac{\partial x}{\partial \eta} & \frac{\partial y}{\partial \eta} \end{bmatrix}^e \begin{Bmatrix} \frac{\partial \psi_i^e}{\partial x} \\ \frac{\partial \psi_i^e}{\partial y} \end{Bmatrix} \equiv \mathbf{J}^e \begin{Bmatrix} \frac{\partial \psi_i^e}{\partial x} \\ \frac{\partial \psi_i^e}{\partial y} \end{Bmatrix} \qquad (10.3.6)$$

which gives the relation between the derivatives of ψ_i^e with respect to the global and local coordinates. The matrix $\mathbf{J}^e$ is called the *Jacobian matrix* of the transformation (10.3.1):

$$\mathbf{J}^e = \begin{bmatrix} \frac{\partial x}{\partial \xi} & \frac{\partial y}{\partial \xi} \\ \frac{\partial x}{\partial \eta} & \frac{\partial y}{\partial \eta} \end{bmatrix}^e \tag{10.3.7}$$

Note from the expression given for K_{ij}^e in Eq. (10.3.5) that we must relate $\partial\psi_i^e/\partial x$ and $\partial\psi_i^e/\partial y$ to $\partial\psi_i^e/\partial\xi$ and $\partial\psi_i^e/\partial\eta$, whereas Eq. (10.3.6) provides the inverse relations. Therefore, Eq. (10.3.6) must be inverted:

$$\begin{Bmatrix} \frac{\partial \psi_i^e}{\partial x} \\ \frac{\partial \psi_i^e}{\partial y} \end{Bmatrix} = (\mathbf{J}^e)^{-1} \begin{Bmatrix} \frac{\partial \psi_i^e}{\partial \xi} \\ \frac{\partial \psi_i^e}{\partial \eta} \end{Bmatrix}, \quad \det \mathbf{J}^e \equiv J^e \neq 0 \tag{10.3.8}$$

Although it is possible to write the relationship in Eq. (10.3.8) directly by means of the chain rule,

$$\begin{aligned} \frac{\partial \psi_i^e}{\partial x} &= \frac{\partial \psi_i^e}{\partial \xi}\frac{\partial \xi}{\partial x} + \frac{\partial \psi_i^e}{\partial \eta}\frac{\partial \eta}{\partial x} \\ \frac{\partial \psi_i^e}{\partial y} &= \frac{\partial \psi_i^e}{\partial \xi}\frac{\partial \xi}{\partial y} + \frac{\partial \psi_i^e}{\partial \eta}\frac{\partial \eta}{\partial y} \end{aligned} \tag{10.3.9}$$

it is not possible to evaluate $\partial\xi/\partial x$, $\partial\xi/\partial y$, $\partial\eta/\partial x$ and $\partial\eta/\partial y$ directly from the transformation equation (10.3.1).

The transformation equation (10.3.1) allows direct evaluation of $\partial x/\partial\xi$, $\partial x/\partial\eta$,$\partial y/\partial\xi$ and $\partial y/\partial\eta$, and therefore $\mathbf{J}^e$, as follows. Using the transformation (10.3.1), we can write

$$\begin{aligned} \frac{\partial x}{\partial \xi} &= \sum_{j=1}^{m} x_j \frac{\partial \hat{\psi}_j^e}{\partial \xi}, & \frac{\partial y}{\partial \xi} &= \sum_{j=1}^{m} y_j \frac{\partial \hat{\psi}_j^e}{\partial \xi} \\ \frac{\partial x}{\partial \eta} &= \sum_{j=1}^{m} x_j \frac{\partial \hat{\psi}_j^e}{\partial \eta}, & \frac{\partial y}{\partial \eta} &= \sum_{j=1}^{m} y_j \frac{\partial \hat{\psi}_j^e}{\partial \eta} \end{aligned} \tag{10.3.10a}$$

and

$$\mathbf{J}^e = \begin{bmatrix} \frac{\partial x}{\partial \xi} & \frac{\partial y}{\partial \xi} \\ \frac{\partial x}{\partial \eta} & \frac{\partial y}{\partial \eta} \end{bmatrix} = \begin{bmatrix} \sum_{i=1}^{m} x_i^e \frac{\partial \hat{\psi}_i^e}{\partial \xi} & \sum_{i=1}^{m} y_i^e \frac{\partial \hat{\psi}_i^e}{\partial \xi} \\ \sum_{i=1}^{m} x_i^e \frac{\partial \hat{\psi}_i^e}{\partial \eta} & \sum_{i=1}^{m} y_i^e \frac{\partial \hat{\psi}_i^e}{\partial \eta} \end{bmatrix}$$

$$= \begin{bmatrix} \frac{\partial \hat{\psi}_1^e}{\partial \xi} & \frac{\partial \hat{\psi}_2^e}{\partial \xi} & \cdots & \frac{\partial \hat{\psi}_m^e}{\partial \xi} \\ \frac{\partial \hat{\psi}_1}{\partial \eta} & \frac{\partial \hat{\psi}_2^e}{\partial \eta} & \cdots & \frac{\partial \hat{\psi}_m^e}{\partial \eta} \end{bmatrix} \begin{bmatrix} x_1^e & y_1^e \\ x_2^e & y_2^e \\ \vdots & \vdots \\ x_m^e & y_m^e \end{bmatrix} \tag{10.3.10b}$$

Thus, given the global coordinates (x_j^e, y_j^e) of element nodes and the interpolation functions $\hat{\psi}_j^e$ used for geometry, the Jacobian matrix can be evaluated using Eq. (10.3.10b). Note that $\hat{\psi}_j^e$ are different, in general, from ψ_j^e used in the approximation of the dependent variables. Only in isoparametric formulations, they are the same.

The computation of the global derivatives of ψ_i^e (i.e., derivatives of ψ_i^e with respect to x and y) in Eq. (10.3.8) requires the inverse of the Jacobian matrix. A necessary and sufficient condition for $(\mathbf{J}^e)^{-1}$ to exist is that the determinant $J^e = |\mathbf{J}^e|$, called the Jacobian, be nonzero at every point $(\xi\ \eta)$ in $\hat{\Omega}$:

$$J^e \equiv \det(\mathbf{J}^e) = \frac{\partial x}{\partial \xi}\frac{\partial y}{\partial \eta} - \frac{\partial x}{\partial \eta}\frac{\partial y}{\partial \xi} > 0 \tag{10.3.11}$$

The transformation should be algebraically simple so that the Jacobian matrix can be easily evaluated. Transformations of the form in Eq. (10.3.1) satisfy these requirements.

Example 10.3.1

The four-node master element is shown in Fig. 10.3.3(a). Consider the three-element mesh of quadrilaterals shown in Fig. 10.3.3(b). Elements 1 and 2 have counterclockwise element node numbering consistent with the node numbering in the master element and element 3 has node numbering opposite to that of the master element. Investigate the effect of node numbering and element convexity on the transformations from the master element to each of the three elements.

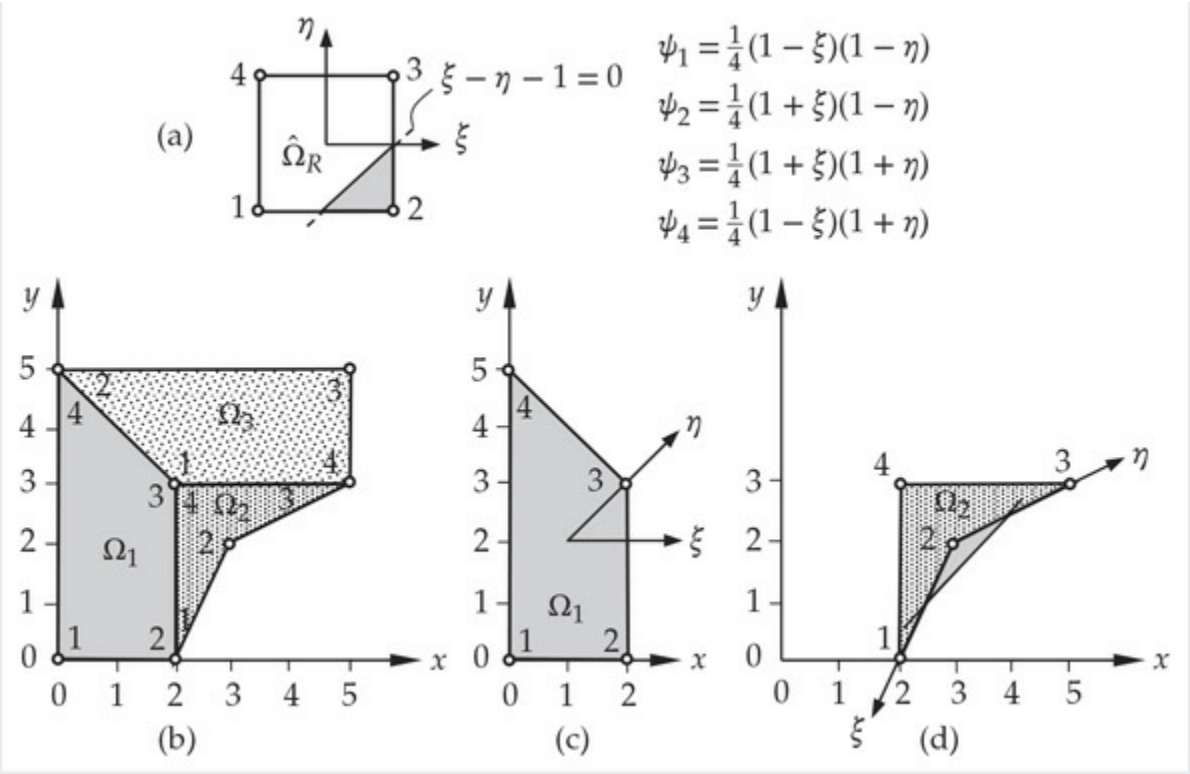

Fig. 10.3.3 Examples of transformations of the master rectangular element $\hat{\Omega}_R$.

Solution: The interpolation functions of the linear master element are shown in Fig. 10.3.3(a). First we compute the derivatives of $\hat{\psi}_i$:

$$\begin{aligned}
&\frac{\partial \hat{\psi}_1}{\partial \xi} = -\tfrac{1}{4}(1-\eta), \quad \frac{\partial \hat{\psi}_2}{\partial \xi} = \tfrac{1}{4}(1-\eta), \quad \frac{\partial \hat{\psi}_3}{\partial \xi} = \tfrac{1}{4}(1+\eta), \quad \frac{\partial \hat{\psi}_4}{\partial \xi} = -\tfrac{1}{4}(1+\eta) \\
&\frac{\partial \hat{\psi}_1}{\partial \eta} = -\tfrac{1}{4}(1-\xi), \quad \frac{\partial \hat{\psi}_2}{\partial \eta} = -\tfrac{1}{4}(1+\xi), \quad \frac{\partial \hat{\psi}_3}{\partial \eta} = \tfrac{1}{4}(1+\xi), \quad \frac{\partial \hat{\psi}_4}{\partial \eta} = \tfrac{1}{4}(1-\xi)
\end{aligned} \tag{1}$$

Then we compute the elements of the Jacobian matrix:

$$\frac{\partial x}{\partial \xi} = \sum_{i=1}^{4} x_i \frac{\partial \hat{\psi}_i}{\partial \xi} = \tfrac{1}{4}[-x_1(1-\eta) + x_2(1-\eta) + x_3(1+\eta) - x_4(1+\eta)]$$

$$\frac{\partial x}{\partial \eta} = \sum_{i=1}^{4} x_i \frac{\partial \hat{\psi}_i}{\partial \eta} = \tfrac{1}{4}[-x_1(1-\xi) - x_2(1+\xi) + x_3(1+\xi) + x_4(1-\xi)]$$

$$\frac{\partial y}{\partial \xi} = \sum_{i=1}^{4} y_i \frac{\partial \hat{\psi}_i}{\partial \xi} = \tfrac{1}{4}[-y_1(1-\eta) + y_2(1-\eta) + y_3(1+\eta) - y_4(1+\eta)] \tag{2}$$

$$\frac{\partial y}{\partial \eta} = \sum_{i=1}^{4} y_i \frac{\partial \hat{\psi}_i}{\partial \eta} = \tfrac{1}{4}[-y_1(1-\xi) - y_2(1+\xi) + y_3(1+\xi) + y_4(1-\xi)]$$

Elements 1 and 3 are *convex* domains in the sense that the line segment connecting any two arbitrary points of a convex domain lies entirely in the element. Clearly, element 2 is not convex because, for example, the line segment joining nodes 1 and 3 is not entirely inside the element.

Element 1. We have $x_1 = x_4 = 0$, $x_2 = x_3 = 2$; $y_1 = y_2 = 0$, $y_3 = 3$, $y_4 = 5$ [see Fig. 10.3.3(c)]. The transformation and Jacobian are given by

$$x = 2\hat{\psi}_2 + 2\hat{\psi}_3 = 1 + \xi, \qquad y = 3\hat{\psi}_3 + 5\hat{\psi}_4 = (1+\eta)(2 - \tfrac{1}{2}\xi) \tag{3}$$

$$J = \det \mathbf{J} = \begin{vmatrix} \frac{\partial x}{\partial \xi} & \frac{\partial y}{\partial \xi} \\ \frac{\partial x}{\partial \eta} & \frac{\partial y}{\partial \eta} \end{vmatrix} = \begin{vmatrix} 1 & -\frac{1}{2}(1+\eta) \\ 0 & 2 - \frac{1}{2}\xi \end{vmatrix} = \tfrac{1}{2}(4 - \xi) > 0 \tag{4}$$

Clearly, the Jacobian is linear in ξ, and for all values of ξ in $-1 \le \xi \le 1$, it is positive. Therefore, the transformation in Eq. (3) is invertible:

$$1 + \xi = x, \quad 1 + \eta = \frac{2y}{5 - x}$$

Element 2. Here we have $x_1 = x_4 = 2$, $x_2 = 3$, $x_3 = 5$, $y_1 = 0$, $y_2 = 2$, and $y_3 = y_4 = 3$ [see Fig. 10.3.3(d)]. The transformation and the Jacobian are given by

$$x = 3 + \xi + \tfrac{1}{2}\eta + \tfrac{1}{2}\xi\eta, \qquad y = 2 + \tfrac{1}{2}\xi + \eta - \tfrac{1}{2}\xi\eta \tag{5}$$

$$J = \begin{vmatrix} \frac{\partial x}{\partial \xi} & \frac{\partial y}{\partial \xi} \\ \frac{\partial x}{\partial \eta} & \frac{\partial y}{\partial \eta} \end{vmatrix} = \begin{vmatrix} 1 + \frac{1}{2}\eta & \frac{1}{2}(1-\eta) \\ \frac{1}{2}(1+\xi) & 1 - \frac{1}{2}\xi \end{vmatrix} = \tfrac{3}{4}(1 + \eta - \xi) \tag{6}$$

The Jacobian is *not* nonzero everywhere in the master element. It is zero

along the line $\xi = 1 + \eta$, and it is negative in the shaded area of the master element [see Fig. 10.3.3(a)]. Moreover, this area is mapped into the shaded area outside element 2. Thus, elements with any interior angle greater than π should not be used in any finite element mesh.

Element 3. We have $x_1 = 2$, $x_2 = 0$, $x_3 = x_4 = 5$, $y_1 = y_4 = 3$, and $y_2 = y_3 = 5$ [see Fig. 10.3.3(b)]. The transformation and the Jacobian become (note that the nodes are numbered clockwise)

$$x = 3 - \tfrac{1}{2}\xi + 2\eta + \tfrac{1}{2}\xi\eta, \quad y = 4 + \xi \tag{7}$$

$$J = \begin{vmatrix} \frac{\partial x}{\partial \xi} & \frac{\partial y}{\partial \xi} \\ \frac{\partial x}{\partial \eta} & \frac{\partial y}{\partial \eta} \end{vmatrix} = \begin{vmatrix} -\frac{1}{2}(1-\eta) & 1 \\ 2 + \frac{1}{2}\xi & 0 \end{vmatrix} = -(2 + \tfrac{1}{2}\xi) < 0 \tag{8}$$

The negative Jacobian indicates that a right-hand coordinate system is mapped into a left-hand coordinate system. Such coordinate transformations should be avoided.

The above example illustrates, for the four-node master element, that non-convex elements are not admissible in finite element meshes. In general, any interior angle θ (see Fig. 10.3.4) should not be too small or too large because the Jacobian $J = (|d\mathbf{r}_1||d\mathbf{r}_2| \sin\theta)/d\xi d\eta$ will be very small. Similar restrictions hold for higher-order master elements. Additional restrictions also exist for higher-order elements. For example, for higher-order triangular and rectangular elements the placing of the side and interior nodes is restricted. For the eight-node rectangular element, it can be shown that the side nodes should be placed at a distance greater than or equal to a quarter of the length of the side from either corner node (see Fig. 10.3.4).

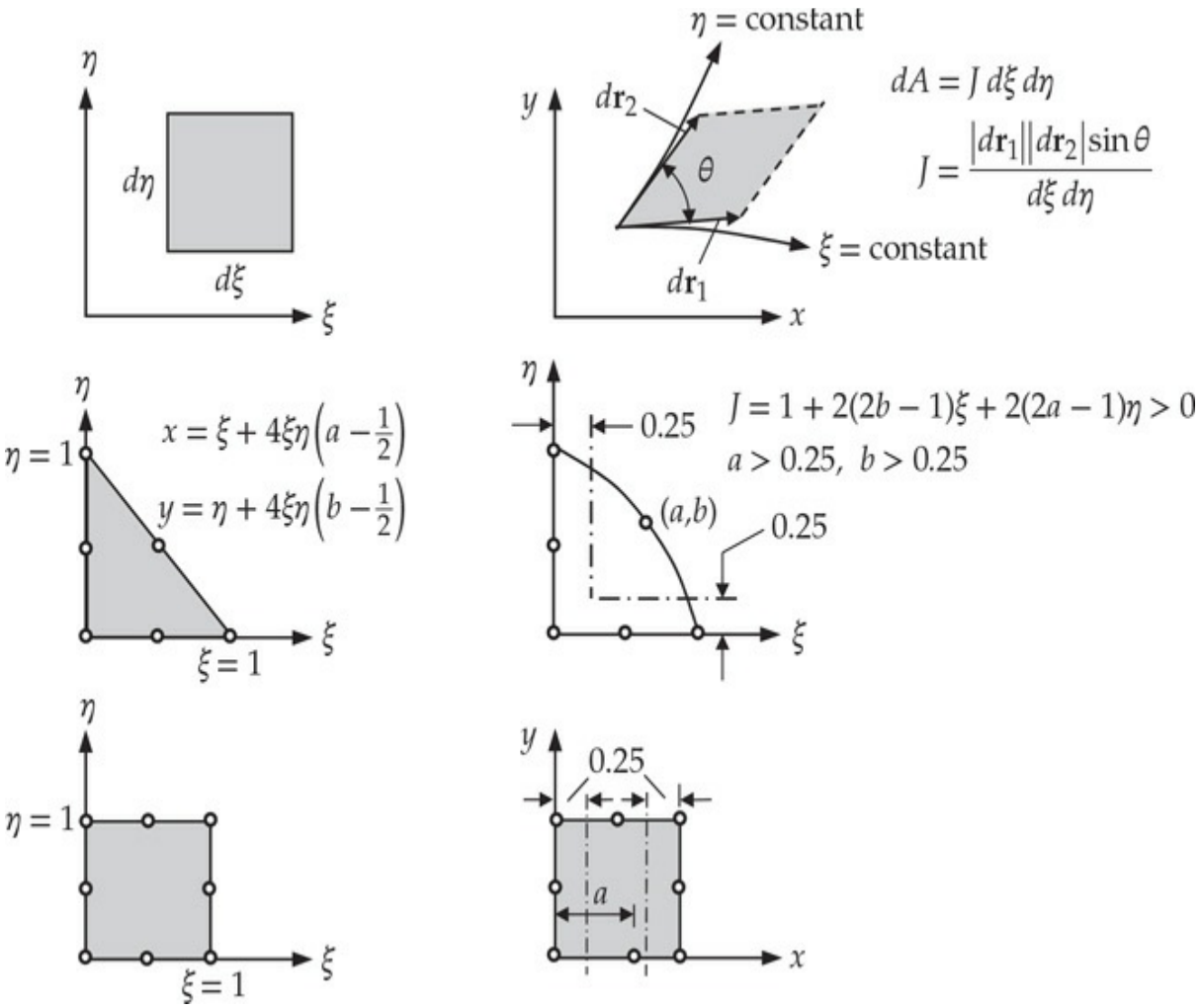

Fig. 10.3.4 Some restrictions on element transformations.

Returning to numerical evaluation of integrals, we have from Eq. (10.3.8),

$$\begin{Bmatrix} \dfrac{\partial \psi_i^e}{\partial x} \\ \dfrac{\partial \psi_i^e}{\partial y} \end{Bmatrix} = (\mathbf{J}^e)^{-1} \begin{Bmatrix} \dfrac{\partial \psi_i^e}{\partial \xi} \\ \dfrac{\partial \psi_i^e}{\partial \eta} \end{Bmatrix} \equiv \mathbf{J}^{*e} \begin{Bmatrix} \dfrac{\partial \psi_i^e}{\partial \xi} \\ \dfrac{\partial \psi_i^e}{\partial \eta} \end{Bmatrix} \tag{10.3.12}$$

where J_{ij}^{*e} is the element in position (i, j) of the inverse of the Jacobian matrix,

$$(\mathbf{J}^e)^{-1} \equiv \mathbf{J}^{*e} = \begin{bmatrix} J_{11}^{*e} & J_{12}^{*e} \\ J_{21}^{*e} & J_{22}^{*e} \end{bmatrix} \tag{10.3.13}$$

The element area $dA = dx\, dy$ in element Ω_e is transformed to

$$dA \equiv dx\, dy = J^e\, d\xi\, d\eta \tag{10.3.14}$$

in the master element $\hat{\Omega}$. The matrix **J** can be viewed as a mapping of points from Ω_e into points in $\hat{\Omega}$ and $\mathbf{J}^* = \mathbf{J}^{-1}$ as a mapping of points from $\hat{\Omega}$ to points in Ω_e. If the determinant J is a constant, for example, it represents the increase or decrease of an area element from $\hat{\Omega}$ to Ω_e.

Equations (10.3.8), (10.3.10b), (10.3.13), and (10.3.14) provide the necessary relations to transform integral expressions on any element Ω_e to an associated master element $\hat{\Omega}$. For instance, consider the integral expression in Eq. (10.3.5). Suppose that the mesh of finite elements is generated by a master element $\hat{\Omega}$.
Then we can write K_{ij}^e over the master element as

$$
\begin{aligned}
K_{ij}^e &= \int_{\Omega_e} \left(a_{11} \frac{\partial \psi_i}{\partial x} \frac{\partial \psi_j}{\partial x} + a_{22} \frac{\partial \psi_i}{\partial y} \frac{\partial \psi_j}{\partial y} + a_{00} \psi_i \psi_j \right) dx dy \\
&= \int_{\hat{\Omega}} \left[\hat{a}_{11} \left(J_{11}^* \frac{\partial \psi_i}{\partial \xi} + J_{12}^* \frac{\partial \psi_i}{\partial \eta} \right) \left(J_{11}^* \frac{\partial \psi_j}{\partial \xi} + J_{12}^* \frac{\partial \psi_j}{\partial \eta} \right) \right. \\
&\quad \left. + \hat{a}_{22} \left(J_{21}^* \frac{\partial \psi_i}{\partial \xi} + J_{22}^* \frac{\partial \psi_i}{\partial \eta} \right) \left(J_{21}^* \frac{\partial \psi_j}{\partial \xi} + J_{22}^* \frac{\partial \psi_j}{\partial \eta} \right) + \hat{a}_{00} \psi_i \psi_j \right] J \, d\xi d\eta \\
&\equiv \int_{\hat{\Omega}} F_{ij}(\xi, \eta) \, d\xi d\eta
\end{aligned}
\tag{10.3.15a}
$$

where

$$
\begin{aligned}
F_{ij}^e = &\left[\hat{a}_{11} \left(J_{11}^* \frac{\partial \psi_i}{\partial \xi} + J_{12}^* \frac{\partial \psi_i}{\partial \eta} \right) \left(J_{11}^* \frac{\partial \psi_j}{\partial \xi} + J_{12}^* \frac{\partial \psi_j}{\partial \eta} \right) \right. \\
&\left. + \hat{a}_{22} \left(J_{21}^* \frac{\partial \psi_i}{\partial \xi} + J_{22}^* \frac{\partial \psi_i}{\partial \eta} \right) \left(J_{21}^* \frac{\partial \psi_j}{\partial \xi} + J_{22}^* \frac{\partial \psi_j}{\partial \eta} \right) + \hat{a}_{00} \psi_i \psi_j \right] J
\end{aligned}
\tag{10.3.15b}
$$

Here J_{ij}^{*e} are the elements of the inverse of the Jacobian matrix in Eq. (10.3.13) and $\hat{a}_{ij} = a_{ij}(x(\xi, \eta), y(\xi, \eta))$. Equations (10.3.8), (10.3.10b), and (10.3.13)–(10.3.15b) are valid for master elements of both rectangular and triangular geometries. The master triangular and rectangular elements for linear and quadratic triangular and quadrilateral elements are shown in Fig. 10.3.5.

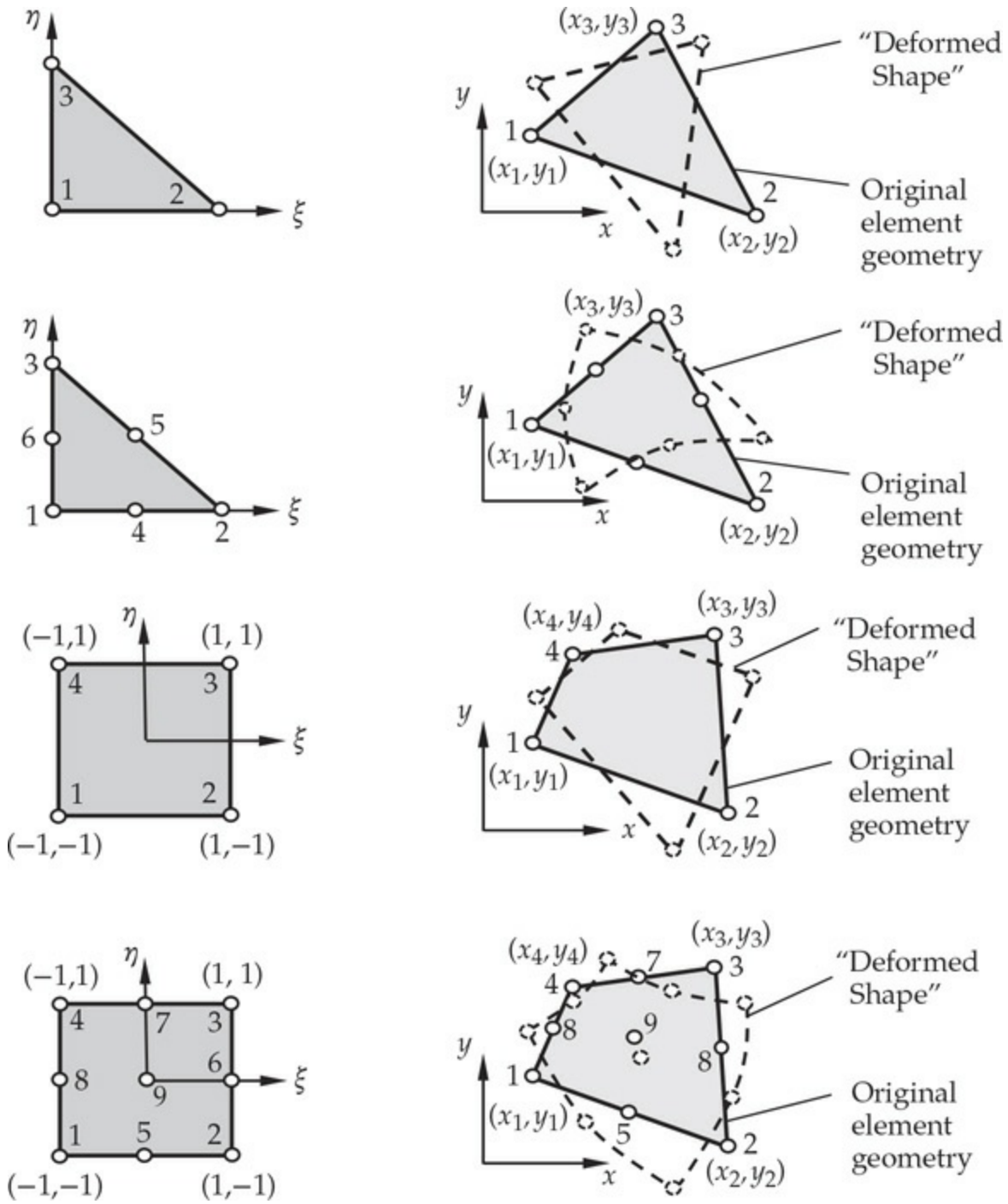

Fig. 10.3.5 Linear and quadratic master finite elements and their typical counterparts in the problem coordinate system. “Deformed Shape” refers to structural problems where the geometry of the body undergoes changes; element geometries do not change in heat transfer and fluid mechanics type–applications.

10.3.3 Numerical Integration over Master Rectangular Element

Quadrature formulas for integrals defined over a rectangular master

element $\hat{\Omega}_R$ (such as those shown in Fig. 10.3.5) can be derived from the one-dimensional quadrature formulas presented in Section 8.2. We have

$$\int_{\hat{\Omega}_R} F(\xi,\eta)d\xi d\eta = \int_{-1}^{1}\left[\int_{-1}^{1} F(\xi,\eta)d\eta\right]d\xi \approx \int_{-1}^{1}\left[\sum_{J=1}^{N} F(\xi,\eta_J)W_J\right]d\xi$$

$$\approx \sum_{I=1}^{M}\sum_{J=1}^{N} F(\xi_I,\eta_J)W_I W_J \qquad (10.3.16)$$

where M and N denote the number of quadrature points in the ξ and η directions, (ξ_I, η_J) are the Gauss points, and W_I and W_J are the corresponding Gauss weights (see Table 8.2.2). The selection of the number of Gauss points is based on the same formula as that given in Section 8.2.5.2: a polynomial of degree p is integrated exactly employing $N = \text{int}[\frac{1}{2}(p+1)]$; that is, the smallest integer greater than $\frac{1}{2}(p+1)$. In most cases, the interpolation functions are of the same degree in both ξ and η, and therefore one has $M = N$. When the integrand is of different degree in ξ and η, the number of Gauss points is selected on the basis of the largest-degree polynomial. The minimum allowable quadrature rule is one that computes the mass of the element exactly when the density is a constant.

The $N \times N$ Gauss point locations are given by the *tensor product* of one-dimensional Gauss points in each of the coordinate directions, ξ_I and η_J:

$$\begin{Bmatrix} \xi_1 \\ \xi_2 \\ \vdots \\ \xi_N \end{Bmatrix} \{\eta_1, \eta_2, \ldots, \eta_N\} \equiv \begin{bmatrix} (\xi_1,\eta_1) & (\xi_1,\eta_2) & \cdots & (\xi_1,\eta_N) \\ (\xi_2,\eta_1) & (\xi_2,\eta_2) & \cdots & (\xi_2,\eta_N) \\ \vdots & & \ddots & \vdots \\ (\xi_N,\eta_1) & (\xi_N,\eta_2) & \cdots & (\xi_N,\eta_N) \end{bmatrix} \qquad (10.3.17)$$

The values of ξ_I (the same values are valid for η_I) for $I = 1, 2, \ldots, 10$ are presented in Table 8.2.2.

Table 10.3.1 contains information on the selection of the integration order and the location of the Gauss points for linear, quadratic, and cubic rectangular master elements. The maximum degree of the polynomial refers to the degree of the highest polynomial in ξ or η that is present in the integrands of the element matrices of the type in Eq. (10.3.15a). Note that the polynomial degree of coefficients as well as J_{ij}^{*e} and J^e should be

accounted for in determining the total polynomial degree of the integrand. Of course, the coefficients a_{11}, a_{22}, and a_{00}, and J_{ij}^{*e}, in general, may not be polynomials. In those cases, their functional variations must be approximated by a suitable polynomial in order to determine the polynomial degree of the integrand.

Table 10.3.1 Residual order and the Gauss point locations for linear, quadratic, and cubic master elements (nodes are not shown).

Order of the Gauss rule	Residual order*	Location of Gauss points[1]
2×2	$O(h^4)$	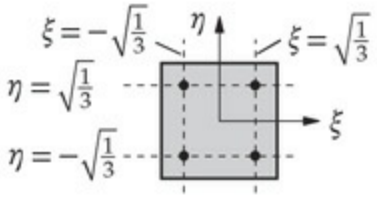
3×3	$O(h^6)$	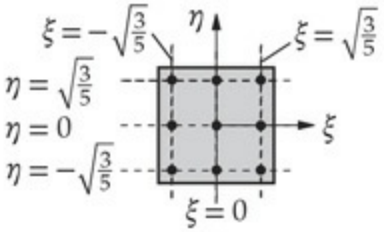
4×4	$O(h^8)$	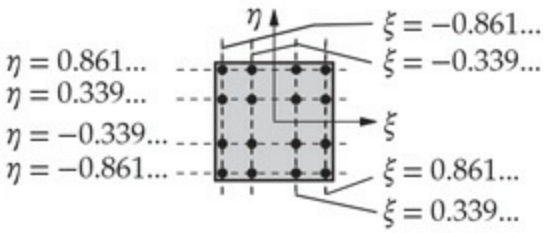

*$O(h^p)$ means polynomial of order $p-1$ is exactly evaluated by the Gauss rule.
[1]See Table 8.2.2 for the integration points and weights for each coordinate direction.

The next two examples illustrate the evaluation of the Jacobian and element matrices on rectangular elements.

Example 10.3.2

Consider the quadrilateral element Ω_1 shown in Fig. 10.3.3(b). Express $\partial\psi_i/\partial x$ and $\partial\psi_i/\partial y$ in terms of (ξ, η) using linear master square element.

Solution: The interpolation functions of the master element are [see Fig. 10.3.3(a)]

$$\psi_i = \tfrac{1}{4}(1+\xi\xi_i)(1+\eta\eta_i), \quad \frac{\partial\psi_i}{\partial\xi} = \tfrac{1}{4}\xi_i(1+\eta\eta_i), \quad \frac{\partial\psi_i}{\partial\eta} = \tfrac{1}{4}\eta_i(1+\eta\eta_i) \tag{1}$$

where (ξ_i, η_i) are the local coordinates of the ith node in the master element: $(\xi_1, \eta_1) = (-1, -1)$, $(\xi_2, \eta_2) = (1, -1)$, $(\xi_3, \eta_3) = (1, 1)$, and $(\xi_4, \eta_4) = (-1, 1)$. The Jacobian matrix is given by

$$\mathbf{J} = \begin{bmatrix} \frac{\partial x}{\partial\xi} & \frac{\partial y}{\partial\xi} \\ \frac{\partial x}{\partial\eta} & \frac{\partial y}{\partial\eta} \end{bmatrix} = \frac{1}{4}\begin{bmatrix} -(1-\eta) & 1-\eta & 1+\eta & -(1+\eta) \\ -(1-\xi) & -(1+\xi) & 1+\xi & 1-\xi \end{bmatrix}\begin{bmatrix} 0.0 & 0.0 \\ 2.0 & 0.0 \\ 2.0 & 3.0 \\ 0.0 & 5.0 \end{bmatrix}$$

$$= \begin{bmatrix} 1 & -\frac{1}{2}(1+\eta) \\ 0 & \frac{1}{2}(4-\xi) \end{bmatrix} \tag{2}$$

The inverse of the Jacobian matrix is given by

$$\mathbf{J}^{-1} = \begin{bmatrix} 1 & \frac{1+\eta}{4-\xi} \\ 0 & \frac{2}{4-\xi} \end{bmatrix}, \quad J^*_{11} = 1, \; J^*_{21} = 0, \; J^*_{12} = \frac{1+\eta}{4-\xi}, \; J^*_{22} = \frac{2}{4-\xi} \tag{3}$$

From Eq. (10.3.8), we have

$$\frac{\partial\psi_i}{\partial x} = \frac{\partial\psi_i}{\partial\xi} + \frac{1+\eta}{4-\xi}\frac{\partial\psi_i}{\partial\eta}, \quad \frac{\partial\psi_i}{\partial y} = \frac{2}{4-\xi}\frac{\partial\psi_i}{\partial\eta} \tag{4}$$

Thus, we have

$$\begin{aligned} \frac{\partial\psi_i}{\partial x} &= \tfrac{1}{4}\xi_i(1+\eta\eta_i) + \tfrac{1}{4}\left(\tfrac{1+\eta}{4-\xi}\right)(1+\xi\xi_i)\eta_i \\ \frac{\partial\psi_i}{\partial y} &= \frac{1}{2(4-\xi)}(1+\xi\xi_i)\eta_i \end{aligned} \tag{5}$$

Example 10.3.3

Consider the quadrilateral element in Fig. 10.3.6. Compute the following element matrices using the Gauss quadrature:

$$\begin{aligned} S^{00}_{ij} &= \int_\Omega \psi_i\psi_j\,dx\,dy, & S^{11}_{ij} &= \int_\Omega \frac{\partial\psi_i}{\partial x}\frac{\partial\psi_j}{\partial x}\,dx\,dy \\ S^{22}_{ij} &= \int_\Omega \frac{\partial\psi_i}{\partial y}\frac{\partial\psi_j}{\partial y}\,dx\,dy, & S^{12}_{ij} &= \int_\Omega \frac{\partial\psi_i}{\partial x}\frac{\partial\psi_j}{\partial y}\,dx\,dy \end{aligned} \tag{1}$$

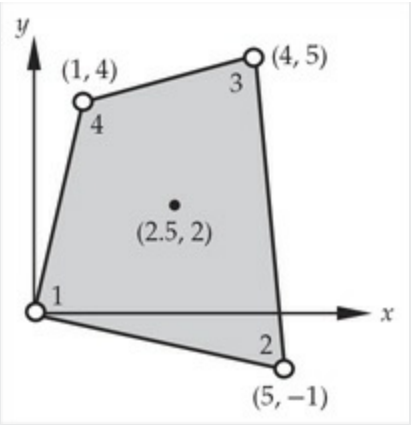

Fig. 10.3.6 Geometry of the linear quadrilateral element used in **Example 10.3.3**.

Solution: The transformation equations are

$$\begin{aligned} x &= 0\cdot\hat{\psi}_1 + 5\hat{\psi}_2 + 4\hat{\psi}_3 + 1\cdot\hat{\psi}_4 = \tfrac{1}{2}(5 + 4\xi - \xi\eta) \\ y &= 0\cdot\hat{\psi}_1 - 1\cdot\hat{\psi}_2 + 5\hat{\psi}_3 + 4\hat{\psi}_4 = \tfrac{1}{2}(4 + 5\eta + \xi\eta) \end{aligned} \tag{2}$$

The Jacobian matrix and its inverse are

$$\begin{aligned} \mathbf{J} &= \begin{bmatrix} \frac{\partial x}{\partial \xi} & \frac{\partial y}{\partial \xi} \\ \frac{\partial x}{\partial \eta} & \frac{\partial y}{\partial \eta} \end{bmatrix} = \frac{1}{2}\begin{bmatrix} 4-\eta & \eta \\ -\xi & 5+\xi \end{bmatrix} \\ J &= \tfrac{1}{4}\left[(4-\eta)(5+\xi) + \xi\eta\right] = \tfrac{1}{4}(20 + 4\xi - 5\eta) \end{aligned} \tag{3}$$

$$\mathbf{J}^{-1} = \frac{1}{2J}\begin{bmatrix} 5+\xi & -\eta \\ \xi & 4-\eta \end{bmatrix}, \quad J_{11}^{*} = \frac{2(5+\xi)}{20+4\xi-5\eta}, \quad J_{12}^{*} = -\frac{2\eta}{20+4\xi-5\eta}$$
$$J_{21}^{*} = \frac{2\xi}{20+4\xi-5\eta}, \quad J_{22}^{*} = \frac{2(4-\eta)}{20+4\xi-5\eta} \tag{4}$$

The matrix **J** transforms base vectors $\hat{\mathbf{e}}_x = (1,0)$ and $\hat{\mathbf{e}}_x = (1,0)$ in the *xy*-system to the base vectors $\hat{\mathbf{e}}_\xi$ and $\hat{\mathbf{e}}_\eta$ in the $\xi\eta$-system:

$$\begin{aligned} \frac{1}{2}\begin{bmatrix} 4-\eta & \eta \\ -\xi & 5+\xi \end{bmatrix}\begin{Bmatrix} 1 \\ 0 \end{Bmatrix} &= \frac{1}{2}\begin{Bmatrix} 4-\eta \\ -\xi \end{Bmatrix} \\ \frac{1}{2}\begin{bmatrix} 4-\eta & \eta \\ -\xi & 5+\xi \end{bmatrix}\begin{Bmatrix} 0 \\ 1 \end{Bmatrix} &= \frac{1}{2}\begin{Bmatrix} \eta \\ 5+\xi \end{Bmatrix} \end{aligned} \tag{5}$$

Therefore, we have

$$\hat{\mathbf{e}}_\xi = \tfrac{1}{2}\left[(4-\eta)\hat{\mathbf{e}}_x - \xi\hat{\mathbf{e}}_y\right], \quad \hat{\mathbf{e}}_\eta = \tfrac{1}{2}\left[\eta\hat{\mathbf{e}}_x + (5+\xi)\hat{\mathbf{e}}_y\right] \tag{6}$$

Hence, the area element $dxdy$ in the xy-system is related to the area element $d\xi d\eta$ in the $\xi\eta$-system by

$$dxdy = \frac{1}{4}\begin{vmatrix} 4-\eta & \eta \\ -\xi & 5+\xi \end{vmatrix} d\xi d\eta = J\, d\xi d\eta \tag{7}$$

The coefficients S_{ij}^{00} and S_{ij}^{11}, for example, can be expressed in natural coordinates (for numerical evaluation) as

$$S_{ij}^{00} = \int_{\Omega_e} \psi_i \psi_j \, dx\, dy = \int_{-1}^{1}\int_{-1}^{1} \psi_i \psi_j J \, d\xi \, d\eta$$

$$S_{ij}^{11} = \int_{\Omega_e} \frac{\partial \psi_i}{\partial x}\frac{\partial \psi_j}{\partial x}\, dx\, dy$$

$$= \int_{-1}^{1}\int_{-1}^{1} \left(J_{11}^{*}\frac{\partial \psi_i}{\partial \xi} + J_{12}^{*}\frac{\partial \psi_i}{\partial \eta}\right)\left(J_{11}^{*}\frac{\partial \psi_j}{\partial \xi} + J_{12}^{*}\frac{\partial \psi_j}{\partial \eta}\right) J \, d\xi \, d\eta$$

where $\partial\psi_i/\partial\xi$ and $\partial\psi_i/\partial\eta$ are given in Eq. (1) of **Example 10.3.1**. Note that the integrand of S_{ij}^{00} is a polynomial of the order $p = 3$ in each coordinate ξ and η. Hence, $N = M = [(p + 1)/2] = 2$ will evaluate S_{ij}^{00} exactly. For example, consider the coefficient S_{11}^{00}:

$$S_{11}^{00} = \int_{\Omega_e} \psi_1 \psi_1 \, dx\, dy = \int_{-1}^{1}\int_{-1}^{1} \psi_1 \psi_1 J \, d\xi \, d\eta$$

$$= \frac{1}{64}\int_{-1}^{1}\int_{-1}^{1} (1-\xi)^2(1-\eta)^2(20 + 4\xi - 5\eta) d\xi \, d\eta$$

$$= \frac{1}{64}\sum_{I=1}^{2}\left[\sum_{J=1}^{2}(1-\xi_I)^2(1-\eta_J)^2(20 + 4\xi_I - 5\eta_J)\right] W_I W_J \tag{8}$$

where (ξ_I, η_J) are the Gauss points

$$(\xi_1, \eta_1) = \left(-\frac{1}{\sqrt{3}}, -\frac{1}{\sqrt{3}}\right), \quad (\xi_1, \eta_2) = \left(-\frac{1}{\sqrt{3}}, \frac{1}{\sqrt{3}}\right)$$

$$(\xi_2, \eta_1) = \left(\frac{1}{\sqrt{3}}, -\frac{1}{\sqrt{3}}\right), \quad (\xi_2, \eta_2) = \left(\frac{1}{\sqrt{3}}, \frac{1}{\sqrt{3}}\right) \tag{9}$$

We have ($W_1 = W_2 = 1$)

$$S_{11}^{00} = \frac{1}{64}\left[\left(1+\frac{1}{\sqrt{3}}\right)^4\left(20+\frac{1}{\sqrt{3}}\right)+\left(1+\frac{1}{\sqrt{3}}\right)^2\left(1-\frac{1}{\sqrt{3}}\right)^2\left(20-\frac{9}{\sqrt{3}}\right)\right.$$
$$\left.+\left(1-\frac{1}{\sqrt{3}}\right)^2\left(1+\frac{1}{\sqrt{3}}\right)^2\left(20+\frac{9}{\sqrt{3}}\right)+\left(1-\frac{1}{\sqrt{3}}\right)^4\left(20-\frac{1}{\sqrt{3}}\right)\right]$$
$$= \frac{1}{64}\left[\frac{1120}{9}+\frac{160}{9}+\frac{32}{3\sqrt{3}}\left(-\frac{4}{\sqrt{3}}+\frac{5}{\sqrt{3}}\right)\right] = \frac{1312}{576} = 2.27778 \tag{10}$$

Similarly, consider the coefficient S_{12}^{11}:

$$S_{12}^{11} = \int_{\Omega_e} \frac{\partial\psi_1}{\partial x}\frac{\partial\psi_2}{\partial x}\,dx\,dy$$
$$= \int_{-1}^{1}\int_{-1}^{1}\left(J_{11}^{*}\frac{\partial\psi_1}{\partial\xi}+J_{12}^{*}\frac{\partial\psi_1}{\partial\eta}\right)\left(J_{11}^{*}\frac{\partial\psi_2}{\partial\xi}+J_{12}^{*}\frac{\partial\psi_2}{\partial\eta}\right)J\,d\xi\,d\eta$$
$$= \frac{1}{64}\int_{-1}^{1}\int_{-1}^{1}\left[-(10+2\xi)(1-\eta)+2\eta(1-\xi)\right]\left[(10+2\xi)(1-\eta)+2\eta(1-\xi)\right]$$
$$\times\frac{1}{(20+4\xi-5\eta)}\,d\xi\,d\eta$$
$$= \frac{1}{64}\int_{-1}^{1}\int_{-1}^{1}\left[-(10+2\xi)^2(1-\eta)^2+4\eta^2(1-\xi)^2\right]\frac{1}{(20+4\xi-5\eta)}\,d\xi\,d\eta \tag{11}$$

which is a ratio of polynomials. Hence, we do not expect to obtain the "exact" value of the integral for any number of of Gauss points. A 2 × 2 Gauss rule gives

$$S_{12}^{11} = \frac{1}{64}\int_{-1}^{1}\int_{-1}^{1}\left[-(10+2\xi)^2(1-\eta)^2 + 4\eta^2(1-\xi)^2\right]\frac{1}{(20+4\xi-5\eta)}\,d\xi\,d\eta$$

$$\approx \sum_{i,j=1}^{2}\left[-(10+2\xi_i)^2(1-\eta_j)^2 + 4\eta_j^2(1-\xi_i)^2\right]\frac{W_iW_j}{64\,(20+4\xi_i-5\eta_j)}$$

$$= \left[-\left(10-\frac{2}{\sqrt{3}}\right)^2\left(1+\frac{1}{\sqrt{3}}\right)^2 + \frac{4}{3}\left(1+\frac{1}{\sqrt{3}}\right)^2\right]\frac{1}{64\left(20+\frac{1}{\sqrt{3}}\right)}$$

$$+ \left[-\left(10+\frac{2}{\sqrt{3}}\right)^2\left(1+\frac{1}{\sqrt{3}}\right)^2 + \frac{4}{3}\left(1-\frac{1}{\sqrt{3}}\right)^2\right]\frac{1}{64\left(20+\frac{9}{\sqrt{3}}\right)}$$

$$+ \left[-\left(10-\frac{2}{\sqrt{3}}\right)^2\left(1-\frac{1}{\sqrt{3}}\right)^2 + \frac{4}{3}\left(1+\frac{1}{\sqrt{3}}\right)^2\right]\frac{1}{64\left(20-\frac{9}{\sqrt{3}}\right)}$$

$$+ \left[-\left(10+\frac{2}{\sqrt{3}}\right)^2\left(1-\frac{1}{\sqrt{3}}\right)^2 + \frac{4}{3}\left(1-\frac{1}{\sqrt{3}}\right)^2\right]\frac{1}{64\left(20-\frac{1}{\sqrt{3}}\right)} = -0.36892$$

In practice, we can obtain accurate values up to a desired decimal point by approximating J. If $J^{-1} = 4\,(20 + 4\xi - 5\eta)^{-1}$ is expanded using the Binomial series (it is necessary that $x^2 < 1$)

$$J^{-1} = \tfrac{1}{5}(1 - 0.2\xi + 0.25\eta)^{-1} = 0.2(1-x)^{-1} \approx 0.2(1 - x + x^2 - x^3\cdots),\quad x = 0.2\xi - 0.25\eta$$

and retaining linear terms only, the integrand becomes cubic polynomial in each ξ and η. Hence, we may use the two-point Gauss integration to evaluate the integral. A 3 × 3 integration gives $S_{12}^{11} = -0.36998$ and 4 × 4 gives $S_{12}^{11} = -0.37000$. The coefficients of $\mathbf{S}^{11}$, $\mathbf{S}^{22}$, and $\mathbf{S}^{12}$ are the same up to four decimal points when 3 × 3 and 4 × 4 Gauss quadrature rules are used. The values are accurate enough to yield good solutions for most problems (of course, the results depend on the problem).

Evaluating all of the integrals in Eq. (1) using 2 × 2 quadrature rule, we obtain

$$\mathbf{S}^{00} = \begin{bmatrix} 2.27778 & 1.25000 & 0.55556 & 1.00000 \\ 1.25000 & 2.72222 & 1.22222 & 0.55556 \\ 0.55556 & 1.22222 & 2.16667 & 0.97222 \\ 1.00000 & 0.55556 & 0.97222 & 1.72222 \end{bmatrix} \text{(exact)}$$

$$\mathbf{S}^{11} = \begin{bmatrix} 0.40995 & -0.36892 & -0.20479 & 0.16376 \\ -0.36892 & 0.34516 & 0.25014 & -0.22639 \\ -0.20479 & 0.25014 & 0.43155 & -0.47690 \\ 0.16376 & -0.22639 & -0.47690 & 0.53953 \end{bmatrix} \text{(inexact)}$$

$$\mathbf{S}^{22} = \begin{bmatrix} 0.26237 & 0.16389 & -0.13107 & -0.29520 \\ 0.16389 & 0.22090 & -0.23991 & -0.14489 \\ -0.13107 & -0.23991 & 0.27619 & 0.09478 \\ -0.29520 & -0.14489 & 0.09478 & 0.34530 \end{bmatrix} \text{(inexact)}$$

$$\mathbf{S}^{12} = \begin{bmatrix} 0.24731 & 0.25156 & -0.25297 & -0.24589 \\ -0.24844 & -0.25090 & 0.25172 & 0.24762 \\ -0.25297 & -0.24828 & 0.24671 & 0.25454 \\ 0.25411 & 0.24762 & -0.24546 & -0.25627 \end{bmatrix} \text{(inexact)}$$

These matrices would have been exact if the element had its sides parallel to the coordinate system (i.e., for a rectangular element).

10.3.4 Integration over a Master Triangular Element

In the preceding section we discussed numerical integration on quadrilateral elements which can be used to represent very general geometries as well as field variables in a variety of problems. Here we discuss numerical integration on triangular elements. Since quadrilateral elements can be geometrically distorted, it is possible to distort a quadrilateral element to obtain a required triangular element by moving the position of the corner nodes to one of the neighboring nodes. In actual computation, this is achieved by assigning the same global node number to two corner nodes of the quadrilateral element. Thus, master triangular elements can be obtained in a natural way from associated master rectangular elements.

We choose the unit right-angle triangle shown in Fig. 10.3.5 as the master triangular element. An arbitrary triangular element Ω_e can be generated from the master triangular element $\hat{\Omega}_T$ by transformation of the form (10.3.1)

$$x = \sum_{i=1}^{n} x_i^e \hat{\psi}_i(L_1, L_2, L_3), \quad y = \sum_{i=1}^{n} y_i^e \hat{\psi}_i(L_1, L_2, L_3) \tag{10.3.18}$$

where (x_i^e, y_i^e) are the global coordinates of node i of element Ω_e and $\hat{\psi}_i(L_1, L_2, L_3)$ are the interpolation functions of the master triangular element $\hat{\Omega}_T$, which can be expressed in terms of either the natural coordinates (ξ, η) or the area coordinates (L_1, L_2, L_3). The derivatives of ψ_i^e (used to represent the solution u over Ω_e) with respect to the global coordinates (x, y) can be computed from [see Eq. (10.3.8)]:

$$\begin{Bmatrix} \frac{\partial \psi_i^e}{\partial x} \\ \frac{\partial \psi_i^e}{\partial y} \end{Bmatrix} = (\mathbf{J}^e)^{-1} \begin{Bmatrix} \frac{\partial \psi_i^e}{\partial L_1} \\ \frac{\partial \psi_i^e}{\partial L_2} \end{Bmatrix}, \quad \mathbf{J}^e = \begin{bmatrix} \frac{\partial x}{\partial L_1} & \frac{\partial y}{\partial L_1} \\ \frac{\partial x}{\partial L_2} & \frac{\partial y}{\partial L_2} \end{bmatrix} \tag{10.3.19}$$

Note that only two of the three area coordinates can be treated as linearly independent, because $L_3 = 1 - L_1 - L_2$, $L_1 = 1 - L_2 - L_3$, or $L_2 = 1 - L_1 - L_3$. The interpolation functions for the linear and higher-order triangular elements were expressed in terms of the area coordinates in **Example 10.2.1**.

For example, in the case of a linear triangular element, the transformation (10.3.18) becomes $(\hat{\psi}_i = L_i, i = 1, 2, 3)$

$$x = \sum_{i=1}^{3} x_i^e L_i, \quad y = \sum_{i=1}^{3} y_i^e L_i \tag{10.3.20}$$

where L_i are the area coordinates of the linear master triangular element shown in Fig. 10.3.5 [see Eq. (10.2.14)]:

$$L_1 = \hat{\psi}_1 = 1 - \xi - \eta = 1 - L_2 - L_3, \quad L_2 = \hat{\psi}_2 = \xi, \quad L_3 = \hat{\psi}_3 = \eta \tag{10.3.21}$$

If we choose L_2 and L_3 as linearly independent (then $L_1 = 1 - L_2 - L_3$), the Jacobian matrix for the linear triangular element is given by

$$\mathbf{J}^e = \begin{bmatrix} \frac{\partial x}{\partial L_2} & \frac{\partial y}{\partial L_3} \\ \frac{\partial x}{\partial L_2} & \frac{\partial y}{\partial L_3} \end{bmatrix} = \begin{bmatrix} x_2^e - x_1^e & y_2^e - y_1^e \\ x_3^e - x_1^e & y_3^e - y_1^e \end{bmatrix} = \begin{bmatrix} \gamma_3^e & -\beta_3^e \\ -\gamma_2^e & \beta_2^e \end{bmatrix} \tag{10.3.22}$$

where β_i^e and γ_i^e are the constants defined in Eq. (9.2.24b). We have used the fact that

$$\frac{\partial x}{\partial L_2} = \frac{\partial}{\partial L_2}\left(x_1^e L_1 + x_2^e L_2 + x_3^e L_3\right) = -x_1^e + x_2^e$$
$$\frac{\partial y}{\partial L_2} = \frac{\partial}{\partial L_2}\left(y_1^e L_1 + y_2^e L_2 + y_3^e L_3\right) = -y_1^e + y_2^e$$

and so on. The inverse of the Jacobian matrix is given by

$$(\mathbf{J}^e)^{-1} = \frac{1}{J^e}\begin{bmatrix} \beta_2^e & \beta_3^e \\ \gamma_2^e & \gamma_3^e \end{bmatrix}, \quad J^e = \beta_2^e\gamma_3^e - \gamma_2^e\beta_3^e = 2A_e \tag{10.3.23}$$

where A_e is the area of the element Ω_e. The inverse transformation from element Ω_e to $\hat{\Omega}_T$ is given by inverting Eq. (10.3.18):

$$\begin{aligned} \xi &= \frac{1}{2A_e}[(x - x_1^e)(y_3^e - y_1^e) - (y - y_1^e)(x_3^e - x_1^e)] \\ \eta &= \frac{1}{2A_e}[(x - x_1^e)(y_1^e - y_2^e) + (y - y_1^e)(x_2^e - x_1^e)] \end{aligned} \tag{10.3.24}$$

Returning to the general case, after transformation, integrals on $\hat{\Omega}_T$ have the form

$$\int_{\Omega_e} G(\xi,\eta)\,d\xi\,d\eta = \int_{\hat{\Omega}_T} \hat{G}(L_1, L_2, L_3)\,dL_1 dL_2 \tag{10.3.25}$$

which can be approximated by the quadrature formula

$$\int_{\hat{\Omega}_T} \hat{G}(L_1, L_2, L_3) dL_1 dL_2 \approx \frac{1}{2}\sum_{I=1}^{N} \hat{G}(\mathbf{S}_I)\, W_I \tag{10.3.26}$$

where W_I and $\mathbf{S}_I = (\xi_I, \eta_I)$ denote the weights and integration points of the quadrature rule. Table 10.3.2 contains the location of integration points and weights for one-, three-, four-, and seven-point quadrature rules over master triangular elements. For evaluation of integrals whose integrands are polynomials of degree higher than five (in any of the area coordinates), the reader should consult books on numerical integration (e.g., see Carnahan et al. [1] and Froberg [2]).

Table 10.3.2 Quadrature points and weights for triangular elements.

Number of integration points	Residual order	Gauss points* and weights	ξ	η	W	Location of Gauss points
1	$O(h^2)$	a	$\frac{1}{3}$	$\frac{1}{3}$	1	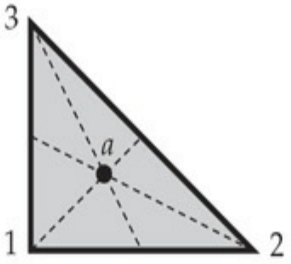
3	$O(h^3)$	a	$\frac{1}{2}$	0	$\frac{1}{3}$	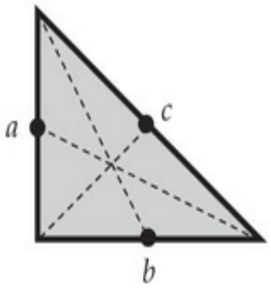
		b	0	$\frac{1}{2}$	$\frac{1}{3}$	
		c	$\frac{1}{2}$	$\frac{1}{2}$	$\frac{1}{3}$	
4	$O(h^4)$	a	$\frac{1}{3}$	$\frac{1}{3}$	$-\frac{27}{48}$	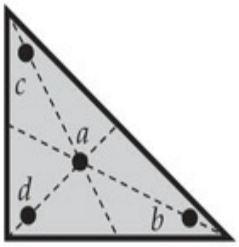
		b	0.2	0.6	$\frac{25}{48}$	
		c	0.2	0.2	$\frac{25}{48}$	
		d	0.6	0.2	$\frac{25}{48}$	
7**	$O(h^6)$	a	$\frac{1}{3}$	$\frac{1}{3}$	0.225	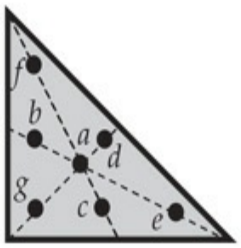
		b	α_1	β_1	W_2	
		c	β_1	α_1	W_2	
		d	β_1	β_1	W_2	
		e	α_2	β_2	W_3	
		f	β_2	α_2	W_3	
		g	β_2	β_2	W_3	

*Gauss point locations, $a : (\xi_1, \eta_1)$; $b : (\xi_2, \eta_2)$; $c : (\xi_3, \eta_3)$; and so on.

**$\alpha_1 = 0.059715871789$, $\alpha_2 = 0.797426985353$, $\beta_1 = 0\,470142064105$, $\beta_2 = 0.101286507323$, $W_2 = 0.125939180544$, $W_3 = 0.132394152788$

Example 10.3.4

Consider the quadratic triangular element shown in Fig. 10.3.7. Calculate $\partial\psi_1/\partial x$, $\partial\psi_1/\partial y$, $\partial\psi_4/\partial x$, and $\partial\psi_4/\partial y$ at the point $(x, y) = (2, 4)$ and evaluate the integral of the product $(\partial\psi_1/\partial x)(\partial\psi_4/\partial x)$. Assume isoparametric formulation.

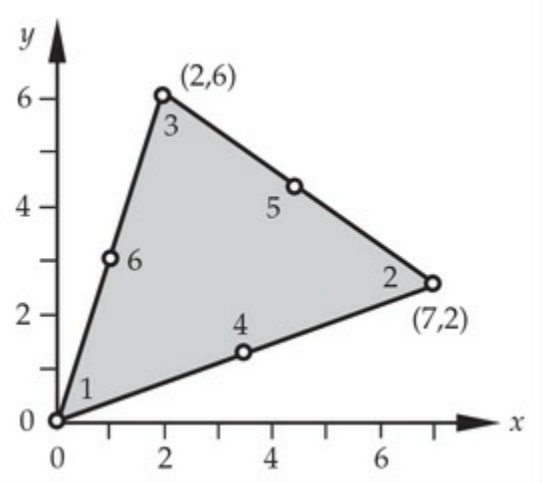

Fig. 10.3.7 A quadratic triangular element in the global (x, y) coordinate system.

Solution: We shall use L_1 ad L_2 as the independent coordinates with $L_3 = 1 - L_1 - L_2$. For the quadratic element at hand, we have (the geometry in this case is exactly represented by three vertices)

$$\begin{aligned} x &= x_1L_1 + x_2L_2 + x_3L_3 = 7L_2 + 2L_3 = 2 - 2L_1 + 5L_2 \\ y &= y_1L_1 + y_2L_2 + y_3L_3 = 2L_2 + 6L_3 = 6 - 6L_1 - 4L_2 \end{aligned} \tag{1}$$

and the Jacobian matrix becomes ($\partial x/\partial L_1 = -2$, $\partial x/\partial L_2 = 5$, $\partial y/\partial L_1 = -6$, and $\partial y/\partial L_2 = -4$):

$$\mathbf{J} = \begin{bmatrix} -2 & -6 \\ 5 & -4 \end{bmatrix}, \quad \mathbf{J}^{-1} = \frac{1}{38}\begin{bmatrix} -4 & 6 \\ -5 & -2 \end{bmatrix}, \quad J = 2A = 38 \tag{2}$$

where A is the area of the triangle. The global derivatives of the interpolation
functions are

$$\begin{Bmatrix} \frac{\partial \psi_1}{\partial x} \\ \frac{\partial \psi_1}{\partial y} \end{Bmatrix} = \frac{1}{38}\begin{bmatrix} -4 & 6 \\ -5 & -2 \end{bmatrix}\begin{Bmatrix} \frac{\partial \psi_1}{\partial L_1} \\ \frac{\partial \psi_1}{\partial L_2} \end{Bmatrix} = -\frac{(4L_1 - 1)}{38}\begin{Bmatrix} 4 \\ 5 \end{Bmatrix}$$
$$\begin{Bmatrix} \frac{\partial \psi_4}{\partial x} \\ \frac{\partial \psi_4}{\partial y} \end{Bmatrix} = \frac{1}{38}\begin{bmatrix} -4 & 6 \\ -5 & -2 \end{bmatrix}\begin{Bmatrix} \frac{\partial \psi_4}{\partial L_1} \\ \frac{\partial \psi_4}{\partial L_2} \end{Bmatrix} = \frac{4}{38}\begin{Bmatrix} 6L_1 - 4L_2 \\ -2L_1 - 5L_2 \end{Bmatrix} \tag{3}$$

where we have used $\psi_1 = L_1(2L_1 - 1)$ and $\psi_4 = 4L_1 L_2$ [see **Example 10.2.1** and Fig. 10.2.4 (a)] and

$$\frac{\partial \psi_1}{\partial L_1} = 4L_1 - 1, \quad \frac{\partial \psi_1}{\partial L_2} = 0, \quad \frac{\partial \psi_4}{\partial L_1} = 4L_2, \quad \frac{\partial \psi_4}{\partial L_2} = 4L_1 \tag{4}$$

For the point (2, 4), the area coordinates can be calculated from Eq. (1):

$$2 = 7L_2 + 2L_3, \quad 4 = 2L_2 + 6L_3$$

whose solution, with $L_1 = 1 - L_2 - L_3$, is

$$L_1 = \frac{5}{19}, \quad L_2 = \frac{2}{19}, \quad L_3 = \frac{12}{19} \tag{5}$$

Evaluating $\partial\psi_1/\partial x$, $\partial\psi_1/\partial y$, $\partial\psi_4/\partial x$, and $\partial\psi_4/\partial y$ at the point (2, 4) (or, equivalently, at $L_1 = 5/19$ and $L_2 = 2/19$), we obtain

$$\frac{\partial \psi_1}{\partial x} = -\frac{4}{38}\left(\frac{20}{19} - 1\right) = -\frac{2}{361}, \quad \frac{\partial \psi_1}{\partial y} = -\frac{5}{38}\left(\frac{20}{19} - 1\right) = -\frac{5}{722}$$
$$\frac{\partial \psi_4}{\partial x} = \frac{60}{(19)^2} - \frac{16}{(19)^2} = \frac{44}{361}, \quad \frac{\partial \psi_4}{\partial y} = -\frac{20}{(19)^2} - \frac{20}{(19)^2} = -\frac{40}{361} \tag{6}$$

The integral of $(\partial\psi_1/\partial x)(\partial\psi_4/\partial x)$ over the quadratic element is ($J = 38$)

$$\int_{\hat{\Omega}_T} \frac{\partial \psi_1}{\partial x}\frac{\partial \psi_4}{\partial x}\, dx\, dy = -\frac{4J}{361}\int_0^1 \int_0^{1-L_2} (4L_1 - 1)(6L_1 - 4L_2)\, dL_1\, dL_2$$

Since the integrand is quadratic in L_1 and bilinear in L_1 and L_2, we use the three-point quadrature (see Table 10.3.2) to evaluate the integral exactly:

$$-\frac{4J}{361}\int_0^1\int_0^{1-L_2}(4L_1-1)(6L_1-4L_2)\,dL_1\,dL_2$$
$$=-\frac{1}{2}\frac{4\times 38}{361}\frac{1}{3}\left[\left(\tfrac{4}{2}-1\right)\left(\tfrac{6}{2}-0\right)+(0-1)\left(0-\tfrac{4}{2}\right)+\left(\tfrac{4}{2}-1\right)\left(\tfrac{6}{2}-\tfrac{4}{2}\right)\right]$$
$$=-\frac{8}{19} \qquad (7)$$

The result can be verified using the exact integration formula in Eq. (10.2.12):

$$\int_{\hat{\Omega}_T}\frac{\partial\psi_1}{\partial x}\frac{\partial\psi_4}{\partial x}dx\,dy=\frac{4}{361}\left[6\times\frac{1}{3!}-4\times\frac{1}{3!}-24\times\frac{2!}{4!}+16\times\frac{1}{4!}\right]2A=-\frac{8}{19}$$

The area A of the triangle is equal to 19, and therefore we obtain the same result as above.

10.4 Modeling Considerations

10.4.1 Preliminary Comments

Finite element analysis involves assumptions concerning the representation of the system and/or its behavior. Valid assumptions can be made only if one has a qualitative understanding of how the process or system works. A good knowledge of the basic principles governing the process and the finite element theory enables the development of a good numerical model (e.g., selection of element type, representation of the domain using a suitable mesh, representation of loads and boundary conditions, and so on). Here we discuss several aspects of finite element analysis, including element geometries, mesh refinements, and load representations.

10.4.2 Element Geometries

Recall from Section 10.3 that the numerical evaluation of integrals over actual elements involves a coordinate transformation from the actual element to a master element. The transformation is acceptable if and only if every point in the actual element is mapped uniquely into a point in the master element and vice versa. Such mappings are termed one-to-one. This

requirement can be expressed as [see Eq. (10.3.11)]

$$J^e \equiv [\mathbf{J}^e] > 0 \quad \text{everywhere in the element } \Omega_e \tag{10.4.1}$$

where $\mathbf{J}^e$ is the Jacobian matrix in Eq. (10.3.10b). Geometrically, the Jacobian J^e represents the ratio of an area element in the actual element Ω^e to the corresponding area element in the master element $\hat{\Omega}$,

$$dA \equiv dxdy = J^e \, d\xi dn$$

Thus, if J^e is zero then a nonzero area element in Ω_e is mapped into zero area $\hat{\Omega}$; and if $J^e < 0$, a right-hand coordinate system is mapped into a left-hand coordinate system. Both are not acceptable.

In general, the Jacobian is a function of ξ and η, implying that the physical element Ω_e is nonuniformly mapped into the master element (i.e., the element is distorted). Excessive distortion of elements is not good because a nonzero area element in Ω_e can be mapped into nearly zero area. To ensure $J^e > 0$ and keep within the extreme limits of acceptable distortion, certain geometric shapes of real elements must be avoided. For example, the interior angle at each vertex of a triangular element should not be equal to either 0° or 180°. Indeed, in practice the angle should reasonably be larger than 0° and smaller than 180° to avoid numerical ill-conditioning of element matrices (or J is very small). Although the acceptable range depends on the problem, the range 15°–165° can be used as a guide. Figure 10.4.1 shows elements with unacceptable vertex angles for straight-sided and curved-sided elements.

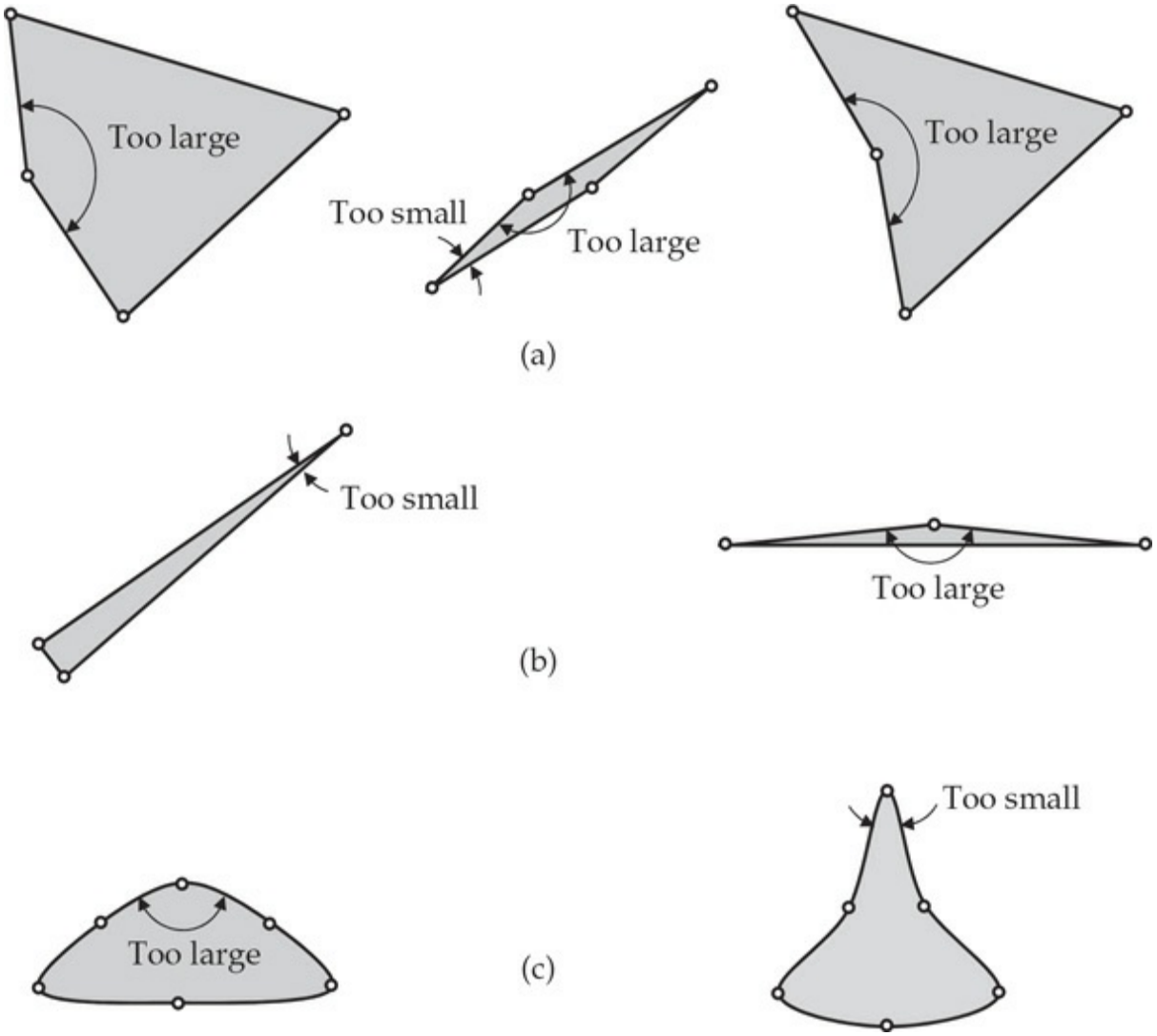

Fig. 10.4.1 Finite elements with unacceptable vertex angles: (a) linear quadrilateral elements; (b) linear triangular elements; and (c) quadratic triangular elements.

For higher-order Lagrange elements (i.e., the C^0 elements), the locations of the interior nodes contribute to the element distortion, and therefore they are constrained to lie within certain distance from the vertex (or corner) nodes (see Fig. 10.4.2). For example, in the case of a quadratic element the mid-side node should be at a distance not less than one-fourth of the length of the side from the corner nodes. When the mid-side node is located exactly at a distance of one-fourth of the side length from a vertex, the element exhibits special properties (see **Problem 10.19**). Such elements, called *quarter-point elements*, are sometimes used in fracture mechanics problems to represent an inverse square-root singularity in the gradient of the solution at the nearest corner node.

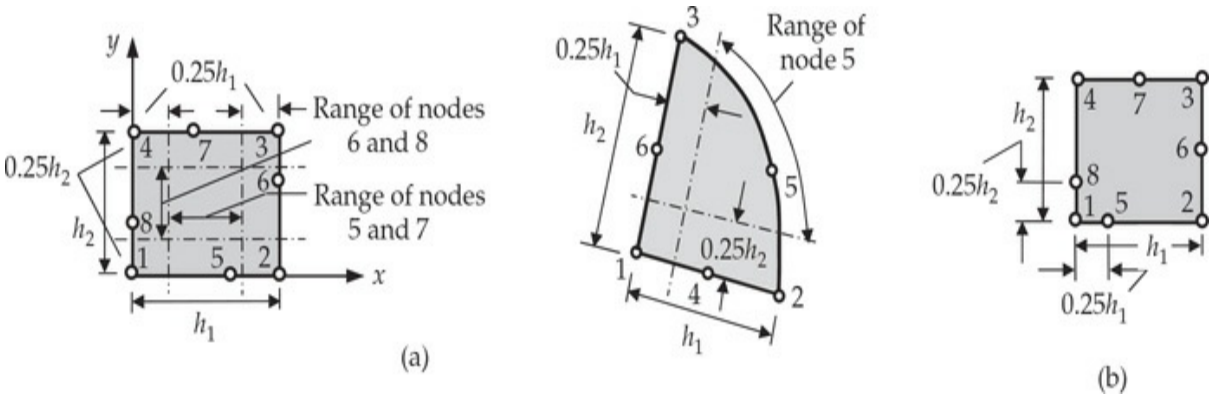

Fig. 10.4.2 Range of acceptable locations of the midside nodes for quadratic elements.

10.4.3 Mesh Refinements

Generation of a finite element mesh for a given problem should follow the guidelines listed below:

1. The mesh should represent the geometry of the computational domain and load representations accurately.
2. The mesh should be such that large gradients in the solution are adequately represented.
3. The mesh should not contain elements with unacceptable geometries (both aspect ratios and included angles), especially in regions of large gradients.

Within the above guidelines, the mesh used can be *coarse* (i.e., have few elements) or *refined* (i.e., have many elements), and may consist of one or more orders and types of elements (e.g., linear and quadratic, triangular and quadrilateral). A judicious choice of element order and type could save computational cost while giving accurate results. It should be noted that the choice of elements and mesh is problem-dependent. What works well for one problem may not work well for another problem. An analyst with physical insight into the process being simulated (i.e., a qualitative understanding of the solution) can make a better choice of elements and mesh for the problem at hand. One should start with a coarse mesh that meets the three requirements listed above, exploit symmetries available in the problem, and evaluate the results thus obtained in light of physical understanding and approximate analytical and/or experimental information. These results can be used to guide subsequent mesh refinements and analyses.

Generation of meshes of single element type is easy because elements of the same degree are compatible with each other (see Fig. 10.4.3). Combining elements of different order, say linear to quadratic elements, may be necessary to accomplish local mesh refinements. Figure 10.4.4 contains element connections that do not satisfy the C^0 continuity along the connecting sides (the solution is not single-valued along the interface). There are two ways to do this. One way is to use a transition element, which has different number of nodes on different sides [see Fig. 10.4.5(a)]. The other way is to impose a condition that constrains the midside node to have the same value as that experienced at the node by the lower-order element [see Fig. 10.4.5(b)]. However, such combinations do not enforce interelement continuity of the solution along the entire interface.

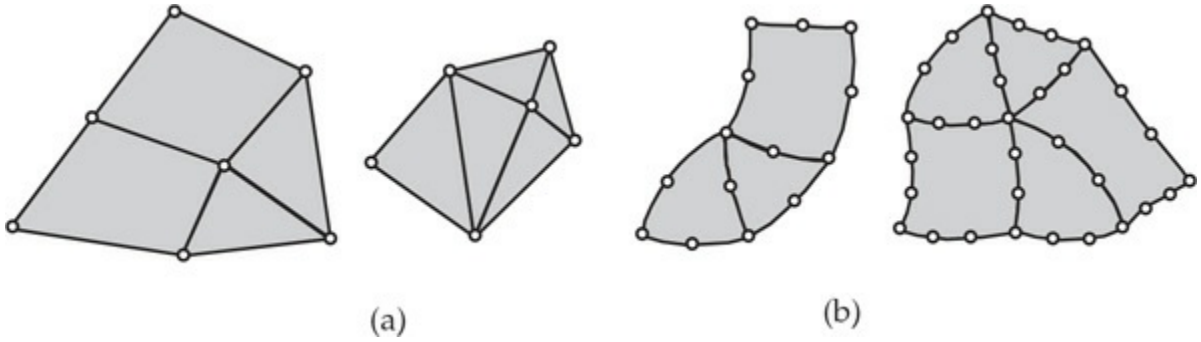

Fig. 10.4.3 Connecting elements of the same order. The C^0 elements of the same order ensure the C^0 continuity along the element interfaces: (a) linear elements; (b) quadratic and cubic elements.

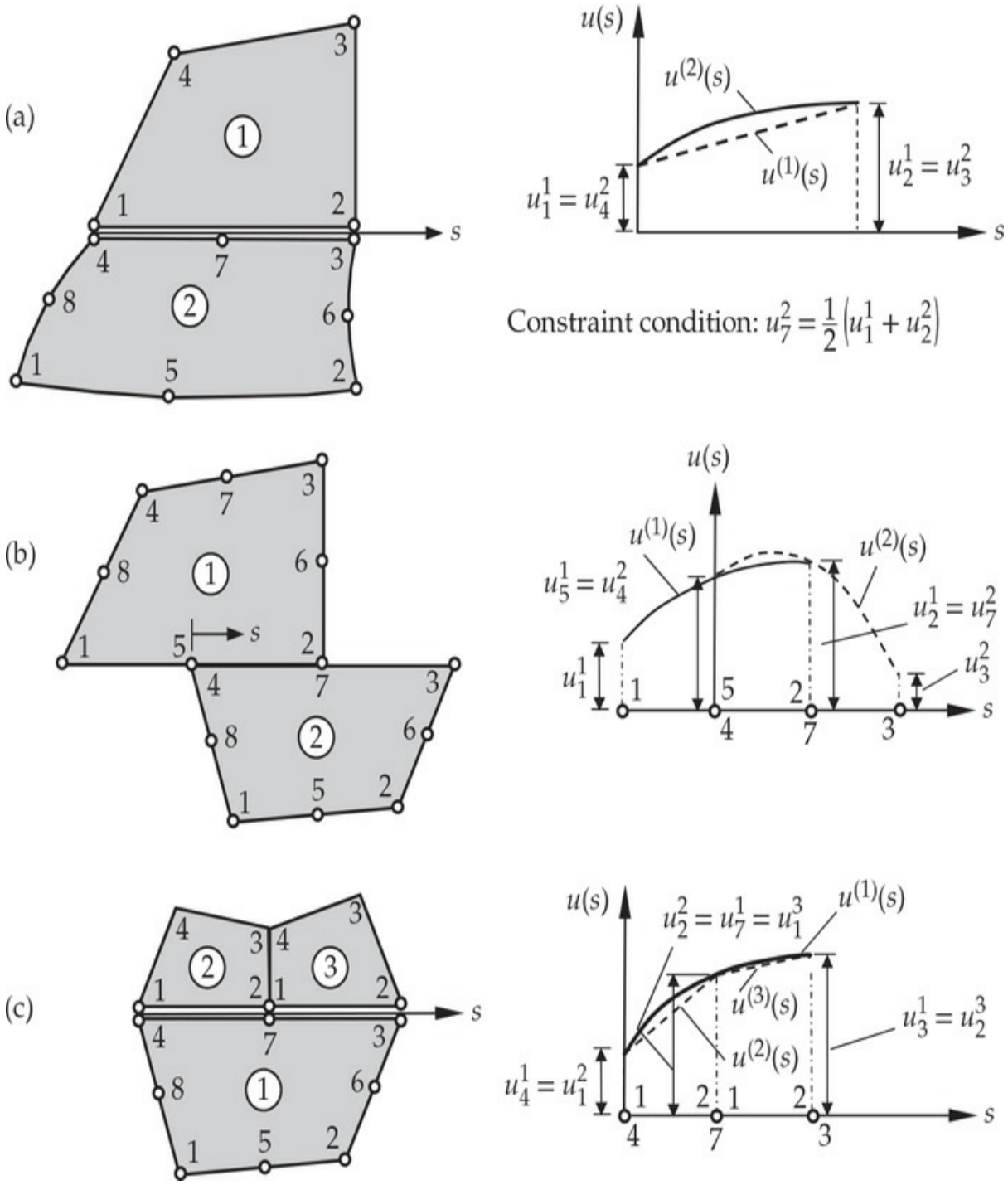

Fig. 10.4.4 Various types of incompatible connections of finite elements. In all cases the inter-element continuity of the function is violated along the connecting sides.

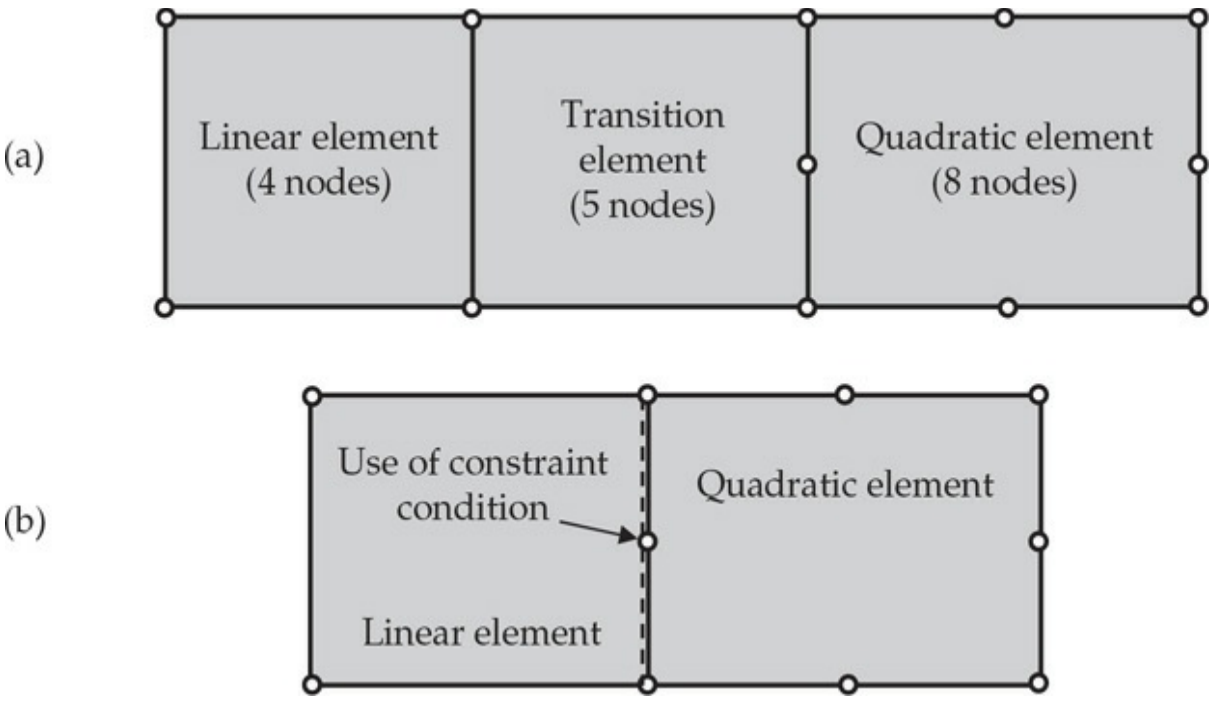

Fig. 10.4.5 Combining different order elements: (a) use of a transition element that has three sides linear and one side quadratic; and (b) use of a linear constraint equation to connect a linear side to a quadratic side.

Mesh refinements involve several options. Refine the mesh by subdividing existing elements into two or more elements of the same type [see Fig. 10.4.6(a)]. This is called the *h-refinement*. Alternatively, existing elements can be replaced by elements of higher order [see Fig. 10.4.6(b)]. This type of refinement is called the *p-refinement*. The *h, p-refinement* is one in which elements are subdivided into two or more elements in some places and replaced with higher-order elements in other places. Generally, local mesh refinements should be such that very small elements are not placed adjacent to those of very large aspect ratios (see Fig. 10.4.7). Use of transition elements and constraint conditions in local mesh refinements is a common practice. Figure 10.4.8 shows few examples of such refinements.

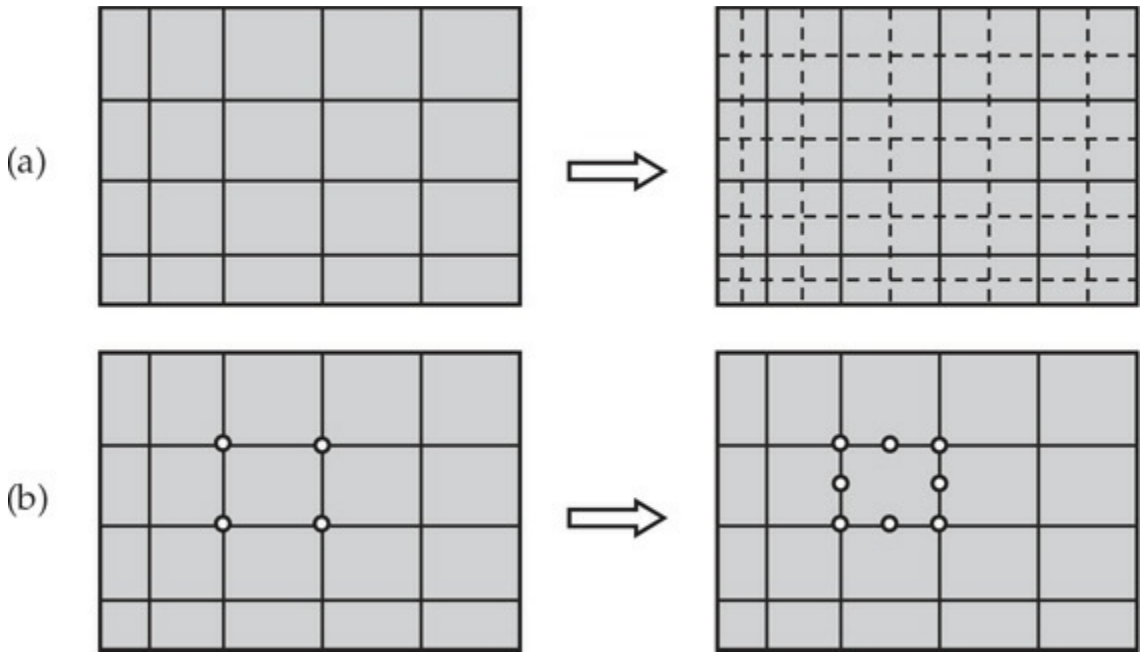

Fig. 10.4.6 The (a) *h*-refinement and (b) *p*-refinement.

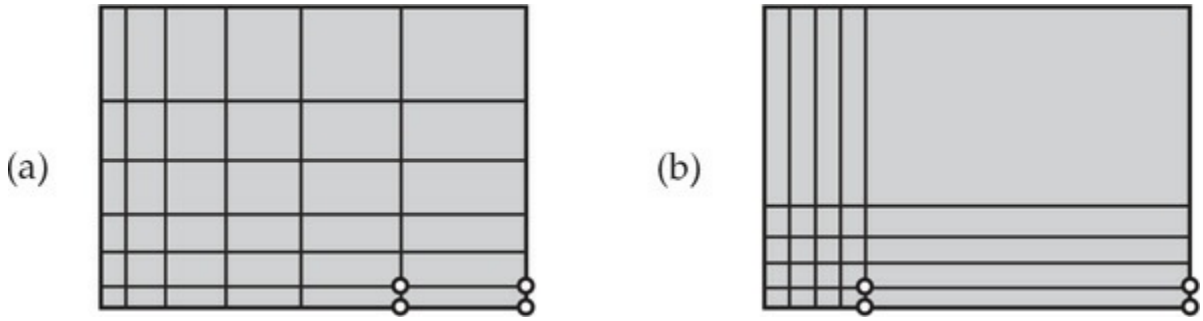

Fig. 10.4.7 Finite element mesh refinements. Mesh shown in (a) is acceptable and mesh shown in (b) is not unacceptable.

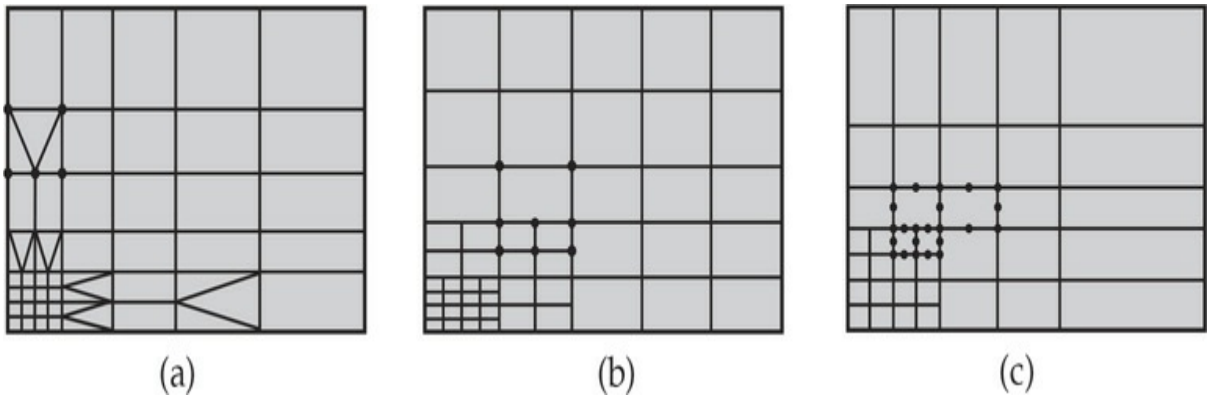

Fig. 10.4.8 Some examples of local mesh refinements. (a) Mesh refinements with compatible connections. (b) Mesh refinements with transition elements (constraint conditions) between linear elements. (c) Mesh refinements with transition elements between linear and quadratic

elements.

10.4.4 Load Representation

Computation of the nodal contributions of a distributed boundary source was discussed in Chapter 9 (see Section 9.2.7.3). Representation of the load (flux) on a curved boundary can be improved by the use of higher-order elements (see Fig. 10.4.9). Of course, *h*-version or *p*-version mesh refinement of the domain will improve the representation of the boundary flux.

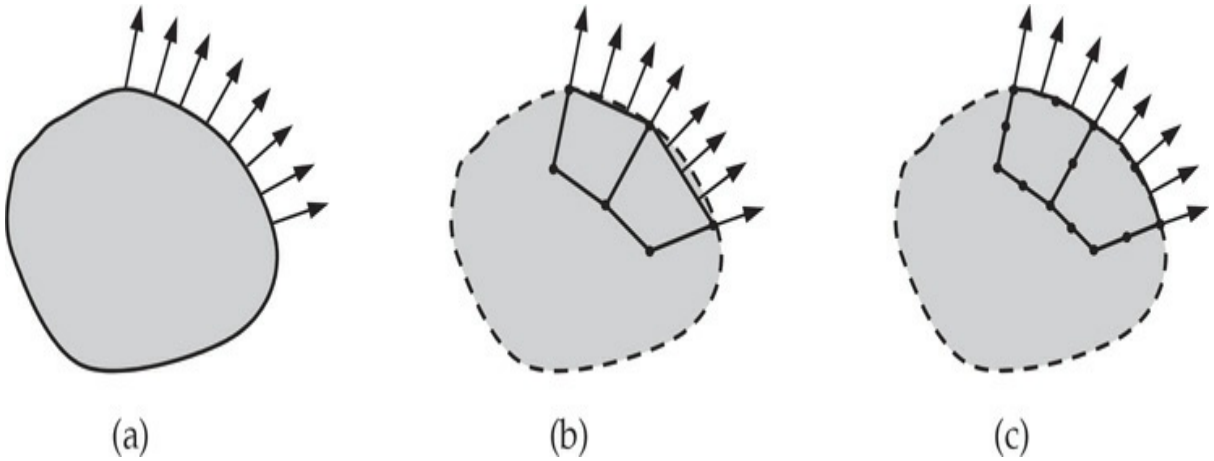

Fig. 10.4.9 Approximation of the boundary fluxes in the finite element method. (a) Distribution of flux on a curved boundary. (b) Approximation by linear elements. (c) Approximation by quadratic elements.

Another situation where representation of boundary forces is subject to different interpretations is the force due to contact between two bodies. For example, a solid plate in contact with a circular disc generates a reactive force that can be represented either as a point load of locally distributed force. Representation of the contact force between deformable bodies as a point load is an approximation of the true distribution. A sinusoidal distribution might be more realistic representation of the actual force (see Fig. 10.4.10).

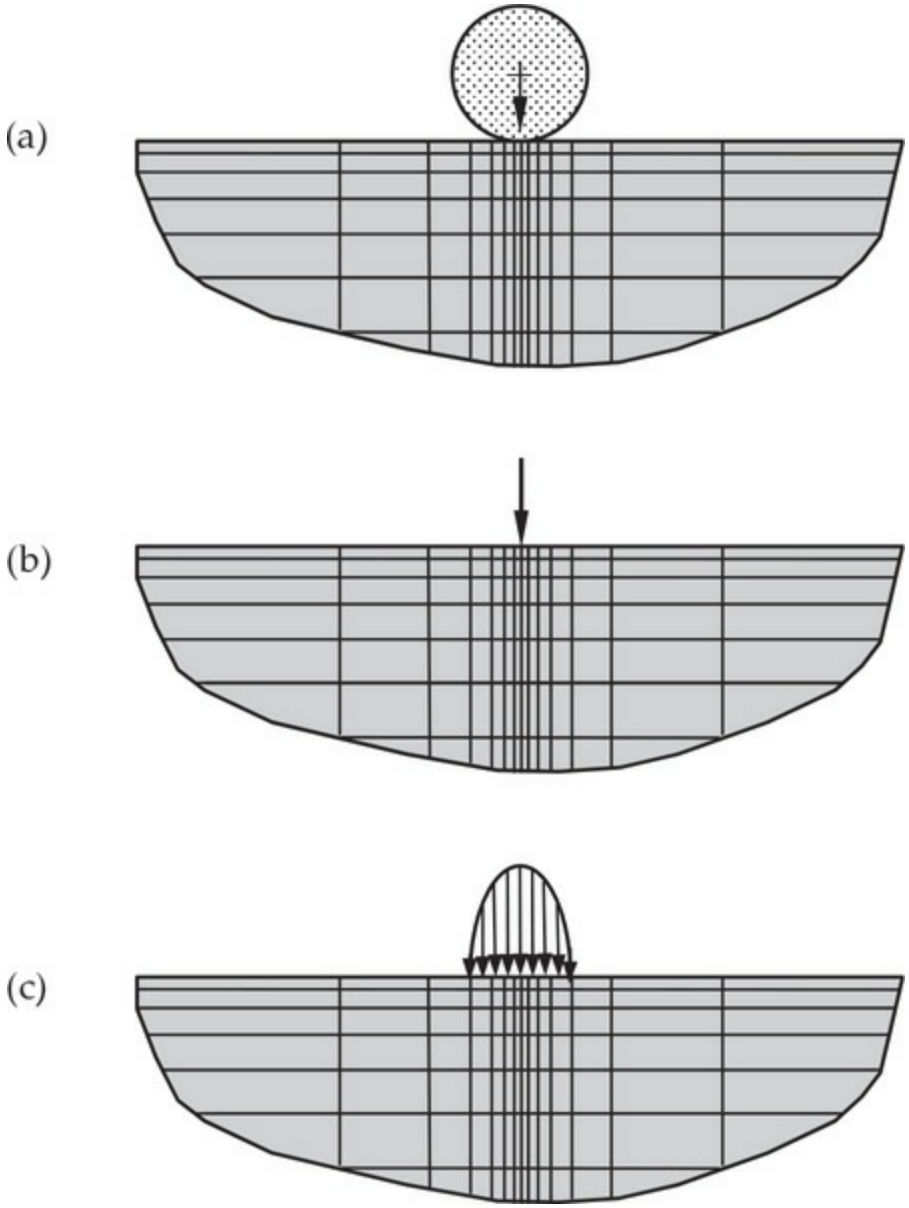

Fig. 10.4.10 Representation of contact pressure developed between two bodies; (a) geometry of the bodies in contact; (b) representation of the contact pressure as a point load; and (c) representation of the contact pressure as a distributed surface load. In the latter case, often the surface area of the distributed force is unknown.

In closing this section, we note that modeling is both an art and science, which can be improved by experience and understanding of physical interactions involved in the process. The modeling guidelines presented herein are to encourage good modeling practice, and they should be followed to determine a good "working" model.

10.5 Computer Implementation and FEM2D

10.5.1 Overview of Program FEM2D

In this section the use of a model computer program **FEM2D** is discussed. The program **FEM2D** contains linear and quadratic triangular and rectangular elements, and it can be used for the solution of heat conduction and convection problems (Chapter 9), laminar flows of viscous incompressible fluids using the penalty function formulation (Chapter 11), and plane elasticity problems (Chapter 12); FEM2D can also be used to solve plate bending problems using classical and shear deformation theories, which are not covered in the current edition of the book. A flowchart of **FEM2D** is presented in Fig. 10.5.1.

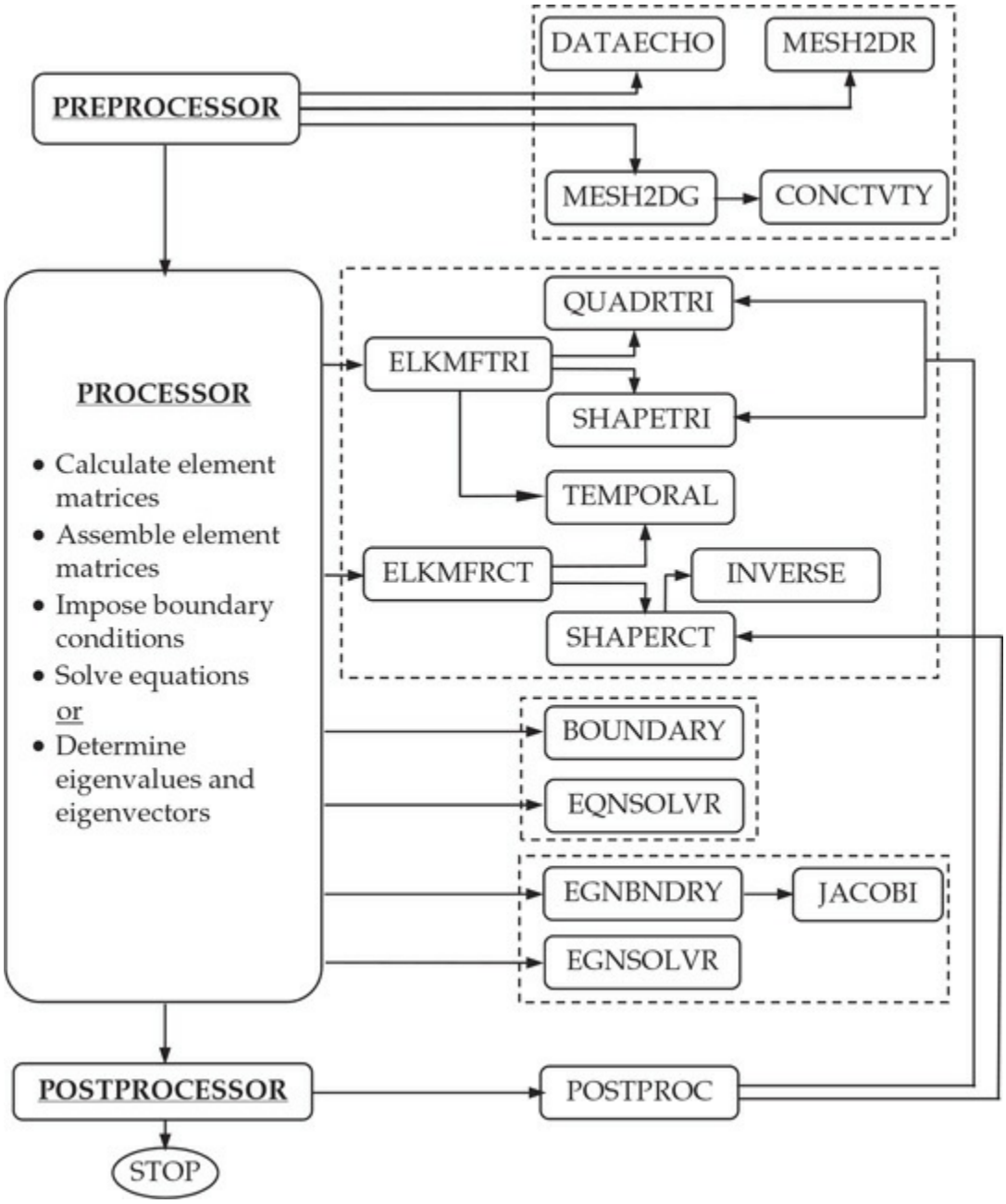

Fig. 10.5.1 Flowchart of the computer program **FEM2D**.

In two dimensions, the element calculations are more involved than in one dimension, owing to the following considerations:

1. Various geometric shapes of elements and approximation of the geometry as well as the solution.
2. Single as well as multivariable problems (i.e., problems with more than one unknown)
3. Integrations performed over areas.
4. Mixed-order (i.e., full and reduced order) integrations used in

certain formulations (e.g., penalty function formulations of viscous incompressible fluids and shear-deformable plates).

A brief description of the roles of the subroutines used (in the alphabetical order) in program **FEM2D** is presented next.

- **BOUNDARY**: Subroutine to impose specified (essential, natural, and mixed) boundary conditions on the primary and secondary variables.
- **CONCTVTY**: Subroutine called from the mesh generator **MESH2DG**.
- **DATAECHO**: Subroutine to echo the input data to the program (to facilitate the user to check the input data).
- **EGNBNDRY**: Subroutine to impose specified homogeneous (essential and mixed) boundary conditions on the primary variables when an eigenvalue problem is solved.
- **EGNSOLVR**: Subroutine to determine eigenvalues and eigenvectors (using Jacobi iteration method).
- **ELKMFRCT**: Subroutine to compute the element matrices **K**, **M**, and **F** for various field problems when quadrilateral elements are used.
- **ELKMFTRI**: Subroutine to compute the element matrices **K**, **M**, and **F** for various field problems when triangular elements are used.
- **EQNSOLVR**: Subroutine to solve a banded symmetric system of algebraic equations using the Gauss elimination method.
- **INVERSE**: Subroutine to invert a 3 × 3 matrix explicitly.
- **JACOBI**: Subroutine called inside **EGNSOLVR**.
- **MESH2DG**: Subroutine to generate mesh for non-rectangular domains.
- **MESH2DR**: Subroutine to generate mesh for rectangular domains only.
- **POSTPROC**: Subroutine to post-compute the solution, gradient of solution, and stresses for various field problems.
- **QUADRTRI**: Subroutine to generate the quadrature points and weights for triangular elements.
- **SHAPERCT**: Subroutine to compute the shape (interpolation) functions and their global derivatives for linear and quadratic (eight- and nine-node) quadrilateral elements.
- **SHAPETRI**: Subroutine to compute the shape (interpolation) functions and their global derivatives for linear and quadratic

triangular elements.

- **TEMPORAL**: Subroutine to compute the equivalent coefficient matrices and column vectors for parabolic and hyperbolic equations when time-dependent analysis is carried [i.e., matrices of fully discretized systems in Eqs. (9.5.13a) and (9.5.21a)].

10.5.2 Preprocessor

In the preprocessor unit, the program **MESH2DR** is used to generate triangular-and rectangular-element meshes of rectangular domains. The subroutine requires minimal input but is not general enough to generate finite element meshes of arbitrary domains. The subroutine **MESH2DG** is more general and can be used to generate meshes for nonrectangular domains. The subroutines **MESH2DR** and **MESH2DG** generate the connectivity array NOD and nodal global coordinates array GLXY. Of course, one can read the mesh information generated by a commercial code.

10.5.3 Element Computations (Processor)

Element calculations for linear and quadratic triangular (**ELKMFTRI**) and quadrilateral (**ELKMFRCT**) elements can be carried out according to the concepts presented in Chapters 8 and 9. The principal steps involved are as follows.

1. Development of a subroutine for the evaluation of the interpolation functions and their derivatives with respect to the global coordinates [see Eqs. (10.3.7)–(10.3.11)].
2. Numerical integration of the coefficients of the element matrices using numerical quadrature formulas [see Eqs. (10.3.16) and (10.3.26)].
3. Setting up of the element matrices required for the class of problems being solved (e.g., static, transient, and eigenvalue problems).

We begin with the notation used for shape functions and their derivatives with respect to the natural (local) coordinates (ξ, η) and global coordinates (x, y) for quadrilateral elements. The variable names adopted are very transparent and thus easy to see how the theoretical developments are translated into Fortran statements. We use the following notation:

XI(I)	Natural coordinate ξ_I of element node I
ETA(I)	Natural coordinate η_I of element node I
ELXY(I, 1)	Global coordinate x of element node I
ELXY(I, 2)	Global coordinate y of element node I
GLXY(I, 1)	Global coordinate x of the Ith node of the mesh
GLXY(I, 2)	Global coordinate y of the Ith node of the mesh
SF(I)	Interpolation function ψ_I of the Ith node of an element
DSF(1, I)	Derivative of SF(I) with respect to ξ: DSF(1, I) = $\partial\psi_I/\partial\xi$
DSF(2, I)	Derivative of SF(I) with respect to η: DSF(2, I) = $\partial\psi_I/\partial\eta$
GDSF(1, I)	Global derivative with respect to x: GDSF(1, I) = $\partial\psi_I/\partial x$
GDSF(2, I)	Global derivative with respect to y: GDSF(2, I) = $\partial\psi_I/\partial y$
DET	Determinant J of the Jacobian matrix **J**
CONST	Product of Jacobian J with the weights corresponding to the Gauss integration point (ξ_{NI}, η_{NJ}) = DET * GAUSWT(NI, NGP) * GAUSWT(NJ, NGP)

The subroutines **SHAPETRI** and **SHAPERCT** (called in a do-loop based on the number of quadrature points) contain the expressions of the interpolation functions and their derivatives for various-order triangular (TRI) and rectangular (RCT) elements, respectively. The derivatives of the interpolation functions with respect to global coordinates [see Eq. (10.3.9)] are also computed in these subroutines.

Once the arrays SF and GDSF are available in do-loops on a number of Gauss points in each coordinate direction, it is simple to evaluate the matrix coefficients using the Gauss quadrature formula in Eq. (10.3.16). For example, $S_{ij}^{\alpha\beta}$ of Eq. (9.2.39),

$$S_{ij}^{\alpha\beta} = \int_{\Omega^e} \frac{\partial\psi_i}{\partial x_\alpha}\frac{\partial\psi_j}{\partial x_\beta}\,dx\,dy \tag{10.5.1}$$

where $x_1 = x$ and $x_2 = y$, can be translated into Fortran statements by

```
S00(I,J) = S00(I,J) + SF(I) * SF(J) * CONST
S11(I,J) = S11(I,J) + GDSF(1,I) * GDSF(1,J) * CONST
S12(I,J) = S12(I,J) + GDSF(1,I) * GDSF(2,J) * CONST
S21(I,J) = S21(I,J) + GDSF(2,I) * GDSF(1,J) * CONST
S22(I,J) = S22(I,J) + GDSF(2,I) * GDSF(2,J) * CONST
```

(10.5.2)

The summed values of S00(I, J), S11(I, J), and so on, over the number of

Gauss points yields their numerical values.

To set up the element coefficient matrices of a given problem, we make use of the element matrices defined above. As an example, consider the problem described by the Poisson equation in Eq. (9.2.1). The element coefficient matrix and the source vector for the problem are given by Eqs. (9.2.19b) and (9.2.19c). The element matrix K_{ij} [denoted ELK(I, J)] can be expressed in terms of $S_{ij}^{\alpha\beta}$ (α, β = 0, 1, 2) by

$$\begin{aligned}\text{ELK(I, J)} = &\text{A00} * \text{S00(I, J)} + \text{A11} * \text{S11(I, J)} + \text{A12} * \text{S12(I, J)} \\ &+ \text{A21} * \text{S12(J, I)} + \text{A22} * \text{S22(I, J)}\end{aligned}$$

where a_{00} = A00, a_{11} = A11, a_{12} = A12, a_{21} = A21, and a_{22} = A22 are the coefficients of the differential equation (9.2.1) (a_{ij} can be functions of x and y).

In multivariable problems, the element matrices are themselves defined in terms of submatrices, as was the case for the Timoshenko beam element [see Eq. (5.3.15)]. In such cases, the element equations may be rearranged to reduce the half-bandwidth of the assembled coefficient matrix. For example, consider the element equations (5.3.15) associated with the Timoshenko beam theory. For quadratic interpolation of w and ϕ_x (see Fig. 10.5.2), the element has a total of six degrees of freedom.

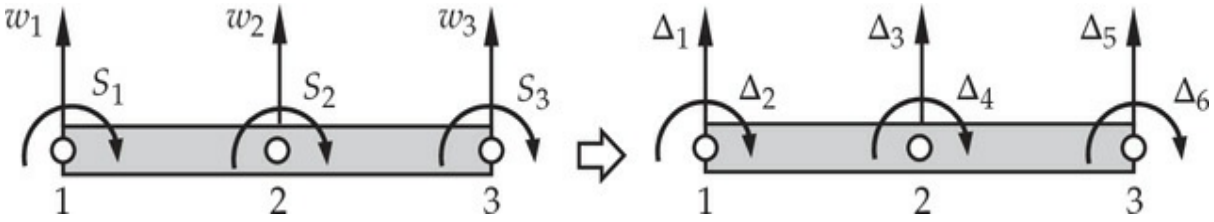

Fig. 10.5.2 Quadratic Timoshenko beam finite element with nodal degrees of freedom.

The element nodal displacement vector is given by

$$\begin{Bmatrix} w_1 \\ w_2 \\ w_3 \\ S_1 \\ S_2 \\ S_3 \end{Bmatrix} \tag{10.5.3}$$

Thus, at any node, the difference between the label number of the first degree of freedom and that of the second degree of freedom is 3 (in a general case, the difference is *n*, where *n* is the number of nodes per element). This difference contributes to an increase in the half-bandwidth of the assembled coefficient matrix and hence in computational cost when Gauss elimination methods are used to solve the equations. To remedy this situation, we reorder the element nodal degrees of freedom as follows:

$$\begin{Bmatrix} w_1 \\ S_1 \\ w_2 \\ S_2 \\ w_3 \\ S_3 \end{Bmatrix} \tag{10.5.4}$$

In reordering the nodal degrees of freedom, we must retain the symmetry, if one is present, of the system of algebraic equations. This is accomplished by renumbering the equations in the same way as the nodal degrees of freedom. To illustrate how this can be done, we consider the element equations of the Timoshenko beam element when both *w* and ϕx are interpolated using quadratic interpolation functions:

$$\begin{bmatrix} \mathbf{K}^{11} & \mathbf{K}^{12} \\ \mathbf{K}^{21} & \mathbf{K}^{22} \end{bmatrix} \begin{Bmatrix} \mathbf{w} \\ \mathbf{S} \end{Bmatrix} = \begin{Bmatrix} \mathbf{F}^1 \\ \mathbf{F}^2 \end{Bmatrix} \tag{10.5.5}$$

which is a set of six equations in six unknowns (each of the submatrices are of order 3 × 3). In expanded form, we have

$$\begin{bmatrix} K_{11}^{11} & K_{12}^{11} & K_{13}^{11} & K_{11}^{12} & K_{12}^{12} & K_{13}^{12} \\ K_{21}^{11} & K_{22}^{11} & K_{23}^{11} & K_{21}^{12} & K_{22}^{12} & K_{23}^{12} \\ K_{31}^{11} & K_{32}^{11} & K_{33}^{11} & K_{31}^{12} & K_{32}^{12} & K_{33}^{12} \\ K_{11}^{21} & K_{12}^{21} & K_{13}^{21} & K_{11}^{22} & K_{12}^{22} & K_{13}^{22} \\ K_{21}^{21} & K_{22}^{21} & K_{23}^{21} & K_{21}^{22} & K_{22}^{22} & K_{23}^{22} \\ K_{31}^{21} & K_{32}^{21} & K_{33}^{21} & K_{31}^{22} & K_{32}^{22} & K_{33}^{22} \end{bmatrix} \begin{Bmatrix} w_1 \\ w_2 \\ w_3 \\ S_1 \\ S_2 \\ S_3 \end{Bmatrix} = \begin{Bmatrix} F_1^1 \\ F_2^1 \\ F_3^1 \\ F_1^2 \\ F_2^2 \\ F_3^2 \end{Bmatrix} \tag{10.5.6}$$

or, more explicitly, we have

$$
\begin{aligned}
&K_{11}^{11}w_1 + K_{12}^{11}w_2 + K_{13}^{11}w_3 + K_{11}^{12}S_1 + K_{12}^{12}S_2 + K_{13}^{12}S_3 = F_1^1\\
&K_{21}^{11}w_1 + K_{22}^{11}w_2 + K_{23}^{11}w_3 + K_{21}^{12}S_1 + K_{22}^{12}S_2 + K_{23}^{12}S_3 = F_2^1\\
&K_{31}^{11}w_1 + K_{32}^{11}w_2 + K_{33}^{11}w_3 + K_{31}^{12}S_1 + K_{32}^{12}S_2 + K_{33}^{12}S_3 = F_3^1\\
&K_{11}^{21}w_1 + K_{12}^{21}w_2 + K_{13}^{21}w_3 + K_{11}^{22}S_1 + K_{12}^{22}S_2 + K_{13}^{22}S_3 = F_1^2\\
&K_{21}^{21}w_1 + K_{22}^{21}w_2 + K_{23}^{21}w_3 + K_{21}^{22}S_1 + K_{22}^{22}S_2 + K_{23}^{22}S_3 = F_2^2\\
&K_{31}^{21}w_1 + K_{32}^{21}w_2 + K_{33}^{21}w_3 + K_{31}^{22}S_1 + K_{32}^{22}S_2 + K_{33}^{22}S_3 = F_3^2
\end{aligned}
\tag{10.5.7}
$$

Here (w_i, S_i) are the degrees of freedom (transverse deflection and rotation) at element node i (i = 1, 2, 3). Now letting

$$
\Delta_1 = w_1,\quad \Delta_2 = S_1,\quad \Delta_3 = w_2,\quad \Delta_4 = S_2,\quad \text{so on} \tag{10.5.8}
$$

and rearranging the algebraic equations 1 through 6 in (10.5.7) as equations 1, 4, 2, 5, 3, and 6, respectively, we obtain

$$
\begin{aligned}
&K_{11}^{11}w_1 + K_{11}^{12}S_1 + K_{12}^{11}w_2 + K_{12}^{12}S_2 + K_{13}^{11}w_3 + K_{13}^{12}S_3 = F_1^1\\
&K_{11}^{21}w_1 + K_{11}^{22}S_1 + K_{12}^{21}w_2 + K_{12}^{22}S_2 + K_{13}^{21}w_3 + K_{13}^{22}S_3 = F_1^2\\
&K_{21}^{11}w_1 + K_{21}^{12}S_1 + K_{22}^{11}w_2 + K_{22}^{12}S_2 + K_{23}^{11}w_3 + K_{23}^{12}S_3 = F_2^1\\
&K_{21}^{21}w_1 + K_{21}^{22}S_1 + K_{22}^{21}w_2 + K_{22}^{22}S_2 + K_{23}^{21}w_3 + K_{23}^{22}S_3 = F_2^2\\
&K_{31}^{11}w_1 + K_{31}^{12}S_1 + K_{32}^{11}w_2 + K_{32}^{12}S_2 + K_{33}^{11}w_3 + K_{33}^{12}S_3 = F_3^1\\
&K_{31}^{21}w_1 + K_{31}^{22}S_1 + K_{32}^{21}w_2 + K_{32}^{22}S_2 + K_{33}^{21}w_3 + K_{33}^{22}S_3 = F_3^2
\end{aligned}
\tag{10.5.9}
$$

or, in matrix form

$$
\begin{bmatrix}
K_{11}^{11} & K_{11}^{12} & K_{12}^{11} & K_{12}^{12} & K_{13}^{11} & K_{13}^{12}\\
K_{11}^{21} & K_{11}^{22} & K_{12}^{21} & K_{12}^{22} & K_{13}^{21} & K_{13}^{22}\\
K_{21}^{11} & K_{21}^{12} & K_{22}^{11} & K_{22}^{12} & K_{23}^{11} & K_{23}^{12}\\
K_{21}^{21} & K_{21}^{22} & K_{22}^{21} & K_{22}^{22} & K_{23}^{21} & K_{23}^{22}\\
K_{31}^{11} & K_{31}^{12} & K_{32}^{11} & K_{32}^{12} & K_{33}^{11} & K_{33}^{12}\\
K_{31}^{21} & K_{31}^{22} & K_{32}^{21} & K_{32}^{22} & K_{33}^{21} & K_{33}^{22}
\end{bmatrix}
\begin{Bmatrix} w_1\\ S_1\\ w_2\\ S_2\\ w_3\\ S_3 \end{Bmatrix}
=
\begin{Bmatrix} F_1^1\\ F_1^2\\ F_2^1\\ F_2^2\\ F_3^1\\ F_3^2 \end{Bmatrix}
\tag{10.5.10}
$$

The above discussion applies to any number of degrees of freedom per node (NDF). Computer implementation of the rearrangement of nodal

degrees of freedom and the associated equations is straightforward, and the Fortran statements of the procedure are given in Box 10.5.1. The logic is general in the sense that it holds for any NDF and NPE ($\mathbf{K}^{\alpha\beta}$, $\alpha, \beta = 1, 2, \ldots, \text{NDF}$).

The Fortran source code and executable files of **FEM2D** can be downloaded from the website http://mechanics.tamu.edu/. They give a more complete understanding on how various computational steps of finite element analysis are carried out. The program can be modified and extended to include one's own finite element formulations. In the next section, we illustrate the capabilities and limitations of the educational program **FEM2D**.

Box 10.5.1: Rearranging finite element equations of the form (10.5.5) to the form (10.5.10) (for the case of NDF = 2 and NPE = 3).

```
      II=1
            DO 200 I=1,NPE
               ELF(II)   =ELF1(I)
               ELF(II+1)=ELF2(I)
               JJ=1
               DO 100 J=1,NPE
                  ELK(II,JJ)      = ELK11(I,J)
                  ELK(II,JJ+1)    = ELK12(I,J)
                  ELK(II+1,JJ)    = ELK21(I,J)
                  ELK(II+1,JJ+1)  = ELK22(I,J)
  100          JJ=NDF*J+1
  200       II=NDF*I+1
```

10.5.4 Applications of FEM2D

10.5.4.1 Types of problems

The computer program **FEM2D** is developed to solve the following four types of problems:

Type 1 (ITYPE = 0): Single-variable problems, including convective-type boundary conditions for heat transfer problems from Chapter 9,

$$c_1\frac{\partial u}{\partial t} + c_1\frac{\partial^2 u}{\partial t^2} - \frac{\partial}{\partial x}\left(a_{11}\frac{\partial u}{\partial x}\right) - \frac{\partial}{\partial y}\left(a_{22}\frac{\partial u}{\partial y}\right) + a_{00}u = f \qquad (10.5.11a)$$

with

$$c_1 = c_0 + c_x x + c_y y, \quad a_{11} = a_{10} + a_{1x} x + a_{1y} y$$
$$a_{22} = a_{20} + a_{2x} x + a_{2y} y, \quad f_0 = f_0 + f_x x + f_y y \qquad (10.5.11b)$$
$$a_0 = \text{constant}, a_0$$

Type 2 (ITYPE = 1): Viscous incompressible fluid flows using the penalty function formulation of Chapter 11.

Type 3 (ITYPE = 2): Plane elasticity problems of Chapter 12.

Type 4 (ITYPE > 2): Plate bending problems using classical plate theory (ITYPE = 4 and 5) and shear deformation plate theory (ITYPE = 3). Only rectangular plate bending elements are considered (plate bending is not included in this edition of the book).

The first category of problems is quite general and includes, as special cases, many other field problems of engineering and science. As a special case, axisymmetric problems can also be analyzed. The last three categories are specific to linear (i.e., Stokes) viscous incompressible fluid flow, linear elasticity, and linear plate bending.

The type of gradient of the solution computed (in subroutine **POSTPROC**) for single-variable problems (Type 1) differs for different physical problems. For heat transfer problems, we wish to compute the x and y components of heat flux

$$q_x = -a_{11} \frac{\partial u}{\partial x}, \quad q_y = -a_{22} \frac{\partial u}{\partial y} \qquad (10.5.12)$$

The same definition applies to the calculation of the velocity components in the velocity potential formulation of inviscid fluid flows [i.e., q_x and q_y are the velocity components v_x and v_y, respectively]. In the stream function formulation, the velocity components (v_x, v_y) are defined by

$$v_x = a_{22} \frac{\partial u}{\partial y}, \quad v_y = -a_{11} \frac{\partial u}{\partial x} \qquad (10.5.13)$$

The (total) stresses (σ_{xx}, σ_{yy}, σ_{xy}) for multivariable problems are computed using the constitutive equations, with the strains (or strain rates for fluid flow problems) computed at the reduced Gauss points. The spatial variation of the derivatives of the solution is dependent on the element type.

For heat transfer problems (i.e., ITYPE = 0), the variable ICONV is used to indicate the presence (ICONV = 1) or absence (ICONV = 0) of convective boundaries. When convective boundaries are involved (i.e., ICONV = 1), the elements whose boundaries coincide with such a boundary will have additional contributions to their coefficient matrices [see Eqs. (9.4.6a), (9.4.6b), (9.4.15a), (9.4.15b), (9.5.6b), and (9.5.6c)]. The array IBN is used to store elements that have convective boundaries, and the array INOD is used to store the pairs of element local nodes (of elements in array IBN) that are on the convective boundary (to specify the side of the element on the convective boundary). If an element has more than one of its sides on the convective boundary, they should be repeated as many times as the number of sides on the convective boundary.

A complete list of the input variables to the program **FEM2D** and their description are presented in Table 10.5.1, which has the capability to analyze six classes (ITYPE = 0, 1, 2, . . . , 5) of problems discussed in this book. The variables in an input should be separated by a space (comma is not required); if all of the variables of a given input are not entered on the same line, the program will read it from the next line (blank lines are skipped).

Table 10.5.1 Description of the input data to the program **FEM2D**.

- **Input 1** *TITLE*

  TITLE — Title of the problem being solved (80 characters)

- **Input 2** *ITYPE, IGRAD, ITEM, NEIGN*

  ITYPE — Problem type
  ITYPE = 0: Single variable problems
  ITYPE = 1: Viscous incompressible flow problems
  ITYPE = 2: Plane elasticity problems
  ITYPE = 3: Plate bending problems by FSDT
  ITYPE = 4: Plate bending problems by CPT(N)
  ITYPE = 5: Plate bending problems by CPT(C)

  IGRAD — Indicator for computing the gradient of the solution or stresses in the postprocessor
  IGRAD = 0: No postprocessing is required
  IGRAD > 0: Postprocessing is required

  When ITYPE = 0 and IGRAD = 1, the gradient is computed as in Eq. 10.5.12; for ITYPE = 0 and IGRAD > 1 the gradient is computed by Eq. 10.5.13

  ITEM — Indicator for dynamic analysis
  ITEM = 0: Static analysis is required
  ITEM > 0: Either eigenvalue or transient analysis is required:
  ITEM = 1 Parabolic equation
  ITEM = 2 Hyperbolic equation

  NEIGN — Indicator for eigenvalue analysis
  NEIGN = 0: Static or transient analysis
  NEIGN > 0: Eigenvalue analysis:
  NEIGN = 1 Vibration analysis
  NEIGN > 1 Stability of plates

  *** Skip Input 3 if NEIGN = 0 ***

- **Input 3** *NVALU NVCTR*

  NVALU — Number of eigenvalues to be printed

  NVCTR — Indicator for printing eigenvectors:
  NVCTR = 0: Do not print eigenvectors
  NVCTR > 0: Print eigenvectors

- **Input 4** *IELTYP NPE MESH NPRNT*

  IELTYP — Element type used in the analysis
  IELTYP = 0 Triangular elements
  IELTYP > 0 Quadrilateral elements

  NPE — Nodes per element
  NPE = 3: Linear triangle (IELTYP = 0)
  NPE = 4: Linear quadrilateral (IELTYP > 0)
  NPE = 6: Quadratic triangle (IELTYP = 0)
  NPE = 8 or 9: Quadratic quadrilateral (IELTYP > 0)

  MESH — Indicator for mesh generation by the program
  MESH = 0, Mesh is not generated by the program
  MESH = 1, Mesh is generated by the program for rectangular domains by **MESH2DR**
  MESH >1: Mesh is generated by the program for non-rectangular domains by **MESH2DG**

NPRNT	Indicator for printing certain output NPRNT = 0: Do not print NOD and element and global matrices NPRNT = 1: Print NOD and element 1 matrices (ELK and ELF) NPRNT = 2: Print NOD and global matrices (GLK and GLF) NPRNT > 2: Combination of NPRNT = 1 and 2
	*** Skip Input 5 if MESH = 1 ***

- **Input 5** *NEM, NNM*

NEM	Number of elements in the mesh when the user inputs the mesh or the mesh is generated by **MESH2DG**
NNM	Number of nodes in the mesh when the user inputs the mesh or the mesh is generated by **MESH2DG**
	*** Skip Inputs 6 and 7 if MESH ≠ 0 ***

- **Input 6** *(NOD(N,I),I=1,NPE)*

NOD(N,I)	Connectivity for the Nth element (I=1,NPE)

- **Input 7** *((GLXY(I,J),J=1,2),I=1,NNM)*

GLXY(I, J)	Global x and y coordinates of the Ith global node in the mesh (J = 1, x coordinate; J = 2, y coordinate)
	*** Inputs 8–11 are read in **MESH2DG** (for MESH > 1) ***

- **Input 8** *NRECL*

NRECL	Number of line records to be read in the mesh
	*** Read the following variables NRECL times:***

- **Input 9** *NOD1 NODL NODINC X1 Y1 XL YL RATIO*

NOD1	First global node number of the line segment
NODL	Last global node number of the line segment
NODINC	Node increment on the line
X1	The global x coordinate of NOD1
Y1	The global y coordinate of NOD1
XL	The global x coordinate of NODL
YL	The global y coordinate of NODL
RATIO	The ratio of the first element length to the last element length

- **Input 10** *NRECEL*

NRECEL	Number of rows of elements to be read in the mesh
	*** Read the following variables NRECEL times: ***

- **Input 11** *NEL1 NELL IELINC NODINC NPE NODE(I)*

NEL1	First element number of the row
NELL	Last element number of the row
IELINC	Increment of element number in the row
NODINC	Increment of the global node number in the row
NPE	Number of nodes in each element
NODE(I)	Connectivity array of the first element in the row (I=1,NPE)
	*** Skip Inputs 12–14 if MESH ≠ 1 ***

- **Input 12** *NX, NY*

NX	Number of elements in the x direction
NY	Number of elements in the y direction

- **Input 13** *X0, (DX(I), I=1,NX)*

  X0 — The x coordinate of global node 1
  DX(I) — The x dimension of the Ith subdivision (I=1, NX)

- **Input 14** *Y0,(DY(I), I=1,NY)*

  Y0 — The y coordinate of global node 1
  DY(I) — The y dimension of the Ith subdivision (I=1, NY)

- **Input 15** *NSPV*

  NSPV — The number of specified primary variables

  *** Skip Input 16 if NSPV = 0 ***

- **Input 16** *((ISPV(I,J), J=1,2), I=1,NSPV)*

  ISPV(I,J) — Node number and local degree of freedom (DOF) number of the Ith specified primary variable
  ISPV(I, 1) = Node number
  ISPV(I, 2) = Local DOF number
  The do-loops on I and J are: [(J=1, 2), I=1, NSPV]

  *** Skip Input 17 if NSPV = 0 or NEIGN ≠ 0 ***

- **Input 17** *(VSPV(I), I=1,NSPV)*

  VSPV(I) — Specified value of the Ith primary variable (I=1, NSPV)

  *** Skip Input 18 if NEIGN ≠ 0 ***

- **Input 18** *NSSV*

  NSSV — Number of (nonzero) specified secondary variables

  *** Skip Input 19 if NSSV=0 or NEIGN ≠ 0 ***

- **Input 19** *((ISSV(I,J), J=1,2), I=1,NSSV)*

  ISSV(I, J) — Node number and local DOF number of the Ith specified secondary variable
  ISSV(I, 1) = Node number
  ISSV(I, 2) = Local DOF number
  The loops on I and J are: ((J=1, 2), I=1, NSSV)

  *** Skip Input 20 if NSSV = 0 or NEIGN ≠ 0 ***

- **Input 20** *(VSSV(I), I=1,NSSV)*

  VSSV(I) — Specified value of the Ith secondary variable (I=1, NSSV)

  *** Inputs 21–27 are for single variable problems (ITYPE = 0) ***

- **Input 21** *A10, A1X, A1Y*

  A10, A1X, A1Y — Coefficients of the differential equation:
  a11 = A10 + A1X*X + A1Y*Y

- **Input 22** *A20, A2X, A2Y*

  A20, A2X, A2Y — Coefficients of the differential equation:
  a22 = A20 + A2X*X + A2Y*Y

- **Input 23** *A00*

  A00 — Coefficient of the differential equation

- **Input 24** *ICONV*

  ICONV — Indicator for convection boundary conditions
  ICONV = 0: No convection; ICONV > 0: Convection is present

- **Input 25** *NBE*

  NBE — Number of elements with convection

  *** The following inputs are read for each I, I = 1, NBE ***

- **Input 26** *(IBN(I), (INOD(I,J), J=1,2), BETA(I), TINF(I), I=1,NBE)*

  IBN(I) — Ith element number with convection
  INOD(I, J) — Local node numbers of the side with convection
  (J = 1, 2; for quadratic elements, give the end nodes)
  BETA(I) — Film coefficient for convection on Ith element
  TINF(I) — Ambient temperature of the Ith element

  *** Input 27 is for viscous fluid flows (ITYPE = 1) only ***

- **Input 27** *VISCSITY, PENALTY*

  VISCSITY — Viscosity of the fluid
  PENALTY — Value of the penalty parameter

  *** Inputs 28 and 29 are for plane elasticity (ITYPE = 2) only.

- **Input 28** *LNSTRS*

  LNSTRS — Flag for plane stress or plane strain problems
  LNSTRS = 0: Plane strain; LNSTRS > 0: Plane stress

- **Input 29** *E1, E2, ANU12, G12, THKNS*

  E1 — Young's modulus along the global x axis
  E2 — Young's modulus along the global y axis
  ANU12 — Poisson's ratio in the xy plane
  G12 — Shear modulus in the xy plane
  THKNS — Thickness of the plane elastic body analyzed

  *** Input 30 is for plate bending problems (ITYPE = 3 to 5) only ***

- **Input 30** *E1, E2, ANU12, G12, G13, G23, THKNS*

  E1 — Young's modulus along the global x axis
  E2 — Young's modulus along the global y axis
  ANU12 — Poisson's ratio in the xy plane
  G12 — Shear modulus in the xy plane
  G13 — Shear modulus in the xz plane
  G23 — Shear modulus in the yz plane
  THKNS — Thickness of the plate analyzed

  *** Remaining Inputs are for all problem types ***
  *** Skip Input 31 if NEIGN ≠ 0 ***

- **Input 31** *F0, FX, FY*

  F0, FX, FY — Coefficients to define the source term:
  f(x, y) = F0 + FX*x + FY*y

  *** Inputs 32–36 are for transient analysis (ITEM ≠ 0) only. ***
  *** Skip Input 32 if ITEM = 0 ***

- **Input 32** *C0, CX, CY*

  C0, CX, CY — Coefficients defining the temporal parts of the differential equations, as defined below:
  C1 = C0 + CX*X + CY*Y when ITYPE = 0 or 1
  C1 = (C0 + CX*X + CY*Y)*THKNS when ITYPE = 2
  I0 = C0*THKNS, I2 = C0*(THKNS**3)/12, and
  CX and CY are not used when NEIGN ≤ 1 and ITYPE = 3 to 5
  when ITYPE = 3 and NEIGN > 1

  *** Skip Input 33 if ITEM = 0 or NEIGN ≠ 0 ***

- **Input 33** *NTIME, NSTP, INTVL, INTIAL*

  NTIME — Number of time steps for the transient solution
  NSTP — Time step number at which the source is removed
  INTVL — Time step interval at which to print the solution
  INTIAL — Indicator for nature of initial conditions
  INTIAL = 0: zero initial conditions; INTIAL > 0: non-zero initial conditions

  *** Skip Input 34 if ITEM = 0 or NEIGN ≠ 0 ***

- **Input 34** *DT, ALFA, GAMA, EPSLN*

  DT — Time step used for the transient solution

  ALFA — Parameter in the alfa-family of time approximation used for parabolic equations:

  ALFA = 0: The forward difference scheme (CS)†
  ALFA = 0.5: The Crank–Nicolson scheme (stable)
  ALFA = 2/3: The Galerkin scheme (stable)
  ALFA = 1: The backward difference scheme (stable)
  † CS = conditionally stable; for all schemes with ALFA < 0.5, the time step DT is restricted to DT < 2/[MAXEGN*(1-2*ALFA)], where MAXEGN is the maximum eigenvalue of the discrete problem

  GAMA — Parameter in the Newmark time integration scheme used for hyperbolic equations:
  GAMA = 0.5: Constant-average acceleration (stable)
  GAMA = 1/3: Linear acceleration scheme (C.S.)
  GAMA = 0.0: The central difference scheme (C.S.)

  ALFA = 0.5 for all schemes; for schemes for which ALFA ≤ 0.5 and GAMA < ALFA, DT is restricted to: DT < 2/SQRT[MAXEGN*(ALFA-GAMA)], MAXEGN being the maximum eigenvalue of the discrete system

  EPSLN — A small parameter to check if the solution has reached a steady state

  *** Skip Input 35 if ITEM or INTIAL = 0, or NEIGN ≠ 0 ***

- **Input 35** *(GLU(I), I=1,NEQ)*

  GLU(I) — Vector of initial value of the primary variables (I=1, NEQ), where NEQ = Number of nodal values in the mesh

  *** Skip Input 36 if ITEM ≤ 1, NEIGN ≠ 0, or INTIAL = 0 ***

- **Input 36** *(GLV(I), I=1,NEQ)*

  GLV(I) — Vector of the initial values of the first derivative of the primary variables (velocity) (I=1, NEQ)

10.5.4.2 Description of mesh generators

In this section, the input data to **FEM2D** for several example problems are given. The example problems are selected from those discussed in earlier sections of this chapter. A major limitation of the program lies in the mesh generation [i.e., the computation of arrays NOD(I, J) and GLXY(I, J) for arbitrary domains]. For such problems, the user is required to input the mesh information, which can be a tedious job if many elements are used. Of course, the program can be modified to accept any other mesh generation subroutines.

The program **MESH2DR** is restricted to rectangular domains with sides parallel to the global x and y axes. The subroutine requires the following input data, as evidenced by Inputs 12, 13, and 14 of Table 10.5.1:

NX	Number of elements in the x direction
NY	Number of elements in the y direction
(X_0, Y_0)	Global coordinates of global node 1, which is located at the lower left corner of the domain (see Fig. 10.5.3)
DX(I)	Array of element lengths along the x direction
DY(I)	Array of element lengths along the y direction

The node and element numbering schemes for triangular and rectangular element meshes generated by **MESH2DR** are shown in Fig. 10.5.3.

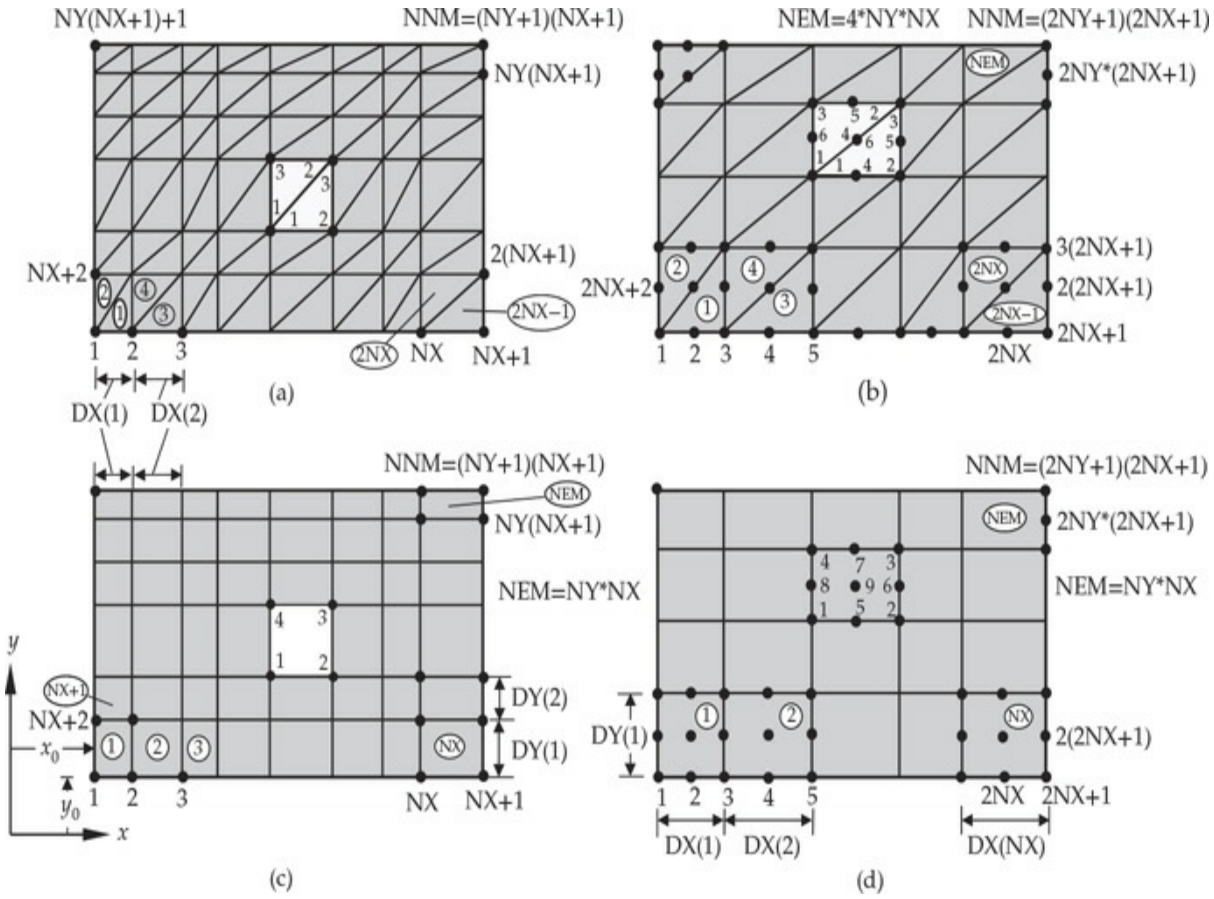

Fig. 10.5.3 Element numbering and global and element node numbering systems used in **MESH2DR** for mesh generation of rectangular domains. (a) Mesh of linear triangles. (b) Mesh of quadratic triangles. (c) Mesh of linear rectangles. (d) Mesh of nine-node rectangles.

The subroutine **MESH2DG**, relatively more general than **MESH2DR**, requires the user to sketch a desired mesh with certain regularity of node and element numbering. It exploits the regularity to generate the mesh. The program **MESH2DG** requires Inputs 5 and 8 through 11 of Table 10.5.1 (all variables are read from the subroutine). The type of data being read in **MESH2DG** should give some indication of the restrictions of the program. The node and element numbering should be regular along the lines and rows being read. Figure 10.5.4(a)–(d) shows typical examples of meshes of linear and quadratic triangular and quadrilateral elements. For each of these meshes, the input data required for **MESH2DG** is listed in Boxes 10.5.2–10.5.5.

Box 10.5.2: Input data to generate the mesh shown in Fig. 10.5.4(a).

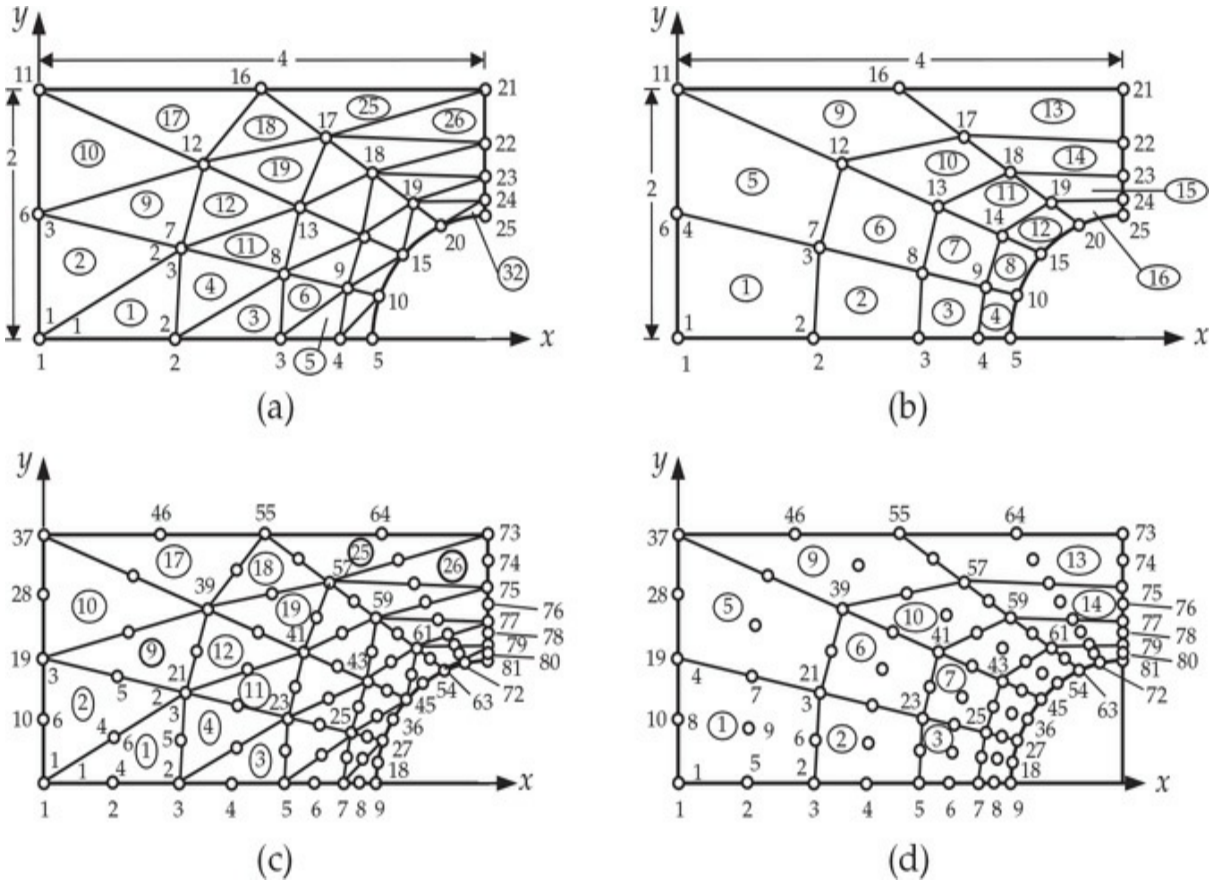

Fig. 10.5.4 An example of mesh generation using **MESH2DG**. (a) Mesh of linear triangles. (b) Mesh of linear rectangles. (c) Mesh of quadratic triangles. (d) Mesh of nine-node quadratic rectangles.

```
 0   3   2   0                                  IELTYP,NPE,MESH,NPRNT
32  25                                          NEM, NNM
 5                                              NRECL
 1   5  1 0.0 0.0 3.0     0.0     6.0  NOD1,NODL,NODINC,
 6  10  1 0.0 1.0 3.07612 0.38268 6.0  X1,Y1,XL,YL,RATIO
11  15  1 0.0 2.0 3.29289 0.7071  6.0  for each of the
16  20  1 2.0 2.0 3.61732 0.92388 6.0  five line segments
21  25  1 4.0 2.0 4.0     1.0     6.0
 8                                              NRECEL
 1   7  2  1  3   1   2   7              NEL1,NELL,IELINC,
 2   8  2  1  3   1   7   6              NODINC,NPE,NOD(I,J),
 9  15  2  1  3   6   7  12              for each of the
10  16  2  1  3   6  12  11              eight rows of elements
17  23  2  1  3  11  12  16
18  24  2  1  3  12  17  16
25  31  2  1  3  16  17  21
26  32  2  1  3  17  22  21
```

Box 10.5.3: Input data to generate the mesh shown in Fig. 10.5.4(b).

```
 1   4   2   0                                  IELTYP,NPE,MESH,NPRNT
16  25                                          NEM, NNM
 5                                              NRECL
 1   5  1 0.0 0.0 3.0      0.0      6.0        NOD1,NODL,NODINC, ...
 6  10  1 0.0 1.0 3.07612  0.38268  6.0
11  15  1 0.0 2.0 3.29289  0.7071   6.0
16  20  1 2.0 2.0 3.61732  0.92388  6.0
21  25  1 4.0 2.0 4.0      1.0      6.0
 4                                              NRECEL
 1   4   1   1   4    1   2    7    6          NEL1,NELL,IELINC,NODINC
 5   8   1   1   4    6   7   12   11          etc.
 9  12   1   1   4   11  12   17   16
13  16   1   1   4   16  17   22   21
```

Box 10.5.4: Input data to generate the mesh shown in Fig. 10.5.4(c).

```
 0   6   2   0                                  IELTYP,NPE,MESH,NPRNT
32  81                                          NEM, NNM
 9                                              NRECL
 1   9 1 0.0 0.0 3.0      0.0       6.0
10  18 1 0.0 0.5 3.01921  0.19509   6.0
19  27 1 0.0 1.0 3.07612  0.38268   6.0
28  36 1 0.0 1.5 3.16853  0.55557   6.0        NOD1,NODL,NODINC,
37  45 1 0.0 2.0 3.29289  0.7071    6.0        X1,Y1,XL,YL,RATIO
46  54 1 1.0 2.0 3.44443  0.83147   6.0        for each of nine
55  63 1 2.0 2.0 3.61732  0.92388   6.0        line segments
64  72 1 3.0 2.0 3.80491  0.98078   6.0
73  81 1 4.0 2.0 4.0      1.0       6.0
 8                                              NRECEL
 1   7  2  2  6  1  3 21  2 12 11
 2   8  2  2  6  1 21 19 11 20 10
 9  15  2  2  6 19 21 39 20 30 29
10  16  2  2  6 19 39 37 29 38 28              NEL1,NELL,IELINC,NODINC,
17  23  2  2  6 37 39 55 38 47 46              NPE,NOD(I,J)
18  24  2  2  6 39 57 55 48 56 47
25  31  2  2  6 55 57 73 56 65 64
26  32  2  2  6 57 75 73 66 74 65
```

Box 10.5.5: Input data to generate the mesh shown in Fig. 10.5.4(d).

```
 2   9   2   0                                    IELTYP,NPE,MESH,NPRNT
16  81                                           NEM, NNM
 9                                               NRECL
 1   9  1 0.0 0.0 3.0      0.0      6.0
10  18  1 0.0 0.5 3.01921 0.19509 6.0
19  27  1 0.0 1.0 3.07612 0.38268 6.0
28  36  1 0.0 1.5 3.16853 0.55557 6.0            NOD1,NODL,NODINC,
37  45  1 0.0 2.0 3.29289 0.7071  6.0            X1,Y1,XL,YL,RATIO
46  54  1 1.0 2.0 3.44443 0.83147 6.0            for each line segment
55  63  1 2.0 2.0 3.61732 0.92388 6.0
64  72  1 3.0 2.0 3.80491 0.98078 6.0
73  81  1 4.0 2.0 4.0     1.0     6.0
 4                                               NRECEL
 1   4 1 2 9  1  3 21 19  2 12 20 10 11
 5   8 1 2 9 19 21 39 37 20 30 38 28 29          NEL1,NELL,IELINC,NODINC,
 9  12 1 2 9 37 39 57 55 38 48 56 46 47          NPE,NOD(I,J)
13  16 1 2 9 55 57 75 73 56 66 74 64 65
```

10.5.5 Illustrative Examples

Here we consider several examples from Chapter 9 (i.e., Type 1 or ITYPE = 0 problems) to illustrate the use of FEM2D in their solution. Additional examples will be considered in Chapters 11–12. As the problems considered were already discussed previously, only input data to FEM2D is discussed here.

Example 10.5.1

We consider the Poisson equation of **Example 9.4.1**

$$-\nabla^2 u = 1 \text{ in } \Omega, \quad u = 0 \text{ on } \Gamma$$

where Ω is a square of two units and Γ denotes the boundary of Ω. Due to the biaxial symmetry, we can use a quadrant of the domain to solve the problem using the finite element method. Analyze the problem using two different meshes: (1) mesh of linear triangles [Fig. 10.5.5(a)] and (2) mesh of linear rectangles [Fig. 10.5.5(b)] in the computational domain.

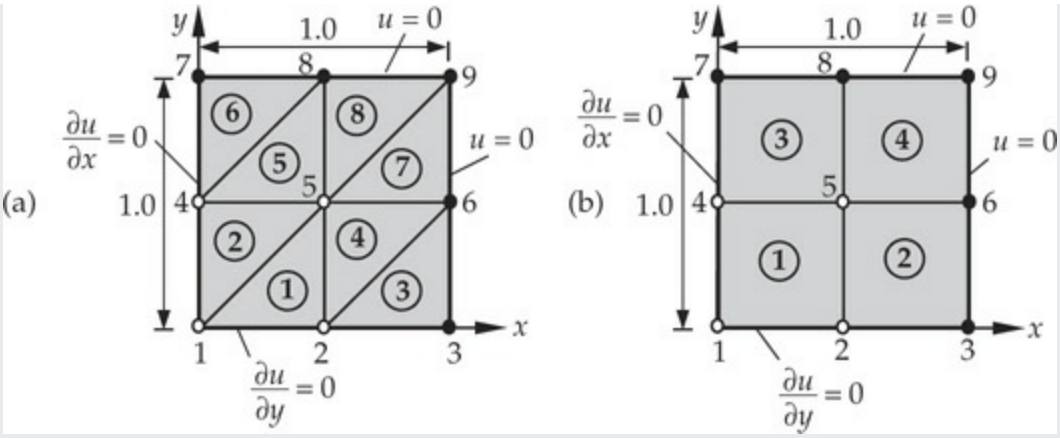

Fig. 10.5.5 Finite element meshes of (a) linear triangles and (b) linear rectangles.

Solution: The problem is one of static in nature and belongs to Type 1. Hence, we have ITYPE = 0, IGRAD = 1, ITEM = 0, and NEIGN = 0. We have 2 × 2 mesh of triangles and rectangles to analyze, and both meshes have the same nodes.

For the 2 × 2 mesh of triangles, we have IELTYP = 0, NPE = 3, MESH = 1 (chose to generate the mesh using the subroutine **MESH2DR**), and NPRNT = 0 (no printing of NOD array and element matrices). For the 2 × 2 mesh of rectangles, we have IELTYP = 1, NPE = 4, MESH = 1 , and NPRNT = 0. The rest of the input data for the mesh of triangles and rectangles is the same.

The number of subdivisions and their lengths along each direction are NX = 2, NY = 2, X0 = 0.0, Y0 = 0.0, DX(1) = 0.5, DX(2) = 0.5, DY(1) = 0.5, DY(2) = 0.5. The number of specified primary variables (NSPV), the node numbers, the specified local degree of freedom (ISPV), and their specified values (VSPV) for the problem are: NSPV = 5, ISPV(I, J) = (3, 1; 6, 1; 7, 1; 8, 1; 9, 1), and VSPV(I) = (0.0, 0.0, 0.0, 0.0, 0.0). There are no specified secondary variables, NSSV=0. The coefficients a^{11} and a^{22} of the differential equation are A10 = 1.0, A1X=0.0, A1Y=0.0, A20=1.0, A2X=0.0, A2Y =0.0, and A00 = 0.0; there is no convection ICONV = 0; and the source is F0 = 1.0, FX = 0.0, and FY = 0.0.

The input data to **FEM2D** for mesh of triangles and rectangles are presented in Box 10.5.6, and the corresponding (edited) output in Box 10.5.7. The numerical results of this problem were discussed in **Example 9.4.1**.

Box 10.5.6: Input data for the Poisson equation of **Example 10.5.1**.

```
Example 9.4.1: Poisson's equation in a square
0   1   0   0          ITYPE,IGRAD,ITEM,NEIGN
0   3   1   0          IELTYP,NPE,MESH,NPRNT  1  4  1  0 (for rectangles)
2   2                  NX,NY
0.0  0.5 0.5           X0,DX(I)
0.0  0.5 0.5           Y0,DY(I)
5                      NSPV
3 1  6 1  7 1  8 1  9 1 ISPV
0.0  0.0  0.0  0.0  0.0 VSPV
0                      NSSV
1.0   0.0  0.0         A10, A1X, A1Y
1.0   0.0  0.0         A20, A2X, A2Y
0.0                    A00
0                      ICONV
1.0   0.0  0.0         F0, FX, FY
```

Example 10.5.2

Consider an isotropic, thin, square plate of 1 m × 1 m. The left side of the plate (i.e., $x = 0$) is maintained at 100°C, the boundary $y = 1$ m is maintained at 500°C, and boundaries $x = 1$ m and $y = 0$ are exposed to an ambient temperature of 100°C. Assume a film coefficient of $\beta = 10$ W/(m$^{2\circ}$C) and no internal heat generation ($f = 0$). Using conductivities $k_x = k_y = 12.5$ W/(m°C) and a uniform 8 × 8 mesh of quadrilateral elements (see Fig. 10.5.6), analyze the problem with FEM2D.

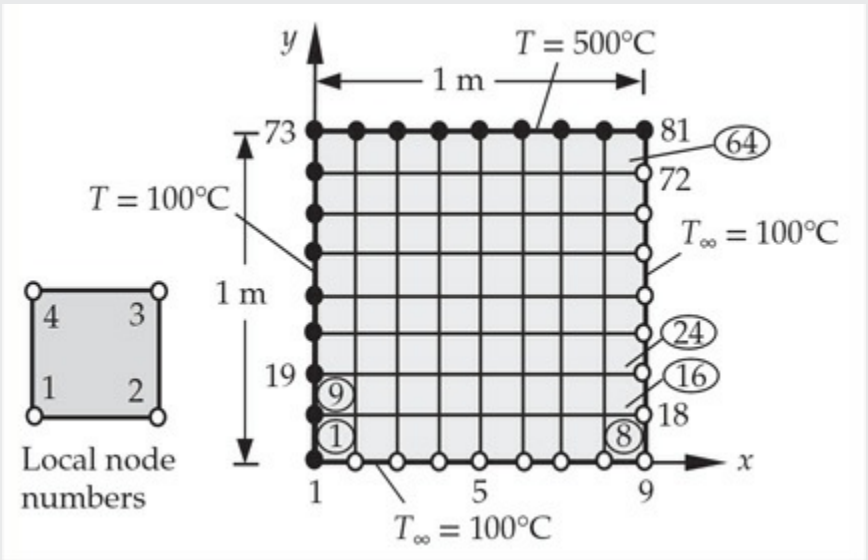

Fig. 10.5.6 The 8 × 8 finite element mesh used for convective heat

transfer problem of **Example 10.5.2**.

Solution: The governing equation is the same as that in Eq. (9.4.1). The input variables associated with convective boundary conditions are ICONV=1, NBE = 16, {IBN(I), BETA(I), TINF(I)} = 1, 10.0, 100.0; 2, 10.0, 100.0, and so on. INOD(I,J) = 1, 2; 1, 2; and so on (element 8 has two sides, 1-2 and 2-3, exposed to convection). The coefficients a_{11}, a_{22}, and a_{00} are A10 = 12.5, A1X = 0.0, A1Y = 0.0, A20 = 12.5, A2X = 0.0, A2Y = 0.0, and A00 = 0.0. The source is zero: F0 = 0.0, FX = 0.0, and FY = 0.0.

Box 10.5.7: Edited output for the Poisson equation of **Example 10.5.1**.

Node	x-coord.	y-coord.	Primary DOF
1	0.00000E+00	0.00000E+00	0.31250E+00
2	0.50000E+00	0.00000E+00	0.22917E+00
3	0.10000E+01	0.00000E+00	0.00000E+00
4	0.00000E+00	0.50000E+00	0.22917E+00
5	0.50000E+00	0.50000E+00	0.17708E+00
6	0.10000E+01	0.50000E+00	0.00000E+00
7	0.00000E+00	0.10000E+01	0.00000E+00
8	0.50000E+00	0.10000E+01	0.00000E+00
9	0.10000E+01	0.10000E+01	0.00000E+00

x-coord.	y-coord.	-a11(du/dx)	-a22(du/dy)	Flux Mgntd	Orient.
0.3333E+00	0.1667E+00	0.1667E+00	0.1042E+00	0.1965E+00	32.01
0.1667E+00	0.3333E+00	0.1042E+00	0.1667E+00	0.1965E+00	57.99
0.8333E+00	0.1667E+00	0.4583E+00	0.0000E+00	0.4583E+00	0.00
0.6667E+00	0.3333E+00	0.3542E+00	0.1042E+00	0.3692E+00	16.39
0.3333E+00	0.6667E+00	0.1042E+00	0.3542E+00	0.3692E+00	73.61
0.1667E+00	0.8333E+00	0.0000E+00	0.4583E+00	0.4583E+00	90.00
0.8333E+00	0.6667E+00	0.3542E+00	0.0000E+00	0.3542E+00	0.00
0.6667E+00	0.8333E+00	0.0000E+00	0.3542E+00	0.3542E+00	90.00

Box 10.5.8 contains the input data for the 8 × 8 mesh of linear quadrilateral elements (8Q4). The output for this problem is not included here but the results are included in the form of figures. The results also include the results obtained with 4 × 4 mesh of nine-node quadrilateral elements (4Q9), which is nodally equivalent to the 8 × 8 mesh, with the following changes to the input file: IELTYP = 2; NPE = 9; DX(I) = {0.25, 0.25, 0.25, 0.25}; DY(I) = {0.25, 0.25, 0.25, 0.25}; and NBE = 8. Plots of temperature variations and heat flow

$$q_x = -k_x \frac{\partial T}{\partial x}, \quad q_y = -k_y \frac{\partial T}{\partial y}$$

along the boundaries are shown in Figs. 10.5.7 and 10.5.8. Note that q_x is linear in y and constant in x, and q_y is linear in y and constant in x (for constant k_x and k_y). A nonuniform mesh with smaller elements in the high-gradient region gives more accurate results.

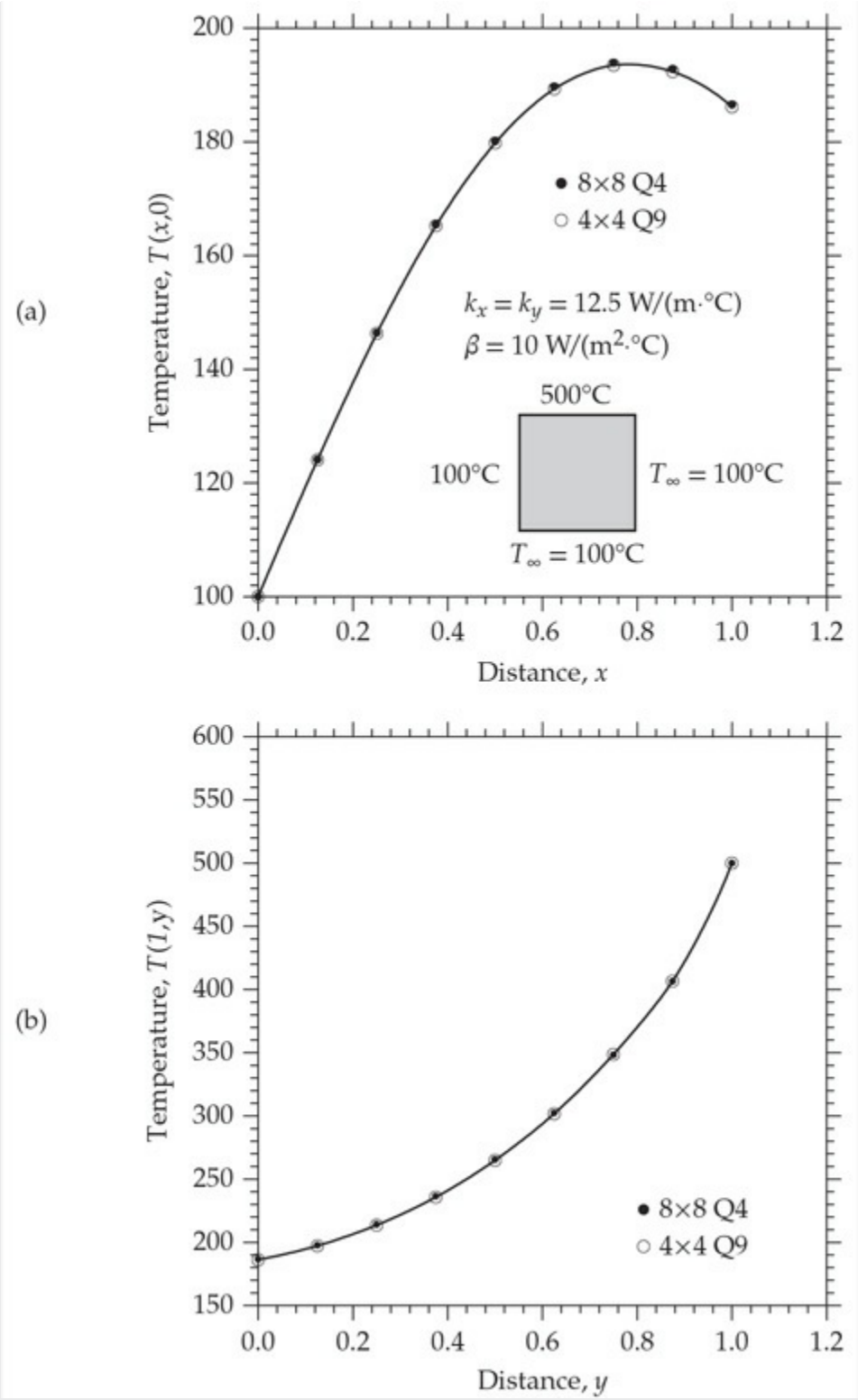

Fig. 10.5.7 Temperature variations along the boundaries (a) y=0 and (b) x=1 for the convective heat transfer problem of **Example 10.5.2**: 4Q9 = 4×4 mesh of nine-node quadrilateral elements; 8Q4 = 8×8 mesh of four-node quadrilateral elements.

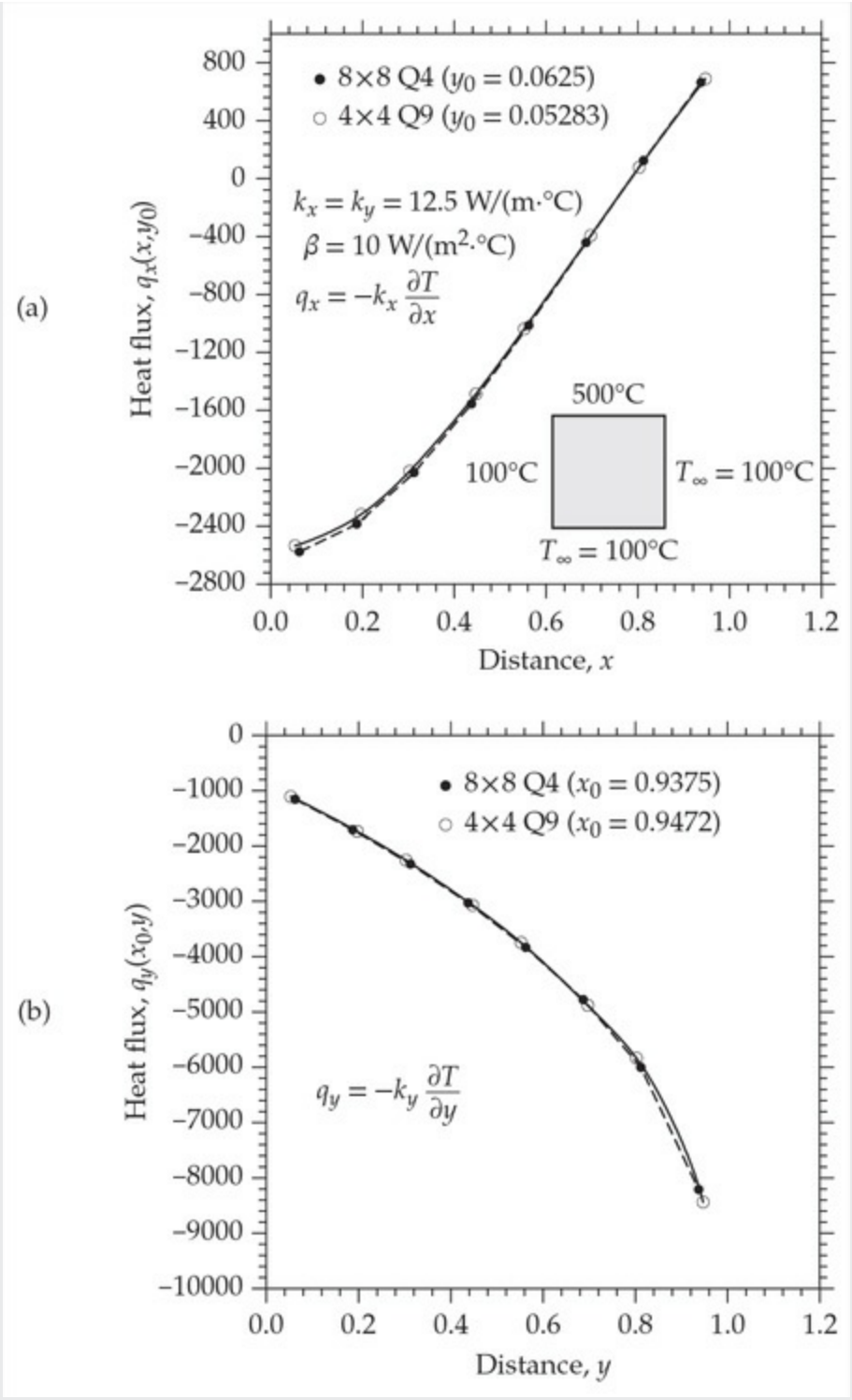

Fig. 10.5.8 Variations of the heat flux components. (a) $q_x(x, y_0)$ (y_0 = 0.05283 and y_0 = 0.0625) boundaries (at the Gauss points nearest to the boundaries) and (b) q_y (x_0, y) (x_0 = 0.9472 and x_0 = 0.9375).

Box 10.5.8: The input to program **FEM2D** for the problem of **Example 10.5.2**.

```
Example 10.5.2: Convective heat transfer in a square region
0   1   0   0          ITYPE,IGRAD,ITEM,NEIGN
1   4   1   0          IELTYP,NPE,MESH,NPRNT
8   8                  NX,NY
0.0 0.125 0.125 0.125 0.125 0.125 0.125 0.125 0.125 X0,DX(I)
0.0 0.125 0.125 0.125 0.125 0.125 0.125 0.125 0.125 Y0,DY(I)
17                     NSPV
 1 1  10 1  19 1  28 1  37 1  46 1  55 1  64 1 73 1
74 1  75 1  76 1  77 1  78 1  79 1  80 1  81 1  ISPV(I,J)
100.0 100.0 100.0 100.0 100.0 100.0 100.0 100.0 500.0
500.0 500.0 500.0 500.0 500.0 500.0 500.0 500.0 VSPV(I)
0                      NSSV
12.5  0.0  0.0         A10, A1X, A1Y
12.5  0.0  0.0         A20, A2X, A2Y
 0.0                   A00
1                      ICONV
16                     NBE,IBN(I),INoDE(I,J),BETA(I),TINF(I)
 1 1 2 10.0 100.0  2 1 2 10.0 100.0  3 1 2 10.0 100.0
 4 1 2 10.0 100.0  5 1 2 10.0 100.0  6 1 2 10.0 100.0
 7 1 2 10.0 100.0  8 1 2 10.0 100.0  8 2 3 10.0 100.0
16 2 3 10.0 100.0 24 2 3 10.0 100.0 32 2 3 10.0 100.0
40 2 3 10.0 100.0 48 2 3 10.0 100.0 56 2 3 10.0 100.0
64 2 3 10.0 100.0
 0.0  0.0  0.0              F0, FX, FY
```

The temperature values along the x-axis are as follows:

Node	x	y	Temperature
1	0.00000E+00	0.00000E+00	0.10000E+03
2	0.12500E+00	0.00000E+00	0.12408E+03
3	0.25000E+00	0.00000E+00	0.14640E+03
4	0.37500E+00	0.00000E+00	0.16545E+03
5	0.50000E+00	0.00000E+00	0.18011E+03
6	0.62500E+00	0.00000E+00	0.18970E+03
7	0.75000E+00	0.00000E+00	0.19392E+03
8	0.87500E+00	0.00000E+00	0.19280E+03
9	0.10000E+01	0.00000E+00	0.18657E+03

The program can also be used to analyze axisymmetric problems. For example, consider a finite cylinder of radius R_0 = 1 m and length L = 1 m. The bottom and top of the cylinder are maintained at T_0 = 100°C, while the surface is exposed to an ambient temperature T_∞ = 100°C (β = 10W/(m^2·°C). For this case, the governing differential equation is given by Eq. (9.2.71) with $\hat{a}_{11} = k_r$, $\hat{a}_{22} = k_z$, and $\hat{a}_{00} = 0$. The coefficients A10,

A1X, A1Y, A20, A2X, A2Y, and A00 for **FEM2D** are: A10 = 0.0, A1X = $2\pi k_r$, A1Y = 0.0, A20 = 0.0, A2X = $2\pi k_z$, A2Y = 0.0, A00 = 0.0. The uniform heat generation f_0 (if not zero) is entered as F0 = 0.0, FX = $2\pi f_0$, and FY = 0.0. For an $m \times n$ mesh of linear elements, the number of elements with convective boundary will be n.

Example 10.5.3

Consider the flow of an inviscid fluid around a cylinder (see **Example 9.4.6**). The governing equation is given by $-\nabla_2 u = 0$, where u is either the velocity potential $u = \phi$ or the stream function $u = \Psi$. Use the velocity potential and stream function formulations to determine the velocity fields.

Solution: Since the domain is not rectangular, we should use subroutine **MESH2DG** (i.e., set MESH = 2). We consider the mesh of 25 nodes and 32 triangular elements shown in Fig. 10.5.4(a) and 25 nodes and 16 quadrilateral elements shown in Fig. 10.5.4(b) (they are nodally equivalent). We have ITYPE = 0; IGRAD=1 in the velocity potential formulation because ($-\boldsymbol{\Delta}\phi = \mathbf{v}$) and IGRAD = 2 in the stream function formulation; ITEM = 0 and NEIGN = 0; IELTYP = 0 for triangles and IELTYP = 1 for quadrilaterals; and MESH = 2 and NPRNT = 0. The coefficients are

$$\text{A10} = 1.0,\ \text{A20} = 1.0,\ \text{A1X} = 0.0,\ \text{A1Y} = 1.0,\ \text{A2X} = 0.0,\ \text{A2Y} = 0.0,\ \text{A00} = 0.0,$$

$$\text{F0} = 0.0,\ \text{FX} = 0.0,\ \text{and FY} = 0.0$$

The input for **MESH2DG** are given in Box 10.5.2 for triangular mesh and Box 10.5.3 for the mesh of quadrilateral elements. In the stream function formulation, we have NSPV = 13 and NSSV = 0; and in the velocity potential formulation, we have NSPV = 5 and NSSV = 3. The partial input of the problem is given in Box 10.5.9. A detailed discussion of the numerical results is presented in **Example 9.4.6**.

Box 10.5.9: The input for the problem of **Example 10.5.3**.

```
Example 10.5.3(a): Flow around a cylinder (VEL. POTENTIAL)
    0   1   0   0                   ITYPE,IGRAD,ITEM,NEIGN
    0   3   2   0                   IEL, NPE, MESH, NPRNT
   *** See Box 10.5.2 for the MESH2DG input ***
    5                               NSPV
   21 1  22 1  23 1  24 1  25 1     ISPV(I,J)
    0.0   0.0   0.0   0.0   0.0     VSPV(I)
    3                               NSSV
    1 1   6 1  11 1                 ISSV(I,J)
    0.5   1.0   0.5                 VSSV(I)
    1.0  0.0  0.0                   A10, A1X, A1Y
    1.0  0.0  0.0                   A20, A2X, A2Y
    0.0                             A00
    0                               ICONV
    0.0  0.0  0.0                   F0, FX, FY

Example 10.5.3(b): Flow around a cylinder (STRM FUNCN)
    0   2   0   0                   ITYPE,IGRAD,ITEM,NEIGN
    1   4   2   0                   IELTYP,NPE,MESH,NPRNT
    *** See Box 10.5.3 for the MESH2DG input ***
   13                               NSPV
    1 1   2 1   3 1   4 1   5 1  10 1  15 1  20 1  25 1
    6 1  11 1  16 1  21 1           ISPV(I,J)
    0.0   0.0   0.0   0.0   0.0   0.0   0.0   0.0   0.0
    1.0   2.0   2.0   2.0           VSPV(I)
    0                               NSSV
    1.0  0.0  0.0                   A10, A1X, A1Y
    1.0  0.0  0.0                   A20, A2X, A2Y
    0.0                             A00
    0                               ICONV
```

Example 10.5.4

Consider the eigenvalue and transient problems discussed in **Examples 9.5.1** and **9.5.2**. Develop the input data files for the eigenvalue and transient analyses.

Solution: The governing differential equation is

$$\frac{\partial u}{\partial t} - \left(\frac{\partial^2 u}{\partial x^2} + \frac{\partial^2 u}{\partial y^2} \right) = 1$$

$$\frac{\partial u}{\partial x}(0, y, t) = 0, \quad \frac{\partial u}{\partial y}(x, 0, t) = 0, \quad u(x, 1, t) = 0, \quad u(1, y, t) = 0$$

$$u(x, y, 0) = 0$$

For eigenvalue analysis, we set ITEM = 1 and NEIGN = 1; for the transient analysis, we set ITEM = 1 (parabolic equation) and NEIGN = 0. In addition, we must input NVALU (number of eigenvalues to be printed) and NVCTR (if eigenvectors to be printed) for eigenvalue analysis.

For the transient analysis, we set NTIME = 20, NSTP = 21, (> NTIME), INTVL = 1, INTIAL = 0, DT = 0.05, ALFA = 0.5, GAMA = 0.5 (not used by the program for parabolic equations, but a value must be read), C0 = 1.0, CX = 0.0, and CY = 0.0. The parameter NSTP allows removal of the source (i.e., *f*) at a given time step. For example, if NSTP = 5, then at the fifth time step and at each subsequent time steps *f* will be set equal to zero. In the present case, the source *f* = 1 is kept at all times; hence, we must choose NSTP to be greater than NTIME (say NSTP = 21).

The input files and partial output for the eigenvalue and transient analyses are presented in Boxes 10.5.10 and 10.5.11, respectively. For a discussion of the numerical results of these two problems, see **Examples 9.5.1** and **9.5.2**.

Box 10.5.10: The input data for the eigenvalue and transient analysis of a parabolic equation (**Example 10.5.4**).

```
Example 10.5.4:  EIGENVALUE ANALYSIS of a parabolic equation
  0   0   1   1                          ITYPE,IGRAD,ITEM,NEIGN
 16   0                                  NVALU, NVCTR
  1   4   1   0                          IELTYP,NPE,MESH,NPRNT
  4   4                                  NX,NY
  0.0  0.25   0.25   0.25   0.25         X0,DX(I)
  0.0  0.25   0.25   0.25   0.25         Y0,DY(I)
  9                                      NSPV
   5 1  10 1   15 1  20 1   21 1
  22 1  23 1   24 1  25 1                ISPV
  1.0   0.0  0.0                        A10, A1X, A1Y
  1.0   0.0  0.0                        A20, A2X, A2Y
  0.0                                    A00
  0                                      ICONV
  1.0  0.0  0.0                          C0, CX, CY

Example 10.5.4: TRANSIENT ANALYSIS of a parabolic equation
  0   0   1   0                          ITYPE,IGRAD,ITEM,NEIGN
  1   4   1   0                          IELTYP,NPE,MESH,NPRNT
  4   4                                  NX,NY
  0.0  0.25   0.25   0.25   0.25         X0,DX(I)
  0.0  0.25   0.25   0.25   0.25         Y0,DY(I)
  9                                      NSPV
   5 1  10 1  15 1  20 1  21 1  22 1
  23 1  24 1  25 1                       ISPV
  0.0 0.0 0.0 0.0 0.0 0.0 0.0 0.0 0.0 VSPV
  0                                      NSSV
  1.0  0.0  0.0                          A10, A1X, A1Y
  1.0   0.0  0.0                         A20, A2X, A2Y
  0.0                                    A00
  0                                      ICONV
  1.0  0.0  0.0                          F0, FX, FY
  1.0  0.0  0.0                          C0, CX, CY
  20    21    1    0                    NTIME,NSTP,INTVL,INTIAL
  0.05  0.5  0.5  1.0E-3                 DT,ALFA,GAMA,EPSLN
```

Box 10.5.11: Partial output of program **FEM2D** for the eigenvalue analysis of a parabolic equation (**Example 10.5.4**).

```
OUTPUT FROM FEM2D FOR THE EIGENVALUE ANALYSIS

 E I G E N V A L U E (  1) =   0.343256E+03
 E I G E N V A L U E (  2) =   0.253701E+03
 E I G E N V A L U E (  3) =   0.253701E+03
 E I G E N V A L U E (  4) =   0.196500E+03
 E I G E N V A L U E (  5) =   0.196500E+03
 E I G E N V A L U E (  6) =   0.174127E+03
 E I G E N V A L U E (  7) =   0.174127E+03
 E I G E N V A L U E (  8) =   0.164145E+03
 E I G E N V A L U E (  9) =   0.106945E+03
 E I G E N V A L U E ( 10) =   0.106945E+03
 E I G E N V A L U E ( 11) =   0.845720E+02
 E I G E N V A L U E ( 12) =   0.845720E+02
 E I G E N V A L U E ( 13) =   0.497442E+02
 E I G E N V A L U E ( 14) =   0.273714E+02
 E I G E N V A L U E ( 15) =   0.273714E+02
 E I G E N V A L U E ( 16) =   0.499854E+01
```

Box 10.5.12: Partial output of program **FEM2D** for the transient analysis of a parabolic equation (**Example 10.5.4**).

```
EDITED OUTPUT FROM FEM2D FOR THE TRANSIENT ANALYSIS

 *TIME* = 0.50000E-01     Time Step Number =  1

 Node     x-coord.       y-coord.     Primary DOF
   1   0.00000E+00    0.00000E+00    0.49867E-01
   2   0.25000E+00    0.00000E+00    0.49718E-01
   3   0.50000E+00    0.00000E+00    0.48620E-01
   4   0.75000E+00    0.00000E+00    0.41808E-01
   5   0.10000E+01    0.00000E+00    0.00000E+00
   6   0.00000E+00    0.25000E+00    0.49718E-01
   7   0.25000E+00    0.25000E+00    0.49582E-01
   8   0.50000E+00    0.25000E+00    0.48509E-01
   9   0.75000E+00    0.25000E+00    0.41748E-01
                         ...

 *TIME* = 0.10000E+01     Time Step Number = 20

 Node     x-coord.       y-coord.     Primary DOF
   1   0.00000E+00    0.00000E+00    0.29621E+00
   2   0.25000E+00    0.00000E+00    0.28037E+00
   3   0.50000E+00    0.00000E+00    0.23065E+00
   4   0.75000E+00    0.00000E+00    0.14053E+00
   5   0.10000E+01    0.00000E+00    0.00000E+00
   6   0.00000E+00    0.25000E+00    0.28037E+00
   7   0.25000E+00    0.25000E+00    0.26565E+00
   8   0.50000E+00    0.25000E+00    0.21920E+00
   9   0.75000E+00    0.25000E+00    0.13424E+00
```

The hyperbolic equations governing vibration and transient response of rectangular membranes were discussed in **Examples 9.5.3** and **9.5.4**. They can be analyzed using **FEM2D** with minor changes (e.g., ITEM = 2 and initial conditions on velocity through vector GLV) to the input data given in Box 10.5.10. This is left as an exercise to the reader.

10.6 Summary

In this chapter four major topics have been discussed: (1) Lagrange interpolation functions for triangular and rectangular elements; (2) numerical integration to evaluate integral expressions over triangular and rectangular elements; (3) some modeling guidelines; and (4) computer

implementation of 2-D problems through finite element program, FEM2D. Interpolation functions for linear, quadratic, and cubic triangular elements are developed using the area coordinates as well as natural coordinates. Linear, quadratic and cubic interpolation functions of Lagrange and serendipity family of rectangular elements are also developed using the natural coordinate system. A systematic description of numerical evaluation of integral expressions involving interpolation functions and their derivatives with respect to global coordinates has been presented. Lastly, computer implementation of the finite element models of two-dimensional problems (FEM2D) is discussed, and a number of illustrative examples, taken from Chapter 9, are presented for the reader to familiarize with the use of FEM2D. The finite element analysis of problems in coming chapters will be carried out with FEM2D.

Problems

INTERPOLATION AND NUMERICAL INTEGRATION

10.1 Show that the interpolation functions for the three-node equilateral triangular element given in Fig. P10.1 are

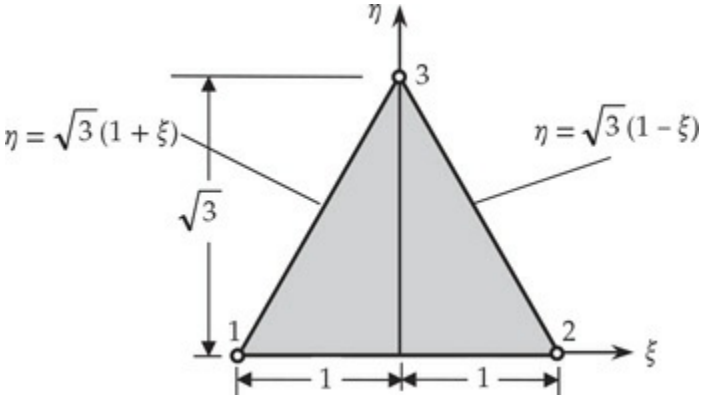

Fig. P10.1

$$\psi_1 = \frac{1}{2}\left(1 - \xi - \frac{1}{\sqrt{3}}\eta\right), \quad \psi_2 = \frac{1}{2}\left(1 + \xi - \frac{1}{\sqrt{3}}\eta\right), \quad \psi_3 = \frac{1}{\sqrt{3}}\eta$$

10.2 Calculate the interpolation functions $\Psi_i(x, y)$ for the quadratic triangular element shown in Fig. P10.2. *Hint:* Use the results of **Example 10.2.1**.

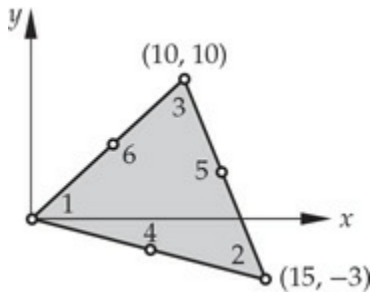

Fig. P10.2

10.3 Determine the interpolation function Ψ_{14} in terms of the area coordinates L_i for the triangular element shown in Fig. P10.3. *Answer*: $32L_1\,L_2\,L_3\,(4L_2 - 1)$.

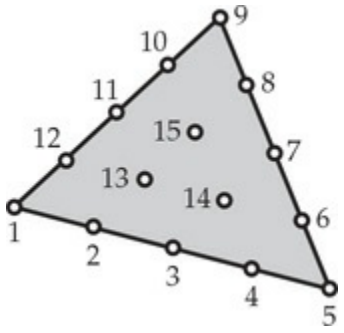

Fig. P10.3

10.4 Derive the interpolation function of nodes 1, 2, and 7 of the cubic serendipity element shown in Fig. P10.4.

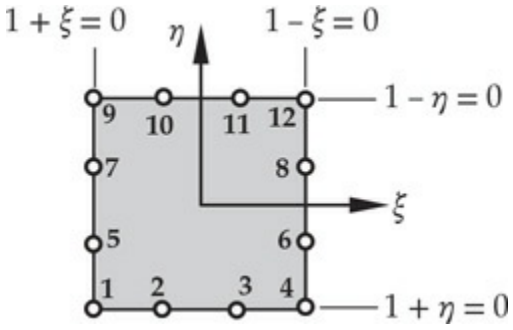

Fig. P10.4

10.5 Consider the five-node element shown in Fig. P10.5. Using the basic linear and quadratic interpolations along the coordinate directions ξ and η derive the interpolation functions for the element. Note that the element can be used as a transition element connecting four-node elements to eight or nine-node elements.

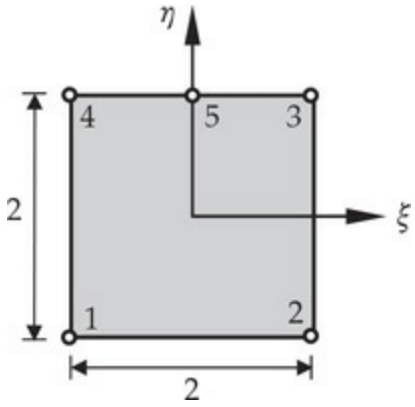

Fig. P10.5

10.6 Derive the interpolation functions of the transition element shown in Fig. P10.6.

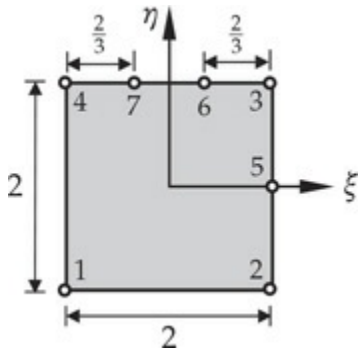

Fig. P10.6

10.7 (*Nodeless variables*) Consider the four-node rectangular element with interpolation of the form

$$u = \sum_{i=1}^{4} u_i \psi_i + \sum_{i=1}^{4} c_i \phi_i$$

where u_i are the nodal values and c_i are arbitrary constants. Determine the form of ψ_i and ϕ_i for the element.

10.8–10.10 Determine the Jacobian matrix, its inverse, and the transformation equations for the elements given in Fig. P10.8–P10.10.

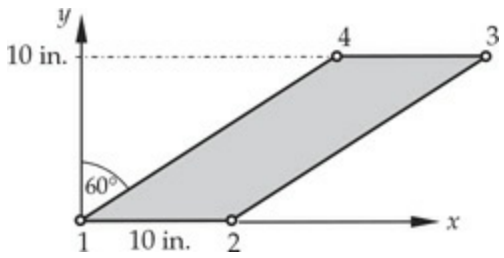

Fig. P10.8

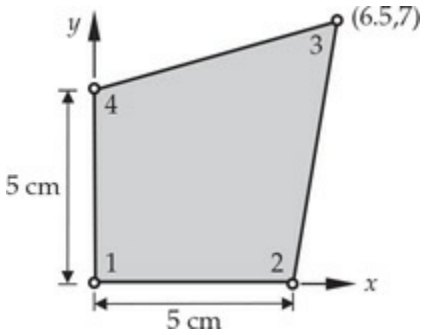

Fig. P10.9

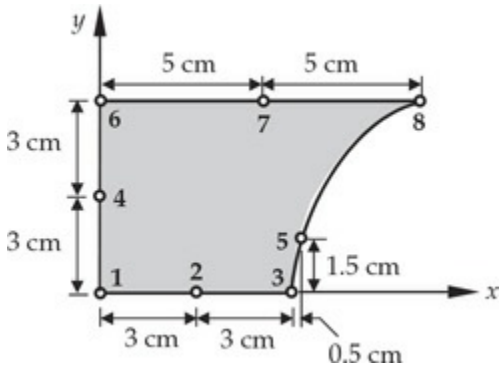

Fig. P10.10

10.11 For a 12-node serendipity (cubic) element, as illustrated in Fig. P10.11, show that the Jacobian $J = J11$ is

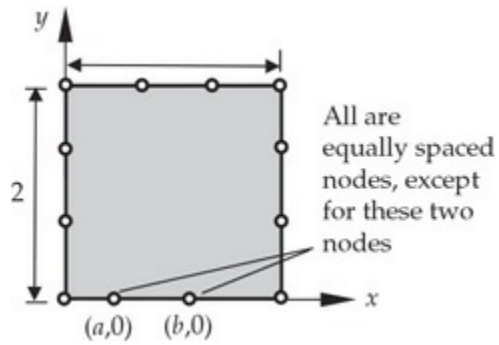

Fig. P10.11

$$J = 0.4375 + 0.84375(b-a) + 0.5625\eta - 0.84375(b-a)\eta$$
$$+ 1.125\xi - 0.5625(a+b)\xi - 1.125\eta\xi + 0.5625(a+b)\eta\xi$$
$$+ 1.6875\xi^2 - 2.53125(b-a)\xi^2 - 1.6875\eta\xi^2 + 2.53125(b-a)\eta\xi^2$$

What can you conclude from the requirement $J > 0$?

10.12 Using the Gauss quadrature, determine the contribution of a constant distributed source to nodal points of the four-node finite element in Fig. P10.9.

10.13 Determine Jacobian of the eight-node rectangular element of Fig. P10.12 in terms of the parameter a.

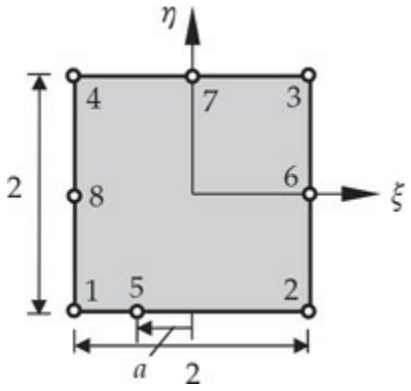

Fig. P10.12

10.14 Determine the conditions on the location of node 3 of the quadrilateral element shown in Fig. P10.13. Show that the transformation equations are given by

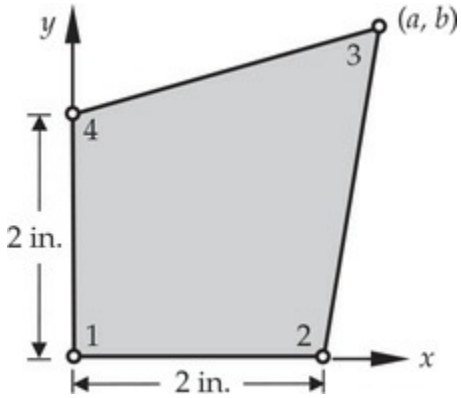

Fig. P10.13

$$x = \frac{1}{4}(1+\xi)[2(1-\eta) + a(1+\eta)]$$
$$y = \frac{1}{4}(1+\eta)[2(1-\xi) + b(1+\xi)]$$

10.15 Determine the global derivatives of the interpolation functions for node 3 of the element shown in Fig. P10.10.

10.16 Let the transformation between the global coordinates (x,y) and local normalized coordinates (ξ, η) in a Lagrange element Ω_e be

$$x = \sum_{i=1}^{m} x_i \hat{\psi}_i(\xi,\eta), \qquad y = \sum_{i=1}^{m} y_i \hat{\psi}_i(\xi,\eta)$$

where (x_i, y_i) denote the global coordinates of the element nodes. The differential lengths in the two coordinates are related by

$$dx_e = \frac{\partial x_e}{\partial \xi} d\xi + \frac{\partial x_e}{\partial \eta} d\eta, \qquad dy_e = \frac{\partial y_e}{\partial \xi} \xi + \frac{\partial y_e}{\partial \eta} d\eta$$

or

$$\begin{Bmatrix} dx_e \\ dy_e \end{Bmatrix} = \begin{bmatrix} \frac{\partial x_e}{\partial \xi} & \frac{\partial x_e}{\partial \eta} \\ \frac{\partial y_e}{\partial \xi} & \frac{\partial y_e}{\partial \eta} \end{bmatrix} \begin{Bmatrix} d\xi \\ d\eta \end{Bmatrix} = [\mathcal{J}] \begin{Bmatrix} d\xi \\ d\eta \end{Bmatrix}$$

In the finite element literature the transpose of $[\mathcal{J}]$ is called the Jacobian matrix, **J.** Show that the derivatives of the interpolation function $\psi_i^e(\xi,\eta)$ with respect to the global coordinates (x, y) are related to their derivatives with respect to the local coordinates (ξ, η) by

$$\begin{Bmatrix} \frac{\partial \psi_i^e}{\partial x} \\ \frac{\partial \psi_i^e}{\partial y} \end{Bmatrix} = \mathbf{J}^{-1} \begin{Bmatrix} \frac{\partial \psi_i^e}{\partial \xi} \\ \frac{\partial \psi_i^e}{\partial \eta} \end{Bmatrix}$$

$$\begin{Bmatrix} \frac{\partial^2 \psi_i^e}{\partial x^2} \\ \frac{\partial^2 \psi_i^e}{\partial y^2} \\ \frac{\partial^2 \psi_i^e}{\partial x \partial y} \end{Bmatrix} = \begin{bmatrix} \left(\frac{\partial x_e}{\partial \xi}\right)^2 & \left(\frac{\partial y_e}{\partial \xi}\right)^2 & 2\frac{\partial x_e}{\partial \xi}\frac{\partial y_e}{\partial \xi} \\ \left(\frac{\partial x_e}{\partial \eta}\right)^2 & \left(\frac{\partial y_e}{\partial \eta}\right)^2 & 2\frac{\partial x_e}{\partial \eta}\frac{\partial y_e}{\partial \eta} \\ \frac{\partial x_e}{\partial \xi}\frac{\partial x_e}{\partial \eta} & \frac{\partial y_e}{\partial \xi}\frac{\partial y_e}{\partial \eta} & \frac{\partial x_e}{\partial \eta}\frac{\partial y_e}{\partial \xi} + \frac{\partial x_e}{\partial \xi}\frac{\partial y_e}{\partial \eta} \end{bmatrix}^{-1}$$
$$\times \left(\begin{Bmatrix} \frac{\partial^2 \psi_i^e}{\partial \xi^2} \\ \frac{\partial^2 \psi_i^e}{\partial \eta^2} \\ \frac{\partial^2 \psi_i^e}{\partial \xi \partial \eta} \end{Bmatrix} - \begin{bmatrix} \frac{\partial^2 x_e}{\partial \xi^2} & \frac{\partial^2 y_e}{\partial \xi^2} \\ \frac{\partial^2 x_e}{\partial \eta^2} & \frac{\partial^2 y_e}{\partial \eta^2} \\ \frac{\partial^2 x_e}{\partial \xi \partial \eta} & \frac{\partial^2 y_e}{\partial \xi \partial \eta} \end{bmatrix} \begin{Bmatrix} \frac{\partial \psi_i^e}{\partial x} \\ \frac{\partial \psi_i^e}{\partial y} \end{Bmatrix} \right)$$

10.17 (Continuation of **Problem 10.16**) Show that the Jacobian can be computed from the equation

$$\mathbf{J} = \begin{bmatrix} \frac{\partial \psi_1^e}{\partial \xi} & \frac{\partial \psi_2^e}{\partial \xi} & \cdots & \frac{\partial \psi_n^e}{\partial \xi} \\ \frac{\partial \psi_1^e}{\partial \eta} & \frac{\partial \psi_2^e}{\partial \eta} & \cdots & \frac{\partial \psi_n^e}{\partial \eta} \end{bmatrix} \begin{bmatrix} x_1^e & y_1^e \\ x_2^e & y_2^e \\ \vdots & \vdots \\ x_n^e & y_n^e \end{bmatrix}$$

10.18 Find the Jacobian matrix for the nine-node quadrilateral element shown in Fig. P10.18. What is the determinant of the Jacobian matrix?

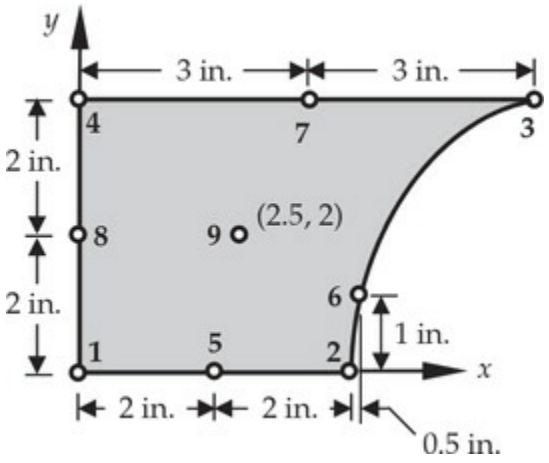

Fig. P10.18

10.19 For the eight-node element shown in Fig. P10.19, show that the x-coordinate along the side 1–2 is related to the ξ-coordinate by the relation

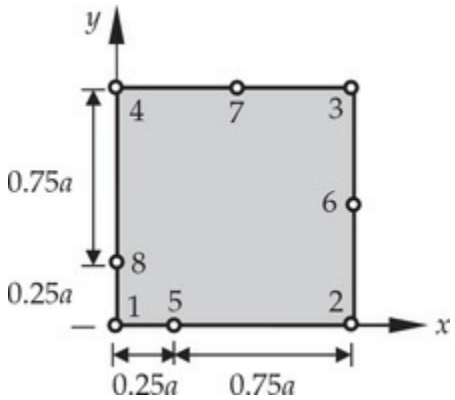

Fig. P10.19

$$x = -\tfrac{1}{2}\xi(1-\xi)x_1^e + -\tfrac{1}{2}\xi(1+\xi)x_2^e + (1-\xi^2)x_5^e$$

and that the following relations hold:

$$\xi = 2\left(\frac{x}{a}\right)^{1/2} - 1, \quad \frac{\partial x}{\partial \xi} = (xa)^{1/2}$$

Also, show that

$$u_h(x,0) = -\left[2\left(\frac{x}{a}\right)^{1/2} - 1\right]\left[1 - \left(\frac{x}{a}\right)^{1/2}\right] u_1^e + \left[-1 + 2\left(\frac{x}{a}\right)^{1/2}\right]\left(\frac{x}{a}\right)^{1/2} u_2^e + 4\left[\left(\frac{x}{a}\right)^{1/2} - \frac{x}{a}\right] u_5^e$$

$$\left.\frac{\partial u_h}{\partial x}\right|_{(x,0)} = -\frac{1}{(xa)^{1/2}}\left\{\frac{1}{2}\left[3 - 4\left(\frac{x}{a}\right)^{1/2}\right] u_1^e + \frac{1}{2}\left[-1 + 4\left(\frac{x}{a}\right)^{1/2}\right] u_2^e + 2\left[1 - 2\left(\frac{x}{a}\right)^{1/2}\right] u_5^e\right\}$$

Thus, $\partial u_e/\partial x$ grows at a rate of $(xa)^{-1/2}$ as x approaches zero along the side 1–2. In other words, we have a $x^{-1/2}$ singularity at node 1. Such elements are used in fracture mechanics problems.

10.20 Using the tensor product of the one-dimensional Hermite cubic interpolation functions, obtain the Hermite cubic interpolation functions (16 of them) for the four-node rectangular element.

COMPUTER PROBLEMS USING FEM2D

10.21 Investigate the convergence of solutions to **Problem 9.18** using 2 × 2, 4 × 4, and 8 × 8 meshes of linear triangular elements and equivalent meshes of linear rectangular elements, and compare the results (in tabular form) with the analytical solution.

10.22 Repeat **Problem 10.21** with nodally equivalent quadratic element meshes.

10.23 Repeat **Problem 10.21** for the case $u_0(x) = 1$ (see **Problem 9.19** for the analytical solution).

10.24 Repeat **Problem 10.23** with nodally equivalent quadratic element meshes.

10.25 Investigate the convergence of the solution to **Problem 9.22** using 8 × 8 mesh of linear triangular elements and equivalent mesh of quadratic triangular elements. *Answer:* For the 4 × 4 mesh of quadratic triangles, the values of $u(x, 0.125)$ at nodes 11 through 17 are 0.1145, 0.1977, 0.2829, 0.3787, 0.4880, 0.6111 and 0.7436.

10.26 Repeat **Problem 10.25** using rectangular elements. *Answer:* For the 4 × 4 mesh of quadratic rectangles, the values of $u(x, 0.125)$ at nodes 11 through 17 are 0.1165, 0.1982, 0.2834, 0.3789, 0.4884, 0.6114 and 0.7449.

10.27 Analyze the axisymmetric problem in **Problem 9.26** using 8 × 2 mesh of linear rectangular elements and equivalent mesh of quadratic elements, and compare the solution with the exact solution. *Answer:* For 8 × 2 mesh the values of $T(r, 0)$ at r = 0.0 0.005, 0.01, and 0.015 are: U_1 = 150.53, U_3 = 147.05, U_5 = 137.59, and U_7 = 121.91. The exact values are T_1 = 150.0, T_2 = 146.875, T_3 = 137.50, and T_4 = 121.875.

10.28 Analyze the axisymmetric problem in **Problem 9.27** using 8 × 8 mesh of linear rectangular elements.

10.29 Determine the critical time step for a conditionally stable scheme to analyze **Problem 9.18** as a parabolic equation (take c = 1.0) using (a) 8 × 8 uniform mesh of linear rectangular elements in the symmetric half of the domain. *Answer:* $\Delta t_{cr} = 2.172 \times 10^{-3}$ for the 8 × 8 mesh of linear elements.

10.30 Determine the transient response of **Problem 9.18**, treating it as a parabolic equation (c_1 = 1.0) and using a 8 × 8 mesh of linear rectangular elements. Assume zero initial conditions. Use α = 0.5 and $\Delta t = 10^{-3}$. Investigate the stability of the solution when α = 0.0 and $\Delta t = 10^{-3}$. The number of time steps should be such that the solution reaches its peak value or a steady state (use $\in = 10^{-4}$). Plot $u(0.5, 0.5, t)$ as a function of time t and $u(0.5, y, t)$ as a function of y for various times.

10.31 Analyze **Problem 9.22** for transient response (take c = 1.0) using a 4 × 4 mesh of linear rectangular elements and a 2 × 2 mesh of nine-node quadratic rectangular elements. Assume zero initial conditions. Investigate the stability and accuracy of the Crank–Nicolson scheme (α = 0.5) and the forward difference scheme (α = 0). Plot $u(0.5, 0.5, t)$ as a function of time t and $u(0.5, y, t)$ as a function of y for various times.

10.32 Analyze **Problem 9.27** for transient response (take c = 104) using a 4 × 4 mesh of nine-node quadratic rectangular elements. Assume zero initial conditions and plot $u(0.0, 0.02, t)$ (solution at node 73) as a function of time t for the Crank–Nicolson scheme (α = 0.5) and the forward difference scheme (α = 0).

10.33 Analyze the heat transfer problem in **Problem 9.28** using an 8 × 16 mesh of linear triangular elements and an equivalent mesh of linear rectangular elements.

10.34 Analyze **Problem 9.30** for nodal temperatures and heat flow across the boundaries using a mesh of 8 × 8 linear rectangular elements and an equivalent mesh of quadratic elements.

10.35 Analyze **Problem 9.35** for nodal temperature and heat flows across the boundary. Take k = 5 W/(m·°C).

10.36 Consider heat transfer in a rectangular domain with a central heated circular cylinder [see Fig. P10.36 for the geometry]. Analyze the problem using the mesh of linear quadrilateral elements shown in Fig. 10.5.4(b).

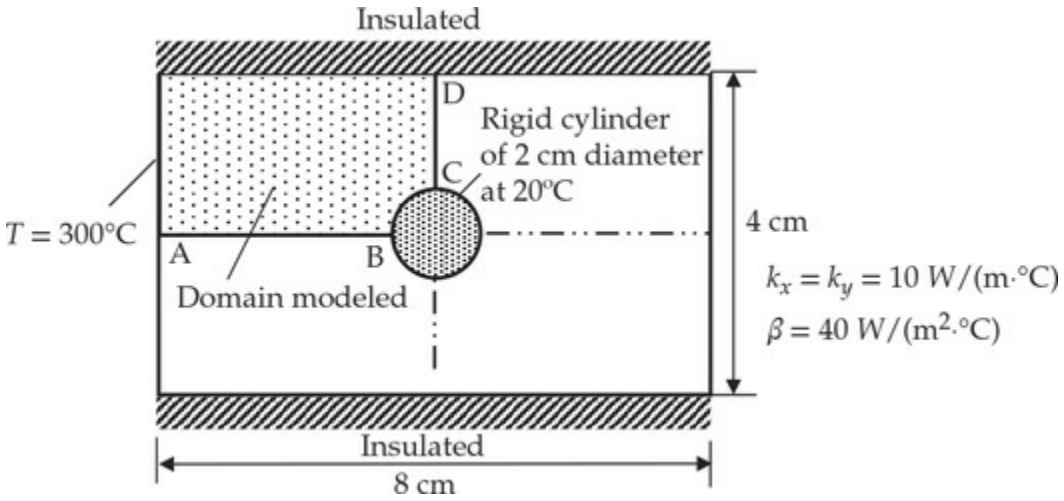

Fig. P10.36

10.37 Analyze the heat transfer problem in Fig. P9.32 with a 4 × 4 mesh of nine-node quadratic rectangular elements.

10.38 Analyze the problem in Fig. P9.35 for transient response using (a) α = 0 and (b) α = 0.5. Use $c_1 = \rho c_p = 10^2$.

10.39 Analyze the axisymmetric problem in Fig. P9.26 using the Crank–Nicolson method. Use an 8 × 1 mesh of linear rectangular elements. Use $c = \rho c_p = 3.6 \times 10^6$ J/(m^3 ·K).

10.40 Analyze the groundwater flow in **Problem 9.38** using the mesh of linear triangular elements of Fig. 9.4.14.

10.41 Analyze the flow around a cylinder of elliptical cross section (see Fig. P9.41) with the stream function formulation. Use the symmetry and the mesh of linear triangles from Fig. 9.4.18.

10.42 Analyze the torsion of a circular cross-section bar shown in Fig.

P10.42(a).

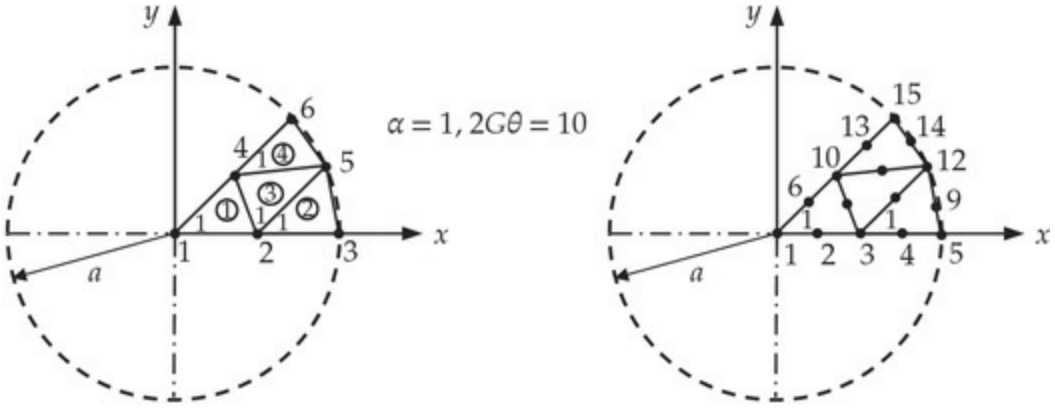

(a) Mesh of four linear triangles (b) Mesh of four quadratic triangles

Fig. P10.42

10.43 Analyze the torsion of the circular cross-section bar of **Problem 10.42** using a mesh of quadratic triangles shown in Fig. P10.42(b).

10.44 Analyze the torsion of an elliptical cross-section bar shown in Fig. P9.44.

10.45 Analyze the rectangular membrane problem in Fig. P10.45(a) with 4 × 4 mesh of linear rectangular elements in the computational domain (i.e., exploit the symmetry). Take $a_{11} = a_{22} = 1$ and $f_0 = 1$.

10.46 Repeat **Problem 10.45** with equivalent mesh of nine-node quadratic elements shown in Fig. P10.45(b).

10.47 Determine the eigenvalues (frequencies) of the rectangular membrane in Fig. P10.45(a) using a 4 × 4 mesh of linear rectangular elements in the half-domain. Use $c = 1.0$.

10.48 Determine the transient response of the problem in Fig. P10.45 (use the results of **Problem**

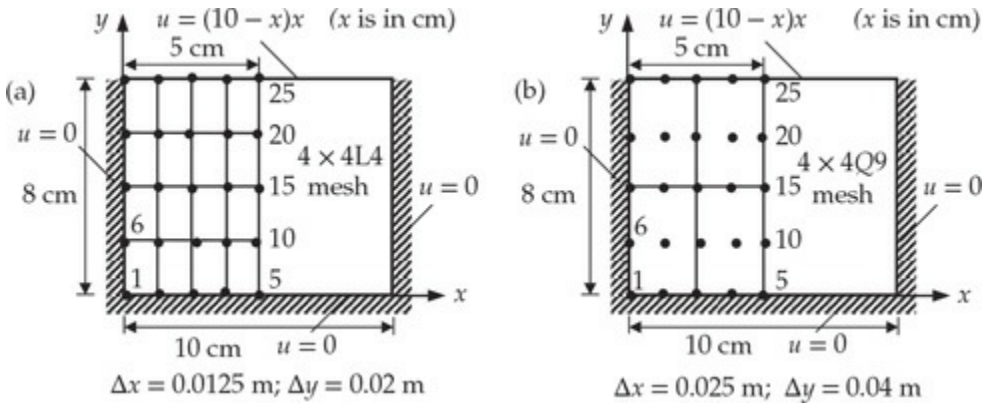

Fig. P10.45

10.47 to estimate the time step) using (a) mesh of linear elements and (b) mesh of quadratic elements (see Fig. P10.45). Assume zero initial conditions, $c = 1$ and $f0 = 1$. Use $\alpha = \gamma = 0.5$, and plot the deflection $u(0.05, 0.04, t)$ versus time t.

10.49 Determine the minimum and maximum eigenvalues and the associated eigenvectors of the circular membrane shown in Fig. P9.49 with a mesh of four quadratic triangular elements. Use $c = 1.0$.

10.50 Determine the transient response of the circular membrane in Fig. P9.49 (see **Problem 10.49** for maximum eigenvalue) using the mesh of quadratic elements. Assume zero initial conditions, $c = 1$ and $f_0 = 1$. Use $\alpha = \gamma = 0.5$, and plot the center deflection $u(0, 0, t)$ versus time t.

References for Additional Reading

1. B. Carnahan, H. A. Luther, and J. O. Wilkes, *Applied Numerical Methods*, John Wiley & Sons, New York, NY, 1969.
2. C. E. Froberg, *Introduction to Numerical Analysis*, Addison-Wesley, Reading, MA, 1969.
3. D. S. Burnett, *Finite Element Analysis from Concepts to Applications*, Addison-Wesley, Reading, MA, 1987.
4. G. R. Cowper, "Gaussian Quadrature Formulas for Triangles," *International Journal for Numerical Methods in Engineering*, **7**, 405–408, 1973.
5. P. C. Hammer, O. P. Marlowe, and A. H. Stroud, "Numerical Integration over Simplexes and Cones," *Mathematics Tables Aids Comp.*, National Research Council (Washington), **10**, 130–137, 1956.
6. B. M. Irons, "Quadrature Rules for Brick-Based Finite Elements," *International Journal for Numerical Methods in Engineering*, **3**, 293–294, 1971.
7. A. N. Loxan, N. Davids, and A. Levenson, "Table of the Zeros of the Legendre Polynomials of Order 1–16 and the Weight Coefficients for Gauss' Mechanical Quadrature Formula," *Bulletin of the American Mathematical Society*, **48**, 739–743, 1942.
8. C. T. Reddy and D. J. Shippy, "Alternative Integration Formulae for

Triangular Finite Elements," *International Journal for Numerical Methods in Engineering*, **17**, 133–139, 1981.

9. P. Silvester, "Newton–Cotes Quadrature Formulae for *N*-Dimensional Simplexes," *Proceedings of 2nd Canadian Congress of Applied Mechanics* (Waterloo, Ontario, Canada), 1969.
10. A. H. Stroud and D. Secrest, *Gaussian Quadrature Formulas*, Prentice-Hall, Engelwood Cliffs, NJ, 1966.

11 Flows of Viscous Incompressible Fluids

Advances are made by answering questions. Discoveries are made by questioning answers.

— Bernhard Haisch

11.1 Introduction

In Chapter 9 we considered the finite element analysis of second-order partial differential equations in one dependent unknown. The equation is valid for two-dimensional flows of inviscid (i.e., non-viscous) fluids. In this chapter, we consider flows of viscous incompressible fluids in two dimensions, whose governing equations are described by a set of three *coupled* partial differential equations expressed in terms of three dependent variables, namely, two velocity components and pressure. The word "coupled" is used here to imply that the same dependent variables appear in more than one equation of the set, and no equation can be solved independently of the other(s) in the set.

A brief introduction to fluids was given in Sections 4.3 and 9.4.4. The finite element analysis of flows of viscous fluids that can be modeled as one-dimensional systems was discussed in Section 4.3. In Section 9.4.4, finite element models of two-dimensional flows of inviscid, incompressible fluids (i.e., potential flows) were considered. The potential flow problems were cast in terms of either the stream function $u = \psi$ or the velocity potential $u = \phi$, and the governing equation in each case was shown to be the Laplace equation, $\nabla^2 u = 0$.

The two-dimensional flows of viscous, incompressible fluids are governed by a set of coupled partial differential equations in terms of the velocity field and pressure. The description of motion adopted in fluid mechanics is known as the *spatial description* or the *Eulerian description*, where focus is placed on fixed spatial location rather than a fixed volume of material. In the spatial description, the motion is referred to a fixed region occupied by a body of matter (with no interest in the body of matter

—where it comes from and where it goes) and its influence on the space it instantly occupies. A typical variable or property (e.g., velocity, density) is measured at the current position **x** occupied by a material particle at that instant of time. The coordinates, **x**, are termed the *spatial coordinates*. For a fixed value of **x**, a variable $\phi(\mathbf{x}, t)$ gives the value of ϕ associated with a fixed point **x** at time t, which will be the value of ϕ associated with different material particles occupying the spatial location **x** at different times. Thus, a change in time t in spatial description implies that a different value ϕ is observed at the *same* spatial location **x**, now probably occupied by a different material particle. This total time rate of change is denoted by D/Dt and it is called the *material time derivative*, defined by

$$\begin{aligned}\frac{D}{Dt}[\phi(\mathbf{x},t)] &= \frac{\partial}{\partial t}[\phi(\mathbf{x},t)] + \frac{dx_i}{dt}\frac{\partial}{\partial x_i}[\phi(\mathbf{x},t)] \\ &= \frac{\partial \phi}{\partial t} + v_i\frac{\partial \phi}{\partial x_i} = \frac{\partial \phi}{\partial t} + \mathbf{v}\cdot\boldsymbol{\nabla}\phi \end{aligned} \tag{11.1.1}$$

where **v** is the velocity vector and $\mathbf{v} = d\mathbf{x}/dt = \dot{\mathbf{x}}$. Thus, the time derivative (11.1.1) in the spatial description consists of two parts. The first part is the instantaneous change of the property ϕ with time at the spatial location **x**. The second part is the additional change in the property at **x** brought about by the material particle that happens to occupy the position **x** at that instant. The second term is sometimes referred to as the *convective part* of the material time derivative, and it is a source of spatial nonlinearity in fluid mechanics (other source of nonlinearity is the constitutive equations, i.e., non-Newtonian fluids). In this book, we limit our discussion to *slow* flows of *viscous* and *incompressible* fluids in a closed domain Ω:

$$\begin{aligned} \text{Slow (inertial effects are negligible):} \quad & \mathbf{v}\cdot\nabla\mathbf{v} \approx 0 \\ \text{Viscous:} \quad & \mu \neq 0 \\ \text{Incompressible:} \quad & \frac{D\rho}{Dt} = 0 \ \ (\rho = \text{constant}) \end{aligned}$$

where μ is the viscosity and ρ is the mass density. Toward developing the finite element models of the flows of viscous incompressible fluids, we begin with a review of the pertinent equations governing low-velocity flows of viscous incompressible fluids (see Reddy [1–3] and Reddy and Gartling [4] for additional details).

11.2 Governing Equations

We assume that one of the dimensions, say, along the z direction (into the plane of the paper) of the domain is very long and there is no flow along that direction, and that the velocity components in the other two directions (v_x and v_y) do not vary with the z direction. Under these conditions, the flow can be approximated as two-dimensional. The governing equations of such flows in rectangular Cartesian coordinates (x, y) are summarized below.

Conservation of Linear Momentum

$$\rho\frac{\partial v_x}{\partial t} - \frac{\partial \sigma_{xx}}{\partial x} - \frac{\partial \sigma_{xy}}{\partial y} - f_x = 0 \tag{11.2.1}$$

$$\rho\frac{\partial v_y}{\partial t} - \frac{\partial \sigma_{xy}}{\partial x} - \frac{\partial \sigma_{yy}}{\partial y} - f_y = 0 \tag{11.2.2}$$

Conservation of Mass (for incompressible medium)

$$\frac{\partial v_x}{\partial x} + \frac{\partial v_y}{\partial y} = 0 \tag{11.2.3}$$

Constitutive Equations

$$\sigma_{xx} = \tau_{xx} - P, \quad \sigma_{xy} = \tau_{xy}, \quad \sigma_{yy} = \tau_{yy} - P \tag{11.2.4}$$

$$\tau_{xx} = 2\mu\frac{\partial v_x}{\partial x}, \quad \tau_{xy} = \mu\left(\frac{\partial v_x}{\partial y} + \frac{\partial v_y}{\partial x}\right), \quad \tau_{yy} = 2\mu\frac{\partial v_y}{\partial y} \tag{11.2.5}$$

Boundary Conditions. Specify one element of each of the following pairs at each point on the boundary Γ:

$$(v_x, t_x) \ \ (v_y, t_y) \ \text{ for any } \ t > 0 \tag{11.2.6}$$

$$t_x = \sigma_{xx}n_x + \sigma_{xy}n_y, \quad t_y = \sigma_{xy}n_x + \sigma_{yy}n_y \tag{11.2.7}$$

Initial Conditions. Specify velocities at time $t = 0$ at each point in the domain Ω and on the boundary Γ:

$$v_x(x, y, 0) = v_x^0(x, y), \ v_y(x, y, 0) = v_y^0(x, y) \tag{11.2.8}$$

Here (v_x, v_y) are the velocity components, (σ_{xx}, σ_{yy}, σ_{xy}) the Cartesian components of the total stress tensor σ, P the pressure, (τ_{xx}, τ_{xy}, τ_{yy}) the Cartesian components of the viscous stress tensor τ, μ the viscosity, f_x and f_y the components of body force vector, (t_x, t_y) the components of stress vector on the boundary, and (v_x^0, v_y^0) the specified initial values of the velocity components.

Using the constitutive relations in Eqs. (11.2.4) and (11.2.5), the momentum and continuity equations in a flow domain Ω can be expressed as

$$\rho\frac{\partial v_x}{\partial t} - \frac{\partial}{\partial x}\left(2\mu\frac{\partial v_x}{\partial x}\right) - \frac{\partial}{\partial y}\left[\mu\left(\frac{\partial v_x}{\partial y} + \frac{\partial v_y}{\partial x}\right)\right] + \frac{\partial P}{\partial x} - f_x = 0 \tag{11.2.9}$$

$$\rho\frac{\partial v_y}{\partial t} - \frac{\partial}{\partial x}\left[\mu\left(\frac{\partial v_x}{\partial y} + \frac{\partial v_y}{\partial x}\right)\right] - \frac{\partial}{\partial y}\left(2\mu\frac{\partial v_y}{\partial y}\right) + \frac{\partial P}{\partial y} - f_y = 0 \tag{11.2.10}$$

$$\frac{\partial v_x}{\partial x} + \frac{\partial v_y}{\partial y} = 0 \tag{11.2.11}$$

and the boundary stress components in (11.2.7) become

$$\begin{aligned} t_x &= \left(2\mu\frac{\partial v_x}{\partial x} - P\right)n_x + \mu\left(\frac{\partial v_x}{\partial y} + \frac{\partial v_y}{\partial x}\right)n_y \\ t_y &= \mu\left(\frac{\partial v_x}{\partial y} + \frac{\partial v_y}{\partial x}\right)n_x + \left(2\mu\frac{\partial v_y}{\partial y} - P\right)n_y \end{aligned} \tag{11.2.12}$$

on Γ. Thus, we have three coupled partial differential equations (11.2.9)–(11.2.11) among three unknowns (v_x, v_y, P).

In the present study, we shall consider two different finite element models of Eqs. (11.2.9)–(11.2.11). The first one is a natural and direct formulation of Eqs. (11.2.9)–(11.2.11) in (v_x, v_y, P), and it is known as the *velocity–pressure formulation* or *mixed formulation*. The second model is based on the interpretation that (a) the continuity equation (11.2.11) is an additional relation among the velocity components (i.e., a constraint among v_x and v_y), and (b) satisfying the constraint in a least-squares (i.e., approximate) sense. This particular method of including the constraint in the formulation is known as the penalty function method, and the

formulation is termed the *penalty formulation*. It is informative to note that the velocity–pressure formulation is the same as the Lagrange multiplier formulation, and the Lagrange multiplier turns out to be the negative of the pressure.

11.3 Velocity–Pressure Formulation

11.3.1 Weak Formulation

The weak forms of Eqs. (11.2.9)–(11.2.11) over an element Ω_e can be obtained by the three-step procedure discussed in Chapter 9. We multiply the three equations (11.2.1)–(11.2.3) wherein (σ_{xx}, σ_{xy}, σ_{yy}) are known in terms of (v_x, v_y, P) through Eqs. (11.2.4) and (11.2.5), each with a different weight function (w_1, w_2, $-w_3$, respectively), integrate over the element, and integrate by parts to obtain the following weak forms (the negative sign on w_3 is necessary to make the coefficient matrix symmetric):

$$
\begin{aligned}
0 &= \int_{\Omega_e} w_1 \left[\rho \frac{\partial v_x}{\partial t} - \frac{\partial \sigma_{xx}}{\partial x} - \frac{\partial \sigma_{xy}}{\partial y} - f_x \right] dx\, dy \\
&= \int_{\Omega_e} \left[\rho w_1 \frac{\partial v_x}{\partial t} + \frac{\partial w_1}{\partial x} \sigma_{xx} + \frac{\partial w_1}{\partial y} \sigma_{xy} - w_1 f_x \right] dx\, dy \\
&\quad - \oint_{\Gamma_e} w_1 \left(\sigma_{xx} n_x + \sigma_{xy} n_y \right) ds
\end{aligned} \tag{11.3.1}
$$

$$
\begin{aligned}
0 &= \int_{\Omega_e} w_2 \left[\rho \frac{\partial v_y}{\partial t} - \frac{\partial \sigma_{xy}}{\partial x} - \frac{\partial \sigma_{yy}}{\partial y} - f_y \right] dx\, dy \\
&= \int_{\Omega_e} \left[\rho w_2 \frac{\partial v_y}{\partial t} + \frac{\partial w_2}{\partial x} \sigma_{xy} + \frac{\partial w_2}{\partial y} \sigma_{yy} - w_2 f_y \right] dx\, dy \\
&\quad - \oint_{\Gamma_e} w_2 \left(\sigma_{xy} n_x + \sigma_{yy} n_y \right) ds
\end{aligned} \tag{11.3.2}
$$

$$
0 = - \int_{\Omega_e} w_3 \left(\frac{\partial v_x}{\partial x} + \frac{\partial v_y}{\partial y} \right) dx\, dy \tag{11.3.3}
$$

The weight functions (w_1, w_2, w_3) can be interpreted physically as follows. Since the first equation is the momentum equation and $f_x\,dxdy$ denotes the force, w_1 must be like the x-component of velocity, v_x, so that the product $f_x w_1$ gives the power. Similarly, w_2 must be like the y-component of velocity, v_y. The third equation represents the volume change in an element of dimensions dx and dy. Therefore, w_3 must be like a force that causes the volume change. Volume changes occur under the action of hydrostatic pressure (acts toward the surface, hence negative), hence w_3 is like P:

$$w_1 \sim v_x\,,\; w_2 \sim v_y \text{ and } \quad w_3 \sim P \tag{11.3.4}$$

This interpretation is useful in developing the finite element model because w_1, for example, will be replaced by the ith interpolation function used in the approximation of v_x. Similarly, w_3 will be replaced by the ith interpolation function used in the approximation of P. When different interpolations are used for (v_x, v_y) and P, this interpretation becomes necessary. Expressing in terms of (v_x, v_y, P), the weak forms in Eqs. (11.3.1)–(11.3.3) become

$$0 = \int_{\Omega_e} \left[\rho w_1 \frac{\partial v_x}{\partial t} + \frac{\partial w_1}{\partial x}\left(2\mu \frac{\partial v_x}{\partial x} - P\right) + \mu \frac{\partial w_1}{\partial y}\left(\frac{\partial v_x}{\partial y} + \frac{\partial v_y}{\partial x}\right) - w_1 f_x \right] dxdy$$
$$- \oint_{\Gamma_e} w_1 t_x\, ds \tag{11.3.5}$$

$$0 = \int_{\Omega_e} \left[\rho w_2 \frac{\partial v_y}{\partial t} + \mu \frac{\partial w_2}{\partial x}\left(\frac{\partial v_x}{\partial y} + \frac{\partial v_y}{\partial x}\right) + \frac{\partial w_2}{\partial y}\left(2\mu \frac{\partial v_y}{\partial y} - P\right) - w_2 f_y \right] dxdy$$
$$- \oint_{\Gamma_e} w_2 t_y\, ds \tag{11.3.6}$$

$$0 = -\int_{\Omega_e} w_3 \left(\frac{\partial v_x}{\partial x} + \frac{\partial v_y}{\partial y}\right) dxdy \tag{11.3.7}$$

Note that there is no boundary integral involving w_3 because no integration by parts is used. This implies that P is not a primary variable; it is a part of the secondary variables (t_x and t_y). This in turn requires that P not necessarily be made continuous across interelement boundaries. If P by

itself is not specified in a problem (but t_x and t_y are specified), then P is arbitrarily set to a value at some node to determine the constant state of the pressure. Thus, P can be determined only within an arbitrary constant. The minus sign in the third statement is inserted because $P \sim w_3$, which makes the resulting finite element model symmetric.

The problem described by weak forms in Eqs. (11.3.5)–(11.3.7) can be restated as a variational problem of finding (v_x, v_y, P) such that

$$\begin{aligned} B_t(\mathbf{w},\mathbf{v}) + B_v(\mathbf{w},\mathbf{v}) - \bar{B}_p(\mathbf{w},P) &= l(\mathbf{w}) \\ -B_p(w_3,\mathbf{v}) &= 0 \end{aligned} \tag{11.3.8}$$

holds for all (w_1, w_2, w_3) and $t > 0$. Here, we use the notation

$$\mathbf{w} = \begin{Bmatrix} w_1 \\ w_2 \end{Bmatrix}, \quad \mathbf{v} = \begin{Bmatrix} v_x \\ v_y \end{Bmatrix}, \quad \mathbf{f} = \begin{Bmatrix} f_x \\ f_y \end{Bmatrix}, \quad \mathbf{t} = \begin{Bmatrix} t_x \\ t_y \end{Bmatrix} \tag{11.3.9}$$

Since w_i are linearly independent of each other, sum of the three equations in (11.3.5)–(11.3.7) is the same as the three individual equations. Thus, the bilinear forms $B_t(\mathbf{w},\mathbf{v})$, $B_v(\mathbf{w},\mathbf{v})$, $\bar{B}_p(\mathbf{w},P)$, and $B_p(w_3,\mathbf{v})$, and the linear form $l(\mathbf{w})$ are defined by

$$\begin{aligned} B_t(\mathbf{w},\mathbf{v}) &= \int_{\Omega_e} \rho \mathbf{w}^{\mathrm{T}} \dot{\mathbf{v}}\, dxdy \\ B_v(\mathbf{w},\mathbf{v}) &= \int_{\Omega_e} (\mathbf{D}\mathbf{w})^{\mathrm{T}} \mathbf{C} (\mathbf{D}\mathbf{v})\, dxdy \\ \bar{B}_p(\mathbf{w},P) &= \int_{\Omega_e} \left(\mathbf{D}_1^{\mathrm{T}}\mathbf{w}\right)^{\mathrm{T}} P\, dxdy \\ B_p(w_3,\mathbf{v}) &= \int_{\Omega_e} (w_3)^{\mathrm{T}} \left(\mathbf{D}_1^{\mathrm{T}}\mathbf{v}\right) dxdy \\ l(\mathbf{w}) &= \int_{\Omega_e} \mathbf{w}^{\mathrm{T}}\mathbf{f}\, dxdy + \oint_{\Gamma_e} \mathbf{w}^{\mathrm{T}}\mathbf{t}\, ds \end{aligned} \tag{11.3.10a}$$

where

$$\mathbf{D}=\begin{bmatrix} \frac{\partial}{\partial x} & 0 \\ 0 & \frac{\partial}{\partial y} \\ \frac{\partial}{\partial y} & \frac{\partial}{\partial x} \end{bmatrix},\quad \mathbf{D}_1=\begin{Bmatrix} \frac{\partial}{\partial x} \\ \frac{\partial}{\partial y} \end{Bmatrix},\quad \mathbf{C}=\mu\begin{bmatrix} 2 & 0 & 0 \\ 0 & 2 & 0 \\ 0 & 0 & 1 \end{bmatrix} \tag{11.3.10b}$$

The transpose of a scalar (or 1 × 1 matrix) used in Eq. (11.3.10a) may look a bit strange at the moment, but it is necessary to obtain the correct form of the finite element model, as will be seen shortly.

11.3.2 Finite Element Model

An examination of the weak form reveals that v_x and v_y are the primary variables that should be made continuous at interelement boundaries, while P is a nodal variable that need not be made continuous across the interelement boundaries. Therefore, the Lagrange family of finite elements can be used for (v_x, v_y, P). The weak form shows that the minimum continuity requirements on (v_x, v_y, P) are

(v_x, v_y) — linear in x and y P — a constant

Thus, there are different continuity requirements on the interpolation of the velocity field and pressure. Let (element label "e" on variables is omitted)

$$v_x(x,y,t)=\sum_{j=1}^{n} v_x^j(t)\psi_j(x,y),\quad v_y(x,y,t)=\sum_{j=1}^{n} v_y^j(t)\psi_j(x,y) \tag{11.3.11a}$$

$$P(x,y,t)=\sum_{J=1}^{m} P_J(t)\phi_J(x,y) \tag{11.3.11b}$$

where ψ_j (j = 1, 2,. . . , n) and ϕJ (J = 1, 2,. . . , m) are interpolation functions of different order. In view of the fact that pressure appears without a derivative while (v_x, v_y) appear with derivatives with respect to x and y, one often takes $n = m + 1$. If the degree of the approximation functions is high, one may use the same degree of interpolation for P and (v_x, v_y).

Substituting Eqs. (11.3.11a) and (11.3.11b) into Eqs. (11.3.5)–(11.3.7), we obtain the following semidiscrete finite element model:

$$\begin{bmatrix} 2\mathbf{S}^{11}+\mathbf{S}^{22} & \mathbf{S}^{21} & -\mathbf{S}^{10} \\ \mathbf{S}^{12} & \mathbf{S}^{11}+2\mathbf{S}^{22} & -\mathbf{S}^{20} \\ -(\mathbf{S}^{10})^{\mathrm{T}} & -(\mathbf{S}^{20})^{\mathrm{T}} & 0 \end{bmatrix} \begin{Bmatrix} \mathbf{v}_x \\ \mathbf{v}_y \\ \mathbf{P} \end{Bmatrix} + \begin{bmatrix} \mathbf{M} & 0 & 0 \\ 0 & \mathbf{M} & 0 \\ 0 & 0 & 0 \end{bmatrix} \begin{Bmatrix} \dot{\mathbf{v}}_x \\ \dot{\mathbf{v}}_y \\ \dot{\mathbf{P}} \end{Bmatrix} = \begin{Bmatrix} \mathbf{F}^1 \\ \mathbf{F}^2 \\ 0 \end{Bmatrix} \tag{11.3.12}$$

The coefficient matrices shown in Eq. (11.3.12) are defined by

$$\begin{aligned} M_{ij} &= \int_{\Omega_e} \rho_0 \psi_i^e \psi_j^e \, dxdy \\ S_{ij}^{\alpha\beta} &= \int_{\Omega_e} \mu \frac{\partial \psi_i^e}{\partial x_\alpha} \frac{\partial \psi_j^e}{\partial x_\beta} \, dxdy; \quad \alpha,\beta = 1,2 \\ S_{iJ}^{\alpha 0} &= \int_{\Omega_e} \mu \frac{\partial \psi_i^e}{\partial x_\alpha} \phi_J^e \, dxdy; \quad \alpha = 1,2 \\ F_i^1 &= \int_{\Omega_e} \psi_i^e f_x \, dxdy + \oint_{\Gamma_e} \psi_i^e t_x \, ds \\ F_i^2 &= \int_{\Omega_e} \psi_i^e f_y \, dxdy + \oint_{\Gamma_e} \psi_i^e t_y \, ds \end{aligned} \tag{11.3.13}$$

We note that $\mathbf{K}^{33} = 0$ because the continuity equation does not contain P. Therefore, the assembled equations will also have zeros in diagonal elements corresponding to the nodal values of P (i.e., the system of equations is not positive-definite).

The vector form of the finite element model in Eq. (11.3.12) can be obtained as follows: The finite element approximations in Eqs. (11.3.11a) and (11.3.11b) are expressed as

$$\begin{aligned} &\mathbf{v} = \begin{Bmatrix} v_x \\ v_y \end{Bmatrix} = \mathbf{\Psi}\boldsymbol{\Delta}, \quad \mathbf{w} = \begin{Bmatrix} w_1 \\ w_2 \end{Bmatrix} = \mathbf{\Psi}\delta\boldsymbol{\Delta} \\ &P = \mathbf{\Phi}^{\mathrm{T}}\mathbf{P}, \qquad\qquad w_3 = \mathbf{\Phi}^{\mathrm{T}}\delta\mathbf{P} \end{aligned} \tag{11.3.14a}$$

where δ denotes the variational symbol (see Reddy [5] for the properties of the variational operator δ) and $\mathbf{w} = \delta\mathbf{v}$ denote the virtual variation of $\mathbf{v}$ and

δP_i is the virtual variation of P_i. Various symbols used in Eq. (11.3.14a) are defined as

$$\boldsymbol{\Psi} = \begin{bmatrix} \psi_1 & 0 & \psi_2 & 0 & \cdots & \psi_n & 0 \\ 0 & \psi_1 & 0 & \psi_2 & \cdots & 0 & \psi_n \end{bmatrix}$$

$$\boldsymbol{\Delta} = \begin{Bmatrix} v_x^1 & v_y^1 & v_x^2 & v_y^2 & \cdots & v_x^n & v_y^n \end{Bmatrix}^{\mathrm{T}} \tag{11.3.14b}$$

$$\boldsymbol{\Phi} = \begin{Bmatrix} \phi_1 & \phi_2 & \cdots & \phi_m \end{Bmatrix}^{\mathrm{T}}, \quad \mathbf{P} = \begin{Bmatrix} P_1 & P_2 & \cdots & P_m \end{Bmatrix}^{\mathrm{T}}$$

Substituting Eq. (11.3.14a) into Eq. (11.3.8) and noting that δv_x^i and δv_y^i are arbitrary and linearly independent, we obtain

$$\mathbf{M}\dot{\boldsymbol{\Delta}} + \mathbf{K}^{11}\boldsymbol{\Delta} + \mathbf{K}^{12}\mathbf{P} = \mathbf{F}^1, \quad \mathbf{K}^{21}\boldsymbol{\Delta} = 0 \tag{11.3.15}$$

where

$$\mathbf{M} = \int_{\Omega_e} \rho \boldsymbol{\Psi}^{\mathrm{T}} \boldsymbol{\Psi}\, dxdy, \quad \mathbf{K}^{11} = \int_{\Omega_e} \mathbf{B}_v^{\mathrm{T}} \mathbf{C} \mathbf{B}_v\, dxdy$$

$$\mathbf{K}^{12} = \int_{\Omega_e} \mathbf{B}_p^{\mathrm{T}} \boldsymbol{\Phi}^{\mathrm{T}}\, dxdy, \quad \mathbf{K}^{21} = \int_{\Omega_e} \boldsymbol{\Phi} \mathbf{B}_p\, dxdy \tag{11.3.16}$$

$$\mathbf{F}^1 = \int_{\Omega_e} \boldsymbol{\Psi}^{\mathrm{T}} \mathbf{f}\, dxdy + \oint_{\Gamma_e} \boldsymbol{\Psi}^{\mathrm{T}} \mathbf{t}\, ds \tag{11.3.17}$$

$$\mathbf{B}_v = \mathbf{D}\boldsymbol{\Psi}, \qquad \mathbf{B}_p = \mathbf{D}_1^{\mathrm{T}} \boldsymbol{\Psi} \tag{11.3.18}$$

Note that $\mathbf{M}$ and $\mathbf{K}^{11}$ are of the order $2n \times 2n$, $\mathbf{K}^{12}$ is of the order $2n \times m$, $\mathbf{K}^{21}$ is of the order $m \times 2n$ and $\mathbf{F}^1$ is of the order $2n \times 1$.

11.4 Penalty Function Formulation

11.4.1 Preliminary Comments

The penalty function method was introduced in Section 6.4.3 in connection with algebraic constraint equations. It can also be used to reformulate a problem with differential constraints as one without constraints. Since the basic idea of the method was already introduced (see

Example 6.4.1), we proceed directly to its application to the viscous flow problem at hand. The question one may ask is: where is the constraint in the flow problem? There are no constraint conditions in the way the equations were presented. We have three equations (11.2.9)–(11.2.11) in three unknowns (v_x, v_y, P). Since the pressure P is uncoupled from the continuity equation (11.2.11) [which has the consequence of yielding nonpositive-definite system of finite element equations (11.3.12)], we would like to eliminate it from the set of governing equations. The elimination of pressure leads to a constraint equation among the velocity components, as described next.

11.4.2 Formulation of the Flow Problem as a Constrained Problem

The equations governing flows of viscous incompressible fluids can be viewed as equivalent to minimizing a quadratic functional with a constraint. Here we present the formulation, in the interest of simplicity, for the static case, since the constraint condition does not involve time derivative terms. Then, we add the time derivative terms to study transient problems.

We begin with unconstrained problem described by the weak forms of the mixed model, namely, Eq. (11.3.8) without the time-derivative terms

$$B_v(\mathbf{w},\mathbf{v}) - \bar{B}_p(\mathbf{w},P) = l(\mathbf{w}); \quad -B_p(w_3,\mathbf{v}) = 0 \tag{11.4.1}$$

where $B_v(\cdot,\cdot)$, $\bar{B}_p(\cdot,\cdot)$, $B_p(\cdot,\cdot)$ and $l(\cdot)$ are defined in Eqs. (11.3.10a) and (11.3.10b). Now, suppose that the velocity field (v_x, v_y) is such that the continuity equation (11.2.3) is satisfied identically. Then the weight functions (w_1, w_2), being (virtual) variations of the velocity components, also satisfy the continuity equation

$$\frac{\partial w_1}{\partial x} + \frac{\partial w_2}{\partial y} = 0 \tag{11.4.2}$$

As a result, variational problem in (11.4.1) now can be stated as follows: among all (v_x, v_y) that satisfy the continuity equation (11.2.3), find the one that satisfies the variational problem

$$B_v(\mathbf{w},\mathbf{v}) = l(\mathbf{w}) \tag{11.4.3}$$

for all admissible weight functions (w_1, w_2); i.e., that which satisfies the condition (11.4.2).

The variational problem in Eq. (11.4.3) is a constrained variational problem, because the solution (v_x, v_y) is constrained to satisfy the continuity equation (11.2.3). We note that $B_v(\cdot\,,\,\cdot)$ is symmetric (because **C** is symmetric):

$$B_v(\mathbf{w},\mathbf{v}) = B_v(\mathbf{v},\mathbf{w}) \tag{11.4.4}$$

and it is linear in **w** as well as **v**, while $l(\cdot)$ is linear in **w**. Hence, the quadratic functional is given by the expression [see Eq. (2.4.25)]

$$I_v(\mathbf{v}) = \tfrac{1}{2}B_v(\mathbf{v},\mathbf{v}) - l(\mathbf{v}) \tag{11.4.5}$$

Now we can state that the equations governing steady flows of viscous incompressible fluids are equivalent to

$$\begin{aligned} &\text{Minimize } I_v(\mathbf{v}) \\ &\text{subjected to the constraint } G(\mathbf{v}) \equiv \frac{\partial v_x}{\partial x} + \frac{\partial v_y}{\partial y} = 0 \end{aligned} \tag{11.4.6}$$

The constrained problem (11.4.6) can be reformulated as an unconstrained problem using the Lagrange multiplier method or the penalty function method. These are discussed next.

11.4.3 Lagrange Multiplier Model

In the Lagrange multiplier method the constrained problem (11.4.6) is reformulated as one of finding the stationary points of the unconstrained functional

$$I_L(\mathbf{v},\lambda) \equiv I_v(\mathbf{v}) + \int_{\Omega_e} \lambda G(\mathbf{v})\, dxdy \tag{11.4.7}$$

where $\lambda(x, y)$ is the *Lagrange multiplier*. The necessary condition for I_L to have a stationary value is that

$$\delta I_L = \delta_{v_x} I_L + \delta_{v_y} I_L + \delta_\lambda I_L = 0 \;\rightarrow\; \delta_{v_x} I_L = 0\,,\; \delta_{v_y} I_L = 0\,,\; \delta_\lambda I_L = 0 \tag{11.4.8}$$

where δ_{v_x}, δ_{v_y} and δ_λ denote the partial variations (see Reddy [5]) with

respect to v_x, v_y and λ, respectively. Calculating the first variations in (11.4.8), we obtain

$$0=\int_{\Omega_e}\left[\frac{\partial\delta v_x}{\partial x}\left(2\mu\frac{\partial v_x}{\partial x}+\lambda\right)+\mu\frac{\partial\delta v_x}{\partial y}\left(\frac{\partial v_x}{\partial y}+\frac{\partial v_y}{\partial x}\right)\right]dxdy$$
$$-\int_{\Omega_e}\delta v_x f_x\,dxdy-\oint_{\Gamma_e}\delta v_x t_x\,ds \tag{11.4.9}$$

$$0=\int_{\Omega_e}\left[\mu\frac{\partial\delta v_y}{\partial x}\left(\frac{\partial v_x}{\partial y}+\frac{\partial v_y}{\partial x}\right)+\frac{\partial\delta v_y}{\partial y}\left(2\mu\frac{\partial v_y}{\partial y}+\lambda\right)\right]dxdy$$
$$-\int_{\Omega_e}\delta v_y f_y\,dxdy-\oint_{\Gamma_e}\delta v_y t_y\,ds \tag{11.4.10}$$

$$0=\int_{\Omega_e}\delta\lambda\left(\frac{\partial v_x}{\partial x}+\frac{\partial v_y}{\partial y}\right)dxdy \tag{11.4.11}$$

where

$$t_x=\left(2\mu\frac{\partial v_x}{\partial x}+\lambda\right)n_x+\mu\left(\frac{\partial v_x}{\partial y}+\frac{\partial v_y}{\partial x}\right)n_y$$
$$t_y=\mu\left(\frac{\partial v_x}{\partial y}+\frac{\partial v_y}{\partial x}\right)n_x+\left(2\mu\frac{\partial v_y}{\partial y}+\lambda\right)n_y \tag{11.4.12}$$

or, in vector form

$$B_v(\mathbf{w},\mathbf{v})+\bar{B}_p(\mathbf{w},\lambda)=l(\mathbf{w}),\quad B_p(\delta\lambda,\mathbf{v})=0 \tag{11.4.13}$$

and the bilinear forms are the same as those in Eqs. (11.3.10a) and (11.3.10b). A comparison of Eq. (11.4.13) with Eq. (11.3.8) [or comparison of Eqs. (11.3.5)– (11.3.7) with (11.4.9)–(11.4.11)] reveals that $\lambda = -P$. Hence, the Lagrange multiplier formulation is the same as the velocity–pressure formulation.

11.4.4 Penalty Model

In the penalty function method, the constrained problem (11.4.6) is reformulated as an unconstrained problem as follows: minimize the

modified functional

$$I_P(\mathbf{v}) \equiv I_v(\mathbf{v}) + \frac{\gamma_e}{2}\int_{\Omega_e}[G(\mathbf{v})]^2 d\mathbf{x} \tag{11.4.14}$$

where γ_e is called the *penalty parameter*. Note that the constraint is included in a least-squares sense into the functional. Seeking the minimum of the modified functional I_P (**v**) is equivalent to seeking the minimum of both I_v (**v**) and G(**v**), the latter with respect to the weight γ_e. The larger the value of γ_e, the more exactly the constraint is satisfied. The necessary condition for the minimum of I_P is

$$\delta I_P = 0 \rightarrow \delta I_{v_x} = 0, \quad \delta I_{v_y} = 0 \tag{11.4.15}$$

We have

$$0 = \int_{\Omega_e}\left[2\mu\frac{\partial\delta v_x}{\partial x}\frac{\partial v_x}{\partial x} + \mu\frac{\partial\delta v_x}{\partial y}\left(\frac{\partial v_x}{\partial y} + \frac{\partial v_y}{\partial x}\right) - \delta v_x f_x\right]dxdy$$

$$-\oint_{\Gamma_e}\delta v_x t_x\, ds + \int_{\Omega_e}\gamma_e\frac{\partial\delta v_x}{\partial x}\left(\frac{\partial v_x}{\partial x} + \frac{\partial v_y}{\partial y}\right)dxdy \tag{11.4.16}$$

$$0 = \int_{\Omega_e}\left[2\mu\frac{\partial\delta v_y}{\partial y}\frac{\partial v_y}{\partial y} + \mu\frac{\partial\delta v_y}{\partial x}\left(\frac{\partial v_x}{\partial y} + \frac{\partial v_y}{\partial x}\right) - \delta v_y f_y\right]dxdy$$

$$-\oint_{\Gamma_e}\delta v_y t_y\, ds + \int_{\Omega_e}\gamma_e\frac{\partial\delta v_y}{\partial y}\left(\frac{\partial v_x}{\partial x} + \frac{\partial v_y}{\partial y}\right)dxdy \tag{11.4.17}$$

or, in vector form

$$B_p(\mathbf{w},\mathbf{v}) = l(\mathbf{w}) \tag{11.4.18}$$

where ($w_1 = \delta v_x$ and $w_2 = \delta v_y$)

$$B_p(\mathbf{w},\mathbf{v}) = B_v(\mathbf{w},\mathbf{v}) + \int_{\Omega_e}\gamma_e\left(\mathbf{D}_1^{\mathrm{T}}\mathbf{w}\right)^{\mathrm{T}}\mathbf{D}_1^{\mathrm{T}}\mathbf{v}\, d\mathbf{x}$$

$$l(\mathbf{w}) = \int_{\Omega_e}\mathbf{w}^{\mathrm{T}}\mathbf{f}\, dxdy + \oint_{\Gamma_e}\mathbf{w}^{\mathrm{T}}\mathbf{t}\, ds \tag{11.4.19}$$

and $B_v(\cdot,\cdot)$ and $\mathbf{D}_1$ are defined in Eqs. (11.3.10a) and (11.3.10b). We note that the pressure does not appear explicitly in the weak forms (11.4.16) and (11.4.17), although it is a part of the boundary stresses [see Eq. (11.4.12)]

A comparison of the weak forms in (11.4.16) and (11.4.17) with those in (11.4.9) and (11.4.10) show that

$$\lambda = \gamma_e \left(\frac{\partial v_x}{\partial x} + \frac{\partial v_y}{\partial y} \right) = -P \quad \text{or} \quad P = -\gamma_e \mathbf{D}_1^{\mathrm{T}} \mathbf{v} \tag{11.4.20}$$

where $\mathbf{v} = \mathbf{v}(\gamma_e)$ is the solution of Eqs. (11.4.16) and (11.4.17). Thus, an approximation for the pressure can be post-computed using (11.4.20).

The time derivative terms can be added to equations (11.4.9)–(11.4.11) as well as to (11.4.16) and (11.4.17) without affecting the above discussion. For the penalty model, we have

$$\begin{aligned} 0 = \int_{\Omega_e} \Bigg[& \rho \delta v_x \frac{\partial v_x}{\partial t} + 2\mu \frac{\partial \delta v_x}{\partial x} \frac{\partial v_x}{\partial x} + \mu \frac{\partial \delta v_x}{\partial y} \left(\frac{\partial v_x}{\partial y} + \frac{\partial v_y}{\partial x} \right) \\ & + \gamma_e \frac{\partial \delta v_x}{\partial x} \left(\frac{\partial v_x}{\partial x} + \frac{\partial v_y}{\partial y} \right) \Bigg] dx\, dy - \int_{\Omega_e} \delta v_x f_x \, dx dy - \oint_{\Gamma_e} \delta v_x t_x \, ds \end{aligned} \tag{11.4.21}$$

$$\begin{aligned} 0 = \int_{\Omega_e} \Bigg[& \rho \delta v_y \frac{\partial v_y}{\partial t} + 2\mu \frac{\partial \delta v_y}{\partial y} \frac{\partial v_y}{\partial y} + \mu \frac{\partial \delta v_y}{\partial x} \left(\frac{\partial v_x}{\partial y} + \frac{\partial v_y}{\partial x} \right) \\ & + \gamma_e \frac{\partial \delta v_y}{\partial y} \left(\frac{\partial v_x}{\partial x} + \frac{\partial v_y}{\partial y} \right) \Bigg] dx dy - \int_{\Omega_e} f_y \delta v_y \, dx dy - \oint_{\Gamma_e} \delta v_y t_y \, ds \end{aligned} \tag{11.4.22}$$

or

$$B_t(\mathbf{w}, \mathbf{v}) + B_p(\mathbf{w}, \mathbf{v}) = l(\mathbf{w}) \tag{11.4.23}$$

where $B_t(\cdot,\cdot)$ is defined in Eq. (11.3.10a), and $B_p(\cdot,\cdot)$ and $l(\cdot)$ are defined in Eq. (11.4.19).

The penalty finite element model can be constructed using Eqs. (11.4.21) and (11.4.22) [or Eq. (11.4.23)] by substituting $\delta v_x = \psi_i$ and $\delta v_y = \psi_i$ and approximations (11.3.11a) for (v_x, v_y). We obtain

$$\begin{bmatrix} \mathbf{M} & 0 \\ 0 & \mathbf{M} \end{bmatrix} \begin{Bmatrix} \dot{\mathbf{v}}_x \\ \dot{\mathbf{v}}_y \end{Bmatrix} + \begin{bmatrix} \mathbf{K}^{11} & \mathbf{K}^{12} \\ \mathbf{K}^{21} & \mathbf{K}^{22} \end{bmatrix} \begin{Bmatrix} \mathbf{v}_x \\ \mathbf{v}_y \end{Bmatrix} = \begin{Bmatrix} \mathbf{F}^1 \\ \mathbf{F}^2 \end{Bmatrix} \tag{11.4.24}$$

where

$$\begin{aligned} \mathbf{K}^{11} &= 2\mathbf{S}^{11} + \mathbf{S}^{22} + \bar{\mathbf{S}}^{11}, \quad \mathbf{K}^{12} = \mathbf{S}^{21} + \bar{\mathbf{S}}^{12} \\ \mathbf{K}^{22} &= \mathbf{S}^{11} + 2\mathbf{S}^{22} + \bar{\mathbf{S}}^{22}, \quad \mathbf{K}^{21} = \mathbf{S}^{12} + \bar{\mathbf{S}}^{21} \end{aligned} \tag{11.4.25}$$

with the coefficients

$$\begin{aligned} M_{ij} &= \int_{\Omega_e} \rho \psi_i^e \psi_j^e \, dxdy \\ S_{ij}^{\alpha\beta} &= \int_{\Omega_e} \mu \frac{\partial \psi_i^e}{\partial x_\alpha} \frac{\partial \psi_j^e}{\partial x_\beta} \, dxdy; \quad \alpha, \beta = 1, 2 \\ \bar{S}_{ij}^{\alpha\beta} &= \int_{\Omega_e} \gamma_e \frac{\partial \psi_i^e}{\partial x_\alpha} \frac{\partial \psi_j^e}{\partial x_\beta} \, dxdy; \quad \alpha, \beta = 1, 2 \\ F_i^1 &= \int_{\Omega_e} \psi_i^e f_x \, dxdy + \oint_{\Gamma_e} \psi_i^e t_x \, ds \\ F_i^2 &= \int_{\Omega_e} \psi_i^e f_y \, dxdy + \oint_{\Gamma_e} \psi_i^e t_y \, ds \end{aligned} \tag{11.4.26}$$

In vector form, the finite element model is given by

$$\mathbf{M}\dot{\mathbf{\Delta}} + \left(\mathbf{K}_v + \mathbf{K}_p\right)\mathbf{\Delta} = \mathbf{F} \tag{11.4.27}$$

where ($\mathbf{M}$, $\mathbf{K}v$ and $\mathbf{K}_p$ are of the order $2n \times 2n$ and $\mathbf{F}$ is of the order $2n \times 1$)

$$\begin{aligned} &\mathbf{M} = \int_{\Omega_e} \rho \mathbf{\Psi}^{\mathrm{T}} \mathbf{\Psi} \, dxdy, \quad \mathbf{K}_v = \int_{\Omega_e} \mathbf{B}_v^{\mathrm{T}} \mathbf{C} \mathbf{B}_v \, dxdy \\ &\mathbf{K}_p = \int_{\Omega_e} \gamma_e \mathbf{B}_p^{\mathrm{T}} \mathbf{B}_p \, d\mathbf{x}, \qquad \mathbf{F} = \int_{\Omega_e} \mathbf{\Psi}^{\mathrm{T}} \mathbf{f} \, dxdy + \oint_{\Gamma_e} \mathbf{\Psi}^{\mathrm{T}} \mathbf{t} \, ds \\ &\mathbf{B}_v = \mathbf{D}\mathbf{\Psi}, \qquad\qquad \mathbf{B}_p = \mathbf{D}_1^{\mathrm{T}} \mathbf{\Psi} \end{aligned} \tag{11.4.28}$$

11.4.5 Time Approximation

For the unsteady case, Eqs. (11.3.15) and (11.4.27) are further approximated using a time approximation scheme. Equations (11.3.15) and (11.4.27) are of the form [see Eq. (7.4.25a)]

$$\mathbf{M}\dot{\boldsymbol{\Delta}} + \mathbf{K}\boldsymbol{\Delta} = \mathbf{F} \tag{11.4.29}$$

where Δ denotes the vector of nodal velocities and pressure in the velocitypressure formulation and only velocities in the penalty formulation. Using the α-family of approximation [see Eqs. (7.4.25a)–(7.4.29b)], we reduce Eq. (11.4.27) (with $\mathbf{K} = \mathbf{K}_v + \mathbf{K}_p$) to

$$\hat{\mathbf{K}}\boldsymbol{\Delta}^{s+1} = \tilde{\mathbf{K}}\boldsymbol{\Delta}^{s} + \hat{\mathbf{F}}^{s,s+1} \tag{11.4.30}$$

where

$$\hat{\mathbf{K}} = \mathbf{M} + a_1\mathbf{K}^{s+1}, \quad \tilde{\mathbf{K}}^{s} = \mathbf{M} - a_2\mathbf{K}^{s} \tag{11.4.31}$$

$$\hat{\mathbf{F}}^{s,s+1} = a_1\mathbf{F}^{s+1} + a_2\mathbf{F}^{s}, \quad a_1 = \alpha\Delta t, \quad a_2 = (1-\alpha)\Delta t \tag{11.4.32}$$

where **M** and **K** for the penalty model are defined in Eq. (11.4.28).

11.5 Computational Aspects

11.5.1 Properties of the Matrix Equations

Some of the properties of the matrix equations in Eqs. (11.3.15) and (11.4.27) are listed below.

1. The matrix equations (11.3.15) and (11.4.27) represent discrete analogs of conservation of mass and momentum. An inspection of the structure of the individual matrices shows that **M** and **K** are symmetric.
2. A negative aspect of the mixed finite element model is the presence of zeroes on the matrix diagonals corresponding to the pressure variables [see Eq. (11.3.15)]. Direct equation solving methods must use some type of pivoting strategy, while the use of iterative solvers is severely handicapped by poor convergence behavior attributable mainly to the form of the constraint equation.
3. The computer implementation of the mixed model is somewhat complicated by the fact that the element contains variable degrees of freedom. For example, for quadratic approximation of the velocity

field and bilinear continuous approximation of the pressure, the element has three degrees of freedom (v_x, v_y, P) at the corner nodes and two degrees of freedom (v_x, v_y) at the mid-side and interior nodes. This complicates the calculation of element matrices as well as the assembly of element equations to form the global system of equations.

4. Equations (11.3.15) and (11.4.27) represent a set of ordinary differential equations in time. The fact that the pressure does not appear explicitly in the continuity equation makes the system time-singular in the pressure and precludes the use of purely explicit time-integration methods.
5. The choice of the penalty parameter is largely dictated by the ratio of the magnitude of penalty terms to the viscous terms, the mesh, and the precision of the computer. Generally, a value of $\gamma = 10^4\,\mu$ to $\gamma = 10^{12}\,\mu$, where μ denotes the viscosity, gives good results. It is found that the pressure is more sensitive to the value of γ than the velocity field.

11.5.2 Choice of Elements

As is clear from the weak forms, both finite element models require only the C^0-continuous functions to approximate the field variables (i.e., velocities and pressure). Thus, any of the Lagrange and serendipity family of interpolation functions are admissible for the interpolation of the velocity field in mixed and penalty finite element models.

The choice of interpolation functions used for the pressure variable in the mixed finite element model is further constrained by the special role the pressure plays in incompressible flows. Recall that the pressure can be interpreted as a Lagrange multiplier that serves to enforce the incompressibility constraint on the velocity field. From Eq. (11.3.11b) it is seen that the approximation functions ϕ_J used for pressure are the weighting functions for the continuity equation. In order to prevent an overconstrained system of discrete equations, the interpolation used for pressure must be at least one order lower than that used for the velocity field (i.e., unequal order interpolation). Further, pressure need not be made continuous across elements because the pressure variable does not constitute a primary variable of the weak form presented in Eqs. (11.3.5)–(11.3.7).

Commonly used elements for two-dimensional flows of viscous

incompressible fluids are shown in Fig. 11.5.1. In the case of linear elements, pressure is treated as discontinuous between elements; otherwise, the whole domain will have the same pressure. Two different pressure approximations have been used when the velocities are approximated by quadratic Lagrange functions. The first is a continuous bilinear approximation, in which the pressure is defined at the corner nodes of the element and is made continuous across element boundaries. The second pressure approximation involves a discontinuous (between elements) linear variation defined on the element by $\mathbf{\Omega} = \{1\ x\ y\}^T$. Here the unknowns are not nodal point values of the pressure but correspond to the coefficients in $P = a \cdot 1 + b \cdot x + c \cdot y$.

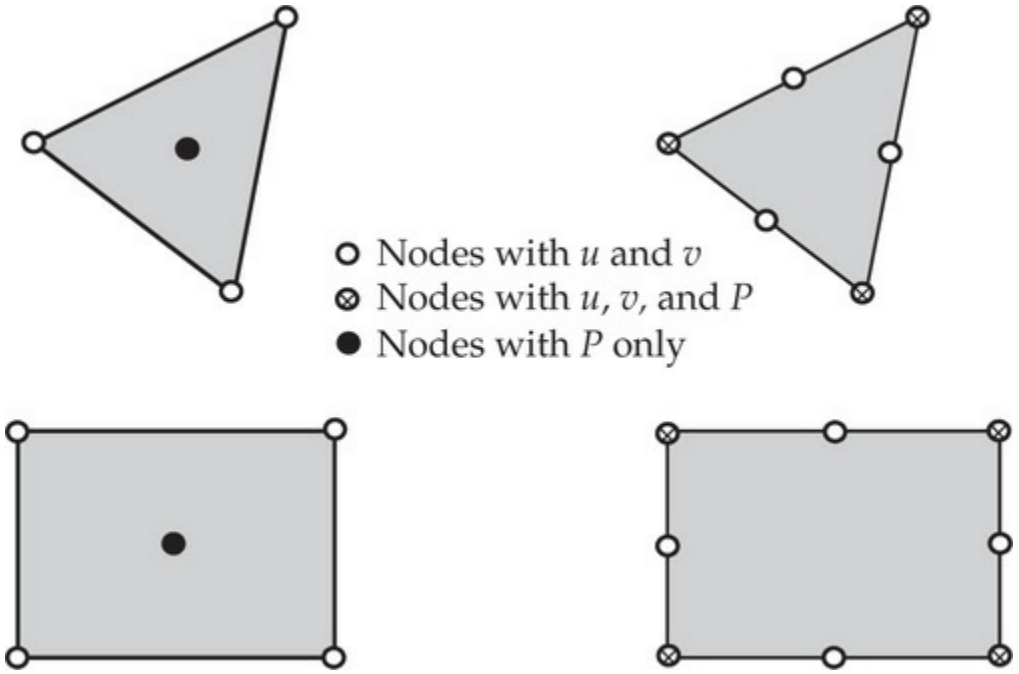

Fig. 11.5.1 The triangular and quadrilateral elements used for the mixed and penalty finite element models.

When the eight-node quadratic element is used to represent the velocity field, a continuous, bilinear pressure approximation may be selected. When a discontinuous pressure variation is utilized with this element, the constant pressure representation over each element must be used. The quadratic quadrilateral elements shown in Fig. 11.5.1 are known to give reliable solutions for velocity and pressure fields. Other elements may yield acceptable solutions for the velocity field but the pressure field is often in error.

11.5.3 Evaluation of Element Matrices in the Penalty Model

The numerical evaluation of the coefficient matrices appearing in equation (11.4.24) requires special consideration. This aspect is discussed here for the steady-state case. For the steady-state flows with constant material properties, Eq. (11.4.24) is of the form

$$\left(\mathbf{K}_v + \mathbf{K}_p\right)\boldsymbol{\Delta} = \mathbf{F} \tag{11.5.1}$$

where $\mathbf{K}_v$ is the contribution from the viscous terms and $\mathbf{K}_p$ is the contribution from the penalty terms (and depends on γ), which comes from the incompressibility constraint. In theory, as we increase the value of γ, the conservation of mass is satisfied more exactly. However, in practice, for some large value of γ, the contribution from the viscous terms would be negligibly small compared to the penalty terms. Thus, if $\mathbf{K}_p$ is a non-singular (i.e., invertible) matrix, the solution of Eq. (11.5.1) for a large value of γ is trivial, $\Delta = 0$. While the solution satisfies the continuity equation, it does not satisfy the momentum equations. In this case the discrete problem (11.5.1) is said to be overconstrained or "locked". If $\mathbf{K}_p$ is singular, then the sum $(\mathbf{K}_v + \mathbf{K}_p)$ is non-singular (because $\mathbf{K}_v$ is non-singular), and a non-trivial solution to the problem is obtained.

The numerical problem described above is eliminated by proper evaluation of the integrals in $\mathbf{K}_v$ and $\mathbf{K}_p$. It is found that if the coefficients of $\mathbf{K}_p$ (i.e., penalty matrix coefficients) are evaluated using a numerical integration rule of an order less than that required to integrate them exactly, the finite element equations (11.5.1) give acceptable solutions for the velocity field. This technique of underintegrating the penalty terms is known in the literature as *reduced integration*. For example, if a linear quadrilateral element is used to approximate the velocity field, the matrix coefficients $\mathbf{K}_v$ (as well as $\mathbf{M}$ for unsteady problems) are evaluated using the 2×2 Gauss quadrature, and $\mathbf{K}_p$ is evaluated using the onepoint (1×1) Gauss quadrature. The one-point quadrature yields a singular $\mathbf{K}_p$. Therefore, Eq. (11.5.1) can be solved because $(\mathbf{K}_v + \mathbf{K}_p)$ is non-singular and can be inverted (after assembly and imposition of boundary conditions) to obtain a good finite element solution of the original problem. When a quadratic quadrilateral element is used, the 3×3 Gauss quadrature is used to evaluate $\mathbf{K}_v$, and $\mathbf{M}$, and the 2×2 Gauss quadrature is used to evaluate $\mathbf{K}_p$. Of course, as the degree of interpolation goes up, or very refined meshes are used, the resulting equations become less sensitive to locking.

In the penalty finite model, the pressure is computed by evaluating Eq. (11.4.20) at integration points corresponding to the reduced Gauss quadrature rule. This is equivalent to using an interpolation for pressure that is one order less than the one used for the velocity field. The pressure computed using equation (11.4.20) at the reduced integration points is not always reliable and accurate. The pressures predicted using the linear elements, especially for coarse meshes, are seldom acceptable. Quadratic elements are known to yield more reliable results.

11.5.4 Post-computation of Stresses

The analysis of a flow problem generally includes calculation of not only the velocity field and pressure but also the computation of the stress field. A brief discussion of the stress calculation is presented here.

For a plane two-dimensional flow, the stress components (σ_{xx}, σ_{yy}, σ_{xy}) are given by

$$\sigma_{xx} = 2\mu\frac{\partial v_x}{\partial x} - P, \quad \sigma_{yy} = 2\mu\frac{\partial v_y}{\partial y} - P, \quad \sigma_{xy} = \mu\left(\frac{\partial v_x}{\partial y} + \frac{\partial v_y}{\partial x}\right) \tag{11.5.2}$$

where μ is the viscosity of the fluid. Substitution of the finite element approximations (11.3.11a) and (11.3.11b) for the velocity field and pressure into Eqs. (11.5.2)
yields

$$\sigma_{xx} = 2\mu\sum_{j=1}^{n}\frac{\partial \psi_j}{\partial x}v_x^j - P, \quad \sigma_{yy} = 2\mu\sum_{j=1}^{n}\frac{\partial \psi_j}{\partial y}v_y^j - P$$
$$\sigma_{xy} = \mu\sum_{j=1}^{n}\left(\frac{\partial \psi_j}{\partial y}v_x^j + \frac{\partial \psi_j}{\partial x}v_y^j\right) \tag{11.5.3}$$

where P is calculated from

$$P(x,y) = \sum_{J=1}^{m}\phi_J(x,y)P_J \tag{11.5.4}$$

in the mixed model, and from

$$P_\gamma(x,y) = -\gamma \sum_{j=1}^{n} \left(\frac{\partial \psi_j}{\partial x} v_x^j + \frac{\partial \psi_j}{\partial y} v_y^j \right) \tag{11.5.5}$$

in the penalty model.

The spatial derivatives of the interpolation functions in Eqs. (11.5.3) and (11.5.5) must be evaluated using the reduced Gauss point rule. Thus, the stresses (as well as the pressure) are computed using the one-point Gauss rule for linear elements and with the 2 × 2 Gauss rule for the quadratic elements.

11.6 Numerical Examples

A number of simple examples of two-dimensional Stokes flows of viscous incompressible fluids are presented in this section. The examples presented herein were solved using the mixed and reduced integration penalty finite element models. Program FEM2D has only the penalty finite element model. The objective here is to evaluate the accuracy of the penalty and mixed finite element models by comparing with the available analytical results and to illustrate the effect of the penalty parameter on the accuracy of the solutions.

Example 11.6.1

Consider the slow flow of a viscous incompressible material squeezed between two long parallel plates [see Fig. 11.6.1(a)]. When the length of the plates is very large compared to both the width and the distance between the plates, we have a case of plane flow. Although this is a moving boundary problem, we wish to determine the velocity and pressure fields for a fixed distance between the plates, assuming that a state of plane flow exists. Exploit the biaxial symmetry (prove it to yourself), and use (a) 10 × 6 mesh of the four-node linear elements (L4) and (b) and 5 × 3 mesh of nine-node quadratic elements in the penalty model, and (c) 5 × 3 nonuniform mesh in the mixed model (with quadratic interpolation of velocities and linear interpolation of pressure), as shown in Fig. 11.6.1(b), to analyze the problem for velocity and pressure fields.

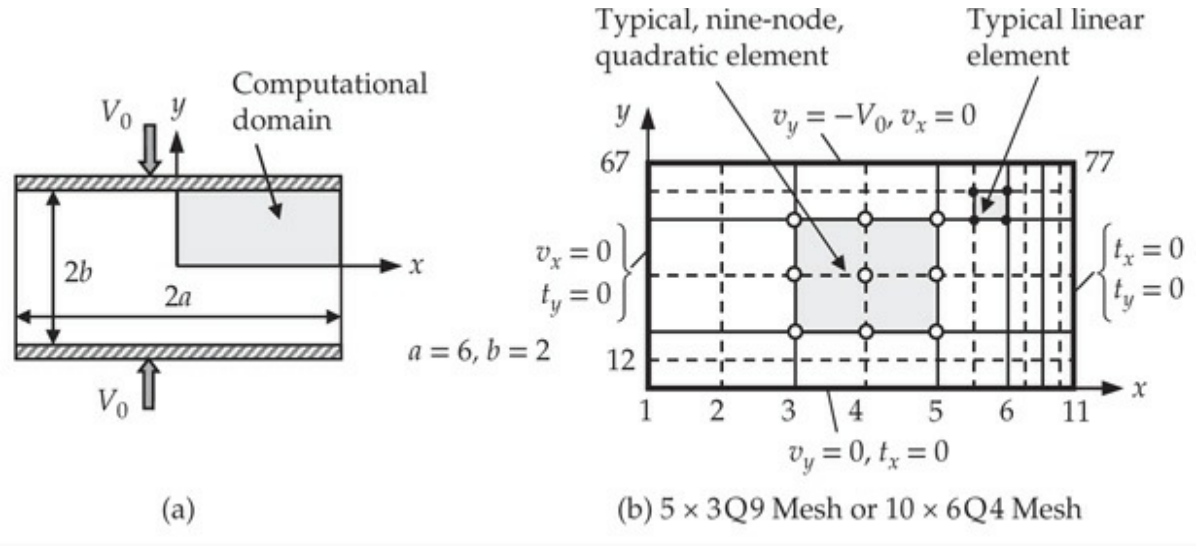

Fig. 11.6.1 (a) Geometry, computational domain, and (b) the finite element mesh used for the analysis of slow flow of viscous incompressible fluid between parallel plates.

Solution: Let V_0 be the velocity with which the two plates are moving toward each other (i.e., squeezing out the fluid), and let $2b$ and $2a$ denote, respectively, the distance between and the length of the plates [see Fig. 11.6.1(a)]. Due to the biaxial symmetry present in the problem, it suffices to model only a quadrant of the domain.

As a first mesh, we use a 5 × 3 nonuniform mesh of nine-node quadratic elements in the mixed model, and a 10 × 6 mesh of the four-node linear elements (Q4) and 5 × 3 mesh of nine-node quadratic elements (Q9) in the penalty model [see Fig. 11.6.1(b)]. The nonuniform mesh, with smaller elements near the free surface (i.e., at $x = a$), is used to approximate accurately the singularity in the shear stress at the point $(a, b) = (6, 2)$.

At every boundary point, we must know one element of each of the two pairs: (v_x, t_x) and (v_y, t_y). The velocity boundary conditions are shown in Fig. 11.6.1(b). The velocity field at $x = 6$ (outflow boundary) is not known; if we do not impose any boundary conditions there, it amounts to requiring $t_x = t_y = 0$ in the integral sense. In the mixed finite element model, it is necessary to specify the pressure at least at one node. In the present case, the node at $(x, y) = (a, 0)$ is specified to have zero pressure. In summary, we have the following boundary conditions:

$$\begin{aligned} &\text{At } x=0: \ v_x=0, \ t_y=-\sigma_{xy}=0; \quad \text{At } y=0: \ v_y=0, \ t_x=-\sigma_{xy}=0 \\ &\text{At } x=a: \ t_x=\sigma_{xx}=0, \ t_y=\sigma_{xy}=0; \quad \text{At } y=b: \ v_x=0, \ v_y=-V_0 \end{aligned} \tag{1}$$

The FEM2D program variables for the problem at hand are: ITYPE=1, IGRAD=1, ITEM = 0, and NEIGN = 0. The following element lengths are used to generate the 10 × 4 mesh four-node quadrilateral elements (IELTYP = 1 and NPE = 4): DX(I)={ 1.0 1.0 1.0 1.0 0.5 0.5 0.25 0.25 0.25 0.25 }; DY(I)= {0.25 0.25 0.5 0.5 0.25 0.25}. The only changes for the 5 × 3 mesh of nine-quadratic quadrilateral elements are that IELTYP = 2 and NPE = 9, and the element lengths: DX(I)={ 2.0 2.0 1.0 0.5 0.5 }, DY(I)= {0.5 1.0 0.5}. The meshes used for penalty and mixed models have exactly the same number of nodes, although the total number of degrees of freedom are not the same due to the pressure variable in the mixed model. The input data for the 10 × 6 mesh of bilinear quadrilateral elements is presented in Box 11.6.1 and an edited output is shown in Box 11.6.2.

The problem at hand has no exact solution because of singularities. An approximate analytical solution to this two-dimensional problem is provided by Nadai [6], and it is given by

$$v_x(x,y)=\frac{3V_0x}{2b}\left(1-\frac{y^2}{b^2}\right),\quad v_y(x,y)=-\frac{3V_0y}{2b}\left(3-\frac{y^2}{b^2}\right)$$
$$P(x,y)=\frac{3\mu V_0}{2b^3}(a^2+y^2-x^2) \tag{2}$$

Box 11.6.1: Input file for viscous fluid squeezed between two parallel plates.

```
Ex 11.6.1: Viscous fluid squeezed between two parallel plates
    1   1   0   0                  ITYPE,IGRAD,ITEM,NEIGN
    1   4   1   0                  IELTYP,NPE,MESH,NPRNT
   10   6                                                 NX, NY
    0.0  1.0 1.0 1.0 1.0 0.5 0.5 0.25 0.25 0.25 0.25     X0, DX(I)
    0.0  0.25 0.25 0.5 0.5 0.25 0.25                     Y0, DY(I)
   39                              NSPV
 1 1  1 2  2 2  3 2  4 2  5 2  6 2  7 2  8 2  9 2 10 2 11 2
12 1 23 1 34 1 45 1 56 1 67 1 67 2 68 1 68 2 69 1 69 2 70 1
70 2 71 1 71 2 72 1 72 2 73 1 73 2 74 1 74 2 75 1 75 2 76 1
76 2 77 1 77 2           ISPV(I,J)
 0.0  0.0  0.0  0.0  0.0  0.0  0.0  0.0  0.0  0.0  0.0  0.0
 0.0  0.0  0.0  0.0  0.0  0.0 -1.0  0.0 -1.0  0.0 -1.0  0.0
-1.0  0.0 -1.0  0.0 -1.0  0.0 -1.0  0.0 -1.0  0.0 -1.0  0.0
-1.0  0.0 -1.0                     VSPV(I)
    0                              NSSV
  1.0   1.0E8                      AMU, PENLTY
  0.0   0.0   0.0                  F0, FX, FY
```

Box 11.6.2: Edited output file for viscous fluid squeezed between two parallel plates.

```
      NUMERICAL INTEGRATION DATA:
         Full quadrature (IPDF x IPDF) rule, IPDF =   2
         Reduced quadrature (IPDR x IPDR),   IPDR =   1
         Quadrature rule used in postproc.,  ISTR =   1

      S O L U T I O N :
       Node    x-coord.       y-coord.     Value of u     Value of v
         1   0.00000E+00   0.00000E+00   0.00000E+00   0.00000E+00
         2   0.10000E+01   0.00000E+00   0.75757E+00   0.00000E+00
         3   0.20000E+01   0.00000E+00   0.15135E+01   0.00000E+00
         4   0.30000E+01   0.00000E+00   0.22756E+01   0.00000E+00
         5   0.40000E+01   0.00000E+00   0.30541E+01   0.00000E+00
         6   0.45000E+01   0.00000E+00   0.34648E+01   0.00000E+00
         7   0.50000E+01   0.00000E+00   0.38517E+01   0.00000E+00
         8   0.52500E+01   0.00000E+00   0.40441E+01   0.00000E+00
         9   0.55000E+01   0.00000E+00   0.41712E+01   0.00000E+00
        10   0.57500E+01   0.00000E+00   0.42654E+01   0.00000E+00
        11   0.60000E+01   0.00000E+00   0.42549E+01   0.00000E+00

 x-coord.     y-coord.     sigma-x     sigma-y     sigma-xy     Pressure
0.5000E+00  0.1250E+00 -0.5880E+01 -0.8886E+01 -0.2540E-01  0.7383E+01
0.1500E+01  0.1250E+00 -0.5496E+01 -0.8500E+01 -0.6883E-01  0.6998E+01
0.2500E+01  0.1250E+00 -0.4749E+01 -0.7766E+01 -0.1222E+00  0.6257E+01
0.3500E+01  0.1250E+00 -0.3549E+01 -0.6645E+01 -0.1727E+00  0.5097E+01
0.4250E+01  0.1250E+00 -0.2405E+01 -0.5612E+01 -0.2331E+00  0.4009E+01
0.4750E+01  0.1250E+00 -0.1425E+01 -0.4578E+01 -0.2232E+00  0.3001E+01
0.5125E+01  0.1250E+00 -0.8476E+00 -0.3693E+01 -0.2172E+00  0.2271E+01
0.5375E+01  0.1250E+00 -0.3336E+00 -0.2640E+01 -0.1705E+00  0.1487E+01
0.5625E+01  0.1250E+00 -0.1971E+00 -0.1546E+01 -0.7399E-01  0.8717E+00
0.5875E+01  0.1250E+00  0.7635E-02 -0.2151E-01 -0.4168E-01  0.6935E-02
```

The velocities v_x (x, 0) obtained with the two finite element models compare well with the analytical solution, as shown in Table 11.6.1. The nine-node element gives very good results for both the penalty and mixed models. The influence of the penalty parameter on the accuracy of the solution is clear from the results. Whether the element is linear or quadratic, it is necessary to use a large value of the penalty parameter.

Table 11.6.1 Comparison of finite element solution v_x (x,0) with the analytical solution for fluid squeezed between plates.

	$\gamma = 1$		$\gamma = 100$		$\gamma = 10^8$			
x	Four -node	Nine* -node	Four -node	Nine -node	Four -node	Nine -node	Mixed model Nine -node	Series solution
1.00	0.0303	0.0310	0.6563	0.6513	0.7576	0.7505	0.7497	0.7500
2.00	0.0677	0.0691	1.3165	1.3062	1.5135	1.4992	1.5031	1.5000
3.00	0.1213	0.1233	1.9911	1.9769	2.2756	2.2557	2.2561	2.2500
4.00	0.2040	0.2061	2.6960	2.6730	3.0541	3.0238	3.0203	3.0000
4.50	0.2611	0.2631	3.0718	3.0463	3.4648	3.4307	3.4292	3.3750
5.00	0.3297	0.3310	3.4347	3.3956	3.8517	3.8029	3.8165	3.7500
5.25	0.3674	0.3684	3.6120	3.5732	4.0441	3.9944	3.9893	3.9375
5.50	0.4060	0.4064	3.7388	3.6874	4.1712	4.1085	4.1204	4.1250
5.75	0.4438	0.4443	3.8316	3.7924	4.2654	4.2160	4.2058	4.3125
6.00	0.4793	0.4797	3.8362	3.7862	4.2549	4.1937	4.2364	4.5000

Figure 11.6.2 contains plots of the velocity $v_x(x, y)$ for $x = 4$ and $x = 6$ obtained with mixed and penalty formulations, and Fig. 11.6.3 contains plots of pressure $P(x, y)$, for $y = y_0$, where y_0 is the y-coordinate of the Gauss point nearest to the centerline or the top plate. These results were obtained with two different meshes of bilinear elements (Q4): 10×6 and 20×16. The pressure in the penalty model was computed using Eq. (11.5.5) with the 2×2 Gauss rule for the quadratic rectangular element and the one-point formula for the linear element, whereas in the mixed model (as well as the analytical solution) it is computed at the nodes. If the pressure in the penalty model were computed using the full quadrature rule for rectangular elements, we would have obtained erroneous values. In general, the same integration rule as that used for the evaluation of the penalty terms in the coefficient matrix must be used to compute the pressure. The oscillations in pressure computed nearest to the top plate are due to the singularity in the boundary conditions at $(x, y) = (6, 2)$. Also, one should think that the finite element solutions are in error when compared to Nadai's approximate solution; rather one may see that Nadai's solution [6] is not a bad approximation of the true solution.

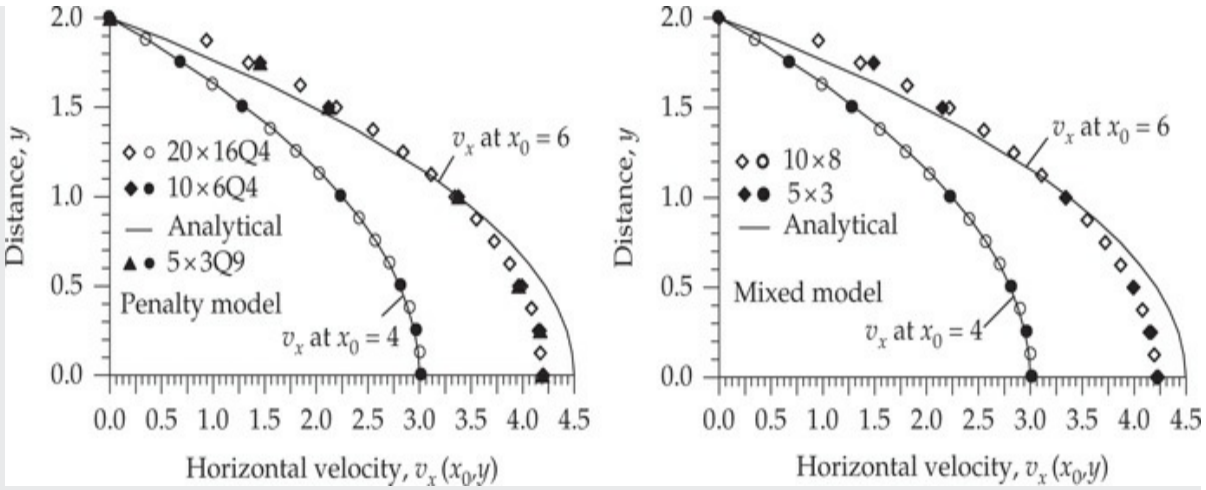

Fig. 11.6.2 Velocity fields for fluid squeezed between parallel plates.

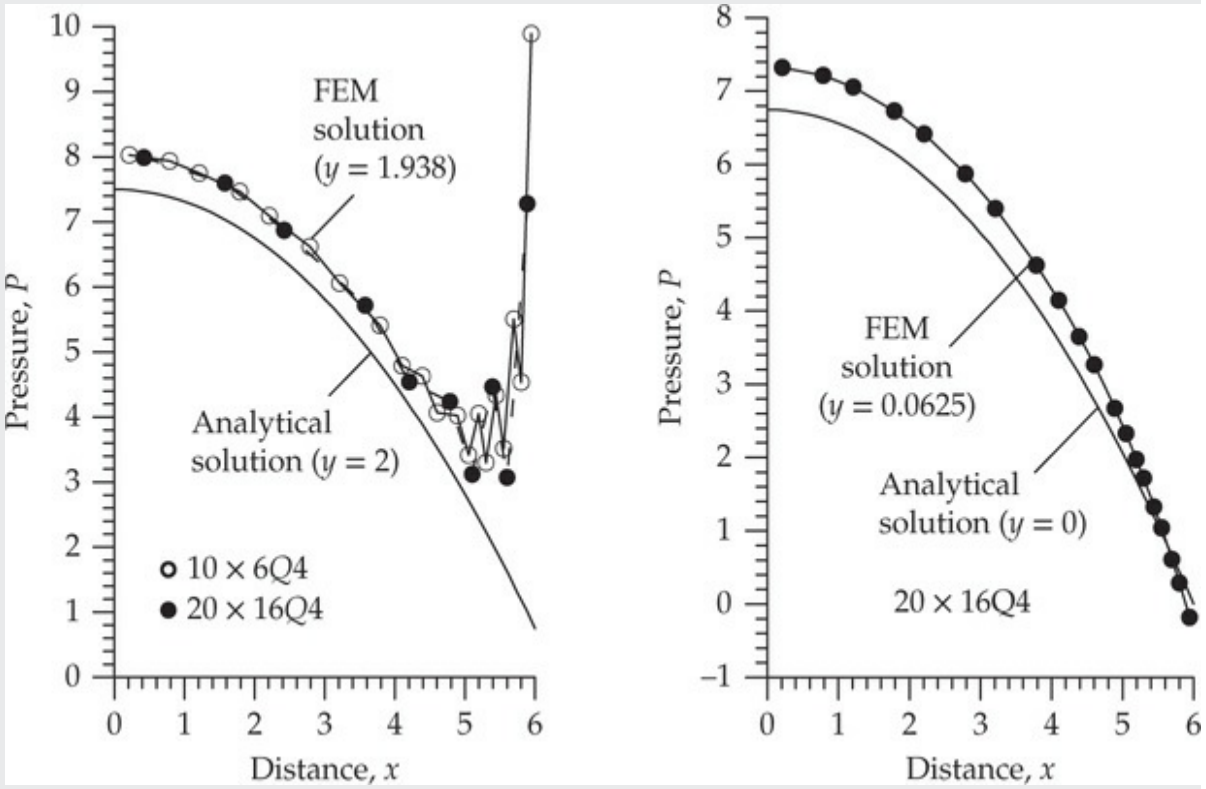

Fig. 11.6.3 Pressures for fluid squeezed between parallel plates.

Example 11.6.2

The slider (or slipper) bearing consists of a short sliding pad moving at a velocity $u = V_0$ relative to a stationary pad inclined at a small angle with respect to the stationary pad, and the small gap between the two pads is filled with a lubricant [see Fig. 11.6.4(a)]. Since the ends of the bearing

are generally open, the pressure there is atmospheric, P_0. If the upper pad is parallel to the base plate, the pressure everywhere in the gap must be atmospheric (because dP/dx is a constant for flow between parallel plates), and the bearing cannot support any transverse load. If the upper pad is inclined to the base pad, a pressure distribution, in general, a function of x and y, is set up in the gap. For large values of V_0, the pressure generated can be of sufficient magnitude to support heavy loads normal to the base pad. Using the 16 × 8 mesh of four-node quadrilateral elements shown in Fig. 11.6.4(b) and the penalty finite element model, determine the velocity and pressure distributions in the gap, and plot (a) horizontal velocity v_x (x_0, y) as a function of y for x_0 = 0, 0.18 and x_0 = 0.36 and (b) pressure and shear stress as a function of x for y = 0.

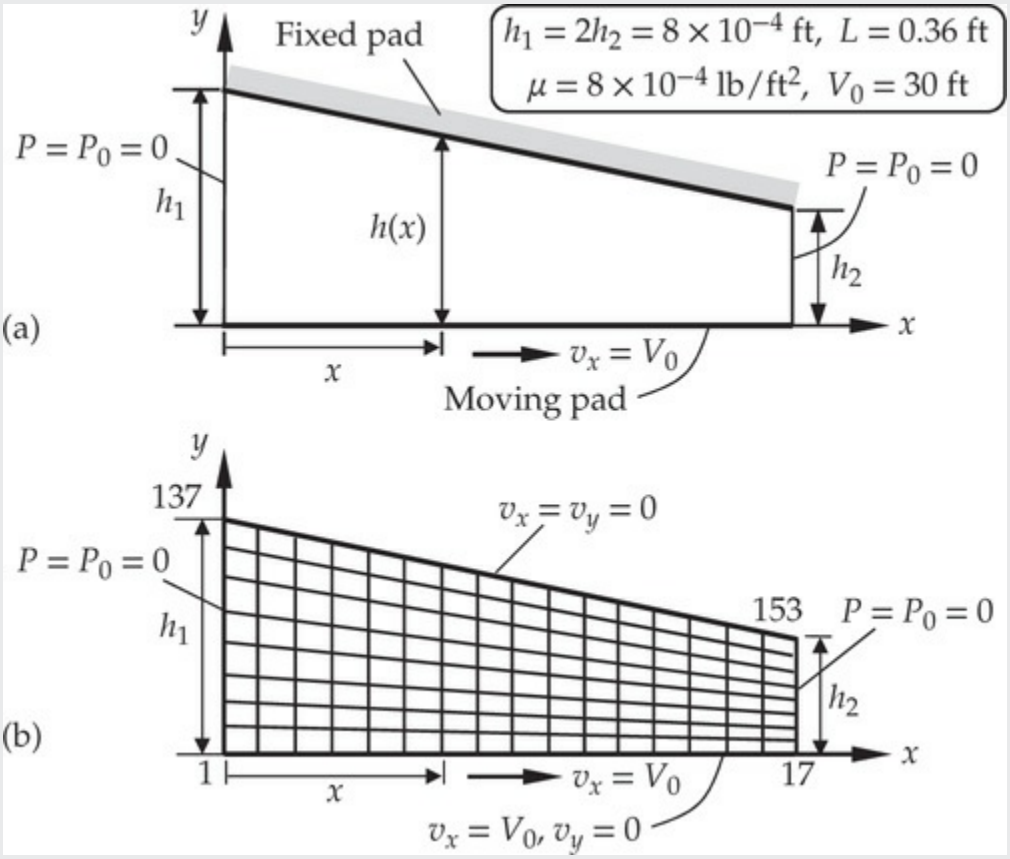

Fig. 11.6.4 Schematic and the finite element mesh for slider bearing.

Solution: Since the domain is nonrectangular, the mesh is generated using MESH2DG in FEM2D program. Figure 11.6.4(b) shows the mesh (graded uniformly) and the boundary conditions.

Schlichting [7] developed an analytical solution of the problem by assuming that the width of the gap and the angle of inclination are small

so that $v_y = 0$ and the pressure is not a function of y. Assuming a two-dimensional state of flow and a small angle of inclination, and neglecting the normal stress gradient (in comparison with the shear stress gradient), the equations governing the flow of the lubricant between the pads is reduced to

$$\mu \frac{\partial^2 v_x}{\partial y^2} = \frac{dP}{dx}, \quad \frac{dP}{dx} = \frac{6\mu V_0}{h^2}\left(1 - \frac{H}{h}\right), \quad 0 < x < L \tag{1}$$

where $H = 2h_1h_2 / (h_1 + h_2)$. The solution of Eq. (1), subject to the boundary conditions

$$v_x(x,0) = V_0, \quad v_x(x,h) = 0 \tag{2}$$

is given by

$$v_x(x,y) = \left(V_0 - \frac{h^2}{2\mu}\frac{dP}{dx}\frac{y}{h}\right)\left(1 - \frac{y}{h}\right) \tag{3}$$

$$P(x) = \frac{6\mu V_0 L(h_1 - h)(h - h_2)}{h^2(h_1^2 - h_2^2)} \tag{4}$$

$$\sigma_{xy}(x,y) = \mu\frac{\partial v_x}{\partial y} = \frac{dP}{dx}\left(y - \frac{h}{2}\right) - \mu\frac{V_0}{h} \tag{5}$$

where

$$h(x) = h_1 + \frac{h_2 - h_1}{L}x \tag{6}$$

In the finite element analysis we do not make any assumptions concerning v_y and the pressure gradient and solve the problem using FEM2D with a mesh of 16 × 8 linear quadrilateral elements to analyze the problem. The mesh and boundary conditions are shown in Fig. 11.6.4(b). The penalty parameter is chosen to be $\gamma = \mu \times 10^8$ The FEM2D program variables for the problem are

ITYPE=1, IGRAD=1, ITEM = 0, NEIGN = 0, IELTYP = 1, NPE = 4, NEM = 128, and NNM = 153

The input data to FEM2D is presented in Box 11.6.3, and an edited output is shown in Box 11.6.4.

Box 11.6.3: Input file for flow of viscous fluid in a wall-driven cavity.

```
Example 11.6.2: Flow of LUBRICANT in slider bearing(MESH:16x8Q4)
    1   1   0   0                   ITYPE,IGRAD,ITEM,NEIGN
    1   4   2   0                   IELTYP,NPE,MESH,NPRNT
  128 153                           NEM, NNM
    9                               NRECL
    1  17   1   0.0  0.0     0.36  0.0     1.0
   18  34   1   0.0  1.0E-4  0.36  0.5E-4  1.0
   35  51   1   0.0  2.0E-4  0.36  1.0E-4  1.0
   52  68   1   0.0  3.0E-4  0.36  1.5E-4  1.0
   69  85   1   0.0  4.0E-4  0.36  2.0E-4  1.0
   86 102   1   0.0  5.0E-4  0.36  2.5E-4  1.0
  103 119   1   0.0  6.0E-4  0.36  3.0E-4  1.0
  120 136   1   0.0  7.0E-4  0.36  3.5E-4  1.0
  137 153   1   0.0  8.0E-4  0.36  4.0E-4  1.0
    8
    1  16   1   1   4     1   2  19  18
   17  32   1   1   4    18  19  36  35
   33  48   1   1   4    35  36  53  52
   49  64   1   1   4    52  53  70  69
   65  80   1   1   4    69  70  87  86
   81  96   1   1   4    86  87 104 103
   97 112   1   1   4   103 104 121 120
  113 128   1   1   4   120 121 138 137
   68                               NSPV
  1  1   1  2   2  1   2  2   3  1   3  2   4  1   4  2   5  1
  5  2   6  1   6  2   7  1   7  2   8  1   8  2   9  1   9  2
 10  1  10  2  11  1  11  2  12  1  12  2  13  1  13  2  14  1
 14  2  15  1  15  2  16  1  16  2  17  1  17  2 137  1 137  2
138  1 138  2 139  1 139  2 140  1 140  2 141  1 141  2 142  1
142  2 143  1 143  2 144  1 144  2 145  1 145  2 146  1 146  2
147  1 147  2 148  1 148  2 149  1 149  2 150  1 150  2 151  1
151  2 152  1 152  2 153  1 153  2
 30.0    0.0   30.0    0.0   30.0    0.0   30.0    0.0   30.0
  0.0   30.0    0.0   30.0    0.0   30.0    0.0   30.0    0.0
 30.0    0.0   30.0    0.0   30.0    0.0   30.0    0.0   30.0
  0.0   30.0    0.0   30.0    0.0   30.0    0.0    0.0    0.0
  0.0    0.0    0.0    0.0    0.0    0.0    0.0    0.0    0.0
  0.0    0.0    0.0    0.0    0.0    0.0    0.0    0.0    0.0
  0.0    0.0    0.0    0.0    0.0    0.0    0.0    0.0    0.0
  0.0    0.0    0.0    0.0    0.0
    0                               NSSV
  8.0E-04  8.0E04                   AMU,PENALTY
  0.0   0.0   0.0                   F0, FX, FY
```

Table 11.6.2 contains a comparison of the finite element solutions and analytical solutions for the velocity, and pressure and shear stress values are compared in Table 11.6.3. Figure 11.6.5 contains plots of the horizontal velocity v_x at $x = 0$ ft, $x = 0.18$ ft and $x = 0.36$ ft, and Fig. 11.6.6 contains plots of pressure and shear stress as a function of x at $y = 0$. The finite element solutions for the pressure and shear stress were computed at the center of the first row of elements along the moving block. The results are in good agreement with the approximate analytical solutions (1)–(6), validating the assumptions made in the development of the analytical solution.

Table 11.6.2 Comparison of the finite element solutions with the analytical solutions for velocities v_x in the slider bearing problem $(\bar{y} = y \times 10^4)$.

$v_x(0, y)$			$v_x(0.18, y)$			$v_x(0.36, y)$		
$\bar{y}$	FEM	Analy.	$\bar{y}$	FEM	Analy.	$\bar{y}$	FEM	Analy.
0.0	30.000	30.000	0.00	30.000	30.000	0.00	30.000	30.000
1.0	22.923	22.969	0.75	25.139	25.156	0.50	29.564	29.531
2.0	16.799	16.875	1.50	20.596	20.625	1.00	28.182	28.125
3.0	11.626	11.719	2.25	16.372	16.406	1.50	25.853	25.781
4.0	7.403	7.500	3.00	12.465	12.500	2.00	22.577	22.500
5.0	4.130	4.219	3.75	8.874	8.906	2.50	18.354	18.281
6.0	1.805	1.875	4.50	5.600	5.625	3.00	13.184	13.125
7.0	0.429	0.469	5.25	2.642	2.656	3.50	7.066	7.031
8.0	0.000	0.000	6.00	0.000	0.000	4.00	0.000	0.000

Table 11.6.3 Comparison of finite element solutions with the analytical solutions for pressure and shear stress in the slider bearing problem.

		Shear stress, $-\bar{\sigma}_{xy}$		Pressure $\bar{P}$	
$\bar{x}$	$\bar{y}$	FEM	Analy.	FEM	Analy.
0.1125	0.49219	0.5661	0.5630	0.085	0.084
0.3375	0.47656	0.5660	0.5630	0.255	0.253
0.5625	0.46094	0.5647	0.5619	0.423	0.419
0.7875	0.44531	0.5617	0.5592	0.588	0.582
1.0125	0.42969	0.5569	0.5546	0.747	0.739
1.2375	0.41406	0.5497	0.5477	0.897	0.888
1.4625	0.39844	0.5397	0.5380	1.037	1.026
1.6875	0.38281	0.5262	0.5248	1.159	1.147
1.9125	0.36719	0.5084	0.5074	1.260	1.247
2.1375	0.35156	0.4853	0.4847	1.331	1.317
2.3625	0.33594	0.4556	0.4556	1.364	1.349
2.5875	0.32031	0.4177	0.4183	1.344	1.330
2.8125	0.30469	0.3693	0.3708	1.256	1.243
3.0375	0.28906	0.3076	0.3103	1.076	1.065
3.2625	0.27344	0.2289	0.2331	0.774	0.767
3.4875	0.25781	0.1282	0.1344	0.308	0.307

$\bar{x} = 10x, \quad \bar{y} = y \times 10^4, \quad \bar{\sigma}_{xy} = -\sigma_{xy} \times 10^{-2}, \quad \bar{P} = P \times 10^{-4}.$

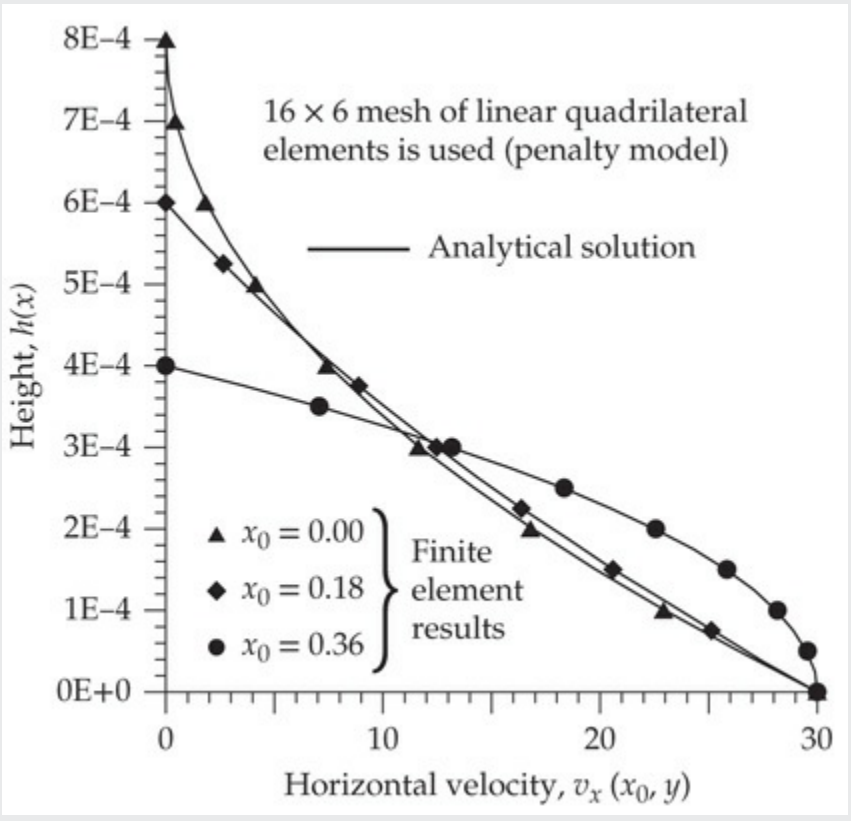

Fig. 11.6.5 Velocity distributions for the slider bearing problem.

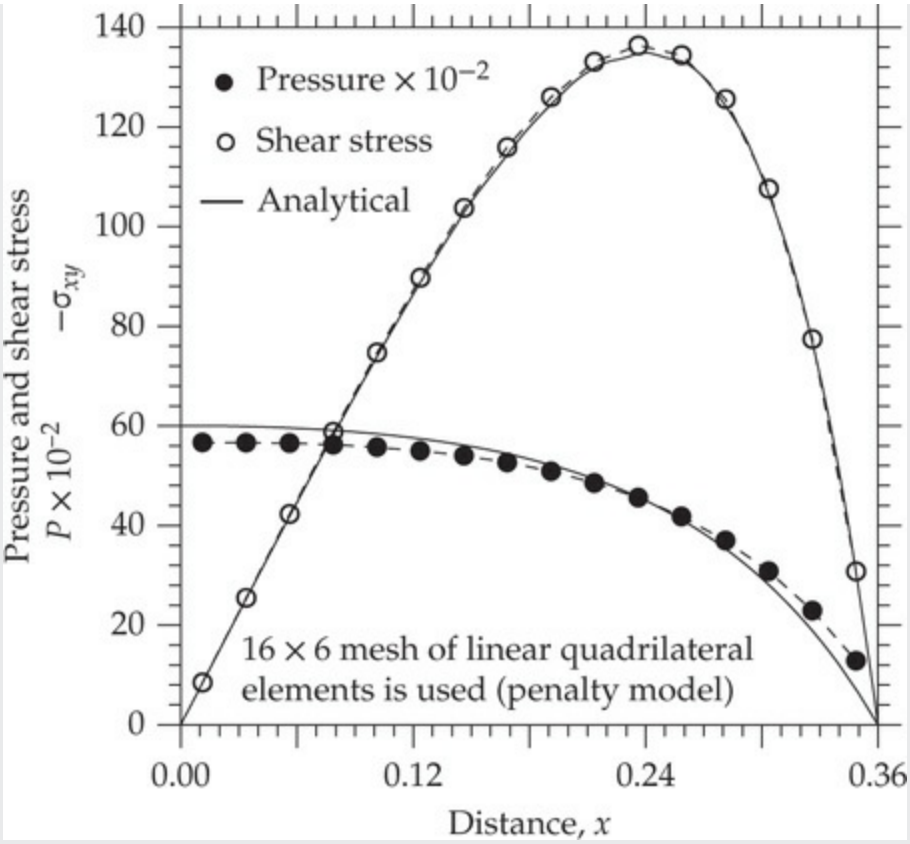

Fig. 11.6.6 Pressure and shear stress distributions for the slider bearing problem.

Box 11.6.4: Edited output file for flow of viscous fluid in a wall-driven cavity.

Node	x-coord.	y-coord.	Value of v_x	Value of v_y
18	0.00000E+00	0.10000E-03	0.22923E+02	-0.21223E-02
19	0.22500E-01	0.96875E-04	0.23145E+02	0.21177E-02
20	0.45000E-01	0.93750E-04	0.23368E+02	-0.21320E-02
21	0.67500E-01	0.90625E-04	0.23618E+02	0.19997E-02
22	0.90000E-01	0.87500E-04	0.23875E+02	-0.21601E-02
23	0.11250E+00	0.84375E-04	0.24161E+02	0.18828E-02
24	0.13500E+00	0.81250E-04	0.24459E+02	-0.22078E-02
25	0.15750E+00	0.78125E-04	0.24789E+02	0.17632E-02
26	0.18000E+00	0.75000E-04	0.25139E+02	-0.22763E-02
27	0.20250E+00	0.71875E-04	0.25526E+02	0.16366E-02
28	0.22500E+00	0.68750E-04	0.25942E+02	-0.23676E-02
29	0.24750E+00	0.65625E-04	0.26404E+02	0.14974E-02
30	0.27000E+00	0.62500E-04	0.26907E+02	-0.24854E-02
31	0.29250E+00	0.59375E-04	0.27468E+02	0.13384E-02
32	0.31500E+00	0.56250E-04	0.28087E+02	-0.26361E-02
33	0.33750E+00	0.53125E-04	0.28783E+02	0.11498E-02
34	0.36000E+00	0.50000E-04	0.29564E+02	-0.28290E-02
120	0.00000E+00	0.70000E-03	0.42885E+00	0.18940E-02
122	0.45000E-01	0.65625E-03	0.87306E+00	0.15087E-02
124	0.90000E-01	0.61250E-03	0.13795E+01	0.10557E-02
126	0.13500E+00	0.56875E-03	0.19627E+01	0.52105E-03
128	0.18000E+00	0.52500E-03	0.26424E+01	-0.11365E-03
130	0.22500E+00	0.48125E-03	0.34454E+01	-0.87392E-03
132	0.27000E+00	0.43750E-03	0.44092E+01	-0.17960E-02
134	0.31500E+00	0.39375E-03	0.55887E+01	-0.29327E-02
136	0.36000E+00	0.35000E-03	0.70661E+01	-0.43638E-02

Example 11.6.3

Consider the laminar flow of a viscous, incompressible fluid ($\mu = 1$ for computational purposes) in a unit square cavity bounded by three motionless walls (two side walls and the bottom) and the top (lid) moving at a constant velocity in its own plane, as depicted in Fig. 11.6.7. Singularities exist at each corner where the moving lid meets a fixed wall. Use the penalty finite element model and examine the influence of the penalty parameter γ on the velocities for uniform meshes (a) 8 × 8 linear and (b) 4 × 4 nine-node quadratic elements (both are quadrilateral elements) first, and then determine the velocity and pressure fields in the cavity and plot centerline velocities as a function of the distance for various meshes, including a refined mesh of 16 × 20 linear elements.

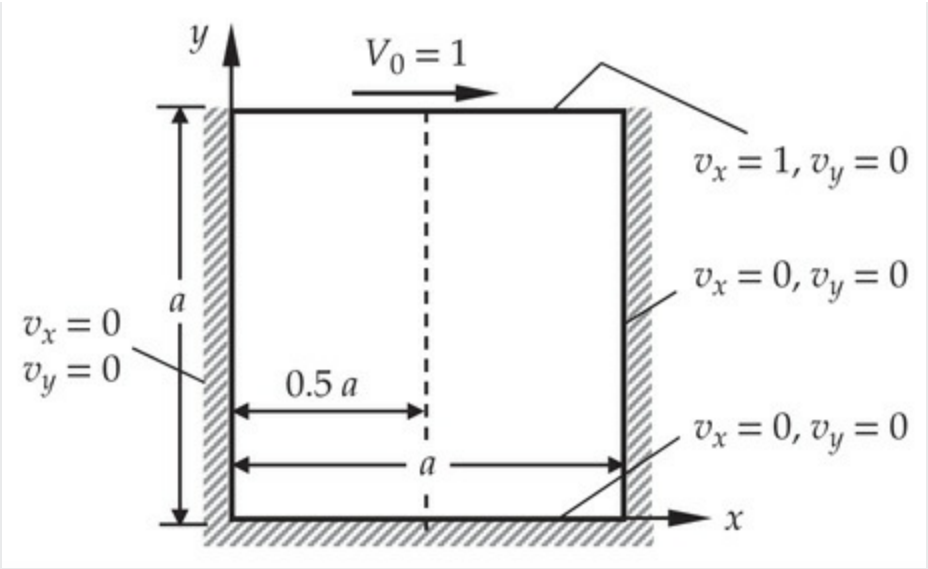

Fig. 11.6.7 Boundary conditions for lid-driven cavity problem.

Solution: This example is one that has been extensively studied by analytical, numerical, and experimental methods, and it is often used as a benchmark problem to test a new numerical method or formulation. At the singular points, namely at the top corners of the lid, we assume that v_x (x, 1) = V_0 = 1.0. The parameters for FEM2D for this problem when 8 × 8 mesh is used are

ITYPE=1, IGRAD=1, ITEM = 0, NEIGN = 0, IELTYP = 1, NPE = 4, MESH = 1, and NX = NY = 8

The input data to FEM2D is presented in Box 11.6.5 and an edited output is shown in Box 11.6.6. The penalty parameter γ is taken to be γ = 1.0, 102, 108 to investigate its influence on the solution. The numerical values of the centerline velocity v_x (0.5, y) are tabulated in Table 11.6.4. It is clear that low values of the penalty parameter adversely affect the accuracy of the solution but when $\gamma > 10^2$, the solution is relatively insensitive to the values of the penalty parameter, γ.

Table 11.6.4 Velocity v_x (0.5,y) obtained with various values of the penalty parameter γ.

	Mesh: 8 × 8Q4			Mesh: 4 × 4Q9		
y	$\gamma = 1$	$\gamma = 10^2$	$\gamma = 10^8$	$\gamma = 1$	$\gamma = 10^2$	$\gamma = 10^8$
0.125	−0.0030	−0.0557	−0.0579	−0.0034	−0.0589	−0.0615
0.250	−0.0045	−0.0938	−0.0988	−0.0037	−0.0984	−0.1039
0.375	−0.0267	−0.1250	−0.1317	0.0240	−0.1320	−0.1394
0.500	−0.0773	−0.1354	−0.1471	0.0720	−0.1442	−0.1563
0.625	−0.1796	−0.0818	−0.0950	0.1678	−0.0983	−0.1118
0.750	0.3624	0.0958	0.0805	0.3439	0.0641	0.0481
0.875	0.6419	0.4601	0.4501	0.6245	0.4295	0.4186

Box 11.6.5: Input file for flow of a viscous fluid in a wall-driven cavity.

```
Example 11.6.3: Flow in a wall-driven cavity(MESH:8x8Q4)
    1   1   0   0                  ITYPE,IGRAD,ITEM,NEIGN
    1   4   1   0                  IELTYP,NPE,MESH,NPRNT
    8   8                          NX, NY
0.0 0.125 0.125 0.125 0.125
    0.125 0.125 0.125 0.125        X0, DX(I)
0.0 0.125 0.125 0.125 0.125
    0.125 0.125 0.125 0.125        Y0, DY(I)
    64                             NSPV
  1 1   1 2   2 1   2 2   3 1   3 2   4 1   4 2   5 1   5 2
  6 1   6 2   7 1   7 2   8 1   8 2   9 1   9 2  10 1  10 2
 18 1  18 2  19 1  19 2  27 1  27 2  28 1  28 2  36 1  36 2
 37 1  37 2  45 1  45 2  46 1  46 2  54 1  54 2  55 1  55 2
 63 1  63 2  64 1  64 2  72 1  72 2  73 1  73 2  74 1  74 2
 75 1  75 2  76 1  76 2  77 1  77 2  78 1  78 2  79 1  79 2
 80 1  80 2  81 1  81 2
  0.0   0.0   0.0   0.0   0.0   0.0   0.0   0.0   0.0   0.0
  0.0   0.0   0.0   0.0   0.0   0.0   0.0   0.0   0.0   0.0
  0.0   0.0   0.0   0.0   0.0   0.0   0.0   0.0   0.0   0.0
  0.0   0.0   0.0   0.0   0.0   0.0   0.0   0.0   0.0   0.0
  0.0   0.0   0.0   0.0   0.0   0.0   1.0   0.0   1.0   0.0
  1.0   0.0   1.0   0.0   1.0   0.0   1.0   0.0   1.0   0.0
  1.0   0.0   1.0   0.0
  0                              NSSV
  1.0E0 1.0E08                   AMU,PENALTY
  0.0   0.0   0.0                F0, FX, FY
```

Box 11.6.6: Edited output file for flow of a viscous fluid in a wall-driven

cavity.

Node	x-coord.	y-coord.	Value of v_x	Value of v_y
14	0.50000E+00	0.12500E+00	-0.57928E-01	-0.33191E-10
23	0.50000E+00	0.25000E+00	-0.98791E-01	-0.24444E-09
32	0.50000E+00	0.37500E+00	-0.13171E+00	-0.34246E-09
41	0.50000E+00	0.50000E+00	-0.14712E+00	-0.10088E-09
50	0.50000E+00	0.62500E+00	-0.94970E-01	0.41647E-09
59	0.50000E+00	0.75000E+00	0.80460E-01	0.74580E-09
68	0.50000E+00	0.87500E+00	0.45006E+00	0.35967E-09
77	0.50000E+00	0.10000E+01	0.10000E+01	0.00000E+00
37	0.00000E+00	0.50000E+00	0.00000E+00	0.00000E+00
38	0.12500E+00	0.50000E+00	-0.30461E-01	0.12639E+00
39	0.25000E+00	0.50000E+00	-0.87409E-01	0.14488E+00
40	0.37500E+00	0.50000E+00	-0.13051E+00	0.90721E-01
41	0.50000E+00	0.50000E+00	-0.14712E+00	-0.10088E-09
42	0.62500E+00	0.50000E+00	-0.13051E+00	-0.90721E-01
43	0.75000E+00	0.50000E+00	-0.87409E-01	-0.14488E+00
44	0.87500E+00	0.50000E+00	-0.30461E-01	-0.12639E+00
45	0.10000E+01	0.50000E+00	0.00000E+00	0.00000E+00

x-coord.	y-coord.	sigma-x	sigma-y	sigma-xy	Pressure
0.6250E-01	0.9375E+00	0.1343E+02	0.1128E+02	0.8000E+01	-0.1236E+02
0.1875E+00	0.9375E+00	0.5548E+01	0.2425E+01	0.5848E+01	-0.3986E+01
0.3125E+00	0.9375E+00	0.2559E+01	0.1110E+01	0.4876E+01	-0.1835E+01
0.4375E+00	0.9375E+00	0.7806E+00	0.3036E+00	0.4400E+01	-0.5421E+00
0.5625E+00	0.9375E+00	-0.7806E+00	-0.3036E+00	0.4400E+01	0.5421E+00
0.6875E+00	0.9375E+00	-0.2559E+01	-0.1110E+01	0.4876E+01	0.1835E+01
0.8125E+00	0.9375E+00	-0.5548E+01	-0.2425E+01	0.5848E+01	0.3986E+01
0.9375E+00	0.9375E+00	-0.1343E+02	-0.1128E+02	0.8000E+01	0.1236E+02

The linear solution for the horizontal velocity along the vertical centerline obtained with the two meshes is shown in Fig. 11.6.8, and the variation of pressure along the top wall (computed at the reduced Gauss points) is shown in Fig. 11.6.9. Figure 11.6.10 contains plots of center velocity v_x (0.5, y) as a function of y for 8 × 8 and 16 × 20 meshes of linear elements.

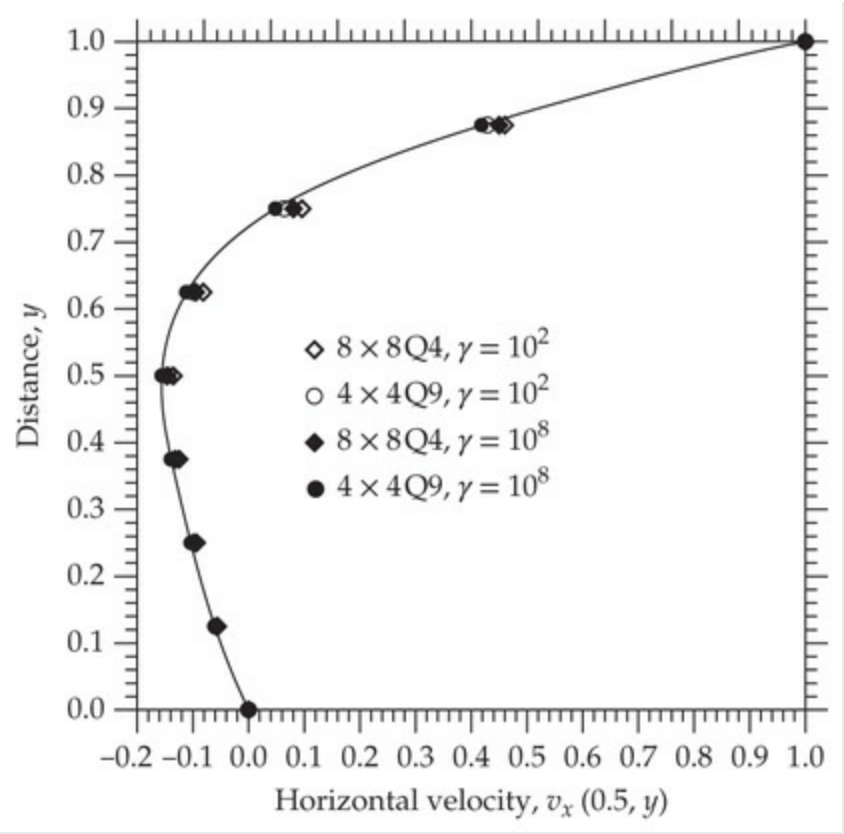

Fig. 11.6.8 Plots of horizontal velocity v_x (0.5,y) versus y.

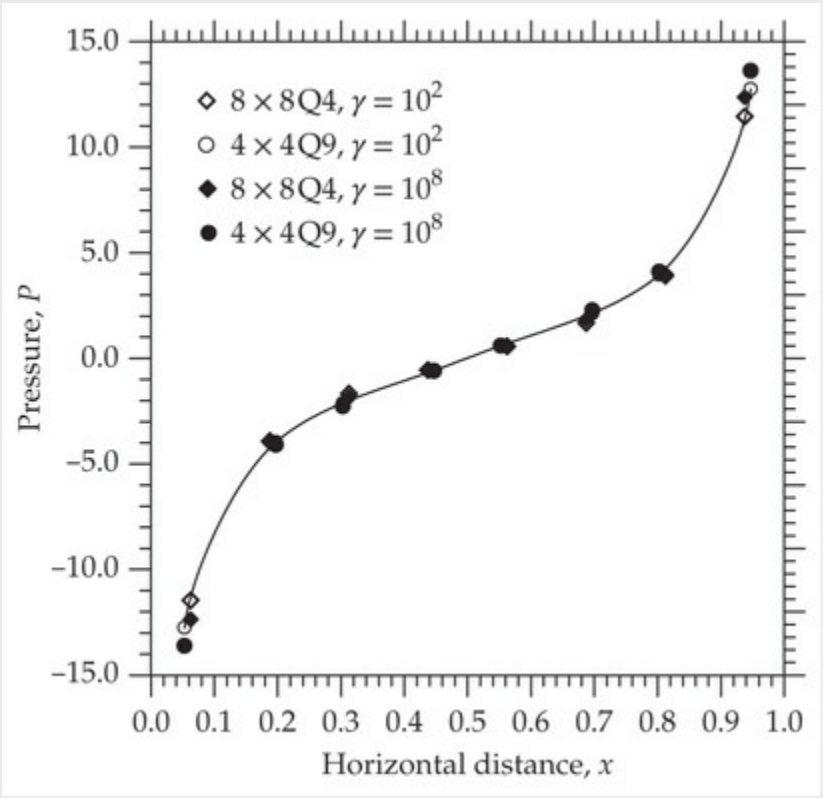

Fig. 11.6.9 Plots of pressure $P(x, 0.9375)$ along the top wall of the cavity.

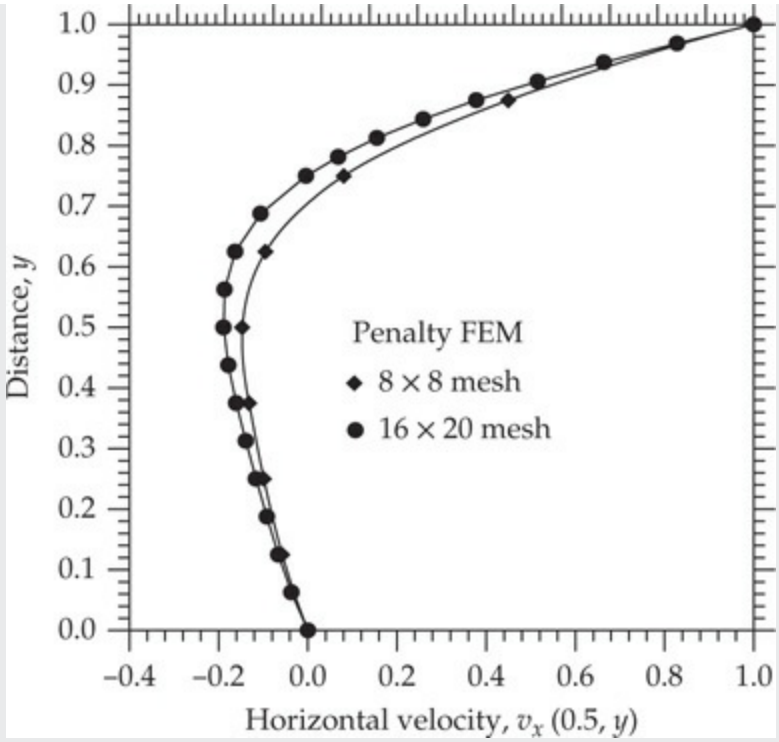

Fig. 11.6.10 Velocity v_x (0.5,y) versus y for 8 × 8Q4 and 16 × 20Q4 meshes.

Example 11.6.4

Consider the problem of a viscous fluid squeezed between two parallel plates [see Fig. 11.6.1(a)]. Assuming that the initial conditions on the velocity field are zero, determine the transient solution of the problem using 6 × 4 uniform mesh of nine-node quadratic elements, the Crank–Nicolson scheme ($\alpha = 0.5$), and time step $\Delta t = 0.1$. Plot the velocity field v_x (6, y, t) as a function of y for various values of time t.

Solution: Since the solution is driven by the velocity v_y (b, x, t) = −1, which is not a function of time, the solution will reach a steady state. The input parameters for FEM2D are ITYPE = 1, IGRAD = 1, ITEM = 1, NEIGN = 0, IELTYP = 2, NPE = 9, MESH = 1, NX = 6, NY = 4, AMU = 1.0, PNLTY = 10^8, NTIME = 20, NSTP = 50, INTVL = 1, INTIAL = 0, DT = 0.1, ALPHA = 0.5, and EPSLN = 10^{-3}. The input file is presented in Box 11.6.7 and an edited output is included in Box 11.6.8.

Box 11.6.7: Input file for the transient analysis of fluid squeezed between plates.

```
EX 11.6.4: Transient Analysis of fluid squeezed between plates
    1   1   1   0                   ITYPE,IGRAD,ITEM,NEIGN
    2   9   1   0                   IEL, NPE, MESH, NPRNT
    6   4                           NX, NY
    0.0  1.0  1.0  1.0  1.0  1.0  1.0          X0, DX(I)
    0.0  0.5  0.5  0.5  0.5                     Y0, DY(I)
    47                                          NSPV
   1 1   1 2   2  2   3  2   4  2   5  2   6  2  7  2  8  2  9  2
  10 2  11 2  12  2  13  2  14  1  27  1  40  1  53 1  66 1  79 1
  92 1 105 1 105  2 106  1 106  2 107  1 107  2 108 1 108 2 109 1
 109 2 110 1 110  2 111  1 111  2 112  1 112  2 113 1 113 2 114 1
 114 2 115 1 115  2 116  1 116  2 117  1 117  2 ISPV(I,J)
   0.0   0.0    0.0    0.0    0.0    0.0    0.0   0.0   0.0   0.0
   0.0   0.0    0.0    0.0    0.0    0.0    0.0   0.0   0.0   0.0
   0.0   0.0   -1.0    0.0   -1.0    0.0   -1.0   0.0  -1.0   0.0
  -1.0   0.0   -1.0    0.0   -1.0    0.0   -1.0   0.0  -1.0   0.0
  -1.0   0.0   -1.0    0.0   -1.0    0.0   -1.0  VSPV(I)
   0                              NSSV
   1.0   1.0E8                    AMU, PENLTY
   0.0   0.0   0.0                F0, FX, FY
   1.0   0.0   0.0                C0, CX, CY
   20    50    1     0            NTIME,NSTP,INTVL,INTIAL
   0.1   0.5   0.25  1.0D-3       DT, ALFA, GAMA, EPSLN
```

Box 11.6.8: Edited output file for viscous fluid squeezed between parallel plates.

```
*TIME* = 0.10000E+00     Time Step Number =  1
Node     x-coord.       y-coord.    Value of v_x  Value of v_y
 13    0.60000E+01    0.00000E+00    0.29963E+01    0.00000E+00
 26    0.60000E+01    0.25000E+00    0.30183E+01   -0.55915E-01
 39    0.60000E+01    0.50000E+00    0.30546E+01   -0.10483E+00
 52    0.60000E+01    0.75000E+00    0.31440E+01   -0.17523E+00
 65    0.60000E+01    0.10000E+01    0.32155E+01   -0.20870E+00
 78    0.60000E+01    0.12500E+01    0.33633E+01   -0.30396E+00
 91    0.60000E+01    0.15000E+01    0.32150E+01   -0.27701E+00
104    0.60000E+01    0.17500E+01    0.29827E+01   -0.51843E+00

*TIME* = 0.10000E+01     Time Step Number = 10
 13    0.60000E+01    0.00000E+00    0.42052E+01    0.00000E+00
 26    0.60000E+01    0.25000E+00    0.41576E+01    0.36780E-01
 39    0.60000E+01    0.50000E+00    0.39978E+01    0.70817E-01
 52    0.60000E+01    0.75000E+00    0.37384E+01    0.77266E-01
 65    0.60000E+01    0.10000E+01    0.33503E+01    0.74066E-01
 78    0.60000E+01    0.12500E+01    0.28552E+01   -0.17315E-01
 91    0.60000E+01    0.15000E+01    0.21638E+01   -0.13685E+00
104    0.60000E+01    0.17500E+01    0.14416E+01   -0.54946E+00
*TIME* = 0.14000E+01     Time Step Number = 14
 13    0.60000E+01    0.00000E+00    0.42203E+01    0.00000E+00
 26    0.60000E+01    0.25000E+00    0.41706E+01    0.40836E-01
 39    0.60000E+01    0.50000E+00    0.40057E+01    0.77788E-01
 52    0.60000E+01    0.75000E+00    0.37397E+01    0.85478E-01
 65    0.60000E+01    0.10000E+01    0.33420E+01    0.80067E-01
 78    0.60000E+01    0.12500E+01    0.28490E+01   -0.13515E-01
 91    0.60000E+01    0.15000E+01    0.21455E+01   -0.13368E+00
104    0.60000E+01    0.17500E+01    0.14390E+01   -0.54872E+00
```

Figure 11.6.11 contains plots of the horizontal velocity v_x (6, y, t) as a function of y for various values of time t. The transient solution reaches a steady state around t = 1.4 (for a difference of 10^{-3} between the solutions at two consecutive time steps).

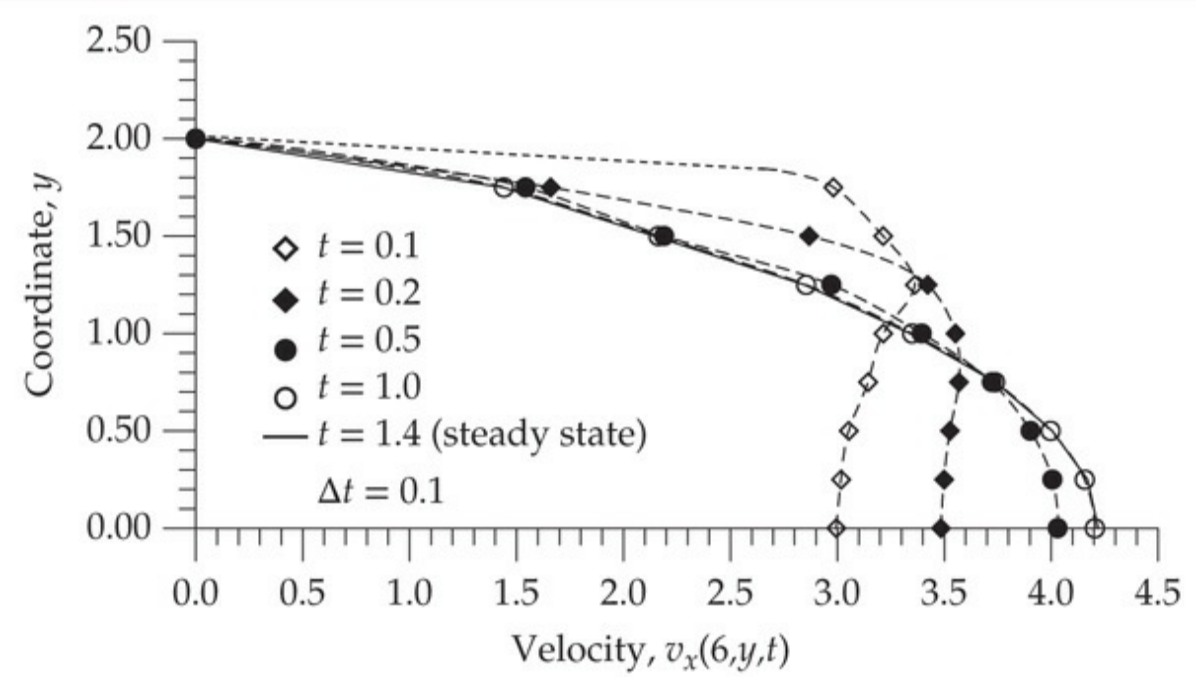

Fig. 11.6.11 Velocity v_x (6, y,t) versus y for various times.

Example 11.6.5

Investigate the motion of a viscous fluid (μ = 1.0) inside a lid-driven cavity of **Example 11.6.3**. Use nonuniform 16 × 20Q4 mesh in the domain with the following element lengths in the x and y directions (16 elements of length 0.0625 in the x direction; 12 elements of length 0.0625 and 8 elements of length 0.03125 in the y direction): {DX}={0.0625, 0.0625,. . . , 0.0625}; {DY}={0.0625,. . . , 0.0625, 0.03125,. . . , 0.03125}. Employ the Crank–Nicolson scheme (γ = 0.5) and the penalty finite element model with γ = 10^8, and obtain the transient solutions with two different time steps: Δt = 0.01 and Δt = 0.001.

Solution: The input file to FEM2D for the problem is presented in Box 11.6.9 and an edited output is included in Box 11.6.10. Table 11.6.5 contains the velocity field v_x (0.5, y, t) × 10 for various times t = 0.01, 0.05, and 1.4. The solution is declared to reach a steady-state when

Table 11.6.5 The horizontal velocity v_x (0.5,y,t) × 10 as a function of $\bar{y} = 10y$ for the wall-driven cavity problem for different times and time steps.

$\bar{y}$	$t = 0.01$		$t = 0.05$		$t = 1.4$		Steady
$\Delta t \rightarrow$	10^{-2}	10^{-3}	10^{-2}	10^{-3}	10^{-2}	10^{-3}	state
0.6250	−0.1342	−0.1953	−0.3103	−0.3247	−0.3688	−0.3684	−0.3688
1.2500	−0.1936	−0.3140	−0.5624	−0.5841	−0.6631	−0.6623	−0.6631
1.8750	−0.2314	−0.3940	−0.7888	−0.8163	−0.9198	−0.9918	−0.9198
2.5000	−0.2691	−0.4651	−1.0122	−1.0435	−1.1593	−1.1582	−1.1593
3.1250	−0.3157	−0.5475	−1.2346	−1.2746	−1.3886	−1.3877	−1.3886
3.7500	−0.3759	−0.6536	−1.4790	−1.5053	−1.6028	−1.6020	−1.6028
4.3750	−0.4516	−0.7902	−1.6964	−1.7151	−1.7820	−1.7816	−1.7820
5.0000	−0.5435	−0.9605	−1.8536	−1.8643	−1.8895	−1.8894	−1.8895
5.6250	−0.6465	−1.1577	−1.8846	−1.8878	−1.8652	−1.8656	−1.8652
6.2500	−0.7474	−1.3479	−1.7011	−1.6946	−1.6250	−1.6257	−1.6250
6.8750	−0.8097	−1.4428	−1.1889	−1.1653	−1.0572	−1.0581	−1.0572
7.5000	−0.7536	−1.1523	−0.2093	−0.1693	−0.0382	−0.0393	−0.0382
7.8125	−0.6325	−0.7744	0.5100	0.5471	0.6820	0.6809	0.6820
8.1250	−0.4077	−0.1695	1.4014	1.4197	1.5526	1.5516	1.5526
8.4375	−0.0054	0.7336	2.4885	2.4716	2.5965	2.5956	2.5965
8.7500	0.6329	1.9318	3.7259	3.6716	3.7823	3.7816	3.7824
9.0625	1.7000	3.5232	5.1185	5.0707	5.1617	5.1609	5.1616
9.3750	3.3334	5.3837	6.5139	6.5756	6.6409	6.6405	6.6410
9.6875	5.9470	7.5970	7.9975	8.2488	8.2838	8.2835	8.2838

$$\mathcal{E} = \sqrt{\frac{\sum_I^{\text{NEQ}} |U_I^{s+1} - U_I^s|^2}{\sum_I^{\text{NEQ}} |U_I^{s+1}|^2}} < \epsilon$$

Box 11.6.9: Input file for the flow of a viscous fluid in a wall-driven cavity.

```
EX 11.6.5: Transient analysis of the lid-driven cavity problem
    1    1    1    0                          ITYPE,IGRAD,ITEM,NEIGN
    1    4    1    0                          IELTYP, NPE, MESH, NPRNT
   16   20                                    NX, NY
0.0   0.0625 0.0625 0.0625 0.0625 0.0625 0.0625
      0.0625 0.0625 0.0625 0.0625 0.0625 0.0625
      0.0625 0.0625 0.0625 0.0625             X0, DX(I)
0.0   0.0625 0.0625 0.0625 0.0625 0.0625 0.0625
      0.0625 0.0625 0.0625 0.0625 0.0625 0.0625
      0.03125 0.03125 0.03125 0.03125
      0.03125 0.03125 0.03125 0.03125         Y0, DY(I)
144                                           NSPV
  1 1    1 2    2 1    2 2    3 1    3 2    4 1    4 2    5 1
  5 2    6 1    6 2    7 1    7 2    8 1    8 2    9 1    9 2
 10 1   10 2   11 1   11 2   12 1   12 2   13 1   13 2   14 1
 14 2   15 1   15 2   16 1   16 2   17 1   17 2   18 1   18 2
 34 1   34 2   35 1   35 2   51 1   51 2   52 1   52 2   68 1
 68 2   69 1   69 2   85 1   85 2   86 1   86 2  102 1  102 2
103 1  103 2  119 1  119 2  120 1  120 2  136 1  136 2  137 1
137 2  153 1  153 2  154 1  154 2  170 1  170 2  171 1  171 2
187 1  187 2  188 1  188 2  204 1  204 2  205 1  205 2  221 1
221 2  222 1  222 2  238 1  238 2  239 1  239 2  255 1  255 2
256 1  256 2  272 1  272 2  273 1  273 2  289 1  289 2  290 1
290 2  306 1  306 2  307 1  307 2  323 1  323 2  324 1  324 2
340 1  340 2  341 1  341 2  342 1  342 2  343 1  343 2  344 1
344 2  345 1  345 2  346 1  346 2  347 1  347 2  348 1  348 2
349 1  349 2  350 1  350 2  351 1  351 2  352 1  352 2  353 1
353 2  354 1  354 2  355 1  355 2  356 1  356 2  357 1  357 2
  0.0    0.0    0.0    0.0    0.0    0.0    0.0    0.0    0.0
  0.0    0.0    0.0    0.0    0.0    0.0    0.0    0.0    0.0
  0.0    0.0    0.0    0.0    0.0    0.0    0.0    0.0    0.0
  0.0    0.0    0.0    0.0    0.0    0.0    0.0    0.0    0.0
  0.0    0.0    0.0    0.0    0.0    0.0    0.0    0.0    0.0
  0.0    0.0    0.0    0.0    0.0    0.0    0.0    0.0    0.0
  0.0    0.0    0.0    0.0    0.0    0.0    0.0    0.0    0.0
  0.0    0.0    0.0    0.0    0.0    0.0    0.0    0.0    0.0
  0.0    0.0    0.0    0.0    0.0    0.0    0.0    0.0    0.0
  0.0    0.0    0.0    0.0    0.0    0.0    0.0    0.0    0.0
  0.0    0.0    0.0    0.0    0.0    0.0    0.0    0.0    0.0
  0.0    0.0    0.0    0.0    0.0    0.0    0.0    0.0    0.0
  0.0    0.0    1.0    0.0    1.0    0.0    1.0    0.0    1.0
  0.0    1.0    0.0    1.0    0.0    1.0    0.0    1.0    0.0
  1.0    0.0    1.0    0.0    1.0    0.0    1.0    0.0    1.0
  0.0    1.0    0.0    1.0    0.0    1.0    0.0    1.0    0.0
    0                                         NSSV
    1.0    1.0E8                              AMU, PENLTY
    0.0    0.0    0.0                         F0, FX, FY
    1.0    0.0    0.0                         C0,  CX,  CY
    150    151    1    0                      NTIME,NSTP,INTVL,INTIAL
    0.001 0.5    0.5  1.0E-6                  DT,ALFA,GAMA,EPSLN
```

Box 11.6.10: Edited output file for viscous fluid squeezed between parallel plates.

TIME = 0.10E+00 Time Step Number =100 Difference = 0.82510E-04

Node	x-coord.	y-coord.	Value of u	Value of v
26	0.50000E+00	0.62500E-01	-0.36506E-01	-0.16666E-07
43	0.50000E+00	0.12500E+00	-0.65653E-01	-0.15158E-07
60	0.50000E+00	0.18750E+00	-0.91155E-01	-0.78388E-08
77	0.50000E+00	0.25000E+00	-0.11506E+00	-0.89954E-08
94	0.50000E+00	0.31250E+00	-0.13807E+00	-0.55894E-08
111	0.50000E+00	0.37500E+00	-0.15966E+00	-0.55408E-08
128	0.50000E+00	0.43750E+00	-0.17785E+00	-0.38310E-08
145	0.50000E+00	0.50000E+00	-0.18892E+00	-0.44778E-08
162	0.50000E+00	0.56250E+00	-0.18682E+00	-0.30558E-08
179	0.50000E+00	0.62500E+00	-0.16308E+00	-0.32317E-08
196	0.50000E+00	0.68750E+00	-0.10650E+00	-0.25332E-08
213	0.50000E+00	0.75000E+00	-0.47054E-02	-0.29066E-08
230	0.50000E+00	0.78125E+00	0.67315E-01	-0.20648E-08
247	0.50000E+00	0.81250E+00	0.15441E+00	-0.19906E-08
264	0.50000E+00	0.84375E+00	0.25887E+00	-0.15246E-08
281	0.50000E+00	0.87500E+00	0.37756E+00	-0.83728E-09
298	0.50000E+00	0.90625E+00	0.51561E+00	-0.45414E-09
315	0.50000E+00	0.93750E+00	0.66371E+00	0.59333E-10
332	0.50000E+00	0.96875E+00	0.82817E+00	0.15004E-09

where NEQ is the number of nodal values in the mesh and ε is the specified tolerance. The solution has reached a steady state at $t = 0.14$, for both time steps, if we set $\varepsilon = 10^{-6}$. The evolution of the horizontal velocity component v_x (0.5, y, t) with time is shown in Fig. 11.6.12 (Δt = 0.001). Graphically, the solution at $t = 0.1$ is already close to the steady state solution (for the scale used in the figure).

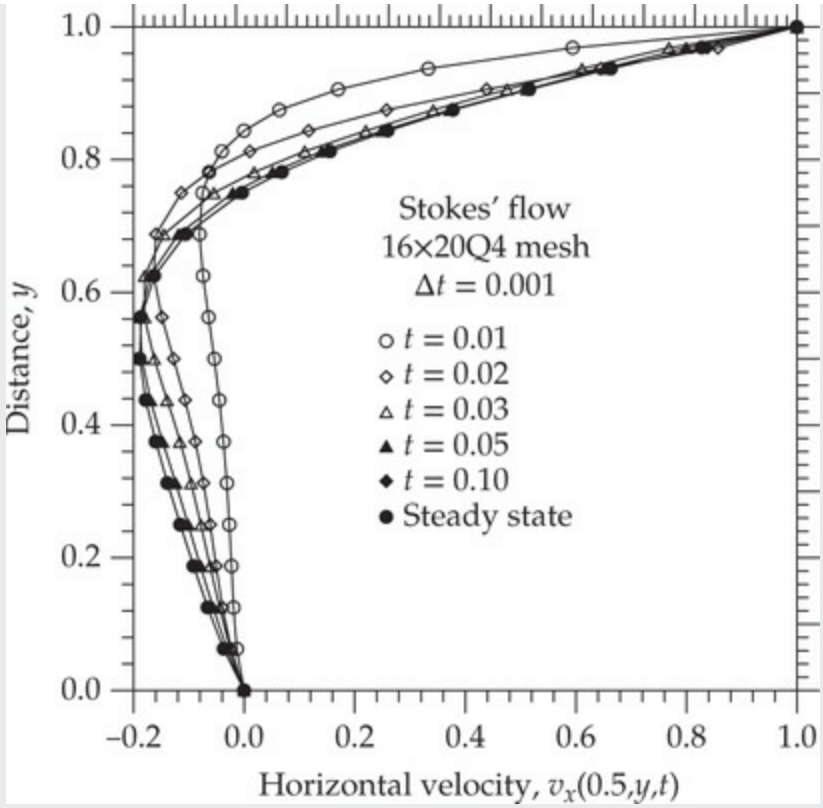

Fig. 11.6.12 The horizontal velocity field v_x (0.5,y,t) × 10 versus time t for the wall-driven cavity problem (16 × 20Q4 mesh).

11.7 Summary

Finite element models of the equations governing two-dimensional flows of viscous, incompressible fluids are developed. Two different types of finite element models are presented: (1) the velocity–pressure finite element model, with (v_x, v_y, P) as the primary nodal degrees of freedom, and (2) the penalty finite element model with (v_x, v_y) as the primary nodal degrees of freedom. In the penalty function method, the pressure is calculated from the velocity field in the post-computation. The coefficient matrix in the penalty finite element model is evaluated using mixed integration: full integration for the viscous terms and reduced integration for the penalty terms [i.e., terms associated with the incompressibility or divergence-free condition on the velocity field ($\nabla \cdot \mathbf{v} = 0$)]. Both triangular and quadrilateral elements are discussed. In general, triangular elements do not yield accurate pressure fields and are not used in the present study when numerical results are discussed. The linear and

quadratic quadrilateral elements are more reliable for pressure as well as for velocity fields in the penalty finite element model. Several numerical examples of steady-state and transient solutions of flows of viscous incompressible fluids in two dimensions are presented with the help of FEM2D (using the penalty finite element model; see [3, 4, 8] for more applications).

Problems

Formulations and Data Preparation

11.1 Consider Eqs. (11.2.1) and (11.2.2) in cylindrical coordinates (r, θ, z). For axisymmetric flows of viscous incompressible fluids (i.e., flow field is independent of the θ coordinate), we have

$$\rho \frac{\partial u}{\partial t} = \frac{1}{r}\frac{\partial}{\partial r}(r\sigma_{rr}) - \frac{\sigma_{\theta\theta}}{r} + \frac{\partial \sigma_{rz}}{\partial z} + f_r \tag{1}$$

$$\rho \frac{\partial w}{\partial t} = \frac{1}{r}\frac{\partial}{\partial r}(r\sigma_{rz}) + \frac{\partial \sigma_{zz}}{\partial z} + f_z \tag{2}$$

$$\frac{1}{r}\frac{\partial}{\partial r}(ru) + \frac{\partial w}{\partial z} = 0 \tag{3}$$

where ($u = v_r$ and $w = v_z$)

$$\sigma_{rr} = -P + 2\mu\frac{\partial u}{\partial r}, \quad \sigma_{\theta\theta} = -P + 2\mu\frac{u}{r}, \quad \sigma_{zz} = -P + 2\mu\frac{\partial w}{\partial z}, \quad \sigma_{rz} = \mu\left(\frac{\partial u}{\partial z} + \frac{\partial w}{\partial r}\right) \tag{4}$$

Develop the semidiscrete finite element model of the equations using the pressure-velocity formulation.

11.2 Develop the semidiscrete finite element model of the equations in **Problem 11.1** using the penalty function formulation.

11.3 Write the fully discretized finite element equations of the finite element models in **Problems 11.1** and **11.2**. Use the α-family of approximation.

11.4 The equations governing unsteady slow flow of viscous, incompressible fluids in the (x, y) plane can be expressed in terms of vorticity ωz and stream function ψ:

$$\rho\frac{\partial\omega_z}{\partial t}-\mu\nabla^2\omega_z=0,\quad -2\omega_z-\nabla^2\psi=0 \tag{1}$$

Develop the semidiscrete finite element model of the equations. Discuss the meaning of the secondary variables.

11.5–11.7 For the viscous flow problems given in Figs. P11.5–P11.7, give the specified primary and secondary degrees of freedom and their values.

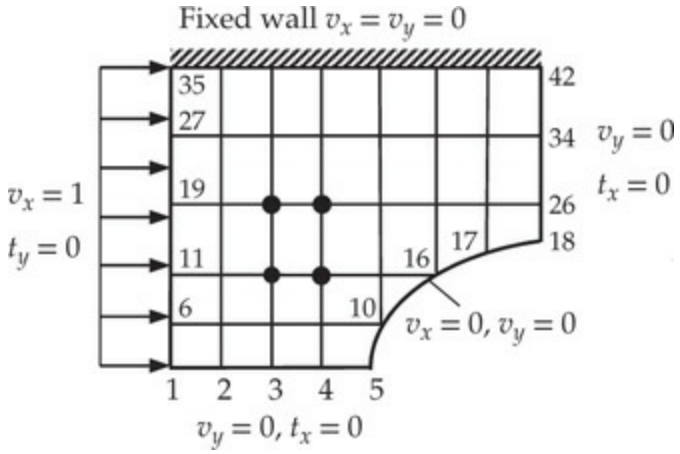

Fig. P11.5

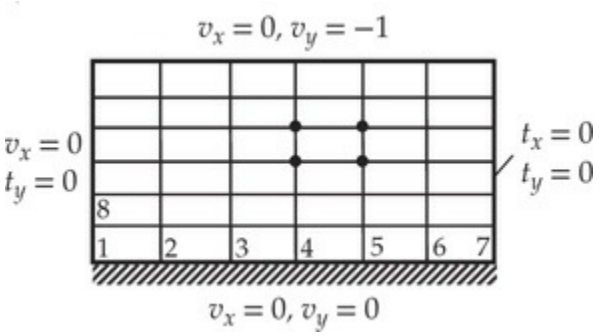

Fig. P11.6

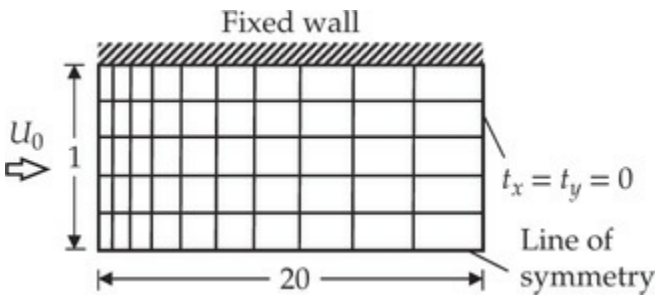

Fig. P11.7

11.8 Consider the flow of a viscous incompressible fluid in a square

cavity (Fig. P11.8). The flow is induced by the movement of the top wall (or lid) with a velocity $v_x = \sin \pi x$. For a 6 × 4 mesh of linear elements with $DX = \{0.1, 0.2, 0.2, 0.2, 0.2, 0.1\}$ and $DY = \{0.35, 0.35, 0.2, 0.1\}$, give the primary and secondary degrees of freedom.

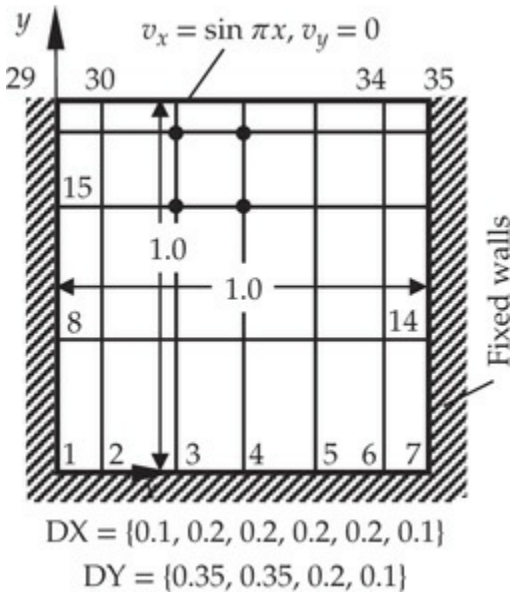

Fig. P11.8

11.9 Consider the flow of a viscous incompressible fluid in a 90° plane tee. Using the symmetry and the mesh shown in Fig. P11.9, write the specified primary and secondary variables for the computational domain.

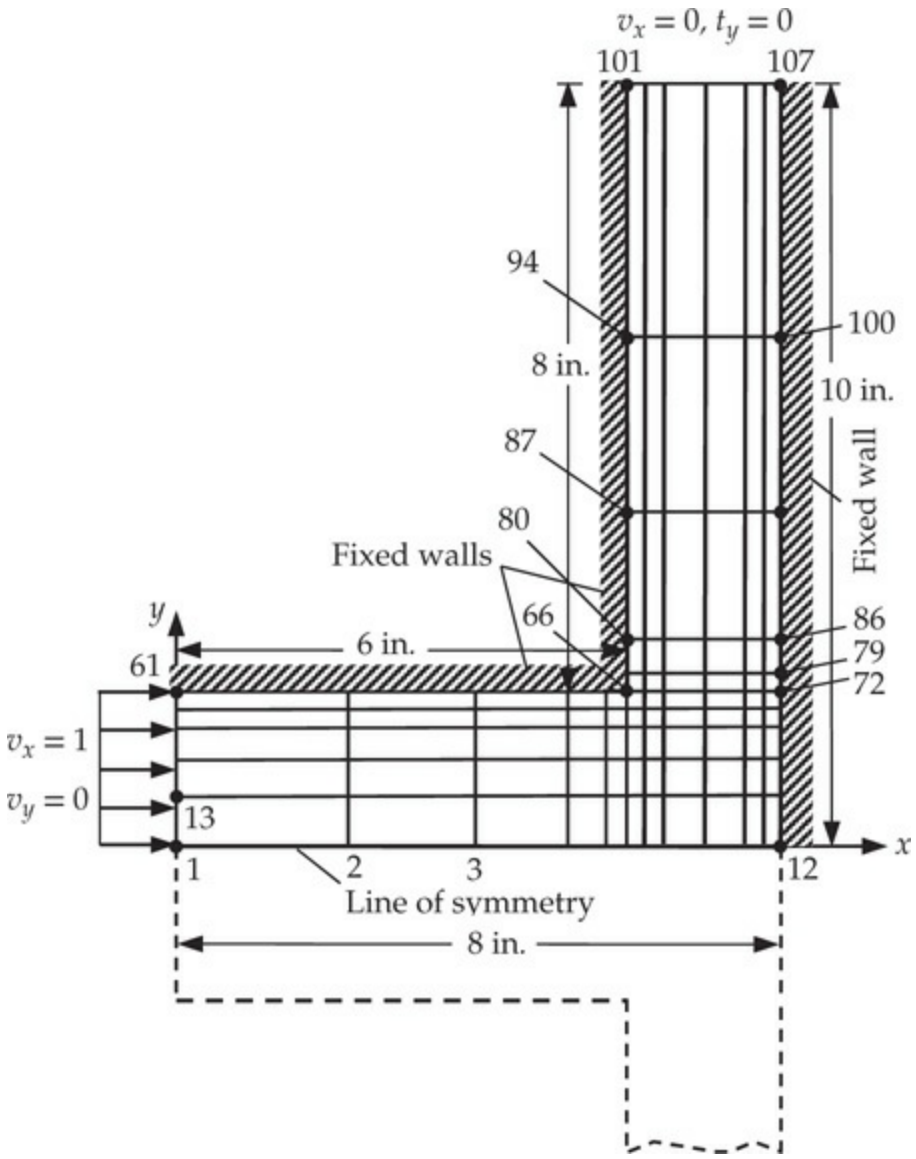

Fig. P11.9

11.10 Repeat **Problem 11.9** for the geometry shown in Fig. P11.10.

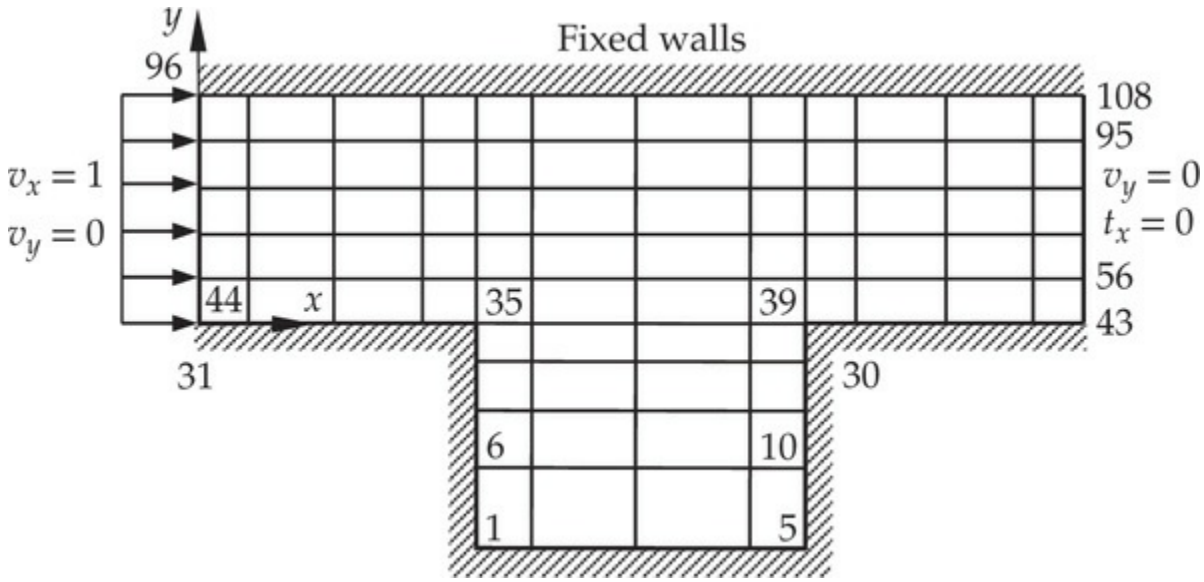

Fig. P11.10

COMPUTATIONAL EXERCISES

Use a value of the penalty parameter that has no influence on the graphical presentation of the results.

11.11 Analyze the problem of viscous fluid being squeezed between parallel plates (see **Example 11.6.1**) using a nonuniform mesh of 10 × 8Q9 elements: four subdivisions of length 1.0, two subdivision of length 0.5, and four subdivisions of length 0.25 along the x axis; and eight subdivisions of length 0.25 in the y direction. Use a penalty parameter of $\gamma = 10^8$. Plot the velocity $v_x(x_0, y)$ versus y for $x_0 = 4$ and $x_0 = 6$. Also plot the pressure $P(x,y_0)$ versus x for $y_0 = 0.05283$ and $y_0 = 1.947$.

11.12 Repeat **Problem 11.11** using a nonuniform mesh of 20 × 16Q4 elements that is nodally the same as the nonuniform mesh of 10 × 8Q9 elements.

11.13 Analyze the flow of a viscous fluid in a slider bearing (see **Example 11.6.2**) using a mesh consisting of six Q9 (quadratic) elements and 35 nodes (see Fig. P11.13). Use the following input data to generate the mesh with MESH2DG:

```
    5                                   NRECL
 1   7   1   0.0   0.0      0.36   0.0      1.0
 8  14   1   0.0   5.0E-5   0.36   5.0E-5   1.0
15  21   1   0.0   4.0E-4   0.36   2.0E-4   1.0
22  28   1   0.0   6.0E-4   0.36   3.0E-4   1.0
29  35   1   0.0   8.0E-4   0.36   4.0E-4   1.0
 2                          NRECEL
 1   3   1   2   9     1   3  17  15   2  10  16   8   9
 4   6   1   2   9    15  17  31  29  16  24  30  22  23
```

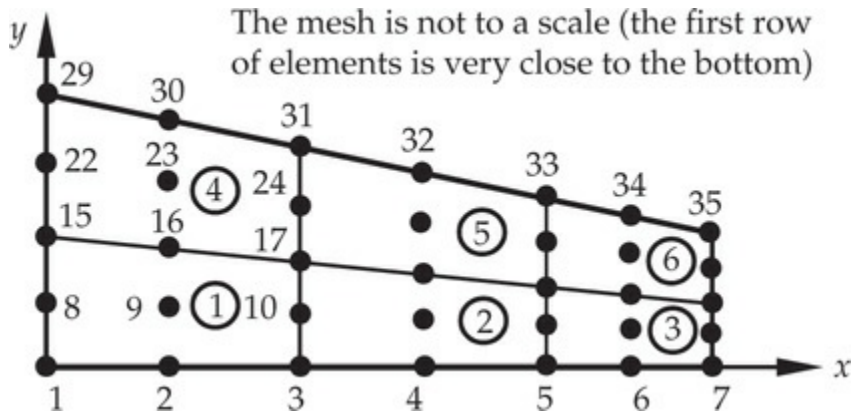

Fig. P11.13

11.14 Analyze the flow of a viscous fluid in a slider bearing (see **Example 11.6.2**) using a mesh of 24 Q4 (linear) elements and 35 nodes (nodally equivalent to the mesh used in **Problem 11.13**). Use the following input data to generate the mesh with MESH2DG:

```
 24   35                                NEM, NNM
 5                                      NREC
 1    7   1   0.0   0.0      0.36   0.0      1.0
 8   14   1   0.0   5.0E-5   0.36   5.0E-5   1.0
15   21   1   0.0   4.0E-4   0.36   2.0E-4   1.0
22   28   1   0.0   6.0E-4   0.36   3.0E-4   1.0
29   35   1   0.0   8.0E-4   0.36   4.0E-4   1.0
 4
 1    6   1   1   4     1   2   9   8
 7   12   1   1   4     8   9  16  15
13   18   1   1   4    15  16  23  22
19   24   1   1   4    22  23  30  29
```

11.15 Analyze the flow of a viscous fluid in a slider bearing (see **Example 11.6.2**) using a mesh of 32 Q9 (quadratic quadrilateral) elements and 153 nodes. Use the following input data to generate the mesh with MESH2DG:

```
  9                                          NREC
  1   17    1    0.0   0.0      0.36   0.0      1.0
 18   34    1    0.0   1.0E-4   0.36   0.5E-4   1.0
 35   51    1    0.0   2.0E-4   0.36   1.0E-4   1.0
 52   68    1    0.0   3.0E-4   0.36   1.5E-4   1.0
 69   85    1    0.0   4.0E-4   0.36   2.0E-4   1.0
 86  102    1    0.0   5.0E-4   0.36   2.5E-4   1.0
103  119    1    0.0   6.0E-4   0.36   3.0E-4   1.0
120  136    1    0.0   7.0E-4   0.36   3.5E-4   1.0
137  153    1    0.0   8.0E-4   0.36   4.0E-4   1.0
  4
  1    8    1    2    9      1    3   37   35    2   20   36   18   19
  9   16    1    2    9     35   37   71   69   36   54   70   52   53
 17   24    1    2    9     69   71  105  103   70   88  104   86   87
 25   32    1    2    9    103  105  139  137  104  122  138  120  121
```

11.16 Analyze the viscous flow inside a square cavity (see **Example 11.6.3**) using a 16 × 20 mesh of linear quadrilateral elements. Present the results in graphical form for v_x (0.5, y) vs. y, $P(x, y) \times 10^{-2}$ vs. x, and $-\sigma_{xy}$ (x, y) vs. x at the bottom of the cavity (i.e., Gauss point closest to $y = 0$). Use the following element lengths along x and y directions: 16 subdivisions of length 0.0625 along the x axis; and 12 subdivisions of length 0.0625 and 8 subdivisions of length 0.03125 in the y direction.

11.17 Repeat **Problem 11.16** with nine-node quadratic quadrilateral elements and compare the results in graphical form for v_x (0.5, y) vs. y, $P(x, y) \times 10^{-2}$ vs. x, and $-\sigma_{xy}$ (x, y) vs. x at the bottom of the cavity (i.e., Gauss point closest to $y = 0$) obtained with the two meshes.

11.18 Analyze the problem of a viscous incompressible fluid being squeezed through a 4:1 contraction, as shown in Fig. P11.18. Take $L_1 = 10$, $L = 6$, $R_1 = 4$, and $R_2 = 1$, and linear quadrilateral elements. The inlet velocity v_x (y) is the fully developed solution of the flow between parallel plates. Plot the velocity v_x (x, y) and pressure along the horizontal centerline.

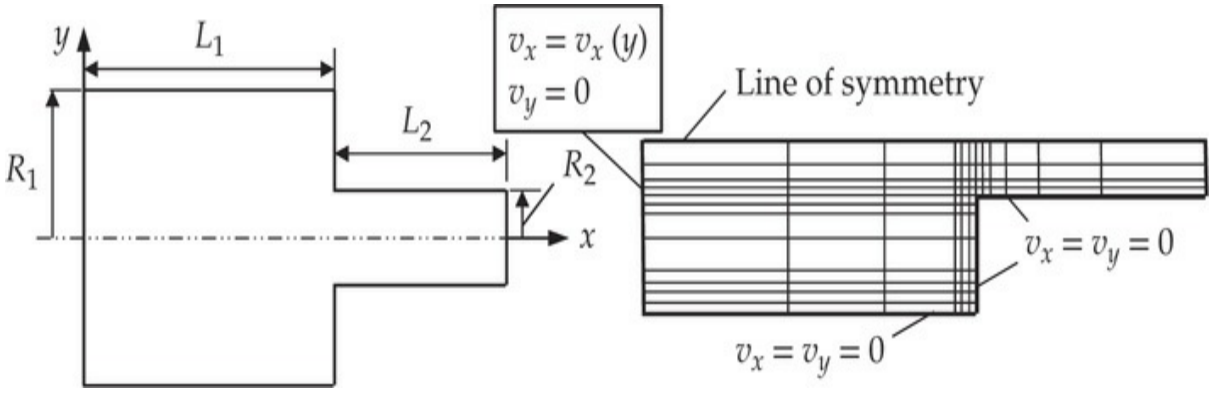

Fig. P11.18

11.19 Analyze the problem of a viscous fluid squeezed between parallel plates (see **Example 11.6.4**) for its transient solution using a uniform 6 × 4Q9 mesh, zero initial conditions, $c_1 = 1.0$, $\Delta t = 0.1$, $\alpha = 0.5$, $\gamma = 10^8$, and $\varepsilon = 10^{-3}$.

11.20 Analyze the cavity problem in **Problem 11.17** (mesh 8 × 10Q9) for its transient solution. Use $\rho = 1.0$, zero initial conditions, penalty parameter $\gamma = 10^8$, time parameter $\alpha = 0.5$, and a time step of $\Delta t = 0.005$ to capture the evolution of v_x (0.5, y, t) with time.

References for Additional Reading

1. J. N. Reddy, *An Introduction to Continuum Mechanics*, 2nd ed., Cambridge University Press, New York, NY, 2013.
2. J. N. Reddy, *Principles of Continuum Mechanics*, 2nd ed., Cambridge University Press, New York, NY, 2018.
3. J. N. Reddy, *An Introduction to Nonlinear Finite Element Analysis*, 2nd ed., Oxford University Press, Oxford, UK, 2015.
4. J. N. Reddy and D. K. Gartling, *The Finite Element Method in Heat Transfer and Fluid Dynamics*, 3rd ed., CRC Press, Boca Raton, FL, 2001.
5. J. N. Reddy, *Energy Principles and Variational Methods in Applied Mechanics*, 3rd ed., John Wiley & Sons, New York, NY, 2017.
6. A. Nadai, *Theory of Flow and Fracture of Solids*, Vol. II, McGraw-Hill, New York, NY, 1963.
7. H. Schlichting, *Boundary Layer Theory* (translated by J. Kestin), 7th ed., McGraw-Hill, New York, NY, 1979.

8. P. M. Gresho and R. L. Sani, *Incompressible Flow and the Finite Element Method*, John Wiley & Sons, Chichester, UK, 1998.
9. R. B. Bird, W. E. Stewart, and E. N. Lightfoot, *Transport Phenomena*, John Wiley & Sons, New York, NY, 1960.
10. J. T., Oden, “RIP methods for Stokesian flows,” in R. H. Gallagher, O.C. Zienkiewicz, J. T. Oden, and D. Norrie (eds.), *Finite Element Method in Flow Problems*, Vol. IV, John Wiley & Sons, London, UK, 1982.

12 Plane Elasticity

The most beautiful thing we can experience is the mysterious. It is the source of all true art and science.

— Albert Einstein

12.1 Introduction

Elasticity is a subject of solid mechanics that deals with stress and deformation of solid continua. Linearized elasticity is concerned with small deformations (i.e., strains and displacements are very small compared to unity) in linear elastic solids (i.e., obey Hooke's law). A class of problems in elasticity, due to geometry, boundary conditions, and external applied loads, have their solutions (i.e., displacements and stresses) not dependent on one of the coordinates. Such problems are called plane elasticity problems. The plane elasticity problems considered here are grouped into *plane strain* and *plane stress* problems. Both classes of problems are described by a pair of *coupled* partial differential equations expressed in terms of the two components of the displacement vector. The governing equations of plane strain problems differ from those of the plane stress problems only in the coefficients of the differential equations.

The description of motion of an elastic body, occupying the volume Ω with closed boundary Γ [see Fig. 12.1.1(a) for the notation], is based on the material description, also known as the Lagrangian description. The equations of motion of three-dimensional linearized elasticity (i.e., strains are assumed to be infinitesimal and the material obeys Hooke's law) are

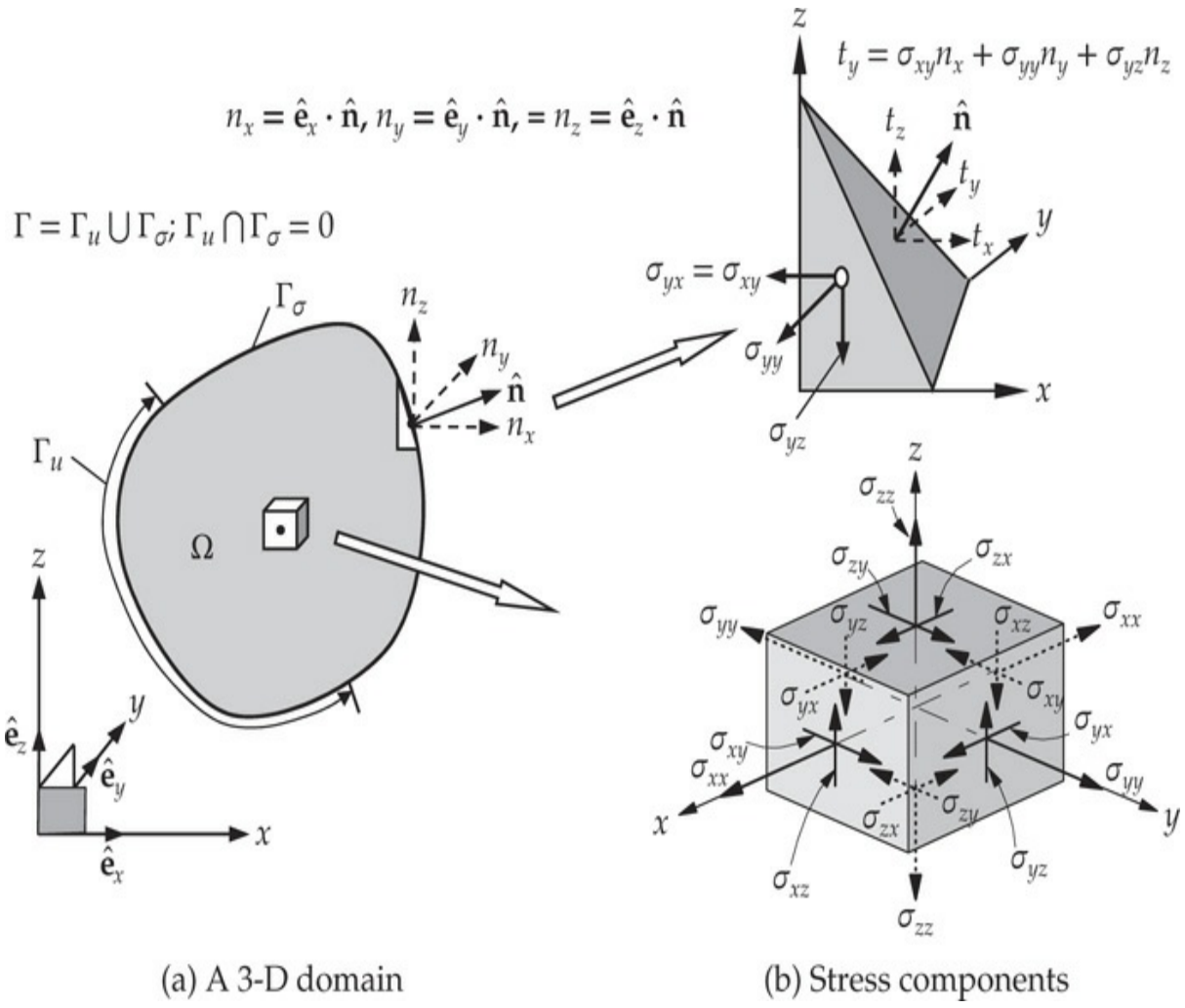

Fig. 12.1.1 Stress and strain components at a point enclosed in a point cube whose faces are perpendicular to the axes (x, y, z).

$$\begin{aligned}
\frac{\partial \sigma_{xx}}{\partial x} + \frac{\partial \sigma_{yx}}{\partial y} + \frac{\partial \sigma_{zx}}{\partial z} + f_x &= \rho \frac{\partial^2 u_x}{\partial t^2} \\
\frac{\partial \sigma_{xy}}{\partial x} + \frac{\partial \sigma_{yy}}{\partial y} + \frac{\partial \sigma_{zy}}{\partial z} + f_y &= \rho \frac{\partial^2 u_y}{\partial t^2} \quad \text{in } \Omega \\
\frac{\partial \sigma_{xz}}{\partial x} + \frac{\partial \sigma_{yz}}{\partial y} + \frac{\partial \sigma_{zz}}{\partial z} + f_z &= \rho \frac{\partial^2 u_z}{\partial t^2}
\end{aligned} \tag{12.1.1}$$

where (u_x, u_y, u_z) are components of the displacement vector **u** along the x, y, and z (material) coordinates, respectively, σ_{ξ_η} are the components of the stress tensor σ acting on a plane perpendicular to the ξ axis and in the direction of the η, axis [see Fig. 12.1.1(b) for the notation], (f_x, f_y, f_z) are the components of the body force vector **f**, measured per unit volume, and

ρ is the mass density. The equations of motion are derived using the principle of balance of linear momentum (or Newton's second law of motion; see Reddy [1]). The principle of balance of angular momentum, in the absence of body moments or couples, leads to the symmetry of the stress tensor:

$$\sigma_{xy} = \sigma_{yx}, \quad \sigma_{xz} = \sigma_{zx}, \quad \sigma_{yz} = \sigma_{zy} \tag{12.1.2}$$

Thus, there are only six independent stress components in 3-D elasticity. The three equations of motion have nine unknowns, namely, three displacements and six stresses. To have three unknowns in three equations, we express the six stresses in terms of three displacements by using the stress–strain relations and strain–displacement relations. Hooke's law for an orthotropic medium, whose material coordinates coincide with the (x, y, z) coordinates, can be expressed as

$$\begin{Bmatrix} \sigma_{xx} \\ \sigma_{yy} \\ \sigma_{zz} \\ \sigma_{yz} \\ \sigma_{xz} \\ \sigma_{xy} \end{Bmatrix} = \begin{bmatrix} C_{11} & C_{12} & C_{13} & 0 & 0 & 0 \\ C_{21} & C_{22} & C_{23} & 0 & 0 & 0 \\ C_{31} & C_{32} & C_{33} & 0 & 0 & 0 \\ 0 & 0 & 0 & C_{44} & 0 & 0 \\ 0 & 0 & 0 & 0 & C_{55} & 0 \\ 0 & 0 & 0 & 0 & 0 & C_{66} \end{bmatrix} \begin{Bmatrix} \varepsilon_{xx} \\ \varepsilon_{yy} \\ \varepsilon_{zz} \\ 2\varepsilon_{yz} \\ 2\varepsilon_{xz} \\ 2\varepsilon_{xy} \end{Bmatrix} \tag{12.1.3}$$

In Eq. (12.1.3), $C_{ij} = C_{ji}$ are the material parameters, called material stiffness coefficients, of a linear elastic medium. The stiffness coefficients C_{ij} can be expressed in terms of the nine engineering material constants (E_1, E_2, E_3, G_{23}, G_{13}, G_{12}, ν_{23}, ν_{13}, and ν_{12}) as follows:

$$\begin{aligned}
C_{11} &= \frac{1-\nu_{23}\nu_{32}}{E_2E_3\Delta}, \quad C_{12} = \frac{\nu_{21}+\nu_{31}\nu_{23}}{E_2E_3\Delta} = \frac{\nu_{12}+\nu_{32}\nu_{13}}{E_1E_3\Delta} \\
C_{13} &= \frac{\nu_{31}+\nu_{21}\nu_{32}}{E_2E_3\Delta} = \frac{\nu_{13}+\nu_{12}\nu_{23}}{E_1E_2\Delta} \\
C_{22} &= \frac{1-\nu_{13}\nu_{31}}{E_1E_3\Delta}, \quad C_{23} = \frac{\nu_{32}+\nu_{12}\nu_{31}}{E_1E_3\Delta} = \frac{\nu_{23}+\nu_{21}\nu_{13}}{E_1E_2\Delta} \\
C_{33} &= \frac{1-\nu_{12}\nu_{21}}{E_1E_2\Delta}, \quad C_{44} = G_{23} \quad C_{55} = G_{13} \quad C_{66} = G_{12} \\
\Delta &= \frac{1-\nu_{12}\nu_{21}-\nu_{23}\nu_{32}-\nu_{31}\nu_{13}-2\nu_{21}\nu_{32}\nu_{13}}{E_1E_2E_3}
\end{aligned} \tag{12.1.4}$$

where E_i are Young's moduli, G_{ij} are the shear moduli, and ν_{ij} are the Poisson ratios.

The strain–displacement relations of linear elasticity are

$$\varepsilon_{xx} = \frac{\partial u_x}{\partial x}, \quad \varepsilon_{yy} = \frac{\partial u_y}{\partial y}, \quad \varepsilon_{zz} = \frac{\partial u_z}{\partial z},$$
$$2\varepsilon_{yz} = \frac{\partial u_y}{\partial z} + \frac{\partial u_z}{\partial y}, \quad 2\varepsilon_{xz} = \frac{\partial u_x}{\partial z} + \frac{\partial u_z}{\partial x}, \quad 2\varepsilon_{xy} = \frac{\partial u_x}{\partial y} + \frac{\partial u_y}{\partial x} \tag{12.1.5}$$

where ε_{xx}, ε_{yy}, and so on are the strain components in the rectangular Cartesian system [the same notation as for the stresses shown in Fig. 12.1.1(b)]. The finite element model of 3-D elasticity equations [i.e., Eq. (12.1.1) expressed in terms of the displacements] will be considered in Chapter 13.

The primary objective of this chapter is three-fold: (1) present a review of the governing equations of linearized 2-D elasticity in terms of the displacement components, (2) develop the weak forms of the governing equations, and (3) construct displacement finite element models. As discussed next, there are two types of plane elasticity problems. In both cases, the forces applied, boundary conditions imposed, and material properties are *not* functions of the (thickness) coordinate z. The problems in which the domains are so thin that the stresses σ_{xz}, σ_{yz}, and σ_{zz} are negligible are termed *plane stress* problems. The second type of plane elasticity problem is one in which the body is very long in the z direction so that displacements are assumed not to depend on the z coordinate. In this case we use a slice of the body to analyze the problem. Problems of this nature are called *plane strain* problems.

The governing equations of plane elasticity in terms of the stresses are obtained by setting the components associated with the z direction to zero. The weak-form development and construction of displacement finite element models follow the same procedure as in the case of viscous incompressible fluids discussed in Chapter 11. In fact, the governing equations of the two fields are quite similar, as we shall see shortly. We utilize suitable approximation functions from the library of two-dimensional finite element interpolation functions.

12.2 Governing Equations

12.2.1 Plane Strain

Plane strain problems are the mathematical models of the actual body whose geometry, boundary conditions, and loads do not vary along the length coordinate z. Consequently, the displacement field is only a function of the coordinates (x, y). Then it suffices to use a slice of unit thickness, cut from the body (see Fig. 12.2.1), as the domain. Other examples of plane strain include earthdam and long cylinder under internal and/or external pressure.

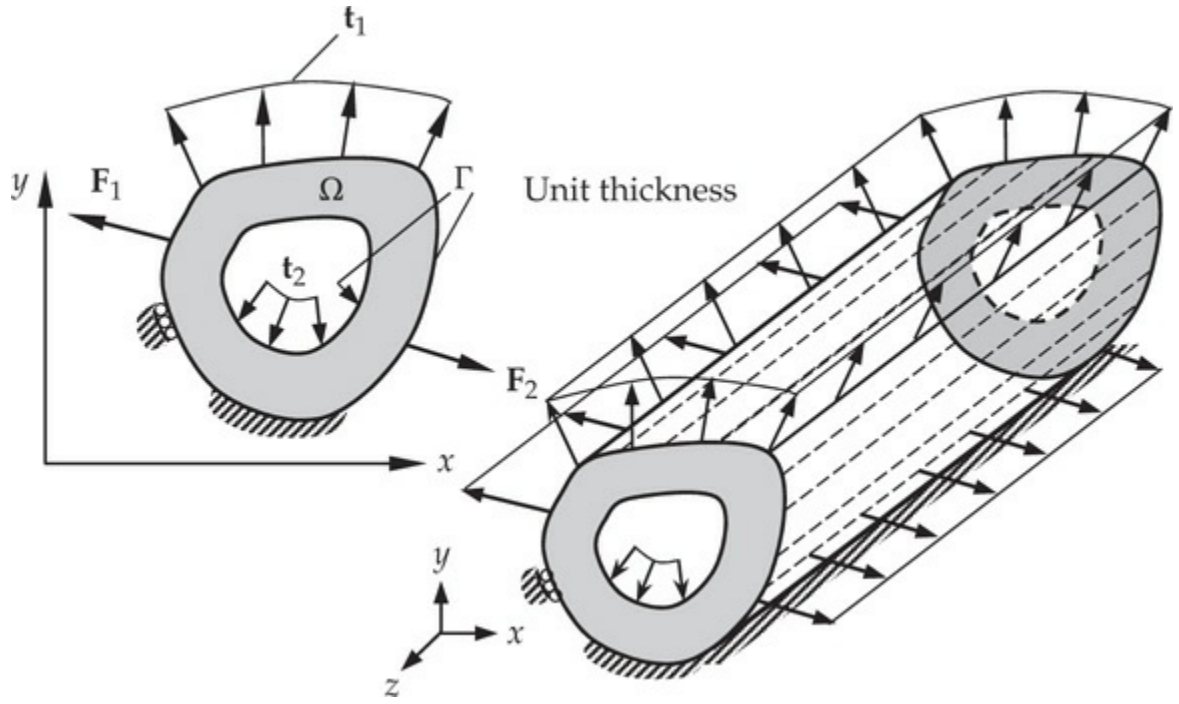

Fig. 12.2.1 A hollow cylindrical member with applied loads in the plane of the cross section.

Thus, the displacement field of a plane strain problem is of the form

$$u_x = u_x(x, y), \quad u_y = u_y(x, y), \quad u_z = 0 \tag{12.2.1}$$

The displacement field in Eq. (12.2.1) results in the following strain field:

$$\varepsilon_{xz} = \varepsilon_{yz} = \varepsilon_{zz} = 0$$
$$\varepsilon_{xx} = \frac{\partial u_x}{\partial x}, \quad 2\varepsilon_{xy} = \frac{\partial u_x}{\partial y} + \frac{\partial u_y}{\partial x}, \quad \varepsilon_{yy} = \frac{\partial u_y}{\partial y} \tag{12.2.2}$$

Clearly, the body is in a state of plane strain. For an orthotropic material, with principal material axes (x_1, x_2, x_3) coinciding with the (x, y, z)

coordinates, the stress components are given by

$$\sigma_{xz} = \sigma_{yz} = 0, \quad \sigma_{zz} = E_3 \left(\frac{\nu_{13}}{E_1} \sigma_{xx} + \frac{\nu_{23}}{E_2} \sigma_{yy} \right) \tag{12.2.3}$$

$$\begin{Bmatrix} \sigma_{xx} \\ \sigma_{yy} \\ \sigma_{xy} \end{Bmatrix} = \begin{bmatrix} \bar{c}_{11} & \bar{c}_{12} & 0 \\ \bar{c}_{12} & \bar{c}_{22} & 0 \\ 0 & 0 & \bar{c}_{66} \end{bmatrix} \begin{Bmatrix} \varepsilon_{xx} \\ \varepsilon_{yy} \\ 2\varepsilon_{xy} \end{Bmatrix} \tag{12.2.4a}$$

where $\bar{c}_{ij}$ are the elastic stiffness coefficients ($E_3 = E_2$ and $\nu_{23} \approx \nu_{12} = \nu_{13}$)

$$\begin{aligned} \bar{c}_{11} &= \frac{(1 - \nu_{23}\nu_{32})E_1}{\Delta}, \qquad \bar{c}_{22} = \frac{(1 - \nu_{13}\nu_{31})E_2}{\Delta} \\ \bar{c}_{12} &= \frac{(\nu_{12} + \nu_{13}\nu_{32})E_2}{\Delta}, \quad \bar{c}_{66} = G_{12} \\ \Delta &= 1 - \nu_{23}\nu_{32} - \nu_{13}\nu_{31} - \nu_{12}\nu_{21} - 2\nu_{12}\nu_{23}\nu_{31} \end{aligned} \tag{12.2.4b}$$

and E_1 and E_2 are principal (Young's) moduli in the x and y directions, respectively, G_{12} the shear modulus in the xy plane, and ν_{12} the Poisson ratio (i.e., the negative of the ratio of the transverse strain in the y direction to the strain in the x direction when stress is applied in the x direction). Poisson's ratio ν_{21} can be computed from the reciprocal relation

$$\nu_{21} = \frac{E_2}{E_1} \nu_{12} \quad \left(\nu_{ij} E_j = \nu_{ji} E_i, \quad \text{no sum on repeated indices} \right) \tag{12.2.5}$$

Additional engineering constants E_3, ν_{23}, and ν_{13} are required to compute σ_{zz}. For an isotropic material, we have $E_1 = E_2 = E_3 = E$, $\nu_{12} = \nu_{21} = \nu_{13} = \nu_{23} = \nu$, and $G_{12} = G = E/2(1 + \nu)$. Hence

$$\bar{c}_{11} = \bar{c}_{22} = \frac{(1 - \nu)E}{(1 + \nu)(1 - 2\nu)}, \quad \bar{c}_{12} = \nu/(1 - \nu)\bar{c}_{11}, \quad \bar{c}_{66} = G \tag{12.2.6}$$

The equations of motion in terms of the stress components reduce to the following two equations:

$$\rho \frac{\partial^2 u_x}{\partial t^2} - \frac{\partial \sigma_{xx}}{\partial x} - \frac{\partial \sigma_{xy}}{\partial y} - f_x = 0 \tag{12.2.7}$$

$$\rho \frac{\partial^2 u_y}{\partial t^2} - \frac{\partial \sigma_{xy}}{\partial x} - \frac{\partial \sigma_{yy}}{\partial y} - f_y = 0 \tag{12.2.8}$$

An example of a plane strain problem is provided by the long cylindrical member under external loads that are independent of z, as shown in Fig. 12.2.1. For cross sections sufficiently far from the ends, it is clear that the displacement u_z is zero and that u_x and u_y are independent of z, that is, a state of plane strain exists.

12.2.2 Plane Stress

A state of *plane stress* is defined as one in which the following stress field exists:

$$\begin{gathered} \sigma_{xz} = \sigma_{yz} = \sigma_{zz} = 0 \\ \sigma_{xx} = \sigma_{xx}(x, y), \quad \sigma_{xy} = \sigma_{xy}(x, y), \quad \sigma_{yy} = \sigma_{yy}(x, y) \end{gathered} \tag{12.2.9a}$$

An example of a plane stress problem is provided by a thin plate under external loads applied in the xy plane (or parallel to it) that are independent of z, as shown in Fig. 12.2.2. The top and bottom surfaces of the plate are assumed to be traction-free, and the specified boundary forces are in the xy plane so that $f_z = 0$ and $u_z = 0$.

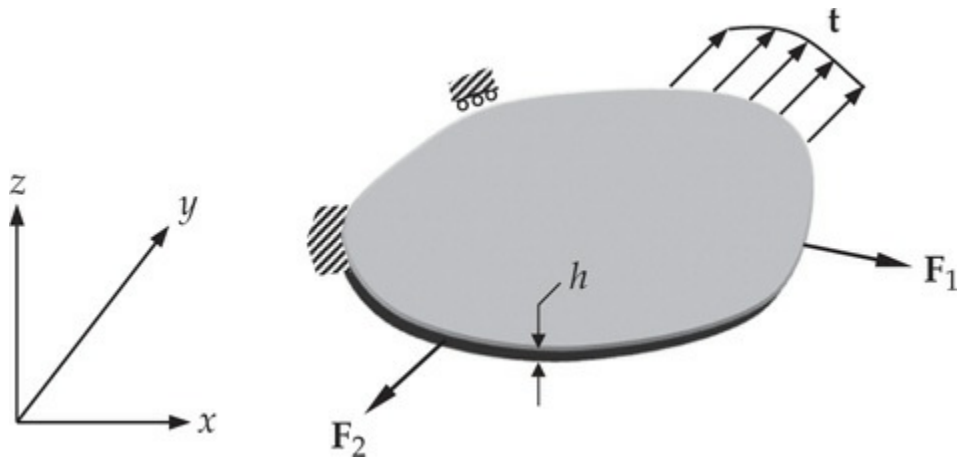

Fig. 12.2.2 A thin plate in a state of plane stress with applied loads in the plane of the plate.

The strain field associated with the stress field in Eq. (12.2.9a) is

$$\begin{Bmatrix} \varepsilon_{xx} \\ \varepsilon_{yy} \\ 2\varepsilon_{xy} \end{Bmatrix} = \begin{bmatrix} s_{11} & s_{12} & 0 \\ s_{12} & s_{22} & 0 \\ 0 & 0 & s_{66} \end{bmatrix} \begin{Bmatrix} \sigma_{xx} \\ \sigma_{yy} \\ \sigma_{xy} \end{Bmatrix} \tag{12.2.9b}$$

$$\varepsilon_{xz} = \varepsilon_{yz} = 0, \quad \varepsilon_{zz} = s_{13}\sigma_{xx} + s_{23}\sigma_{yy} \tag{12.2.9c}$$

where s_{ij} are the elastic compliances

$$\begin{aligned} s_{11} &= \frac{1}{E_1}, \quad s_{22} = \frac{1}{E_2}, \quad s_{33} = \frac{1}{E_3} \\ s_{12} &= -\nu_{21}s_{22} = -\nu_{12}s_{11}, \quad s_{66} = \frac{1}{G_{12}} \\ s_{13} &= -\nu_{31}s_{33} = -\nu_{13}s_{11}, \quad s_{23} = -\nu_{32}s_{33} = -\nu_{23}s_{22} \end{aligned} \tag{12.2.10}$$

The inverse of (12.2.9b) is given by

$$\begin{Bmatrix} \sigma_{xx} \\ \sigma_{yy} \\ \sigma_{xy} \end{Bmatrix} = \begin{bmatrix} Q_{11} & Q_{12} & 0 \\ Q_{12} & Q_{22} & 0 \\ 0 & 0 & Q_{66} \end{bmatrix} \begin{Bmatrix} \varepsilon_{xx} \\ \varepsilon_{yy} \\ 2\varepsilon_{xy} \end{Bmatrix} \tag{12.2.11}$$

where Q_{ij} are the plane stress-reduced elastic stiffness coefficients

$$\begin{aligned} Q_{11} &= \frac{E_1}{(1-\nu_{12}\nu_{21})}, \quad Q_{22} = \frac{E_2}{(1-\nu_{12}\nu_{21})} \\ Q_{12} &= \nu_{12}Q_{22} = \nu_{21}Q_{11}, \quad Q_{66} = G_{12} \end{aligned} \tag{12.2.12}$$

The equations of motion of a plane stress problem are the same as those listed in Eqs. (12.2.7) and (12.2.8). Note that the equations of motion of plane stress and plane strain will differ from each other only on account of the difference in the constitutive equations for the two cases.

12.2.3 Summary of Equations

The governing equations for the two types of plane elasticity problems discussed in the preceding pages are summarized below, both in expanded form and vector form.

Equations of Motion

$$\frac{\partial \sigma_{xx}}{\partial x} + \frac{\partial \sigma_{xy}}{\partial y} + f_x = \rho \frac{\partial^2 u_x}{\partial t^2}$$
$$\frac{\partial \sigma_{xy}}{\partial x} + \frac{\partial \sigma_{yy}}{\partial y} + f_y = \rho \frac{\partial^2 u_y}{\partial t^2} \qquad (12.2.13a)$$

or

$$\mathbf{D}^{\mathrm{T}}\boldsymbol{\sigma} + \mathbf{f} = \rho \ddot{\mathbf{u}} \qquad (12.2.13b)$$

where f_x and f_y denote the components of the body force vector (measured per unit volume) along the $x$and y-directions, respectively, ρ is the mass density of the material, and $\mathbf{D}^{\mathrm{T}}$ is the transpose of $\mathbf{D}$:

$$\mathbf{D} = \begin{bmatrix} \partial/\partial x & 0 \\ 0 & \partial/\partial y \\ \partial/\partial y & \partial/\partial x \end{bmatrix}, \quad \boldsymbol{\sigma} = \begin{Bmatrix} \sigma_{xx} \\ \sigma_{yy} \\ \sigma_{xy} \end{Bmatrix}, \quad \mathbf{f} = \begin{Bmatrix} f_x \\ f_y \end{Bmatrix}, \quad \mathbf{u} = \begin{Bmatrix} u_x \\ u_y \end{Bmatrix} \qquad (12.2.13c)$$

Strain-Displacement Relations

$$\varepsilon_{xx} = \frac{\partial u_x}{\partial x}, \quad \varepsilon_{yy} = \frac{\partial u_y}{\partial y}, \quad 2\varepsilon_{xy} = \frac{\partial u_x}{\partial y} + \frac{\partial u_y}{\partial x} \qquad (12.2.14a)$$

or

$$\boldsymbol{\varepsilon} = \mathbf{D}\mathbf{u}, \quad \boldsymbol{\varepsilon} = \begin{Bmatrix} \varepsilon_{xx} \\ \varepsilon_{yy} \\ 2\varepsilon_{xy} \end{Bmatrix} \qquad (12.2.14b)$$

Stress-Strain (or *Constitutive*) *Relations*

$$\begin{Bmatrix} \sigma_{xx} \\ \sigma_{yy} \\ \sigma_{xy} \end{Bmatrix} = \begin{bmatrix} c_{11} & c_{12} & 0 \\ c_{12} & c_{22} & 0 \\ 0 & 0 & c_{66} \end{bmatrix} \begin{Bmatrix} \varepsilon_{xx} \\ \varepsilon_{yy} \\ 2\varepsilon_{xy} \end{Bmatrix} \qquad (12.2.15a)$$

or

$$\boldsymbol{\sigma} = \mathbf{C}\boldsymbol{\varepsilon}, \quad \mathbf{C} = \begin{bmatrix} c_{11} & c_{12} & 0 \\ c_{12} & c_{22} & 0 \\ 0 & 0 & c_{66} \end{bmatrix} \qquad (12.2.15b)$$

where c_{ij} ($c_{ji} = c_{ij}$) are the elasticity (material) constants for an orthotropic medium with the material principal directions (x_1, x_2, x_3) coinciding with the coordinate axes (x, y, z) used to describe the problem. The c_{ij} can be expressed in terms of the engineering constants (E_1, E_2, ν_{12}, G_{12}) for an orthotropic material by Eq. (12.2.4b) for plane strain ($c_{ij} = \bar{c}_{ij}$) and by Eq. (12.2.12) for plane stress problems ($c_{ij} = Q_{ij}$).

Boundary Conditions

The natural boundary conditions are

$$\left.\begin{aligned} t_x &\equiv \sigma_{xx} n_x + \sigma_{xy} n_y = \hat{t}_x \\ t_y &\equiv \sigma_{xy} n_x + \sigma_{yy} n_y = \hat{t}_y \end{aligned}\right\} \quad \text{on } \Gamma_\sigma \tag{12.2.16a}$$

or

$$\mathbf{t} \equiv \boldsymbol{\sigma}\mathbf{N} = \hat{\mathbf{t}} \ \text{ on } \Gamma_\sigma, \quad \mathbf{N} = \left\{ \begin{array}{c} n_x \\ n_y \end{array} \right\}, \quad \boldsymbol{\sigma} = \left[\begin{array}{cc} \sigma_{xx} & \sigma_{xy} \\ \sigma_{xy} & \sigma_{yy} \end{array} \right] \tag{12.2.16b}$$

The essential (or geometric) boundary conditions are

$$u_x = \hat{u}_x, \quad u_y = \hat{u}_y \quad \text{or} \quad \mathbf{u} = \hat{\mathbf{u}} \ \text{ on } \Gamma_u \tag{12.2.17}$$

where (n_x, n_y) denote the components (called the direction cosines) of the unit normal vector $\hat{\mathbf{n}}$ on the boundary Γ; Γ_σ and Γu are (disjoint) portions of the boundary; $\hat{t}_x$ and $\hat{t}_y$ denote the components of the specified traction vector, and $\hat{u}_x$ and $\hat{u}_y$ are the components of specified displacement vector. Only one element of each pair, (u_x, t_x) and (u_y, t_y), may be specified at a boundary point.

Equations (12.2.13a) and (12.2.13b) can be expressed in terms of only the displacements u_x and u_y by substituting Eqs. (12.2.14a) and (12.2.14b) into Eqs. (12.2.15a) and (12.2.15b), and the result into Eqs. (12.2.13a) and (12.2.13b):

$$\begin{aligned} &-\frac{\partial}{\partial x}\left(c_{11}\frac{\partial u_x}{\partial x} + c_{12}\frac{\partial u_y}{\partial y}\right) - \frac{\partial}{\partial y}\left[c_{66}\left(\frac{\partial u_x}{\partial y} + \frac{\partial u_y}{\partial x}\right)\right] = f_x - \rho\frac{\partial^2 u_x}{\partial t^2} \\ &-\frac{\partial}{\partial x}\left[c_{66}\left(\frac{\partial u_x}{\partial y} + \frac{\partial u_y}{\partial x}\right)\right] - \frac{\partial}{\partial y}\left(c_{12}\frac{\partial u_x}{\partial x} + c_{22}\frac{\partial u_y}{\partial y}\right) = f_y - \rho\frac{\partial^2 u_y}{\partial t^2} \end{aligned} \tag{12.2.18a}$$

or

$$-\mathbf{D}^{\mathrm{T}}\mathbf{C}\mathbf{D}\mathbf{u} = \mathbf{f} - \rho\ddot{\mathbf{u}} \tag{12.2.18b}$$

The boundary stress vector components can also be expressed in terms of the displacements:

$$t_x = \left(c_{11}\frac{\partial u_x}{\partial x} + c_{12}\frac{\partial u_y}{\partial y}\right)n_x + c_{66}\left(\frac{\partial u_x}{\partial y} + \frac{\partial u_y}{\partial x}\right)n_y \tag{12.2.19a}$$

$$t_y = c_{66}\left(\frac{\partial u_x}{\partial y} + \frac{\partial u_y}{\partial x}\right)n_x + \left(c_{12}\frac{\partial u_x}{\partial x} + c_{22}\frac{\partial u_y}{\partial y}\right)n_y \tag{12.2.19b}$$

or

$$\mathbf{t} = \hat{\mathbf{n}} \cdot \mathbf{C}\,\mathbf{D}\mathbf{u}, \quad \hat{\mathbf{n}} = \begin{bmatrix} n_x & 0 & n_y \\ 0 & n_y & n_x \end{bmatrix} \tag{12.2.19c}$$

12.3 Virtual Work and Weak Formulations

12.3.1 Preliminary Comments

Here, we study two different ways of constructing the weak forms of the plane elasticity equations (12.2.18a) and (12.2.18b). The first one uses the principle of virtual displacements (or the principle of minimum total potential energy), expressed in terms of matrices relating displacements to strains, strains to stresses, and the equations of motion. This approach is used in most finite element textbooks on solid mechanics and structural mechanics. The second approach follows a procedure consistent with the previous chapters and employs the weak formulation of Eqs. (12.2.18a) and (12.2.18b) to construct the finite element model. Of course, both methods give, mathematically, the *same* finite element model, but differ in their algebraic forms. We first discretize the domain Ω into a set of finite elements, $\Omega = \cup_{e=1}^{N}\Omega_e$. Over a typical element Ω_e, we develop the virtual work and weak-form statements.

12.3.2 Principle of Virtual Displacements in Vector Form

Here, we use (the time-dependent version of) the principle of virtual

displacements (see Section 2.3.6 and Reddy [2]) applied to a plane elastic finite element Ω_e with volume $V_e = \Omega_e \times (-h_e/2, h_e/2)$ (see Fig. 12.3.1)

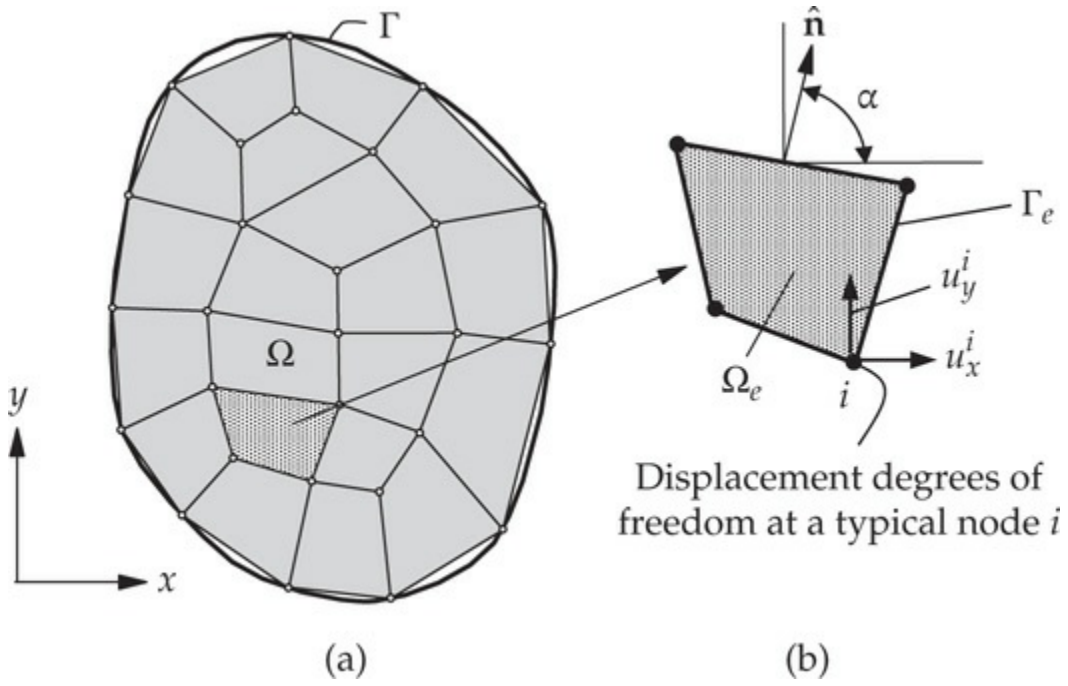

Fig. 12.3.1 (a) Finite element discretization of a plane elastic domain and (b) a typical finite element.

$$0 = \int_{V_e} (\sigma_{ij}\delta\varepsilon_{ij} + \rho\ddot{u}_i\delta u_i)dV - \int_{V_e} f_i\delta u_i\, dV - \oint_{S_e} \hat{t}_i\delta u_i\, dS \tag{12.3.1}$$

where $S_e = \Gamma_e \times (-h_e/2, h_e/2)$ is the surface of the volume element V_e; and h_e is the thickness of the finite element Ω_e; δ denotes the variational operator (see Reddy [2]); σ_{ij} and ε_{ij} are the components of stress and strain tensors, respectively and f_i and $\hat{t}_i$ are the components of the body force and boundary stress vectors, respectively. The correspondence between the (x, y) components and (x_1, x_2) components of the stress and strain tensors is given by

$$\begin{aligned} &\sigma_{11} = \sigma_{xx},\ \ \sigma_{12} = \sigma_{xy},\ \ \sigma_{22} = \sigma_{yy},\ \ \varepsilon_{11} = \varepsilon_{xx},\ \ \varepsilon_{12} = \varepsilon_{xy},\ \ \varepsilon_{22} = \varepsilon_{yy} \\ &u_1 = u_x,\ \ u_2 = u_y,\ \ f_1 = f_x,\ \ f_2 = f_y,\ \ t_1 = t_x,\ \ t_2 = t_y \end{aligned} \tag{12.3.2}$$

The first term in Eq. (12.3.1) corresponds to the virtual strain energy stored in the body, the second term corresponds to the kinetic energy stored in the body, the third term represents the virtual work done by the body forces, and the fourth term represents the virtual work done by the

surface tractions. Consistent with the assumptions of plane elasticity, we assume that all quantities in (12.3.1) are independent of the thickness coordinate, z. Hence, we obtain

$$0 = \int_{\Omega_e} h_e \left[\sigma_{xx}\delta\varepsilon_{xx} + \sigma_{yy}\delta\varepsilon_{yy} + 2\sigma_{xy}\delta\varepsilon_{xy} + \rho\left(\ddot{u}_x\delta u_x + \ddot{u}_y\delta u_y\right)\right] dxdy$$
$$- \int_{\Omega_e} h_e \left(f_x\delta u_x + f_y\delta u_y\right) dxdy - \oint_{\Gamma e} h_e \left(\hat{t}_x\delta u_x + \hat{t}_y\delta u_y\right) dS \qquad (12.3.3)$$

wherein, now, f_x and f_y are body forces per unit area and t_x and t_y are boundary forces per unit length. When the stresses are expressed in terms of strains through Eq. (12.2.15b) and strains in terms of displacements by Eq. (12.2.14b), Eq. (12.3.3) takes the form [note that $\delta\varepsilon = \mathbf{D}\delta\mathbf{u}$ and $(\mathbf{AB})^{\mathrm{T}} = \mathbf{B}^{\mathrm{T}}\,\mathbf{A}^{\mathrm{T}}$]

$$0 = \int_{\Omega_e} h_e \left[(\mathbf{D}\delta\mathbf{u})^{\mathrm{T}}\,\mathbf{C}\,(\mathbf{D}\mathbf{u}) + \rho(\delta\mathbf{u})^{\mathrm{T}}\ddot{\mathbf{u}}\right] dxdy$$
$$- \int_{\Omega_e} (\delta\mathbf{u})^{\mathrm{T}} h_e\,\mathbf{f}\,dxdy - \oint_{\Gamma_e} h_e\,(\delta\mathbf{u})^{\mathrm{T}}\mathbf{t}\,dS \qquad (12.3.4)$$

12.3.3 Weak-Form Formulation

Here we present an alternative procedure to the virtual work statement in Eq. (12.3.4), namely, weak formulation of the plane elasticity equations (12.2.13a) and (12.2.13b), wherein σ_{xx}, σ_{yy} and σ_{xy} are known in terms of the displacements u_x and u_y as where

$$\sigma_{xx} = c_{11}\frac{\partial u_x}{\partial x} + c_{12}\frac{\partial u_y}{\partial y}, \quad \sigma_{xy} = c_{66}\left(\frac{\partial u_x}{\partial y} + \frac{\partial u_y}{\partial x}\right), \quad \sigma_{yy} = c_{12}\frac{\partial u_x}{\partial x} + c_{22}\frac{\partial u_y}{\partial y} \qquad (12.3.5)$$

The weak-form approach, which has been used throughout the book thus far, does not require knowledge of the principles of virtual displacements or the total minimum potential energy (which are concepts restricted to solid and structural mechanics fields) but only needs the governing differential equations and their physical meaning. We use the three-step procedure for each of the two differential equations: multiply the first equation with a weight function w_1 and the second equation with weight function w_2 and integrate by parts to trade the differentiation equally

between the weight functions and the dependent variables (u_x, u_y) in each case. The weight functions w_1 and w_2 have the meaning of first variations of u_x and u_y, respectively: $w_1 \sim \delta u_x$ and $w_2 \sim \delta u_y$. We obtain

$$0 = \int_{\Omega_e} h_e \left(\frac{\partial w_1}{\partial x}\sigma_{xx} + \frac{\partial w_1}{\partial y}\sigma_{xy} - w_1 f_x + \rho w_1 \ddot{u}_x \right) dxdy - \oint_{\Gamma_e} h_e w_1 \left(\sigma_{xx} n_x + \sigma_{xy} n_y \right) dS \tag{12.3.6}$$

$$0 = \int_{\Omega_e} h_e \left(\frac{\partial w_2}{\partial x}\sigma_{xy} + \frac{\partial w_2}{\partial y}\sigma_{yy} - w_2 f_y + \rho w_2 \ddot{u}_y \right) dxdy - \oint_{\Gamma_e} h_e w_2 \left(\sigma_{xy} n_x + \sigma_{yy} n_y \right) dS \tag{12.3.7}$$

The last step of the development is to identify the primary and secondary variables of the formulation and rewrite the boundary integrals in terms of the secondary variables. Examination of the boundary integrals in Eqs. (12.3.6) and (12.3.7) reveals that the expressions in the parentheses constitute the secondary variables. By comparing these expressions with those in Eq. (12.2.16a), it follows that the boundary tractions t_x and t_y are the secondary variables. Thus, the final weak forms are given by

$$0 = \int_{\Omega_e} h_e \left[\frac{\partial w_1}{\partial x}\left(c_{11}\frac{\partial u_x}{\partial x} + c_{12}\frac{\partial u_y}{\partial y} \right) + c_{66}\frac{\partial w_1}{\partial y}\left(\frac{\partial u_x}{\partial y} + \frac{\partial u_y}{\partial x} \right) + \rho w_1 \ddot{u}_x \right] dxdy$$
$$- \int_{\Omega_e} h_e w_1 f_x \, dxdy - \oint_{\Gamma_e} h_e w_1 t_x \, dS \tag{12.3.8a}$$

$$0 = \int_{\Omega_e} h_e \left[c_{66}\frac{\partial w_2}{\partial x}\left(\frac{\partial u_x}{\partial y} + \frac{\partial u_y}{\partial x} \right) + \frac{\partial w_2}{\partial y}\left(c_{12}\frac{\partial u_x}{\partial x} + c_{22}\frac{\partial u_y}{\partial y} \right) + \rho w_2 \ddot{u}_y \right] dxdy$$
$$- \int_{\Omega_e} h_e w_2 f_y \, dxdy - \oint_{\Gamma_e} h_e w_2 t_y \, dS \tag{12.3.8b}$$

12.4 Finite Element Model

12.4.1 General Comments

Here, we develop the finite element model of the plane elasticity equations using both the vector form in Eq. (12.3.4) as well as the expanded forms

(12.3.8a) and (12.3.8b) so that readers with different backgrounds can follow the development. An examination of the weak forms in Eqs. (12.3.8a) and (12.3.8b) reveals that (1) u_x and u_y are the primary variables, which must be carried as the primary nodal degrees of freedom; and (2) only the first derivatives of u_x and u_y with respect to x and y appear in the weak forms. Therefore, u_x and u_y must be approximated by at least linear Lagrange family of interpolation functions. The simplest elements that satisfy those requirements are the linear triangular and linear quadrilateral elements. Although u_x and u_y are independent of each other, they are the components of the displacement vector. Therefore, both components should be approximated using the same type and degree of interpolation.

Let u_x and u_y be approximated by the finite element interpolations (the element label e is omitted in the interest of brevity)

$$u_x \approx \sum_{j=1}^{n} u_x^j \psi_j(x,y), \qquad u_y \approx \sum_{j=1}^{n} u_y^j \psi_j(x,y) \tag{12.4.1}$$

At the moment, we will not restrict ψ_j to any specific element so that the finite element formulation to be developed is valid for any admissible element. For example, if a linear triangular element (n = 3) is used, we have two (u_x^i, u_y^i) (i = 1, 2, 3) degrees of freedom per node and a total of six nodal displacements per element [see Fig. 12.4.1(a)]. For a linear quadrilateral element (n = 4), there are a total of eight nodal displacements per element [see Fig. 12.4.1(b)]. Since the first derivatives of ψ_i for a triangular element are element-wise constant, all strains (ε_{xx}, ε_{yy}, ε_{xy}) computed for the linear triangular element are element-wise constant. Therefore, the linear triangular element for plane elasticity problems is known as the *constant-strain-triangular (CST) element*. For a quadrilateral element the first derivatives of ψ_i are not constant: $\partial\psi_i/\partial\xi$ is linear in η, and constant in ξ, and $\partial\psi_i/\partial\eta$ is linear in ξ and constant in η.

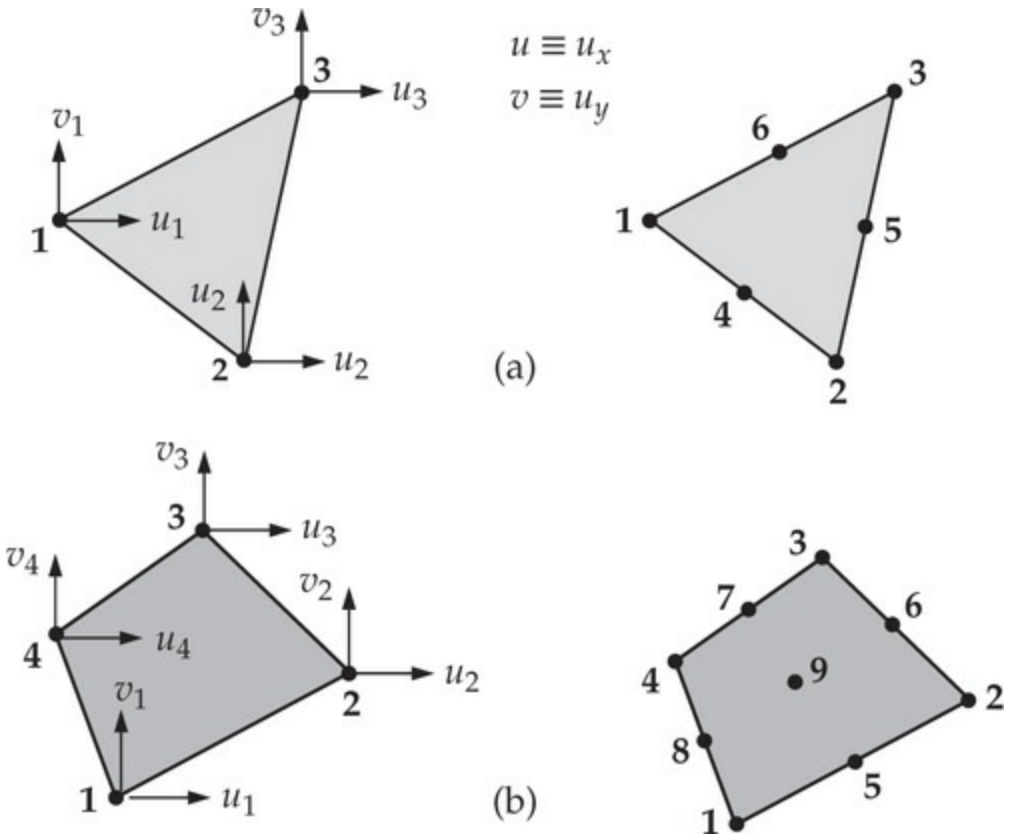

Fig. 12.4.1 Linear and quadratic (a) triangular and (b) quadrilateral elements for plane elasticity.

12.4.2 FE Model Using the Vector Form

The finite element approximation in Eq. (12.4.1) can be expressed in vector form as

$$\mathbf{u} = \begin{Bmatrix} u_x \\ u_y \end{Bmatrix} = \boldsymbol{\Psi}\boldsymbol{\Delta}, \quad \mathbf{w} = \delta\mathbf{u} = \begin{Bmatrix} w_1 = \delta u_x \\ w_2 = \delta u_y \end{Bmatrix} = \boldsymbol{\Psi}\,\delta\boldsymbol{\Delta} \tag{12.4.2a}$$

where $\boldsymbol{\Psi}$ is a $2 \times 2n$ matrix and Δ is a $2n \times 1$ vector of nodal degrees of freedom:

$$\boldsymbol{\Psi} = \begin{bmatrix} \psi_1 & 0 & \psi_2 & 0 & \dots & \psi_n & 0 \\ 0 & \psi_1 & 0 & \psi_2 & \dots & 0 & \psi_n \end{bmatrix}$$
$$\boldsymbol{\Delta} = \begin{Bmatrix} u_x^1 & u_y^1 & u_x^2 & u_y^2 & \dots & u_x^n & u_y^n \end{Bmatrix}^{\mathrm{T}} \tag{12.4.2b}$$

The strains are

$$\boldsymbol{\varepsilon} = \mathbf{D}\mathbf{u} = \mathbf{D}\boldsymbol{\Psi}\boldsymbol{\Delta} \equiv \mathbf{B}\boldsymbol{\Delta}, \quad \boldsymbol{\sigma} = \mathbf{C}\mathbf{B}\boldsymbol{\Delta} \tag{12.4.3}$$

where **D** is defined earlier in Eqs. (12.2.13c), and **B** is a $3 \times 2n$ matrix

$$\mathbf{B} = \mathbf{D}\boldsymbol{\Psi} = \begin{bmatrix} \frac{\partial \psi_1}{\partial x} & 0 & \frac{\partial \psi_2}{\partial x} & 0 & \cdots & \frac{\partial \psi_n}{\partial x} & 0 \\ 0 & \frac{\partial \psi_1}{\partial y} & 0 & \frac{\partial \psi_2}{\partial y} & \cdots & 0 & \frac{\partial \psi_n}{\partial y} \\ \frac{\partial \psi_1}{\partial y} & \frac{\partial \psi_1}{\partial x} & \frac{\partial \psi_2}{\partial y} & \frac{\partial \psi_2}{\partial x} & \cdots & \frac{\partial \psi_n}{\partial y} & \frac{\partial \psi_n}{\partial x} \end{bmatrix} \tag{12.4.4}$$

To obtain the vector form of the finite element model, we substitute the finite element expansion (12.4.2a) into the virtual work statement (12.3.4) and obtain

$$\begin{aligned} 0 &= \int_{\Omega_e} h_e (\delta\boldsymbol{\Delta}^e)^{\mathrm{T}} \left(\mathbf{B}^{\mathrm{T}}\mathbf{C}\mathbf{B}\boldsymbol{\Delta}^e + \rho\boldsymbol{\Psi}^{\mathrm{T}}\boldsymbol{\Psi}\ddot{\boldsymbol{\Delta}}^e \right) dxdy \\ &\quad - \int_{\Omega_e} h_e (\delta\boldsymbol{\Delta}^e)^{\mathrm{T}} \boldsymbol{\Psi}^{\mathrm{T}} \mathbf{f}\, dxdy - \oint_{\Gamma_e} h_e (\delta\boldsymbol{\Delta}^e)^{\mathrm{T}} \boldsymbol{\Psi}^{\mathrm{T}} \mathbf{t}\, dS \\ &= (\delta\boldsymbol{\Delta}^e)^{\mathrm{T}} \left(\mathbf{K}^e\boldsymbol{\Delta}^e + \mathbf{M}^e\ddot{\boldsymbol{\Delta}}^e - \mathbf{f}^e - \mathbf{Q}^e \right) \end{aligned} \tag{12.4.5}$$

Since the above equation holds for any *arbitrary* variations $\delta\Delta$, it follows (from the Fundamental Lemma of variational calculus) that the coefficient of $\delta\Delta$ in the expression (12.4.5) should be identically zero, giving the result

$$\mathbf{M}^e\ddot{\boldsymbol{\Delta}}^e + \mathbf{K}^e\boldsymbol{\Delta}^e = \mathbf{f}^e + \mathbf{Q}^e \tag{12.4.6}$$

where

$$\begin{aligned} \mathbf{K}^e &= \int_{\Omega_e} h_e\, \mathbf{B}^{\mathrm{T}}\mathbf{C}\mathbf{B}\, dxdy, \qquad \mathbf{M}^e = \int_{\Omega_e} \rho h_e\, \boldsymbol{\Psi}^{\mathrm{T}}\boldsymbol{\Psi}\, dxdy \\ \mathbf{f}^e &= \int_{\Omega_e} h_e\, \boldsymbol{\Psi}^{\mathrm{T}}\mathbf{f}\, dxdy, \qquad \mathbf{Q}^e = \oint_{\Gamma_e} h_e\, \boldsymbol{\Psi}^{\mathrm{T}}\, \mathbf{t}\, dS \end{aligned} \tag{12.4.7}$$

The element mass matrix $\mathbf{M}^e$ and stiffness matrix $\mathbf{K}^e$ are of order $2n \times 2n$ and the element body-force vector $\mathbf{f}^e$ and the vector of internal forces $\mathbf{Q}^e$ is of order $2n \times 1$, where n is the number of nodes in a Lagrange finite element (a triangle or quadrilateral).

12.4.3 FE Model Using Weak Form

Substituting Eq. (12.4.1) for u_x and u_y and $w_1 = \psi_i$ and $w_2 = \psi_i$ [to obtain the ith algebraic equation associated with each of the weak statements in Eqs. (12.3.8a) and (12.3.8b)], and writing the resulting algebraic equations in matrix form, we obtain

$$\begin{bmatrix} \mathbf{M}^{11} & 0 \\ 0 & \mathbf{M}^{22} \end{bmatrix} \begin{Bmatrix} \ddot{\mathbf{u}}_x \\ \ddot{\mathbf{u}}_y \end{Bmatrix} + \begin{bmatrix} \mathbf{K}^{11} & \mathbf{K}^{12} \\ (\mathbf{K}^{12})^{\mathrm{T}} & \mathbf{K}^{22} \end{bmatrix} \begin{Bmatrix} \mathbf{u}_x \\ \mathbf{u}_y \end{Bmatrix} = \begin{Bmatrix} \mathbf{F}^1 \\ \mathbf{F}^2 \end{Bmatrix} \tag{12.4.8a}$$

or

$$\mathbf{M}\ddot{\boldsymbol{\Delta}} + \mathbf{K}\boldsymbol{\Delta} = \mathbf{F} \tag{12.4.8b}$$

where

$$\begin{aligned}
M_{ij}^{11} &= M_{ij}^{22} = \int_{\Omega_e} \rho h \psi_i \psi_j \, dx dy \\
K_{ij}^{11} &= \int_{\Omega_e} h \left(c_{11} \frac{\partial \psi_i}{\partial x} \frac{\partial \psi_j}{\partial x} + c_{66} \frac{\partial \psi_i}{\partial y} \frac{\partial \psi_j}{\partial y} \right) dx dy \\
K_{ij}^{12} &= K_{ji}^{21} = \int_{\Omega_e} h \left(c_{12} \frac{\partial \psi_i}{\partial x} \frac{\partial \psi_j}{\partial y} + c_{66} \frac{\partial \psi_i}{\partial y} \frac{\partial \psi_j}{\partial x} \right) dx \, dy \\
K_{ij}^{22} &= \int_{\Omega_e} h \left(c_{66} \frac{\partial \psi_i}{\partial x} \frac{\partial \psi_j}{\partial x} + c_{22} \frac{\partial \psi_i}{\partial y} \frac{\partial \psi_j}{\partial y} \right) dx dy \\
F_i^1 &= \int_{\Omega_e} h \psi_i f_x \, dx \, dy + \oint_{\Gamma_e} h \psi_i t_x \, dS \equiv f_i^1 + Q_i^1 \\
F_i^2 &= \int_{\Omega_e} h \psi_i f_y \, dx dy + \oint_{\Gamma_e} h \psi_i t_y \, dS \equiv f_i^2 + Q_i^2
\end{aligned} \tag{12.4.9}$$

The body forces f_x and f_y are measured per unit volume and the surface tractions t_x and t_y are measured per unit area. The coefficient matrix $\mathbf{K}^{\alpha\beta}$ corresponds to the coefficient of βth variable in the αth equation. Equations (12.3.8a) and (12.3.8b) are labeled as the first and second equations, respectively, and u_x and u_y are numbered as variables 1 and 2, respectively. Then, for example, K^{12} is the coefficient of u_y (second variable) in the first finite element equation.

12.4.4 Eigenvalue and Transient Problems

For natural vibration study of plane elastic bodies, we seek a periodic solution of the form

$$\boldsymbol{\Delta} = \boldsymbol{\Delta}_0 e^{-i\omega t} \quad (i = \sqrt{-1}) \tag{12.4.10}$$

where ω is the frequency of natural vibration. Then Eq. (12.4.5) or (12.4.8b) reduces to an eigenvalue problem

$$(-\omega^2 \mathbf{M}^e + \mathbf{K}^e)\boldsymbol{\Delta}_0^e = \mathbf{Q}^e \tag{12.4.11}$$

For transient analysis, using the time-approximation schemes discussed in Section 7.4.5 (Newmark integration scheme), Eq. (12.4.5) or (12.4.8b) can be reduced to the following system of algebraic equations:

$$\hat{\mathbf{K}}^{s+1}\boldsymbol{\Delta}^{s+1} = \hat{\mathbf{F}}^{s,s+1} \tag{12.4.12a}$$

where

$$\begin{aligned} \hat{\mathbf{K}}^{s+1} &= \mathbf{K}^{s+1} + a_3 \mathbf{M}^{s+1} \\ \hat{\mathbf{F}}^{s,s+1} &= \mathbf{F}^{s+1} + \mathbf{M}^{s+1}\left(a_3 \boldsymbol{\Delta}^s + a_4 \dot{\boldsymbol{\Delta}}^s + a_5 \ddot{\boldsymbol{\Delta}}^s\right) \\ a_3 &= \frac{2}{\gamma(\Delta t)^2}, \quad a_4 = \Delta t\, a_3, \quad a_5 = \frac{1}{\gamma} - 1 \end{aligned} \tag{12.4.12b}$$

where **K**, **M** and **F** = **f** + **Q** are the vectors appearing in Eq. (12.4.9) and γ is the parameter in the (α, γ)-family of approximation [see Eqs. (7.4.33) and (7.4.34)]. For γ = 0 (centered difference scheme), the alternative formulation of Eq. (9.5.22) must be used. For additional details, the reader should consult Section 7.4.5.

12.4.5 Evaluation of Integrals

For the linear triangular (i.e., CST) element, the ψ_i^e and its derivatives are given by

$$\psi_i^e = \frac{1}{2A_e}(\alpha_i^e + \beta_i^e x + \gamma_i^e y), \quad \frac{\partial \psi_i^e}{\partial x} = \frac{\beta_i^e}{2A_e}, \quad \frac{\partial \psi_i^e}{\partial y} = \frac{\gamma_i^e}{2A_e} \tag{12.4.13}$$

Since the derivatives of ψ_i^e are constant, we have

$$\mathbf{B}^e = \frac{1}{2A_e}\begin{bmatrix} \beta_1^e & 0 & \beta_2^e & 0 & \cdots & \beta_n^e & 0 \\ 0 & \gamma_1^e & 0 & \gamma_2^e & \cdots & 0 & \gamma_n^e \\ \gamma_1^e & \beta_1^e & \gamma_2^e & \beta_2^e & \cdots & \gamma_n^e & \beta_n^e \end{bmatrix}_{(3\times 2n)} \tag{12.4.14}$$

where A_e is the area of the triangular element. Since $\mathbf{B}^e$ and $\mathbf{C}^e$ are independent of x and y, the element stiffness matrix in Eq. (12.4.9) for the CST element is given by

$$\mathbf{K}^e = h_e A_e (\mathbf{B}^e)^{\mathrm{T}} \mathbf{C}^e \mathbf{B}^e \quad (2n \times 2n) \tag{12.4.15a}$$

For the case in which the body force components f_x and f_y are element-wise constant (say, equal to f_{x0}^e and f_{y0}^e respectively), the load vector $\mathbf{F}^e$ has the form

$$\mathbf{f}^e = \int_{\Omega_e} h_e (\mathbf{\Psi}^e)^{\mathrm{T}} \mathbf{f}_0^e \, dxdy = \frac{A_e h_e}{3}\begin{Bmatrix} f_{x0}^e \\ f_{y0}^e \\ f_{x0}^e \\ f_{y0}^e \\ f_{x0}^e \\ f_{y0}^e \end{Bmatrix}_{(6\times 1)} \tag{12.4.15b}$$

For a general quadrilateral element, it is not easy to compute the coefficients of the stiffness matrix by hand. In such cases we use the numerical integration discussed in Section 10.3. However, for a linear rectangular element of sides a and b, the element coefficient matrices in Eq. (9.2.52) can be used to obtain the stiffness matrix. For example, the submatrices in Eq. (12.4.8a) for the linear element are given by

$$\mathbf{M}^{11} = \mathbf{M}^{22} = \frac{\rho hab}{36}\begin{bmatrix} 4 & 2 & 1 & 2 \\ 2 & 4 & 2 & 1 \\ 1 & 2 & 4 & 2 \\ 2 & 1 & 2 & 4 \end{bmatrix}$$

$$\mathbf{K}^{11} = hc_{11}\frac{b}{6a}\begin{bmatrix} 2 & -2 & -1 & 1 \\ -2 & 2 & 1 & -1 \\ -1 & 1 & 2 & -2 \\ 1 & -1 & -2 & 2 \end{bmatrix} + hc_{66}\frac{a}{6b}\begin{bmatrix} 2 & 1 & -1 & -2 \\ 1 & 2 & -2 & -1 \\ -1 & -2 & 2 & 1 \\ -2 & -1 & 1 & 2 \end{bmatrix} \tag{12.4.16a}$$

$$\mathbf{K}^{12} = \frac{h}{4}\left(c_{12}\begin{bmatrix} 1 & 1 & -1 & -1 \\ -1 & -1 & 1 & 1 \\ -1 & -1 & 1 & 1 \\ 1 & 1 & -1 & -1 \end{bmatrix} + c_{66}\begin{bmatrix} 1 & -1 & -1 & 1 \\ 1 & -1 & -1 & 1 \\ -1 & 1 & 1 & -1 \\ -1 & 1 & 1 & -1 \end{bmatrix}\right)$$

$$\mathbf{K}^{22} = hc_{66}\frac{b}{6a}\begin{bmatrix} 2 & -2 & -1 & 1 \\ -2 & 2 & 1 & -1 \\ -1 & 1 & 2 & -2 \\ 1 & -1 & -2 & 2 \end{bmatrix} + hc_{22}\frac{a}{6b}\begin{bmatrix} 2 & 1 & -1 & -2 \\ 1 & 2 & -2 & -1 \\ -1 & -2 & 2 & 1 \\ -2 & -1 & 1 & 2 \end{bmatrix}$$

For a linear quadrilateral element with constant body force components (f_{x0}, f_{y0}), the load vector is given by

$$\mathbf{f}^e = \frac{A_e h_e}{4}\begin{Bmatrix} f^e_{x0} \\ f^e_{y0} \\ f^e_{x0} \\ f^e_{y0} \\ \vdots \end{Bmatrix}_{(8\times 1)} \tag{12.4.16b}$$

The vector $\mathbf{Q}^e$ is computed only when a portion of the boundary Γ_e of an element Ω_e falls on the boundary Γ_σ of the domain Ω on which tractions are specified (i.e., known). Computation of $\mathbf{Q}^e$ involves the evaluation of line integrals (for any type of element), as explained in Section 9.2.7; also, see **Example 9.2.4**. For plane elasticity problems, the surface tractions t_x and t_y take the place of q_n in the single-variable problems. However, it should be noted that t_x and t_y are the horizontal and vertical components

(i.e., parallel to the coordinate lines x and y) of the traction vector **t**, which, in general, is oriented at an angle to the boundary line (or curve), which itself is oriented at an angle to the global coordinate axis x. In practice, it is convenient to express the surface traction **t** in the element coordinates. In that case, $\mathbf{Q}^e$ can be evaluated in the element coordinates and then transformed to the global coordinates for assembly. If $\mathbf{Q}^e$ denotes the element load vector referred to the element coordinates, then the corresponding load vector referred to the global coordinates is given by

$$\mathbf{F}^e = \mathbf{R}\mathbf{Q}^e \tag{12.4.17a}$$

where **R** is the transformation matrix

$$\mathbf{R}^e = \begin{bmatrix} \cos\alpha & \sin\alpha & 0 & 0 \\ -\sin\alpha & \cos\alpha & 0 & 0 \\ 0 & 0 & \cos\alpha & \sin\alpha \\ 0 & 0 & -\sin\alpha & \cos\alpha \\ & & & \ddots \end{bmatrix}_{2n\times 2n} \tag{12.4.17b}$$

and α is the angle between the global x-axis and the traction vector **t**.

Example 12.4.1

As a specific example, first consider the structure shown in Fig. 12.4.2(a). Side 2–3 of element 7 is subjected to linearly varying normal force:

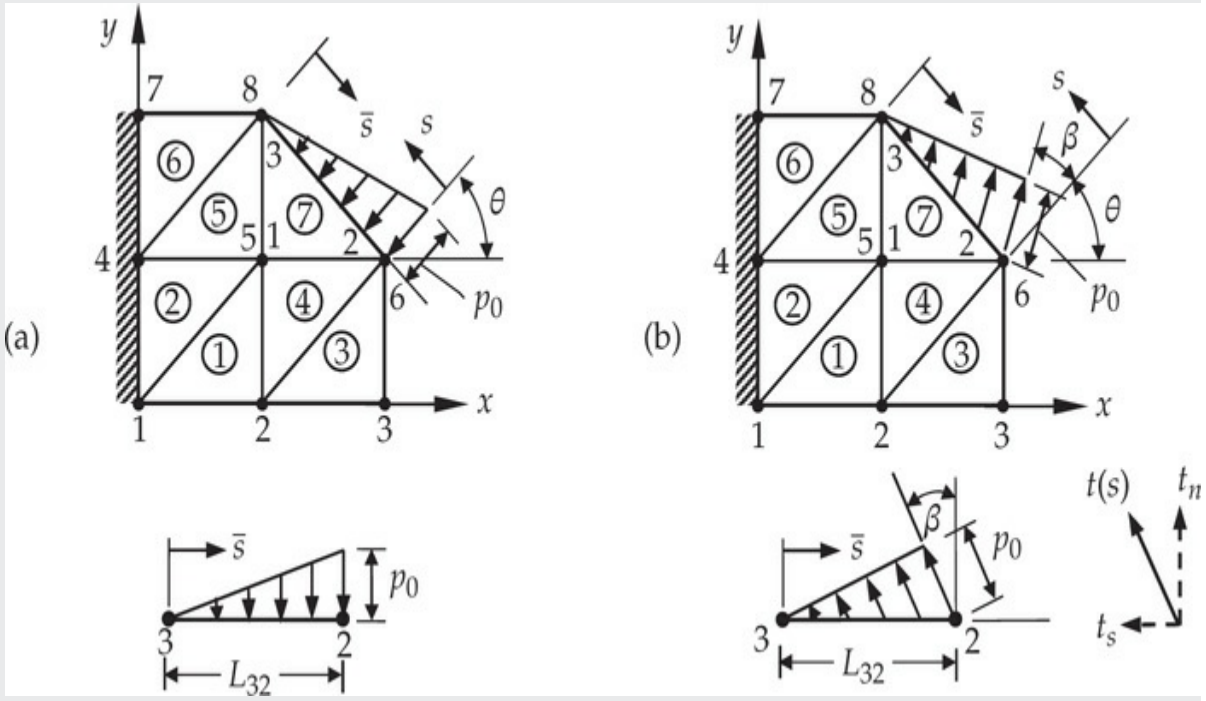

Fig. 12.4.2 Plane elasticity problem with (a) traction normal to the boundary and (b) traction in an arbitrary direction.

$$t_n \neq 0, \quad t_s = 0 \tag{1}$$

where the subscripts n and s refer to normal and tangential directions, respectively. We have (for $e = 7$)

$$\mathbf{Q}^e = \oint_{\Gamma_e} h_e \boldsymbol{\Psi}^{\mathrm{T}} \begin{Bmatrix} t_n \\ t_s \end{Bmatrix} ds = \int_{\Gamma^e_{12}} h_e \boldsymbol{\Psi}^{\mathrm{T}} \begin{Bmatrix} t_n \\ t_s \end{Bmatrix} ds + \int_{\Gamma^e_{23}} h_e \boldsymbol{\Psi}^{\mathrm{T}} \begin{Bmatrix} t_n \\ 0 \end{Bmatrix} ds + \int_{\Gamma^e_{31}} h_e \boldsymbol{\Psi}^{\mathrm{T}} \begin{Bmatrix} t_n \\ t_s \end{Bmatrix} ds \tag{2}$$

The first and third integrals cannot be evaluated because we do not know t_n and t_s on these sides of the element. However, by internal stress equilibrium, the contributions of these integrals cancel with like contributions from the neighboring elements (elements 4 and 5) in the assembled force vector of the structure. Thus, we must compute only the integral over side 2–3 of the element. We have (for $e = 7$)

$$\mathbf{Q}^{(7)}_{2-3} = \int_0^{L_{23}} h \boldsymbol{\Psi}^{\mathrm{T}} \begin{Bmatrix} t_n \\ 0 \end{Bmatrix} ds, \quad t_n = -p_0 \left(1 - \frac{s}{L_{23}}\right) \tag{3}$$

where the minus sign in front of p_0 is added to account for the direction of the applied traction, which is acting toward the body in the present case. The local coordinate system s used in the above expression is chosen along the side connecting node 2 to node 3, with its origin at node 2. One is not restricted to this choice. If one feels that it is convenient to choose the local coordinate system $\bar{s}$, which is taken along side 3–2, with its origin at node 3 of element 7, we can write

$$\mathbf{Q}^{(7)}_{3-2} = \int_0^{L_{23}} h \boldsymbol{\Psi}^{\mathrm{T}} \begin{Bmatrix} t_n \\ 0 \end{Bmatrix} d\bar{s}, \quad t_n = -\frac{p_0 \bar{s}}{L_{23}} \tag{4}$$

wherein now $\boldsymbol{\Psi}^e$ is expressed in terms of the local coordinate $\bar{s}$. We have

$$\mathbf{Q}_{3-2}^{(7)} = \int_0^{L_{23}} h \begin{Bmatrix} 0 \\ 0 \\ \psi_2^7 t_n \\ 0 \\ \psi_3^7 t_n \\ 0 \end{Bmatrix} d\bar{s} = -\frac{L_{23} p_0 h}{6} \begin{Bmatrix} 0 \\ 0 \\ 2 \\ 0 \\ 1 \\ 0 \end{Bmatrix} \tag{5}$$

The global components of this force vector are [set $\alpha = 90 - \theta$ in Eq. (12.4.17b)]

$$\mathbf{Q}_{3-2}^{(7)} = -\frac{L_{23} p_0 h}{6} \begin{Bmatrix} 0 \\ 0 \\ 2\sin\theta \\ 2\cos\theta \\ \sin\theta \\ \cos\theta \end{Bmatrix} \tag{6}$$

Next, consider the case in which the tractions are oriented at an angle β, as shown in Fig. 12.4.2(b). Then one may resolve the applied traction into normal and tangential components

$$t_n = t(s)\cos\beta, \quad t_s = t(s)\sin\beta \tag{7}$$

and repeat the procedure described above.

The same procedure applies to linear quadrilateral elements. In general, the loads due to specified boundary stresses can be computed using an appropriate local coordinate system and one-dimensional interpolation functions. When higher-order elements are involved, the corresponding order of one-dimensional interpolation functions must be used.

12.4.6 Assembly of Finite Element Equations

The assembly procedure for multi-degree of freedom problems is the same as that used for a single degree of freedom problem (see Section 9.2), except that the procedure should be applied to both degrees of freedom at each node. For example, consider the plane elastic structure and the finite element mesh used in Fig. 12.4.3(a). There are eight nodes in the mesh; hence, the total size of the assembled stiffness matrix will be 16 × 16, and the force vector will be 16 × 1. The first two rows and columns of the global stiffness matrix, for example, correspond to the global degrees (1,2)

of freedom at global node 1, which has contributions from nodes 2 and 3 of elements 1 and 2, respectively, as indicated in Fig. 12.4.3(b). Thus, the contributions to global coefficients K_{IJ} (I, J = 1, 2) come from $K^1_{ij}\ (i,j=3,4)$ and $K^2_{ij}\ (i,j=5,6)$.

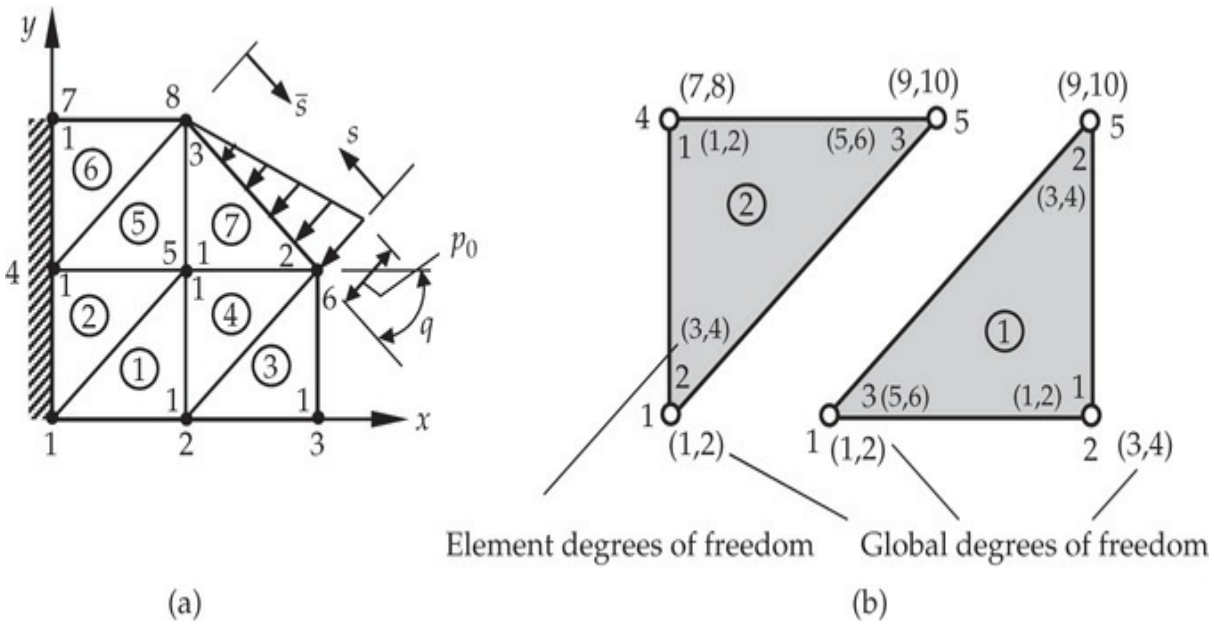

Fig. 12.4.3 Plane elasticity problem with global and local displacement degrees of freedom.

For instance, the global stiffness matrix coefficients K_{11}, K_{12}, K_{13}, K_{15}, K_{22}, K_{33}, and K_{34} are known in terms of the element coefficients as follows:

$$K_{11}=K^1_{55}+K^2_{33},\quad K_{22}=K^1_{66}+K^2_{44},\quad K_{12}=K^1_{56}+K^2_{34},\quad K_{13}=K^1_{51}$$
$$K_{33}=K^1_{11}+K^3_{55}+K^4_{33},\quad K_{34}=K^1_{12}+K^3_{56}+K^4_{34},\quad K_{15}=0$$

Note that K_{34}, for example, denotes the coupling stiffness coefficient between the third (u_x) and fourth (u_y) global displacement degrees of freedom, both are at global node 2. On the other hand, K_{13} denotes the coupling coefficient between the first displacement degree of freedom (u_x) at global node 1 and third global displacement degree (u_x) of freedom at global node 2. Similar arguments apply for the assembly of the force vector.

With regard to the specification of the displacements (the primary degrees of freedom) and forces (the secondary degrees of freedom) in a

finite element mesh, one has the following four distinct possibilities:

Case 1: u_x and u_y are specified (and t_x and t_y are unknown and are determined in the post-computation).

Case 2: u_x and t_y are specified (and t_x is unknown and is determined in the post-computation; and u_y is unknown and is determined as a part of the solution for unknown displacement degrees of freedom).

Case 3: t_x and u_y are specified (and u_x is unknown and is determined as a part of the solution for unknown displacement degrees of freedom; and t_y is unknown and is determined in the post-computation).

Case 4: t_x and t_y are specified (and u_x and u_y are unknown and are determined as a part of the solution for unknown displacement degrees of freedom).

In general, only one of the quantities of each of the pairs (u_x, t_x) and (u_y, t_y) is known at a nodal point in the mesh. As discussed in Chapter 10, we are required to make a decision as to which degree of freedom is known when singular points (i.e., points at which both displacement and force degrees of freedom are known or when two different values of the same degree of freedom are specified) are encountered.

For time-dependent problems, the initial displacement and velocity must be specified for each component of the displacement field:

$$\mathbf{u} = \mathbf{u}^0, \quad \dot{\mathbf{u}} = \mathbf{v}^0 \tag{12.4.18}$$

12.4.7 Post-computation of Strains and Stresses

The strains and stresses can be post-computed using the strain–displacement relations (12.2.14a) and stress–strain relations (12.2.15a), once the nodal displacements are known from the primary calculation. From Eqs. (12.4.3) to (12.4.4), we have

$$\boldsymbol{\varepsilon}(\mathbf{x}, t) = \mathbf{B}(\mathbf{x})\,\boldsymbol{\Delta}(t), \quad \boldsymbol{\sigma}(\mathbf{x}, t) = \mathbf{C}\,\mathbf{B}(\mathbf{x})\,\boldsymbol{\Delta}(t) \tag{12.4.19}$$

where $\mathbf{x} = (x, y)$ is the location where the strains and stresses are calculated at time t. In explicit form, the stresses, for example, at (x_0, y_0) in a typical finite element Ω_e at time $t = t_s$ are given by [see Eq. (12.3.5); $u_j = u_x^j$ and $v_j = u_y^j$]

$$\sigma_{xx}(x_0,y_0,t_s)=\sum_{j=1}^{n}\left[c_{11}u_j^e(t_s)\frac{\partial\psi_j^{(e)}}{\partial x}+c_{12}v_j^e(t_s)\frac{\partial\psi_j^{(e)}}{\partial y}\right]_{(x_0,y_0)}$$

$$\sigma_{xy}(x_0,y_0,t_s)=\sum_{j=1}^{n}\left[c_{66}\left(u_j^e(t_s)\frac{\partial\psi_j^{(e)}}{\partial y}+v_j^e(t_s)\frac{\partial\psi_j^{(e)}}{\partial x}\right)\right]_{(x_0,y_0)} \tag{12.4.20}$$

$$\sigma_{yy}(x_0,y_0,t_s)=\sum_{j=1}^{n}\left[c_{12}u_j^e(t_s)\frac{\partial\psi_j^{(e)}}{\partial x}+c_{22}v_j^e(t_s)\frac{\partial\psi_j^{(e)}}{\partial y}\right]_{(x_0,y_0)}$$

Of course, one can calculate the strains and stresses at any desired point (x, y). However, as shown by Barlow [3,4], calculation of the strains and stresses (which are lower-order polynomials than the displacements) at reduced Gauss points is found to be a better representation of the actual strain and stress fields in the structure (i.e., the reduced Gauss points are optimal points for accurate stresses). Thus, for linear elements the stresses are calculated at the center of the master element, and for quadratic elements they are computed at the 2 × 2 Gauss point locations of the master element. When stresses are needed at a node, different techniques of extrapolation have been discussed in the literature (see, e.g., [5]).

12.5 Elimination of Shear Locking in Linear Elements

12.5.1 Background

The linear finite elements of elasticity have limitations in predicting certain kinematics of deformation. For example, consider pure bending (i.e., subjected to end couples) of a thin and long plane elastic sheet of isotropic material. Figure 12.5.1(a) shows a mesh of linear rectangular elements while Fig. 12.5.1(b) shows a mesh of quadratic rectangular elements. A linear rectangular element can only deform, in general, to become a quadrilateral (with straight sides). For the loading shown, the linear element can become a trapezoid by stretching the top and compressing the bottom of the element, as shown in Fig. 12.5.1(c), whereas the actual deformation should make all horizontal lines become curves (i.e., arc of a circle). On the other hand, a typical quadratic

rectangular element in the mesh can deform to have the sides become quadratic curves. In the present case, a quadratic element will deform as shown in Fig. 12.5.1(d). Thus, the mesh of linear elements will produce a deformation that exhibits nonzero shear strain γ_{xy}, whereas the shear strain should be zero everywhere because it is a case of pure bending. The mesh of quadratic elements will not have nonzero shear strain. Since the mesh of linear elements cannot "bend," it behaves as a stiff structure. Such a state is known as *shear locking* (different from the shear locking encounter in Timoshenko beams).

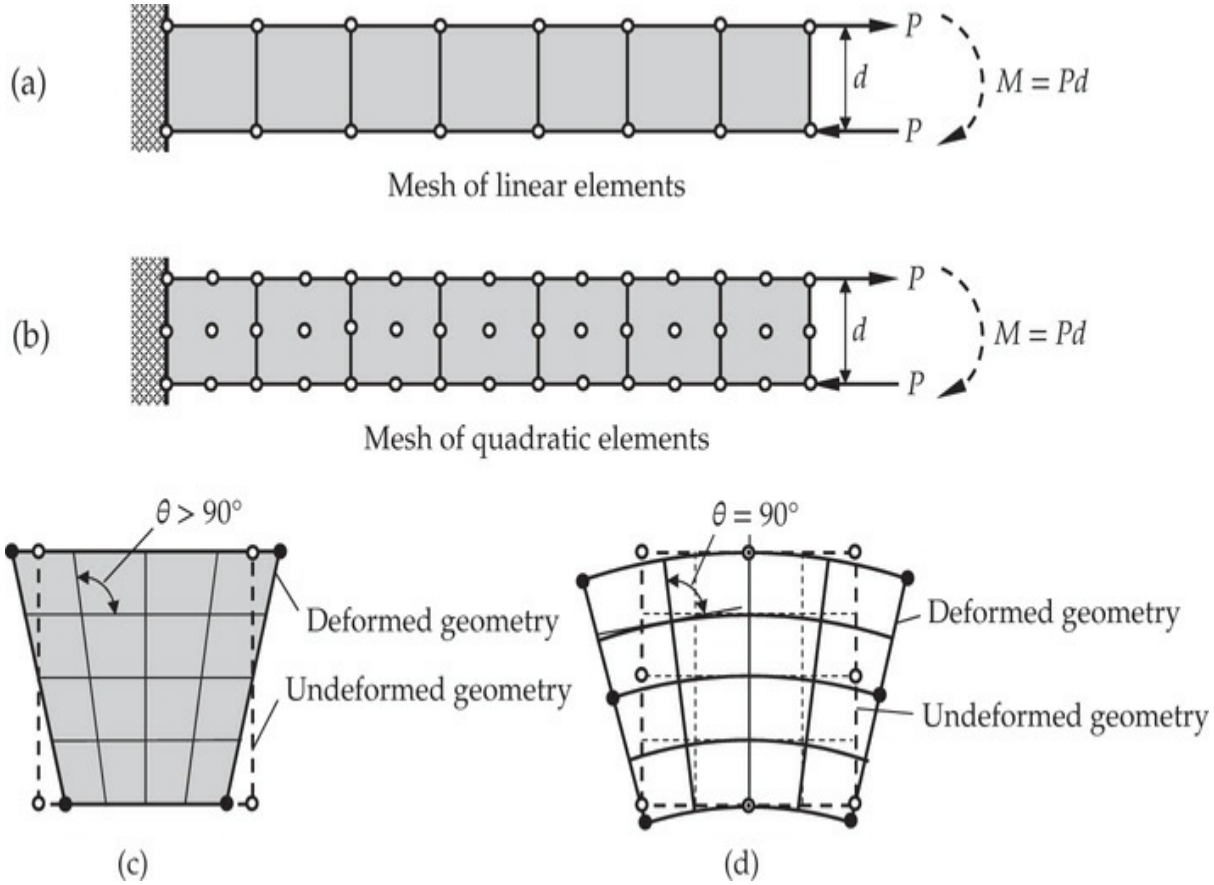

Fig. 12.5.1 A plate strip subjected to a couple (i.e., pure bending). (a) A mesh of linear rectangular elements. (b) A mesh of quadratic rectangular elements. (c) Undeformed and deformed shape of linear elements. (d) Undeformed and deformed shape of quadratic elements.

To overcome the shear locking of linear elements without increasing the order of the stiffness matrix, we can add quadratic terms to the displacement expansions (to be able to capture the bending deformation) through "nodeless" variables and eliminate the nodeless variables through static condensation so that the element will have only the nodal

displacement degrees of freedom active. The procedure is discussed next.

12.5.2 Modification of the Stiffness Matrix of Linear Finite Elements

Consider the displacement expansion of the form [see Eq. (12.4.2a)]

$$\mathbf{u} = \boldsymbol{\Psi}\boldsymbol{\Delta} + \begin{bmatrix} 1-\xi^2 & 1-\eta^2 \\ 1-\xi^2 & 1-\eta^2 \end{bmatrix} \begin{Bmatrix} \alpha_1 \\ \alpha_2 \end{Bmatrix} \equiv \boldsymbol{\Psi}\boldsymbol{\Delta} + \boldsymbol{\Phi}\boldsymbol{\alpha} \tag{12.5.1}$$

where $\boldsymbol{\Psi}$ and $\boldsymbol{\Delta}$ are as defined in Eq. (12.4.2b) and α_1 and α_2 are nodeless variables (have the units of the displacement). Substituting the expansion from Eq. (12.5.1) into the strain vector, we obtain

$$\boldsymbol{\varepsilon} = \mathbf{D}\mathbf{u} = \mathbf{B}\boldsymbol{\Delta} + \bar{\mathbf{B}}\boldsymbol{\alpha} = \{\mathbf{B}\ \bar{\mathbf{B}}\} \begin{Bmatrix} \boldsymbol{\Delta} \\ \boldsymbol{\alpha} \end{Bmatrix} \tag{12.5.2}$$

where $\mathbf{B}$ is defined by Eq. (12.4.4) and $\bar{\mathbf{B}}$ is defined by

$$\bar{\mathbf{B}} = \mathbf{D}\boldsymbol{\Phi} \tag{12.5.3}$$

Using Eq. (12.5.2) in Eq. (12.3.4) (without the mass term), we obtain the finite element equations for a static case:

$$\begin{bmatrix} \mathbf{K}^{\Delta\Delta} & \mathbf{K}^{\Delta\alpha} \\ \mathbf{K}^{\alpha\Delta} & \mathbf{K}^{\alpha\alpha} \end{bmatrix} \begin{Bmatrix} \boldsymbol{\Delta} \\ \boldsymbol{\alpha} \end{Bmatrix} = \begin{Bmatrix} \mathbf{F}^{\Delta} \\ \mathbf{F}^{\alpha} \end{Bmatrix} \tag{12.5.4}$$

where

$$\begin{aligned} \mathbf{K}^{\Delta\Delta} &= \int_{\Omega_e} h_e\, \mathbf{B}^{\mathrm{T}}\mathbf{C}\mathbf{B}\, dxdy, \quad \mathbf{K}^{\Delta\alpha} = \int_{\Omega_e} h_e\, \mathbf{B}^{\mathrm{T}}\mathbf{C}\bar{\mathbf{B}}\, dxdy \\ \mathbf{K}^{\alpha\Delta} &= \int_{\Omega_e} h_e\, \bar{\mathbf{B}}^{\mathrm{T}}\mathbf{C}\mathbf{B}\, dxdy, \quad \mathbf{K}^{\alpha\alpha} = \int_{\Omega_e} h_e\, \bar{\mathbf{B}}^{\mathrm{T}}\mathbf{C}\bar{\mathbf{B}}\, dxdy \\ \mathbf{F}^{\Delta} &= \int_{\Omega_e} h_e\, \boldsymbol{\Psi}^{\mathrm{T}}\mathbf{f} + \oint_{\Gamma_e} h_e\, \boldsymbol{\Psi}^{\mathrm{T}} h_e\, \mathbf{t}\, dS, \quad \mathbf{F}^{\alpha} = \int_{\Omega_e} h_e\, \boldsymbol{\Phi}^{\mathrm{T}}\mathbf{f}\, dxdy \end{aligned} \tag{12.5.5}$$

We note that at the element level $\mathbf{F}^{\alpha}$ is always known. Now solving for α from the second set of equations in (12.5.4), we obtain

$$\mathbf{K}^{\alpha\Delta}\boldsymbol{\Delta} + \mathbf{K}^{\alpha\alpha}\boldsymbol{\alpha} = \mathbf{F}^{\alpha} \Rightarrow \boldsymbol{\alpha} = (\mathbf{K}^{\alpha\alpha})^{-1}\left(\mathbf{F}^{\alpha} - \mathbf{K}^{\alpha\Delta}\boldsymbol{\Delta}\right) \tag{12.5.6}$$

Then substituting this result into the first equation for α in (12.5.4), we arrive at

$$\hat{\mathbf{K}}\boldsymbol{\Delta} = \hat{\mathbf{F}} \tag{12.5.7}$$

where

$$\hat{\mathbf{K}} = \mathbf{K}^{\Delta\Delta} - \mathbf{K}^{\Delta\alpha}(\mathbf{K}^{\alpha\alpha})^{-1}\mathbf{K}^{\alpha\Delta}, \quad \hat{\mathbf{F}} = \mathbf{F}^{\Delta} - \mathbf{K}^{\Delta\alpha}(\mathbf{K}^{\alpha\alpha})^{-1}\mathbf{F}^{\alpha} \tag{12.5.8}$$

Thus, the size of the effective stiffness matrix $\hat{\mathbf{K}}$ of a linear element remains the same as before (8 × 8).

12.6 Numerical Examples

Here we consider a couple of computational examples of plane elasticity problems to illustrate assembly of the element coefficients to obtain global coefficients, load computation, and imposition of boundary conditions, and show the influence of mesh and type of elements on the accuracy. The stresses are evaluated at the reduced Gauss points of the elements. These examples are analyzed using the program **FEM2D**.

Example 12.6.1

Consider a thin elastic plate subjected to a uniformly distributed edge load, as shown in Fig. 12.6.1. Use a = 120 in., b = 160 in., h = 0.036 in., v = 0.25, $E = 30 \times 10^6$ lb in.$^{-2}$, p_0 = 10 lb/in., and $f_x = f_y = 0$. Determine the static solution to the problem using various meshes of linear and quadratic (a) triangles and (b) rectangles.

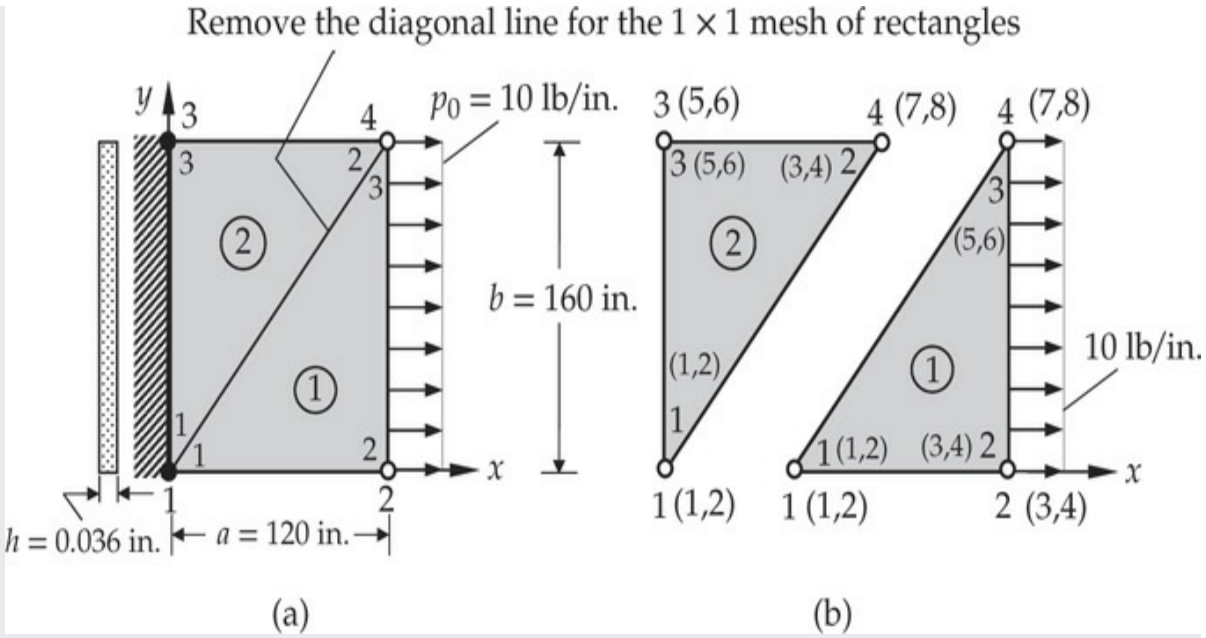

Fig. 12.6.1 Geometry and finite element mesh of a plane elasticity problem by the CST elements.

Solution: First we illustrate the assembly of element coefficients and computation of specified nodal forces using 1 × 1 meshes of linear (a) triangles and (b) rectangles. Then we use various meshes of linear and quadratic elements to analyze the problem and investigate convergence of displacements and stresses with mesh refinements.

For the 1 × 1 mesh of linear triangles, the correspondence between the global and local nodes and the local and global nodal displacement degrees of freedom are shown in Fig. 12.6.1 and Table 12.6.1. Based on this information, one can obtain the global stiffness and force coefficients in terms of the element coefficients, which are known from either Eq. (12.4.15a) (linear triangles) or from Eq. (12.4.8a) with $\mathbf{K}^{\alpha\beta}$ defined in Eq. (12.4.16a) (for linear rectangles). Algebraic form of the global stiffness coefficients in terms of the element stiffness coefficients are presented in Table 12.6.1. As explained earlier, if the global degrees of freedom I and J do not correspond to the degrees of freedom of the same element, the coefficient K_{IJ} is zero. For example, K_{53}, K_{54}, K_{63}, and K_{64} are zero because the global degrees of freedom (5,6) and (3,4) do not belong to the same element. The force coefficients can be assembled in the same way; for example, we have $F_7 = F_3^2 + F_5^1$ and $F_8 = F_4^2 + F_6^1$.

Table 12.6.1 Correspondence between the global stiffness coefficients and element stiffness coefficients for the mesh shown in **Example 12.6.1**.

Nodal correspondence		Stiffness correspondence	
Global Node (DOF)	Local Node (DOF)	Global	Local
1 (1, 2)	1 of element 1 (1, 2)	K_{11}	$K_{11}^1 + K_{11}^2$
		K_{22}	$K_{22}^1 + K_{22}^2$
	1 of element 2 (1, 2)	K_{12}	$K_{12}^1 + K_{12}^2$
2 (3, 4)	2 of element 1 (3, 4)	K_{33}	K_{33}^1
		K_{44}	K_{44}^1
		K_{34}	K_{34}^1
3 (5, 6)	3 of element 2 (5,6)	K_{55}	K_{55}^2
		K_{66}	K_{66}^2
		K_{56}	K_{56}^2
4 (7, 8)	2 of element 2 (3, 4)	K_{77}	$K_{55}^1 + K_{33}^2$
		K_{88}	$K_{66}^1 + K_{44}^2$
	3 of element 1 (5, 6)	K_{78}	$K_{56}^1 + K_{34}^2$

The specified global degrees of freedom for the 1 × 1 mesh are

$$U_1 = U_2 = U_5 = U_6 = 0 \tag{1}$$

The rows and columns 1, 2, 5, and 6 of the assembled **K** can be deleted (since the specified boundary conditions are homogeneous) to obtain the following condensed equations for the unknown displacements:

$$\begin{bmatrix} K_{33}^1 & K_{34}^1 & K_{35}^1 & K_{36}^1 \\ K_{43}^1 & K_{44}^1 & K_{45}^1 & K_{46}^1 \\ K_{53}^1 & K_{54}^1 & K_{55}^1 + K_{33}^2 & K_{56}^1 + K_{34}^2 \\ K_{63}^1 & K_{64}^1 & K_{65}^1 + K_{43}^2 & K_{66}^1 + K_{44}^2 \end{bmatrix} \begin{Bmatrix} U_3 \\ U_4 \\ U_7 \\ U_8 \end{Bmatrix} = \begin{Bmatrix} F_3 \\ F_4 \\ F_7 \\ F_8 \end{Bmatrix} \tag{2}$$

where the known forces F_3, F_4, F_7, and F_8 are (p_0 is the force per unit length, and $f_x = f_y = 0$)

$$F_3 = (Q_2^1)^{(1)} = \frac{p_0 b}{2} = 800\,\text{lb}, \quad F_7 = (Q_3^1)^{(1)} + (Q_2^1)^{(2)} = \frac{p_0 b}{2} = 800\,\text{lb}$$
$$F_4 = (Q_2^2)^{(1)} = 0, \quad F_8 = (Q_3^2)^{(1)} + (Q_2^2)^{(2)} = 0 \tag{3}$$

Here $(Q_i^j)^{(e)}$ denotes the force in the x_j-direction ($x_1 = x$ and $x_2 = y$) at local node i of element e. The numerical form of the condensed equations is

$$10^4 \begin{bmatrix} 93.0 & -36.0 & -16.2 & 14.4 \\ -36.0 & 72.0 & 21.6 & -43.2 \\ -16.2 & 21.6 & 93.0 & 0.0 \\ 14.4 & -43.2 & 0.0 & 72.0 \end{bmatrix} \begin{Bmatrix} U_3 \\ U_4 \\ U_7 \\ U_8 \end{Bmatrix} = \begin{Bmatrix} 800.0 \\ 0.0 \\ 800.0 \\ 0.0 \end{Bmatrix} \tag{4}$$

Solving the equations, we obtain

$$\begin{Bmatrix} U_3 \\ U_4 \\ U_7 \\ U_8 \end{Bmatrix} = 10^{-4} \begin{Bmatrix} 11.291 \\ 1.964 \\ 10.113 \\ -1.080 \end{Bmatrix} \text{ in.} \tag{5}$$

Similar procedure applies to the 1 × 1 mesh of (i.e., single) rectangular element. The condensed assembled equations for the unknown displacement degrees of freedom are

$$\begin{bmatrix} K_{33}^1 & K_{34}^1 & K_{35}^1 & K_{36}^1 \\ K_{43}^1 & K_{44}^1 & K_{45}^1 & K_{46}^1 \\ K_{53}^1 & K_{54}^1 & K_{55}^1 & K_{56}^1 \\ K_{63}^1 & K_{64}^1 & K_{65}^1 & K_{66}^1 \end{bmatrix} \begin{Bmatrix} U_3 \\ U_4 \\ U_7 \\ U_8 \end{Bmatrix} = \begin{Bmatrix} F_3 \\ F_4 \\ F_7 \\ F_8 \end{Bmatrix} \tag{6}$$

or

$$10^4 \begin{bmatrix} 62.0 & -18.0 & -14.8 & -3.6 \\ -18.0 & 48.0 & 3.6 & -19.2 \\ -14.8 & 3.6 & 62.0 & 18.0 \\ -3.6 & -19.2 & 18.0 & 48.0 \end{bmatrix} \begin{Bmatrix} U_3 \\ U_4 \\ U_7 \\ U_8 \end{Bmatrix} = \begin{Bmatrix} 800.0 \\ 0.0 \\ 800.0 \\ 0.0 \end{Bmatrix} \tag{7}$$

The solution of these equations is

$$\begin{Bmatrix} U_3 \\ U_4 \\ U_7 \\ U_8 \end{Bmatrix} = 10^{-4} \begin{Bmatrix} 10.853 \\ 2.326 \\ 10.853 \\ -2.326 \end{Bmatrix} \text{ in.} \tag{8}$$

Table 12.6.2 contains the finite element solutions (deflections and stresses) of isotropic and orthotropic plates obtained with 1 × 1 mesh. The results were obtained using the computer code **FEM2D**. Note that the finite element solutions (e.g., displacements) obtained with mesh of triangles do not exhibit symmetry about the $y = b/2$ line. This is because

of the unsymmetry of the triangular element mesh used. One-element mesh of rectangular element yields results symmetric about the $y = b/2$ line.

Table 12.6.2 Finite element results for isotropic and orthotropic thin plates using 1 × 1 meshes of triangular and rectangular elements† (msi = 10^6 psi, $\bar{U}_i = U_i \times 10^4$.

Mesh	Material	$\bar{U}_3$	$\bar{U}_4$	$\bar{U}_7$	$\bar{U}_8$
Isotropic					
1 × 1	$E = 30$ msi	11.291	1.964	10.113	−1.080
	$\nu = 0.25$	10.853	2.326	10.853	−2.326
Orthotropic					
1 × 1	$E_1 = 31$ msi, $E_2 = 2.7$ msi	10.767	1.666	10.651	−1.579
	$G_{12} = 0.75$ msi, $\nu_{12} = 0.28$	10.728	2.675	10.728	−2.675

†The first row corresponds to mesh of triangles and the second row to rectangular element.

As an example, the input data for the 16 × 16 mesh of linear triangular elements is presented in Box 12.6.1. Box 12.6.1 also contains the data statements that are different for the 8 × 8 mesh of quadratic triangular elements. We note that the nodal forces, $\mathbf{f}^e$, for quadratic elements follow the form shown in Eq. (3.4.38). The same input files are valid for rectangular elements by changing IELTYP to 1 (or 2) and NPE to 4 (or 9). An edited output for the case of 8 × 8 mesh of quadratic triangular elements is presented in Box 12.6.2.

Box 12.6.1: A typical input file to program **FEM2D** for **Example 12.6.1**.

```
Example 12.6.1: Plane elastic plate with uniform edge load
    2   1   0   0                    ITYPE,IGRAD,ITEM,NEIGN
    0   3   1   0                    IELTYP,NPE,MESH,NPRNT
    16   16                                        NX, NY
    0.0   7.5  7.5  7.5  7.5  7.5  7.5  7.5  7.5
          7.5  7.5  7.5  7.5  7.5  7.5  7.5  7.5  X0, DX(I)
    0.0  10.0 10.0 10.0 10.0 10.0 10.0 10.0 10.0
         10.0 10.0 10.0 10.0 10.0 10.0 10.0 10.0  Y0, DY(I)
    34                                            NSPV
     1 1   1 2  18 1  18 2  35 1  35 2  52 1  52 2
    69 1  69 2  86 1  86 2 103 1 103 2 120 1 120 2
   137 1 137 2 154 1 154 2 171 1 171 2 188 1 188 2
   205 1 205 2 222 1 222 2 239 1 239 2 256 1 256 2
   273 1 273 2                                    ISPV
   0.0   0.0   0.0   0.0   0.0   0.0   0.0   0.0
   0.0   0.0   0.0   0.0   0.0   0.0   0.0   0.0
   0.0   0.0   0.0   0.0   0.0   0.0   0.0   0.0
   0.0   0.0   0.0   0.0   0.0   0.0   0.0   0.0
   0.0   0.0                                    VSPV
    17                                          NSSV
    17 1  34 1  51 1  68 1  85 1 102 1 119 1 136 1
   153 1 170 1 187 1 204 1 221 1 238 1 255 1 272 1
   289 1    ISSV
   50.0 100.0 100.0 100.0 100.0 100.0 100.0 100.0
  100.0 100.0 100.0 100.0 100.0 100.0 100.0 100.0
   50.0                                         VSSV
    1                                           LNSTRS
30.0E06 30.0E06 0.25 12.0E06 0.036          E1,E2,ANU12,G12,THKNS
    0.0       0.0     0.0                       F0, FX, FY

Statements that are different for the 8 by 8 mesh of quadratic triangles

Example 12.6.1: Plane elastic plate with uniform edge load
    2   1   0   0                    ITYPE,IGRAD,ITEM,NEIGN
    0   6   1   0                    IELTYP,NPE,MESH,NPRNT
    8   8                                         NX, NY
    0.0  15.0 15.0 15.0 15.0 15.0 15.0 15.0 15.0  X0, DX(I)
    0.0  20.0 20.0 20.0 20.0 20.0 20.0 20.0 20.0  Y0, DY(I)
    .
    .
    .
  33.3333 133.3333 66.6667 133.3333 66.6667
          133.3333 66.6667 133.3333 66.6667
          133.3333 66.6667 133.3333 66.6667
          133.3333 66.6667 133.3333 33.3333       VSSV    etc.
```

Box 12.6.2: Edited output from program **FEM2D** for **Example 12.6.1**.

```
Example 12.6.1: Plane elastic plate with uniform edge load

            OUTPUT  from  program *** FEM2D *** by J. N. REDDY
                A  2-D  ELASTICITY   PROBLEM  IS  ANALYZED

     MATERIAL PROPERTIES OF THE SOLID ANALYZED:
        Thickness of the body, THKNS .............=  0.3600E-01
        Modulus of elasticity, E1 ................=  0.3000E+08
        Modulus of elasticity, E2 ................=  0.3000E+08
        Poisson s ratio, ANU12 ...................=  0.2500E+00
        Shear modulus, G12 .......................=  0.1200E+08

        ***PLANE STRESS assumption is selected by user**
        ******* A STEADY-STATE PROBLEM is analyzed *******
        *** A mesh of   TRIANGLES    is chosen by user ***

     FINITE ELEMENT MESH INFORMATION:
        Element type: 0 = Triangle; >0 = Quad.)..=   0
        Number of nodes per element, NPE .........=   6
        No. of primary deg. of freedom/node, NDF =   2
        Number of elements in the mesh, NEM .....= 128
        Number of nodes in the mesh, NNM .........= 289
        Number of equations to be solved, NEQ ...= 578
        Half bandwidth of the matrix GLK, NHBW ..=  74
        Mesh subdivisions, NX and NY .............=   8    8

        No. of specified PRIMARY variables, NSPV =  34
        No. of speci.  SECONDARY variables, NSSV =  17

     NUMERICAL INTEGRATION DATA:

        Full Integration polynomial degree, IPDF =   3
        Number of full integration points,  NIPF =   4
        Reduced Integration polynomial deg.,IPDR =   2
        No.  of reduced integration points, NIPR =   3
        Integ. poly. deg. for stress comp., ISTR =   1
        No. of integ. pts. for stress comp.,NSTR =   1

     S O L U T I O N :

     Node     x-coord.      y-coord.     Value of u_x   Value of u_y
      17    0.12000E+03   0.00000E+00   0.11168E-02    0.19946E-03
     102    0.12000E+03   0.50000E+02   0.10922E-02    0.78970E-04
     119    0.12000E+03   0.60000E+02   0.10888E-02    0.53118E-04
     136    0.12000E+03   0.70000E+02   0.10867E-02    0.26853E-04
     153    0.12000E+03   0.80000E+02   0.10860E-02    0.41578E-06

    x-coord.     y-coord.       sigma-x       sigma-y       sigma-xy

  0.10000E+02  0.66667E+01   0.3168E+03   0.1938E+02   0.3147E+02
  0.50000E+01  0.13333E+02   0.2935E+03   0.5637E+02   0.4273E+02
  0.50000E+01  0.73333E+02   0.2636E+03   0.5984E+02   0.3277E+01
```

Deflections and stresses obtained with various uniform meshes of (a) triangular elements and (b) rectangular elements are presented in Table 12.6.3. Mesh $m \times n$ means that m elements in the x-direction and n elements in the y-direction are used. The mesh in FEM2D is generated according to the convention shown in Fig. 10.5.3. Meshes of rectangular elements (provided that the mesh is symmetric about the $y = b/2$ line) always yield results symmetric about the $y = b/2$ line. As the mesh of triangles is refined, the solution will become symmetric about $y = b/2$ line within a certain degree of error. Maximum stress locations are different for different meshes (especially for the triangles) and hence the question of convergence with mesh refinements is not meaningful.

Table 12.6.3 Deflections and stresses obtained with various meshes of triangles and rectangles in an isotropic plate subjected to uniform edge load [nL = $n \times n$ mesh of linear elements; nQ9 = $n \times n$ mesh of nine-node quadratic elements $(\bar{u} = u \times 10^4)$].

Element type	Mesh	$\bar{u}_x(120,0)$	$\bar{u}_y(120,0)$	σ_{xx}	σ_{yy}	σ_{xy}
	1L	11.291	1.964	285.9 (80, 53.33)†	67.42 (40, 106.7)	10.80 (80, 53.33)
	2L	11.372	2.175	294.1 (40, 26.67)	69.36 (20, 53.33)	23.20 (40, 26.67)
	4L	11.284	2.126	306.2 (20, 13.33)	73.75 (10, 146.7)	35.93 (20, 13.33)
Triangles	8L	11.209	2.054	331.6 (10, 6.67)	81.31 (5, 153.33)	48.04 (10, 6.67)
	4Q6	11.166	2.009	294.3 (20, 13.33)	54.48 (10, 66.67)	28.16 (10, 26.67)
	16L	11.179	2.014	372.5 (5, 3.33)	91.94 (2.5, 156.7)	58.90 (5, 3.33)
	8Q6	11.168	1.995	316.8 (10, 6.67)	59.84 (5, 73.33)	42.73 (5, 13.33)
	1L	10.853	2.326	277.8 (60, 80)	25.84 (60, 80)	0.0 (60, 80)
	2L	11.078	2.021	277.8 (30, 40)	37.46 (30, 40)	13.23 (30, 40)
	4L	11.150	2.009	288.1 (15, 20)	49.74 (15, 60)	27.73 (15, 20)
Rectangles	8L	11.162	1.997	308.0 (7.5, 10)	56.53 (7.5, 50)	40.97 (7.5, 10)
	4Q9	11.165	1.992	312.3 (6.34, 8.45)	58.17 (6.34, 71.55)	41.88 (6.34, 8.45)
	16L	11.166	1.992	339.5 (3.75, 5)	61.20 (3.75, 75)	53.14 (3.75, 5)
	8Q9	11.167	1.990	346.1 (3.17, 4.23)	61.80 (3.17, 84.23)	53.58 (3.17, 4.23)

†Location of the stress. One-point Gauss location for all triangles, one-point Gauss location for linear rectangles, and 2 × 2 Gauss locations for the quadratic rectangles are used.

Example 12.6.2

Consider an isotropic ($E = 30 \times 10^6$ psi, $v = 0.25$) steel plate ($a = 12$ in., b

= 1.5 in., h = 0.1 in.) fixed to a rigid wall at the right end, as shown in Fig. 12.6.2(a). Assuming that the body forces are zero, determine the maximum deflection and stress in the structure when it is subjected to an edge stress τ_0 = 150 psi. Investigate the convergence of the results with various uniform meshes of rectangles.

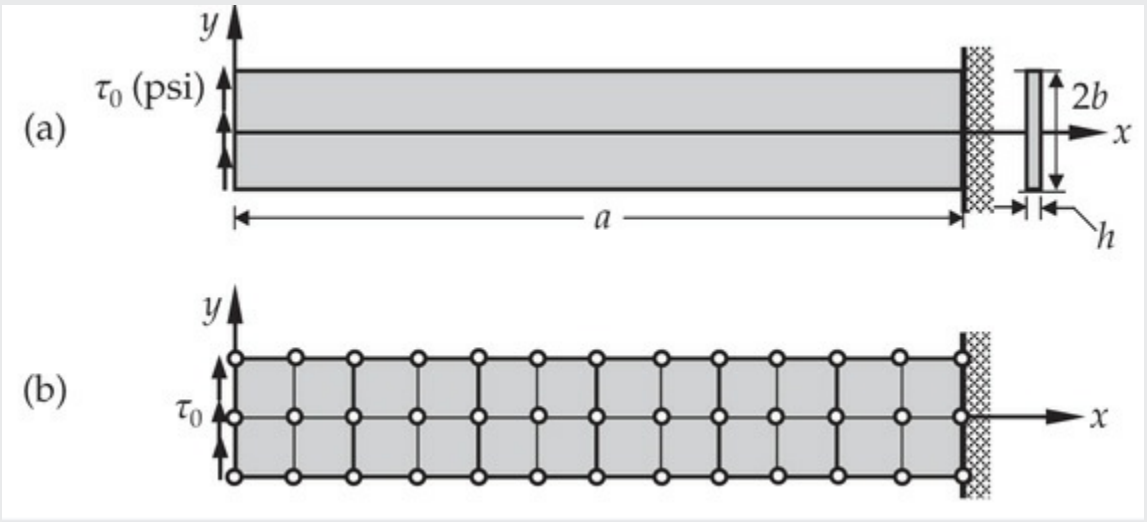

Fig. 12.6.2 Problem domain and a typical finite element mesh for the thin elastic plate considered in **Example 12.6.2**.

Solution: Clearly, the problem is one of a plane stress type, and it has no exact solution. The geometric boundary conditions of the problem are

$$u_x(a, y) = 0, \quad u_y(a, y) = 0 \tag{1}$$

and the traction boundary conditions are

$$\begin{aligned} &t_x = t_y = 0 \text{ at } y = -b \text{ for any } x \\ &t_x = 0, \quad t_y = -h\tau_0 \text{ at } x = 0 \text{ for any } y \\ &t_x = 0, \quad t_y = 0 \text{ at } y = b \text{ for any } x \end{aligned} \tag{2}$$

A typical finite element mesh (12 × 2) is shown in Fig. 12.6.2(b). The mesh shown consists of linear rectangular elements. Equivalent triangular element meshes are obtained by joining node 1 to node 3 of each rectangular element. Equivalent meshes of nine-node quadratic Lagrange elements are obtained by considering a 2 × 2 mesh of linear elements equivalent to a nine-node quadratic element.

The specified boundary conditions on the primary and nonzero secondary variables for the 12 × 2 mesh of linear elements (rectangles without shear correction) are given by

$$U_{25} = U_{26} = U_{51} = U_{52} = U_{77} = U_{78} = 0.0$$

$$F_2 = \frac{(\tau_0 h)b}{2}, \quad F_{28} = (\tau_0 h)b, \quad F_{54} = \frac{(\tau_0 h)b}{2} \tag{3}$$

For the equivalent 6 × 1 mesh of nine-node quadratic elements, the nonzero forces are (the displacement boundary conditions remain the same):

$$F_2 = \frac{(\tau_0 h)b}{3}, \quad F_{28} = \frac{4(\tau_0 h)b}{3}, \quad F_{54} = \frac{(\tau_0 h)b}{3} \tag{4}$$

The input data for the 12 × 2 mesh of linear rectangular elements (IELTYP = 1, NPE = 4) is presented in Box 12.6.3. The same input file is valid for the 6 × 1 mesh of nine-node quadratic rectangular elements (IELTYP = 2, NPE = 9), with the arrays DX(I) and DY(I) changed to

```
0.0   2.0   2.0   2.0   2.0   2.0   2.0              X0,DX(I)
0.0   3.0                                            Y0,DY(I)
```

and the VSSV array changed to

```
  7.5     30.0     7.5                                VSSV
```

An edited output for 12 × 2 mesh of linear rectangular elements is presented in Box 12.6.4.

Box 12.6.3: The input file to program **FEM2D** for **Example 12.6.2**.

```
Example 12.6.2: A cantilevered plate (12x2Q4)
    2   1   0   0                      ITYPE,IGRAD,ITEM,NEIGN
    1   4   1   0                      IELTYP,NPE,MESH,NPRNT
   12   2                                        NX, NY
    0.0  1.0  1.0  1.0  1.0  1.0  1.0
         1.0  1.0  1.0  1.0  1.0  1.0            X0,DX(I)
    0.0  1.5  1.5                               Y0,DY(I)
    6                                           NSPV
    13  1  13  2  26 1   26 2   39 1  39 2      ISPV
    0.0    0.0    0.0    0.0    0.0   0.0      VSPV
    3                                           NSSV
    1  2   14  2  27  2                        ISSV
    11.25  22.5   11.25                        VSSV
    1                                           LNSTRS
    30.0E06 30.0E06 0.25 12.0E06 0.1     E1,E2,ANU12,G12,THKNS
     0.0     0.0    0.0                      F0, FX, FY
```

Box 12.6.4: Edited output file from program **FEM2D** for **Example 12.6.2**.

```
                A  2-D  ELASTICITY   PROBLEM  IS  ANALYZED

    MATERIAL PROPERTIES OF THE SOLID ANALYZED:

       Thickness of the body, THKNS ............=  0.1000E+00
       Modulus of elasticity, E1 ...............=  0.3000E+08
       Modulus of elasticity, E2 ...............=  0.3000E+08
       Poisson s ratio, ANU12 ..................=  0.2500E+00
       Shear modulus, G12 ......................=  0.1200E+08

    FINITE ELEMENT MESH INFORMATION:

       Element type: 0 = Triangle; >0 = Quad.)..=   1
       Number of nodes per element, NPE ........=   4
       No. of primary deg. of freedom/node, NDF =   2
       Number of elements in the mesh, NEM .....=  24
       Number of nodes in the mesh, NNM ........=  39
       Number of equations to be solved, NEQ ...=  78
       Half bandwidth of the matrix GLK, NHBW ..=  30
       Mesh subdivisions, NX and NY ............=  12    2
       No. of specified PRIMARY variables, NSPV =   6
       No. of speci.  SECONDARY variables, NSSV =   3

     Node  DOF     Value
        1    2   0.11250E+02
       14    2   0.22500E+02
       27    2   0.11250E+02

    NUMERICAL INTEGRATION DATA:

       Full quadrature (IPDF x IPDF) rule, IPDF =   2
       Reduced quadrature (IPDR x IPDR),   IPDR =   1
       Quadrature rule used in postproc.,  ISTR =   1

    S O L U T I O N :

    Node     x-coord.       y-coord.    Value of u_x    Value of u_y
      1    0.00000E+00    0.00000E+00   -0.67656E-03    0.37472E-02
     14    0.00000E+00    0.15000E+01    0.17746E-17    0.37464E-02
     27    0.00000E+00    0.30000E+01    0.67656E-03    0.37472E-02

   x-coord.      y-coord.      sigma-x       sigma-y       sigma-xy
 0.11500E+02   0.75000E+00    0.1640E+04    0.1923E+03   -0.1500E+03
 0.11500E+02   0.22500E+01   -0.1640E+04   -0.1923E+03   -0.1500E+03
```

Table 12.6.4 contains a comparison of the finite element solutions u_y (0, 0) and σ_{xx} (x, y) obtained with various meshes. The linear element has the slowest convergence compared to the quadratic element.

Table 12.6.4 Comparison of the finite element solution with the elasticity solution for a cantilever beam subjected to a uniform shear load at the free end (**Example 12.6.2**).

Element*	Mesh	u_y (in.)	Stress (psi)	
		$\times 10^{-2}$	(x, y)	$\sigma_{xx}(x, y)$
Q4	12×2	0.37464	(11.500, 0.7500)	1640
Q9	6×1	0.39694	(11.577, 0.6340)	2003
Q4	24×4	0.39316	(11.750, 0.3750)	2623
Q9	12×2	0.39972	(11.789, 0.3170)	2817
Q4	48×8	0.39842	(11.875, 0.1875)	3252
Q9	24×4	0.40370	(11.894, 0.1585)	3276
EBT	6H	0.38400	(12.000,0.0000)	3600
TBT-RIE	6Q	0.40200	(12.000,0.0000)	3600
TBT-IIE	6C	0.40200	(12.000,0.0000)	3600

*Q4 = Four-node (linear) rectangular element; Q9 = nine-node (quadratic) rectangular elements; EBT = Euler–Bernoulli beam element (Hermite cubic); TBT = Timoshenko beam element (RIE = reduced integration element—quadratic; IIE = interdependent interpolation element—Hermite cubic for deflection and interdependent quadratic for rotation); all beam finite solutions coincide with the respective exact beam theory solutions.

Example 12.6.3

Consider an isotropic, hollow circular cylinder of internal radius $a = 10$ in. and outside radius $b = 15$ in. The cylinder is held between rigid (smooth) supports such that $u_z = 0$ at $z = \pm L/2$, and subjected to internal pressure $p_0 = 2 \times 10^3$ psi, as shown in Fig. 12.6.3(a). Determine the displacements and stresses in the cylinder using the finite element method. Take $E = 28 \times 10^6$ psi and $\nu = 0.3$.

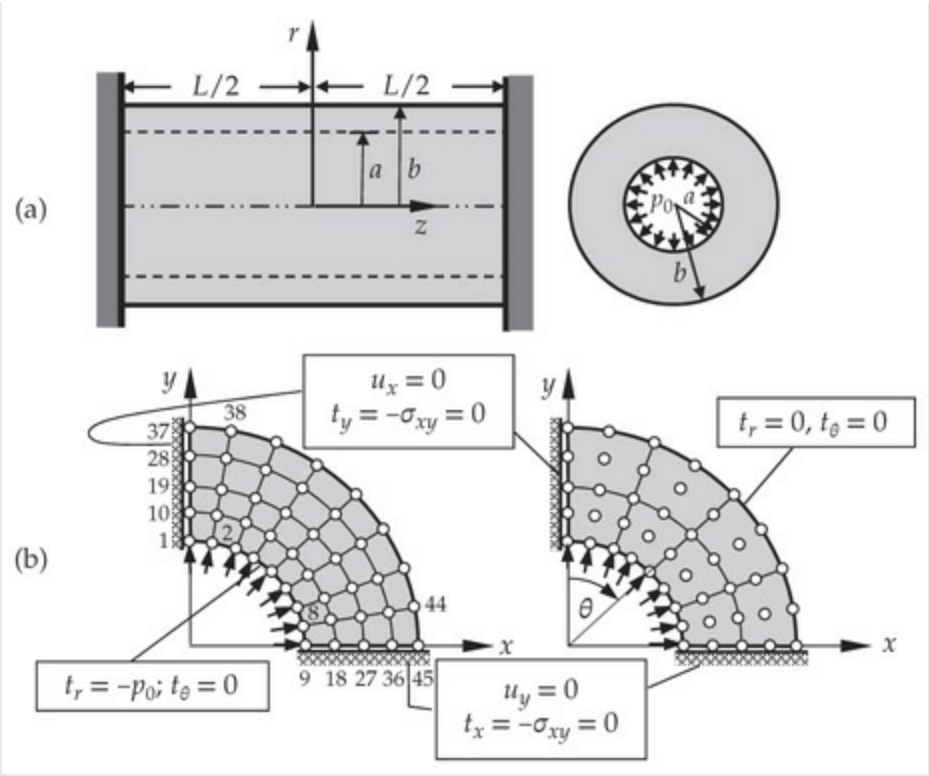

Fig. 12.6.3 A cylindrical pressure vessel.

Solution: Because of the geometry, material (isotropic), and boundary conditions, we find that the problem has symmetry about $z = 0$; but the plane $z = 0$ has exactly the same boundary conditions as the plane $z = \pm L/2$. Therefore, we find that the problem has symmetry about $z = L/4$. This way, it is clear that we can consider any section of unit length of the cylinder to formulate the problem. Thus, it is a plane strain problem.

From the finite element analysis point of view, we can exploit the biaxial symmetry and use a quadrant as the computational domain (unit thickness into the plane of the paper). The boundary conditions of the computational domain are:

$$u_x(0,y) = 0,\ t_y(0,y) = -\sigma_{xy}(0,y) = 0; \quad u_y(x,0) = 0,\ t_x(x,0) = -\sigma_{xy}(x,0) = 0$$
$$t_r(a,\theta) = -p_0,\ t_\theta(a,\theta) = 0; \quad t_r(b,\theta) = 0,\ t_\theta(b,\theta) = 0 \tag{1}$$

where (r, θ) are the cylindrical coordinates.

Finite element meshes of 8 × 4 linear and 4 × 2 quadratic quadrilateral elements are shown in Fig. 12.6.3(b). The specified displacement boundary conditions are:

$$U_1 = U_{19} = U_{37} = U_{55} = U_{73} = 0; \quad U_{18} = U_{36} = U_{54} = U_{72} = U_{90} = 0 \tag{2}$$

The contribution of p_0 to the global nodes at $r = R_i$ is computed as

follows. For the linear mesh, the length of the boundary segment (on which p_0 acts) of a typical element is $h_e = a\,\Delta\theta_e$, where $\Delta\theta_e = \pi/(2 \times 8) = 0.19635$. Hence, the x and y components of forces at the nodes of the boundary segment are

$$f^e_{xi} = f^e_i \sin\theta_e, \quad f^e_{yi} = f^e_i \cos\theta_e, \quad f^e_i = \frac{p_0 h_e}{2} = 1963.4954 \text{ lb} \tag{3}$$

where θ_e is measured clockwise from the y-axis, as shown in Fig. 12.6.4(a). Therefore, the assembled nonzero force components are

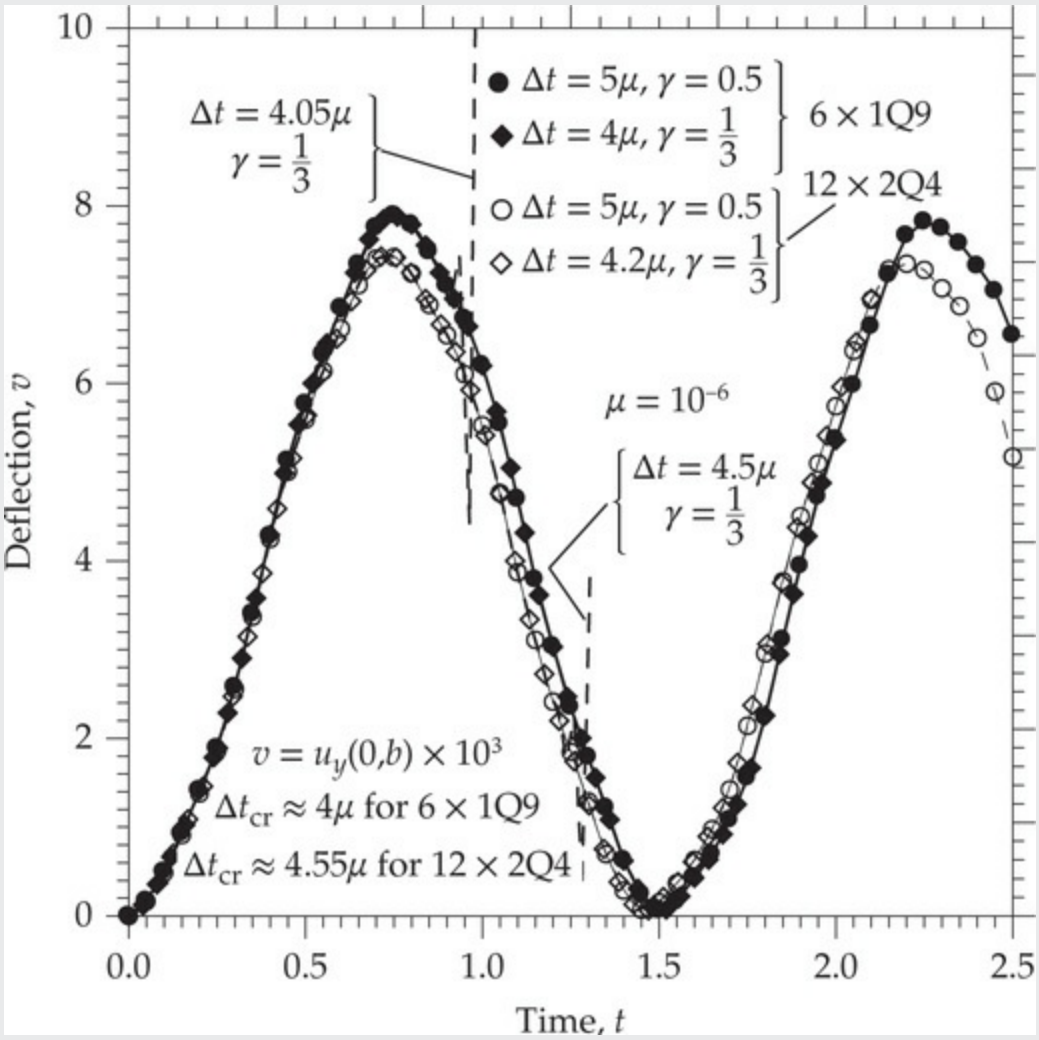

Fig. 12.6.4 The transient response of a cantilevered plate ($\mu = 10^{-6}$).

$$F^y_1 = 1963.5, \quad F^x_2 = 766.12, \quad F^y_2 = 3851.6, \quad F^x_3 = 1502.8, \quad F^y_3 = 3628, \quad F^x_4 = 2181.8$$
$$F^y_4 = 3265.2, \quad F^x_5 = 2766.8, \quad F^y_5 = 2776.8, \quad F^x_6 = 3265.2, \quad F^y_6 = 2181.8, \quad F^x_7 = 3628$$
$$F^y_7 = 1502.8, \quad F^x_8 = 3851.6, \quad F^y_8 = 766.12, \quad F^x_9 = 1963.5 \tag{4}$$

For the mesh of quadratic elements [$\Delta\theta_e = \pi/(2 \times 4) = 0.3927$], the x and y components of forces at the nodes of the boundary segment are

$$f_{xi}^e = f_i^e \sin\theta_e, \quad f_{yi}^e = f_i^e \cos\theta_e, \quad f_i^e = \frac{p_0 h_e}{6} = 1309.0 \text{ lb} \tag{5}$$

Thus, the nonzero force components are

$$F_1^y = 1309, \quad F_2^x = 1021.5, \quad F_2^y = 5135.4, \quad F_3^x = 1001.9, \quad F_3^y = 2418.7, \quad F_4^x = 2909$$
$$F_4^y = 4353.6, \quad F_5^x = 1851.2, \quad F_5^y = 1851.2, \quad F_6^x = 4353.6, \quad F_6^y = 2909, \quad F_7^x = 2418.7$$
$$F_7^y = 1001.9, \quad F_8^x = 5135.4, \quad F_8^y = 1021.5, \quad F_9^x = 1309 \tag{6}$$

The input data for the 8 × 4 mesh of linear rectangular elements (IELTYP = 1, NPE = 4) is presented in Box 12.6.5. The same input file is valid for the 4 × 2 mesh of nine-node quadratic rectangular elements (IELTYP = 2, NPE = 9). The difference between the two inputs is in the nodal forces. An edited output for 4 × 2 mesh of nine-node quadrilateral elements is presented in Box 12.6.6.

The problem has the exact solution (see Reddy [1]): the radial displacement u_r and radial stress σ_{rr} in the cylinder are given by

$$u_r = \frac{1}{2(\mu+\lambda)}\left(\frac{p_0 a^2}{b^2 - a^2}\right) r + \frac{a^2 b^2}{2\mu}\left(\frac{p_0}{b^2 - a^2}\right)\frac{1}{r} \tag{7}$$

$$\sigma_{rr} = \left(\frac{p_0 a^2}{b^2 - a^2}\right) - \left(\frac{p_0 a^2}{b^2 - a^2}\right)\frac{b^2}{r^2}, \quad \sigma_{\theta\theta} = \left(\frac{p_0 a^2}{b^2 - a^2}\right) + \left(\frac{p_0 a^2}{b^2 - a^2}\right)\frac{b^2}{r^2} \tag{8}$$

The finite element solution for the displacement $U_2 = U_{17}$ is in excellent agreement with the exact solution $u_r(a) = 0.19686 \times 10^{-2}$ in. The x and y components of stresses are related to the the radial and hoop stresses by (the exact values at $r = 0$ are $\sigma_{rr} = -2000$ psi and $\sigma_{\theta\theta} = 5200$ psi)

$$\sigma_{xx} = \sigma_{rr}\cos^2\theta + \sigma_{\theta\theta}\sin^2\theta, \quad \sigma_{yy} = \sigma_{rr}\sin^2\theta + \sigma_{\theta\theta}\cos^2\theta \tag{9}$$

For example, the exact values of the stresses at the location $(x, y) = (0.87776, 10.491)$ are $\sigma_{xx} = 4803$ psi and $\sigma_{yy} = -1603$ psi, whereas the values obtained using the 4 × 2 mesh of quadratic elements are $\sigma_{xx} = 4807$ psi and $\sigma_{yy} = -1604$ psi.

Box 12.6.5: The input file to program **FEM2D** for **Example 12.6.3**.

```
Example 12.6.3: Cylinder with internal pressure (8x4Q4)
    2   1   0   0                       ITYPE,IGRAD,ITEM,NEIGN
    2   9   0   0                       IELTYP,NPE,MESH,NPRNT
    8  45                               NEM NNM
    1    3   21   19    2   12   20   10   11
    3    5   23   21    4   14   22   12   13
    5    7   25   23    6   16   24   14   15
    7    9   27   25    8   18   26   16   17
   19   21   39   37   20   30   38   28   29
   21   23   41   39   22   32   40   30   31
   23   25   43   41   24   34   42   32   33
   25   27   45   43   26   36   44   34   35  NOD(I,J)

          0.00000E+00   0.10000E+02
          0.19509E+01   0.98079E+01
          0.38268E+01   0.92388E+01
          0.55557E+01   0.83147E+01
          0.70711E+01   0.70711E+01
          0.83147E+01   0.55557E+01
          0.92388E+01   0.38268E+01
          0.98079E+01   0.19509E+01
          0.10000E+02   0.0
          0.00000E+00   0.11250E+02
          0.21948E+01   0.11034E+02
          0.43052E+01   0.10394E+02
          0.62502E+01   0.93540E+01
          0.79550E+01   0.79550E+01
          0.93540E+01   0.62502E+01
          0.10394E+02   0.43052E+01
          0.11034E+02   0.21948E+01
          0.11250E+02   0.0
          0.00000E+00   0.12500E+02
          0.24386E+01   0.12260E+02
          0.47835E+01   0.11548E+02
          0.69446E+01   0.10393E+02
          0.88388E+01   0.88388E+01
          0.10393E+02   0.69446E+01
          0.11548E+02   0.47835E+01
          0.12260E+02   0.24386E+01
```

```
          0.12500E+02   0.0
          0.00000E+00   0.13750E+02
          0.26825E+01   0.13486E+02
          0.52619E+01   0.12703E+02
          0.76391E+01   0.11433E+02
          0.97227E+01   0.97227E+01
          0.11433E+02   0.76391E+01
          0.12703E+02   0.52619E+01
          0.13486E+02   0.26825E+01
          0.13750E+02   0.0
          0.00000E+00   0.15000E+02
          0.29264E+01   0.14712E+02
          0.57403E+01   0.13858E+02
          0.83336E+01   0.12472E+02
          0.10607E+02   0.10607E+02
          0.12472E+02   0.83336E+01
          0.13858E+02   0.57403E+01
          0.14712E+02   0.29264E+01
          0.15000E+02   0.0                      X(I), Y(I)
10                                                NSPV
1  1   10 1   19 1   28 1   37 1
9  2   18 2   27 2   36 2   45 2                  ISPV(I)
0.0     0.0    0.0    0.0    0.0
0.0     0.0    0.0    0.0    0.0                  VSPV(I)
16                                                NSSV
1  2    2  1    2  2    3  1    3  2
4  1    4  2    5  1    5  2    6  1    6  2
7  1    7  2    8  1    8  2    9  1              ISSV(I)
                  0.13090E+04
     0.10215E+04   0.51354E+04
     0.10019E+04   0.24187E+04
     0.29090E+04   0.43536E+04
     0.18512E+04   0.18512E+04
     0.43536E+04   0.29090E+04
     0.24187E+04   0.10019E+04
     0.51354E+04   0.10215E+04
     0.13090E+04                                  VSPV(I)
0                                                 LNSTRS
28.0E06 28.0E06 0.3 10.76923E06 1.0     E1,E2,ANU12,G12,THKNS
 0.0     0.0    0.0                       F0, FX, FY
```

Box 12.6.6: Edited output from program **FEM2D** for **Example 12.6.3**.

```
        OUTPUT  from  program *** FEM2D *** by J. N. REDDY

            A  2-D  ELASTICITY   PROBLEM  IS  ANALYZED

MATERIAL PROPERTIES OF THE SOLID ANALYZED:

   Thickness of the body, THKNS .............=  0.1000E+01
   Modulus of elasticity, E1 ................=  0.2800E+08
   Modulus of elasticity, E2 ................=  0.2800E+08
   Poisson s ratio, ANU12 ...................=  0.3000E+00
   Shear modulus, G12 .......................=  0.1077E+08
    **PLANE STRAIN assumption is selected by user**

CONTINUOUS SOURCE COEFFICIENTS:

   Coefficient, F0  .........................=  0.0000E+00
   Coefficient, FX  .........................=  0.0000E+00
   Coefficient, FY  .........................=  0.0000E+00

   ******* A STEADY-STATE PROBLEM is analyzed *******

   *** A mesh of QUADRILATERALS is chosen by user ***

FINITE ELEMENT MESH INFORMATION:

   Element type: 0 = Triangle; >0 = Quad.)..=   2
   Number of nodes per element, NPE .........=   9
   No. of primary deg. of freedom/node, NDF =   2
   Number of elements in the mesh, NEM .....=   8
   Number of nodes in the mesh, NNM .........=  45
   Number of equations to be solved, NEQ ...=  90
   Half bandwidth of the matrix GLK, NHBW ..=  42
   No. of specified PRIMARY variables, NSPV =  10
   No. of speci.  SECONDARY variables, NSSV =  16
 Node  DOF     Value
    1   2   0.13090E+04
    2   1   0.10215E+04
    2   2   0.51354E+04
    3   1   0.10019E+04
    3   2   0.24187E+04
    4   1   0.29090E+04
    4   2   0.43536E+04
```

```
         5   1   0.18512E+04
         5   2   0.18512E+04
         6   1   0.43536E+04
         6   2   0.29090E+04
         7   1   0.24187E+04
         7   2   0.10019E+04
         8   1   0.51354E+04
         8   2   0.10215E+04
         9   1   0.13090E+04

    NUMERICAL INTEGRATION DATA:
       Full quadrature (IPDF x IPDF) rule, IPDF =   3
       Reduced quadrature (IPDR x IPDR),   IPDR =   2
       Quadrature rule used in postproc.,  ISTR =   2

    S O L U T I O N :
    Node    x-coord.      y-coord.     Value of u_x   Value of u_y
      1   0.00000E+00   0.10000E+02   0.00000E+00    0.19669E-02
      2   0.19509E+01   0.98079E+01   0.38421E-03    0.19315E-02
      3   0.38268E+01   0.92388E+01   0.75271E-03    0.18172E-02
      4   0.55557E+01   0.83147E+01   0.10941E-02    0.16375E-02
      5   0.70711E+01   0.70711E+01   0.13908E-02    0.13908E-02
      6   0.83147E+01   0.55557E+01   0.16375E-02    0.10941E-02
      7   0.92388E+01   0.38268E+01   0.18172E-02    0.75271E-03
      8   0.98079E+01   0.19509E+01   0.19315E-02    0.38421E-03
      9   0.10000E+02   0.00000E+00   0.19669E-02    0.00000E+00
     10   0.00000E+00   0.11250E+02   0.00000E+00    0.18195E-02

  x-coord.      y-coord.      sigma-x       sigma-y       sigma-xy
0.87776E+00   0.10491E+02   0.4807E+04   -0.1604E+04   -0.5305E+03
0.99808E+00   0.11930E+02   0.4075E+04   -0.8773E+03   -0.4146E+03
0.32039E+01   0.10029E+02   0.4243E+04   -0.1040E+04   -0.1891E+04
0.36431E+01   0.11404E+02   0.3643E+04   -0.4453E+03   -0.1458E+04
0.48258E+01   0.93569E+01   0.3493E+04   -0.2901E+03   -0.2642E+04
0.54873E+01   0.10639E+02   0.3057E+04    0.1413E+03   -0.2044E+04
0.67978E+01   0.80391E+01   0.2132E+04    0.1071E+04   -0.3205E+04
0.77297E+01   0.91411E+01   0.2014E+04    0.1185E+04   -0.2476E+04
0.80391E+01   0.67978E+01   0.1071E+04    0.2132E+04   -0.3205E+04
0.91411E+01   0.77297E+01   0.1185E+04    0.2014E+04   -0.2476E+04
0.93569E+01   0.48258E+01  -0.2901E+03    0.3493E+04   -0.2642E+04
0.10639E+02   0.54873E+01   0.1413E+03    0.3057E+04   -0.2044E+04
0.10029E+02   0.32039E+01  -0.1040E+04    0.4243E+04   -0.1891E+04
0.11404E+02   0.36431E+01  -0.4453E+03    0.3643E+04   -0.1458E+04
0.10491E+02   0.87776E+00  -0.1604E+04    0.4807E+04   -0.5305E+03
0.11930E+02   0.99808E+00  -0.8773E+03    0.4075E+04   -0.4146E+03
```

Now suppose that the cylinder is replaced with a hollow disc of internal radius a = 10 in., external radius b = 15 in., and thickness h = 0.1 in., and subjected to internal pressure (say, due to shrink fit) p_0 psi. Then the problem becomes one of plane stress. The input data file for the problem remains the same, with the exception of thickness being 0.1 in. and LNSTRS = 1. The exact value of the radial displacement is u_r (a, θ) = 0.02071 in. The values obtained with the linear and quadratic meshes are 0.02075 in. and 0.02070 in., respectively.

The last example of this chapter deals with free vibration and transient analysis of the cantilevered plate of **Example 12.6.2**.

Example 12.6.4

Consider the cantilever beam shown in Fig. 12.6.2(a). Determine the transient response using meshes of (a) 12 × 2Q4 and (b) 6 × 1Q9 elements with the linear acceleration (α = 0.5 and γ = 1/3) and constant average acceleration (α = 0.5 and γ = 1/2) schemes. Use a mass density of ρ = 15.2 slugs/ft^3 = 7.3302 × 10^{-4} lb-s/in^4 (a slug is equal to lb-s/ft) and zero initial conditions on the displacement and velocity.

Solution: The linear acceleration scheme has a time step restriction of

$$\Delta t < \Delta t_{cri} = \sqrt{\frac{12}{\lambda_{\max}}} \tag{1}$$

Therefore, first we determine the value of the critical time step by conducting free vibration analysis to find the maximum eigenvalue λ_{max} for the two meshes. Box 12.6.7 contains the input data for the eigenvalue analysis for the 12 × 2Q4 mesh. The maximum eigenvalues obtained for the 12 × 2Q4 and 6 × 1Q9 meshes are λ_{max} = 604662.4 × 10^6 and λ_{max} = 750440.3 × 10^6, respectively. Hence, the critical time steps for the two meshes are Δ_{cr} = 4.4548 × 10^{-6} and Δ_{cr} = 3.9988 × 10^{-6}, respectively. The input data for the transient analysis is presented in Box 12.6.8.

Box 12.6.7: Input file for natural vibration (**Example 12.6.4**).

```
Example 12.6.4: Natural vibration of a cantilevered plate
   2   0   2   1                      ITYPE,IGRAD,ITEM,NEIGN
   33  0                              NVALU,NVCTR
   1   4   1   0                      IELTYP,NPE,MESH,NPRNT
  12   2                                        NX, NY
   0.0  1.0  1.0  1.0  1.0  1.0  1.0
        1.0  1.0  1.0  1.0  1.0  1.0            X0,DX(I)
   0.0  1.5  1.5                               Y0,DY(I)
   6                                           NSPV
   13  1  13  2  26 1   26 2   39 1  39 2      ISPV
   1                                           LNSTRS
   30.0E06 30.0E06 0.25 12.0E06 0.1     E1,E2,ANU12,G12,THKNS
    7.3302E-04  0.0    0.0                     C0, CX, CY
```

Figure 12.6.4 contains plots of the tip deflection $v \equiv u_y\,(0, b, t) \times 10^3$ versus time $t \times 10^3$ as predicted by the 12 × 2 Q4 and 6 × 1 Q9 meshes of rectangular elements and the two time approximation schemes: (1) $\alpha = \gamma = \frac{1}{2}$ and (2) $\alpha = \frac{1}{2}$ and $\gamma = \frac{1}{3}$. When the time step used is slightly greater than the critical time step for a mesh, the solution is stable for the first several time steps but it eventually becomes unstable for the linear acceleration scheme. For constant average acceleration scheme (which is stable), a larger time step (than the critical) yields stable and accurate solutions.

Box 12.6.8: Input file for natural vibration (**Example 12.6.4**).

```
Example 12.6.4: Transient analysis of a cantilevered plate
  2   1   2   0                                ITYPE,IGRAD,ITEM,NEIGN
  1   4   1   0                                IELTYP,NPE,MESH,NPRNT
 12   2                                        NX, NY
  0.0  1.0  1.0  1.0  1.0  1.0  1.0
       1.0  1.0  1.0  1.0  1.0  1.0            X0,DX(I)
  0.0  1.5  1.5                                Y0,DY(I)
  6                                            NSPV
  13 1  13 2  26 1  26 2  39 1  39 2           ISPV
  0.0   0.0   0.0   0.0   0.0   0.0           VSPV
  3                                            NSSV
  1  2   14  2  27  2                         ISSV
  11.25  22.5   11.25                         VSSV
  1                                            LNSTRS
  30.0E06  30.0E06  0.25  12.0E06  0.1        E1,E2,ANU12,G12,THKNS
  0.0  0.0  0.0                                F0, FX, FY
  7.3302E-04  0.0   0.0                        C0, CX, CY
  500  501  100   0                           NTIME,NSTP,INTVL,INTIAL
  4.2E-06 0.5 0.33333333 1.0E-6              DT,ALFA,GAMA,EPSLN
```

12.7 Summary

In this chapter equations of linearized two-dimensional problems of elasticity are introduced and their finite element models are formulated. The plane strain and plane stress problems, which differ only in the use of constitutive relations, are discussed. The governing equations are expressed in terms of the displacements, and their weak form and finite element model are developed in two alternative ways:

1. The vector/matrix formulation ($\mathbf{B}^T\mathbf{C}\mathbf{B}$) using the principle of virtual displacements, which is most common in finite element books on solid and structural mechanics.
2. The weak-form formulation, which is used throughout the book.

Linear and quadratic triangular and rectangular elements for plane elasticity are presented. Shear locking that occurs in the case of linear elements is discussed. The eigenvalue and time-dependent problems of plane elasticity are also presented. Several numerical examples are presented to illustrate the evaluation of element stiffness matrices and load

vectors and solution by the FEM2D program.

Problems

IDENTIFICATION OF BOUNDARY CONDITIONS AND LOADS

12.1 Show that the plane strain stress–strain constitutive relations for an orthotropic material are given by those in Eqs. (12.2.4a) and (12.2.4b).

12.2–12.4 Compute the contribution of the boundary forces to the global force DOF in the plane stress elasticity problems given in Figs. P12.2–P12.4. Give nonzero forces for at least two global nodes. *Answer for Problem 12.2*: $F_7^x = h\left(\frac{17p_1 + p_0}{72}\right)$ and $F_{14}^x = h\left(\frac{5p_1 + p_0}{12}\right)$.

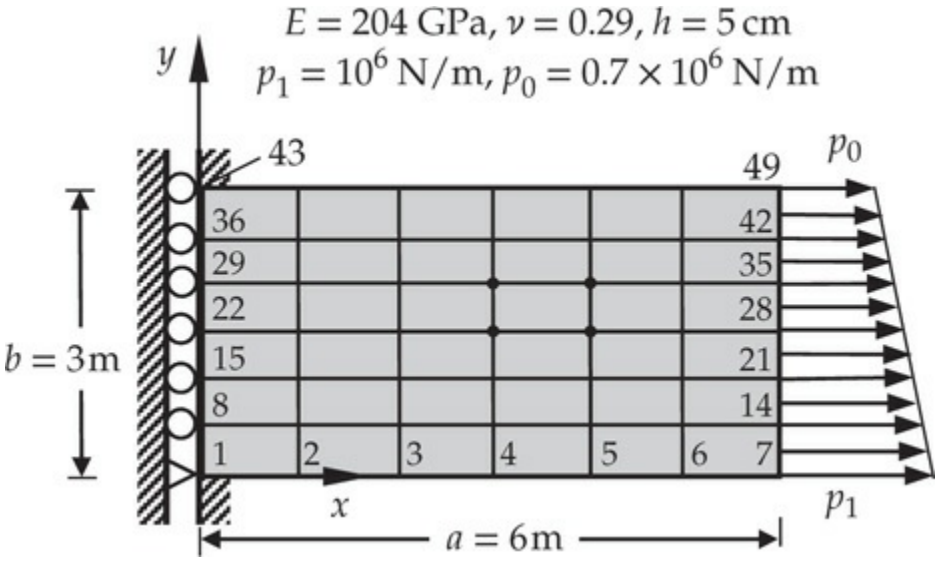

Fig. P12.2

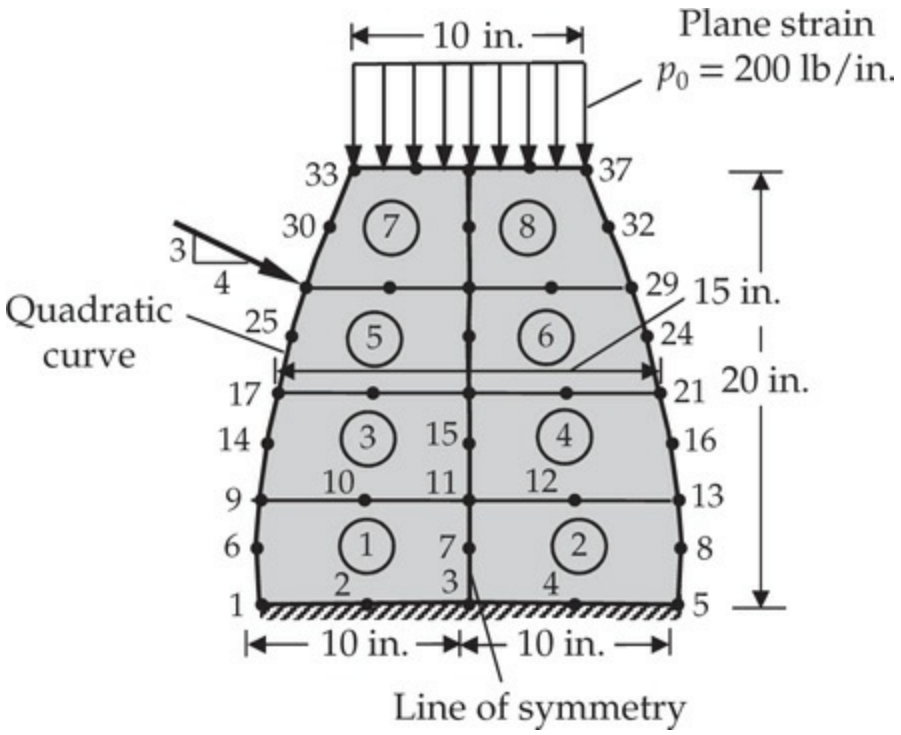

Fig. P12.3

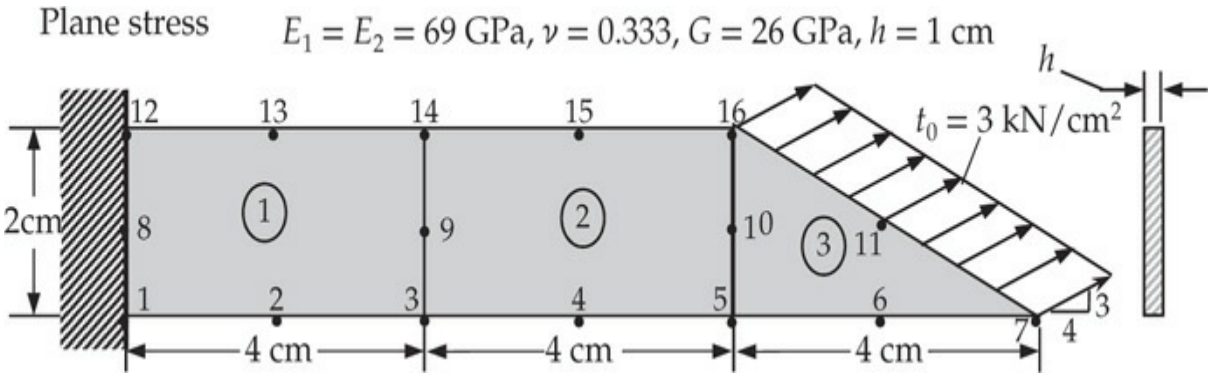

Fig. P12.4

12.5–12.7 Give the connectivity matrices and the specified primary degrees of freedom for the plane elasticity problems given in Figs. P12.2–P12.4. Give only the first three rows of the connectivity matrix.

12.8 Consider the cantilevered beam of length 6 cm, height 2 cm, thickness 0.2 cm, and material properties $E = 3 \times 10^7$ N/cm^2 and $\nu = 0.3$, and subjected to a bending moment of 600 N-cm at the free end, as shown in Fig. P12.8. Replace the moment by an equivalent distributed force at $x = 6$ cm, and model the domain by a nonuniform 10×4 mesh of linear rectangular elements. Identify the specified displacements

and global forces. *Answer:* $F_{11}^x = -37.5$ N and $F_{22}^x = -45$ N.

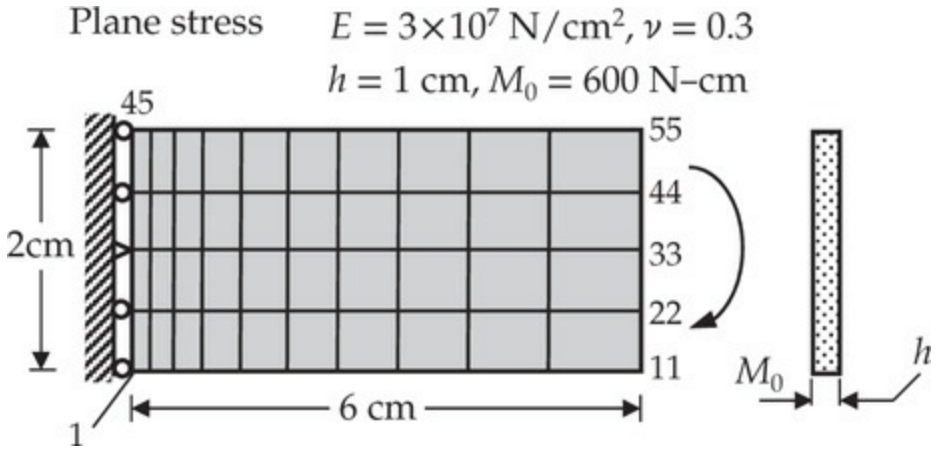

Fig. P12.8

12.9 Consider the ("transition") element shown in Fig. P12.9. Define the generalized displacement vector of the element by $\{u\} = \{u_1, v_1, \theta_1, u_2, v_2, u_3, v_3\}^T$ and represent the displacement components u and v by

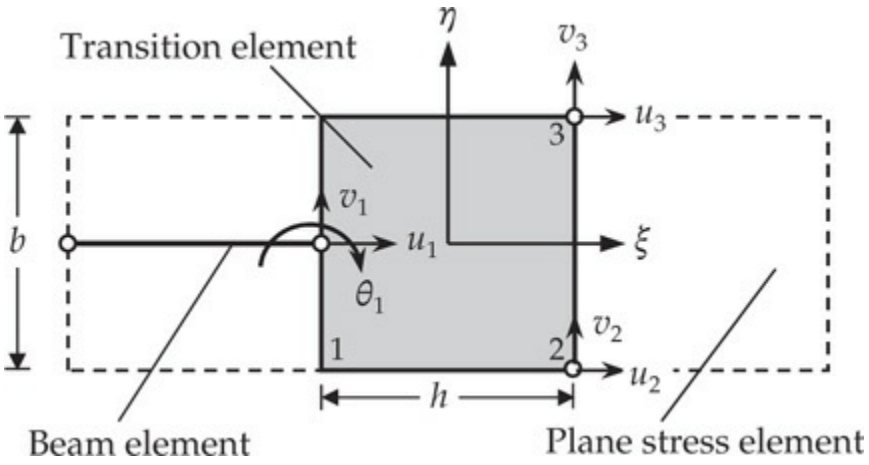

Fig. P12.9

$$u = \psi_1 u_1 + \psi_2 u_2 + \psi_3 u_3 + \frac{h}{2}\eta\psi_1\theta_1, \quad v = \psi_1 v_1 + \psi_2 v_2 + \psi_3 v_3$$

where ψ_1 is the interpolation function for the beam, and ψ_2 and ψ_3 are the interpolation functions for nodes 2 and 3:

$$\psi_1 = \frac{1}{2}(1-\xi), \quad \psi_2 = \frac{1}{4}(1+\xi)(1-\eta), \quad \psi_3 = \frac{1}{4}(1+\xi)(1+\eta)$$

Derive the stiffness matrix for the element.

12.10 Consider a square, isotropic, elastic body of thickness h shown in Fig. P12.10. Suppose that the displacements are approximated by

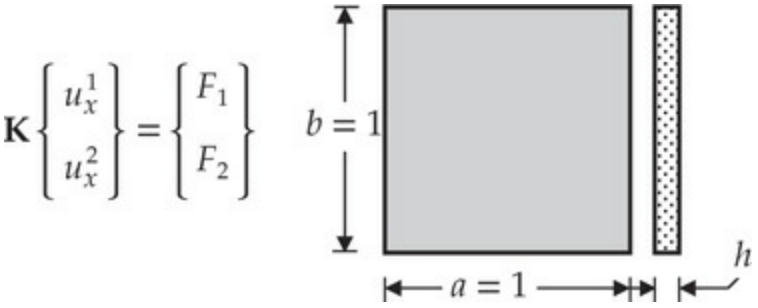

Fig. P12.10

$$u_x(x,y) = (1-x)yu_x^1 + x(1-y)u_x^2, \quad u_y(x,y) = 0$$

Assuming that the body is in a plane state of stress, derive the 2 × 2 stiffness matrix for the unit square.

12.11–12.15 For the plane stress elasticity problems shown in Figs. P12.11–P12.15, give the boundary degrees of freedom and compute the contribution of the specified forces to the nodes. *Answer for Problem 12.11:* $F_{37}^y = -37.5$ kN and $F_{38}^y = -75$ kN.

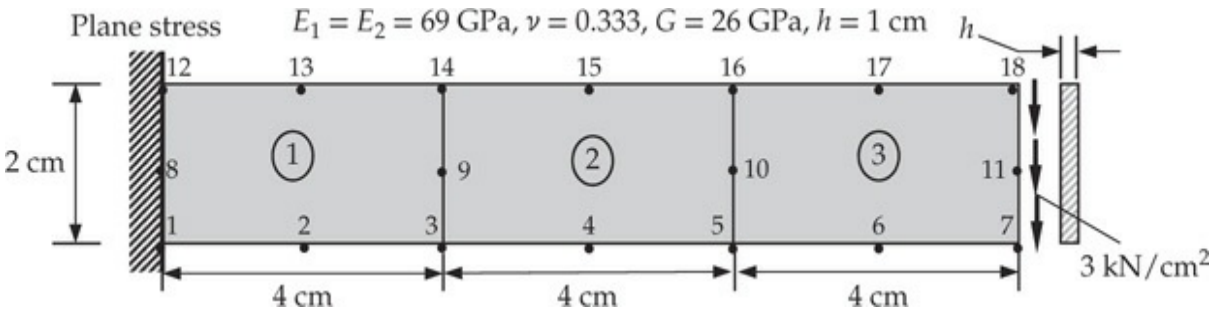

Fig. P12.11

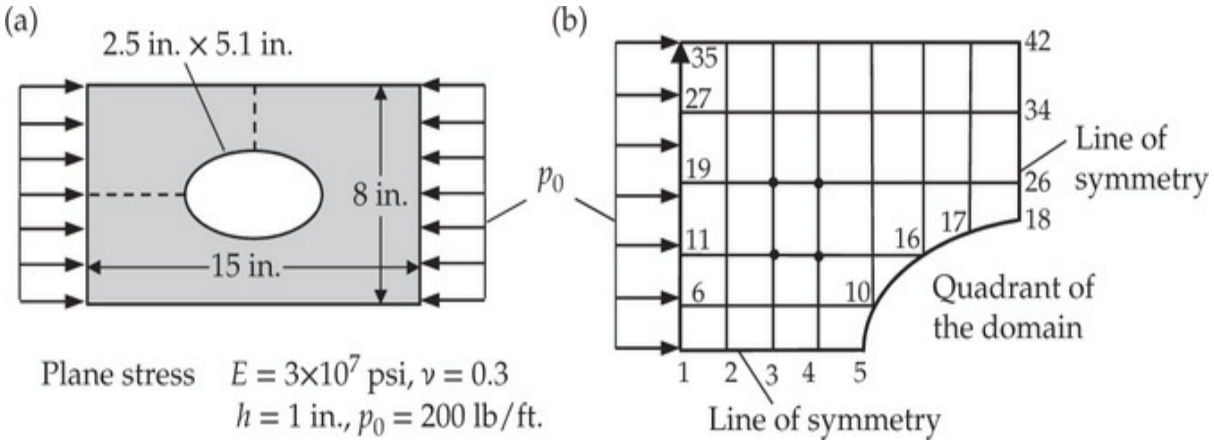

Fig. P12.12

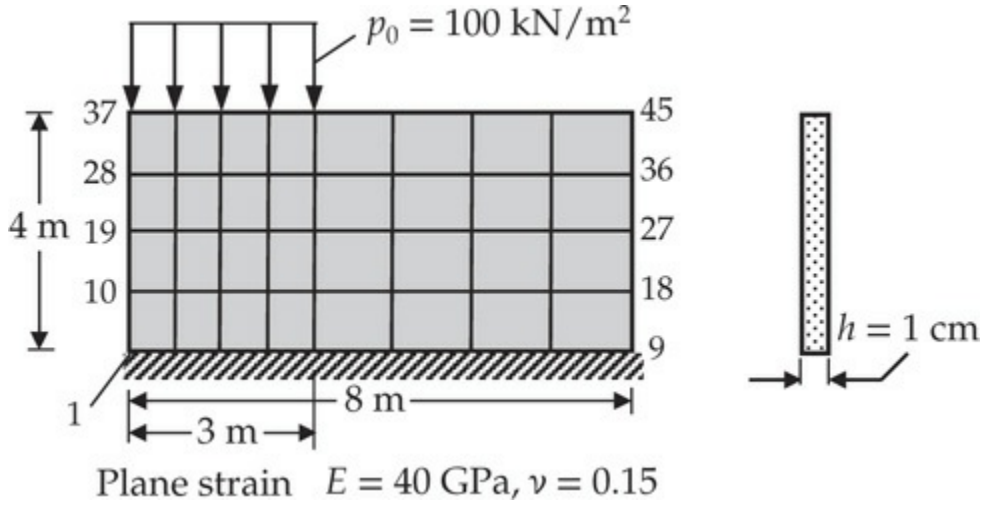

Fig. P12.13

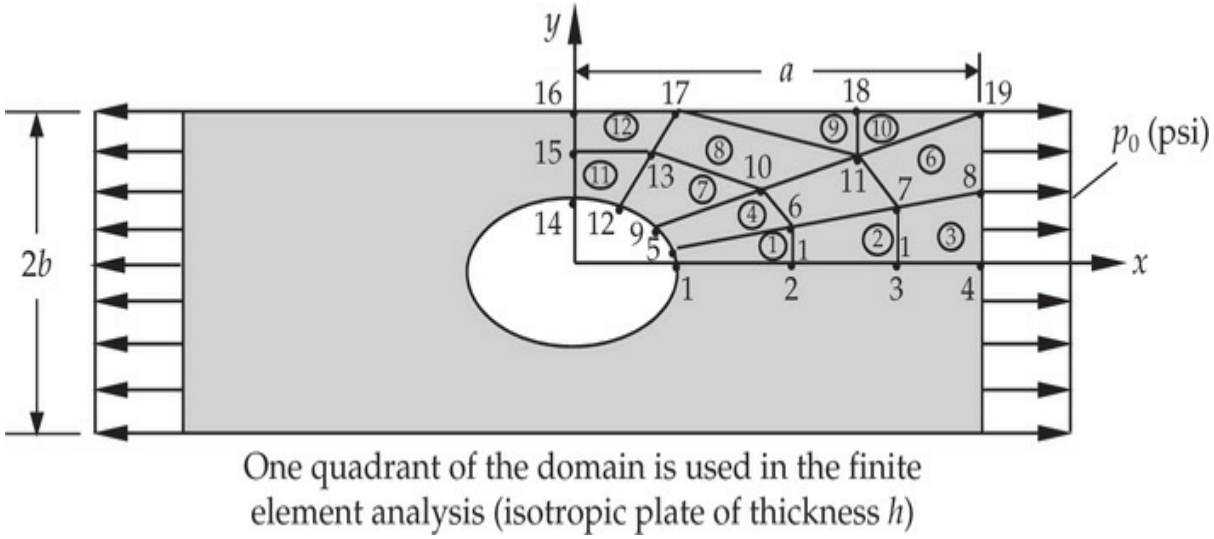

Fig. P12.14

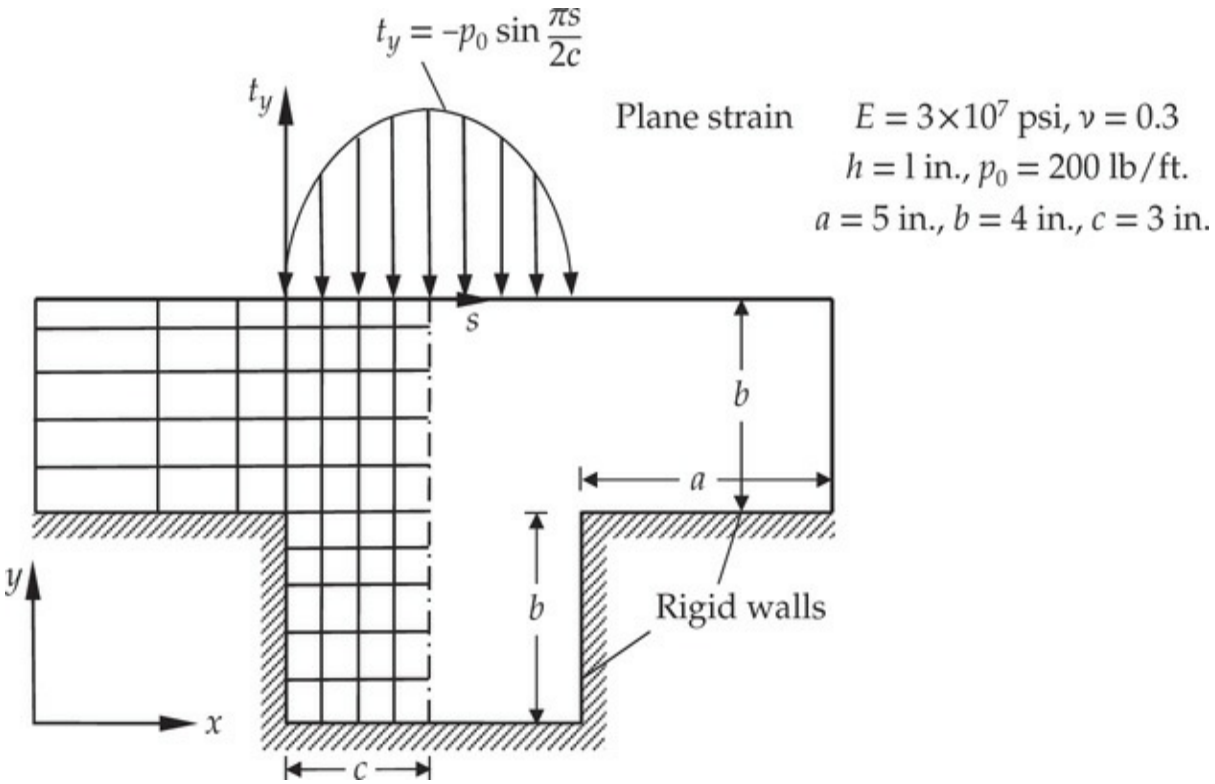

Fig. P12.15

12.16 Analyze the plane elasticity (plane stress) problem in Fig. P12.2 for displacements and stresses with the mesh shown.

12.17 Repeat **Problem 12.16** using the equivalent mesh of triangular elements.

12.18 Repeat **Problem 12.16** using nodally equivalent mesh of quadratic quadrilateral elements.

12.19 Repeat **Problem 12.16** using nodally equivalent mesh of quadratic triangular elements.

12.20 Analyze the plane elasticity problem shown in Fig. P12.11 for displacements and stresses.

12.21 Analyze the plane elasticity problem in Fig. P12.11 for natural frequencies. Use a density of $\rho = 0.0088$ kg/cm^3.

12.22 Analyze the plane elasticity problem in Fig. P12.11 for the transient response. Use $\alpha = \frac{1}{2}, \gamma = \frac{1}{2}$, and $\Delta t = 10^{-5}$. Assume zero initial conditions.

References for Additional Reading

1. J. N. Reddy, *An Introduction to Continuum Mechanics*, 2nd ed.,

Cambridge University Press, New York, NY, 2013.

2. J. N. Reddy, *Energy Principles and Variational Methods in Applied Mechanics*, 3rd ed., John Wiley & Sons, New York, NY, 2017.
3. J. Barlow, "Optimal Stress Locations in Finite Element Models," *International Journal for Numerical Methods in Engineering*, **10**, 243–251, 1976.
4. J. Barlow, "More on Optimal Stress Points—Reduced Integration Element Distortions and Error Estimation," *International Journal for Numerical Methods in Engineering*, **28**, 1487–1504, 1989.
5. M. Vaz, Jr., P.A. Muñoz-Rojas, and G. Filippini, "On the Accuracy of Nodal Stress Computation in Plane Elasticity using Finite Volumes and Finite Elements," *Computers and Structures*, 87(17–18):1044–1057, 2009.
6. R. G. Budynas, *Advanced Strength and Applied Stress Analysis*, McGraw-Hill, New York, NY, 1977.
7. J. N. Reddy and M. L. Rasmussen, *Advanced Engineering Analysis*, John Wiley & Sons, New York, NY, 1982.
8. K. Rektorys, *Variational Methods in Mathematics, Science and Engineering*, D. Reidel Publishing, Boston, MA, 1980.
9. K. Rektorys, *The Method of Discretization in Time*, D. Reidel Publishing, Boston, MA, 1982.
10. W. S. Slaughter, *The Linearized Theory of Elasticity*, Birkhäuser, Boston, MA, 2002.
11. S. P. Timoshenko and J. N. Goodier, *Theory of Elasticity*, 3rd ed., McGraw-Hill, New York, NY, 1970.
12. A. C. Ugural and S. K. Fenster, *Advanced Strength and Applied Elasticity*, American Elsevier, New York, NY, 1975.
13. E. Volterra and J. H. Gaines, *Advanced Strength of Materials*, Prentice-Hall, Engelwood Cliffs, NJ, 1971.

13 3-D Finite Element Analysis

I do not feel obliged to believe that the same God who has endowed us with sense, reason, and intellect has asked us to forgo their use.

— Galileo Galilei

13.1 Introduction

The introduction to the finite element method presented in the preceding chapters is sufficient to provide the essential background for the development of finite element models and the associated computer programs for most linear boundary, initial, and eigenvalue problems in one and two dimensions. The background should also help one to intelligently use commercially available finite element software. The determination of temperature distributions, effects of flows around and inside bodies, and stress distributions in complex geometries has become a routine part of engineering analysis, due in large part to the finite element method and availability of general purpose computer programs.

The physical problems considered here involve general three-dimensional geometries. As in the case of two-dimensional problems, a three-dimensional region Ω (see Fig. 13.1.1) is discretized into an appropriate collection of finite elements. As an example, two-dimensional and corresponding three-dimensional finite element discretizations are presented in Fig. 13.1.2. The admissible geometries of finite elements in three dimensions are basically extensions of two-dimensional elements to three dimensions. However in three dimensions, element geometries include combinations of triangular and quadrilateral shapes to form three-dimensional geometries, as illustrated in Fig. 13.1.3. More details of three-dimensional elements will be presented in Section 13.5.

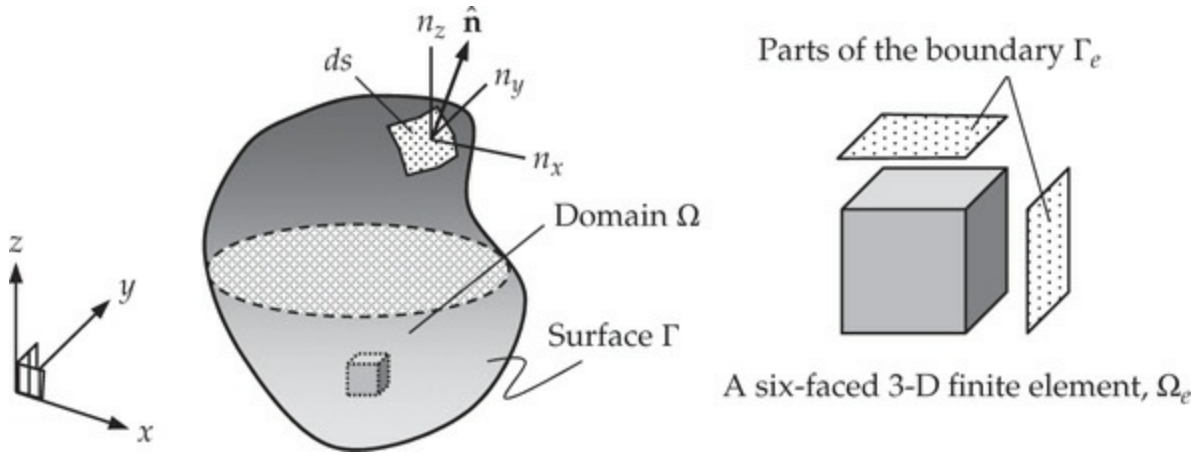

Fig. 13.1.1 A three-dimensional domain Ω, its boundary Γ with unit normal $\hat{\mathbf{n}}$, and a typical three-dimensional finite element.

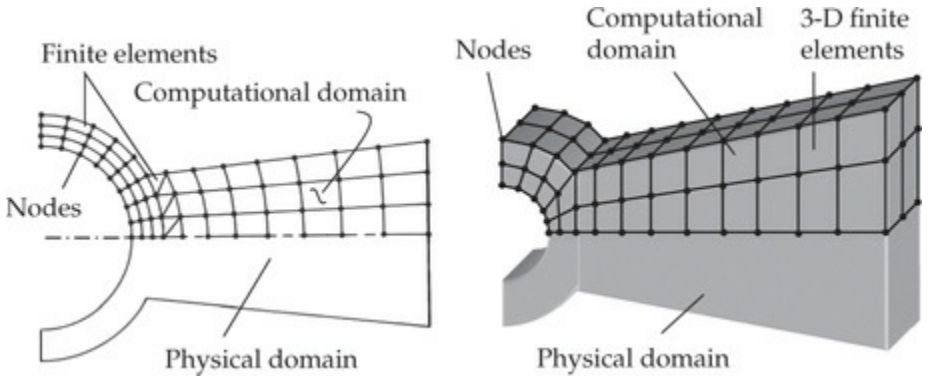

Fig. 13.1.2 Finite element discretization of a (a) two-dimensional domain and (b) three-dimensional domain.

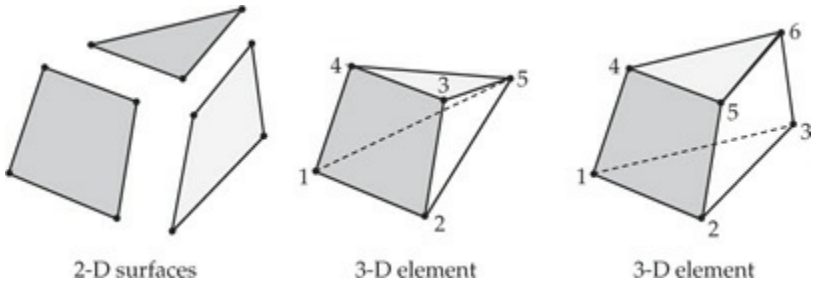

Fig. 13.1.3 Three-dimensional finite elements built from two-dimensional geometries.

In the remainder of the chapter, we discuss extensions of the developments presented in Chapters 9–12 to three dimensions to familiarize the reader with the governing equations, weak forms, and finite element models of heat transfer (and related diffusion) problems, flows of viscous incompressible fluids, and stress and deformation in three dimensions. Only the rectangular Cartesian coordinate system (x, y, z) is

used to write the governing equations and develop finite element models.

13.2 Heat Transfer

13.2.1 Preliminary Comments

In this section we present the finite element analysis of 3-D conduction heat transfer (and related diffusion type problems). Conduction heat transfer plays a major role in industrial design and manufacturing of thermal systems. The conduction problem also provides a convenient framework to discuss various advanced aspects of the finite element method and numerical algorithms. The introduction to the finite element method presented in Chapter 3 aids the development presented here for the general 3-D heat conduction problem.

13.2.2 Governing Equations

Heat transfer in 3-D orthotropic (with principal material coordinates assumed to coincide with the x, y, and z coordinates) solids is governed by

$$\rho c_v \frac{\partial T}{\partial t} - \frac{\partial}{\partial x}\left(k_x \frac{\partial T}{\partial x}\right) - \frac{\partial}{\partial y}\left(k_y \frac{\partial T}{\partial y}\right) - \frac{\partial}{\partial z}\left(k_z \frac{\partial T}{\partial z}\right) = g \text{ in } \Omega \text{ for } t > 0 \qquad (13.2.1)$$

where (k_x, k_y, k_z) denote conductivities in the x, y, and z directions, respectively, ρ is the mass density, c_v is the specific heat at constant volume, T is the temperature, and g is the internal heat generation per unit volume. The boundary conditions are of the form (for any time t)

$$T = \hat{T} \quad \text{on} \quad \Gamma_1, \quad k_x \frac{\partial T}{\partial x} n_x + k_y \frac{\partial T}{\partial y} n_y + k_z \frac{\partial T}{\partial z} n_z + \beta(T - T_\infty) = \hat{q} \quad \text{on} \quad \Gamma_2 \qquad (13.2.2)$$

where $\hat{T}$ and $\hat{q}$ are specified functions of position on the portions Γ_1 and Γ_2, respectively, of the surface Γ of the domain Ω (see Fig. 13.1.1); β is the convection coefficient and T_∞ is the ambient temperature. The boundary segments Γ_1 and Γ_2 are such that their union is the total boundary Γ and their intersection is null. The initial condition is

$$T(x, y, z, 0) = T_0(x, y, z) \text{ for any } (x, y, z) \text{ in } \Omega \qquad (13.2.3)$$

13.2.3 Weak Form

Suppose that the domain Ω is divided into a set of finite elements Ω_e with closed boundary Γ_e. The specific shapes of finite elements in 3-D will be discussed in the sequel. Let T_h^e be the finite element approximation of T over the element Ω_e. The weak form of Eq. (13.2.1) over a three-dimensional finite element Ω_e is obtained using the usual three-step procedure. We obtain (the element label "e" is inserted to imply that all quantities are defined over the element only)

$$
\begin{aligned}
0 &= \int_{\Omega_e} w_i^e \left[\rho_e c_v^e \frac{\partial T_h^e}{\partial t} - \frac{\partial}{\partial x}\left(k_x^e \frac{\partial T_h^e}{\partial x}\right) - \frac{\partial}{\partial y}\left(k_y^e \frac{\partial T_h^e}{\partial y}\right) - \frac{\partial}{\partial z}\left(k_z^e \frac{\partial T_h^e}{\partial z}\right) - g_e \right] dv \\
&= \int_{\Omega_e} \left(\rho_e c_v^e w_i^e \frac{\partial T_h^e}{\partial t} + k_x^e \frac{\partial w_i^e}{\partial x}\frac{\partial T_h^e}{\partial x} + k_y^e \frac{\partial w_i^e}{\partial y}\frac{\partial T_h^e}{\partial y} + k_z^e \frac{\partial w_i^e}{\partial z}\frac{\partial T_h^e}{\partial z} - w_i^e g_e \right) dv \\
&\quad - \oint_{\Gamma^e} w_i^e \left(k_x^e \frac{\partial T_h^e}{\partial x} n_x + k_y^e \frac{\partial T_h^e}{\partial y} n_y + k_z^e \frac{\partial T_h^e}{\partial z} n_z \right) ds \\
&= \int_{\Omega_e} \left(\rho_e c_v^e w_i^e \frac{\partial T_h^e}{\partial t} + k_x \frac{\partial w_i^e}{\partial x}\frac{\partial T_h^e}{\partial x} + k_y \frac{\partial w_i^e}{\partial y}\frac{\partial T_h^e}{\partial y} + k_z \frac{\partial w_i^e}{\partial z}\frac{\partial T_h^e}{\partial z} - w_i^e g_e \right) dv \\
&\quad + \oint_{\Gamma^e} \beta_e w_i^e T_h^e \, ds - \oint_{\Gamma^e} w_i^e \left(\hat{q}_n^e + \beta_e T_\infty^e \right) ds
\end{aligned}
\tag{13.2.4}
$$

where w_i^e is a set of weight functions, which will be replaced, in the weak-form Galerkin model, by the interpolation functions ψ_i^e used to approximate T by T_h^e over Ω_e. We note that the convection on the boundary of the element is included.

13.2.4 Finite Element Model

We assume a finite element interpolation of the form

$$
T(x,y,z,t) \approx T_h^e(x,y,z,t) = \sum_{j=1}^{n} T_j^e(t)\psi_j^e(x,y,z) \tag{13.2.5}
$$

over the element Ω_e. Substituting $w_i = \psi_i^e$ and Eq. (13.2.5) into Eq. (13.2.4), we obtain the finite element model

$$\mathbf{M}^e\dot{\mathbf{T}}^e + \mathbf{K}^e\mathbf{T}^e = \mathbf{f}^e + \mathbf{Q}^e \equiv \mathbf{F}^e \tag{13.2.6}$$

where

$$M_{ij}^e = \int_{\Omega_e} \rho_e c_v^e \psi_i^e \psi_j^e \, d\Omega_e$$

$$K_{ij}^e = \int_{\Omega_e} \left(k_x^e \frac{\partial \psi_i^e}{\partial x}\frac{\partial \psi_j^e}{\partial x} + k_y^e \frac{\partial \psi_i^e}{\partial y}\frac{\partial \psi_j^e}{\partial y} + k_z^e \frac{\partial \psi_i^e}{\partial z}\frac{\partial \psi_j^e}{\partial z} \right) d\Omega_e + \oint_{\Gamma^e} \beta_e \psi_i^e \psi_j^e \, d\Gamma_e$$

$$f_i^e = \int_{\Omega_e} f\psi_i^e \, d\Omega_e, \quad Q_i^e = \oint_{\Gamma^e} (\hat{q}_n^e + \beta_e T_\infty^e)\psi_i^e \, d\Gamma_e \tag{13.2.7}$$

Note that the boundary Γ_e of a three-dimensional element is a collection of surface (i.e., two-dimensional) elements, as shown in Fig. 13.1.3. Numerical integration of volume and surface integrals is carried out in the same way as described in Chapter 10. Additional information is presented in Section 13.5.

13.3 Flows of Viscous Incompressible Fluids

13.3.1 Governing Equations

Here we develop the penalty finite element model of the Stokes equations governing three-dimensional flows of incompressible fluids. The governing equations consist of three momentum equations and a continuity equation:

$$\rho\frac{\partial v_x}{\partial t} - 2\mu\frac{\partial^2 v_x}{\partial x^2} - \mu\frac{\partial}{\partial y}\left(\frac{\partial v_x}{\partial y} + \frac{\partial v_y}{\partial x}\right) - \mu\frac{\partial}{\partial z}\left(\frac{\partial v_x}{\partial z} + \frac{\partial v_z}{\partial x}\right) + \frac{\partial P}{\partial x} - f_x = 0 \tag{13.3.1}$$

$$\rho\frac{\partial v_y}{\partial t} - 2\mu\frac{\partial^2 v_y}{\partial y^2} - \mu\frac{\partial}{\partial x}\left(\frac{\partial v_x}{\partial y} + \frac{\partial v_y}{\partial x}\right) - \mu\frac{\partial}{\partial z}\left(\frac{\partial v_y}{\partial z} + \frac{\partial v_z}{\partial y}\right) + \frac{\partial P}{\partial y} - f_y = 0 \tag{13.3.2}$$

$$\rho\frac{\partial v_z}{\partial t} - 2\mu\frac{\partial^2 v_z}{\partial z^2} - \mu\frac{\partial}{\partial x}\left(\frac{\partial v_x}{\partial z} + \frac{\partial v_z}{\partial x}\right) - \mu\frac{\partial}{\partial y}\left(\frac{\partial v_y}{\partial z} + \frac{\partial v_z}{\partial y}\right) + \frac{\partial P}{\partial z} - f_z = 0 \tag{13.3.3}$$

$$\frac{\partial v_x}{\partial x} + \frac{\partial v_y}{\partial y} + \frac{\partial v_z}{\partial z} = 0 \tag{13.3.4}$$

where (v_x, v_y, v_z) are the components of the velocity vector $\mathbf{v}$, P is the hydrostatic pressure, (f_x, f_y, f_z) are the components of the body force vector $\mathbf{f}$, and ρ is the mass density.

13.3.2 Weak Forms

There are four unknowns (v_x, v_y, v_z, P) in four equations. It is possible to construct a mixed finite element model of these equations, but here we consider only the penalty finite element model of the equations. In developing the penalty finite element model, we replace the pressure P in the momentum equations with

$$P = -\gamma \left(\frac{\partial v_x}{\partial x} + \frac{\partial v_y}{\partial y} + \frac{\partial v_z}{\partial z} \right) \tag{13.3.5}$$

and omit the continuity equation, Eq. (13.3.4). Recall from Section 11.4 that γ is the penalty parameter. The variational problem of the resulting equations can be cast in vector form as [see Section 11.4.4, and in particular Eqs. (11.4.23) and (11.4.24)]:

$$B_t(\mathbf{w}, \mathbf{v}) + B_p(\mathbf{w}, \mathbf{v}) = l(\mathbf{w}) \tag{13.3.6}$$

where the bilinear forms $B_t(\mathbf{w}, \mathbf{v})$ and $B_p(\mathbf{w}, \mathbf{v})$, and the linear form $l(\mathbf{w})$ are defined [see Eqs. (11.3.10a) and (11.4.19)] as follows:

$$\mathbf{w} = \begin{Bmatrix} w_1 \\ w_2 \\ w_3 \end{Bmatrix}, \quad \mathbf{v} = \begin{Bmatrix} v_x \\ v_y \\ v_z \end{Bmatrix}, \quad \mathbf{f} = \begin{Bmatrix} f_x \\ f_y \\ f_z \end{Bmatrix}, \quad \mathbf{t} = \begin{Bmatrix} t_x \\ t_y \\ t_z \end{Bmatrix} \tag{13.3.7}$$

$$B_t(\mathbf{w}, \mathbf{v}) = \int_{\Omega_e} \rho \mathbf{w}^{\mathrm{T}} \dot{\mathbf{v}} \, dv$$

$$B_p(\mathbf{w}, \mathbf{v}) = \int_{\Omega_e} (\mathbf{D}\mathbf{w})^{\mathrm{T}} \mathbf{C} (\mathbf{D}\mathbf{v}) \, dv + \int_{\Omega_e} \gamma_e \left(\mathbf{D}_1^{\mathrm{T}} \mathbf{w}\right)^{\mathrm{T}} \mathbf{D}_1^{\mathrm{T}} \mathbf{v} \, dv \tag{13.3.8}$$

$$l(\mathbf{w}) = \int_{\Omega_e} \mathbf{w}^{\mathrm{T}} \mathbf{f} \, dv + \oint_{\Gamma_e} \mathbf{w}^{\mathrm{T}} \mathbf{t} \, ds$$

Here the matrix differential operators **D** and $\mathbf{D}_1$ and **C** are defined by [see Eq. (11.3.10b)]

$$\mathbf{D}=\begin{bmatrix} \frac{\partial}{\partial x} & 0 & 0 \\ 0 & \frac{\partial}{\partial y} & 0 \\ 0 & 0 & \frac{\partial}{\partial z} \\ \frac{\partial}{\partial y} & \frac{\partial}{\partial x} & 0 \\ \frac{\partial}{\partial z} & 0 & \frac{\partial}{\partial x} \\ 0 & \frac{\partial}{\partial z} & \frac{\partial}{\partial y} \end{bmatrix}, \quad \mathbf{D}_1=\begin{Bmatrix} \frac{\partial}{\partial x} \\ \frac{\partial}{\partial y} \\ \frac{\partial}{\partial z} \end{Bmatrix}, \quad \mathbf{C}=\mu\begin{bmatrix} 2 & 0 & 0 & 0 & 0 & 0 \\ 0 & 2 & 0 & 0 & 0 & 0 \\ 0 & 0 & 2 & 0 & 0 & 0 \\ 0 & 0 & 0 & 1 & 0 & 0 \\ 0 & 0 & 0 & 0 & 1 & 0 \\ 0 & 0 & 0 & 0 & 0 & 1 \end{bmatrix} \tag{13.3.9}$$

13.3.3 Finite Element Model

We assume finite element approximation of the form

$$\mathbf{v}=\begin{Bmatrix} v_x \\ v_y \\ v_z \end{Bmatrix}=\mathbf{\Psi\Delta}, \quad \mathbf{w}=\begin{Bmatrix} w_1 \\ w_2 \\ w_3 \end{Bmatrix} \tag{13.3.10}$$

where

$$\mathbf{\Psi}=\begin{bmatrix} \psi_1 & 0 & 0 & \psi_2 & 0 & 0 & \dots & \psi_n & 0 & 0 \\ 0 & \psi_1 & 0 & 0 & \psi_2 & 0 & 0 & \dots & \psi_n & 0 \\ 0 & 0 & \psi_1 & 0 & 0 & \psi_2 & 0 & 0 & \dots & \psi_n \end{bmatrix}_{(3\times 3n)}$$

$$\mathbf{\Delta}=\begin{Bmatrix} v_x^1 & v_y^1 & v_z^1 & v_x^2 & v_y^2 & v_z^2 & \dots & v_x^n & v_y^n & v_z^n \end{Bmatrix}^{\mathrm{T}}_{(3n\times 1)} \tag{13.3.11}$$

Substituting Eq. (13.3.10) into the variational statement in Eq. (13.3.6), we obtain the following ($3n \times 3n$, where n is the number of nodes in the element) finite element equations:

$$\mathbf{M}^e\dot{\mathbf{\Delta}}^e+\left(\mathbf{K}_v^e+\mathbf{K}_p^e\right)\mathbf{\Delta}^e=\mathbf{F}^e \tag{13.3.12}$$

where $\mathbf{K}_v^e$ is the contribution of the viscous terms (i.e., terms containing the element viscosity μ_e), $\mathbf{K}_p^e$ is the contribution of the penalty terms (i.e., terms containing the element penalty parameter γe), and $\mathbf{K}_v^e$ and $\mathbf{K}_p^e$ are of the order $3n \times 3n$; and $\mathbf{F}^e$ is the contribution of the body forces (f_x, f_y, f_z) as

well as the boundary stresses (t_x, t_y, t_z) (**F** is of the order $3n \times 1$):

$$\mathbf{M}^e = \int_{\Omega_e} \rho \boldsymbol{\Psi}^{\mathrm{T}} \boldsymbol{\Psi}\, dv, \quad \mathbf{K}_v^e = \int_{\Omega_e} \mathbf{B}_v^{\mathrm{T}} \mathbf{C} \mathbf{B}_v\, dv, \quad \mathbf{K}_p^e = \int_{\Omega_e} \gamma_e \mathbf{B}_p^{\mathrm{T}} \mathbf{B}_p\, dv$$

$$\mathbf{F}^e = \int_{\Omega_e} \boldsymbol{\Psi}^{\mathrm{T}} \mathbf{f}\, dv + \oint_{\Gamma_e} \boldsymbol{\Psi}^{\mathrm{T}} \mathbf{t}\, ds \tag{13.3.13}$$

$$\mathbf{B}_v = \mathbf{D}\boldsymbol{\Psi}, \quad \mathbf{B}_p = \mathbf{D}_1^{\mathrm{T}} \boldsymbol{\Psi}$$

where dv is a volume element and ds is the surface element in the 3-D finite element, Ω_e, and its closed surface, Γ_e, respectively.

If we use the weak-form approach of Chapter 11, we obtain (prove to yourself)

$$\begin{bmatrix} \mathbf{M}^{11} & 0 & 0 \\ 0 & \mathbf{M}^{22} & 0 \\ 0 & 0 & \mathbf{M}^{33} \end{bmatrix} \begin{Bmatrix} \dot{\mathbf{v}}_x \\ \dot{\mathbf{v}}_y \\ \dot{\mathbf{v}}_z \end{Bmatrix} + \begin{bmatrix} \mathbf{K}^{11} & \mathbf{K}^{12} & \mathbf{K}^{13} \\ \mathbf{K}^{21} & \mathbf{K}^{22} & \mathbf{K}^{23} \\ \mathbf{K}^{31} & \mathbf{K}^{32} & \mathbf{K}^{33} \end{bmatrix} \begin{Bmatrix} \mathbf{v}_x \\ \mathbf{v}_y \\ \mathbf{v}_z \end{Bmatrix} = \begin{Bmatrix} \mathbf{F}^1 \\ \mathbf{F}^2 \\ \mathbf{F}^3 \end{Bmatrix} \tag{13.3.14}$$

where, for example,

$$M_{ij}^{11} = \int_{\Omega_e} \rho \psi_i^e \psi_j^e\, dxdydz, \quad K_{ij}^{12} = \int_{\Omega_e} \left(\mu \frac{\partial \psi_i^e}{\partial y} \frac{\partial \psi_j^e}{\partial x} + \gamma \frac{\partial \psi_i^e}{\partial x} \frac{\partial \psi_j^e}{\partial y} \right) dxdydz$$

$$K_{ij}^{11} = \int_{\Omega_e} \left[\mu \left(2 \frac{\partial \psi_i^e}{\partial x} \frac{\partial \psi_j^e}{\partial x} + \frac{\partial \psi_i^e}{\partial y} \frac{\partial \psi_j^e}{\partial y} + \frac{\partial \psi_i^e}{\partial z} \frac{\partial \psi_j^e}{\partial z} \right) + \gamma \frac{\partial \psi_i^e}{\partial x} \frac{\partial \psi_j^e}{\partial x} \right] dxdydz \tag{13.3.15}$$

13.4 Elasticity

13.4.1 Governing Equations

Here, we develop the finite element models of three-dimensional elasticity problems [see Eqs. (12.1.1)–(12.1.5)]. We write the governing equations of a linearized 3-D elastic medium, Eqs. (12.1.1)–(12.1.5), in vector form and then develop the weak forms and finite element models in vector forms (see Sections 12.3.2 and 12.4.2).

Strain-Displacement Relations

$$\varepsilon_{xx} = \frac{\partial u_x}{\partial x}, \quad \varepsilon_{yy} = \frac{\partial u_y}{\partial y}, \quad \varepsilon_{zz} = \frac{\partial u_z}{\partial z}$$
$$2\varepsilon_{xy} = \frac{\partial u_x}{\partial y} + \frac{\partial u_y}{\partial x}, \quad 2\varepsilon_{xz} = \frac{\partial u_x}{\partial z} + \frac{\partial u_z}{\partial x}, \quad 2\varepsilon_{yz} = \frac{\partial u_y}{\partial z} + \frac{\partial u_z}{\partial y} \tag{13.4.1}$$

or

$$\boldsymbol{\varepsilon} = \mathbf{D}\mathbf{u}, \quad \boldsymbol{\varepsilon} = \begin{Bmatrix} \varepsilon_{xx} \\ \varepsilon_{yy} \\ \varepsilon_{zz} \\ 2\varepsilon_{yz} \\ 2\varepsilon_{xz} \\ 2\varepsilon_{xy} \end{Bmatrix}, \quad \mathbf{D}^{\mathrm{T}} = \begin{bmatrix} \frac{\partial}{\partial x} & 0 & 0 & 0 & \frac{\partial}{\partial z} & \frac{\partial}{\partial y} \\ 0 & \frac{\partial}{\partial y} & 0 & \frac{\partial}{\partial z} & 0 & \frac{\partial}{\partial x} \\ 0 & 0 & \frac{\partial}{\partial z} & \frac{\partial}{\partial y} & \frac{\partial}{\partial x} & 0 \end{bmatrix} \tag{13.4.2}$$

where (ε_{xx}, ε_{yy}, ε_{zz}, ε_{xy}, ε_{xz}, ε_{yz}) are the components of the strain tensor ε, (u_x, u_y, u_z) are the components of the displacement vector **u**.

Equations of Motion

$$\begin{aligned} \frac{\partial \sigma_{xx}}{\partial x} + \frac{\partial \sigma_{xy}}{\partial y} + \frac{\partial \sigma_{xz}}{\partial z} + f_x &= \rho \frac{\partial^2 u_x}{\partial t^2} \\ \frac{\partial \sigma_{xy}}{\partial x} + \frac{\partial \sigma_{yy}}{\partial y} + \frac{\partial \sigma_{yz}}{\partial z} + f_y &= \rho \frac{\partial^2 u_y}{\partial t^2} \\ \frac{\partial \sigma_{xz}}{\partial x} + \frac{\partial \sigma_{yz}}{\partial y} + \frac{\partial \sigma_{zz}}{\partial z} + f_z &= \rho \frac{\partial^2 u_z}{\partial t^2} \end{aligned} \tag{13.4.3}$$

or

$$\mathbf{D}^{\mathrm{T}}\boldsymbol{\sigma} + \mathbf{f} = \rho\ddot{\mathbf{u}} \tag{13.4.4}$$

where f_x, f_y, and f_z denote the components of the body force vector **f** (measured per unit volume) along the x, y, and z directions, respectively, ρ is the mass density of the material, and

$$\boldsymbol{\sigma} = \begin{Bmatrix} \sigma_{xx} \\ \sigma_{yy} \\ \sigma_{zz} \\ \sigma_{yz} \\ \sigma_{xz} \\ \sigma_{xy} \end{Bmatrix}, \quad \mathbf{f} = \begin{Bmatrix} f_x \\ f_y \\ f_z \end{Bmatrix}, \quad \mathbf{u} = \begin{Bmatrix} u_x \\ u_y \\ u_z \end{Bmatrix} \tag{13.4.5}$$

Stress-Strain (or Constitutive) Relations for an Orthotropic Material

$$\begin{Bmatrix} \sigma_{xx} \\ \sigma_{yy} \\ \sigma_{zz} \\ \sigma_{yz} \\ \sigma_{xz} \\ \sigma_{xy} \end{Bmatrix} = \begin{bmatrix} c_{11} & c_{12} & c_{13} & 0 & 0 & 0 \\ c_{12} & c_{22} & c_{23} & 0 & 0 & 0 \\ c_{13} & c_{23} & c_{33} & 0 & 0 & 0 \\ 0 & 0 & 0 & c_{44} & 0 & 0 \\ 0 & 0 & 0 & 0 & c_{55} & 0 \\ 0 & 0 & 0 & 0 & 0 & c_{66} \end{bmatrix} \begin{Bmatrix} \varepsilon_{xx} \\ \varepsilon_{yy} \\ \varepsilon_{zz} \\ 2\varepsilon_{yz} \\ 2\varepsilon_{xz} \\ 2\varepsilon_{xy} \end{Bmatrix} \quad \text{or} \quad \boldsymbol{\sigma} = \mathbf{C}\boldsymbol{\varepsilon} \tag{13.4.6}$$

where c_{ij} ($c_{ji} = c_{ij}$) are the elasticity (material) constants for an orthotropic medium with the material principal directions (x_1, x_2, x_3) coinciding with the coordinate axes (x, y, z) used to describe the problem. The c_{ij} can be expressed in terms of the engineering constants (E_1, E_2, E_3, ν_{12}, ν_{13}, ν_{23}, G_{12}, G_{13}, G_{23}) for an orthotropic material by Eq. (12.1.4).

Boundary Conditions

$$\text{Natural} \qquad \left.\begin{aligned} t_x &\equiv \sigma_{xx} n_x + \sigma_{xy} n_y + \sigma_{xz} n_z = \hat{t}_x \\ t_y &\equiv \sigma_{xy} n_x + \sigma_{yy} n_y + \sigma_{yz} n_z = \hat{t}_y \\ t_z &\equiv \sigma_{xz} n_x + \sigma_{yz} n_y + \sigma_{zz} n_z = \hat{t}_z \end{aligned}\right\} \quad \text{on } \Gamma_\sigma \tag{13.4.7}$$

$$\text{Essential} \qquad \mathbf{u} = \hat{\mathbf{u}} \quad \text{on } \Gamma_u \tag{13.4.8}$$

13.4.2 Principle of Virtual Displacements

The principle of virtual displacements for a three-dimensional elastic body Ω_e can be expressed in vector form as in Eq. (12.3.4):

$$0 = \int_{\Omega_e} \left[(\mathbf{D}\delta\mathbf{u})^{\mathrm{T}} \mathbf{C} (\mathbf{D}\mathbf{u}) + \rho \delta\mathbf{u}^{\mathrm{T}} \ddot{\mathbf{u}} \right] dV - \int_{\Omega_e} (\delta\mathbf{u})^{\mathrm{T}} \mathbf{f}\, dV - \oint_{\Gamma_e} (\delta\mathbf{u})^{\mathrm{T}} \mathbf{t}\, dS \tag{13.4.9}$$

where δ denotes the variational operator and $\delta(\cdot)$ is the variation of the enclosed quantity.

13.4.3 Finite Element Model

The finite element approximation is assumed to be in the form

$$\mathbf{u} = \begin{Bmatrix} u_x \\ u_y \\ u_z \end{Bmatrix} = \boldsymbol{\Psi}\boldsymbol{\Delta}, \quad \mathbf{w} = \delta\mathbf{u} = \begin{Bmatrix} w_1 = \delta u_x \\ w_2 = \delta u_y \\ w_3 = \delta u_z \end{Bmatrix} = \boldsymbol{\Psi}\delta\boldsymbol{\Delta} \tag{13.4.10}$$

where

$$\boldsymbol{\Psi} = \begin{bmatrix} \psi_1 & 0 & 0 & \psi_2 & 0 & 0 & \dots & \psi_n & 0 & 0 \\ 0 & \psi_1 & 0 & 0 & \psi_2 & 0 & \dots & 0 & \psi_n & 0 \\ 0 & 0 & \psi_1 & 0 & 0 & \psi_2 & 0 & \dots & 0 & \psi_n \end{bmatrix}$$

$$\boldsymbol{\Delta} = \begin{Bmatrix} u_x^1 & u_y^1 & u_z^1 & u_x^2 & u_y^2 & u_z^2 & \dots & u_x^n & u_y^n & u_z^n \end{Bmatrix}^{\mathrm{T}} \tag{13.4.11}$$

Substituting Eq. (13.4.10) into the statement of the principle of virtual work (13.4.9), we arrive at the finite element model of a three-dimensional elastic finite element:

$$\mathbf{M}^e\ddot{\boldsymbol{\Delta}}^e + \mathbf{K}^e\boldsymbol{\Delta}^e = \mathbf{f}^e + \mathbf{Q}^e \tag{13.4.12}$$

where

$$\mathbf{K}^e = \int_{\Omega_e} \mathbf{B}^{\mathrm{T}}\mathbf{C}\mathbf{B}\, dV, \quad \mathbf{M}^e = \int_{\Omega_e} \rho\boldsymbol{\Psi}^{\mathrm{T}}\boldsymbol{\Psi}\, dV$$
$$\mathbf{f}^e = \int_{\Omega_e} \boldsymbol{\Psi}^{\mathrm{T}}\mathbf{f}\, dV, \qquad \mathbf{Q}^e = \oint_{\Gamma_e} \boldsymbol{\Psi}^{\mathrm{T}}\mathbf{t}\, dS \tag{13.4.13}$$

The element mass matrix $\mathbf{M}^e$ and stiffness matrix $\mathbf{K}^e$ are of order $3n \times 3n$ and the element load vector $\mathbf{f}^e$ and the vector of internal forces $\mathbf{Q}^e$ are of order $3n \times 1$, where n is the number of nodes in a typical finite element, Ω^e.

13.5 Element Interpolation Functions and Numerical

13.5.1 Fully Discretized Models and Computer Implementation

The semidiscrete finite element models in Eqs. (13.2.6), (13.3.12), and (13.4.12) can be transformed to fully discretized finite element models using the steps outlined in Chapter 7 for parabolic [Eqs. (7.4.29a) and (7.4.29b)] and hyperbolic [Eqs. (7.4.37a) and (7.4.37b)] equations. The associated eigenvalue problems can also be derived as discussed in Eqs. (7.4.25c) and (7.4.32c), respectively.

Computer implementation of the three classes of problems described in Sections 13.2–13.4 is straightforward, and follows the ideas presented in Chapter 10. In fact, the computer program **FEM2D** can be readily modified to **FEM3D** with modest effort. The element subroutine **ELKMF*** undergoes changes to reflect the 3-D terms in the definition of the coefficient matrices. Another change is in the subroutine **SHAPE3D** in which the interpolation functions and their global derivatives are evaluated. In the next section, interpolation functions for a number of commonly used three-dimensional finite elements are presented. We note that in going from two dimensions to three dimensions, we increase the number of geometries (i.e., shapes) that can be used to define finite element interpolation functions.

13.5.2 Three-Dimensional Finite Elements

The element matrices in Eqs. (13.2.7), (13.3.13), and (13.4.13) require the use of C^0 (i.e., the Lagrange) family of interpolation functions. The interpolation functions can be derived as described in Chapter 10 for two-dimensional elements, and the three-dimensional interpolation functions have the same interpolation properties as those of two-dimensional elements:

$$\sum_{i=1}^{n} \psi_i^e(\xi,\eta,\zeta) = 1, \quad \psi_i^e(\xi_j,\eta_j,\zeta_j) = \delta_{ij} \tag{13.5.1}$$

In this section, a number of commonly used three-dimensional elements are presented (see [1–4]).

13.5.2.1 Hexahedral (brick) elements

Brick elements represent the most commonly used finite elements in 3-

D problems, and the straight-sided, (tri)linear, eight-node brick element shown in Fig. 13.5.1 is the most cost-effective choice. Note that an actual element (and its deformed shape in the case of elasticity problems) have eight points in 3-D space connected by planes, while the master element is a cube of dimensions 2 × 2 × 2 units. The interpolation functions of the linear element are derived from the trilinear polynomial

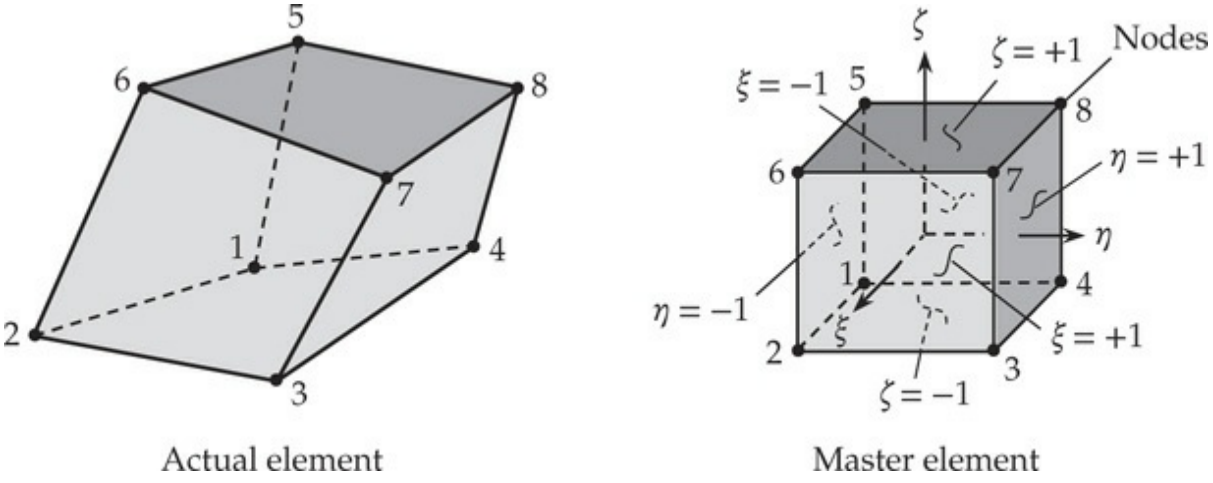

Fig. 13.5.1 The linear (eight-node) brick element.

$$\psi_i^e(\xi,\eta,\zeta) = c_0 + c_1\xi + c_2\eta + c_3\zeta + c_4\xi\eta + c_5\xi\zeta + c_6\eta\zeta + c_7\xi\eta\zeta \tag{13.5.2}$$

using the interpolation properties in Eq. (13.5.1). In the case of the trilinear brick element the interpolation functions can be obtained using the products of one-dimensional functions in terms of the normalized (natural) coordinates (ξ, η, ζ):

$$\psi_{ijk}(\xi,\eta,\zeta) \equiv \psi_i(\xi)\,\psi_j(\eta)\,\psi_k(\zeta), \quad i,j,k = 1,2 \tag{13.5.3}$$

where, for example, $\psi_i(\xi)$ is defined by

$$\psi_1(\xi) = \tfrac{1}{2}(1-\xi), \quad \psi_2(\xi) = \tfrac{1}{2}(1+\xi) \tag{13.5.4}$$

Then denoting

$$\begin{aligned} &\psi_{111} = \psi_1, \quad \psi_{211} = \psi_2, \quad \psi_{221} = \psi_3, \quad \psi_{121} = \psi_4 \\ &\psi_{112} = \psi_5, \quad \psi_{212} = \psi_6, \quad \psi_{222} = \psi_7, \quad \psi_{122} = \psi_8 \end{aligned} \tag{13.5.5}$$

we obtain

$$\Psi^e = \frac{1}{8}\begin{Bmatrix} (1-\xi)(1-\eta)(1-\zeta) \\ (1+\xi)(1-\eta)(1-\zeta) \\ (1+\xi)(1+\eta)(1-\zeta) \\ (1-\xi)(1+\eta)(1-\zeta) \\ (1-\xi)(1-\eta)(1+\zeta) \\ (1+\xi)(1-\eta)(1+\zeta) \\ (1+\xi)(1+\eta)(1+\zeta) \\ (1-\xi)(1+\eta)(1+\zeta) \end{Bmatrix} \tag{13.5.6}$$

The quadratic shape functions for the 20-node serendipity element (see Fig. 13.5.2) are given in Eq. (13.5.7).

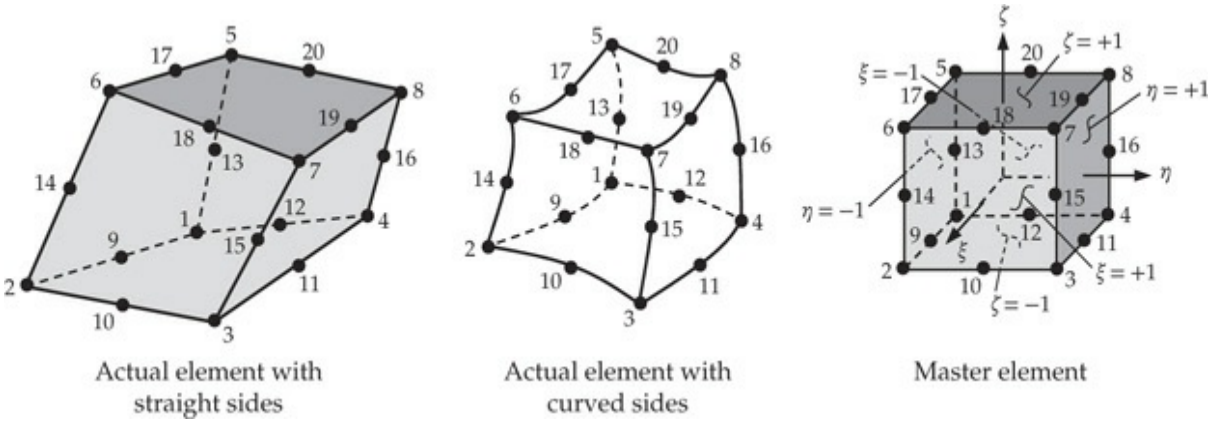

Fig. 13.5.2 The (20-node) quadratic brick element.

$$\boldsymbol{\Psi}^e = \frac{1}{8}\begin{Bmatrix} (1-\xi)(1-\eta)(1-\zeta)(-\xi-\eta-\zeta-2) \\ (1+\xi)(1-\eta)(1-\zeta)(\xi-\eta-\zeta-2) \\ (1+\xi)(1+\eta)(1-\zeta)(\xi+\eta-\zeta-2) \\ (1-\xi)(1+\eta)(1-\zeta)(-\xi+\eta-\zeta-2) \\ (1-\xi)(1-\eta)(1+\zeta)(-\xi-\eta+\zeta-2) \\ (1+\xi)(1-\eta)(1+\zeta)(\xi-\eta+\zeta-2) \\ (1+\xi)(1+\eta)(1+\zeta)(\xi+\eta+\zeta-2) \\ (1-\xi)(1+\eta)(1+\zeta)(-\xi+\eta+\zeta-2) \\ 2(1-\xi^2)(1-\eta)(1-\zeta) \\ 2(1+\xi)(1-\eta^2)(1-\zeta) \\ 2(1-\xi^2)(1+\eta)(1-\zeta) \\ 2(1-\xi)(1-\eta^2)(1-\zeta) \\ 2(1-\xi)(1-\eta)(1-\zeta^2) \\ 2(1+\xi)(1-\eta)(1-\zeta^2) \\ 2(1+\xi)(1+\eta)(1-\zeta^2) \\ 2(1-\xi)(1+\eta)(1-\zeta^2) \\ 2(1-\xi^2)(1-\eta)(1+\zeta) \\ 2(1+\xi)(1-\eta^2)(1+\zeta) \\ 2(1-\xi^2)(1+\eta)(1+\zeta) \\ 2(1-\xi)(1-\eta^2)(1+\zeta) \end{Bmatrix} \tag{13.5.7}$$

As in the case of the two-dimensional quadratic (nine-node) Lagrange element, a brick element with 27 nodes may also be constructed; the shape functions are not shown for this element.

The transformation between the actual element Ω_e and the master element Ω [or equivalently, between (x, y, z) and (ξ, η, ζ)] is accomplished by a coordinate transformation of the form

$$x = \sum_{i=1}^{n} x_i^e \phi_i^e(\xi,\eta,\zeta), \quad y = \sum_{i=1}^{n} y_i^e \phi_i^e(\xi,\eta,\zeta), \quad z = \sum_{i=1}^{n} z_i^e \phi_i^e(\xi,\eta,\zeta) \tag{13.5.8}$$

where n is the number of nodes in the element.

13.5.2.2 Tetrahedral elements

The standard tetrahedral elements are a three-dimensional version of the triangular elements. The 4-node linear and 10-node quadratic tetrahedral elements are shown in Figs. 13.5.3(a) and (b), respectively. The volume coordinates, L_i, are used to describe the interpolation functions for linear and quadratic elements, where $L_1 + L_2 + L_3 + L_4 = 1$. The interpolation functions are

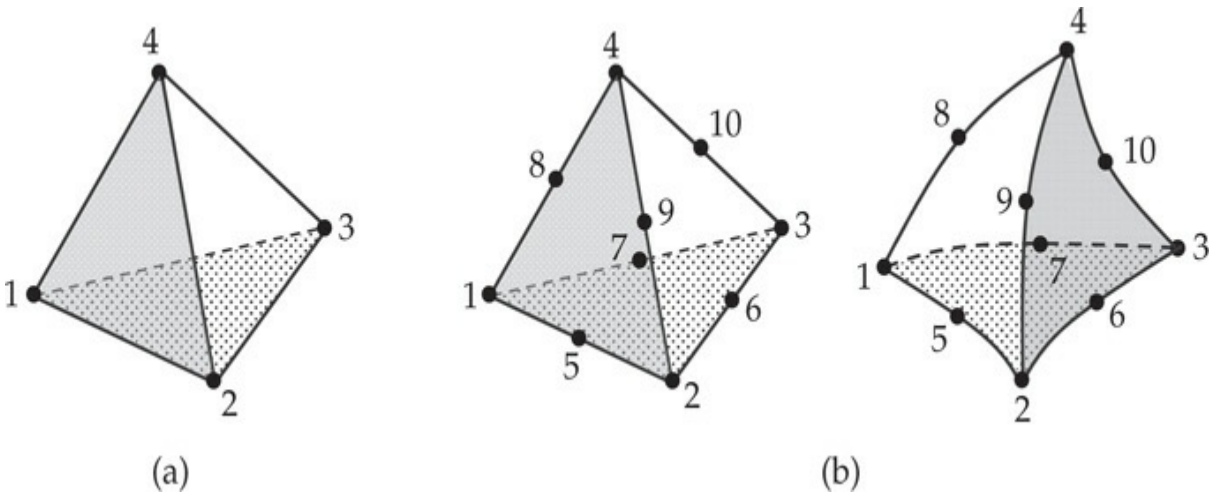

Fig. 13.5.3 Linear and quadratic tetrahedral elements.

$$\boldsymbol{\Psi}^e = \begin{Bmatrix} L_1 \\ L_2 \\ L_3 \\ L_4 \end{Bmatrix}; \quad \boldsymbol{\Psi}^e = \begin{Bmatrix} L_1(2L_1 - 1) \\ L_2(2L_2 - 1) \\ L_3(2L_3 - 1) \\ L_4(2L_4 - 1) \\ 4L_1L_2 \\ 4L_2L_3 \\ 4L_3L_1 \\ 4L_1L_4 \\ 4L_2L_4 \\ 4L_3L_4 \end{Bmatrix} \tag{13.5.9}$$

Other higher-order tetrahedrons may be defined that have nodes at the element centroid and the center of each triangular face.

13.5.2.3 Prism elements

A prism or wedge element is often useful in three-dimensional geometries, especially, for transitioning between hexahedral and tetrahedral elements. The shape functions for the six-node linear element [see Fig. 13.5.4(a)] are given by

$$\boldsymbol{\Psi}^e = \frac{1}{2}\begin{Bmatrix} L_1(1-\zeta) \\ L_2(1-\zeta) \\ L_3(1-\zeta) \\ L_1(1+\zeta) \\ L_2(1+\zeta) \\ L_3(1+\zeta) \end{Bmatrix} \tag{13.5.10}$$

The interpolation functions for the 15-node quadratic prism element [see Fig. 13.5.4(b)] are

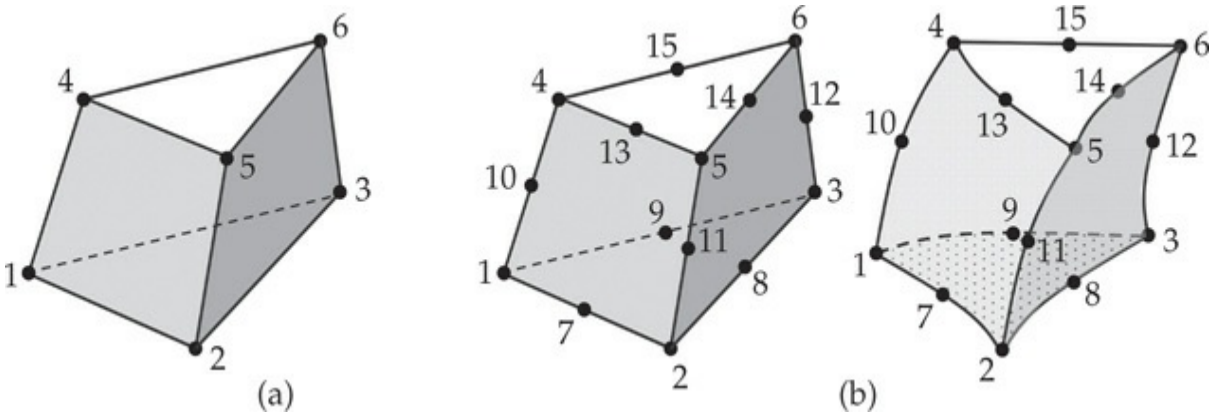

Fig. 13.5.4 (a) The six-node linear prism element. (b) The 15-node quadratic prism element.

$$\boldsymbol{\Psi}^e = \frac{1}{2}\begin{Bmatrix} L_1[(2L_1-1)(1-\zeta)-(1-\zeta^2)] \\ L_2[(2L_2-1)(1-\zeta)-(1-\zeta^2)] \\ L_3[(2L_3-1)(1-\zeta)-(1-\zeta^2)] \\ L_1[(2L_1-1)(1+\zeta)-(1-\zeta^2)] \\ L_2[(2L_2-1)(1+\zeta)-(1-\zeta^2)] \\ L_3[(2L_3-1)(1+\zeta)-(1-\zeta^2)] \\ 4L_1L_2(1-\zeta) \\ 4L_2L_3(1-\zeta) \\ 4L_3L_1(1-\zeta) \\ 2L_1(1-\zeta^2) \\ 2L_2(1-\zeta^2) \\ 2L_3(1-\zeta^2) \\ 4L_1L_2(1+\zeta) \\ 4L_2L_3(1+\zeta) \\ 4L_3L_1(1+\zeta) \end{Bmatrix} \tag{13.5.11}$$

The area coordinates, L_i , are used to describe the functional variation in the triangular cross section of the prism elements, while a standard normalized coordinate, ζ, describes the variation in the vertical direction. Note that $L_1 + L_2 + L_3 = 1$.

13.5.3 Numerical Integration

The evaluation of the various finite element coefficient matrices in Eqs. (13.2.7), (13.3.13), and (13.4.13) require the integration of the product of interpolation functions and their spatial derivatives over the area or volume of the element. The numerical integration ideas described in Section 10.3 can be easily extended to three dimensions. Here we give the pertinent equations for the three-dimensional case.

In evaluating the element matrices numerically, the geometry of the elements can be described by the transformation equations in Eq. (13.5.8). Under these transformations, the master tetrahedral, prism, and hexahedral elements transform to arbitrary tetrahedral, prism, and hexahedral elements. The definition of the Jacobian matrix and the numerical quadrature rules described in Chapter 10 can be extended to the three-dimensional case. For an isoparametric formulation, the following relations, based on the chain rule of differentiation, can be derived for brick elements:

$$\begin{Bmatrix} \frac{\partial \psi_i}{\partial \xi} \\ \frac{\partial \psi_i}{\partial \eta} \\ \frac{\partial \psi_i}{\partial \zeta} \end{Bmatrix} = \begin{bmatrix} \frac{\partial x}{\partial \xi} & \frac{\partial y}{\partial \xi} & \frac{\partial z}{\partial \xi} \\ \frac{\partial x}{\partial \eta} & \frac{\partial y}{\partial \eta} & \frac{\partial z}{\partial \eta} \\ \frac{\partial x}{\partial \zeta} & \frac{\partial y}{\partial \zeta} & \frac{\partial z}{\partial \zeta} \end{bmatrix} \begin{Bmatrix} \frac{\partial \psi_i}{\partial x} \\ \frac{\partial \psi_i}{\partial y} \\ \frac{\partial \psi_i}{\partial z} \end{Bmatrix} = \begin{bmatrix} J_{11} & J_{12} & J_{13} \\ J_{21} & J_{22} & J_{23} \\ J_{31} & J_{32} & J_{33} \end{bmatrix} \begin{Bmatrix} \frac{\partial \psi_i}{\partial x} \\ \frac{\partial \psi_i}{\partial y} \\ \frac{\partial \psi_i}{\partial z} \end{Bmatrix} \tag{13.5.12}$$

Inverting Eq. (13.5.12), we obtain the global spatial derivatives of the interpolation functions in terms of the local derivatives:

$$\begin{Bmatrix} \frac{\partial \psi_i}{\partial x} \\ \frac{\partial \psi_i}{\partial y} \\ \frac{\partial \psi_i}{\partial z} \end{Bmatrix} = \begin{bmatrix} J^*_{11} & J^*_{12} & J^*_{13} \\ J^*_{21} & J^*_{22} & J^*_{23} \\ J^*_{31} & J^*_{32} & J^*_{33} \end{bmatrix} \begin{Bmatrix} \frac{\partial \psi_i}{\partial \xi} \\ \frac{\partial \psi_i}{\partial \eta} \\ \frac{\partial \psi_i}{\partial \zeta} \end{Bmatrix} \tag{13.5.13}$$

where $\mathbf{J}^*$ is the inverse of the Jacobian matrix $\mathbf{J}$. The components J^*_{ij} are complicated functions of the components of $\mathbf{J}$ that can in principle be

obtained by analytically inverting the 3 × 3 Jacobian matrix. In practice, the Jacobian is usually inverted numerically at each integration point.

In performing numerical integration over the element volume, it is necessary to transform the integrand and limits of integration from the global coordinates to the local element coordinates. The differential elemental volume transforms according to (J is the determinant of the Jacobian matrix)

$$d\mathbf{x} = dx\,dy\,dz = J\,d\xi\,d\eta\,d\zeta \tag{13.5.14}$$

The integration limits for the integrals transform to the limits on the local coordinates (ξ, η, ζ), that is, −1 to +1. In the previous equations the (ξ, η, ζ) coordinates for a brick element were used for purposes of explanation. Similar relations for a tetrahedral element can be derived by replacing (ξ, η, ζ) with (L_1, L_2, L_3). The variable L_4 does not enter the formulae due to the relation $L_4 = 1 - (L_1 + L_2 + L_3)$.

To illustrate numerical integration further, we consider the matrix coefficient

$$K_{12}^e = \int_{\Omega^e} a(x,y)\frac{\partial \psi_1^e}{\partial x}\frac{\partial \psi_2^e}{\partial y}\,dxdydz \tag{13.5.15}$$

to be evaluated using a brick element. Transforming the integral to one posed on the master element, we obtain

$$K_{12}^e = \int_{-1}^{+1}\int_{-1}^{+1}\int_{-1}^{+1} \hat{a}(\xi,\eta,\zeta)\left(J_{11}^*\frac{\partial \psi_1}{\partial \xi} + J_{12}^*\frac{\partial \psi_1}{\partial \eta} + J_{13}^*\frac{\partial \psi_1}{\partial \zeta}\right) \times \left(J_{21}^*\frac{\partial \psi_2}{\partial \xi} + J_{22}^*\frac{\partial \psi_2}{\partial \eta} + J_{23}^*\frac{\partial \psi_2}{\partial \zeta}\right) J\,d\xi d\eta d\zeta \tag{13.5.16}$$

where $\hat{a} = a(x(\xi, \eta, \zeta), y(\xi, \eta, \zeta), z(\xi, \eta, \zeta))$.

Each element of a coefficient matrix is of the form

$$K_{ij}^e = \int_{-1}^{+1}\int_{-1}^{+1}\int_{-1}^{+1} F_{ij}(\xi,\eta,\zeta)\,d\xi d\eta d\zeta \tag{13.5.17}$$

The Gauss quadrature formula in Eq. (10.3.16) can be readily extended to three dimensions to evaluate the integral expression K_{ij}^e in Eq. (13.5.17):

$$\int_{-1}^{+1}\int_{-1}^{+1}\int_{-1}^{+1} F_{ij}(\xi,\eta,\zeta)\,d\xi d\eta d\zeta \approx \sum_{I=1}^{M}\sum_{J=1}^{N}\sum_{K=1}^{P} F_{ij}(\xi_I,\eta_J,\zeta_K)\,W_I W_J W_K \qquad (13.5.18)$$

For brick elements it is typical to take $M = N = P = 2$ or 3, depending on whether it is a linear or quadratic element. Other element types (e.g., tetrahedral elements) are also evaluated using quadrature formulae similar to that in Eq. (10.3.26). For additional discussion of quadrature rules and their utilization, the reader may consult [5–7].

13.6 Numerical Examples

In this section we present one example of each of the areas covered in this chapter: (1) heat conduction, (2) flow of viscous incompressible fluid, and (3) deformation of a solid in three dimensions. The problems were analyzed using programs **FEM3D**, **FLOPEN3D**, and **ELAST3D**, which are extensions of **FEM2D**. These programs are not discussed here.

Example 13.6.1

Consider an isotropic slab of dimensions 1 × 1 × 10 m. The left face is maintained at a temperature of 100°C while the bottom, top and the right faces are maintained at 0°C, as shown in Fig. 13.6.1(a). The front and back faces are assumed to be insulated. There is no internal heat generation. Analyze the problem using a mesh of brick elements.

Solution: Since only temperature boundary conditions are involved, the solution will be independent of the conductivity of the medium. Using the symmetry, a quadrant of the domain is modeled using a mesh of 4 × 2 × 2 eight-node brick elements [see Fig. 13.6.1(b)]. The resulting temperature field is presented in Fig. 13.6.1(c). As one might expect, the three-dimensional solution is the same as the two-dimensional (in the *xy*-plane) solution, because the two-dimensional problem is equivalent to assuming that the slab is infinitely long in the *z*-direction. Thus, all planes parallel to the plane $z = 0$ have the same temperature distribution. The three-dimensional solution would have been different from the two-dimensional one if we had specified, for example, temperature on the front and back faces (AEFB and DHGC).

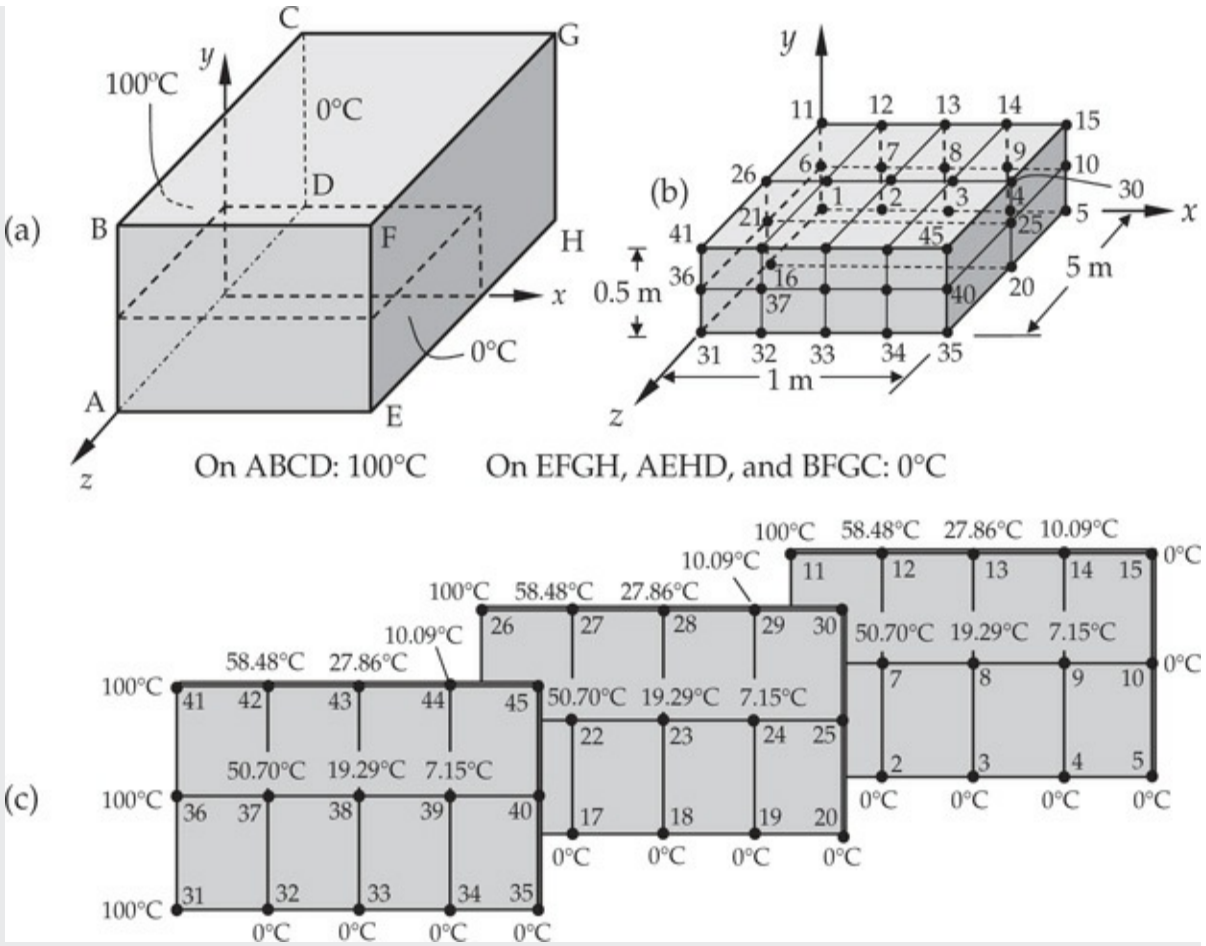

Fig. 13.6.1 Heat conduction in an isotropic slab. (a) Geometry and boundary conditions. (b) Computational domain. (c) Predicted nodal temperatures.

Example 13.6.2

Consider the Couette flow of viscous incompressible fluid between two parallel flat walls, as shown in Fig. 13.6.2(a). Assuming a constant pressure gradient, $-\partial P/\partial x = 1$ N/m^2, across the left and right boundaries and that the top plate is moving at a constant velocity of $v_x(x, 6, z) = 3.0$ m/s, determine the 3-D flow field using the 3-D penalty finite element model with a mesh of 2 × 6 × 2 eight-node brick elements.

Solution: The full domain is used as the computational domain with a mesh of 2 × 6 × 2 eight-node brick elements, as shown in Fig. 13.6.2(b). The velocity boundary conditions are as follows:

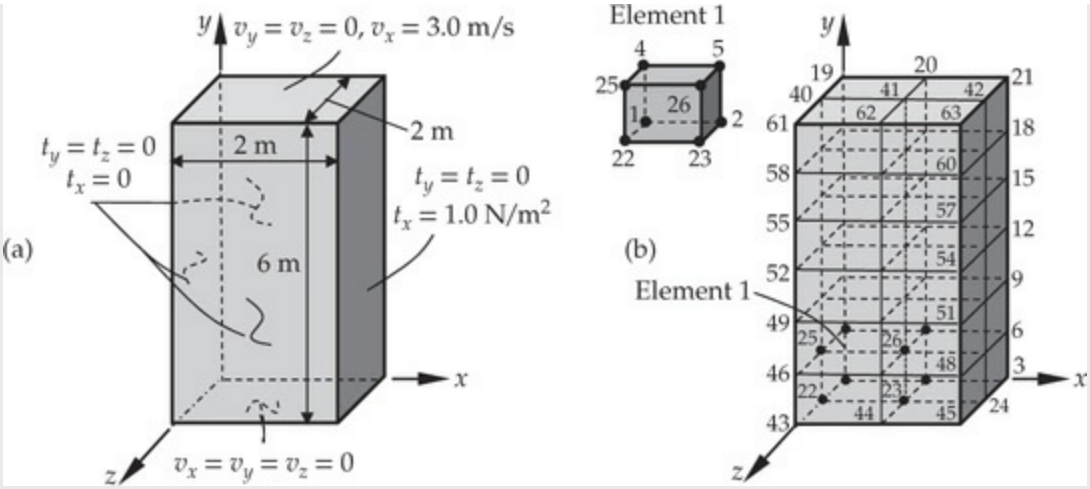

Fig. 13.6.2 Couette flow between two parallel flat plates. (a) Geometry and boundary conditions. (b) Computational domain with a finite element mesh.

$$\begin{aligned} v_x(x,0,z) &= 0.0, \quad v_y(x,0,z) = 0.0, \quad v_z(x,0,z) = 0.0 \\ v_x(x,6,z) &= 3.0, \quad v_y(x,6,z) = 0.0, \quad v_z(x,6,z) = 0.0 \end{aligned} \tag{1}$$

The stress boundary conditions require (t_x, t_y, t_z) to be zero on $x = 0$ plane, $z = 0$ plane, and $z = 2$ plane; also, (t_y, t_z) are zero on $x = 2$ plane. The contribution of the nonzero pressure gradient, $t_x = -\partial P/\partial x = 1.0$, acting on the $x = 2$ plane to the nodes on the plane can be calculated using the formula:

$$f_i^e = \frac{abt_x}{4} \tag{2}$$

where a and b are the y and z dimensions of the two-dimensional surface. Thus, the x-components of the nonzero global nodal forces are

$$\begin{gathered} F_6^x = F_{48}^x = F_9^x = F_{51}^x = F_{12}^x = F_{54}^x = F_{15}^x = F_{57}^x = F_{18}^x = F_{60}^x = 0.5 \\ F_{27}^x = F_{30}^x = F_{33}^x = F_{36}^x = F_{39}^x = 1.0 \end{gathered} \tag{3}$$

The horizontal velocity $v_x(x_0, y, 1.0)$ as a function of y is presented in Fig. 13.6.3 for x_0= 0.0, 1.0, and 2.0. It is clear that there is 3-D effect. In a 2-D analysis, all three velocity profiles would have been the same as the velocity field is only a function of y. These velocity profiles are also different from those on the $z = 0$ or $z = 2$ planes (not shown here), further proving that the flow is three dimensional.

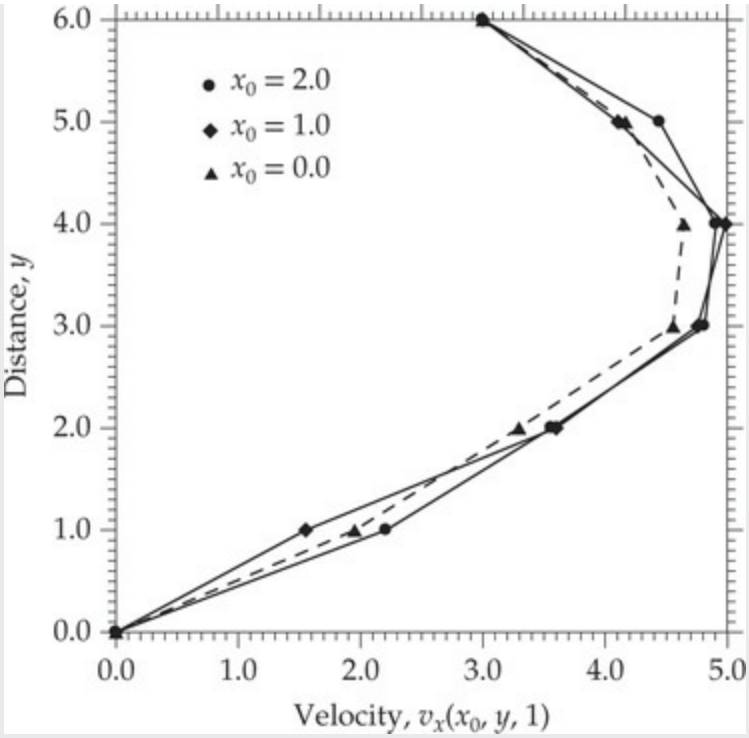

Fig. 13.6.3 Plots of the *x*-component of the velocity field as a function of *y* for the Couette flow between two parallel flat plates.

Example 13.6.3

Consider a steel (E = 200 GPa and ν = 0.28) beam of dimensions $a \times b \times L = 10 \times 10 \times 60$ cm and density ρ (or specific weight $\gamma = \rho g = 77$ kN/m^3, where g is the gravitational constant) is attached to a rigid support at the top, as shown in Fig. 13.6.4(a). Determine the maximum displacement and stress in the beam using the 3-D finite element model and a mesh of 2 × 2 × 6 eight-node brick elements.

Solution: The full domain is used as the computational domain with the mesh shown in Fig. 13.6.4(b). The displacement boundary conditions are

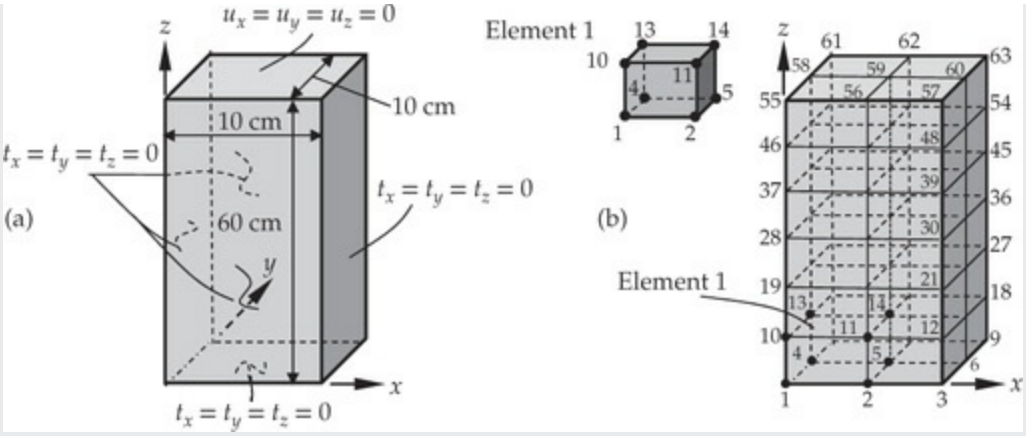

Fig. 13.6.4 Rectangular beam hanging under its own weight. (a) Geometry and boundary conditions. (b) Computational domain with a finite element mesh.

$$u_x(x, y, L) = 0.0, \quad u_y(x, y, L) = 0.0, \quad u_z(x, y, L) = 0.0 \tag{1}$$

The stress boundary conditions require (t_x, t_y, t_z) to be zero on all surfaces except for the $z = L$ plane (where the displacements are specified). The beam deforms under its own weight, that is $f_x = f_y = 0$ and $f_y = -\gamma$. The approximate analytical solution for the displacement u_z and stress σ_{zz} is

$$u_z(x, y, z) = \frac{\gamma}{2E}\left[z^3 - L^2 + \nu\,(x^2 + y^2)\right], \quad \sigma_{zz} = \gamma z \tag{2}$$

The finite element solution for the vertical displacement $u_z(0.05, 0.05, 0) = -0.0677 \times 10^{-6}$ m is about 2.3% in error compared to the analytical solution, -0.0693×10^{-6}, whereas the stress $\sigma_{zz} = 42.35$ kN/m^3 computed at the Gauss point (0.075, 0.075, 0.55) matches with the analytical solution at the same point.

13.7 Summary

This chapter was dedicated to the finite element formulation of 3-D heat transfer, 3-D flows of viscous incompressible fluids, and 3-D elasticity. Starting with the governing equations, weak forms were derived and finite element models were developed for the three cases. A library of interpolation functions of some commonly used three-dimensional finite elements have been presented and numerical integration to evaluate integrals of finite element interpolation functions has been discussed.

Some simple numerical examples of 3-D problems were presented to illustrate the use of 3-D finite elements.

Problems

13.1 Develop the mixed finite element model of the Stokes equations governing the flows of viscous incompressible fluids in three dimensions. Assume the following form of the finite element approximation of the velocity vector **v** and pressure P:

$$v_i(\mathbf{x},t) = \sum_{m=1}^{M} \psi_m(\mathbf{x}) v_i^m(t) = \boldsymbol{\Psi}^T \mathbf{v}_i \tag{1}$$

$$P(\mathbf{x},t) = \sum_{l=1}^{L} \phi_l(\mathbf{x}) P_l(t) = \boldsymbol{\Phi}^T \mathbf{P} \tag{2}$$

where $\boldsymbol{\psi}$ and $\boldsymbol{\Phi}$ are (column) vectors of interpolation (or shape) functions, $\mathbf{v}_i$ and $\mathbf{P}$ are vectors of nodal values of velocity components and pressure, respectively, and the superscript $(\cdot)^T$ denotes a transpose of the enclosed vector or matrix. In particular, show that the vector form of the mixed finite element model is

$$-\mathbf{Q}^T\mathbf{v} = 0, \quad \mathbf{M}\dot{\mathbf{v}} + \mathbf{K}\mathbf{v} - \mathbf{Q}\mathbf{P} = \mathbf{F} \tag{3}$$

and define all matrices.

13.2 Develop a penalty finite element model by treating Eq. (13.3.5) as an additional equation and then use it to eliminate **P** from the second equation of Eq. (3) of **Problem 13.1**. This is known as the consistent penalty finite element model.

13.3 The equations governing nonisothermal flows of an incompressible Newtonian fluid are given by

$$\frac{\partial v_i}{\partial x_i} = 0 \tag{1}$$

$$\rho_0 \frac{\partial v_i}{\partial t} - \frac{\partial}{\partial x_j}\left[-P\delta_{ij} + \mu\left(\frac{\partial v_i}{\partial x_j} + \frac{\partial v_j}{\partial x_i}\right)\right] + \rho_0 g_i \beta (T - T_0) = 0 \tag{2}$$

$$\rho_0 c_v \frac{\partial T}{\partial t} - \frac{\partial}{\partial x_i}\left(k_{ij}\frac{\partial T}{\partial x_j}\right) - Q = 0 \tag{3}$$

where v_i denotes the velocity component, P is the pressure, ρ_0 is the density, g_i is the gravitational force components, T is the temperature, c_v is the specific heat of the fluid at constant volume, β is the coefficient of thermal expansion, Q is the rate of internal heat generation, μ is the shear viscosity of the fluid, and k_{ij} are the components of the thermal conductivity tensor. Develop the mixed finite element model by assuming finite element approximations of the form

$$T(\mathbf{x},t)=\sum_{m=1}^{M}\theta_m(\mathbf{x})T_m(t)=\boldsymbol{\Theta}^T\mathbf{T} \tag{4a}$$

$$v_i(\mathbf{x},t)=\sum_{n=1}^{N}\psi_n(\mathbf{x})v_i^n(t)=\boldsymbol{\Psi}^T\mathbf{v}_i \tag{4b}$$

$$P(\mathbf{x},t)=\sum_{l=1}^{L}\phi_l(\mathbf{x})P_l(t)=\boldsymbol{\Phi}^T\mathbf{P} \tag{4c}$$

where $\boldsymbol{\Theta}$, $\boldsymbol{\psi}$, and $\boldsymbol{\Phi}$ are vectors of interpolation functions, and $\mathbf{T}$, $\mathbf{v}_i$, and $\mathbf{P}$ are vectors of nodal values of temperature, velocity components, and pressure, respectively.

13.4 Derive the interpolation functions ψ_1, ψ_5, and ψ_8 for the eight-node brick element using the procedure described in Chapter 10 for rectangular elements.

13.5 Evaluate the source vector components f_i^e and coefficients K_{ij}^e over a master brick element when f is a constant, f_0, and $k_x = k_y = k_z = k$, a constant in Eq. (13.2.7).

References for Additional Reading

1. J. N. Reddy and D. K. Gartling, *The Finite Element Method in Heat Transfer and Fluid Dynamics,* 3rd ed., CRC Press, Boca Raton, FL, 2010.
2. K. S. Surana and J. N. Reddy, *The Finite Element Method for Boundary Value Problems, Mathematics and Computations,* CRC Press, Boca Raton, FL, 2017.
3. K. S. Surana and J. N. Reddy, *The Finite Element Method for Initial Value Problems, Mathematics and Computations,* CRC Press, Boca

Raton, FL, 2018.

4. O. C. Zienkiewicz and R. L. Taylor, *The Finite Element Method*, 4th ed., *Vol. 2*: *Solid and Fluid Mechanics, Dynamics and Non-linearity*, McGraw-Hill, London, UK, 1989.
5. G. R. Cowper, "Gaussian Quadrature Formulae for Triangles," *International Journal for Numerical Methods in Engineering*, **7**, 405–408, 1973.
6. P. M. Gresho, and R. L. Sani, *Incompressible Flow and the Finite Element Method*, John Wiley & Sons, Chichester, UK, 1998.
7. P. C. Hammer, O. P. Marlowe, and A. H. Stroud, "Numerical Integration over Simplexes and Cones," *Mathematics Tables Aids Computation*, National Research Council, Washington, D.C., **10**, 130–137, 1956.
8. B. M. Irons, "Quadrature Rules for Brick-Based Finite Elements," *International Journal for Numerical Methods in Engineering*, **3**, 293–294, 1971.
9. J. N. Reddy, *Energy Principles and Variational Methods in Applied Mechanics*, 3rd ed., John Wiley & Sons, New York, NY, 2017.
10. J. N. Reddy, *An Introduction to Nonlinear Finite Element Analysis*, 2nd ed., Oxford University Press, Oxford, UK, 2015.
11. J. N. Reddy, "Penalty-Finite-Element Analysis of 3-D Navier–Stokes Equations," *Computer Methods in Applied Mechanics and Engineering*, **35**, 87–106, 1982.
12. M. P. Reddy and J. N. Reddy, "Finite-Element Analysis of Flows of Non-Newtonian Fluids in Three-Dimensional Enclosures," *International Journal of Non-Linear Mechanics*, **27**, 9–26, 1992.

Index

Please note that index links point to page beginnings from the print edition. Locations are approximate in e-readers, and you may need to page down one or more times after clicking a link to get to the indexed material.

Table of Contents

Differential Equations